

AD _____

Award Number:

W81XWH-06-2-0044

TITLE:

Advanced Medical Countermeasures Consortium

PRINCIPAL INVESTIGATOR:

Milton Smith, M.D.

CONTRACTING ORGANIZATION:

**The University of Michigan
Ann Arbor, MI 48109**

REPORT DATE:
October 2010

TYPE OF REPORT:

Final

PREPARED FOR: U.S. Army Medical Research and Materiel Command
Fort Detrick, Maryland 21702-5012

DISTRIBUTION STATEMENT:

X Approved for public release; distribution unlimited

The views, opinions and/or findings contained in this report are those of the author(s) and should not be construed as an official Department of the Army position, policy or decision unless so designated by other documentation.

REPORT DOCUMENTATION PAGE

Form Approved
OMB No. 0704-0188

Public reporting burden for this collection of information is estimated to average 1 hour per response, including the time for reviewing instructions, searching existing data sources, gathering and maintaining the data needed, and completing and reviewing this collection of information. Send comments regarding this burden estimate or any other aspect of this collection of information, including suggestions for reducing this burden to Department of Defense, Washington Headquarters Services, Directorate for Information Operations and Reports (0704-0188), 1215 Jefferson Davis Highway, Suite 1204, Arlington, VA 22202-4302. Respondents should be aware that notwithstanding any other provision of law, no person shall be subject to any penalty for failing to comply with a collection of information if it does not display a currently valid OMB control number. **PLEASE DO NOT RETURN YOUR FORM TO THE ABOVE ADDRESS.**

1. REPORT DATE (DD-MM-YYYY) 01-10-2010			2. REPORT TYPE Final		3. DATES COVERED (From - To) 21 AUG 2006 - 24 SEP 2010	
4. TITLE AND SUBTITLE The development of therapeutic and diagnostic countermeasures by the Advanced Medical Countermeasures Consortium					5a. CONTRACT NUMBER	
6. AUTHOR(S) Milton Smith, M.D. (Amax a subcontractor)					5d. PROJECT NUMBER W81XWH-06-2-0044	
					5e. TASK NUMBER	
					5f. WORK UNIT NUMBER	
7. PERFORMING ORGANIZATION NAME(S) AND ADDRESS(ES) The University of Michigan Ann Arbor, MI 48109					8. PERFORMING ORGANIZATION REPORT NUMBER	
9. SPONSORING / MONITORING AGENCY NAME(S) AND ADDRESS(ES) U.S. Army Medical Research and Material Command Fort Detrick, MD 21702-5012					10. SPONSOR/MONITOR'S ACRONYM(S)	
					11. SPONSOR/MONITOR'S REPORT NUMBER(S)	
12. DISTRIBUTION / AVAILABILITY STATEMENT Approved for public release, distribution unlimited.						
13. SUPPLEMENTARY NOTES						
14. ABSTRACT A diverse cadre of weapons of mass destruction was utilized by the group to examine pathogenesis and methods of intervention. It was determined that oxidative stress is significant component of the pathogenesis of biological and chemical weapons. Antioxidants had an ameliorate effect on both chemical and biological agents, and has the potential to be used as an ancillary treatment. Antigen presenting cells may be useful for detecting subclinical infectious disease. Dendritic cells are able to differentiate between different types of pathogens thus generating a specific signature for the pathogen.						
15. SUBJECT TERMS liposomes, antioxidants, complement, mustard gas, anthrax, ricin, antigen presenting cells, subclinical diagnosis						
16. SECURITY CLASSIFICATION OF:			17. LIMITATION OF ABSTRACT UU	18. NUMBER OF PAGES 537	19a. NAME OF RESPONSIBLE PERSON USAMRMC	
a. REPORT U	b. ABSTRACT U	c. THIS PAGE U			19b. TELEPHONE NUMBER (include area code)	

Table of Contents

Introduction.....	4
Statement of Work.....	4
Body.....	5
Key Research Accomplishments.....	7
Reportable outcomes.....	7
Conclusion.....	8
References	8

Introduction

The Advanced Medical Countermeasures Consortium had the goal developing treatment and diagnostic countermeasures against various weapons of mass destruction. Our approach to these tasks were different in that we looked for common properties in the pathogenesis that would assist us in developing candidate countermeasures. In our experiments we used diverse agents: chemical (CEES- a mustard analogue), biological (anthrax, spike protein, Y. Pestis), and a toxin (Ricin). The Amaox portion of the annual summary will highlight the accomplishments of the group.

Statement of Work

Task 1

Telephone contact and/or visitations with the investigators. These contacts with the investigators will be on going throughout the project.

Frequent telephone contact was made with all of the investigators. Communication with all of the investigators was timely and effective.

Task 2

Develop experimental modifications based on newly gained information from the members of the group. No modifications were necessary.

Task 3

Continue guidance of the development of the APC Biosensor and STIMAL

APC Biosensor-The results the research was encouraging. Late in the cycle of the research it was learned that current approach using gene expression was not the best approach. We now believe that improved, and more cost effective approach would be examine exosomes as a method of diagnostics.

Antioxidant liposomes- they have shown an ameliorative effect chemical and biological weapons.

Task 4

Act as an interface between governmental agencies and the Consortium. In this cycle there were no occurrences where this was necessary.

Task 5

Assurance that reports and other paper work involving the consortium are done in a timely manner. This has been done.

Task 6

Arrange for annual meetings for and Chair the Consortium meetings. In this last year of operation a final meeting was unnecessary.

Task 7

Design experimental goals for both technologies as it applies to the individual projects in each funding cycle. This was successfully done.

Comments on administrative and logistical matters.

Dr. Crawford has not discussed or submitted his annual report to Amaox or to the University of Michigan at this time. The status of the report is unknown.

Body/summary

Liposomes

Enhancement of serum/tissue antioxidant levels have an ameliorative effect on acute lung injury (Misopoulos, 2008), paraquat poisoning (Suntres2002), and CEES (a mustard gas analogue) (McClintock). Liposome encapsulation of antioxidants, in comparison to the free molecules, confer several advantages such as increased half-life, tissue targeting, and solubilizing vitamin E in blood. The liposome encapsulated antioxidants were developed to significantly enhance blood and tissue levels of antioxidants. The liposome encapsulated antioxidants can be administered intravenously, topically or by aerosol.

Stone- East Tennessee State University

Mustard gas is known to affect primarily three organ systems, the skin, eyes and lungs. Dermal exposure to CEES induces multiple inflammatory biomarkers as well as mast cells (Tiwari-Singh,2009). It was hypothesized that mast cells could be important in mustard gas pathogenesis. Dr. Stone utilized RBL-2H3 mast cell lines exposed to CEES to assess if any changes occurred as a consequence of oxidative stress (OS). Proteins undergoing OS are known to have glutathionylation (a post translational modification) that occurs by the attachment of a GSH (glutathione) molecule. After exposure to CEES high levels of caspase-3 levels were found and apoptosis. Liposomes that were utilized by Dr. Rest in his studies with Bacillus anthracis were supplied by Dr. Stone.

Ward-University of Michigan

The causative agent is the coronavirus (SARS-CoV); Spiked protein (SP) is one of the four components of the virus (Rota, 2003). Spike protein, one of the four components of the SARS-CoV virus, was utilized as one of the agents to create an acute lung injury. Spiked protein was chosen since the actual virus can only be used in designated centers. The bronchioalveolar (BAL) fluids in ALI frequently contain proinflammatory cytokines, chemokines, and complement activation products. In the ALI model the amount of leakage of albumin into the BAL is a measure of the extent of lung injury. LPS alone induced a 44% leak of protein which was independent of complement C5a. SP by itself caused a small increase in the leakage of albumin; whereas the LPS in combination with SP caused a leakage of 77%. Neutrophils were the predominant inflammatory cells four hours after the LPS + SP. Multiplex analysis revealed a 5 fold increase in MCP-1 (CCL2), 45% increase in K.C. (CSCL1) and a 2.2 fold increase in IL-12. The data is suggestive of a C5a predominant mediated inflammatory response.

Rest-Drexel University

In 1994 Hanna had begun to explore the role of oxidants in macrophages that were exposed to lethal toxin, one of the primary components of pathogenesis from BA. These macrophages exposed to lethal toxin produce superoxide anion and underwent cytolysis (Hanna,1994). Antioxidants such as NAC or methionine were effective in inhibiting cytolysis. The early work by Hanna gave us the impetus to further explore the effects NAC on BA and innate were exposed to Bacillus anthracis (BA) strain 7702 spores and the vegetative bacteria under a variety of conditions. In untreated macrophages that were incubated with BA there was a time sensitive progression in the numbers of vegetative bacteria, eventually the macrophages were overwhelmed, and died. This was in contrast to the macrophages that had been treated with NAC, wherein more than 90% remained viable. In the treated sample the number of intracellular, and extracellular bacteria were significantly lower at the end of the assay in comparison to the untreated. The NAC treated macrophages were more efficient killers of vegetative BA and spores, as opposed to the untreated group. NAC also accelerated the germination of spores. It was determined that it was not NAC itself that was enhancing macrophage killing of BA, but the effect that NAC had on macrophages. The

supernatant from the macrophages that were treated with NAC also had bactericidal activity against other bacteria as well.

Suntres-Northern Ontario Medical School

Antioxidants are able to scavenge oxidants at both the extracellular and intracellular compartments. They are also able to inhibit with signal transduction for inflammatory cytokines, thereby reducing inflammatory cytokine production. In rats given vitamin E succinate or butylated hydroxyanisole their lives were extended after being challenged with a lethal dose of ricin (Muldoon, 1994). In U937 cells that had been exposed to Ricin and N-acetylcysteine (NAC) inhibited apoptosis (Oda, 1999). The antioxidant liposomes were proven to be safe when administered in a number of animal models. The largest limiting factor to the administration of the liposomes was the viscosity. Liposomes were developed using Dipalmitoyl-sn-Glycero-3-Phosphocholine (DPPC). The liposomes were found to be stable in plasma and bronchoalveolar lavage. In the rat model that was administered ricin by the intravenous route. The control liposomes (DPPC) and the NAC liposome (DPPC + N-acetylcysteine) were administered 4 hours after the administration of ricin. In the liver the ricin caused the appearance of fat vacuoles in periportal hepatocytes. In the rats treated with liposome encapsulated NAC less: neutrophils appeared in the lung, thickening of the alveolar capillaries and hemorrhage.

Crawford- Parcels Laboratory

Diagnostics- At the point at which the pathogen enters the host is the beginning of the subclinical (or incubation) disease process. DC are recruited to areas where there is a danger signal (Shi, 2003; Galluchi, 2001). These danger signals are areas of inflammation where cells are dying or where pathogens have entered the host. The dendritic cells contain TLR or toll like receptors that are pattern-recognition receptors (PRRs) on their surface (Zitvogel, 2008). The PRRs are able to recognize molecules that are shared by groups for related microbes and are not found in mammalian cells. The molecules are recognized are the pathogen-associated molecular patterns or PAMPs (e.g. Lipopolysaccharide from gram negative cell walls or peptidoglycan and lipoteichoic acids from gram- positive cell wall). Dendritic cells (DC) have a unique characteristic in that they sample multiple sites within the host. They initiate innate and adaptive immune responses. When dendritic cells are exposed to pathogens they undergo gene expression that is specific for a class of pathogen (Huang 2001). Gene changes have been noted as early as 30 minutes after exposure for infectious agents (Das et al., 2008).

Huang described specific transcriptomes of pathogens that were recognized by dendritic cells and were able to differentiate between pathogens (Huang, 2001). The early studies using in human primary dendritic cells exposed to chemical and biological agents there was consistent differential gene expression for those agents. For example, for the chemical agents there was a specific gene expression for azide versus CEES. Similarly there were specific differential responses for the biological agents such as anthrax or adenovirus. These differential responses were consistent using either proteomics or genomics analysis. Qualitative differences were seen in APCs taken from infected asymptomatic animals versus controls. In most recent in vitro studies DC were exposed to BA or Y. Pestis to determine pathogen-induced transcriptomes. The 2 hour time point was chosen since DC exposed to spores will induce several inflammatory transcriptomes (Brittingham,2005). Global microarrays were used to show clusters that were specific to the pathogen. The response to Y. Pestis showed an upregulation of 164 specific genes; in contrast to BA there were 154 specific genes. There were 106 genes that were expressed that were common to both pathogens.

Key Research Accomplishments

- C5a antibody reduces lung damage by spiked protein + LPS
- N-acetyl cysteine (NAC) is sporicidal.
- Macrophages treated with NAC become more efficient at killing bacillus anthracis
- The supernatant from NAC treated macrophages is bactericidal to other bacteria
- Antioxidants have an ameliorative effect on animals exposed to Ricin
- Liposome encapsulated antioxidants improve ameliorative effects over the free molecule in exposures to chemical and biological weapons
- Macrophages exposed to CEES undergo oxidative stress
- Antigen presenting cell gene expression can be used to differentiate between pathogens

Reportable outcomes

Victor Paromov, Sudha Kumari, Marianne Brannon, Sasidhar K. Naga, Hongsong Yang, Milton Smith, William L. Stone. "The Protective Effect of Antioxidant Liposomes in a Human Epidermal Model Exposed to a Mustard Gas Analog" *BMC Cell Biology*, 2009 (in preparation)

Mukherjee S, Stone WL, Yang H, Smith MG, Das SK. Protection of half sulfur mustard gas induced lung injury in guinea pigs by antioxidant liposomes: *Biochem Mol Toxicol*. 2009, 23(2):143-53.

Mukhopadhyay S, Mukherjee S, Stone WL, Smith M, Das SK. Role of MAPK/AP-1 signaling pathway in the protection of CEES-induced lung injury by antioxidant liposomes: *Toxicology*. 2009 Jul 10; 261(3):143-51. Epub 2009 May 21.

Mukhopadhyay, S., S. Mukherjee, et al. "Antioxidant liposomes protect against CEES-induced lung injury by decreasing SAF-1/MAZ-mediated inflammation in the guinea pig lung." *J Biochem Mol Toxicol* 24(3): 187-94, 2010

Suntres Z., Stone W., et. Al. (2005). "Ricin- Induced Toxicity: Role of oxidative stress." *Med CBR Def*, Volume 3

Manuscripts in preparation

- Bernui, M. E, Smith, M., and R. F. Rest. N-Acetylcysteine Inhibits Bacillus anthracis Spore Germination by Altering Specific Germination-pathway Components. Submitted, 2010.
- Bernui, M. E., Stone, W., Smith, M., and R. F. Rest. N-acetylcysteine (NAC) and STIMAL® (liposome-encapsulated NAC) Increase the Ability of Human Macrophages to Kill Bacillus anthracis. Submitted, 2010
- Suntres, Z.E., Smith, M.G., Alipour, M., Omri, A., Pucaj, K. Acute toxicity of liposomal antioxidants in rodents (in preparation).
- Suntres, Z.E., Smith, M.G., Alipour, M., Omri, A., Pucaj, K. Acute toxicity of liposomal antioxidants in beagle dogs (in preparation).
- Buonocore, C., Alipour M., Omri, A., Smith, M.G., Suntres, Z.E. Role of reactive oxygen species in ricin-induced toxicity. (in preparation)

- Buonocore, C., Alipour M., Omri, A., Smith, M.G., Suntres, Z.E. Treatment of ricin-induced toxicity with liposomal N-acetylcysteine. (in preparation).
- Suntres, Z.E., Smith, M.G., Alipour, M., Omri, A., Pucaj, K. Acute toxicity of liposomal antioxidants in rodents (in preparation).
- Suntres, Z.E., Smith, M.G., Alipour, M., Omri, A., Pucaj, K. Acute toxicity of liposomal antioxidants in beagle dogs (in preparation).
- Buonocore, C., Alipour M., Omri, A., Smith, M.G., Suntres, Z.E. Role of reactive oxygen species in ricin-induced toxicity. (in preparation)
- Buonocore, C., Alipour M., Omri, A., Smith, M.G., Suntres, Z.E. Treatment of ricin-induced toxicity with liposomal N-acetylcysteine. (in preparation).

Presentations made:

TMTI (Transformational Medical Technologies Innovation)

BARDA (Biomedical Advanced Research and Development Authority)

Numerous presentations to Congressional staffers

Advanced Medical Countermeasures meetings

Conclusions

The nexus between the different weapons of mass destruction may be their inducement of oxidative stress (Ermakov, 2009; McClintok, 2006, Hanna, 1994). In Dr. Rest's work the antioxidant NAC was used to treat macrophages infected with anthrax; there was the enhancement of the macrophages killing of vegetative bacteria and decreased spore growth. At this juncture it is unknown what the mechanism of action is responsible for the antioxidants being sporicidal and increasing the efficiency of macrophage killing. In the Ricin (Suntres, 2005) and CEES (McClintock, 2006) models the antioxidants had an ameliorative effect. One consequence of macrophages exposed to CEES is that proteins undergo glutathionylation. Achieving a better understanding of which proteins have undergone oxidative stress will elucidate the mechanism of action of CEES and the protective effect that antioxidants have displayed. Inhibition of complement C5a results in less lung damage in animal models that have been exposed to spike protein and LPS. The changes in that occur in the APC represents the host-pathogen response. Although it is not proven as yet, these detectable changes may be the earliest recognized in an infected animal thus far?

References

Brittingham, K. C., G. Ruthel, et al. (2005). "Dendritic cells endocytose Bacillus anthracis spores: implications for anthrax pathogenesis." J Immunol 174(9): 5545-52.

Das, R., R. Hammamieh, et al. (2008). "Early indicators of exposure to biological threat agents using host gene profiles in peripheral blood mononuclear cells." BMC Infect Dis 8: 104.

Ermakov, A. V., M. S. Konkova, et al. (2009). "Oxidative stress as a significant factor for development of an adaptive response in irradiated and nonirradiated human lymphocytes after inducing the bystander effect by low-dose X-radiation." Mutat Res 669(1-2): 155-61.

- Gallucci, S. and P. Matzinger (2001). "Danger signals: SOS to the immune system." Curr Opin Immunol 13(1): 114-9.
- Gu, J. and C. Korteweg (2007). "Pathology and pathogenesis of severe acute respiratory syndrome." Am J Pathol 170(4): 1136-47.
- Hanna, P. C., B. A. Kruskal, et al. (1994). "Role of macrophage oxidative burst in the action of anthrax lethal toxin." Mol Med 1(1): 7-18.
- Hoesel, L. M., M. A. Flierl, et al. (2008). "Ability of antioxidant liposomes to prevent acute and progressive pulmonary injury." Antioxid Redox Signal 10(5): 973-81.
- Huang, Q., D. Liu, et al. (2001). "The plasticity of dendritic cell responses to pathogens and their components." Science 294(5543): 870-5.
- Kadowaki, N., S. Ho, et al. (2001). "Subsets of human dendritic cell precursors express different toll-like receptors and respond to different microbial antigens." J Exp Med 194(6): 863-9.
- Kam, Y. W., Y. Okumura, et al. (2009). "Cleavage of the SARS coronavirus spike glycoprotein by airway proteases enhances virus entry into human bronchial epithelial cells in vitro." PLoS One 4(11): e7870.
- Karginov, V. A., T. M. Robinson, et al. (2004). "Treatment of anthrax infection with combination of ciprofloxacin and antibodies to protective antigen of Bacillus anthracis." FEMS Immunol Med Microbiol 40(1): 71-4.
- McClintock, S. D., L. M. Hoesel, et al. (2006). "Attenuation of half sulfur mustard gas-induced acute lung injury in rats." J Appl Toxicol 26(2): 126-31.
- Mitsopoulos, P., A. Omri, et al. (2008). "Effectiveness of liposomal-N-acetylcysteine against LPS-induced lung injuries in rodents." Int J Pharm 363(1-2): 106-11.
- Muldoon, D. F., D. Bagchi, et al. (1994). "The modulating effects of tumor necrosis factor alpha antibody on ricin-induced oxidative stress in mice." J Biochem Toxicol 9(6): 311-8.
- Oda, T., N. Sadakata, et al. (1999). "Specific efflux of glutathione from the basolateral membrane domain in polarized MDCK cells during ricin-induced apoptosis." J Biochem 126(4): 715-21.
- Rota, P. A., M. S. Oberste, et al. (2003). "Characterization of a novel coronavirus associated with severe acute respiratory syndrome." Science 300(5624): 1394-9.
- Shetron-Rama, L. M., A. C. Herring-Palmer, et al. "Transport of Bacillus anthracis from the lungs to the draining lymph nodes is a rapid process facilitated by CD11c+ cells." Microb Pathog 49(1-2): 38-46.
- Shi, Y., J. E. Evans, et al. (2003). "Molecular identification of a danger signal that alerts the immune system to dying cells." Nature 425(6957): 516-21.
- Sinha, J., N. Das, et al. (2001). "Liposomal antioxidants in combating ischemia-reperfusion injury in rat brain." Biomed Pharmacother 55(5): 264-71.
- Suntres, Z., W. Stone, et al. (2005). "Ricin-induced Tissue Toxicity: The Role of Oxidative Stress." Journal Medical CBR Defense 3(December 23).

Suntres, Z. E. (2002). "Role of antioxidants in paraquat toxicity." Toxicology 180(1): 65-77.

Tewari-Singh, N., S. Rana, et al. (2009). "Inflammatory biomarkers of sulfur mustard analog 2-chloroethyl ethyl sulfide-induced skin injury in SKH-1 hairless mice." Toxicol Sci 108(1): 194-206.

Zitvogel, L. and G. Kroemer (2008). "Introduction: the immune response against dying cells." Curr Opin Immunol 20(5): 501-3.

Peter A. Ward, M.D.

University of Michigan Medical School,

Ann Arbor, MI

REPORT DOCUMENTATION PAGE

Form Approved
OMB No. 0704-0188

Public reporting burden for this collection of information is estimated to average 1 hour per response, including the time for reviewing instructions, searching existing data sources, gathering and maintaining the data needed, and completing and reviewing this collection of information. Send comments regarding this burden estimate or any other aspect of this collection of information, including suggestions for reducing this burden to Department of Defense, Washington Headquarters Services, Directorate for Information Operations and Reports (0704-0188), 1215 Jefferson Davis Highway, Suite 1204, Arlington, VA 22202-4302. Respondents should be aware that notwithstanding any other provision of law, no person shall be subject to any penalty for failing to comply with a collection of information if it does not display a currently valid OMB control number. **PLEASE DO NOT RETURN YOUR FORM TO THE ABOVE ADDRESS.**

1. REPORT DATE (DD-MM-YYYY) 29/09/2010		2. REPORT TYPE Final		3. DATES COVERED (From - To) 09/21/2006 – 09/24/2010	
4. TITLE AND SUBTITLE An Overview of the Continuation of the Work of the Mustard Gas Consortium for the Use of the Free and Liposome-Encapsulated Antioxidants as a Counter Measure to Mustards.				5a. CONTRACT NUMBER	
				5b. GRANT NUMBER W81XWH-06-2-0044	
				5c. PROGRAM ELEMENT NUMBER PE 62384BP	
6. AUTHOR(S) Peter A. Ward, M.D.				5d. PROJECT NUMBER	
				5e. TASK NUMBER	
				5f. WORK UNIT NUMBER	
7. PERFORMING ORGANIZATION NAME(S) AND ADDRESS(ES) The Regents and the University of Michigan Division of Research Development and Administration 3003 South State St. Ann Arbor, MI 48109-1274				8. PERFORMING ORGANIZATION REPORT NUMBER	
9. SPONSORING / MONITORING AGENCY NAME(S) AND ADDRESS(ES) U.S. Army Medical Research and Materiel Command Fort Detrick, MD 21702-5012				10. SPONSOR/MONITOR'S ACRONYM(S)	
				11. SPONSOR/MONITOR'S REPORT NUMBER(S)	
12. DISTRIBUTION / AVAILABILITY STATEMENT Approved for public release, distribution unlimited.					
13. SUPPLEMENTARY NOTES					
14. ABSTRACT The <u>purpose</u> of these studies was to determine how the mustard compound, CEES, causes both acute lung injury (ALI) and progressive lung injury, resulting in pulmonary fibrosis. Using liposomes to deliver antioxidants (N-acetyl-cysteine, glutathione or α , γ tocopherol), we assessed the ability of these interventions to block lung injury caused by CEES. The <u>scope</u> of the studies involved the use of animal models of ALI as well as the use of lung macrophages. <u>Major</u> findings included ALI caused by CEES. The resultant lung injury (acute pulmonary edema, hemorrhage, PMN accumulation) could be greatly attenuated by PMN depletion, complement blockade, or liposomes containing antioxidants. The use of α , γ tocopherol liposomes prevented pulmonary fibrosis after CEES. Companion in vitro studies with lung macrophages showed that CEES caused production of cytokines/chemokines. Finally, we found that the combination of spike protein (from SARS coronavirus) and LPS induced an acute lung inflammatory response resulting in ALI. Antioxidant interventions greatly attenuated such outcomes. The <u>significance</u> of these findings suggests that ALI resulting from exposure to CEES or coronaviral products can be greatly attenuated by antioxidants, which mean bear on humans exposed to such agents.					
15. SUBJECT TERMS Acute lung injury, acute respiratory distress syndrome, lung inflammation, CEES, SARS coronavirus, PMNs, complement, pulmonary fibrosis, antioxidant liposomes.					
16. SECURITY CLASSIFICATION OF:			17. LIMITATION OF ABSTRACT U	18. NUMBER OF PAGES 128	19a. NAME OF RESPONSIBLE PERSON USAMRMC
a. REPORT U	b. ABSTRACT U	c. THIS PAGE U			19b. TELEPHONE NUMBER (include area code)

Table of Contents

	<u>Page</u>
Front Cover.....	1
Report Document Page.....	2
Table of Contents.....	3
Introduction.....	4
Statement of Work.....	4
Body.....	4
Key Research Accomplishments.....	6
Reportable Outcomes.....	6
Conclusion.....	9
References.....	9
Appendices.....	9

Introduction

This research program, extending from August 2006 to September 2010, takes advantage of our long standing expertise in the inflammatory response, mechanisms of acute lung injury (ALI), role of oxidants and mechanisms for delivery of antioxidants, and the role of complement in ALI. In the enclosed report we will describe the use of in vivo models of ALI in rodents and ways in which we decipher pathways leading to ALI, how antioxidants can be delivered to the lung (especially using liposomes as delivery vehicles) in order to protect against the harmful effects of CEES, and the in vitro and in vivo analysis of the coronavirus, SARS-CoV, and its components that, in the mouse model of ALI, induces a complement dependent induction of ALI. Since in SARS infections (and other intrapulmonary bacterial and viral infections) in humans cause a major complication, namely, development of ALI which may progress to the acute respiratory distress syndrome (ARDS) which in the case of SARS and Hantavirus infection in lung is often lethal. The end result in these types of infections or in CEES induced ALI, is that the lung is subjected to an intense acute inflammatory response that may be lethal. In the case of CEES, the outcome may be irreversible pulmonary damage (interstitial fibrosis).

Statement of Work

Related to CEES-induced lung injury:

Task 1: To assess the ability of CEES to produce ALI and assess both the short term and long term consequences.

Task 2: To determine the inflammatory components (complement, PMNs, cytokines/chemokines) relevant to CEES-triggered ALI in lungs and their pathophysiological role.

Task 3: To determine the ability of liposome-based antioxidants to attenuate both short term (hours) and long term (3 wks.) lung injury.

Related to mechanisms of SARS coronavirus-induced ALI:

Task 4: Using spike protein (a surface component of SARS coronavirus), to determine the extent to which this protein, together with a costimulus (LPS), can induce ALI in mouse lungs.

Task 5: To determine in this viral model of ALI the relevant mediators (PMNs, complement, cytokines/chemokines) related to development of ALI.

Body (Research Accomplishments):

(Please note: All references related to publications are listed in the Publication Section)

Task 1: We have shown that intravenous administration of CEES into young adult Long Evans rats results in ALI characterized in 4-6 hr by greatly increased pulmonary edema with alveolar flooding (quantitated by albumin content of BALF), intraalveolar hemorrhage and fibrin deposition, and the presence of large numbers of PMNs. Based on morphological features, these changes subsided within 12-24 hr., with substantial clearing of the alveolar compartment

of edema fluid, RBCs and PMNs. However, over the next three weeks there was progressive deposition of collagen within the distal interstitial and airway compartment of lung culminating in alveolar collapse and dense bands of interstitial collagen. Collagen presence was also documented in lung extracts that contained substantial amounts of hydroxyproline. (See publications 1-5.)

Task 2: To determine the inflammatory mediators responsible for CEES-induced ALI, we assessed the requirements of PMNs using PMN depletion (by an mAb), the role of complement (using complement-depleting procedures that drastically reduced serum levels of C3), and the role of oxidants (using antioxidant liposomes). The data showed that PMN depletion or complement consumptive depletion dramatically reduced the albumin leak into lung after airway instillation of CEES. Reduced evidence of ALI was also supported by morphological observations. These data indicate that CEES-induced ALI is fundamentally caused by the unleashing of a violent acute inflammatory response involving complement activation which sets the stage for massive PMN accumulation, followed by destruction of the vascular endothelial-alveolar epithelial barrier. The role of oxidants has also been documented based on the protective effects of antioxidant liposomes (containing NAC, GSH, catalase or superoxidase dismutase [reviewed in publications, 2,6]). While we have noted the appearance of numerous cytokines and chemokines in BALF from rats with CEES-induced ALI, we have not determined the relevance of each to the development of ALI. In vitro, we demonstrated that rat alveolar macrophages incubated with either LPS or CEES responded with production of a variety of cytokines and chemokines, indicating that CEES can directly activate lung macrophages in a manner that is oxidant-dependent (publication 6).

Task 3: In these studies we have demonstrated that liposomes containing either NAC or GSH have the ability to greatly attenuate ALI caused by airway administration of CEES (publications 1,2,6), but such interventions did not attenuate CEES-induced pulmonary fibrosis that peaked at 3 weeks, based on morphological and biochemical (extractable OH-proline) measurements. In striking contrast, liposomes containing α,γ -tocopherol failed to attenuate ALI caused by CEES but dramatically attenuated the 3 week fibrotic response to CEES (publication 6). We do not understand why α,γ -tocopherol liposomes had no effect on ALI but were highly protective as related to the fibrotic response to CEES. Also, we do not know how long between CEES administration and development of fibrosis that intervention with α,γ -tocopherol liposomes would still be effective. Many of the other studies deal with underlying mechanisms related to development of ALI (e.g. role of complement, and catecholamines [publications 7-11], role of C5a receptors [publications 12,13,16], cross talk between Fc γ R_s and TCR4 in ALI [publication 14], and silencing of C5aR in airway epithelial cells [publication 15]). We have recently published reports describing how oxidants reversibly and irreversibly injure the lung (publication 17) and the relationship between the innate immune system (complement) and hyperinflammatory responses in the setting of experimental sepsis (publications 18,19).

Tasks 4, 5: In order to assess how the SARS coronavirus triggers in humans a highly damaging and potentially lethal ALI, we have used the spike protein, which is a surface constituent of the SARS virus, and have shown in vivo in C57Bl/6 mice that airway instillation of a combination of spike protein and LPS produces ALI in lungs of mice and induces a substantial albumin leak as well as buildup of PMNs in lung and the appearance of cytokines and chemokines in BALF. In addition, this injury could be greatly attenuated in the presence of neutralizing antibody to C5a (see Annual Report for 2009-2010 for details). Such data suggest that the SARS coronavirus appears to trigger intense ALI that in humans can be life-threatening.

Key Research Accomplishments

- Acute lung inflammatory injury (ALI) induced by CEES, with dependency on complement (C5a), oxidants and PMNs.
- Ability of antioxidant liposomes containing N-acetylcysteine or glutathione to attenuate ALI due to CEES.
- Ability of α,γ tocopherol liposomes to attenuate CEES-induced pulmonary fibrosis but not ALI, suggesting that ALI and fibrosis follow different pathophysiological pathways.
- Ability of catecholamines to enhance the acute lung inflammatory response.
- Ability of spike protein (of SARS coronavirus) with a costimulus (LPS) to cause ALI in mouse lungs in a complement (C5a) and PMN-dependent manner, associated with cytokine/chemokine production both in vitro and in vivo.

Reportable Outcomes

Personnel that received pay from this research effort for the following time periods:

Year	Personnel
2006	Peter A. Ward, Ren-Feng Guo, Firas Zetoune, Hongwei Gao, Daniel Rittirsch
2007	Peter A. Ward, Ren-Feng Guo, Firas Zetoune, Daniel Rittirsch, Beverly Schumann
2008	Peter A. Ward, Daniel Rittirsch, Ren-Feng Guo, Firas Zetoune, Gelareh Atefi, Ketong Zhu, Beverly Schumann
2009	Peter A. Ward, Ketong Zhu, Gelareh Atefi, Firas Zetoune, Beverly Schumann
2010	Peter A. Ward, Ketong Zhu, Gelareh Atefi, Markus Bosmann, Beverly Schumann

Publications: 08/06 – 08/07

1. McClintock, S.D., Hoesel, L.M., Das, S.K., Till, G.O., Neff, T., Kunkel, R.G., Smith, M.G., and **Ward, P.A.**: Attenuation of half sulfur mustard gas-induced acute lung injury in rats. *J Appl Toxicol.* 2006, 26:126-311.
2. Guo, R.F. and **Ward, P.A.**: Role of oxidants in lung injury during sepsis. *Antioxidants and Redox Signaling* 2007, 9:1-12.
3. Smith, M.G., Stone, W., Guo, R.F., **Ward, P.A.**, Suntres, Z., Mukherjee, S., and Das, S.K. Vesicants and Oxidative Stress. In *Chemical Warfare Agents. Chemistry, Pharmacology, Toxicology, and Therapeutics*, J.A. Romano, Jr., B.J. Lukey, H. Salem (eds). 2nd Edition, CRC Press, Boca Raton, FL. pp.247 – 312, 2007.

Publications: 08/07 – 08/08

4. Wrann, C.D., Tabriz, N.A., Barkhausen, T., Klos, A., van Griensven, M., Pape, H.C., Kendoff, D.O., Guo, R., **Ward, P.A.**, Krettek, C., Riedemann, N.C.: The phosphatidylinositol 3-kinase signaling pathway exerts protective effects during sepsis

by controlling C5a-mediated activation of innate immune functions. *J. Immunol.* 2007; 178:5940-5948.

5. **Ward, P.A.**: New therapeutic approaches for influenza A H5N1 infected humans. (Invited Editorial) *Crit Care Med.* 2007; 35:1437-1438.
6. Hoesel, L. M., Flierl, M.A., Niederbichler, A.D., Rittirsch, D., Sarma, J.V., McClintock, S.D., Reuben, J.S., Pianko, M.J., Stone, W., Yang, H., Smith, M., **Ward, P.A.**: Ability of anti-oxidant liposomes to prevent acute and progressive pulmonary injury. *Antioxid Redox Signal.* 2008, 10:973-981.
7. Flierl, M.A., Rittirsch, D., Huber-Lang, M., Sarma, J.V., **Ward, P.A.**: Catecholamines – Crafty weapons in the inflammatory arsenal of immune/inflammatory cells or opening Pandora’s box? *Mol Med.* 2008, 14:195-204.
8. Rittirsch, D., Flierl, M.A., Day, D.E., Nadeau, B.A., McGuire, S.R., Hoesel, L.M., Ipaktchi, K., Zetoune, F.S., Sarma, J.V., Leng, L., Huber-Lang, M.S., Neff, T.A., Bucala, R., **Ward, P.A.**: Acute lung injury induced by lipopolysaccharide is independent of complement activation. *J Immunol.* 2008 180:7664-7672.

Publications: 08/08 – 08/09

9. Albrecht, E.A., Sarma, J.V., **Ward, P.A.**: Activation by C5a of endothelial cell caspase 8 and cFLIP. *Inflamm Res*, 2009 58:30-37. PMID: 19115040.
10. Flierl, M.A., Rittirsch, D., Nadeau, B.A., Sarma, J.V., Day, D.E., Lentsch, A.B., Huber-Lang, M.S., **Ward, P.A.**: Upregulation of phagocyte-derived catecholamines augments the acute inflammatory response. *PLoS One.* 2009 4(2):e4414. [Epub 2009 Feb 12] PMID: 19212441.
11. Flierl, M.A., Stahel, P.F., Rittirsch, D., Huber-Lang, M., Niederbichler, A.D., Hoesel, L.M., Touban, B.M., Morgan, S.J., Smith, W.R., **Ward, P.A.**, Ipaktchi, K.: Inhibition of complement C5a prevents breakdown of the blood-brain barrier and pituitary dysfunction in experimental sepsis. *Crit Care*, 2009 Feb 5 13: R12 [Epub ahead of print]. PMID: 19196477.
12. **Ward, P.A.**: Functions of C5a receptors. *J. Mol Med.* 2009 87 :375-378. PMID: 19189071.
13. Rittirsch, D., Flierl, M.A., Day, D.E., Nadeau, B.A., Zetoune, F.S., Sarma, J.V., Werner, C.M., Wanner, G.A., Simmen, H.P., Huber-Lang, M.S., **Ward, P.A.**: Cross-talk between TLR4 and Fcγ receptor III (CD16) pathways. *PLoS Pathogens.* Epub 2009 Jun 5, 5(6):e10000464. PMID: 19503602. PMCID: 2685003.

Publications: 08/09 – 08/10

14. **Ward, P.A.** Oxidative stress: acute and progressive lung injury. *Ann N Y Acad Sci.* 2010 Aug;1203:53-59.
15. **Ward, P.A.**, Zetoune, F.S., Sarma, J.V. Defective innate immunity and hyper-inflammatory responses in sepsis. *Proceedings of the 8th World Congress on Trauma, Shock, Inflammation and Sepsis, TSIS 2010, March 9-13th, pp. 9-12.*
16. **Ward, P.A.** The harmful role of C5a on innate immunity in sepsis. *J Innate Immun.* 2010;2(5):439-45. Epub 2010 Jun 26.

Reportable Outcomes

Invited Presentations 08/06 – 08/07:

1. NIH/NIAID Radiation Combined Injury Workshop, March 26-27, 2007, Bethesda, MD: “Factors affecting the outcomes of sepsis.”
2. Advanced Medical Countermeasures Consortial Meeting, June 28, 2007, Crystal City, VA: “Protective effects of anti-oxidant liposomes in acute and progressive lung injury after CEES.”
3. BARDA 2007 Industry Day Conference, August 3, 2007, Washington, DC: “Protective effects of anti-oxidant liposomes.”

Invited Presentations 08/07 – 08/08:

4. Invited plattform presentation at Biosciences 2008 (Hunt Valley, MD), “Liposomal blockade of lung injury after exposure to 2-chloroethyl ethyl sulfide (CEES)”, June 4, 2008.
5. Progress report, presented at Advanced Medical Countermeasures Consortium, Hunt Valley, (MD), June 4, 5, 2008.

Invited Presentations 08/08 – 08/09:

6. Invited Speaker, “How to get into High Impact Journals as an Author” – Pre-Meeting, November 6; “Adrenergic Regulation of Acute Lung Injury”, November 9, ISRD 2008, 5th Intl Symposium on Respiratory Diseases, Shanghai, China, November 9, 2008.
7. Invited Speaker, “Phagocyte-derived Catecholamines Regulate Lung Inflammation”, American Thoracic Society Intl. Conference, San Diego, CA, May 20, 2009.
8. Invited Discussion Leader, “Evidence for Association of TLR4 and FcγRIII (CD16) In Vitro and In Vivo”, Gordon Research Conference: Phagocytes – Innate Immune Cell: Pathogen Interactions, Waterville Valley, NH, June 11, 2009.
9. Invited Speaker, “Regulation of IL-17 Production In Vitro and In Vivo”, 6th Intl Innate Immunity Conference, Heraklion, Crete, Greece, June 25, 2009.
10. Chair, CounterACT Research Review Committee, NIH 3rd Annual CounterACT Research Symposium, Washington, DC, April 13-16, 2009.
11. Invited Speaker, “Role of IL-17 in Sepsis”, 22nd Congress of the International Society on Thrombosis and Haemostasis, Boston, MA, July 11-12, 2009.

Invited Presentations 08/09 – 08/10:

12. Invited Speaker, “The Molecular Basis for Sepsis”, University of Illinois Chicago Pharmacology Research Seminar, Chicago, IL, September 16, 2009.
13. Invited Speaker, “Role of IL-17 in Unrestrained Inflammation”, IRFG/IBPRG 2009 Conference, University of Calgary, Alberta, Canada, October 2, 2009.
14. Invited Speaker, “The Molecular Basis for Sepsis”, Institute of Infection, Inflammation and Immunity Research Day, University of Calgary, Alberta, Canada, October 5, 2009.
15. Marie T. Bonazinga Award and Lecture “The Molecular Determinants of Sepsis”, SLB-ICS-ISICR 2009 Tri-Society Annual Conference, Lisbon, Portugal, October 18, 2009.
16. Invited Speaker, “Oxidative Stress: Acute and Progressive Lung Injury”, New York Academy of Sciences, New York, NY, October 29, 2009.

17. Invited Speaker, "Autonomic Regulation of the Lung Injury Response (Anti-inflammatory Activities of Bronchodilators)", ISRD 2009-6th Intl. Symposium on Respiratory Diseases, Shanghai, China, November 6, 2009.
18. Invited Moderator, "Basic Science: Sepsis", Society of Critical Care Medicine, 39th Critical Care Congress, Miami Beach, FL, January 11, 2010.
19. Invited Speaker and Moderator, "Defective Innate Immunity and Hyper-inflammatory Responses in Sepsis", 8th World Congress on Trauma, Shock, Inflammation and Sepsis, Munich, Germany, March 9-13, 2010.
20. Invited Speaker, Endotoxemia, C5a receptors and IL-17A – "Roles of IL-17A, LPS and Complement", 7th International Innate Immunity Conference, Rhodes, Greece, July 3 – 10, 2010.
21. Invited Speaker, "Complement Based Therapies", XXIII International Complement Workshop, New York City, NY, August 1, 2010.
22. Invited Chair, Session: Animal Models of Disease, XXIII International Complement Workshop, New York City, NY, August 4, 2010.

Conclusions

CEES induces both short term lung injury (ALI) as well as long term lung injury (fibrosis). ALI is predominately due to an intense acute inflammatory response, which is characterized by alveolar flooding and hemorrhage along with buildup of PMNs. The damage is linked to PMNs, complement, cytokines/chemokines and oxidants. Appropriate liposomes containing antioxidants (GSH, NAC, catalase, superoxide dismutase, tocopherols) can avert both the short term and the long term (fibrotic) lung damage induced by exposure to CEES. This information may be relevant to the treatment of humans exposed to mustard gas compounds.

Another recent focus of study has been trying to understand the pathogenesis of ALI and ARDS induced in humans after exposure to SARS coronavirus. Using spike protein (a surface molecule on the SARS virus) together with LPS, we have found that ALI develops in mice (C57Bl/6) after intrapulmonary exposure to spike protein + LPS, resulting in a PMN and C5a-dependent inflammatory response that is also associated with intrapulmonary cytokines and chemokines. This suggests that pulmonary complications (the chief clinical problem in SARS patients) of SARS infection are due to an unregulated acute lung inflammatory response.

References:

Listed as publications in section on Reportable Outcomes

Appendices:

Original Research Communication

Ability of Antioxidant Liposomes to Prevent Acute and Progressive Pulmonary Injury

LASZLO M. HOESEL,² MICHAEL A. FLIERL,¹ ANDREAS D. NIEDERBICHLER,²
DANIEL RITTIRSCH,¹ SHANNON D. MCCLINTOCK,¹ JAYNE S. REUBEN,³
MATTHEW J. PIANKO,¹ WILLIAM STONE,⁴ HONGSONG YANG,⁴ MILTON SMITH,⁵
J. VIDYA SARMA,¹ and PETER A. WARD¹

ABSTRACT

We recently showed that acute oxidant-related lung injury (ALI) in rats after application of 2-chloroethyl ethyl sulfide (CEES) is attenuated by the airway instillation of antioxidants. We investigated whether intratracheal administration of antioxidant-containing liposomes immediately after instillation of CEES would attenuate short-term as well as long-term (fibrotic) effects of CEES-induced lung injury. In the acute injury model (4 h after injury), *N*-acetylcysteine (NAC)-containing liposomes were protective and reduced to baseline levels both the lung permeability index and the appearance of proinflammatory mediators in bronchoalveolar lavage fluids from CEES-exposed lungs. Similar results were obtained when rat alveolar macrophages were incubated *in vitro* with either CEES or lipopolysaccharide in the presence of NAC-liposomes. When lung fibrosis 3 weeks after CEES was quantitated by using hydroxyproline content, liposomes containing NAC or NAC + glutathione had no effects, but liposomes containing α/γ -tocopherol alone or with NAC significantly suppressed the increase in lung hydroxyproline. The data demonstrate that delivery of antioxidants *via* liposomes to CEES-injured lungs is, depending on liposomal content, protective against ALI, prevents the appearance of proinflammatory mediators in bronchoalveolar fluids, and suppresses progressive fibrosis. Accordingly, the liposomal strategy may be therapeutically useful in CEES-induced lung injury in humans. *Antioxid. Redox Signal.* 10, 973–981.

INTRODUCTION

OXIDANT-MEDIATED acute lung injury (ALI) is known to occur in a variety of conditions [including exposure to mustard gas and its derivatives such as 2-chloroethyl ethyl sulfide (CEES)] (8). CEES is a chemical agent that initiates cell injury associated with an imbalance between oxidants and antioxidants. On a subcellular level, it is known that sulfur mustard leads to an increase of gene expression involved in inflammation, apoptosis, and cell-cycle regulation (5). In addition

to acute lung injury, lung exposure to sulfur mustard or its derivatives also leads to progressive lung injury, being represented by extensive interstitial fibrosis, which is well described in humans exposed to mustard gas compounds (18, 25) and in rats exposed to CEES (29). No specific therapy exists for the treatment of humans exposed to inhaled mustard gas compounds, although in the case of ALI in rats after exposure to CEES, we previously showed that protective strategies were associated with liposomes containing antioxidant enzymes (catalase, superoxide dismutase) or liposomes containing iron chelators or

Departments of Pathology¹ and Surgery,² University of Michigan Medical School, Ann Arbor, Michigan.

³Department of Biomedical Sciences, Baylor College of Dentistry The Texas A and M University System, Dallas, Texas.

⁴Department of Pediatrics, East Tennessee State University, Johnson City, Tennessee.

⁵AMAOX, Ltd., Melbourne, Florida.

nonspecific reducing agents (30). When given at the time of lung exposure to CEES, these agents reduced the intensity of acute lung injury (ALI), as defined by albumin leak into lung, by as much as 70%. Delayed instillation of these liposomes for as long as 90 min was still protective. These findings are consistent with the hypothesis that CEES upsets the redox balance in lung, leading to a loss of reducing equivalents in the lung (23, 26).

In a recent study, we showed that liposomes containing antioxidants, such as GSH or α -tocopherol given intratracheally at the time of injury, were also protective against ALI, as measured 4 h after airway instillation of CEES (29). Collectively, our studies have suggested that ALI occurring after airway exposure to CEES is associated with an intense lung-damaging inflammatory response featuring involvement of the complement system and neutrophils [polymorphonuclear leukocytes (PMNs)], both of which intensified inflammatory injury. In other words, exposure of lung to CEES triggered a lung-damaging inflammatory response. Instillation into CEES-exposed lungs of antioxidant liposomes was remarkably protective, even when liposomal delivery was delayed for 90 min after CEES instillation, suggesting that time for effective treatment of lungs may exist after exposure to CEES. Finally, it was also shown that CEES exposure of rat lung led to pulmonary fibrosis, although the effectiveness of antioxidant liposomes in that setting is not known.

Lipopolysaccharide (LPS), a major component of the cell wall of gram-negative bacteria, is known to trigger inflammatory reactions in lung similar to the effects of CEES (16, 51). Stimulation of macrophages by LPS results in activation of nuclear transcription factors [nuclear factor κ B (NF- κ B)] and release of proinflammatory cytokines (10, 20, 37, 38). Further, it has been shown that systemic administration of NAC may attenuate LPS-induced injury (15). In the context of CEES, LPS has been reported to enhance the cytotoxic effects of CEES (40). In the current study, we further explore the ability of antioxidant liposomes to protect against acute and progressive lung injury in rat lungs exposed to CEES. The data suggest that introduction of antioxidant interventions is protective in the lung.

MATERIALS AND METHODS

Chemicals

Except where noted, all chemicals and reagents were purchased from the Sigma Chemical Co. (St. Louis, MO).

Animal model

Adult male (275–325 g) specific pathogen-free Long-Evans rats (Harlan Co., Indianapolis, IN) were used in these studies. Intraperitoneal ketamine (100 mg/kg body weight) (Fort Dodge Animal Health, Fort Dodge, IA) was used for anesthesia, and intraperitoneal xylazine (13 mg/kg body weight) (Bayer Corp., Shawnee Mission, KS) for sedation. The experimental procedure for CEES-induced lung injury in rats was described previously (30). In brief, after induction of anesthesia, the trachea was surgically exposed, and a slightly curved P50 catheter was inserted into the trachea past the bifurcation to facilitate a unilateral, left-lung injury. A small volume of CEES (2 μ l/rat; ~6

mg/kg) was solubilized in ethanol (58 μ l/rat) and then added to a syringe containing Dulbecco's phosphate-buffered saline (DPBS) (340 μ l/rat). This solution was injected *via* the intratracheal catheter into the left-lung mainstem bronchus. Animals were killed at indicated time points by exsanguinations *via* the inferior vena cava. All animal experiments were in accordance with the standards in The Guide for the Care and Use of Laboratory Animals, approved by the University Committee on Use and Care of Animals (UCUCA), and were supervised by veterinarians from the Unit for Laboratory and Animal Care of the University of Michigan Medical School.

Permeability index

The lung permeability index was determined as described later. Studies not requiring the use of a radiolabeled marker (125 I-BSA) proceeded identically, substituting DPBS (intravenously) for the radiomarker. For experiments where indicated, 0.5 mg bovine serum albumin (BSA) was mixed with 0.5 μ Ci 125 I-BSA, and the material (in 0.5 ml) was injected intravenously into rats. Animals were killed 4 h later, and the pulmonary arterial circulation was flushed with 10 ml of cold DPBS. The lungs were then surgically dissected, and the amount of radioactivity (125 I-labeled BSA) in lung parenchyma determined by gamma counting. For calculations of the permeability index, the amount of radioactivity remaining in perfused lungs was divided by the amount of radioactivity present in 1.0 ml of blood obtained from the inferior vena cava at the time of death, as described elsewhere (30). 125 I-BSA present in lung is a quantitative measure of the degree of vascular endothelial and alveolar epithelial damage, in which much of the 125 I-BSA can be lavaged from the distal airway compartment, indicating loss of the vascular and epithelial barrier function (24).

Liposome preparation

Dipalmitoylphosphatidylcholine (DPPC; Avanti Polar Lipids, Alabaster, AL) was dissolved 20 mg/ml in a 2:1 vol/vol chloroform/methanol solution. The DPPC solution was then dried under a thin stream of nitrogen in a round-bottom flask to form a thin lipid film on the walls of the tube. Once the film had been dried, the tube was then placed on a vacuum for at least 1 h to dry further and to remove any excess organic compounds from the lipid film.

The following compounds, being encapsulated within the liposomes, were prepared in Dulbecco's phosphate-buffered saline (DPBS), pH adjusted to 7.4. *N*-Acetylcysteine (NAC, 30 mg/ml), glutathione (GSH, 30 mg/ml), vitamin E (α + γ -tocopherol, each at 1.3 mg/ml) were then added to the lipid film. The tube was then vortexed to free the lipid film from the walls of the tube and then placed in a heated water bath (41°C). When sizing the liposomes, it was necessary to keep them at a temperature above their transition phase (41°C). Vortexing the liposomes once they were above the transition-phase temperature resulted in large multilamellar vesicles. To reduce the size of the liposomes and to produce uniform small unilamellar vesicles, the lipid suspension was then passed 10 times through polycarbonate membrane filters in a Liposofast Basic miniextruder (Avestin, Inc., Ottawa, Ontario, Canada). The resulting liposomes were uniform in size, measuring 100 nm in diame-

ter. It is well known that the pharmacokinetics of liposome uptake is dependent on particle-size distribution (11, 12). Uniformity and size of the liposomes was confirmed by light microscopy. Liposomes were injected intratracheally (volume of 100 μ l per rat) through the same catheter setup immediately after the CEES instillation. This translates into 3 mg NAC, 3 mg GSH, and 0.13 mg α - or γ -tocopherol, respectively (the same doses apply where combinations of antioxidant agents were given). The same conditions were used when soluble NAC was used. *N*-Acetylcysteine (NAC, 30 mg/ml) was prepared in Dulbecco's phosphate-buffered saline (DPBS); pH adjusted to 7.4 and 100 μ l of the suspension per rat was injected intratracheally.

Cytokine measurements in bronchoalveolar lavage fluid

To determine the concentration of various inflammatory cytokines in the lungs, bronchoalveolar lavage fluids (BALFs) were obtained selectively from the left, (injured) lung lobe at indicated time points after administration of CEES. After centrifugation, IL-1 β , IL-6, TNF- α , and CINC-1 were measured in the supernatant fluids by using commercially available ELISA kits and by following the manufacturer's instructions (R&D Systems, Minneapolis, MN).

In vitro stimulation of alveolar macrophages

Alveolar macrophages were obtained from normal rat lungs by bronchoalveolar lavage. After pooling, gentle centrifugation and counting of the cells (with a yield of $\sim 10 \times 10^6$ cells per lung), macrophages resuspended in RPMI medium containing 0.5% BSA were incubated for 1 h to allow for settling. To create an *in vitro* situation similar to the *in vivo* CEES model, 2.5×10^6 cells/ml media were incubated with 500 μ M CEES with or without antioxidant liposomes (50 μ l) for 4 h. In additional experiments, plated macrophages were incubated with 100 ng/ml lipopolysaccharide (LPS) from *Escherichia coli* (serotype O111:B4) and 50 μ l liposomes. After centrifugation, IL-1 β , IL-6, TNF- α , and CINC-1 were measured in the supernatants by using commercially available ELISA kits and by following the manufacturer's instructions (R&D Systems, Minneapolis, MN).

Hydroxyproline assays

Hydroxyproline is a modified amino acid found at a uniquely high percentage in collagen. Therefore, we determined hy-

droxyproline content of the lungs as a quantitative measure of collagen deposition, as described previously. Although the accuracy of this assay may potentially be affected by proteins containing collagen-like motifs (*e.g.*, surfactant), its usefulness for determining tissue collagen content has been established and well accepted (31). Rats were killed 3 weeks after exposure to CEES, and the pulmonary circulation was flushed with 10 ml cold DPBS. The left (injured) lung was surgically removed. The isolated lobes were homogenized in 1 ml of PBS, and hydrolyzed by the addition of 1 ml of 12N HCl. Samples were then baked at 110°C for 12 h. Aliquots were then assayed by adding chloramine-T solution for 20 min followed by development with Ehrlich's reagent at 65°C for 15 min, as previously described (47). Absorbance was measured at 550 nm, and the amount of hydroxyproline was determined against a standard curve generated by using known concentrations of pure hydroxyproline.

Morphologic assessment of lung injury

Morphologically to assess lung injury, lungs were fixed by gentle intratracheal instillation of 10 ml buffered (pH 7.2) formalin (10%) at the indicated time points after airway instillation of CEES. Tissues were embedded in paraffin. Lung sections were then obtained for histologic examination by using hematoxylin and eosin stain. In addition, lung sections were stained with Masson trichrome to assess deposition of fibrin and collagen (28).

Statistical analysis

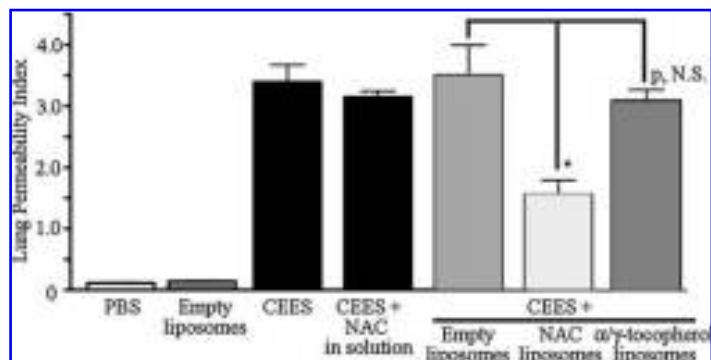
Results are presented as mean \pm SEM in the text and figures. Groups ($n = 5$ rats) were subjected to one-way analysis of variance (ANOVA), and when significance was found, Tukey's *post hoc* test was applied. A value of $p < 0.05$ was considered significant.

RESULTS

Protective effects of NAC-containing liposomes in ALI

Because NAC-containing liposomes are known to protect against acute (4-h) CEES-induced injury in rat lungs when

FIG. 1. Permeability indices in rat lungs 4 h after airway delivery of PBS (control) or empty liposomes, or CEES (6 mg/kg) in the absence of liposomes or in the presence of empty liposomes, NAC-containing (30 mg/ml), or α/γ -tocopherol-containing (1.3 mg/ml) liposomes. An additional group of animals received soluble NAC dissolved in PBS (fourth bar, CEES + NAC in solution) by using the same conditions used for preparation of NAC-liposomes. The permeability index was the ratio of 125 I-albumin in left lung parenchyma to the radioactivity present in 1.0 ml blood (vena cava) obtained at the time of death. For each bar, $n = 6$ animals. * $p < 0.05$.



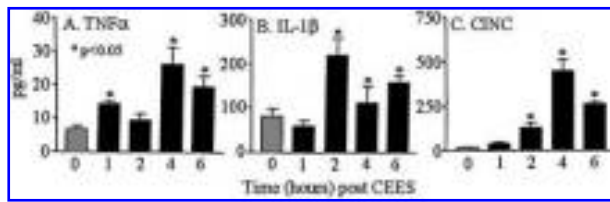


FIG. 2. Appearance of TNF- α , IL-1 β , and CINC-1 (as measured by ELISA) in BAL fluids from the left (injured) lung as a function of time after intratracheal instillation of CEES into rat lungs. For each bar, $n = 6$ animals. $*p < 0.05$ when compared with 0 time values.

given intratracheally immediately after instillation of CEES (29), experiments were designed to assess the protective effects of empty liposomes, NAC in solution (PBS), NAC-liposomes, and α/γ -tocopherol liposomes. As shown in Fig. 1, control lungs (receiving PBS or empty liposomes) showed very little evidence of albumin leak (permeability index), with values < 0.15 . CEES caused an intense leak of serum albumin, with the permeability index ~ 3.4 , whereas CEES instillation followed by NAC in PBS (pH 7.4) showed a very modest reduction in the permeability index ($< 10\%$). Empty liposomes or liposomes loaded with α/γ -tocopherol, given into the upper airways immediately after CEES, did not reduce the permeability index (same as with CEES alone), whereas in the case of NAC-liposomes, a 59% reduction in the permeability index was found ($p < 0.05$).

Time course for mediators in BAL fluids after CEES

To establish the time course for appearance of inflammatory mediators in BAL fluids from rats given CEES into the left lung

at time 0, BAL samples were obtained at 0, 1, 1.5, 2, 4, and 6 h after CEES administration. Mediators were measured with ELISA (Fig. 2). Time courses for TNF- α , IL-1 β , and CINC-1 indicated that, as a general rule, these proinflammatory mediators peaked between 2 and 4 h after instillation of CEES into rat lungs. For subsequent experiments, the 4-h time point was selected.

Reductions in BAL Mediators in CEES lungs after antioxidant liposomes

We previously showed that liposomes containing NAC prevent the ALI that follows airway administration of CEES (30). CEES was used to induce ALI in the absence of liposomes or in the presence of empty liposomes or NAC-containing liposomes, the last of which are known to be protective in the ALI CEES model (29). In the current studies, we sought to determine to what extent protective liposomes would affect BAL levels of cytokines and chemokines. BAL fluids were obtained 4 hours after airway administration of CEES in the absence or presence of empty liposomes or NAC-liposomes, as indicated in Fig. 3. CEES caused ~ 20 -fold, fourfold, 2.5-fold, and 1.6-fold increases in CINC-1, IL-1 β , IL-6, and TNF- α , respectively, in BAL fluids. The presence of empty liposomes with CEES caused little or no change when compared with the values found with CEES alone. Conversely, NAC-liposomes caused the levels of BAL mediators to decrease to virtually baseline levels in all cases.

Effects of antioxidant liposomes on in vitro production of cytokines and chemokines by lung macrophages

Two different *in vitro* experiments were used in which alveolar macrophages ($2.5 \times 10^{-6}/\text{ml}$) from normal rat lungs were

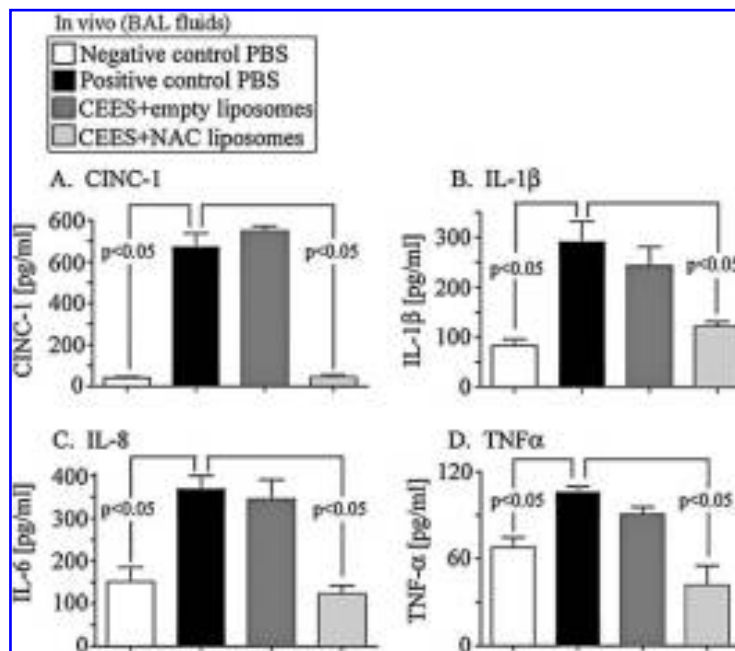
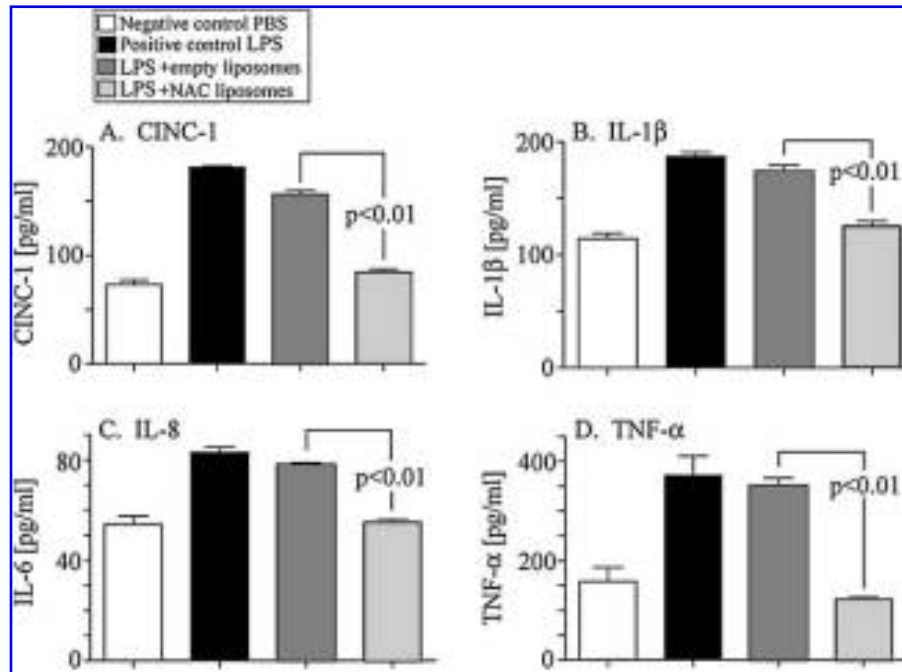


FIG. 3. Levels of rat CINC-1 (A), IL-1 β (B), IL-6 (C), and TNF- α (D) in BAL fluids from left lung 4 h after instillation of PBS (control) or CEES. As indicated, CEES was instilled, followed by airway instillation of empty liposomes (lips) or NAC-liposomes. For each bar, $n = 8$ animals.

FIG. 4. Effects of LPS and liposomes on levels of proinflammatory mediators in 4-h culture fluids of alveolar macrophages (2.5×10^6) incubated with PBS (negative control) or with LPS (100 ng/ml) alone (positive control), or with empty liposomes or NAC-containing liposomes. Mediators CINC-1 (A), IL-1 β (B), IL-6 (C), and TNF- α (D) were measured with ELISA. Each sample was measured in quadruplicate. For each bar, $n = 6$ animals.

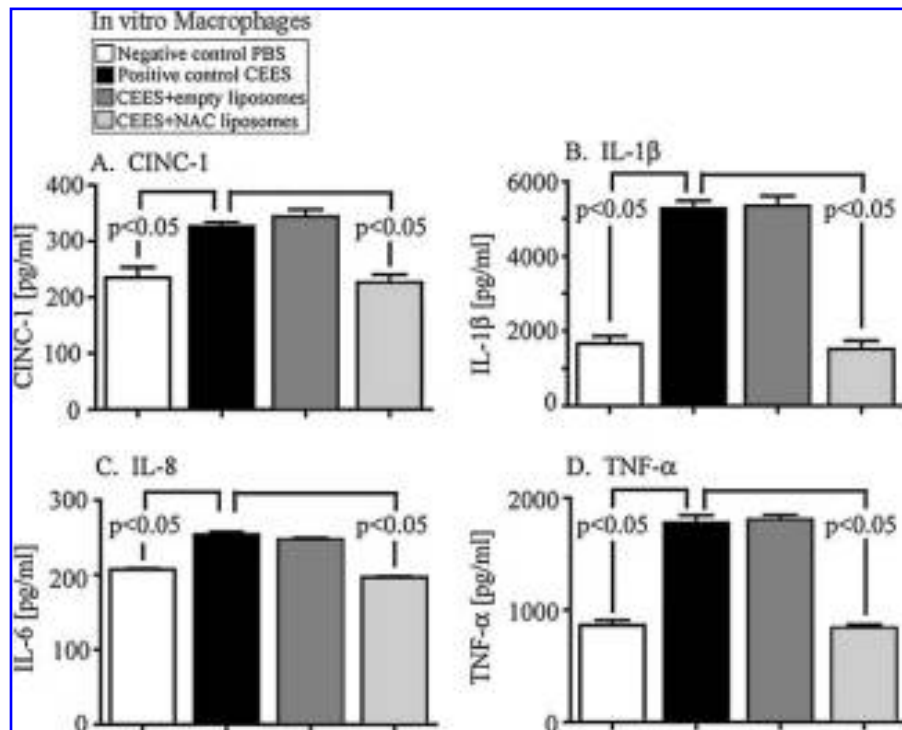


used. In the first set of experiments, cells were exposed to LPS (100 ng/ml) for 4 hours in the absence or presence of empty or NAC-liposomes. Supernatant fluids were then measured for the presence of proinflammatory mediators, as shown in Fig. 4. In each case, LPS addition in the absence or presence of empty liposomes induced a substantial increase (over negative controls) of CINC-1, IL-1 β , IL-6, and TNF- α . The presence of NAC-liposomes caused the mediator levels to decrease to baseline lev-

els. Addition of empty liposomes did not induce mediator release from nonstimulated alveolar macrophages (data not shown).

In the second set of *in vitro* experiments (Fig. 5), the effect of CEES alone or in the presence of empty or NAC-containing liposomes on mediator release from alveolar macrophages was assessed. Empty liposomes did not perturb the levels of mediators released, remaining at baseline levels in nonstimulated

FIG. 5. *In vitro* effects of CEES and liposomes on levels of proinflammatory mediators in 4-h culture fluids of alveolar macrophages (2.5×10^6) incubated with PBS (negative control), CEES (500 μ M) alone (positive control), or with empty liposomes or NAC-containing liposomes. Mediators CINC-1 (A), IL-1 β (B), IL-6 (C), and TNF- α (D) were measured with ELISA. Each sample was measured in quadruplicate. For each bar, $n = 6$ animals.



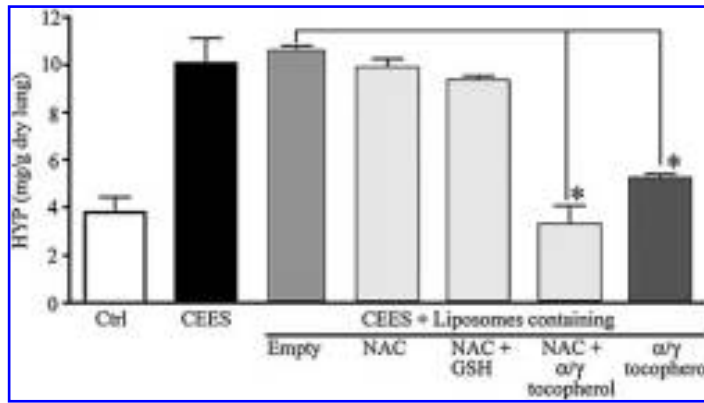


FIG. 6. Collagen levels (as measured by hydroxyproline content) in left lung homogenates 3 weeks after airway instillation of PBS (control) or CEES alone or together with empty liposomes or liposomes containing NAC, NAC + GSH, NAC + α , γ -tocopherol, or α , γ -tocopherol alone. For each bar, $n = 8$ animals. * $p < 0.05$ when compared with the CEES group.

macrophages (data not shown). Furthermore, in all cases, the addition of empty liposomes had no effect on mediator release when compared with CEES-stimulated macrophages not otherwise manipulated (Fig. 5). In contrast, the addition of NAC-containing liposomes to CEES-stimulated macrophages caused total suppression of the increase in levels of IL-6, IL-1 β , TNF- α , and CINC-1 release, declining to levels equivalent to negative controls. Clearly, NAC-liposomes suppress release of proinflammatory mediators *in vitro* and *in vivo* after exposure of alveolar macrophages to either CEES (Fig. 5) or LPS (Fig. 4). The mechanisms by which CEES induces release of proinflammatory mediators from alveolar macrophages and the protective effects of NAC-liposomes are not known but may be linked to NF- κ B activation or suppressed NF- κ B activation.

Ability of anti-oxidant liposomes to protect from CEES-induced pulmonary fibrosis

We recently showed that CEES administration into rat lung induces intense pulmonary fibrosis within 3 weeks, as defined by histologic changes (29). In the current studies, we assessed whether antioxidant liposomes would prevent this outcome. Accordingly, CEES was administered into rat lungs in the absence of liposomes or together with empty liposomes or liposomes containing NAC, NAC + GSH, or NAC + α/γ -tocopherol or α/γ -tocopherol alone. Three weeks later, lungs were obtained, and collagen content (hydroxyproline, HYP) was assessed, as described earlier (31). As shown in Fig. 6, hydroxyproline content (mg/gm dry lung) increased 2.5-fold 3 weeks after CEES exposure of lungs in the absence of liposomes or in the presence of empty liposomes or liposomes containing NAC or NAC + GSH. No protective effects on hydroxyproline build-up were found. Strikingly, when liposomes containing NAC + α/γ -tocopherol were used, the build-up of hydroxyproline was completely abrogated ($p < 0.05$). Liposomes containing only α/γ -tocopherol also suppressed HYP buildup but not to the same extent as when α/γ -tocopherol liposomes were used ($p < 0.05$).

Morphologic correlates in lung

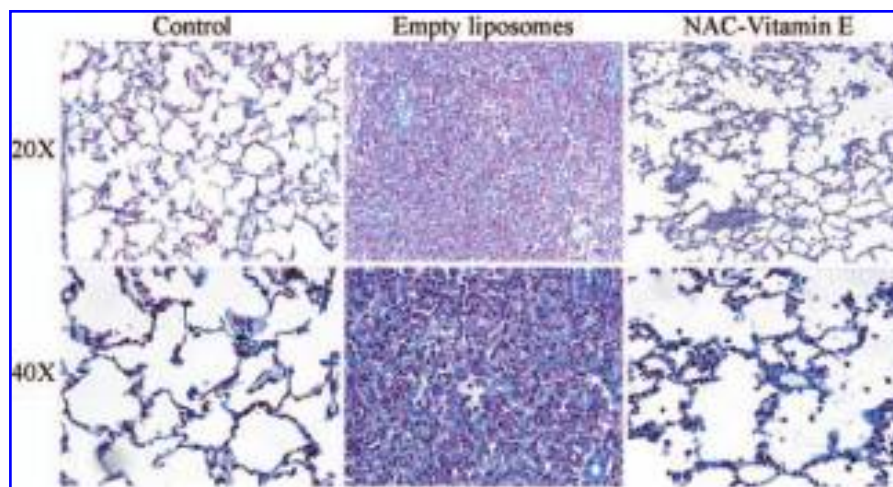
As shown in Fig. 7, sham lungs demonstrated normal architecture (A), whereas lungs exposed 3 weeks earlier to CEES showed extensive interstitial fibrosis (shown by blue staining in Masson-trichrome-stained sections), inflammatory cell in-

filtrates (neutrophils and mononuclear cells), and alveolar collapse (B). In contrast, CEES-exposed lungs from rats also given liposomes with NAC and α/γ -tocopherol had preservation of alveolar spaces and limited inflammatory cellular infiltrates, both in alveolar walls and in alveolar spaces (C). These data support the biochemical data shown in Fig. 6.

DISCUSSION

These studies establish that antioxidant liposomes can protect against CEES-induced ALI in rats after airway instillation of appropriate liposomes. ALI, as defined by breakdown of the vascular endothelial and alveolar epithelial barriers with leak of 125 I-albumin into lung parenchyma, occurred in rats after airway exposure to CEES. In the setting of CEES, development of ALI is related to complement activation, PMN influx, generation predominantly by activated lung macrophages of proinflammatory cytokines and chemokines, and release of oxidants and proteases from PMNs and macrophages (9, 50). In other words, ALI caused by exposure to CEES is fundamentally caused by triggering of an extremely robust intrapulmonary inflammatory response, which is complement dependent (5). The vascular (endothelial) and airway (alveolar epithelial) barriers are breached by this intense inflammatory response, resulting in alveolar flooding and hemorrhage. It is possible that interaction of CEES with endothelial and epithelial cells also directly results in tissue damage (32). Some of the mechanisms of CEES-induced cell injury have recently been established. CEES is an alkylating agent and has variably toxic, mutagenic, carcinogenic, and teratogenic effects. However, the mechanisms of its delayed toxic effects (retardation in the rate of cell division, disruption of mitoses, chromosomal breakages, and other abnormalities of chromosomes) and of its carcinogenic actions are not understood (5). A review of the evidence linking sulfur mustard to oxidative stress has been described (32). Direct evidence for free radical formation in rat lung lavage after inhalation of sulfur mustard vapor has been obtained by using electron paramagnetic resonance (EPR) and spin-trapping techniques (1). These studies show a rapid formation of ascorbyl radicals followed by the formation of carbon-centered radicals. Evidence for free radical-mediated lung damage in CEES-exposed mice (*i.e.*, increased lipid peroxidation, as well as decreased GSH and increased oxidized GSH) has also been described (17). Interestingly, it has been shown that CEES is

FIG. 7. Histologic features of control lung (airway instillation of PBS), CEES lung with empty liposomes, or CEES lung with liposomes containing NAC + α/γ -tocopherol (vitamin E). Lungs were obtained 3 weeks after airway instillation of CEES. (Masson Trichome staining of paraffin-embedded sections, 20 \times and 40 \times magnification).



an alkylating agent that will react with nonprotein thiols (NAC or GSH) as well as protein thiol groups. Mustard gas is known to form metabolites (by the β -lyase pathway) derived from its covalent conjugation with GSH. Sulfur mustard metabolites from the glutathione (GSH)/ β -lyase pathway are specific markers for exposure to sulfur mustard (6, 7). This may represent another mechanism by which antioxidant liposomes protect against CEES-induced lung injury.

In the setting of our lung-injury model, all of these changes result in acute lung injury (4 h), followed by alveolar collapse and interstitial pulmonary fibrosis 3 weeks later. These outcomes can be averted by liposomes that contain the combination of NAC and α/γ -tocopherol or α/γ -tocopherol alone, whereas liposomes containing α/γ -tocopherol did not attenuate the acute lung injury. In contrast, liposomes containing NAC or NAC + GSH did not attenuate long-term fibrosis (3 weeks) but proved to be efficacious in protecting against CEES-induced ALI (4 h). Why liposomes containing certain antioxidants or combinations thereof are effective in the acute injury but not in the long-term injury, and *vice versa*, is not clear. It seems that tocopherol and NAC affect different aspects of the acute reaction, whereas tocopherol is more effective in preventing the progression to fibrosis. One possible explanation might be the hydrophobic nature of α/γ -tocopherol, which allows insertion into membranes (cell membrane, endoplasmic reticulum, and mitochondrial membranes), producing a relatively long-lasting effect, whereas internalization of NAC might lead to a relatively short life span (48). Similar to our results, it has been reported that the instillation of liposomes containing both GSH and α -tocopherol (but not GSH alone) resulted in the highest level of GSH retention in lung tissue, suggesting an effective antioxidant formulation for treating oxidative lung injury (43). In addition, it has been shown that tocopherol may also modulate signal-transduction pathways (2, 35, 52). Precisely what products of the macrophage can be linked to the development of pulmonary fibrosis after lung exposure to CEES remains to be defined, but a likely candidate mediator known to be released by macrophages is TGF- β (4). The protective effects of NAC-liposomes after acute exposure of lung to CEES liposomes may be associated with the dramatic disappearance of proinflammatory mediators in BAL fluids appearing after exposure to CEES (Fig. 3). Suppression of mediator appearance may be related to the ability of intracellular NAC to suppress NF- κ B ac-

tivation within macrophages, preventing generation of proinflammatory mediators. However, it should be noted that we did not directly measure a "restoration of redox balance," but other investigators, by using *in vitro* model systems, have shown that NAC protects against CEES toxicity by blocking the CEES-induced loss of intracellular GSH (22). We therefore assume that the administration of antioxidant liposomes affects the redox status in lung cells. It remains to be shown in future experiments whether antioxidant agents indeed restore the redox balance within the different lung cells.

Liposomal use for drug delivery has been studied extensively [reviewed in (13)]. The main cellular targets for lung oxidant stress are epithelial cells lining the alveoli (including type I and II alveolar cells), endothelial cells lining the pulmonary capillaries, and alveolar macrophages. Liposomal drugs may be administered orally, intravenously, or intratracheally, but only the latter two routes improve drug delivery (13). Intravenously administered liposomal drugs may be absorbed by pulmonary endothelial cells, but providing effective methods of drug delivery is still challenging.

For intratracheal instillation, the uptake and subcellular distribution of liposomal α -tocopherol (but not γ -tocopherol) in lung tissue was examined (41). Recovery of α -tocopherol in the lung was maximal 1 hour after liposomal instillation and resulted in a 16-fold increase in pulmonary total α -tocopherol concentration 72 h after instillation. α -Tocopherol was recovered largely from cytosolic, nuclear, microsomal, and mitochondrial fractions, providing evidence that α -tocopherol levels present in the membranes of these subcellular fractions were sufficient to protect against oxidant-induced lipid peroxidation. Evidence suggests that liposomes given into the airways are avidly taken up by phagocytes of the reticuloendothelial system (21, 27, 39, 46). Once internalized, they release their contents intracellularly (34, 36). In addition, alveolar types I and II as well as pulmonary endothelial cells have been shown to be able to internalize intratracheally administered liposomes (3, 33). In the current studies, we focused on alveolar macrophages (which are the chief sources of lung cytokines and chemokines) being affected by NAC-liposomes (Fig. 3); however, to what extent other lung cells such as alveolar epithelial cells have been altered remains to be determined.

The implications from the current studies (especially *in vitro* data) are that liposomal delivery most likely enhances a reduc-

ing environment in lung macrophages, which may be otherwise compromised when these cells come into contact with CEES or LPS. Delivery of NAC in liposomes may be protective in the setting of CEES-induced lung injury by phagocytosis of liposomes into lung macrophages and possibly by other lung cells as well (21, 27, 39). Once ingested by macrophages, the liposomal contents are released into the interior of the macrophages (34, 36). NAC may be distributed into the cytosol component, whereas α/γ -tocopherol is distributed into membranes within cells (see earlier). Phosphonate-containing liposomes have been used in rodents selectively to deplete the lung of macrophages, whereas other types of lung cells are not affected (49). It seems in the CEES model of ALI that the release of proinflammatory mediators (cytokines and chemokines) from lung macrophages is blocked by the use of NAC-liposomes, subsequently resulting in intracellular release of NAC and blockade of NF- κ B activation within macrophages. However, it seems plausible that an attenuated oxidative stress within macrophages may also indirectly result in protection of adjacent alveolar epithelial and endothelial cells. Whether the use of other liposomes with antioxidant properties (*e.g.*, GSH, α/γ -tocopherol) would also suppress the release into CEES-treated lungs of proinflammatory mediators remains to be determined, but it seems likely, because such liposomes protect against ALI after airway exposure (44). As suggested earlier, it is likely that NAC liposomes are phagocytized by lung macrophages, resulting in release of NAC into the cytosol, resulting in blockade of NF- κ B activation, which is required for production and release of mediators by macrophages. The trigger in this situation is likely CEES, which causes NF- κ B activation in macrophage-type cells (9, 14).

Lipopolysaccharide (LPS) is known to induce acute lung injury with features similar to changes in CEES-induced acute lung injury (50). Because both types of injury result in an inflammatory response and its accompanying oxidative stress, we extended our experiments to *in vitro* exposure of alveolar macrophages to LPS or CEES (Figs. 3 and 4). *In vivo* experiments have shown that administration of liposomes containing NAC or α -tocopherol protects rats from ALI induced by LPS or paraquat (19, 42, 44, 45). We show in this report that liposomes containing NAC significantly suppressed the release of proinflammatory cytokines from alveolar macrophages exposed to either LPS or CEES, suggesting similar pathways being activated under both conditions. This confirms the *in vivo* data (Fig. 3), underscoring the hypothesis that augmentation of the pulmonary antioxidant status can attenuate both LPS- and CEES-induced oxidative stress.

Taken together, restoration of the redox balance may be crucial in the setting of ALI induced by CEES for attenuation of early, acute injury, and may also set the stage for attenuating the long-term effects of CEES (pulmonary fibrosis). Liposome-mediated delivery of antioxidant agents, particularly NAC and α/γ -tocopherol, is a powerful tool to diminish CEES-induced acute and long-term lung injury.

ABBREVIATIONS

ALI, acute lung injury; ANOVA, analysis of variance; BALF, bronchoalveolar lavage fluid; BSA, bovine serum al-

bumin; 125 I-BSA, iodine 125-labeled bovine serum albumin; CINC-1, cytokine-induced neutrophil chemoattractant-1; CEES, chloroethyl ethyl sulfide; DPBS, Dulbecco's phosphate-buffered saline; DPPC, dipalmitoylphosphatidylcholine; ELISA, enzyme-linked immunosorbent assay; GSH, glutathione; HYP, hydroxyproline; IL-1 β , interleukin-1 β ; IL-6, interleukin-6; LPS, lipopolysaccharide; NAC, *N*-acetylcysteine; NF- κ B, nuclear factor κ -B; PMN, polymorphonuclear leukocyte; RPMI, Roswell Park Memorial Institute; TGF- β , transforming growth factor- β ; TNF- α , tumor necrosis factor- α .

ACKNOWLEDGMENTS

This work was supported by DOD grants DAMD17-03-2-0054 and W81XWH-06-2-0044 and NIH grants GM-029507 and HL-31963.

REFERENCES

1. Anderson DR, Yourick JJ, Arroyo CM, Young GD, and Harris LW. Use of EPR spin-trapping techniques to detect radicals from rat lung lavage fluid following sulfur mustard vapor exposure. *Med Defense Biosci Rev Proc* 1: 113–121, 1993.
2. Azzi A, Gysin R, Kempna P, Munteanu A, Negis Y, Villacorta L, Visarius T, and Zingg JM. Vitamin E mediates cell signaling and regulation of gene expression. *Ann N Y Acad Sci* 1031: 86–95, 2004.
3. Baker RR, Czopf L, Jilling T, Freeman BA, Kirk KL, and Matalon S. Quantitation of alveolar distribution of liposome-entrapped antioxidant enzymes. *Am J Physiol* 263: L585–L594, 1992.
4. Bartram U and Speer CP. The role of transforming growth factor beta in lung development and disease. *Chest* 125: 754–765, 2004.
5. Bignold LP. Alkylating agents and DNA polymerases. *Anticancer Res* 26: 1327–1336, 2006.
6. Black RM, Brewster K, Clarke RJ, Hambrook JL, Harrison JM, and Howells DJ. Biological fate of sulphur mustard, 1,1'-thiobis(2-chloroethane): isolation and identification of urinary metabolites following intraperitoneal administration to rat. *Xenobiotica* 22: 405–418, 1992.
7. Boyer AE, Ash D, Barr DB, Young CL, Driskell WJ, Whitehead RD Jr, Ospina M, Preston KE, Woolfitt AR, Martinez RA, Silks LA, and Barr JR. Quantitation of the sulfur mustard metabolites 1,1'-sulfonylbis[2-(methylthio)ethane] and thiodiglycol in urine using isotope-dilution gas chromatography-tandem mass spectrometry. *J Analyt Toxicol* 28: 327–332, 2004.
8. Calvet JH, Jarreau PH, Levame M, D'Ortho MP, Lorino H, Harf A, and Macquin-Mavier I. Acute and chronic respiratory effects of sulfur mustard intoxication in guinea pig. *J Appl Physiol* 76: 681–688, 1994.
9. Chatterjee D, Mukherjee S, Smith MG, and Das SK. Signal transduction events in lung injury induced by 2-chloroethyl ethyl sulfide, a mustard analog. *J Biochem Mol Toxicol* 17: 114–121, 2003.
10. Chen CC, Wang JK, and Lin SB. Antisense oligonucleotides targeting protein kinase C- α , - β I, or - δ but not - ϵ inhibit lipopolysaccharide-induced nitric oxide synthase expression in RAW 264.7 macrophages: involvement of a nuclear factor kappa B-dependent mechanism. *J Immunol* 161: 6206–6214, 1998.
11. Chono S, Tanino T, Seki T, and Morimoto K. Influence of particle size on drug delivery to rat alveolar macrophages following pulmonary administration of ciprofloxacin incorporated into liposomes. *J Drug Target* 14: 557–566, 2006.
12. Chono S, Tanino T, Seki T, and Morimoto K. Uptake characteristics of liposomes by rat alveolar macrophages: influence of particle size and surface mannose modification. *J Pharm Pharmacol* 59: 75–80, 2007.

13. Christofidou-Solomidou M and Muzykantov VR. Antioxidant strategies in respiratory medicine. *Treat Respir Med* 5: 47–78, 2006.
14. Das SK, Mukherjee S, Smith MG, and Chatterjee D. Prophylactic protection by *N*-acetylcysteine against the pulmonary injury induced by 2-chloroethyl ethyl sulfide, a mustard analogue. *J Biochem Mol Toxicol* 17: 177–184, 2003.
15. Davreux CJ, Soric I, Nathens AB, Watson RW, McGilvray ID, Suintres ZE, Shek PN, and Rotstein OD. *N*-Acetyl cysteine attenuates acute lung injury in the rat. *Shock* 8: 432–438, 1997.
16. Downey JS and Han J. Cellular activation mechanisms in septic shock. *Front Biosci* 3: d468–d476, 1998.
17. Elsayed NM and Omaye ST. Biochemical changes in mouse lung after subcutaneous injection of the sulfur mustard 2-chloroethyl 4-chlorobutyl sulfide. *Toxicology* 199: 195–206, 2004.
18. Emad A and Rezaian GR. Immunoglobulins and cellular constituents of the BAL fluid of patients with sulfur mustard gas-induced pulmonary fibrosis. *Chest* 115: 1346–1351, 1999.
19. Fan J, Shek PN, Suintres ZE, Li YH, Oreopoulos GD, and Rotstein OD. Liposomal antioxidants provide prolonged protection against acute respiratory distress syndrome. *Surgery* 128: 332–338, 2000.
20. Fujihara M, Connolly N, Ito N, and Suzuki T. Properties of protein kinase C isoforms (beta II, epsilon, and zeta) in a macrophage cell line (J774) and their roles in LPS-induced nitric oxide production. *J Immunol* 152: 1898–1906, 1994.
21. Gonzalez-Rothi RJ, Straub L, Cacace JL, and Schreiber H. Liposomes and pulmonary alveolar macrophages: functional and morphologic interactions. *Exp Lung Res* 17: 687–705, 1991.
22. Han S, Espinoza LA, Liao H, Boulares AH, and Smulson ME. Protection by antioxidants against toxicity and apoptosis induced by the sulphur mustard analog 2-chloroethylethyl sulphide (CEES) in Jurkat T cells and normal human lymphocytes. *Br J Pharmacol* 141: 795–802, 2004.
23. Husain K, Dube SN, Sugendran K, Singh R, Das Gupta S, and Soman SM. Effect of topically applied sulphur mustard on antioxidant enzymes in blood cells and body tissues of rats. *J Appl Toxicol* 16: 245–248, 1996.
24. Johnson KJ and Ward PA. Acute immunologic pulmonary alveolitis. *J Clin Invest* 54: 349–357, 1974.
25. Khateri S, Ghanei M, Keshavarz S, Soroush M, and Haines D. Incidence of lung, eye, and skin lesions as late complications in 34,000 Iranians with wartime exposure to mustard agent. *J Occup Environ Med* 45: 1136–1143, 2003.
26. Kopff M, Zakrzewska I, Strzelczyk M, Klem J, and Dubiecki W. Superoxide dismutase and catalase activity in psoriatic patients treated topically with ointment containing 2-chloroethyl-3-chloropropyl sulfide. *Pol J Pharmacol* 46: 439–444, 1994.
27. Lentsch AB, Czermak BJ, Bless NM, Van Rooijen N, and Ward PA. Essential role of alveolar macrophages in intrapulmonary activation of NF-kappaB. *Am J Respir Cell Mol Biol* 20: 692–698, 1999.
28. Luna L. *Manual histology staining methods: AFIP*. New York: McGraw-Hill, 1968.
29. McClintock SD, Hoesel LM, Das SK, Till GO, Neff T, Kunkel RG, Smith MG, and Ward PA. Attenuation of half sulfur mustard gas-induced acute lung injury in rats. *J Appl Toxicol* 26: 126–131, 2006.
30. McClintock SD, Till GO, Smith MG, and Ward PA. Protection from half-mustard-gas-induced acute lung injury in the rat. *J Appl Toxicol* 22: 257–262, 2002.
31. Moore BB, Coffey MJ, Christensen P, Sitterding S, Ngan R, Wilke CA, McDonald R, Phare SM, Peters-Golden M, Paine R 3rd, and Toews GB. GM-CSF regulates bleomycin-induced pulmonary fibrosis via a prostaglandin-dependent mechanism. *J Immunol* 165: 4032–4039, 2000.
32. Naghii MR. Sulfur mustard intoxication, oxidative stress, and antioxidants. *Mil Med* 167: 573–575, 2002.
33. Poelma DL, Zimmermann LJ, Scholten HH, Lachmann B, and van Iwaarden JF. In vivo and in vitro uptake of surfactant lipids by alveolar type II cells and macrophages. *Am J Physiol Lung Cell Mol Physiol* 283: L648–L654, 2002.
34. Popescu MC, Swenson CE, and Ginsberg RS. Liposome-mediated treatment of viral, bacterial and protozoal infections. In: *Liposomes: from biophysics to therapeutics*, edited by Ostro MJ. New York: Marcel Dekker, 1987, pp 219–251.
35. Rimbach G, Minihane AM, Majewicz J, Fischer A, Pallauf J, Virgili F, and Weinberg PD. Regulation of cell signalling by vitamin E. *Proc Nutr Soc* 61: 415–425, 2002.
36. Roerdink F, Regts J, Daemen T, Bakker-Woudenberg I, and Scherphof G. Liposomes as drug carriers to liver macrophages: fundamentals and therapeutic aspects. In: *Targeting of drugs with synthetic systems*, edited by Senior J and Poste G. New York: Plenum Press, 1986, pp 193–206.
37. Shapira L, Sylvia VL, Halabi A, Soskolne WA, Van Dyke TE, Dean DD, Boyan BD, and Schwartz Z. Bacterial lipopolysaccharide induces early and late activation of protein kinase C in inflammatory macrophages by selective activation of PKC-epsilon. *Biochem Biophys Res Commun* 240: 629–634, 1997.
38. Shapira L, Takashiba S, Champagne C, Amar S, and Van Dyke TE. Involvement of protein kinase C and protein tyrosine kinase in lipopolysaccharide-induced TNF-alpha and IL-1 beta production by human monocytes. *J Immunol* 153: 1818–1824, 1994.
39. Shephard EG, Joubert JR, Finkelstein MC, and Kuhn SH. Phagocytosis of liposomes by human alveolar macrophages. *Life Sci* 29: 2691–2698, 1981.
40. Stone WL, Qui M, and Smith M. Lipopolysaccharide enhances the cytotoxicity of 2-chloroethyl ethyl sulfide. *BMC Cell Biol* 4: 1, 2003.
41. Suintres ZE, Hepworth SR, and Shek PN. Pulmonary uptake of liposome-associated alpha-tocopherol following intratracheal instillation in rats. *J Pharm Pharmacol* 45: 514–520, 1993.
42. Suintres ZE and Shek PN. Alleviation of paraquat-induced lung injury by pretreatment with bifunctional liposomes containing alpha-tocopherol and glutathione. *Biochem Pharmacol* 52: 1515–1520, 1996.
43. Suintres ZE and Shek PN. Incorporation of alpha-tocopherol in liposomes promotes the retention of liposome-encapsulated glutathione in the rat lung. *J Pharm Pharmacol* 46: 23–28, 1994.
44. Suintres ZE and Shek PN. Prophylaxis against lipopolysaccharide-induced acute lung injury by alpha-tocopherol liposomes. *Crit Care Med* 26: 723–729, 1998.
45. Suintres ZE and Shek PN. Treatment of LPS-induced tissue injury: role of liposomal antioxidants. *Shock* 6(suppl 1): S57–S64, 1996.
46. Thepen T, Van Rooijen N, and Kraal G. Alveolar macrophage elimination in vivo is associated with an increase in pulmonary immune response in mice. *J Exp Med* 170: 499–509, 1989.
47. Thrall RS, McCormick JR, Jack RM, McReynolds RA, and Ward PA. Bleomycin-induced pulmonary fibrosis in the rat: inhibition by indomethacin. *Am J Pathol* 95: 117–130, 1979.
48. Traber MG and Atkinson J. Vitamin E, antioxidant and nothing more. *Free Radic Biol Med* 43: 4–15, 2007.
49. Van Rooijen N and Sanders A. Liposome mediated depletion of macrophages: mechanism of action, preparation of liposomes and applications. *J Immunol Methods* 174: 83–93, 1994.
50. Ward PA. Role of complement, chemokines, and regulatory cytokines in acute lung injury. *Ann N Y Acad Sci* 796: 104–112, 1996.
51. Wright SD, Ramos RA, Tobias PS, Ulevitch RJ, and Mathison JC. CD14, a receptor for complexes of lipopolysaccharide (LPS) and LPS binding protein. *Science* 249: 1431–1433, 1990.
52. Zingg JM and Azzi A. Non-antioxidant activities of vitamin E. *Curr Med Chem* 11: 1113–1133, 2004.

Address reprint requests to:

Peter A. Ward, M.D.

Department of Pathology

University of Michigan Medical School

1301 Catherine Road

Ann Arbor, MI 48109-0602

E-mail: pward@umich.edu

Date of first submission to ARS Central, August 13, 2007; date of final revised submission, November 14, 2007; date of acceptance, November 15, 2007.

Activation by C5a of endothelial cell caspase 8 and cFLIP

E. A. Albrecht¹, J. V. Sarma², P. A. Ward^{2*}

¹Department of Biology and Physics, Kennesaw State University, Kennesaw, GA 30144

²Department of Pathology, University of Michigan Medical School, Ann Arbor, MI 48109, Fax +734-764-4308, e-mail pward@umich.edu

Received 23 July 2008; returned for revision 10 September 2008; received for final revision 29 September 2008; accepted by M. Parnham 18 September 2008

Published Online First 8 January 2009

Abstract. *Objectives and design:* In this study, we examine the relationship between C5a and activation of cysteine aspartic acid protease 8 (caspase 8) in human umbilical vein endothelial cells (HUVEC).

Materials or subjects: Primary cultures of HUVEC were used.

Treatments: Recombinant human C5a (50 ng/ml) was used in the presence or absence of 10 µg/ml cycloheximide (CHX).

Methods: HUVEC were treated with C5a alone and in the presence of CHX, then monitored for cell viability, poly-ADP-ribose 1 (PARP-1) and caspase 8 activities. Gene and protein expressions were assessed for caspase 8 and the caspase 8 homologue, FLICE –inhibitory protein (cFLIP).

Results: We found a 43.1 ± 6.9 percent reduction in viability of HUVEC stimulated for 18 h with 50 ng/ml C5a in the presence of 10 µg/ml CHX (p<0.05). In contrast, the cell viability of cells stimulated for 18 h with 50 ng/ml C5a or 10 µg/ml CHX alone was not significantly different compared to the non-stimulated control. Treatment of HUVEC with C5a induced an increase in caspase 8 activity but did not significantly affect cFLIP levels.

Conclusions: These data suggest caspase 8 activation induced by C5a leads to cell death if protein synthesis of anti-apoptotic protein(s) is blocked.

Key words: Complement factor 5a (C5a) – Cycloheximide (CHX) – Caspase 8 – Caspase 8 homologue FLICE – Inhibitory protein (cFLIP)

Introduction

The endothelium plays an important role in inflammatory syndromes, such as sepsis and atherosclerosis [1, 2, 3, 4, 5]. In the case of sepsis, high levels of pro-inflammatory media-

tors (C5a, TNFα, LPS, IL6, and FasL) are produced and can be linked to altered apoptotic cell death. Although research has focused on myeloid cells (e.g., neutrophils, lymphocyte, macrophages), recent reports suggest that non-myeloid cells play an important role during inflammatory syndromes. For example, apoptosis of endothelial cells has been reported in regions of atherosclerotic plaques, suggesting endothelial cells are capable of apoptosis under specific stimuli [6]. Other studies have found elevated levels of shed apoptotic endothelial cells or endothelial cell microparticles in the sera of septic and multiple sclerosis patients [7, 8].

Primary cell culture studies have shown that endothelial cells are resistant to cell death when stimulated with TNFα, IL-1 or LPS [9, 10, 11, 12]. This resistance has been attributed to cyto-protective proteins, which modulate apoptotic reactions at proximal (e.g. cFLIP), intermediate (e.g., Bcl-2, Bcl-x), and distal (e.g. BIRC2, TNFAIP3) apoptotic cascade locations. This has been supported with cecal ligation and puncture (CLP) models showing endothelial apoptosis corresponds to suppressed levels of Bcl-2 [13]. The protein cFLIP has received attention because of its upstream inhibition of apoptosis. Although the mechanism by which cFLIP attenuates cell death has not been fully elucidated, it has been suggested that cFLIP acts as a competitive inhibitor to caspase 8 by blocking caspase 8 binding to the death induced signaling complex (DISC) [14]. This is supported by other reports suggesting that cFLIP is cleaved into a p43 subunit that attaches to DISC, preventing the processing of caspase 8 into its active form [15, 16]. Overall, this action results in a reduction of the long or “inactive” form of cFLIP. However, several cell types (HUVEC, human aortic endothelial cells, HL60, Jurkat) stimulated by either TNFα, FasL, or LPS initiate activation of MAP kinase 1 (MEK1), phosphatidylinositol 3-kinase/Akt, and NF B pathways, resulting in gene transcription and protein synthesis of cFLIP so that cytosolic levels remain constant [17, 18, 19]. It appears that maintaining cytosolic levels of cFLIP, along with other anti-apoptotic proteins, is important for endothelial cell survival after exposure to apoptosis inducing agents.

Correspondence to: P. A. Ward

There is increasing evidence that anaphylatoxins (C5a, C3a) promote pro-inflammatory conditions contributing to altered cellular apoptosis [20, 21, 22, 23]. C5a is known as a potent stimulus, inducing chemotaxis, release of granules, and the generation of reactive oxygen species from phagocytic cells. Yet, recent studies have suggested that C5a plays a role in the apoptotic process during systemic inflammatory conditions. C5a is thought to have an anti-apoptotic effect on neutrophils, during sepsis. Studies suggest that the ligation of C5aR (CD88) activates PI-3K and MAPK survival signaling pathways in neutrophils, thus suppressing the apoptotic response [23]. Expression of C5aR was initially thought to be restricted to monocytes/macrophages and polymorphonuclear cells, but it now appears to include several other cell types, including endothelial cells [24, 25, 26]. The actions of C5a-C5aR in non-myeloid cells *in vivo* are less clear. Although, it has been demonstrated that C5a produces robust gene expression response in human umbilical vein endothelial cells (HUVEC), including genes associated with cell adherence (E-selectin, ICAM-1, VCAM-1), chemokines (IL-1, IL-6), growth factors (e.g. VEGF, PDGF), and apoptosis (caspase 3, caspase 8, cFLIP) [27].

For this study we chose to investigate the relationship between C5a induced stimulation of HUVEC and activation of caspase-8 and cFLIP. Our data suggest that C5a stimulation alone did not significantly affect cell viability compared to non-stimulated controls. However, preincubation of cells with cycloheximide (CHX) followed by C5a stimulation significantly reduced cell viability. In addition, we found caspase 8 activity increased after C5a stimulation, which coincided with reduced cytosolic levels of cFLIP.

Material and Methods

Endothelial Cell Culture

Primary HUVEC were isolated and plated in T-75 flasks coated with 1% gelatin (Sigma, St. Louis, MO). Cells were cultured in medium 199 (Gibco BRL, Grand Island, NY) containing endothelial growth supplement (Sigma, St. Louis, MO), 20% fetal bovine calf serum (Hyclone, Logan, UT), 5% penicillin/streptomycin (Gibco BRL, Grand Island, NY) and 25 µg/ml heparin (Sigma, St. Louis, MO). All experiments were performed using the first 3–4 cell passages. A CHX pre-incubation period of 30 min was used for experimental conditions where CHX and C5a were used in combination.

Cell Viability Assay

HUVEC were plated into 12 well plates at 1×10^5 cells/well and allowed to attach for 24 h. Prior to experimentation, media was removed and replaced with 0.5 ml of fresh media. Confluent, HUVEC were stimulated with C5a (50 ng/ml), C5a (50 ng/ml) with CHX (10 µg/ml). Controls included non-stimulated cells and cells incubated with CHX (10 µg/ml) for 18 h. After 18 h, the media was removed, replaced with 0.5 ml fresh media. Next, 100 µl of CellTiter 96[®] AQueous One Solution Reagent (Promega, Madison, WI) was added to each well, incubated at 37°C for 2 h, then read at 490 nm.

Caspase-8 Activity Assay

Caspase-8 activity was detected using a caspase-8 fluorescent assay kit (BD Bioscience, Palo Alto, CA). HUVEC were plated into 12 well

plates at 1×10^5 cells/well and allowed to attach for 24 h at 37°C prior to experimentation. Cell supernatant fluids were removed and replaced with 0.5 ml of fresh medium then stimulated with C5a (50 ng/ml) alone or with CHX (10 µg/ml) for 18 h. Controls included non-stimulated cells and cells incubated with CHX (10 µg/ml) alone for 18 h. After stimulation, the cells were washed with 37°C HBSS, lysed with lysis buffer (BD biosciences, San Jose, CA) and incubated on ice for 10 min. Cell lysates were centrifuge at 10000 rpm for 3 min and 250 µl of the supernatant was added to 250 µl of reaction buffer containing 25 µl of Caspase-8 substrate. This solution was incubated for 1 h and 30 min at 37°C, then read in a microplate reader with a 400 nm excitation and 550 emission filter. Quantitation of sample was performed as described in the kit protocol, using a 7-amino-4-trifluoromethyl coumarin (AFC) standard curve. Samples were normalized by calculating the relative fluorescent units per microgram of protein (RUF/µg).

RT-PCR

HUVEC were stimulated with C5a alone or in the presence of CHX for 0, 4, and 8 h. CHX control involved incubating HUVEC with CHX for 8 h. One microgram total RNA was reverse transcribed with superscript reverse transcriptase (Invitrogen, Carlsbad, CA) using random and poly dT primers for first-strand cDNA synthesis. This was repeated for each timepoint. Primers for each gene of interest were designed using Primer Select software and included: cFLIP: forward primer, 5'-GGGGACTTGGCTGAAGTCTCTA-3', reverse primer, 5'-AAATCCTCACCAATCTCTGCCATCA-3'; Caspase-8: forward primer, 5'-CACTAGAAAGGAGGAGATGGAAAAG-3', reverse primer, 5'-CTATCCTGTTCTCTTGGAGAGTCC-3'; GAPDH: forward primer, 5'-CGGAGTCAACGGATTGGTTCGTAT-3', reverse primer, 5'-AGCCTTCTCCATGGTGGTGAAGA-3'. Polymerase Chain Reactions (PCR) were run on Gene Amp PCR system 9700 (Applied Biosystems, Foster City, CA) using a "hot start" method with the following conditions: 94°C for 5 min, 94°C for 1 min, 60–65°C for 1 min, 72°C for 1 min, 72°C for 10 min. GAPDH reaction mixture was run for 26, 28, and 35 cycles to ensure that the reaction product was in the linear range. PCR products were examined in 1% agarose gel. The RT product volumes were readjusted and the reaction was repeated with GAPDH primers at 28 cycles. After RT product adjustment, the selected gene primers were amplified with 28 and 35 cycles, and then examined by agarose gel electrophoresis to confirm product size.

Western Blots

To examine the ability of C5a to induce proteins in HUVEC, we employed Western-blotting techniques. HUVEC were grown to confluence, then stimulated with human C5a (50 ng/ml) in the presence or absence of CHX (10 µg/ml) at 37°C for 2, 8 or 18 h. After stimulation, the supernatant fluids were removed and the monolayer was washed twice with PBS. Monolayers were then placed on ice and lysed using NP40 buffer (50 mM Tris-HCl pH 8.0, 1% NP40) containing protease inhibitors (Roche, Mannheim, Germany). The lysate was then collected with sterile cell scrapers and sonicated. The resulting cell lysate was centrifuged at 13,500x g for 10 min and the supernatant fluid removed. This was repeated for each time point. The protein concentrations were estimated using a BioRad protein colorimetric assay. The standardized supernatants were combined with sample buffer, sterile glycerol and stored at -80°C. The cell lysates were subjected to 10 and 15% sodium dodecyl sulfate poly acrylamide gel electrophoresis (SDS-PAGE) and transferred to methanol activated PVDF membranes. The membranes were blocked for 1 h with 5% non-fat dry milk dissolved in TBST (1 M Tris pH 8, 1 M NaCl, 0.1% Tween 20). A dilution of 1:1000 for anti-rabbit antibodies to full length PARP-1 (Cell Signaling Technology, Danvers, MA) was used for immunoblotting. Detection of cFLIP was performed using a 1:2000 dilution of anti-rabbit antibodies to full length cFLIP (Gene Therapy Systems, San Diego, CA) or a 1:1000 dilution of anti-rabbit antibodies (AVIVA Systems Biology, San Diego, CA) to short and long forms of cFLIP. Caspase 8 was immunoblotted using a 1:2000 dilution of anti-

mouse antibodies (Cell Signaling Technology, Danvers, MA) which detected both the inactive (55kDa) and active (p41/43 kDa) fragments or anti-mouse antibodies which detect only the inactive form of caspase 8 (NeoMarkers, Fremont, CA). After an overnight incubation at 4 °C, the membranes were washed thrice with TBST and incubated with their respective secondary anti-rabbit or anti-mouse antibodies coupled to horseradish peroxidase for 2h at room temperature. The membranes were then washed twice with TBST followed by an additional wash with TBS. The immunoreactive bands were visualized using enhanced chemiluminescence (ECL) Western blotting detection agents according to manufacturer's directions.

Statistical Analysis

Statistical analysis of the responses obtained from cell viability and caspase 8 activity were carried out using unpaired student t test and InStat 3 (Graphpad, San Diego, CA) software. P values of <0.05 were considered to be significant.

Results

C5a promotes cell death in HUVEC when in the presence of cycloheximide

Several apoptotic (e.g., caspase 3, NFkB1, caspase 8) and anti-apoptotic genes (e.g., BIRC3, TNFAIP3, cFLIP) are induced in HUVEC when stimulated by C5a [27]. With this in mind, we chose to examine more closely the ability of C5a to induce an apoptotic response in HUVEC. To do this, we used CHX, a known inhibitor of protein synthesis. We tested the cytotoxicity of CHX on endothelial cells (data not shown) and determined a CHX concentration of 10 µg/ml would be used for the duration of the study. In addition, we used a C5a concentration of 50 ng/ml, based on data from our previous study [27].

HUVEC stimulated with 50 ng/ml C5a or 10 µg/ml CHX for 18h maintained cell viability of 95.7 ± 0.49 and $90.7 \pm 6.2\%$, respectively. These results were not significantly different compared to the non-stimulated control (Fig. 1A and B). In contrast, cells stimulated with C5a in the presence of CHX showed a significant reduction ($43.1 \pm 6.9\%$) in cell viability compared to non-stimulated cells. This result is complemented by brightfield images (Fig. 1B), where cells stimulated with C5a in the presence of CHX displayed apoptotic morphology (e.g., cell rounding) (frame 1d). Cells stimulated with C5a (frame b) or CHX alone (frame c) maintained cobble-stone appearances, similar to the non-stimulated cells (frame a). Next, we subjected HUVEC to increasing concentrations of C5a (1–100 ng/ml) for 18h in the presence of CHX (10 µg/ml). Figure 1C shows the dose dependent loss of cell viability in HUVEC.

PARP-1 protein levels are rapidly decreased in response to C5a and CHX, while caspase 8 activity increases

The loss of cell viability when HUVEC are co-incubated with C5a and CHX, suggests initiation of apoptotic cascades, which are usually constrained by anti-apoptotic proteins. To examine this possibility, we monitored caspase 8

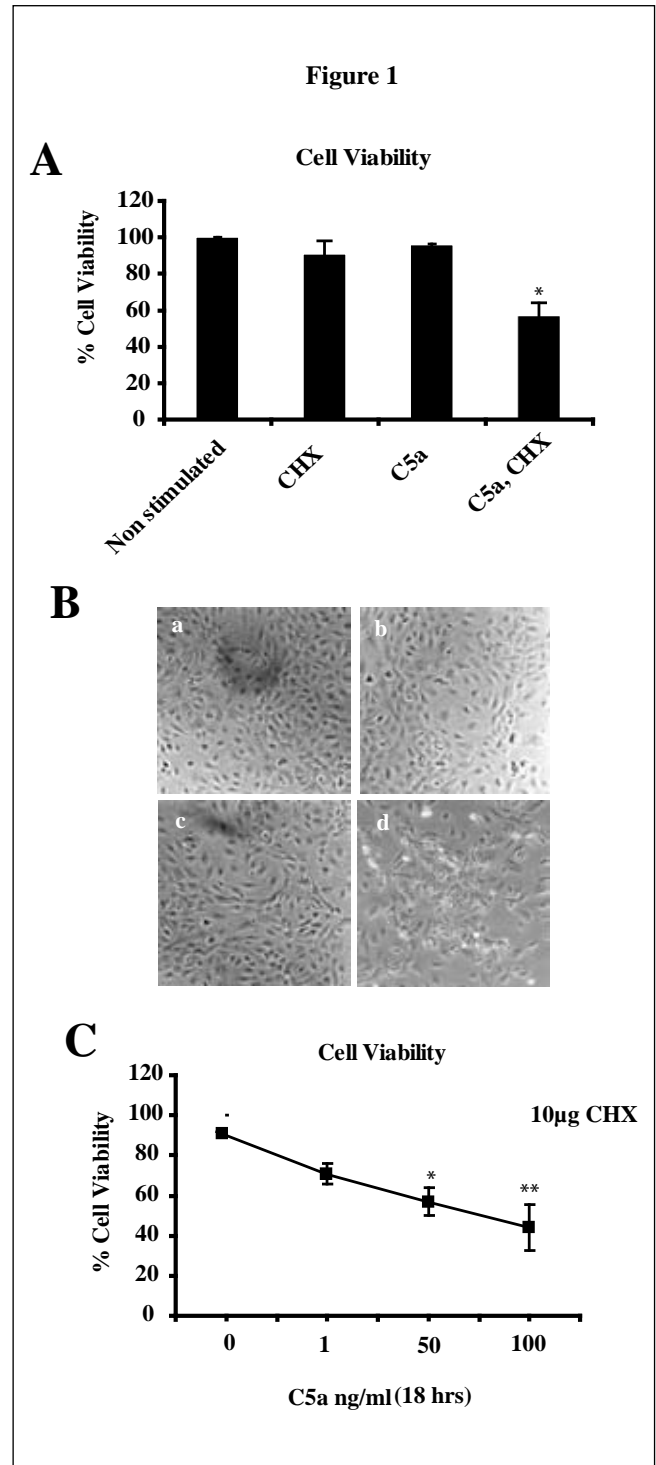


Fig 1. C5a induces loss of HUVEC viability in the presence of CHX. **A)** MTS assay for cell viability. Cells were treated with C5a (50 ng/ml), CHX (10 µg/ml), or C5a (50 ng/ml) plus CHX (10 µg/ml) for 18h. *P<0.05 vs. C5a treated. **B)** Brightfield images, 200X magnification: a) non-stimulated control b) CHX (10 µg/ml) 18h c) C5a (50 ng/ml), 18h d) C5a (50 ng/ml) with CHX (10 µg/ml), 18h. Percentage of viability was expressed as the proportion of untreated cells. **C)** Dose dependent response with MTS assay. Cells were stimulated with C5a (1–100 ng/ml) for 18h in the presence of CHX (10 µg/ml). *P<0.05 vs. control conditions (CHX 10 µg/ml); **P<0.01 vs. control conditions (CHX 10 µg/ml). The results shown are the mean \pm S.E. of experiments done in triplicate and are representative of three separate experiments.

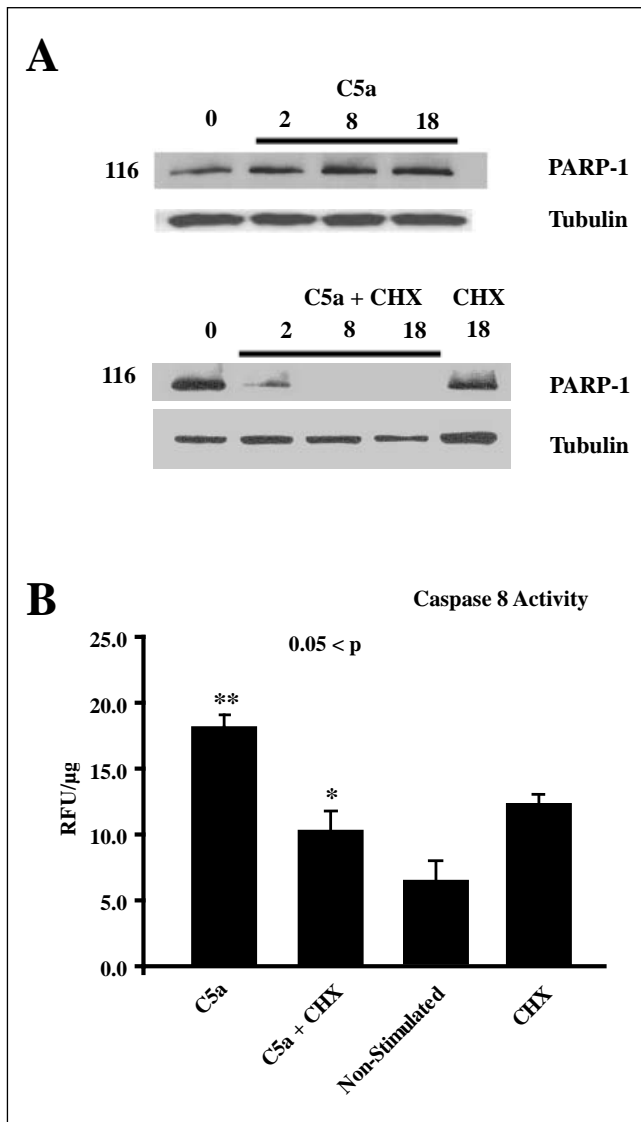


Fig 2. C5a stimulation of HUVEC initiates apoptotic pathway activity. **A)** Western blots for protein expression of PARP. Cell lysates were collected after 2, 8, 18 h following stimulation with C5a (50 ng/ml) alone or with C5a (50 ng/ml) and CHX (10 μg/ml). Control lysates were collected from cells without C5a stimulation (Non-stimulated). Loading conditions were confirmed by β-tubulin content. **B)** Caspase-8 activity assay. Cell lysates are collected after 18 h and analyzed for Caspase-8 activity following stimulation with C5a (50 ng/ml) alone or with C5a (50 ng/ml) and CHX (10 μg/ml). Control lysates were from cells without C5a stimulation (Non-stimulated) and cell stimulated with CHX (10 μg/ml) for 18 h. *P < 0.05 vs. C5a; **P < 0.05 vs. Non Stimulated. Data are ± S.E. of three separate experiments.

enzymatic activity and PARP-1 protein levels under similar experimental conditions. Caspase-8 serves as an upstream apoptotic initiator in the CD95/Fas and TNFα pathways. Accordingly, it is possible under the experimental conditions that C5a initiates apoptotic cascade(s). PARP-1, a regulator of DNA repair, was selected as a complementary marker of apoptosis [28]. Western blot analysis was used to examine full length PARP-1 levels, with the antibody which was specific for the full length form of PARP-1. Cell lysates were

collected 0, 2, 8 and 18 h after C5a addition, in the presence or absence of CHX (Fig. 2). PARP-1 levels remained constant after stimulation with C5a alone (Fig. 2A upper frame). In contrast, cells stimulated with C5a and CHX showed reductions in or loss of PARP-1 at all timepoints, while treatment of cells with CHX alone still resulted in the presence of PARP-1.

Next, we measured caspase-8 activity in HUVEC using 7-amino-4-trifluoromethyl coumarin (AFC) under the same experimental conditions. The active form of caspase 8 targets the AFC complex, so that caspase activity may be measured by fluorescent emission. Cell lysates were collected after 18 h and assayed for the active fragment (p41/43) of caspase 8 (Fig. 2B). Non-stimulated HUVEC demonstrated a low level of caspase 8 activity (6.3 ± 2.9 RFU/μg). Cells stimulated with C5a for 18 h produced 18.3 ± 0.9 RFU/μg of protein, compared to 10.3 ± 1.7 RFU/μg for cells stimulated with C5a and CHX. This data suggests that C5a induces caspase 8 activity in HUVEC, but does not result in PARP cleavage. Although cells stimulated with CHX alone or in combination with C5a showed elevated levels of caspase 8 activity, they were not significant compared to the non-stimulated control.

C5a induces increase in gene expression of caspase 8 and cFLIP

The influence of C5a on the gene expression of caspase-8 and cFLIP was assessed. We wanted to determine if the elevated caspase-8 activity observed in Figure 2B was linked with increased caspase-8 gene expression. In addition, we monitored the gene expression of cFLIP, which has been identified as a competitive inhibitor for caspase-8. We predicted that changes in caspase-8 gene expression would correspond to similar changes in cFLIP gene expression. As depicted in Figure 3A, caspase-8 gene expression increased 4 and 8 h after C5a stimulation. The gene expression for cFLIP was unchanged after 4 h, but dramatically increased after 8 h of C5a stimulation. Cells stimulated with C5a in the presence of CHX demonstrated a robust increase in caspase-8 gene expression after 4 and 8 h (Fig. 3B). Interestingly, cells treated with C5a and CHX had a greater increase in caspase-8 gene expression at 4 h compared to those stimulated with C5a alone. In contrast, C5a and CHX treated cells showed limited increase in cFLIP gene expression at 8 h. This suggests that C5a induces caspase-8 gene more rapidly than cFLIP, but cFLIP gene expression is moderately repressed in the presences of CHX. Basal gene expression levels of cFLIP were unchanged by CHX alone.

C5a promotes activation of caspase-8 and cFLIP

We investigated the activity of caspase-8 and its known competitive inhibitor, cFLIP, after cell stimulation with C5a. To better understand the apoptotic response elicited by C5a, we collected cell lysates after 18 h incubation with C5a (50 ng/ml) in the presence or absence of CHX (10 μg/ml). We selected antibodies which recognized only the inactive (long) form of cFLIP so that we could monitor the loss of the pro-

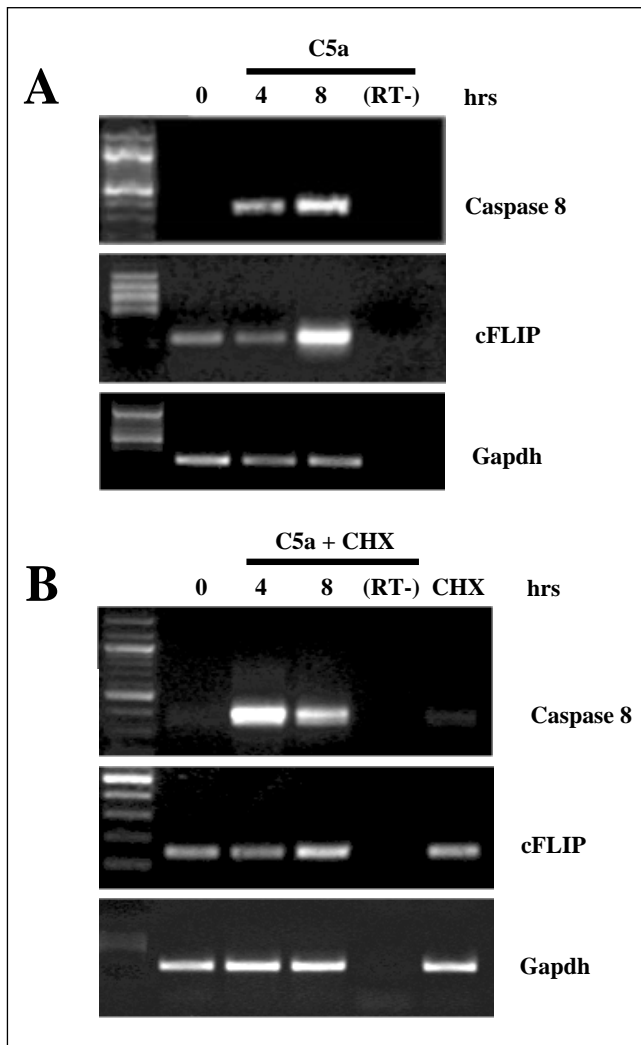


Fig 3. C5a induces increased gene expression of caspase-8 and cFLIP in HUVEC. **A)** RT-PCR of Caspase-8 and cFLIP gene expressions after 0, 4, and 8 h of stimulation by C5a (50 ng/ml). **B)** RT-PCR of Caspase-8 and cFLIP gene expressions after 0, 4, and 8 h of stimulation by C5a (50 ng/ml) with CHX (10 µg/ml). RT- samples were run under identical conditions for each time course, but without enzyme (Superscripts) for 8 h. GAPDH was used as a loading control. Data are representative of three separate experiments.

forms more closely (Fig. 4A and B). Controls included cells treated with CHX alone for 18 h and nonstimulated cells (Fig. 4A). Cell stimulation with C5a promoted a slight loss of full length cFLIP (Fig. 4B) compared to non-stimulated controls. HUVEC stimulated with C5a and CHX demonstrated a nearly total loss of cFLIP after 18 h. To monitor changes in the cytosolic levels of caspase 8, we utilized an antibody that recognizes the inactive (55 kDa) and active (p41/p43) fragments of caspase 8. HUVEC stimulated with C5a alone showed slight increase in the precursor form, correlating with increased levels of “active” p41/p43 fragments. This caspase activation complemented the AFC assay data (Fig 2B) showing increased caspase activation after 18 h of C5a and CHX stimulation. To follow the relationship between cFLIP and caspase 8 activation over time, cell lysates were

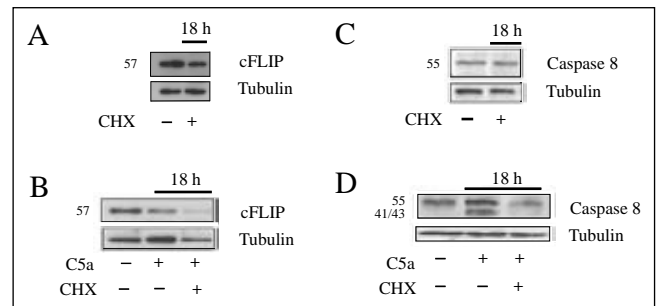


Fig 4. Western blotting of Caspase-8 and cFLIP. **A)** Cell lysates were collected 18 h following C5a (50 ng/ml) alone or in the presence of CHX (10 µg/ml). Control included non-stimulated (-) and 18 h CHX (10 µg/ml) treatment (+). The activity of cFLIP was monitored by the loss of the full length form. C5a treatment caused diminished cytosolic cFLIP levels compared to untreated controls. The combination of C5a and CHX caused cFLIP cytosolic level to be virtually undetectable **B)** Cell lysates were collected at 18 h following stimulation with C5a (50 ng/ml) alone or in the presence of CHX (10 µg/ml). Control included nonstimulated (-) and 18 h CHX (10 µg/ml) treated (+). Activation of caspase 8 was monitored by the appearance of the cleaved forms (p43/41). Data are representative of three separate experiments.

collected following 2, 8, and 18 h after stimulation with C5a (50 ng/ml). First, we utilized antibodies that recognize pro-forms (inactive) and fragmented (active) forms of caspase 8 and cFLIP, to determine if C5a stimulation co-activated both caspase 8 and cFLIP. HUVEC stimulated with C5a showed a progressive increase in the active caspase 8 fragment (p41/43 kDa) (Fig. 5). In addition, there was a clear increase in the pro-form of caspase 8, especially at 8 and 18 h. Thus, it appears, that C5a induced gene activation, (described in Figure 3A), leads to increased caspase 8 production and activation. Similarly, C5a stimulation initiated cFLIP cleavage, which increased the 43 kDa active fragment levels over time. This suggests that C5a stimulation promotes caspase 8 and cFLIP activation (cleavage) events.

Discussion

During an inflammatory response, escalating levels of pro-inflammatory mediators such as IL-1, IL-6, TNF α , and C5a interact with endothelial cells, causing robust gene activation and the initiation of apoptotic intracellular signaling. Although early classification of an apoptotic state involves increased caspase 8 activity, other indicators such as external expression of phosphatidylserine or mitochondrial damage may be used to fully characterize an apoptotic state.

Several reports have shown that endothelial cells are resilient to apoptosis induced by IL-6, LPS and TNF α unless the cells are also co-incubated with either cycloheximide or actinomycin D [29, 30, 31, 32]. But the relationship between C5a receptor ligation and the initiation of apoptotic cascades is less clear. Thus, we chose to investigate the relationship between C5a receptor ligation on endothelial cells and the activation of caspase 8 and cFLIP. HUVEC were stimulated with 50 ng/ml of C5a, based on an earlier study demonstrating that this concentration provided optimal transcription that could not be attributed to contaminating LPS [33].

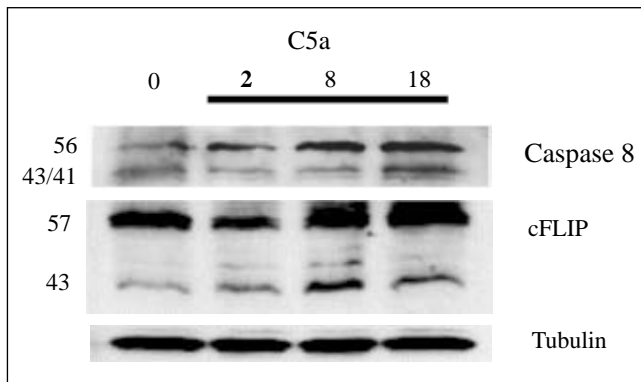


Fig 5. Western blotting of Caspase-8 and cFLIP from HUVEC lysates. Cell lysates were collected 2, 8, 18h following C5a (50ng/ml). The active fragment of caspase 8 and cFLIP increased over time.

The present study provides evidence that C5a in the presence of CHX, much like other potent inflammatory mediators, reduces cell viability. Figure 1 shows the phenotypic morphology and dose dependent relationship between cell viability and C5a concentration. After 18h, C5a in the presence of CHX caused a significant reduction in cell viability (Fig. 1A). In addition, the dose dependent relationship between C5a and cell death suggested that C5a may be activating apoptotic signaling cascades. To examine this, we assayed the activity of early and late enzymes of apoptosis (caspase 8 and PARP-1). We found endothelial cells stimulated with C5a/CHX rapidly lost full length PARP-1 after 2h, while PARP-1 level of cells stimulated with C5a alone remained unchanged (Fig. 2A), suggesting that upstream inhibition of apoptotic signaling may be occurring, but not leading to DNA damage unless anti-apoptotic mechanisms are inhibited. To determine if caspase activity was present, we stimulated the endothelial cells with C5a alone and with C5a in the presence of CHX for 18h then assay caspase 8 activity using an AFC fluorescent probe. We predicted that suppression of anti-apoptotic protein synthesis by CHX would cause elevated levels of caspase activity. Our results showed an increase in caspase activity for both C5a treated and CHX/C5a treated cells. We found the caspase 8 activity of cells stimulated with C5a alone, was higher than C5a/CHX stimulated cells. This may represent the decrease in viability indicated in figure 1, thus as cells quickly progress toward complete cell death the activities of the caspase begin to decline. In contrast, C5a alone stimulation does not induce down stream apoptotic responses and continued apoptotic progression allowing for an extended elevation of caspase activity. The CHX control (Fig. 2B) showed increase caspase activity compared to the non-stimulated control, suggesting that CHX does contribute to caspase 8 activation and can be cytotoxic to HUVEC, even at low concentrations.

Next, we wanted to determine if C5a stimulation of HUVEC induces the activation of the key upstream apoptotic modulators, caspase 8 and cFLIP. Changes in gene activation of cFLIP suggest that C5a is activating apoptotic signaling in a caspase dependent manner. More recent studies have suggested that caspase activity and their corresponding inhibitors have non death functions [34, 35]. For example,

caspase-8 has been shown to be involved in T-cell proliferation. This function appears to be dependent on the intracellular location of the active caspase 8 molecule. Thus, caspase activity resulting from endothelial C5aR ligation, may also include non-death associated functions.

We found an increase in caspase 8 for cells stimulated with C5a alone and in the presence of CHX (Fig 3). The gene expression of caspase 8 increased after 4h and continued through 8 h. Similarly, C5a and C5a /CHX elevated the gene expression of cFLIP after 8h of stimulation. The time course of gene activation show that caspase 8 and cFLIP gene expression are staggered, with changes in cFLIP activation lagging behind caspase 8. Thus, the consumption of caspase 8 and cFLIP may include signals to replace or elevate cytosolic protein levels of these apoptotic proteins. Several studies have demonstrated that endothelial cells exposed to TNF- α , or Fas-ligand initiate survival pathways involving NF- κ B and phosphatidylinositol 3-Kinase/Akt [17, 18, 19]. Each pathway has been implicated in controlling cFLIP levels, and critical for endothelial cell survival. C5a, like other inflammatory mediators, may induce similar responses in endothelial cells. Evidence for this comes from our previous study, where we found that C5a stimulated HUVEC displayed robust gene activation, including NF- κ B and NF- κ BIA [27]. Complementary to this, Schraufstatter et al., reported that C5a receptors expressed on HUVEC are capable of activating EGFR [36], which has been shown to induce NF- κ B. Thus, transactivation of EGFR by C5aR, may provide an additional route of NF- κ B signal transduction in endothelial cells.

To evaluate protein changes for caspase 8 and cFLIP, we collected cell lysates after 18h of C5a stimulation with or without CHX. The antibody utilized in Figure 4A and B recognized the full length of cFLIP, thus a loss of protein expression would indicate C5a directly or indirectly targeted cFLIP activation. We found C5a moderately reduced cFLIP protein levels after 18h. Similarly, HUVEC stimulated with C5a in the presence of CHX showed a greater loss of cytosolic full length cFLIP (Figure 4B). Although cFLIP is known to be CHX sensitive, our controls demonstrated that at CHX concentrations $\geq 10\mu\text{g/ml}$ the levels of cFLIP remain unchanged (Fig 4A).

To examine the changes in cytosolic caspase 8 protein expression we used an antibody that recognizes the inactive and active form of the proteins (Fig. 4C and D). The data suggest that stimulation with C5a alone induces moderate increases in the active form (p43/41) through the 18h time point. Changes in the levels of caspase 8 stimulated with C5a/CHX for 18h was less obvious. This pattern complemented our AFC fluorometric assay result suggesting that C5a combined with CHX causes a progressive decrease in active and inactive caspase 8. Additionally, we monitored the activation of caspase 8 and cFLIP in the presence of C5a alone. Figure 5 shows the simultaneous activation of caspase 8 and cFLIP over time. Formation of the active fragments of each molecule occurs in a progressively and also corresponds to an increase in full length caspase 8. This activity highlights the importance of cFLIP as an anti-apoptotic molecule in HUVEC during C5a stimulation.

Interestingly, C5a induces both the activation of apoptotic and anti-apoptotic signaling cascades. Other apoptosis

studies involving TNF- α follow this same pattern, where elevated caspase activity, caused anti-apoptotic signaling to be reduced by inhibiting NF- κ B [37, 38]. However, inhibiting the synthesis of new anti-apoptotic proteins such as A20, cIAP2, and TRAF1, by CHX may precede influences on gene expression.

We have previously shown in experimental sepsis that C5a induces apoptosis of thymocytes [39] and adrenal medullary cells [40]. C5a also induces dysfunction of cardiomyocytes [41], signaling paralysis in blood neutrophils [42]. Although we have not examined the status of endothelial cell apoptosis, we have previously shown that C5a reacting with endothelial cells will induce upregulation of genes related to cell adhesion molecules and cytokines/chemokines [27], which would collectively be expected to convert the endothelial cell to a proinflammatory state. In addition, we found that several proapoptotic and anti-inflammatory genes were also upregulated. In the setting of sepsis, evidence for endothelial and epithelial cell apoptosis has been reported [43]. We have shown that C5a blockade can improve burn-induced cardiac dysfunction [44] and it is possible that C5a blockade can prevent endothelial cell death during sepsis.

Collectively, this study suggests that HUVEC stimulated with C5a alone may initiate apoptotic and anti-apoptotic proteins. Previous studies have suggested that *de novo* synthesis of anti-apoptotic proteins is essential for endothelial cell survival when exposed to pro-apoptotic molecules [45, 46, 47]. Our results suggest that C5a stimulation may initiate similar events.

References

- [1] Reinhart K, Bayer O, Brunkhorst F, Meisner M. Markers of endothelial damage in organ dysfunction and sepsis. *Crit. Care Med.* 2002; 30: 302–12.
- [2] Hack C, Zeerleder S. The endothelium in sepsis: source of and a target for inflammation. *Crit. Care Med.* 2001; 29: 21–7.
- [3] Hotchkiss R, Tinsley K, Swanson P, Karl I. Endothelial cell apoptosis in sepsis. *Crit. Care Med.* 2002; 30: 225–8.
- [4] Srinivasan SR, Radhakrishnamurthy B, Vijayagopal P, Berenson GS. Proteoglycans, lipoproteins, and atherosclerosis. *Adv Exp Med Biol.* 1991; 285: 373–81.
- [5] Bäck M. Inflammatory signaling through leukotriene receptors in atherosclerosis. *Curr Atheroscler Rep.* 2008; 10(3): 244–51.
- [6] Kaplanski G, Marin V, Fabrigoule M. Thrombin-activated human endothelial cells supported monocyte adhesion in vitro following expression of intercellular adhesion molecule-1(ICAM-1;CD54) and vascular cell adhesion molecule-1 (VCAM-1; CD106). *Blood* 1998; 92: 1259–67.
- [7] Mutunga M, Fulton B, Bullock R, Batchelor A, Gascoigne A, Gillespie J, Baudouin S. Circulating endothelial cells in patients with septic shock. *Am J Respir Crit Care Med.* 2001; 163: 195–200.
- [8] Minagar A, Jy W, Jimenez J, Sheremata W, Mauro L, Mao W, et al. Elevated plasma endothelial microparticles in multiple sclerosis. *Neurology* 2001; 56: 1319–24.
- [9] Hull C, McLean G, Wong F, Duriez P, Karsan A. Lipopolysaccharide signals an endothelial apoptosis pathway through TNF receptor-associated factor 6-mediated activation of c-Jun NH₂-terminal kinase. *J Immunol.* 2002; 169: 2611–8.
- [10] Hu X, Ester Y, Harlan J, Wong F, Karsan A. Lipopolysaccharide induces the antiapoptotic molecules A1 and A20 in microvascular endothelial cells. *Blood* 1998; 92: 2758–65.
- [11] Pohlman T, Harlan J. Human endothelial cell response to lipopolysaccharide, interleukin-1, and tumor necrosis factor is regulated by protein synthesis. *Cell Immunol* 1989; 119: 41–9.
- [12] Harlan J, Harker L, Striker G, Weaver L. Effects of lipopolysaccharide on human endothelial cells in culture. *Thromb Res* 1983; 29: 15–26.
- [13] Zhou M, Simms H, Wang P. Adrenomedullin and adrenomedullin binding protein-1 attenuate vascular endothelial cell apoptosis in sepsis. *Ann Surg* 2004; 240: 321–30.
- [14] Rasper D, Vaillancourt J, Hadano S, Houtzager V, Seiden I, Keen S, et al. Cell death attenuation by ‘Ursurpin’, a mammalian DED-caspase homologue that precludes caspase 8 recruitment and inactivation by the CD-95 (Fas, APO-1) receptor complex. *Cell Death Differ* 1998; 5: 271–88.
- [15] Scaffidi C, Schmitz I, Krammer P, Peter M. The role of c-FLIP in modulation of CD95-induced apoptosis. *J Biol Chem* 1999; 274: 1541–8.
- [16] Thome M, Schneider P, Hofmann K, Fickenscher H, Meinel E, Neipel F, et al. Viral FLICE-inhibitory proteins (FLIPs) prevent apoptosis induced by death receptors. *Nature* 1997; 386: 517–21.
- [17] Bortol R, Tazzari P, Cappellini A, Tabelini G, Billi A, Baregge R, et al. Constitutively active Akt1 protects HL60 leukemia cells from TRAIL-induced apoptosis through a mechanism involving NF- κ B activation and cFLIP_L up-regulation. *Leukemia* 2003; 17: 379–89.
- [18] Okada Y, Masahiko K, Hisanori M, Yoshinari I, Akihiro Morkawa, Kunio O, Kimura H. Reduced expression of Flice-inhibitory protein (FLIP) and NF B is associated with death receptor-induced cell death in human aortic endothelial cells (HAECs). *Cytokine* 2001; 15(2): 66–74.
- [19] Suhara T, Mano T, Oliveira B, Walsh K. Phosphatidylinositol 3-kinase/Akt signaling controls endothelial cell sensitivity to fas-mediated apoptosis via regulation of FLICE-inhibitory protein (FLIP). *Circ Res* 2001; 89: 13–9.
- [20] Reidemann N, Gou R, Neff T, Laudes I, Keller K, Sarma V, et al. Increased C5a receptor expression in sepsis. *J. Clin. Invest.* 2002; 110: 101–8.
- [21] Wesche D, Lomas-Neira J, Perl M, Chung C, Ayala A. Leukocyte apoptosis and its significance in sepsis and shock. *J Leuk Biol.* 2005; 78: 325–37.
- [22] Perianayagam M, Balakrishnan V, King A, Pereira B, Jaber B. C5a delays apoptosis of human neutrophils by a phosphatidylinositol 3-kinase signaling pathway. *Kidney International* 2002; 61: 456–63.
- [23] Guo R, Sun L, Hongwei G, Shi K, Rittirsch D, Sarma V, et al. In vivo regulation of neutrophil apoptosis by C5a during sepsis. *J Leuko Biol* 2006; 80: 1575–83.
- [24] Gasque P, Singhrao S K, Neal JW, Gotze O, Morgan BP. Expression of the receptor for complement C5a (CD88) is up-regulated on reactive astrocytes, microglia, and endothelial cells in the inflamed human central nervous system. *Am. J. Pathol.* 1997; 150.
- [25] Foreman KE, Vaporciyan AA, Bonish BK, Jones ML, Johnson K J, Glovsky MM, et al. C5a-induced expression of P-selectin in endothelial cells. *J. Clin. Invest.* 1994; 94: 1147–55.
- [26] Monsinjon I, Gasque P, Chan P, Ischenko A, Brady J, Fontaine M. Regulation by complement C3a and C5a anaphylatoxins of cytokine production in human umbilical vein endothelial cells. *Faseb J* 2003; 17: 1003–14.
- [27] Albrecht E, Chinnaiyan A, Sooryanarayana V, Kumar-Sinha C, Barrette T, Sarma V, et al. C5a-induced gene expression in human umbilical vein endothelial cells. *Am J Pathol* 2004; 164: 849–59.
- [28] Bouchard V, Rouleau M, Poirier G. PARP-1, a determinant of cell survival in response to DNA damage. *Exp Hematology* 2003; 31: 446–54.
- [29] Zen H, Karsan A, Stempien-Otero A, Yee E, Tupper J, Li X, et al. NF- κ B activation is required for human endothelial survival during exposure to tumor necrosis factor- but not to interleukin-1 or lipopolysaccharide. *J Biol Chem.* 1999; 274: 28808–15.
- [30] Duriez P, Wong F, Dorovini-Zis K, Shahidi R, Karsan A. A1 Functions at the mitochondria to delay endothelial apoptosis in response to tumor necrosis factor. *J Biol Chem.* 2000; 275: 18099–107.
- [31] Eissner G, Kohlhuber F, Grell M, Ueffing M, Scheurich P, Hieke A, et al. Critical involvement of transmembrane tumor necrosis factor- in endothelial programmed cell death mediated by ionizing radiation and bacterial endotoxin. *Blood* 1995; 86: 4184–93.

- [32] Miura M, Friedlander R, Yuan J. Tumor necrosis factor-induced apoptosis is mediated by a CrmA-sensitive cell death pathway. *Proc Natl. Acad. Sci. USA* 1995; 92: 8318–22.
- [33] Schindler R, Gelfand J, Dinarello C. Recombinant C5a stimulates transcription rather than translation of interleukin-1(IL-1) and tumor necrosis factor: translational signal provided by lipopolysaccharide of IL-1 itself. *Blood* 1990; 76: 1631–8.
- [34] Malfait J, Beyaert R. Non-apoptotic functions of caspase-8. *Biochem Pharmacol.* 2008; Aug 6. [Epub ahead of print]
- [35] Koenig A, Russell JQ, Rodgers WA, Budd RC. Spatial differences in active caspase-8 defines its role in T-cell activation versus cell death. *Cell Death Differ.* 2008; Jul 11. [Epub ahead of print]
- [36] Schraufstatter IU, Trieu K, Sikora L, Sriramarao P, DiScipio R. Complement c3a and c5a induce different signal transduction cascades in endothelial cells. *J Immunol.* 2002; 169(4): 2102–10.
- [37] Irmeler, M., Martinon F, Holler N, Steiner V, Ruegg C, Wajant H, Tschoep J. Caspase-induced inactivation of the anti-apoptotic TRAF1 during Fas ligand-mediated apoptosis. *FEBS Lett.* 2000; 468: 129–33.
- [38] Levkau B, Scatena M, Giachelli C.M, Ross R, Raines E. Apoptosis overrides survival signals through a caspase-mediated dominant negative NF-kappa B loop. *Nat. Cell Biol.* 1999; 1: 227–33.
- [39] Guo, R.F., Huber-Lang, M., Wang, X., Sarma, V., Padgaonkar, V.A., Craig, R.A., Riedemann, N.C., McClintock, S.D., Hlaing, T., Shi, M.M., and Ward, P.A.: Protective effects of anti-C5a in sepsis-induced thymocyte apoptosis. *J Clin Invest.* 2000; 106: 1271–80.
- [40] Flierl, M.A., Rittirsch, D., Chen, A.J., Nadeau, B.A., Day, D.E., Sarma, J.V., Huber-Lang, M.S. and Ward, P.A. The complement anaphylatoxin C5a induces apoptosis in adrenomedullary cells during experimental sepsis. *PLoS ONE* 2008 On-Line Vol 3/issue 7/e2560.
- [41] Niederbichler, A.D., Hoesel, L.M., Westfall, M.V., Gao, H., Ipaktchi, K.R., Sun, L., Zetoune, F.S., Su, G.L., Arbabi, S., Sarma, J.V., Wang, S.C., Hemmila, M.R., and Ward, P.A.: An essential role for complement C5a in the pathogenesis of septic cardiac dysfunction. *J Experimental Medicine.* 2006; 203(1): 53–61.
- [42] Huber-Lang, M.S., Younkun, E.M., Sarma, J.V., McGuire, S.R., Lu, K.T., Guo, R.F., Padgaonkar, V.A., Curnutte, J.T., Erickson, R., and Ward, P.A.: Complement-induced impairment of innate immunity during sepsis. *J Immunol.* 2002; 169(6): 3223–31
- [43] Weche DE, Lomas-Neira JL, Perl M, Chung C-S, and Ayala A. Leukocyte apoptosis and its significance in sepsis and shock. *J. Leukoc. Biol.* 2005; 78: 325–7.
- [44] Hoesel, LM, Niederbichler AD, Schaefer J, Ipaktchi KR, Gao H, Rittirsch D, Pianko MJ, Vogt PM, Sarma JV, Su GL, Arbabi S, Westfall MV, Wang Sc, Hemmila MR and Ward PA. C5a-blockade improves burn-induced cardiac dysfunction. *J. Immunol.* 2007; 178: 7902–10
- [45] Kay J, Korner A. Effects of cycloheximide on protein and ribonucleic acid synthesis in cultured human lymphocytes. *Biochem J.* 1966; 100: 815–22.
- [46] Kreuz S, Siegmund D, Scheurich P, Wajant H. NF-kB inducers up-regulate cFLIP, a cycloheximide-sensitive inhibitor of death receptor signaling. *Mol Cell Biol.* 2001; 21: 3964–73.
- [47] Choi K, Wong F, Harlan J, Chaundhary P, Hood L, Karsan A. Lipopolysaccharide mediates endothelial apoptosis by a FADD-dependent pathway. *J Biol Chem.* 1998; 273: 20185–8.

Grant Support: NIH, GM-29507, GM-61656, HL-31963

To access this journal online:
<http://www.birkhauser.ch/IR>

Acute Lung Injury Induced by Lipopolysaccharide Is Independent of Complement Activation¹

Daniel Rittirsch,* Michael A. Flierl,* Danielle E. Day,* Brian A. Nadeau,*
Stephanie R. McGuire,* Laszlo M. Hoesel,*[†] Kyros Ipaktchi,[†] Firas S. Zetoune,*
J. Vidya Sarma,* Lin Leng,[¶] Markus S. Huber-Lang,[§] Thomas A. Neff,[‡] Richard Bucala,[¶]
and Peter A. Ward^{2*}

Although acute lung injury (ALI) is an important problem in humans, its pathogenesis is poorly understood. Airway instillation of bacterial LPS, a known complement activator, represents a frequently used model of ALI. In the present study, pathways in the immunopathogenesis of ALI were evaluated. ALI was induced in wild-type, C3^{-/-}, and C5^{-/-} mice by airway deposition of LPS. To assess the relevant inflammatory mediators, bronchoalveolar lavage fluids were evaluated by ELISA analyses and various neutralizing Abs and receptor antagonists were administered in vivo. LPS-induced ALI was neutrophil-dependent, but it was not associated with generation of C5a in the lung and was independent of C3, C5, or C5a. Instead, LPS injury was associated with robust generation of macrophage migration inhibitory factor (MIF), leukotriene B₄ (LTB₄), and high mobility group box 1 protein (HMGB1) and required engagement of receptors for both MIF and LTB₄. Neutralization of MIF or blockade of the MIF receptor and/or LTB₄ receptor resulted in protection from LPS-induced ALI. These findings indicate that the MIF and LTB₄ mediator pathways are involved in the immunopathogenesis of LPS-induced experimental ALI. Most strikingly, complement activation does not contribute to the development of ALI in the LPS model. *The Journal of Immunology*, 2008, 180: 7664–7672.

To investigate the molecular mechanisms of acute lung injury (ALI),³ which is a major problem in humans, various experimental models of ALI have been used, the most common being the endotoxin (bacterial LPS) model. In experimental ALI, the lung parenchyma is damaged by the generation and release of proteases and reactive oxygen and nitrogen species produced by activated lung macrophages and transmigrated neutrophils in the interstitial and alveolar compartments. The end results are microvascular injury and diffuse alveolar damage with intrapulmonary hemorrhage, edema, and fibrin deposition (1, 2), which are also features in patients with ALI and the acute respiratory distress syndrome (ARDS) (3, 4).

Clinical studies (5, 6) as well as experimental studies (4, 7) have suggested an important role for complement activation products in the pathophysiology of ALI/ARDS. For the full development of

injury in other experimental ALI models (e.g., intrapulmonary IgG immune complex deposition), local activation of complement is usually required (7). In particular, generation of C5a amplifies production of proinflammatory cytokines (7–10), leading to intrapulmonary accumulation and activation of neutrophils and macrophages.

However, in the LPS-induced model of ALI, it is not clear to what extent activation of the complement system contributes to the development of lung injury, even though LPS is known to be an activator of the complement system via the classical and the alternative pathways (11–13). As a so-called pathogen-associated molecular pattern, LPS is recognized by TLR4, which is up-regulated on bronchial epithelial cells and lung macrophages during LPS-induced ALI and is considered to play a crucial role in innate immune responses (14, 15). The interaction of LPS with TLR4 ultimately leads to release of proinflammatory mediators and the subsequent recruitment of leukocytes into lungs (3, 10, 14, 16, 17).

Because the role of complement activation and its contribution to the development of experimental ALI after LPS challenge is unclear, the immunopathogenesis of the LPS model of ALI was investigated for specific mediator pathways involved in events leading to lung injury. LPS-induced ALI was neutrophil-dependent and required participation of macrophage migration inhibitory factor (MIF) and leukotriene B₄ (LTB₄). Unexpectedly, the development of ALI after LPS administration was independent of complement activation.

Materials and Methods

Animals

Adult male (22–25 g) specific pathogen-free C57BL/6 mice were used in these studies. Additionally, lung injury was used in C3^{-/-} (on a C57BL/6 genetic background) (18), C5^{+/+}, and C5^{-/-} mice (congenic strains B10.D2/oSn and B10.D2/nSn, respectively) (19). All studies were done in accordance with the University of Michigan committee on the use and care of animals.

*Department of Pathology and [†]Department of Traumatology, University of Michigan Medical School, Ann Arbor, MI 48109; [‡]Department of Anesthesiology, University Hospital Zurich, Zurich, Switzerland; [§]Department of Traumatology, Hand, Plastic, and Reconstructive Surgery, University Hospital Ulm, Ulm, Germany; and [¶]Department of Medicine and Pathology, Yale University School of Medicine, The Anlyan Center, New Haven, CT 06520

Received for publication August 23, 2007. Accepted for publication April 3, 2008.

The costs of publication of this article were defrayed in part by the payment of page charges. This article must therefore be hereby marked *advertisement* in accordance with 18 U.S.C. Section 1734 solely to indicate this fact.

¹ This work was supported by National Institutes of Health Grants GM-29507 and HL-31963 (to P.A.W.), AI43210 (to R.B.), and Deutsche Forschungsgemeinschaft Grant HU 823/2-2 (to M.S.H.-L.).

² Address correspondence and reprint requests to Dr. Peter A. Ward, Department of Pathology, University of Michigan Medical School, 1301 Catherine Road, Ann Arbor, MI 48109. E-mail address: pward@umich.edu

³ Abbreviations used in this paper: ALI, acute lung injury; ARDS, acute respiratory distress syndrome; BAL, bronchoalveolar lavage; HMGB1, high mobility group box 1 protein; KC, CXCL1; LIX, LPS-induced CXC chemokine; LTB₄, leukotriene B₄; MIF, migration inhibitory factor; MPO, myeloperoxidase; WT, wild type.

Copyright © 2008 by The American Association of Immunologists, Inc. 0022-1767/08/\$2.00

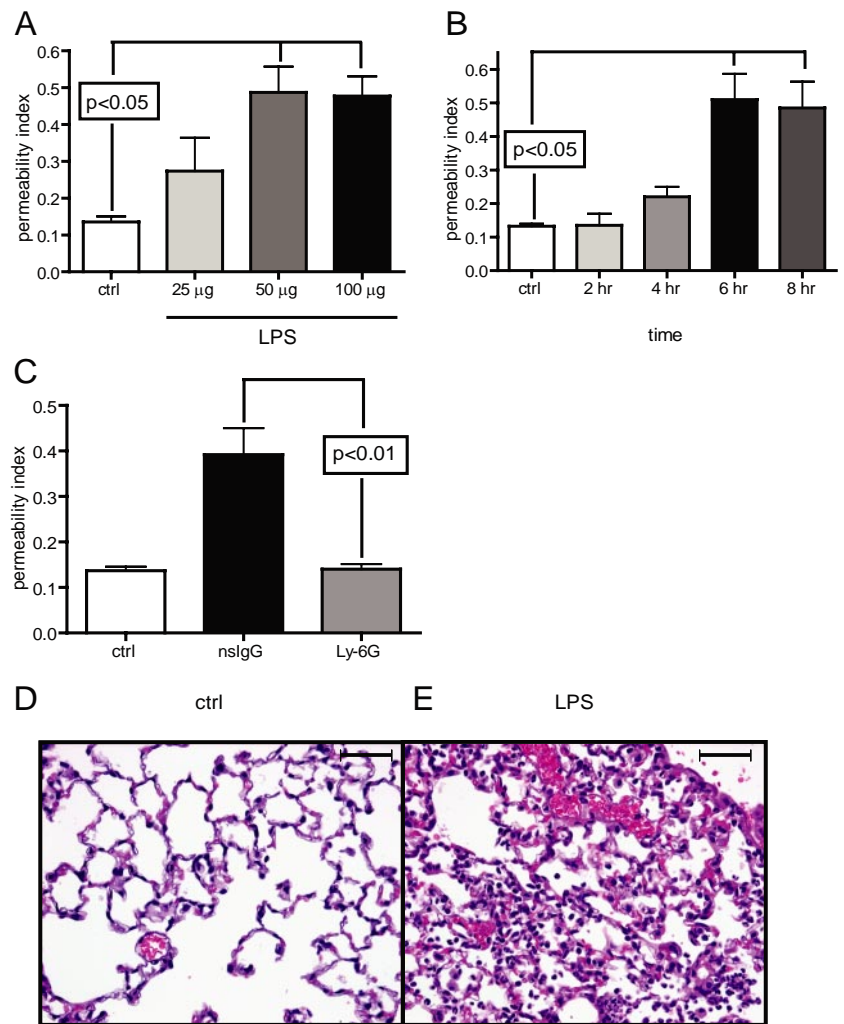


FIGURE 1. Parameters of acute lung injury as reflected by leak of ^{125}I -albumin into lung parenchyma (permeability index) as a function of the dose (25–100 μg) of LPS used (A) or as a function of time (0–8 h) after LPS administration (B). C, Effects of systemic neutrophil depletion on LPS-induced ALI. For each bar, $n \geq 5$ mice. Histologic features in control lung (D) and lungs injured by deposition of LPS (E). H&E, $\times 40$ (scale bar = 100 μm).

LPS lung injury

For LPS lung injury, unless otherwise indicated, 50 μg LPS from *Escherichia coli* (serotype O111:B4; Sigma-Aldrich) in 40 μl PBS was given intratracheally. Sham-operated animals underwent the same procedure with intratracheal injection of PBS. Permeability index as a quantitative marker for vascular leakage was determined as described elsewhere (20). For retrieval of bronchoalveolar lavage (BAL) fluids, airways were flushed with 0.8 ml PBS. If not otherwise noted, the permeability index was determined and BAL fluids were collected 6 h after lung injury induction.

Neutrophil depletion

Neutropenia was induced using monoclonal anti-mouse Ly-6G Ab (RB6–8C5; eBioscience). Control animals received injections of nonspecific ChromPure Rat IgG (nsIgG; Jackson ImmunoResearch Laboratories). Mice were given a single injection of 25 μg Ly-6G Ab or nsIgG in 100 μl of sterile saline i.v. 24 h before lung injury induction (21).

Lung myeloperoxidase (MPO) activity in lung extracts

After 6 h, mouse lungs were perfused through the right ventricle with 2 ml PBS, snap frozen in liquid nitrogen, and stored at -80°C . To measure MPO activity, whole lungs were homogenized in 50 mmol/L potassium phosphate buffer containing 0.5% hexadecyltrimethylammonium bromide and 5 mmol/L EDTA. After centrifugation at $12,000 \times g$ for 10 min at 4°C , the supernatant fluids were incubated in a 50 mmol/L potassium phosphate buffer containing the substrate, H_2O_2 (1.5 mol/L) and *o*-dianisidine dihydrochloride (167 $\mu\text{g}/\text{ml}$; Sigma-Aldrich). The enzymatic activity was determined spectrophotometrically by measuring the change in absorbance at 460 nm over 3 min (Molecular Devices) (10).

Leukocyte count in BAL fluids

Immediately after collection of BAL fluids, RBC were lysed with 1% acetic acid and total white cell count of each BAL sample was determined

using a Neubauer hemocytometer (Hauser Scientific). Cell differentials were analyzed (300 cells for each experimental condition) after cytopsin centrifugation ($500 \times g$, 3 min), methanol fixation (10 min), and Papanheim's staining.

Anti-C5a treatment

Rabbit anti-rat C5a IgG (40 μg) (22) or nonspecific rabbit IgG (40 μg) (Jackson ImmunoResearch Laboratories) was given intratracheally together with LPS.

Blockade of MIF or MIF receptor

Neutralizing mAb against mouse MIF was purified from mouse ascites fluids (ImmunoPure IgG purification kit, Pierce). Ten to 80 μg anti-MIF mAb (IgG1) or irrelevant mouse IgG1 (Jackson ImmunoResearch Laboratories) was mixed with LPS. For blockade of the MIF receptor, mice were treated with ISO-1 (35 mg/kg body weight i.p.; Calbiochem) or vehicle (aqueous 5% DMSO) 30 min before lung injury induction.

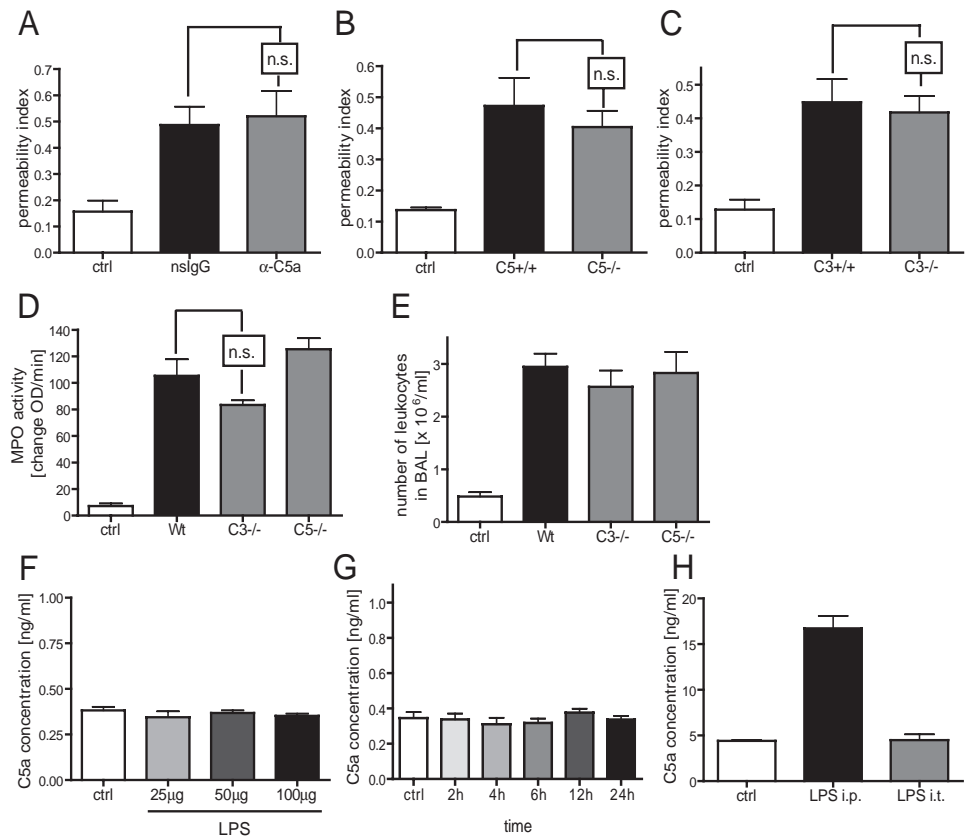
Blockade of LTB4 receptor

For in vivo blockade of the LTB4 receptor BLT1, the synthetic receptor antagonist U-75302 (BIOMOL) or vehicle (DMSO) was given intratracheally together with endotoxin (23).

ELISA for mouse C5a and C3a

To measure the concentration of mouse C5a in BAL fluids, ELISA plates were coated with purified monoclonal anti-mouse C5a IgG (BD Pharmingen, capture Ab, 5 $\mu\text{g}/\text{ml}$). After blocking, BAL fluids and recombinant mouse C5a (as standards) were applied and biotinylated monoclonal anti-mouse C5a Ab was used subsequently (BD Pharmingen, detection Ab, 500 ng/ml) followed by incubation with streptavidin-peroxidase (400 ng/ml). *O*-phenylenediamine dihydrochloride was then added, the color reaction

FIGURE 2. A, Effects of anti-C5a (40 μg IgG) administered intratracheally on ALI in the LPS model (50 μg). Lung injury induced by LPS in $\text{C5}^{-/-}$ mice (B) or $\text{C3}^{-/-}$ mice (C). Lung MPO content in WT and $\text{C3}^{-/-}$ and $\text{C5}^{-/-}$ mice (D). E, Number of leukocytes in BAL from $\text{C3}^{-/-}$ and $\text{C5}^{-/-}$ mice in comparison to WT animals with ALI. F, BAL C5a content in LPS-injured lungs as a function of dose of LPS, as measured at 6 h. G, Time-course for BAL C5a content (determined by ELISA) after airway deposition of 50 μg LPS. H, Plasma C5a levels after intraperitoneal vs intratracheal administration of LPS. For each bar, $n \geq 5$ mice.



was stopped with 3 M sulfuric acid, and the absorbance was read at 490 nm (24).

ELISA for mouse IL-6, TNF- α , LPS-induced CXC chemokine (LIX), CXCL1 (KC), MIP-2, high mobility group box 1 protein (HMGB1), MIF, and LTB4

For measurement of IL-6, TNF- α , MIP-2, LIX, and KC in BAL fluids, ELISA kits (DuoSet, R&D Systems) were used according to the manufacturer's protocol. For quantification of HMGB1 in BAL fluids, a commercially available ELISA assay (Shino-Test) was used. Measurement of MIF was done using purified rabbit anti-MIF IgG (5 $\mu\text{g}/\text{ml}$, Cell Sciences). As detection Ab, purified rabbit anti-MIF IgG was biotinylated using the EZ-link NHS-PEO solid-phase biotinylation kit (Pierce). After washing and blocking of wells, BAL fluids or standards (recombinant mouse MIF, R&D Systems) were applied in various dilutions. Biotinylated detection Ab (500 ng/ml) was added and development was performed as described above (ELISAs for C5a and C3a). LTB4 concentrations in BAL fluids were determined by using a commercially available ELISA kit (Cayman Chemical).

Statistical analysis

All values were expressed as means \pm SEM. Data sets were analyzed by one-way ANOVA followed by Tukey multiple comparison test with GraphPad Prism 4 software (GraphPad Software). Results were considered statistically significant when $p < 0.05$.

Results

Characterization of lung injury after deposition of LPS

Lung injury as defined by the permeability index (albumin leak) was studied as a function of dose of LPS, which was administered directly into the airways of mice. As shown in Fig. 1A, the dose of the inflammatory stimulus was related to an increase in the permeability index. There was no significant difference in the permeability index between the 50 μg and the 100 μg dose. In all subsequent experiments, unless otherwise indicated, the dose of LPS used was 50 μg . The injury peaked 6 h after LPS administration (Fig. 1B). In the current study we used the mAb Ly-6G to induce >95% depletion of blood neutrophils (without affecting the number of blood monocytes), as recently described (21). The permeability index rose to a level of 0.39 ± 0.06 6 h after intratracheal instillation of 50 μg LPS, as contrasted to a value of 0.14 ± 0.01 in the uninjured lungs (Fig. 1C). In neutrophil-depleted mice (Ly-6G), the permeability index remained at baseline (0.14 ± 0.01), indicating that for LPS to induce lung injury blood neutrophils must be available (Fig. 1C).

The histological patterns of ALI due to LPS are shown in Fig. 1, D and E. Fig. 1D depicts a control lung, in which PBS was

Table I. Cytokine/chemokine concentrations in BAL fluids (pg/ml)^a

Cytokine/Chemokine	Control PBS	WT LPS	$\text{C3}^{-/-}$ LPS ^b	$\text{C5}^{-/-}$ LPS ^b
IL-6	69.12 \pm 11.63	1200 \pm 161.4	1491 \pm 195.1	1797 \pm 242.2
TNF- α	396.2 \pm 41.65	5028 \pm 472.6	3763 \pm 332.2	5404 \pm 728.5
MIP-2	15.44 \pm 1.577	764.3 \pm 191.0	1124 \pm 207.5	927.9 \pm 385.1
KC	87.7 \pm 12.1	4671 \pm 1609	7583 \pm 832.1	2158 \pm 668.8
LIX	300.8 \pm 10.3	1262 \pm 73	953.9 \pm 67.84	1132 \pm 234.8

^a $n \geq 5$ for each group.

^b All values in column are not significant when compared with WT LPS data.

Table II. Mediator concentrations in BAL fluids^a

Mediator	Control PBS	LPS	Unit
HMGB1	48.4 ± 1.3	141.3 ± 22.7*	ng/ml
MIF	0.6 ± 0.2	4.6 ± 0.8*	μg/ml
LTB4	n.d.	426.2 ± 38.5*	pg/ml

^a $n \geq 5$ for each group. All p values are based on comparison to control PBS data. *, $p < 0.05$. n.d., Not detectable.

administered intratracheally. The lung was essentially normal in appearance. In Fig. 1E, LPS-induced ALI was characterized by interstitial and intraalveolar deposits of neutrophils and fibrin, prominence of alveolar macrophages, and intraalveolar hemorrhage.

Complement activation is not required in the LPS model of ALI

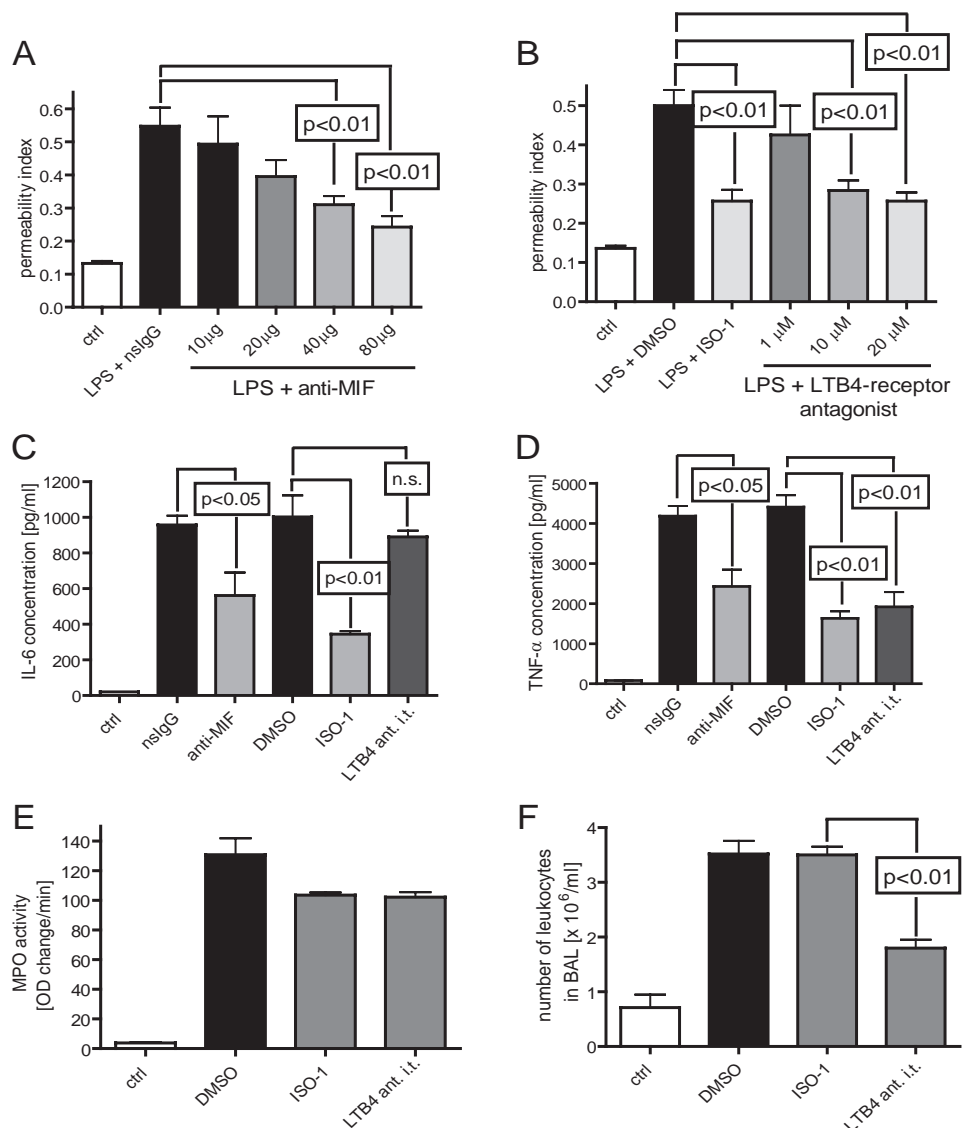
Previous studies have shown a requirement for C5 for the full expression of lung injury following deposition of IgGIC in mouse lung (24). Contrarily, in LPS-induced ALI blockade of C5a with 40 μg anti-C5a-IgG, which was given together with the LPS, did not suppress lung injury (Fig. 2A), nor was there reduced injury in the absence of C5 (Fig. 2B) or C3 (Fig. 2C). In accord, the absence

of C3 or C5 neither affected accumulation of leukocytes in lung as indicated by assessment of lung myeloperoxidase activity (Fig. 2D) nor their appearance in the alveolar space (Fig. 2E). Using a self-developed ELISA with which C5a has been detected in mouse BAL fluids (24), no increase of C5a in BAL was found as a function of the dose (25–100 μg) of LPS used (Fig. 2F) or as a function of time (0–24 h) after LPS administration (Fig. 2G). Additionally, there was no increase in C5a plasma levels after intratracheal injection of LPS, indicating that systemic complement activation in terms of a possible LPS clearance mechanism does not occur during ALI (Fig. 2H). In contrast, in wild-type mice (WT) injected i.p. with 10 μg LPS in 200 μl PBS, C5a plasma levels rose 4-fold as compared with WT mice not given LPS (Fig. 2H), indicating that the LPS used in the present study is capable of activating mouse complement if given i.p. Collectively, these data suggest that ALI following airway deposition of LPS is complement-independent.

Appearance of proinflammatory mediators in experimental ALI

The levels of proinflammatory mediators were quantitated in BAL fluids after airway deposition of LPS. The lung cytokines IL-6 and TNF-α and the chemokines MIP-2, KC, and LIX, which are chiefly derived from lung macrophages in a NF-κB-dependent fashion, are known to play important roles in ALI (25, 26). It has

FIGURE 3. A, Intensity of lung injury (measured as permeability index) in the LPS model with isotype-matched IgG1 or with anti-MIF mAb (each at 40 μg mixed with LPS). B, Effects of ISO-1 (the MIF receptor antagonist, 35 mg/kg body weight, administered i.p. 30 min before lung injury induction) or the LTB4 receptor antagonist (1–20 μM) after admixture with the intratracheally administered LPS. Effects of MIF or LTB4 blockade on the buildup of IL-6 (C) and TNF-α (D). For the interventions indicated in C and D, 40 μg neutralizing mAb to mouse MIF or 20 μM of the LTB4 receptor antagonist was mixed with the LPS; when the MIF receptor antagonist (ISO-1) was used, 35 mg/kg body weight was injected i.p. 30 min before intratracheal administration of 50 μg LPS. E, Lung MPO content in LPS-injured lungs of the LPS-treated animals of the ISO-1 (35 mg/kg body weight) or the LTB4 receptor antagonist (20 μM). F, Effects of MIF or LTB4 blockade on the total white cell count in BAL fluids. For each bar, $n \geq 5$ mice.



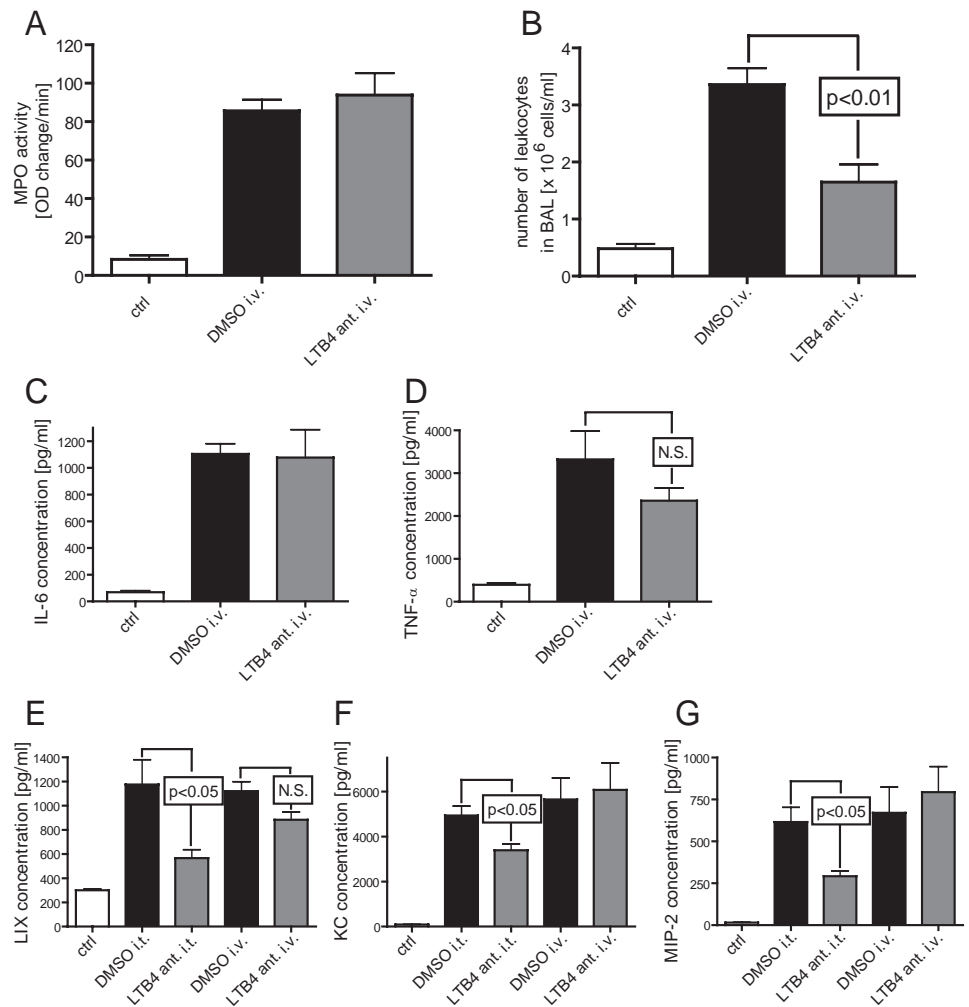


FIGURE 4. Effects of LTB4 blockade by the LTB4 antagonist when administered i.v. in comparison to intratracheal administration on lung MPO content (A) and appearance of leukocytes in BAL fluids (B). Levels of IL-6 (C) and TNF- α (D) in BAL fluids after i.v. application of the LTB4 antagonist. Concentrations of the chemoattractants LIX (E), KC (F), and MIP-2 (G) in BAL fluids after i.v. vs intratracheal administration of the LTB4 antagonist in lung injury. For each bar, $n \geq 5$ mice.

been shown that PMN recruitment is mediated by neutrophil chemoattractants such as KC, MIP-2, and LIX. In particular, PMN infiltration into lung following exposure to LPS is dependent on interaction of CXCR2 with its ligands (e.g., KC, MIP-2) (26). As shown in Table I, the cytokine/chemokine levels were substantially elevated in BAL fluids of LPS-injured lungs of WT mice. As is evident, there was no difference in cytokine/chemokine levels in BAL fluids from C3^{-/-} or C5^{-/-} mice when compared with WT mice with lung injury. Consistent with the findings described above (Fig. 2), these data support the conclusion that complement is not required for the full inflammatory response during LPS-induced ALI.

Requirements for MIF and LTB4 in the LPS model of ALI

BAL fluids from WT mice after LPS-induced lung injury were screened for the mediators HMGB1, MIF, and LTB4, which have been described to play important roles in the pulmonary inflammatory response (16, 27, 28). HMGB1, which is known to be a distal mediator in ALI and the blockade of which has shown protective effects in the LPS model (16), showed a robust increase in BAL fluids after LPS administration (Table II). MIF was also found at increased levels in BAL fluids from LPS-injured lungs as compared with the PBS controls (Table II). Finally, measurement of LTB4 in BAL fluids revealed no detectable levels in controls, but readily detectable levels of LTB4 in LPS-injured lungs (Table II), suggesting that LTB4, HMGB1, and MIF contribute to the development of LPS-induced lung injury.

Because no complement requirement could be demonstrated in the LPS model (Fig. 2) and MIF and LTB4 levels were robustly elevated in LPS-induced ALI (Table II), the possible roles of these mediators in the development of ALI were evaluated. In particular, we were interested in whether these mediators might be required for PMN recruitment, which was found to be necessary for the development of lung injury (Fig. 1C). As shown in Fig. 3, neutralization of MIF (10–80 μ g anti-MIF IgG intratracheally) reduced the index of lung injury as a function of dose (Fig. 3A), while intraperitoneal administration of the MIF receptor antagonist ISO-1 also significantly suppressed injury (Fig. 3B). When the LTB4 receptor antagonist (1–20 μ M) was administered intratracheally together with LPS, there was a dose-dependent reduction in the permeability index (Fig. 3B). We assessed how neutralization of MIF, blockade of the MIF receptor, or blockade of the LTB4 receptor (20 μ M) might affect production of IL-6 and TNF- α . In Fig. 3C, protective interventions with anti-MIF or ISO-1 reduced the BAL levels of IL-6 by 48 and 71%, respectively. In contrast, the use of the LTB4 receptor antagonist did not significantly reduce the levels of IL-6. When BAL levels of TNF- α were determined, using the same BAL samples used for IL-6 assays, similar data were obtained, except for mice treated with the LTB4 receptor antagonist in which TNF- α levels were also significantly suppressed (Fig. 3D). In summary, these data suggest that MIF and LTB4 promote production of proinflammatory cytokines during ALI induced by LPS.

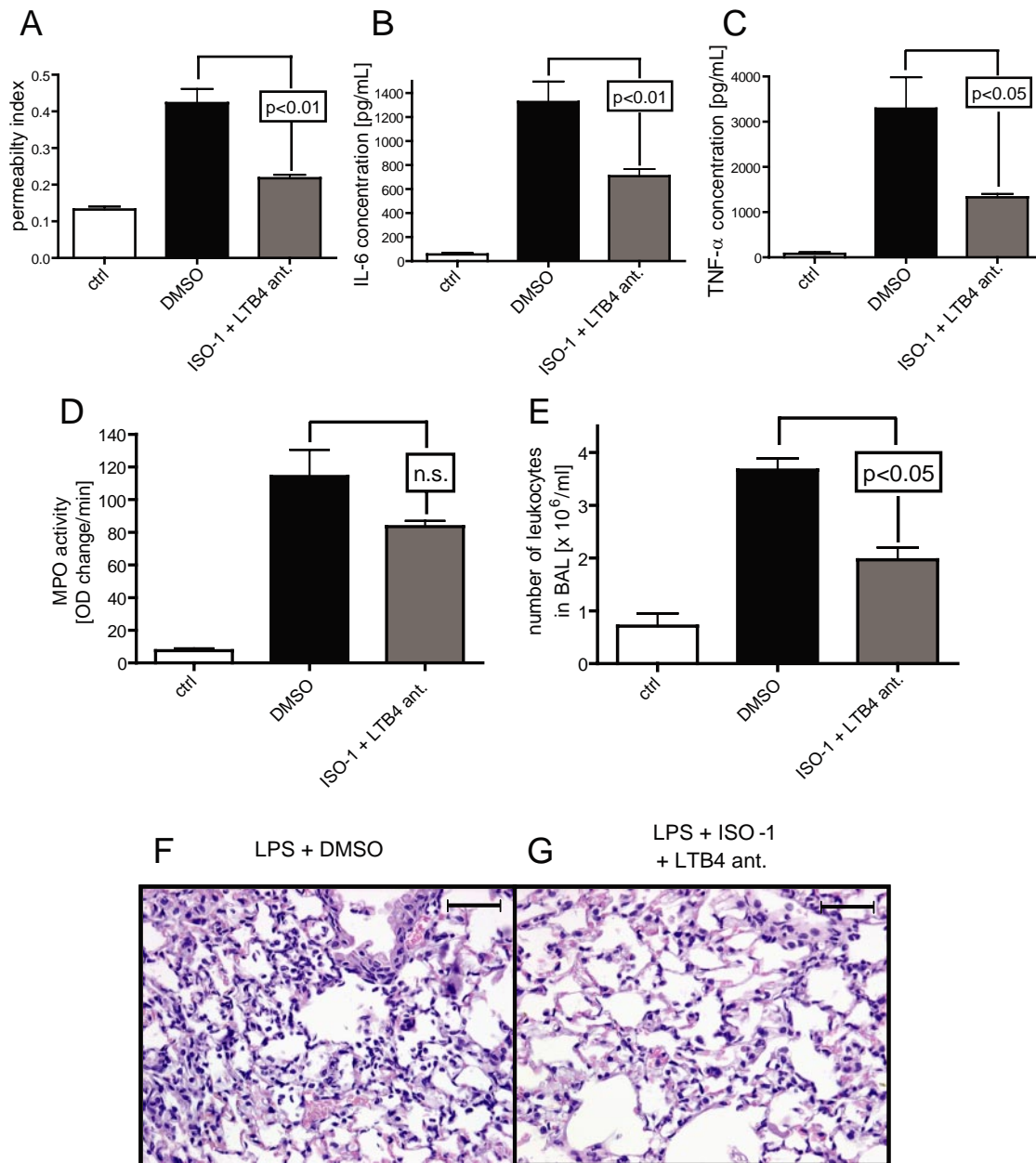


FIGURE 5. A, Effects of a dual blockade of MIF (ISO-1; 35 mg/kg body weight) and LTB4 (receptor antagonist; 20 μ M) on LPS-induced ALI. Intensity of lung injury as determined by lung permeability. Levels of proinflammatory cytokines IL-6 (B) and TNF- α (C) in the combined presence of ISO-1 and the LTB4 antagonist. D, Buildup of lung MPO after intratracheal LPS administration and ISO-1 + LTB4 antagonist. E, Total leukocyte count in BAL fluids. For each bar, $n \geq 5$ mice. Effect of the LTB4 antagonist + ISO-1 on lung histology (G) in comparison to deposition of LPS + DMSO (F). H&E, $\times 40$ (scale bar = 100 μ m).

Finally, lung MPO levels after LPS administration were assessed (Fig. 3E). When the protective interventions (ISO-1, LTB4 receptor antagonist) were used with the doses described above, minor reductions in MPO content were found, but these were not significantly different from MPO content in LPS lungs that were not otherwise manipulated. However, the number of leukocytes in BAL fluids was significantly reduced in the presence of the LTB4 antagonist, but not when ISO-1 was administered (Fig. 3F). In all groups treated with LPS, there was no difference in cell differentials, with predominantly PMNs and 10–15% macrophages (data not shown). Collectively, these data suggest that protective interventions directed at receptors for MIF or LTB4 reduce the development of ALI but do not interfere with neutrophil accumulation in lung after administration of LPS. LTB4 appears to promote

transmigration of PMNs into the alveolar space, while MIF seems to accentuate proinflammatory mediator release from macrophages and neutrophils rather than interfering with their migration.

Similar to the results displayed in Fig. 3, E and F, where the LTB4 antagonist was given intratracheally, i.v. administration of the antagonist did not alter buildup of lung MPO (Fig. 4A), but resulted in reduced numbers of leukocytes present in the airway compartment (Fig. 4B). In accord with Fig. 3C (intratracheal application), i.v. treatment with the LTB4 antagonist also did not affect the secretion of IL-6 (Fig. 4C). TNF- α levels in BAL fluids were not substantially reduced by LTB4 blockade when the antagonist was injected i.v. (Fig. 4D), although intratracheal administration significantly suppressed TNF- α production (Fig. 3D). A similar pattern was found for the chemokines LIX, KC, and MIP-2,

with the latter two being ligands for CXCR2, which is known to mediate PMN recruitment into lungs. Only intratracheal administration of the LTB4 antagonist resulted in decreased chemokine levels in BAL fluids of LPS-injured mice, whereas its i.v. application had no effect on local chemokine production (Fig. 4E–G). In summary, these data suggest that LTB4 might trigger the release of chemoattractants from alveolar macrophages rather than directly recruiting PMNs into the lung. However, leukocyte transmigration into the alveolar space seems to depend on direct interaction of LTB4 with the recruited cells because the number of leukocytes was significantly reduced, regardless of whether the LTB4 antagonist was administered via the intratracheal or the i.v. route.

Dual inhibition of LTB4 and MIF in the LPS model of ALI

When blockade of MIF was used together with inhibition of LTB4 (Fig. 5), the intensity of lung injury was reduced to an extent similar to that found when either antagonist was administered alone (70% reduction vs 67% by ISO-1 or LTB4 antagonist, respectively) (Fig. 5A). Moreover, concentrations of IL-6 (Fig. 5B) and TNF- α (Fig. 5C) in BAL fluids were significantly suppressed in the presence of ISO-1 and the LTB4 antagonist, but they were still elevated in comparison to control animals. Dual inhibition of MIF and LTB4 failed to significantly reduce the buildup of lung MPO (Fig. 5D). In contrast, as in the case of the single inhibition of LTB4 (Fig. 3F), the number of leukocytes in BAL fluids was clearly lower when the LTB4 antagonist + ISO-1 were given (Fig. 5E), but without any further accentuation of this effect by the additional blockade of MIF. These findings were underpinned by lung histology. In the presence of the LTB4 antagonist and ISO-1, the bulk of PMNs only accumulated in the lung interstitium (Fig. 5G), whereas in LPS-injured lungs without inhibitors, PMNs were also present in the alveolar compartment (Fig. 5F). Taken together, these data suggest that MIF and LTB4 promote lung injury via different mechanisms and that dual inhibition of both mediators does not result in a synergistic effect on the attenuation of inflammatory response.

Discussion

ALI and ARDS, as well as chronic obstructive pulmonary disease, represent fundamentally disordered inflammation in the lung and continue to be prevalent clinical problems (2). Despite extensive efforts in both the clinical and laboratory settings, the molecular mechanisms of these inflammatory disorders are poorly understood. LPS and related products are known to be present in BAL fluids from patients with ARDS (29). Therefore, lung injury induction by LPS in rodents represents a frequently used ALI model, mimicking many features of ALI/ARDS in humans. In this study, the LPS model was evaluated for immunopathological events leading to lung injury.

It is well established that following the intrapulmonary deposition of IgG immune complexes, generation of C5a plays an important role in the pathogenesis of ALI (7, 24). However, activation of the complement system was not required for the full development of LPS-induced lung injury suggesting that there is differential regulation of local complement activation in the lung depending on the nature of the inflammatory stimulus. In the present study, neither the blockade of C5a nor the absence of C5 or C3 influenced the intensity of lung injury in the LPS model, and no increase of BAL C5a was found after LPS administration (Fig. 2). This is in accord with an earlier report (30), but contrasts with a recent publication that describes altered complement levels and expression in LPS-induced ALI (31). However, in the latter report, only the expression of nonactivated complement proteins was presented, making it far from certain if activation of the complement

cascade actually occurred. In another conflicting report, C3 and C5b-9 deposition on the endothelium of pulmonary vessels has been reported, but complement depletion had no effect on lung MPO activity and TNF- α levels, which again raises the question of whether complement activation had effectively proceeded (32). In various studies, patients with ARDS showed evidence for complement activation, the extent of which correlated with the degree and outcome of ARDS (5, 6, 33). In contrast, in another study published some years ago, C5a could not be detected in BAL fluids from patients with ARDS using the methods available at that time (34). Although hepatic production is the main source for complement proteins, virtually all complement proteins can be locally synthesized in the lung by type II alveolar pneumocytes, alveolar macrophages, and lung fibroblasts (35, 36). However, while the total pulmonary complement protein concentration is comparable to levels found in serum, its activity in normal lung is markedly reduced due to the complement-inhibitory activity of surfactant protein A and C1 inhibitor, both being abundantly present and active in the lung (37, 38). Reduced lung activity of both surfactant protein A and C1 inhibitor can be related to the development of ARDS in humans (39, 40). In other words, pulmonary activation of the complement system underlies a complex and distinct regulation. Therefore, presence of complement proteins in the lung does not necessarily imply their local activation.

There is also diverse information regarding the role of the complement system in the setting of endotoxemia. The febrile response induced by infusion of LPS seems related to generation of C5a, and endotoxic C5^{-/-} mice had reduced evidence for organ failure when compared with C5^{+/+} mice (41, 42). In contrast, C3- and C4-deficient mice infused with LPS showed greatly increased mortality, suggesting that systemic *in vivo* clearance of LPS requires C3 and C4 (43). In line with the above-mentioned observations, in this study robust complement activation (as indicated by increased plasma levels of C5a) only occurred when LPS was injected i.p., but not when it was administered via the intratracheal route (Fig. 2F–H). These observations suggest that complement may be necessary for systemic clearance of LPS from the blood compartment *in vivo*, but not in the local setting of the lung as described in this report, where LPS failed to induce activation of the complement system. In other words, different mechanisms of endotoxin clearance might be involved that are dependent on the entry route of LPS.

Finally, although our data strongly suggest that the complement activation does not contribute in the development of ALI after LPS exposure, we were able to identify MIF and LTB4 as key mediators in the pathogenesis of LPS-induced ALI. MIF has been found in BAL fluids from humans with ARDS and may play a role in sustaining the pulmonary inflammatory response (27). In the present study we sought to evaluate the role of MIF in experimental ALI. MIF functions as a pleiotropic proinflammatory protein and plays a key role in systemic and local inflammatory responses (44). It is abundantly produced by monocytes/macrophages, can induce and enhance the production of other cytokines, and regulates apoptosis of leukocytes (44–46). Previous studies suggest the participation of MIF in neutrophil accumulation in lung after intraperitoneal injection of LPS (47). Intratracheal administration of neutralizing mAb to MIF or use of the MIF receptor antagonist ISO-1 attenuated the capillary leak and tissue damage in ALI. Blockade of MIF suppressed proinflammatory cytokine release in LPS-induced ALI, but did not interfere with PMN accumulation or their transmigration into the alveolar space. The chief effects of MIF in experimental ALI may be enhancement of the proinflammatory response (27), up-regulation of TLR4 (48), glucocorticoid antagonism (27), or a combination of all the above.

Because of its importance in the pathogenesis of airway hyper-responsiveness, the role of LTB₄ and interaction with its receptor (BLT1) in acute lung injury was evaluated (28). LTB₄ is a chemotactic factor for neutrophils and appears to be responsible for neutrophil accumulation in lung tissue during acute asthmatic exacerbation (49, 50). Additionally, LTB₄ enhances the release of active oxygen species and the respiratory burst of neutrophils via its priming effects (51, 52). In the present LPS model, LTB₄ levels in BAL fluids were substantially elevated when compared with noninjured lungs. Furthermore, blockade of the LTB₄ receptor BLT1 strikingly reduced lung injury. Interestingly, these protective effects in the LPS model were not linked to altered accumulation of neutrophils based on lung MPO content, which does not distinguish between interstitial and intraalveolar PMNs. However, the transmigration of PMNs from the interstitium to the airway compartment seems to be LTB₄-dependent (Figs. 3 and 4). These findings are consistent with previous studies describing that intratracheal instillation of LTB₄, which is also a major product of alveolar macrophages, can recruit active PMNs into airspace (53, 54). Although the precise mechanisms involved are largely unknown, reactive oxygen species and the expression of neutrophil elastase seem to be involved in the regulation of transepithelial migration of PMNs into the alveolar compartment in response to LTB₄ (54, 55).

In summary, the immunopathogenesis of LPS-induced ALI underlies a complex regulation regarding mediators and pathways involved in neutrophil mobilization and priming. Most strikingly, LPS-induced ALI is independent of activation of the complement system and, instead, is orchestrated by MIF and LTB₄.

Acknowledgments

We thank Beverly Schumann and Sue Scott for excellent secretarial assistance in preparation of the manuscript.

Disclosures

The authors have no financial conflicts of interest.

References

- Johnson, K. J., and P. A. Ward. 1974. Acute immunologic pulmonary alveolitis. *J. Clin. Invest.* 54: 349–357.
- Flierl, M. A., D. Rittirsch, L. M. Hoesel, H. Gao, M. Huber-Lang, and P. A. Ward. 2006. Acute lung injury: a challenging transfer from bench to bedside. *Med. Hypothesis Res.* 3: 727–738.
- Kabir, K., J. P. Gelinak, M. Chen, D. Chen, D. Zhang, X. Luo, J. H. Yang, D. Carter, and R. Rabinovici. 2002. Characterization of a murine model of endotoxin-induced acute lung injury. *Shock* 17: 300–303.
- Ward, P. A. 1996. Rous-Whipple Award lecture: role of complement in lung inflammatory injury. *Am. J. Pathol.* 149: 1081–1086.
- Hammerschmidt, D. E., L. J. Weaver, L. D. Hudson, P. R. Craddock, and H. S. Jacob. 1980. Association of complement activation and elevated plasma C5a with adult respiratory distress syndrome: pathophysiological relevance and possible prognostic value. *Lancet* 1: 947–949.
- Solomkin, J. S., L. A. Cotta, P. S. Satoh, J. M. Hurst, and R. D. Nelson. 1985. Complement activation and clearance in acute illness and injury: evidence for C5a as a cell-directed mediator of the adult respiratory distress syndrome in man. *Surgery* 97: 668–678.
- Mulligan, M. S., E. Schmid, B. Beck-Schimmer, G. O. Till, H. P. Friedl, R. B. Brauer, T. E. Hugli, M. Miyasaka, R. L. Warner, K. J. Johnson, and P. A. Ward. 1996. Requirement and role of C5a in acute lung inflammatory injury in rats. *J. Clin. Invest.* 98: 503–512.
- Warren, J. S., K. R. Yabroff, D. G. Remick, S. L. Kunkel, S. W. Chensue, R. G. Kunkel, K. J. Johnson, and P. A. Ward. 1989. Tumor necrosis factor participates in the pathogenesis of acute immune complex alveolitis in the rat. *J. Clin. Invest.* 84: 1873–1882.
- Shanley, T. P., J. L. Foreback, D. G. Remick, T. R. Ulich, S. L. Kunkel, and P. A. Ward. 1997. Regulatory effects of interleukin-6 in immunoglobulin G immune-complex-induced lung injury. *Am. J. Pathol.* 151: 193–203.
- Speyer, C. L., H. Gao, N. J. Rancilio, T. A. Neff, G. B. Huffnagle, J. V. Sarma, and P. A. Ward. 2004. Novel chemokine responsiveness and mobilization of neutrophils during sepsis. *Am. J. Pathol.* 165: 2187–2196.
- Oishi, K., N. L. Koles, G. Guelde, and M. Pollack. 1992. Antibacterial and protective properties of monoclonal antibodies reactive with *Escherichia coli* O111:B4 lipopolysaccharide: relation to antibody isotype and complement-fixing activity. *J. Infect. Dis.* 165: 34–45.
- Mintz, C. S., D. R. Schultz, P. I. Arnold, and W. Johnson. 1992. *Legionella pneumophila* lipopolysaccharide activates the classical complement pathway. *Infect. Immun.* 60: 2769–2776.
- Vukajlovich, S. W., J. Hoffman, and D. C. Morrison. 1987. Activation of human serum complement by bacterial lipopolysaccharides: structural requirements for antibody independent activation of the classical and alternative pathways. *Mol. Immunol.* 24: 319–331.
- Medzhitov, R., and C. Janeway, Jr. 2000. Innate immune recognition: mechanisms and pathways. *Immunol. Rev.* 173: 89–97.
- Saito, T., T. Yamamoto, T. Kazawa, H. Gejyo, and M. Naito. 2005. Expression of Toll-like receptor 2 and 4 in lipopolysaccharide-induced lung injury in mouse. *Cell Tissue Res.* 321: 75–88.
- Abraham, E., J. Arcaroli, A. Carmody, H. Wang, and K. J. Tracey. 2000. HMG-1 as a mediator of acute lung inflammation. *J. Immunol.* 165: 2950–2954.
- Reutershan, J., A. Basit, E. V. Galkina, and K. Ley. 2005. Sequential recruitment of neutrophils into lung and bronchoalveolar lavage fluid in LPS-induced acute lung injury. *Am. J. Physiol.* 289: L807–L815.
- Circolo, A., G. Garnier, W. Fukuda, X. Wang, T. Hidvegi, A. J. Szalai, D. E. Briles, J. E. Volanakis, R. A. Wetsel, and H. R. Colten. 1999. Genetic disruption of the murine complement C3 promoter region generates deficient mice with extrahepatic expression of C3 mRNA. *Immunopharmacology* 42: 135–149.
- Wheat, W. H., R. Wetsel, A. Falus, B. F. Tack, and R. C. Strunk. 1987. The fifth component of complement (C5) in the mouse: analysis of the molecular basis for deficiency. *J. Exp. Med.* 165: 1442–1447.
- Neff, T. A., R. F. Guo, S. B. Neff, J. V. Sarma, C. L. Speyer, H. Gao, K. D. Bernacki, M. Huber-Lang, S. McGuire, L. M. Hoesel, et al. 2005. Relationship of acute lung inflammatory injury to Fas/FasL system. *Am. J. Pathol.* 166: 685–694.
- Hoesel, L. M., T. A. Neff, S. B. Neff, J. G. Younger, E. W. Olle, H. Gao, M. J. Pianko, K. D. Bernacki, J. V. Sarma, and P. A. Ward. 2005. Harmful and protective roles of neutrophils in sepsis. *Shock* 24: 40–47.
- Huber-Lang, M. S., J. V. Sarma, S. R. McGuire, K. T. Lu, R. F. Guo, V. A. Padgaonkar, E. M. Younkin, I. J. Laudes, N. C. Riedemann, J. G. Younger, and P. A. Ward. 2001. Protective effects of anti-C5a peptide antibodies in experimental sepsis. *FASEB J.* 15: 568–570.
- Noiri, E., T. Yokomizo, A. Nakao, T. Izumi, T. Fujita, S. Kimura, and T. Shimizu. 2000. An in vivo approach showing the chemotactic activity of leukotriene B(4) in acute renal ischemic-reperfusion injury. *Proc. Natl. Acad. Sci. USA* 97: 823–828.
- Huber-Lang, M., J. V. Sarma, F. S. Zetoune, D. Rittirsch, T. A. Neff, S. R. McGuire, J. D. Lambris, R. L. Warner, M. A. Flierl, L. M. Hoesel, et al. 2006. Generation of C5a in the absence of C3: a new complement activation pathway. *Nat. Med.* 12: 682–687.
- Kelley, J. 1990. Cytokines of the lung. *Am. Rev. Respir. Dis.* 141: 765–788.
- Reutershan, J., M. A. Morris, T. L. Burcin, D. F. Smith, D. Chang, M. S. Saprito, and K. Ley. 2006. Critical role of endothelial CXCR2 in LPS-induced neutrophil migration into the lung. *J. Clin. Invest.* 116: 695–702.
- Donnelly, S. C., C. Haslett, P. T. Reid, I. S. Grant, W. A. Wallace, C. N. Metz, L. J. Bruce, and R. Bucala. 1997. Regulatory role for macrophage migration inhibitory factor in acute respiratory distress syndrome. *Nat. Med.* 3: 320–323.
- Miyahara, N., S. Miyahara, K. Takeda, and E. W. Gelfand. 2006. Role of the LTB₄/BLT1 pathway in allergen-induced airway hyperresponsiveness and inflammation. *Allergol. Int.* 55: 91–97.
- Martin, T. R., G. D. Rubinfeld, J. T. Ruzinski, R. B. Goodman, K. P. Steinberg, D. J. Leturcq, A. M. Moriarty, G. Raghur, R. P. Baughman, and L. D. Hudson. 1997. Relationship between soluble CD14, lipopolysaccharide binding protein, and the alveolar inflammatory response in patients with acute respiratory distress syndrome. *Am. J. Respir. Crit. Care Med.* 155: 937–944.
- Burrell, R., R. C. Lantz, and D. E. Hinton. 1988. Mediators of pulmonary injury induced by inhalation of bacterial endotoxin. *Am. Rev. Respir. Dis.* 137: 100–105.
- Bolger, M. S., D. S. Ross, H. Jiang, M. M. Frank, A. J. Ghio, D. A. Schwartz, and J. R. Wright. 2007. Complement levels and activity in the normal and LPS-injured lung. *Am. J. Physiol.* 292: L748–L759.
- Rabinovici, R., C. G. Yeh, L. M. Hillebrand, D. E. Griswold, M. J. DiMartino, J. Vernick, K. L. Fong, and G. Feuerstein. 1992. Role of complement in endotoxin/platelet-activating factor-induced lung injury. *J. Immunol.* 149: 1744–1750.
- Pittet, J. F., R. C. Mackersie, T. R. Martin, and M. A. Matthay. 1997. Biological markers of acute lung injury: prognostic and pathogenetic significance. *Am. J. Respir. Crit. Care Med.* 155: 1187–1205.
- Parsons, P. E., A. A. Fowler, T. M. Hyers, and P. M. Henson. 1985. Chemotactic activity in bronchoalveolar lavage fluid from patients with adult respiratory distress syndrome. *Am. Rev. Respir. Dis.* 132: 490–493.
- Hetland, G., E. Johnson, and U. Aasebo. 1986. Human alveolar macrophages synthesize the functional alternative pathway of complement and active C5 and C9 in vitro. *Scand. J. Immunol.* 24: 603–608.
- Strunk, R. C., D. M. Eidlen, and R. J. Mason. 1988. Pulmonary alveolar type II epithelial cells synthesize and secrete proteins of the classical and alternative complement pathways. *J. Clin. Invest.* 81: 1419–1426.
- Watford, W. T., J. R. Wright, C. G. Hester, H. Jiang, and M. M. Frank. 2001. Surfactant protein A regulates complement activation. *J. Immunol.* 167: 6593–6600.
- Watford, W. T., A. J. Ghio, and J. R. Wright. 2000. Complement-mediated host defense in the lung. *Am. J. Physiol.* 279: L790–L798.

39. Seeger, W., A. Gunther, H. D. Walmrath, F. Grimminger, and H. G. Lasch. 1993. Alveolar surfactant and adult respiratory distress syndrome: pathogenetic role and therapeutic prospects. *Clin. Invest.* 71: 177–190.
40. Carvalho, A. C., S. DeMarinis, C. F. Scott, L. D. Silver, A. H. Schmaier, and R. W. Colman. 1988. Activation of the contact system of plasma proteolysis in the adult respiratory distress syndrome. *J. Lab. Clin. Med.* 112: 270–277.
41. Li, S., S. A. Boackle, V. M. Holers, J. D. Lambris, and C. M. Blatteis. 2005. Complement component C5a is integral to the febrile response of mice to lipopolysaccharide. *Neuroimmunomodulation* 12: 67–80.
42. Barton, P. A., and J. S. Warren. 1993. Complement component C5 modulates the systemic tumor necrosis factor response in murine endotoxin shock. *Infect. Immun.* 61: 1474–1481.
43. Fischer, M. B., A. P. Prodeus, A. Nicholson-Weller, M. Ma, J. Murrow, R. R. Reid, H. B. Warren, A. L. Lage, F. D. Moore, Jr., F. S. Rosen, and M. C. Carroll. 1997. Increased susceptibility to endotoxin shock in complement C3- and C4-deficient mice is corrected by C1 inhibitor replacement. *J. Immunol.* 159: 976–982.
44. Nishihira, J. 2000. Macrophage migration inhibitory factor (MIF): its essential role in the immune system and cell growth. *J. Interferon Cytokine Res.* 20: 751–762.
45. Leng, L., and R. Bucala. 2005. Macrophage migration inhibitory factor. *Crit. Care Med.* 33: S475–S477.
46. Kudrin, A., M. Scott, S. Martin, C. W. Chung, R. Donn, A. McMaster, S. Ellison, D. Ray, K. Ray, and M. Binks. 2006. Human macrophage migration inhibitory factor: a proven immunomodulatory cytokine? *J. Biol. Chem.* 281: 29641–29651.
47. Makita, H., M. Nishimura, K. Miyamoto, T. Nakano, Y. Tanino, J. Hirokawa, J. Nishihira, and Y. Kawakami. 1998. Effect of anti-macrophage migration inhibitory factor antibody on lipopolysaccharide-induced pulmonary neutrophil accumulation. *Am. J. Respir. Crit. Care Med.* 158: 573–579.
48. Roger, T., J. David, M. P. Glauser, and T. Calandra. 2001. MIF regulates innate immune responses through modulation of Toll-like receptor 4. *Nature* 414: 920–924.
49. Rae, S. A., and M. J. Smith. 1981. The stimulation of lysosomal enzyme secretion from human polymorphonuclear leucocytes by leukotriene B₄. *J. Pharm. Pharmacol.* 33: 616–617.
50. Lamblin, C., P. Gosset, I. Tillie-Leblond, F. Saulnier, C. H. Marquette, B. Wallaert, and A. B. Tonnel. 1998. Bronchial neutrophilia in patients with noninfectious status asthmaticus. *Am. J. Respir. Crit. Care Med.* 157: 394–402.
51. Suda, N., I. Morita, T. Kuroda, and S. Murota. 1992. Priming effects of leukotriene B₄ on endothelial cell injury induced by TPA-activated leukocytes. *Inflammation* 16: 307–314.
52. Sibelius, U., K. Hattar, S. Hoffmann, K. Mayer, U. Grandel, A. Schenkel, W. Seeger, and F. Grimminger. 2002. Distinct pathways of lipopolysaccharide priming of human neutrophil respiratory burst: role of lipid mediator synthesis and sensitivity to interleukin-10. *Crit. Care Med.* 30: 2306–2312.
53. Martin, T. R., B. P. Pistoresse, E. Y. Chi, R. B. Goodman, and M. A. Matthay. 1989. Effects of leukotriene B₄ in the human lung: recruitment of neutrophils into the alveolar spaces without a change in protein permeability. *J. Clin. Invest.* 84: 1609–1619.
54. Woo, C. H., M. H. Yoo, H. J. You, S. H. Cho, Y. C. Mun, C. M. Seong, and J. H. Kim. 2003. Transepithelial migration of neutrophils in response to leukotriene B₄ is mediated by a reactive oxygen species-extracellular signal-regulated kinase-linked cascade. *J. Immunol.* 170: 6273–6279.
55. Young, R. E., M. B. Voisin, S. Wang, J. Dangerfield, and S. Nourshargh. 2007. Role of neutrophil elastase in LTB₄-induced neutrophil transmigration in vivo assessed with a specific inhibitor and neutrophil elastase deficient mice. *Br. J. Pharmacol.* 151: 628–637.

Attenuation of half sulfur mustard gas-induced acute lung injury in rats

Shannon D. McClintock,¹ Laszlo M. Hoesel,¹ Salil K. Das,² Gerd O. Till,¹ Thomas Neff,¹ Robin G. Kunkel,¹ Milton G. Smith¹ and Peter A. Ward^{1,*}

¹ The University of Michigan Medical School, Department of Pathology, Ann Arbor, MI 48109, USA

² Meharry Medical School, Department of Biochemistry, Nashville, TN, USA

³ Amaox, Ltd, Paw Paw, MI 49079, USA

Received 12 January 2005; Revised 29 June 2005; Accepted 9 August 2005

ABSTRACT: Airway instillation into rats of 2-chloroethyl ethyl sulfide (CEES), the half molecule of sulfur mustard compound, results in acute lung injury, as measured by the leak of plasma albumin into the lung. Morphologically, early changes in the lung include alveolar hemorrhage and fibrin deposition and the influx of neutrophils. Following lung contact with CEES, progressive accumulation of collagen occurred in the lung, followed by parenchymal collapse. The co-instillation with CEES of liposomes containing pegylated (PEG)-catalase (CAT), PEG-superoxide dismutase (SOD), or the combination, greatly attenuated the development of lung injury. Likewise, the co-instillation of liposomes containing the reducing agents, N-acetylcysteine (NAC), glutathione (GSH), or resveratrol (RES), significantly reduced acute lung injury. The combination of complement depletion and airway instillation of liposomes containing anti-oxidant compounds maximally attenuated CEES-induced lung injury by nearly 80%. Delayed airway instillation of anti-oxidant-containing liposomes (containing NAC or GSH, or the combination) significantly diminished lung injury even when instillation was delayed as long as 1 h after lung exposure to CEES. These data indicate that CEES-induced injury of rat lungs can be substantially diminished by the presence of reducing agents or anti-oxidant enzymes delivered via liposomes. Copyright © 2005 John Wiley & Sons, Ltd.

KEY WORDS: CEES; anti-oxidant liposomes; neutrophils; fibrosis; macrophages

Introduction

As is well known, mustard gas [bis (2-chloroethyl ethyl) sulfide], also known as sulfur mustard (HD), has long been known to be a vesicant in humans and, when inhaled, causes extreme lung damaging reactions (Eisenmenger *et al.*, 1991; Khateri *et al.*, 2003; Lakshmana Rao *et al.*, 1999). In human survivors, progressive lung dysfunction due to pulmonary fibrosis is well documented (Emad and Rezaian, 1999). Not unexpectedly, HD is radiomimetic, teratogenic and mutagenic (Angelov *et al.*, 1996; Dube *et al.*, 1998). Currently, there is no effective therapy for either the vesicant-inducing properties of HD or for the outcomes that can lead to acute and progressive lung injury and death.

2-Chloroethyl ethyl sulfide (CEES) is less toxic than HD and can be used in the absence of facilities required for HD studies. In rats CEES has been shown

to induce acute lung injury in a dose-dependent and time-dependent manner (McClintock *et al.*, 2002). CEES-induced acute lung injury is complement- and neutrophil-dependent, suggesting that some of the CEES-induced injury is due to engagement of the inflammatory response in lung in an unknown manner (McClintock *et al.*, 2002). Furthermore, lung injury is attenuated after intravenous treatment with the anti-oxidant, N-acetylcysteine (NAC), or airway delivery of anti-oxidants or anti-oxidant enzymes (McClintock *et al.*, 2002). These data have suggested that CEES compromises the redox potential in the lung, putting it at risk of oxidant-mediated injury.

Liposomal delivery of drugs or chemical compounds is a way to achieve high tissue levels of a desired compound (Fan *et al.*, 2000; Freeman *et al.*, 1985; Suntres and Shek, 1996). In the lung, airway delivery of liposomes results in macrophage uptake of liposomes by a phagocytic pathway (Gonzalez-Rothi *et al.*, 1991; Shephard *et al.*, 1981; Sone *et al.*, 1980). As far as is known, liposomes are not internalized by any other lung cells. The current studies demonstrated that liposomes containing anti-oxidants or anti-oxidant enzymes cause a reduction in acute lung injury in rats following airway delivery of CEES. Furthermore, delivery of such liposomes, when delayed 1 h after CEES administration, still provides significant attenuation of acute lung injury.

* Correspondence to: Dr Peter A. Ward, The University of Michigan Medical School, Department of Pathology, 1301 Catherine Rd, Ann Arbor, MI 48109, USA.

E-mail: pward@umich.edu

Contract/grant sponsor: USAMRMC DAMD; Contract/grant number: 17-03-2-0054.

These findings may have important therapeutic implications for HD-induced acute lung injury in humans.

Materials and Methods

Chemicals

Except where noted, all chemicals and reagents were purchased from the Sigma Chemical Co. (St Louis, MO).

Animal Model

Adult male (275–325 g) specific pathogen-free Long-Evans rats (Harlan Co., Indianapolis, IN) were used in these studies. Intraperitoneal ketamine (100 mg kg⁻¹ body weight) (Fort Dodge Animal Health, Fort Dodge, IA) was used for anesthesia and intraperitoneal xylazine (13 mg kg⁻¹ body weight) (Bayer Corp. Shawnee Mission, KS) was used for sedation when required (delayed time point liposome administration). The experimental procedure for CEES-induced lung injury in rats has been described previously (McClintock *et al.*, 2002). Briefly, after induction of anesthesia, ¹²⁵I-labeled bovine serum albumin (¹²⁵I-BSA, 0.5 μ Ci per rat) was injected intravenously as a quantitative marker for vascular leakage. The trachea was then surgically exposed and a slightly curved P50 catheter was inserted into the trachea past the bifurcation so as to facilitate a unilateral, left-lung injury. A small volume of CEES (2 μ l per rat; about 6 mg kg⁻¹) was solubilized in ethanol (58 μ l per rat) and then added to a syringe containing Dulbecco's phosphate buffered saline (DPBS) (340 μ l per rat). This solution was injected via the intratracheal catheter, into the left lung main stem bronchus. Studies, not requiring the usage of a radio-labeled marker, proceeded identically substituting DPBS for the radioactive injection. For all studies, except the time response experiment, animals were killed 4 h later, the pulmonary arterial circulation was flushed with 10 ml of cold DPBS, the lungs were surgically dissected, placed in counting vessels, and the amount of radioactivity (¹²⁵I-labeled BSA) determined by gamma counting. For calculations of the permeability index, the amount of radioactivity (¹²⁵I-labeled BSA) remaining in the lungs in which the vasculature was perfused with saline was divided by the amount of radioactivity present in 1.0 ml of blood obtained from the inferior vena cava at the time of killing as described elsewhere (McClintock *et al.*, 2002). ¹²⁵I-BSA present in the lung after thorough flushing of the vasculature is a quantitative measure of the degree of vascular endothelial and alveolar epithelial damage, in which much of the ¹²⁵I-BSA can be lavaged from the distal airway compartment, indicating the loss of the vascular and epithelial barriers (Johnson and Ward, 1974).

All animal experiments were in accordance with the standards in The Guide for the Care and Use of Laboratory Animals, and were supervised by veterinarians from the Unit for Laboratory and Animal Care of the University of Michigan Medical School.

Complement Depletion

Cobra venom factor (CVF) was purified from crude, lyophilized cobra venom (*Naja atra*) by ion exchange chromatography (Ballow and Cochrane, 1969). Complement depletion of experimental animals was achieved by intraperitoneal injections of 25 units of CVF per rat at time zero and 24 h later, resulting in undetectable levels of serum hemolytic complement activity as confirmed by CH50 assay (Mayer, 1961). Experiments were performed 24 h after the second CVF injection.

Liposome Preparation

Dipalmitoylphosphatidylcholine (DPPC, Avanti Polar Lipids) was dissolved 20 mg ml⁻¹ in a 2 : 1 v/v chloroform/methanol solution. When α -tocopherol (α T) was also included in the liposomes, it was added just after the chloroform/methanol solvent to provide a 7 : 3 molar ratio (DPPC : α -T) after first being carefully dissolved in a small volume of ethanol. The DPPC or (DPPC : α -T) solution was then dried under a thin stream of nitrogen in a round bottom flask to form a thin lipid film on the walls of the tube. Once the film had been dried, the tube was then placed on a vacuum for at least 1 h to further dry and remove any excess organic compounds from the lipid film.

The compounds being encapsulated in the liposomes were exclusively prepared in Dulbecco's phosphate buffered saline (DPBS), pH adjusted to 7.4 and then added to the lipid film. The tube was then vortexed to free the lipid film from the walls of the tube, and then placed in a heated water bath (41 °C). When sizing the liposomes, it is necessary to keep them at a temperature above their transition phase. The transition phase temperature for DPPC is 41 °C. Vortexing the liposomes once they are above the transition phase temperature results in large multilamellar vesicles. To reduce the size of the vesicles and to produce uniform small unilamellar vesicles, the lipid suspension was then passed ten times through polycarbonate membrane filters in a Liposofast Basic mini extruder available from Avestin, Inc. (Ottawa, Ontario). The resulting liposomes were uniform in size measuring 100 nm in diameter. According to the manufacturer, the use of an extruder is an efficient method for producing liposomes that are of relatively uniform size. Liposomes were checked via light microscopy for uniformity and size. Liposomes were injected intratracheally in a volume

of 100 μ l per rat through the same catheter setup used for CEES instillation at the time point designated by each individual experimental protocol.

Morphological Assessment of Lung Injury

In order morphologically to assess lung injury, lungs were fixed by intratracheal instillation of 10 ml buffered (pH 7.2) formalin (10%) at the indicated time points following airway instillation of CEES. Lung sections were then obtained for histological examination by staining with hematoxylin and eosin. In addition, lung sections were stained with trichrome in order to assess the deposition of fibrin and collagen (Luna, 1968).

Statistical Analysis

The results are presented as mean \pm SEM in the text and figures. Groups ($n \geq 5$) were subjected to one-way analysis of variance and when significance was found, Student's *t*-test with the Bonferroni correction for multiple comparisons was applied. A value of $P < 0.05$ was considered significant.

Results

Histopathologic Features of Lung Response to CEES

Following airway instillation of CEES into rat lungs, tissues were obtained at 0, 6, 12 and 24 h as well 3 and 6 days and 6 weeks after exposure to CEES. Lung sections were stained with trichrome stain to evaluate lung deposition of fibrin and collagen. Composite results are shown in Fig. 1 (frames A–I). At time 0, trichrome stains revealed the usual perivascular and septal evidence of collagen (frames A, B). As early as 6 h, increased evidence of trichrome stained deposition in alveolar walls was likely related to fibrin deposition (frame C). By 24 h after lung instillation of CEES, dense interstitial and intra-alveolar accumulations of trichrome positive (blue dye) were evident throughout the affected lungs, suggestive of increased deposition of fibrin and collagen fibers (frame D). Intra-alveolar hemorrhage, edema and intra-alveolar accumulation of macrophages and mononuclear cells were found at 24 h (frame E). By 3 days, dense interstitial deposits of fibrin and collagen occurred (frame F). By day 6, extensive confluent collagen deposits were found in the lung, together with a collapse of alveolar

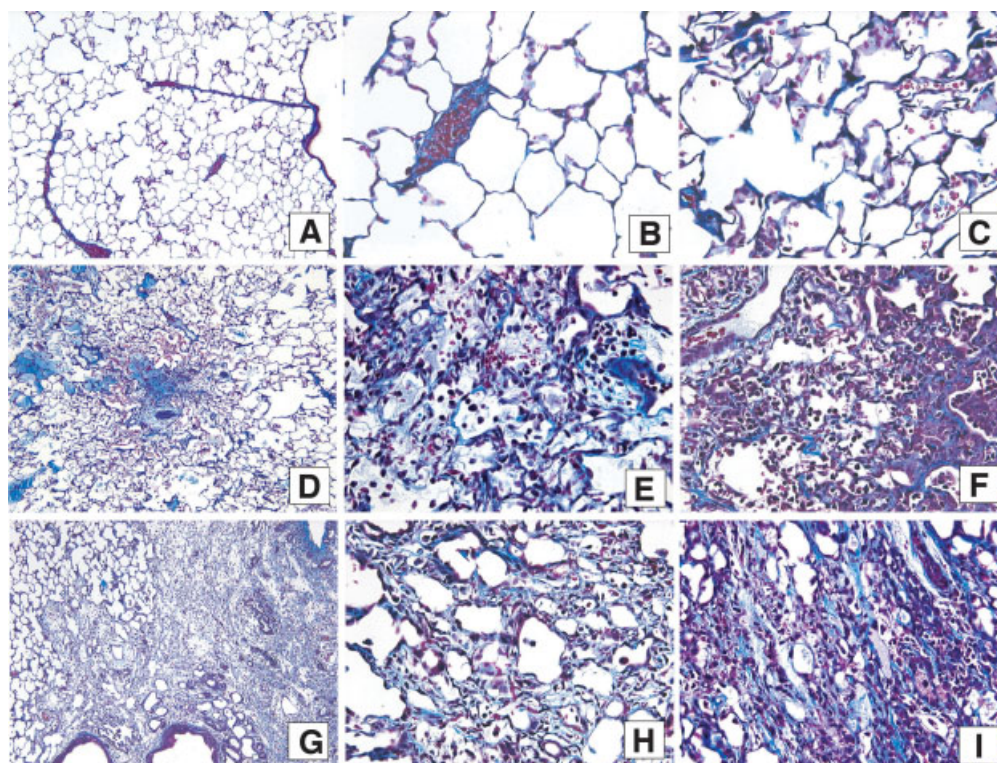


Figure 1. Tissue sections of lungs with trichrome stain. Lungs were obtained after airway instillation of CEES at time 0 (A, B, 10 \times and 40 \times); 6 h (C, 40 \times); 24 h (D, E, 10 \times and 40 \times); 3 days (F, 10 \times), 6 days (G, 10 \times and H, 40 \times); and 3 weeks (I, 40 \times). All tissue sections were reacted with trichrome stain

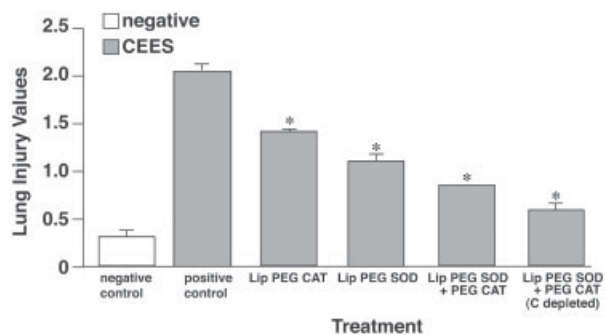


Figure 2. Attenuative effects of liposomes loaded with anti-oxidant enzymes. Rats received either saline followed by unloaded liposomes (negative control), CEES followed by airway delivery of unloaded liposomes (positive control), or CEES with liposomes containing either pegylated (PEG)-CAT or PEG-SOD, individually or the combination, or the combination of liposomes in complement depleted animals induced by the earlier intraperitoneal injection of purified cobra venom factor. Liposomes were administered immediately after CEES instillation. For each bar $n \geq 6$. Lung injury values are represented by the leak of ^{125}I -albumin from the vascular compartment into the airway compartment 4 h after airway delivery of CEES (see text). * Represents P values of <0.05 when compared with the positive control group

structures and the appearance of honeycombing (frames G, H). By week 3, little recognizable lung structure remained in the face of dense collagen deposits and parenchymal collapse, together with numerous interstitial macrophages and mononuclear cells (frame I).

Attenuation of CEES-Induced Acute Lung Injury by Anti-Oxidant Enzymes in Liposomes

As shown in Fig. 2, the airway instillation of CEES together with unloaded liposomes resulted 4 h later in approximately a 10-fold increase in lung injury, as defined by the leakage of ^{125}I -albumin from blood into the lung. When instilled into the lung immediately after CEES, polyethyleneglycol (PEG)-linked catalase-containing liposomes (LIP-PEG-CAT) attenuated injury by 40%. Liposomes containing PEG-superoxide dismutase (PEG-SOD) diminished injury by 57%. The combination of PEG-SOD and PEG-CAT in liposomes further reduced injury by 71%. With the combination of PEG-SOD and PEG-CAT liposomes given to complement-depleted animals, the injury was reduced by 86%. These data indicate that anti-oxidant enzymes have powerful attenuative effects on CEES-induced acute lung injury. Since, as described above, airway delivery of liposomes results in their phagocytosis by lung macrophages, it seems likely that the attenuative effects of liposomes

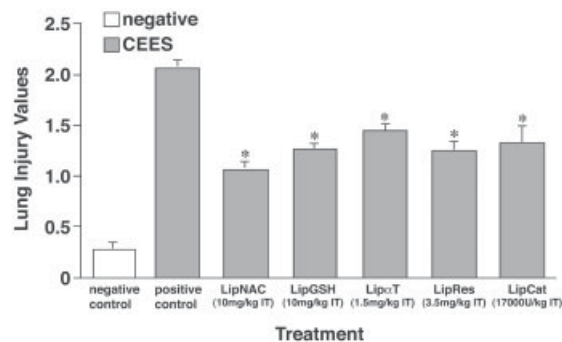


Figure 3. Attenuative effects of liposomes loaded with reducing agents in CEES lung injury. The positive and negative controls are similar to those described in Fig. 1. When used, liposomes were injected intratracheally immediately after the airway instillation of CEES. Lung injury was determined by the permeability index. αT , α -tocopherol

containing anti-oxidant enzymes are due to the bolstering of anti-oxidant defenses in lung macrophages.

Attenuative Effects of Liposomes Containing Reducing Agents

In an additional set of experiments (shown in Fig. 3), there was approximately a 10-fold increase in leakage of albumin from the circulation into the lungs of animals receiving airway instillation of CEES 4 h earlier together with unloaded liposomes. When liposomes containing NAC (Lip-NAC) were instilled immediately after CEES, injury was attenuated by 60%. Liposomes containing glutathione (GSH) led to a 48% reduction in lung injury. Liposomes containing α -tocopherol (αT) reduced injury by 37%. Liposomes containing the reducing agent present in red wine, resveratrol (RES), reduced injury by 48%, while liposomes containing PEG-CAT reduced injury by 44%. These data indicate that reducing agents presented in liposomes have significantly attenuative effects against CEES-induced acute lung injury. The data also indicate that the non-derivatized form of catalase (CAT) also has attenuative effects when given within liposomes.

Additive Effects of Complement Depletion and Liposomes Containing Reducing Agents

Previous studies in our laboratory have shown that complement depletion resulted in a 43% reduction of lung injury (McClintock *et al.*, 2002). As shown in Fig. 4, approximately a 10-fold increase in the leakage of ^{125}I -albumin into the lungs occurred following instillation of CEES together with unloaded liposomes. When the animals were complement (C) depleted, the instillation

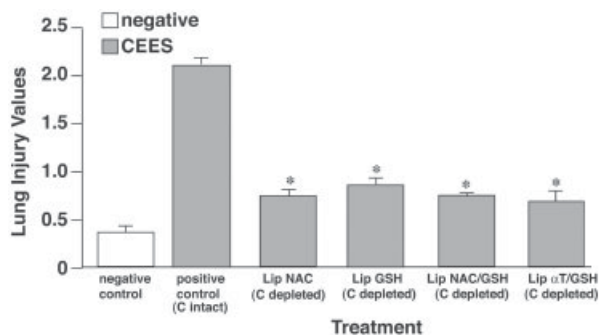


Figure 4. Enhanced effects of anti-oxidant containing liposomes in complement depleted rats. The negative and positive control groups are similar to those described in Fig. 1. Complement depletion was induced in four groups of animals by the prior intraperitoneal injection of purified cobra venom factor (CVF). Liposomes containing the various anti-oxidant compounds were given immediately after airway instillation of CEES. For each group, $n \geq 6$

of liposomes containing NAC reduced injury by 79%, those containing GSH reduced injury by 72% in complement-depleted rats, liposomes containing the combination of NAC and GSH reduced injury by 78% in complement-depleted rats. Complement-depleted animals receiving liposomes containing αT together with GSH showed an 82% reduction in lung injury as measured by leakage of albumin from the blood. Thus, the combination of complement depletion and anti-oxidant liposomes seems significantly to attenuate CEES-induced acute lung injury in an additive manner.

Effects of Delayed Lung Instillation of Anti-Oxidant Liposomes

As shown in Fig. 5, in CEES treated animals instillation of liposomes containing reducing agents was done either 10 min before the airway instillation of CEES or at 30, 60 and, in one case, 90 min following the airway instillation of CEES. As shown in Fig. 5, over the course of the first 60 min after instillation of CEES, there were significant attenuative effects of liposomes containing NAC or GSH, or the combination. Under these circumstances, injury was reduced between 55% and 77%, respectively. In the case of liposomes containing the combination of NAC and GSH, even when delivery was delayed until 90 min following instillation of CEES, there was a 55% reduction in the development of acute lung injury. These data indicate that delayed airway administration of anti-oxidant-containing liposomes results in significant reduction of CEES-induced lung injury, even when delivery is delayed by at least an hour following exposure of lungs to CEES.

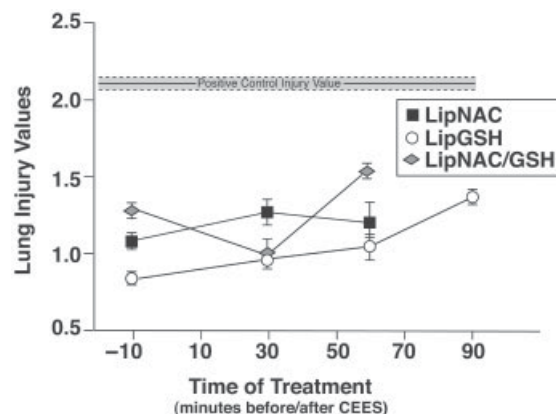


Figure 5. Attenuative effects of anti-oxidant containing liposomes when airway instillation was given at various time points before or after airway delivery of CEES. The dotted line near the top represents the positive control value. Lung injury values (permeability indices) in the negative control are not shown but were <0.5 , as described in Figs 1–3

Discussion

The data described in this report indicate that CEES instillation into the lung produces acute lung injury in a manner that seems related to the loss of the redox balance in the lung, although this has not been demonstrated directly. This conclusion is based on the attenuative effects of reducing agents (NAC, GSH, αT , resveratrol) or anti-oxidant enzymes (SOD, CAT) or various combinations, all presented in liposomes alone or in combination. Since it is well known that liposomes given into the airways are phagocytized by macrophages and internalized (Gonzalez-Rothi *et al.*, 1991; Lentsch *et al.*, 1999; Shephard *et al.*, 1981), the implications from the current studies are that liposomal delivery selectively enhances a reducing environment in lung macrophages, which may be compromised when these cells came into contact with CEES.

The morphological features described in this report are consistent with our earlier report of an accumulation of myeloperoxidase (MPO) in the lung after CEES instillation (McClintock *et al.*, 2002). The presence of alveolar hemorrhage and edema implies a severe disruption of vascular and distal airway barrier. These changes are consistent with the concept that CEES induces an acute lung-damaging inflammatory response that is complement-dependent. Beneficial effects of neutrophil and complement depletion as demonstrated previously indicate that the inflammatory response to CEES contributes to the development of lung injury (McClintock *et al.*, 2002). Masson's trichrome staining revealed an accumulation of fibrin and/or collagen within the alveolar spaces. Deposition of fibrin reflects a non-specific reaction to tissue damage. It remains to be shown

that CEES-exposure causes rapid development of interstitial fibrosis, as confirmed biochemically by collagen accumulation. It is hypothesized that epithelial and endothelial damage following CEES-exposure results in disruption of tissues, resulting in collagen accumulation in the interstitial and alveolar spaces. It appears likely that following lung exposure to CEES collagen deposition occurs in a widespread manner, resulting in parenchymal collapse and the honeycombing changes that occur in humans with pulmonary fibrosis. Numerous macrophages and mononuclear cells in areas of collagen deposition in the lung may be associated with the release of mediators (such as TGF β) that promote lung production of collagen.

How CEES functions as a powerful oxidant and what lung cells are targets of CEES is unclear. The extensive leakage of albumin into the lung after exposure to airway administration of CEES infers that the blood–gas barrier has been seriously compromised, causing a functional impairment (or destruction) of both vascular endothelial and alveolar epithelial cells. The subsequent alveolar flooding with plasma components leaking into the distal airway compartment could seriously compromise blood–gas exchange, resulting in hypoxia.

The permeability index after instillation of CEES and empty liposomes was found to be similar to CEES instillation alone (as reported in McClintock *et al.*, 2002) implying that empty liposomes do not cause any lung damage by themselves. The fact that the combination of complement depletion and liposomal delivery of GSH or NAC enhances the attenuation when compared with the use of either type of liposomes given to complement-intact rats (Figs 3 and 4) suggests that it may be both the loss of reducing potential in the lung as well as an engagement of complement activation products (e.g. C5a) that leads to intense acute lung injury. Whether complement activation products are directly responsible for lung injury or are functioning to enhance cytokine and chemokine expression remains to be determined. In a recent study it was shown that neutrophil depletion prior to CEES delivery was also capable of reducing CEES-induced lung injury (McClintock *et al.*, 2002), suggesting that activated neutrophils enter into the sequence of destructive events after CEES instillation into the lung.

A matter of considerable interest is that delayed delivery (for as long as 60 min) of liposomes containing NAC or GSH, or the combination, into lungs after CEES instillation still provides substantial attenuation from the massive leak of albumin into the lung. It should be noted that there is not much increased albumin leak into the lung in the first 60 min after administration of CEES (McClintock *et al.*, 2002). In fact, compared with values at 1 h, the permeability index at 2, 4 and 6 h after instillation of CEES rose 2 fold, 2.9 fold, 7.7 fold and 16.2 fold, respectively, when compared with uninjured lung values. Accordingly, the development of extensive lung

injury after airway instillation of CEES requires considerable time for full development of lung injury. This would be in accord with the concept that CEES triggers in the lung an acute inflammatory response, which itself serves to cause lung damage. Since this sequence requires several hours before the large increases in lung permeability (albumin leak into lung) are seen, this may explain why delayed administration of anti-oxidant liposomes can still bring about significant attenuative effects. Understanding more fully the molecular events that lead to CEES-induced intense acute lung injury may provide even better strategies for effective therapeutic intervention after exposure of lung to HD and related compounds.

References

- Angelov A, Belchen L, Angelov G. 1996. Experimental sulfur mustard gas poisoning and protective effect of different medicines in rats and rabbits. *Indian Vet. J.* **73**: 546–551.
- Ballow M, Cochrane CG. 1969. Two anticomplementary factors in cobra venom: hemolysis of guinea pig erythrocytes by one of them. *J. Immunol.* **103**: 944–952.
- Dube SN, Husain K, Sugendran K, Vijayaraghavan R, Somani SM. 1998. Dose response of sulphur mustard: behavioral and toxic signs in rats. *Indian J. Physiol. Pharmacol.* **42**: 389–394.
- Eisenmenger W, Drasch G, von Clarmann M, Kretschmer E, Roider G. 1991. Clinical and morphological findings on mustard gas [bis(2-chloroethyl)sulfide] poisoning. *J. Forensic Sci.* **36**: 1688–1698.
- Emad A, Rezaian GR. 1999. Immunoglobulins and cellular constituents of the BAL fluid of patients with sulfur mustard gas-induced pulmonary fibrosis. *Chest* **115**: 1346–1351.
- Fan J, Shek PN, Suntres ZE, Li YH, Oreopoulos GD, Rotstein OD. 2000. Liposomal antioxidants provide prolonged protection against acute respiratory distress syndrome. *Surgery* **128**: 332–338.
- Freeman BA, Turrens JF, Mirza Z, Crapo JD, Young SL. 1985. Modulation of oxidant lung injury by using liposome-entrapped superoxide dismutase and catalase. *Fed. Proc.* **44**: 2591–2595.
- Gonzalez-Rothi RJ, Straub L, Cacace JL, Schreier H. 1991. Liposomes and pulmonary alveolar macrophages: functional and morphologic interactions. *Exp. Lung Res.* **17**: 687–705.
- Johnson KJ, Ward PA. 1974. Acute immunologic pulmonary alveolitis. *J. Clin. Invest.* **54**: 349–357.
- Khateri S, Ghanei M, Keshavarz S, Soroush M, Haines D. 2003. Incidence of lung, eye, and skin lesions as late complications in 34,000 Iranians with wartime exposure to mustard agent. *J. Occup. Environ. Med.* **45**: 1136–1143.
- Lakshmana Rao PV, Vijayaraghavan R, Bhaskar AS. 1999. Sulphur mustard induced DNA damage in mice after dermal and inhalation exposure. *Toxicology* **139**: 39–51.
- Lentsch AB, Czermak BJ, Bless NM, Van Rooijen N, Ward PA. 1999. Essential role of alveolar macrophages in intrapulmonary activation of NF-kappaB. *Am. J. Respir. Cell Mol. Biol.* **20**: 692–698.
- Luna L. 1968. *Manual of Histologic Staining Methods of the AFIP*, 3rd edn. McGraw-Hill: New York.
- Mayer MM. 1961. Complement and complement fixation. In *Experimental Immunology*, Kabat EA, Mayer MM (eds). Springfield: Thomas, 133–240.
- McClintock SD, Till GO, Smith MG, Ward PA. 2002. Protection from half-mustard-gas-induced acute lung injury in the rat. *J. Appl. Toxicol.* **22**: 257–262.
- Shephard EG, Joubert JR, Finkelstein MC, Kuhn SH. 1981. Phagocytosis of liposomes by human alveolar macrophages. *Life Sci.* **29**: 2691–2698.
- Sone S, Poste G, Fidler IJ. 1980. Rat alveolar macrophages are susceptible to activation by free and liposome-encapsulated lymphokines. *J. Immunol.* **124**: 2197–2202.
- Suntres ZE, Shek PN. 1996. Treatment of LPS-induced tissue injury: role of liposomal antioxidants. *Shock* **6** (Suppl 1): S57–S64.

Catecholamines—Crafty Weapons in the Inflammatory Arsenal of Immune/Inflammatory Cells or Opening Pandora’s Box^S?

Michael A Flierl,¹ Daniel Rittirsch,¹ Markus Huber-Lang,² J Vidya Sarma,¹ and Peter A Ward¹

¹Department of Pathology, University of Michigan Medical School, Ann Arbor, MI, USA; ²Departments of Traumatology, Hand, Plastic, and Reconstructive Surgery, University of Ulm Medical School, 89075 Ulm, Germany

It is well established that catecholamines (CAs), which regulate immune and inflammatory responses, derive from the adrenal medulla and from presynaptic neurons. Recent studies reveal that T cells also can synthesize and release catecholamines which then can regulate T cell function. We have shown recently that macrophages and neutrophils, when stimulated, can generate and release catecholamines *de novo* which, then, in an autocrine/paracrine manner, regulate mediator release from these phagocytes via engagement of adrenergic receptors. Moreover, regulation of catecholamine-generating enzymes as well as degrading enzymes clearly alter the inflammatory response of phagocytes, such as the release of proinflammatory mediators. Accordingly, it appears that phagocytic cells and lymphocytes may represent a major, newly recognized source of catecholamines that regulate inflammatory responses.

Online address: <http://www.molmed.org>

doi: 10.2119/2007-00105.Flierl

INTRODUCTION

Norepinephrine and epinephrine are key hormones to prepare the body for one of its most primeval reactions: the “fight or flight” response. Catecholamines (CAs) increase the contractility and conduction velocity of cardiomyocytes, leading to increased cardiac output and a rise in blood pressure, which leads to increased vascular tone and resistance. This results in an increased “pre-load” in the right atrium, causing the heart rate to drop due to the Starling-mechanism. Moreover, catecholamines facilitate breathing (bronchi become dilated), and the body’s metabolic reserves are mobilized (lipolysis

and glycogenolysis) to provide vital energy. Past concepts held the adrenal medulla and the nervous system to be responsible for the production, storage, and release of catecholamines. Recent findings suggest that such assertions need to be re-evaluated. Because the brain and the immune system are some of the body’s major adaptive systems (1) and communicate with each other extensively in an attempt to regulate body homeostasis (2), a common “language” is needed to facilitate this crosstalk. Key systems involved in this crosstalk are the hypothalamic-pituitary-adrenal (HPA) axis and the autonomic nervous system,

consisting of the adrenergic sympathetic nervous system, the vagus-mediated parasympathetic nervous system, and the enteric nervous system (1-3). Over many decades, an increasing body of evidence has accumulated demonstrating that lymphocytes and phagocytes not only are capable of synthesizing and releasing neuropeptides, but also neurotransmitters and hormones. Furthermore, these cells express adrenergic and cholinergic functions. Thus, coexisting in the nervous as well as in the immune system, these mediators become an universal language of a neuro-endocrine-immune modulating network (4), which enables the nervous, endocrine, and immune system to regulate and fine-tune their functional responses positively or negatively, and thereby allows the body to adapt rapidly to various changes of internal and external environments. We are beginning now to understand that catecholamines are an integral part, and potent modulators, of these neuro-endocrine-immune/inflammatory interactive networks. Through direct communication via sympathetic nerve fibers that innervate lymphoid organs (5), catecholamines can modulate mouse lymphocyte proliferation, differentiation, (6) and cytokine pro-

Footnote S: Zeus ordered Hephaestus to create the first woman on earth, Pandora. She was bestowed with exceptional beauty and many talents by the Greek Gods. When Prometheus stole fire from heaven, furious Zeus provided Pandora with a jar (Pandora’s box) and gave her

to Epimetheus, Prometheus’ brother. Not under any circumstances was she to open that box, but intrigued by natural inquisitiveness, she did, and all evil contained escaped and spread over the earth. The only thing remaining at the bottom of the box was Hope.

Address correspondence and reprint requests to Peter A. Ward, M.D., Department of Pathology, The University of Michigan Medical School, 1301 Catherine Road, Ann Arbor, Michigan 48109-0602. Phone: 734-647-2921, Fax: 734-763-4782; E-mail: pward@umich.edu. Submitted October 18, 2007; Accepted for publication December 3, 2007; Epub (www.molmed.org) ahead of print December 5, 2007.

duction of rodent Th cells (7) and human peripheral blood mononuclear cells (PBMCs) (8). These interactions are facilitated by adrenergic receptors expressed on murine lymphocytes (7), rat natural killer (NK) cells (9), rodent macrophages and neutrophils (10,11), and human PBMCs (12). Consequently, we need to understand better the sources, distribution, and roles of catecholamines and their receptors in immunity and inflammation.

IMMUNE CELLS—A NEW, DIFFUSELY EXPRESSED ADRENERGIC ORGAN

The first evidence that catecholamines might originate from sources other than neuronal or endocrine tissue was reported more than ten years ago when the presence of endogenous catecholamines was reported in human lymphocytes (13). Lymphocytes were described not only to contain intracellular levels of catecholamines, but these catecholamines were secreted, negatively regulating lymphocyte proliferation, differentiation, and apoptosis via an au-

tochrine loop in mice and humans (13,14). Shortly thereafter, parallel experiments identified dopamine and norepinephrine in human PBMCs (15,16). In line with these findings, additional studies confirmed the presence of catecholamines in various other cells, including murine bone marrow derived mast cells (17), rodent macrophages and neutrophils (11,18), and in a macrophage cell line (19). Surprisingly high levels of the epinephrine-synthesizing enzyme, phenylethanolamine-N-methyl transferase (PNMT), were found in the thymus of young mice, which were comparable to levels in the brainstem (Figure 1A; 20). Interestingly, PNMT levels were found to be two-fold higher in the lymphocyte-harboring cortex of the thymus than in the medulla. Low PNMT activity and PNMT mRNA also could be detected in the marginal zone of the white pulp of the spleen (20), which contains significant amounts of lymphocytes also, suggesting the presence of epinephrine-generating cell population(s) in lym-

phoid organs. As the morphology of these findings correlate perfectly with the lymphocyte-rich sites of lymphoid organs, it is reasonable to assume that the epinephrine-producing cell population might be lymphocytes. The mere presence of catecholamines in cells, however, left the unanswered question as to whether these catecholamines originated from extracellular sources and simply were taken up actively and stored by lymphocytes and phagocytes or whether such cells might have synthesized catecholamines *de novo*. Affirmation of the presence of the intracellular machinery for catecholamine production in human lymphocytes was obtained indirectly when human hematopoietic cell lines and human T and B cell hybridomas were cultured over a long period of time, with subsequent detection of catecholamines inside the cells. Based on the cell culture protocols, it was highly unlikely that these intracellular catecholamines could have originated from extracellular sources (21).

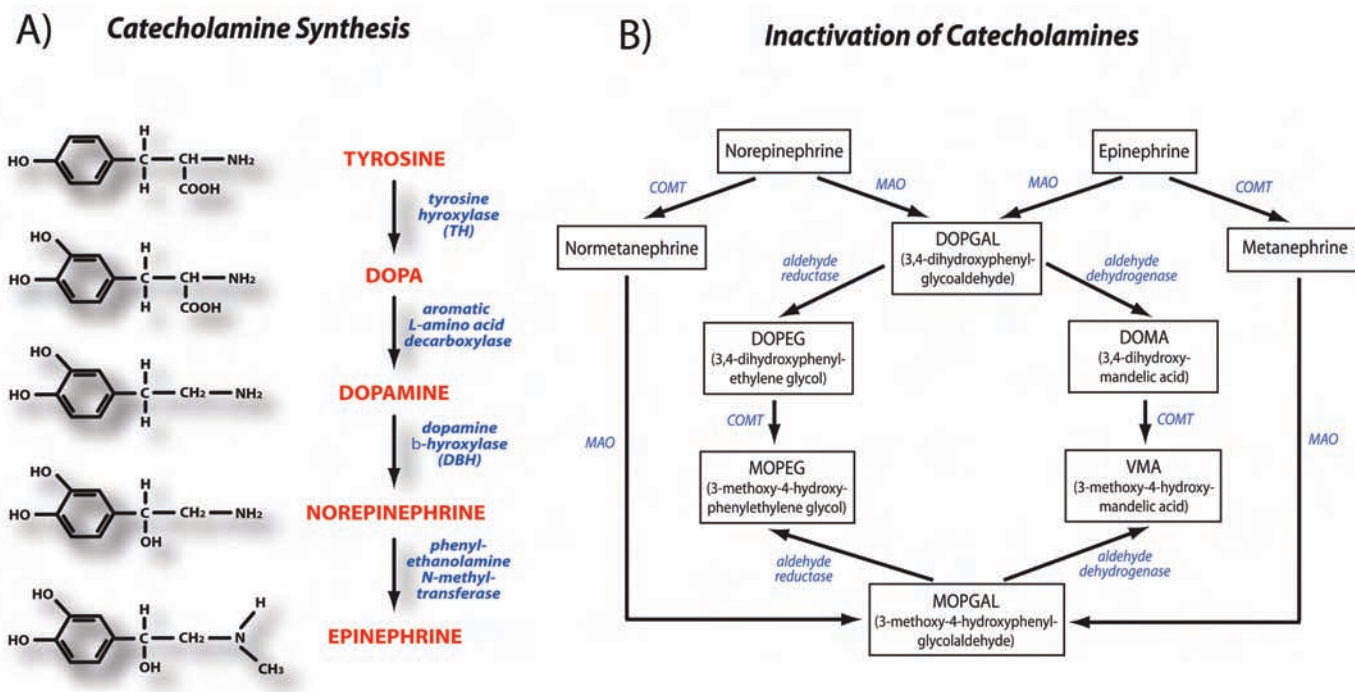


Figure 1. Pathways for synthesis of catecholamines (A) and various metabolizing pathways of catecholamines (B).

Evidence for *de novo* Synthesis, Storage, Release, and Inactivation of Catecholamines by Immune/Inflammatory Cells

Synthesis. The synthesis of catecholamines relies on two key enzymes: tyrosine-hydroxylase (TH), which is known to be the rate-limiting step in catecholamine synthesis, and dopamine- β -hydroxylase (DBH), which converts dopamine to norepinephrine (3; Figure 1A). The intracellular presence of these hydroxylases and changes in expression of these enzymes strongly implies the ability of cells to synthesize catecholamines *de novo*. Recently, rat phagocytes were found to contain mRNA for both TH and DBH, which clearly were inducible by cell contact with bacterial lipopolysaccharide (LPS) (11). In parallel, rat lymphocytes (22,23) and human PBMCs (24) contain inducible mRNA for these catecholamine-generating enzymes, upregulation of which results in increased levels of dopamine, norepinephrine, and epinephrine when rat lymphocytes were stimulated (22). In contrast, pharmacological inhibition of TH and DBH in rat and human lymphocytes decreased intracellular catecholamine levels in a dose-dependent manner (22,25). Blockade of the conversion of dopamine to norepinephrine (by DBH-inhibition) increased intracellular levels of dopamine and other norepinephrine precursor molecules in human PBMCs (25). Therefore, it is not surprising that the addition of tyrosine and *L*-DOPA to lymphocyte cultures increases catecholamine levels in these cells in a dose-dependent manner (25). Shortly after exposure of human PBMCs to [3 H]-*L*-DOPA, [3 H]-norepinephrine, and [3 H]-dopamine were detected in these cells, suggesting an active uptake mechanism of catecholamine-precursor molecules from the extracellular fluids into human PBMCs (25). Interestingly, these metabolic events are highly selective, because, in contrast to *L*-dopa, *D*-dopa failed to alter catecholamine synthesis in human PBMCs (25). However, human PBMC presents a highly heterogenous group of

cells (lymphocytes, monocytes, etc.), making it difficult to draw definitive conclusions about its various cell types.

In summary, these findings suggest that, like neurons and endocrine cells, lymphocytes actively transport tyrosine and *L*-dopa from extracellular sources into the cell to produce catecholamines via catalysis by TH and DBH. Thus, it now is becoming clear that lymphocytes and phagocytes not only possess the ability to produce, store, release, and reuptake catecholamines *de novo*, but that these cells also are capable of exquisitely regulating their catecholamine-synthesis in response to various extracellular stimuli. But, the question remains: how significant is the relative abundance of immune cell-derived catecholamines in comparison to the main catecholamine-producing organ, the adrenal medulla or presynaptic neurons? The adrenomedullary baseline production of epinephrine and norepinephrine in rodents is about 730pg/mL/min and 102pg/mL/min, respectively (26). In a recent study, 10^7 rat neutrophils produced about 100pg/mL and 20pg/mL while 10^7 rat macrophages released nearly 375pg/mL of epinephrine and 50pg/mL of norepinephrine when stimulated with 50ng/mL LPS (11). However, it is important to note that the kinetics of phagocytic catecholamine release is biphasic due to release of stored material versus *de novo* biosynthesis (11). This means that, during inflammatory processes, phagocytic catecholamine levels are linked to a very delicate and dynamic regulation within a local milieu, making it difficult to determine precisely the relative contributions to catecholamines by phagocytes as opposed to the adrenal medulla during inflammation. There do not appear to be definitive publications describing the amount of catecholamines secreted by lymphocytes or presynaptic neurons.

Storage and release of catecholamines. Catecholamines are found throughout adrenergic neurons, but the highest concentrations of these biogenic amines are found in the peripheral presynaptic nerve terminals where these amines are stored in membrane-bound granules and

protected from enzymatic destruction (27,28). After depolarizing stimulation of these neurons, rapid secretory release of stored catecholamines occurs. One of the main modes to remove catecholamines that have been released by presynaptic neurons is cellular reuptake of these amines (*see below*). In neurons, this process is known to be inhibited by reserpine. In rodent and human lymphocytes, trace amounts of intracellular catecholamines have been found. In the resting rodent lymphocyte, norepinephrine was the highest content (2.53×10^{-20} M/cell), followed by dopamine (1.29×10^{-20} M/cell) and epinephrine (1.00×10^{-20} M/cell) (22). To date, it seems unclear which role these intracellular baseline catecholamine stores play, because it is only after mitogen stimulation such as phytohaemagglutinin (PHA) (29), concanavalin A (conA) (22), or lipopolysaccharide (LPS) (11), that lymphocyte- or phagocyte-derived catecholamines increase to significant amounts for secretion, affecting cells in an autocrine/paracrine fashion. Incubation of human PBMCs with reserpine markedly reduced intracellular accumulation of catecholamines, while catecholamine levels in culture supernatant fluids significantly increased (21), suggesting that human PBMCs employ a mechanism similar to neurons, resulting in catecholamine release followed by reuptake. Moreover, studies have revealed that, in accordance with chromaffin cells from the adrenal medulla, secretion of norepinephrine by human lymphocytes depends on acetylcholine and calcium (30,31). Acetylcholine (ACh) facilitated norepinephrine release from peripheral human lymphocytes, as did inflow of calcium into human lymphocytes. Yet, in clear contrast to mechanisms employed by chromaffin cells, blockade of nicotinic receptors on lymphocytes blocked ACh-induced release of norepinephrine release only by about 50% and blocking of Ca^{2+} -channels attenuated the ACh-induced norepinephrine release by no more than 30% (30,31). Therefore, it is clear that we lack a detailed understand-

ing of the molecular mechanisms involved in catecholamine release by lymphocytes. A recent report identified interferons (IFNs) as molecular regulators of catecholamine synthesis in human PBMCs (29). When human PBMCs were stimulated with phytohaemagglutinin, catecholamine production and release was increased by addition of IFN β , while the opposite was the case when stimulated PBMCs were exposed to IFN γ which reduced even the mRNA expression of TH. In turn, stimulation with norepinephrine caused mouse Th1 cells to produce two- to four-fold more IFN γ (6), suggesting a negative feedback loop of IFN γ on norepinephrine production. Thus, IFNs seem to emerge as the first physiological compounds that mediate production of catecholamines by human PBMCs. However, PBMCs are a highly heterogeneous population of various cell types, making it difficult to draw definitive conclusions from these findings. Thus, achieving a more complete comprehension of the involvement of various ion channels, neurotransmitters, and other mediators triggering catecholamine-release clearly is needed.

Reuptake and degradation of catecholamines by immune/inflammatory cells. Following release of epinephrine and norepinephrine, their activities are terminated by (1) reuptake into nerve terminals, (2) dilution into extracellular fluids and uptake at extraneuronal sites, and (3) metabolic transformation (inactivation) of these catecholamines (32). Two enzymes are essential in the initial steps of metabolic inactivation (Figure 1B): monoamine oxidase (MAO) and catechol-O-methyl transferase (COMT) (33,34). MAO and COMT produce physiologically inactive catecholamine-metabolites, but neither of these enzymes plays an important role in the rapid termination of the physiological actions of secreted catecholamines. Rather, this is achieved by active reuptake into presynaptic nerve terminals (27). Human lymphocytes also have been shown to express some of these reuptake transporters. Dopamine-

specific binding sites, as well as a dopamine-selective reuptake system, have been demonstrated on human lymphocyte membranes (35,36). Selective blockade of these monoamine transporters suppressed both the dopamine binding to the specific sites and the uptake of [3 H]-dopamine. Dopamine-transporter (DAT) mRNA, DAT immunoreactivity, and vesicular monoamine transporter immunoreactivity have been detected on cell membranes and in vesicle-like structures of human lymphocytes (37,38), suggesting DAT on lymphocytes similar to that on neurons. There is some evidence that, in addition to DATs, human PBMCs also may express a norepinephrine transporter (NAT), which would allow for active uptake of catecholamines (12). Nevertheless, the presence of NAT on immune cells remains debatable and additional confirmation is needed for definitive proof (39,40).

As mentioned above, the physiological actions of released catecholamines are terminated primarily by rapid cellular reuptake. Yet, their final intracellular inactivation still relies on the mitochondria-bound MAO and the cytosolic COMT. Several studies have demonstrated the presence of MAO and COMT in human lymphocytes (34,41). Furthermore, metabolites of dopamine, norepinephrine, and epinephrine have been detected in rat lymphocytes (21). Recently, both mRNA and protein for MAO and COMT were found in rat macrophages and rat neutrophils and could be induced by LPS (11). When MAO was inhibited by pargyline, the content of intracellular dopamine, norepinephrine, and epinephrine levels increased in activated human and rat lymphocytes, while intracellular catecholamine metabolites decreased (12,22). Thus, immune cells seem to possess not only the full cellular machinery for *de novo* synthesis, release, and inactivation of catecholamines, but also are capable of intracellular catecholamine-inactivation by MAO and COMT, utilizing the same classical metabolic pathway described in nervous and endocrine systems.

Modulation of Immune/Inflammatory Cell Functions by Catecholamines

Endogenous catecholamines as modulators of immune/inflammatory cells.

There is a large body of evidence indicating that, in addition to being crucial neurotransmitters and hormones, catecholamines are important immunomodulators during health and disease (3,42-45; Figure 2). Surprisingly, first reports of the immunomodulating functions of catecholamines were published as early as 1904, describing a robust leukocytosis following subcutaneous administration of epinephrine (46). However, it was not until the mid 1990s that it was reported that lymphocyte-derived catecholamines modulate lymphocyte functions in an autocrine and paracrine manner, providing these cells with a potent tool to fine tune their actions and crosstalk with nearby cells (13). Because the expression of TH and DBH mRNA has been found to be inducible by various stimuli when compared with non-stimulated lymphocytes, it seems likely that the catecholamine synthesis in lymphocytes and phagocytes depends on the functional state of these cells, and that there are diverse cell triggers (11,19,22,23). These auto-regulatory interactions between endogenous catecholamines and immune/inflammatory cells can alter a wide array of cell functions, in part through adrenoceptors or dopaminergic receptors expressed on these cells (10,11,47,48) (*see below*). For instance, it has been observed that the neurotransmitter dopamine, at physiological concentrations, inhibits the proliferation (by downregulating tyrosine kinases) (49-51) and the cytotoxicity of human CD4 $^+$ and CD8 $^+$ T cells *in vitro* by acting through the D1/D5, D2, and D3 receptors, making dopamine an important regulator of human T cell functions (52,53). Moreover, exposure of human PBMCs to norepinephrine triggered a very distinct profile of mRNA expression and cytokine production in individual lymphocyte populations, augmenting Th1 (IL-2) and Th2 (IL-4, IL-5, IL-13) type cytokine production, while expression of MIP-1 α and

MCP-1 mRNA remained unaffected (8). Similar results were obtained when cells were exposed to dopamine. Thus, it seems likely that catecholamines very selectively activate different lymphocyte subpopulations, leading to a pattern of very distinct expression of inflammatory mediators. It also was demonstrated that catecholamines activate resting T cells by stimulating the release of pro- and anti-inflammatory mediators and alter the expression of surface integrins.

Regulation of immune cell-derived catecholamines. Immune cells seem to regulate their activity and the function of surrounding cells via endogenous catecholamines by two different mechanisms: (a) released catecholamines act in an autocrine/paracrine feedback fashion and (b) catecholamines produced by the adrenal medulla directly activate and modulate intracellular functions of immune/inflammatory cells.

Receptor-mediated autocrine/paracrine mechanisms. It is well established now that immune/inflammatory cells express multiple receptors for catecholamines. Numerous types of adrenergic receptors have been identified on human and rodent PBMCs, macrophages, neutrophils, and lymphocytes (10,11,48,54,55). Dopamine receptor subtypes also have been described on these cells (50,56,57). Adrenoceptors are G-protein coupled, seven-transmembrane spanning receptors (58). Upon interaction with their ligand, intracellular second messengers such as cyclic AMP, calcium ions, diacylglycerol, and inositol 1,4,5-triphosphate become activated and/or inhibited. Therefore, secreted endogenous catecholamines are able to activate the releasing cell itself as well as nearby cells in an autocrine/paracrine manner, stimulating cellular adrenergic/dopaminergic receptors, activating intracellular second messengers, and ultimately regulating cell functions (18,59). Rodent phagocytes have been demonstrated to regulate their release of inflammatory mediators via autocrine/paracrine interactions of endogenous catecholamines with adrenergic receptors expressed on their cell sur-

faces (10,11,18). Blockade of α - and β -adrenoceptors on human or rodent macrophages, neutrophils, and lymphocytes significantly inhibited the cytokine/chemokine production of these cells (10,11,18,60). These findings make it tempting to speculate that the inflammatory cytokine/chemokine network might be one of the important mediator systems tightly controlled by catecholamines via adrenergic receptors. Yet, it remains to be determined if catecholamine secretion by immune cells is a ubiquitous phenomenon or if it is, rather, an ultimate weapon of immune cells facing overpowering pathogenic insults. The physiological counterpart of the adrenergic system, the cholinergic system, also is known to be an integral part of human macrophage and lymphocyte regulation. Human macrophages are known to control their cytokine release via interactions of acetylcholine with nicotinic acetylcholine receptors expressed on cell membranes (61,62). Stimulation of the $\alpha 7$ subunit of the nicotinic acetylcholine receptors on macrophages greatly inhibited production of tumor necrosis factor (TNF) α , interleukin-(IL-)1 β , HMGB1 (and other cytokines), by transducing a cellular signal that inhibits the nuclear activity of NF- κ B and activates the transcription factor STAT3 via phosphorylation by JAK2 (63). Human peripheral blood lymphocytes also have been shown to express various cholinergic products including acetylcholine, choline acetyltransferase (ChAT), acetylcholinesterase (AChE), and vesicular acetylcholine transporter (VAChT), as well as M₂-M₅ muscarinic cholinergic receptors (38). As evaluated by confocal microscopy, acetylcholine and VAChT were clustered in punctiform intracellular areas (which most likely correspond to cytoplasmic storage vesicles), while ChAT and AChE were spread diffusely throughout the cytoplasm. As expected, muscarinic receptors were localized in the cell membranes (38). To date, however, it is not clear how these lymphocytic cholinergic markers may contribute to the regulation of immune functions.

Receptor-independent intracellular regulatory mechanisms. Following termination of their actions and cellular reuptake, catecholamines are oxidized intracellularly by the mitochondrion-associated MAO and the ubiquitous cytosolic COMT. During inactivation, catecholamines are degraded into various products including large quantities of reactive oxygen species and other cytotoxic oxidative metabolites, which are known to induce cellular apoptosis in mouse lymphocytes, human PBMCs, and PC12 cell lines (14,64-67). Newly synthesized intracellular catecholamines might not be released immediately but stored inside the cells, which may put cells in jeopardy of receptor-independent and oxidative stress-induced apoptosis (39). This theory is supported by the finding that stress-induced apoptosis can be blocked by the anti-oxidant ascorbic acid (19). Therefore, it seems likely that catecholamines use intracellular oxidative mechanisms to exert autoregulatory functions on immune cells. Even more importantly, a catecholamine-specific transporter has been described on nuclear membranes of lymphocytes, which actively transports catecholamines from the cytoplasm into the cell nucleus where catecholamines interact with nuclear receptors such as steroid receptors (16,68), influence transcription processes via interaction with nuclear factor (NF)- κ B, and modulate apoptosis (69) by facilitating the expression of proto-oncogene *Bax* while attenuating *Bcl-2* expression (16,17). It is noteworthy that the mitochondria-associated MAO and the cytosolic COMT fail to enter the nucleus, posing the important but so far unanswered question of how and by what mechanism intranuclear actions of catecholamines are terminated.

IMMUNE CELL-DERIVED CATECHOLAMINES DURING SHOCK AND SEPSIS

Foolishly Unlocking Pandora's Box?

Even though catecholamines are used frequently, sometimes even as last-resort

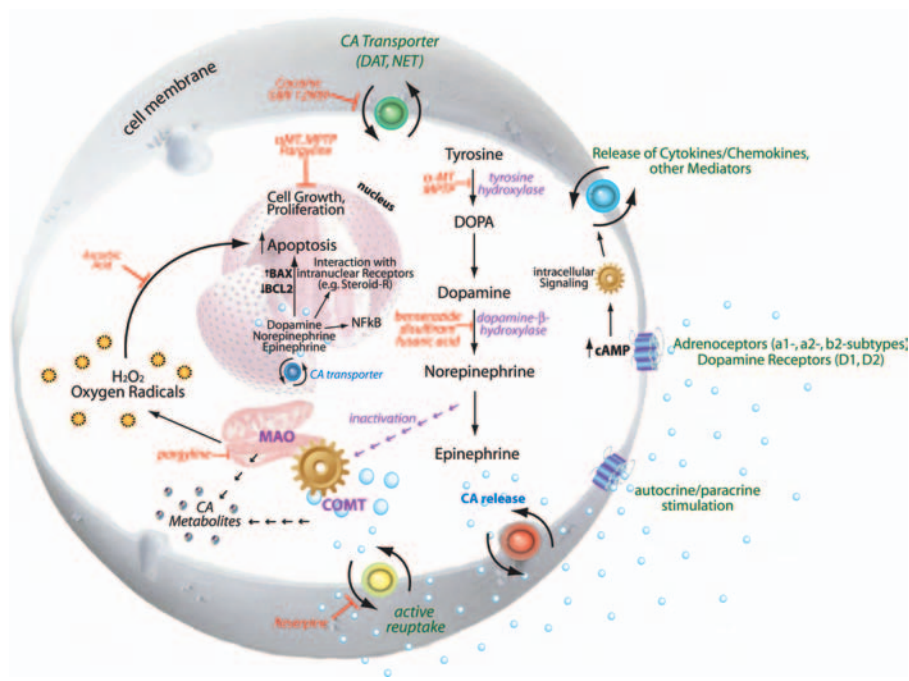


Figure 2. Summary of the various interactions between catecholamines and lymphocytes/phagocytes. Most of these actions have been demonstrated in lymphocytes (see text).

drugs to stabilize cardiovascular functions in the critically ill patient, there are several potentially fatal consequences of lymphocyte/phagocyte-derived or exogenously administered catecholamines, in addition to the above described immunomodulatory properties, that need to be taken into account.

Shock. The state of shock leads to a strong activation of the sympathetic nervous system resulting in a massive increase of circulating catecholamines. When endogenous catecholamine-release fails to stabilize cardiovascular parameters, therapeutic catecholamines frequently are administered. Therefore, it is essential to understand the immunomodulatory effects of endogenously released or administered catecholamines in the setting of shock. As expected, hemorrhagic shock induces a robust increase of circulating epinephrine and norepinephrine in an experimental animal model (70). While these increases were paralleled by an elevated number of circulating natural killer

(NK) cells and an elevated CD4/CD8⁺ ratio, levels of circulating CD8⁺ lymphocytes significantly decreased. Moreover, an increased rate of splenocyte apoptosis was noted 24 h after induction of hemorrhage. All of these effects could be abolished by administration of nonselective or β_1 -selective adrenergic blockade without affecting serum cytokine concentrations of TNF α or IL-10 (70). In addition, when noradrenergic neurons were depleted within the central nervous system, cellular cytokine release was affected significantly during hemorrhagic shock (71-73). Thus, hemorrhagic shock leads to vigorous increases in circulating catecholamines, which finally modulate immune cell functions via adrenergic receptors expressed on these cells. Surprisingly, it has been shown that massive, trauma-induced activation of the sympathetic nervous system with subsequent robust release of norepinephrine leads to increased *in vivo* growth of bacteria within the gastrointestinal system in an experimental

animal model, which most likely contributes to the high incidence of systemic bacterial inflammation and sepsis following trauma hemorrhage (74). Most importantly (or shockingly), it was discovered that catecholamines *directly* stimulate bacterial growth. It was reported that catecholamines enhanced growth of several gram-negative bacteria and the production of bacterial growth factor in cultured *E. coli* (75-77). However, to date, it is unclear under precisely what conditions catecholamines inhibit or augment bacterial growth, because norepinephrine and epinephrine failed to demonstrate uniform effects on bacterial growth (78).

Sepsis and septic shock. One of the most challenging subtypes of shock clinically is the septic shock, which is characterized by impaired functions of heart and vessel tone, despite high concentrations of circulating catecholamines (79). Yet, administration of catecholamines often becomes the choice of last resort to maintain blood pressure in patients with septic shock (80). In an experimental model of sepsis, infusion of epinephrine was associated with profound alterations of cellular immune functions analogous to those observed in hemorrhagic shock: all lymphocyte subsets decreased, while the splenocyte apoptosis rate and number of circulating NK cells increased (81). Moreover, splenocyte proliferation and cytokine release was inhibited, whereas apoptosis-rate of splenic lymphocytes was increased (81). In parallel, infusion of dopamine decreased the survival rate of septic mice. Thus, there seems to be a universal pattern for catecholamine effects during sepsis, which might be modulated by cellular adrenoceptors: splenocytes are driven into apoptosis, lymphocyte counts decrease (perhaps due to apoptosis), while NK cell numbers increase. Dopamine is another commonly used drug to prevent renal failure and treat moderate hypotension in the critically ill (82). Dopamine also is an agonist of α - and β -adrenergic receptors, but exerts its effects mainly via

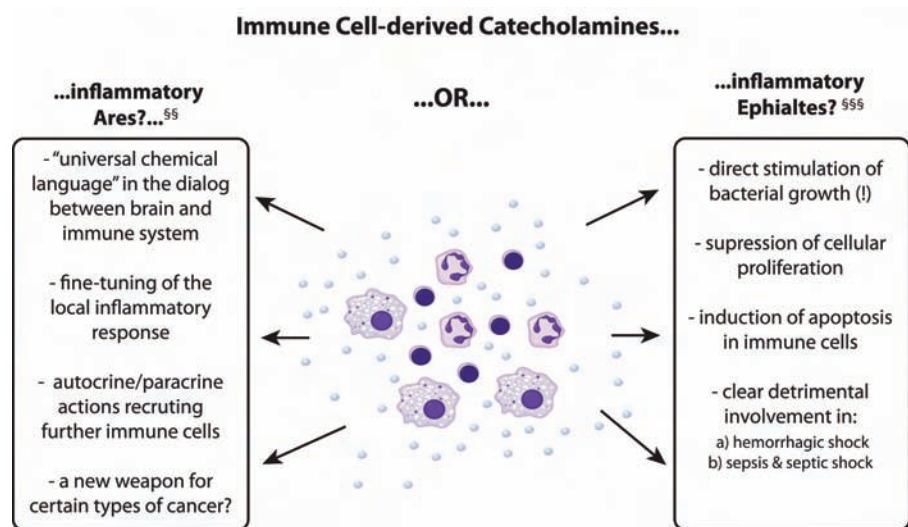


Figure 3. Lymphocyte- and phagocyte-derived catecholamines seem to be a double-edged sword. Some of these bidirectional actions during inflammation are listed.

specific dopaminergic receptors that can be found on a large number of cells including lymphocytes (83). In physiological concentrations, dopamine inhibits the proliferation and cytotoxicity of human CD4⁺ and CD8⁺ lymphocytes in vivo and in vitro via the dopamine receptors (52,84-86), paralleling the adverse effects of epinephrine and norepinephrine.

Lately, the gut has also been identified as an alternate source of catecholamines during sepsis in rodents, releasing norepinephrine into the portal vein and thereby altering the functional state of hepatocytes and Kupffer cells, unexpectedly contributing to hepatocellular dysfunction during sepsis (87-90). This mechanism also seems to be mediated via α_2 -adrenoceptors (88).

Unfortunately, there are only a few human studies investigating the immunomodulatory effects of catecholamines in septic patients. Yet, evidence now is emerging that the pro- and anti-inflammatory "cytokine-/chemokine storm" occurring in septic patients seems to be modulated, at least in part, by epinephrine. In parallel to various animal studies, immunosuppressive actions of catecholamines seem to be co-

regulated by the β -adrenoceptor in humans (91,92). Thus, catecholamines clearly contribute to the severe immunodysregulation occurring during septic shock.

It is important to be aware of these adverse effects of catecholamines in critically ill patients. Although catecholamines are textbook drugs for various settings in patients suffering from severe trauma, hemorrhagic shock, sepsis or septic shock, their administration needs to be evaluated carefully on an individual basis to maximize benefit and minimize adverse effects of catecholamine administration.

Footnote §§: Ares, son of Zeus and Hera, is the Greek God of savage war, bloodlust and slaughter.

Footnote §§§: Ephialtes guided Xerxes' Persian forces around the allied Greek troops who were blocking the pass of Thermopylae in 480 BC, leading to the last stand of the Leonidas and his 500 Spartans. The malicious treacherousness of this ancient character is still being remembered today, as Ephialtes literally means "nightmare" in Modern-Greek.

Or Skilled Hephaestus^{§§§§} Going to Work?

Despite all these potentially harmful actions described above, there are several benefits of endogenous catecholamines (Figure 3). First of all, in addition to neuropeptides, the neuro-endocrine-immune network produces powerful mediators enabling rapid communication and fine-tuning of the nervous, endocrine, and immune systems. A recent report allows a brief foretaste of how exquisite this fine-tuning might in fact be. Blockade of diverse adrenoceptors on rat phagocytes variably inhibited expression of different cytokines and chemokines (11). TNF α production was inhibited completely by blockade of the α_2 -adrenoceptor or high-dose blockade of the β_2 -adrenoceptor, while remaining completely unaffected by α_1 - or β_1 -adrenoceptor blockade. In sharp contrast, IL-1 β levels were suppressed greatly by pharmacological blockade of either α_1 -, α_2 -, β_1 -, or β_2 -adrenoceptors. IL-6 and CINC-1 production by phagocytes was regulated by either α_2 -, β_1 -, or β_2 -adrenoceptors, respectively. Because norepinephrine has higher affinity for the α -adrenergic receptors and epinephrine for β -adrenoceptors, it might well be that these two catecholamines display dissimilar effects on phagocytes which could define a very distinct inflammatory mediator pattern best suited for a particular inflammatory setting. A better understanding of these observations might provide us with many new pharmacological targets to dampen inflammation. Finally,

Footnote §§§§: Hephaestus, son of Zeus and Hera, is the Greek God of technology, blacksmiths, metallurgy and fire. His skilled craftsmanship is thought to have created many of the splendid equipment of the Greek Gods, and most of the power-imbued metalworks that appear in Greek mythology: Hermes' winged helmet and sandals, Aegis' breastplate, Aphrodite's legendary girdle, Achilles' armor, Heracles' bronze clappers, Helios' chariot and Eros' famed bow and arrow.

recent research reports suggest that catecholamines might be cytotoxic for human neuroblastoma cells (93,94). While specific types of cancer might present an appealing new target for catecholamine-dependent immunomodulation, this needs to be further evaluated.

CONCLUSIONS

Besides the adrenomedullary chromaffin cells and neurons, lymphocytes, and phagocytes represent a third category of catecholamine-producing cells. They are able to synthesize and release endogenous catecholamines *de novo* which can modify various pathological responses, all of which challenges traditional paradigms. The wide distribution of immune cells throughout the body, combined with their ability to migrate to the site of inflammation, underscores the dynamic role of immune/inflammatory cells. Targeting lymphocyte/phagocyte-derived catecholamines will pose an extremely challenging quest for researchers. Because catecholamines are not proteins, usage of neutralizing antibodies seem an unlikely strategy. The fact that immune cells utilize the very same molecular pathways as the adrenal medulla and neurons defies classical immunological approaches such as blocking catecholamine-producing enzymes by antibodies or RNA-silencing to inhibit immune/inflammatory cell-derived catecholamines. Moreover, myriad actions of endogenous catecholamines occur inside the cell and perhaps even in the nucleus, further complicating a selective targeting attempt. However, extending our understanding for extra- and intracellular adrenergic regulation of lymphocytes and phagocytes, its implications and its possibilities might deepen our understanding of the pathogenesis of diverse diseases and ultimately might result in great curative advances.

ACKNOWLEDGMENTS

The authors thank Beverly Schumann and Sue Scott for the preparation of this manuscript. This work was supported by NIH grants GM-29507, GM-61656, and

HL-31963, and DOD grant W81XWH-06-2-0044 (P.A.W.) and Deutsche Forschungsgemeinschaft grants DFG HU 823/2-1, DFG HU 823/2-2, and DFG HU 823/2-3 (M.H.-L.).

REFERENCES

1. Sternberg EM. (2006) Neural regulation of innate immunity: a coordinated nonspecific host response to pathogens. *Nat. Rev. Immunol.* 6:318-28.
2. Tracey KJ. (2002) The inflammatory reflex. *Nature.* 420:853-9.
3. Elenkov IJ, Wilder RL, Chrousos GP, Vizi ES. (2000) The sympathetic nerve—an integrative interface between two supersystems: the brain and the immune system. *Pharmacol. Rev.* 52:595-638.
4. Blalock JE. (2005) The immune system as the sixth sense. *J. Intern. Med.* 257:126-38.
5. Straub RH. (2004) Complexity of the bidirectional neuroimmune junction in the spleen. *Trends Pharmacol. Sci.* 25:640-6.
6. Swanson MA, Lee WT, Sanders VM. (2001) IFN-gamma production by Th1 cells generated from naive CD4+ T cells exposed to norepinephrine. *J. Immunol.* 166:232-40.
7. Sanders VM *et al.* (1997) Differential expression of the beta2-adrenergic receptor by Th1 and Th2 clones: implications for cytokine production and B cell help. *J. Immunol.* 158:4200-10.
8. Torres KC *et al.* (2005) Norepinephrine, dopamine and dexamethasone modulate discrete leukocyte subpopulations and cytokine profiles from human PBMC. *J. Neuroimmunol.* 166:144-57.
9. Peng YP, Qiu YH, Jiang JL, Wang JJ. (2004) Effect of catecholamines on IL-2 production and NK cytotoxicity of rats in vitro. *Acta Pharmacol. Sin.* 25:1354-60.
10. Spengler RN, Allen RM, Remick DG, Strieter RM, Kunkel SL. (1990) Stimulation of alpha-adrenergic receptor augments the production of macrophage-derived tumor necrosis factor. *J. Immunol.* 145: 1430-4.
11. Flierl MA *et al.* (2007) Phagocyte-derived catecholamines enhance acute inflammatory injury. *Nature.* 449:721-5.
12. Marino F *et al.* (1999) Endogenous catecholamine synthesis, metabolism storage, and uptake in human peripheral blood mononuclear cells. *Exp. Hematol.* 27:489-95.
13. Bergquist J, Tarkowski A, Ekman R, Ewing A. (1994) Discovery of endogenous catecholamines in lymphocytes and evidence for catecholamine regulation of lymphocyte function via an autocrine loop. *Proc. Natl. Acad. Sci. U. S. A.* 91: 12912-6.
14. Josefsson E, Bergquist J, Ekman R, Tarkowski A. (1996) Catecholamines are synthesized by mouse lymphocytes and regulate function of these cells by induction of apoptosis. *Immunology.* 88:140-6.
15. Bergquist J, Silberring J. (1998) Identification of catecholamines in the immune system by electro-spray ionization mass spectrometry. *Rapid Commun. Mass Spectrom.* 12:683-8.
16. Bergquist J, Josefsson E, Tarkowski A, Ekman R, Ewing A. (1997) Measurements of catecholamine-mediated apoptosis of immunocompetent cells by capillary electrophoresis. *Electrophoresis.* 18: 1760-6.
17. Freeman JG *et al.* (2001) Catecholamines in murine bone marrow derived mast cells. *J. Neuroimmunol.* 119:231-8.
18. Spengler RN, Chensue SW, Giacherio DA, Blenk N, Kunkel SL. (1994) Endogenous norepinephrine regulates tumor necrosis factor-alpha production from macrophages in vitro. *J. Immunol.* 152:3024-31.
19. Brown SW *et al.* (2003) Catecholamines in a macrophage cell line. *J. Neuroimmunol.* 135:47-55.
20. Warthan MD *et al.* (2002) Phenylethanolamine N-methyl transferase expression in mouse thymus and spleen. *Brain Behav. Immun.* 16:493-9.
21. Cosentino M *et al.* (2000) HPLC-ED measurement of endogenous catecholamines in human immune cells and hematopoietic cell lines. *Life Sci.* 68:283-95.
22. Qiu YH, Cheng C, Dai L, Peng YP. (2005) Effect of endogenous catecholamines in lymphocytes on lymphocyte function. *J. Neuroimmunol.* 167:45-52.
23. Qiu YH, Peng YP, Jiang JM, Wang JJ. (2004) Expression of tyrosine hydroxylase in lymphocytes and effect of endogenous catecholamines on lymphocyte function. *Neuroimmunomodulation.* 11:75-83.
24. Cosentino M *et al.* (2002) Stimulation with phytohaemagglutinin induces the synthesis of catecholamines in human peripheral blood mononuclear cells: role of protein kinase C and contribution of intracellular calcium. *J. Neuroimmunol.* 125:125-33.
25. Musso NR, Breni S, Setti M, Indiveri F, Lotti G. (1996) Catecholamine content and in vitro catecholamine synthesis in peripheral human lymphocytes. *J. Clin. Endocrinol. Metab.* 81:3553-7.
26. Chritton SL *et al.* (1997) Adrenomedullary secretion of DOPA, catecholamines, catechol metabolites, and neuropeptides. *J. Neurochem.* 69:2413-20.
27. Molinoff PB, Axelrod J. (1971) Biochemistry of catecholamines. *Annu. Rev. Biochem.* 40:465-500.
28. Shore PA. (1972) Transport and storage of biogenic amines. *Annu. Rev. Pharmacol.* 12:209-26.
29. Cosentino M *et al.* (2005) Interferon-gamma and interferon-beta affect endogenous catecholamines in human peripheral blood mononuclear cells: implications for multiple sclerosis. *J. Neuroimmunol.* 162:112-21.
30. Kilpatrick DL, Slepets RJ, Corcoran JJ, Kirshner N. (1982) Calcium uptake and catecholamine secretion by cultured bovine adrenal medulla cells. *J. Neurochem.* 38:427-35.
31. Musso NR, Breni S, Indiveri F, Lotti G. (1998) Acetylcholine-induced, calcium-dependent norepinephrine outflow from peripheral human lymphocytes. *J. Neuroimmunol.* 87:82-7.
32. Axelsson J. (1971) Catecholamine functions. *Annu. Rev. Physiol.* 33:1-30.
33. Zhu BT. (2002) Catechol-O-Methyltransferase (COMT)-mediated methylation metabolism of

- endogenous bioactive catechols and modulation by endobiotics and xenobiotics: importance in pathophysiology and pathogenesis. *Curr. Drug Metab.* 3:321-49.
34. Balsa MD, Gomez N, Unzeta M. (1989) Characterization of monoamine oxidase activity present in human granulocytes and lymphocytes. *Biochim. Biophys. Acta.* 992:140-4.
 35. Faraj BA, Olkowski ZL, Jackson RT. (1991) Binding of [3H]-dopamine to human lymphocytes: possible relationship to neurotransmitter uptake sites. *Pharmacology.* 42:135-41.
 36. Faraj BA., Olkowski ZL, Jackson RT. (1995) A cocaine-sensitive active dopamine transport in human lymphocytes. *Biochem. Pharmacol.* 50:1007-14.
 37. Mill J, Asherson P, Browes C, D'Souza U, Craig I. (2002) Expression of the dopamine transporter gene is regulated by the 3' UTR VNTR: Evidence from brain and lymphocytes using quantitative RT-PCR. *Am. J. Med. Genet.* 114:975-9.
 38. Amenta F *et al.* (2001) Identification of dopamine plasma membrane and vesicular transporters in human peripheral blood lymphocytes. *J. Neuroimmunol.* 117:133-42.
 39. Cosentino M *et al.* (2003) Unravelling dopamine (and catecholamine) physiopharmacology in lymphocytes: open questions. *Trends Immunol.* 24:581-2; author reply 582-3.
 40. Gordon J, Barnes NM. (2003) Lymphocytes transport serotonin and dopamine: agony or ecstasy? *Trends Immunol.* 24:438-43.
 41. Bidart JM, Motte P, Assicot M, Bohuon C, Bellet D. (1983) Catechol-O-methyltransferase activity and amergic binding sites distribution in human peripheral blood lymphocyte subpopulations. *Clin. Immunol. Immunopathol.* 26:1-9.
 42. Madden KS, Sanders VM, Felten DL. (1995) Catecholamine influences and sympathetic neural modulation of immune responsiveness. *Annu. Rev. Pharmacol. Toxicol.* 35:417-48.
 43. Sanders VM, Kohm AP. (2002) Sympathetic nervous system interaction with the immune system. *Int. Rev. Neurobiol.* 52:17-41.
 44. Sanders VM, Straub RH. (2002) Norepinephrine, the beta-adrenergic receptor, and immunity. *Brain Behav. Immun.* 16:290-332.
 45. Ottaway CA, Husband AJ. (1994) The influence of neuroendocrine pathways on lymphocyte migration. *Immunol. Today.* 15:511-7.
 46. Loeper M, Crouzon O. (1904) L'action de l'adrénaline sur le sang. *Arch. Med. Exp. Anat. Pathol.* 16:83-108.
 47. Zoukos Y *et al.* (1994) Increased expression of high affinity IL-2 receptors and beta-adrenoceptors on peripheral blood mononuclear cells is associated with clinical and MRI activity in multiple sclerosis. *Brain.* 117(Pt 2):307-15.
 48. Rouppe van der Voort C, Kavelaars A., van de Pol M, Heijnen CJ. (2000) Noradrenaline induces phosphorylation of ERK-2 in human peripheral blood mononuclear cells after induction of alpha(1)-adrenergic receptors. *J. Neuroimmunol.* 108:82-91.
 49. Ghosh MC *et al.* (2003) Dopamine inhibits cytokine release and expression of tyrosine kinases, Lck and Fyn in activated T cells. *Int. Immunopharmacol.* 3: 1019-26.
 50. Levite M *et al.* (2001) Dopamine interacts directly with its D3 and D2 receptors on normal human T cells, and activates beta1 integrin function. *Eur. J. Immunol.* 31:3504-12.
 51. Cosentino, M *et al.* (2007) Human CD4+CD25+ regulatory T cells selectively express tyrosine hydroxylase and contain endogenous catecholamines subserving an autocrine/paracrine inhibitory functional loop. *Blood.* 109:632-42.
 52. Saha B, Mondal AC, Majumder J, Basu S, Dasgupta PS. (2001) Physiological concentrations of dopamine inhibit the proliferation and cytotoxicity of human CD4+ and CD8+ T cells in vitro: a receptor-mediated mechanism. *Neuroimmunomodulation.* 9:23-33.
 53. Kipnis J *et al.* (2004) Dopamine, through the extracellular signal-regulated kinase pathway, downregulates CD4+CD25+ regulatory T-cell activity: implications for neurodegeneration. *J. Neurosci.* 24:6133-43.
 54. Van Tits LJ *et al.* (1990) Catecholamines increase lymphocyte beta 2-adrenergic receptors via a beta 2-adrenergic, spleen-dependent process. *Am. J. Physiol.* 258:E191-202.
 55. Anstead MI, Hunt TA, Carlson SL, Burki NK. (1998) Variability of peripheral blood lymphocyte beta-2-adrenergic receptor density in humans. *Am. J. Respir. Crit. Care Med.* 157:990-2.
 56. Besser MJ, Ganor Y, Levite M. (2005) Dopamine by itself activates either D2, D3 or D1/D5 dopaminergic receptors in normal human T-cells and triggers the selective secretion of either IL-10, TNFalpha or both. *J. Neuroimmunol.* 169:161-71.
 57. McKenna F *et al.* (2002) Dopamine receptor expression on human T- and B-lymphocytes, monocytes, neutrophils, eosinophils and NK cells: a flow cytometric study. *J. Neuroimmunol.* 132:34-40.
 58. Pierce KL, Premont RT, Lefkowitz RJ. (2002) Seven-transmembrane receptors. *Nat. Rev. Mol. Cell Biol.* 3:639-50.
 59. Engler KL, Rudd ML, Ryan JJ, Stewart JK, Fischer-Stenger K. (2005) Autocrine actions of macrophage-derived catecholamines on interleukin-1 beta. *J. Neuroimmunol.* 160:87-91.
 60. Starkie RL, Rolland J, Febbraio MA. (2001) Effect of adrenergic blockade on lymphocyte cytokine production at rest and during exercise. *Am. J. Physiol. Cell Physiol.* 281:C1233-40.
 61. Borovikova LV *et al.* (2000) Vagus nerve stimulation attenuates the systemic inflammatory response to endotoxin. *Nature.* 405:458-62.
 62. Wang H *et al.* (2003) Nicotinic acetylcholine receptor alpha7 subunit is an essential regulator of inflammation. *Nature.* 421:384-8.
 63. Tracey KJ. (2007) Physiology and immunology of the cholinergic antiinflammatory pathway. *J. Clin. Invest.* 117:289-96.
 64. Cosentino M *et al.* (2004) Dopaminergic modulation of oxidative stress and apoptosis in human peripheral blood lymphocytes: evidence for a D1-like receptor-dependent protective effect. *Free Radic. Biol. Med.* 36:1233-40.
 65. Del Rio MJ, Velez-Pardo C. (2002) Monoamine neurotoxins-induced apoptosis in lymphocytes by a common oxidative stress mechanism: involvement of hydrogen peroxide (H₂O₂), caspase-3, and nuclear factor kappa-B (NF-kappaB), p53, c-Jun transcription factors. *Biochem. Pharmacol.* 63:677-88.
 66. Jones DC, Gunasekar PG, Borowitz JL, Isom GE. (2000) Dopamine-induced apoptosis is mediated by oxidative stress and is enhanced by cyanide in differentiated PC12 cells. *J. Neurochem.* 74: 2296-304.
 67. Burke WJ, Kristal BS, Yu BP, Li SW, Lin TS. (1998) Norepinephrine transmitter metabolite generates free radicals and activates mitochondrial permeability transition: a mechanism for DOPEGAL-induced apoptosis. *Brain Res.* 787:328-32.
 68. Buu NT. (1993) Uptake of 1-methyl-4-phenylpyridinium and dopamine in the mouse brain cell nuclei. *J. Neurochem.* 61:1557-60.
 69. Bergquist J, Ohlsson B, Tarkowski A. (2000) Nuclear factor-kappa B is involved in the catecholaminergic suppression of immunocompetent cells. *Ann. N. Y. Acad. Sci.* 917:281-9.
 70. Oberbeck R *et al.* (2002) Influence of beta-adrenoceptor antagonists on hemorrhage-induced cellular immune suppression. *Shock.* 18:331-5.
 71. Cunnick JE, Lysle DT, Kucinski BJ, Rabin BS. (1990) Evidence that shock-induced immune suppression is mediated by adrenal hormones and peripheral beta-adrenergic receptors. *Pharmacol. Biochem. Behav.* 36:645-51.
 72. Molina PE. (2001) Noradrenergic inhibition of TNF upregulation in hemorrhagic shock. *Neuroimmunomodulation.* 9:125-33.
 73. Molina PE, Abumrad NN. (1999) Central sympathetic modulation of tissue cytokine response to hemorrhage. *Neuroimmunomodulation.* 6:193-200.
 74. Lyte M, Bailey MT. (1997) Neuroendocrine-bacterial interactions in a neurotoxin-induced model of trauma. *J. Surg. Res.* 70:195-201.
 75. Freestone PP *et al.* (2002) Growth stimulation of intestinal commensal *Escherichia coli* by catecholamines: a possible contributory factor in trauma-induced sepsis. *Shock.* 18:465-70.
 76. Lyte M., Frank CD, Green BT. (1996) Production of an autoinducer of growth by norepinephrine cultured *Escherichia coli* O157:H7. *FEMS Microbiol. Lett.* 139:155-9.
 77. Kinney KS, Austin CE, Morton DS, Sonnenfeld G. (2000) Norepinephrine as a growth stimulating factor in bacteria-mechanistic studies. *Life Sci.* 67: 3075-85.
 78. Belay T, Sonnenfeld G. (2002) Differential effects of catecholamines on in vitro growth of pathogenic bacteria. *Life Sci.* 71:447-56.
 79. Annane D *et al.* (1999) Inappropriate sympathetic activation at onset of septic shock: a spectral analysis approach. *Am J Respir Crit Care Med.* 160: 458-65.

80. Annane D, Bellissant E, Cavaillon JM. (2005) Septic shock. *Lancet*. 365:63-78.
81. Oberbeck R *et al.* (2004) Adrenergic modulation of survival and cellular immune functions during polymicrobial sepsis. *Neuroimmunomodulation*. 11:214-23.
82. Oberbeck R. (2006) Catecholamines: physiological immunomodulators during health and illness. *Curr. Med. Chem*. 13:1979-89.
83. Basu S, Dasgupta PS. (2000) Dopamine, a neurotransmitter, influences the immune system. *J. Neuroimmunol*. 102:113-24.
84. Tsao CW, Lin YS, Cheng JT. (1997) Effect of dopamine on immune cell proliferation in mice. *Life Sci*. 61:PL 361-71.
85. Beck G *et al.* (2004) Clinical review: immunomodulatory effects of dopamine in general inflammation. *Crit. Care*. 8:485-91.
86. McCorkle FM, Taylor RL Jr. (1994) Continuous administration of dopamine alters cellular immunity in chickens. *Comp. Biochem. Physiol. C. Pharmacol. Toxicol. Endocrinol*. 109:289-93.
87. Yang S, Koo DJ, Zhou M, Chaudry IH, Wang P. (2000) Gut-derived norepinephrine plays a critical role in producing hepatocellular dysfunction during early sepsis. *Am. J. Physiol. Gastrointest. Liver Physiol*. 279:G1274-81.
88. Yang S, Zhou M, Chaudry IH, Wang P. (2001) Norepinephrine-induced hepatocellular dysfunction in early sepsis is mediated by activation of alpha2-adrenoceptors. *Am. J. Physiol. Gastrointest. Liver Physiol*. 281:G1014-21.
89. Zhou M, Das P, Simms HH, Wang P. (2005) Gut-derived norepinephrine plays an important role in up-regulating IL-1beta and IL-10. *Biochim. Biophys. Acta*. 1740:446-52.
90. Zhou M, Hank Simms H, Wang P. (2004) Increased gut-derived norepinephrine release in sepsis: up-regulation of intestinal tyrosine hydroxylase. *Biochim. Biophys. Acta*. 1689:212-8.
91. Bergmann M *et al.* (1999) Attenuation of catecholamine-induced immunosuppression in whole blood from patients with sepsis. *Shock*. 12:421-7.
92. Bergmann M, Sautner T. (2002) Immunomodulatory effects of vasoactive catecholamines. *Wien. Klin. Wochenschr*. 114:752-61.
93. Chan AS, Ng LW, Poon LS, Chan WW, Wong YH. (2007) Dopaminergic and adrenergic toxicities on SK-N-MC human neuroblastoma cells are mediated through G protein signaling and oxidative stress. *Apoptosis*. 12:167-79.
94. Moussa CE, Tomita Y, Sidhu A. (2006) Dopamine D1 receptor-mediated toxicity in human SK-N-MC neuroblastoma cells. *Neurochem. Int*. 48:226-34.

Cross-Talk between TLR4 and Fc γ ReceptorIII (CD16) Pathways

Daniel Rittirsch^{1,2}, Michael A. Flierl¹, Danielle E. Day¹, Brian A. Nadeau¹, Firas S. Zetoune¹, J. Vidya Sarma¹, Clement M. Werner², Guido A. Wanner², Hans-Peter Simmen², Markus S. Huber-Lang³, Peter A. Ward^{1*}

1 Department of Pathology, University of Michigan Medical School, Ann Arbor, Michigan, United States of America, **2** Department of Traumatology, University Hospital Zurich, Zurich, Switzerland, **3** Department of Traumatology, Hand-, Plastic-, and Reconstructive Surgery, University Hospital Ulm, Ulm, Germany

Abstract

Pathogen-pattern-recognition by Toll-like receptors (TLRs) and pathogen clearance after immune complex formation via engagement with Fc receptors (FcRs) represent central mechanisms that trigger the immune and inflammatory responses. In the present study, a linkage between TLR4 and Fc γ R was evaluated *in vitro* and *in vivo*. Most strikingly, *in vitro* activation of phagocytes by IgG immune complexes (IgGIC) resulted in an association of TLR4 with Fc γ RIII (CD16) based on co-immunoprecipitation analyses. Neutrophils and macrophages from TLR4 mutant (mut) mice were unresponsive to either lipopolysaccharide (LPS) or IgGIC *in vitro*, as determined by cytokine production. This phenomenon was accompanied by the inability to phosphorylate tyrosine residues within immunoreceptor tyrosine-based activation motifs (ITAMs) of the FcR γ -subunit. To transfer these findings *in vivo*, two different models of acute lung injury (ALI) induced by intratracheal administration of either LPS or IgGIC were employed. As expected, LPS-induced ALI was abolished in TLR4 mut and TLR4^{-/-} mice. Unexpectedly, TLR4 mut and TLR4^{-/-} mice were also resistant to development of ALI following IgGIC deposition in the lungs. In conclusion, our findings suggest that TLR4 and Fc γ RIII pathways are structurally and functionally connected at the receptor level and that TLR4 is indispensable for Fc γ RIII signaling via FcR γ -subunit activation.

Citation: Rittirsch D, Flierl MA, Day DE, Nadeau BA, Zetoune FS, et al. (2009) Cross-Talk between TLR4 and Fc γ ReceptorIII (CD16) Pathways. PLoS Pathog 5(6): e1000464. doi:10.1371/journal.ppat.1000464

Editor: Danny C. Douek, NIH/NIAID, United States of America

Received: October 31, 2008; **Accepted:** May 4, 2009; **Published:** June 5, 2009

Copyright: © 2009 Rittirsch et al. This is an open-access article distributed under the terms of the Creative Commons Attribution License, which permits unrestricted use, distribution, and reproduction in any medium, provided the original author and source are credited.

Funding: This work was supported by National Institutes of Health grants GM-29507, GM-61656 (www.nigms.nih.gov) and HL-31963 (www.nhlbi.nih.gov) to PAW, and German Research Foundation grant HU 823/2-2 (www.dfg.de) to MSH-L. The funders had no role in study design, data collection and analysis, decision to publish, or preparation of the manuscript.

Competing Interests: The authors have declared that no competing interests exist.

* E-mail: pward@umich.edu

Introduction

The immune system is traditionally divided into innate and adaptive entities. Adaptive immunity is organized around T cells and B cells and requires a process of maturation and clonal selection of lymphocytes. In contrast, innate immunity can be immediately activated during the onset of infection in order to control replication of pathogenic microbes and bring about their clearance from tissues or blood. As an important aspect of innate immunity, pattern-recognition receptors (PRRs) collectively recognize lipid, carbohydrate, peptide, and nucleic-acid structures of invading microorganisms [1]. PRRs comprise the toll-like receptor family (TLR), which consists of at least 12 different evolutionarily conserved membrane proteins that trigger innate immune responses [2]. Initially identified in 1997, TLR4 represents the most thoroughly investigated TLR [3]. TLR4 is essential for responses to bacterial lipopolysaccharide (LPS), a well-known pathogen-associated molecular pattern (PAMP) [3,4]. Besides LPS, various endogenous ligands, such as hyaluronan and high mobility group box 1 protein (HMGB1), appear to engage TLR4 [5,6]. After binding of LPS to the TLR4/MD-2/CD14 receptor complex, activation of the intracellular signaling pathway is initiated, ultimately leading to NF- κ B activation and its translocation to the nucleus, resulting in subsequent cytokine/chemokine production and release [7].

As part of the adaptive immune system, antibodies of high affinity binding specifically recognize and neutralize intruding pathogens or their products. After antibody binding to antigen, the Fc domain of immunoglobulin (Ig) is recognized by Fc receptors (FcRs) which are predominantly expressed on immune and inflammatory cells and thereby link antibody-mediated (humoral) immune responses to cellular effector functions [8,9]. Specific FcRs exist for all classes of immunoglobulins. Binding of IgGs to Fc γ Rs on phagocytes triggers a wide variety of cellular functions including phagocytosis, release of inflammatory mediators, and clearance of immune complexes [8]. Fc γ Rs specifically bind IgG and are divided into four subclasses. Fc γ RI (CD64), Fc γ RIII (CD16), and Fc γ RIV are activating receptors, while Fc γ RII (CD32) mediates inhibitory functions. The cellular response is determined by the balance between activating (ITAM, immunoreceptor tyrosine-based activation motif) and inhibitory (ITIM, immunoreceptor tyrosine-based inhibitory motif) signals [10,11,12,13].

Despite extensive research in the past, the highly complex regulation of innate and adaptive immunity and their interactions are still poorly understood. It has been suggested that adaptive immune responses are controlled by innate immune recognition and vice versa [14,15,16]. In particular, TLRs and Fc γ Rs are considered to be important regulators of immune responses [13,17]. Recently, evidence has emerged that there is indirect interaction between TLR4 and Fc γ R pathways. TLR4 has been

Author Summary

The immune system is traditionally divided into innate and adaptive entities. Pattern-recognition receptors (PRRs) collectively recognize molecular structures of invading microorganisms, followed by initiation of immune responses. PRRs comprise the toll-like receptor (TLR) family, including TLR4, which is essential for responses to bacterial lipopolysaccharide (LPS). As part of the adaptive immune system, Fc receptors (FcRs) on immune cells recognize antigen-antibody complexes and link antibody-mediated immune responses to cellular effector functions. Here, we describe cross-talk between the pathogen-recognition-receptor toll-like receptor 4 (TLR4) and receptors for IgG immune complexes (IgGIC), Fcγ receptors (FcγRs). We found that TLR4 is involved in FcγRIII (CD16) signaling and that heterodimerization of TLR4 and FcγRIII occurs in the presence of IgGIC but not LPS. Consequently, dysfunctional TLR4 signaling results in unresponsiveness of immune cells *in vitro* to both LPS and IgGIC, resulting in absence of acute lung injury after intratracheal administration of LPS or intrapulmonary immune complex deposition. In summary, we describe that TLR4 and FcγRIII pathways are structurally and functionally connected. These findings provide new insights of the interplay between innate and adaptive immunity, which closely interact with each other at the receptor level and post receptor signaling pathways.

shown to up-regulate FcγR expression in experimental immune complex arthritis; inhibition of TLR4 resulted in attenuation of *in vivo* cytokine release in models of glomerulonephritis and rheumatoid arthritis [18,19,20]. In the present study, we addressed the question as to whether there is a direct link between TLR4 and FcγR pathways *in vitro* and *in vivo*.

Results

Exclusion of LPS Contamination of Reagents

In the past, the investigation of TLR4 faced the problem of LPS contamination, which imposed considerable restrictions on the interpretation of data [5]. Therefore, the LPS concentration was determined in reagents used for lung injury induction by deposition of IgG immune complexes (IgGIC), such as DPBS, anti-BSA IgG and BSA, although none of these reagents had been prepared using bacterial (*E.coli*) systems. Using Limulus Amebocyte Lysate Kinetic-QCL assay, LPS levels were not detectable ($<5 \times 10^{-3}$ units/ml) in any of the reagents (data not shown), suggesting that *in vitro* stimulation by IgGIC is based upon a genuine agonist effect that is not due to LPS contamination. In addition to determination of LPS contamination (see above), DPBS, anti-BSA IgG and BSA were subjected to endotoxin removal by solid-phase polymyxin. Using the polymyxin-treated reagents, immune complexes were generated and then applied in *in vitro* experiments or the reagents were administered in mice for the formation of immune complexes *in vivo*. Furthermore, commercially available, preformed peroxidase/anti-peroxidase immune complexes (PAP IgGIC) were used at the same concentration in order to confirm the results using BSA IgGIC or polymyxin-treated BSA IgGIC. The results of both, polymyxin-treated BSA IgGIC and PAP IgGIC, are presented in the corresponding figures. In summary, using different *in vitro* and *in vivo* approaches, it is highly unlikely that any of the effects following IgGIC stimulation in the present study are based on LPS contamination of the reagents.

Association between TLR4 and FcγRIII after IgG Immune Complex Activation

In order to assess whether crosstalk between TLR4 and FcγR might occur at the receptor level, neutrophils (PMNs) and macrophages from wild-type (Wt) mice were incubated *in vitro* with IgGIC, LPS, or the combination of the two. After incubation, cell lysates were immunoprecipitated (IP) with anti-TLR4 and then analyzed for FcγRII/III by immunoblotting (IB). As shown in Figure 1A,B, immunoprecipitated TLR4 was associated with FcγR after cell exposure to IgGIC. Inversely, LPS incubation did not result in an association of both receptors as indicated by the absence of bands for FcγR, whereas the combination of LPS+IgGIC seemed to enhance the signal for FcγR co-immunoprecipitated by anti-TLR4 IgG (Figure 1A,B). The band for FcγR under the conditions described above indicated a protein mass of 55 kDa, in accord with the reported molecular weight for FcγRIII [21,22]. In contrast, there was no band at the 40 kDa position (data not shown), the molecular weight of FcγRII, which is also recognized by the anti-FcγR antibody (mAb, clone 2.4G2) used for Western blot analyses [23,24]. In accord with Figure 1A,B, reverse direction immunoprecipitation using FcγRIII antibody followed TLR4 Western blots revealed bands at around 90 kDa, consistent with the reported molecular weight of TLR4 (Figure 1C,D). However, under these conditions bands also occurred after stimulation of phagocytes with LPS (Figure 1C,D), which may suggest that FcγRIII and TLR4 heterodimerize upon LPS stimulation, although to a lesser extent as compared to IgGIC treated cells. When PMNs and macrophages from FcγRIII^{-/-} mice were exposed to the same *in vitro* conditions (IgGIC, LPS, LPS+IgGIC), the band for FcγRIII failed to appear, confirming its specificity (Figure 1E,F). In order to examine whether the interaction between TLR4 and FcγRIII was specific for these two receptors or whether there also might be multimerization with other TLRs or Fc receptors, lysates from Wt phagocytic cells under various conditions (see above) were subjected to immunoprecipitation with anti-TLR6 or anti-CD23 (anti-FcεRII), followed by Western blots for FcγRIII or TLR4, respectively (Figure 1G–J). In both combinations, specific bands for either FcγRIII (after immunoprecipitation with anti-TLR6; Figure 1G,H) or TLR4 (immunoprecipitation of cell lysates with anti-TLR6; Figure 1I,J) failed to appear, whereas the strong bands in the lower panels (loading controls) demonstrate that immunoprecipitation of the samples worked properly. In addition, macrophages from Wt mice were incubated with polymyxin-treated BSA IgGIC and PAP IgGIC, followed by immunoprecipitation with anti-TLR4 and Western blotting with anti-FcγRIII. As shown in Figure 1K, receptor heterodimerization occurred under these conditions as well, confirming the results shown in Figure 1A,B.

In summary, these findings indicate that association of TLR4 and FcγRIII occurs following activation of phagocytes with IgGIC and/or LPS and that this receptor association is a specific phenomenon for FcγRIII and TLR4.

Attenuated *In Vitro* Cytokine Production by TLR4 Mutant PMNs and Macrophages Following IgGIC or LPS Exposure

Elicited peritoneal neutrophils (PMNs) and macrophages were obtained from Wt and TLR4 mut mice. The cells were incubated *in vitro* with IgGIC or LPS. Subsequently, supernatant fluids were collected and evaluated by ELISA for interleukin-6 (IL-6) and tumour necrosis factor alpha (TNFα) levels (Figure 2). PMNs from Wt mice showed significant release of IL-6 and TNFα after exposure to either IgGIC or LPS. In the case of TLR4 mut PMNs, cytokine responses to IgGIC or LPS were lost (Figure 2A–D).

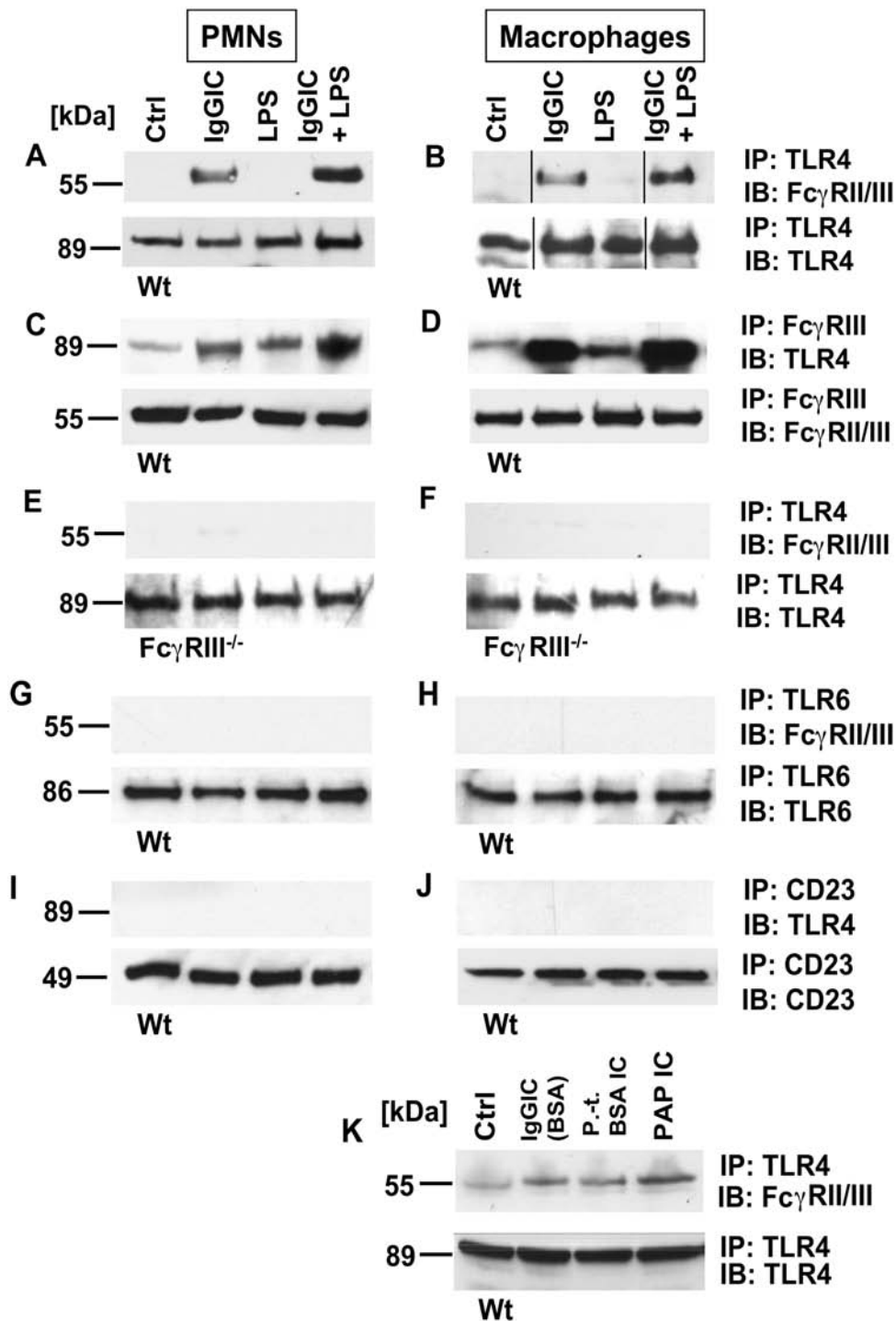


Figure 1. Association between TLR4 and FcγRIII. Peritoneal PMNs and macrophages (3×10^6 cells/ml) from Wt mice and Fcγ-subunit^{-/-} mice were incubated *in vitro* for 30 min with either IgG immune complexes (IgGIC; 100 μg/ml), LPS (20 ng/ml), or the combination. (A,B) Western blot analysis (IB) for FcγRIII of Wt PMN or macrophage lysates co-immunoprecipitated (IP) with anti-TLR4. (C,D) Reverse direction immunoprecipitation using anti-FcγRIII/III IgG followed by Western blot analysis for TLR4. (E,F) Western blot analysis for FcγRIII of PMNs or macrophages from FcγRIII^{-/-} co-immunoprecipitated (IP) with anti-TLR4. (G,H) Samples were immunoprecipitated with anti-TLR6 IgG and probed for FcγRIII. (I,J) Immunoprecipitation with anti-CD23 followed by Western blots using anti-TLR4 IgG. (K) Western blots (IB) of cell lysates of Wt macrophages that were incubated for 30 min with BSA IgG immune complexes (IgGIC; 100 μg/ml), polymyxin-treated BSA IgG immune complexes (p.-t. BSA IC; 100 μg/ml) or peroxidase/anti-peroxidase IgGIC immune complexes (PAP IC; 100 μg/ml). IB for FcγRIII of Wt macrophage lysates co-immunoprecipitated (IP) with anti-TLR4. Corresponding loading controls are displayed in lower panels.
doi:10.1371/journal.ppat.1000464.g001

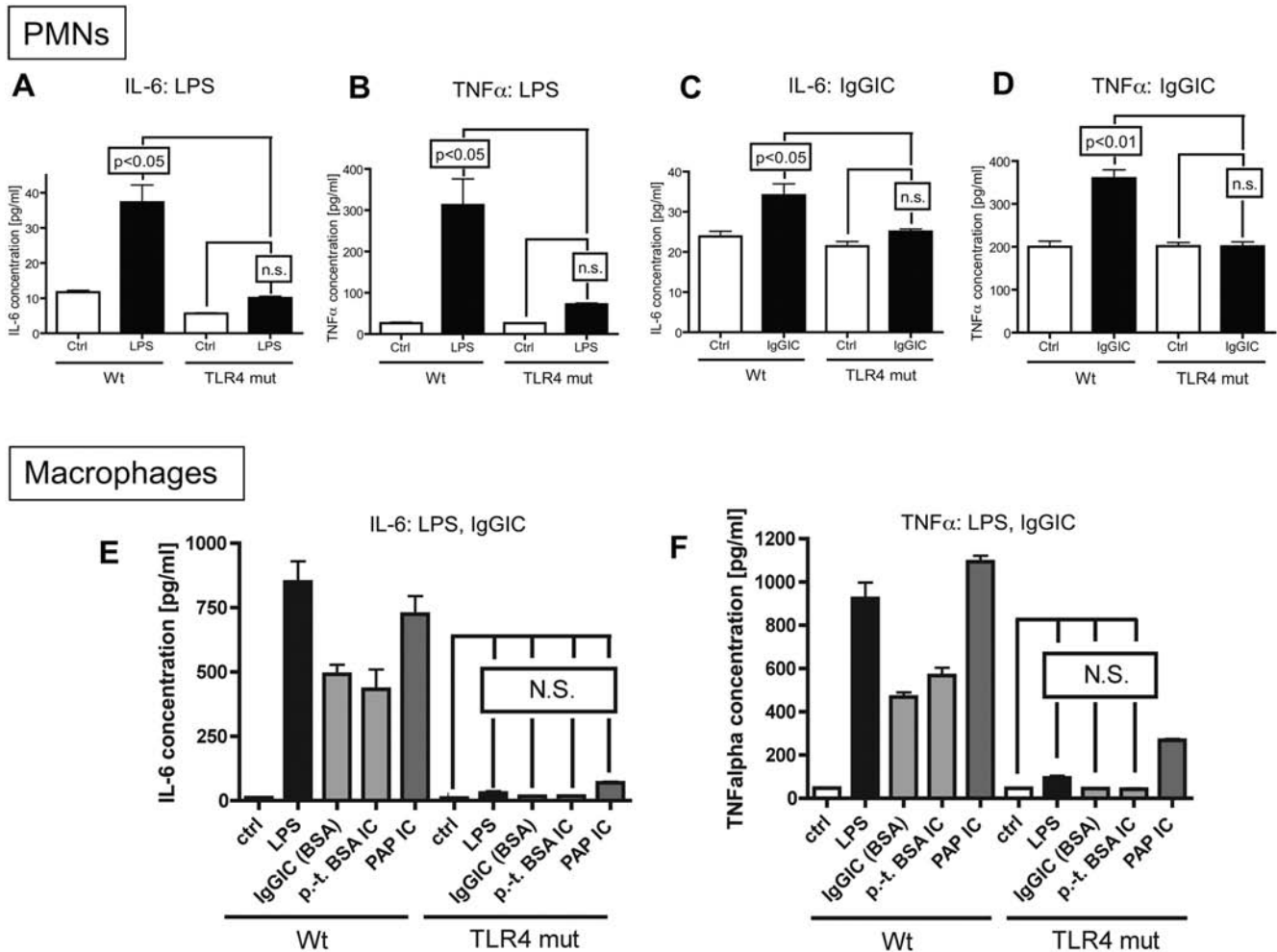


Figure 2. *In vitro* cytokine responses of elicited peritoneal PMNs and macrophages to LPS and IgGIC. *In vitro* cytokine responses of elicited peritoneal PMNs (A–D) and macrophages (E,F). Cells (3×10^6 cells/ml) from either Wt or TLR4 mut mice were incubated for 4 hr with LPS (20 ng/ml) or IgGIC (100 μ g/ml), respectively. In addition, macrophages were incubated with polymyxin-treated BSA IgG immune complexes (p.-t. BSA IC, 100 μ g/ml) or peroxidase/anti-peroxidase IgGIC immune complexes (PAP IC, 100 μ g/ml). (A) IL-6 release from PMNs after LPS stimulation. (B) TNF α levels after incubation of PMNs with LPS. (C) Concentration of IL-6 in supernatants when PMNs were exposed to IgGIC. (D) Production of TNF α by PMNs and macrophages in the presence of IgGIC. Ctrl = control levels of non-stimulated cells. (E) Release of IL-6 by macrophages into supernatant fluids after stimulation with LPS, IgGIC, p.-t. BSA IC, or PAP IC. (F) TNF α production by macrophages exposed to LPS, IgGIC, p.-t. BSA IC, or PAP IC. The experiments were performed in triplicates for each condition (each bar) with $n \geq 3$ donors of cells for each mouse strain, Wt or TLR4 mut. Differences between controls and stimulated cells were—if not otherwise noted—statistically significant ($p < 0.05$). doi:10.1371/journal.ppat.1000464.g002

When peritoneal macrophages were employed in the same protocol, similar results were found (Figure 2E,F). There was a 4-fold increase in IL-6 after exposure of Wt macrophages to LPS, and a 3-fold increase in IL-6 after IgGIC exposure (Figure 2E). Likewise, there was a robust release of TNF α by Wt macrophages into supernatant fluids after stimulation with IgGIC or LPS. When TLR4 mut macrophages were used under the same conditions, IL-6 and TNF α responses to IgGIC or LPS were greatly abolished (Figure 2E,F). Similar results were found when macrophages were incubated with polymyxin-treated BSA IgGIC or PAP IgGIC indicating that the results are reproducible and not based on LPS contamination of the reagents (Figure 2E,F). Thus, the lack of a functional TLR4 is associated with the *in vitro* inability of PMNs and macrophages to respond to LPS or IgGIC.

In order to assess if the impaired response of TLR4 mut cells observed *in vitro* might be due to a general impairment of the inflammatory response, peritoneal PMNs and macrophages from Wt and TLR4 mut mice were exposed to opsonized zymosan

particles as well as to Pam3Cys, which is a specific ligand for TLR2 [25,26,27]. As displayed in Figure S1, Wt cells showed a significant increase of IL-6 (Figure S1A,C,E,G) and TNF α (Figure S1B,D,F,H) release when incubated *in vitro* with Pam3Cys or opsonized zymosan particles. In contrast to the findings described above (incubation with LPS or IgGIC), PMNs (Figure S1A–D) and macrophages (Figure S1E–H) from TLR4 mut mice showed full responses for IL-6 and TNF α when incubated with opsonized zymosan particles or Pam3Cys. These data indicate that the ability to produce cytokines in response to non-TLR4 agonists is intact in TLR4 mut cells and that the impairment of the inflammatory response to LPS and IgGIC is specific for the non-functional TLR4 protein.

In another set of experiments, cells from Fc γ RIII-deficient mice were tested for responsiveness to LPS. Peritoneal PMNs and macrophages from Wt and Fc γ RIII $^{-/-}$ were incubated with LPS and opsonized zymosan (as a positive control) under the same conditions described above and supernatant fluids were analyzed for IL-6 and TNF α levels by ELISA. As shown in Figure 3,

phagocytes from FcγRIII^{+/+} and FcγRIII^{-/-} mice robustly produced cytokines when incubated with LPS, opsonized zymosan or IgGIC. There was no difference in cytokine secretion between the FcγRIII^{+/+} and FcγRIII^{-/-} cells, except for LPS-induced TNFα release by FcγRIII^{-/-} PMNs, which was lower as compared to FcγRIII^{+/+} PMNs, but significantly elevated above baseline levels. As expected, FcγRIII^{+/+} macrophages robustly

released IL-6 and TNFα into supernatant fluids when stimulated with IgGIC, whereas macrophages from FcγRIII^{-/-} mice were unresponsive to IgGIC (Figure 3C,D).

These results suggest that FcγRIII-deficient phagocytes can respond to LPS and that FcγRIII is not required for direct TLR4 signaling, while FcγRIII is essential for the mediation of IgGIC-induced responses.

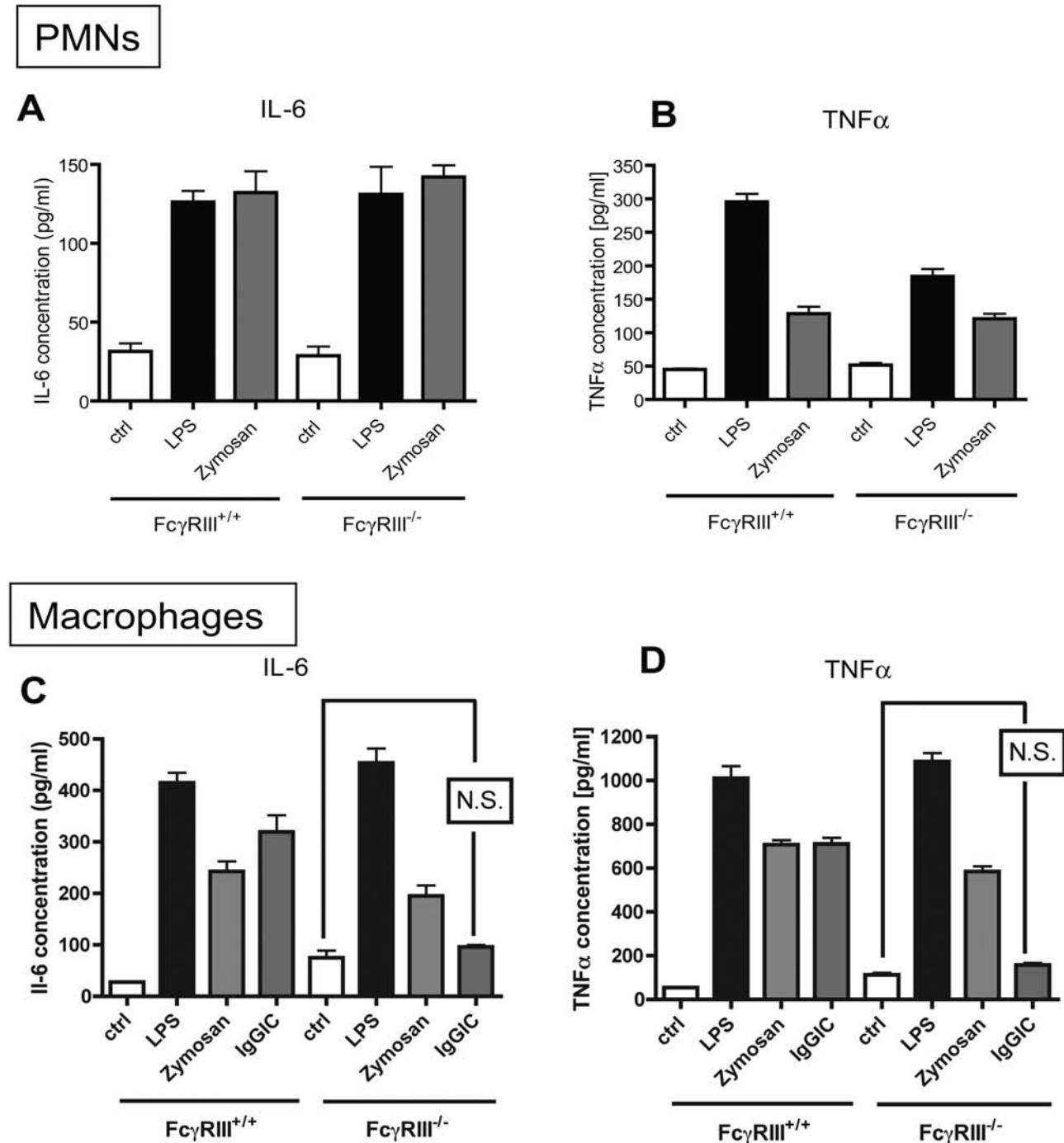


Figure 3. Responsiveness of FcγRIII-deficient phagocytes to LPS. Peritoneal PMNs (A,B) and macrophages (C,D) from Wt and FcγRIII^{-/-} mice were incubated to LPS (100 ng/ml) or Zymosan (300 μg/ml), or IgG immune complexes (IgGIC; 100 μg/ml; macrophages only), and supernatant fluids were analyzed for IL-6 and TNFα levels. Ctrl=control levels of non-stimulated cells. For each condition, n≥4. Differences between controls and stimulated cells were—if not otherwise noted—statistically significant (p<0.05). doi:10.1371/journal.ppat.1000464.g003

Phosphorylation of FcR γ -Subunit Requires the Integrity of TLR4

After binding of LPS, TLR4 engages intracellular signaling pathways via the adaptor molecules MyD88 and TRIF [27]. In the case of Fc γ R-immune-complex interaction, intracellular pathways are activated by tyrosine phosphorylation of the FcR γ -subunit ITAM region [8,28]. This subunit is known to be the common adaptor of Fc γ RI, Fc γ RIII and Fc ϵ RI [29,30], the first two being essential for development of IgGIC induced acute lung injury [31]. In order to evaluate the mechanism behind the impaired response of TLR4 mut cells to IgGIC, tyrosine phosphorylation of the FcR γ -subunit was investigated *in vitro*. When peritoneal PMNs (Figure 4A) or macrophages (Figure 4B) from Wt mice were exposed to IgGIC, rapid tyrosine phosphorylation (PY) of the FcR γ -subunit occurred over the first 30 min, as indicated by robust bands in the Western blots. In striking contrast, phosphorylation of the FcR γ -subunit failed to occur when TLR4 mut cells were used. Here, the intensity of the bands was comparable to those in non-stimulated cells (Figure 4A,B). When LPS was used as a stimulus (Figure 4C,D), slight phosphorylation of the FcR γ -subunit occurred in Wt cells (but not in TLR4 mut cells), indicating that TLR4 has little ability to activate the FcR γ -subunit as an intracellular signaling event (Figure 4C,D). Furthermore, the above mentioned results were

confirmed in macrophages by using polymyxin-treated BSA IgGIC for stimulation under the same conditions in order to exclude LPS contamination of the reagents (Figure 4E). Collectively, these data suggest that the integrity of TLR4 seems to be required for a proper function of Fc γ R activation via phosphorylation of the FcR γ -subunit, further suggesting communication between the TLR4 and Fc γ R signaling pathways.

Acute Lung Injury in Wt, TLR4 Mutant, and TLR4^{-/-} Mice

Using the LPS and IgGIC models of ALI, Wt, TLR4 mut, TLR4^{+/+} and TLR4^{-/-} mice were evaluated for responses following lung deposition of IgGIC or LPS. While Fc γ Rs play a key role in the IgG immune complex (IgGIC) model of ALI [31,32], TLR4 is critical for the development of lung injury in the LPS model [33,34,35]. As indicated in Figure 5A, LPS-induced lung injury, as defined by the permeability index (leak of plasma albumin into the extravascular lung compartment), showed a 4-fold increase in Wt mice (compared to controls, ctrl) and remained at the control level in LPS-challenged TLR4 mut mice. In the case of IgGIC (Figure 5B), the permeability index rose 5-fold above control (basal) levels in Wt mice. However, TLR4 mut mice unexpectedly showed no evidence of injury after deposition of IgGIC (Figure 5B). TLR4^{-/-} mice behaved similar to TLR4 mut mice in terms of lung injury, with virtually no lung injury in response to deposition of either LPS or IgGIC (Figure 5A,B). When

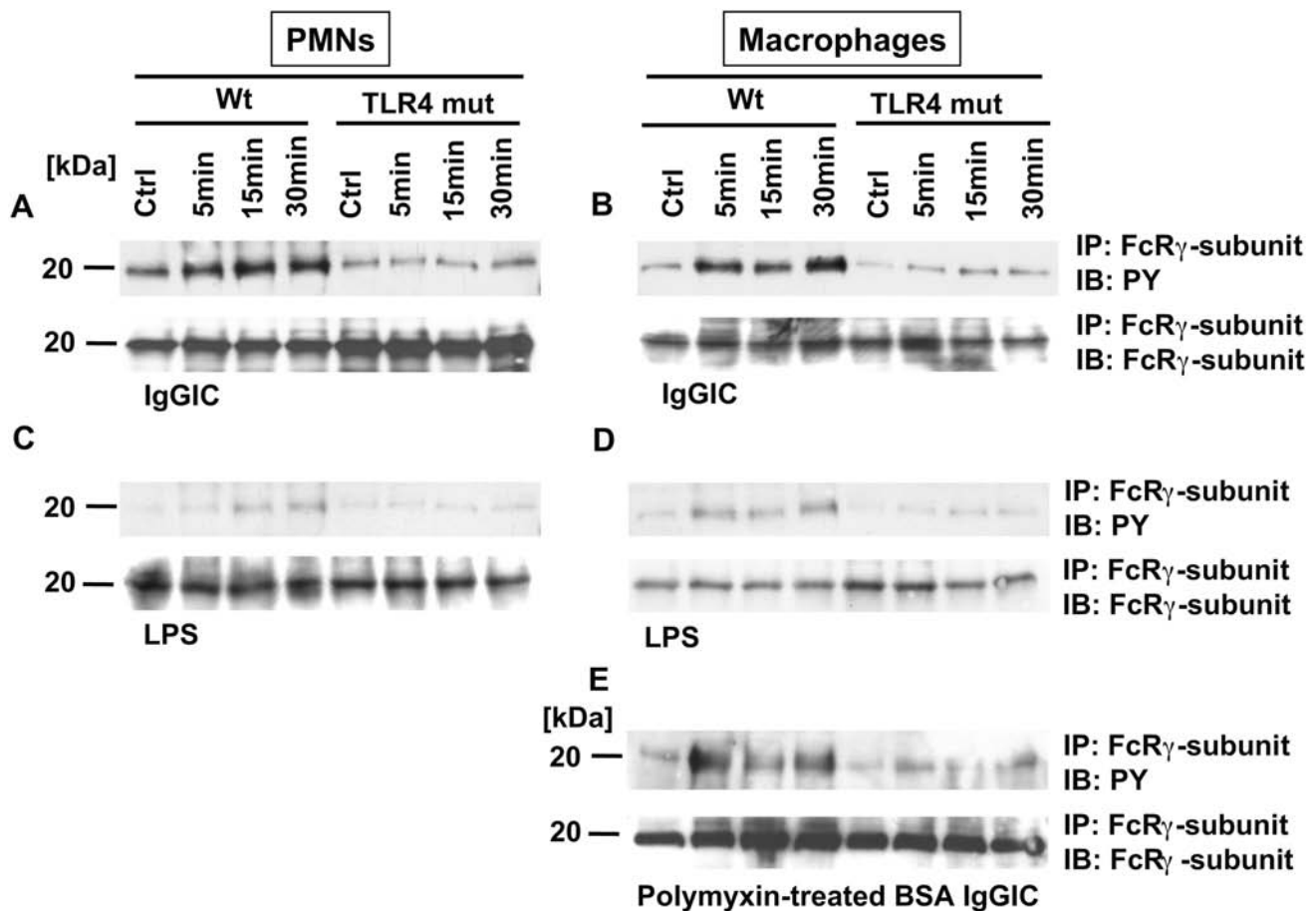


Figure 4. Western blot analysis for tyrosine-phosphorylated (PY) FcR γ -subunit of PMN or macrophage lysates after *in vitro* incubation. (A,B) 3×10^6 cells/ml from either Wt or TLR4 mut mice were incubated for 5, 15, and 30 min with IgG immune complexes (IgGIC; 100 μ g/ml). (C,D) The same protocol was used for stimulation with LPS (20 ng/ml). (E) Lysates from either Wt or TLR4 mut mice that were incubated with polymyxin-treated BSA immune complexes (100 μ g/ml) under the same conditions as described above. Corresponding loading controls are displayed in the lower panels.

doi:10.1371/journal.ppat.1000464.g004

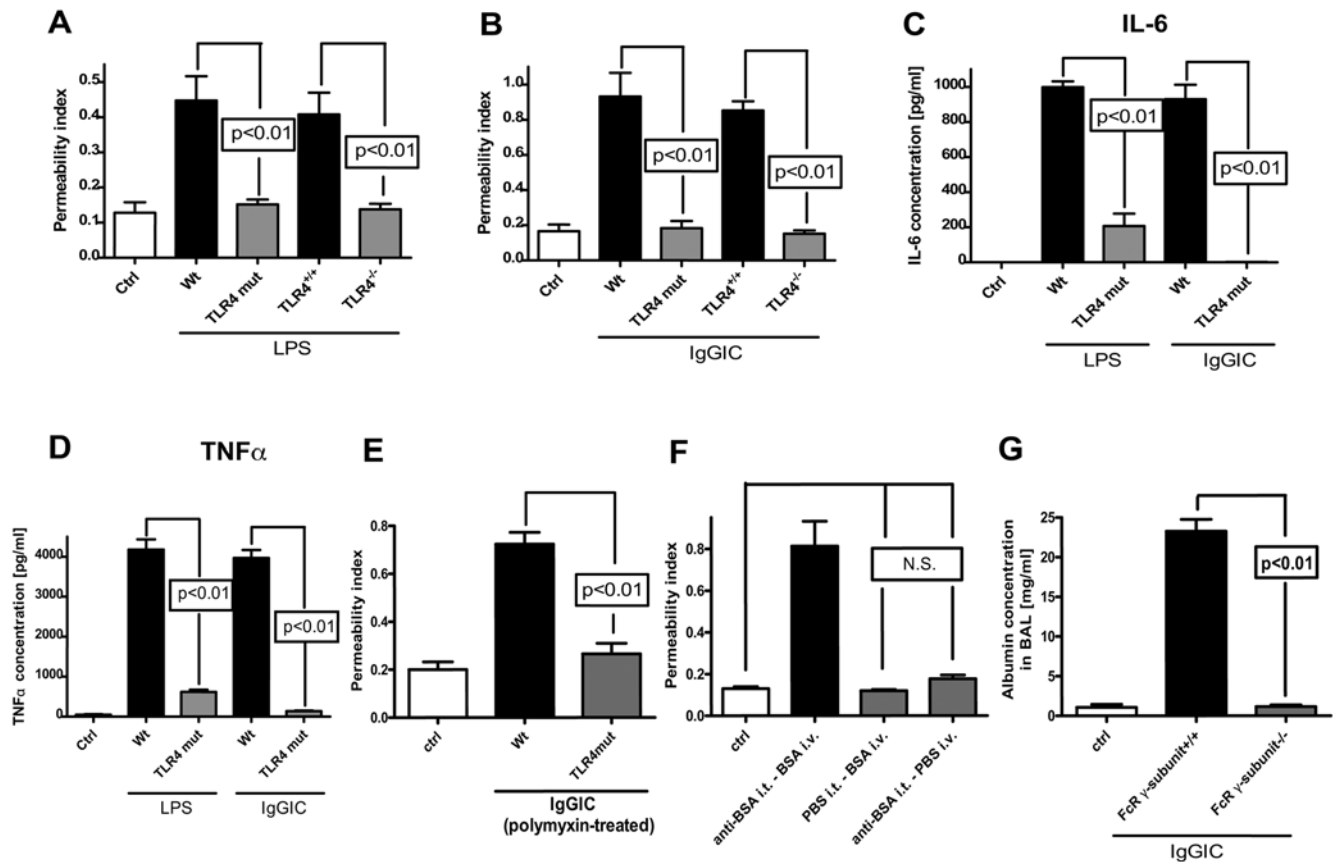


Figure 5. Parameters of acute lung injury in Wt and TLR4 mut mice. (A) Lung injury (as measured by leak of ¹²⁵I-BSA into lung) in Wt, TLR4 mut, TLR4^{+/+}, and TLR4^{-/-} mice receiving LPS intratracheally. (B) Permeability indices in Wt, TLR4 mut, TLR4^{+/+}, and TLR4^{-/-} mice after intrapulmonary immune complex formation following administration of BSA (i.v.) and anti-BSA IgG (i.t.). (C) IL-6 levels in BAL fluids after IgG immune complex (IgGIC)- or LPS-induced lung injury using Wt and TLR4 mut mice. (D) TNFα in BAL fluids from the same mice described in frame (C). For each bar, n ≥ 5. (E) Lung injury induced by IgG immune complexes (IgGIC) in Wt and TLR4 mut mice after endotoxin removal by polymyxin. (F) Lung permeability after intratracheal (i.t.) administration of anti-BSA IgG and intravenous (i.v.) injection of BSA, PBS i.t., and BSA i.v. or anti-BSA i.t. and PBS i.v. (G) IgGIC-induced lung injury in FcRγ-subunit^{-/-} mice in comparison to Wt mice (FcRγ-subunit^{+/+}). For each bar, n ≥ 5. doi:10.1371/journal.ppat.1000464.g005

IL-6 levels were measured in bronchoalveolar lavage (BAL) fluids, LPS and IgGIC induced high levels of IL-6 in Wt mice and very low levels in TLR4 mut mice (Figure 5C). Similar patterns were found for TNFα levels (Figure 5D).

Similarly, induction of ALI by intrapulmonary deposition of polymyxin-treated BSA IgGIC in Wt and TLR4 mut mice (Figure 5E) revealed no difference to the results displayed in Figure 5B; when polymyxin-treated reagents were administered for intrapulmonary IgGIC formation lung permeability rose 3.5 fold in Wt mice whereas mice TLR4 mut mice did not show a significant increase. Thus, these findings support the conclusion that lung injury induction by IgGICs is not linked to contamination of the reagents with endotoxin. In addition, reagents that were used for the formation of IgGIC were administered separately *in vivo* at the same concentration as they were used in combination for intrapulmonary IgGIC deposition (Figure 5F). When BSA was injected intravenously, followed by intratracheal PBS injection lung permeability was not different from control mice. Similarly, intratracheal injection of anti-BSA and subsequent intravenous DPBS injection (containing a trace amount of I¹²⁵-labelled BSA) did not result in increased lung permeability. In striking contrast, the combination of anti-BSA (i.t.) and by BSA (i.v.) injection lead

to the development of acute lung injury, as also shown in Figure 5B and 5E. These data indicate that the development of lung injury in the IgG model is dependent on the *in vivo* formation of immune complexes and may not be explained by putative LPS contamination of the reagents since their separate, independent administration failed to increase lung permeability. Finally, IgGIC lung injury was induced in FcR γ-subunit-deficient mice, which do not express FcγRI and FcγRIII on the surface of PMNs and macrophages [36]. In contrast to Wt mice (FcR γ-subunit^{+/+}), FcR γ-subunit^{-/-} mice did not develop acute lung injury after intrapulmonary IgGIC deposition, as determined by lung permeability (Figure 5G). These findings suggest that the IgGIC-induced lung injury using anti-BSA and BSA is strictly dependent on the FcγR-mediated signalling, and not on LPS-induced activation of TLR4. However, the caveat remains that there is always a concern about LPS contamination in the context of sensitive assays and *in vivo* responses. In particular, the possibility that LPS was present at concentrations below the detection limit of the available assays, which would not result in any *in vivo* (and *in vitro*) responses alone, but would be responsible for putative synergistic effects and an augmentation of IgGIC-induced inflammatory responses cannot be entirely excluded.

Expression of FcγRIII, FcRγ-Subunit, and C5aR in Wt and TLR4 Mutant Mice

It is well established that engagement of FcγRIII with IgGIC as well as activation of the complement system with generation of C5a and its interaction with C5aR play crucial roles in the pathogenesis of IgGIC-induced ALI [31,37,38]. Therefore, elicited peritoneal PMNs were evaluated by flow cytometry for surface expression of FcγRII/III and C5aR protein. As shown in Figure 6A,F, the levels of each receptor on the surface of PMNs were the same in Wt versus TLR4 mut cells. The original flow cytometry data of FcγRII/III expression on Wt and TLR4 mut PMNs are displayed in Figure 6B,C. In addition, the total content of FcγRIII and FcRγ-subunit in cell lysates from Wt and TLR4 mut PMN (Figure 6D) and macrophages (Figure 6E) were analyzed by Western blotting. In accordance with the flow cytometry results (Figure 6A,B), unstimulated phagocytes from both mouse strains expressed the same levels of FcγRII/III and FcRγ-subunit. The analysis for the house keeping protein GAPDH (lower bands) indicates equal loading of the cell lysates. Thus, the inability of TLR4 mut mice to respond to IgGIC or LPS is not associated with reduced surface content of FcγR protein on PMNs, consistent with the findings that there is cross-talk between FcγR and TLR4 signaling pathways such that downstream

production of IL-6 and TNFα upon IgGIC stimulation requires participation of both pathways. Collectively, these data indicate that TLR4 is required for proper FcγRIII functions.

Discussion

The mechanisms by which the recognition of pathogens leads to host responses are inadequately understood. The modulation of immune responses is inter alia mediated by cell surface receptors that are associated with signaling molecules that contain ITAMs (immunoreceptor tyrosine-based activation motifs), TREMs (triggering receptors expressed on myeloid cells) and OSCARs (human osteoclast-associated receptors) [1]. Intracellular signaling after TLR4 activation is mediated through the adaptor proteins, MyD88 and TRIF, whereas FcγRI and FcγRIII both contain the FcRγ-subunit, which is phosphorylated at tyrosine residues by Src and Syk kinases upon FcγR activation [28,30,39,40]. Interestingly, ligation of FcRγ-subunit containing FcRs results in inhibition of IL-12 production by monocytes in response to TLR ligands [41]. The specificity of IL-12 downregulation appears to be based on inhibition at the transcription level [41]. Moreover, TLRs are considered to control activation of acquired immunity [14], supporting the hypothesis for an instructive role of innate immunity in adaptive immune responses [15].

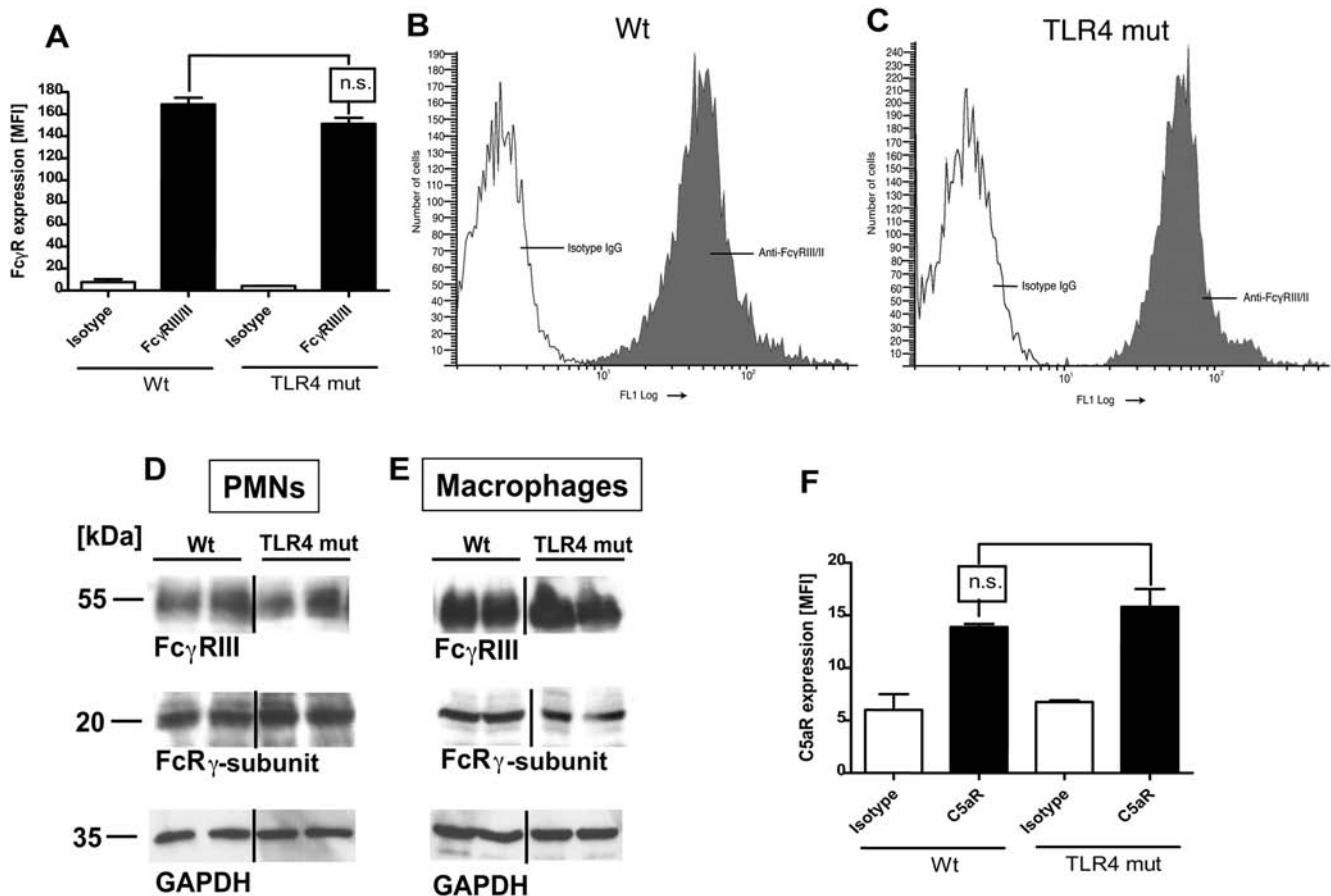


Figure 6. Expression levels of FcγRIII/III, FcRγ-subunit, and C5aR on phagocytes from Wt and TLR4 mut mice. (A) Summary of flow cytometry analyses of FcγRII/III expression on blood PMNs. (B,C) Original flow cytometry results for FcγRII/III expression on the surface of PMNs from Wt (B) or TLR4 mut (C) mice. (D,E) Analysis of the expression of FcγRIII (upper bands) and FcRγ-subunit (middle bands) in cell lysates [(D), PMNs; (E), macrophages] from Wt or TLR4 mut mice by Western blotting. The lower bands represent the analysis for GAPDH as loading controls. (F) Surface expression of C5aR protein on PMNs from Wt or TLR4 mut mice as assessed by flow cytometry. MFI, mean fluorescence intensity. Studies were done in three separate and independent experiments, with each sample run in duplicates. doi:10.1371/journal.ppat.1000464.g006

In the present study, we describe that TLR4 and FcγRIII associate, possibly by heterodimerization, following stimulation with IgGIC *in vitro* (Figure 1). Binding of IgGICs to the extracellular domain of FcγRs causes clustering of these receptors, followed by phosphorylation of tyrosine residues within the ITAM region, and subsequent activation of intracellular signaling cascades [28,30,40]. TLR signaling is initiated by dimerization of TLRs, which can form homo- or heterodimers [42]. Previously, it has been suggested that TLR4 co-associates with FcγRIII after activation of human monocytes [43]. Based on our findings, it is possible that TLR4 and FcγRIII multimerize into clusters following stimulation by LPS or IgGIC, a mechanism known as capping [44], which is required for engagement of intracellular signaling pathways. TLR4 may represent the central component for such signaling or “docking platforms” [45] and interconnect intracellular signaling pathways via association to adaptor proteins. As demonstrated in the present study, dysfunction of TLR4 results in impaired signaling in FcγRIII pathways (Figure 4).

The mutation that is responsible for the endotoxin tolerance of C3H/HeJ mice has recently been demonstrated to cause suppressed tyrosine phosphorylation by Src tyrosine kinases (Lyn) in the toll-IL-1 resistance (TIR) domain of TLR4, resulting in signaling-incompetence [45]. Altered or suppressed TLR4 tyrosine phosphorylation correlated with impaired MyD88 association and suppressed IRAK-1 activation [45]. In addition, our data suggest that this mutation in the TLR gene not only hinders phosphorylation of its own TIR domain but also blocks the tyrosine phosphorylation of the ITAM-containing Fcγ-subunit, the consequence of which ultimately leads to impaired signaling after engagement of FcγRIII.

In the LPS model of acute lung injury, TLR4 mut or TLR4^{-/-} mice were, as expected, highly protected from the development of tissue damage in the LPS-induced model of acute lung injury (Figure 5). It is well established that mice with mutation in the TLR4 gene or genetic deficiency of TLR4 are non-responsive to LPS [4], including LPS-mediated lung injury [33,34,35]. In the present study, TLR4 mut and TLR4^{-/-} mouse strains unexpectedly also showed greatly attenuated susceptibility to IgGIC-induced lung injury (Figure 5). For this model, it is known that, besides complement activation, FcγRs are critical for initiation and development of IgGIC alveolitis [31,32], particularly through engagement and activation of ITAM-containing FcγRs (FcγRI and FcγRIII) [31]. In accordance, mice with targeted disruption of the Fcγ-subunit showed an impaired inflammatory response in the reverse passive Arthus reaction [46]. In our study, TLR4 mut mice not only were resistant to lung injury, but also failed to locally release cytokines *in vivo* after intrapulmonary IgGIC deposition, as indicated by baseline levels of IL-6 and TNFα in BAL fluids (Figure 5). In companion experiments, *in vitro* exposure of TLR4 mut phagocytes to IgGIC resulted in complete suppression of proinflammatory cytokines (TNFα, IL-6) in comparison to phagocytes from Wt mice (Figure 2). Furthermore, TLR4 mut cells showed impaired tyrosine phosphorylation of the Fcγ-subunit when exposed to IgGIC, in striking contrast to Wt cells (Figure 4). The fact that TLR4 mut PMNs and macrophages responded with cytokine release when incubated with opsonized zymosan particles or with Pam3Cys (Figure 3) indicates that 1.) the mutation in the TLR4 gene does not lead to a global impairment of the cellular inflammatory/immune response and 2.) the intracellular signaling pathways are intact since other TLRs (such as TLR2 and TLR6), which share common pathways, could be activated *in vitro*. On the other hand, phagocytes from FcγRIII-deficient mice are fully responsive to LPS (Figure 3), suggesting that TLR4 signaling does not depend on the functional integrity of FcγRIII, whereas TLR4 is required for FcγRIII signaling.

Especially in the field of immunology, there is an increasing number of reports describing effects of receptor interactions. Examples include a previous study suggesting cross-talk between IFN-gamma and IFN-alpha receptors with signaling pathways [47]. In brief, signalling by IFN-gamma was shown to depend on the IFN-alpha/beta receptor components. A more recent publication describes that signalling triggered by NKG2D and DAP10 is coupled to the interleukin 15 receptor signalling pathway, suggesting that coupling of activating receptors to other receptor systems may regulate cell type-specific signaling events [48]. In the case of innate immunity, it has been proposed several times that there is a link between TLR4 and the complement system, especially to the C5a signalling pathway, which can negatively regulate TLR4-induced responses [49,50]. Under physiological conditions, receptor interactions and cross-talk between signalling pathways might represent important regulatory mechanisms of the immune system to provide distinct but fine-tuned responses. In the case of TLR4 and FcγRIII, cross-talk may provide an optimal and rapid response against invading microorganisms by mediating an interplay between adaptive and innate immunity. However, in certain conditions, such as systemic inflammation (sepsis) or autoimmune diseases that are characterized by a loss of inhibitory action or uncontrolled activation of signalling pathways, a loss of control over otherwise carefully orchestrated receptor interactions can become instruments of harm.

Taken together, the present findings strongly suggest that (i) there is a direct link between TLR4 and FcγR pathways, (ii) phosphorylation of tyrosine residues in the ITAM-containing Fcγ-subunit requires the presence and integrity of TLR4 during cellular activation after binding of IgGICs to FcγRs, and (iii) presence of IgGICs results in an association between TLR4 and FcγRIII (CD16) on phagocytic cells. These data imply that innate and adaptive immunity are closely connected at the receptor level and post receptor signaling pathways, which might have ramifications for a variety of inflammatory conditions, such as IgGIC-mediated autoimmune diseases (rheumatoid arthritis or glomerulonephritis), ischemia/perfusion injury, trauma or systemic inflammation (sepsis), etc.

Materials and Methods

Animals

Adult male (22–25 g) specific pathogen-free C3H/OuJ (Wt) and C3H/HeJ (TLR4 mut) mice with a missense mutation in the TLR4-gene were used in these studies [4]. In addition, lung injury was employed in mice lacking the genes for TLR4 (TLR4^{-/-}; C57BL/10ScCr) and the corresponding wild-type mice (TLR4^{+/+}; C57BL/ScSn) [4]. In some *in vitro* experiments, cells from FcγRIII-deficient (FcγRIII^{-/-}; B6.129P2-Fcγ3^{tm1Sjv}/J), FcR γ-subunit-deficient (FcRγ-subunit^{-/-}; B6.129P2-Fcer1g^{tm1Rav}N12) and appropriate Wt mice (C57BL/6) were used [51].

Ethics Statement

All studies were performed in accordance with the University of Michigan Committee on Use and Care of Animals.

In Vitro Incubation of Peritoneal PMNs and Macrophages

Mouse peritoneal leukocytes were harvested 5 h (PMNs) or 5 days (macrophages) after intraperitoneal injection of thioglycolate into untreated Wt and TLR4 mut mice by peritoneal lavage with PBS. 3 × 10⁶ cells / sample were incubated in HBSS for up to 4 h at 37°C in the presence of LPS (20 ng/ml; serotype O111:B4; Sigma, St. Louis, MO), BSA IgG immune complexes (IgGIC, 100 μg/ml; MP Biomedicals), polymyxin-treated BSA IgG immune complexes (p.-t.

BSA IC, 100 µg/ml), peroxidase/anti-peroxidase IgG immune complexes (PAP IC, 100 µg/ml; MP Biomedicals), opsonized zymosan particles (300 µg/ml; Sigma) or Pam3Cys (1 µg/ml; InvivoGen). After incubation, supernatant fluids were collected for assessment of cytokines by ELISA and pellets were lysed with RIPA buffer (Upstate) for immunoprecipitation analyses.

Immunoprecipitation and Western Blotting

After incubation of peritoneal PMNs or macrophages with either IgG immune complexes (100 µg/ml; prepared as described elsewhere [52] or LPS (20 ng/ml) for 5 to 30 min, supernatant fluids were removed and pellets were lysed with 1X RIPA buffer containing Vanadate and protease inhibitors (Roche Diagnostics). Protein concentrations were determined in cell lysates using BCA protein assay (Pierce). Equal protein amounts of supernatants were then incubated overnight with preblocked protein A and G beads (Santa Cruz) in the presence of anti-FcRγ-subunit IgG (Upstate) or anti-TLR4 IgG (Santa Cruz), respectively. Reverse direction immunoprecipitation included anti-FcγRIII IgG (Santa Cruz).

After centrifugation, pellets were resuspended in Laemmli sample buffer (Biorad) followed by boiling of the samples. After a final spin step, supernatant fluids were electrophoretically separated under reducing conditions in SDS-PAGE and transferred onto PVDF membrane. The membrane was blocked in 5% bovine milk in TBST and then probed for TLR4 or FcγRIII using polyclonal anti-TLR4 IgG (1 µg/ml, Santa Cruz) or monoclonal anti-FcγRII/III IgG (1 µg/ml; clone 2.4G2; BD Pharmingen). Alternatively, membranes containing the samples co-immunoprecipitated with anti-FcRγ-subunit IgG were incubated with anti-phospho-tyrosine monoclonal antibody (1 µg/ml; clone 4G10, Upstate). As secondary antibodies, HRP-conjugated donkey anti-goat IgG (1:80,000; Jackson ImmunoResearch), HRP-conjugated goat anti-rat IgG (1:10,000; Amersham) HRP-conjugated donkey anti-rabbit IgG (1:10,000; Amersham) and HRP-conjugated sheep anti-mouse IgG (1:20,000; Amersham) were added and the blot was developed using ECL-procedure (Amersham).

ELISA for Mouse IL-6, TNFα

For measurement of IL-6 and TNFα in BAL fluids and supernatant fluids after *in vitro* incubation of mouse PMNs and macrophages, commercially available ELISA-kits ("Duo set", R&D Systems) were used according to the manufacturer's protocol.

Immune Complex Lung Injury

To induce IgGIC lung injury, tracheae of mice were surgically exposed and 125 µg rabbit anti-BSA IgG (MP Biomedicals) was administered using a 30 gauge needle (volume of 42 µl/mouse) followed by intravenous injection of BSA (500 µg; Sigma). For determination of the permeability index as a quantitative marker for vascular leakage, ¹²⁵I-labelled bovine serum albumin (1 µCi ¹²⁵I-BSA/mouse) was injected intravenously. After the development of acute lung injury, the pulmonary vasculature was flushed with 2.0 ml PBS. The amount of lung radioactivity was then measured as a ratio of radioactivity present in 100 µl blood recovered from the inferior vena cava at the time of animal euthanasia and that in lung. For bronchoalveolar lavage retrieval, lung injury was performed as described above, but without the intravenous injection of ¹²⁵I-BSA. The airways were flushed with 0.8 ml ice cold PBS using a blunt 20 gauge needle and BAL fluids were recovered for further studies.

LPS Lung Injury

50 µg LPS from *E.coli* (serotype O111:B4; Sigma) were given intratracheally (volume of 42 µl/mouse). When lung permeability

was measured, a trace amount of ¹²⁵I-BSA was injected intravenously, as described above. The permeability index was determined and BAL fluids were collected as described for the IgGIC model.

Detection of Possible LPS Contamination

Reagents other than LPS, such as DPBS, BSA, anti-BSA IgG that were used for the *in vivo* and *in vitro* experiments were tested for LPS-contamination. For quantification of LPS content, samples were conducted in Limulus Amebocyte Lysate Kinetic-QCL assay (Cambrex) according to the manufacturer's protocol and as described elsewhere [53]. In addition, reagents used for immune complex formation (DPBS, BSA, anti-BSA IgG) were subjected to endotoxin removal (Pierce) prior to induction of lung injury or preparation of immune complexes used stimulation of phagocytes *in vitro*.

Analysis of FcγR and C5aR on PMNs

Flow cytometric analysis was conducted after whole blood collection of untreated wild-type and TLR4 mut mice in a citrate-containing syringe. Rabbit anti-mouse C5aR serum (1:10 dilution; Lampire) was incubated with mouse whole blood. Non-specific rabbit serum (Jackson ImmunoResearch) was added to control samples in equal amounts. For detection of FcγR on PMNs, mouse whole blood was either incubated with 1 µg monoclonal anti-FcγRII/III IgG (clone 2.4G2; BD Pharmingen) or with the appropriate isotype IgG control (Jackson ImmunoResearch). After washing, cells were suspended in Phycoerythrin (PE)-labeled anti-rabbit IgG (Invitrogen) diluted 1:200 in staining buffer and incubated at room temperature for 45 min. Erythrocytes were lysed by addition of 1 × FACS lysing solution (BD Pharmingen) for 10 min. After washing, the leukocytes were resuspended in a 1%-paraformaldehyde fixing solution and analyzed on a flow cytometer (BD Pharmingen).

Statistical Analysis

All values were expressed as mean ± SEM. Data sets were analyzed by one-way analysis of variance (ANOVA); differences in mean values among experimental groups were then compared using Tukey multiple comparison test. Results were considered statistically significant when $P < 0.05$.

Supporting Information

Figure S1 Cytokine response of PMNs and macrophages to Zymosan and Pam3Cys. *In vitro* cytokine responses to non-TLR4 agonists of elicited peritoneal phagocytes from Wt or TLR4 mut mice. PMNs (A–D) and macrophages (E–H) (3×10^6 cells/ml) were incubated (for 4 hr) with serum-opsonized zymosan particles (300 µg/ml) or Pam3Cys (1 µg/ml). Ctrl = control levels of non-stimulated cells. For each condition $n \geq 3$. Differences between controls and stimulated cells were found to be statistically significant ($p < 0.05$).

Found at: doi:10.1371/journal.ppat.1000464.s001 (0.50 MB EPS)

Acknowledgments

We thank Beverly Schumann and Sue Scott for excellent secretarial assistance in preparation of the manuscript.

Author Contributions

Conceived and designed the experiments: DR MAF JVS MSHL PAW. Performed the experiments: DR MAF DED BAN FSZ. Analyzed the data: DR MAF DED BAN FSZ JVS CMW GAW HPS MSHL PAW. Contributed reagents/materials/analysis tools: DR FSZ. Wrote the paper: DR PAW.

References

- Trinchieri G, Sher A (2007) Cooperation of Toll-like receptor signals in innate immune defence. *Nat Rev Immunol* 7: 179–190.
- Akira S, Uematsu S, Takeuchi O (2006) Pathogen recognition and innate immunity. *Cell* 124: 783–801.
- Medzhitov R, Janeway C Jr (2000) Innate immunity. *N Engl J Med* 343: 338–344.
- Poltorak A, He X, Smirnova I, Liu MY, Van Huffel C, et al. (1998) Defective LPS signaling in C3H/HeJ and C57BL/10ScCr mice: mutations in Tlr4 gene. *Science* 282: 2085–2088.
- Jiang D, Liang J, Li Y, Noble PW (2006) The role of Toll-like receptors in non-infectious lung injury. *Cell Res* 16: 693–701.
- Yu M, Wang H, Ding A, Golenbock DT, Latz E, et al. (2006) HMGB1 signals through toll-like receptor (TLR) 4 and TLR2. *Shock* 26: 174–179.
- May MJ, Ghosh S (1998) Signal transduction through NF-kappa B. *Immunol Today* 19: 80–88.
- Gessner JE, Heiken H, Tamm A, Schmidt RE (1998) The IgG Fc receptor family. *Ann Hematol* 76: 231–248.
- Selvaraj P, Fidadara N, Nagarajan S, Cimino A, Wang G (2004) Functional regulation of human neutrophil Fc gamma receptors. *Immunol Res* 29: 219–230.
- Ravetch JV, Luster AD, Weinshank R, Kochan J, Pavlovic A, et al. (1986) Structural heterogeneity and functional domains of murine immunoglobulin G Fc receptors. *Science* 234: 718–725.
- Miettinen HM, Rose JK, Mellman I (1989) Fc receptor isoforms exhibit distinct abilities for coated pit localization as a result of cytoplasmic domain heterogeneity. *Cell* 58: 317–327.
- Amigorena S, Bonmerot C, Drake JR, Choquet D, Hunziker W, et al. (1992) Cytoplasmic domain heterogeneity and functions of IgG Fc receptors in B lymphocytes. *Science* 256: 1808–1812.
- Nimmerjahn F, Ravetch JV (2008) Fc gamma receptors as regulators of immune responses. *Nat Rev Immunol* 8: 34–47.
- Schnare M, Barton GM, Holt AC, Takeda K, Akira S, et al. (2001) Toll-like receptors control activation of adaptive immune responses. *Nat Immunol* 2: 947–950.
- Fearon DT, Locksley RM (1996) The instructive role of innate immunity in the acquired immune response. *Science* 272: 50–53.
- Kim KD, Zhao J, Auh S, Yang X, Du P, et al. (2007) Adaptive immune cells temper initial innate responses. *Nat Med* 13: 1248–1252.
- Iwasaki A, Medzhitov R (2004) Toll-like receptor control of the adaptive immune responses. *Nat Immunol* 5: 987–995.
- Abdollahi-Roodsaz S, Joosten LA, Roelofs MF, Radstake TR, Matera G, et al. (2007) Inhibition of Toll-like receptor 4 breaks the inflammatory loop in autoimmunity destructive arthritis. *Arthritis Rheum* 56: 2957–2967.
- van Lent PL, Blom AB, Grevers L, Sloetjes A, van den Berg WB (2007) Toll-like receptor 4 induced Fc gamma R expression potentiates early onset of joint inflammation and cartilage destruction during immune complex arthritis: Toll-like receptor 4 largely regulates Fc gamma R expression by interleukin 10. *Ann Rheum Dis* 66: 334–340.
- Banas MC, Banas B, Hudkins KL, Wietecha TA, Iyoda M, et al. (2008) TLR4 links podocytes with the innate immune system to mediate glomerular injury. *J Am Soc Nephrol* 19: 704–713.
- Santiago A, Satriano J, DeCandido S, Holthofer H, Schreiber R, et al. (1989) A specific Fc gamma receptor on cultured rat mesangial cells. *J Immunol* 143: 2575–2582.
- Huizinga TW, van der Schoot CE, Jost C, Klaassen R, Kleijer M, et al. (1988) The PI-linked receptor FcRIII is released on stimulation of neutrophils. *Nature* 333: 667–669.
- Warmerdam PA, van de Winkel JG, Gosselin EJ, Capel PJ (1990) Molecular basis for a polymorphism of human Fc gamma receptor II (CD32). *J Exp Med* 172: 19–25.
- Gruel N, Chapiro J, Fridman WH, Teillaud JL (2001) Purification of soluble recombinant human Fc gamma RII (CD32). *Prep Biochem Biotechnol* 31: 341–354.
- Wang X, Wang Y, Kim HP, Nakahira K, Ryter SW, et al. (2007) Carbon monoxide protects against hyperoxia-induced endothelial cell apoptosis by inhibiting reactive oxygen species formation. *J Biol Chem* 282: 1718–1726.
- Zhang X, Kimura Y, Fang C, Zhou L, Sfyroera G, et al. (2007) Regulation of Toll-like receptor-mediated inflammatory response by complement in vivo. *Blood* 110: 228–236.
- Takeda K, Kaisho T, Akira S (2003) Toll-like receptors. *Annu Rev Immunol* 21: 335–376.
- Strzelecka A, Kwiatkowska K, Sobota A (1997) Tyrosine phosphorylation and Fc gamma receptor-mediated phagocytosis. *FEBS Lett* 400: 11–14.
- Orloff DG, Ra CS, Frank SJ, Klausner RD, Kinet JP (1990) Family of disulphide-linked dimers containing the zeta and eta chains of the T-cell receptor and the gamma chain of Fc receptors. *Nature* 347: 189–191.
- Duchemin AM, Ernst LK, Anderson CL (1994) Clustering of the high affinity Fc receptor for immunoglobulin G (Fc gamma RI) results in phosphorylation of its associated gamma-chain. *J Biol Chem* 269: 12111–12117.
- Baumann U, Kohl J, Tschernig T, Schwertler-Strumpf K, Verbeek JS, et al. (2000) A codominant role of Fc gamma RI/III and C5aR in the reverse Arthus reaction. *J Immunol* 164: 1065–1070.
- Chouchakova N, Skokowa J, Baumann U, Tschernig T, Philippens KM, et al. (2001) Fc gamma RIII-mediated production of TNF-alpha induces immune complex alveolitis independently of CXC chemokine generation. *J Immunol* 166: 5193–5200.
- Saito T, Yamamoto T, Kazawa T, Gejyo H, Naito M (2005) Expression of toll-like receptor 2 and 4 in lipopolysaccharide-induced lung injury in mouse. *Cell Tissue Res* 321: 75–88.
- Andonegui G, Bonder CS, Green F, Mullaly SC, Zbytniuk L, et al. (2003) Endothelium-derived Toll-like receptor-4 is the key molecule in LPS-induced neutrophil sequestration into lungs. *J Clin Invest* 111: 1011–1020.
- Jeyaseelan S, Chu HW, Young SK, Freeman MW, Worthen GS (2005) Distinct roles of pattern recognition receptors CD14 and Toll-like receptor 4 in acute lung injury. *Infect Immun* 73: 1754–1763.
- Takai T, Li M, Sylvestre D, Clynes R, Ravetch JV (1994) FcR gamma chain deletion results in pleiotropic effector cell defects. *Cell* 76: 519–529.
- Mulligan MS, Schmid E, Beck-Schimmer B, Till GO, Friedl HP, et al. (1996) Requirement and role of C5a in acute lung inflammatory injury in rats. *J Clin Invest* 98: 503–512.
- Ward PA (1996) Rous-Whipple Award Lecture. Role of complement in lung inflammatory injury. *Am J Pathol* 149: 1081–1086.
- Durden DL, Rosen H, Cooper JA (1994) Serine/threonine phosphorylation of the gamma-subunit after activation of the high-affinity Fc receptor for immunoglobulin G. *Biochem J* 299(Pt 2): 569–577.
- Pfefferkorn LC, Yeaman GR (1994) Association of IgA-Fc receptors (Fc alpha R) with Fc epsilon RI gamma 2 subunits in U937 cells. Aggregation induces the tyrosine phosphorylation of gamma 2. *J Immunol* 153: 3228–3236.
- Grazia Cappiello M, Sutterwala FS, Trinchieri G, Mosser DM, Ma X (2001) Suppression of Il-12 transcription in macrophages following Fc gamma receptor ligation. *J Immunol* 166: 4498–4506.
- Akira S, Takeda K (2004) Toll-like receptor signalling. *Nat Rev Immunol* 4: 499–511.
- Pfeiffer A, Bottcher A, Orso E, Kapinsky M, Nagy P, et al. (2001) Lipopolysaccharide and ceramide docking to CD14 provokes ligand-specific receptor clustering in rafts. *Eur J Immunol* 31: 3153–3164.
- Holifield BF, Ishihara A, Jacobson K (1990) Comparative behavior of membrane protein-antibody complexes on motile fibroblasts: implications for a mechanism of capping. *J Cell Biol* 111: 2499–2512.
- Medvedev AE, Piao W, Shoenfelt J, Rhee SH, Chen H, et al. (2007) Role of TLR4 tyrosine phosphorylation in signal transduction and endotoxin tolerance. *J Biol Chem* 282: 16042–16053.
- Kohl J, Gessner JE (1999) On the role of complement and Fc gamma-receptors in the Arthus reaction. *Mol Immunol* 36: 893–903.
- Takaoka A, Mitani Y, Suemori H, Sato M, Yokochi T, et al. (2000) Cross talk between interferon-gamma and -alpha/beta signaling components in caveolar membrane domains. *Science* 288: 2357–2360.
- Hornig T, Bezbradica JS, Medzhitov R (2007) NKG2D signaling is coupled to the interleukin 15 receptor signaling pathway. *Nat Immunol* 8: 1345–1352.
- Hawlich H, Belkaid Y, Baelder R, Hildeman D, Gerard C, et al. (2005) C5a negatively regulates toll-like receptor 4-induced immune responses. *Immunity* 22: 415–426.
- Rittirsch D, Flierl MA, Nadeau BA, Day DE, Huber-Lang M, et al. (2008) Functional roles for C5a receptors in sepsis. *Nat Med* 14: 551–557.
- Hazenbos WL, Gessner JE, Hofhuis FM, Kuipers H, Meyer D, et al. (1996) Impaired IgG-dependent anaphylaxis and Arthus reaction in Fc gamma RIII (CD16) deficient mice. *Immunity* 5: 181–188.
- Czermak BJ, Breckwoldt M, Ravage ZB, Huber-Lang M, Schmal H, et al. (1999) Mechanisms of enhanced lung injury during sepsis. *Am J Pathol* 154: 1057–1065.
- Niederbichler AD, Hoessel LM, Westfall MV, Gao H, Ipakchi KR, et al. (2006) An essential role for complement C5a in the pathogenesis of septic cardiac dysfunction. *J Exp Med* 203: 53–61.

MARCH
9TH - 13TH, 2010
MUNICH, GERMANY

**8TH WORLD CONGRESS ON
TRAUMA, SHOCK,
INFLAMMATION AND SEPSIS
TSIS 2010**

SELECTED PAPERS

Editor **Eugen Faist**

MONDUZZI EDITORE | PROCEEDINGS

Defective Innate Immunity and Hyper-Inflammatory Responses in Sepsis

P. A. Ward, F. S. Zetoune and J. V. Sarma

University of Michigan Medical School, Department of Pathology, Ann Arbor, Michigan, U.S.A.

Summary

Polymicrobial sepsis following cecal ligation and puncture (CLP) in rodents leads to defective innate immunity. Surface receptors on blood neutrophils for C5a are greatly reduced after CLP, associated with defective chemotaxis and phagocytosis. Changes indicative of a hyper-inflammatory state after CLP include increased β_1 and β_2 integrins, increased chemokine receptors on PMNs, and increased ICAM-1 on endothelial cells. Following CLP, PMNs contribute to clearance of bacteria from blood but are also involved in the development of multiorgan failure.

Introduction

It is well known that in human and rodent sepsis PMNs are a first line of defense for containment of bacterial dissemination. However, during sepsis there is also loss in regulation of the inflammatory response, as reflected by the “cytokine storm” featuring high plasma levels of chemokines and cytokines, buildup of PMNs in organs, development and progression of multiorgan failure, septic shock and lethality¹.

There is abundant evidence that, in rodents with CLP as well as in septic humans, robust activation of the complement system occurs, with appearance of the anaphylatoxins, C3a and C5a, and consumptive depletion of serum/plasma complement. In vivo blockade of C5a greatly attenuates all of the features of CLP-induced sepsis and greatly improves survival². Presented below is evidence for the development of a hyper-inflammatory state in sepsis following CLP.

Material and Methods

Induction of CLP-induced sepsis in rats and mice has been recently described using Long Evans rats and C57Bl/6 mice³. In general, the moderate to severe form of CLP was employed, in which approximately 80% of animals are dead be-

tween 3-7 days. Content of β_1 and β_2 integrins (CD29 and CD18) and C5a receptor (C5aR, CD88) on rat blood PMNs was determined by flow cytometry⁴. Lung vascular ICAM-1 was quantitated by binding of ¹²⁵I-anti-mouse ICAM-1 to the pulmonary vascular endothelium⁴. Serum levels of soluble mouse ICAM-1 were determined by commercial ELISA kits. Systemic depletion of mouse PMNs was accomplished as described⁵. Endpoints for organ damage were the standard biochemical measurements of serum transaminases (AST, ALT), blood urea nitrogen (BUN) and creatinine.

Results

Changes in C5aR Content on Blood PMNs after CLP

As measured by flow cytometry, some animals (n=11) had preserved C5aR content on PMNs over a 7-day period after CLP, whereas other animals (n=12) had PMNs with clearly reduced levels of C5aR. Animals maintaining near normal levels of C5aR on blood PMNs had 100% survival, whereas rats whose blood PMNs lost $\geq 50\%$ of C5aR showed only 20% survival⁶. Loss of C5aR from blood PMNs was a reliable prognostic indicator after CLP.

Increased Levels of β_1 and β_2 Integrins on Rat Blood PMNs after CLP

When blood PMNs were quantitatively evaluated for integrin content, there was a time dependent increase in both β_1 (CD29) and β_2 (CD18) content on PMN surfaces after CLP. The increased integrin content on blood PMNs implies that cells are not only activated, but that these leukocytes are more reactive with their “counter-receptors” such as fibronectin (in the case of CD29) and ICAM-1 (in the case of CD18)⁷.

Changes in CCRs on Blood PMNs After CLP

CCRs are receptors on leukocytes reactive with chemokine ligands (CCLs), the interaction of which leads to a variety of proinflammatory responses such as leukocyte (lymphocytes, monocytes) activation, chemotaxis and release of proinflammatory mediators. CCR content on PMNs is very limited and PMNs are unresponsive to chemokines. PMNs are highly responsive to CXCLs, such as CXCL1 (Gro α), CXCL7 (NAP) and CXCL8 (IL-8). Following CLP, blood PMNs showed increased expression of mRNA and protein for CCR1, CCR2 and CCR5. The implications for “gain of function” in CLP PMNs comes from the finding that, after CLP, the binding of MCP-1 to mouse blood PMNs rose from a baseline value of 33% to 91% 6 hr after CLP. Gain of function was shown by the fact that blood PMNs 6 hr after CLP showed dose-dependent chemotactic responses to both MCP-1 and MIP-1 α . These data suggest that CLP causes increased expression of CCRs on blood PMNs, endowing these cells with functional responsiveness to appropriate CCLs.

Evidence for Increased ICAM-1 Levels on Endothelial Cells after CLP

There is evidence that CLP in mice leads to changes in endothelial cells in a manner that leads to buildup of PMNs in a variety of organs. There is increased content of ICAM-1 in the lung vasculature⁷. Vascular ICAM-1 content in lung rose by nearly 50% after CLP. Sham lungs had levels of ICAM-1 that were nearly 35 fold greater than VCAM-1 content. At each time point after CLP, ICAM-1 levels increased. Similar changes in ICAM-1 occurred in kidneys, liver and heart. These data likely explain the buildup of myeloperoxidase (MPO) in organs after CLP. It is possible that increased ICAM-1 content in organs may be linked to development of the multiorgan failure of sepsis.

PMNs in the Setting of Sepsis Have Both Protective and Harmful Effects

It is well established in both human sepsis and in polymicrobial sepsis in rodents that there is a buildup of PMNs in organs and tissues. PMNs are known to be the first line of defense against invading bacteria. Innate immune responses provided by PMNs represent crucial defenses. PMN depletion was induced by employing a mAb, anti-mouse Ly-gG, which binds to a PMN specific epitope, resulting in PMN depletion⁵. Survival rates 24 hr after CLP in mice treated with class matched IgG were 80%, whereas mice that were PMN depleted 24 hr before CLP had a survival rate that fell to 50% ($p < 0.05$). If PMN depletion was delayed until 12 hr after CLP, the survival rate was 100%, suggesting that 12 hr after CLP PMN removal is protective. PMN depletion 24 hr before CLP caused an increase in blood CFUs (24 hr after CLP) by approximately 1000 fold, while, surprisingly, if PMN depletion was delayed until 12 hr after CLP, there was a nearly 1000 fold decrease in CFUs. Such data suggest that PMNs have both protective and harmful effects in the setting of CLP.

When PMN depletion was delayed until 12 hr after CLP, there were substantial reductions in the cytokine storm 24 hr after CLP. Serum levels of IL-1 β fell by 65%, IL-6 by 76%, IL-2 by 74%, IL-10 by 81% and TNF α by 83%. This might be related to PMNs being a source for the cytokines, or it could be an indirect result from reduced intensity of sepsis (reduced blood CFUs, improved survival) or some other effect. In mice depleted of PMNs either 24 hr before CLP or 12 hr after CLP, serum transaminases, before CLP caused a 36% rise in ALT, while PMN depletion 12 hr after CLP reduced ALT levels by 51%. In the case of serum AST, similar changes occurred. As for renal function, BUN levels fell by 9% with early PMN depletion whereas later depletion (+12 hr) reduced BUN levels by 65%. Creatinine levels fell 38% when early depletion occurred, whereas PMN depletion 12 hr after CLP caused a 79% reduction in serum creatinine. Therefore, PMN depletion reduces evidence of liver and renal dysfunction caused by CLP, especially when PMN depletion was done 12 hr after CLP.

Conclusions

In sepsis, PMNs subserve two functions: in early hours after CLP, containment of invading bacteria; in the later phases of sepsis, PMNs contribute to development of the cytokine storm and multiorgan failure. Sepsis unleashes an intense proinflammatory condition featuring elevations in β_1 and β_2 integrins on PMNs as well as expression of functional receptors for chemokines. There is an upregulation of ICAM-1 on the vasculature. These data underscore the protective and the harmful roles of PMNs in sepsis and development of a strong proinflammatory phenotype which likely contributes to the multiorgan failure of sepsis.

References

1. Rittirsch D, Flierl MA, Ward PA. Harmful molecular mechanisms in sepsis. *Nat Rev Immunol*. 2008 Oct;8(10):776-87. Review. PMID: 18802444; PMCID: PMC2786961.
2. Ward PA. The dark side of C5a in sepsis. *Nat Rev Immunol*. 2004 Feb;4(2):133-42. Review. PMID: 15040586.
3. Rittirsch D, Huber-Lang MS, Flierl MA, Ward PA. Immunodesign of experimental sepsis by cecal ligation and puncture. *Nat Protoc*. 2009;4(1):31-6. PMID: 19131954; PMCID: PMC2754226.
4. Speyer CL, Gao H, Rancilio NJ, Neff TA, Huffnagle GB, Sarma JV, Ward PA. Novel chemokine responsiveness and mobilization of neutrophils during sepsis. *Am J Pathol*. 2004 Dec;165(6):2187-96. PMID: 15579460.
5. Hoesel LM, Neff TA, Neff SB, Younger JG, Olle EW, Gao H, Pianko MJ, Bernacki KD, Sarma JV, Ward PA. Harmful and protective roles of neutrophils in sepsis. *Shock*. 2005 Jul;24(1):40-7. PMID: 15988319.
6. Guo RF, Riedemann NC, Bernacki KD, Sarma VJ, Laudes IJ, Reuben JS, Younkin EM, Neff TA, Paulauskis JD, Zetoune FS, Ward PA. Neutrophil C5a receptor and the outcome in a rat model of sepsis. *FASEB J*. 2003 Oct;17(13):1889-91. PMID: 12897064.
7. Laudes IJ, Guo RF, Riedemann NC, Speyer C, Craig R, Sarma JV, Ward PA. Disturbed homeostasis of lung intercellular adhesion molecule-1 and vascular cell adhesion molecule-1 during sepsis. *Am J Pathol*. 2004 Apr;164(4):1435-45. PMID: 15039231.

Functions of C5a receptors

Peter A. Ward

Received: 16 December 2008 / Revised: 14 January 2009 / Accepted: 15 January 2009 / Published online: 3 February 2009
© Springer-Verlag 2009

Abstract The split product of the complement protein, C5, is C5a and is an extremely potent pro-inflammatory peptide that interacts with two C5a receptors, C5aR and C5L2, present on surfaces of phagocytes as well as other cell types. The former is a well-established receptor that initiates G-protein-coupled signaling via mitogen-activated protein kinase pathways. Its *in vivo* blockade greatly reduces inflammatory injury. Much less is known about C5L2, occupancy of which by C5a does not initiate increased intracellular Ca^{2+} . There are numerous conflicting reports suggesting that C5L2 is a “default receptor” that attenuates C5a-dependent biological responses by competing with C5aR for binding of C5a. However, there are other reports suggesting that C5L2 plays an active, positive role in inflammatory responses. Better definition of C5L2 is needed if its *in vivo* blockade, along with C5aR, is to be considered in complement-dependent inflammatory diseases.

Keywords Complement · C5a · C5aR · C5L2 · Inflammation

Introduction

The initial structural characterization in 1991 [1, 2] of the rhodopsin-like receptor for C5a, C5aR [1], and the receptor for *N*-formyl Met-Leu-Phe [2] provided key biochemical information that would permit development of antibodies and synthetic inhibitors to these receptors, for which C5aR binds C5a with high affinity and initiates G-protein-

dependent cascade of cell responses (increased intracellular Ca^{2+} , granule fusion with the cell membrane, enzyme release, on oxidative burst [H_2O_2 production], etc.). Similar signaling events occur with receptor–ligand interaction involving the formyl peptide receptor. C5aR is now known to be crucial in the initiation of acute inflammatory responses [3, 4]. Both C5a receptors, C5aR and C5L2, have been the subject of a recent review [5]. In the early 2000s, a second receptor for C5a, C5L2, was described, based on its ability to bind C5a and C5a *des Arg* with high affinity in the absence of an intracellular Ca^{2+} signal [6]. However, signaling as assessed by phosphoprotein appearance in myeloid-derived cells (neutrophils [PMNs], macrophages, monocytes, and dendritic cells) could not be measured [7]. Functional responses, such as chemotaxis, enzyme release, the respiratory burst, etc., were also undetectable after ligation of C5L2 with C5a, leading to the designation of C5L2 as a “default” or “scavenger” receptor [6]. In other words, C5L2 competed with C5aR for binding of C5a, and the balance in C5a occupancy between the two receptors would determine the outcome (pro-inflammatory or anti-inflammatory).

C3a *des Arg* as a controversial ligand for C5L2

Between 2002 and 2005, C5L2 was described as having the ability to bind with C3a *des Arg* with high affinity [8–10]. Under such conditions, C3a *des Arg* caused cell lines transfected with C5L2 as well as normal adipose cells to show increased synthesis of triglycerides and increased uptake of glucose [9]. Accordingly, C3a *des Arg* was named “acylation stimulating protein.” It should be pointed out that C3a *des Arg* was isolated from activated human serum and required $>1 \mu\text{M}$ for the observed activity. The possibility of contaminating C5a or C5a *des Arg* needs to

P. A. Ward (✉)
Department of Pathology,
The University of Michigan Medical School,
1301 Catherine Road,
Ann Arbor, MI 48109-0602, USA
e-mail: pward@umich.edu

Table 1 Consequences of loss of C5a receptor function

Condition	Receptor absence or blockade ^a		Reference(s)
	C5aR	C5L2	
IgG immune complex lung	Reduced injury	Enhanced injury	[7, 12]
MAPK activation in cells	Reduced injury	Controversial	[5, 6, 14]
Experimental asthma	Reduced injury	Reduced injury	[14]
CLP: survival	Enhanced injury	Enhanced injury	[15]
CLP: IL-6 levels	Reduced injury	Enhanced injury	[13]
CLP: pro-inflammatory mediators	Reduced injury	Reduced injury	[15]
CLP: HMGB1 levels	Unaltered injury	Reduced injury	[15]
Endotoxemia		Reduced survival	[14]

^a Knockout or blockade by antibody

be considered. In addition, recombinant C3a *des Arg* or the truncated form of the peptide should be employed in order to determine if the functional activity on adipocytes can be confirmed. It was also suggested that C5L2 would bind C4a, and it was confirmed that C5L2 bound C5a and C5a *des Arg* with high affinity [6, 10, 11]. In 2006, investigators from Germany and the UK, using transfected cell lines (HEK 293 and RBL cells), described their inability to demonstrate the binding of either C3a or C3a *des Arg* C5L2 to these cells. It was argued that "...C5L2 is not a receptor C3a or C3a *des Arg*⁷⁷" [11]. One possible explanation may be that adipocytes have unique binding and functional responses to C3a and C3a *des Arg* that are not seen in other cell types. Resolution of this controversy is critically needed.

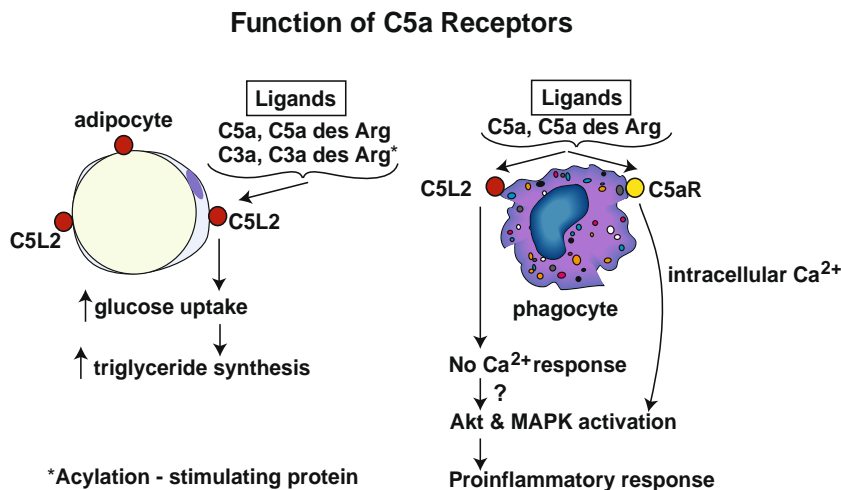
Biological responses of C5aR and C5L2

Evidence for the roles of C5aR and C5L2 is summarized in Table 1 and Fig. 1. Using a model of acute lung injury (ALI) in mice following distal airway deposition of IgG immune complexes, the inflammatory outcome was measured by morphological changes, albumin leak, and mediator presence (e.g., interleukin 6 [IL-6], tumor necrosis

factor alpha [TNF- α]). Genetic absence of C5aR in C57Bl/6 mice was associated with greatly reduced evidence of ALI as well as reduced PMN accumulation [12] and reduced levels of pro-inflammatory mediators. C5L2^{-/-} mice undergoing the same type of lung inflammatory injury (IgG immune complexes) showed amplified inflammation injury [7]. In these C5L2^{-/-} mice, increased PMN content in bronchoalveolar lavage fluids was found, together with higher levels of IL-6 and TNF- α . When blocking antibody to C5L2 was employed in mice with cecal ligation and puncture (CLP), plasma levels of IL-6 were nearly threefold higher than in mice in which C5L2 was not blocked [13]. Collectively, these two experimental systems suggested that the lack of availability of C5L2 results in enhanced inflammatory responses via engagement of C5a exclusively with C5aR, in line with C5L2 acting as a "scavenger" or "default" receptor, functioning as a counterbalance to the pro-inflammatory effects of C5aR. However, in a recent report also using ovalbumin-anti-ovalbumin IgG immune complexes, reduced inflammatory injury in airways has been described in C5L2^{-/-} mice [14].

In vitro signaling in C5L2^{-/-} macrophages or PMNs showed reduced activation (phosphorylation) of mitogen-activated protein kinases (MAPKs; p38, ERK1/2, JNK)

Fig. 1 Function of C5aR receptors



after incubation with C3a or C5a [14]. Production of TNF- α or IL-6 in C5L2^{-/-} cells stimulated with lipopolysaccharide (LPS) or LPS+C5a was also reduced. This is in contrast to an earlier report in which cells transfected with C5L2 showed little, if any, activation of MAPKs after incubation with C5a [7]. While there remains great confusion regarding the relationship between C5L2 and activation of signaling pathways, it is possible that differences in the types of cells being studied, problems with transgenic expression of C5L2 and linkage with signaling pathways, and the possibility that C5aR and C5L2 may interact in some unknown manner (such as heterodimerization) are issues that have not been adequately addressed but may be important in resolving the current confusion about the functionality of C5L2.

In the setting of experimental asthma in mice several years ago, it was described that C5^{-/-} mice are protected against experimental asthma [15], suggesting that activation products of C5 are harmful in this model. Recent studies suggest that, in C5aR^{-/-} mice, the upper airway inflammatory response and airway hyper-responsiveness (AHR) are significantly diminished, suggesting that C5aR induces "... marked enhancement of TH2 polarized responses" [16]. In C5L2^{-/-} mice undergoing ovalbumin-induced asthma, development of AHR and peribronchiolar inflammation was reduced, suggesting that C5L2 contributes positively to the lung inflammatory response [14]. Finally, in the same study, PMN accumulation in dorsal subcutaneous air pouches of C5L2^{-/-} mice was reduced (by more than twofold). Collectively, these data from the Toronto group suggest a linkage between C5L2, MAPK signaling, and phagocyte activation and mobilization. However, essentially, none of these reported phenotypes are seen in the mice studied in the Gerard lab (C. Gerard, J. Köhl, unpublished data).

Substantial work has been done to define the possible role of C5aR and C5L2 in the setting of experimental sepsis, using knockout mice or mice in which C5aR or C5L2 was blocked with an antibody (to the N-terminal region of each receptor) or with a synthetic inhibitor of both receptors. Using survival as the endpoint, evidence was obtained that both receptors contributed to adverse events resulting in mortality after CLP [17]. Absence or blockade of either receptor greatly reduced plasma levels of pro-inflammatory cytokines (IL-1 β , IL-6, macrophage inflammatory protein [MIP]-1 α , and MIP-2), but interestingly, there was no effect on TNF- α levels in the plasma of CLP mice, suggesting that cytokines and chemokines are individually regulated. These studies also showed that C5L2 absence either in vivo or in vitro resulted in little, if any, expression of HMGB1, either in plasma of CLP mice or in supernatant fluids from mouse macrophages or human blood PMNs or peripheral mononuclear cells stimulated with C5a, LPS, or the combination [17]. Collectively, these

data suggest that, in the setting of sepsis, C5L2 contributes to adverse events related to the "cytokine storm," lethality, and production of HMGB1, which is known to be linked to the adverse events in CLP-induced sepsis [18].

As indicated above, C5L2^{-/-} mice have been reported to be hypersusceptible to lethal endotoxemia, although the explanation for this observation is not apparent [14]. This would seem to be reverse of the role of C5L2 in the setting of CLP-induced sepsis in which C5L2 contributes to pro-inflammatory, harmful events [17]. In the setting of septic shock in humans, C5L2 content on blood PMNs falls, likely because of internalization of C5aC5L2 complexes [19]. Similar changes occur in blood PMNs from CLP rats. Loss of C5L2 on blood PMNs after CLP was prevented if animals were given blocking antibody to C5a at the time of CLP. It has been suggested that C5L2 may have anti-inflammatory properties in the central nervous system [20]. The biological role of C5L2 has been the subject of a recent review [21]. Finally, a recent study suggests that C5a and C5a *des Arg* binding to cells results in a clathrin-dependent pathway of rapid internalization of these ligands that then become degraded, whereas internalization involving C5aR is slower, with suggestions that undegraded C5a and C5a *des Arg* may be released into the extravascular environment [22].

Conclusions

It is clear that there are two C5a receptors, C5aR and C5L2, each of which has high affinity binding for C5a and C5a *des Arg*. What is confusing is the extent to which C3a and C3a *des Arg* bind to C5L2. It is also known that C5aR interacts with C5a in a G-protein-dependent manner, which results in increased intracellular Ca²⁺ together with MAPK and Akt activation, followed by a series of functional responses such as chemotaxis, enzyme release, Mac-1 upregulation, degranulation, a respiratory burst, etc. The role of C5aR in the setting of sepsis also seems obvious: C5aR interacting with C5a contributes to adverse events in ALI after deposition of IgG immune complexes and in CLP-induced sepsis, including the intensified pro-inflammatory state and lethality. As for C5L2, there is much confusion and less certainty about its role. Clearly, it binds both C5a and C5a *des Arg*, but no increased intracellular Ca²⁺ occurs. Beyond this, its role is controversial. Interestingly, it has been recently shown that the vast majority of C5L2 exists intracellularly in endosomal compartments and is translocated to the cell surface after cell activation (Gerard, C., personal communication). It remains to be determined what signaling pathway is engaged by C5L2. Whether C3a *des Arg* is a ligand for C5L2 is strongly debated (see above). There is disagreement as to whether C5a reacting with C5L2 activates MAPK signaling. There is mixed evidence about

the role of C5L2 in cytokine and chemokine production. This may be a matter of the mediator in question (e.g., IL-6 vs. IL-1 β vs. TNF- α , etc.) It seems likely that C5a interaction with C5L2 triggers HMGB1 release, which is known to participate in the adverse consequences of experimental sepsis. As mentioned above, it is possible that some type of interaction between C5aR and C5L2 occurs, such as heterodimerization, or that C5a interaction with C5aR results in signaling events that alter cell responsiveness of C5L2 to C5a.

Acknowledgment We thank Professor Craig Gerard (Dept. Pediatrics, Children's Hospital of Boston, MA) for helpful suggestions for the manuscript. This work is supported in part by National Institute of Health grants: HL-31963, GM-61656 and GM-029507.

References

- Gerard NP, Gerard C (1991) The chemotactic receptor for human C5a anaphylatoxin. *Nature* 349:614–617
- Boulay F, Tardif M, Brouchon L, Vignais P (1990) Synthesis and use of a novel N-formyl peptide derivative to isolate a human N-formyl peptide receptor cDNA. *Biochem Biophys Res Commun* 168:1103–1109
- Strainic MG, Liu J, Huang D, An F, Lalli PN, Muqim N, Shapiro VS, Dubyak GR, Heeger PS, Medof ME (2008) Locally produced complement fragments C5a and C3a provide both costimulatory and survival signals to naïve CD4+ T cells. *Immunity* 28:425–435
- Hawlish H, Wills-Karp M, Karp CL, Köhl J (2004) The anaphylatoxins bridge innate and adaptive immune responses in allergic asthma. *Mol Immunol* 41:123–131
- Lee H, Whitfield PL, Mackay CR (2008) Receptors for complement C5a. The importance of C5aR and the enigmatic role of C5L2. *Immunol Cell Biol* 86:153–160
- Okinaga S, Slattery D, Humbles A, Zsengeller Z, Morteau O, Kinrade MB, Brodbeck RM, Krause JE, Choe HR, Gerard NP, Gerard C (2003) C5L2, a non-signaling C5a binding protein. *Biochemistry* 42:9406–9415
- Gerard N, Lu B, Liu P, Craig S, Fujiwara Y, Okinaga S, Gerard C (2005) An anti-inflammatory function for the complement anaphylatoxin C5a-binding protein, C5L2. *JBC* 280:39677–39680
- Kalant D, Cain SA, Maslowska M, Sniderman AD, Cianflone K, Monk PN (2003) The chemoattractant receptor-like protein C5L2 binds the C3a des-arg⁷⁷/acylation-stimulating protein. *J Biol Chem* 278:11123–11129
- Kalant D, MacLaren, Cui W, Samanta R, Monk PN, Laporte SA, Cianflone K (2005) C5L2 is a functional receptor for acylation-stimulating protein. *J Biol Chem* 280:23936–23944
- Cain SA, Monk PN (2002) The orphan receptor C5L2 has high affinity binding sites for complement fragments C5a and C5a des-arg⁷⁴. *J Biol Chem* 277:7165–7169
- Johswich K, Martin M, Thalmann J, Rheinheimer C, Monk PN, Klos A (2006) Ligand specificity of the anaphylatoxin C5L2 receptor and its regulation on myeloid and epithelial cell lines. *J Biol Chem* 281:39088–39095
- Hopken UE, Lu B, Gerard NP, Gerard C (1997) Impaired inflammatory responses in the reverse Arthus reaction through genetic deletion of the C5a receptor. *J Exp Med* 186:749–756
- Gao H, Neff TA, Guo TA, Speyer CL, Sarma JV, Tomlins S, Man Y, Riedemann NC, Hoesel LM, Younkin E, Zetoune FS, Ward PA (2005) Evidence for a functional role of the second C5a receptor C5L2. *FASEB J* 19:1003–1005
- Chen NJ, Mirsos C, Suh D, Lu YC, Lin WJ, McKerlie C, Lee T, Baribault H, Tian H, Yeh WC (2007) C5L2 is critical for the biological activities of the anaphylatoxins C5a and C3a. *Nat Lett* 446:203–207
- Karp CL, Grupe A, Schadt E, Ewart SL, Keane-Moore M, Cuomo PJ, Köhl J, Wahl L, Kuperman D, Germer S, Aud D, Peltz G, Wills-Karp (2000) Identification of complement factor 5 as a susceptibility locus for experimental allergic asthma. *Nat Immunol* 1:221–226
- Köhl J, Baelder R, Lewkowich IP, Pandey MK, Hawlish H, Wang L, Best J, Herman NS, Sproles AA, Zwirner J, Whitsett JA, Gerard C, Sfyroera G, Lambris JD, Wills-Karp M (2006) A regulatory role for the C5a anaphylatoxin in type 2 immunity in asthma. *J Clin Invest* 116:628–632
- Rittirsch D, Flierl MA, Nadeau BA, Day DE, Huber-Lang M, Mackay CR, Zetoune FS, Gerard NP, Cianflone K, Koehl J, Gerard C, Sarma JV, Ward PA (2008) Functional roles for C5a receptors in sepsis. *Nat Med* 14:551–557
- Yang H, Wang H, Czura CJ, Tracey KJ (2005) The cytokine activity of HMGB1. *J Leuk Biol* 78:1–8
- Huber-Lang M, Sarma JV, Rittirsch D, Schreiber H, Weiss M, Flierl M, Younkin E, Schneider M, Suger-Wiedeck H, Gebhard F, McClintock SD, Neff T, Zetoune F, Bruckner U, Guo RF, Monk PN, Ward PA (2005) Changes in the novel orphan, C5a receptor (C5L2), during experimental sepsis and sepsis in humans. *J Immunol* 174:1104–1110
- Gavrilyuk V, Kalinin S, Hilbush BS, Middlecamp A, McGuire S, Pelligrino D, Weinberg G, Feinstien DL (2005) Identification of complement 5a-like receptor (C5L2) from astrocytes: characterization of anti-inflammatory properties. *J Neurochem* 92:1140–1149
- Johswich K, Kos A (2007) C5L2 – an anti-inflammatory molecule or a receptor for acylation stimulating protein (C3a-desArg)? Review. *Advances in experimental medicines and biology*. In: Lambris JD (ed) *Current topics in innate immunity*. Springer, New York, pp 159–180
- Scola A-M et al (2008) The human complement fragment receptor, C5L2, is a recycling decoy receptor. *Mol Immunol*. doi:10.1016/j.molimm.2008.11.001

Research

Open Access

Inhibition of complement C5a prevents breakdown of the blood-brain barrier and pituitary dysfunction in experimental sepsis

Michael A Flierl¹, Philip F Stahel¹, Daniel Rittirsch^{2,5}, Markus Huber-Lang³, Andreas D Niederbichler⁴, L Marco Hoesel⁵, Basel M Touban¹, Steven J Morgan¹, Wade R Smith¹, Peter A Ward⁵ and Kyros Ipaktchi¹

¹Department of Orthopaedic Surgery, Denver Health Medical Center, University of Colorado School of Medicine, 777 Bannock Street, Denver, CO 80204, USA

²Department of Trauma Surgery, University Hospital Zurich, Rämistrasse 100, 8091 Zurich, Switzerland

³Department of Trauma, Hand-, Plastic-, and Reconstructive Surgery, University Hospital Ulm, Steinhövelstrasse 9, 89075 Ulm, Germany

⁴Department of Plastic, Hand, and Reconstructive Surgery, University Medical Center Hannover (MHH), Carl-Neuberg-Strasse 1, 30625 Hannover, Germany

⁵Department of Pathology, University of Michigan Medical School, 1301 Catherine Road, Ann Arbor, MI 48109, USA

Corresponding author: Philip F Stahel, philip.stahel@dhha.org

Received: 27 Oct 2008 Revisions requested: 9 Jan 2009 Revisions received: 12 Jan 2009 Accepted: 6 Feb 2009 Published: 6 Feb 2009

Critical Care 2009, **13**:R12 (doi:10.1186/cc7710)

This article is online at: <http://ccforum.com/content/13/1/R12>

© 2009 Flierl et al.; licensee BioMed Central Ltd.

This is an open access article distributed under the terms of the Creative Commons Attribution License (<http://creativecommons.org/licenses/by/2.0>), which permits unrestricted use, distribution, and reproduction in any medium, provided the original work is properly cited.

Abstract

Introduction Septic encephalopathy secondary to a breakdown of the blood-brain barrier (BBB) is a known complication of sepsis. However, its pathophysiology remains unclear. The present study investigated the effect of complement C5a blockade in preventing BBB damage and pituitary dysfunction during experimental sepsis.

Methods Using the standardised caecal ligation and puncture (CLP) model, Sprague-Dawley rats were treated with either neutralising anti-C5a antibody or pre-immune immunoglobulin (Ig) G as a placebo. Sham-operated animals served as internal controls.

Results Placebo-treated septic rats showed severe BBB dysfunction within 24 hours, accompanied by a significant upregulation of pituitary C5a receptor and pro-inflammatory cytokine expression, although gene levels of growth hormone were significantly attenuated. The pathophysiological changes in placebo-treated septic rats were restored by administration of neutralising anti-C5a antibody to the normal levels of BBB and pituitary function seen in the sham-operated group.

Conclusions Collectively, the neutralisation of C5a greatly ameliorated pathophysiological changes associated with septic encephalopathy, implying a further rationale for the concept of pharmacological C5a inhibition in sepsis.

Introduction

Sepsis remains a leading cause of morbidity and mortality in the intensive care unit (ICU), and one of the top 10 causes of death worldwide [1,2]. The underlying pathophysiological cascade of sepsis is highly complex and far from fully understood [3-5]. From an immunological standpoint, the activation of the complement cascade, a potent arm of the innate immune response, has been associated with fatal outcomes in septic

patients [6-9]. Particularly, the complement anaphylatoxin C5a, a small inflammatory peptide derived from complement activation, has been characterised as a 'key' mediator of sepsis and septic organ dysfunction [10-14], and was recently labelled as 'too much of a good thing' or to reveal 'a dark side in sepsis' [15,16].

ACTH: adrenocorticotrophic hormone; BBB: blood-brain barrier; C5aR: C5a receptor; C5L2: C5a like receptor 2; CLP: caecal ligation and puncture; CNS: central nervous system; C_T: cycle threshold; EB: Evans Blue; ELISA: enzyme immunosorbent assay; GAPDH: glyceraldehyde 3-phosphate dehydrogenase; GH: growth hormone; ICAM: intracellular adhesion molecule; ICU: intensive care unit; Ig: immunoglobulin; IL: interleukin; MSH: melanocyte-stimulating hormone; PBS: phosphate buffered saline; PCR: polymerase chain reaction; POMC: proopiomelanocortin; RIPA: radio immunoprecipitation assay; TBST: Tris-buffered saline Tween-20; TNF: tumour necrosis factor; VCAM: vascular adhesion molecule

Although intentionally beneficial, disproportionate activation of complement during sepsis has been found to contribute to thymocyte and adrenomedullary apoptosis [17,18], paralysis of innate immunity [19,20], deterioration of the coagulation/fibrinolytic system [21] and multiple organ failure [22]. Accordingly, blockade of C5a or its receptors has been shown to prevent multiple organ failure and to greatly attenuate mortality after caecal ligation and puncture (CLP)-induced sepsis [10,11,14,19,22].

Encephalopathy syndrome is a well described complication of sepsis in the ICU. This phenomenon is thought to represent a consequence of inflammation-mediated dysfunction of the blood-brain barrier (BBB), thus allowing neurotoxic mediators to extravasate from the peripheral circulation into the sub-arachnoid space or into the brain parenchyma. Noteworthy, the focus of research studies have only addressed in more depth the neuro-inflammatory and metabolic intracerebral changes in sepsis [23-29]. The complement anaphylatoxin C5a has been characterised as a mediator of BBB dysfunction in a variety of central nervous system (CNS) disorders, including traumatic brain injury and bacterial meningitis [30-32]. In addition, the detection of the C5a receptor (C5aR) on neurons and the observed upregulation of neuronal C5aR expression under inflammatory conditions [31,33-35] renders the brain more vulnerable to C5a-mediated neuropathophysiological sequelae secondary to a disruption of the BBB [30,31,36,37]. The complement cascade has only recently been implicated in the pathophysiology of septic encephalopathy [38].

Based on the established functions of C5a in the pathophysiology of sepsis and on experimental data which imply C5a is a potent mediator of BBB damage and neuroinflammation, we designed the present study to investigate the effect of antibody-mediated C5a-blockade on preventing the development of encephalopathy in experimental sepsis. We hypothesised that blockade of C5a would reverse the dysfunction of the BBB and restore the immunological and endocrinological homeostasis in the septic brain.

Materials and methods

Experimental CLP model

All procedures were performed in accordance with the National Institutes of Health guidelines and University Committee on Use and Care of Animals, University of Michigan (UCUCA approval #8575, 08/11/2008). Specific pathogen-free, adult male Sprague-Dawley rats (Harlan Inc., Indianapolis, IN, USA) weighing 300 to 350 g were used in all experiments. Sepsis was induced by the CLP procedure as previously described [39]. In brief, rats were anaesthetised with isoflurane (3%, oxygen flow 3 L/minute). After abdominal midline incision, the caecum was exposed, ligated and punctured through with a 18-gauge needle, and a small portion of faeces was expressed to ensure potency of the punctures. After repositioning of the bowel, the abdomen was closed in

layers using 4-0 surgical sutures (Ethicon Inc., Somerville, NJ, USA) and metallic clips. Sham animals underwent the same procedure except for ligation and puncture of the caecum. Before and after the surgery, animals had unrestricted access to food and water. Where indicated, animals intravenously received 500 µg anti-C5a antibody or 500 µg preimmune immunoglobulin (Ig) G in 500 µl sterile Dulbecco's PBS immediately after CLP or sham procedure, as previously described [13].

Anti-C5a antibody

The neutralising anti-rat C5a antibody used in this study was previously characterised [10,22]. In short, rat C5a peptide corresponding to amino acid residues 17 to 36 was coupled to keyhole limpet haemocyanin and used as an antigen to immunise rabbits. After several immunisations, the antibody was affinity purified from serum using the synthetic peptide coupled to beads. Cross-reactivity with recombinant rat C5a was confirmed by Western blotting.

Albumin immunohistochemistry

Rat brains were surgically removed, embedded in optimal cutting temperature compound (Miles, Elkhart, IN, USA) and stored at -80°C. Frozen sections (10 µm) were prepared from the embedded tissue and incubated with rabbit anti-rat albumin antibody (Bethyl Laboratories, Montgomery, TX, USA) at a dilution of 1/100 overnight. After washing, sections were incubated with a 1/200 dilution of peroxidase-conjugated goat anti-rabbit IgG for two hours (Jackson ImmunoResearch Laboratories, West Grove, PA, USA). After thorough washing, sections were stained using the ImmPACT DAB staining kit (Vector Laboratories, Burlingame, CA, USA). Tissue sections were then mounted with Crystal Mount mounting medium (Sigma, St. Louis, MO, USA) and addition of coverslips. Staining was assessed using light microscopy (BX41, Olympus, Center Valley, PA, USA) and digital imaging (Adobe Photoshop, Adobe, San Jose, CA, USA). For each experimental condition, three animals were used. The immunostainings displayed are representative for three independent experiments.

Intracerebral Evans Blue assessment

The extent of BBB dysfunction was assessed 24 hours after induction of CLP by assessment of Evans Blue (EB) extravasation in four animals per experimental condition. Briefly, 20 µl of a 2% solution of EB in saline was injected into the tail vein one hour before harvesting of brains (i.e. at t = 23 hours after CLP), and allowed to circulate for 60 minutes. Subsequently, the chest was surgically opened under anaesthesia and the intravascular dye was removed by saline perfusion (40 to 50 ml) through the left heart ventricle. The brain/pituitary was then removed and weighed before homogenisation and placed in 4 mL 99.5% formamide per gram of tissue in polyethylene tubes (BD Bioscience, Rockville, MD, USA). Tubes were placed for 48 hours on a shaker (Barnstead International, Dubuque, IA, USA) at room temperature for EB extraction. Supernatants

were collected and the absorbance read in a plate reader (Biotek Instruments, Winooski, VT, USA) at 620 nm and compared with an EB standard curve and formamide blanks. The result are expressed as microgram EB per milligram tissue.

Isolation of total RNA and quantitative real-time PCR

Total RNA was isolated from five to seven pituitary glands per experimental condition using the TRIzol method (Life Technologies Inc., Gaithersburg, MD, USA) according to the manufacturer's instructions. Digestion of any contaminating DNA was achieved by treatment of samples with RNase-Free DNase (Promega Corp., Madison, WI, USA). Reverse transcription was performed with 5 µg RNA using the Superscript II RNase H⁻ Reverse Transcriptase (GIBCO BRL; Life Technologies Inc., Gaithersburg, MD, USA) according to the manufacturer's protocol. Real-time PCR was then performed as previously described [13]. Reactions were prepared in duplicates using the iQ SYBR green Supermix reagent (Bio Rad Laboratories, Hercules, CA, USA). An amplification plot was generated using two-fold dilutions of the cDNA generated from a known amount (1 µg) of mRNA. The cycle threshold (C_T) was set above the baseline fluorescence. Plotting the log of the dilutions versus the C_T values then generated a standard curve. Quantitation of samples was determined using the standard curves. Genes analysed were C5aR, the adrenocorticotropic hormone (ACTH)-precursor proopiomelanocortin (POMC) and growth hormone (GH).

The following primer pairs were used:

C5aR: 5' primer, 5'-TATAGTCCTGCCCTCGCTCAT-3'; 3' primer, 5'-TCACCACTTTGAGCGTCTTGG-3'.

POMC: 5' primer, 5'-AGCCTCTGTCCAGTCCTGAG-3'; 3' primer, 5'-CTTAGTCACTGCTCCTAAC-3'.

GH: 5' primer, 5'-CTCGGACCGCGTCTATGAGA-3'; and 3' primer, 5'-TGAGGATCGCCCAATACGG-3'.

TNF: 5' primer, 5'-GTGATCGGTCCCAACAAGGA-3'; and 3' primer, 5'-AGGGTCTGGGCCATGGAA-3'.

IL-6: 5' primer, 5'-ATATGTTCTCAGGGAGATCTTGGAA-3'; and 3' primer, 5'-GTGCATCATCGCTGTTTCATACA-3'.

GAPDH: 5' primer, 5'-GCCTCGTCTCATAGACAAGATG-3'; and 3' primer, 5'-CAGTAGACTCCACGACATAC-3'.

Western blot analysis of C5aR

Following decapitation, rat brains were immediately removed surgically, the pituitary identified and excised, homogenised in ice-cold radio immunoprecipitation assay (RIPA) buffer (Upstate, Temecula, CA, USA) and subjected to BCA Protein Assay analysis (Thermo Scientific, Rockford, IL, USA) for equal protein loading. Total protein from pituitary lysates (50

µg) was separated by electrophoresis in a denaturing 12% polyacrylamide gel and then transferred to a polyvinylidene fluoride membrane. Equal loading was confirmed by detection of glyceraldehyde 3-phosphate dehydrogenase (GAPDH) (Santa Cruz, Santa Cruz, CA, USA) as a 'housekeeping' protein. Non-specific binding sites were blocked with Tris-buffered saline Tween-20 (TBST) plus 5% nonfat dry milk for one hour at room temperature. Following washing in TBST, the membrane was incubated with rabbit anti-rat C5aR antibody (kindly provided by P.A. Ward, University of Michigan [14,40,41]) at a 1/500 dilution overnight. After three washes in TBST, the membrane was incubated in a 1/10,000 dilution of horseradish peroxidase-conjugated donkey anti-rabbit IgG as the secondary antibody (Amersham, Piscataway, NJ, USA). The membrane was developed by enhanced chemiluminescence technique according to the manufacturer's protocol (Amersham, Piscataway, NJ, USA). Pituitary tissue was harvested from five animals and assessed by Western blotting. Due to the lane restrictions (n = 10) of a typical Western mini gel, two (sham groups) or three (CLP groups) samples were compared, in order to be able to evaluate samples directly 'side-by-side'. The blot depicted is representative of three independent experiments.

ELISA of pituitary hormone levels

Rat whole blood was collected into syringes containing anticoagulant citrate dextrose (Baxter, Deerfield, IL, USA) in a 9:1 ratio by puncture of the inferior vena cava 24 hours after CLP or sham surgery. Samples were centrifuged (2500 rpm for 10 minutes at 4°C), plasma was obtained and immediately stored at -80°C. Levels of GH and corticosterone were determined using commercially available ELISA kits (both Diagnostic Systems Laboratories, Webster, TX, USA) according to the manufacturer's instructions. For plasma measurements of GH and corticosterone, five to seven samples were assessed for each experimental group.

Statistical analysis

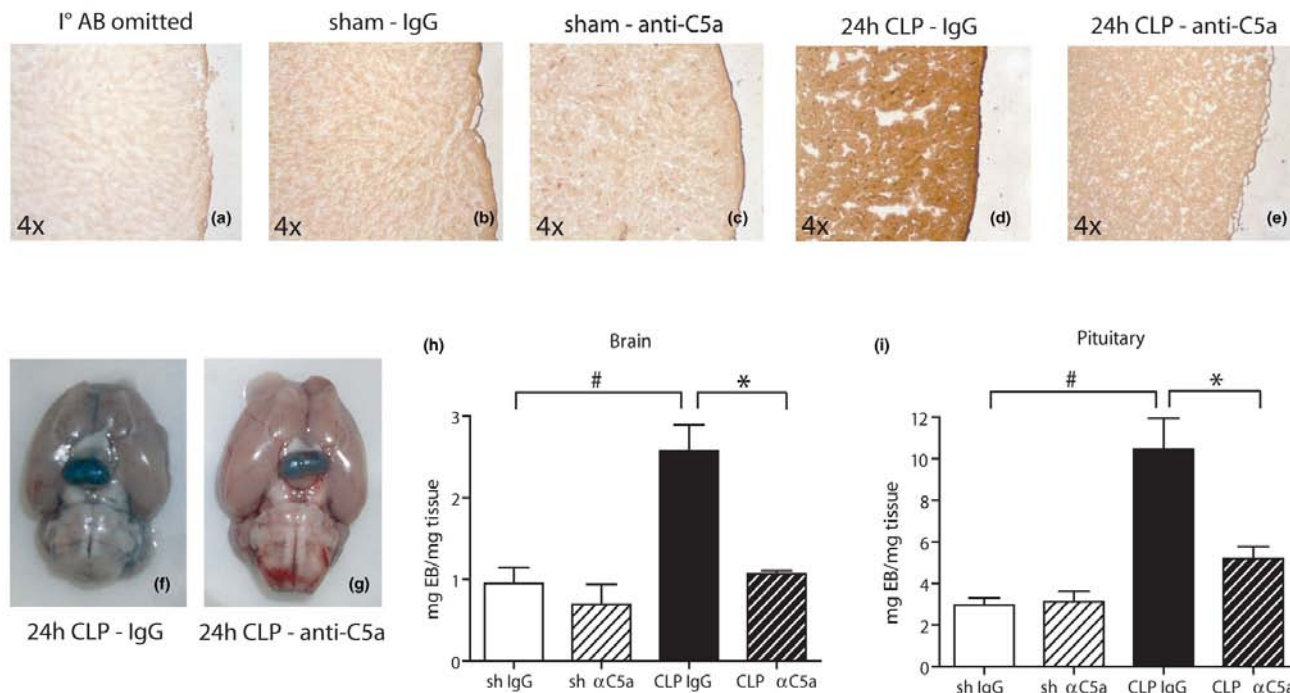
All values are expressed as mean ± standard deviation. Data were analysed with a one-way analysis of variance, and individual group means were then compared with the Tukey multiple comparison test. Differences were considered statistically significant at p < 0.05.

Results

Anti-C5a prevents BBB breakdown during experimental sepsis

As depicted in Figure 1, as a negative control, primary antibody was omitted in a section obtained from a preimmune IgG-treated animal (panel a) and little straining of brain tissue for albumin was noted. Sham animals treated with either pre-immune IgG (panel b) or anti-C5a (panel c) displayed comparable levels of baseline immunostaining for albumin. However, there was a significant increase in diffuse cerebral albumin accumulation 24 hours after CLP in animals treated with pre-

Figure 1



Anti-C5a ameliorates impairment of the blood-brain barrier after caecal ligation and puncture (CLP). (a-e) Brains were surgically removed, snap-frozen and tissue sections (10 μm) were obtained. Cerebral extravasation of rat albumin was assessed by immunohistochemistry 24 hours after CLP or sham procedure, three samples per experimental condition. Stains displayed are representative of three independent experiments. (f, g) Comparison of Evans Blue extravasation into the cerebellum and pituitary in IgG-treated or anti-C5a treated rats 24 hours post CLP. Displayed depictions are representative of four animals. (h, i) Quantification of Evans Blue extravasation into the brain or pituitary by determination of mg Evans Blue/mg tissue ratio in different groups at indicated time-points, four for each experimental condition. # p < 0.05 between sham and 24 hours CLP animals; * p < 0.05 between IgG-treated and anti-C5a-treated rats.

immune IgG (panel d). In contrast, when rats received anti-C5a immediately after the CLP procedure, cerebral albumin build-up was dramatically reduced to sham levels (panels b and e).

Similar results were found when breakdown of the BBB was analysed by EB extravasation 24 hours after CLP. Animals treated with preimmune IgG displayed robust EB extravasation in the cerebral and pituitary areas (panel f), while anti-C5a-treated littermates exhibited far less buildup of EB (panel g). Panels h and i show quantified EB extravasation 24 hours after CLP as mg EB/mg tissue ratio and confirm the observations made in panels f and g on a quantitative level.

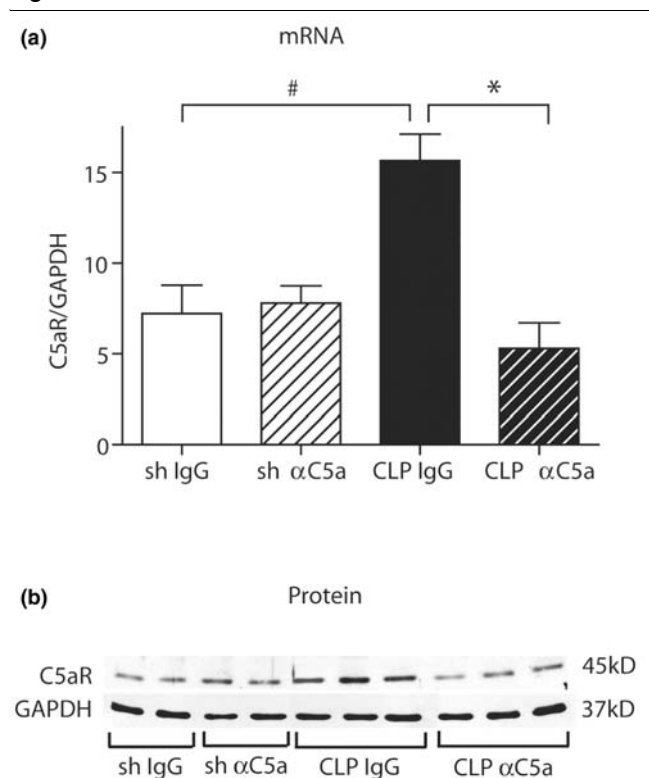
C5aR is upregulated in the pituitary gland of septic rats

Rat pituitary glands were surgically removed, total RNA was isolated and analysed by quantitative real-time PCR. There was a significant increase of pituitary C5aR expression 24 hours after CLP in animals receiving preimmune IgG, while anti-C5a-treated littermates displayed expression levels comparable with sham animals (Figure 2a). Similar results were found when pituitaries were homogenised and obtained pro-

teins were subjected to Western blot analysis. Protein expression of C5aR in the pituitary was markedly increased in IgG-treated animals 24 hours after CLP, while rats that were administered anti-C5a revealed C5aR protein expression similar to sham controls (Figure 2b). Such patterns of increased C5aR expression in CLP mice have been described in lung, liver, kidney and heart [12].

C5a-blockade partially reverses cytokine upregulation in the pituitary gland

Following isolation of pituitary total RNA, quantitative real-time PCR was performed for TNF and IL-6. Sham animals treated with either preimmune IgG or anti-C5a displayed similar expression of mRNA for both proinflammatory mediators. However, 24 hours after the CLP procedure, mRNA expression for TNF and IL-6 was substantially increased in IgG-treated rats (Figure 3). Elevated mRNA levels were partially reduced to sham levels when animals were administered anti-C5a immediately after CLP.

Figure 2

Pituitary expression of C5a receptor (R) during experimental sepsis in IgG or anti-C5a IgG treated sham animals and septic littermates 24 hours after caecal ligation and puncture (CLP) procedure. **(a)** Following total RNA isolation from pituitary tissue, pituitary C5aR mRNA expression was assessed by real-time PCR. For each bar, sample size was five to seven. **(b)** Five pituitary tissue samples were removed at indicated time-points, homogenised and C5aR protein expression was analysed by Western blotting. For sham groups, two samples were taken; for CLP groups, three samples were taken. Blot is representative for three independent experiments. GAPDH = glyceraldehyde 3-phosphate dehydrogenase. # $p < 0.05$ between sham and 24 hours CLP animals; * $p < 0.05$ between IgG-treated and anti-C5a-treated rats.

Pituitary dysfunction is reversed by C5a blockade

Pituitary glands were surgically removed, total RNA was isolated and analysed for POMC and GH by quantitative real-time PCR. mRNA expression for both, POMC and GH was dramatically reduced 24 hours after CLP in IgG-treated rats (Figures 4a,b). Anti-C5a administration completely reversed these changes, resulting in POMC and GH mRNA expression levels equivalent to sham groups. Plasma samples were obtained 24 hours after CLP or sham procedure and subjected to ELISA analysis for GH and corticosterone, the main glucocorticoid of rodents. When compared with sham animals, IgG-treated rats had with significantly increased plasma levels of GH and corticosterone 24 hours after CLP. Again, these changes were reversed by administration of anti-C5a immediately after CLP (Figures 4c,d).

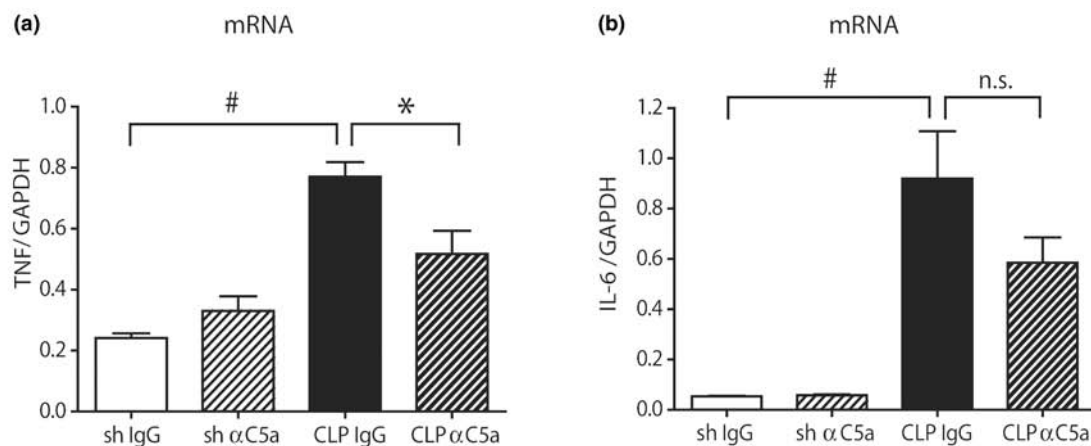
Discussion

Under physiological conditions, the BBB maintains the cerebral micro-environment by tightly regulating the passage of molecules into and out of the brain to protect the brain from microorganisms and neurotoxic substances. During sepsis, however, blood-borne proinflammatory mediators are released, coincidental with diffuse endothelial activation and subsequent upregulation of vascular adhesion molecule-1 (VCAM-1), intracellular adhesion molecule-1 (ICAM-1), E-selectin on cerebral endothelia [42-45], facilitating adhesion and transmigration of neutrophils and monocytes into the brain tissue. Especially the anaphylatoxin C5a is known to be a strong inducer of ICAM-1, VCAM-1 and various selectins [46-50]. In addition, cerebral endothelia produce IL-1 β , TNF and IL-6 [51-53], all of which have been shown to directly induce a disruption of the BBB *in vitro* [54]. Thus, these mediators interact with surrounding brain cells, relaying into the brain inflammatory response and jeopardising the functional integrity of the BBB [55-57]. In the present study, we found that, during experimental sepsis, the antibody-mediated blockade of anaphylatoxin C5a prevented breakdown of the blood-brain barrier, reducing cerebral and pituitary edema formation, as assessed by extravasation of albumin and EB (Figure 1).

Although the CNS itself was traditionally thought to be immunologically privileged, recent studies have demonstrated that the CNS is a rich source of inflammatory mediators, such as cytokines, chemokines and complement components [58-64], and has therefore been termed both 'culprit' and 'victim' during sepsis [57]. Thus, during sepsis, the BBB is exposed to harmful proinflammatory mediators deriving from two different compartments, the brain as well as the systemic circulation. This results in an extrinsic, as well as intrinsic, attack on the BBB, accelerating the deterioration of its barrier function. As described above, we demonstrate significant upregulation of pituitary expression of TNF and IL-6 mRNA following CLP (Figure 3), indicating that the pituitary might be an additional source of cerebral proinflammatory mediators. Blood-derived proinflammatory mediators reach the hypophyseal circulation via the anterior hypophyseal arteries and cytokines can diffuse into the pituitary because these areas are free from CNS BBB [65]. Therefore, we decided that mRNA analysis for TNF and IL-6 might shed a more accurate light on the origin of these proinflammatory mediators.

Resident cells of the brain, such as neurons, astrocytes and microglia, are capable of synthesising essentially all complement proteins, complement regulatory molecules and complement receptors [31,66-70]. It has been reported that the pituitary expresses the complement receptors C3aR, C5aR and C5a-like receptor 2 (C5L2), and that these molecules may contribute to regulation of the immune response [71,72]. We found upregulation of C5aR in the pituitary based on mRNA and protein levels following CLP and reversal of these changes by administration of anti-C5a (Figure 2). Upregulation

Figure 3



Expression of inflammatory mediators in the pituitary. Pituitary tissue samples were surgically removed, snap-frozen, homogenised and total RNA was extracted. Samples were then analysed by quantitative real-time PCR analysis. Expression of (a) TNF and (b) IL-6 mRNA in the pituitary 24 hours after sham procedure or caecal ligation and puncture (CLP). Five to seven samples were taken per experimental condition. GAPDH = glyceraldehyde 3-phosphate dehydrogenase. # $p < 0.05$ between sham and 24 hours CLP animals; * $p < 0.05$ between IgG-treated and anti-C5a-treated rats.

of C5aR during sepsis has been described in various organs, such as lung, liver, kidney and heart [12]. Such upregulation infers that these tissues may develop highly undesirable outcomes after encounters with C5a.

Sepsis is known to induce an abnormal pituitary response [73]. Hormonal changes in cortisol, mineralocorticoids, thyroid hormones, GH and vasopressin have all been described during sepsis. Although the acute phase of sepsis is characterised by high levels of GH, GH insufficiency is reported in the late stage of sepsis [73,74]. In line with these findings, we have found elevated levels of GH protein 24 hours after CLP, while pituitary mRNA expression is significantly reduced, most likely because of a negative feedback mechanism.

Hypercortisolism during the early stages of sepsis is usually followed by cortisol insufficiency in 60% of septic patients [73]. Significantly increased levels of corticosterone occurred in rats following CLP (Figure 4). In the current study, pituitary POMC mRNA expression was completely abolished during experimental sepsis (Figure 4). POMC is a polypeptide precursor of multiple molecules, including ACTH and melanocyte-stimulating hormones (MSH) α , β and γ [75]. Interestingly, MSH- α has recently emerged as a molecule with potent anti-inflammatory effects, which orchestrates descending neurogenic anti-inflammatory pathways and ameliorates the inflammatory response of immune cells [76]. At a molecular level, MSH- α decreases the intracellular production of pro-inflammatory cytokines and chemokines by inhibiting nuclear factor- κ B activation and reduces cellular expression of VCAM-1, ICAM-1 and E-selectin [76]. During human sepsis, plasma concentrations of MSH- α have been found to be significantly decreased during the early course of the disease and gradu-

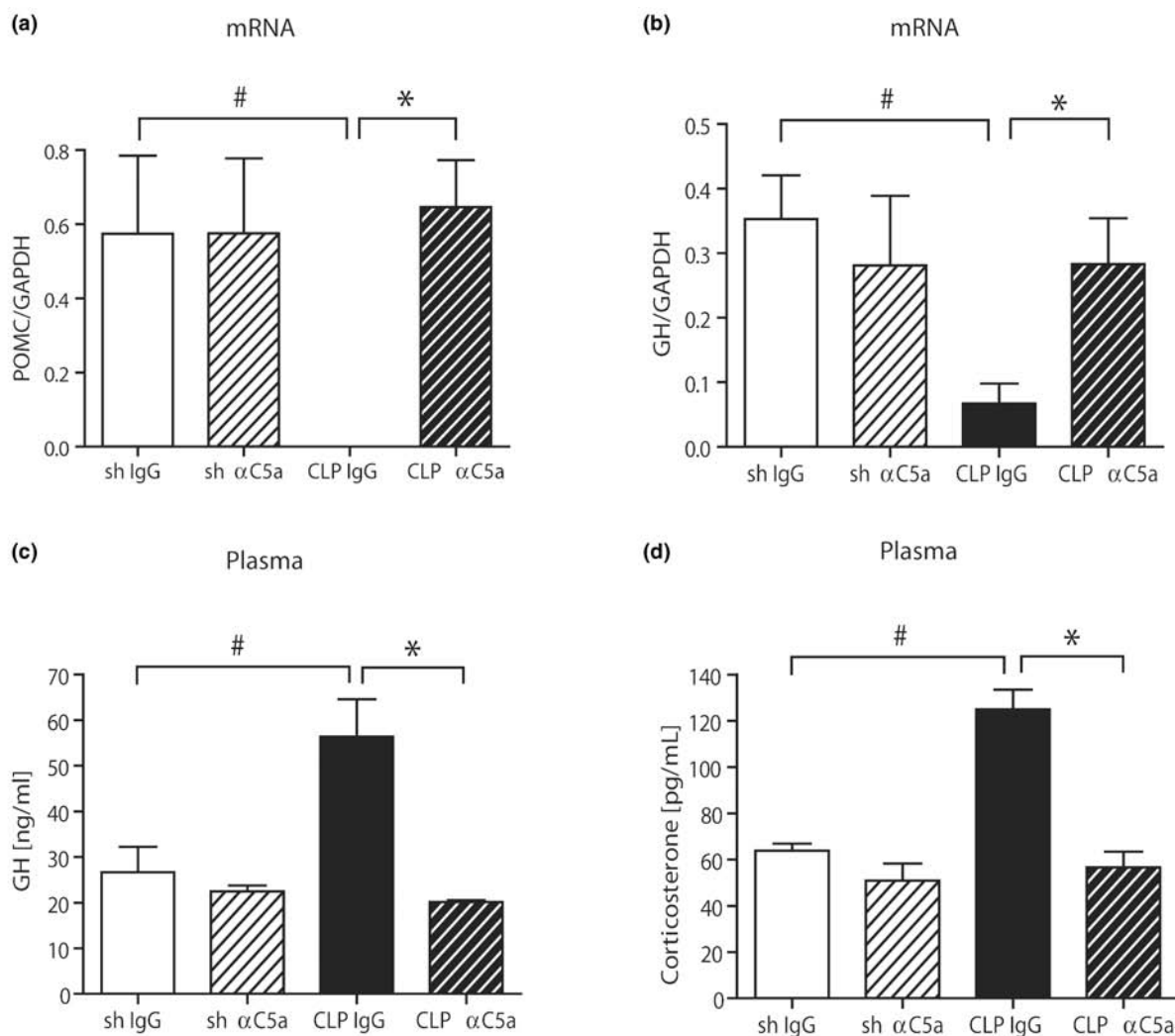
ally recovered as a function of time [77]. More importantly, its concentrations negatively correlated with plasma concentrations of TNF and IL-1 β [77]. Thus, it is tempting to speculate, whether the observed pituitary upregulation of TNF and IL-6 mRNA (Figure 3) is related to the complete absence of POMC expression (Figure 4), which will result in a lack of pituitary MSH- α production with uninhibited proinflammatory activation of pituitary cells.

It remains to be determined if our findings can be extrapolated into humans. Several reports have stressed the disconnection between rodent and human sepsis [78-80], making it difficult to draw definitive conclusions from an experimental study for the clinical setting. Moreover, in the current study, the C5a-neutralising antibody was administered immediately after the CLP procedure. Follow-up studies need to address the effects of delayed anti-C5a treatment, because diagnosis of the sepsis syndrome in patients might be delayed due to several comorbidities. Thus, it is imperative to address if anti-C5a treatment also reverses BBB and pituitary dysfunction after onset of CLP, which would greatly enhance the therapeutic impact of a potential C5a-blockade in humans.

Conclusions

We describe amelioration of BBB breakdown and partial reversal of pituitary dysfunction by neutralisation of C5a during experimental sepsis. Similarly, blockade of C5aR has recently been described to reduce the LPS-induced activation in the paraventricular nucleus and the central amygdala [81]. Thus, as we are beginning to gain novel insights into the crucial role of C5a in the development of sepsis-induced BBB dysfunction, we might be able to immunomodulate its detrimental effects and improve the outcome of septic encephalopathy.

Figure 4



Evaluation of pituitary function after caecal ligation and puncture (CLP). Pituitary tissue samples were removed from four to five mice, snap-frozen, homogenised in Trizol and total RNA was extracted. Assessment of mRNA expression of (a) proopiomelanocortin (POMC) and (b) growth hormone (GH) 24 hours after CLP or sham operation by real-time PCR. Whole blood samples were drawn at given time-points by puncture of the inferior vena cava, plasma was obtained by centrifugation and subjected to ELISA analysis. Samples were assessed for (c) GH or (d) corticosterone under identical conditions. For all graphs, there were five to seven samples per experimental condition. GAPDH = glyceraldehyde 3-phosphate dehydrogenase. # $p < 0.05$ between sham and 24 hours CLP animals; * $p < 0.05$ between IgG-treated and anti-C5a-treated rats.

Key messages

- Anti-C5a prevents break-down of the BBB during experimental sepsis.
- The C5aR is robustly upregulated in the pituitary gland during CLP-induced sepsis.
- Pituitary mRNA expression of proinflammatory TNF and IL-6 is upregulated during experimental sepsis.
- Experimental sepsis induces pituitary dysfunction which is ameliorated by a neutralising anti-C5a antibody.

Competing interests

The authors declare that they have no competing interests.

Authors' contributions

MAF, PFS, MHL, PAW and KI designed the study and supervised the experiments. MAF, DR, AND, LMH and BMT performed the experiments. MAF, PFS, SJM, WRS and KI analysed the data and drafted the manuscript. All authors revised the manuscript for important scientific content, read and approved the final manuscript.

References

- Dombrovskiy VY, Martin AA, Sunderram J, Paz HL: **Rapid increase in hospitalization and mortality rates for severe sepsis in the United States: a trend analysis from 1993 to 2003.** *Crit Care Med* 2007, **35**:1244-1250.
- Kung HC, Hoyert DL, Xu J, Murphy SL: **Deaths: final data for 2005.** *Natl Vital Stat Rep* 2008, **56**:1-120.
- Rittirsch D, Flierl MA, Ward PA: **Harmful molecular mechanisms in sepsis.** *Nat Rev Immunol* 2008, **8**:776-787.
- Levy MM, Fink MP, Marshall JC, Abraham E, Angus D, Cook D, Cohen J, Opal SM, Vincent JL, Ramsay G: **2001 SCCM/ESICM/ACCP/ATS/SIS International Sepsis Definitions Conference.** *Crit Care Med* 2003, **31**:1250-1256.
- Annane D, Bellissant E, Cavaillon JM: **Septic shock.** *Lancet* 2005, **365**:63-78.
- Nakae H, Endo S, Inada K, Takakuwa T, Kasai T, Yoshida M: **Serum complement levels and severity of sepsis.** *Res Commun Chem Pathol Pharmacol* 1994, **84**:189-195.
- Nakae H, Endo S, Inada K, Yoshida M: **Chronological changes in the complement system in sepsis.** *Surg Today* 1996, **26**:225-229.
- Stove S, Welte T, Wagner TO, Kola A, Klos A, Bautsch W, Kohl J: **Circulating complement proteins in patients with sepsis or systemic inflammatory response syndrome.** *Clin Diagn Lab Immunol* 1996, **3**:175-183.
- Hack CE, Nuijens JH, Felt-Bersma RJ, Schreuder WO, Eerenberg-Belmer AJ, Paardekooper J, Bronsveld W, Thijs LG: **Elevated plasma levels of the anaphylatoxins C3a and C4a are associated with a fatal outcome in sepsis.** *Am J Med* 1989, **86**:20-26.
- Czermak BJ, Sarma V, Pierson CL, Warner RL, Huber-Lang M, Bless NM, Schmal H, Friedl HP, Ward PA: **Protective effects of C5a blockade in sepsis.** *Nat Med* 1999, **5**:788-792.
- Huber-Lang MS, Sarma JV, McGuire SR, Lu KT, Guo RF, Padgaonkar VA, Younkin EM, Laudes IJ, Riedemann NC, Younger JG, Ward PA: **Protective effects of anti-C5a peptide antibodies in experimental sepsis.** *Faseb J* 2001, **15**:568-570.
- Riedemann NC, Guo RF, Neff TA, Laudes IJ, Keller KA, Sarma VJ, Markiewski MM, Mastellos D, Strey CW, Pierson CL, Lambris JD, Zetoune FS, Ward PA: **Increased C5a receptor expression in sepsis.** *J Clin Invest* 2002, **110**:101-108.
- Niederbichler AD, Hoesel LM, Westfall MV, Gao H, Ipaktchi KR, Sun L, Zetoune FS, Su GL, Arbabi S, Sarma JV, Wang SC, Hemmila MR, Ward PA: **An essential role for complement C5a in the pathogenesis of septic cardiac dysfunction.** *J Exp Med* 2006, **203**:53-61.
- Rittirsch D, Flierl MA, Nadeau BA, Day DE, Huber-Lang M, Mackay CR, Zetoune FS, Gerard NP, Cianflone K, Kohl J, Gerard C, Sarma JV, Ward PA: **Functional roles for C5a receptors in sepsis.** *Nat Med* 2008, **14**:551-557.
- Gerard C: **Complement C5a in the sepsis syndrome – too much of a good thing?** *N Engl J Med* 2003, **348**:167-169.
- Ward PA: **The dark side of C5a in sepsis.** *Nat Rev Immunol* 2004, **4**:133-142.
- Guo RF, Huber-Lang M, Wang X, Sarma V, Padgaonkar VA, Craig RA, Riedemann NC, McClintock SD, Hlaing T, Shi MM, Ward PA: **Protective effects of anti-C5a in sepsis-induced thymocyte apoptosis.** *J Clin Invest* 2000, **106**:1271-1280.
- Flierl MA, Rittirsch D, Chen AJ, Nadeau BA, Day DE, Sarma JV, Huber-Lang MS, Ward PA: **The complement anaphylatoxin C5a induces apoptosis in adrenomedullary cells during experimental sepsis.** *PLoS ONE* 2008, **3**:e2560.
- Huber-Lang MS, Riedemann NC, Sarma JV, Younkin EM, McGuire SR, Laudes IJ, Lu KT, Guo RF, Neff TA, Padgaonkar VA, Lambris JD, Spruce L, Mastellos D, Zetoune FS, Ward PA: **Protection of innate immunity by C5aR antagonist in septic mice.** *Faseb J* 2002, **16**:1567-1574.
- Huber-Lang MS, Younkin EM, Sarma JV, McGuire SR, Lu KT, Guo RF, Padgaonkar VA, Curnutte JT, Erickson R, Ward PA: **Complement-induced impairment of innate immunity during sepsis.** *J Immunol* 2002, **169**:3223-3231.
- Laudes IJ, Chu JC, Sikranth S, Huber-Lang M, Guo RF, Riedemann N, Sarma JV, Schmaier AH, Ward PA: **Anti-c5a ameliorates coagulation/fibrinolytic protein changes in a rat model of sepsis.** *Am J Pathol* 2002, **160**:1867-1875.
- Huber-Lang M, Sarma VJ, Lu KT, McGuire SR, Padgaonkar VA, Guo RF, Younkin EM, Kunkel RG, Ding J, Erickson R, Curnutte JT, Ward PA: **Role of C5a in multiorgan failure during sepsis.** *J Immunol* 2001, **166**:1193-1199.
- Semmler A, Hermann S, Mormann F, Weberpals M, Paxian SA, Okulla T, Schafers M, Kummer MP, Klockgether T, Heneka MT: **Sepsis causes neuroinflammation and concomitant decrease of cerebral metabolism.** *J Neuroinflammation* 2008, **5**:38.
- Piazza O, Russo E, Cotena S, Esposito G, Tufano R: **Elevated S100B levels do not correlate with the severity of encephalopathy during sepsis.** *Br J Anaesth* 2007, **99**:518-521.
- Alexander JJ, Jacob A, Cunningham P, Hensley L, Quigg RJ: **TNF is a key mediator of septic encephalopathy acting through its receptor, TNF receptor-1.** *Neurochem Int* 2008, **52**:447-456.
- Wratten ML: **Therapeutic approaches to reduce systemic inflammation in septic-associated neurologic complications.** *Eur J Anaesthesiol Suppl* 2008, **42**:1-7.
- Handa O, Stephen J, Cepinskas G: **Role of eNOS-derived nitric oxide (NO) in activation and dysfunction of cerebrovascular endothelial cells during early onsets of sepsis.** *Am J Physiol Heart Circ Physiol* 2008, **295**:H1712-1719.
- Toklu HZ, Uysal MK, Kabasakal L, Sirvanci S, Ercan F, Kaya M: **The effects of riluzole on neurological, brain biochemical, and histological changes in early and late term of sepsis in rats.** *J Surg Res* 2008.
- Hofer S, Bopp C, Hoerner C, Plaschke K, Faden RM, Martin E, Bardenheuer HJ, Weigand MA: **Injury of the blood brain barrier and up-regulation of icam-1 in polymicrobial sepsis.** *J Surg Res* 2008, **146**:276-281.
- Faustmann PM, Krause D, Dux R, Dermietzel R: **Morphological study in the early stages of complement C5a fragment-induced experimental meningitis: activation of macrophages and astrocytes.** *Acta Neuropathol* 1995, **89**:239-247.
- Nataf S, Stahel PF, Davoust N, Barnum SR: **Complement anaphylatoxin receptors on neurons: new tricks for old receptors?** *Trends Neurosci* 1999, **22**:397-402.
- Stahel PF, Barnum SR: **The role of the complement system in CNS inflammatory diseases.** *Expert Rev Clin Immunol* 2006, **2**:445-456.
- Stahel PF, Frei K, Eugster HP, Fontana A, Hummel KM, Wetsel RA, Ames RS, Barnum SR: **TNF-alpha-mediated expression of the receptor for anaphylatoxin C5a on neurons in experimental Listeria meningoencephalitis.** *J Immunol* 1997, **159**:861-869.
- Osaka H, McGinty A, Hoepken UE, Lu B, Gerard C, Pasinetti GM: **Expression of C5a receptor in mouse brain: role in signal transduction and neurodegeneration.** *Neuroscience* 1999, **88**:1073-1082.
- O'Barr SA, Caguioa J, Gruol D, Perkins G, Ember JA, Hugli T, Cooper NR: **Neuronal expression of a functional receptor for the C5a complement activation fragment.** *J Immunol* 2001, **166**:4154-4162.
- Ernst JD, Hartiala KT, Goldstein IM, Sande MA: **Complement (C5)-derived chemotactic activity accounts for accumulation of polymorphonuclear leukocytes in cerebrospinal fluid of rabbits with pneumococcal meningitis.** *Infect Immun* 1984, **46**:81-86.
- Williams CA, Schupf N, Hugli TE: **Anaphylatoxin C5a modulation of an alpha-adrenergic receptor system in the rat hypothalamus.** *J Neuroimmunol* 1985, **9**:29-40.
- Jacob A, Hensley LK, Safratovich BD, Quigg RJ, Alexander JJ: **The role of the complement cascade in endotoxin-induced septic encephalopathy.** *Lab Invest* 2007, **87**:1186-1194.
- Baker CC, Chaudry IH, Gaines HO, Baue AE: **Evaluation of factors affecting mortality rate after sepsis in a murine cecal ligation and puncture model.** *Surgery* 1983, **94**:331-335.
- Laudes IJ, Chu JC, Huber-Lang M, Guo RF, Riedemann NC, Sarma JV, Mahdi F, Murphy HS, Speyer C, Lu KT, Lambris JD, Zetoune FS, Ward PA: **Expression and function of C5a receptor in mouse microvascular endothelial cells.** *J Immunol* 2002, **169**:5962-5970.
- Riedemann NC, Neff TA, Guo RF, Bernacki KD, Laudes IJ, Sarma JV, Lambris JD, Ward PA: **Protective effects of IL-6 blockade in sepsis are linked to reduced C5a receptor expression.** *J Immunol* 2003, **170**:503-507.
- Wong D, Dorovini-Zis K: **Expression of vascular cell adhesion molecule-1 (VCAM-1) by human brain microvessel endothelial cells in primary culture.** *Microvasc Res* 1995, **49**:325-339.

43. Hess DC, Thompson Y, Sprinkle A, Carroll J, Smith J: **E-selectin expression on human brain microvascular endothelial cells.** *Neurosci Lett* 1996, **213**:37-40.
44. Hess DC, Bhutwala T, Sheppard JC, Zhao W, Smith J: **ICAM-1 expression on human brain microvascular endothelial cells.** *Neurosci Lett* 1994, **168**:201-204.
45. Rieckmann P, Michel U, Albrecht M, Bruck W, Wockel L, Felgenhauer K: **Cerebral endothelial cells are a major source for soluble intercellular adhesion molecule-1 in the human central nervous system.** *Neurosci Lett* 1995, **186**:61-64.
46. Mulligan MS, Schmid E, Till GO, Hugli TE, Friedl HP, Roth RA, Ward PA: **C5a-dependent up-regulation in vivo of lung vascular P-selectin.** *J Immunol* 1997, **158**:1857-1861.
47. Foreman KE, Vaporciyan AA, Bonish BK, Jones ML, Johnson KJ, Glovsky MM, Eddy SM, Ward PA: **C5a-induced expression of P-selectin in endothelial cells.** *J Clin Invest* 1994, **94**:1147-1155.
48. Albrecht EA, Chinnaiyan AM, Varambally S, Kumar-Sinha C, Barrette TR, Sarma JV, Ward PA: **C5a-induced gene expression in human umbilical vein endothelial cells.** *Am J Pathol* 2004, **164**:849-859.
49. Mulligan MS, Schmid E, Beck-Schimmer B, Till GO, Friedl HP, Brauer RB, Hugli TE, Miyasaka M, Warner RL, Johnson KJ, Ward PA: **Requirement and role of C5a in acute lung inflammatory injury in rats.** *J Clin Invest* 1996, **98**:503-512.
50. Schmid E, Piccolo MT, Friedl HP, Warner RL, Mulligan MS, Hugli TE, Till GO, Ward PA: **Requirement for C5a in lung vascular injury following thermal trauma to rat skin.** *Shock* 1997, **8**:119-124.
51. Breder CD, Hazuka C, Ghayur T, Klug C, Huginin M, Yasuda K, Teng M, Saper CB: **Regional induction of tumor necrosis factor alpha expression in the mouse brain after systemic lipopolysaccharide administration.** *Proc Natl Acad Sci USA* 1994, **91**:11393-11397.
52. Fabry Z, Fitzsimmons KM, Herlein JA, Moninger TO, Dobbs MB, Hart MN: **Production of the cytokines interleukin 1 and 6 by murine brain microvessel endothelium and smooth muscle pericytes.** *J Neuroimmunol* 1993, **47**:23-34.
53. Reyes TM, Fabry Z, Coe CL: **Brain endothelial cell production of a neuroprotective cytokine, interleukin-6, in response to noxious stimuli.** *Brain Res* 1999, **851**:215-220.
54. de Vries HE, Blom-Roosemalen MC, van Oosten M, de Boer AG, van Berkel TJ, Breimer DD, Kuiper J: **The influence of cytokines on the integrity of the blood-brain barrier in vitro.** *J Neuroimmunol* 1996, **64**:37-43.
55. Papadopoulos MC, Davies DC, Moss RF, Tighe D, Bennett ED: **Pathophysiology of septic encephalopathy: a review.** *Crit Care Med* 2000, **28**:3019-3024.
56. Sharshar T, Carlier R, Bernard F, Guidoux C, Brouland JP, Nardi O, de la Grandmaison GL, Aboab J, Gray F, Menon D, Annane D: **Brain lesions in septic shock: a magnetic resonance imaging study.** *Intensive Care Med* 2007, **33**:798-806.
57. Sharshar T, Hopkinson NS, Orlikowski D, Annane D: **Science review: The brain in sepsis – culprit and victim.** *Crit Care* 2005, **9**:37-44.
58. Hanisch UK: **Microglia as a source and target of cytokines.** *Glia* 2002, **40**:140-155.
59. Ghirnikar RS, Lee YL, Eng LF: **Inflammation in traumatic brain injury: role of cytokines and chemokines.** *Neurochem Res* 1998, **23**:329-340.
60. Ransohoff RM, Tani M: **Do chemokines mediate leukocyte recruitment in post-traumatic CNS inflammation?** *Trends Neurosci* 1998, **21**:154-159.
61. Stahel PF, Kariya K, Shohami E, Barnum SR, Eugster H, Trentz O, Kossmann T, Morganti-Kossmann MC: **Intracerebral complement C5a receptor (CD88) expression is regulated by TNF and lymphotoxin-alpha following closed head injury in mice.** *J Neuroimmunol* 2000, **109**:164-172.
62. Gasque P, Dean YD, McGreal EP, VanBeek J, Morgan BP: **Complement components of the innate immune system in health and disease in the CNS.** *Immunopharmacology* 2000, **49**:171-186.
63. Boos L, Campbell IL, Ames R, Wetsel RA, Barnum SR: **Deletion of the complement anaphylatoxin C3a receptor attenuates, whereas ectopic expression of C3a in the brain exacerbates, experimental autoimmune encephalomyelitis.** *J Immunol* 2004, **173**:4708-4714.
64. Lynch NJ, Willis CL, Nolan CC, Roscher S, Fowler MJ, Weihe E, Ray DE, Schwaeble WJ: **Microglial activation and increased synthesis of complement component C1q precedes blood-brain barrier dysfunction in rats.** *Mol Immunol* 2004, **40**:709-716.
65. Porter JC, Sissom JF, Arita J, Reymond MJ: **Hypothalamic-hypophysial vasculature and its relationship to secretory cells of the hypothalamus and pituitary gland.** *Vitam Horm* 1983, **40**:145-174.
66. Rancan M, Morganti-Kossmann MC, Barnum SR, Saft S, Schmidt OI, Ertel W, Stahel PF: **Central nervous system-targeted complement inhibition mediates neuroprotection after closed head injury in transgenic mice.** *J Cereb Blood Flow Metab* 2003, **23**:1070-1074.
67. Stahel PF, Kossmann T, Morganti-Kossmann MC, Hans VH, Barnum SR: **Experimental diffuse axonal injury induces enhanced neuronal C5a receptor mRNA expression in rats.** *Brain Res Mol Brain Res* 1997, **50**:205-212.
68. Gasque P, Singhrao SK, Neal JW, Gotze O, Morgan BP: **Expression of the receptor for complement C5a (CD88) is up-regulated on reactive astrocytes, microglia, and endothelial cells in the inflamed human central nervous system.** *Am J Pathol* 1997, **150**:31-41.
69. Francis K, van Beek J, Canova C, Neal JW, Gasque P: **Innate immunity and brain inflammation: the key role of complement.** *Expert Rev Mol Med* 2003, **5**:1-19.
70. Davoust N, Jones J, Stahel PF, Ames RS, Barnum SR: **Receptor for the C3a anaphylatoxin is expressed by neurons and glial cells.** *Glia* 1999, **26**:201-211.
71. Francis K, Lewis BM, Akatsu H, Monk PN, Cain SA, Scanlon MF, Morgan BP, Ham J, Gasque P: **Complement C3a receptors in the pituitary gland: a novel pathway by which an innate immune molecule releases hormones involved in the control of inflammation.** *Faseb J* 2003, **17**:2266-2268.
72. Lewis BM, Francis K, Monk P, Scanlon MF, Ham J: **Complement C5a inhibits the secretion of macrophage migration inhibitory factor in anterior pituitary cell lines.** *Endocrine Abstracts* 2006, **11**:P602.
73. Maxime V, Siami S, Annane D: **Metabolism modulators in sepsis: the abnormal pituitary response.** *Crit Care Med* 2007, **35**:S596-601.
74. Ross R, Miell J, Freeman E, Jones J, Matthews D, Preece M, Buchanan C: **Critically ill patients have high basal growth hormone levels with attenuated oscillatory activity associated with low levels of insulin-like growth factor-I.** *Clin Endocrinol (Oxf)* 1991, **35**:47-54.
75. Raffin-Sanson ML, de Keyzer Y, Bertagna X: **Proopiomelanocortin, a polypeptide precursor with multiple functions: from physiology to pathological conditions.** *Eur J Endocrinol* 2003, **149**:79-90.
76. Brzoska T, Luger TA, Maaser C, Abels C, Bohm M: **Alpha-melanocyte-stimulating hormone and related tripeptides: biochemistry, antiinflammatory and protective effects in vitro and in vivo, and future perspectives for the treatment of immune-mediated inflammatory diseases.** *Endocr Rev* 2008, **29**:581-602.
77. Catania A, Cutuli M, Garofalo L, Airaghi L, Valenza F, Lipton JM, Gattinoni L: **Plasma concentrations and anti-L-cytokine effects of alpha-melanocyte stimulating hormone in septic patients.** *Crit Care Med* 2000, **28**:1403-1407.
78. Rittirsch D, Hoesel LM, Ward PA: **The disconnect between animal models of sepsis and human sepsis.** *J Leukoc Biol* 2007, **81**:137-143.
79. Esmon CT: **Why do animal models (sometimes) fail to mimic human sepsis?** *Crit Care Med* 2004, **32**:S219-222.
80. Poli-de-Figueiredo LF, Garrido AG, Nakagawa N, Sannomiya P: **Experimental models of sepsis and their clinical relevance.** *Shock* 2008, **30**(Suppl 1):53-59.
81. Crane JW, Buller KM: **Systemic blockade of complement C5a receptors reduces lipopolysaccharide-induced responses in the paraventricular nucleus and the central amygdala.** *Neurosci Lett* 2007, **424**:10-15.

animal models of SCA may also be useful for a better understanding of what should or should not be done for resuscitation. Since left ventricular function before VF is a major determinant for successful resuscitation, a model of VF in chronic myocardial infarction with no acute ischemia and a model of VF associated with nonischemic induced heart failure may also be useful (6).

There is no doubt that acute coronary artery occlusion is frequent in SCA, and it may be found in 50% of patients (7). This may affect up to 85% to 90% of patients with both ST segment elevation and chest pain before SCA, but coronary occlusion is poorly predicted in other settings by clinical and electrocardiographic findings. One further question is whether a coronary angiography should be systematically performed early after SCA. Immediate coronary angiography can be followed if necessary by coronary angioplasty. It seems reasonable to perform coronary angiography in patients with a sufficiently high hope of survival. A score using several simple items may help to identify these patients: those with age <75, those with early initial intervention (in the first 10 mins), those with ventricular tachyarrhythmia rather than asystole on initial surface electrocardiogram, and those with no need to use epinephrine (8, 9). Those in whom shock will develop in the first 48 hrs should also undergo coronary angiography. In these latter

patients, shock or refrillation after resuscitation is possibly still related to ischemia rather than to myocardial damage, hypotension, or epinephrine use, and revascularization may bring some benefit.

Treatment of ventricular arrhythmias during acute myocardial infarction has been a controversial topic for several decades. Primary VF accounts for the majority of early deaths in myocardial infarction. VF is a less common cause of death in the hospital with the early use of revascularization strategies in conjunction with β -blockers. Secondary VF occurring in the setting of congestive heart failure or cardiogenic shock can also contribute to death from myocardial infarction. We now hope that the use of targeted models of cardiac arrest will clarify several unsolved issues, improve our strategies of acute management, and decrease the midterm mortality for more patients with SCA.

Laurent Fauchier, MD, PhD
Axel de Labriolle, MD
Services de Cardiologie
Pôle Thorax
Cardiovasculaire
Hémostase
Centre Hospitalier
Universitaire Trousseau
Tours, France

REFERENCES

1. Cobb LA, Fahrenbruch CE, Olsufka M, et al: Changing incidence of out-of-hospital ven-

tricular fibrillation. *JAMA* 2002; 288: 3008–3013

2. ECC Committee, Subcommittees and Task Forces of the American Heart Association. 2005 American Heart Association Guidelines for Cardiopulmonary Resuscitation and Emergency Cardiovascular Care. *Circulation* 2005; 112(24 Suppl):IV1–IV203
3. White RD: Waveforms for defibrillation and cardioversion: Recent experimental and clinical studies. *Curr Opin Crit Care* 2004; 10: 202–207
4. Niemann JT, Rosborough JP, Youngquist S, et al: Is all ventricular fibrillation the same? A comparison of ischemically induced and electrically induced ventricular fibrillation in a porcine cardiac arrest and resuscitation model. *Crit Care Med* 2007; 35:1356–1361
5. Zipes DP, Wellens HJ: Sudden cardiac death. *Circulation* 1998; 98:2334–2351
6. Mehta D, Curwin J, Gomes A, et al: Sudden death in coronary artery disease. Acute ischemia versus myocardial substrate. *Circulation* 1997; 96:3215–3233
7. Spaulding CM, Joly L, Rosenberg A, et al: Immediate coronary angiography in survivors of out-of-hospital cardiac arrest. *N Engl J Med* 1997; 336:1629–1633
8. Weaver WD, Hill D, Fahrenbruch CE, et al: Use of the automatic external defibrillator in the management of out-of-hospital cardiac arrest. *N Engl J Med* 1988; 319:661–666
9. Morrison LJ, Visentin LM, Kiss A, et al: Validation of a rule for termination of resuscitation in out-of-hospital cardiac arrest. *N Engl J Med* 2006; 355:478–487

New therapeutic approaches for influenza A H5N1 infected humans*

The article by Dr. Arabi and colleagues (1) in this issue of *Critical Care Medicine* is based on a literature review of papers published in English and featuring humans with avian influenza A (H5N1) virus pulmonary infection. The potential use of a neuraminidase inhibitor to impede viral

entry into cells is suggested. Such an approach is based on the known requirements of avian and human influenza A viruses for binding to cell surfaces via sialic acid residues covalently linked to galactose. These structures are found on epithelial cells in respiratory bronchioles and on alveolar epithelial cells (2). It is now fairly clear that, like the severe acute respiratory syndrome coronavirus, the H5N1 influenza A RNA virus proliferates chiefly in the lung for a period of several weeks, although extrapulmonary viral replication may also occur in the intestine and perhaps in other organs (3). The results of viral replication in the lung are alveolar epithelial cell damage and/or de-

struction, resulting in massive intra-alveolar edema and hemorrhage together with intense fibrin deposition along alveolar walls, all of which lead to serious problems with gas exchange between the vascular and alveolar compartments and severe hypoxemia (4). Collectively, these morphologic changes have been described as diffuse alveolar damage and the adult respiratory distress syndrome. To date, the only therapeutic strategy in such circumstances is the use of supportive interventions (artificial ventilation, vasopressor support).

Not unexpectedly, there is evidence that diffuse alveolar damage caused by the H5N1 virus also triggers up-regulation of

*See also p. 1397.

Key Words: H5N1 influenza A lung injury; fibrin; alveolar injury; coagulation; tumor necrosis factor- α ; activated protein C; acute respiratory distress syndrome

Copyright © 2007 by the Society of Critical Care Medicine and Lippincott Williams & Wilkins

DOI: 10.1097/01.CCM.0000259174.45444.AF

tissue factor, which is a potent procoagulatory factor and may be linked to extensive fibrin deposition along alveolar walls as well as the consumptive coagulopathy occurring during H5N1 infection. There is evidence that H5N1 infection in mouse lung results in generation of multiple cytokines and chemokines (e.g., interleukin-6, interleukin-1 β , tumor necrosis factor [TNF]- α , macrophage inflammatory protein-1 α). Interestingly, mice genetically deficient in TNF- α -1 receptor have a greatly reduced mortality even though viral replication in the lung is not affected (5).

Such data suggest that two therapeutic strategies might be considered in the case of humans with influenza A H5N1 infection: activated protein C (APC) and blockade of TNF- α or its receptor. APC blocks several different activated coagulation factors and also has anti-inflammatory properties. APC has been approved for use in humans with high-grade sepsis (6). Therapeutic use of APC is contraindicated if there is evidence of severe consumptive coagulopathy, thrombocytopenia, or other signs that the clotting system has been extensively activated. The use of APC might

diminish the consumptive coagulopathy occurring during H5N1 infection, especially as it involves the lungs. Blocking antibody to TNF- α and the TNF- α receptor blocking agent, soluble TNF α RI (sTNF α RI), are known to be effective in the treatment of patients with rheumatoid arthritis ((7). In patients with rheumatoid arthritis, sTNF α RI seems to be well tolerated and is largely without evidence of toxicity. If the data in knockout mice can be extrapolated to humans with H5N1 infection, either blockade of TNF- α (with antibody) or use of sTNF α RI might be therapeutically effective. It is clear that there is an urgent need for reliable, specific, and sensitive tests for early detection of H5N1 infection. There is an equally urgent need for highly effective drugs to block H5N1 entry into cells and intracellular replication. In the meantime, in H5N1-infected patients, perhaps the use of APC or sTNF α RI might provide some therapeutic benefit, but clinical trials are obviously required.

Peter A. Ward, MD
Department of Pathology
University of Michigan
Medical School

Ann Arbor, MI

REFERENCES

1. Arabi Y, Gomersall CD, Ahmed QA, et al: The critically ill avian influenza A (H5N1) patient. *Crit Care Med* 2007; 35:1397–1403
2. Shinya K, Ebin M, Yamada S, et al: Influenza virus receptors in the human airway. *Brief Communications, Nature* 2006; 440:435–436
3. Uiprasertkul M, Puthavathana P, Sangsiriwut K, et al: Influenza A H5N1 replication sites in humans. *Emerg Infect Dis* 2005; 11:1036–1041
4. Wai-Fu N, Ka-Fai T, Lam WL, et al: The comparative pathology of severe acute respiratory syndrome and avian influenza A subtype H5N1—A review. *Human Pathol* 2006; 37: 381–390
5. Szretter KJ, Gangappa S, Lu X, et al: Role of host cytokine responses in the pathogenesis of avian H5N1 influenza viruses in mice. *J Virol* 2007; 81:2736–2744
6. Bernard GR, Vincent JL, Laterre PF, et al: Efficacy and safety of recombinant human activated protein C for severe sepsis. *N Engl J Med* 2001; 344:699–709
7. Moreland LW, Baumgartner SW, Schiff MH, et al: Treatment of rheumatoid arthritis with a recombinant human tumor necrosis factor receptor (p75)-Fc fusion protein. *N Engl J Med* 1997; 337:141–147

ANNALS OF THE NEW YORK ACADEMY OF SCIENCES

Issue: *Oxidative/Nitrosative Stress and Disease***Oxidative stress: acute and progressive lung injury**

Peter A. Ward

University of Michigan Medical School, Department of Pathology, Ann Arbor, Michigan

Address for correspondence: Peter A. Ward, M.D., Department of Pathology, The University of Michigan Medical School, 1301 Catherine Road, 7520 MSRB I, Ann Arbor, MI 48109-5602. pward@umich.edu

Oxidative stress in lung often occurs in humans during acute lung injury (ALI) and in the acute respiratory distress syndrome. The lung inflammatory response may proceed to the development of pulmonary fibrosis, a devastating complication that occurs in premature infants after prolonged exposure to high oxygen concentrations. Oxidant-related ALI can be induced by airway deposition of lipopolysaccharide or IgG immune complexes, resulting in activation of recruited neutrophils and residential macrophages, whose oxidants and proteases produce reversible ALI. In the presence of a powerful trigger of leukocytes (phorbol myristate acetate), or following intrapulmonary deposition of enzymes that generate oxidants, extensive endothelial and epithelial damage and destruction occurs, overwhelming repair mechanisms of lung and resulting in pulmonary fibrosis. How residential or circulating stem cells participate in regeneration of damaged/destroyed cells may provide clues regarding therapy in humans who are experiencing lung inflammatory damage.

Keywords: acute lung injury; pulmonary fibrosis; oxidants; antioxidants; inflammation; macrophages

Introduction

It is well known that oxidant production within lung can lead to acute lung injury (ALI) and sometimes progressive lung injury which often results in irreversible fibrosis.¹⁻⁴ The sources of oxidants may be extrinsic or intrinsic. Agents such as paraquat, when inhaled, can be metabolized into free radicals which may be intensely lung-damaging often resulting in pulmonary fibrosis.⁵ Intrinsically generated oxidants may be derived from mitochondria, but the most important source of damaging oxidants is phagocytic cells (residential macrophages and recruited neutrophils [PMNs]) that can generate toxic oxygen metabolites from assembly on cell surfaces of NADPH oxidase (also known as NOX2). Similar pathways leading to oxidant generation can occur in endothelial and alveolar epithelial cells, but the majority of oxidants in lung arises from stimulated phagocytic cells.^{6,7}

Defenses against toxic oxygen metabolites in lung include superoxide dismutase (SOD), catalase, glutathione peroxidase, and glutathione, which is present in mM concentrations in lung lining fluids.

These antioxidant enzymes are inducible in a variety of situations such as during hyperoxia, in the presence of lipopolysaccharide (LPS), etc.^{8,9} Enzymes such as SOD can be induced in lung by hyperoxia, bacterial LPS, to name just a few examples. SOD dismutates the superoxide anion (O_2^*) to H_2O_2 . Catalase converts H_2O_2 to H_2O , while glutathione peroxidase is a selenium-containing enzyme that catalyzes conversion of H_2O_2 to H_2O in the presence of glutathione, which is then converted to its oxidized form, GSSG. The presence of these antioxidant enzymes and reducing factors in lung illustrates how the lung adapts to maintain a redox balance and can respond to oxidizing conditions that may threaten the structural and functional integrity of the lung. It is understandable why the lung is so responsive to such threats, because it is the single organ in the body that is exposed to the highest concentrations of O_2 . In the following, we describe how enzyme and substrate combinations as well as inflammatory events in lung featuring oxidant production by phagocytes can be used to evaluate under what conditions oxidant production in lung results in outcomes.

doi: 10.1111/j.1749-6632.2010.05552.x

Ann. N.Y. Acad. Sci. 1203 (2010) 53-59 © 2010 New York Academy of Sciences.

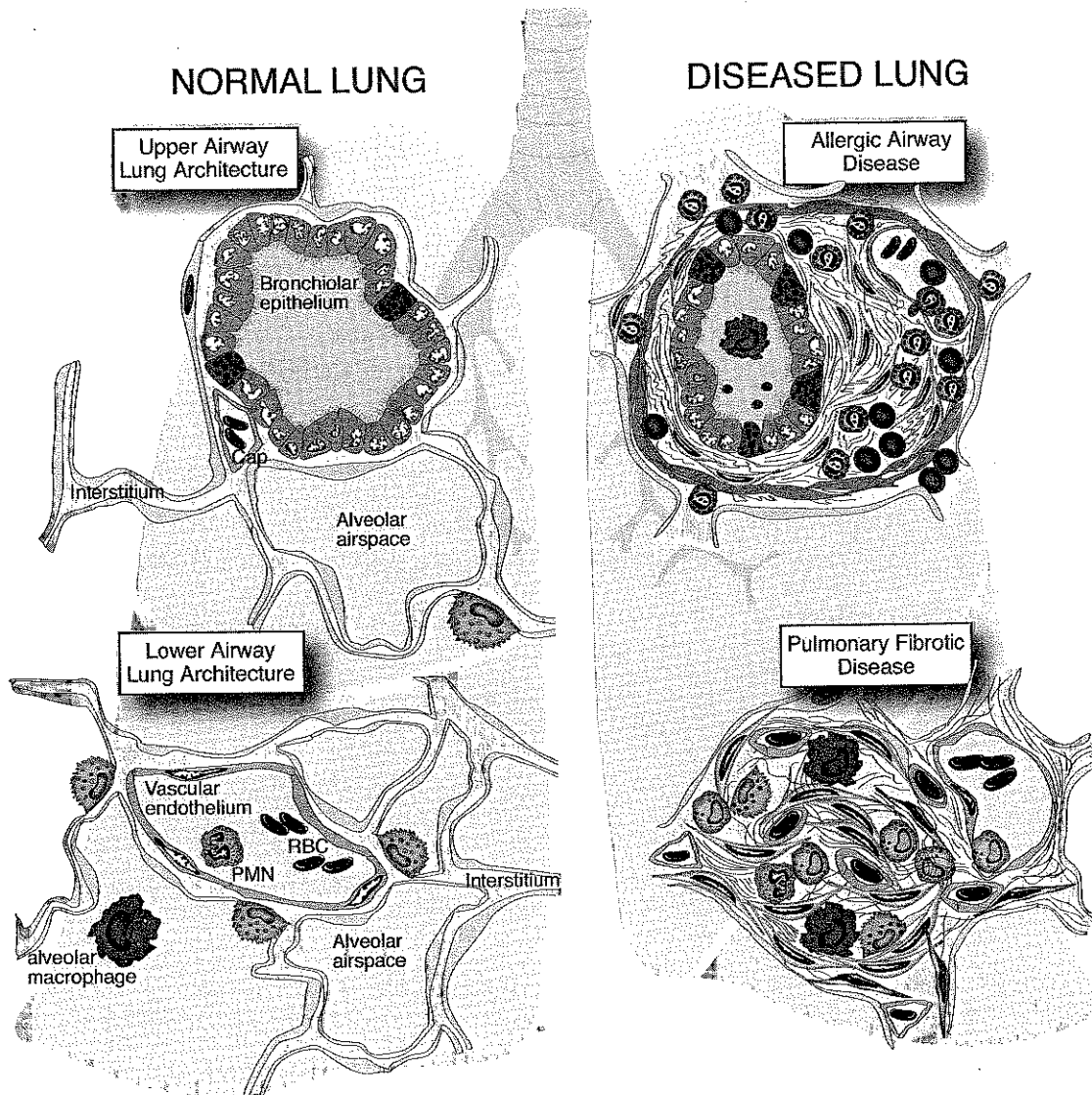


Figure 1. Representation of upper and lower airways of normal lung (left) and inflammatory changes in upper airways of asthmatic lung (upper right) and fibrosis and inflammatory cells in distal airways (lower right).

Inflammatory responses involving upper and lower airways

The architecture of normal upper and lower airways is schematically shown in Figure 1 (left upper and lower frames). Upper airways contain bronchioles lined by ciliated epithelial cells and occasional goblet cells that produce mucous, all being surrounded by smooth muscle cells. The distal (lower) airways contain capillaries, the interstitial compartment and the alveolar compartment, which is lined by alveolar

epithelial cells (Types I and II) (left lower frame). In disease states such as asthma (upper right frame), the upper airways are altered with the appearance of inflammatory cells (eosinophils, mast cells, lymphocytes, and occasional neutrophils [PMNs]) in the wall, greatly increased amounts of smooth muscle cells and large amounts of mucous secreted into the airway lumen. When oxidant injury overwhelms the repair capacity of the distal airway compartment (lower right frame), alveolar collapse may result together with extensive fibrotic scars, which effectively

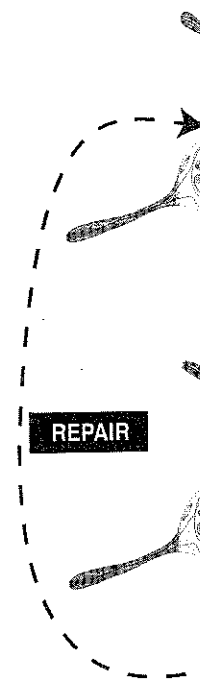


Figure 2. Schematic of repair process reversed by regenerative result will be pulmonary

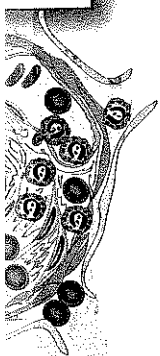
destroy the air exchange and the capillary system

Generation of reactive oxidants

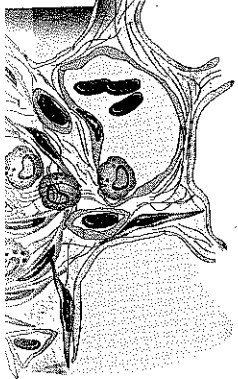
Oxidants can be generated and recruited PMNs (e.g., paraquat) and products in lung. Toxic oxidants generated by enzyme/substrate in lung. Toxic oxygen hydrogen peroxide products [e.g., hypochlorite] by natural enzymes are present in pulmonary levels elevated when the oxidants (such as hydroxyl radicals)

LUNG

Airway
base



Fibrotic
base



upper airways of asthmatic

(left lower frame). In (upper right frame), with the appearance of lymphocytes, mast cells, lymphocytes (PMNs) in the airway compartment. The collapse of smooth muscle and mucous secreted into the airway compartment may result in scars, which effectively

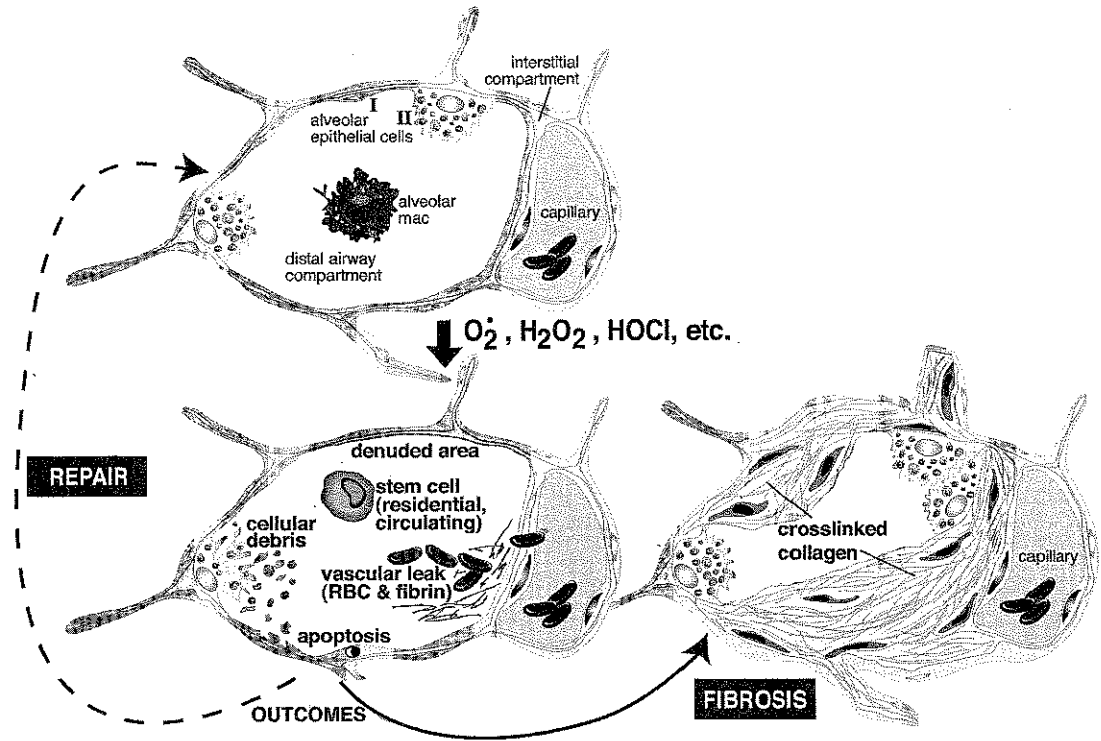


Figure 2. Schematic of events before (upper frame) and after instillation of PMA into rat lungs (lower frames). If injury can be reversed by regenerative capacities of lung (lower left frame), the lung is restored to the preinjury state. If injury is too intense, the result will be pulmonary fibrosis (lower right frame).

destroy the air exchange between affected airways and the capillary system.

Generation of intrinsically generated lung oxidants

Oxidants can be generated by lung macrophages and recruited PMNs. Although certain chemicals (e.g., paraquat) are metabolized into highly toxic products in lung, we will restrict our comments to oxidants generated by phagocytic cells in the lung or by enzyme/substrate combinations delivered to lung. Toxic oxygen products can be generated when macrophages or PMNs undergo stimulation by factors such as bacterial LPS or IgG immune complexes (IgGIC). Toxic oxygen products (superoxide, $O_2^{\bullet-}$; hydrogen peroxide, H_2O_2 or its peroxidative products [e.g., hypochlorous acid, HOCl]) can be intercepted by naturally occurring or induced antioxidants such as SOD or catalase. Those antioxidant enzymes are present naturally in lung but the intrapulmonary levels of these enzymes can be greatly elevated when the lung faces a large burden of oxidants (such as hyperoxia) that compromise the re-

dox balance of lung.⁸ It is possible with phorbol myristate acetate (PMA) to very powerfully activate lung macrophages, which overwhelms the antioxidant reserves of the lung and results in catastrophic parenchymal damage,⁹ as described below. In the case of LPS or IgGIC induced injury, lung damage is limited and reversible, and the lung architecture is restored to normal in a matter of a few days.^{10,11} In the case of PMA, damage is so intense as to overwhelm the repair and regenerative abilities of lung, leading to pulmonary fibrosis. Under such conditions, there is extensive damage/destruction of alveolar epithelial cells and vascular endothelial cells, resulting in intense alveolar edema ("alveolar flooding") and intraalveolar hemorrhage. The reversibility or irreversibility of ALI seems to be due to the extent of damage/destruction of vascular endothelial and alveolar epithelial cells. In the latter case, lung residential or blood borne stem cells may enhance the regenerative capacity of the lung (Fig. 2). If this capacity is overwhelmed, there will be collapse of alveoli and development of dense cross-linked collagen, which will, in the same locale, ablate gas

exchange between the alveolar compartment and the capillaries.

Acute and progressive lung injury after lung exposure to PMA

As indicated above, airway instillation of PMA (20 μ g) results in intense parenchymal damage of the lung due to intense damage/destruction of endothelial cells and alveolar epithelial cells. The sources of these damaging oxidants are lung macrophages in the absence of PMN recruitment. Damage or destruction of endothelial and epithelial cells of the distal airways results in the breakdown of both barriers, with intense hemorrhage and flooding of the alveolar compartment, together with diffuse fibrin deposition (as described later). Such types of outcomes can be greatly attenuated in the presence of catalase but not SOD, suggesting that the toxic oxidants are H_2O_2 and/or its peroxidative products such as HOCl. Interestingly, the development of PMA-induced ALI is not affected by PMN depletion in blood, supporting the interpretation that lung macrophages are the source of the highly damaging oxidants.⁹

Lung injury resulting from extrinsic, oxidant-generating enzymes

ALI can also be induced by introducing into the distal airway system appropriate oxidant-generating enzymes. This strategy allows one to further define the nature of the most lung-damaging oxidants. A powerful oxidant generating system includes the use of glucose and glucose oxidase (which generate H_2O_2) in the presence of peroxidases (lactoperoxidase, myeloperoxidase). The combination of xanthine and xanthine oxidase generates O_2^{\bullet} . The permeability index was employed as the endpoint (albumin leak into lung as a sensitive and quantitative endpoint of ALI). The combination of xanthine and xanthine oxidase resulted in a nearly 10-fold increase in injury, suggesting that O_2^{\bullet} may be directly injurious to lung. When the combination of glucose and glucose oxidase was used to generate H_2O_2 , albumin leak was barely double the background level. On the other hand, in the copresence of either lactoperoxidase or myeloperoxidase, the albumin leak was increased five to ninefold over background levels. The expected products from either peroxidase in the presence of H_2O_2 would be hypohalides, such as HOCl, HOBr, and HOI. These

data suggest that H_2O_2 *per se* is not especially toxic, but that its products generated by a peroxidase are the key toxic products damaging the lung. Such data are consistent with many reports indicating that nucleated mammalian cells can withstand mM concentrations of H_2O_2 without exhibiting evidence of damage.^{12,13}

The toxic products generated by glucose, glucose oxidase and lactoperoxidase. In the copresence of catalase, injury dropped by approximately 95%, which is consistent with the conclusion that peroxidative products of H_2O_2 represent the key toxic products. As expected, SOD did not affect lung damage generated by glucose, glucose oxidase and lactoperoxidase, because no generation of O_2^{\bullet} would be expected. Not shown in is the fact that PMN depletion had no protective effects on lung injury generated by either xanthine + xanthine oxidase or by glucose + glucose oxidase + lactoperoxidase, all of which indicates that recruitment of PMNs into lung under such conditions does not contribute significantly to the oxidant burden in lung.

Morphology of oxidant-mediated ALI

Morphological features of ALI following intrapulmonary generation of oxidants following airway instillation of glucose, glucose oxidase (28 units), lactoperoxidase (1.7 units) were evaluated by scanning electron microscopy (SEM) and transmission electron microscopy (TEM). As shown in Figure 3 employing SEM, normal lung (frame A) contained smooth intact alveolar walls in which capillaries could be identified. In some areas small projections from the alveolar walls could be seen, representing alveolar type II epithelial cells. Four hours after initiation of lung injury (frame B), the morphology was dramatically different. Alveolar spaces contained RBCs, together with tenuous white fibrous collections of fibrin. In some areas these collections were confluent, resulting in thick fibrin deposits. In other areas, discontinuities due to dropout of alveolar epithelial and vascular endothelial cells could be seen. 48 h after the onset of injury (frame C), extensive collections of fibrin remained together with leukocytes and RBCs. By 5 days (frame D) residual RBCs were still present in alveolar spaces, which were undergoing collapse, associated with residual fibrin and thick bands of collagen (frame E and



Figure 3. Scanning electron microscopy (SEM) and lactoperoxidase (S)

inset in frame E). cells could also be

Based on TEM lungs and at the A, B (4 h) show in capillaries along the presence of I with extensive f edema fluid, prot tegrating cells (al alveolar compart alveolar membra hours after injury hemorrhage, ede evident in alveol tion of alveolar were evident. By gen could be see with collapse of broblasts and evi

not especially toxic, by a peroxidase are of the lung. Such data suggest that nutrients withstand mM concentrations of inhibiting evidence of

ed by glucose, glucose. In the context of the conclusion that SOD did not affect the generation of O_2^{\bullet} is the fact that the effects on lung injury + xanthine oxidase + lactoperoxidase that recruitment of conditions does not oxidant burden in

Mediated ALI

Following intrapulmonary instillations following airway instillations of glucose oxidase (28 units), lungs were re-evaluated by scanning electron microscopy (SEM) and transmission electron microscopy (TEM) as shown in Figure 3 (frame A) contained normal lung tissue in which capillaries were seen, representative of normal cells. Four hours after injury (frame B), the morphology of alveolar spaces contained extensive white fibrous areas with these collections of fibrin deposits. In addition to dropout of alveolar endothelial cells could be seen, injury (frame C), examined together with alveolar spaces (frame D) residual alveolar spaces, which were associated with residual collagen (frame E and

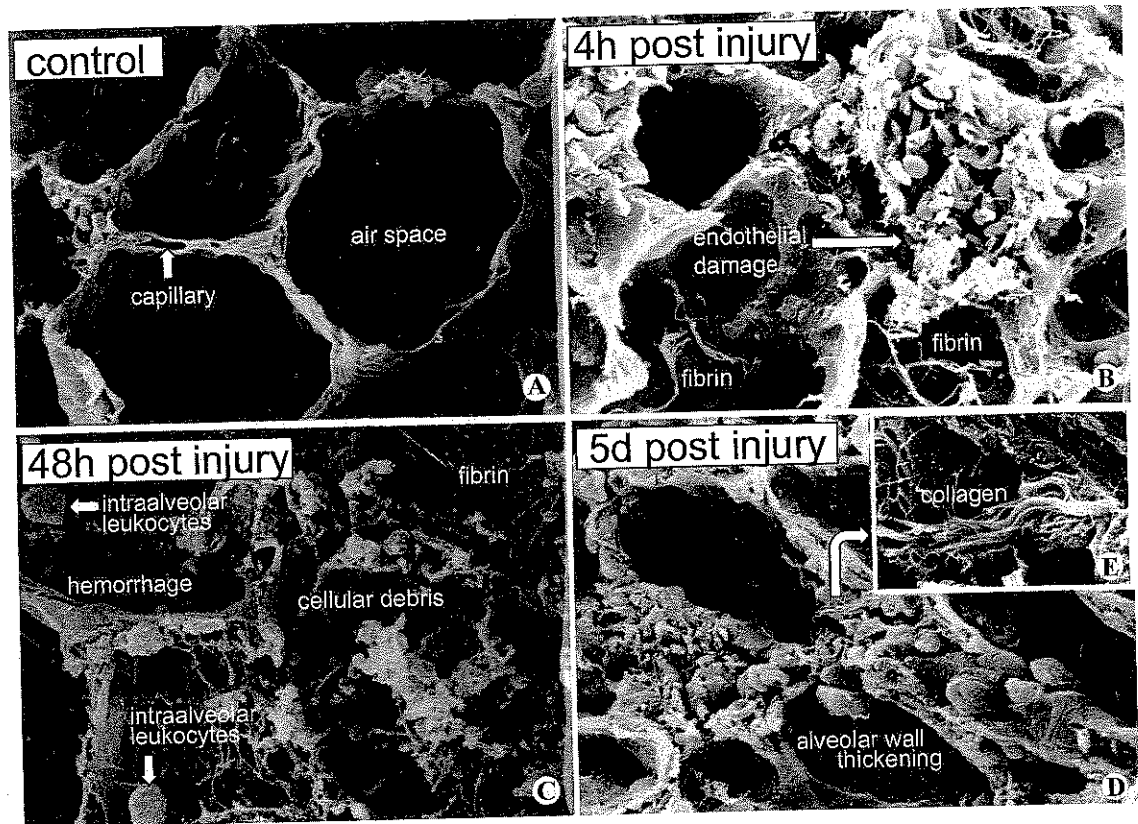


Figure 3. Scanning electron micrographs of control lung and lungs 4 and 48 h after airway instillation of glucose, glucose oxidase, and lactoperoxidase (see text for details) (1100 \times).

inset in frame E). Regenerating alveolar epithelial cells could also be seen.

Based on TEM analysis of tissues from the same lungs and at the same timepoints (Fig. 4), frames A, B (4 h) showed extensive cell debris, platelets in capillaries along the endothelial surfaces, and the presence of RBCs in alveolar spaces, together with extensive fibrin deposits and evidence of edema fluid, protein, and some PMNs. Also, disintegrating cells (alveolar epithelial cells) within the alveolar compartment were found, and denuded alveolar membranes were also evident. Forty-eight hours after injury (frame C), extensive intraalveolar hemorrhage, edema fluid, and fibrin deposits were evident in alveolar spaces. In addition, disintegration of alveolar walls and extensive cellular debris were evident. By day 5 (frame D), extensive collagen could be seen in the lung parenchyma together with collapse of alveolar spaces, prominence of fibroblasts and evidence of proliferating Type II alve-

olar epithelial cells. In the same areas prominent regenerating Type II alveolar epithelial cells were present.

Discussion

These data indicate that ALI resulting from generation of intrapulmonary oxidants derived from either activated lung macrophages or from oxidant generating enzymes delivered into the lung can induce ALI that may be reversible or irreversible (the latter resulting in pulmonary fibrosis). Reversibility occurs when oxidants are derived from phagocytic cells (macrophages and PMNs) and when the stimulant (e.g., LPS, IgGIC) results in limited oxidant generation. On the other hand, if the stimulant (such as PMA) is especially powerful, it appears that macrophage generated oxidants overcome the limit of natural antioxidant enzymes in lung (catalase, SOD, and glutathione peroxidase) as well as constitutive GSH. Under such conditions the regenerative

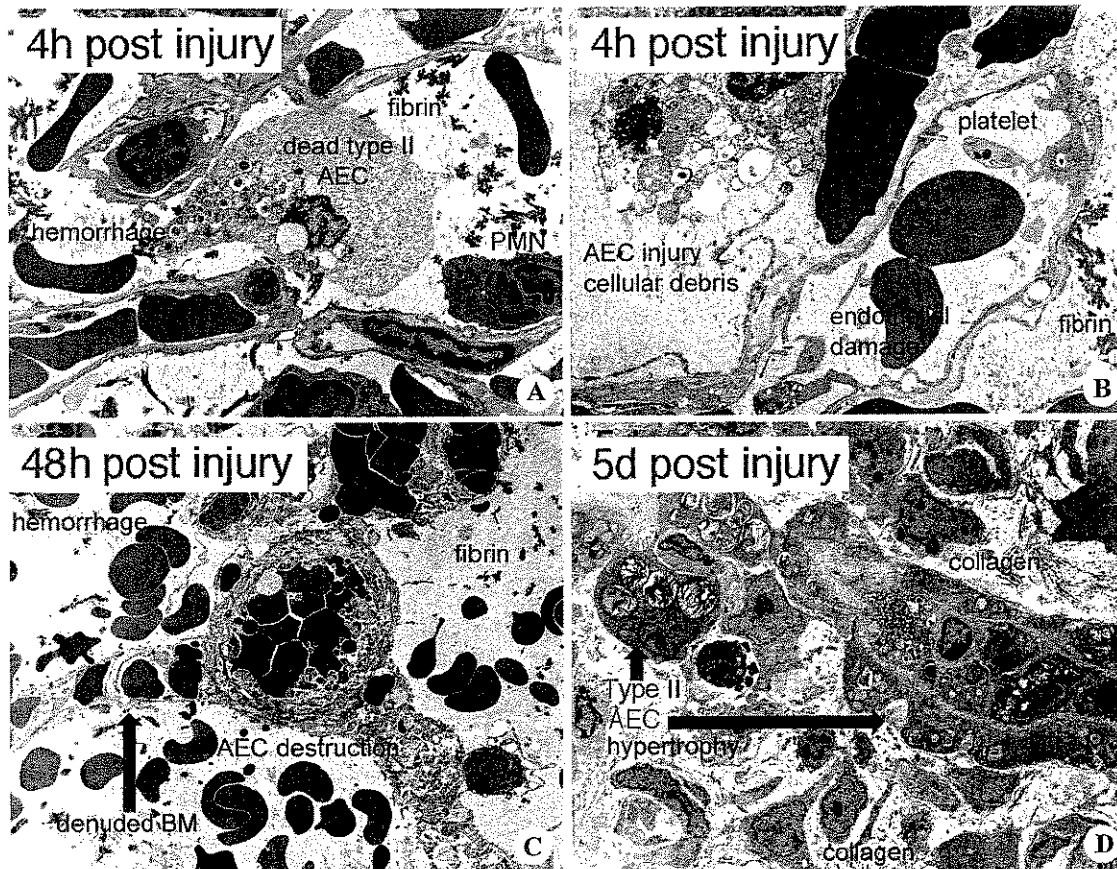


Figure 4. Transmission electron micrographs of lungs 4 and 48 h and 5 days following the same treatments described in legend to Figure 3 (Frame A, 3200 \times ; B, 5000 \times ; C, 1650 \times ; D, 1300 \times).

capacity of lung is overwhelmed and the outcome is development of pulmonary fibrosis.

The use of extrinsic enzymes (glucose oxidase, xanthine oxidase, and lactoperoxidase) has allowed a provisional determination of the oxidants that are especially lung damaging. It appears that O_2^{\bullet} generated by xanthine oxidase + xanthine can be intensely lung-damaging, although it is difficult to relate this to O_2^{\bullet} produced by macrophages and PMNs in lung, because O_2^{\bullet} is rapidly converted to H_2O_2 by SOD and can also interact with $\bullet NO$. The production of H_2O_2 by glucose oxidase + glucose, not surprisingly resulted in very limited lung damage, because *in vitro* studies usually show that mM levels of H_2O_2 are required to produce cell damage.^{12,13} However, the presence of lactoperoxidase or myeloperoxidase, which converts H_2O_2 into organochloride, organiodine, and organochloride products which are extremely lung damaging prod-

uct(s) and can lead to irreversible lung injury and pulmonary fibrosis (Figs. 3 and 4). Because MPO is naturally present in substantial quantities in PMNs and can be readily secreted, it seems likely that HOCl may be the lung-damaging product that leads to irreversible lung damage and fibrosis in the experimental protocols employed.

Conclusions

It is well known that oxidant generation in lung can be highly lung damaging. Natural sources of oxidants in lung are macrophages and recruited neutrophils. In most cases, limited oxidant production from these phagocytes allows the development of reversible lung injury. However, an extremely strong stimulus of phagocytes (PMA) may overwhelm the regenerative capacity of lung, with resultant parenchymal collapse and fibrosis. Use of substrates and enzymes allows the probing of the

most toxic oxidants such as xanthine and plus glucose oxidase or myeloperoxidase in the lung beyond its regenerative capacity, leading to a fibrotic outcome. The engagement of antioxidant systems is a topic relevant to oxidant damage in human lungs.

Conflicts of interest

The author declares:

References

1. MacNee, W. & I. Raj. Idiopathic pulmonary fibrosis. *Am Rev Respir Dis* 1988; 138: 1100-1108.
2. Kinnula, V.L., C.L. Fagan. Oxidative stress in pulmonary fibrosis. *Am Rev Respir Dis* 1997; 155: 417-422.
3. Johnson, L.N. & M. M. Pulmonary injury, oxidative stress, and fibrosis. *Antioxid. Redox Signal* 2000; 2: 1-10.
4. Vivekananda, J., A. I. Inflammatory injury: oxidative stress induces fibro-



ments described in legend

sible lung injury and d 4). Because MPO is il quantities in PMNs eems likely that HOCl oduct that leads to ir- fibrosis in the experi-

t generation in lung 3. Natural sources of hages and recruited ited oxidant produc- ows the development owever, an extremely es (PMA) may over- city of lung, with re- and fibrosis. Use of vs the probing of the

most toxic oxidants in the lung setting. Reagents such as xanthine and xanthine oxidase or glucose plus glucose oxidase in the copresence of lactoperoxidase or myeloperoxidase can severely damage the lung beyond its regenerative capacity, resulting in a fibrotic outcome. Understanding the dynamic between oxidant production in lung and engagement of antioxidant defenses provide information relevant to oxidant-mediated damage in human lungs.

Conflicts of interest

The author declares no conflicts of interest.

References

1. MacNee, W. & I. Rahman. 1995. Oxidants/antioxidants in idiopathic pulmonary fibrosis. *Thorax* 50(Suppl 1): S53-S58.
2. Kinnula, V.L., C.L. Fattman, R.J. Tan & T.D. Oury. 2005. Oxidative stress in pulmonary fibrosis: a possible role for redox modulatory therapy. *Am. J. Respir. Crit. Care Med.* 172: 417-422.
3. Johnson, L.N. & M. Koval. 2009. Cross-talk between pulmonary injury, oxidant stress, and gap junctional communication. *Antioxid. Redox. Signal.* 11: 355-367.
4. Vivekananda, J., A. Lin, J.J. Coalson & R.J. King. 1994. Acute inflammatory injury in the lung precipitated by oxidant stress induces fibroblasts to synthesize and release transforming growth factor- α . *J. Biol. Chem.* 269: 25057-25061.
5. Bus, J.S., S.D. Aust & J.E. Gibson. 1976. Paraquat toxicity: proposed mechanism of action involving lipid peroxidation. *Environ. Health Perspect.* 16: 139-46.
6. Johnson, K.J., J.C. Fantone III, J. Kaplan & P.A. Ward. 1981. In vivo damage of rat lungs by oxygen metabolites. *J. Clin. Invest.* 67: 983-993.
7. Fantone, J.C. & P.A. Ward. 1982. Role of oxygen-derived free radicals and metabolites in leukocyte-dependent inflammatory reactions. *Am. J. Pathol.* 107: 395-418.
8. Quinlan, T., S. Spivack & B.T. Mossman. 1994. Regulation of antioxidant enzymes in lung after oxidant injury. *Environ. Health Perspect.* 102(Suppl 2): 79-87.
9. Johnson, K.J. & P.A. Ward. 1982. Acute and progressive lung injury after contact with phorbol myristate acetate. *Am. J. Pathol.* 107: 29-35.
10. Rittirsch, D., M.A. Flierl, D.E. Day, et al. 2008. Acute lung injury induced by lipopolysaccharide is independent of complement activation. *J. Immunol.* 180: 7664-7672. PMID: 18490769.
11. Rittirsch, D., M.A. Flierl, D.E. Day, et al. 2009. Cross-talk between TLR4 and Fcy receptor III (CD16) pathways. *PLoS Pathog.* 5: e10000464. Epub 2009 Jun 5.
12. Elner, S.G., V.M. Elner, M.G. Field, et al. 2008. Retinal flavoprotein autofluorescence as a measure of retinal health. *Trans. Am. Ophthalmol. Soc.* 106: 215-222.
13. Rauen, U., T. Li, I. Ioannidis & H. de Groot. 2007. Nitric oxide increases toxicity of hydrogen peroxide against rat liver endothelial cells and hepatocytes by inhibition of hydrogen peroxide degradation. *Am. J. Physiol. Cell Physiol.* 292: C1440-C1449.

Forum Review

Role of Oxidants in Lung Injury During Sepsis

REN-FENG GUO and PETER A. WARD

ABSTRACT

The role of oxidative stress has been well appreciated in the development of sepsis-induced acute lung injury (ALI). Oxidative stress in sepsis-induced ALI is believed to be initiated by products of activated lung macrophages and infiltrated neutrophils, promptly propagating to lung epithelial and endothelial cells. This leads to tissue damage and organ dysfunction. On stimulation, neutrophils (PMNs) enable their migration machinery. The lung undergoes changes favoring adhesion and transmigration of PMNs, resulting in PMN accumulation in lung, which is a characteristic of sepsis-induced ALI. Oxidative stress turns on the redox-sensitive transcription factors (NF- κ B, AP-1), resulting in a large output of proinflammatory cytokines and chemokines, which further aggravate inflammation and oxidative stress. During the process, transcription factor nuclear factor-erythroid 2-p45-related factor 2 (Nrf2) and heme oxygenase (HO) appear to play the counterbalancing roles to limit the propagation of oxidative stress and inflammatory responses in lung. Many antioxidants have been tested to treat sepsis-induced ALI in animal models and in patients with sepsis. However, the results are inconclusive. In this article, we focus on the current understanding of the pathogenesis of sepsis-induced ALI and novel antioxidant strategies for therapeutic purposes. *Antioxid. Redox Signal.* 9, 1991–2002.

INTRODUCTION

DESPITE TECHNICAL DEVELOPMENTS in intensive care units (ICUs) and advanced supportive treatment, the death rate in septic patients remains high, with a range of lethality ranging from 30 to 50% (3). The acute respiratory distress syndrome (ARDS) has been defined as a severe form of acute lung injury (ALI), featuring pulmonary inflammation and increased capillary leak (98). ARDS may arise in a number of clinical situations, especially in patients with sepsis. As a common complication of sepsis, it has been considered a leading cause for death in sepsis. A well-described pathophysiologic model of ARDS is one form of acute lung inflammation mediated by inflammatory cells and mediators as well as oxidative stress (22).

Oxidative stress is caused by an imbalance between the production of reactive oxygen species (ROS) and the biologic scavenger system, which can readily detoxify the reactive oxygen intermediates under normal physiologic conditions. Oxidative-induced damage has been considered to be one of the underly-

ing mechanisms that contribute to multiple organ failure in sepsis (7, 35, 102). Because of the natural oxidizing nature of the atmosphere and the direct exposure to many atmospheric pollutants, the lung is at high risk of oxidative injury. It has been recognized that oxidative stress can not only directly cause tissue damage, but it also can affect the molecular mechanisms that control lung inflammation. In the healthy lung, airway lining fluids and extracellular spaces are maintained in a highly reduced state (with millimolar levels of reduced glutathione, GSH) to preserve normal physiologic functions. Under normal conditions, the levels of antioxidants and oxidants in lung are balanced in favor of a reducing state. Decreases in antioxidants or increases in oxidants can disrupt this equilibrium and can cause oxidative stress. An imbalance in the oxidant-antioxidant system has been recognized as one of the first events that ultimately lead to inflammatory reactions in the lung (17).

Oxidative stress has been found to occur in many forms of lung disorders, such as pneumonia, ARDS, idiopathic pulmonary fibrosis, lung transplantation, chronic obstructive pul-

monary disease, cystic fibrosis, bronchiectasis ischemia–reperfusion, and lung cancer (10, 18, 79). Based on composition, oxidants can be divided into two main categories, ROS and reactive nitrogen species (RNS). Superoxide, hydroxyl radicals, and hydrogen peroxide are generally classified as ROS in contrast to nitric oxide and peroxynitrite, which are nitrogen based. These molecules naturally function as neurotransmitters, second messengers, and as a part of the chemical host defense against infection. It is only when their concentrations become excessive, especially extracellularly, that the potential for adverse responses can occur. High ROS/RNS levels lead to alterations in normal cell function and eventually compromise local tissue and systemic homeostatic mechanisms. In this review, we focus on the understanding of the roles of oxidative stress in sepsis-induced ALI and potential therapeutic strategies by using antioxidants.

DETECTION OF OXIDATIVE STRESS IN LUNG

It is clear that a better understanding of the oxidative state in the lung is important for the diagnosis and treatment of lung diseases. Many methods have been developed for detection of free radicals from oxygen, ROS, RNS, and their byproducts to assess the presence of oxidative stress. The techniques include established standard protocols and advanced methods using high-performance liquid chromatography (HPLC), mass spectrometry, and electron paramagnetic resonance. Described later are the most frequently used methods for evaluation of lung oxidative status.

Monitoring oxidative stress in live cells

ROS in live cells can be detected by using a fluorogenic marker for ROS and observing under fluorescence microscopy. One frequently used marker is carboxy- H_2DCFDA , a cell-permeable fluorogenic marker, which is oxidized during oxidative stress in live cells and emits bright green fluorescence (97). $NO\cdot$ production by lung cells can be measured by using the $NO\cdot$ fluorescent indicator, DAF-2 (89). On reaction with an active intermediate (N_2O_3) formed during the oxidation of $NO\cdot$ to nitrite, DAF-2 is converted to its fluorescent triazole form, which can be measured by fluorescent plate readers at excitation and emission wavelengths of 485 and 538 nm, respectively.

Hydrogen peroxide (H_2O_2) and superoxide products in bronchoalveolar fluids

H_2O_2 fluids in bronchoalveolar fluids (BALs) can be measured by the simple assay for detecting the presence of peroxides in both aqueous and lipid environments. The basis of these assays is the complexing of ferrous ion (Fe^{2+}) by H_2O_2 in the presence of xylenol orange. Peroxides will oxidize Fe^{2+} to Fe^{3+} , and Fe^{3+} will form a colored complex with xylenol orange that can be read at 560 nm (46, 47). Superoxide radical generation can be estimated by nitroblue-tetrazolium reduction assay (60).

Antioxidant status in lung

The antioxidant status in the lungs can be evaluated by lung levels of superoxide dismutase (SOD) and catalase (CAT) and their activities. SOD activity can be assessed by the OxyScan SOD-525 assay, which measures the activity of all forms of SOD. The method is based on the SOD-mediated increase in the rate of autooxidation of 5,6,6a,11b-tetrahydro-3,9,10-trihydroxybenzofluorene in aqueous alkaline solution to yield a chromophore with maximum absorbance at 525 nm. Catalase (CAT) activity can be determined by a two-step reaction scheme (catalase-520 assay). First, catalase reacts with a known quantity of H_2O_2 to generate H_2O and $O_2\cdot^-$. In the presence of horseradish peroxidase (HRP), the remaining H_2O_2 reacts with 3,5-dichloro-2-hydroxybenzenesulfonic acid and 4-aminophenazone to form a chromophore with a color intensity. Lipid peroxidation levels in lung can be measured by thiobarbituric acid–reactive substances assay (25). The GSH/GSSG ratio, a useful measure of oxidative stress, can be determined by a colorimetric method by using Biotex GSH/GSSG-412.

Protein oxidation and lipid peroxidation in lung

The levels of protein carbonyls and nitrotyrosine are widely used for the detection of oxidative modification of proteins. Protein carbonyls are considered to be one of the most reliable methods to evaluate the protein damage mediated by oxidative stress. Nitrotyrosine levels in tissues and BAL fluids correlate with oxidant stress in animal and human studies (33). Protein carbonyls can be measured through the reaction with dinitrophenylhydrazine (DNPH) (57). The proteins are first precipitated by the addition of 20% trichloroacetic acid and then redissolved in DNPH. Nitrotyrosine is often determined by enzyme-linked immunosorbent assay (ELISA), Western blotting, and immunohistochemistry with specific antibodies. Lipid peroxidation, oxidized lipids, and lipid mediators are believed to play an important role in lung inflammatory diseases. The detection of products of lipid peroxidation has been widely used to estimate the overall status of oxidative stress in lung. Among them, thiobarbituric acid reactants (TBARs) and malondialdehyde (MDA) are commonly used indicators (16).

DNA damage

The most common type of damage caused by reactive oxygen species in the body is oxidative damage to DNA. Hydroxydeoxyguanosine (8-OHdG), a product of this type of DNA damage, is used as a biomarker for oxidative stress. It can be measured by the immunohistochemical procedure and an HPLC system equipped with an electrochemical detector (HPLC-ECD) (63). More recently, it has been reported that capillary electrophoresis-mass spectrometry (CE/MS) can be also used for the analysis 8-OHdG to study oxidative stress (101).

Analysis of expired air for oxidation products

Studies have shown that expired $NO\cdot$ and CO can serve as biomarkers for oxidative stress, whereas ethane can serve as a marker of lipid peroxidation (73). CO can be detected electrochemically, and it can also be measured by a laser spectrophotometer and near-infrared CO analyzers. The levels of exhaled

NO[•] can be assessed by chemiluminescence. Ethane content can be detected by using gas chromatography. Oxidative stress in lung appears to be an important factor in predicting or assessing (or both) lung injury. Methods for detection of oxidative stress have a broad range from well-established protocols to newly developed technologies. It is very difficult to measure oxygen free radicals directly because of their short half-lives and reactivity with other molecules. Radical spin-trapping agents have been used to form stable radical adducts, which can be detected by electron paramagnetic resonance spectroscopy (EPR). Trapping agents are generally nitron- or nitroso-containing molecules, such as 5,5-dimethyl-1-pyrroline-*n*-oxide (DMPO), that react with oxygen free radicals to form stable nitroxide free radicals (72). The sampling procedure to collect exhaled breath condensate can be used to measure H₂O₂, leukotrienes, isoprostanes, and 3-nitrotyrosine in lung inflammation (73). Given the nature of complexity and importance of lung biology, it is essential to develop sensitive and reliable tools to monitor the status of lung oxidative stress. A standardized protocol is also required for clinical application.

EVIDENCE OF OXIDATIVE STRESS IN SEPSIS-INDUCED ALI

Low antioxidant and high plasma levels of oxygen free radicals have been well documented in patients with sepsis and in animal models of sepsis (30, 35, 96). Many oxidative indicators have been reported in lungs from septic patients and animals. In patients with sepsis, protein carbonyls were significantly elevated in both blood and BAL fluids during the initial phase of sepsis, decreasing within a few days but remaining above control values (102). In the same study, myeloperoxidase (MPO) activity was also markedly increased in BAL fluids from septic patients. Strong correlations were found between carbonyl concentrations in BAL fluid and plasma, when compared with protein carbonyls, TBARS, and MPO in lung, suggesting that neutrophil oxidants might be chiefly responsible for oxidative stress in lungs during sepsis. All patients with ARDS had higher levels of hypoxanthine, a prooxidant substrate for xanthine oxidase (75). Hypoxanthine levels were 2 times higher in nonsurvivors than those in survivors. Nonsurvivor ARDS patients appeared to have higher levels of oxidative stress and damage when compared with survivors. Surprisingly, hypoxanthine levels were normal in patients in intensive care with sepsis but no lung injury. These data suggest that oxidative stress plays an essential role in the pathogenesis of ALI in sepsis, and directly contributes to the bad outcome.

Oxidative stress in animal models of sepsis has been also well described. In rodent sepsis models induced by cecal ligation and puncture (CLP), the activities of enzymatic antioxidants, including SOD, CAT, and glutathione peroxidase (GSH-PX), in lung were significantly decreased during the early- and late-sepsis phases (21), indicating that sepsis sets up an environment favorable for oxidative stress in lung. As expected, MDA concentrations and nitrate (NO₃⁻)/nitrite (NO₂⁻) levels were also elevated in the septic lung. In addition, MPO activity was found to be enhanced, and a large number of neutrophil infiltrates were observed by histology in lungs from septic animals. Many other

oxidative indicators in lung, including 8-isoprostane, exhaled NO[•], superoxide anion, glutathione, protein carbonyls, and TBARS, were all changed in favor of an oxidative-stress status during experimental sepsis (2, 19, 51, 59, 85, 86, 96).

NEUTROPHIL ACCUMULATION IN LUNG DURING SEPSIS

The pathophysiology of the sepsis-induced ALI/ARDS is very complicated and not completely defined. However, increased production of ROS/RNS from PMNs has been proposed as one of the significant mechanisms underlying the development of lung inflammation. Additionally, the contribution by lung macrophages may be an important source for ROS/RNS. Sepsis-induced ALI is characterized by the activation of a variety of cells, including inflammatory cells such as PMNs and macrophages, and increased levels of inflammatory mediators. PMN infiltrates occur in lungs from both humans and animals with sepsis. The number of neutrophils in BAL fluids from patients with ARDS is significantly increased and associated with poor survival (1, 61, 100). Circulating PMNs infiltrate and accumulate in the lung *via* transmigration through the endothelium, interstitium, and alveolar epithelium to enter the alveolar compartment or be sequestered in lung capillaries. Upregulation of chemoattractant molecules (chemokines) occurs, establishing a concentration gradient that directs the neutrophils into the lung. Adhesion molecules, including integrins, selectins, and ICAMs, are also involved in the migration process (40). These events are described in Fig. 1.

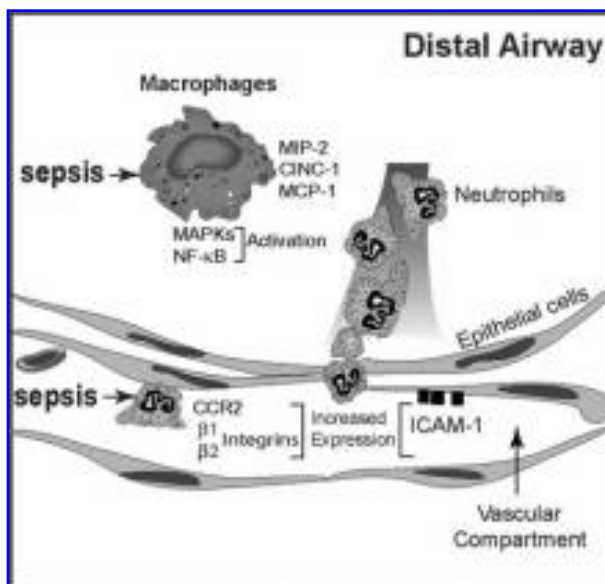


FIG. 1. The mechanism of PMN accumulation in the lung during sepsis. In rat and mouse models of sepsis, activated alveolar macrophages release MIP-2 (rat), CINC-1 (rat), and MCP-1 (mouse), which chemoattract PMNs into the lung. Increased levels of CCR2 as well as β_1 and β_2 integrins on PMNs, together with enhanced expression of ICAM-1 on endothelial cells, facilitate PMN adhesion and migration.

Local production of CXC chemokines is essential for the accumulation of PMNs in the lung under conditions of acute inflammation. For PMN chemoattractants, although sufficient local concentrations of CXC chemokines are necessary for PMN recruitment, the dictating factor is the ratio of lung-to-blood chemokine concentrations (11). In experimental sepsis, lung production of two important CXC chemokines, MIP-2 and CINC-1, increased but lagged behind in comparison with the levels of MIP-2 and CINC in blood (38). As a result, lung levels of CXC chemokines increased when blood levels of those decreased. The discrepancy might be important for CXC chemokines to create a gradient difference between the two compartments (vascular and alveolar), which is necessary for initiation of PMN migration. CXC chemokines have been implicated in all steps in the extravasation process of leukocytes, including rolling, adhesion, and transmigration *in vivo* (104). Thus, the role of blood CXC chemokines may primarily focus on the activation of PMNs and endothelial cells, setting the stage for PMN migration, whereas local CXC chemokines chiefly function chemotactically during sepsis. In addition, blood CXC chemokines produced in the early stage of experimental sepsis may provide vital signals for PMN survival, given the fact that CXC chemokines and C5a reduce PMN apoptosis (23, 39). Under such conditions, the greatly prolonged life span of PMNs may be related to the development of the symptoms of sepsis. The reason for higher BAL levels of CXC chemokines is likely the activation of lung macrophages. It is clear that a phase exists in which alveolar macrophages are prone to activation during the early stage of sepsis, and then may go into a refractory (deactivation) stage (38, 82). Conversely, PMNs quickly enter into this refractory phase, and their capability for producing CXC chemokines and other inflammatory mediators is greatly compromised. It was found that CXC chemokine macrophage-inflammatory protein-2 (MIP-2) production in both alveolar macrophages and PMNs was dependent on mitogen-activated protein (MAP) kinases (p38 and p42/p44) and NF- κ B pathways (38). Interestingly, alveolar macrophages still maintain, and even increase, their capacity for activation of p38 and p42/p44 MAPKs during sepsis, whereas septic blood PMNs become nonresponsive to stimulations. Paralysis of signaling pathways in PMNs is likely caused, at least in part, by overproduction of C5a in sepsis. In addition, the CC chemokine, MCP-1, seems to also play an important role in attracting PMNs into lung (89). PMNs in sepsis used a novel migration pathway that is CC chemokine receptor CCR2 dependent. Ordinarily, PMNs do not express CCR2, but in sepsis, this receptor is clearly expressed (88).

Sepsis involves widespread upregulation of both PMN and endothelial adhesion molecules (74). In a rat model of sepsis, it was observed that the content of β_1 and β_2 integrins on circulating PMNs was elevated after CLP. The increased expression of β_1 integrin on blood PMNs followed β_2 integrin elevation, which was seen as early as 3 h after CLP. Rapid elevation of β_2 integrin may represent an important role in host defense by directing PMNs into inflamed organs. Several lines of evidence support such a role for β_2 integrin in the mobilization of PMNs into tissues. Patients with inherited deficiencies of β_2 integrin are much more susceptible to bacterial infection (41). In a canine model of lung inflammation (i.v. infusion of TNF- α), anti-CD11b treatment reduced PMN accumulation early (within

the first 24 h), but not later (>24 h) (74), suggesting that leukocyte trafficking may differ between the early and late stages of inflammation. Expression of β_1 integrin in PMN migration is amplified in sepsis. Fully activated β_1 integrin at the later stage of sepsis may alter the balance of integrin cooperativity. It was previously shown that blood PMNs from septic, but not control, patients expressed $\alpha_4\beta_1$ integrin, which caused increased adhesiveness to immobilized VCAM-1 (43). Anti- β_1 integrin antibody interferes with cell motility of septic PMNs from CLP rats, indicating that sepsis alters the trafficking of PMNs into the lung by engaging a β_1 integrin-dependent pathway (37). The adhesion molecule, ICAM-1, is also involved in PMN migration during sepsis. Absence or blockade of this molecule impairs the ability of PMNs to migrate into organ tissues and reduces consequent secondary organ damage, resulting in improved clinical indicators and overall survival (42). We previously demonstrated that PMN migration into lung during sepsis is ICAM-1 dependent, but not VCAM-1 dependent, perhaps related to VCAM-1 shedding that occurs during the course of sepsis development (54).

Figure 1 illustrates a simplified version of pathways for PMN migration in the lung during sepsis. CCR2 and β_1 and β_2 adhesion molecules on PMNs are upregulated during the course of sepsis, whereas PMN capability to produce CXC chemokines is reduced. In lung, activated macrophages release a large amount of PMN chemoattractants and other inflammatory cytokines, whereas ICAM-1 is activated on endothelial cells, setting the stage for PMN migration. These processes are tightly regulated by MAPKs and NF- κ B pathways.

ROLE OF OXIDANTS IN SEPSIS-INDUCED ALI

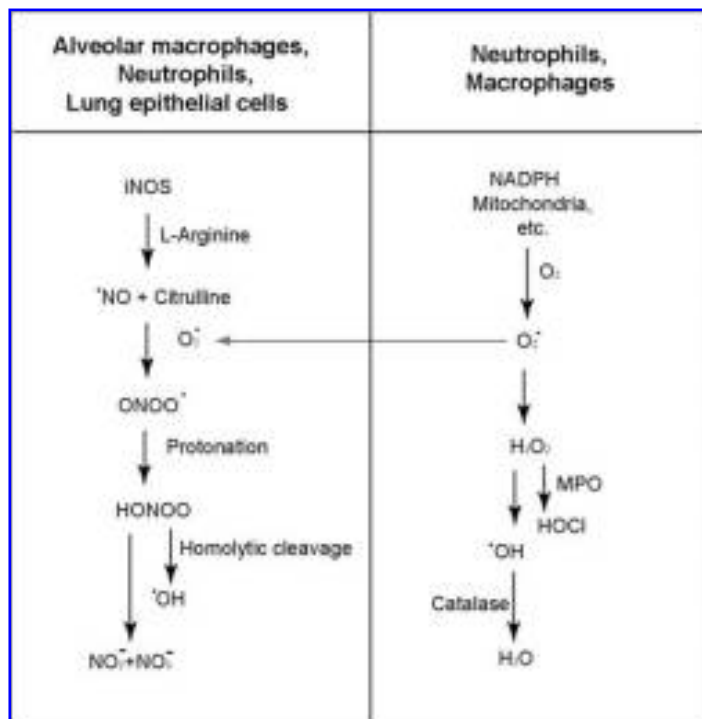
Inflammation occurs after activation of PMNs and macrophages, resulting in ROS/RNS generation and the release of lysosomal enzymes and cationic proteins. Oxidative stress is initiated by ROS such as superoxide (O_2^-) and hydrogen peroxide (H_2O_2). These oxidants are not very harmful *per se*, but can be converted into more dangerous oxidants, causing harmful reactions in tissues (16). Generation of superoxide-derived products continues to be the main pathway responsible for the production of ROS. O_2^- can be generated through various enzymatic systems, including the mitochondrial respiratory chain, xanthine oxidase, cyclooxygenase, and NADPH oxidase (16). The NADPH oxidase pathway is well defined in phagocytic cells. Activation of the oxidase can be initiated by a variety of inflammatory mediators and is likely to be a major source of oxidant generation in sepsis-induced lung injury. Translocation of cytosolic subunits of NADPH oxidase components from the cytoplasm to the cell membrane occurs in PMNs, macrophages, and monocytes on cell stimulation, thus representing a potential therapeutic target in the treatment of ROS-mediated lung injury during sepsis. NADPH oxidase catalyzes the transfer of an additional electron to molecular oxygen (O_2) to form the O_2^- anion. Because NADPH oxidase adds single electrons to O_2 , oxygen-derived intermediates are also produced. Reduction of Fe^{3+} to Fe^{2+} or Cu^{2+} to Cu^+ by superoxide in the Fenton re-

action facilitates the generation of hydroxyl radicals (OH^\cdot). In the presence of Fe^{2+} , superoxide is reduced to H_2O_2 , which can then be metabolized in the presence of transition metals and chloride to form hypochlorous acid (HOCl). This reaction is catalyzed by MPO and provides a practical marker for PMN accumulation in tissue. Although it is not a free radical, H_2O_2 can permeate cellular membranes, thus extending the damage beyond the originating cell. These products injure cells of the lung and airway and interfere with gas exchange.

NO^\cdot is an abundant signaling molecule. Like H_2O_2 , it is able to cross cell membranes to alter various physiologic processes through binding and activation of guanylate cyclase. *Via* this intermediate, NO^\cdot functions as a secondary messenger in the maintenance of systemic vascular tone. NO^\cdot also affects platelet aggregation and can stimulate immune responses, activate genes, and cause apoptosis (32, 50). It is fairly unreactive with bioorganic molecules; however, it does react with aromatic amino acids to form stable nitrotyrosine adducts in proteins and peptides, which may impair cell function. NO^\cdot is synthesized by three nitric oxide synthase (NOS) isozymes, so named by the origin of the cell in which they were originally discovered. Two of the three forms (nNOS and eNOS) are constitutively expressed and generate small amounts of NO^\cdot , which generally are not sufficient to cause cellular damage. Binding to calcium and calmodulin is required for NOS activation, serving as factors that regulate NOS activity. In contrast, the third isoform (iNOS) is an inducible calcium-independent enzyme that produces copious amounts of NO^\cdot for several hours to even days after induction. It is during circumstances that initiate induction of this third NOS form that the physiologic roles of NO^\cdot are superseded by its implication as the culprit behind various injurious inflammatory responses and potentially cytotoxic events.

In the setting of lung, all three NOS isozymes are present. Various forms of NO^\cdot can be observed as *S*-nitrosothiol, nitrate, and nitrite in exhaled air and bronchoalveolar lavage from human lungs (24, 95). Upregulation of iNOS amplifies the conversion of L-arginine to L-citrulline and NO^\cdot formation. In the presence of superoxide, NO^\cdot is converted to peroxynitrite (ONOO^-), which is then protonated to form an unstable species, peroxynitrous acid (ONOOH). The presence of iNOS has been reported in alveolar macrophages, PMNs, and endothelial and lung epithelial cells (99). Accordingly, these cells are all potential sources of peroxynitrite. ONOO^- reacts with protein thiols and is thought to be the predominant mechanism by which NO^\cdot production leads to cytotoxicity. Peroxynitrous acid is degraded to form the hydroxyl radical, NO_3^- and NO_2^- by hemolytic cleavage, or it can react with CO_2 to form peroxycarboxylate (ONOOCO_2^-). Detection of NO_3^- and nitrite NO_2^- serves as a convenient experimental marker for NO^\cdot production. Activation of infiltrating and resident phagocytes can cause an increase in both NO^\cdot and superoxide, resulting in apoptosis. On a molecular level, the resulting peroxynitrite interacts with DNA to cause DNA fragmentation, and with membrane lipids to cause peroxidation of the endothelial or alveolar epithelial cell plasma membranes. Low concentrations of NO^\cdot suppress peroxidation, but as superoxide levels increase, cell membrane injury becomes intensified. Reduced amounts of NO^\cdot serve to decrease endothelial cell membrane permeability, thus limiting PMN transmigration from the vascular compartment into the lung tissue. NO^\cdot is an endogenous inhibitor of leukocyte adhesion to endothelial cells, but this phenomenon is reversed by increasing amounts of superoxide anion. The potential pathways that generate oxidants in sepsis-induced ALI are illustrated in Fig. 2.

FIG. 2. Mechanisms for production of reactive oxygen species in sepsis-induced ALI.



Role of NO[•] in sepsis-induced ALI

Sepsis and ALI are associated with a high level of NO[•] production after activation of iNOS. NO[•] has been implicated in the pathophysiology of ALI in humans and animal models of ALI. However, NOS inhibition with nonselective inhibitors, such as N^G-monomethyl-L-arginine (L-NMMA), in animals with sepsis and ALI has resulted in worsened outcomes (65, 71), suggesting complex roles of NO[•] in the pathogenesis of sepsis. The results obtained from iNOS-deficient mice have been controversial. In the CLP-induced sepsis model, no pulmonary protein leak developed in iNOS-deficient mice, despite increased pulmonary MPO activity (27). By using the same model, it has been demonstrated that pulmonary oxidant stress is completely iNOS dependent and is associated with tyrosine nitration, and that pulmonary oxidant stress and nitrosative stress are dependent on the presence of iNOS in inflammatory cells (macrophages and PMNs), with no apparent contribution of iNOS in pulmonary parenchymal cells (80, 81). Therefore, the authors proposal that iNOS inhibition targeted specifically to inflammatory cells may be an effective therapeutic approach in sepsis and acute lung injury. In the bacterial lipopolysaccharide (LPS) model of ALI, lung-injury parameters such as MPO levels and albumin leak into lung were not affected by eNOS deficiency, but substantially were intensified in mice with iNOS deficiency. In LPS-induced lung injury in iNOS-deficient mice, BAL levels of CXC chemokines (MIP-2, KC) did not show any difference when compared with wild-type (WT) mice, but CC chemokines (MCP-1, MCP-3) were enhanced. Blockade of MCP-1 in iNOS-deficient mice reduced lung MPO to the levels present in WT mice. Thus, iNOS appears to play a protective role in this ALI model by limiting PMN accumulation in lung (89). Reasons for the discrepancy for iNOS-deficient effects from two ALI models are not clear. Tissue-specific KO conditions and reliable specific inhibitors for iNOS may help clarify the role of NO[•] in sepsis-induced ALI, thereby assisting in the design of future clinical trials. Nevertheless, the role of NO[•] in oxidative stress in lung is indisputable.

Role of O₂^{•-} in sepsis-induced ALI

Generation of O₂^{•-} by the NADPH oxidase complex of PMNs is crucial for host defense responses, and it is essential for killing invading microorganisms. However, O₂^{•-} may also exert harmful effect in tissues. NADPH oxidase is a multisubunit complex in which gp91^{phox} and p47^{phox} are essential for O₂^{•-} generation. O₂^{•-} can work as a "double-edged sword," so it is not surprising that the results from p47^{phox}^{-/-} and gp91^{phox}^{-/-} mice are perplexing in the setting of sepsis (31). More PMN infiltrates and higher bacterial loads were seen in lungs from p47^{phox}^{-/-} and gp91^{phox}^{-/-} mice compared with WT mice after live *Escherichia coli* challenge, whereas lung microvascular injury was prevented in these mice. Thus, PMN infiltration in lung tissue did not result in overt lung microvascular injury, when the O₂^{•-} generation was impaired. In the same study, it was found that increased bacterial load in NADPH-deficient mice was a critical factor for activating the release of chemokines, which subsequently enhanced PMN sequestration and migration into lung tissue. A selective SOD mimetic, M40401, was found to be protective in a live *E. coli* model of

sepsis, but it improved survival only in severe sepsis and was less effective and even harmful with less-severe sepsis (19). Another SOD mimetic, "Tempol," has been reported to improve survival in CLP-induced septic rats, reduce the plasma levels of NO[•] and IL-1 β , and decrease the levels of organ O₂^{•-} and tissue injury (59). It seems that O₂^{•-} is indispensable for killing bacteria, but also leads to tissue damage during sepsis.

NO[•] and O₂^{•-} appear to play dual roles in the pathogenesis of sepsis-induced ALI. They may function by totally different mechanisms at different stages of sepsis. Thus, in clinical trials that involve antioxidant inhibitors, a compelling need exists to monitor closely the bacterial load and oxidative status. For example, it might be reasonable to scavenge O₂^{•-} at a stage when the systemic bacterial load is partially contained during sepsis.

OXIDANT-RELATED MOLECULAR EVENTS IN SEPSIS-INDUCED ALI

NF- κ B and activator protein-1 (AP-1)

NF- κ B and AP-1 are two well-defined redox-sensitive transcription factors. Oxidative stress activates multiple stress kinase pathways and transcription factors (NF- κ B, AP-1) by modifying cysteine residues subsequently regulating gene expression for proinflammatory cytokines as well as the protective antioxidant molecules (76). Activation of NF- κ B occurs in lung macrophages and in lung tissue during sepsis (28, 45, 62). NF- κ B is a heteromeric dimer composed of a complex of proteins from the RelA family. NF- κ B is constitutively relegated to the cytosolic compartment. The dimer most commonly comprises p50 (NF- κ B1) and p65 (RelA) subunits bound to members of the inhibitor κ B (I κ B) family. Activation of NF- κ B occurs in response to an appropriate stimulus. After phosphorylation and ubiquitination of an I κ B subunit, it is subsequently degraded by a 28S proteasome. This allows the heterodimer complex to translocate to the nucleus and bind to specific DNA promoter sequences. Access to DNA is dependent on the degree of histone coiling, which is in turn regulated by the degree of acetylation of histone core residues. As the DNA becomes more acetylated, it unwinds, thus allowing binding of transcription factors, initiating gene transcription. H₂O₂ and TNF- α have both been shown to increase histone acetylation, providing a potential mechanism for oxidant-mediated inflammation (56). This effect may be antagonized by NO[•], which has been shown to be capable of maintaining levels of I κ B, thus hindering NF- κ B activation (95). Whether this is achieved by decreasing I κ B degradation or increasing its synthesis has yet to be determined. Depletion of glutathione leads to ubiquitination of NF- κ B and subsequent activation (77, 78). As glutathione levels increase, I κ B degradation is inhibited so that NF- κ B does not become activated. NF- κ B also regulates iNOS and the inducible form of cyclooxygenase (COX-2). Thus, regulation of the inflammatory response may proceed through a negative-feedback loop via NF- κ B and nitric oxide. An endogenous protease inhibitor, secretory leukocyte protease inhibitor (SLPI), inhibits I κ B degradation, suppressing NF- κ B activation. PMN accumulation, ROS activity, and levels of IL-1 and IL-8 were shown to decrease in LPS-treated rabbits that in-

haled NO⁻ (48). These decreases correlated with a concomitant decrease in NF- κ B activation. Depletion of lung macrophages in rats by airway instillation of liposome-encapsulated dichloromethylene diphosphonate suppressed activation of NF- κ B and resultant BAL levels of TNF- α and MIP-2 (55). PMN accumulation and vascular permeability were also decreased, suggesting that activation of alveolar macrophages served as the source of an initial inflammatory stimulus. Activated alveolar macrophages and infiltrated PMNs generate ROS and cytokines, propagating the cycle of oxidant stress and inflammation. This scenario is likely to be the key event that drives pulmonary oxidant stress and inflammation during sepsis-induced ALI.

The promoter regions of various cytokines and chemokines contain binding sites for AP-1, suggesting that AP-1 plays a critical role in coordinating the gene expression of various inflammatory mediators. Like NF- κ B, AP-1 activation occurs in lung during sepsis and likely modulates inflammation (4). AP-1 is a complex multisubunit protein composed of members of the Jun and Fos families. Much is known regarding its role in events regulating cell proliferation, transformation, differentiation, and apoptosis (49). AP-1 activation was found to be detectable in alveolar macrophages as well as in whole-lung lysates. Macrophage depletion or anti-TNF- α treatment significantly decreased the level of AP-1 activation in lung after IgG immune complex deposition, but complement depletion had no effect (36). AP-1 also responds to oxidative and cellular stress, DNA damage resulting from UV irradiation, and exposure to proinflammatory cytokines (TNF- α , IFN- γ , and TGF- β). TNF- α has been shown to activate AP-1 upstream of MAPK kinase pathways. Activation of AP-1 appears to occur concurrent with activation of other transcription factors, including Elk-1, ATF-2, and CEBP (58, 78). The AP-1 family of transcription factors has been found to play a critical role in regulating the stress-inducible protein heme oxygenase-1 (HO-1) gene after LPS treatment in rat lung (12), suggesting that AP-1 may also participate in the negative regulatory loop of the inflammatory chain.

Nuclear factor-erythroid 2-p45-related factor 2 (Nrf2)

Nrf2 is a transcription factor that is expressed in many organs, including lung. Nrf2 is directly involved in transcriptional activation of ARE-driven redox-related genes including GST, NADPH/quinine reductase, UDP-glucosyltransferases, epoxide hydrolase, heme oxygenase-1, glutathione peroxidase-2, peroxiredoxins, and glutathione reductase (GSSG-R). Therefore, it appears to be an important modulator in regulation of redox status in cells. Nrf2 has been reported as a critical intracellular molecule for regulation of the innate immune response and survival in mouse models of sepsis. Disruption of Nrf2 dramatically worsened the survival of mice in response to endotoxin and CLP-induced septic shock. Inflammation in these Nrf2-deficient mice was greatly intensified after LPS challenge. In response to LPS, Nrf2-deficient cells showed greater activation of NF- κ B, which appeared to be regulated *via* the modulation of the oxidant-antioxidant system (93). In addition, these mice have been shown to be more susceptible to hyperoxic lung injury and lung inflammation induced by the oxidant butylated hydroxytoluene (BHT) (14, 15). Activation of Nrf2 by a chem-

ical agonist, CDDO-Im, attenuated LPS-induced inflammatory responses and oxidative stress in lung, and decreased mortality in Nrf2-sufficient mice (94). Nrf2 appears to be an important transcription factor that limits progression of oxidative stress during sepsis-induced ALI. Therefore, activation or overexpression of this molecule in lung appears to be an attractive strategy for antioxidative defense.

Heme oxygenase-1 (HO-1)

Cumulative evidence has demonstrated that the stress-inducible protein, HO-1, is an auxiliary antioxidant molecule, closely involved in the regulation of lung oxidative status and inflammatory responses. LPS induces high mRNA levels of HO-1 expression in the rat lung, which correlates with increased HO-1 protein levels and enzyme activity (12, 13). Redox-sensitive transcription factor AP-1 plays a critical role in regulating HO-1 gene activation after LPS exposure. In a murine model of sepsis, mice treated with a lethal dose of LPS and subsequently exposed to the HO-1 enzymatic product, CO, had significantly improved survival and lower serum IL-6 and IL-1 β levels than controls. The same effect was obtained when endogenous CO was induced through overexpression of HO-1 (68). Interestingly, AP-1 binding was decreased by CO exposure. CO, ferrous iron, and biliverdin are main enzymatic products of HO activation. With the rat model of CLP-induced sepsis, biliverdin treatment offered a potent defense against lethal endotoxemia, as well as in the lungs, and effectively abrogated the lung inflammatory response. Biliverdin administration before a lethal dose of LPS led to a significant improvement in long-term survival, reduced lung permeability and lung alveolitis, and decreased proinflammatory cytokine IL-6. In the same case, augmentation of IL-10, a potent antiinflammatory cytokine in lung injury, occurred (84). Iron (Fe) released as a result of HO-1 activation returns to a transient chelatable pool, where it may potentially promote oxidative stress and inflammation. However, this pathway can be effectively inhibited by ferritin generated through HO-1. Apparently, HO-1 works as a strong negative regulator in the development of oxidative stress and lung inflammatory responses during sepsis-induced ALI. Endogenous CO indeed increased in patients with severe sepsis (103), suggesting that the HO-1 pathway has been activated, and provides a protective role in patients with sepsis.

Other important molecular events in sepsis-induced ALI

Cellular oxidative stress regulates cell function from many perspectives, including receptor function, enzymatic activity, transcription factor activation, and gene expression. As described earlier, it has been documented that protein modifications frequently occur during sepsis. Oxidation-involved molecular events such as tyrosine phosphorylation, activation of MAP kinases, protein kinase C, phospholipase A₂, are found in the lung during sepsis and are likely contribute to the pathogenesis of sepsis (45, 53, 69, 90). Other oxidation-involved events such as protein carbonylation, tyrosine chlorination, and tyrosine nitration are also reported in sepsis (20, 66). How these events regulate the development of sepsis-induced ALI has yet to be defined.

As depicted in Fig. 3, oxidative stress in the lung activates NF- κ B and AP-1 pathways during sepsis-induced ALI, which in turn leads to amplified inflammatory responses. AP-1 and Nrf2 activation result in HO-1 expression, leading to CO production in the lung during sepsis. CO together with enzymatic antioxidants generated from Nrf2 activation may play an anti-inflammatory role in sepsis-induced ALI.

ANTIOXIDANT TREATMENT IN SEPSIS-INDUCED ALI

In an earlier study in patients with sepsis-induced ALI, it was found that oral intake of an antioxidant mixture reduced lung microvascular permeability, improved oxygenation and cardiopulmonary function, and reduced proinflammatory eicosanoid synthesis and lung inflammation (29). These findings provide hope for antioxidant strategies in the treatment of sepsis.

Both enzymatic antioxidants and nonenzymatic antioxidants have been widely tested in humans and animals with sepsis. *N*-acetylcysteine (NAC), a nonenzymatic antioxidant, is one of the most extensively tested antioxidants. NAC possesses powerful antioxidative roles by directly scavenging oxygen radicals (H_2O_2 , OH, HOCl) and indirectly replenishing the cellular glutathione system. In the models of sepsis-induced ALI, NAC has been shown to be highly protective in lung inflammatory responses by reducing the levels of inflammatory mediators, inhibiting PMN activation and sequestration, suppressing the prothrombotic state, and preventing hypoxic pulmonary vasoconstriction (HPV) (6, 26). However, clinical trails have resulted in controversial findings. Although NAC improves the degree of organ-failure indexes in patients with septic shock, it reduces cardiac performance and tissue oxygenation (5). It was even harmful when initiation of NAC treatment occurred >24 h after hospital admission (67). A later clinical trial suggested

that NAC treatment aggravated sepsis-induced organ failure, in particular cardiovascular failure (87). In a recent preclinical trial study using a porcine model of endotoxemia, NAC failed to improve any of the variables of the systemic, pulmonary, or hepatosplanchnic hemodynamics, gas exchange, and metabolism, although it significantly elevated glutathione levels (96). More experimental and clinical studies with new management approaches are required to take advantage of the potential therapeutic utility of NAC.

Tocopherol (vitamin E) is another nonenzymatic antioxidant that has potential for treatment of sepsis-induced ALI (83, 92). Tocopherol can directly scavenge ROS and upregulate the activities of antioxidant enzymes. It can terminate the chain reaction of lipid peroxidation by scavenging lipid peroxy radicals. In the mouse model of endotoxin-induced ALI, liposomal tocopherol administration significantly decreased the number of PMNs in airspaces and reduced lung injury, as evidenced by decreased lactate dehydrogenase activity in airways and reduced lung edema. Tocopherol failed to inhibit NF- κ B and AP-1 activation, as well as the endotoxin-induced expression of proinflammatory cytokines in lung tissue. In patients with ARDS, the antioxidative system is severely compromised, as evidenced by decreased plasma levels of α -tocopherol, ascorbate, β -carotene, and selenium (64). The early administration of α -tocopherol and ascorbic acid (vitamin C) in humans reduced the incidence of organ failure and shortened the ICU length of stay (70). Vitamin C is known to scavenge $O_2^{\cdot -}$ by forming the semi-dehydroascorbate free radical that is subsequently reduced by GSH. Thus, oral intake of combined antioxidants appears to be beneficial in the setting of sepsis-induced ALI.

The antioxidant enzyme SOD, with a biologic function of dismutating $O_2^{\cdot -}$ to H_2O_2 , holds promise for the treatment of sepsis-induced ALI. Extracellular (EC)-SOD-deficient mice showed increased evidence of ALI that occurs after hemorrhagic shock, accompanied by increased lung PMN accumulation and MPO activity (8). Overexpression of pulmonary EC-SOD in the mouse lung significantly attenuated lung injury that occurs after hemorrhagic shock (9). Overexpression of EC-SOD in lung also attenuated influenza-induced lung injury by both ameliorating inflammation and attenuating oxidative stress (91). Unlike nonenzymatic antioxidants, antioxidant enzymes such SOD and CAT have high affinities and rates of reaction, which can effectively detoxify ROS in numerous cycles, representing a highly efficient mechanism in detoxification. Similar to SOD, CAT provided impressive protection against acute lung injury induced in experimental animals after administration of LPS. EUK-8, a low-molecular-weight salen-manganese complex that exhibits both SOD-like and CAT-like activities *in vitro*, significantly attenuated several features of lung dysfunction caused by endotoxin, including arterial hypoxemia, pulmonary hypertension, decreased dynamic pulmonary compliance, and pulmonary edema (34). Because of the obvious gap between human diseases and animals models, further clinical data are needed to assess the role of the SOD/CAT approach in sepsis-induced ALI.

Other antioxidants that have shown therapeutic merits in the animal models of sepsis-induced ALI include methylene blue (21), resveratrol (52), tempol (59), β -glucan (85), M4041 (19), melatonin (86), and AT1-receptor inhibitor (44). However,

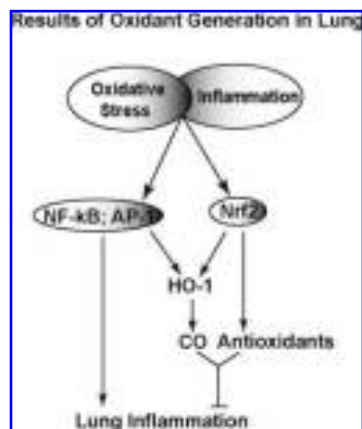


FIG. 3. Molecular events in sepsis-induced ALI. Oxidative stress and inflammation in lung activate the transcription factors, NF- κ B and AP-1, leading to amplified inflammatory responses. AP-1 and Nrf2 activation result in HO-1 expression, resulting in CO production. CO, together with enzymatic antioxidants generated from Nrf2 activation, results in an anti-inflammatory outcome in sepsis-induced ALI.

these compounds have been tested only in animals. More experimental and clinical data are expected in the coming years to validate these compounds by using various animal models and eventually in humans with sepsis.

SUMMARY

Sepsis and sepsis-induced ALI represent unsolved clinical problems due to the extremely complicated pathogenesis, which involves an imbalance of the pro- and antiinflammatory networks, complement activation, endothelial cell activation, PMN and macrophage activation, oxidative stress, and transcription factor activation. Blockade of only one of the inflammatory mediators has not resulted in a satisfactory outcome in human clinical trials, perhaps because of the complexity of the inflammatory network and the redundancy of inflammatory mediators. As oxidative stress works through the initiation and progression phases in the development of sepsis, the importance of oxidant stress in sepsis-induced ALI in humans has been appreciated. The disappointing results of NAC clinical trials may reflect the inability to reestablish a redox balance in the setting of sepsis in patients. It has been realized that severity of sepsis alters the effects of O₂^{•-} inhibition in sepsis (19). Further improvement of antioxidant interventions requires better understanding of the mechanisms and characteristics of oxidant stress in the specific setting of a disease condition and the development of more-effective delivery strategies. In addition, the redox-sensitive transcription factor, NF- κ B, seems to be a logical target for therapy in ARDS patients. However, blockade of NF- κ B inevitably turns off some gene expression, which may lead to immunosuppression. To this end, a local inhibition of lung NF- κ B activation may be a less detrimental therapeutic strategy. Therapeutic strategies should be directed at the improvement of net proinflammatory, prooxidant, and cytotoxic imbalances that develop in ARDS.

ACKNOWLEDGMENTS

This work is supported by the National Institutes of Health (grants GM-61656, HL-31963, and GM-02507).

ABBREVIATIONS

ALI, acute lung injury; AP-1, activator protein-1; BAL, bronchoalveolar fluid; BHT, butylated hydroxytoluene; CAT, catalase; CE/MS, capillary electrophoresis-mass spectrometry; CLP, cecal ligation and puncture; COX, cyclooxygenase; DMPO, 5,5-dimethyl-1-pyrroline-*n*-oxide; DNP, dinitrophenylhydrazine; EPR, electron paramagnetic resonance spectroscopy; Fe²⁺, ferrous ion; GSH-PX, glutathione peroxidase; GSSG-R, glutathione reductase; HO-1, heme oxygenase-1; HPLC, high-performance liquid chromatography; HPV, hypoxic pulmonary vasoconstriction; HRP, horseradish peroxidase; H₂O₂, hydrogen peroxide; HOCl, hypochlorous acid; L-NMMA, NO₃⁻ nitrate; LPS, lipopolysaccharide; MIP-2, mac-

rophage-inflammatory protein-2; MAP, mitogen-activated protein; MPO, myeloperoxidase; MDA, malondialdehyde; NAC, N-acetylcysteine; NO₂⁻, nitrite; N^G-monomethyl-L-arginine; NOS, nitric oxide synthase; Nrf2, nuclear factor-erythroid 2-p45-related factor 2; O₂^{•-}, superoxide; OH⁻, hydroxyl radical; 8-OHdG, hydroxydeoxyguanosine; ONOO⁻, peroxynitrite; ONOOH, peroxyntrous acid; ONOOCO₂⁻, peroxycarboxylate; RNS, reactive nitrogen species; ROS, reactive oxygen species; SOD, superoxide dismutase; SLPI, secretory leukocyte protease inhibitor; TBARS, thiobarbituric acid-reactive substances; vitamin C, ascorbic acid; vitamin E, tocopherol.

REFERENCES

1. Aggarwal A, Baker CS, Evans TW, and Haslam PL. G-CSF and IL-8 but not GM-CSF correlate with severity of pulmonary neutrophilia in acute respiratory distress syndrome. *Eur Respir J* 15: 895-901, 2000.
2. Andrades M, Ritter C, Moreira JC, and Dal-Pizzol F. Oxidative parameters differences during non-lethal and lethal sepsis development. *J Surg Res* 125: 68-72, 2005.
3. Angus DC, Linde-Zwirble WT, Lidicker J, Clermont G, Carcillo J, and Pinsky MR. Epidemiology of severe sepsis in the United States: analysis of incidence, outcome, and associated costs of care. *Crit Care Med* 29: 1303-1310, 2001.
4. Armstead VE, Opentanova IL, Minchenko AG, and Lefer AM. Tissue factor expression in vital organs during murine traumatic shock: role of transcription factors AP-1 and NF-kappaB. *Anesthesiology* 91: 1844-1852, 1999.
5. Atkinson MC. The use of N-acetylcysteine in intensive care. *Crit Care Resusc* 4: 21-27, 2002.
6. Baboolal HA, Ichinose F, Ullrich R, Kawai N, Bloch KD, and Zapol WM. Reactive oxygen species scavengers attenuate endotoxin-induced impairment of hypoxic pulmonary vasoconstriction in mice. *Anesthesiology* 97: 1227-1233, 2002.
7. Borrelli E, Roux-Lombard P, Grau GE, Girardin E, Ricou B, Dayer J, and Suter PM. Plasma concentrations of cytokines, their soluble receptors, and antioxidant vitamins can predict the development of multiple organ failure in patients at risk. *Crit Care Med* 24: 392-397, 1996.
8. Bowler RP, Arcaroli J, Abraham E, Patel M, Chang LY, and Crapo JD. Evidence for extracellular superoxide dismutase as a mediator of hemorrhage-induced lung injury. *Am J Physiol Lung Cell Mol Physiol* 284: L680-L687, 2003.
9. Bowler RP, Arcaroli J, Crapo JD, Ross A, Slot JW, and Abraham E. Extracellular superoxide dismutase attenuates lung injury after hemorrhage. *Am J Respir Crit Care Med* 164: 290-294, 2001.
10. Bowler RP and Crapo JD. Oxidative stress in allergic respiratory diseases. *J Allergy Clin Immunol* 110: 349-356, 2002.
11. Call DR, Nemzek JA, Ebong SJ, Bolgos GL, Newcomb DE, and Remick DG. Ratio of local to systemic chemokine concentrations regulates neutrophil recruitment. *Am J Pathol* 158: 715-721, 2001.
12. Camhi SL, Alam J, Otterbein L, Sylvester SL, and Choi AM. Induction of heme oxygenase-1 gene expression by lipopolysaccharide is mediated by AP-1 activation. *Am J Respir Cell Mol Biol* 13: 387-398, 1995.
13. Camhi SL, Alam J, Wiegand GW, Chin BY, and Choi AM. Transcriptional activation of the HO-1 gene by lipopolysaccharide is mediated by 5' distal enhancers: role of reactive oxygen intermediates and AP-1. *Am J Respir Cell Mol Biol* 18: 226-234, 1998.
14. Chan K and Kan YW. Nrf2 is essential for protection against acute pulmonary injury in mice. *Proc Natl Acad Sci U S A* 96: 12731-12736, 1999.
15. Cho HY, Jedlicka AE, Reddy SP, Zhang LY, Kensler TW, and Kleeberger SR. Linkage analysis of susceptibility to hyperoxia. Nrf2 is a candidate gene. *Am J Respir Cell Mol Biol* 26: 42-51, 2002.

16. Christofidou-Solomidou M and Muzykantov VR. Antioxidant strategies in respiratory medicine. *Treat Respir Med* 5: 47–78, 2006.
17. Crapo JD. Oxidative stress as an initiator of cytokine release and cell damage. *Eur Respir J Suppl* 44: 4s–6s, 2003.
18. Crapo JD. Redox active agents in inflammatory lung injury. *Am J Respir Crit Care Med* 168: 1027–1028, 2003.
19. Cui X, Parent C, Macarthur H, Ochs SD, Gerstenberg E, Solomon S, Fitz Y, Danner RL, Banks SM, Natanson C, Salvemini D, and Eichacker PQ. Severity of sepsis alters the effects of superoxide anion inhibition in a rat sepsis model. *J Appl Physiol* 97: 1349–1357, 2004.
20. Dalle-Donne I, Giustarini D, Colombo R, Rossi R, and Milzani A. Protein carbonylation in human diseases. *Trends Mol Med* 9: 169–176, 2003.
21. Demirbilek S, Sizanli E, Karadag N, Karaman A, Bayraktar N, Turkmen E, and Ersoy MO. The effects of methylene blue on lung injury in septic rats. *Eur Surg Res* 38: 35–41, 2006.
22. Demling RH. The modern version of adult respiratory distress syndrome. *Annu Rev Med* 46: 193–202, 1995.
23. Dunican AL, Leuenroth SJ, Ayala A, and Simms HH. CXC chemokine suppression of polymorphonuclear leukocytes apoptosis and preservation of function is oxidative stress independent. *Shock* 13: 244–250, 2000.
24. Dweik RA, Laskowski D, Abu-Soud HM, Kaneko F, Hutte R, Stuehr DJ, and Erzurum SC. Nitric oxide synthesis in the lung: regulation by oxygen through a kinetic mechanism. *J Clin Invest* 101: 660–666, 1998.
25. Erdinçler DS, Seven A, İnci F, Beger T, and Candan G. Lipid peroxidation and antioxidant status in experimental animals: effects of aging and hypercholesterolemic diet. *Clin Chim Acta* 265: 77–84, 1997.
26. Fan J, Shek PN, Suntres ZE, Li YH, Oreopoulos GD, and Rotstein OD. Liposomal antioxidants provide prolonged protection against acute respiratory distress syndrome. *Surgery* 128: 332–338, 2000.
27. Farley KS, Wang LF, Razavi HM, Law C, Rohan M, McCormack DG, and Mehta S. Effects of macrophage inducible nitric oxide synthase in murine septic lung injury. *Am J Physiol Lung Cell Mol Physiol* 290: L1164–L1172, 2006.
28. Feng X, Yan W, Liu X, Duan M, Zhang X, and Xu J. Effects of hydroxyethyl starch 130/0.4 on pulmonary capillary leakage and cytokines production and NF-kappaB activation in CLP-induced sepsis in rats. *J Surg Res* 135: 129–136, 2006.
29. Gadek JE, DeMichele SJ, Karlstad MD, Pacht ER, Donahoe M, Albertson TE, Van Hoozen C, Wennberg AK, Nelson JL, and Noursalehi M. Effect of enteral feeding with eicosapentaenoic acid, gamma-linolenic acid, and antioxidants in patients with acute respiratory distress syndrome. Enteral Nutrition in ARDS Study Group. *Crit Care Med* 27: 1409–1420, 1999.
30. Galley HF, Howdle PD, Walker BE, and Webster NR. The effects of intravenous antioxidants in patients with septic shock. *Free Radic Biol Med* 23: 768–774, 1997.
31. Gao XP, Standiford TJ, Rahman A, Newstead M, Holland SM, Dinauer MC, Liu QH, and Malik AB. Role of NADPH oxidase in the mechanism of lung neutrophil sequestration and microvessel injury induced by Gram-negative sepsis: studies in p47phox^{-/-} and gp91phox^{-/-} mice. *J Immunol* 168: 3974–3982, 2002.
32. Gaston B, Drazen JM, Loscalzo J, and Stamler JS. The biology of nitrogen oxides in the airways. *Am J Respir Crit Care Med* 149: 538–551, 1994.
33. Gole MD, Souza JM, Choi I, Hertkorn C, Malcolm S, Foust RF 3rd, Finkel B, Lanken PN, and Ischiropoulos H. Plasma proteins modified by tyrosine nitration in acute respiratory distress syndrome. *Am J Physiol Lung Cell Mol Physiol* 278: L961–L967, 2000.
34. Gonzalez PK, Zhuang J, Doctrow SR, Malfroy B, Benson PF, Menconi MJ, and Fink MP. Role of oxidant stress in the adult respiratory distress syndrome: evaluation of a novel antioxidant strategy in a porcine model of endotoxin-induced acute lung injury. *Shock* 6(suppl 1): S23–S26, 1996.
35. Goode HF, Cowley HC, Walker BE, Howdle PD, and Webster NR. Decreased antioxidant status and increased lipid peroxidation in patients with septic shock and secondary organ dysfunction. *Crit Care Med* 23: 646–651, 1995.
36. Guo RF, Lentsch AB, Sarma JV, Sun L, Riedemann NC, McClintock SD, McGuire SR, Van Rooijen N, and Ward PA. Activator protein-1 activation in acute lung injury. *Am J Pathol* 161: 275–282, 2002.
37. Guo RF, Riedemann NC, Laudes IJ, Sarma VJ, Kunkel RG, Dilleley KA, Paulauskis JD, and Ward PA. Altered neutrophil trafficking during sepsis. *J Immunol* 169: 307–314, 2002.
38. Guo RF, Riedemann NC, Sun L, Gao H, Shi KX, Reuben JS, Sarma VJ, Zetoune FS, and Ward PA. Divergent signaling pathways in phagocytic cells during sepsis. *J Immunol* 177: 1306–1313, 2006.
39. Guo RF, Sun L, Gao H, Shi KX, Rittirsch D, Sarma VJ, Zetoune FS, and Ward PA. In vivo regulation of neutrophil apoptosis by C5a during sepsis. *J Leukoc Biol* 80: 1575–1583, 2006.
40. Guo RF and Ward PA. Mediators and regulation of neutrophil accumulation in inflammatory responses in lung: insights from the IgG immune complex model. *Free Radic Biol Med* 33: 303–310, 2002.
41. Hawkins HK, Heffelfinger SC, and Anderson DC. Leukocyte adhesion deficiency: clinical and postmortem observations. *Pediatr Pathol* 12: 119–130, 1992.
42. Hildebrand F, Pape HC, Harwood P, Muller K, Hoevel P, Putz C, Siemann A, Krettek C, and van Griensven M. Role of adhesion molecule ICAM in the pathogenesis of polymicrobial sepsis. *Exp Toxicol Pathol* 56: 281–290, 2005.
43. Ibbotson GC, Doig C, Kaur J, Gill V, Ostrovsky L, Fairhead T, and Kubes P. Functional alpha4-integrin: a newly identified pathway of neutrophil recruitment in critically ill septic patients. *Nat Med* 7: 465–470, 2001.
44. Imai Y, Kuba K, Rao S, Huan Y, Guo F, Guan B, Yang P, Sarao R, Wada T, Leong-Poi H, Crackower MA, Fukamizu A, Hui CC, Hein L, Uhlhig S, Slutsky AS, Jiang C, and Penninger JM. Angiotensin-converting enzyme 2 protects from severe acute lung failure. *Nature* 436: 112–116, 2005.
45. Jarrar D, Kuebler JF, Rue LW, 3rd, Matalon S, Wang P, Bland KI, and Chaudry IH. Alveolar macrophage activation after trauma-hemorrhage and sepsis is dependent on NF-kappaB and MAPK/ERK mechanisms. *Am J Physiol Lung Cell Mol Physiol* 283: L799–L805, 2002.
46. Jiang ZY, Hunt JV, and Wolff SP. Ferrous ion oxidation in the presence of xylenol orange for detection of lipid hydroperoxide in low density lipoprotein. *Anal Biochem* 202: 384–389, 1992.
47. Jiang ZY, Woollard AC, and Wolff SP. Lipid hydroperoxide measurement by oxidation of Fe²⁺ in the presence of xylenol orange: comparison with the TBA assay and an iodometric method. *Lipids* 26: 853–856, 1991.
48. Kang JL, Park W, Pack IS, Lee HS, Kim MJ, Lim CM, and Koh Y. Inhaled nitric oxide attenuates acute lung injury via inhibition of nuclear factor-kappa B and inflammation. *J Appl Physiol* 92: 795–801, 2002.
49. Karamouzis MV, Konstantinopoulos PA, and Papavassiliou AG. The activator protein-1 transcription factor in respiratory epithelium carcinogenesis. *Mol Cancer Res* 5: 109–120, 2007.
50. Kobzik L, Bredt DS, Lowenstein CJ, Drazen J, Gaston B, Sugaaraker D, and Stamler JS. Nitric oxide synthase in human and rat lung: immunocytochemical and histochemical localization. *Am J Respir Cell Mol Biol* 9: 371–377, 1993.
51. Koksai GM, Sayilgan C, Aydin S, Oz H, and Uzun H. Correlation of plasma and tissue oxidative stresses in intra-abdominal sepsis. *J Surg Res* 122: 180–183, 2004.
52. Kolgazi M, Sener G, Cetinel S, Gedik N, and Alican I. Resveratrol reduces renal and lung injury caused by sepsis in rats. *J Surg Res* 134: 315–321, 2006.
53. Kuklin V, Kirov M, Sovershaev M, Andreassen T, Ingebretsen OC, Ytrehus K, and Bjertnaes L. Tezosentan-induced attenuation of lung injury in endotoxemic sheep is associated with reduced activation of protein kinase C. *Crit Care* 9: R211–R217, 2005.
54. Laudes IJ, Guo RF, Riedemann NC, Speyer C, Craig R, Sarma JV, and Ward PA. Disturbed homeostasis of lung intercellular adhesion molecule-1 and vascular cell adhesion molecule-1 during sepsis. *Am J Pathol* 164: 1435–1445, 2004.

55. Lentsch AB, Czermak BJ, Bless NM, Van Rooijen N, and Ward PA. Essential role of alveolar macrophages in intrapulmonary activation of NF-kappaB. *Am J Respir Cell Mol Biol* 20: 692–698, 1999.
56. Lentsch AB and Ward PA. Activation and regulation of NF-kappaB during acute inflammation. *Clin Chem Lab Med* 37: 205–208, 1999.
57. Levine RL, Garland D, Oliver CN, Amici A, Climent I, Lenz AG, Ahn BW, Shattiel S, and Stadtman ER. Determination of carbonyl content in oxidatively modified proteins. *Methods Enzymol* 186: 464–478, 1990.
58. Li QJ, Vaingankar S, Sladek FM, and Martins-Green M. Novel nuclear target for thrombin: activation of the Elk1 transcription factor leads to chemokine gene expression. *Blood* 96: 3696–3706, 2000.
59. Liaw WJ, Chen TH, Lai ZZ, Chen SJ, Chen A, Tzao C, Wu JY, and Wu CC. Effects of a membrane-permeable radical scavenger, Tempol, on intraperitoneal sepsis-induced organ injury in rats. *Shock* 23: 88–96, 2005.
60. Libon C, Forestier F, Cotte-Laffitte J, Labarre C, and Quero AM. Effect of acute oral administration of alcohol on superoxide anion production from mouse alveolar macrophages. *J Leukoc Biol* 53: 93–98, 1993.
61. Martin TR, Pistoresse BP, Hudson LD, and Maunder RJ. The function of lung and blood neutrophils in patients with the adult respiratory distress syndrome: implications for the pathogenesis of lung infections. *Am Rev Respir Dis* 144: 254–262, 1991.
62. Meduri GU, Muthiah MP, Carratu P, Eltorkey M, and Chrousos GP. Nuclear factor-kappaB- and glucocorticoid receptor alpha-mediated mechanisms in the regulation of systemic and pulmonary inflammation during sepsis and acute respiratory distress syndrome: evidence for inflammation-induced target tissue resistance to glucocorticoids. *Neuroimmunomodulation* 12: 321–338, 2005.
63. Mei N, Tamae K, Kunugita N, Hirano T, and Kasai H. Analysis of 8-hydroxydeoxyguanosine 5'-monophosphate (8-OH-dGMP) as a reliable marker of cellular oxidative DNA damage after gamma-irradiation. *Environ Mol Mutagen* 41: 332–338, 2003.
64. Metnitz PG, Bartens C, Fischer M, Fridrich P, Steltzer H, and Druml W. Antioxidant status in patients with acute respiratory distress syndrome. *Intensive Care Med* 25: 180–185, 1999.
65. Minnard EA, Shou J, Naama H, Cech A, Gallagher H, and Daly JM. Inhibition of nitric oxide synthesis is detrimental during endotoxemia. *Arch Surg* 129: 142–147; discussion 147–148, 1994.
66. Mohiuddin I, Chai H, Lin PH, Lumsden AB, Yao Q, and Chen C. Nitrotyrosine and chlorotyrosine: clinical significance and biological functions in the vascular system. *J Surg Res* 133: 143–149, 2006.
67. Molnar Z, Shearer E, and Lowe D. N-Acetylcysteine treatment to prevent the progression of multisystem organ failure: a prospective, randomized, placebo-controlled study. *Crit Care Med* 27: 1100–1104, 1999.
68. Morse D, Pischke SE, Zhou Z, Davis RJ, Flavell RA, Loop T, Otterbein SL, Otterbein LE, and Choi AM. Suppression of inflammatory cytokine production by carbon monoxide involves the JNK pathway and AP-1. *J Biol Chem* 278: 36993–36998, 2003.
69. Nagase T, Uozumi N, Aoki-Nagase T, Terawaki K, Ishii S, Tomita T, Yamamoto H, Hashizume K, Ouchi Y, and Shimizu T. A potent inhibitor of cytosolic phospholipase A2, arachidonyl trifluoromethyl ketone, attenuates LPS-induced lung injury in mice. *Am J Physiol Lung Cell Mol Physiol* 284: L720–L726, 2003.
70. Nathens AB, Neff MJ, Jurkovich GJ, Klotz P, Farver K, Ruzinski JT, Radella F, Garcia I, and Maier RV. Randomized, prospective trial of antioxidant supplementation in critically ill surgical patients. *Ann Surg* 236: 814–822, 2002.
71. Nava E, Palmer RM, and Moncada S. Inhibition of nitric oxide synthesis in septic shock: how much is beneficial? *Lancet* 338: 1555–1557, 1991.
72. Olea-Azar C, Rigol C, Mendizabal F, Morello A, Maya JD, Moncada C, Cabrera E, Di Maio R, Gonzalez M, and Cerecetto H. ESR spin trapping studies of free radicals generated from nitro-furan derivative analogues of nifurtimox by electrochemical and *Trypanosoma cruzi* reduction. *Free Radic Res* 37: 993–1001, 2003.
73. Paredi P, Kharitonov SA, and Barnes PJ. Analysis of expired air for oxidation products. *Am J Respir Crit Care Med* 166: S31–S37, 2002.
74. Parent C and Eichacker PQ. Neutrophil and endothelial cell interactions in sepsis: the role of adhesion molecules. *Infect Dis Clin North Am* 13: 427–447, 1999.
75. Quinlan GJ, Lamb NJ, Tilley R, Evans TW, and Gutteridge JM. Plasma hypoxanthine levels in ARDS: implications for oxidative stress, morbidity, and mortality. *Am J Respir Crit Care Med* 155: 479–484, 1997.
76. Rahman I, Biswas SK, Jimenez LA, Torres M, and Forman HJ. Glutathione, stress responses, and redox signaling in lung inflammation. *Antioxid Redox Signal* 7: 42–59, 2005.
77. Rahman I, Gilmour PS, Jimenez LA, Biswas SK, Antonicelli F, and Arouma OL. Ergothioneine inhibits oxidative stress- and TNF-alpha-induced NF-kappa B activation and interleukin-8 release in alveolar epithelial cells. *Biochem Biophys Res Commun* 302: 860–864, 2003.
78. Rahman I, Gilmour PS, Jimenez LA, and MacNee W. Oxidative stress and TNF-alpha induce histone acetylation and NF-kappaB/AP-1 activation in alveolar epithelial cells: potential mechanism in gene transcription in lung inflammation. *Mol Cell Biochem* 234–235: 239–248, 2002.
79. Rahman I and Kelly F. Biomarkers in breath condensate: a promising new non-invasive technique in free radical research. *Free Radic Res* 37: 1253–1266, 2003.
80. Razavi HM, Wang L, Weicker S, Quinlan GJ, Mumby S, McCormack DG, and Mehta S. Pulmonary oxidant stress in murine sepsis is due to inflammatory cell nitric oxide. *Crit Care Med* 33: 1333–1339, 2005.
81. Razavi HM, Wang L, Weicker S, Rohan M, Law C, McCormack DG, and Mehta S. Pulmonary neutrophil infiltration in murine sepsis: role of inducible nitric oxide synthase. *Am J Respir Crit Care Med* 170: 227–233, 2004.
82. Reddy RC, Chen GH, Newstead MW, Moore T, Zeng X, Tateda K, and Standiford TJ. Alveolar macrophage deactivation in murine septic peritonitis: role of interleukin 10. *Infect Immun* 69: 1394–1401, 2001.
83. Rocksen D, Ekstrand-Hammarstrom B, Johansson L, and Bucht A. Vitamin E reduces transendothelial migration of neutrophils and prevents lung injury in endotoxin-induced airway inflammation. *Am J Respir Cell Mol Biol* 28: 199–207, 2003.
84. Sarady-Andrews JK, Liu F, Gallo D, Nakao A, Overhaus M, Ollinger R, Choi AM, and Otterbein LE. Biliverdin administration protects against endotoxin-induced acute lung injury in rats. *Am J Physiol Lung Cell Mol Physiol* 289: L1131–L1137, 2005.
85. Sener G, Toklu H, Ercan F, and Erkanli G. Protective effect of beta-glucan against oxidative organ injury in a rat model of sepsis. *Int Immunopharmacol* 5: 1387–1396, 2005.
86. Sener G, Toklu H, Kapucu C, Ercan F, Erkanli G, Kacmaz A, Tilki M, and Yegen BC. Melatonin protects against oxidative organ injury in a rat model of sepsis. *Surg Today* 35: 52–59, 2005.
87. Spapen HD, Diltor MW, Nguyen DN, Hendrickx I, and Huyghens LP. Effects of N-acetylcysteine on microalbuminuria and organ failure in acute severe sepsis: results of a pilot study. *Chest* 127: 1413–1419, 2005.
88. Speyer CL, Gao H, Rancilio NJ, Neff TA, Huffnagle GB, Sarma JV, and Ward PA. Novel chemokine responsiveness and mobilization of neutrophils during sepsis. *Am J Pathol* 165: 2187–2196, 2004.
89. Speyer CL, Neff TA, Warner RL, Guo RF, Sarma JV, Riedemann NC, Murphy ME, Murphy HS, and Ward PA. Regulatory effects of iNOS on acute lung inflammatory responses in mice. *Am J Pathol* 163: 2319–2328, 2003.
90. Spitzer JA and Zhang P. Protein tyrosine kinase activity and the influence of gender in phagocytosis and tumor necrosis factor secretion in alveolar macrophages and lung-recruited neutrophils. *Shock* 6: 426–433, 1996.
91. Suliman HB, Ryan LK, Bishop L, and Folz RJ. Prevention of influenza-induced lung injury in mice overexpressing extracellular superoxide dismutase. *Am J Physiol Lung Cell Mol Physiol* 280: L69–L78, 2001.

92. Suntres ZE and Shek PN. The pulmonary uptake of intravenously administered liposomal alpha-tocopherol is augmented in acute lung injury. *J Drug Target* 4: 151–159, 1996.
93. Thimmulappa RK, Lee H, Rangasamy T, Reddy SP, Yamamoto M, Kensler TW, and Biswal S. Nrf2 is a critical regulator of the innate immune response and survival during experimental sepsis. *J Clin Invest* 116: 984–995, 2006.
94. Thimmulappa RK, Scollick C, Traore K, Yates M, Trush MA, Liby KT, Sporn MB, Yamamoto M, Kensler TW, and Biswal S. Nrf2-dependent protection from LPS induced inflammatory response and mortality by CDDO-Imidazolide. *Biochem Biophys Res Commun* 351: 883–889, 2006.
95. Thomassen MJ and Kavuru MS. Human alveolar macrophages and monocytes as a source and target for nitric oxide. *Int Immunopharmacol* 1: 1479–1490, 2001.
96. Vassilev D, Hauser B, Bracht H, Ivanyi Z, Schoaff M, Asfar P, Vogt J, Wachter U, Schelzig H, Georgieff M, Bruckner UB, Radermacher P, and Froba G. Systemic, pulmonary, and hepatopulmonary effects of N-acetylcysteine during long-term porcine endotoxemia. *Crit Care Med* 32: 525–532, 2004.
97. Wan XS, Zhou Z, Ware JH, and Kennedy AR. Standardization of a fluorometric assay for measuring oxidative stress in irradiated cells. *Radiat Res* 163: 232–240, 2005.
98. Ware LB and Matthay MA. The acute respiratory distress syndrome. *N Engl J Med* 342: 1334–1349, 2000.
99. Warner RL, Paine R 3rd, Christensen PJ, Marletta MA, Richards MK, Wilcoxon SE, and Ward PA. Lung sources and cytokine requirements for in vivo expression of inducible nitric oxide synthase. *Am J Respir Cell Mol Biol* 12: 649–661, 1995.
100. Weiland JE, Davis WB, Holter JF, Mohammed JR, Dorinsky PM, and Gadek JE. Lung neutrophils in the adult respiratory distress syndrome: clinical and pathophysiologic significance. *Am Rev Respir Dis* 133: 218–225, 1986.
101. Weiss DJ and Lunte CE. Detection of a urinary biomarker for oxidative DNA damage 8-hydroxydeoxyguanosine by capillary electrophoresis with electrochemical detection. *Electrophoresis* 21: 2080–2085, 2000.
102. Winterbourn CC, Buss IH, Chan TP, Plank LD, Clark MA, and Windsor JA. Protein carbonyl measurements show evidence of early oxidative stress in critically ill patients. *Crit Care Med* 28: 143–149, 2000.
103. Zegdi R, Perrin D, Burdin M, Boiteau R, and Tenailon A. Increased endogenous carbon monoxide production in severe sepsis. *Intens Care Med* 28: 793–796, 2002.
104. Zhang XW, Liu Q, Wang Y, and Thorlacius H. CXC chemokines, MIP-2 and KC, induce P-selectin-dependent neutrophil rolling and extravascular migration in vivo. *Br J Pharmacol* 133: 413–421, 2001.

Address reprint requests to:
Ren-Feng Guo, M.D.
Department of Pathology
The University of Michigan Medical School
1301 Catherine Road
Ann Arbor, MI 48109-0602
E-mail: grf@med.umich.edu

Date of first submission to ARS Central, June 15, 2007; date of acceptance, June 23, 2007.

The Harmful Role of C5a on Innate Immunity in Sepsis

Peter A. Ward

Department of Pathology, University of Michigan Medical School, Ann Arbor, Mich., USA

Key Words

Sepsis · C5a · C5a receptors · Defective signaling

Abstract

There is accumulating evidence in humans and in experimental sepsis that robust activation of the complement system occurs along with development of defects in the innate immune system. In this report we review evidence that the complement activation product, C5a, appears in the plasma of rodents following cecal ligation and puncture (CLP). C5a interacts with its receptors (C5aR, C5L2) on phagocytes (polymorphonuclear neutrophils, PMNs, macrophages), ultimately paralyzing the ERK1/2 pathway of the mitogen-activated protein kinase signaling pathway. C5a is also interactive with its receptors on a variety of other cell types in various organs. Interaction of C5a with receptors on PMNs results in compromised innate immunity, with intense suppression of phagocytosis, chemotaxis and the respiratory burst. Endothelial cells acquire a pro-inflammatory phenotype (increased ICAM-1 and tissue factor expression), while macrophages are primed and produce large amounts of cytokines/chemokines. All of these outcomes are C5a and C5a receptor dependent. CLP also unleashes activation of clotting (and fibrinolytic) factors in a C5a-dependent manner. Finally, thymocytes upregulate C5aR and react with C5a, re-

sulting in apoptosis via the intrinsic (mitochondrial) pathway. Collectively, these findings suggest that interception of C5a in sepsis preserves innate immune functions and may be a strategy for treatment of septic humans.

Copyright © 2010 S. Karger AG, Basel

Introduction

The defensive responses in sepsis involve engagement of the innate immune system in an attempt to contain and remove offending microorganisms by locally triggering a robust acute inflammatory response at the site of infection. In sepsis, this response often becomes systemically expressed. There is strong evidence that both the Toll-like receptor and complement systems are brought into play as the body tries to contain the offending microorganisms. It is well known that these responses may result in a successful assault on the microorganisms, resulting in their containment and cessation of the inflammatory response, with return to homeostasis. Unfortunately, for 30–50% of septic patients in North America, the inflammatory response continues and becomes greatly exaggerated, resulting in septic shock and lethality [1]. In the course of progression of the septic state, there is evidence for a ‘cytokine storm’ which is defined by the pres-

Table 1. Evidence for harmful effects of C5a in sepsis

-
- 1 Protective effects of neutralizing polyclonal antibodies to C5a in CLP rats:
 - a Enhanced survival
 - b Reduced defects in innate immune system
 - c Reduced multiorgan failure
 - d Reduced intensity of coagulopathy

 - 2 Protective effects of absence or blockade of C5a receptors in CLP mice:
 - a Requirement for blockade or absence of both C5aR and C5L2
 - b Improved survival
 - c Reduced cytokine storm
 - d Role of C5L2 in production of HMGB1

 - 3 Unexpected effects of CLP in C5^{-/-} mice
-

ence in serum/plasma of numerous pro-inflammatory cytokines and chemokines. Precisely why this occurs and to what extent these mediators are responsible for development of multiorgan failure (involving heart, lungs, kidneys and liver) is entirely unknown. We will provide a brief review for the role of the complement system in the setting of sepsis both in humans and in animals with an emphasis on generation of C5a and its engagement with C5a receptors (C5aR, C5L2), the result of which leads to a large number of life-threatening outcomes in a variety of organs.

Evidence for Complement Activation in Humans with Sepsis

It has been known for some time that in septic humans there is robust activation of the complement system, as signified by the loss of the hemolytic activity of complement (CH50) and by the appearance in plasma of complement activation products, namely, the complement anaphylatoxins, C3a and C5a, which can be measured by ELISA technology [2, 3]. In humans, the levels of C5a can rise to levels as high as 100 nM [2]. Coincident with complement activation is impairment of innate immune functions of blood neutrophils (polymorphonuclear neutrophils, PMNs), involving chemotaxis, phagocytosis and the respiratory burst (associated with activation of NADPH oxidase, NOX2) [4]. Of considerable interest is the finding that the impaired chemotactic responses are globally affected, since neutrophils (PMNs) develop defective responses not only to C5a but also to the structurally unrelated and bacterially derived che-

motactic molecule, N-formyl-Met-Leu-Phe [2, 4]. Such data suggest that signaling pathways involving G protein-coupled receptors, which seem to converge downstream, have become defective, resulting in global dysfunction of innate immune responses in PMNs. It is important to emphasize that reports describing defects in innate immune responses of blood leukocytes from septic humans have often involved relatively small groups of patients and frequently have lacked sequential measurements over time in order to define the kinetics of such events. The absence of such information makes it very difficult to compare various reports and to know to what extent findings in sepsis can be put into a reliable framework of knowledge.

Complement Activation and Role of C5a in Experimental Sepsis

We will deal with evidence for the adverse roles of C5a as well as C5a receptors (C5aR, C5L2) in experimental sepsis. Several decades ago, monkeys infused intravenously with live *Escherichia coli* showed evidence of complement activation [5]. The copresence of a rabbit polyclonal antibody to C5a in this model resulted in neutralization of C5a, attenuating some of the features of sepsis such as shock, oxygen consumption and development of the acute respiratory distress syndrome [6]. There were suggestions that mortality rates in the anti-C5a-treated monkeys were reduced, but the number of monkeys was too small to obtain statistical significance that would link C5a neutralization to attenuated pathophysiological changes and improved survival.

Most of the work dealing with the role of C5a and C5a receptors in the setting of sepsis (cecal ligation and puncture, CLP) has been done in our own laboratories, using the rat and rodent models of CLP. Technical details of the CLP model in rodents have been recently described [7]. The data outlining evidence for the linkage between C5a and its receptors in the setting of sepsis are briefly summarized in table 1. The first strong hint for the adverse role of C5a in CLP rats came from the finding that intravenous infusion of neutralizing polyclonal antibody to rat C5a was highly protective, caused reduced evidence of multiorgan failure and resulted in dramatically improved survival (from 0% survival in the unprotected to 50% survival in rats treated with neutralizing antibody to C5a) [4, 8]. In successive studies, treatment of either CLP rats or mice with neutralizing antibodies (polyclonal or monoclonal antibodies, mAb) to C5a resulted

in improvements in survival and was found to be related to amount of antibody infused (intravenously) at the time of CLP as well as the time of administration of the antibody [9]. Such treatment greatly reduced evidence of multiorgan dysfunction [10]. Several important observations arose from these studies. When the rabbit polyclonal IgG was employed and given intravenously at the time of CLP, the protective effects in rats (survival over a 10-day period) were directly related to the dose of antibody employed (200, 400, 600 μ g). The antibodies that were affinity purified were directed towards three different peptide regions of rat C5a: the N-terminal area (residues 1–16), the mid-region of C5a (residues 17–36) and the C-terminal region (residues 58–77). The most protective antibodies were those directed at the mid- and C-terminal regions of C5a. By the use of these synthetic peptides for each of the three regions of C5a, it was possible to demonstrate that they could reduce chemotactic responses of rat PMNs to intact C5a, thereby establishing that C5a binds to C5aR at at least three different sites, which seems unusual for a G protein-coupled receptor-ligand interaction. Such data infer that at least three different regions on C5a could be targeted to reduce the ability of C5a to interact with its receptor(s). The use of 600 μ g of antibody targeted at the mid- or C-terminal regions of C5a improved survival over 10 days from 23% in rats receiving pre-immune IgG to 83–90% survival in rats given antibodies to the mid- or C-terminal or mid-regions of C5a.

Another fascinating outcome of these studies was the fact that the polyclonal antibodies to C5a, when added to normal rat serum, did not inhibit C5b-9-dependent lysis of sensitized rabbit red cells [11]. In other words, the antibodies behaved like mAbs that could recognize C5a only after it had been cleaved from C5 but not when it was still present in intact C5. This implies that C5a, when released from its parent molecule, undergoes a conformational change that results in expression of a unique epitope. Such observations are important, since, if such an anti-C5a were to be used in humans, it would neutralize C5a but would not cause C5 depletion, resulting in loss of C5b-9 generation and compromising the lytic ability of C5b-9 for Gram-negative bacteria.

Finally, these studies showed that the protective effects of anti-C5a antibodies to the mid- or C-terminal regions of rat C5a were, as expected, time dependent based on induction of CLP. When given at time 0 of CLP, 90% survival was found; when delayed until 6 h after CLP, survival was still approximately 60%; when infusion of anti-C5a was delayed until 12 h after CLP, survival was still

40–50%. Such data infer that there is a substantial ‘window’ after onset of sepsis when antibody-induced neutralization of C5a is still efficacious. Similar data have been found using mouse neutralizing mAbs to rat C5a (data not shown). In addition to being highly protective (defined as greatly improved survival), these interventions substantially reduced the intensity of multiorgan failure as defined by diminished levels of plasma lactate, transaminases, creatinine and blood urea nitrogen [4, 10].

The time frame for sepsis development after CLP occurs in a short period of approximately 3 days in rodents. The early phase (in the first 36 h) is the ‘hyperdynamic’ phase featuring, among other things, fever, tachycardia, increased cardiac output and leukocytosis. The late phase (between 36 and 72 h) is the ‘hypodynamic’ phase characterized by hypothermia, shock, bradycardia, tachypnea and falling core body temperature, among other things. In humans, the sequence of pathophysiological events in sepsis is more spread out, often occurring over 4–6 days. Based on the protective effects of delayed infusion of anti-C5a into CLP rats (described above), it is possible that such a therapeutic approach in septic humans might still be effective when patients enter the phase of septic shock.

Another strategy used in CLP mice was employment of a cyclical inhibitor of C5aR (and also C5L2), which blocks the ability of C5a to react with its receptors [12]. This compound was highly effective in enhancing survival of CLP mice [13]. The intensity of the coagulopathy of sepsis was greatly attenuated in CLP rats (for example, clotting times were minimally prolonged, thrombocytopenia was reduced and plasma levels of fibrin split products as well as thrombin-antithrombin complexes were greatly reduced) as a result of neutralization of C5a after CLP [14].

Roles of C5a Receptors in Experimental Sepsis

Based on the key role of C5a in sepsis (as described above), the crucial issue deals with the possible coordinate roles of C5aR and C5L2 in the setting of experimental sepsis. Aside from interception of C5a in sepsis (as described above), blockade of C5a receptors is an alternative approach. However, it is essential to know which receptor is dominant in sepsis or whether both participate, in order to assess a receptor blocking strategy. Figure 1 shows a scheme in which CLP-induced sepsis in rodents induces complement activation, resulting in C5a produc-

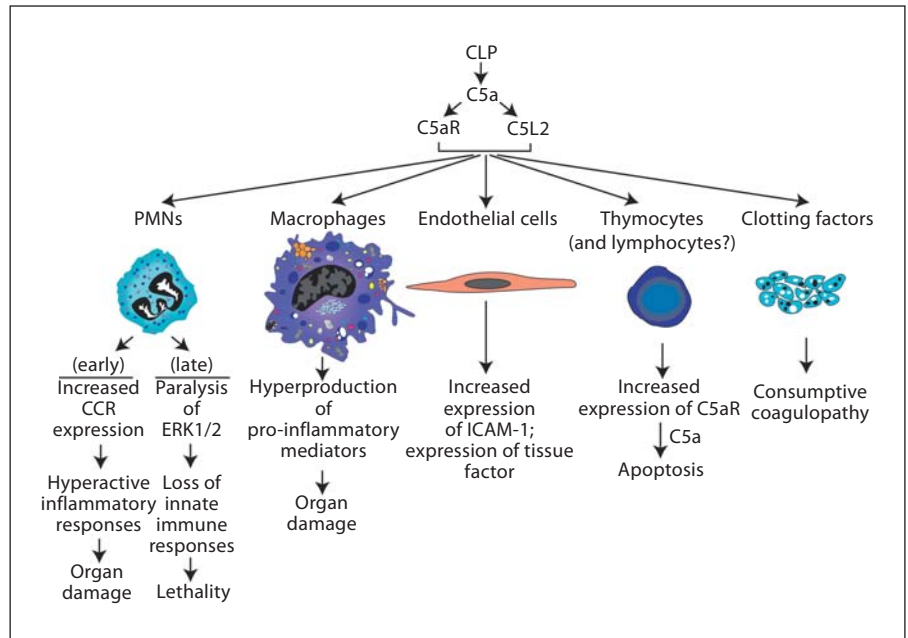


Fig 1. Roles of C5a and C5a receptors in experimental sepsis.

tion and engagement of both C5aR and C5L2 in a variety of cell targets that bear these receptors (PMNs, macrophages, endothelial cells, thymocytes and perhaps lymphocytes, as well as organs such as lung, liver, spleen, heart and kidneys). As indicated above, sepsis is associated with the appearance of C5a (and C5a desArg) as well as C3a (and C3a desArg) in plasma. C5a and C5a desArg interact with C5aR (CD88) and C5L2, each of which is a seven-membrane spanning receptor. C5L2 also appears to interact with C3a desArg [17]. Engagement of C5aR with C5a causes C5aR to engage with the G protein system, resulting in a rapid cytosolic Ca^{2+} transient and rapid intracellular translocation of the C5a·C5aR complex. Because of an amino acid substitution in the DRY region of the second intracellular loop of C5L2, engagement of this receptor with C5a does not result in G protein-coupled activation and, thereby, no Ca^{2+} transient occurs [15–19]. Somewhat surprisingly, the bulk of C5L2 appears to be chiefly within intracellular granules of PMNs [20, 21]. As C5a·C5aR translocates into the cytoplasm, it appears to associate with C5L2, whereupon signal transduction occurs in a manner that may represent the competing influences of C5aR (positive outcomes) and C5L2 (negative outcomes). These interactions and subsequent responses of phagocytes appear to be contained by the binding of β -arrestin to the C5a receptors [20]. On balance, while activation of C5aR clearly leads to ERK1/2 activation, the extent to which C5L2 interacting with C5a

affects ERK1/2 activation is a subject of considerable contention. In PMNs from C5L2^{-/-} mice, in nonmyeloid cells transfected to express C5L2 or in wild-type (Wt) PMNs in which C5L2 has been blocked with an antibody, one group argues that under such conditions engagement of C5L2 seems to attenuate ERK1/2 activation linked to C5a·C5aR engagement [20]. It seems clear that ERK1/2 activation (phosphorylation) is linked to C5a interacting with C5aR [22]. In contrast, another group reports that, in the absence of C5L2, reduced activation of ERK1/2 occurs [23]. It is currently not possible to reconcile these divergent views.

There is strong evidence recently obtained that both C5aR and C5L2 contribute to the adverse outcomes of sepsis. As indicated above, in CLP mice treated with a synthetic, cyclic inhibitor which blocks both C5aR and C5L2 [13], infusion of a competing peptide that blocks both receptors [24] or after the use of mice lacking one of the two C5a receptors and also treated with a blocking antibody to the other receptors [24], there was considerably improved survival following CLP. Our group has also described in CLP mice that antibody-induced blockade of C5L2 resulted in significantly increased (by 3-fold) levels of IL-6 in the plasma, suggesting that C5L2 in some manner regulates the cytokine appearance in plasma under conditions of CLP [25]. When Wt, C5aR^{-/-} and C5L2^{-/-} mice (all on a C57Bl/6 background) were used in the mild and severe CLP models of sepsis [7], it was fairly

clear that in the severe form of sepsis the absence of C5aR together with antibody-induced blockade of C5L2 resulted in significantly improved survival (going from 0% survival up to 80%) [24]. In the mild form of sepsis, absence of C5L2 as compared to Wt mice also led to improved survival (from 40 to 80%) in C5L2^{-/-} mice [24]. Interestingly, in either C5aR^{-/-} or C5L2^{-/-} mice, levels of various cytokines and chemokines in the cytokine storm were in general substantially reduced ($\geq 80\%$) after CLP. This pattern suggests that the sepsis-induced cytokine storm may occur in a sequential fashion and in a manner that requires C5a engagement of both C5aR and C5L2. Another important observation obtained from these studies was that C5L2^{-/-} mice after CLP had greatly reduced levels of HMGB1, which is a well-known transcription factor that appears in plasma after CLP or endotoxemia and whose blockade in these models of sepsis is protective [26]. Interestingly, in C5aR^{-/-} mice after CLP, there was no reduction in plasma levels of HMGB1 [24]. Furthermore, peritoneal exudate macrophages from Wt or C5aR^{-/-} mice produced HMGB1 when stimulated with LPS, whereas macrophages from C5L2^{-/-} mice showed no HMGB1 production. Accordingly, HMGB1 expression from LPS-stimulated peritoneal macrophages is a function of C5L2 but not C5aR. However, as described above, the bulk of cytokines and chemokines expressed in plasma after CLP requires participation of both C5aR and C5L2.

Early after CLP, PMNs show a gain of function by expressing CCL1, CCL2 and CCL5 [27], which would be expected to lead to pro-inflammatory outcomes. Ordinarily, these receptors are expressed in small amounts, if at all, on PMNs and these cells respond very poorly to ligands for these receptors, based on chemotaxis as the functional endpoint. Blood PMNs after CLP show increased binding of MCP-1 and MIP-1 α and acquire the ability to respond chemotactically *in vitro* to these chemokines [27]. Non-CLP PMNs are ordinarily nonresponsive to these chemokines. In addition, CLP causes blood PMNs to show increased expression of β_1 integrins (CD29) and β_2 integrins (CD18), indicating a hyperresponsiveness to the 'counter receptors' for these integrins [28]. Collectively, these data demonstrate that, in the early stages after CLP, blood PMNs develop an exaggerated ability to respond to a variety of inflammatory mediators. As indicated above, as time progresses after CLP, the MAPK (ERK1/2) pathways in PMNs become paralyzed in a C5a-dependent manner [4] and lose innate immune functions (phagocytosis, chemotaxis, respiratory burst), causing an inability to clear gut-derived bacteria from

blood and from the peritoneal cavity. In rodents with CLP, these bacteria are both Gram-positive and -negative). Under these conditions, the respiratory burst in blood PMNs becomes defective and assembly of NADPH oxidase (NOX2) is greatly impaired due to an inability to translocate from the cytosol critical subunits (such as p47^{phox}) of the oxidase to the cell membrane, indicating that the ability to generate H₂O₂ for MPO-dependent killing of ingested bacteria is greatly reduced (fig. 1) [4]. It is clear that such defects are C5a dependent and can be largely averted after CLP by *in vivo* neutralization of C5a [4]. Macrophage interaction with C5a does not result in impairment of signaling pathways for reasons that are not understood. This may be due to the fact that binding sites for C5a on macrophages are far fewer when compared to the number of sites on PMNs. The chief effect of C5a on macrophages is their 'priming' and greatly enhanced production of pro-inflammatory mediators, likely related to the cytokine storm in sepsis which is followed by multi-organ failure. Endothelial cells during sepsis have increased expression of ICAM-1 as well as tissue factor, both being linked to interaction of these cells with C5a [29]. In this manner, endothelial cells bind many more PMNs resulting in increased translocation of PMNs into organs. As well, endothelial cells with their increased surface content of tissue factors now enhance the likelihood of intravascular clots. Thymocytes as early as 3 h after sepsis have increased expression of C5aR and then undergo apoptosis via the internal (mitochondrial) pathway of apoptosis [30]. Whether this also occurs in T and B cells which become apoptotic very early in the setting of sepsis [31] is unclear. Finally, sepsis induces the well-known phenomenon of consumptive coagulopathy. This is characterized by platelet activation together with activation and consumption depletion of clotting factors, as the clotting cascade is activated following the conversion of prothrombin to thrombin. These events lead to reduction of clotting factors in blood, platelet depletion and presence of thrombin-antithrombin complexes and fibrin split products, among others. Concurrent with activation and depletion of clotting factors during sepsis is activation of the fibrinolytic system, whose function is to bring about conversion of plasminogen to plasmin, which is the major serine protease that degrades fibrin into fibrin split products. Removal of fibrin from the luminal surfaces of vessels or from extravascular locales is critical, inefficient removal of fibrin deposits can lead to more and more fibrin deposition, resulting in vascular occlusion and thrombus formation as well as fibrosis in areas of peripheral lung if fibrin breakdown is insufficient. In

vivo blockade of C5a in CLP rats reverses most of the features of coagulopathy [loss of clotting factors, thrombocytopenia, prolonged clotting times, continued presence of products of clotting (such as thrombin-antithrombin complexes) and fibrin split products, among others] [14]. How and why C5a interception after CLP curtails the consumptive coagulopathy of sepsis is not at all understood. Such outcomes might be linked to the well-known interconnections between the complement and the clotting cascades [32]. In general, the ability of C5a neutralization to greatly reduce the complications of experimental sepsis has great appeal, since the only FDA-approved drug for human sepsis is recombinant activated protein C, which is intrinsically an anticoagulant. Using an anticoagulant in a condition (sepsis) in which consumptive coagulation is occurring means that strict limitations in its use are mandatory.

Unexpected Effects of CLP in C5^{-/-} Mice

There have been several lessons learned about molecular events occurring in sepsis vis-à-vis the role of C5, C5 activation products (C5a, C5b-9) and C5a receptors. Based on all of the evidence presented above, the predictions to be drawn from the use of C5^{-/-} mice would be that, since no C5a can be generated, these mice should be well protected from the adverse events of sepsis, assuming that C5a and its receptors are 'major players' in the harmful outcomes of experimental sepsis. The surprise which we recently uncovered was that C5^{-/-} mice had no survival advantage compared to Wt CLP mice [33]. Using the high-grade intensity of CLP [7], by day 5 all mice in both groups (Wt, C5^{-/-}) were dead. Clearly, absence of C5 conferred no survival advantage. When plasma samples were examined for mediator content, in C5^{-/-} CLP mice

TNF- α levels were elevated by 64% compared to Wt mice, while other mediators (IL-1 β , IL-6, MCP-1 and MIP-2) were reduced by 36–89%. Clearly, the absence of C5 in some manner caused downward deflection in the cytokine storm. One of the most interesting differences between the Wt and C5aR^{-/-} CLP mice was that blood colony-forming units (CFUs) in Wt mice were around 2×10^5 CFUs/ml blood, while the CFUs in blood from C5^{-/-} mice were $\geq 900 \times 10^5$ CFUs/ml blood. In the absence of C5, no C5b-9 which can be formed, loss of which seems to be associated with a serious derangement in bacterial clearance. Therefore, the protective effects of C5b-9 have been lost in the absence of C5, suggesting that in experimental sepsis, C5a, which is robustly produced in CLP, has widespread harmful effects (as emphasized in fig. 1), while C5b-9 has protective effects by reducing CFU content in blood. As a result, the absence of C5 prevents the harmful effects of C5a, but the protective effects of C5b-9 are nullified in C5^{-/-} mice after CLP. Such observations imply that great caution is often needed in interpreting data from knockout mice. Another example of problems interpreting data from knockout mice was our observation that C3^{-/-} mice developed full-fledged lung injury after intrapulmonary deposition of IgG immune complexes [32]. The surprising finding was the presence of C5a in their lungs. It was ultimately shown that C5a was generated by the interaction of thrombin with C5, also underscoring the linkages between the complement and clotting systems. The data described above suggest that it may be inadvisable to use C5-depleting antibodies in the setting of sepsis in humans.

Acknowledgement

This research was supported in part by NIH grant GM-61656.

References

- 1 Dellinger RP, Levy MM, Carlet JM, Bion J, Parker MM, Jaeschke R, Reinhart K, Angus DC, Brun-Buisson C, Beale R, Calandra T, Dhainaut JF, Gerlach H, Harvey M, Marini JJ, Marshall J, Ranieri M, Ramsay G, Sevransky J, Thompson BT, Townsend S, Vender JS, Zimmerman JL, Vincent JL: Surviving Sepsis Campaign: international guidelines for management of severe sepsis and septic shock. *Intensive Care Med* 2008;34:17–60.
- 2 Solomkin JS, Jenkins MK, Nelson RD, Chenoweth D, Simmons RL: Neutrophil dysfunction in sepsis. II. Evidence for the role of complement activation products in cellular deactivation. *Surgery* 1981;90:319–327.
- 3 Goya T, Morisaki T, Torisu M: Immunologic assessment of host defense impairment in patients with septic multiple organ failure: relationship between complement activation and changes in neutrophil function. *Surgery* 1994;115:145–155.
- 4 Huber-Lang MS, Younkin EM, Sarma JV, McGuire SR, Lu KT, Guo RF, Padgaonkar VA, Curnutte JT, Erickson R, Ward PA: Complement-induced impairment of innate immunity during sepsis. *J Immunol* 2002; 169:3223–3231.
- 5 Hangen DH, Stevens JH, Satoh PS, Hall EW, O'Hanley PT, Raffin TA: Complement levels in septic primates treated with anti-C5a antibodies. *J Surg Res* 1989;46:195–199.

- 6 Stevens JH, O'Hanley P, Shapiro JM, Mihm FG, Satoh PS, Collins JA, Raffin TA: Effects of anti-C5a antibodies on the adult respiratory distress syndrome in septic primates. *J Clin Invest* 1986;77:1812-1816.
- 7 Rittirsch D, Huber-Lang M, Flierl M, Ward PA: Immunodesign of experimental sepsis by cecal ligation and puncture. *Nat Protoc* 2009;4:31-36.
- 8 Czermak BJ, Sarma V, Pierson CL, Warner RL, Huber-Lang M, Bless NM, Schmal H, Friedl HP, Ward PA: Protective effects of C5a blockade in sepsis. *Nat Med* 1999;5:788-792.
- 9 Huber-Lang MS, Sarma JV, McGuire SR, Lu KT, Guo RF, Padgaonkar VA, Younkin EM, Laudes IJ, Riedemann NC, Younger JG, Ward PA: Protective effects of anti-C5a peptide antibodies in experimental sepsis. *FASEB J* 2001;15:568-570.
- 10 Huber-Lang M, Sarma VJ, Lu KT, McGuire SR, Padgaonkar VA, Guo RF, Younkin EM, Kunkel RG, Ding J, Erickson R, Curnutte JT, Ward PA: Role of C5a in multiorgan failure during sepsis. *J Immunol* 2001;166:1193-1199.
- 11 Huber-Lang MS, Sarma JV, McGuire SR, Lu KT, Padgaonkar VA, Younkin EM, Guo RF, Weber CH, Zuiderweg RR, Zetoune FS, Ward PA: Structure-function relationships of human C5a and C5aR. *J Immunol* 2003;170:6115-6124.
- 12 Finch AM, Wong AK, Paczkowski NJ, Wadi SK, Craik DJ, Fairlie DP, Taylor SM: Low-molecular-weight peptidic and cyclic antagonists of the receptor for the complement factor C5a. *J Med Chem* 1999;42:1965-1974.
- 13 Huber-Lang MS, Riedeman NC, Sarma JV, Younkin EM, McGuire SR, Laudes IJ, Lu KT, Guo RF, Neff TA, Padgaonkar VA, Lambris JD, Spruce L, Mastellos D, Zetoune FS, Ward PA: Protection of innate immunity by C5aR antagonist in septic mice. *FASEB J* 2002;16:1567-1574.
- 14 Laudes IJ, Chu JC, Sikranth S, Huber-Lang M, Guo RF, Riedemann N, Sarma JV, Schmaier AH, Ward PA: Anti-c5a ameliorates coagulation/fibrinolytic protein changes in a rat model of sepsis. *Am J Pathol* 2002;160:1867-1875.
- 15 Lee H, Whitfeld PL, Mackay CR: Receptors for complement C5a. The importance of C5aR and the enigmatic role of C5L2. *Immunol Cell Biol* 2008;86:153-160.
- 16 Okinaga S, Slattery D, Humbles A, Zsengeller Z, Morteau O, Kinrade MB, Brodbeck RM, Krause JE, Choe HR, Gerard NP, Gerard C: C5L2, a non-signaling C5a binding protein. *Biochemistry* 2003;42:9406-9415.
- 17 Kalant D, Cain SA, Maslowska M, Sniderman AD, Cianflone K, Monk PN: The chemoattractant receptor-like protein C5L2 binds the C3a des-Arg77/acylation-stimulating protein. *J Biol Chem* 2003;278:11123-11129.
- 18 Kalant D, MacLaren R, Cui W, Samanta R, Monk PN, Laporte SA, Cianflone K: C5L2 is a functional receptor for acylation-stimulating protein. *J Biol Chem* 2005;280:23936-23944.
- 19 Cain SA, Monk PN: The orphan receptor C5L2 has high affinity binding sites for complement fragments C5a and C5a des-Arg(74). *J Biol Chem* 2002;277:7165-7169.
- 20 Bamberg CE, Mackay CR, Lee H, Zahra D, Jackson J, Lim YS, Whitfeld PL, Craig S, Corsini E, Lu B, Gerard C, Gerard NP: The C5a receptor (C5aR) C5L2 is a modulator of C5aR-mediated signal transduction. *J Biol Chem* 2010;285:7633-7644.
- 21 Scola AM, Johswich KO, Morgan BP, Klos A, Monk PN: The human complement fragment receptor, C5L2, is a recycling decoy receptor. *Mol Immunol* 2009;46:1149-1162.
- 22 Riedemann NC, Guo RF, Hollmann TJ, Gao H, Neff TA, Reuben JS, Speyer CL, Sarma JV, Wetsel RA, Zetoune FS, Ward PA: Regulatory role of C5a in LPS-induced IL-6 production by neutrophils during sepsis. *FASEB J* 2004;18:370-372.
- 23 Chen NJ, Mirtsos C, Suh D, Lu YC, Lin WJ, McKelvie C, Lee T, Baribault H, Tian H, Yeh WC: C5L2 is critical for the biological activities of the anaphylatoxins C5a and C3a. *Nature* 2007;446:203-207.
- 24 Rittirsch D, Flierl MA, Nadeau BA, Day DE, Hoesel LM, Zetoune FS, MacKay CR, Cianflone K, Gerard NP, Huber-Lang MS, Köhl J, Gerard C, Sarma JV, Ward PA: Functional roles for C5a receptors in sepsis. *Nat Med* 2008;14:551-557.
- 25 Gao H, Neff TA, Guo RF, Speyer CL, Sarma JV, Tomlins S, Man Y, Riedemann NC, Hoesel LM, Younkin EM, Zetoune FS, Ward PA: Evidence for a functional role of the second C5a receptor, C5L2. *FASEB J* 2005;19:1003-1005.
- 26 Wang H, Bloom O, Zhang M, Vishnubhakat JM, Ombrellino M, Che J, Frazier A, Yang H, Ivanova S, Borovikova L, Manogue KR, Faist E, Abraham E, Andersson J, Andersson U, Molina PE, Abumrad NN, Sama A, Tracey KJ: HMG-1 as a late mediator of endotoxin lethality in mice. *Science* 1999;285:248-251.
- 27 Speyer CL, Gao H, Rancilio NJ, Neff TA, Huffnagle GB, Sarma JV, Ward PA: Novel chemokine responsiveness and mobilization of neutrophils during sepsis. *Am J Pathol* 2004;165:2187-2196.
- 28 Guo RF, Riedemann NC, Laudes IJ, Sarma VJ, Kunkel RG, Dille KA, Paulauskis JD, Ward PA: Altered neutrophil trafficking during sepsis. *J Immunol* 2002;169:307-314.
- 29 Laudes IJ, Guo RF, Riedemann NC, Speyer C, Craig R, Sarma JV, Ward PA: Disturbed homeostasis of lung intercellular adhesion molecule-1 and vascular cell adhesion molecule-1 during sepsis. *Am J Pathol* 2004;164:1435-1445.
- 30 Riedemann NC, Guo RF, Laudes IJ, Keller K, Sarma VJ, Padgaonkar V, Zetoune FS, Ward PA: C5a receptor and thymocyte apoptosis in sepsis. *FASEB J* 2002;16:887-888.
- 31 Hotchkiss RS, Tinsley KW, Swanson PE, Schmiege RE Jr, Hui JJ, Chang KC, Osborne DF, Freeman BD, Cobb JP, Buchman TG, Karl IE: Sepsis-induced apoptosis causes progressive profound depletion of B and CD4+ T lymphocytes in humans. *J Immunol* 2001;166:6952-6963.
- 32 Huber-Lang M, Sarma JV, Zetoune FS, Rittirsch D, Neff TA, McGuire SR, Lambris JD, Warner RL, Flierl MA, Hoesel LM, Gebhard F, Younger JG, Drouin SM, Wetsel RA, Ward PA: Generation of C5a in the absence of C3: a new complement activation pathway. *Nat Med* 2006;12:682-687.
- 33 Flierl MA, Rittirsch D, Nadeau BA, Day DE, Zetoune FS, Sarma JV, Huber-Lang MS, Ward PA: Functions of the complement components C3 and C5 during sepsis. *FASEB J* 2008;22:3483-3490.

The Phosphatidylinositol 3-Kinase Signaling Pathway Exerts Protective Effects during Sepsis by Controlling C5a-Mediated Activation of Innate Immune Functions¹

Christiane D. Wrann,^{2*} Navid A. Tabriz,^{2*} Tanja Barkhausen,* Andreas Klos,[‡] Martijn van Griensven,[†] Hans C. Pape,[§] Daniel O. Kendoff,* Renfeng Guo,[¶] Peter A. Ward,[¶] Christian Krettek,* and Niels C. Riedemann^{3*}

The PI3K/Akt signaling pathway has been recently suggested to have controversial functions in models of acute and chronic inflammation. Our group and others have reported previously that the complement split product C5a alters neutrophil innate immunity and cell signaling during the onset of sepsis and is involved in PI3K activation. We report in this study that in vivo inhibition of the PI3K pathway resulted in increased mortality in septic mice accompanied by strongly elevated serum levels of TNF- α , IL-6, MCP-1, and IL-10 during sepsis as well as decreased oxidative burst activity in blood phagocytes. PI3K inhibition in vitro resulted in significant increases in TLR-4-mediated generation of various proinflammatory cytokines in neutrophils, whereas the opposite effect was observed in PBMC. Oxidative burst and phagocytosis activity was significantly attenuated in both neutrophils and monocytes when PI3K activation was blocked. In addition, PI3K inhibition resulted in strongly elevated TLR-4-mediated generation of IL-1 β and IL-8 in neutrophils when these cells were costimulated with C5a. C5a-induced priming effects on neutrophil and monocyte oxidative burst activity as well as C5a-induced phagocytosis in neutrophils were strongly reduced when PI3K activation was blocked. Our data suggest that the PI3K/Akt signaling pathway controls various C5a-mediated effects on neutrophil and monocyte innate immunity and exerts an overall protective effect during experimental sepsis. *The Journal of Immunology*, 2007, 178: 5940–5948.

During the early inflammatory response to invading microorganisms, crucial innate immune players such as neutrophils and monocytes are set into place to defend the host. During experimental sepsis, neutrophils are activated very early in the onset phase of the inflammatory response as first line of defense, contributing significantly to mediator generation, pathogen phagocytosis, and O²⁻ radical production. In various diseases related to acute inflammation, neutrophils are also thought to be responsible for host tissue damage and organ failure. However, during sepsis it is a well-described phenomenon that neutrophils undergo a status of immune paralysis with regard to their ability to fight invading microorganisms (1), setting the stage for super infection and for high lethality during sepsis (2), whereas the overall $t_{1/2}$ in the serum is prolonged. The latter

observation could be explained by activation of the PI3K pathway in neutrophils (3, 4), which, during sepsis, could at least partially be due to generation of the complement split product C5a (5, 6).

During the onset of experimental sepsis, the complement system is activated via three well-known pathways, leading to generation of the potent inflammatory split product C5a. There is growing evidence for various harmful effects of C5a and C5aR activation during the onset of sepsis (1, 7, 8). Blockade of either C5a or C5aR leads to greatly improved survival in septic rodents (9–11). Earlier work suggested that C5a generation during sepsis plays a critical role for suppression of neutrophil innate immune functions (11–14). We recently demonstrated that C5a has a key function for altering intracellular signaling pathways in neutrophils in vitro and during the onset of sepsis in vivo (2, 15, 16), offering an explanation for the above-mentioned suppression of innate immune functions.

The PI3K signaling pathway, including the downstream Akt kinase, has been described as important inhibitory regulator of neutrophil apoptosis (3, 4). Recent work pointed out an important role of this signaling pathway for neutrophil respiratory burst (17, 18) as well as chemotaxis of neutrophils in response to fMLP (17, 19–21). Various studies then reported the importance of PI3K activation for neutrophil sequestration in inflamed tissue in different animal models (22–25). These results implicated an important role of this signaling pathway for the innate immune response during acute inflammation. We thought to investigate the regulatory potential of this pathway for TLR-4- and C5a-mediated activation of neutrophils and monocytes and for outcome in experimental sepsis.

Materials and Methods

Reagents

Human rC5a and other reagents were purchased from Sigma-Aldrich, if not otherwise indicated.

*Department of Trauma Surgery, Hannover Medical School, Hannover, Germany; [†]Ludwig Boltzmann Institute for Experimental and Clinical Traumatology, Vienna, Austria; [‡]Department of Medical Microbiology, Hannover Medical School, Hannover, Germany; [§]Department of Orthopedic Surgery, Division Orthopedic Traumatology, University of Pittsburgh, Pittsburgh, PA 15213; and [¶]Department of Pathology, University of Michigan Medical School, Ann Arbor, MI 48109

Received for publication October 27, 2006. Accepted for publication February 20, 2007.

The costs of publication of this article were defrayed in part by the payment of page charges. This article must therefore be hereby marked *advertisement* in accordance with 18 U.S.C. Section 1734 solely to indicate this fact.

¹ This work was supported by Hochschulinterne Leistungsfoerderung-1 Grant (Hannover Medical School, Hannover, Germany) and by Deutsche Forschungsgemeinschaft Grant RI 1216/4-1 (German Research Council (Deutsche Forschungsgemeinschaft)).

² C.D.W. and N.A.T. contributed equally to this work.

³ Address correspondence and reprint requests to Dr. Niels C. Riedemann, Department of Trauma Surgery, Medizinische Hochschule Hannover, Carl Neuberg Strasse 1, 30625 Hannover, Germany. E-mail address: nriedeman@yahoo.com

Neutrophil and PBMC isolation from whole blood and *in vitro* stimulation

EDTA/heparin was used as an anticoagulant for the isolation of human neutrophils and PBMC from blood. After Ficoll-Paque gradient centrifugation (Biocoll; Biochrom), PBMC were collected from the buffy coat and neutrophils were separated from the pellet by dextrane (Roth) sedimentation. Hypotonic RBC lysis was achieved, using sterile H₂O. Neutrophils were resuspended in DMEM containing 10% FCS (Biochrom). A final concentration of 6×10^6 cells/ml was used for stimulation at 37°C and 5% CO₂ for the times indicated with C5a (50 or 200 ng/ml) or LPS (20, 50, or 100 ng/ml), or both. Supernatant fluids were collected after pelleting of the cells and frozen at -80°C until used for ELISA analysis. For certain experiments, neutrophils were preincubated for 30 min with 50 μM PI3K inhibitor LY294002 (New England Biolabs), which inhibits downstream phosphorylation of the Akt pathway.

Western blot analysis

Neutrophils were isolated from human blood and stimulated at 37°C *in vitro* with human rC5a (10–100 ng/ml) or LPS (50 ng/ml), or both. Approximately 2×10^6 cells per condition were then used for whole cell lysis using Laemmli buffer containing 5% 2-ME. Lysates were separated on a NuPAGE 4–12% Bis-Tris gel (Invitrogen Life Technologies), and proteins were then transferred to a nitrocellulose membrane. Membranes were incubated overnight with Abs to phosphorylated and nonphosphorylated human/rat Akt, FKHR,⁴ glycogen synthase kinase (GSK)-3β, phosphatase and tensin homolog deleted on chromosome 10, and phosphoinositide-dependent protein kinase 1 (New England Biolabs). For detection of the protein, ECL plus was used (Amersham Biosciences), according to the manufacturer's instructions.

Quantitation of IL-6, TNF-α, IL-1β, IL-12, IL-10, and IL-8 in cell supernatants

Neutrophils were isolated from human whole blood, as outlined above, and stimulated at 37°C *in vitro* with human rC5a (50 or 200 ng/ml) or LPS (50 ng/ml), or both for 6 h in an incubator with 5% CO₂ under sterile conditions. Cell supernatants were then isolated and frozen at -80°C until analyzed for various mediators using a commercially available flow cytometric bead assay, according to the manufacturer's instructions (BD Biosciences). For IL-8 ELISA experiments were conducted using a commercially available IL-8 ELISA kit, according to the manufacturer's instructions (BioSource International).

Cecum ligation and puncture (CLP) in mice and inhibition of the PI3K/Akt pathway *in vivo*

Specific pathogen-free C57BL/6 mice (Own Laboratories, Zentrales Tierlabor Medizinische Hochschule Hannover) were used for all CLP studies. Anesthesia was achieved by i.p. injection of ketamine (Ketanest; Pfizer) and xylazine (Rompun; Bayer). In the CLP model, approximately two-thirds of the cecum was ligated through a 3-cm abdominal midline incision. The ligated part of the cecum was punctured through and through with a 21-gauge needle. After repositioning of the bowel, the abdomen was closed in layers, using a 4.0 surgical suture (Ethicon) and metallic clips. For inhibition of the PI3K/Akt signaling pathway *in vivo*, a specific inhibitor (LY294002; New England Biolabs) was diluted in 200 μl of Dulbecco's PBS (DPBS) solution and injected into the penal vein of mice immediately following CLP to achieve a total blood concentration of 50 μM. Control animals received 200 μl of DPBS, including equal amounts of DMSO, also immediately after CLP. All animal studies were reviewed and approved by the local ethic committee of the state of Lower Saxony, Germany.

Collection of serum samples in mice

After induction of CLP, animals were sacrificed at the indicated time points and blood was drawn from the inferior caval vein. Blood samples were allowed to clot at 5°C for 6 h before centrifugation at 4000 rpm for 15 min at 4°C. Serum was collected and immediately frozen at -80°C until used for ELISA analysis. For experiments using the flow cytometric analysis of oxidative burst in neutrophils and monocytes from whole blood in mice, animals were treated with LY294002, as outlined earlier, and were then sacrificed 90 min thereafter. Next, blood was drawn from the inferior caval vein, and 100 μl of mouse whole blood was used for further flow cyto-

metric analysis of oxidative burst activity, as outlined in the section below. Heparin was used as anticoagulant.

Quantitation of IL-6, TNF-α, IL-10, MCP-1, IL-12, IFN-γ, and keratinocyte-derived chemokine (KC) in serum samples

Serum samples were collected, as outlined above. For quantification of various mediators, a commercially available flow cytometric bead assay was performed, according to the manufacturer's instructions (BD Biosciences). For quantification of mouse KC ELISA experiments were conducted using a commercially available mouse KC ELISA kit, according to the manufacturer's instructions.

Quantitation of oxidative burst and phagocytosis in whole blood cells

To determine the ability of blood neutrophils and monocytes to generate oxygen radicals and to conduct phagocytosis, commercially available flow cytometry-based assays were used, according to the manufacturer's instructions (Phagoburst, Phagotest; ORPEGEN Pharma). The Phagoburst assays use dihydrorhodamine 123 as a fluorogenic substrate and determine the percentage of active cells and their enzymatic activity/degree of activity. For Phagotest analysis, whole blood samples were incubated with FITC-labeled *Escherichia coli* bacteria (3.3×10^7 bacteria/ml) for 10 min in a 37°C warm water bath. Leukocyte surface-bound bacteria were neutralized using quenching solution. Cells were analyzed in a FACSCalibur flow cytometer (BD Biosciences). In a forward/side scatter dot plot, gates were set on granulocytes and monocytes to analyze each population with regard to mean fluorescence intensity (MFI). For oxidative burst measurement in mouse whole blood, samples were collected after inhibitor treatment, as described earlier, and then stimulated with PMA (1.4 μM) for 10 min in a 37°C water bath and processed according to the same protocol explained in this paragraph.

In vitro stimulation of oxidative burst and phagocytosis in blood phagocytes

Heparinized human whole blood was preincubated for 30 min with 50 μM PI3K inhibitor LY294002 (New England Biolabs) or with an equal amount of the vehicle (DMSO) at 37°C and 5% CO₂. Human rC5a was then added at different concentrations (1–10,000 ng/ml), and the blood was further incubated for different time periods (10, 20, and 60 min). In one set of experiments, the cells were then stimulated with either unlabeled opsonized bacteria (*E. coli*) (6.7×10^8 bacteria/ml), PMA (1.4 μM), or the chemotactic peptide fMLP (0.8 μM) for 10 min in a 37°C water bath and processed afterward, according to the protocol explained above. In another set of experiments, the cells were processed immediately after C5a incubation with no further stimulation.

Assessment of bacterial growth in the peritoneal cavity during CLP-induced sepsis in mice

Sepsis was induced with CLP, and animals were treated with or without LY294002, according to the explained protocol, before being sacrificed at 6 h after CLP. The peritoneal cavity was lavaged with 10 ml of sterile 0.9% NaCl. Samples were diluted serially in 0.9% NaCl and incubated in parallel on Columbia 5% sheep blood plates, McConkey plates, and Slanetz-Bartley *Enterococci*-specific indicator plates for 24 h in aerobic atmosphere. The resulting bacterial colonies were further analyzed by biochemical assays, counted, and expressed as CFU per sample.

Statistical analysis

All values were expressed as the mean ± SEM. Significance was assigned where $p < 0.05$. Data sets were analyzed using Student's *t* test or using one-way ANOVA, with individual group means being compared with the Tukey multiple comparison test. Statistical analysis for survival studies was performed using proportional hazards modeling. The software used was GraphPad Prism 3.0 (GraphPad).

Results

Impact of PI3K/Akt inhibition on outcome during sepsis in mice

To determine whether inhibition of the PI3K/Akt pathway had effects on outcome during experimental sepsis in rodents, we conducted CLP experiments in mice receiving either 200 μl of DPBS as control or 200 μl of DPBS containing the PI3K inhibitor LY294002 to achieve a serum concentration of 50 μM. Mice were followed up for 7 days and monitored every 6 h for various signs

⁴ Abbreviations used in this paper: FKHR, forkhead-related transcription factor; CLP, cecum ligation and puncture; DPBS, Dulbecco's PBS; GSK, glycogen synthase kinase; KC, keratinocyte-derived chemokine; MFI, mean fluorescence intensity.

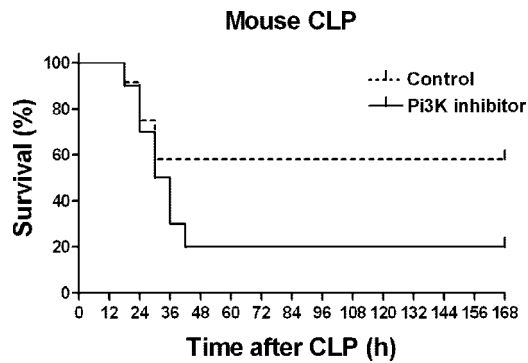


FIGURE 1. Effect of PI3K inhibition on outcome in experimental sepsis CLP study in C57BL/6 mice. CLP was induced with a 21-gauge needle and a two-thirds ligation of the cecum. CLP was induced and mice were treated with LY294002 directly after CLP by penal vein injection with 200 μ l of DPBS containing body weight-adjusted concentrations of LY294002 to reach a calculated serum concentration of \sim 50 μ M. Control groups were treated equally with 200 μ l of DPBS containing no inhibitor. Experiments were conducted with $n = 12$ animals per group.

of sickness. The group of mice receiving LY294002 demonstrated significantly reduced survival as well as earlier and more severe onset of sepsis (Fig. 1) when compared with the control group. These results demonstrated an overall protective effect mediated by the PI3K/Akt signaling pathway during the onset of sepsis.

Impact of *in vivo* PI3K/Akt pathway inhibition on cytokine generation during sepsis and on burst activity in phagocytes

We conducted CLP experiments in mice receiving either 200 μ l of DPBS as control or 200 μ l of DPBS containing the PI3K inhibitor LY294002 to achieve an intravascular concentration of 50 μ M, as described in *Materials and Methods*. Six hours after induction of sepsis, blood was drawn from the caval vein, followed by exsanguinations of the animals. Serum samples were prepared and analyzed for presence of various mediators using a flow cytometric bead assay. As depicted in Fig. 2A, significantly higher serum levels were found in LY294002-treated animals for TNF- α , IL-6, IL-10, and MCP-1, when compared with control mice. For KC, a tendency toward higher levels in LY294002-treated mice (mean value 33,833 pg/ml) was observed when compared with control mice (mean value 26,998 pg/ml), which was not found to be statistically significant. No differences were found for IL-12 and IFN- γ (data not shown). These results demonstrated an inhibitory function of the PI3K/Akt pathway for generation of crucial inflammatory mediators such as TNF- α and IL-6 during the onset phase of sepsis, suggesting an overall negative feedback mechanism on inflammation in this model. We further investigated the effect of *in vivo* inhibition of the PI3K pathway on oxidative burst in neutrophils and monocytes in a whole blood assay. Mice were treated with 200 μ l of DPBS containing LY294002 (50 μ M serum concentration) or no inhibitor. Heparinized whole blood samples were drawn 90 min after treatment and stimulated with PMA (1.4 μ M) for 10 min. The inhibitor treatment resulted in a significant decrease of burst activity in both cell populations, neutrophils and monocytes (Fig. 2B), demonstrating *in vivo* activity of the administered PI3K inhibitor. The number of bursting cells was not affected (data not shown).

Effect of PI3K/Akt inhibition on bacterial growth in the peritoneal cavity during sepsis

Six hours after induction of sepsis and inhibitor treatment with or without LY294002, peritoneal lavage fluids were collected from the mice and cultured and bacterial counts were determined as

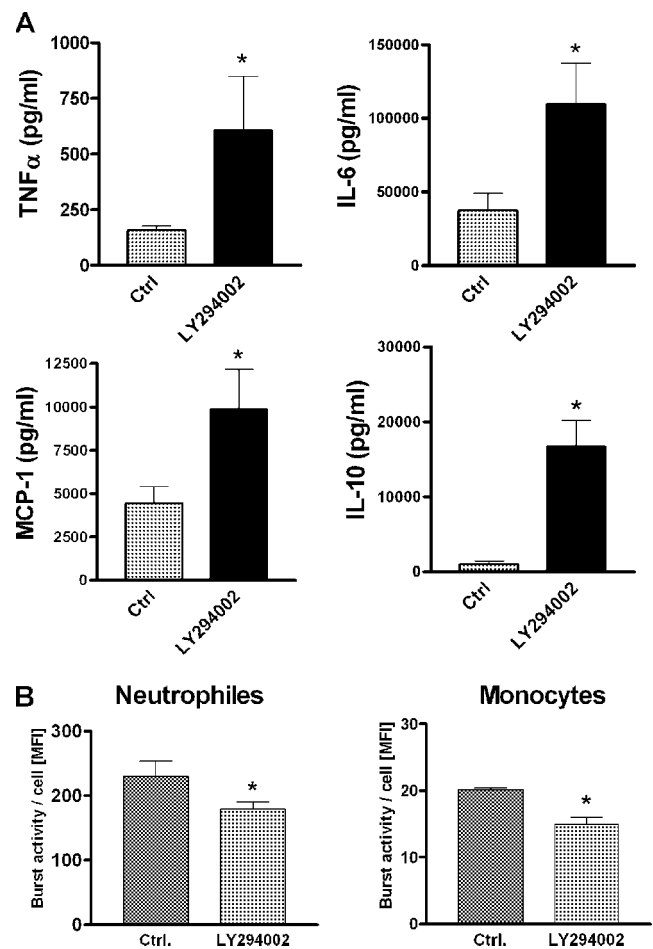


FIGURE 2. Impact of *in vivo* PI3K/Akt pathway inhibition on cytokine generation during sepsis and on burst activity in phagocytes. **A**, Flow cytometric bead ELISA of serum samples from septic animals. Animals underwent CLP and were treated with 200 μ l of DPBS containing LY294002 (50 μ M serum concentration) or no inhibitor directly after CLP. Blood serum samples were drawn 6 h after induction of CLP. The symbol * indicates statistical significant difference from the control group. Data are representative for five to seven animals per group. **B**, Flow cytometric analysis of oxidative burst in whole blood samples gated for neutrophil and monocyte cell populations. Animals were treated with 200 μ l of DPBS containing LY294002 (50 μ M serum concentration) or no inhibitor. Heparinized whole blood samples were drawn 90 min after treatment and stimulated with PMA (1.4 μ M) for 10 min. Fifty thousand cells were analyzed for each experimental point. Oxidative burst activity per single cell is depicted as MFI. Neutrophils are shown in the *left panel* and monocytes in the *right panel*. *, Statistical significant difference from the control group. Data are representative for three to five animals per group.

CFU after 24 h of incubation. The dominating bacteria found in all samples were *Enterococci* spp.; *Staphylococci* and *Lactobacillus* spp. were also detected to a lesser extent in most samples. No statistical significant difference in CFU counts of *Enterococci* spp. could be detected in the LY294002-treated group when compared with the vehicle control group (data not shown). Also, no significant differences in the variety of other bacteria were detected. These results suggested that PI3K inhibition resulted in adverse effects on outcome in septic mice most likely triggered by impaired innate immune functions rather than by direct effects on bacterial growth.

Role of the PI3K/Akt pathway on LPS-induced cytokine generation in neutrophils and PBMC

An earlier study has described the involvement of the PI3K pathway in LPS/TLR-4-dependent TNF- α generation in PBMC,

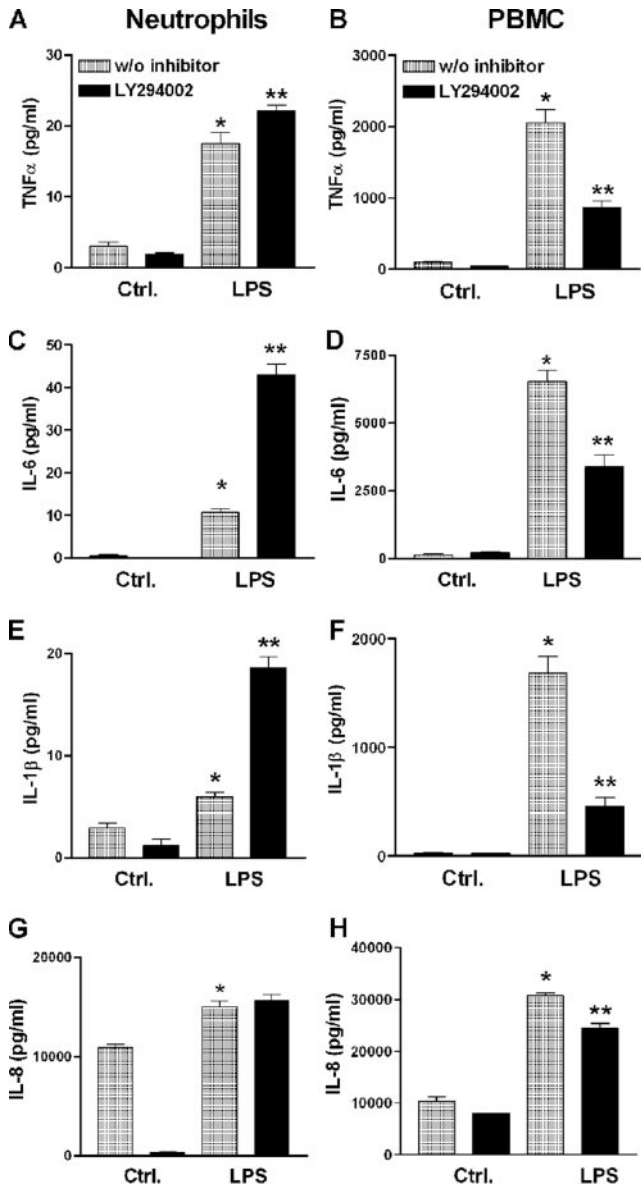


FIGURE 3. Effects of PI3K inhibition on LPS-induced mediator generation in human neutrophils (A, C, E, G) and PBMC (B, D, F, H) in vitro. Flow cytometric bead ELISA of neutrophil and PBMC supernatant fluids. Neutrophils and PBMC were isolated from whole blood and incubated in vitro with LPS (50 ng/ml) or medium control for 6 h at 37°C at a concentration of 6×10^6 cells/ml. Cells were stimulated in the absence or presence of LY294002 after preincubation for 30 min at a concentration of 50 μ M. *, Statistical significant difference from the control group; **, statistical significant difference from the LPS-treated group with no inhibitor. Data are representative of three to four independent experiments, with incubation and analysis being conducted in separate triplicate or quadruplicate samples.

demonstrating reduction of LPS-induced TNF- α generation after PI3K inhibition (26), suggesting a promoting effect of PI3K for TNF- α generation. Because we found in vivo strongly elevated mediator levels 6 h after CLP in serum samples of mice, we thought to investigate LPS-induced in vitro generation of various mediators in neutrophils and PBMC after 6 h of stimulation. Interestingly, we observed that in neutrophils the proinflammatory mediators TNF- α , IL-6, and IL-1 β were significantly increased when PI3K activity was inhibited (Fig. 3, A, C, E, and G), whereas the opposite effect could be seen in PBMC (Fig. 3, B, D, F, and H),

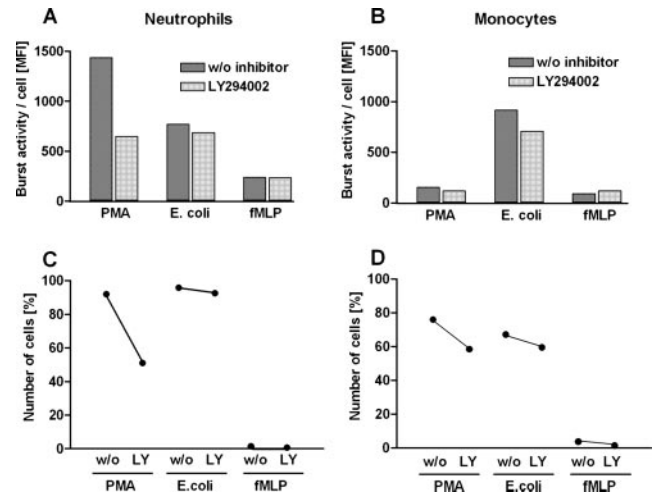


FIGURE 4. Effects of PI3K inhibition on oxidative burst in neutrophils and monocytes in human whole blood. Flow cytometric analysis of oxidative burst in whole blood samples gated for neutrophil and monocyte cell populations. Fifty thousand cells were analyzed for each experimental point. Human whole blood samples were preincubated with LY294002 (50 μ M) or equal amounts of vehicle control and then stimulated with either PMA (1.4 μ M), *E. coli* bacteria (6.7×10^8 /ml), or fMLP (0.8 μ M) for 10 min. Oxidative burst activity per single cell is depicted as MFI (A and B), and numbers of bursting cells are shown in percentages (C and D). Data are representative of two to three independent experiments per graph.

suggesting an inhibitory potential of this signaling pathway for LPS-induced neutrophil mediator generation and a stimulatory function in PBMC. However, under in vivo conditions as described above, an overall inhibitory function of the PI3K pathway was dominating, with respect to TNF- α , IL-6, but also IL-10 and MCP-1 generation, as described earlier.

Effects of PI3K inhibition on oxidative burst in neutrophils and monocytes in vitro

We investigated the role of the PI3K pathway on oxidative burst in neutrophils and monocytes in a whole blood assay, as described in *Materials and Methods*. Whole blood samples were preincubated with 50 μ M LY294002 for 30 min, and oxidative burst was then stimulated with PMA, *E. coli*, as well as fMLP. PI3K inhibition resulted in a strong reduction of PMA- and *E. coli*-induced oxidative burst in neutrophils and in monocytes (Fig. 4, A and B), as well as in reduction of the number of cells initiating oxidative burst (Fig. 4, C and D). The latter effect was more apparent in PMA-induced oxidative burst when compared with *E. coli* as stimulus, especially in neutrophils (Fig. 4C). PMA appeared to be the strongest stimulus for neutrophils, whereas in monocytes, *E. coli* achieved a stronger stimulation of oxidative burst. The induction of oxidative burst by fMLP resulted in only minor initiation of oxidative burst in neutrophils and monocytes. Also, no inhibitory effects could be seen after PI3K inhibition when cells were stimulated with fMLP. Earlier studies have suggested a stimulatory effect of PI3K for fMLP-induced oxidative burst in isolated neutrophils in vitro (17), which could not be confirmed in this whole blood assay (Fig. 4A). Our data suggest an overall promoting effect of the PI3K pathway on PMA- and *E. coli*-induced oxidative burst in neutrophils and monocytes.

Effects of PI3K inhibition on phagocytosis activity in neutrophils and monocytes in vitro

We further thought to investigate whether PI3K inhibition would also affect phagocytosis in neutrophils and monocytes. Whole

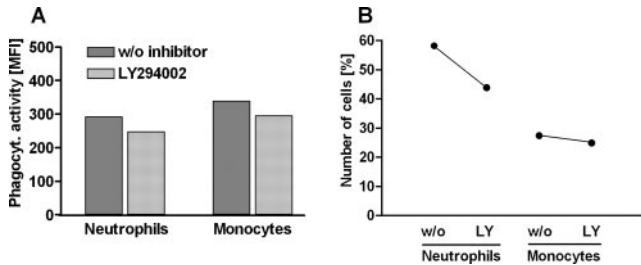


FIGURE 5. Effects of PI3K inhibition on *E. coli*-induced phagocytosis in neutrophils and monocytes in human whole blood. Human whole blood samples were preincubated with LY294002 (50 μ M) or equal amounts of vehicle control and then stimulated with opsonized FITC-conjugated *E. coli* bacteria (3.3×10^7 /ml) for 10 min. Fifty thousand cells were analyzed for each experimental point. Phagocytosis activity per single cell is depicted as MFI (A), and numbers of bursting cells are shown in percentages (B). Data are representative of three independent experiments.

blood samples were collected from healthy donors and subjected to PI3K inhibition by preincubation for 30 min with 50 μ M LY294002 or control containing PBS and equal amounts of DMSO. PI3K inhibition clearly attenuated *E. coli*-induced phagocytosis activity in both neutrophils and monocytes (Fig. 5A), as well as the total number of phagocytosing cells (Fig. 5B), with the latter effect being less prominent in monocytes. Our data suggest a promoting effect of the PI3K signaling pathway for neutrophil and monocyte phagocytosis activity.

Activation of the PI3K/Akt signaling pathway in neutrophils by C5a

It has been described recently that C5a activates the PI3K/Akt signaling pathway in neutrophils *in vitro*, which could be linked to inhibition of apoptosis in neutrophils (4, 5). In monocytes, LPS-induced phosphorylation of Akt, Raf-1, and GSK-3 β has been described before (26). The c-Raf kinase is known to initiate MEK1/2 phosphorylation, thereby initiating activation of the ERK1/2 MAPK pathway. The c-Raf kinase therefore represents an important link between Akt and ERK1/2 MAPK signaling pathways. Another group has described recently that, in macrophages, C5a induces PI3K/Akt activation, leading to downstream activation of ERK1/2 (27). Our group demonstrated earlier rapid phosphorylation of Akt in neutrophils upon stimulation with C5a (2). We thought to investigate in further detail the activation patterns of C5a within the PI3K/Akt signaling pathway in neutrophils. We conducted *in vitro* studies stimulating isolated human neutrophils with C5a at various time points and various concentrations (Fig. 6). We found that C5a was capable of inducing Akt phosphorylation within 2–15 min, peaking at 5-min activation (data not shown). Concentrations of 50–100 ng/ml C5a demonstrated the strongest Akt phosphorylation potential (Fig. 6A). Blockade of the PI3K with LY294002 resulted in complete inhibition of Akt phosphorylation (Fig. 6B). We investigated upstream and downstream activation within the Akt signaling pathway induced by C5a. We found that C5a induced phosphorylation of GSK-3 β as well as the forkhead kinase family member FKHR in a time-dependent manner (Fig. 6C). Induction of the known negative regulator of Akt activation, the so-called phosphatase and tensin homolog deleted on chromosome 10, could also not be detected (data not shown).

Role of PI3K inhibition for C5a-mediated effects on LPS-induced generation of IL-1 β and IL-8 in neutrophils

A recent report described C5a as negative regulator for IL-12 generation in human monocytes, with this effect being dependent on

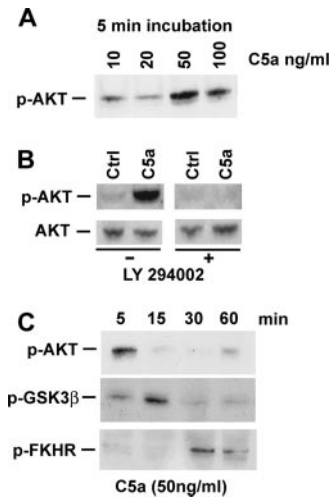


FIGURE 6. Activation of the PI3K pathway in human neutrophils by C5a. Western blot analysis of Akt activation (phosphorylation) in whole cell lysates of human neutrophils. A, Cells were stimulated at 37°C for 5 min with various concentrations of C5a, as depicted. B, Cells were stimulated for 5 min at 37°C in the absence or presence of 50 μ M LY294002. C, Western blot analysis of Akt, GSK-3 β , and FKHR activation in whole cell lysates of isolated human neutrophils. Cells were stimulated at 37°C with C5a (50 ng/ml) for various time points, as depicted. The blots are representative of two to three independent experiments.

C5a-induced PI3K/Akt activation (28). Our group described various regulatory effects of C5a on neutrophil mediator generation in concert with LPS-induced TLR-4 stimulation (2, 15, 16). We thought to investigate in greater detail the involvement of PI3K activation for LPS-induced mediator generation in neutrophils *in vitro*. Human neutrophils were isolated from blood and incubated for 6 h *in vitro* with C5a (50 ng/ml), LPS (50 ng/ml), or both in the absence or presence of the PI3K inhibitor LY294002 (Fig. 7). Stimulation of neutrophils with C5a alone did not result in significant generation of IL-1 β (Fig. 7A). LPS stimulation resulted in minor generation of IL-1 β , which was increased when PI3K signaling was absent. Costimulation of neutrophils with C5a and LPS *per se* did not result in significant increase of IL-1 β generation

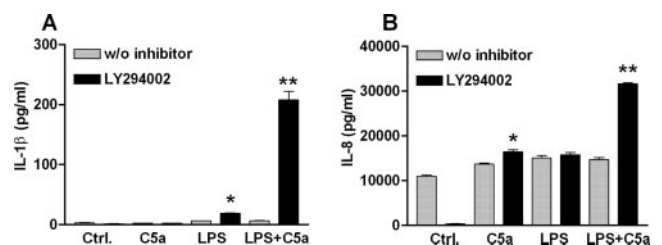
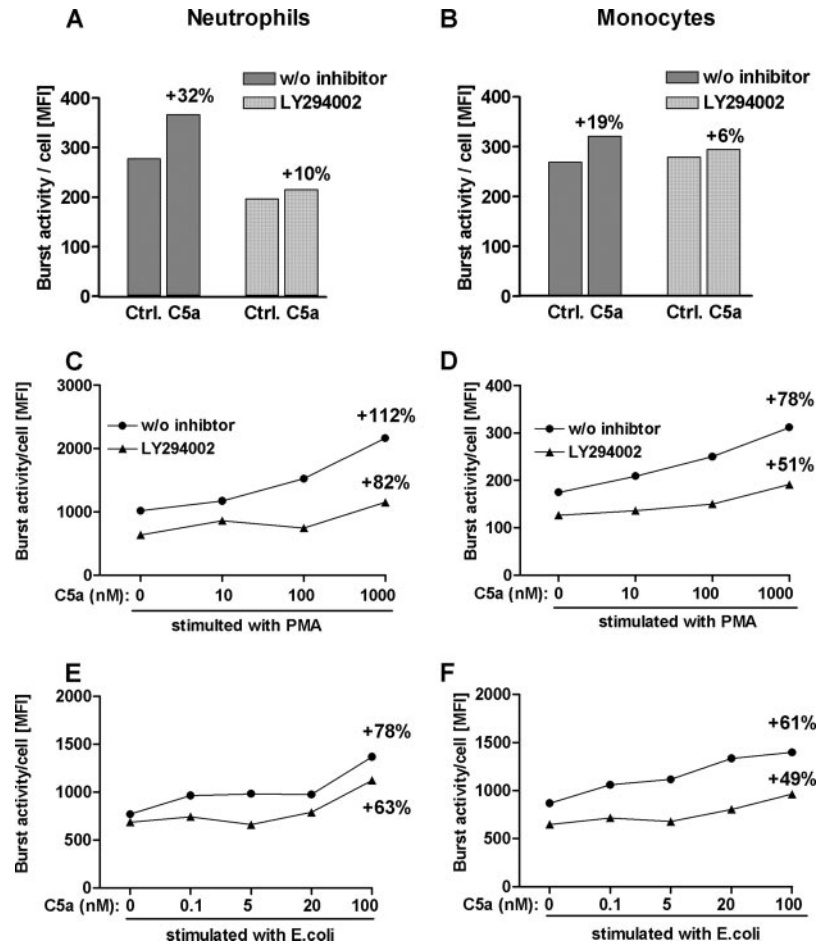


FIGURE 7. Effects of PI3K inhibition on C5a-mediated modulation of TLR-4-dependent generation of IL-1 β and IL-8 in human neutrophils. Flow cytometric bead ELISA of neutrophil supernatant fluids for IL-1 β (A) and IL-8 (B). Neutrophils were isolated from whole blood and incubated *in vitro* with C5a (50 ng/ml), LPS (50 ng/ml), or both for 6 h at 37°C at a concentration of 6×10^6 cells/ml. Cells were stimulated in the absence or presence of LY294002 after preincubation for 30 min at a concentration of 50 μ M. *, Statistical significant difference from the corresponding single treatment group (LPS and C5a, respectively) without LY294002. **, Statistical significant difference from the LPS + C5a-costimulated treatment group with no inhibitor. Data are representative of two to three independent experiments, with incubation and analysis being conducted in separate triplicate or quadruplicate samples.

FIGURE 8. Effects of PI3K inhibition on C5a-mediated modulation of oxidative burst in neutrophils and monocytes in human whole blood. Flow cytometric analysis of oxidative burst in whole blood samples gated for neutrophil and monocyte cell populations. Fifty thousand cells were analyzed for each experimental point. *A* and *B*, Human whole blood samples were preincubated with LY294002 (50 μ M) or equal amounts of vehicle. Samples were then incubated with or without C5a (100 ng/ml) for 60 min, and oxidative burst was measured with no further stimulation. *C–F*, Whole blood samples were preincubated with or without LY294002 (50 μ M) for 30 min and then incubated with different concentrations of C5a (0–10,000 ng/ml) for 20 min before final stimulation with either PMA (1.4 μ M) (*C* and *D*) or *E. coli* bacteria (6.7×10^8 /ml) (*E* and *F*) for 10 min. Oxidative burst activity per single cell is depicted as MFI. Percentages of the maximum increase in oxidative burst activity are calculated compared with control values (0 C5a) and depicted on the *right panels* of the curves. Data are representative of two to three independent experiments.



when compared with LPS-only stimulated cells. This changed dramatically, under conditions of PI3K inhibition. A similar phenomenon could be observed for generation of IL-8 (Fig. 7*B*). PI3K inhibition attenuated baseline IL-8 generation completely. This effect was counteracted by stimulation with C5a or LPS. The latter stimulation led to small, but significant increases in IL-8 generation after PI3K signaling was inhibited, when compared with C5a- or LPS-stimulated neutrophils undergoing no PI3K inhibition. Co-stimulation of neutrophils with LPS and C5a after PI3K blockade resulted in significantly enhanced IL-8 generation when compared with cells with intact PI3K signaling. These results suggested that the PI3K signaling pathway exerts an important inhibitory control function for C5a-mediated boost of TLR-4-dependent generation of the proinflammatory mediator IL-1 β and the potent chemoattractant IL-8.

Role of PI3K inhibition for C5a-mediated effects on oxidative burst generation in neutrophils and monocytes

Generation of oxidative burst represents a crucial function of the innate immune response to invading microorganisms. We thought to investigate the effect of PI3K inhibition on C5a-mediated oxidative burst and on C5a-mediated priming effects in human neutrophils and monocytes. We found that C5a induced oxidative burst in neutrophils and monocytes with regard to the intensity of burst activity per cell (Fig. 8, *A* and *B*), whereas only small effects could be observed on the total number of bursting cells (data not shown). When PI3K activation was inhibited, the observed increase was almost completely abolished in neutrophils and strongly reduced in monocytes, demonstrating involvement of this signaling pathway in C5a-mediated oxidative burst. We further

investigated whether C5a-mediated priming of oxidative burst was dependent on PI3K activation (Fig. 8, *C–F*). Whole blood samples were preincubated with or without LY294002 for 30 min and then treated with various concentrations of C5a for 20 min before being stimulated with either PMA or *E. coli*. PMA-induced oxidative burst was strongly primed by preincubation with C5a in both neutrophils and monocytes (Fig. 8, *C* and *D*). This effect was strongly reduced in both cell populations when PI3K activation was inhibited, suggesting PI3K dependency of this C5a-mediated priming effect for PMA-induced oxidative burst. Similar experiments were conducted using *E. coli* as stimulus for oxidative burst. Low concentrations of C5a (1 ng/ml) achieved a noticeable priming effect for *E. coli*-induced oxidative burst in neutrophils and monocytes (Fig. 8, *E* and *F*). This effect was clearly reduced when PI3K activation was inhibited. However, in neutrophils, preincubation with high doses of C5a (1000 ng/ml) resulted in strongly increased *E. coli*-induced oxidative burst even after inhibition of PI3K activation (Fig. 8*D*), suggesting another pathway being responsible for priming effects induced by high-dose C5a preincubation before *E. coli* stimulation. Similarly, in monocytes, the C5a-induced priming effect for higher doses of C5a (200–1000 ng/ml) was only slightly inhibited when PI3K activation was blocked (Fig. 8*F*).

Role of PI3K inhibition for C5a-mediated effects on phagocytosis in neutrophils and monocytes

The ability of neutrophils and monocytes to conduct phagocytosis represents another crucial function of the innate immune response, which has also been demonstrated to be strongly dependent on C5a/C5aR (29), as well as on C5a and activating Fc γ R in Kupffer cells (30). We thought to investigate whether C5a effects on

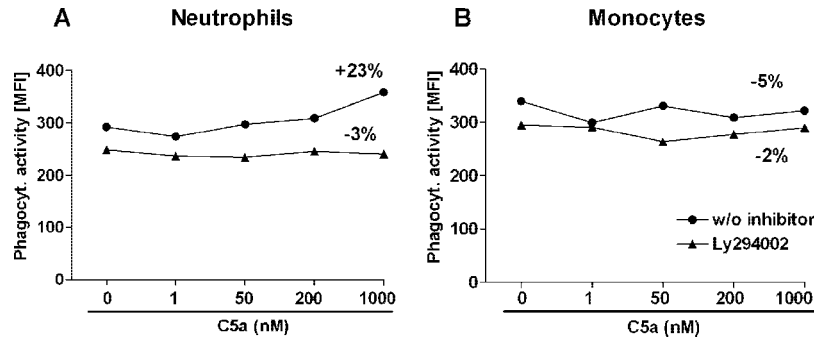


FIGURE 9. Effects of PI3K inhibition on C5a-mediated priming of *E. coli*-induced phagocytosis in neutrophils and monocytes in human whole blood. Flow cytometric analysis of phagocytosis in whole blood samples gated for neutrophil and monocyte cell populations. Fifty thousand cells were analyzed for each experimental point. Samples were preincubated with LY294002 (50 μ M) or equal amounts of vehicle control, and then incubated with different concentrations of C5a (0–1000 ng/ml) for 60 min before being stimulated for 10 min with opsonized FITC-conjugated *E. coli* bacteria (3.3×10^6 /ml). The phagocytosis activity per single cell of neutrophils (A) and monocytes (B) is given as MFI. Percentages of the maximum increase in phagocytosis activity are calculated compared with control values (0 C5a) and depicted on the right panels of the curves. Data are representative of two to three independent experiments.

E. coli-induced phagocytosis were dependent on PI3K signaling in neutrophils and monocytes. Preincubation of neutrophils with C5a resulted in dose-dependent enhancement of the phagocytic process induced by attenuated *E. coli* bacteria. This effect was completely abolished, when the PI3K signaling pathway was blocked, suggesting a strong dependency of this C5a-mediated priming effect on intact PI3K signaling (Fig. 9A). These findings could not be seen in monocytes applying the same experimental setting and assay (Fig. 9B). The number of phagocytosing cells was not considerably affected by C5a in both neutrophils and monocytes (data not shown).

Discussion

The PI3K/Akt signaling pathway has been suggested before to exert protective effects in models of acute inflammation (20, 31, 32), but rather harmful effects in models of chronic inflammation such as systemic lupus (33) or rheumatoid arthritis (34). It has also been described as important inhibitory pathway for apoptosis in neutrophils (5, 6, 35) and as important signaling pathway for LPS-induced B cell activation (36). Overexpression of Akt in lymphocytes prolonged their survival and also improved outcome in experimental sepsis (31), suggesting an important role of this signaling pathway during inflammation. However, until now, only little is known about the function of this pathway for innate immunity during acute inflammation. We demonstrate in this study an overall protective role of this pathway in our acute model of polymicrobial sepsis (Fig. 1) and a controlling inhibitory function for generation of various inflammatory mediators during the onset phase of sepsis (Fig. 2A). We were able to demonstrate that in vivo injection of LY294002 resulted in significant reduction of oxidative burst activity in blood monocytes and neutrophils in mice, offering a possible explanation for observed adverse effects for outcome during sepsis. Recent data demonstrated that inhibition of PI3K with wortmannin reversed the protective effects of glucan phosphate during experimental sepsis, demonstrating a protective effect of this pathway during acute inflammation (32). Our observations are in line with such earlier findings.

We compared the role of the PI3K pathway for TLR4-dependent generation of cytokines in vitro in neutrophils and monocytes. Interestingly, we were able to demonstrate opposing effects in these two cell populations. In neutrophils, PI3K activation appeared to limit the LPS response for generation of TNF- α , IL-6, IL-1 β , and IL-8 (Fig. 3, A, C, E, and G), whereas in monocytes PI3K activation appeared to have a significantly promoting function for LPS-

dependent generation of these mediators (Fig. 3, B, D, F, and H). Similar findings in monocytes have been reported regarding the role of PI3K for LPS-induced TNF- α generation (26). In bone marrow mouse neutrophils, a recent study reported that TLR-2-dependent activation of PI3K occurs, and that inhibitions of this pathway resulted in reduced generation of TNF- α and MIP2. The latter observations are somewhat in contrast to our findings, even though it cannot be excluded that TLR-2-dependent generation of TNF- α in neutrophils is controlled by PI3K differently from the TLR-4-dependent one. Also, another study recently reported crucial differences between mouse and human neutrophils with respect to the importance of various PI3K subunits, making observation regarding PI3K activation in mouse neutrophils difficult to compare with those in humans (18). The same may or may not apply to monocytes.

In the context of mediator generation, the findings in vivo during sepsis in mice (Fig. 2A) clearly demonstrate an inhibitory potential of the PI3K pathway. Our in vitro studies reflect these findings only in neutrophils, but not in PBMC (Fig. 3). The question as to which of these two cell populations is responsible for the cytokine storm in vivo during sepsis is puzzling. Complex interactions between various blood phagocytes and also endothelial cells further complicate this matter. Earlier studies of our own group demonstrated that neutrophil depletion clearly diminished the IL-6 generation in the serum of septic mice (15), suggesting a leading role of neutrophils. However, the question outlined above cannot be finally answered as of yet.

Neutrophils are generally regarded as driving force for acute inflammation, whereas monocytes are thought to be more important in chronic inflammation. In this context, our observations may partially explain why PI3K activation appears to be beneficial in acute inflammatory processes, e.g., by limiting neutrophil activation, whereas being harmful in more chronic inflammatory processes, e.g., by promoting monocyte activation.

As outlined earlier, PI3K activation has been reported before to be involved in regulating oxidative burst and phagocytosis in neutrophils and monocytes (17, 18, 20, 37). However, no studies have been conducted to compare these cell populations directly. We report in this study that PI3K inhibition resulted in impaired oxidative burst and phagocytosis activity in both neutrophils and monocytes (Figs. 4 and 5). In neutrophils, this effect was especially strong for PMA-induced oxidative burst, whereas in monocytes the inhibitory effect was more prominent for *E. coli*-induced oxidative

burst. These findings again suggest different regulatory functions of this pathway in neutrophils when compared with monocytes.

The concept of C5a/C5aR interception during sepsis has evolved in recent years, and C5a has become an interesting target for potential clinical interventions in the field of acute inflammation and especially sepsis (1). Our and other groups have suggested that large amounts of C5a are generated early during the onset of sepsis, but the intracellular regulatory mechanisms controlling C5a-induced effects on innate immune functions are not understood in detail. We have found recently that C5a negatively regulates LPS-induced production of TNF- α by rat neutrophils *in vitro*, but has the opposite effect on macrophages (16). In this study, TNF- α generation in neutrophils was strongly dependent on NF- κ B activation, and treatment of CLP mice with anti-C5a caused enhanced serum levels of TNF- α , apparently by protecting the signaling pathways from C5a-induced dysfunction. We also recently demonstrated involvement of p38 and ERK1/2 activation in generation of IL-6 in neutrophils (15) and reported that the PI3K signaling pathway is involved in LPS-mediated macrophage migration inhibitory factor generation in neutrophils (2). A recent report from another group described C5a as negative regulator for IL-12 generation in human monocytes, with this effect being dependent on C5a-induced PI3K/Akt activation (28). We thought to investigate in greater detail the role of the PI3K/Akt signaling pathway for C5a-induced alterations of mediator generation upon TLR4 stimulation in neutrophils. We found that C5a-mediated effects on LPS-induced IL-1 β and IL-8 generation were controlled in an inhibitory fashion by the PI3K pathway (Fig. 7), offering a partial explanation for the observed rise of serum inflammatory mediators in CLP mice after PI3K inhibition.

Oxidative burst and phagocytosis represent key players of the innate immune response to invading microorganisms. Recent work has demonstrated the importance of C5a for an intact oxidative burst and phagocytosis in neutrophils and monocytes in response to *E. coli* in a new whole blood assay applying flow cytometric analysis (29). The PI3K/Akt pathway has also been described to be an important mediator of neutrophil oxidative burst in other assays using isolated human neutrophils (17). The ability of Kupffer cells to conduct phagocytosis has been described to be regulated by C5a as well as activating Fc γ R in recent studies (30). The PI3K pathway appears to be important late in the process of phagocytosis in neutrophils and monocytes, namely during the phagosome closure after cup formation (37, 38). We thought to investigate in how far C5a-dependent regulation of oxidative burst and phagocytosis was dependent on PI3K activation in neutrophils and peripheral blood monocytes. Our results demonstrated that C5a-mediated priming of *E. coli*- and PMA-induced oxidative burst was largely dependent on intact PI3K signaling in both neutrophils and monocytes. C5a-mediated enhancement of phagocytosis appeared also to be dependent on PI3K activation in neutrophils.

Taken together, our results suggest that the PI3K signaling pathway exerts an overall protective role during the onset of sepsis in rodents by limiting C5a-mediated effects on neutrophil cytokine generation, and promoting oxidative burst and phagocytosis. We further propose that this pathway has opposing regulatory mechanisms in TLR-4-mediated cytokine generation in neutrophils when compared with monocytic cells. Inducing the activation of this pathway may represent a therapeutic approach for limiting acute inflammatory diseases such as sepsis.

Acknowledgment

We thank Gerda Bartling for excellent technical assistance with the microbiological analyses of the peritoneal lavage fluids.

Disclosures

The authors have no financial conflict of interest.

References

- Riedemann, N. C., R. F. Guo, and P. A. Ward. 2003. Novel strategies for the treatment of sepsis. *Nat. Med.* 9: 517–524.
- Riedemann, N. C., R. F. Guo, H. Gao, L. Sun, M. Hoesel, T. J. Hollmann, R. A. Wetsel, F. S. Zetoune, and P. A. Ward. 2004. Regulatory role of C5a on macrophage migration inhibitory factor release from neutrophils. *J. Immunol.* 173: 1355–1359.
- Klein, J. B., A. Buridi, P. Y. Coxon, M. J. Rane, T. Manning, R. Ketritz, and K. R. McLeish. 2001. Role of extracellular signal-regulated kinase and phosphatidylinositol-3 kinase in chemoattractant and LPS delay of constitutive neutrophil apoptosis. *Cell. Signal.* 13: 335–343.
- Hu, Z., and M. M. Sayeed. 2005. Activation of PI3-kinase/PKB contributes to delay in neutrophil apoptosis after thermal injury. *Am. J. Physiol.* 288: C1171–C1178.
- Perianayagam, M. C., V. S. Balakrishnan, A. J. King, B. J. Pereira, and B. L. Jaber. 2002. C5a delays apoptosis of human neutrophils by a phosphatidylinositol 3-kinase-signaling pathway. *Kidney Int.* 61: 456–463.
- Perianayagam, M. C., V. S. Balakrishnan, B. J. Pereira, and B. L. Jaber. 2004. C5a delays apoptosis of human neutrophils via an extracellular signal-regulated kinase and Bad-mediated signalling pathway. *Eur. J. Clin. Invest.* 34: 50–56.
- Ward, P. A. 2004. The dark side of C5a in sepsis. *Nat. Rev. Immunol.* 4: 133–142.
- Guo, R. F., and P. A. Ward. 2005. Role of C5a in inflammatory responses. *Annu. Rev. Immunol.* 23: 821–852.
- Czermak, B. J., V. Sarma, C. L. Pierson, R. L. Warner, M. Huber-Lang, N. M. Bless, H. Schmal, H. P. Friedl, and P. A. Ward. 1999. Protective effects of C5a blockade in sepsis. *Nat. Med.* 5: 788–792.
- Riedemann, N. C., R. F. Guo, T. A. Neff, I. J. Laudes, K. A. Keller, V. J. Sarma, M. M. Markiewski, D. Mastellos, C. W. Strey, C. L. Pierson, et al. 2002. Increased C5a receptor expression in sepsis. *J. Clin. Invest.* 110: 101–108.
- Huber-Lang, M. S., E. M. Younkin, J. V. Sarma, S. R. McGuire, K. T. Lu, R. F. Guo, V. A. Padgaonkar, J. T. Curnutte, R. Erickson, and P. A. Ward. 2002. Complement-induced impairment of innate immunity during sepsis. *J. Immunol.* 169: 3223–3231.
- Huber-Lang, M. S., N. C. Riedemann, J. V. Sarma, E. M. Younkin, S. R. McGuire, I. J. Laudes, K. T. Lu, R. F. Guo, T. A. Neff, V. A. Padgaonkar, et al. 2002. Protection of innate immunity by C5aR antagonist in septic mice. *FASEB J.* 16: 1567–1574.
- Solomkin, J. S., M. K. Jenkins, R. D. Nelson, D. Chenoweth, and R. L. Simmons. 1981. Neutrophil dysfunction in sepsis. II. Evidence for the role of complement activation products in cellular deactivation. *Surgery* 90: 319–327.
- Guo, R. F., N. C. Riedemann, K. D. Bernacki, V. J. Sarma, I. J. Laudes, J. S. Reuben, E. M. Younkin, T. A. Neff, J. D. Paulauskis, F. S. Zetoune, and P. A. Ward. 2003. Neutrophil C5a receptor and the outcome in a rat model of sepsis. *FASEB J.* 17: 1889–1891.
- Riedemann, N. C., R. F. Guo, T. J. Hollmann, H. Gao, T. A. Neff, J. S. Reuben, C. L. Speyer, J. V. Sarma, R. A. Wetsel, F. S. Zetoune, and P. A. Ward. 2004. Regulatory role of C5a in LPS-induced IL-6 production by neutrophils during sepsis. *FASEB J.* 18: 370–372.
- Riedemann, N. C., R. F. Guo, K. D. Bernacki, J. S. Reuben, I. J. Laudes, T. A. Neff, H. Gao, C. Speyer, V. J. Sarma, F. S. Zetoune, and P. A. Ward. 2003. Regulation by C5a of neutrophil activation during sepsis. *Immunity* 19: 193–202.
- Chen, Q., D. W. Powell, M. J. Rane, S. Singh, W. Butt, J. B. Klein, and K. R. McLeish. 2003. Akt phosphorylates p47^{phox} and mediates respiratory burst activity in human neutrophils. *J. Immunol.* 170: 5302–5308.
- Condliffe, A. M., K. Davidson, K. E. Anderson, C. D. Ellison, T. Crabbe, K. Okkenhaug, B. Vanhaesebroeck, M. Turner, L. Webb, M. P. Wymann, et al. 2005. Sequential activation of class IB and class IA PI3K is important for the primed respiratory burst of human but not murine neutrophils. *Blood* 106: 1432–1440.
- Hannigan, M., L. Zhan, Z. Li, Y. Ai, D. Wu, and C. K. Huang. 2002. Neutrophils lacking phosphoinositide 3-kinase γ show loss of directionality during N-formyl-Met-Leu-Phe-induced chemotaxis. *Proc. Natl. Acad. Sci. USA* 99: 3603–3608.
- Hirsch, E., V. L. Katanaev, C. Garlanda, O. Azzolino, L. Pirola, L. Silengo, S. Sozzani, A. Mantovani, F. Altruda, and M. P. Wymann. 2000. Central role for G protein-coupled phosphoinositide 3-kinase γ in inflammation. *Science* 287: 1049–1053.
- Sadhu, C., K. Dick, W. T. Tino, and D. E. Staunton. 2003. Selective role of PI3K δ in neutrophil inflammatory responses. *Biochem. Biophys. Res. Commun.* 308: 764–769.
- Puri, K. D., T. A. Doggett, J. Douangpanya, Y. Hou, W. T. Tino, T. Wilson, T. Graf, E. Clayton, M. Turner, J. S. Hayflick, and T. G. Diacovo. 2004. Mechanisms and implications of phosphoinositide 3-kinase δ in promoting neutrophil trafficking into inflamed tissue. *Blood* 103: 3448–3456.
- Puri, K. D., T. A. Doggett, C. Y. Huang, J. Douangpanya, J. S. Hayflick, M. Turner, J. Penninger, and T. G. Diacovo. 2005. The role of endothelial PI3K γ activity in neutrophil trafficking. *Blood* 106: 150–157.
- Ong, E., X. P. Gao, D. Predescu, M. Broman, and A. B. Malik. 2005. Role of phosphatidylinositol 3-kinase- γ in mediating lung neutrophil sequestration and vascular injury induced by *E. coli* sepsis. *Am. J. Physiol.* 289: L1094–L1103.
- Sadhu, C., B. Masinovsky, K. Dick, C. G. Sowell, and D. E. Staunton. 2003. Essential role of phosphoinositide 3-kinase δ in neutrophil directional movement. *J. Immunol.* 170: 2647–2654.

26. Guha, M., and N. Mackman. 2002. The phosphatidylinositol 3-kinase-Akt pathway limits lipopolysaccharide activation of signaling pathways and expression of inflammatory mediators in human monocytic cells. *J. Biol. Chem.* 277: 32124–32132.
27. Chiou, W. F., H. R. Tsai, L. M. Yang, and W. J. Tsai. 2004. C5a differentially stimulates the ERK1/2 and p38 MAPK phosphorylation through independent signaling pathways to induced chemotactic migration in RAW264.7 macrophages. *Int. Immunopharmacol.* 4: 1329–1341.
28. La Sala, A., M. Gadina, and B. L. Kelsall. 2005. G_i-protein-dependent inhibition of IL-12 production is mediated by activation of the phosphatidylinositol 3-kinase-protein 3 kinase B/Akt pathway and JNK. *J. Immunol.* 175: 2994–2999.
29. Mollnes, T. E., O. L. Brekke, M. Fung, H. Fure, D. Christiansen, G. Bergseth, V. Videm, K. T. Lappégard, J. Kohl, and J. D. Lambris. 2002. Essential role of the C5a receptor in *E. coli*-induced oxidative burst and phagocytosis revealed by a novel lepirudin-based human whole blood model of inflammation. *Blood* 100: 1869–1877.
30. Kumar, V., S. R. Ali, S. Konrad, J. Zwirner, J. S. Verbeek, R. E. Schmidt, and J. E. Gessner. 2006. Cell-derived anaphylatoxins as key mediators of antibody-dependent type II autoimmunity in mice. *J. Clin. Invest.* 116: 512–520.
31. Bommhardt, U., K. C. Chang, P. E. Swanson, T. H. Wagner, K. W. Tinsley, I. E. Karl, and R. S. Hotchkiss. 2004. Akt decreases lymphocyte apoptosis and improves survival in sepsis. *J. Immunol.* 172: 7583–7591.
32. Williams, D. L., C. Li, T. Ha, T. Ozment-Skelton, J. H. Kalbfleisch, J. Preiszner, L. Brooks, K. Breuel, and J. B. Schweitzer. 2004. Modulation of the phosphoinositide 3-kinase pathway alters innate resistance to polymicrobial sepsis. *J. Immunol.* 172: 449–456.
33. Barber, D. F., A. Bartolome, C. Hernandez, J. M. Flores, C. Redondo, C. Fernandez-Arias, M. Camps, T. Ruckle, M. K. Schwarz, S. Rodriguez, et al. 2005. PI3K γ inhibition blocks glomerulonephritis and extends lifespan in a mouse model of systemic lupus. *Nat. Med.* 11: 933–935.
34. Camps, M., T. Ruckle, H. Ji, V. Ardisson, F. Rintelen, J. Shaw, C. Ferrandi, C. Chabert, C. Gillieron, B. Francon, et al. 2005. Blockade of PI3K γ suppresses joint inflammation and damage in mouse models of rheumatoid arthritis. *Nat. Med.* 11: 936–943.
35. Klein, J. B., M. J. Rane, J. A. Scherzer, P. Y. Coxon, R. Kettritz, J. M. Mathiesen, A. Buridi, and K. R. McLeish. 2000. Granulocyte-macrophage colony-stimulating factor delays neutrophil constitutive apoptosis through phosphoinositide 3-kinase and extracellular signal-regulated kinase pathways. *J. Immunol.* 164: 4286–4291.
36. Venkataraman, C., G. Shankar, G. Sen, and S. Bondada. 1999. Bacterial lipopolysaccharide induced B cell activation is mediated via a phosphatidylinositol 3-kinase dependent signaling pathway. *Immunol. Lett.* 69: 233–238.
37. Dewitt, S., W. Tian, and M. B. Hallett. 2006. Localised PtdIns(3,4,5)P₃ or PtdIns(3,4)P₂ at the phagocytic cup is required for both phagosome closure and Ca²⁺ signalling in HL60 neutrophils. *J. Cell Sci.* 119: 443–451.
38. Cox, D., C. C. Tseng, G. Bjekic, and S. Greenberg. 1999. A requirement for phosphatidylinositol 3-kinase in pseudopod extension. *J. Biol. Chem.* 274: 1240–1247.

Upregulation of Phagocyte-Derived Catecholamines Augments the Acute Inflammatory Response

Michael A. Flierl¹, Daniel Rittirsch¹, Brian A. Nadeau¹, J. Vidya Sarma¹, Danielle E. Day¹, Alex B. Lentsch², Markus S. Huber-Lang³, Peter A. Ward^{1*}

1 Department of Pathology, University of Michigan Medical School, Ann Arbor, Michigan, United States of America, **2** The Laboratory of Trauma, Sepsis & Inflammation Research, Department of Surgery, University of Cincinnati College of Medicine, Cincinnati, Ohio, United States of America, **3** Department of Trauma-, Hand- and Reconstructive Surgery, University of Ulm Medical School, Ulm, Germany

Abstract

Following our recent report that phagocytic cells (neutrophils, PMNs, and macrophages) are newly discovered sources of catecholamines, we now show that both epinephrine and norepinephrine directly activate NF κ B in macrophages, causing enhanced release of proinflammatory cytokines (TNF α , IL-1 β , IL-6). Both adrenal-intact (AD+) and adrenalectomized (ADX) rodents were used, because ADX animals had greatly enhanced catecholamine release from phagocytes, facilitating our efforts to understand the role of catecholamines released from phagocytes. Phagocytes isolated from adrenalectomized rats displayed enhanced expression of tyrosine-hydroxylase and dopamine- β -hydroxylase, two key enzymes for catecholamine production and exhibited higher baseline secretion of norepinephrine and epinephrine. The effects of upregulation of phagocyte-derived catecholamines were investigated in two models of acute lung injury (ALI). Increased levels of phagocyte-derived catecholamines were associated with intensification of the acute inflammatory response, as assessed by increased plasma leak of albumin, enhanced myeloperoxidase content in lungs, augmented levels of proinflammatory mediators in bronchoalveolar lavage fluids, and elevated expression of pulmonary ICAM-1 and VCAM-1. In adrenalectomized rats, development of ALI was enhanced and related to α_2 -adrenoceptors engagement but not to involvement of mineralocorticoid or glucocorticoid receptors. Collectively, these data demonstrate that catecholamines are potent inflammatory activators of macrophages, upregulating NF κ B and further downstream cytokine production of these cells. In adrenalectomized animals, which have been used to further assess the role of catecholamines, there appears to be a compensatory increase in catecholamine generating enzymes and catecholamines in macrophages, resulting in amplification of the acute inflammatory response via engagement of α_2 -adrenoceptors.

Citation: Flierl MA, Rittirsch D, Nadeau BA, Sarma JV, Day DE, et al. (2009) Upregulation of Phagocyte-Derived Catecholamines Augments the Acute Inflammatory Response. PLoS ONE 4(2): e4414. doi:10.1371/journal.pone.0004414

Editor: Patricia Bozza, Instituto Oswaldo Cruz and FIOCRUZ, Brazil

Received: September 25, 2008; **Accepted:** December 16, 2008; **Published:** February 12, 2009

Copyright: © 2009 Flierl et al. This is an open-access article distributed under the terms of the Creative Commons Attribution License, which permits unrestricted use, distribution, and reproduction in any medium, provided the original author and source are credited.

Funding: This study was supported by NIH grants GM29507, GM61656 and HL-31963 (P.A.W.), NIH grants DK56029 and AG025881 (A.B.L.) and Deutsche Forschungsgemeinschaft grants HU 823/2-2 and HU 823/2-3 (M.H.-L.). The funding agencies had no role in study design, data collection and analysis, decision to publish, or preparation of the manuscript.

Competing Interests: The authors have declared that no competing interests exist.

* E-mail: pward@umich.edu

Introduction

During an immune response, the central nervous system and the immune system communicate with each other [1]. The major pathway systems involved in this cross-talk are the hypothalamic-pituitary-adrenal (HPA) axis and the autonomic nervous system [1–3]. Activation of the vagus-dominated parasympathetic, cholinergic nervous system is known to greatly attenuate and dampen the inflammatory response via nicotinic cholinergic receptors expressed on macrophages and other immune cells [4,5]. According to its afferent and efferent arms, this effect has been termed “inflammatory reflex” [2] or “cholinergic anti-inflammatory pathway” [6]. In contrast, the role of the sympathetic nervous system (SNS) during inflammation seems to be more complex and less well understood. On the one hand, SNS activation seems to target immune cells that express adrenoceptors, exacerbating the local inflammatory response [7,8], and increase the general immune and proinflammatory mediator response [9–11]. On the other hand, several studies indicate an inhibitory effect of the SNS on the inflammatory response, suppressing the immune

response by decreasing the activity of natural killer cells and T cell immunity [12–15]. In addition, catecholamines released from presynaptic sympathetic nerve terminals lead to localized vasoconstriction, preventing invading pathogens from becoming systemic [3].

Over two decades ago, lymphocytes were described as sources of catecholamines [16]. These lymphocyte-derived catecholamines seem to act in an autocrine/paracrine fashion that affects lymphocyte trafficking [17], vascular perfusion, cell proliferation [18], cytokine production and the functional activity of lymphocytes [19,20]. Recently, phagocytes (macrophages and neutrophils) have also been identified as a newly recognized source of catecholamines that exert a similar autocrine/paracrine regulation of phagocytes following release of norepinephrine or epinephrine [8,20–22]. Additional experiments demonstrated that blockade of these phagocyte-derived catecholamines (by pharmacological blockade of catecholamine generating enzymes or blockade of adrenoceptors) greatly attenuated lung inflammatory injury, while the opposite was the case when the catecholamine-inactivating enzymes catechol-O-methyltransferase (COMT) and monoamine

oxidase (MAO) were inhibited [8]. Therefore, activation of the adrenergic system during an inflammatory response may greatly enhance the local inflammatory response, resulting in neutrophil accumulation [23] and enhanced cytokine production. In the current study, we sought to further define the role of phagocyte-derived catecholamines on inflammation on a molecular level and in a setting of acute inflammatory, single organ injury.

Results

Catecholamines Induce NF κ B Activation and Release of Cytokines in Mouse Macrophages

Following isolation, peritoneal mouse macrophages were stimulated with a range of concentrations of norepinephrine or epinephrine (10^{-12} – 10^{-6} M) for 30 min at 37°C. While unstimulated macrophages exhibited low levels of NF κ B activation, significant NF κ B activation occurred in a dose-dependent manner, peaking at the 10^{-10} M dose of catecholamine (Figure 1A, B). In parallel, a dose-dependent decrease of I κ B α levels in cytosolic fractions of macrophages (Figure 1C, D) was found following exposure to norepinephrine or epinephrine. Similar results were obtained with mouse neutrophils (data not shown).

This suggests induction of intracellular proinflammatory pathways by norepinephrine and epinephrine. To evaluate if this catecholamine-induced activation of NF κ B was followed by increased downstream production of proinflammatory cytokines, peritoneal mouse macrophages were incubated for 4 hrs at 37°C with either HBSS (negative control), LPS (positive control, 20 ng/

ml), or various doses of norepinephrine or epinephrine that lead to NF κ B activation (10^{-11} – 10^{-8} M). The cell supernatant fluids were evaluated for TNF α , IL-1 β and IL-6 and MIP-2 by ELISA. Exposure to norepinephrine or epinephrine not only induced activation of NF κ B (Figure 1), but caused release of TNF α , IL-1 β and IL-6 and MIP-2 from isolated macrophages in a dose dependent manner (Figures 2 and 3). Interestingly, 10^{-10} M norepinephrine or epinephrine alone caused $\geq 50\%$ of the amounts of released LPS cytokines when compared to macrophages incubated with LPS (20 ng/ml).

Increased Baseline-Expression of Catecholamine-generating Enzymes and Upregulation of Catecholamine Secretion in Phagocytes obtained from Adrenalectomized (ADX) Animals

We have recently identified phagocytes as a newly recognized source of norepinephrine and epinephrine [8]. To investigate the inflammatory potential of phagocyte-derived catecholamines, we isolated both blood neutrophils and alveolar macrophages from otherwise healthy and untreated adrenal-intact (AD+) and adrenalectomized (ADX) rats. When mRNA was obtained from isolated, unstimulated cells, phagocytes from ADX animals expressed higher baseline levels for the two key enzymes involved in catecholamine synthesis, tyrosine-hydroxylase (TH) and dopamine- β -hydroxylase (DBH) (Figure 4A, B), as demonstrated by real-time PCR. In parallel, the basal secretion (after 15 min in culture) of norepinephrine and epinephrine from isolated and otherwise untreated blood neutrophils and alveolar macrophages

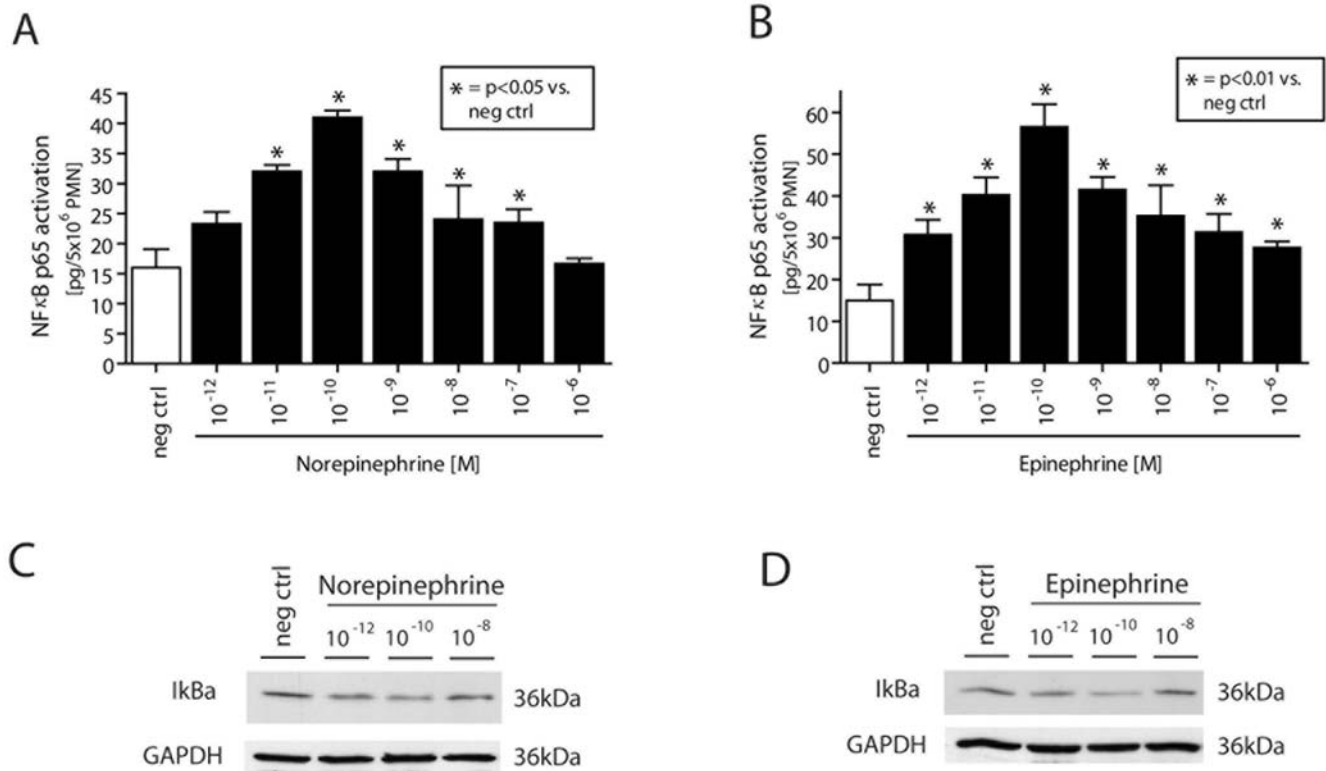


Figure 1. Isolated peritoneal mouse macrophages (A, B) were exposed to various concentrations of norepinephrine or epinephrine for 30 min at 37°C. Then, nuclear proteins were extracted from 10×10^6 cells protein concentrations adjusted and NF κ B p65 activation assessed. Each bar represents $n=4$. In a second set of experiments, following incubation with various concentrations of norepinephrine or epinephrine (30 min, 37°C), peritoneal mouse macrophages (5×10^6 /ml; C, D) were lysed and cytosol subjected to Western blotting analysis for I κ B α . Depicted blots are representative of 3 independent experiments. Neg ctrl, incubation with HBSS. doi:10.1371/journal.pone.0004414.g001

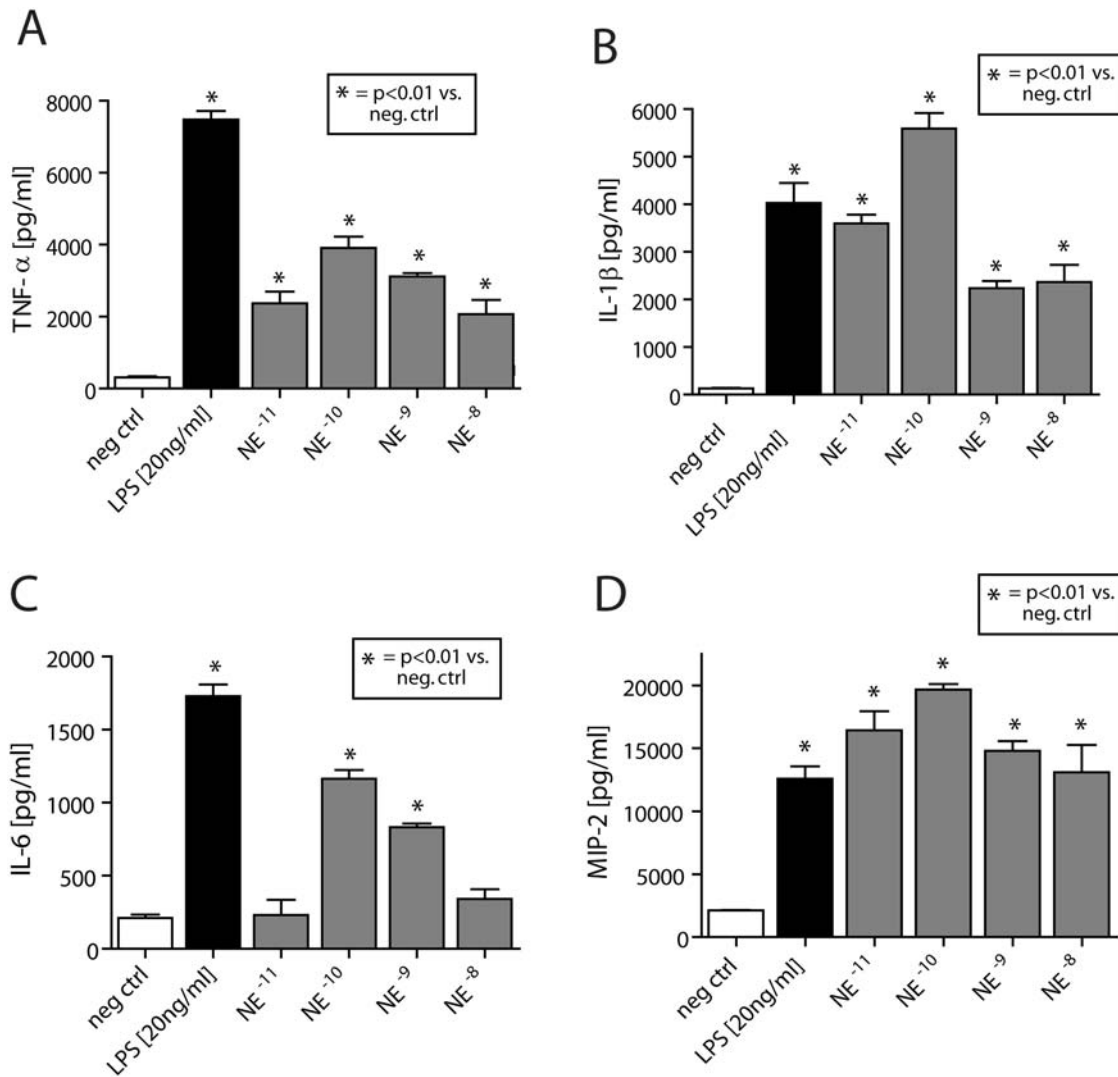


Figure 2. Isolated peritoneal mouse macrophages were exposed to various concentrations of norepinephrine (10^{-11} – 10^{-8} M) or LPS (20 ng/ml, positive control) for 30 min at 37°C. Then, supernatant fluids were obtained and subjected to ELISA analysis for TNF- α (A), IL-1 β (B), IL-6 (C) and MIP-2 (D). Each bar represents n=4–7. Neg ctrl, incubation with HBSS. doi:10.1371/journal.pone.0004414.g002

was significantly increased in phagocytic cells derived from ADX animals when compared to cells from AD+ animals (Figure 4C, D). This may represent a compensatory response in order to maintain intrinsic catecholamine levels in the absence of adrenal glands.

Adrenalectomized Animals Display Elevated Baseline Levels in Plasma of Proinflammatory Mediators

To investigate whether the increased phagocytic baseline production of catecholamines in ADX rats (Figure 4) would result in activation of NF κ B (Figure 1) with subsequent release of TNF α , IL-1 β and IL-6 and MIP-2 by macrophages (Figures 2 and 3) *in vivo*, plasma from healthy and otherwise untreated AD+ or ADX animals was obtained and screened for baseline levels of proinflammatory mediators. As shown in Table 1, ADX animals displayed but statistically significant increase in plasma levels of the proinflammatory cytokines (TNF α , IL-1 β and IL-6), as well as the inflammatory chemokine, CINC-1, when compared to AD+ littermates.

Adrenalectomy Exacerbates Acute Lung Injury

Figures 5 and 6 display data obtained in the immune complex-induced ALI model. As shown in Figure 5, adrenalectomized (ADX) rats showed a greatly enhanced intensity of the acute inflammatory response. The permeability index (an indicator of vascular leakage of albumin) increased nearly 3 fold in ADX rats (Figure 5A) when compared to AD+ rats. Myeloperoxidase (MPO) content in lung homogenates increased nearly 50% in ADX rats (Figure 5B), and bronchoalveolar lavage (BAL) fluids had a higher leukocyte content (by nearly 2 fold), due to increased content of PMNs which accounted for >95% of BAL leukocytes (Figure 5C). The intensified level of injury was also apparent in morphological changes in lungs (Figure 5, frames D–I). While ADX and adrenal-intact rats exhibited comparable features in control (uninjured) lungs (Figure 5D, G), ADX animals had clearly increased evidence of injury as reflected in intensified number of PMNs, fibrin and hemorrhage in the interstitial and alveolar compartments (Figure 3H, I) when compared to lungs from adrenal intact rats (Figure 5E, F).

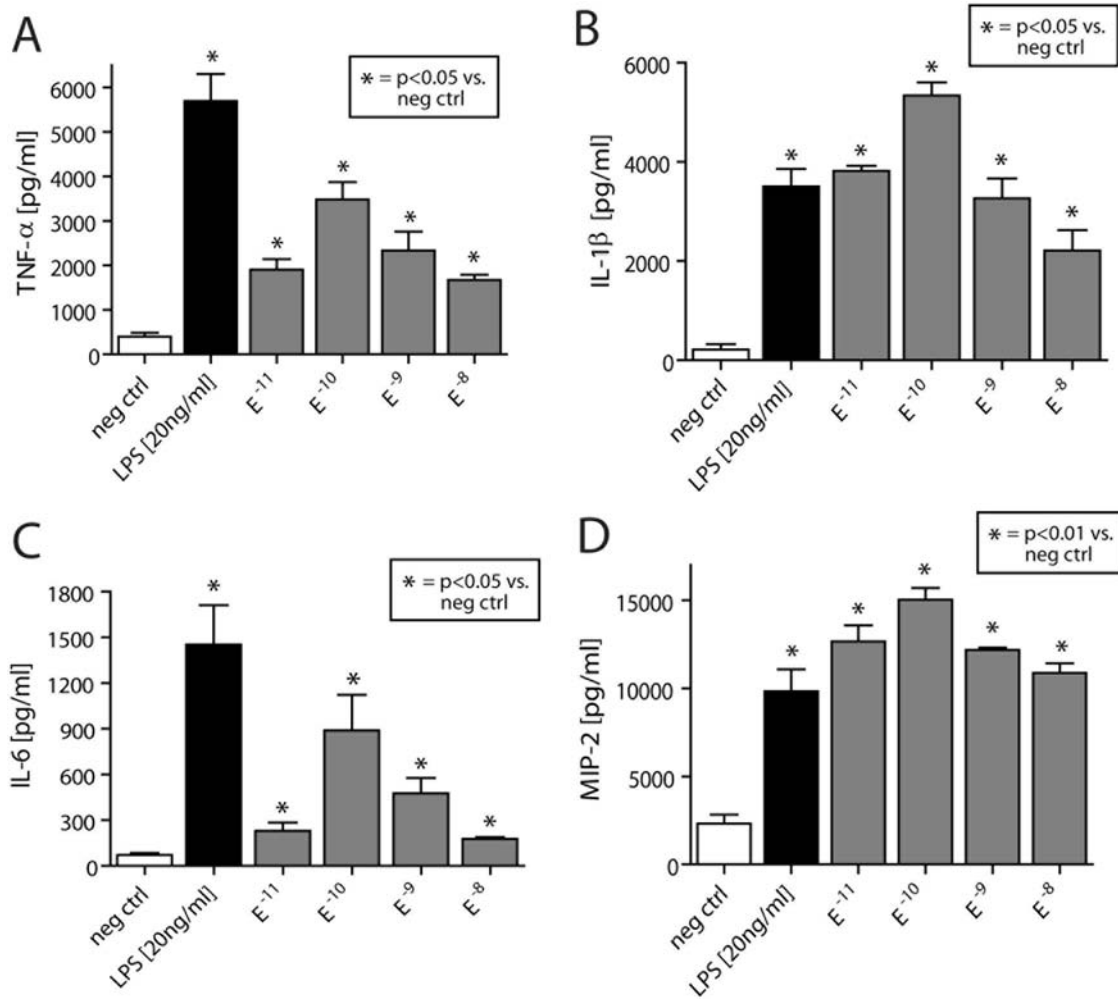


Figure 3. Following isolation, peritoneal mouse macrophages incubated to HBSS (negative control), LPS (20 ng/ml, positive control) or 10^{-11} – 10^{-8} M epinephrine (30 min, 37°C). Obtained supernatants were analyzed for TNF- α (A), IL-1 β (B), IL-6 (C) and MIP-2 (D) using ELISA measurements. n = 4–7 per experimental group. doi:10.1371/journal.pone.0004414.g003

Enhanced lung injury in ADX rats was also reflected in BAL fluid analysis from adrenal-intact and ADX rats, which consistently showed significantly increased levels of proinflammatory cytokines (IL-6, TNF α and IL-1 β) (Figure 6A–C) in ADX animals. In parallel, the levels of norepinephrine in BAL fluids from injured lungs were significantly elevated in ADX animals when compared to adrenal-intact littermates (Figure 6D). As demonstrated by Western blots in lung homogenates, the adhesion molecules ICAM-1 and VCAM-1 were modestly and significantly upregulated during lung injury (Figure 6, lower frames E, F). ADX animals had higher levels of these cell adhesion molecules than their adrenal-intact littermates. Finally, as expected, ADX rats showed evidence suggesting enhanced activation of NF κ B in lung homogenates as assessed by EMSA (data not shown).

To exclude that these results were unique to immune complex-induced ALI, lung injury was also induced in rats by intra-tracheal administration of LPS and subjected to analysis for vascular leakage, MPO content, BAL fluid cytokines measurements and histological analysis. The results, as shown in Figure 7, paralleled the pattern found in IC-induced lung injury, indicating amplified injury in ADX rats as defined by increased albumin leakage (frame A), elevated MPO content (frame B), amplified cytokine levels in BAL

fluids (frames C–E) and enhanced histopathology of inflammation (neutrophils, fibrin) and injury (hemorrhage) (frames F–I).

The α_2 -adrenergic Receptor Mediates the Severity of Acute Lung Injury in ADX Rats

Recently, we have described a central role for α_2 -adrenoceptor in the pathophysiology of experimental acute lung injury [8]. Pharmacological α_2 -adrenoceptor blockade by RX821002 greatly reduced the intensity of ALI, while blockade of all other adrenoceptors failed to change the intensity of lung injury [8]. To determine if α_2 -adrenoceptors or rather the absence of mineralocorticoids and glucocorticoids might account for the increased level of inflammatory lung injury in ADX rats, we administered the specific α_2 -adrenoceptor blocker, (RX 821002), or the competitive aldosterone receptor antagonist (spironolactone) in adrenal-intact and adrenalectomized animals immediately after induction of IC-ALI. The glucocorticoid receptor antagonist, RU 28362, was administered 1 hr before initiation of lung injury. As shown in Figure 8, blockade of the α_2 -adrenergic receptor significantly reduced by 70% ($p < 0.01$) the intensity of the albumin leak into lungs of ADX rats. In AD+ animals, blockade of the α_2 -adrenoceptor reduced the albumin leak following ALI by ~46%,

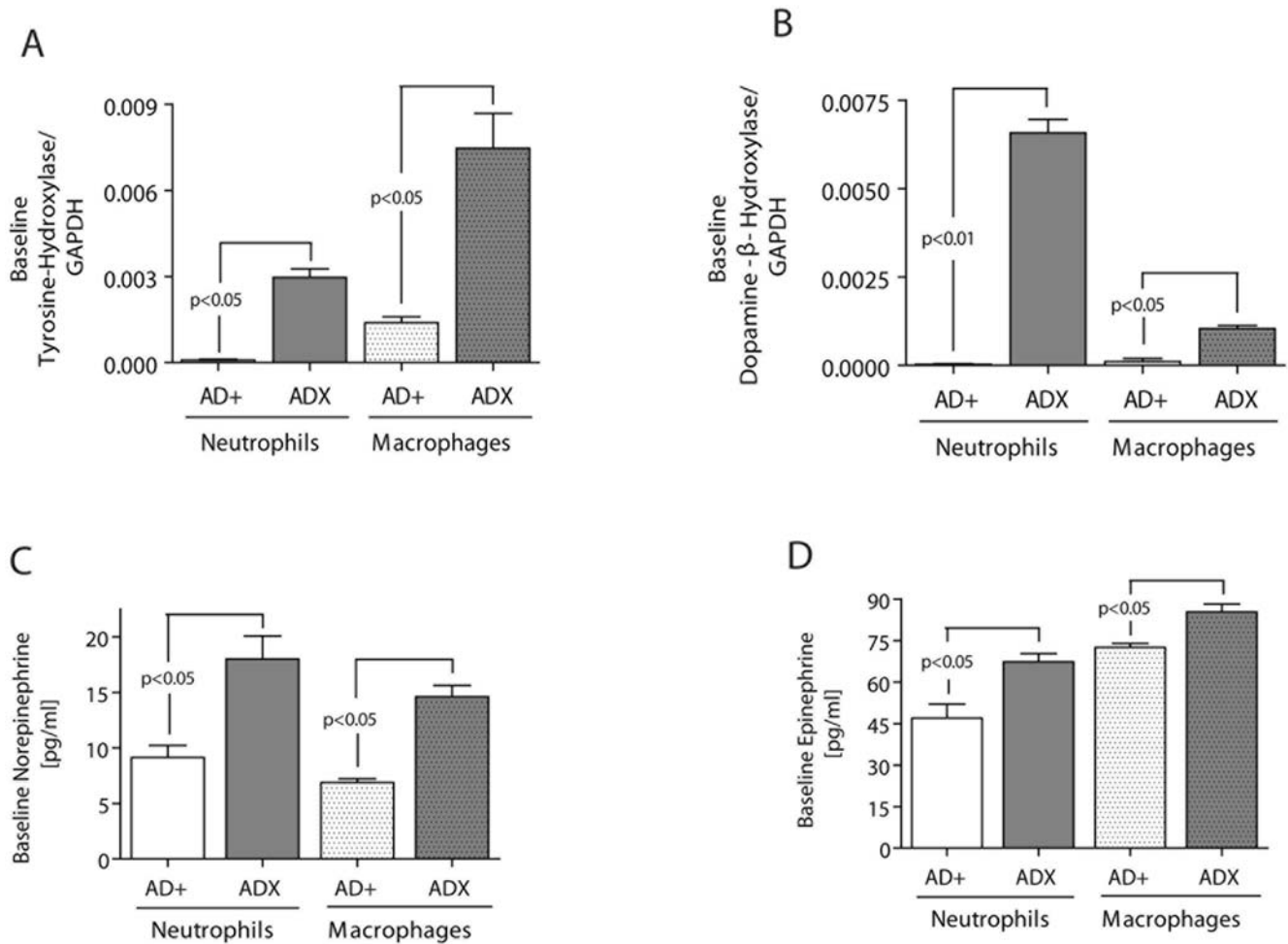


Figure 4. Rat blood neutrophils and rat alveolar macrophages were obtained from AD⁺ and ADX animals and mRNA isolated and subjected to real-time PCR analysis for both key-enzymes of catecholamine synthesis, tyrosine-hydroxylase (rate limiting step) and dopamine- β -hydroxylase (final conversion step) (A, B). Following 15 min culture of unstimulated phagocytes derived from AD⁺ and ADX animals, supernatant fluids were analyzed for norepinephrine (C) and epinephrine (D) by ELISA. Each bar n = 5.
doi:10.1371/journal.pone.0004414.g004

as reported earlier [8]. In contrast, glucocorticoid or mineralocorticoid receptor blockade (by RU 28362 and spironolactone, respectively) neither exacerbated nor reduced the level of injury in both adrenal-intact or ADX animals (Figure 8), suggesting that it is adrenergic receptor engagement rather than cortical mineralocorticoid or glucocorticoid receptor engagement that affects the inflammatory response in ADX animals.

Table 1. Plasma Baseline Levels of Proinflammatory Mediators (pg/ml).

Mediators	AD ⁺	ADX
TNF α	26 \pm 1	34 \pm 2*
IL-1 β	44 \pm 4	61 \pm 2*
IL-6	105 \pm 4	128 \pm 1*
CINC-1	23 \pm 1	27 \pm 1*

For each sample, n = 8–10.

Data are expressed as mean \pm SEM.

* = p < 0.01 vs. AD⁺.

doi:10.1371/journal.pone.0004414.t001

Discussion

There is increasing evidence that the immune system and the central nervous system (CNS) interact to modulate each other via autonomic pathways [2–5]. Immune mediators and cytokines released by the innate immune system rapidly activate neuronal responses, resulting in amplified local immune responses designed to clear pathogens and triggering regional neural and systemic neuroendocrine responses, (including local catecholamine production and systemic glucocorticoid release), both of which seek to return the system to a homeostatic state [1].

Following interaction with adrenergic receptors, the physiological actions of catecholamines can be terminated by cellular reuptake, followed by their intracellular inactivation by monoamine oxidase (MAO) or catechol-O-methyltransferase (COMT). Moreover, there is now evidence for the presence of dopamine and norepinephrine transporters (DAT and NAT, respectively) on lymphocytes, which facilitate the rapid local removal of dopamine or norepinephrine by reuptake [24–27]. Similarly, catecholamine-specific transporters have been described on nuclear membranes of lymphocytes, which actively transport catecholamines from the cytoplasm into the cell nucleus, where catecholamines can interact with nuclear receptors and regulate proliferation or apoptosis [28–

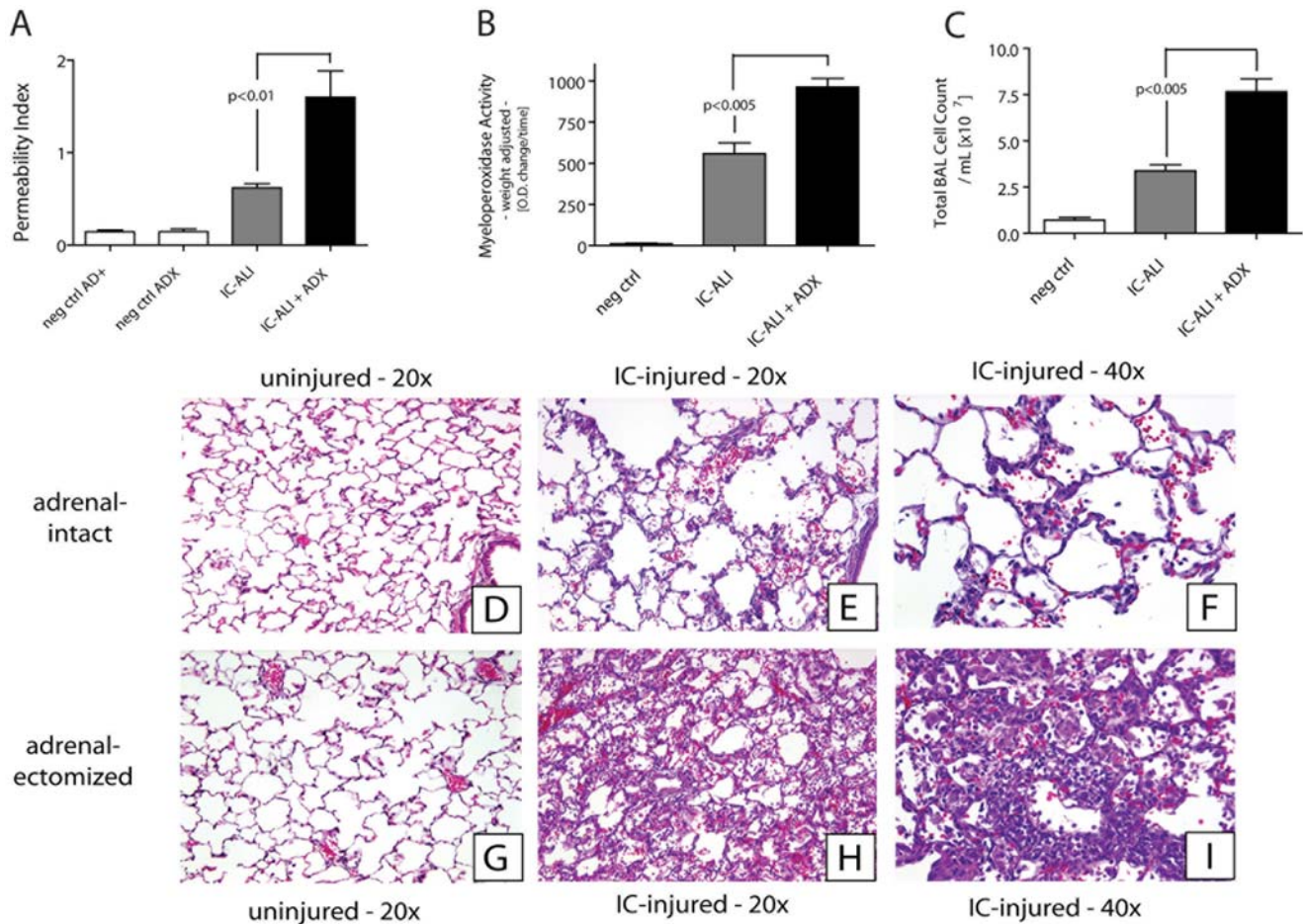


Figure 5. IgG immune complex (IC)-induced lung injury was induced in adrenal-intact (AD⁺) and adrenalectomized (ADX) rats. Vascular leakage (A), content of myeloperoxidase in lung extracts (B) and total white cell content in BAL fluids (C) were assessed. In negative controls, intratracheal administration of anti-BSA was replaced by PBS. Lungs were surgically removed 4 hr after intrapulmonary deposition of IgG immune complexes, tissues fixed in buffered 5% formaldehyde, and paraffin-embedded lung sections were stained with hematoxylin and eosin (D–I). Frames D–F, histology of lungs from adrenal-intact animals; frames G–I represent lungs from adrenalectomized littermates. Sections are representative for at least three rats per group. For each bar n>5 rats. doi:10.1371/journal.pone.0004414.g005

31]. Since mitochondria-associated MAO and the cytosolic COMT do not enter the nucleus, it remains to be determined how and by which mechanism intranuclear actions of catecholamines are terminated. In the present study we describe in macrophages a catecholamine-induced, dose dependent activation of NF κ B p65 and a decrease of cytosolic I κ B α (Figure 1). A similar pattern has been described when alveolar macrophages were exposed *in vitro* to IgG immune complexes [32]. Thus, catecholamines enhance cytokine release by macrophages (Figures 2 and 3) via activation and translocation of NF κ B (Figure 1), indicating that catecholamines are powerful cellular hormones that self-regulate the activation level and the inflammatory potential of inflammatory cells.

It is well established that phagocytes (PMNs and alveolar macrophages) are essential for initiation of acute lung injury in our present models [33–36]. These cells are known to express all adrenergic receptors (both α and β subtypes) and to produce enhanced levels of TNF α in the presence of an α_2 -adrenergic agonist [8,19,20]. Accordingly, in the present study, the mechanism of augmented injury in ADX rodents might be related to an elevated production of phagocyte-derived catecholamines in an attempt to restore systemic catecholamine levels in the absence of

the adrenal glands, resulting in increased catecholamine production by PMNs and macrophages, as suggested in Figure 4. This seems to be followed by direct activation of NF κ B and “priming” of macrophages, leading to an increased baseline production of proinflammatory mediators (Figures 1–3 and Table 1). Upon a “second hit”, such as exposure to LPS, IgG-IC or other inflammatory stimuli, the inflammatory response is greatly accentuated. Another possibility might be a compensatory overactivity of pulmonary sympathetic nerve endings or increased catecholamine production by lymphocytes, resulting in increased norepinephrine levels in BAL fluids. However, we recently demonstrated in the present model of ALI that neither T cells nor sympathetic nerves (by cell depletion or chemical sympathectomy, respectively) are involved in events leading to ALI, but, rather, alveolar macrophages and neutrophils are responsible for increased catecholamine levels in BAL fluids following IC-ALI [8]. Moreover, in a recent study, untreated and healthy bilaterally adrenalectomized rats displayed morphological signs of renal inflammation when compared to untreated adrenal-intact littermates [37], confirming our findings that adrenalectomized rats exhibit a certain proinflammatory priming. Thus, it is now becoming evident, that the sympathetic nervous system may play a

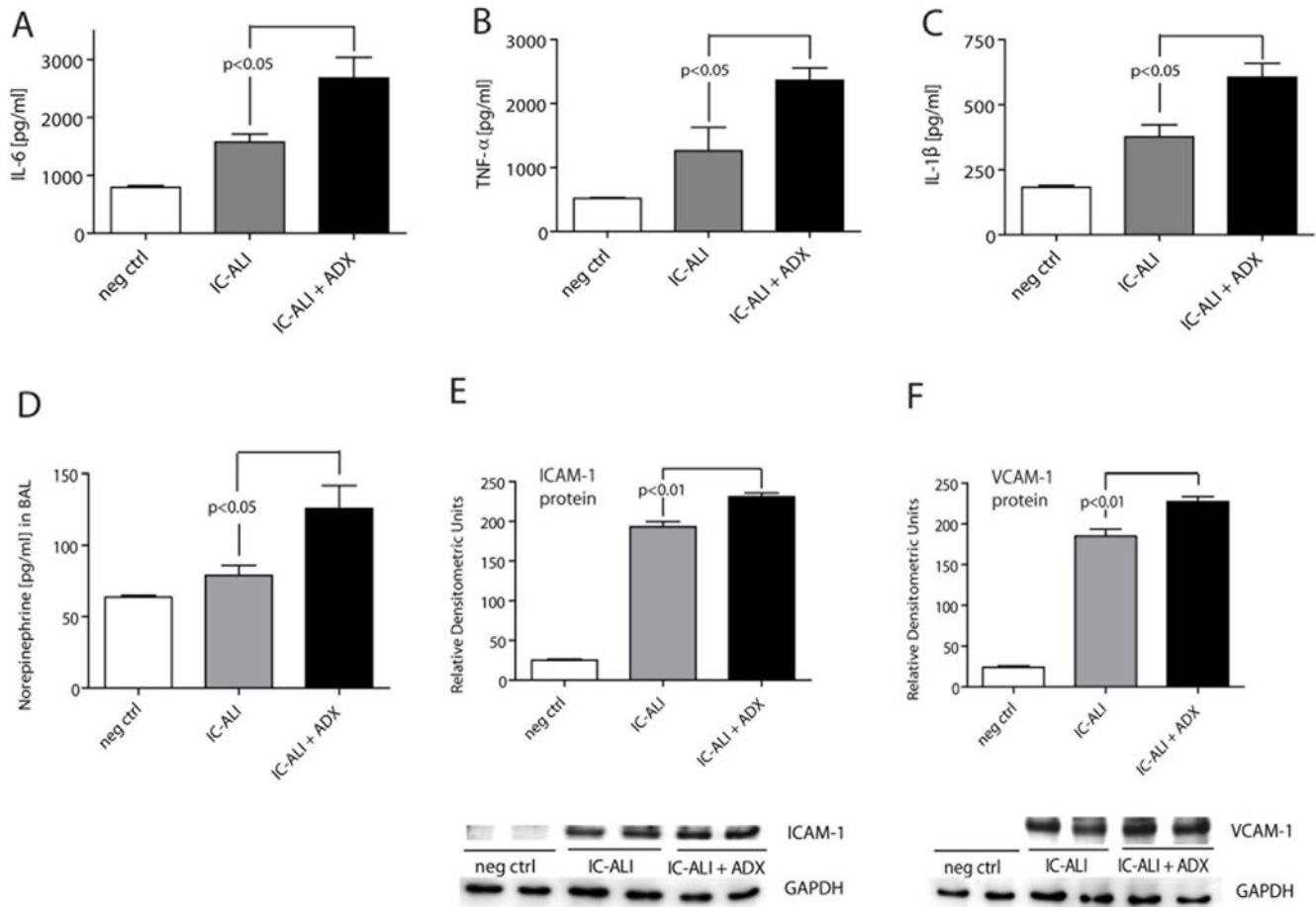


Figure 6. BAL fluids 4 hr after immune complex-induced lung injury, showing content of interleukin-6 (IL-6) (A), tumor necrosis factor α (TNF α) (B), interleukin-1 β (IL-1 β) (C) and norepinephrine (D). Four hours after induction of injury, whole lungs were flushed, surgically removed, homogenized and subjected to Western blot analysis for the adhesion molecules ICAM-1 (E) and VCAM-1 (F). For Western blot studies, experiments were repeated, using 5 different samples per group. Blots shown are of representative bands. For each bar $n \geq 5$ rats. Abbreviations: neg ctrl, negative control; AD+, adrenal-intact animals; ADX, adrenalectomized animals; IC-ALI, immune complex-induced acute lung injury.

doi:10.1371/journal.pone.0004414.g006

dualistic role during the inflammatory response, than previously thought. While it clearly has profound anti-inflammatory effects during *systemic* inflammation as described above [1,3], we are now beginning to understand that the *local* inflammatory response can be immensely boosted through local, cell-derived catecholamine production and subsequent adrenergic signaling in various immune cells [7,8].

Further hormonal key players antagonizing inflammation are glucocorticoids, which are rapidly released from the adrenal cortex following activation of the HPA axis and down-regulate inflammation [38]. It was somewhat surprising that greatly increased levels of ALI occurred in ADX rats and that this was not related to engagement of mineralocorticoid or glucocorticoid receptors (Figure 8). Glucocorticoids ultimately inhibit transcription, which takes up to several hours, whereas lung injury in the current model peaks 4 or 6 hr after initiation. Thus, it seems unlikely that various glucocorticoid effects could have been fully developed in this short period of time. Moreover, rats possess the ability to synthesize steroids in non-adrenal tissues. The rat CNS has been identified as a source of 11 β -hydroxylase and aldosterone synthase [22,39,40]. Other non-adrenal sources include the kidney and vascular tissues [40]. Thus, it seems likely that, in the absence of the adrenal glands, these extra-adrenal sources of corticosterone

and aldosterone compensate for the lack of the adrenal medulla in an attempt to maintain systemic levels of corticoids.

This study suggests that catecholamines activate macrophage NF κ B with subsequent cytokine production in a dose dependent manner. Upregulation of phagocyte-derived catecholamines (by adrenalectomy) results in intensification of the acute inflammatory response.

Materials and Methods

Reagents

Norepinephrine and epinephrine were obtained from Sigma-Aldrich (St. Louis, MO) and were of highest purity. These chemical compounds were synthetically manufactured under sterile conditions and were thus virtually free of endotoxin, RNA or DNA according to the manufacturer.

Animals and Anaesthesia

All investigative procedures and the animal facilities conformed to the Guide of Care and Use of Laboratory Animals published by the US National Institutes of Health. The study was approved by the University Animal Care and Use Committee (UGUCA) and performed according to appropriate guidelines. Specific pathogen-

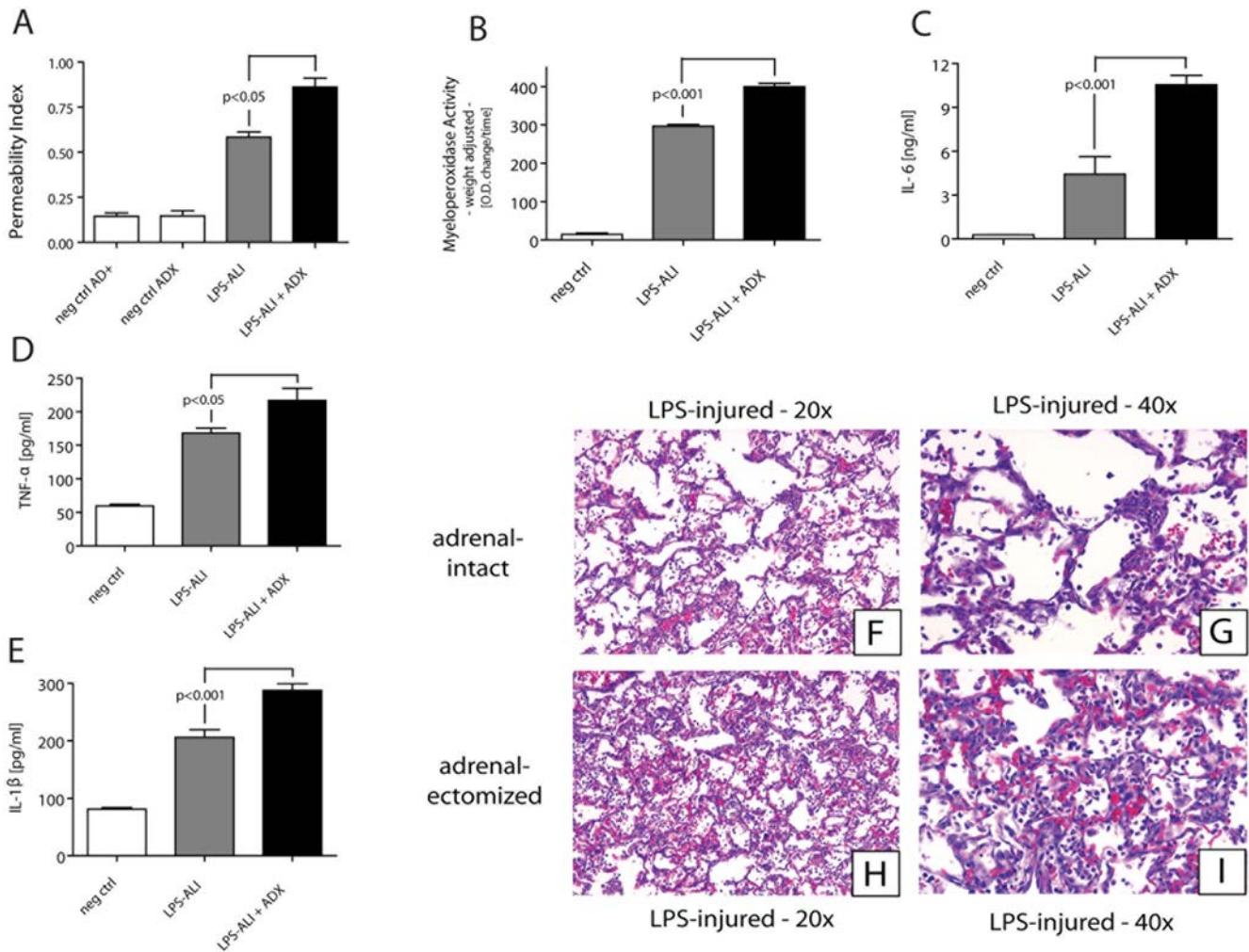


Figure 7. ALI was induced by airway instillation of LPS (300 µg). In parallel to immune complex-induced ALI, vascular leakage (**A**) and myeloperoxidase (MPO) activity in lung extracts (**B**) 6 hr after initiation of injury were measured. Bronchioalveolar lavage fluids obtained 6 hr after introduction of LPS-induced lung injury were assessed for content of IL-6 (**C**), TNF α (**D**), and IL-1 β (**E**). Following surgical removal 6 hr after intrapulmonary LPS deposition, lungs were formalin-fixed, paraffin-embedded and stained with hematoxylin and eosin (**F–I**). Insets F and G show lungs of adrenal-intact animals, while lungs of rats lacking their adrenal glands are presented in insets H and I. For each bar $n > 5$ rats. Abbreviations used: neg ctrl, negative control; AD+, adrenal-intact animals; ADX, adrenalectomized animals; LPS-ALI, LPS-induced acute lung injury. doi:10.1371/journal.pone.0004414.g007

free male C57BL/6 mice (Jackson Laboratories, Bar Harbor, ME) were used for data displayed in Figure 1 and Table 1. Adrenalectomized Long-Evans rats (300–325 g) were obtained from Taconic, Hudson, NY. Un-manipulated, adrenal-intact littermates (300–325 g; Taconic, Hudson, NY) served as controls.

Isolation of mouse macrophages

Peritoneal mouse macrophages were obtained using the thioglycollate method. Mice were injected with 1.5 ml of 2.4% thioglycollate in ddH₂O. Four days later, transmigrated macrophages were harvested by instillation and aspiration of 8 ml PBS (Gibco, Grand Island, NY). Cells were then spun down and subjected to an additional washing step using PBS. Macrophages were then resuspended in HBSS (with Ca²⁺/Mg²⁺). The obtained cell suspension was of high purity, as determined by optical cell differential counts (neutrophils: 0%, macrophages: 97%, lymphocytes: 1%, eosinophils: 2%). Mouse macrophages were exclusively used for the experiments in Figures 1 through 3, since high cell

numbers were needed for these experiments in order to obtain adequate numbers of nuclei. For all other experiments, rat phagocytes were used.

Isolation of rat neutrophils and macrophages

For rat neutrophil isolation, whole blood samples were drawn from the inferior vena cava into syringes containing anticoagulant ACD (Baxter Health Care, Deerfield, IL, USA) (0.1 ml/ml blood). Cells were isolated by using Ficoll-Paque gradient centrifugation (Pharmacia Biotech AB, Uppsala, Sweden) followed by a dextran sedimentation step. After hypotonic lysis of residual blood cells, neutrophils were resuspended in HBSS. The purity of this neutrophil suspension was >95%. Alveolar macrophages were obtained by bronchioalveolar lavage of rats by instilling and withdrawing 10 ml sterile Dulbecco's PBS (without Ca²⁺/Mg²⁺) three times from the lungs via an intratracheal cannula. Cells were then spun down and resuspended in HBSS. The purity of the cell suspension was >95%, with the rest of the cells being lymphocytes.

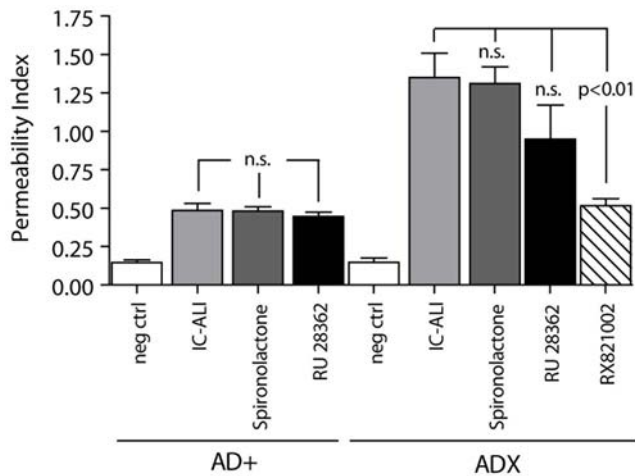


Figure 8. Severity of IgG-IC ALI following pharmacologic blockade of mineralocorticoid and glucocorticoid receptors (by spironolactone and RU 28362, respectively) in adrenal-intact and ADX animals, as assessed by permeability index. The α_2 -adrenergic antagonist RX 821002 was employed in ADX rats. Each bar represents $n \geq 5$ rats. Neg ctrl, negative control with intratracheal instillation of PBS.

doi:10.1371/journal.pone.0004414.g008

Measurement of NF κ B activation

Isolated mouse neutrophils were adjusted to 10×10^6 /ml and resuspended in RPMI medium containing 0.5% BSA (Sigma-Aldrich, St. Louis, MO). Cells were then allowed to settle down for 2 hrs at $37^\circ\text{C}/5\%\text{CO}_2$ to discard non-adherent and non-viable cells. Upon stimulation with various doses of norepinephrine or epinephrine (10^{-12} – 10^{-6} M; both Sigma-Aldrich, St. Louis, MO) for 30 min at $37^\circ\text{C}/5\%\text{CO}_2$, nuclear extracts were obtained using a commercially available kit (“Nuclear Extract Kit”, Active Motif, Carlsbad, CA) according to the manufacturer’s instructions, quantified by BCATM protein measurement (Thermo Scientific, Rockford, IL), protein adjusted and stored at -80°C until further analysis. NF κ B p65 activation was assessed with an ELISA kit (“TransAMTM NF κ B p65”, Active Motif, Carlsbad, CA) according to the manufacturer’s instructions. Recombinant NF κ B p65 protein (Active Motif, Carlsbad, CA) was used to generate the standard curve.

Western Blot analysis for I κ B α

Following isolation and incubation with various concentrations of norepinephrine or epinephrine (30 min, 37°C), peritoneal mouse neutrophils (5×10^6 /ml) were lysed and cytosol was subjected to Western Blotting analysis for I κ B α . Samples were separated in a denaturing polyacrylamide gel and transferred to a PVDF membrane. After blocking with 5% milk-TBST washing in TBST, membranes were then incubated in the appropriate primary antibodies (I κ B α or GAPDH; both from Abcam, Cambridge, MA) at 4°C overnight. After washing, membranes were incubated with the appropriate HRP-conjugated secondary antibodies (Amersham, Arlington Heights, IL) and analyzed by ECL development. Neg ctrl, incubation with HBSS.

Cytokine-production by neutrophils following norepinephrine and epinephrine incubation

Isolated mouse neutrophils were adjusted to 5×10^6 cells/ml and incubated with HBSS (neg ctrl), 20 ng/ml LPS (pos ctrl), norepinephrine (10^{-10} M) or epinephrine (10^{-10} M) for 4 hrs at

$37^\circ\text{C}/5\%\text{CO}_2$. Supernatants were analyzed by ELISA for TNF α , IL-1 β , IL-6 and MIP-2 (all R&D Systems, Minneapolis, MN).

Isolation of total RNA and detection of rat tyrosine-hydroxylase (TH) and rat dopamine- β -hydroxylase (DBH) by real-time quantitative PCR analysis

Total RNA was extracted from isolated phagocytes using Trizol reagent (Life Technologies, Grand Island, NY) according to the manufacturer’s instructions. Reverse transcription was performed with 1 μg RNA using Reverse Transcriptase AMV (Roche, Indianapolis, IN) according to the manufacturer’s instructions. Real-time quantitative PCR was then performed using SYBR[®] Green PCR Master Mix (Applied Biosystems, Foster City, CA). The following primers were used: rat TH: FOR 5’-AGT CTG GCC TTC CGC GTG TTT CAA-3’ and REV 5’-GGG CGC TGG ATA CGA GAG GCA TAG-3’; rat DBH FOR: 5’-CTG CGA CCC CAA GGA TTA TG-3’ and REV 5’-CAG CAC GTG GCG ACA GTA GTT-3’; rat GAPDH: FOR 5’-CGG CAA GTT CAA CGG CAC AGT CA-3’ and REV 5’-CTT TCC AGA GGG GCC ATC CAC AG-3’. Product sizes were 458 bp (TH), 439 bp (DBH), and 424 bp (GAPDH).

Analysis of cell supernatants for catecholamines

EIA kits for Norepinephrine and Epinephrine were obtained from Rocky Mountain Diagnostics, Colorado Springs, CO. Supernatant fluids from phagocytic cells were analyzed according to the manufacturer’s instructions.

IgG immune complex and LPS-induced alveolitis

Intraperitoneal ketamine (100 mg/kg body weight) (Fort Dodge Animal Health, Fort Dodge, IA) was used for anesthesia and intraperitoneal xylazine (13 mg/kg body weight) (Bayer Corp. Shawnee Mission, KS) for sedation. Induction of IgG immune complex-induced alveolitis was performed as previously described [41]. Rats received 2.5 mg of rabbit polyclonal IgG anti-BSA (ICN Biomedicals, Costa Mesa, CA) in 300 μl of PBS intratracheally, followed by i.v. injection of either 10 mg of BSA in 0.5 ml PBS (injury) or 0.5 ml PBS (neg ctrl). For LPS-induced alveolitis, rats received 300 μg of LPS (Sigma Aldrich, St. Louis, MO) in a total volume of 300 μl PBS intratracheally. Maximum level of injury in LPS-alveolitis was reached 6 hr after LPS-instillation. Permeability index was performed as described [41] and quantified by calculating the amount of radioactivity in lungs divided by the amount of radioactivity in 1.0 ml blood.

Lung myeloperoxidase content

Whole-lung MPO activity was quantified as previously described [42].

BAL fluid analysis

BAL fluids were collected by instilling and withdrawing 10 mL of sterile PBS three times from rat lungs. Cellular contents were counted by Coulter cytometry after lysis of erythrocytes. Contents of interleukin IL-6, TNF α , IL-1 β and noradrenaline in BAL fluids were measured using ELISA kits (R&D Systems, Minneapolis, MN and Rocky Mountain Diagnostics, Colorado Springs, CO, respectively).

Morphological assessment of lung injury

Rat lungs were fixed by intratracheal instillation of 10 ml buffered (pH 7.2) formalin (10%). The lungs were further fixed in a 10% buffered formalin solution for histological examination by tissue sectioning and staining with H&E.

Western blot analysis for ICAM-1 and VCAM-1

Flushed whole rat lungs were homogenized in ice-cold RIPA buffer containing a protease-inhibitor cocktail (Roche, Indianapolis, IN). After protein extraction, sonication and protein measurement, samples were separated in a denaturing polyacrylamide gel and transferred to a PVDF membrane. After blocking with 5% milk-TBST washing in TBST, membranes were then incubated in appropriate primary antibodies (ICAM-1, VCAM-1: Santa Cruz Biotechnology, Santa Cruz, CA; GAPDH: Abcam, Cambridge, MA) at 4°C overnight. After washing, membranes were incubated with the appropriate HRP-conjugated secondary antibodies (Amersham, Arlington Heights, IL) and analyzed by ECL development.

Receptor agonists and antagonists

Agonists and antagonists (all Sigma Aldrich, St. Louis, MO) were administered to rats intraperitoneally in a total volume of 1.5 ml. Following agents were used: 1,2-propanediol (vehicle, 1 ml/kg), RX 821002 (α_2 -adrenoceptor antagonist, 2.5 mg/kg), RU 28362 (glucocorticoid receptor antagonist, 150 μ g/kg) and spironolactone (mineralocorticoid receptor antagonist, 50 mg/kg).

References

- Sternberg EM (2006) Neural regulation of innate immunity: a coordinated nonspecific host response to pathogens. *Nat Rev Immunol* 6: 318–328.
- Tracey KJ (2002) The inflammatory reflex. *Nature* 420: 853–859.
- Elenkov IJ, Wilder RL, Chrousos GP, Vizi ES (2000) The sympathetic nerve—an integrative interface between two supersystems: the brain and the immune system. *Pharmacol Rev* 52: 595–638.
- Borovikova LV, Ivanova S, Zhang M, Yang H, Botchkina GI, et al. (2000) Vagus nerve stimulation attenuates the systemic inflammatory response to endotoxin. *Nature* 405: 458–462.
- Wang H, Yu M, Oehani M, Amella CA, Tanovic M, et al. (2003) Nicotinic acetylcholine receptor $\alpha 7$ subunit is an essential regulator of inflammation. *Nature* 421: 384–388.
- Tracey KJ (2007) Physiology and immunology of the cholinergic antiinflammatory pathway. *J Clin Invest* 117: 289–296.
- Flierl MA, Rittirsch D, Huber-Lang M, Sarma JV, Ward PA (2008) Catecholamines—Crafty Weapons in the Inflammatory Arsenal of Immune/Inflammatory Cells or Opening Pandora’s Box? *Mol Med* 14: 195–204.
- Flierl MA, Rittirsch D, Nadeau BA, Chen AJ, Sarma JV, et al. (2007) Phagocyte-derived catecholamines enhance acute inflammatory injury. *Nature* 449: 721–725.
- Madden KS, Sanders VM, Felten DL (1995) Catecholamine influences and sympathetic neural modulation of immune responsiveness. *Annu Rev Pharmacol Toxicol* 35: 417–448.
- Johnson JD, Campisi J, Sharkey CM, Kennedy SL, Nickerson M, et al. (2005) Adrenergic receptors mediate stress-induced elevations in extracellular Hsp72. *J Appl Physiol* 99: 1789–1795.
- Johnson JD, Campisi J, Sharkey CM, Kennedy SL, Nickerson M, et al. (2005) Catecholamines mediate stress-induced increases in peripheral and central inflammatory cytokines. *Neuroscience* 135: 1295–1307.
- Madden KS, Felten SY, Felten DL, Sundaresan PR, Livnat S (1989) Sympathetic neural modulation of the immune system. I. Depression of T cell immunity in vivo and in vitro following chemical sympathectomy. *Brain Behav Immun* 3: 72–89.
- Maestroni GJ, Mazzola P (2003) Langerhans cells beta 2-adrenoceptors: role in migration, cytokine production, Th priming and contact hypersensitivity. *J Neuroimmunol* 144: 91–99.
- Benschop RJ, Nieuwenhuis EE, Tromp EA, Godaert GL, Ballieux RE, et al. (1994) Effects of beta-adrenergic blockade on immunologic and cardiovascular changes induced by mental stress. *Circulation* 89: 762–769.
- Chelmicka-Schorr E, Checinski M, Arnason BG (1988) Chemical sympathectomy augments the severity of experimental allergic encephalomyelitis. *J Neuroimmunol* 17: 347–350.
- Bergquist J, Tarkowski A, Ekman R, Ewing A (1994) Discovery of endogenous catecholamines in lymphocytes and evidence for catecholamine regulation of lymphocyte function via an autocrine loop. *Proc Natl Acad Sci U S A* 91: 12912–12916.
- Kradin R, Rodberg G, Zhao LH, Leary C (2001) Epinephrine yields translocation of lymphocytes to the lung. *Exp Mol Pathol* 70: 1–6.
- Ackerman KD, Madden KS, Livnat S, Felten SY, Felten DL (1991) Neonatal sympathetic denervation alters the development of in vitro spleen cell proliferation and differentiation. *Brain Behav Immun* 5: 235–261.
- Spengler RN, Allen RM, Remick DG, Strieter RM, Kunkel SL (1990) Stimulation of alpha-adrenergic receptor augments the production of macrophage-derived tumor necrosis factor. *J Immunol* 145: 1430–1434.

RX 821002 and spironolactone were administered immediately before induction of IC-induced lung injury, while RU 28362 was administered 1 hr before initiation of lung injury.

Statistical analysis

All values are expressed as means \pm SEM. Data were analyzed with a one-way ANOVA and individual group means were then compared with a Student-Newman-Keuls test. Differences were considered significant when $p \leq 0.05$.

Acknowledgments

We are indebted to Lisa Riggs, Robin Kunkel and Roscoe Warner for their excellent support in the tissue histology studies and illustrations. Further, we thank Beverly Schumann and Sue Scott for their outstanding assistance in the preparation of this manuscript.

Author Contributions

Conceived and designed the experiments: MAF MSHL PAW. Performed the experiments: MAF DR BAN DED AL. Analyzed the data: MAF. Wrote the paper: MAF JVS PAW.

- Spengler RN, Chensue SW, Giacherio DA, Blenk N, Kunkel SL (1994) Endogenous norepinephrine regulates tumor necrosis factor- α production from macrophages in vitro. *J Immunol* 152: 3024–3031.
- Cosentino M, Marino F, Bombelli R, Ferrari M, Lecchini S, et al. (1999) Endogenous catecholamine synthesis, metabolism, storage and uptake in human neutrophils. *Life Sci* 64: 975–981.
- Brown SW, Meyers RT, Brennan KM, Rumble JM, Narasimhachari N, et al. (2003) Catecholamines in a macrophage cell line. *J Neuroimmunol* 135: 47–55.
- Morken JJ, Warren KU, Xie Y, Rodriguez JL, Lyte M (2002) Epinephrine as a mediator of pulmonary neutrophil sequestration. *Shock* 18: 46–50.
- Faraj BA, Olkowski ZL, Jackson RT (1991) Binding of [3 H]-dopamine to human lymphocytes: possible relationship to neurotransmitter uptake sites. *Pharmacology* 42: 135–141.
- Faraj BA, Olkowski ZL, Jackson RT (1995) A cocaine-sensitive active dopamine transport in human lymphocytes. *Biochem Pharmacol* 50: 1007–1014.
- Marino F, Cosentino M, Bombelli R, Ferrari M, Lecchini S, et al. (1999) Endogenous catecholamine synthesis, metabolism storage, and uptake in human peripheral blood mononuclear cells. *Exp Hematol* 27: 489–495.
- Gordon J, Barnes NM (2003) Lymphocytes transport serotonin and dopamine: agony or ecstasy? *Trends Immunol* 24: 438–443.
- Bergquist J, Josefsson E, Tarkowski A, Ekman R, Ewing A (1997) Measurements of catecholamine-mediated apoptosis of immunocompetent cells by capillary electrophoresis. *Electrophoresis* 18: 1760–1766.
- Buu NT (1993) Uptake of 1-methyl-4-phenylpyridinium and dopamine in the mouse brain cell nuclei. *J Neurochem* 61: 1557–1560.
- Josefsson E, Bergquist J, Ekman R, Tarkowski A (1996) Catecholamines are synthesized by mouse lymphocytes and regulate function of these cells by induction of apoptosis. *Immunology* 88: 140–146.
- Saha B, Mondal AC, Majumder J, Basu S, Dasgupta PS (2001) Physiological concentrations of dopamine inhibit the proliferation and cytotoxicity of human CD4+ and CD8+ T cells in vitro: a receptor-mediated mechanism. *Neuroimmunomodulation* 9: 23–33.
- Lentsch AB, Shanley TP, Sarma V, Ward PA (1997) In vivo suppression of NF-kappa B and preservation of I kappa B alpha by interleukin-10 and interleukin-13. *J Clin Invest* 100: 2443–2448.
- Johnson KJ, Ward PA (1974) Acute immunologic pulmonary alveolitis. *J Clin Invest* 54: 349–357.
- Lentsch AB, Ward PA (2001) Regulation of experimental lung inflammation. *Respir Physiol* 128: 17–22.
- Mulligan MS, Schmid E, Beck-Schimmer B, Till GO, Friedl HP, et al. (1996) Requirement and role of C5a in acute lung inflammatory injury in rats. *J Clin Invest* 98: 503–512.
- Ward PA (1996) Rous-Whipple Award Lecture. Role of complement in lung inflammatory injury. *Am J Pathol* 149: 1081–1086.
- Ozturk H, Ozturk H, Gedik S, Uzunlar AK, Ketani A (2007) Effects of specific inhibition of cyclooxygenase-2 on kidney in bilateral adrenalectomized rats. *Int Urol Nephrol* 39: 267–270.
- Weinberg PF, Matthay MA, Webster RO, Roskos KV, Goldstein IM, et al. (1984) Biologically active products of complement and acute lung injury in patients with the sepsis syndrome. *Am Rev Respir Dis* 130: 791–796.
- MacKenzie SM, Clark CJ, Fraser R, Gomez-Sanchez CE, Connell JM, et al. (2000) Expression of 11beta-hydroxylase and aldosterone synthase genes in the rat brain. *J Mol Endocrinol* 24: 321–328.

40. Rudolph AE, Blasi ER, Delyani JA (2000) Tissue-specific corticosteroidogenesis in the rat. *Mol Cell Endocrinol* 165: 221–224.
41. Czermak BJ, Lentsch AB, Bless NM, Schmal H, Friedl HP, et al. (1999) Synergistic enhancement of chemokine generation and lung injury by C5a or the membrane attack complex of complement. *Am J Pathol* 154: 1513–1524.
42. Suzuki K, Ota H, Sasagawa S, Sakatani T, Fujikura T (1983) Assay method for myeloperoxidase in human polymorphonuclear leukocytes. *Anal Biochem* 132: 345–352.

Zach Suntres, Ph.D.

Northern Ontario School of Medicine,

**Thunder Bay, Ontario
Canada**

REPORT DOCUMENTATION PAGE

Form Approved
OMB No. 0704-0188

Public reporting burden for this collection of information is estimated to average 1 hour per response, including the time for reviewing instructions, searching existing data sources, gathering and maintaining the data needed, and completing and reviewing this collection of information. Send comments regarding this burden estimate or any other aspect of this collection of information, including suggestions for reducing this burden to Department of Defense, Washington Headquarters Services, Directorate for Information Operations and Reports (0704-0188), 1215 Jefferson Davis Highway, Suite 1204, Arlington, VA 22202-4302. Respondents should be aware that notwithstanding any other provision of law, no person shall be subject to any penalty for failing to comply with a collection of information if it does not display a currently valid OMB control number. **PLEASE DO NOT RETURN YOUR FORM TO THE ABOVE ADDRESS.**

1. REPORT DATE (DD-MM-YYYY) 29/09/2010		2. REPORT TYPE Final		3. DATES COVERED (From - To) Sept 2006- Sept 2010	
4. TITLE AND SUBTITLE The Toxicological Evaluation of Liposomal Antioxidant Formulations and their use in the treatment of ricin-induced injuries				5a. CONTRACT NUMBER 3000627138	
				5b. GRANT NUMBER W81XH-06-2-0044	
				5c. PROGRAM ELEMENT NUMBER	
6. AUTHOR(S) Dr. Zach Suntres				5d. PROJECT NUMBER	
				5e. TASK NUMBER	
				5f. WORK UNIT NUMBER	
7. PERFORMING ORGANIZATION NAME(S) AND ADDRESS(ES) Northern Ontario School of Medicine 955 Oliver Road Thunder Bay, Ontario Canada P7B-5E1				8. PERFORMING ORGANIZATION REPORT NUMBER	
9. SPONSORING / MONITORING AGENCY NAME(S) AND ADDRESS(ES) U.S. Army Medical Research Fort Detrick, Maryland				10. SPONSOR/MONITOR'S ACRONYM(S)	
				11. SPONSOR/MONITOR'S REPORT NUMBER(S)	
12. DISTRIBUTION / AVAILABILITY STATEMENT Approved for public release; distribution unlimited					
13. SUPPLEMENTARY NOTES					
14. ABSTRACT This research was carried out to evaluate the safety of a liposomal formulation (STIMAL) containing combinations of the antioxidants α -tocopherol, γ -tocopherol, and/or N-acetylcysteine and their effectiveness in the treatment of ricin-induced toxicity. Liposomal formulations containing NAC with alpha- or gamma-tocopherols were found to be stable in the presence body fluids such as plasma and bronchoalveolar lavage suggesting that the liposomal antioxidant formulations can be effective for intravenous administration for the treatment of oxidant-induced tissue injuries because they can overcome structure destabilization as a result of interaction with certain serum components present in blood (following iv injection) and bronchoalveolar lavage (following inhalation). The liposomal antioxidant formulations were also found to be non mutagenic. The dosage range finding study used to determine the maximum tolerated doses (MTD) in male and female Sprague-Dawley rats, as well as the acute toxicity studies, showed that that the highest dose by a single intravenous administration of STIMAL used (660 mg DPPC, 200 mg NAC, 83 mg α -T, and 83 mg γ -T) failed to produce any adverse reactions. The administration of NAC as a liposomal formulation increased the bioavailability of NAC by 2-fold while inclusion of tocopherols in the formulation increased the availability of NAC by 4-5-fold. The factor that limited the administration of higher levels of antioxidants via the liposome delivery system was found to be the viscosity of the preparation Also, the liposomal formulation containing NAC was found to protect against ricin-induced injuries as demonstrated by the changes in hematological, clinical chemistry parameters (decrease in platelets, increase in WBC and neutrophils), biochemical parameters (increases in ALT and AST, lipid peroxidation, myeloperoxidase activity, and nitrotyrosine levels and decreases in glutathione level) as well as liver and lung histopathological findings. These data suggest that the liposomal antioxidant formulations appear to be safe and useful in the treatment of injuries associated with oxidative stress.					
15. SUBJECT TERMS liposomes, antioxidants, toxicity, N-acetylcysteine, alpha-tocopherol, gamma-tocopherol, ricin, oxidative stress, inflammation					
16. SECURITY CLASSIFICATION OF:			17. LIMITATION OF ABSTRACT UU	18. NUMBER OF PAGES 103	19a. NAME OF RESPONSIBLE PERSON USAMRMC
a. REPORT U	b. ABSTRACT U	c. THIS PAGE U			19b. TELEPHONE NUMBER (include area code)

TABLE OF CONTENTS

	<u>Page</u>
Cover Page.....	1
Report Documentation Page (SF-298).....	2
Table of Contents.....	3
Statement of Work	4
Introduction.....	4
Body.....	5
Key Research Accomplishments.....	28
Reportable Outcomes.....	28
Conclusion.....	29
References.....	30
Appendices for.....	31
1. Chromosomal Abberation Test	
2. Acute Study: rats	
3. Acute Study: dogs	
4. Histopathology: dogs	

Statement of Work

The overall objective of this work was to evaluate the pre-clinical safety of three different liposomal formulations containing combinations of the antioxidants α -tocopherol, γ -tocopherol, and/or N-acetylcysteine under Good Laboratory Practices (GLP) conditions and examine the effectiveness of liposomal N-acetylcysteine in the treatment of ricin-induced toxicity. The preclinical safety studies covered the establishment of the pharmacokinetic and the toxicological profile as well as the assessment of the acute toxicity of liposomal antioxidants containing N-acetylcysteine or N-acetylcysteine and α -tocopherol or N-acetylcysteine and γ -tocopherol in both *in vivo* models (rodent [Sprague-Dawley rat] and non-rodent [beagle dog]) and *in vitro* systems (mutagenicity, genotoxicity). At the end of the preclinical safety evaluation, we identified an initial safe dose, recognized possible target organs for toxicity, and, distinguish safety parameters for clinical monitoring. The effectiveness of liposomal N-acetylcysteine against ricin-induced toxicity was assessed by measuring the effects of conventional NAC and liposomal NAC against ricin-induced changes in hematological, biochemical and histological parameters. Briefly, results from the *in vivo* and *in vitro* studies demonstrated that the liposomal antioxidant formulations did not demonstrate any potential for toxicity and were effective against the oxidant- and inflammatory-induced injuries seen following ricin administration.

Introduction

The Advanced Medical Countermeasures Consortium (AMCC) is investigating the role of liposomal antioxidant formulations (STIMAL) as an effective antidote/therapeutic product to protect from exposure to chemical warfare agents, such as mustard gas. Mustard gas-induced organ and tissue injuries are mediated through mechanisms that also involve the activation of the inflammatory response and the inducement of oxidative stress (1,2). Recent studies have focused on the use of antioxidants as a treatment modality for ameliorating the injurious effects of mustard gas. So far, many natural antioxidants exhibit poor bioavailability and cannot easily cross biological barriers such as membranes. Lipophilic compounds are insoluble in water and are located almost exclusively within membranes. Hydrophilic compounds cannot penetrate many biological compartments enclosed by membranes through passive diffusion and largely remain in extracellular compartments. We have demonstrated that the protective effects of antioxidants against several experimental models of oxidant-induced tissue and organ injuries were significantly enhanced following their delivery as liposomal formulations (3-7). Liposomes are phospholipid vesicles composed of lipid bilayers enclosing an aqueous compartment. Hydrophilic molecules (ie. N-acetylcysteine [NAC]) can be encapsulated in the aqueous spaces and lipophilic molecules (α -Tocopherol, γ -Tocopherol) can be incorporated into the lipid bilayers. The relative ease in incorporating hydrophilic and lipophilic antioxidants in liposomes; the possibility of directly delivering liposomes to an accessible body site; and the relative non-immunogenicity and low toxicity of liposomes have rendered the liposomal system

highly attractive for drug delivery (3, 7). The overall objective of this proposal is to evaluate the safety of a liposomal formulation containing combinations of the antioxidants α -tocopherol, γ -tocopherol, and/or N-acetylcysteine. The preclinical safety studies cover the establishment of the basic pharmacology, pharmacokinetics and toxicological profile of the liposomal antioxidants, using animals (acute and subchronic toxicity studies, toxicokinetics) and *in vitro* systems (mutagenicity, genotoxicity, irritation). At the end of the preclinical safety evaluation, it will be possible to identify an initial safe dose, recognize possible target organs for toxicity, and, distinguish safety parameters for clinical monitoring. An example of the efficacy of liposomal antioxidants against oxidant-induced organ injuries is demonstrated in studies examining the protective effect of liposomal NAC against ricin-induced toxicity. Ricin mediates its toxic effects *in vitro* by inhibiting protein synthesis but oxidative stress-mediated mechanisms resulting to apoptosis and cell death have also been implicated. Ricin has been shown to selectively activate phagocytes, known to generate excessive amounts of ROS, which in addition to their direct toxic actions, also exacerbate the inflammatory process and cause further tissue damage (9).

Body

1. Report on *in vitro* studies involving the characterization of liposomal N-acetylcysteine (NAC) formulation.

Experiments were carried out to identify possible liposomal antioxidant formulation to be used in the preclinical safety studies. Results from studies described by the consortium collaborators suggested that liposomes containing N-acetylcysteine (NAC) or glutathione (GSH) and/or alpha/gamma-tocopherol are effective against CEES and other oxidant-induced organ injuries. We have validated the preparation and characterization of liposomes containing different antioxidants.

1.a. **Stability of liposomal NAC in PBS buffer, plasma, and bronchoalveolar lavage (BAL).**

In order for liposomes to be effective in the treatment of oxidant-induced tissue injuries, liposomes have to overcome structure destabilization as a result of interaction with certain serum components present in blood (following *iv* injection) and bronchoalveolar lavage (following inhalation). Thus, the stability of liposomal NAC formulation in biological fluids such as plasma and bronchoalveolar lavage, as well as PBS buffer as a control, was examined and the results are shown in figures 1 and 2. Liposomal NAC with alpha- or gamma-tocopherols showed better stability in PBS buffer than plasma, but the differences were not great. Inclusion of alpha- or gamma-tocopherol in liposomes improved the retention of NAC under all conditions examined.

Figure 1

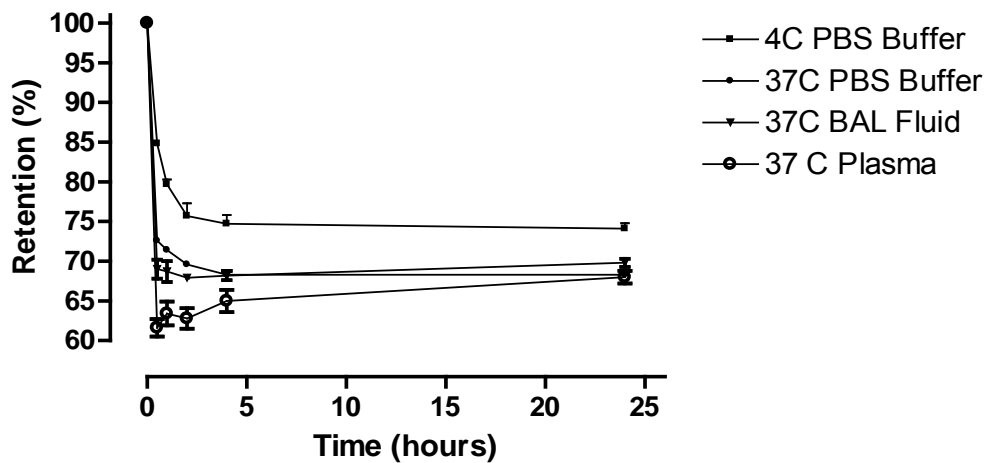
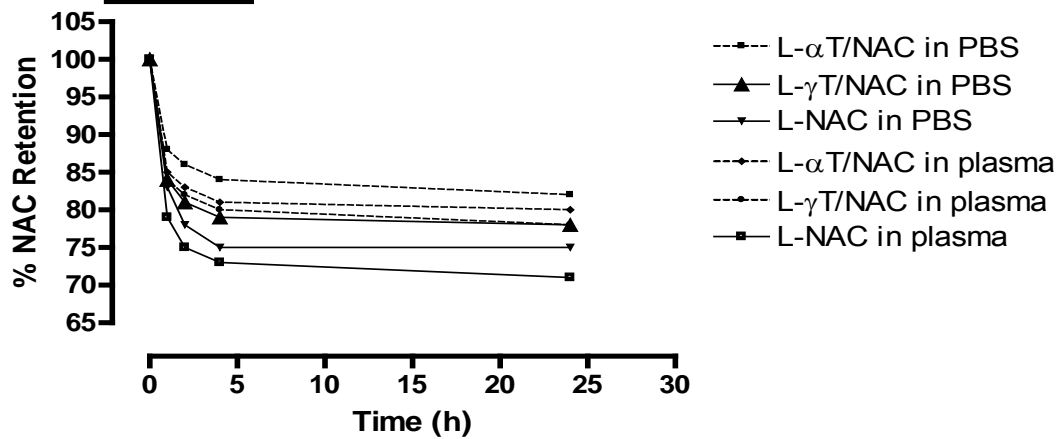


Figure 2



1.b. Improvement of liposomal stability by lyophilization for prolonged storage or shipment purposes.

(i) Storage of lyophilized liposomes

We have found that the stability of the liposomal formulations can be improved significantly when prepared in the powder form following lyophilization. Lyophilization refers to the process whereby a substance is prepared in dry form by freezing and dehydration. Briefly, preformed liposomal formulations can be dehydrated by freeze-drying using a lyophilizator at -45°C (time of freeze-drying depends on volume of sample). The vials containing the liposomal formulations can be stored at -20°C for months or shipped in dry ice.

(ii) Reconstitution Procedure for lyophilized liposomes

In the reconstitution procedure, the vials containing the liposomal formulations can be rehydrated with sterile Phosphate Buffer Saline (PBS) at pH 6.5 as follows (for a 1 ml final solution): An initial volume of 150 μL of PBS is added to the vial until all the liposomal powder is dissolved (vortexing is highly recommended if liposomes are aggregated); the vial is placed in a pre-heated water bath set at 45°C (this temperature should be maintained throughout the rehydration process) for 15 min. Then, an additional volume of 700 μL of PBS is added to the vial, vortexed well, and placed to the water bath at 45°C for an additional 30 min. After heating in the water bath, the mixture is vortexed once more to dissolve any remaining aggregated liposomes. Finally, the sample is centrifuged at 4°C (28000xg or higher) for 30 minutes in order to separate lipids that did not form into liposomes, free drug dispersed in supernatant, and any foam produced during the vortex process. After centrifugation, the supernatant is discarded and the pellet formed (liposomes) can be reconstituted with the required buffer of choice (ex. PBS, 0.9% saline) and diluted to the concentration of preference. The liposomes are ready for use.

1.c. (i) Chromosomal Abberations of liposomal antioxidant formulations in Chinese Hamster Ovary Cells

The purpose of the *in vitro* chromosomal aberration test is to identify agents that cause structural chromosomal aberrations in cultured mammalian cells. Structural aberrations may be of two types, chromosome or chromatid. With the majority of chemical mutagens, induced aberrations are of the chromatid type, but chromosome type aberrations also occur. Chromosomal aberrations are the cause of many human genetic diseases and there is substantial evidence that chromosomal damage and related events causing alterations in oncogenes and tumor suppressor genes of somatic cells are involved in cancer induction in humans and experimental animals.

An increase in polyploidy may indicate that a chemical has the potential to induce numerical aberrations. The *in vitro* chromosomal aberration test may employ cultures of established cell lines, cell strains or primary cell cultures. In our studies, the test substances (empty liposomes

(DPPC), liposomal NAC, liposomal α -tocopherol/NAC and liposomal γ -tocopherol/NAC) were investigated in an *in vitro* chromosome aberration test for their potential to induce structural chromosome aberrations in Chinese hamster ovary cell line WB_L. The experimental design followed the *OECD Guideline for the Testing of Chemicals – 473, In Vitro Mammalian Chromosome Aberration Test* (1997). The liposomal antioxidant formulations consisting of DPPC lipids, with NAC, NAC/alpha-tocopherol or NAC/gamma-tocopherol are not clastogenic in cultured Chinese hamster ovary WB_L cells under the conditions of the test (see Appendix 1 for draft report and results).

(ii) Ames test of mutagenicity. The liposomal antioxidant formulations are not mutagenic to *S. typhimurium* strains, TA98, TA100, TA1535, TA1537, and *E. coli* strain, WP2 *uvrA*, under the conditions of the test.

1.d. Development of Ultrapressure Liquid Chromatography (UPLC) method for the measurement of N-acetylcysteine and other thiols.

We have developed a simple, sensitive, and rapid method that will be used to determine the levels of NAC/GSH in the different organs and tissues of animals. The method uses the Ellman's reagent derivatization procedure. The mobile phase consists of a mixture of methanol and ammonium formate (20:80 v/v) with a C18 reverse phase column as the stationary phase. Ellman's reagent can react stoichiometrically with thiols giving rise to mixed disulphides which have different retention times. The method was found to yield a quantitative recovery of GSH and NAC of more than 96%, to be sensitive (20 pmole/10 ul injection) and rapid (less than 3 min).

1.e Antioxidant effectiveness of liposomal NAC *in vitro*.

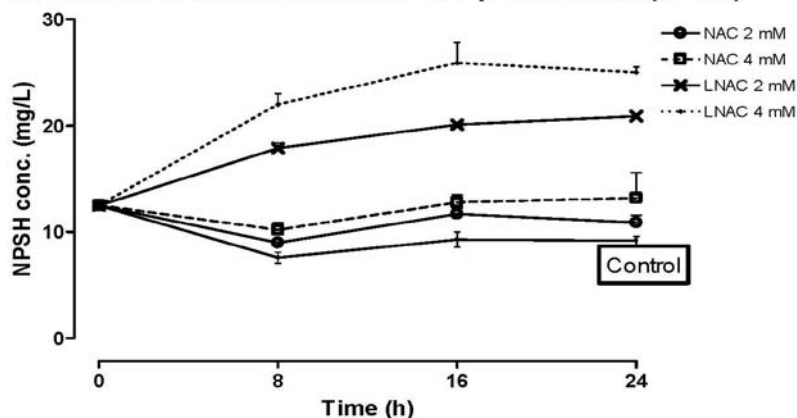
To assess the effectiveness of lipid-encapsulated and free antioxidants, the uptake and antioxidant properties of liposomal NAC and free NAC were examined in an *in vitro* model consisting of cells (hepG2 cell culture) exposed to the oxidant hydrogen peroxide (H₂O₂). The uptake of NAC in cells was assessed by measuring the cellular non-protein thiols (NPSH). The toxicity of liposomal NAC and free NAC as well as the protective effects of the antioxidant formulations against H₂O₂-induced cell injury was assessed by measuring the leakage of lactate dehydrogenase (LDH), an indicator of loss in cell permeability.

Pre-treatment of cells with either NAC or L-NAC (2 or 4 mM NAC for up to 24 h) did not produce any LDH leakage from Hep G2 cells suggesting that both formulations, at the concentrations used, are not toxic.

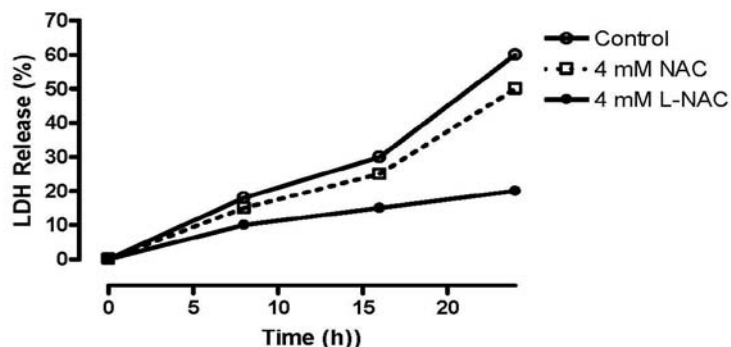
Exposure of hep G2 cells to free NAC was not effective in increasing the cellular thiol levels. On the other hand, cellular thiol levels were significantly increased, in a concentration-dependent and time-dependent manner, when cells were treated with liposomal NAC. Pretreatment of cells with L-NAC conferred protection against H₂O₂-induced cell membrane injury, a treatment effect not seen in cells

pretreated with L-NAC. These data suggest that delivery of NAC as a liposomal formulation increases the intracellular thiol content and decreases cellular susceptibility to oxidative stresses. (see figures below).

Effect of NAC or L-NAC on cellular Non-protein thiols (NPSH)



Effect of H₂O₂ on cells pretreated with NAC or L-NAC



2. Maximum Tolerated Dose studies for four liposomal antioxidant formulations in rodents (rat) and non-rodents (dog)

The up-and-down procedure was used to determine the maximum tolerated dose in both, male and female Sprague-Dawley rats and beagle dogs, respectively. The liposomal formulations tested were: Liposomes consisting of dipalmitoylphosphatidylcholine (DPPC); Liposomal NAC; Liposomal alpha-tocopherol/NAC; and, Liposomal gamma-tocopherol/NAC. The treatments were tested as outlined in the following chart:

Range Finding Chart

Dose Sequence	Dose Level (mg/kg)		Number of Animals and Sex (male / female)
	Severe toxic effect or mortality seen at preceding dose	No effect seen at preceding dose	
1 st	-	a	1 male / 1 female
2 nd	a : m	a x m	1 male / 1 female
3 rd	b : m	b x m	1 male / 1 female
4 th	c : m	c x m	1 male / 1 female
5 th	d : m	d x m	1 male / 1 female

a = initial dose

m = multiplier (1.5 – 3)

The objective of the procedure is that if the first group of animals survives and does not show severe toxic effect, the second group of animals will receive a higher dose. If any animals in the first group die or appear moribund, then the second group of animals will receive a lower dose. The next dose level will be chosen based on the same criteria. Based on the reaction of the previous group, the following group will be dosed at 24 to 72 hour intervals.

Findings.

The dosage range finding study used to determine the maximum tolerated doses (MTD) in male and female Sprague-Dawley rats showed that the highest dose by a single intravenous administration of STIMAL used (consisting of: 660 mg DPPC, 200 mg NAC, 83 mg α -T, and 83 mg γ -T) failed to produce any adverse reactions. Gross necropsy findings were unremarkable.

The dosage range finding study used to determine the maximum tolerated doses (MTD) in male and female beagle dogs was similar to those for the rats. However, during the initial studies, it was decided to reduce the volume of the liposomal formulations administered to dogs by 50% since some dogs experienced emesis (most likely due to the high rate of a large volume/viscosity of the liposomal formulations).

Due to the high viscosity of the dosing formulations the dose level of 200 mg/kg (NAC) (doses for all formulations are based on NAC, the antioxidant encapsulated in liposomes at the highest levels; IV administration to humans is approximately 150 mg/kg NAC) was considered to be the maximum feasible dose (MFD) that can be injected safely to rats by an intravenous route of administration.

3. Single dose acute intravenous toxicity study for four preparations in rodents (Appendix 2)

For the single dose acute intravenous toxicity study, male and female Sprague-Dawley rats were challenged intravenously with the following liposomal formulations:

1. Liposomes (660 mg/kg DPPC) (control)
2. Liposomal NAC (660 mg DPPC/200 mg NAC/kg)
3. Liposomal alpha-tocopherol/NAC (660 mg DPPC/83 mg alpha-tocopherol/200 mg NAC/kg)
4. Liposomal gamma-tocopherol/NAC (660 mg DPPC/83 mg gamma-tocopherol/200 mg NAC/kg).

Animals were monitored on a daily basis within the 14-day experimental period. This study examined a safe dose range of three liposomal antioxidant formulations with plain liposomes being determined as a control group (liposomes/ NAC; liposomes/ α -tocopherol and NAC; and liposomes/ γ -tocopherol and NAC) administered by a single intravenous dose in Sprague-Dawley rats. Endpoints included daily clinical observations, weekly general physical examinations, body weights, food consumption, clinical pathology, gross necropsy and histopathology.

Injections were well-tolerated by animals (for all four formulations), and there were no clinical origins of toxicity associated with the treatment regimens either during injections, after injections or during the 14-day post treatment period.

Rats in all groups gained body weight during the two week observation period, and statistical analysis (ANOVA, $p=0.05$) showed that there was no difference in body weights and body weight gain between the control group (empty liposomes) and the three antioxidant formulations, or amongst antioxidant formulations groups.

Hematology results indicated that RBC counts, reticulocytes, hemoglobin and RBC indices (MCV, MCH and MCHC) were all within the normal ranges for both genders for all test groups. The exception was hematocrit (Hct), which was slightly below the lower limit of the normal historical ranges in males and females, for three test groups and control group which received empty liposomes. These slight decreases in Hct were not considered to be significant as they were just marginally below the normal historical ranges. These differences were most likely due to physiological variations since the control animals appeared to be similarly affected as the test animals.

Platelet counts were within normal ranges for both genders and all groups. WBC counts and differential counts were within the normal physiological range in groups which received empty liposomes, liposome/NAC and α -tocopherol, for both genders. WBC counts, in male rats which were dosed with liposome/NAC and γ -tocopherol were slightly below the lower limit of the normal range, and were also slightly lower than WBC counts in the remaining groups. Neutrophils, lymphocytes and monocytes were within the normal range, but were slightly lower than the counts for these parameters in

other groups. This is consistent with the anti-inflammatory properties of γ -tocopherol. However, it cannot be excluded that this finding is not treatment related but because of its low magnitude, this observation is of limited toxicological significance.

Prothrombin time, APTT and fibrinogen were all within the normal ranges for all groups and both genders, with the exception that APTT for female rats treated with liposomes NAC and γ -tocopherol was approximately one second below the low end of normal range. This finding is not clinically significant.

Mean total protein, albumin and globulin were within the normal ranges in all groups and both genders. A/G ratio was marginally increased in female rats treated with empty liposomes and γ -tocopherol.

Cholesterol, triglycerides and glucose levels were all within the normal ranges for all groups and both genders.

Electrolytes (Na^+ , Cl^- and K^+), calcium and phosphorus values were essentially within the normal ranges for all groups and both genders. There was however a slight “increase” in Cl^- levels in some groups. This finding is mostly likely an artifact known as a “great chloride shift”, and it is not considered treatment related.

Hepatocellular / hepatobiliary panel showed that ALP, Bil(T) and ALT were within normal ranges for all groups and both genders. AST was slightly increased in males which received liposome/NAC and γ -tocopherol. AST is tissue non-specific, and most likely originated from erythrocytes.

BUN and creatinine were within the normal ranges for all groups and both genders.

LDH and CK were increased in some animals in all groups. There were substantial inter-group and intra-group variabilities in the levels of lactate dehydrogenase (LDH) and creatine kinase (CK), including the control group. These differences are nevertheless known variabilities with these enzymes and are related to their release during regular handling of rats, grasping, dosing, etc. (Yerroum *et al*, 1999), blood collection procedures (Friedel *et al*, 1974), or their release from cellular elements during clotting (Friedel *et al*, 1970).

Gross pathology findings were unremarkable.

Histopathology: The tissues listed under Tissue Preservation from all animals were prepared for microscopic examination by embedding in paraffin wax, sectioning and staining with hematoxylin and eosin and evaluated histopathologically.

Tissue Preservation

During necropsy, the following tissues and organs were retained, from all Main Study animals. Neutral buffered 10% formalin was used for fixation and preservation unless otherwise indicated.

Abnormal Tissues	Kidneys	Skin (inguinal)
Adrenals	Liver (sample of central & left lobes)	Spinal Cord
Lungs	Spleen	
Aorta (Thoracic)	Lymph Node (Mandibular)	Sternum & Marrow
Brain	Lymph Node (Mesenteric)	Stomach
Cecum	Mammary Gland (inguinal)	Testes**
Colon	Nasal Turbinates	Thymus
Duodenum	Optic Nerves**+	Thyroid/Parathyroids +
Epididymes**	Ovaries	Tongue
Esophagus	Pancreas	Trachea
Eyes**	Pituitary	Urinary Bladder
Femur & Marrow	Prostate	Uterus (horns, cervix, body)
Heart***	Salivary Glands (Mandibular)	Vagina
Ileum	Seminal Vesicles	
Jejunum	Sciatic Nerve	
	Skeletal Muscle (quadriceps)	

** Fixed in Acid Alcohol (euthanized animals only)

*** Sections of left and right ventricles and atria, septum with papillary muscle

+ Parathyroids & optic nerves examined only if present in routine sections

@ Lungs of euthanized animals infused with formalin

Three femoral bone marrow smears were prepared from each sacrificed animal, and were retained for possible future examination.

No histological findings were considered to be toxicologically significant. Various known background or incidental conditions were noted in the test and control groups.

Several animals in each group had lesions that were considered to be background changes because they occurred in control animals or because they were known spontaneous conditions in rats.

Lung: Some animals in each group had pulmonary granulomas that are attributed to intravenous injections with embolism of hair fibers and keratinocytes into the pulmonary veins and capillaries.

Kidney: Small foci of interstitial nephritis or atrophic basophilic tubules occur spontaneously in rats. Small tubular deposits of crystalline material (nephrocalcinosis) commonly occurs, especially in female rats on some diets. Pyelonephritis and cystitis occurred sporadically in response to urinary tract infections, most common in female rats.

4. Toxicokinetic Study of liposomal NAC, liposomal α -T/NAC and liposomal γ -T/NAC in rats.

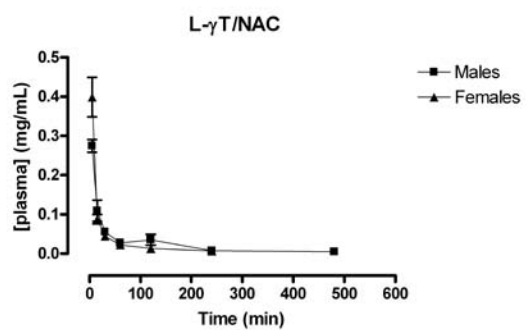
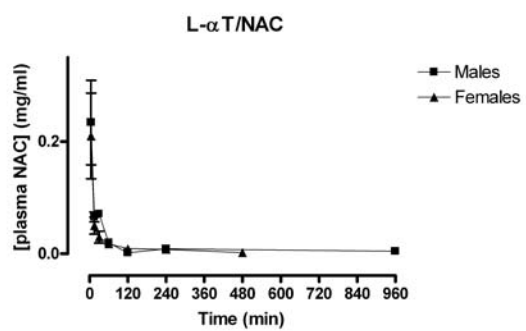
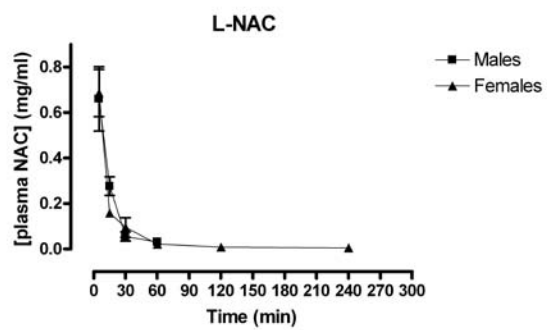
This study examined the pharmacokinetics of test articles LNAC (liposomes consisting of DPPC lipids and N-acetylcysteine; NAC), L- α T/NAC NAT (LNAC and α -tocopherol), L- γ T/NAC (LNAC and γ -tocopherol) and control article EL (empty liposomes consisting of DPPC) when

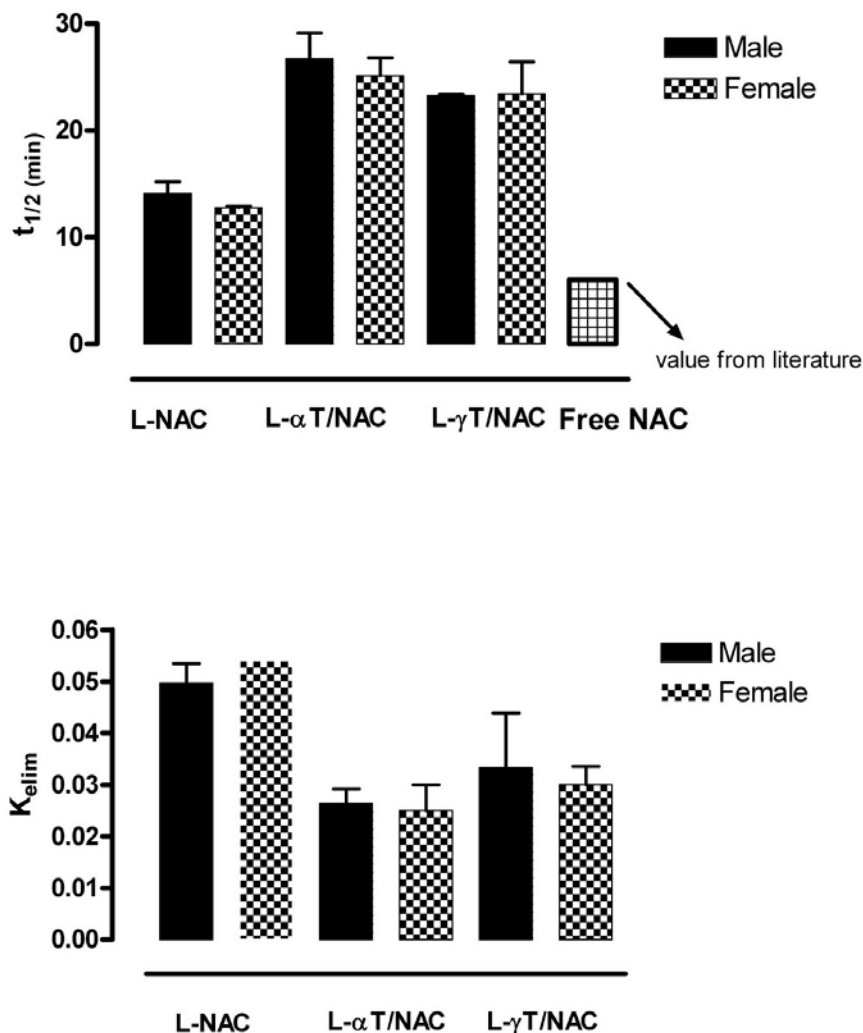
administered to rats. Test and control articles were prepared at the Northern Ontario School of Medicine and were provided to Nucro-Technics lyophilized in microcentrifuge and 15 mL polypropylene tubes. Dosing formulations of all articles were prepared at Nucro-Technics as per written instructions from Dr. Suntres. Animals were dosed with test articles by single intravenous injection (lateral tail vein) equivalent to 200 mg/kg of NAC. An equivalent dose of liposomes (EL) was used as a control dose.

Four groups of rats, each with sub-groups A and B, were used in the study. Each study group consisted of 12 rats (6 male, 6 female), with each sub-group consisting of 3 males and 3 females [strain: CrI:CD[®](SD)BR-Sprague-Dawley (Charles River Canada)]. Group 1 was treated with empty liposomes, group 2 with L-NAC, group 3 with L- α T/NAC and group 4 with L- γ T/NAC. All groups received an equivalent dose of liposomes. Test groups were administered the equivalent of 200 mg/kg NAC (L-NAC), 200 mg/kg NAC and 83.3 mg/kg α -tocopherol (L- α T/NAC) or 200 mg/kg NAC and 71.4 mg/kg γ -tocopherol (L- γ T/NAC) in liposomes. Dosing formulations contained test or control article in sterile PBS, pH 6.5.

Animals were fasted the evening before dosing. Animal body weights were measured and recorded on the day of dosing (pre-dose). Clinical observations of animals were performed during dosing and up to 4 hours post-dose. Animals that appeared in poor health were monitored for a longer duration. Blood samples were collected on 13 occasions for all dosing groups. Samples were collected from all sub-group A animals pre-dose and at 15 minutes, 1, 4, 8, 24 and 72 hours post-dose. Samples were collected from all sub-group B animals at 5 and 30 minutes and at 2, 6, 12 and 48 hours post-dose. Blood plasma was isolated from samples and frozen until plasma analysis. After the final blood collection, surviving animals were sacrificed. Liver, kidneys, lung, spleen, pancreas and heart from these rats were collected and frozen until tissue analysis.

Section 3: Figure 1: Plasma NAC





Results.

NAC disappeared faster from the plasma of animals administered with L-NAC (4 hrs) than animals treated with L- α T/NAC (8 hrs) or L- γ T/NAC (6 hrs) (Section 3: Figure 1). The half-life of NAC in L-NAC, L- α T/NAC or L- γ T/NAC-treated animals was approximately 13 min, 29 min or 26 min, respectively (Section 3: Figure 2). The approximate half-life of free NAC reported in the literature is approximately 6 min. These data suggest that administration of NAC as a liposomal formulation increases the availability of NAC by 2-fold while inclusion of tocopherols in the formulation increases the availability of NAC by 4-5-fold. This is consistent with data reported in previous work where inclusion of tocopherols in liposomes increases the stability of liposomes and decreases solute leakage (Suntres et al, 1994). Observations from both in vitro and in vivo studies have shown that in most cases after parenteral administration, the entrapped agent may be released from liposomes prematurely upon encountering the biological milieu. Such instability of liposomal membranes, resulting in the leakage of the entrapped solute (ie. NAC) has been attributed to interactions of the liposomal lipid bilayers with various

destabilizing serum proteins, degradative enzymes, and oxidative stress. Alpha-tocopherol is known to influence the permeability of phospholipids vesicles by decreasing their vulnerability to the destructive action of plasma proteins and enzymes (Suntres et al., 1994). Consequently, the incorporation of tocopherols in the lipid bilayers of liposomes, not only increases the antioxidant potential of the liposomal formulation (due to their inherent antioxidant properties), but also may enhance the duration of NAC's antioxidant effect.

5. Single dose acute intravenous toxicity study for four preparations in beagle dogs (Appendix 3)

For the single dose acute intravenous toxicity study, male and female beagle dogs were challenged intravenously with the following liposomal formulations:

1. Liposomes (330 mg/kg DPPC) (control)
2. Liposomal NAC (330 mg DPPC/60 mg NAC/kg)
3. Liposomal alpha-tocopherol/NAC (330 mg/25 mg alpha-tocopherol/60 mg NAC/kg)
4. Liposomal gamma-tocopherol/NAC (330 mg/25 mg gamma-tocopherol/60 mg NAC/kg).

Although beagle dogs were able to survive doses of liposomal antioxidants similar to those used in the rat study, the doses were reduced because after the intravenous administration of the formulations, the animals experienced vomiting, an effect from which animals recovered completely after 1 hr post-administration. The most probable cause for this effect was, most likely, the large volume of liposomal formulations administered to the animals and not due to the components of the formulation. A decrease in the injectable volume and rate of administration of the liposomal formulations alleviated the side effect but it resulted in a decrease in the amount of antioxidants delivered to the animals.

The experimental procedures on dogs, carried by technical staff at Nucro-technics (GLP facility), were audited on-site by COL. Peter Schultheiss, Director, Animal Care and Use Review Office, US Army Veterinary Corps on March 14, 2008. Briefly, COL. Schultheiss was satisfied with the experimental protocol and procedures and a full report was communicated to Dr. Peter Ward, Dr. Z. Suntres, and Nucro-Technics.

During the acute study, animals were monitored on a daily basis within the 14-day experimental period. This study examined a safe dose range of three liposomal antioxidant formulations with plain liposomes being determined as a control group (liposomes/ NAC; liposomes/ α -tocopherol and NAC; and liposomes/ γ -tocopherol and NAC) administered by a single intravenous dose in Sprague-Dawley rats. Endpoints included daily clinical observations, weekly general physical examinations, body weights, food consumption, clinical pathology (Appendix 3), gross necropsy and histopathology.

Injections were well-tolerated by animals (for all four formulations), and there were no clinical origins of toxicity associated with the treatment regimens either during

injections, after injections or during the 14-day post treatment period. All data is included in Appendix 3.

Histopathology in male and female dogs (APPENDIX 4)

Results:

A list of grades for all tissues examined, with means are provided in Table 1.

Conditions of possible toxicological significance:

There were no conditions of possible toxicological significance.

Conditions of uncertain significance:

A single female treated with Liposomes/ γ -tocopherol and NAC had a temporary increase in ALT. There were no tissue changes that indicated any unresolved injury.

Conditions lacking toxicological significance:

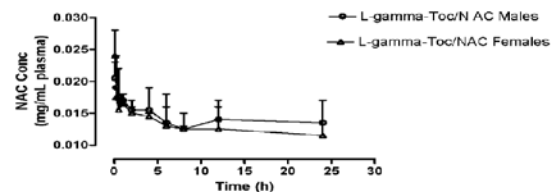
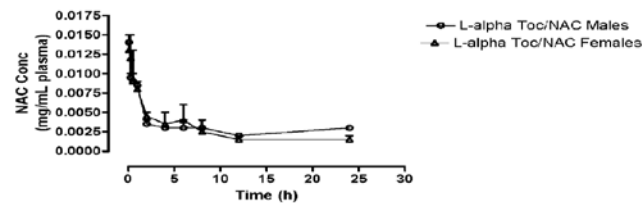
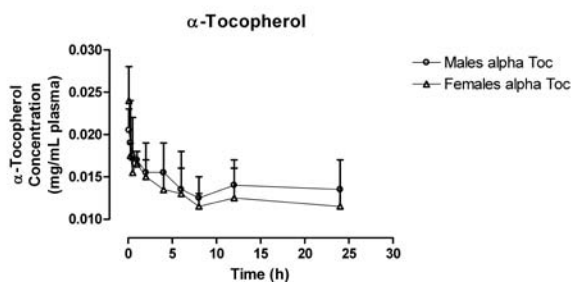
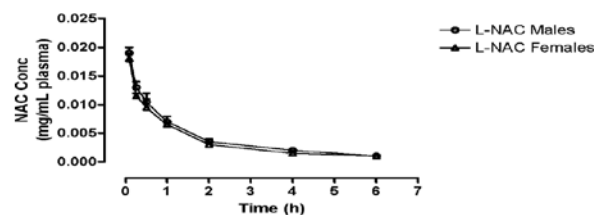
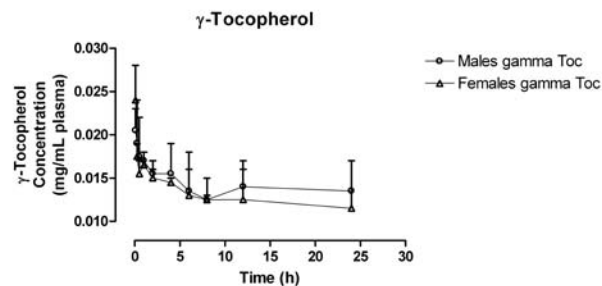
Hypotension which was rapidly resolved occurred during and immediately following treatment in animals in all dose groups.

Conclusions:

The intravenous administration of a single 60 mg/kg dose of Liposomes and NAC or Liposomes/ α -tocopherol and NAC, or Liposomes/ γ -tocopherol and NAC to beagle dogs caused no substantive clinical or pathological effects during the 14-day observation period.

6. Toxicokinetic Study of liposomal NAC, liposomal α -T/NAC and liposomal γ -T/NAC in beagle dogs.

As with the rats, iv administration of the STIMAL significantly improved the retention of antioxidants in the circulation by decreasing the rate of elimination. The incorporation of tocopherols in the liposomal formulation further improve the stability of the formulation, preventing the leakage of NAC and consequently increasing the retention and circulation of NAC in the blood.



N-Acetylcysteine Pharmacokinetics

	L-NAC		L- α T/NC		L- γ T/NAC	
	Male	Female	Male	Female	Male	Female
Half-Life (hr)	0.304	0.285	0.81	0.75	1.15	1.10
K elim	2.28	2.43	0.856	0.925	0.600	0.632
Vd	2610	2720	2790	2680	2720	2860

Pharmacokinetics of Tocopherols

	L- α T/NC		L- γ T/NAC	
	Male	Female	Male	Female
Half-Life (hr)	13.60	13.30	18.10	16.90
K elim	0.051	0.052	0.038	0.041
Vd	3390	2970	1420	1500

7. Investigate the role of oxidative stress and inflammation in the lungs and other organs of animals exposed to ricin and examine the therapeutic effects of liposomal-antioxidants against ricin-induced organ injuries..

The role of oxidative stress and inflammation in animals exposed to ricin was examined by assessing the cellular oxidant/antioxidant balance (measuring the levels of superoxide dismutase, and glutathione (GSH) and the extent of lipid peroxidation (by measuring the levels of 4-hydroxyalkenals)) and the levels of inflammatory cells and inflammatory mediators such as myeloperoxidase and nitrotyrosine.

The therapeutic potential of liposomal NAC formulation was investigated in the lungs, liver, kidneys, and heart of rats exposed to ricin. Plain liposomes (composed of dipalmitoylphosphatidylcholine, DPPC) or DPPC liposomes containing NAC was administered intravenously to animals 4-hours after the administration of ricin. Clinical chemistry, biochemical, hematological and/or histopathological findings were used to compare the effectiveness of the different treatments.

Methods

The amount of ricin chain A purchased from Sigma-Aldrich was 1 mg; the entire amount was utilized. All work was performed within the operationally effective zone of the biosafety cabinet. The contaminated test tubes and pipette tips were placed in a 10% bleach solution. All areas were decontaminated with a 10% bleach solution.

Animals. Male Sprague–Dawley rats (approximate body weight 220–250 g) were housed in stainless-steel cages (in group of 2 rats per cage) with free access to pelleted purina laboratory chow and tap water. The animals were kept at room temperature 22–24° and were exposed to alternate cycles of 12 hr light and darkness. Animals used in this study were treated and cared for in accordance with the guidelines recommended by the Canadian

Council on Animal Care, and the experimental protocol for treating animals will be approved by the institutional animal care committee.

Ricin A (1 or 10 $\mu\text{g}/\text{kg}$ body weight) was administered intravenously with animals being sacrificed 5 or 24 hours later. Control animals received an equivalent volume of saline

Plasma preparation

Blood samples were collected from anesthetized animals by cardiac puncture in EDTA-containing syringes. The collected blood was used for the measurement of clinical and chemistry parameters. The remaining blood was centrifuged immediately, and the isolated plasma was stored at -70° .

Lung, liver, kidney, and heart tissue preparation

Organs were removed from animals immediately after decapitation and rinsed with ice-cold saline to remove excess blood. Following rinsing, organs were weighed quickly. Several lung, liver, kidney, and heart sections were fixed in 10 % formaldehyde and following a 24-hour fixation period, tissues will be sectioned and stained with hematoxylin and eosin. The remaining organs were processed at $0-4^{\circ}\text{C}$. Approximately 1 g of lung tissue sample was homogenized with a Brinkmann Polytron in a sufficient volume of ice-cold 50 mM potassium phosphate buffer, pH 7.4, to produce a 20% homogenate.

Statistical Analysis.

Results are expressed as means \pm SEM obtained from four animals for each marker/parameter. Comparisons among groups were evaluated by one-way ANOVA with a Newman–Keuls test of multiple comparisons. A *P* value of 0.05 or less was considered significant.

Results

Dose- and Time-dependent Effects

Male Sprague–Dawley rats (approximate body weight 220–250 g) were administered ricin chain A at 1 $\mu\text{g}/\text{kg}$ b.wt or 10 $\mu\text{g}/\text{kg}$ b.wt, iv and killed 5 hr post-ricin administration. No toxicity was observed with 1 $\mu\text{g}/\text{kg}$ b.wt as determined by gross necropsy, clinical chemistry and hematological parameters. However, changes in hematological and clinical chemistry parameters (decrease in platelets, hypoalbuminemia, increase in WBC and neutrophils, increases in ALT and AST [liver injury markers] and creatinine kinase (injury markers for heart and skeletal muscle)) were observed at a ricin chain A dose of 10 $\mu\text{g}/\text{kg}$ b.wt. These changes were most evident 24-hr post-ricin chain A exposure (data reported is for the 24-hr exposure period).

Biochemistry: Treatment of animals with 25 mg/kg NAC or liposomal NAC 4 h post-ricin chain A exposure did not have any significant changes on the extent of inflammation as indicated by the changes in the numbers of white blood cells and neutrophils in the circulation. However, the antioxidant formulations decreased the toxic effects of ricin as

evidenced by the biochemical (AST, ALT) (fig 3) and histopathological data, and this protection was most evident following the administration of liposomal NAC.

Administration of ricin resulted in increases in liver injuries as indicated by the increases in aspartame transaminase activity (AST, ALT). In the lung, ricin administration resulted in increases in oxidative stress as indicated by increases in lung tissue lipid peroxidation levels, increases in myeloperoxidase and decreases in GSH concentrations (Fig 4). Treatment of animals with NAC or L-NAC (25 mg/kg b.wt) 4 hr post-ricin administration ameliorated the ricin-induced injury which was most evident following the administration of liposomal-NAC. So far, this data suggest that ricin mediates its toxic effects, at least in part, via oxidant-mediated mechanism(s) and this toxicity can be ameliorated with the antioxidant N-acetylcysteine with the liposomal formulation being the most effective.

Histopathology:

Responses on Liver: Ricin treatment resulted in the appearance of fat vacuoles in periportal hepatocytes . This was less pronounced in animals given NAC in liposomes than in animals given NAC alone. Ricin also increased accumulation of neutrophils in hepatic sinusoids. Neutrophils often were fragmented and engulfed by enlarged Kupffer cells. Kupffer cell responses were prominent in ricin treated rats and this response appeared to be reduced by NAC in liposomes but not by NAC alone. Sinusoidal neutrophilia was reduced by NAC in liposomes but not by NAC alone.

Responses on Lungs: Ricin increased the level of pulmonary congestion, the numbers of neutrophils in pulmonary capillaries, the apparent thickness of the alveolar capillaries and the amount of hemorrhage into the pulmonary alveoli. There was some reduction in these responses by NAC, with L-NAC fairing better than conventional NAC.

Responses on heart: There were no ricin-specific toxic responses observed. The NAC formulations had no evident influence on the heart.

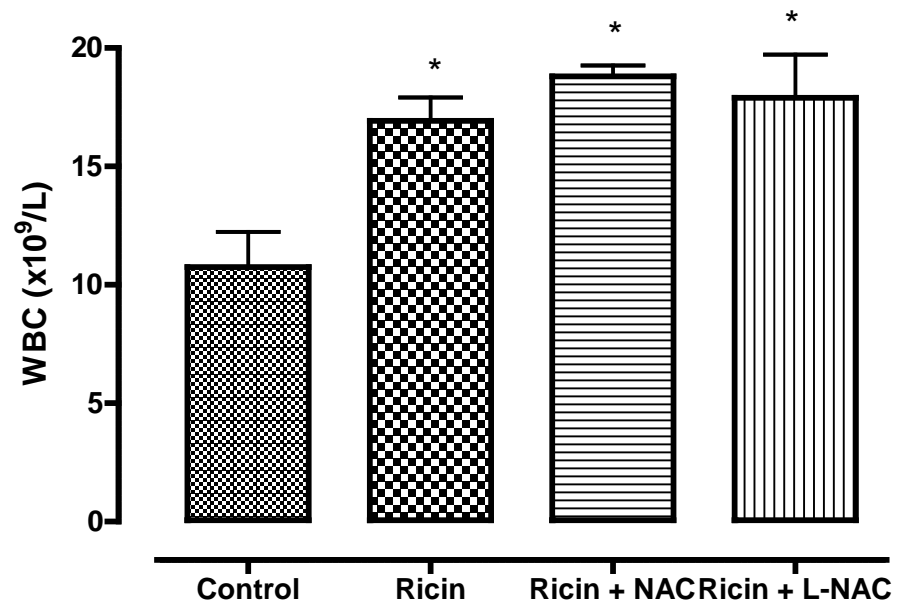


Figure 1: The effect of NAC or L-NAC against ricin-induced changes in the levels of White Blood Cells.

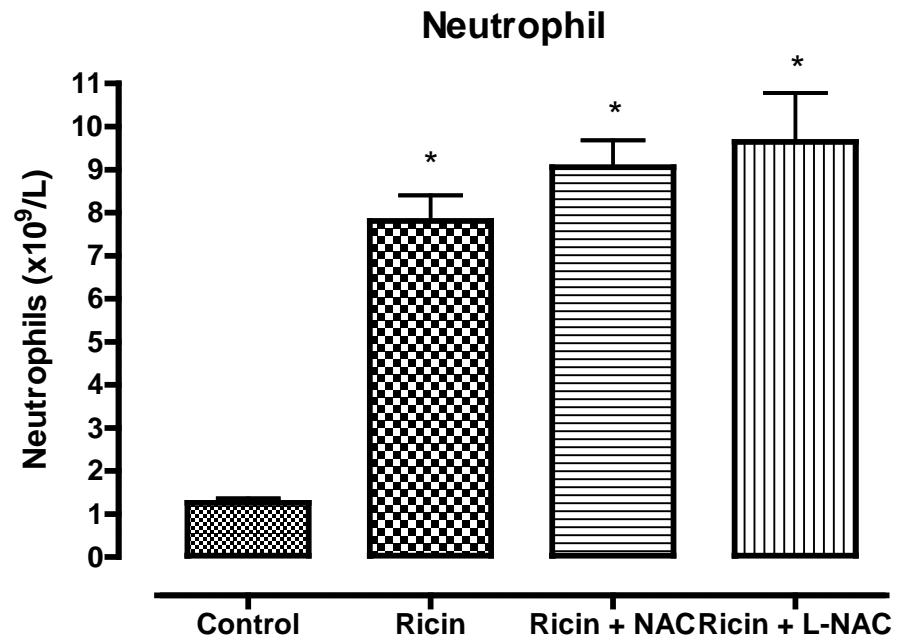


Figure 2: The effect of NAC or L-NAC against ricin-induced changes in the levels of Neutrophils

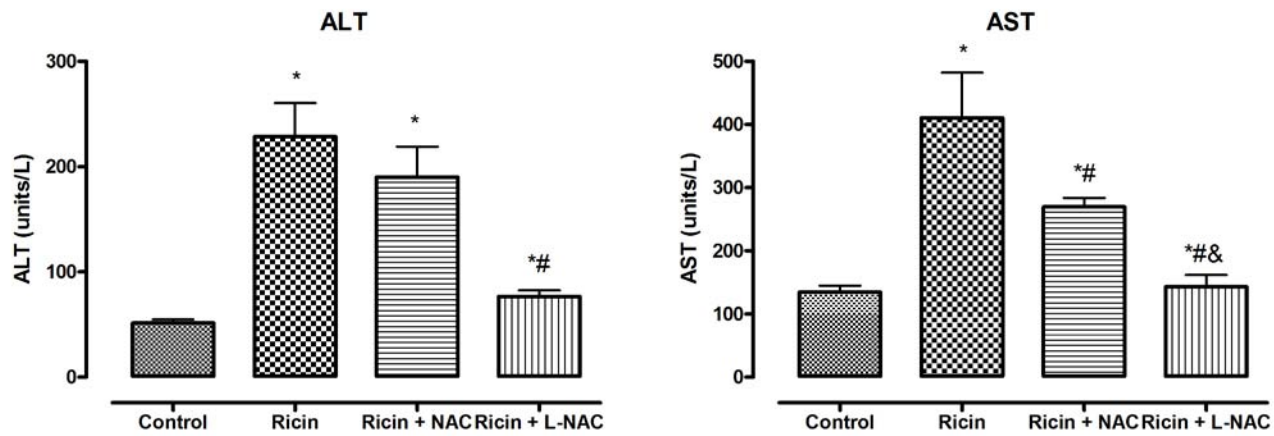
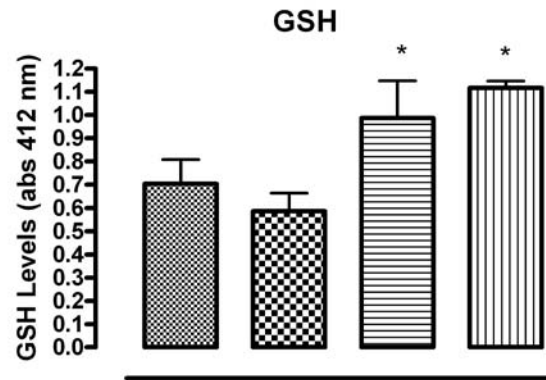
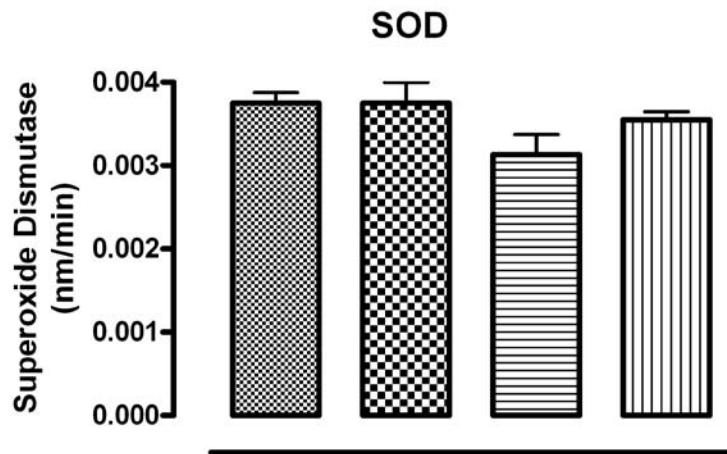
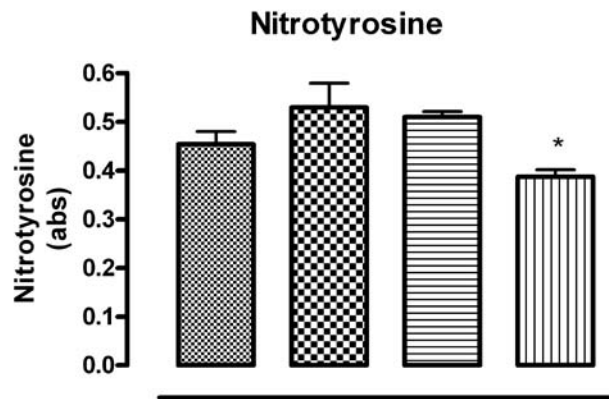


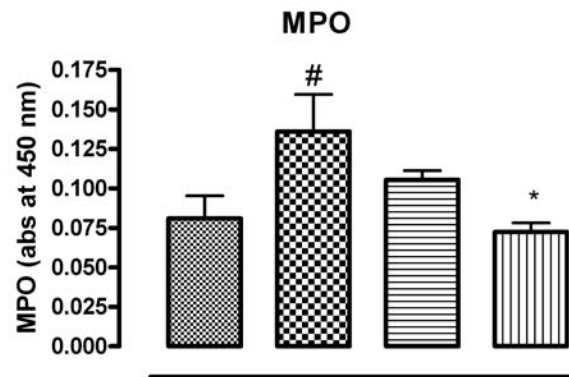
Figure 3: The effect of NAC or L-NAC against ricin-induced changes in the levels of liver enzymes, ALT and AST



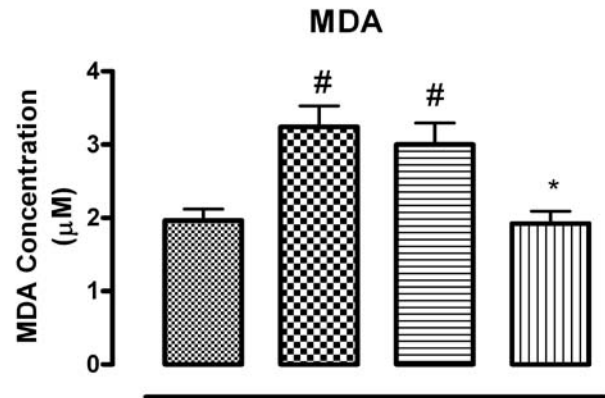
* significantly different from ricin group, $p < 0.05$



* significantly different from Ricin group, $p < 0.05$



* significantly different from Ricin group, $p < 0.05$
 # significantly different from Control group, $p < 0.05$



* significantly different from Ricin group, $p < 0.05$

significantly different from control group, $p < 0.05$

Figure 4: The effect of NAC or L-NAC against ricin-induced changes in the levels of lung antioxidant (SOD and GSH), oxidant (MDA) and inflammatory (nitrotyrosine and MPO) parameters.

Key Research Accomplishments:

- Characterization of liposomal antioxidant formulations (STIMAL formulations: liposomal NAC, liposomal alpha-tocopherol/NAC, liposomal gamma-tocopherol/NAC) with regards to their size, entrapment efficiencies, and stability in buffers and body fluids (plasma, bronchoalveolar lavage) at 4Cor 37C.
- Methodology for improving the stability of the liposomal formulation by lyophilization for prolonged storage or shipment purposes.
- Validation of the non-mutagenic properties of the liposomal antioxidant formulations.
- Determination of maximum tolerated dose of the liposomal antioxidant formulations in rodents and non-rodents.
- Determination of acute toxicity of liposomal antioxidant formulations in rodents.
- Determination of the uptake and antioxidant properties of liposomal NAC and free NAC in an *in vitro* model consisting of cells (hepG2 cell culture) exposed to oxidants.
- Development of Ultrapressure Liquid Chromatography (UPLC) method for the measurement of N-acetylcysteine and other thiols.
- Acute toxicity studies in male and female rodents and non-rodents showed that the intravenous administration of the STIMAL formulations are safe under the conditions investigated.
- Encapsulation of antioxidants within liposomes increases their circulation in both rodents and non-rodents.
- Confirmed the role of inflammation and oxidative stress in ricin toxicity.
- Demonstrated that antioxidants may confer protection against ricin-induced organ injuries.
- Demonstrated that the delivery of N-acetylcysteine as a liposomal formulation offers better protection against ricin-induced organ injuries than its conventional form.

Reportable Outcomes.

Presentations:

1. Advanced Medical Countermeasures Consortial Meeting, June 28, 2007, Crystal City, VA. "Safety of liposomal antioxidants (STIMAL).
2. Progress report, presented at Advanced Medical Countermeasures Consortium, Hunt Valley (MD), June 4-5, 2008.
3. Attended Biosciences Conference 2008 (Hunt Valley, MD).
4. Presented at the Department of Biomolecular Sciences, Laurentian University, 2007 (invited speaker).
5. Presented to the Department of Biology, Lakehead University, 2008 (invited speaker).

Publications:

1. Paromov, V., **Suntres, Z.**, Stone, W., Smith, M. Sulfur Mustard Toxicity if Human Skin: Role of Oxidative Stress and Antioxidant Therapy. *Journal of Burns and Wounds*, 2007.

2. Smith, M.G., Stone, W., Guo, R.F., Ward, P.A., **Suntres, Z.**, Mukherjee, S., and Das, S.K. Vesicants and Oxidative Stress. In Chemical Warfare Agents. Chemistry, Pharmacology, Toxicology, and Therapeutics, J.A. Romano, Jr., B.J. Lukey, H. Salem (eds). 2nd Edition, CRC Press, Boca Raton, FL. pp.247 – 312, 2007.
3. **Suntres, Z.E.**, Smith, M.G., Alipour, M., Omri, A., Pucaj, K. Acute toxicity of liposomal antioxidants in rodents (in preparation).
4. **Suntres, Z.E.**, Smith, M.G., Alipour, M., Omri, A., Pucaj, K. Acute toxicity of liposomal antioxidants in beagle dogs (in preparation).
5. Buonocore, C., Alipour M., Omri, A., Smith, M.G., **Suntres, Z.E.** Role of reactive oxygen species in ricin-induced toxicity. (in preparation)
6. Buonocore, C., Alipour M., Omri, A., Smith, M.G., **Suntres, Z.E.** Treatment of ricin-induced toxicity with liposomal N-acetylcysteine. (in preparation).

Training of one PhD graduate student (Misagh Alipour), one research assistant (Natasha Vermulen) and one undergraduate student (Caroline Buonocoro).

Personnel that received support from this award – Misagh Alipour and Peter Mitsopoulos.

Conclusion.

Liposomal formulations containing NAC with alpha- or gamma-tocopherols are stable in the presence body fluids such as plasma and bronchoalveolar lavage suggesting that the liposomal antioxidant formulations can be effective in the treatment of oxidant-induced tissue injuries because they can overcome structure destabilization as a result of interaction with certain serum components present in blood (following iv injection) and bronchoalveolar lavage (following inhalation). The liposomal antioxidant formulations are non mutagenic. The dosage range finding study used to determine the maximum tolerated doses (MTD) in male and female Sprague-Dawley rats and beagle dogs, as well as the acute toxicity studies, showed that the liposomal antioxidant formulations did not produced any adverse effects assessed clinically, biochemically, and histopathologically and deemed to be potentially safe for their use in Phase I clinical trials. Pharmacokinetic studies showed that intravenous administration of antioxidants as liposomal formulations dramatically increased their circulation time. The antioxidant formulations are able to ameliorate the organ damage associated with inflammation, probably by sequestering the reactive oxygen species generated by the inflammatory cells. The improved protection conferred by L-NAC may be attributed to the higher retention of NAC in tissues.

To-date, no antidote exists for ricin. Ricin poisoning is treated by giving victims supportive medical care to minimize the effects of the poisoning. The results of this study demonstrate that the administration of antioxidants, such as N-acetylcysteine, may prove useful in ameliorating the toxic effects of ricin and other potential chemical and biological toxicants.

References

1. Naghii MR. Sulfur mustard intoxication, oxidative stress, and antioxidants. *Mil. Med.* 2002; 167:573-5.
2. Paromov V, Suntres Z, Stone W, Smith M. Sulfur Mustard Toxicity if Human Skin: Role of Oxidative Stress and Antioxidant Therapy. *Journal of Burns and Wounds*, 2007 (in press).
3. Paromov, V., Suntres, Z., Stone, W., Smith, M. Sulfur Mustard Toxicity if Human Skin: Role of Oxidative Stress and Antioxidant Therapy. *Journal of Burns and Wounds*, 7:60-85, 2007.
4. Stone WL, Smith MG, Therapeutic uses of antioxidant liposomes. *Mol. Biotechnol* 2004; 27:217-30.
5. Suntres ZE, Hepworth SR, Shek PN, Protective effect of liposome-associated α -tocopherol against paraquat-induced acute lung toxicity. *Biochem. Pharmacol.* 1992; 44:1811-18.
6. Suntres ZE, Shek PN, Prevention of phorbol myristate acetate-induced lung injury by α -tocopherol liposomes. *J. Drug Targeting* 1995; 3:201-8.
7. Suntres ZE, Shek PN, Alleviation of paraquat-induced lung injury by pretreatment with bifunctional liposomes containing α -tocopherol and glutathione. *Biochem. Pharmacol.* 1996; 52: 1515-20.
8. Suntres ZE, Role of Antioxidants in Paraquat Toxicity. *Toxicology* 2002; 180: 65-77.
9. Suntres, Z.E., Stone, W., and Smith, MG. Riin-induced tissue-injury: The role of oxidative stress. *J Med CBR Def*, Volume 3, 2005

09/10/08

APPENDIX 1: Chromosomal Abberation Test

DRAFT

**CHROMOSOME ABERRATION TEST OF
Empty liposomes (DPPC), Liposomal NAC, Liposomal
alpha-tocopherol/NAC and Liposomal gamma-
tocopherol/NAC
IN CULTURED CHINESE HAMSTER OVARY CELLS**

Nucro-Technics Project No.:

For Study Sponsor

Northern Ontario School of Medicine

**955 Oliver Road
Thunder Bay, Ontario
P7B 5E1**

09/10/08

Contacting Facility and Sponsorship

TESTING FACILITY:

Nucro-Technics
2000 Ellesmere Road, Unit #16
Scarborough, Ontario, Canada
M1H 2W4

SPONSOR:

Northern Ontario School of Medicine
955 Oliver Road
Thunder Bay, Ontario
P7B 5E1

STUDY MONITOR:

Zack Suntres, Ph.D.
Northern Ontario School of Medicine
Tel. No.: (807) 766-7395
Fax No.: (807) 766-7370
Email: zacharias.suntres@normed.ca

SPONSOR'S REPRESENTATIVE:

Dr. Greg Ross
Associate Dean-Research
Northern Ontario School of Medicine

09/10/08

SUMMARY

The test substances, empty liposomes (DPPC), liposomal NAC, liposomal α -tocopherol/NAC and liposomal γ -tocopherol/NAC were investigated in an *in vitro* chromosome aberration test for their potential to induce structural chromosome aberrations in Chinese hamster ovary cell line WB_L. The experimental design followed the *OECD Guideline for the Testing of Chemicals – 473, In Vitro Mammalian Chromosome Aberration Test* (1997).

1. Test and Control Articles

Test Article #1:

Identity:	Liposomes consisting of DPPC lipids
Color/Form:	Lyophilized white powder
Batch / Lot No.:	will be documented in the report
Purity:	will be documented in the report
Storage Conditions:	-10 to -25°C lyophilized (room temperature reconstituted; see directions for reconstitution)
Handling Precautions:	Handle aseptically, standard laboratory procedures
Supplier:	Northern Ontario School of Medicine

Test Article #2:

Identity:	Liposomes consisting of DPPC lipids and N-acetylcysteine (NAC)
Color/Form:	Lyophilized white powder
Batch / Lot No.:	will be documented in the report
Purity:	will be documented in the report
Storage Conditions:	-10 to -25°C lyophilized (room temperature reconstituted; see directions for reconstitution)
Handling Precautions:	Handle aseptically, standard laboratory procedures
Supplier:	Northern Ontario School of Medicine

Test Article #3:

Identity:	Liposomes consisting of DPPC lipids and α -tocopherol and NAC
Color/Form:	Lyophilized white powder

09/10/08

Batch / Lot No.:	will be documented in the report
Purity:	will be documented in the report
Storage Conditions:	-10 to -25°C lyophilized (room temperature reconstituted; see directions for reconstitution)
Handling Precautions:	Handle aseptically, standard laboratory procedures
Supplier:	Northern Ontario School of Medicine

Test Article #4:

Identity:	Liposomes consisting of DPPC lipids and γ -tocopherol and NAC
Color/Form:	Lyophilized white powder
Batch / Lot No.:	will be documented in the report
Purity:	will be documented in the report
Storage Conditions:	-10 to -25°C lyophilized (room temperature reconstituted; see directions for reconstitution)
Handling Precautions:	Handle aseptically, standard laboratory procedures
Supplier:	Northern Ontario School of Medicine

Test Article Properties

The Sponsor will provide documentation on the strength, stability, and purity on each batch of test article, unless otherwise noted.

Test and Control Article Preparation

The test articles were prepared by Medical Sciences Division of Northern Ontario School of Medicine and provided in lyophilized form.

In Experiments 1 and 2, cultures were exposed to the liposomal formulations for 3 hours in the absence and presence of an S9 metabolic activation system, respectively. S9 was prepared from the livers of rats pre-treated with a combination of phenobarbital and benzoflavone. Cells were harvested at 18 hours, approximately 1.5 normal cell cycle lengths. In Experiment 3, the exposure was extended until harvest time at 18 hours without S9.

Exposure to DPPC liposomes, Liposomal NAC, Liposomal α -tocopherol/NAC or Liposomal γ -tocopherol/NAC for 3 hours with and without S9 did not result in detectable cytotoxicity when evaluated by cell count and mitotic index. Extending

09/10/08

exposure to 18 hours without S9 did not significantly produce any cytotoxicity. One hundred metaphase cells from each of the duplicate cultures of each of the 4 dilutions were analyzed for chromosome aberrations (16 formulations in total). All results were negative.

It was thus concluded that exposure to DPPC liposomes, Liposomal NAC, Liposomal α -tocopherol/NAC or Liposomal γ -tocopherol/NAC did not induce chromosome aberrations in cultured WB_L Chinese hamster ovary cells under the conditions of the test.

09/10/08

Table of Contents

Testing Facility and Sponsorship	1
Report Approval	2
Summary	3
Chromosome Aberration Test	7
Introduction	7
Materials	7
Procedure	8
Results	11
Discussion	12
Conclusion	12
Literature	37

List of Tables (pages 13-36)

Table 1. Relative Cell Growth	
Table 2. Relative Mitotic Index	
Table 3-1. Summary of Chromosome Aberrations – Experiment 1, -S9.....	
Table 3-2. Summary of Chromosome Aberrations – Experiment 2, +S9.....	
Table 3-3. Summary of Chromosome Aberrations – Experiment 3, -S9, 18 hour exposure	

List of Appendices (pg 38-40)

Appendix I. pH and Osmolality of Treatment Media

CHROMOSOME ABERRATION TEST OF LIPOSOMAL ANTIOXIDANT FORMULATIONS IN CULTURED CHINESE HAMSTER OVARY CELLS

1. Introduction

The objective of the study was to test Empty liposomes consisting of DPPC lipids, Liposomal NAC, Liposomal α -tocopherol/NAC or Liposomal γ -tocopherol/NAC for their potential to induce aberrant chromosomes in cultured Chinese hamster ovary (CHO) cell line WB_L. The study design followed the *OECD Guideline for the Testing of Chemicals – 473, In Vitro Mammalian Chromosome Aberration Test* (OECD, 1997).

09/10/08

2. Materials

2.1. Test substance

Liposomes were prepared from dipalmitoylphosphatidylcholine and contained NAC, α -tocopherol/NAC or γ -tocopherol/NAC.

2.2. Cells

Cells grow as an adherent monolayer, with a doubling time of approximately 12 hours (Galloway, S.M., *et al*, 1987). Health status of the cultures was determined by observation under a microscope. The cultures were free of mycoplasma.

2.3. Media and culture conditions

Cells were cultured in McCoy's 5A Medium Modified with 2 mM L-glutamine and 25 mM HEPES supplemented with 10% heat-inactivated fetal bovine serum (Invitrogen Corporation, Burlington, ON, Canada). Sterile Falcon tissue culture flasks (BD Biosciences Bedford, MA, U.S.A.) were used. The cells were incubated in a humidified tissue culture incubator at $37 \pm 2^\circ\text{C}$ and $5 \pm 2\%$ CO_2 . When cells reached approximately 50 - 70 % confluency, they were dislodged with 0.05% trypsin (Invitrogen Corporation, Burlington, ON, Canada), collected by centrifugation, and seeded in fresh medium. Each trypsinization was recorded as one passage. For long-term preservation in liquid nitrogen, a freezing medium containing 8% dimethyl sulfoxide (DMSO) (CASRN: 67-68-5) (Sigma Chemical Co., St. Louis, MO, U.S.A.) was used.

2.4. Controls

A sterile 0.1 M phosphate buffer solution, pH 7.4 (PBS), was prepared at the testing facility and was used to re-constitute the lyophilized liposomal test articles and was used as the negative control. Mitomycin C (MMC), (CASRN: 50-07-7), Lot No. 103K0498 (Sigma Chemical Co., St. Louis, MO, U.S.A.) was used at 0.5 $\mu\text{g}/\text{ml}$ as a positive control for cultures not treated with S9. Cyclophosphamide (CP), (CASRN: 6055-19-2), Lot No. 113K1406, (Sigma Chemical Co., St. Louis, MO, U.S.A.) was used at 7.5 $\mu\text{g}/\text{ml}$ as a positive control for treatment with S9.

09/10/08

2.5. Metabolic activation system

S9 used in the study was the microsomal fraction of a liver homogenate from rats treated with phenobarbital-5, 6-benzoflavone (Moltox Inc. Boone, NC, U.S.A.). Cofactors for the microsomal enzymes include β -nicotinamide adenine dinucleotide phosphate (NADP) and isocitric acid (Sigma Chemical Co., St. Louis, MO, U.S.A.). A 10 x concentrated S9 mix was freshly prepared. The final culture contained 2.4 mg/ml NADP, 4.5 mg/ml isocitric acid and 25 μ l/ml S9 (Galloway, S.M., *et al*, 1987).

3. Procedure

3.1. Preparation of cultures

A continuous culture from passage 13 to 14 was used for Experiments 1 and 2 and a separate culture, passage 10, was used for Experiment 3. On the day before each experiment, approximately 5×10^5 cells were seeded into each T-25 cm² Falcon flask. The cultures were incubated overnight. Duplicate cultures were prepared for each exposure concentration. When examined under an inverted microscope the next day, the cultures appeared healthy, evenly distributed and approximately 20-30 % confluent.

3.2. Test substance preparation and treatment

On each day of an experiment, solutions of each liposomal test article were first prepared separately in 0.1 M phosphate buffer, pH 7.4. The treatment proceeded in a humidified incubator at $37 \pm 2^\circ\text{C}$ and $5 \pm 2\%$ CO₂ for 3 hours in Experiments 1 and 2 or for 18 hours in Experiment 3. At the end of a three-hour treatment, the cells were washed with phosphate buffered saline and the incubation continued in fresh culture medium until harvest time.

The treatment media of the negative control, 5 mg/ml and 10 mg/ml were sampled for measurement of pH and osmolality, using the US Pharmacopeia methods as a reference (USP, 2006a and 2006b).

3.3. Harvest

For all experiments, cultures were harvested 18 hours after the initiation of treatment. Approximately two hours prior to harvesting, Colcemid[®] (Invitrogen Corporation, Burlington, ON, Canada) was added at 0.1 μ g/ml to arrest cells in metaphase. The cells were then harvested and the number of cells was counted using the trypan blue exclusion method. Relative Cell Growth (RCG) was calculated as follows:

09/10/08

$$\text{RCG (\%)} = \frac{\text{Viable cell count in test flask}}{\text{Viable cell count in solvent control flask}} \times 100$$

3.4. Preparation of chromosome slides

The cells were collected by centrifugation, swelled in 0.075 M KCl and fixed in a 3:1 mixture of methanol and glacial acetic acid. They were dripped on to coded slides, air-dried and stained in 10% Giemsa stain (Evans, H.J., 1976).

For each duplicate culture, 500 cells were examined to score mitotic index. The mitotic index (MI) was calculated as the percent of cells at the mitotic stage. Relative mitotic index (RMI) was calculated as:

$$\text{RMI (\%)} = \frac{\text{Test concentration MI}}{\text{Solvent control MI}} \times 100$$

3.5. Analysis of chromosome aberrations

All slides were randomly coded. Well-spread metaphase cells with 19 - 23 chromosomes were analysed for chromosome aberrations as defined in Protocol TOP/176914 (Scott, *et al.*, 1990; OECD, 1997). One hundred cells from each negative control and DPPC liposomes-, liposomal NAC-, liposomal α -tocopherol/NAC- or liposomal γ -tocopherol/NAC-treated culture or 50 cells from a positive control culture were examined (OECD, 1997). The number of each type of aberration, number of aberrations per cell and percent of cells with aberrations were recorded and summarized. If a cell contained >10 aberrations, it counted as ten under “severely damaged cells (*sd*)” (Scott, D., *et al.*, 1990). The number of endoreduplicated and polyploidy cells, chromatid gaps and chromosome gaps were recorded when encountered, but not included in the calculations.

4. Results

Three experiments for each of the four formulations were performed. Scores of structural chromosome aberrations in metaphase cells are summarized in Tables 3-1, 3-2 and 3-3 as percentages of cells with aberrations for each corresponding formulation. In Experiments 1 and 2, the cultures were exposed to DPPC liposomes, liposomal NAC, liposomal α -

09/10/08

tocopherol/NAC or liposomal γ -tocopherol/NAC for 3 hours in the absence and the presence of S9, respectively. In Experiment 3, the exposure time was extended to 18 hours without S9.

No precipitation of the test article was observed in the culture media throughout the experiments. All treatment media maintained a neutral pH (Appendix I). Osmolality measurements of the treatment media were similar to those of the negative controls and were within a physiological range (Appendix I). Under these conditions, the cells appeared healthy during and after DPPC liposomes-, liposomal NAC-, liposomal α -tocopherol/NAC- or liposomal γ -tocopherol/NAC- treatment for 3 hours with and without S9. The cell growth was normal throughout the testing period at all dilutions tested.

The mitotic indices showed no cytotoxic effects in all three different experiments. (Tables 2).

One hundred metaphase cells from each culture were analyzed for chromosome aberrations. As shown in Tables 3-3, the results confirmed a non-mutagenic response under the test conditions.

All concurrent positive controls induced significant numbers of cells with chromosome aberrations. Without S9, mitomycin C at 0.5 μ g/ml induced chromosome aberrations in 85-95 % of cells after three hours of exposure (Tables 3-1) and in 66-67 % of cells after 18 hours of exposure (Tables 3-3). In the presence of S9, treatment with 7.5 μ g/ml of cyclophosphamide for three hours resulted in 65-66 % cells with chromosome aberrations (Table 3-2).

5. Discussion

In each of the three experiments, at least four exposure concentrations were analyzed for structural chromosome aberrations. This complied with the requirement of the current guidelines in terms of the number of concentrations to be scored (OECD, 1997).

In Experiments 1 and 2, the liposomal formulations were considered to be non-toxic. After exposure for three hours with and without S9, no cytotoxicity was observed, as evaluated by cell count and mitotic index and by examining the cultures under an inverted microscope.

In Experiment 3, when extending the exposure time to 18 hours without S9, no cytotoxicity was observed.

6. Conclusion

09/10/08

The liposomal antioxidant formulations consisting of DPPC lipids, with NAC, NAC/alpha-tocopherol or NAC/gamma-tocopherol are not clastogenic in cultured Chinese hamster ovary WB_L cells under the conditions of the test.

Results for DPPC

Table 1. Relative Cell Growth for DPPC Control

	Experiment 1, - S9			Experiment 2, + S9			Experiment 3, - S9		
DPPC (mg/ml)	Cells per flask (x 10⁶)	Mean (x 10 ⁶)	Relative Cell Growth (%)	Cells per flask (x 10⁶)	Mean (x 10 ⁶)	Relative Cell Growth (%)	Cells per flask (x 10⁶)	Mean (x 10 ⁶)	Relative Cell Growth (%)
0	2.65	2.68	100	1.80	1.73	100	3.15	3.40	100
	2.70			1.65			3.65		
5	2.60	2.55	95	1.60	1.50	86	3.25	3.40	100
	2.50			1.40			3.55		
10	2.75	2.77	103	1.40	1.73	100	4.00	3.93	115
	2.80			2.05			3.85		
25	2.50	2.43	91	1.75	1.50	87	2.65	3.05	90
	2.35			1.25			3.45		
50	3.35	3.15	118	1.55	1.78	103	3.25	3.33	98
	2.95			2.00			3.40		

Table 2. Relative Mitotic Index for DPPC Control

	Experiment 1, - S9			Experiment 2, + S9			Experiment 3, - S9		
DPPC (mg/ml)	No. of dividing cells	Mitotic index (%)	Relative mitotic index (%)	No. of dividing cells	Mitotic index	Relative mitotic index (%)	No. of dividing cells	Mitotic index (%)	Relative mitotic index (%)
0	145	29.8	100	145	28.5	100	56	9.9	100
	153			140			43		
5	160	32.3	108	175	33.2	116	55	10.4	105
	163			157			49		
10	146	31.0	104	156	28.3	99	50	8.8	89
	164			127			38		
25	154	32.9	110	139	26.4	83	48	8.8	89
	175			125			40		
50	154	28.9	97	140	26.5	93	51	9.7	98
	135			125			46		

Note: *No. of Dividing Cells* is counted from a total of 500 cells;
Mitotic Index is calculated as the number of dividing cells per hundred cells observed;
Relative Mitotic Index is mitotic index normalized against that of the negative control culture.

Table 3-1. Summary of Chromosome Aberrations - Experiment 1, - S9, 3 hr. exposure for DPPC Control

DPPC (mg/ml)	Cells	Not Computed				Chromatid Type								Chromosome Type				Other Types		No. Aberrations Per Cell	of %	% of Cel with Aberrat
						Simple				Complex				Simple		Complex						
		<i>tg</i>	<i>sg</i>	<i>e</i>	<i>pp</i>	<i>tb</i>	<i>isb</i>	<i>tr</i>	<i>qr</i>	<i>cr</i>	<i>id</i>	<i>ci</i>	<i>sb</i>	<i>d</i>	<i>r</i>	<i>dm</i>	<i>pu</i>	<i>sd</i>				
0	100																			0	0	
	100				1															0	0	
	%				.5															0	0	
5	100																			0	0	
	100																			0	0	
	%																			0	0	
10	100																			0	0	
	100																			0	0	
	%																			0	0	
25	100																			0	0	
	100																			0	0	
	%																			0	0	
50	100				1															0	0	
	100				1															0	0	
	%				1.0															0	0	
Mitomycin C 0.5 □g/ml	50					10	1	30	8	4	5	8	30		2	1		2	2.08	96		
	50	3	1		1	24	3	32	7	4	5	10	20		4	1		4	2.87	88		
	%	3.0	1		1	34	4	62	15	8	10	18	50		6	2		6	2.45	92		

Note: *sd* = 10 aberrations in calculations

Table 3-2. Summary of Chromosome Aberrations - Experiment 2, +S9, 3 hr. exposure for DPPC Control

DPPC (mg/ml)	Cells	Not Computed				Chromosome Type								Other Types		No. of Aberrations Per Cell	% of Cells with Aberrations						
		Simple		Complex		Simple		Complex		<i>pu</i>	<i>sd</i>												
		<i>tg</i>	<i>sg</i>	<i>e</i>	<i>pp</i>	<i>tb</i>	<i>isb</i>	<i>tr</i>	<i>qr</i>			<i>cr</i>	<i>id</i>	<i>ci</i>	<i>sb</i>			<i>d</i>	<i>r</i>	<i>dm</i>			
0	100			1	2																0.01	1.0	
	100	1		1	2																	0	0
	%	0.5		1.0	2.0																	0.005	0.5
5	100	2			4																	0	0
	100				1																	0	0
	%	1.0			2.5																	0	0
10	100	1			2																	0	0
	100	1			4																	0	0
	%	1.0			3.0																	0	0
25	100				3																	0	0
	100				2																	0	0
	%				2.5																	0	0
50	100				2																	0	0
	100			1	2																	0	0
	%			0.5	2.0																	0	0
Cyclophosphamide 7.5 μ g/ml	50	4	3		0	10	6	10	8	3	4	9	5		2	2			2		1.60	68.0	
	50	2	2		1	10	4	8	4	1	3	4	7		1	2			1		1.12	62.0	
	%	6	5		1	20	10	18	12	4	7	13	13		3	4			3		1.36	65.0	

Note: *sd* = 10 aberrations in calculations

Table 3-3. Summary of Chromosome Aberrations - Experiment 3, - S9, 18 hr. exposure for DPPC Control

DPPC (mg/ml)	Cells	Not Computed				Chromatid Type								Chromosome Type				Other Types	No. Aberrations Per Cell	of % of Cells with Aberrations	
		<i>tg</i>	<i>sg</i>	<i>e</i>	<i>pp</i>	Simple				Complex				Simple		Complex					
						<i>tb</i>	<i>isb</i>	<i>tr</i>	<i>qr</i>	<i>cr</i>	<i>id</i>	<i>ci</i>	<i>sb</i>	<i>d</i>	<i>r</i>	<i>dm</i>	<i>pu</i>				<i>sd</i>
0	100				1															0	0
	100				1															0	0
	%				1.0															0	0
5	100				2															0	0
	100	1			2															0	0
	%	0.5			2.0															0	0
10	100				4															0	0
	100	2	1		2															0	0
	%	1.0	0.5		3.0															0	0
25	100	1	1		1						1									0.01	1.0
	100				3															0	0
	%	0.5	0.5		2.0						0.5									0.005	0.5
50	43																			0	0
	157	2		1	3															0	0
	%	1.0		0.5	1.5															0	0
Mitomycin C 0.5 μ g/ml	50	3	1			14	4	20	4	5	6	2	5	2	5	1		1	1.74	69.0	
	50	3	1		1	6	2	11	4	2	6	1	5	1	4	1			0.98	63.0	
	%	6	2		1	20	6	31	8	7	12	3	10	3	9	2		1	1.36	66.0	

sd = 10 aberrations in calculations

DPPC NAC

Table 1. Relative Cell Growth for DPPC/NAC

	Experiment 1, - S9			Experiment 2, + S9			Experiment 3, - S9		
DPPC/NAC (mg/ml)	Cells per flask (x 10⁶)	Mean (x 10 ⁶)	Relative Cell Growth (%)	Cells per flask (x 10⁶)	Mean (x 10 ⁶)	Relative Cell Growth (%)	Cells per flask (x 10⁶)	Mean (x 10 ⁶)	Relative Cell Growth (%)
0	2.70	2.78	100	2.80	2.73	100	3.00	3.25	100
	2.85			2.65			3.50		
5/1.5	2.60	2.65	95	2.60	2.55	91	3.25	3.20	98
	2.70			2.50			3.15		
10/3.0	2.65	2.78	100	2.70	2.68	98	3.45	3.40	105
	2.90			2.65			3.35		
25/7.5	2.60	2.70	97	2.60	2.52	92	3.20	3.35	103
	2.80			2.45			3.50		
50/15	2.65	2.65	95	2.55	2.65	97	3.15	3.08	95
	2.65			2.75			3.00		

Table 2. Relative Mitotic Index for DPPC Control

	Experiment 1, - S9			Experiment 2, + S9			Experiment 3, - S9		
DPPC (mg/ml)	No. of dividing cells	Mitotic index (%)	Relative mitotic index (%)	No. of dividing cells	Mitotic index	Relative mitotic index (%)	No. of dividing cells	Mitotic index (%)	Relative mitotic index (%)
0	145	29.8	100	145	28.5	100	56	9.9	100
	153			140			43		
5	160	32.3	108	175	33.2	116	55	10.4	105
	163			157			49		
10	146	31.0	104	156	28.3	99	50	8.8	89
	164			127			38		
25	154	32.9	110	139	26.4	83	48	8.8	89
	175			125			40		
50	154	28.9	97	140	26.5	93	51	9.7	98
	135			125			46		

Note: *No. of Dividing Cells* is counted from a total of 500 cells;
Mitotic Index is calculated as the number of dividing cells per hundred cells observed;
Relative Mitotic Index is mitotic index normalized against that of the negative control culture.

Table 3-1. Summary of Chromosome Aberrations - Experiment 1, - S9, 3 hr. exposure for DPPC Control/NAC

DPPC/NAC (mg/ml)	Cells	Not Computed				Chromatid Type								Chromosome Type				Other Types		No. Aberrations Per Cell	of % of Cel with Aberra
						Simple				Complex				Simple		Complex					
		<i>tg</i>	<i>sg</i>	<i>e</i>	<i>pp</i>	<i>tb</i>	<i>isb</i>	<i>tr</i>	<i>qr</i>	<i>cr</i>	<i>id</i>	<i>ci</i>	<i>sb</i>	<i>d</i>	<i>r</i>	<i>dm</i>	<i>pu</i>	<i>sd</i>			
0	100																			0	0
	100																			0	0
	%																			0	0
5/1.5	100																			0	0
	100																			0	0
	%																			0	0
10/3.0	100																			0	0
	100																			0	0
	%																			0	0
25/7.5	100																			0	0
	100																			0	0
	%																			0	0
50/15	100																			0	0
	100																			0	0
	%																			0	0
Mitomycin C 0.5 μ g/ml	50					10	1	30	8	4	5	8	30		2	1		2	2.08	96	
	50	3	1		1	24	3	32	7	4	5	10	20		4	1		4	2.87	88	
	%	3.0	1		1	34	4	62	15	8	10	18	50		6	2		6	2.45	92	

Note: *sd* = 10 aberrations in calculations

Table 3-2. Summary of Chromosome Aberrations - Experiment 2, +S9, 3 hr. exposure for DPPC/NAC

DPPC/NAC (mg/ml)	Cells	Not Computed				Chromatid Type						Chromosome Type				Other Types		No. Aberrations Per Cell	of	% of Cells with Aberrations	
						Simple		Complex				Simple		Complex							
		<i>tg</i>	<i>sg</i>	<i>e</i>	<i>pp</i>	<i>tb</i>	<i>isb</i>	<i>tr</i>	<i>qr</i>	<i>cr</i>	<i>id</i>	<i>ci</i>	<i>sb</i>	<i>d</i>	<i>r</i>	<i>dm</i>	<i>pu</i>				<i>sd</i>
0	100			1	1															0	0
	100		1	1	2															0	0
	%		0.5	1.0	1.5															0	0
5/1.5	100				1															0	0
	100				1															0	0
	%				1															0	0
10/3.0	100				2															0	0
	100				1															0	0
	%				1.5															0	0
25/7.5	100				2															0	0
	100				2															0	0
	%				2.0															0	0
50/15.0	100				1															0	0
	100				1															0	0
	%				1.0															0	0
Cyclophosphamide 7.5 μ g/ml	50	4	3		0	10	6	10	8	3	4	9	5		2	2		2		1.60	68.0
	50	2	2		1	10	4	8	4	1	3	4	7		1	2		1		1.12	62.0
	%	6	5		1	20	10	18	12	4	7	13	13		3	4		3		1.36	65.0

Note: *sd* = 10 aberrations in calculations

Table 3-3. Summary of Chromosome Aberrations - Experiment 3, - S9, 18 hr. exposure for DPPC?NAC

DPPC/NAC (mg/ml)	Cells	Not Computed				Chromatid Type						Chromosome Type				Other Types	No. Aberrations Per Cell	of % of Cells with Aberrations			
		<i>tg</i>	<i>sg</i>	<i>e</i>	<i>pp</i>	Simple			Complex			Simple		Complex							
						<i>tb</i>	<i>isb</i>	<i>tr</i>	<i>qr</i>	<i>cr</i>	<i>id</i>	<i>ci</i>	<i>sb</i>	<i>d</i>	<i>r</i>				<i>dm</i>	<i>pu</i>	<i>sd</i>
0	100				2															0	0
	100				2															0	0
	%				2.0															0	0
5/1.5	100	1																		0	0
	100	1																		0	0
	%	1.0																		0	0
10/3.0	100				1															0	0
	100				1															0	0
	%				1.0															0	0
25/7.5	100				1															0	0
	100				1															0	0
	%				1.0															0	0
50/15	43																			0	0
	157			1	1															0	0
	%			0.5	0.5															0	0
Mitomycin C 0.5 μ g/ml	50	3	1			14	4	20	4	5	6	2	5	2	5	1		1	1.74	69.0	
	50	3	1		1	6	2	11	4	2	6	1	5	1	4	1			0.98	63.0	
	%	6	2		1	20	6	31	8	7	12	3	10	3	9	2		1	1.36	66.0	

sd = 10 aberrations in calculations

DPPC-NAC/ α T

Table 1. Relative Cell Growth for DPPC/NAC/alpha-tocopherol

	Experiment 1, - S9			Experiment 2, + S9			Experiment 3, - S9		
DPPC/NAC/ α -T (mg/ml)	Cells per flask (x 10⁶)	Mean (x 10 ⁶)	Relative Cell Growth (%)	Cells per flask (x 10⁶)	Mean (x 10 ⁶)	Relative Cell Growth (%)	Cells per flask (x 10⁶)	Mean (x 10 ⁶)	Relative Cell Growth (%)
0	2.75	2.78	100	2.00	1.97	100	3.15	3.23	100
	2.80			1.95			3.30		
5/1.5/1.0	2.80	2.75	98	1.90	1.87	95	3.15	3.20	99
	2.70			1.85			3.25		
10/3.0/2.0	2.75	2.78	100	1.90	1.95	99	3.25	3.20	99
	2.80			2.00			3.155		
25/7.5/5.0	2.65	2.70	97	1.75	1.85	93	3.30	3.25	101
	2.75			1.95			3.20		
50/15/10	2.75	2.83	102	1.85	1.90	96	3.20	3.13	97
	2.90			2.95			3.05		

Table 2. Relative Mitotic Index for DPPC/NAC/ α -T

	Experiment 1, - S9			Experiment 2, + S9			Experiment 3, - S9		
DPPC/NAC/ α T (mg/ml)	No. of dividing cells	Mitotic index (%)	Relative mitotic index (%)	No. of dividing cells	Mitotic index	Relative mitotic index (%)	No. of dividing cells	Mitotic index (%)	Relative mitotic index (%)
0	150	30.5	100	140	27.0	100	70	12.5	100
	155			130			55		
5/1.5/1.0	160	30.5	100	150	28.5	105	55	11.5	92
	145			135			60		
10/3.0/2.0	140	30.0	98	145	29.5	109	60	13.0	104
	160			150			70		
25/7.5/5.0	140	29.0	95	135	29.5	109	60	11.5	92
	150			165			55		
50/15/10	130	28.0	92	160	30.5	112	60	12.0	96
	150			145			60		

Note: *No. of Dividing Cells* is counted from a total of 500 cells;
Mitotic Index is calculated as the number of dividing cells per hundred cells observed;
Relative Mitotic Index is mitotic index normalized against that of the negative control culture.

Table 3-1. Summary of Chromosome Aberrations - Experiment 1, - S9, 3 hr. exposure for DPPC Control/NAC/ α -T

DPPC/NAC/ α T (mg/ml)	Cells	Not Computed				Chromatid Type								Chromosome Type				Other Types	No. Aberrations Per Cell	of % of Cells with Aberra	
		<i>tg</i>	<i>sg</i>	<i>e</i>	<i>pp</i>	Simple				Complex				Simple		Complex					
						<i>tb</i>	<i>isb</i>	<i>tr</i>	<i>qr</i>	<i>cr</i>	<i>id</i>	<i>ci</i>	<i>sb</i>	<i>d</i>	<i>r</i>	<i>dm</i>	<i>pu</i>				<i>sd</i>
0	100																			0	0
	100																			0	0
	%																			0	0
5/1.5/1.0	100																			0	0
	100																			0	0
	%																			0	0
10/3.0/2.0	100																			0	0
	100																			0	0
	%																			0	0
25/7.5/5.0	100																			0	0
	100																			0	0
	%																			0	0
50/15/10	100																			0	0
	100																			0	0
	%																			0	0
Mitomycin C 0.5 μ g/ml	50					8	1	28	7	3	4	9	27		2				1	1.98	86
	50	2	1		1	24	3	27	6	4	5	12	15		4	1		3	2.62	84	
	%	2.0	1		1	32	4	55	13	7	9	21	42		6	1		4	2.30	85	

Note: *sd* = 10 aberrations in calculations

Table 3-2. Summary of Chromosome Aberrations - Experiment 2, +S9, 3 hr. exposure for DPPC/NAC/ α -T

DPPC/NAC/ γ -T (mg/ml)	Cells	Not Computed				Chromatid Type						Chromosome Type				Other Types		No. Aberrations Per Cell	of	% of Cells with Aberrations	
		Simple		Complex				Simple		Complex		<i>pu</i>	<i>sd</i>								
		<i>tg</i>	<i>sg</i>	<i>e</i>	<i>pp</i>	<i>tb</i>	<i>isb</i>	<i>tr</i>	<i>qr</i>	<i>cr</i>	<i>id</i>			<i>ci</i>	<i>sb</i>	<i>d</i>	<i>r</i>				<i>dm</i>
0	100				1															0	0
	100				1															0	0
	%				1.0															0	0
5/1.5/1.0	100				1															0	0
	100																			0	0
	%				0.5															0	0
10/3.0/2.0	100																			0	0
	100				1															0	0
	%				0.5															0	0
25/7.5/5.0	100																			0	0
	100																			0	0
	%																			0	0
50/15.0/10	100		1																	0	0
	100		0.5																	0	0
	%																			0	0
Cyclophosphamide 7.5 μ g/ml	50	3	3		1	10	8	12	7	3	3	2	4		1	1		2	1.42	66.0	
	50	2	1		1	7	5	6	3	3	4	11	12		1	2			1.08	66.0	
	%	5	4		2	17	13	18	10	6	7	13	16		2	3		2	1.25	66.0	

Note: *sd* = 10 aberrations in calculations

Table 3-3. Summary of Chromosome Aberrations - Experiment 3, - S9, 18 hr. exposure for DPPC/NAC/ α -T

DPPC/NAC/ γ T (mg/ml)	Cells	Not Computed				Chromatid Type						Chromosome Type				Other Types <i>pu sd</i>	No. of Aberrations Per Cell	% of Cells with Aberrations		
		Simple		Complex		Simple		Complex												
		<i>tg</i>	<i>sg</i>	<i>e</i>	<i>pp</i>	<i>tb</i>	<i>isb</i>	<i>tr</i>	<i>qr</i>	<i>cr</i>	<i>id</i>	<i>ci</i>	<i>sb</i>	<i>d</i>	<i>r</i>				<i>dm</i>	
0	100				1														0	0
	100	1			1														0	0
	%	0.5			1.0														0	0
5/1.5/1.0	100	1																	0	0
	100																		0	0
	%	0.5																	0	0
10/3.0/2.0	100				1														0	0
	100				1														0	0
	%				1.0														0	0
25/7.5/5.0	100				1														0	0
	100				1														0	0
	%				1.0														0	0
50/15/10	43				2														0	0
	157				1														0	0
	%				1.5														0	0
Mitomycin C 0.5 \square g/ml	50	3	1			18	4	22	4	6	5	2	5	1	4	1		1	1.64	66.0
	50	2			1	8	4	13	3	2	6	2	4	1	2				0.90	68.0
	%	5	1		1	26	8	35	7	8	11	4	9	2	6	1		1	1.27	67.0

sd = 10 aberrations in calculations

DPPC-NAC/ γ T

Table 1. Relative Cell Growth for DPPC/NAC/gamma-tocopherol

	Experiment 1, - S9			Experiment 2, + S9			Experiment 3, - S9		
DPPC/NAC/ γ -T (mg/ml)	Cells per flask (x 10⁶)	Mean (x 10 ⁶)	Relative Cell Growth (%)	Cells per flask (x 10⁶)	Mean (x 10 ⁶)	Relative Cell Growth (%)	Cells per flask (x 10⁶)	Mean (x 10 ⁶)	Relative Cell Growth (%)
0	2.82	2.80	100	2.10	2.05	100	3.00	3.02	100
	2.78			2.00			3.04		
5/1.5/1.0	2.81	2.82	101	1.90	1.98	97	3.10	3.03	100
	2.83			2.06			2.96		
10/3.0/2.0	2.76	2.75	98	2.03	2.02	98	3.15	3.06	101
	2.74			1.99			2.97		
25/7.5/5.0	2.76	2.72	97	1.90	1.92	94	2.90	2.90	96
	2.68			1.94			2.89		
50/15/10	2.79	2.82	101	1.98	2.04	99	3.00	3.05	101
	2.85			2.08			3.10		

Table 2. Relative Mitotic Index for DPPC/NAC/ γ -T

	Experiment 1, - S9			Experiment 2, + S9			Experiment 3, - S9		
DPPC/NAC/ γ -T (mg/ml)	No. of dividing cells	Mitotic index (%)	Relative mitotic index (%)	No. of dividing cells	Mitotic index	Relative mitotic index (%)	No. of dividing cells	Mitotic index (%)	Relative mitotic index (%)
0	162	31.6	100	159	30.1	100	80	15.5	100
	154			142			75		
5/1.5/1.0	160	31.0	98	150	29.5	98	85	16.5	106
	150			145			80		
10/3.0/2.0	155	30.4	96	155	30.5	101	76	15.0	97
	149			150			74		
25/7.5/5.0	156	32.6	103	146	30.4	101	80	15.5	100
	170			158			75		
50/15/10	148	30.0	95	150	30.5	101	78	15.4	100
	152			155			76		

Note: *No. of Dividing Cells* is counted from a total of 500 cells;
Mitotic Index is calculated as the number of dividing cells per hundred cells observed;
Relative Mitotic Index is mitotic index normalized against that of the negative control culture.

Table 3-1. Summary of Chromosome Aberrations - Experiment 1, - S9, 3 hr. exposure for DPPC Control/NAC/γ-T

DPPC/NAC/γT (mg/ml)	Cells	Not Computed				Chromatid Type								Chromosome Type				Other Types	No. Aberrations Per Cell	of %	% of Cells with Aberrations	
		<i>tg</i>	<i>sg</i>	<i>e</i>	<i>pp</i>	Simple				Complex				Simple		Complex						
						<i>tb</i>	<i>isb</i>	<i>tr</i>	<i>qr</i>	<i>cr</i>	<i>id</i>	<i>ci</i>	<i>sb</i>	<i>d</i>	<i>r</i>	<i>dm</i>	<i>pu</i>					<i>sd</i>
0	100				1																0	0
	100																				0	0
	%				0.5																0	0
5/1.5/1.0	100																				0	0
	100																				0	0
	%																				0	0
10/3.0/2.0	100																				0	0
	100																				0	0
	%																				0	0
25/7.5/5.0	100				1																0	0
	100				1																0	0
	%				1																0	0
50/15/10	100																				0	0
	100																				0	0
	%																				0	0
Mitomycin C 0.5 μg/ml	50					8	1	28	7	3	4	9	27		2				1	1.98	86	
	50	2	1		1	24	3	27	6	4	5	12	15		4	1		3	2.62	84		
	%	2.0	1		1	32	4	55	13	7	9	21	42		6	1		4	2.30	85		

Note: *sd* = 10 aberrations in calculations

Table 3-2. Summary of Chromosome Aberrations - Experiment 2, +S9, 3 hr. exposure for DPPC/NAC/γ-T

DPPC/NAC/γ-T (mg/ml)	Cells	Not Computed				Chromatid Type						Chromosome Type				Other Types		No. Aberrations Per Cell	of	% of Cells with Aberrations		
						Simple			Complex			Simple		Complex		pu	sd					
		tg	sg	e	pp	tb	isb	tr	qr	cr	id	ci	sb	d	r						dm	
0	100																			0		0
	100				1															0		0
	%				0.5															0		0
5/1.5/1.0	100				1															0		0
	100																			0		0
	%				0.5															0		0
10/3.0/2.0	100				1															0		0
	100				1															0		0
	%				1.0															0		0
25/7.5/5.0	100																			0		0
	100																			0		0
	%																			0		0
50/15.0/10	100				1															0		0
	100				1															0		0
	%				1.0															0		0
Cyclophosphamide 7.5 μg/ml	50	3	3		1	10	8	12	7	3	3	2	4		1	1		2		1.42	66.0	
	50	2	1		1	7	5	6	3	3	4	11	12		1	2				1.08	66.0	
	%	5	4		2	17	13	18	10	6	7	13	16		2	3		2		1.25	66.0	

Note: sd = 10 aberrations in calculations

Table 3-3. Summary of Chromosome Aberrations - Experiment 3, - S9, 18 hr. exposure for DPPC/NAC/ γ -T

DPPC/NAC/ γ T (mg/ml)	Cells	Not Computed				Chromatid Type						Chromosome Type				Other Types <i>pu sd</i>	No. of Aberrations Per Cell	% of Cells with Aberrations		
						Simple			Complex			Simple		Complex						
		<i>tg</i>	<i>sg</i>	<i>e</i>	<i>pp</i>	<i>tb</i>	<i>isb</i>	<i>tr</i>	<i>qr</i>	<i>cr</i>	<i>id</i>	<i>ci</i>	<i>sb</i>	<i>d</i>	<i>r</i>				<i>dm</i>	
0	100				2														0	0
	100				1														0	0
	%				1.5														0	0
5/1.5/1.0	100	1																	0	0
	100																		0	0
	%	0.5																	0	0
10/3.0/2.0	100				2														0	0
	100				2														0	0
	%				2.0														0	0
25/7.5/5.0	100																		0	0
	100				1														0	0
	%				0.5														0	0
50/15/10	100																		0	0
	100																		0	0
	%																		0	0
Mitomycin C 0.5 μ g/ml	50	3	1			18	4	22	4	6	5	2	5	1	4	1		1	1.64	66.0
	50	2			1	8	4	13	3	2	6	2	4	1	2				0.90	68.0
	%	5	1		1	26	8	35	7	8	11	4	9	2	6	1		1	1.27	67.0

sd = 10 aberrations in calculations

LITERATURE

- Evans, H.J., Cytological Methods for Detecting Chemical Mutagens. In: *Chemical Mutagens, Principles and Methods for their Detection*, Vol. 4, Ed. A. Hollaender, Plenum Press, New York and London, pp. 1-29, 1976;
- Galloway, S.M., Aardema, M.J., Ishidate, M.Jr., Ivett, J.L., Kirkland, D.J., Morita, T., Mosesso, P., Sofuni, T. Report From Working Group On *In Vitro* Tests For Chromosomal Aberrations. *Mutation Res.*, 312:241-261, 1994;
- Galloway, S.M., Armstrong, M.J., Reuben, C., Colman, S., Brown, B., Cannon, C., Bloom, A.D., Nakamura, F., Ahmed, M., Duk, S., Rimpo, J., Margolin, G.H., Resnick, M.A., Anderson, G. and Zeiger, E. Chromosome Aberrations and Sister Chromatid Exchanges in Chinese Hamster Ovary Cells: Evaluations of 108 Chemicals. *Environ. Mol. Mutagen* 10 (suppl. 10), 1-175, 1987;
- FDA, 21 CFR, Part 58, Good Laboratory Practice for Nonclinical Laboratory Studies, National Archives and Records Administration, 2004;
- OECD Guideline for the Testing of Chemicals. - 473. *In Vitro* Mammalian Chromosome Aberration Test., Adopted 21st July 1997;
- OECD Principles of Good Laboratory Practice, 1998;
- Scott, D., Dean, B.J., Danford, N.D. and Kirkland, D.J. Metaphase Chromosome Aberration Assays *In Vitro* In: *Basic Mutagenicity Tests: UKEMS Recommended Procedures*. Cambridge University Press, pp. 62-86, 1990;
- Scott, D., Galloway, S.M., Marshall, R.R., Ishidate, M. Jr., Brusick, D., Ashby, J. and Myhr, B.C. Genotoxicity Under Extreme Culture Conditions. A Report from ICPEMC Task Group 9. *Mutation Res.*, 257:147-204, 1991;
- US Pharmacopeia 29. <791> pH, 2730-2731, 2006a;
- US Pharmacopeia 29. <785> Osmolality and Osmolarity, 2718-2720, 2006b.

Appendix I. pH and Osmolality of Treatment Media for DPPC

Treatment medium	Experiment	S9	pH	Osmolality (mOsmol/kg)
Negative control	1	-	7.35	265
	2	+	7.42	314
	3	-	7.29	273
25 mg/ml	1	-	7.39	264
	2	+	7.47	319
	3	-	7.27	281
50 mg/ml	1	-	7.41	264

2	+	7.50	320
3	-	7.14	290

Note: The method used as reference: *US Pharmacopeia* (2006) 29 <791> for pH; <785> for osmolality.

Appendix I. pH and Osmolality of Treatment Media for DPPC/NAC

Treatment medium	Experiment	S9	pH	Osmolality (mOsmol/kg)
Negative control	1	-	7.37	260
	2	+	7.44	305
	3	-	7.25	279
25/7.5 mg/ml	1	-	7.40	267
	2	+	7.44	311
	3	-	7.28	280

50/15 mg/ml	1	-	7.43	269
	2	+	7.44	328
	3	-	7.25	305

Note: The method used as reference: *US Pharmacopeia* (2006) 29 <791> for pH; <785> for osmolality.

Appendix I. pH and Osmolality of Treatment Media for DPPC/NAC/αT

Treatment medium	Experiment	S9	pH	Osmolality (mOsmol/kg)
Negative control	1	-	7.34	266
	2	+	7.40	299
	3	-	7.30	283

25/7.5/5.0 mg/ml	1	-	7.38	262
	2	+	7.45	303

	3	-	7.31	290
50/15/10 mg/ml	1	-	7.41	262
	2	+	7.38	324
	3	-	7.27	298

Note: The method used as reference: *US Pharmacopeia* (2006) 29 <791> for pH; <785> for osmolality.

Appendix I. pH and Osmolality of Treatment Media for DPPC/NAC/γT

Treatment medium	Experiment	S9	pH	Osmolality (mOsmol/kg)
Negative control	1	-	7.35	268
	2	+	7.39	296
	3	-	7.31	286

25/7.5/5.0 mg/ml	1	-	7.39	265
	2	+	7.40	298
	3	-	7.32	292
<hr/>				
50/15/10 mg/ml	1	-	7.40	265
	2	+	7.40	315
	3	-	7.33	294
<hr/>				

Note: The method used as reference: *US Pharmacopeia* (2006) 29 <791> for pH; <785> for osmolality.

Appendix 2: Single dose acute intravenous toxicity study for four preparations in rodents

Haematology Group Summaries – End of Treatment Period – Males

Parameters	Unit	Group Means ± S.D. (n = 5)				
		Group 1 Control (Empty Liposome)	Group 2 Liposome/NAC	Group 3 Liposome/ α - toxopherol/NAC	Group 4 Liposome/ γ - toxopherol/NAC	Normal Ranges
RBC	$\times 10^{12} / L$	6.88 ± 0.47	7.30 ± 0.20	7.11 ± 0.38	6.93 ± 0.28	4.9 – 9.8
Hb	g / L	143 ± 5	145 ± 6	145 ± 7	141 ± 2	131 – 184
Hct	%	39.6 ± 1.5	40.5 ± 1.7	40.5 ± 2.0	39.1 ± 0.4	42 – 52
MCV	fL	57.7 ± 2.7	55.5 ± 1.0	57.0 ± 1.4	56.5 ± 1.9	50 – 67
MCH	pg	20.9 ± 1.0	19.8 ± 0.4	20.3 ± 0.4	20.4 ± 0.7	17 – 23
MCHC	g / L	361 ± 5	357 ± 2	357 ± 2	362 ± 3	320 – 366
Platelets	$\times 10^9 / L$	1104 ± 38	1332 ± 93	1134 ± 64	1094 ± 189	474 – 1535
WBC	$\times 10^9 / L$	7.96 ± 1.33	5.58 ± 2.36	9.13 ± 2.76	4.17 ± 0.94	5.0 – 14.0
Neutrophils	$\times 10^9 / L$	0.96 ± 0.19	0.93 ± 0.33	1.31 ± 0.78	0.61 ± 0.10	0.3 – 2.1
Lymphocytes	$\times 10^9 / L$	6.73 ± 1.16	4.44 ± 2.05	7.57 ± 2.51	3.41 ± 0.82	2.5 – 12.8
Monocytes	$\times 10^9 / L$	0.16 ± 0.03	0.11 ± 0.05	0.15 ± 0.03	0.08 ± 0.02	0.1 – 0.4
Eosinophils	$\times 10^9 / L$	0.04 ± 0.02	0.05 ± 0.02	0.04 ± 0.01	0.03 ± 0.02	0 – 0.2
Basophils	$\times 10^9 / L$	0.02 ± 0.01	0.02 ± 0.01	0.03 ± 0.01	0.02 ± 0.01	0 – 0.1
LUC	$\times 10^9 / L$	0.05 ± 0.04	0.03 ± 0.02	0.03 ± 0.01	0.02 ± 0.01	0 – 0.2
Reticulocytes	$\times 10^9 / L$	365.0 ± 26.7	309.9 ± 27.5	338.3 ± 42.4	361.0 ± 69.8	Up to 400

Haematology Group Summaries – End of Treatment Period – Females

Parameters	Unit	Group Means ± S.D. (n = 5)				
		Group 1 Control (Empty Liposome)	Group 2 Liposome/NAC (Group 3 Liposome/ α - toxopherol/NAC	Group 4 Liposome/ γ - toxopherol/NAC	Normal Ranges
RBC	$\times 10^{12} / L$	7.31 ± 0.23	7.30 ± 0.40	7.25 ± 0.05	7.26 ± 0.40	6.6 – 8.7
Hb	g / L	146 ± 5	145 ± 5	146 ± 2	143 ± 4	133 – 157
Hct	%	39.6 ± 1.5	40.1 ± 1.9	39.7 ± 0.6	39.4 ± 0.9	40 – 50
MCV	fL	54.1 ± 2.0	54.9 ± 1.1	54.8 ± 0.5	54.3 ± 2.3	53 – 63
MCH	pg	20.0 ± 0.7	19.9 ± 0.5	20.2 ± 0.3	19.7 ± 0.7	18 – 22
MCHC	g / L	369 ± 5	362 ± 9	369 ± 6	363 ± 3	329 – 374
Platelets	$\times 10^9 / L$	1238 ± 93	1133 ± 75	882 ± 257	1020 ± 164	651 – 1567
WBC	$\times 10^9 / L$	5.23 ± 1.33	5.92 ± 2.05	5.54 ± 1.05	5.59 ± 3.19	4.3 – 15.0
Neutrophils	$\times 10^9 / L$	0.72 ± 0.53	0.72 ± 0.38	0.95 ± 0.36	1.25 ± 0.96	0.1 – 1.6
Lymphocytes	$\times 10^9 / L$	4.27 ± 1.03	5.02 ± 1.66	4.31 ± 1.10	4.06 ± 2.09	2.4 – 10.7
Monocytes	$\times 10^9 / L$	0.12 ± 0.07	0.08 ± 0.06	0.16 ± 0.04	0.16 ± 0.11	0 – 0.3
Eosinophils	$\times 10^9 / L$	0.08 ± 0.03	0.07 ± 0.03	0.08 ± 0.03	0.07 ± 0.04	0 – 0.2
Basophils	$\times 10^9 / L$	0.01 ± 0.00	0.01 ± 0.01	0.02 ± 0.01	0.02 ± 0.01	0 – 0.1
LUC	$\times 10^9 / L$	0.03 ± 0.02	0.02 ± 0.02	0.03 ± 0.01	0.04 ± 0.02	0 – 0.4
Reticulocytes	$\times 10^9 / L$	245.7 ± 20.8	206.7 ± 31.4	240.9 ± 34.6	263.7 ± 32.9	Up to 400

Coagulation Group Summaries – End of Treatment Period

Group	Parameter – Mean ± S.D. (n=5)		
	Prothrombin Time (sec.)	APTT (sec.)	Fibrinogen (g/L)
Group 1 Control (Empty Liposome) Male	17.9 ± 0.6	13.1 ± 2.0	2.92 ± 0.39
Group 2 Liposome/NAC Male	17.5 ± 0.5	15.4 ± 2.6	2.76 ± 0.08
Group 3 Liposome/ α -toxopherol/NAC Male	17.9 ± 0.8	14.3 ± 1.9	2.88 ± 0.18
Group 4 Liposome/ γ -toxopherol/NAC Male	17.4 ± 0.5	12.4 ± 0.8	2.51 ± 0.91
Group 1 Control (Empty Liposome) Female	16.3 ± 0.9	13.2 ± 2.8	2.49 ± 0.25
Group 2 Liposome/NAC Female	17.1 ± 1.6	13.4 ± 1.0	2.08 ± 0.76
Group 3 Liposome/ α -toxopherol/NAC Female	17.2 ± 0.7	13.2 ± 2.7	2.08 ± 0.52
Group 4 Liposome/ γ -toxopherol/NAC Female	16.2 ± 0.7	11.4 ± 1.9	2.50 ± 0.65
Normal Ranges	14.8 - 22.8	12.9 – 29.3	1.5 - 3.9

Serum Chemistry Group Summaries – Males – End of Treatment Period

Parameters	Unit	Group Means \pm S.D. (n=5)				Normal Ranges
		Group 1 Control (Empty Liposome)	Group 2 Liposome/NAC	Group 3 Liposome/ α -tocopherol/NAC	Group 4 Liposome/ γ -tocopherol/NAC	
A/G	-	1.2 \pm 0.0	1.3 \pm 0.1	1.3 \pm 0.1	1.3 \pm 0.1	0.9 – 1.3
ALB	g / L	28 \pm 1	29 \pm 1	29 \pm 1	29 \pm 1	24 – 48
GLOB	g / L	23 \pm 1	24 \pm 1	23 \pm 1	23 \pm 1	22 – 39
ALP	u / L	191 \pm 45	206 \pm 42	207 \pm 45	239 \pm 35	75 – 435
Bil(T)	μ mol / L	3.2 \pm 1.6	2.1 \pm 0.6	2.0 \pm 0.4	2.8 \pm 2.2	0.9 – 7.0
BUN	mmol / L	4.6 \pm 0.9	4.1 \pm 0.6	4.6 \pm 0.4	4.4 \pm 0.6	2.8 – 8.8
Ca	mmol / L	2.50 \pm 0.05	2.49 \pm 0.07	2.41 \pm 0.05	2.52 \pm 0.03	2.5 – 3.1
Cl	mmol / L	113 \pm 1	112 \pm 2	106 \pm 1	105 \pm 1	97 – 109
Creatinine	μ mol / L	40 \pm 3	35 \pm 2	36 \pm 3	34 \pm 4	30 – 65
Glucose	mmol / L	5.8 \pm 0.7	5.5 \pm 0.6	6.7 \pm 0.8	6.7 \pm 0.4	1.0 – 8.6
LDH	u / L	3660 \pm 1576	5621 \pm 1555	4505 \pm 574	3334 \pm 2041	2127 - 6401
P	mmol / L	2.70 \pm 0.15	2.79 \pm 0.12	2.54 \pm 0.08	2.95 \pm 0.07	1.5 – 4.4
K	mmol / L	4.5 \pm 0.2	4.7 \pm 0.2	4.5 \pm 0.1	4.6 \pm 0.3	3.8 – 7.4
Protein (T)	g / L	51 \pm 2	52 \pm 2	52 \pm 2	52 \pm 2	52 – 80
AST	u / L	104 \pm 16	128 \pm 15	108 \pm 9	125 \pm 44	53 – 113
ALT	u / L	51 \pm 4	50 \pm 3	53 \pm 3	55 \pm 5	19 – 60
Na	mmol / L	142 \pm 1	142 \pm 1	141 \pm 1	143 \pm 1	140 – 153
Triglycerides	mmol / L	0.51 \pm 0.20	0.38 \pm 0.12	0.36 \pm 0.21	0.35 \pm 0.26	0.2 – 2.0
CK	u / L	534 \pm 165	713 \pm 152	594 \pm 90	446 \pm 290	228 - 529
Cholesterol	mmol / L	1.26 \pm 0.10	1.41 \pm 0.07	1.41 \pm 0.23	1.28 \pm 0.27	1.3 – 3.2

Serum Chemistry Group Summaries – Females – End of Treatment Period

Parameters	Unit	Group Means \pm S.D. (n=5)				
		Group 1 Control (Empty Liposome)	Group 2 Liposome/NAC	Group 3 Liposome/ α - tocopherol/NAC	Group 4 Liposome/ γ - tocopherol/NAC	Normal Ranges
A/G	-	1.5 \pm 0.1	1.3 \pm 0.2	1.4 \pm 0.1	1.3 \pm 0.2	0.9 – 1.3
ALB	g / L	35 \pm 1	34 \pm 4	34 \pm 2	35 \pm 3	26 – 55
GLOB	g / L	24 \pm 1	25 \pm 1	24 \pm 1	26 \pm 1	23 – 36
ALP	u / L	132 \pm 34	152 \pm 31	116 \pm 15	140 \pm 51	74 – 435
Bil(T)	μ mol /L	3.7 \pm 1.0	4.8 \pm 3.2	3.8 \pm 2.4	5.0 \pm 3.3	0.9 – 7.0
BUN	mmol /L	4.7 \pm 0.4	4.3 \pm 0.5	4.2 \pm 0.2	5.5 \pm 0.8	2.9 – 8.8
Ca	mmol /L	2.54 \pm 0.05	2.55 \pm 0.05	2.51 \pm 0.07	2.59 \pm 0.03	2.5 – 3.1
Cl	mmol /L	115 \pm 2	114 \pm 2	108 \pm 3	106 \pm 1	99 – 110
Creatinine	μ mol /L	35 \pm 4	33 \pm 4	32 \pm 3	34 \pm 7	31 – 68
Glucose	mmol /L	7.1 \pm 0.7	8.9 \pm 2.1	6.6 \pm 1.0	7.2 \pm 2.1	1.0 – 8.1
LDH	u / L	3038 \pm 1247	3321 \pm 541	3039 \pm 1245	3812 \pm 1932	1455 - 3081
P	mmol /L	2.43 \pm 0.09	2.73 \pm 0.17	2.20 \pm 0.09	2.41 \pm 0.09	1.5 – 3.6
K	mmol /L	4.3 \pm 0.2	4.7 \pm 0.5	4.3 \pm 0.3	4.7 \pm 0.5	4.0 – 6.7
Protein (T)	g / L	59 \pm 1	59 \pm 3	58 \pm 2	62 \pm 3	54 – 85
AST	u / L	90 \pm 14	103 \pm 16	101 \pm 31	119 \pm 37	30 - 140
ALT	u / L	43 \pm 4	33 \pm 17	45 \pm 3	46 \pm 6	19 – 60
Na	mmol /L	142 \pm 1	143 \pm 1	143 \pm 1	142 \pm 1	140 – 150
Triglycerides	mmol /L	0.14 \pm 0.05	0.10 \pm 0.00	0.11 \pm 0.03	0.10 \pm 0.00	0.2 – 2.2
CK	u / L	528 \pm 151	751 \pm 455	553 \pm 482	665 \pm 653	158 - 556
Cholesterol	mmol /L	1.46 \pm 0.25	1.64 \pm 0.27	1.54 \pm 0.21	1.64 \pm 0.43	1.2 – 3.8

Appendix 3

APPENDIX 3- Acute toxicity effects following a single administration of the STIMAL formulations in male or female beagle dogs

Body Weights

Haematology Group Summaries – Prestudy

Parameters	Unit	Group Means \pm S.D. (n = 9)			
		Males	Male Normal Ranges	Females	Female Normal Ranges
RBC	$\times 10^{12} / L$	6.60 \pm 0.42	5.24 - 7.63	6.51 \pm 0.45	5.34 - 7.54
Hb	g / L	148 \pm 9	116 - 175	146 \pm 7	119 - 174
Hct	%	45.0 \pm 2.9	34.3 - 51.0	44.2 \pm 2.5	35.1 - 51.0
MCV	fL	68.2 \pm 1.4	61.7 - 71.1	67.9 \pm 1.9	61.7 - 71.9
MCH	pg	22.4 \pm 0.4	21.0 - 24.3	22.4 \pm 0.7	21.1 - 24.4
MCHC	g / L	329 \pm 3	322 - 362	330 \pm 5	323 - 358
Platelets	$\times 10^9 / L$	358 \pm 64	187 - 626	419 \pm 51	223 - 545
WBC	$\times 10^9 / L$	12.31 \pm 2.15	5.47 - 17.95	13.25 \pm 4.20	6.39 - 17.09
Neutrophils	$\times 10^9 / L$	6.92 \pm 1.46	2.48 - 11.15	7.95 \pm 3.84	3.01 - 10.44
Lymphocytes	$\times 10^9 / L$	4.30 \pm 1.03	1.54 - 6.09	4.01 \pm 1.24	1.63 - 6.38
Monocytes	$\times 10^9 / L$	0.66 \pm 0.16	0.16 - 1.23	0.82 \pm 0.31	0.23 - 1.16
Eosinophils	$\times 10^9 / L$	0.23 \pm 0.12	0 - 0.62	0.26 \pm 0.10	0 - 0.51
Basophils	$\times 10^9 / L$	0.15 \pm 0.07	0 - 0.13	0.16 \pm 0.08	0 - 0.13
LUC	$\times 10^9 / L$	0.06 \pm 0.02	0 - 0.10	0.06 \pm 0.03	0 - 0.10
Reticulocytes	$\times 10^9 / L$	78.6 \pm 23.1	10 - 128.4	99.5 \pm 22.5	10 - 123.2

Haematology Group Summaries – Male – 24 hours post-dose

Parameters	Unit	Group Means ± S.D. (n = 2)				Normal Ranges
		Group 1 Empty Liposomes (60 mg/kg)	Group 2 Liposomes + N- acetylcystein (60 mg/kg)	Group 3 Liposomes + α -tocopherol and NAC (60 mg/kg)	Group 4 Liposomes + γ -tocopherol and NAC (60 mg/kg)	
RBC	$\times 10^{12} / L$	5.85 ± 0.24	5.84 ± 0.47	6.60 ± 1.12	6.50 ± 1.22	5.24 - 7.63
Hb	g / L	133 ± 7	134 ± 8	151 ± 23	148 ± 25	116 - 175
Hct	%	39.5 ± 2.7	38.9 ± 2.9	44.2 ± 6.2	43.9 ± 7.6	34.3 - 51.0
MCV	fL	67.5 ± 1.7	66.6 ± 0.5	67.2 ± 1.9	67.6 ± 0.8	61.7 - 71.1
MCH	pg	22.7 ± 0.3	23.0 ± 0.4	23.0 ± 0.5	22.8 ± 0.4	21.0 - 24.3
MCHC	g / L	337 ± 4	345 ± 3	342 ± 3	336 ± 1	322 - 362
Platelets	$\times 10^9 / L$	153 ± 62	215 ± 7	181 ± 10	156 ± 16	187 - 626
WBC	$\times 10^9 / L$	16.99 ± 2.99	15.62 ± 0.20	15.88 ± 5.34	10.29 ± 0.96	5.47 - 17.95
Neutrophils	$\times 10^9 / L$	12.24 ± 1.97	10.29 ± 0.45	13.28 ± 4.88	8.07 ± 1.47	2.48 - 11.15
Lymphocytes	$\times 10^9 / L$	3.65 ± 0.96	4.11 ± 0.59	2.01 ± 0.35	1.52 ± 0.40	1.54 - 6.09
Monocytes	$\times 10^9 / L$	0.53 ± 0.06	0.82 ± 0.04	0.27 ± 0.11	0.34 ± 0.01	0.16 - 1.23
Eosinophils	$\times 10^9 / L$	0.40 ± 0.04	0.25 ± 0.02	0.20 ± 0.09	0.20 ± 0.04	0 - 0.62
Basophils	$\times 10^9 / L$	0.12 ± 0.01	0.09 ± 0.01	0.08 ± 0.04	0.06 ± 0.05	0 - 0.13
LUC	$\times 10^9 / L$	0.05 ± 0.00	0.07 ± 0.00	0.05 ± 0.05	0.11 ± 0.11	0 - 0.10
Reticulocytes	$\times 10^9 / L$	238.0 ± 34.2	262.1 ± 63.9	327.8 ± 147.6	346.8 ± 122.3	10 - 128.4

Haematology Group Summaries – Male – Week 2

Parameters	Unit	Group Means ± S.D. (n = 2)				Normal Ranges
		Group 1 Empty Liposomes (60 mg/kg)	Group 2 Liposomes + N- acetylcystein (60 mg/kg)	Group 3 Liposomes + α -tocopherol and NAC (60 mg/kg)	Group 4 Liposomes + γ -tocopherol and NAC (60 mg/kg)	
RBC	$\times 10^{12} / L$	6.11 ± 0.59	6.65 ± 0.18	6.21 ± 0.44	6.43 ± 0.36	5.24 - 7.63
Hb	g / L	133 ± 14	145 ± 6	137 ± 7	141 ± 6	116 - 175
Hct	%	42.0 ± 4.2	45.5 ± 2.1	42.0 ± 1.4	43.5 ± 2.1	34.3 - 51.0
MCV	fL	68.6 ± 0.9	68.0 ± 1.4	67.4 ± 2.0	68.3 ± 0.4	61.7 - 71.1
MCH	pg	21.8 ± 0.1	21.7 ± 0.3	22.1 ± 0.5	22.0 ± 0.4	21.0 - 24.3
MCHC	g / L	318 ± 1	319 ± 1	327 ± 3	322 ± 3	322 - 362
Platelets	$\times 10^9 / L$	422 ± 97	520 ± 41	426 ± 51	427 ± 156	187 - 626
WBC	$\times 10^9 / L$	12.01 ± 1.05	21.38 ± 0.83	16.61 ± 0.27	17.68 ± 3.86	5.47 - 17.95
Neutrophils	$\times 10^9 / L$	5.91 ± 0.21	12.82 ± 0.52	10.74 ± 1.66	10.26 ± 2.28	2.48 - 11.15
Lymphocytes	$\times 10^9 / L$	4.78 ± 0.73	6.39 ± 0.74	4.28 ± 1.52	5.58 ± 1.23	1.54 - 6.09
Monocytes	$\times 10^9 / L$	0.74 ± 0.19	1.58 ± 0.26	0.98 ± 0.01	1.25 ± 0.02	0.16 - 1.23
Eosinophils	$\times 10^9 / L$	0.45 ± 0.27	0.37 ± 0.32	0.47 ± 0.34	0.40 ± 0.17	0 - 0.62
Basophils	$\times 10^9 / L$	0.08 ± 0.05	0.11 ± 0.01	0.08 ± 0.02	0.08 ± 0.08	0 - 0.13
LUC	$\times 10^9 / L$	0.07 ± 0.03	0.13 ± 0.01	0.09 ± 0.05	0.12 ± 0.06	0 - 0.10
Reticulocytes	$\times 10^9 / L$	47.5 ± 3.5	76.5 ± 3.5	47.5 ± 0.7	67.5 ± 19.1	10 - 128.4

Haematology Group Summaries – Female – 24 hours post-dose

Parameters	Unit	Group Means ± S.D. (n = 2)				Normal Ranges
		Group 1 Empty Liposomes (60 mg/kg)	Group 2 Liposomes + N- acetylcystein (60 mg/kg)	Group 3 Liposomes + α -tocopherol and NAC (60 mg/kg)	Group 4 Liposomes + γ -tocopherol and NAC (60 mg/kg)	
RBC	$\times 10^{12} / L$	6.25 ± 0.49	5.9 ± 0.66	6.88 ± 0.13	6.55 ± 0.04	5.34 - 7.54
Hb	g / L	141 ± 5	136 ± 16	157 ± 6	146 ± 4	119 - 174
Hct	%	41.2 ± 2.0	40.4 ± 4.1	45.7 ± 2.0	43.0 ± 0.4	35.1 - 51.0
MCV	fL	66.0 ± 2.1	68.6 ± 0.6	66.4 ± 1.7	65.6 ± 1.0	61.7 - 71.9
MCH	pg	22.5 ± 1.0	23.1 ± 0.1	22.8 ± 0.3	22.4 ± 0.5	21.1 - 24.4
MCHC	g / L	341 ± 4	336 ± 4	344 ± 4	341 ± 13	323 - 358
Platelets	$\times 10^9 / L$	197 ± 66	244 ± 82	145 ± 81	185 ± 49	223 - 545
WBC	$\times 10^9 / L$	11.63 ± 0.76	15.52 ± 4.24	8.45 ± 1.64	11.85 ± 0.02	6.39 - 17.09
Neutrophils	$\times 10^9 / L$	7.87 ± 1.12	9.23 ± 0.97	5.17 ± 0.34	8.65 ± 0.50	3.01 - 10.44
Lymphocytes	$\times 10^9 / L$	3.01 ± 0.23	4.89 ± 3.34	2.64 ± 1.17	2.31 ± 0.58	1.63 - 6.38
Monocytes	$\times 10^9 / L$	0.41 ± 0.02	0.68 ± 0.15	0.29 ± 0.09	0.32 ± 0.04	0.23 - 1.16
Eosinophils	$\times 10^9 / L$	0.23 ± 0.13	0.53 ± 0.28	0.20 ± 0.10	0.41 ± 0.00	0 - 0.51
Basophils	$\times 10^9 / L$	0.08 ± 0.02	0.12 ± 0.01	0.09 ± 0.02	0.10 ± 0.02	0 - 0.13
LUC	$\times 10^9 / L$	0.05 ± 0.01	0.09 ± 0.04	0.07 ± 0.04	0.06 ± 0.01	0 - 0.10
Reticulocytes	$\times 10^9 / L$	289.4 ± 59.1	268.7 ± 93.2	359.9 ± 8.8	327.5 ± 11.1	10 - 123.2

Haematology Group Summaries – Female – Week 2

Parameters	Unit	Group Means ± S.D. (n = 2)				Normal Ranges
		Group 1 Empty Liposomes (60 mg/kg)	Group 2 Liposomes + N- acetylcystein (60 mg/kg)	Group 3 Liposomes + α -tocopherol and NAC (60 mg/kg)	Group 4 Liposomes + γ -tocopherol and NAC (60 mg/kg)	
RBC	$\times 10^{12} / L$	6.87 ± 0.40	6.66 ± 0.64	6.51 ± 0.77	6.42 ± 0.74	5.34 - 7.54
Hb	g / L	148 ± 3	149 ± 14	143 ± 17	141 ± 14	119 - 174
Hct	%	46.5 ± 0.7	46.5 ± 4.9	43.0 ± 4.2	41.5 ± 6.4	35.1 - 51.0
MCV	fL	67.7 ± 2.1	69.9 ± 0.2	66.0 ± 0.6	65.2 ± 2.5	61.7 - 71.9
MCH	pg	21.6 ± 0.9	22.4 ± 0.1	22.0 ± 0.0	22.1 ± 0.4	21.1 - 24.4
MCHC	g / L	319 ± 4	320 ± 0	334 ± 2	339 ± 18	323 - 358
Platelets	$\times 10^9 / L$	515 ± 86	489 ± 62	492 ± 32	431 ± 11	223 - 545
WBC	$\times 10^9 / L$	12.92 ± 2.81	14.12 ± 3.83	11.29 ± 0.41	12.46 ± 0.78	6.39 - 17.09
Neutrophils	$\times 10^9 / L$	7.33 ± 2.09	7.65 ± 1.99	6.36 ± 0.08	6.82 ± 0.31	3.01 - 10.44
Lymphocytes	$\times 10^9 / L$	4.18 ± 0.69	5.09 ± 2.22	3.71 ± 0.30	4.50 ± 0.42	1.63 - 6.38
Monocytes	$\times 10^9 / L$	1.10 ± 0.08	0.89 ± 0.18	0.88 ± 0.14	0.69 ± 0.05	0.23 - 1.16
Eosinophils	$\times 10^9 / L$	0.15 ± 0.01	0.29 ± 0.18	0.17 ± 0.04	0.31 ± 0.00	0 - 0.51
Basophils	$\times 10^9 / L$	0.08 ± 0.06	0.10 ± 0.00	0.08 ± 0.04	0.08 ± 0.00	0 - 0.13
LUC	$\times 10^9 / L$	0.10 ± 0.06	0.10 ± 0.01	0.10 ± 0.05	0.06 ± 0.01	0 - 0.10
Reticulocytes	$\times 10^9 / L$	42.0 ± 0.0	96.5 ± 78.5	20.0 ± 5.7	47.0 ± 4.2	10 - 123.2

Serum Chemistry Group Summaries – Prestudy

Parameters	Unit	Group Means \pm S.D. (n = 9)			
		Males	Male Normal Ranges	Females	Female Normal Ranges
A/G	-	1.3 \pm 0.1	0.9 - 1.4	1.1 \pm 0.1	0.7 - 1.5
ALB	g / L	29 \pm 2	23 - 34	27 \pm 2	21 - 33
GLOB	g / L	23 \pm 2	21 - 29	23 \pm 2	19 - 32
ALP	u / L	142 \pm 24	69 - 176	129 \pm 26	20 - 248
Bil(T)	μ mol / L	< 1.7	0 - 5.5	2.0 \pm 0.6	0 - 6.8
BUN	mmol / L	4.0 \pm 0.9	2.5 - 7.0	4.1 \pm 0.4	2.1 - 7.7
Ca	mmol / L	2.71 \pm 0.06	2.54 - 2.92	2.61 \pm 0.09	2.54 - 2.92
Cl	mmol / L	113 \pm 2	108 - 122	113 \pm 2	108 - 121
Creatinine	μ mol / L	54 \pm 5	44 - 73	54 \pm 3	42 - 76
Glucose	mmol / L	5.1 \pm 0.1	4.6 - 6.5	4.8 \pm 0.5	4.3 - 6.7
LDH	u / L	296 \pm 158	30 - 749	305 \pm 100	30 - 675
P	mmol / L	2.38 \pm 0.15	1.33 - 3.10	2.15 \pm 0.10	1.37 - 3.08
K	mmol / L	4.7 \pm 0.2	4.0 - 5.5	4.4 \pm 0.3	3.9 - 5.4
Protein (T)	g / L	52 \pm 2	47 - 60	50 \pm 3	29 - 72
AST	u / L	42 \pm 4	21 - 57	49 \pm 14	23 - 55
ALT	u / L	29 \pm 7	22 - 63	27 \pm 7	25 - 56
Na	mmol / L	143 \pm 1	139 - 152	144 \pm 2	140 - 150
Triglycerides	mmol / L	0.19 \pm 0.05	0.10 - 0.55	0.16 \pm 0.06	0.04 - 0.56
CK	u / L	419 \pm 236	100 - 519	456 \pm 391	100 - 489
Cholesterol	mmol / L	4.02 \pm 0.44	2.62 - 5.19	3.08 \pm 0.42	2.39 - 5.19

Serum Chemistry Group Summaries – Male – 24 hours post-dose

Parameters	Unit	Group Means ± S.D. (n = 2)				Normal Ranges
		Group 1 Empty Liposomes (60 mg/kg)	Group 2 Liposomes + N- acetylcystein (60 mg/kg)	Group 3 Liposomes + α -tocopherol and NAC (60 mg/kg)	Group 4 Liposomes + γ -tocopherol and NAC (60 mg/kg)	
A/G	-	1.1 ± 0.1	1.1 ± 0.1	1.1 ± 0.1	0.9 ± 0.0	0.9 - 1.4
ALB	g / L	26 ± 0	26 ± 0	28 ± 1	26 ± 3	23 - 34
GLOB	g / L	25 ± 0	24 ± 1	26 ± 2	29 ± 4	21 - 29
ALP	u / L	194 ± 7	136 ± 27	132 ± 1	184 ± 58	69 - 176
Bil(T)	μ mol / L	1.9 ± 0.3	< 1.7	2.4 ± 0.9	2.7 ± 0.4	0 - 5.5
BUN	mmol / L	3.7 ± 0.1	4.3 ± 1.0	3.3 ± 0.5	2.4 ± 0.0	2.5 - 7.0
Ca	mmol / L	2.68 ± 0.08	2.70 ± 0.06	2.56 ± 0.04	2.67 ± 0.23	2.54 - 2.92
Cl	mmol / L	115 ± 1	113 ± 2	113 ± 2	117 ± 1	108 - 122
Creatinine	μ mol / L	53 ± 5	60 ± 5	50 ± 1	48 ± 6	44 - 73
Glucose	mmol / L	5.0 ± 0.1	5.2 ± 0.1	5.2 ± 0.5	5.2 ± 0.6	4.6 - 6.5
LDH	u / L	490 ± 421	215 ± 60	590 ± 560	482 ± 194	30 - 749
P	mmol / L	2.28 ± 0.02	2.15 ± 0.18	2.14 ± 0.15	2.04 ± 0.25	1.33 - 3.10
K	mmol / L	4.2 ± 0.1	4.2 ± 0.1	4.6 ± 0.8	4.3 ± 0.2	4.0 - 5.5
Protein (T)	g / L	51 ± 0	50 ± 1	54 ± 1	55 ± 6	47 - 60
AST	u / L	83 ± 13	50 ± 3	54 ± 1	54 ± 17	21 - 57
ALT	u / L	105 ± 57	35 ± 4	60 ± 31	35 ± 8	22 - 63
Na	mmol / L	140 ± 0	138 ± 0	140 ± 0	140 ± 2	139 - 152
Triglycerides	mmol / L	0.34 ± 0.01	0.23 ± 0.01	0.26 ± 0.08	0.24 ± 0.06	0.10 - 0.55
CK	u / L	299 ± 83	580 ± 245	220 ± 178	198 ± 63	100 - 519
Cholesterol	mmol / L	5.13 ± 0.37	5.39 ± 0.30	4.41 ± 0.62	6.04 ± 0.96	2.62 - 5.19
GGT	u / L	9 ± 3	7 ± 1	8 ± 2	7 ± 1	4 - 15

Serum Chemistry Group Summaries – Male – Week 2

Parameters	Unit	Group Means \pm S.D. (n = 2)				Normal Ranges
		Group 1 Empty Liposomes (60 mg/kg)	Group 2 Liposomes + N- acetylcystein (60 mg/kg)	Group 3 Liposomes + α -tocopherol and NAC (60 mg/kg)	Group 4 Liposomes + γ -tocopherol and NAC (60 mg/kg)	
A/G	-	1.1 \pm 0.1	1.0 \pm 0.1	1.0 \pm 0.2	1.1 \pm 0.1	0.9 - 1.4
ALB	g / L	28 \pm 0	27 \pm 1	25 \pm 2	26 \pm 4	23 - 34
GLOB	g / L	26 \pm 2	28 \pm 2	28 \pm 4	25 \pm 1	21 - 29
ALP	u / L	177 \pm 1	144 \pm 18	123 \pm 9	136 \pm 23	69 - 176
Bil(T)	μ mol / L	< 1.7	< 1.7	< 1.7	< 1.7	0 - 5.5
BUN	mmol / L	4.1 \pm 1.2	4.7 \pm 0.6	3.6 \pm 0.1	3.7 \pm 0.8	2.5 - 7.0
Ca	mmol / L	2.67 \pm 0.04	2.73 \pm 0.01	2.75 \pm 0.01	2.75 \pm 0.12	2.54 - 2.92
Cl	mmol / L	113 \pm 1	113 \pm 0	114 \pm 0	116 \pm 1	108 - 122
Creatinine	μ mol / L	52 \pm 1	62 \pm 2	55 \pm 1	57 \pm 2	44 - 73
Glucose	mmol / L	4.8 \pm 0.0	4.7 \pm 0.1	4.8 \pm 0.3	4.9 \pm 0.1	4.6 - 6.5
LDH	u / L	304 \pm 54	526 \pm 79	265 \pm 22	355 \pm 284	30 - 749
P	mmol / L	2.22 \pm 0.08	2.26 \pm 0.23	2.23 \pm 0.01	2.30 \pm 0.13	1.33 - 3.10
K	mmol / L	4.6 \pm 0.0	5.1 \pm 0.1	4.8 \pm 0.1	4.6 \pm 0.1	4.0 - 5.5
Protein (T)	g / L	53 \pm 1	54 \pm 1	52 \pm 1	51 \pm 5	47 - 60
AST	u / L	50 \pm 4	49 \pm 6	40 \pm 4	42 \pm 1	21 - 57
ALT	u / L	36 \pm 1	24 \pm 2	24 \pm 14	27 \pm 4	22 - 63
Na	mmol / L	137 \pm 1	138 \pm 1	140 \pm 0	139 \pm 1	139 - 152
Triglycerides	mmol / L	0.22 \pm 0.13	0.13 \pm 0.01	0.14 \pm 0.04	0.18 \pm 0.08	0.10 - 0.55
CK	u / L	340 \pm 125	336 \pm 204	191 \pm 40	260 \pm 35	100 - 519
Cholesterol	mmol / L	3.89 \pm 0.10	4.35 \pm 0.00	3.51 \pm 0.35	4.25 \pm 0.26	2.62 - 5.19

Serum Chemistry Group Summaries – Female – 24 hours post-dose

Parameters	Unit	Group Means ± S.D. (n = 2)				Normal Ranges
		Group 1 Empty Liposomes (60 mg/kg)	Group 2 Liposomes + N- acetylcystein (60 mg/kg)	Group 3 Liposomes + α -tocopherol and NAC (60 mg/kg)	Group 4 Liposomes + γ -tocopherol and NAC (60 mg/kg)	
A/G	-	1.1 ± 0.0	1.1 ± 0.1	1.1 ± 0.1	1.2 ± 0.0	0.7 - 1.5
ALB	g / L	26 ± 1	26 ± 4	26 ± 0	29 ± 3	21 - 33
GLOB	g / L	24 ± 0	24 ± 0	25 ± 4	25 ± 2	19 - 32
ALP	u / L	151 ± 50	125 ± 28	130 ± 21	157 ± 13	20 - 248
Bil(T)	μ mol / L	2.2 ± 0.3	< 1.7	< 1.7	4.0 ± 1.7	0 - 6.8
BUN	mmol / L	4.0 ± 0.3	4.2 ± 0.5	4.4 ± 0.2	3.5 ± 0.2	2.1 - 7.7
Ca	mmol / L	2.65 ± 0.05	2.68 ± 0.01	2.65 ± 0.01	2.67 ± 0.08	2.54 - 2.92
Cl	mmol / L	115 ± 1	118 ± 1	114 ± 1	112 ± 0	108 - 121
Creatinine	μ mol / L	57 ± 3	54 ± 2	58 ± 0	49 ± 3	42 - 76
Glucose	mmol / L	5.2 ± 0.1	5.3 ± 0.5	5.1 ± 0.2	5.3 ± 0.4	4.3 - 6.7
LDH	u / L	360 ± 69	250 ± 4	325 ± 90	254 ± 125	30 - 675
P	mmol / L	2.06 ± 0.04	2.10 ± 0.04	2.00 ± 0.06	1.90 ± 0.12	1.37 - 3.08
K	mmol / L	4.0 ± 0.1	4.2 ± 0.4	4.2 ± 0.1	4.3 ± 0.1	3.9 - 5.4
Protein (T)	g / L	50 ± 0	50 ± 4	51 ± 3	54 ± 5	29 - 72
AST	u / L	77 ± 5	54 ± 8	46 ± 1	74 ± 44	23 - 55
ALT	u / L	52 ± 6	45 ± 8	28 ± 1	225 ± 274	25 - 56
Na	mmol / L	141 ± 1	140 ± 2	142 ± 2	140 ± 2	140 - 150
Triglycerides	mmol / L	0.33 ± 0.04	0.22 ± 0.02	0.34 ± 0.11	0.17 ± 0.00	0.04 - 0.56
CK	u / L	413 ± 120	399 ± 179	344 ± 45	200 ± 91	100 - 489
Cholesterol	mmol / L	3.90 ± 0.58	4.45 ± 0.51	3.87 ± 0.42	4.60 ± 0.33	2.39 - 5.19
GGT	u / L	7 ± 0	5 ± 0	6 ± 1	10 ± 3	3 - 9

Serum Chemistry Group Summaries – Female – Week 2

Parameters	Unit	Group Means ± S.D. (n = 2)				Normal Ranges
		Group 1 Empty Liposomes (60 mg/kg)	Group 2 Liposomes + N- acetylcystein (60 mg/kg)	Group 3 Liposomes + α -tocopherol and NAC (60 mg/kg)	Group 4 Liposomes + γ -tocopherol and NAC (60 mg/kg)	
A/G	-	1.2 ± 0.1	1.3 ± 0.0	1.1 ± 0.1	1.1 ± 0.0	0.7 - 1.5
ALB	g / L	29 ± 1	29 ± 3	25 ± 2	27 ± 3	21 - 33
GLOB	g / L	25 ± 1	23 ± 2	23 ± 0	25 ± 1	19 - 32
ALP	u / L	153 ± 42	122 ± 33	95 ± 3	123 ± 6	20 - 248
Bil(T)	μ mol / L	2.2 ± 0.6	< 1.7	< 1.7	< 1.7	0 - 6.8
BUN	mmol / L	4.5 ± 0.7	4.9 ± 0.5	4.8 ± 1.4	4.2 ± 0.6	2.1 - 7.7
Ca	mmol / L	2.68 ± 0.02	2.62 ± 0.02	2.61 ± 0.18	2.71 ± 0.06	2.54 - 2.92
Cl	mmol / L	115 ± 2	116 ± 1	117 ± 4	115 ± 3	108 - 121
Creatinine	μ mol / L	57 ± 2	49 ± 6	53 ± 1	54 ± 1	42 - 76
Glucose	mmol / L	4.7 ± 0.1	4.7 ± 1.2	4.8 ± 0.1	5.2 ± 0.6	4.3 - 6.7
LDH	u / L	465 ± 190	240 ± 175	184 ± 47	155 ± 25	30 - 675
P	mmol / L	2.18 ± 0.15	2.27 ± 0.00	1.96 ± 0.01	2.04 ± 0.01	1.37 - 3.08
K	mmol / L	4.8 ± 0.1	5.1 ± 0.6	4.3 ± 0.1	4.5 ± 0.1	3.9 - 5.4
Protein (T)	g / L	53 ± 0	51 ± 6	48 ± 1	53 ± 5	29 - 72
AST	u / L	52 ± 3	42 ± 3	40 ± 1	44 ± 1	23 - 55
ALT	u / L	39 ± 4	20 ± 1	26 ± 6	35 ± 12	25 - 56
Na	mmol / L	137 ± 0	138 ± 1	140 ± 1	140 ± 2	140 - 150
Triglycerides	mmol / L	0.15 ± 0.04	0.16 ± 0.04	0.12 ± 0.03	0.12 ± 0.01	0.04 - 0.56
CK	u / L	422 ± 149	226 ± 1	274 ± 139	188 ± 46	100 - 489
Cholesterol	mmol / L	2.90 ± 0.52	3.59 ± 0.15	2.78 ± 0.26	3.27 ± 0.23	2.39 - 5.19

APPENDIX 4

HISTOPATHOLOGY REPORT

Nucro-Technics Project: 197253

DETERMINATION OF THE MAXIMUM TOLERATED DOSE FOLLOWED BY AN ACUTE INTRAVENOUS TOXICITY STUDY OF THREE LIPOSOMAL ANTIOXIDANT FORMULATIONS IN BEAGLE DOGS

Study Design

Group	Treatment	Regimen	Days	Sex	Count	Slide Numbers
1	Control (Empty Liposomes)	0 mg/kg	15	Male Female	2 2	080149 – 080150 080151 – 080152
2	Test 1 (Liposomes and NAC)	60 mg/kg	15	Male Female	2 2	080153 – 080154 080155 – 080156
3	Test 2 (Liposomes/ α -tocopherol and NAC)	60 mg/kg	15	Male Female	2 2	080157 – 080158 080159 – 080160
4	Test 3 (Liposomes/ γ -tocopherol and NAC)	60 mg/kg	15	Male Female	2 2	080161 – 080162 080163 – 080164

The test article was administered once via the *vena cephalica*. Animals were observed for 14 days and necropsy was performed on day 15.

Clinical Observations: Animals in all groups including Empty Liposomes control animals experienced substantial hypotension during and immediately after dosing, but all completely recovered within 15 – 30 minutes after dosing.

Clinical Pathology: Clinical pathology parameters were unremarkable with the exception of one single female dog (#016) dosed with the formulation of Liposomes, γ -tocopherol and NAC, which had approximately a 6-fold increase in ALT at 24 hours after dosing. On Day 5 post-dosing the ALT was approximately 3-fold the normal range, and at the end of the study it was normal.

Gross Necropsy: Necropsy findings were unremarkable.

Histological Methods:

Hematoxylin and Eosin stained sections were provided from all the following tissues: Adrenal Gland; Aorta (thoracic); Brain; Cecum; Colon; Duodenum; Epididymides; Esophagus; Eyes; Heart; Ileum; Jejunum; Kidneys; Liver (sample of central and left lobes); Lungs (left and right diaphragmatic lobes); Lymph Node (Mandibular); Lymph Node (Mesenteric); Mammary Gland (inguinal); Optic Nerves (if present in routine sections); Ovaries; Pancreas; Pituitary; Prostate; Salivary Glands (Mandibular); Sciatic Nerve; Skeletal Muscle (quadriceps); Skin (inguinal); Spinal Cord; Spleen; Sternum and Marrow; Stomach; Testes; Thymus; Thyroid; Parathyroid; Tongue; Trachea; Urinary Bladder; Uterus (horns, cervix, body); Vagina.

Changes observed in tissues were graded on a scale of: None = 0; Minimal = 1; Mild = 2; Moderate = 3; Marked = 4; Severe = 5.

Results:

A list of grades for all tissues examined, with means are provided in Table 1.

Conditions of possible toxicological significance:

There were no conditions of possible toxicological significance.

Conditions of uncertain significance:

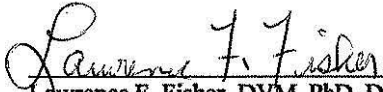
A single female treated with Liposomes/ γ -tocopherol and NAC had a temporary increase in ALT. There were no tissue changes that indicated any unresolved injury.

Conditions lacking toxicological significance:

Hypotension which was rapidly resolved occurred during and immediately following treatment in animals in all dose groups.

Conclusions:

The intravenous administration of a single 60 mg/kg dose of Liposomes and NAC or Liposomes/ α -tocopherol and NAC, or Liposomes/ γ -tocopherol and NAC to beagle dogs caused no substantive clinical or pathological effects during the 14-day observation period.


Lawrence F. Fisher, DVM, PhD, DACVP


Date

Histopathology Findings

Project: 197253 **Animal:** 002 **Sex:** Male **Pathology No.:** 080150 **Duration:** 15 Days
Group: 1 **Treatment:** Empty Liposomes
Regimen: 0 mg/kg

Tissue	Result	Slide No.	Grade	Description (i.e. No significant findings)
Brain (Hindbrain + Brain Stem)	Normal	-1	0	No significant findings
Brain (Forebrain + Mid Brain)	Normal	-2	0	No significant findings
Adrenals	Normal	-3	0	No significant findings
Pituitary	Normal	-3	0	No significant findings
Sciatic Nerve	Normal	-4	0	No significant findings
Cervical Spinal Cord	Normal	-5	0	No significant findings
Thoracic Spinal Cord	Normal	-6	0	No significant findings
Eye (Left)	Normal	-7	0	No significant findings
Optic Nerve - Left (if present)	Normal	-7	0	No significant findings
Eye (Right)	Normal	-8	0	No significant findings
Optic Nerve - Right (if present)	Normal	-8	0	No significant findings
Heart	Normal	-9	0	No significant findings
Lungs (left & right diaphragmatic lobes)	Normal	-10	0	No significant findings
Liver (sample of central & left lobes)	Normal	-11	0	No significant findings
Kidney (Left)	Normal	-12	0	No significant findings
Kidney (Right)	Normal	-13	0	No significant findings
Pancreas	Normal	-14	0	No significant findings
duodenum	Normal	-14	0	No significant findings
Spleen	Normal	-15	0	No significant findings
Jejunum	Normal	-15	0	No significant findings
Stomach	Normal	-16	0	No significant findings
Ileum	Normal	-17	0	No significant findings
Colon	Normal	-17	0	No significant findings
Mesenteric Lymph Nodes	Normal	-18	0	No significant findings
Cecum	Normal	-18	0	No significant findings
Mandibular Lymph Nodes	Normal	-19	0	No significant findings
Muscle (Quadriceps)	Normal	-20	0	No significant findings
Tongue	Normal	-20	0	No significant findings
Skin	Normal	-21	0	No significant findings
Thymus	Normal	-22	0	No significant findings
Lumbar Cord	Normal	-22	0	No significant findings
Thyroid (Left)	Normal	-23	0	No significant findings
Parathyroid - Left	Normal	-23	0	No significant findings
Thyroid (Right)	Normal	-24	0	No significant findings
Parathyroid - Right	Normal	-24	0	No significant findings
Sterum & Marrow	Normal	-25	0	No significant findings
Salivary Glands	Normal	-26	0	No significant findings
Testis - Left	Normal	-27	0	Immature
Epididymis - Left	Normal	-27	0	No significant findings
Testis - Right	Normal	-28	0	Immature
Epididymis - Right	Normal	-28	0	No significant findings
Prostate	Normal	-29	0	Immature
Bladder	Normal	-29	0	No significant findings
Esophagus	Normal	-30	0	No significant findings
Aorta	Normal	-30	0	No significant findings
Trachea	Normal	-31	0	No significant findings
Mediastinal Lymph Nodes	Abnormal	-32	3	Hemorrhage

Histopathology Findings				
Project: 197253	Animal: 003	Sex: Male	Pathology No.: 080153	Duration: 15 Days
Group: 2	Treatment: Liposomes and NAC			
Regimen: 60 mg/kg				

Tissue	Result	Slide No.	Grade	Description (i.e. No significant findings)
Brain (Hindbrain + Brain Stem)	Normal	-1	0	No significant findings
Brain (Forebrain + Mid Brain)	Normal	-2	0	No significant findings
Adrenals	Normal	-3	0	No significant findings
Pituitary	Normal	-3	0	No significant findings
Sciatic Nerve	Normal	-4	0	No significant findings
Cervical Spinal Cord	Normal	-5	0	No significant findings
Thoracic Spinal Cord	Normal	-6	0	No significant findings
Eye (Left)	Normal	-7	0	No significant findings
Optic Nerve - Left (if present)	Normal	-7	0	No significant findings
Eye (Right)	Normal	-8	0	No significant findings
Optic Nerve - Right (if present)	Normal	-8	0	No significant findings
Heart	Normal	-9	0	No significant findings
Lungs (left & right diaphragmatic lobes)	Abnormal	-10	3	Suppurative pneumonia
Liver (sample of central & left lobes)	Normal	-11	0	No significant findings
Kidney (Left)	Normal	-12	0	No significant findings
Kidney (Right)	Normal	-13	0	No significant findings
Pancreas	Normal	-14	0	No significant findings
duodenum	Normal	-14	0	No significant findings
Spleen	Normal	-15	0	No significant findings
Jejunum	Normal	-15	0	No significant findings
Stomach	Normal	-16	0	No significant findings
Ileum	Normal	-17	0	No significant findings
Colon	Normal	-17	0	No significant findings
Mesenteric Lymph Nodes	Normal	-18	0	No significant findings
Cecum	Normal	-18	0	No significant findings
Mandibular Lymph Nodes	Normal	-19	0	No significant findings
Muscle (Quadriceps)	Normal	-20	0	No significant findings
Tongue	Normal	-20	0	No significant findings
Skin	Normal	-21	0	No significant findings
Thymus	Normal	-22	0	No significant findings
Lumbar Cord	Normal	-22	0	No significant findings
Thyroid (Left)	Normal	-23	0	No significant findings
Parathyroid - Left	Normal	-23	0	No significant findings
Thyroid (Right)	Normal	-24	0	No significant findings
Parathyroid - Right	Normal	-24	0	No significant findings
Sterum & Marrow	Normal	-25	0	No significant findings
Salivary Glands	Normal	-26	0	No significant findings
Testis - Left	Normal	-27	0	Immature
Epididymis - Left	Normal	-27	0	No significant findings
Testis - Right	Normal	-28	0	Immature
Epididymis - Right	Normal	-28	0	No significant findings
Prostate	Normal	-29	0	Immature
Bladder	Normal	-29	0	No significant findings
Esophagus	Normal	-30	0	No significant findings
Aorta	Normal	-30	0	No significant findings
Trachea	Normal	-31	0	No significant findings

Histopathology Findings

Project: 197253 **Animal:** 004 **Sex:** Male **Pathology No.:** 080154 **Duration:** 15 Days
Group: 2 **Treatment:** Liposomes and NAC
Regimen: 60 mg/kg

Tissue	Result	Slide No.	Grade	Description (i.e. No significant findings)
Brain (Hindbrain + Brain Stem)	Normal	-1	0	No significant findings
Brain (Forebrain + Mid Brain)	Normal	-2	0	No significant findings
Adrenals	Normal	-3	0	No significant findings
Pituitary	Normal	-3	0	No significant findings
Sciatic Nerve	Normal	-4	0	No significant findings
Cervical Spinal Cord	Normal	-5	0	No significant findings
Thoracic Spinal Cord	Normal	-6	0	No significant findings
Eye (Left)	Normal	-7	0	No significant findings
Optic Nerve - Left (if present)	Normal	-7	0	No significant findings
Eye (Right)	Normal	-8	0	No significant findings
Optic Nerve - Right (if present)	Normal	-8	0	No significant findings
Heart	Normal	-9	0	No significant findings
Lungs (left & right diaphragmatic lobes)	Normal	-10	0	No significant findings
Liver (sample of central & left lobes)	Normal	-11	0	No significant findings
Kidney (Left)	Normal	-12	0	No significant findings
Kidney (Right)	Normal	-13	0	No significant findings
Pancreas	Normal	-14	0	No significant findings
duodenum	Normal	-14	0	No significant findings
Spleen	Normal	-15	0	No significant findings
Jejunum	Normal	-15	0	No significant findings
Stomach	Normal	-16	0	No significant findings
Ileum	Normal	-17	0	No significant findings
Colon	Normal	-17	0	No significant findings
Mesenteric Lymph Nodes	Normal	-18	0	No significant findings
Cecum	Normal	-18	0	No significant findings
Mandibular Lymph Nodes	Normal	-19	0	No significant findings
Muscle (Quadriceps)	Normal	-20	0	No significant findings
Tongue	Normal	-20	0	No significant findings
Skin	Normal	-21	0	No significant findings
Thymus	Normal	-22	0	No significant findings
Lumbar Cord	Normal	-22	0	No significant findings
Thyroid (Left)	Normal	-23	0	No significant findings
Parathyroid - Left	Normal	-23	0	No significant findings
Thyroid (Right)	Normal	-24	0	No significant findings
Parathyroid - Right	Normal	-24	0	No significant findings
Sterum & Marrow	Normal	-25	0	No significant findings
Salivary Glands	Normal	-26	0	No significant findings
Testis - Left	Normal	-27	0	Immature
Epididymis - Left	Normal	-27	0	No significant findings
Testis-Right	Normal	-28	0	Immature
Epididymis - Right	Normal	-28	0	No significant findings
Prostate	Normal	-29	0	Immature
Bladder	Normal	-29	0	No significant findings
Esophagus	Normal	-30	0	No significant findings
Aorta	Normal	-30	0	No significant findings
Trachea	Normal	-31	0	No significant findings

Histopathology Findings

Project: 197253 **Animal:** 005 **Sex:** Male **Pathology No.:** 080157 **Duration:** 15 Days
Group: 3 **Treatment:** Liposomes and α -tocopherol and NAC
Regimen: 60 mg/kg

Tissue	Result	Slide No.	Grade	Description (i.e. No significant findings)
Brain (Hindbrain + Brain Stem)	Normal	-1	0	No significant findings
Brain (Forebrain + Mid Brain)	Normal	-2	0	No significant findings
Adrenals	Normal	-3	0	No significant findings
Pituitary	Normal	-3	0	No significant findings
Sciatic Nerve	Normal	-4	0	No significant findings
Cervical Spinal Cord	Normal	-5	0	No significant findings
Thoracic Spinal Cord	Normal	-6	0	No significant findings
Eye (Left)	Normal	-7	0	No significant findings
Optic Nerve - Left (if present)	Normal	-7	0	No significant findings
Eye (Right)	Normal	-8	0	No significant findings
Optic Nerve - Right (if present)	Normal	-8	0	No significant findings
Heart	Normal	-9	0	No significant findings
Lungs (left & right diaphragmatic lobes)	Normal	-10	0	No significant findings
Liver (sample of central & left lobes)	Normal	-11	0	No significant findings
Kidney (Left)	Normal	-12	0	No significant findings
Kidney (Right)	Normal	-13	0	No significant findings
Pancreas	Normal	-14	0	No significant findings
duodenum	Normal	-14	0	No significant findings
Spleen	Normal	-15	0	No significant findings
Jejunum	Normal	-15	0	No significant findings
Stomach	Normal	-16	0	No significant findings
Ileum	Normal	-17	0	No significant findings
Colon	Normal	-17	0	No significant findings
Mesenteric Lymph Nodes	Normal	-18	0	No significant findings
Cecum	Normal	-18	0	No significant findings
Mandibular Lymph Nodes	Normal	-19	0	No significant findings
Muscle (Quadriceps)	Normal	-20	0	No significant findings
Tongue	Normal	-20	0	No significant findings
Skin	Normal	-21	0	No significant findings
Thymus	Abnormal	-22	2	Involution
Lumbar Cord	Normal	-22	0	No significant findings
Thyroid (Left)	Abnormal	-23	3	Cyst
Parathyroid - Left	Normal	-23	0	No significant findings
Thyroid (Right)	Abnormal	-24	2	C-cell hyperplasia
Parathyroid - Right	Normal	-24	0	No significant findings
Sterum & Marrow	Normal	-25	0	No significant findings
Salivary Glands	Normal	-26	0	No significant findings
Testis - Left	Normal	-27	0	Immature
Epididymis - Left	Normal	-27	0	No significant findings
Testis-Right	Normal	-28	0	Immature
Epididymis - Right	Normal	-28	0	No significant findings
Prostate	Normal	-29	0	Immature
Bladder	Normal	-29	0	No significant findings
Esophagus	Normal	-30	0	No significant findings
Aorta	Normal	-30	0	No significant findings
Trachea	Normal	-31	0	No significant findings

Histopathology Findings

Project: 197253 **Animal:** 006 **Sex:** Male **Pathology No.:** 080158 **Duration:** 15 Days
Group: 3 **Treatment:** Liposomes and α -tocopherol and NAC
Regimen: 60 mg/kg

Tissue	Result	Slide No.	Grade	Description (i.e. No significant findings)
Brain (Hindbrain + Brain Stem)	Normal	-1	0	No significant findings
Brain (Forebrain + Mid Brain)	Normal	-2	0	No significant findings
Adrenals	Normal	-3	0	No significant findings
Pituitary	Normal	-3	0	No significant findings
Sciatic Nerve	Normal	-4	0	No significant findings
Cervical Spinal Cord	Normal	-5	0	No significant findings
Thoracic Spinal Cord	Normal	-6	0	No significant findings
Eye (Left)	Normal	-7	0	No significant findings
Optic Nerve - Left (if present)	Normal	-7	0	No significant findings
Eye (Right)	Normal	-8	0	No significant findings
Optic Nerve - Right (if present)	Normal	-8	0	No significant findings
Heart	Normal	-9	0	No significant findings
Lungs (left & right diaphragmatic lobes)	Normal	-10	0	No significant findings
Liver (sample of central & left lobes)	Normal	-11	0	No significant findings
Kidney (Left)	Normal	-12	0	No significant findings
Kidney (Right)	Normal	-13	0	No significant findings
Pancreas	Normal	-14	0	No significant findings
duodenum	Normal	-14	0	No significant findings
Spleen	Normal	-15	0	No significant findings
Jejunum	Normal	-15	0	No significant findings
Stomach	Normal	-16	0	No significant findings
Ileum	Normal	-17	0	No significant findings
Colon	Normal	-17	0	No significant findings
Mesenteric Lymph Nodes	Normal	-18	0	No significant findings
Cecum	Normal	-18	0	No significant findings
Mandibular Lymph Nodes	Normal	-19	0	No significant findings
Muscle (Quadriceps)	Normal	-20	0	No significant findings
Tongue	Normal	-20	0	No significant findings
Skin	Abnormal	-21	2	Hyperkeratosis, focal
Thymus	Abnormal	-22	2	Involution
Lumbar Cord	Normal	-22	0	No significant findings
Thyroid (Left)	Normal	-23	0	No significant findings
Parathyroid - Left	Normal	-23	0	No significant findings
Thyroid (Right)	Normal	-24	0	No significant findings
Parathyroid - Right	Normal	-24	0	No significant findings
Sterum & Marrow	Normal	-25	0	No significant findings
Salivary Glands	Normal	-26	0	No significant findings
Testis - Left	Normal	-27	0	Immature
Epididymis - Left	Normal	-27	0	No significant findings
Testis-Right	Normal	-28	0	Immature
Epididymis - Right	Normal	-28	0	No significant findings
Prostate	Normal	-29	0	Immature
Bladder	Normal	-29	0	No significant findings
Esophagus	Normal	-30	0	No significant findings
Aorta	Normal	-30	0	No significant findings
Trachea	Normal	-31	0	No significant findings

Histopathology Findings

Project: 197253 **Animal:** 007 **Sex:** Male **Pathology No.:** 080161 **Duration:** 15 Days
Group: 4 **Treatment:** Liposomes and γ -tocopherol and NAC
Regimen: 60 mg/kg

Tissue	Result	Slide No.	Grade	Description (i.e. No significant findings)
Brain (Hindbrain + Brain Stem)	Normal	-1	0	No significant findings
Brain (Forebrain + Mid Brain)	Normal	-2	0	No significant findings
Adrenals	Normal	-3	0	No significant findings
Pituitary	Normal	-3	0	No significant findings
Sciatic Nerve	Normal	-4	0	No significant findings
Cervical Spinal Cord	Normal	-5	0	No significant findings
Thoracic Spinal Cord	Normal	-6	-	
Eye (Left)	Normal	-7	0	No significant findings
Optic Nerve - Left (if present)	Normal	-7	0	No significant findings
Eye (Right)	Normal	-8	0	No significant findings
Optic Nerve - Right (if present)	Normal	-8	0	No significant findings
Heart	Normal	-9	0	No significant findings
Lungs (left & right diaphragmatic lobes)	Normal	-10	0	No significant findings
Liver (sample of central & left lobes)	Normal	-11	0	No significant findings
Kidney (Left)	Normal	-12	0	No significant findings
Kidney (Right)	Normal	-13	0	No significant findings
Pancreas	Normal	-14	0	No significant findings
duodenum	Normal	-14	0	No significant findings
Spleen	Normal	-15	0	No significant findings
Jejunum	Normal	-15	0	No significant findings
Stomach	Normal	-16	0	No significant findings
Ileum	Normal	-17	0	No significant findings
Colon	Normal	-17	0	No significant findings
Mesenteric Lymph Nodes	Normal	-18	0	No significant findings
Cecum	Normal	-18	0	No significant findings
Mandibular Lymph Nodes	Normal	-19	0	No significant findings
Muscle (Quadriceps)	Normal	-20	0	No significant findings
Tongue	Normal	-20	0	No significant findings
Skin	Normal	-21	0	No significant findings
Thymus	Normal	-22	0	No significant findings
Lumbar Cord	Normal	-22	0	No significant findings
Thyroid (Left)	Normal	-23	0	No significant findings
Parathyroid - Left	Absent	-23	-	
Thyroid (Right)	Normal	-24	0	No significant findings
Parathyroid - Right	Normal	-24	0	No significant findings
Sternum & Marrow	Normal	-25	0	No significant findings
Salivary Glands	Normal	-26	0	No significant findings
Testis - Left	Normal	-27	0	Immature
Epididymis - Left	Normal	-27	0	No significant findings
Testis-Right	Normal	-28	0	No significant findings
Epididymis - Right	Normal	-28	0	No significant findings
Prostate	Normal	-29	0	Immature
Bladder	Normal	-29	0	No significant findings
Esophagus	Normal	-30	0	No significant findings
Aorta	Normal	-30	0	No significant findings
Trachea	Normal	-31	0	No significant findings

Histopathology Findings

Project: 197253 **Animal:** 008 **Sex:** Male **Pathology No.:** 080162 **Duration:** 15 Days
Group: 4 **Treatment:** Liposomes and γ -tocopherol and NAC
Regimen: 60 mg/kg

Tissue	Result	Slide No.	Grade	Description (i.e. No significant findings)
Brain (Hindbrain + Brain Stem)	Normal	-1	0	No significant findings
Brain (Forebrain + Mid Brain)	Normal	-2	0	No significant findings
Adrenals	Normal	-3	0	No significant findings
Pituitary	Absent	-3	-	
Sciatic Nerve	Normal	-4	0	No significant findings
Cervical Spinal Cord	Normal	-5	0	No significant findings
Thoracic Spinal Cord	Normal	-6	0	No significant findings
Eye (Left)	Normal	-7	0	No significant findings
Optic Nerve - Left (if present)	Normal	-7	0	No significant findings
Eye (Right)	Normal	-8	0	No significant findings
Optic Nerve - Right (if present)	Absent	-8	-	
Heart	Normal	-9	0	No significant findings
Lungs (left & right diaphragmatic lobes)	Normal	-10	0	No significant findings
Liver (sample of central & left lobes)	Normal	-11	0	No significant findings
Kidney (Left)	Normal	-12	0	No significant findings
Kidney (Right)	Normal	-13	0	No significant findings
Pancreas	Normal	-14	0	No significant findings
duodenum	Normal	-14	0	No significant findings
Spleen	Normal	-15	0	No significant findings
Jejunum	Normal	-15	0	No significant findings
Stomach	Normal	-16	0	No significant findings
Ileum	Normal	-17	0	No significant findings
Colon	Normal	-17	0	No significant findings
Mesenteric Lymph Nodes	Normal	-18	0	No significant findings
Cecum	Normal	-18	0	No significant findings
Mandibular Lymph Nodes	Normal	-19	0	No significant findings
Muscle (Quadriceps)	Normal	-20	0	No significant findings
Tongue	Normal	-20	0	No significant findings
Skin	Normal	-21	0	No significant findings
Thymus	Normal	-22	0	No significant findings
Lumbar Cord	Normal	-22	0	No significant findings
Thyroid (Left)	Abnormal	-23	2	C-cell hyperplasia
Parathyroid - Left	Normal	-23	0	No significant findings
Thyroid (Right)	Normal	-24	0	No significant findings
Parathyroid - Right	Normal	-24	0	No significant findings
Sterum & Marrow	Normal	-25	0	No significant findings
Salivary Glands	Normal	-26	0	No significant findings
Testis - Left	Normal	-27	0	Immature
Epididymis - Left	Normal	-27	0	No significant findings
Testis-Right	Normal	-28	0	Immature
Epididymis - Right	Normal	-28	0	No significant findings
Prostate	Normal	-29	0	Immature
Bladder	Normal	-29	0	No significant findings
Esophagus	Normal	-30	0	No significant findings
Aorta	Normal	-30	0	No significant findings
Trachea	Normal	-31	0	No significant findings

Histopathology Findings				
Project: 197253	Animal: 009	Sex: Female	Pathology No.: 080151	Duration: 15 Days
Group: 1	Treatment: Empty Liposomes			
Regimen: 0 mg/kg				

Tissue	Result	Slide No.	Grade	Description (i.e. No significant findings)
Brain (Hindbrain + Brain Stem)	Normal	-1	0	No significant findings
Brain (Forebrain + Mid Brain)	Normal	-2	0	No significant findings
Adrenals	Normal	-3	0	No significant findings
Pituitary	Absent	-3	-	
Sciatic Nerve	Normal	-4	0	No significant findings
Cervical Spinal Cord	Normal	-5	0	No significant findings
Thoracic Spinal Cord	Normal	-6	0	No significant findings
Eye (Left)	Normal	-7	0	No significant findings
Optic Nerve - Left (if present)	Normal	-7	0	No significant findings
Eye (Right)	Normal	-8	0	No significant findings
Optic Nerve - Right (if present)	Absent	-8	-	
Heart	Normal	-9	0	No significant findings
Lungs (left & right diaphragmatic lobes)	Normal	-10	0	No significant findings
Liver (sample of central & left lobes)	Normal	-11	0	No significant findings
Kidney (Left)	Normal	-12	0	No significant findings
Kidney (Right)	Normal	-13	0	No significant findings
Pancreas	Normal	-14	0	No significant findings
duodenum	Normal	-14	0	No significant findings
Spleen	Normal	-15	0	No significant findings
Jejunum	Normal	-15	0	No significant findings
Stomach	Normal	-16	0	No significant findings
Ileum	Normal	-17	0	No significant findings
Colon	Normal	-17	0	No significant findings
Mesenteric Lymph Nodes	Normal	-18	0	No significant findings
Cecum	Normal	-18	0	No significant findings
Mandibular Lymph Nodes	Normal	-19	0	No significant findings
Muscle (Quadriceps)	Normal	-20	0	No significant findings
Tongue	Normal	-20	0	No significant findings
Skin	Normal	-21	0	No significant findings
Mammary Gland	Normal	-21	0	No significant findings
Thymus	Normal	-22	0	No significant findings
Lumbar Cord	Normal	-22	0	No significant findings
Thyroid (Left)	Normal	-23	0	No significant findings
Parathyroid - Left	Normal	-23	0	No significant findings
Thyroid (Right)	Normal	-24	0	No significant findings
Parathyroid - Right	Normal	-24	0	No significant findings
Sterum & Marrow	Normal	-25	0	No significant findings
Salivary Glands	Normal	-26	0	No significant findings
Uterus (Horns, Cervix, Body)	Normal	-27	0	Immature
Vagina	Normal	-29	0	Immature
Ovaries	Normal	-29	0	Immature
Bladder	Normal	-29	0	No significant findings
Esophagus	Normal	-30	0	No significant findings
Aorta	Normal	-30	0	No significant findings
Trachea	Normal	-31	0	No significant findings

Histopathology Findings				
Project: 197253	Animal: 010	Sex: Female	Pathology No.: 080152	Duration: 15 Days
Group: 1	Treatment: Empty Liposomes			
Regimen: 0 mg/kg				

Tissue	Result	Slide No.	Grade	Description (i.e. No significant findings)
Brain (Hindbrain + Brain Stem)	Normal	-1	0	No significant findings
Brain (Forebrain + Mid Brain)	Normal	-2	0	No significant findings
Adrenals	Normal	-3	0	No significant findings
Pituitary	Normal	-3	0	No significant findings
Sciatic Nerve	Normal	-4	0	No significant findings
Cervical Spinal Cord	Normal	-5	0	No significant findings
Thoracic Spinal Cord	Normal	-6	0	No significant findings
Eye (Left)	Normal	-7	0	No significant findings
Optic Nerve - Left (if present)	Normal	-7	0	No significant findings
Eye (Right)	Normal	-8	0	No significant findings
Optic Nerve - Right (if present)	Normal	-8	0	No significant findings
Heart	Normal	-9	0	No significant findings
Lungs (left & right diaphragmatic lobes)	Normal	-10	0	No significant findings
Liver (sample of central & left lobes)	Normal	-11	0	No significant findings
Kidney (Left)	Normal	-12	0	No significant findings
Kidney (Right)	Normal	-13	0	No significant findings
Pancreas	Normal	-14	0	No significant findings
duodenum	Normal	-14	0	No significant findings
Spleen	Normal	-15	0	No significant findings
Jejunum	Normal	-15	0	No significant findings
Stomach	Normal	-16	0	No significant findings
Ileum	Normal	-17	0	No significant findings
Colon	Normal	-17	0	No significant findings
Mesenteric Lymph Nodes	Normal	-18	0	No significant findings
Cecum	Normal	-18	0	No significant findings
Mandibular Lymph Nodes	Normal	-19	0	No significant findings
Muscle (Quadriceps)	Normal	-20	0	No significant findings
Tongue	Normal	-20	0	No significant findings
Skin	Normal	-21	0	No significant findings
Mammary Gland	Normal	-21	0	No significant findings
Thymus	Normal	-22	0	No significant findings
Lumbar Cord	Normal	-22	0	No significant findings
Thyroid (Left)	Normal	-23	0	No significant findings
Parathyroid - Left	Normal	-23	0	No significant findings
Thyroid (Right)	Abnormal	-24	2	C-cell hyperplasia
Parathyroid - Right	Normal	-24	0	No significant findings
Sterum & Marrow	Normal	-25	0	No significant findings
Salivary Glands	Normal	-26	0	No significant findings
Uterus (Horns, Cervix, Body)	Normal	-27	0	Immature
Vagina	Normal	-29	0	Immature
Ovaries	Normal	-29	0	Immature
Bladder	Normal	-29	0	No significant findings
Esophagus	Normal	-30	0	No significant findings
Aorta	Normal	-30	0	No significant findings
Trachea	Normal	-31	0	No significant findings

Histopathology Findings

Project: 197253 **Animal:** 011 **Sex:** Female **Pathology No.:** 080155 **Duration:** 15 Days
Group: 2 **Treatment:** Liposomes and NAC
Regimen: 60 mg/kg

Tissue	Result	Slide No.	Grade	Description (i.e. No significant findings)
Brain (Hindbrain + Brain Stem)	Normal	-1	0	No significant findings
Brain (Forebrain + Mid Brain)	Normal	-2	0	No significant findings
Adrenals	Normal	-3	0	No significant findings
Pituitary	Normal	-3	0	No significant findings
Sciatic Nerve	Normal	-4	0	No significant findings
Cervical Spinal Cord	Normal	-5	0	No significant findings
Thoracic Spinal Cord	Normal	-6	0	No significant findings
Eye (Left)	Normal	-7	0	No significant findings
Optic Nerve - Left (if present)	Normal	-7	0	No significant findings
Eye (Right)	Normal	-8	0	No significant findings
Optic Nerve - Right (if present)	Normal	-8	0	No significant findings
Heart	Normal	-9	0	No significant findings
Lungs (left & right diaphragmatic lobes)	Normal	-10	0	No significant findings
Liver (sample of central & left lobes)	Normal	-11	0	No significant findings
Kidney (Left)	Normal	-12	0	No significant findings
Kidney (Right)	Normal	-13	0	No significant findings
Pancreas	Normal	-14	0	No significant findings
duodenum	Normal	-14	0	No significant findings
Spleen	Normal	-15	0	No significant findings
Jejunum	Normal	-15	0	No significant findings
Stomach	Normal	-16	0	No significant findings
Ileum	Normal	-17	0	No significant findings
Colon	Normal	-17	0	No significant findings
Mesenteric Lymph Nodes	Normal	-18	0	No significant findings
Cecum	Normal	-18	0	No significant findings
Mandibular Lymph Nodes	Normal	-19	0	No significant findings
Muscle (Quadriceps)	Normal	-20	0	No significant findings
Tongue	Normal	-20	0	No significant findings
Skin	Normal	-21	0	No significant findings
Mammary Gland	Absent	-21	-	
Thymus	Normal	-22	0	No significant findings
Lumbar Cord	Normal	-22	0	No significant findings
Thyroid (Left)	Normal	-23	0	No significant findings
Parathyroid - Left	Absent	-23	-	
Thyroid (Right)	Abnormal	-24	2	C-cell hyperplasia
Parathyroid - Right	Absent	-24	-	
Sterum & Marrow	Normal	-25	0	No significant findings
Salivary Glands	Normal	-26	0	No significant findings
Uterus (Horns, Cervix, Body)	Normal	-27	0	Immature
Vagina	Normal	-28	0	Immature
Ovaries	Normal	-29	0	No significant findings
Bladder	Normal	-29	0	No significant findings
Esophagus	Normal	-30	0	No significant findings
Aorta	Normal	-30	0	No significant findings
Trachea	Normal	-31	0	No significant findings

Histopathology Findings

Project: 197253 **Animal:** 012 **Sex:** Female **Pathology No.:** 080156 **Duration:** 15 Days
Group: 2 **Treatment:** Liposomes and NAC
Regimen: 60 mg/kg

Tissue	Result	Slide No.	Grade	Description (i.e. No significant findings)
Brain (Hindbrain + Brain Stem)	Normal	-1	0	No significant findings
Brain (Forebrain + Mid Brain)	Normal	-2	0	No significant findings
Adrenals	Normal	-3	0	No significant findings
Pituitary	Abnormal	-3	3	Cyst
Sciatic Nerve	Normal	-4	0	No significant findings
Cervical Spinal Cord	Normal	-5	0	No significant findings
Thoracic Spinal Cord	Normal	-6	0	No significant findings
Eye (Left)	Normal	-7	2	No significant findings
Optic Nerve - Left (if present)	Absent	-7	-	
Eye (Right)	Normal	-8	2	No significant findings
Optic Nerve - Right (if present)	Normal	-8	0	No significant findings
Heart	Normal	-9	0	No significant findings
Lungs (left & right diaphragmatic lobes)	Normal	-10	0	No significant findings
Liver (sample of central & left lobes)	Normal	-11	0	No significant findings
Kidney (Left)	Normal	-12	0	No significant findings
Kidney (Right)	Normal	-13	0	No significant findings
Pancreas	Normal	-14	0	No significant findings
duodenum	Normal	-14	0	No significant findings
Spleen	Normal	-15	0	No significant findings
Jejunum	Normal	-15	0	No significant findings
Stomach	Normal	-16	0	No significant findings
Ileum	Normal	-17	0	No significant findings
Colon	Normal	-17	0	No significant findings
Mesenteric Lymph Nodes	Normal	-18	0	No significant findings
Cecum	Normal	-18	0	No significant findings
Mandibular Lymph Nodes	Normal	-19	0	No significant findings
Muscle (Quadriceps)	Normal	-20	0	No significant findings
Tongue	Normal	-20	0	No significant findings
Skin	Normal	-21	0	No significant findings
Mammary Gland	Normal	-21	0	Immature
Thymus	Normal	-22	0	No significant findings
Lumbar Cord	Normal	-22	0	No significant findings
Thyroid (Left)	Normal	-23	0	No significant findings
Parathyroid - Left	Normal	-23	0	No significant findings
Thyroid (Right)	Normal	-24	0	No significant findings
Parathyroid - Right	Normal	-24	0	No significant findings
Sterum & Marrow	Normal	-25	0	No significant findings
Salivary Glands	Normal	-26	0	No significant findings
Uterus (Horns, Cervix, Body)	Normal	-27	0	Immature
Vagina	Normal	-28	0	Immature
Ovaries	Normal	-29	0	No significant findings
Bladder	Normal	-29	0	No significant findings
Esophagus	Normal	-30	0	No significant findings
Aorta	Normal	-30	0	No significant findings
Trachea	Normal	-31	0	No significant findings

Histopathology Findings

Project: 197253 **Animal:** 013 **Sex:** Female **Pathology No.:** 080159 **Duration:** 15 Days
Group: 3 **Treatment:** Liposomes and α -tocopherol and NAC
Regimen: 60 mg/kg

Tissue	Result	Slide No.	Grade	Description (i.e. No significant findings)
Brain (Hindbrain + Brain Stem)	Normal	-1	0	No significant findings
Brain (Forebrain + Mid Brain)	Normal	-2	0	No significant findings
Adrenals	Normal	-3	0	No significant findings
Pituitary	Normal	-3	0	No significant findings
Sciatic Nerve	Normal	-4	0	No significant findings
Cervical Spinal Cord	Normal	-5	0	No significant findings
Thoracic Spinal Cord	Normal	-6	0	No significant findings
Eye (Left)	Normal	-7	0	No significant findings
Optic Nerve - Left (if present)	Normal	-7	0	No significant findings
Eye (Right)	Normal	-8	0	No significant findings
Optic Nerve - Right (if present)	Normal	-8	0	No significant findings
Heart	Normal	-9	0	No significant findings
Lungs (left & right diaphragmatic lobes)	Normal	-10	0	No significant findings
Liver (sample of central & left lobes)	Normal	-11	0	No significant findings
Kidney (Left)	Normal	-12	0	No significant findings
Kidney (Right)	Abnormal	-13	2	Multifocal hemorrhage
Pancreas	Normal	-14	0	No significant findings
duodenum	Normal	-14	0	No significant findings
Spleen	Normal	-15	0	No significant findings
Jejunum	Normal	-15	0	No significant findings
Stomach	Normal	-16	0	No significant findings
Ileum	Normal	-17	0	No significant findings
Colon	Normal	-17	0	No significant findings
Mesenteric Lymph Nodes	Normal	-18	0	No significant findings
Cecum	Normal	-18	0	No significant findings
Mandibular Lymph Nodes	Normal	-19	0	No significant findings
Muscle (Quadriceps)	Normal	-20	0	No significant findings
Tongue	Normal	-20	0	No significant findings
Skin	Normal	-21	0	No significant findings
Mammary Gland	Normal	-21	0	No significant findings
Thymus	Normal	-22	0	No significant findings
Lumbar Cord	Normal	-22	0	No significant findings
Thyroid (Left)	Normal	-23	0	No significant findings
Parathyroid - Left	Normal	-23	0	No significant findings
Thyroid (Right)	Normal	-24	0	No significant findings
Parathyroid - Right	Normal	-24	0	No significant findings
Sterum & Marrow	Normal	-25	0	No significant findings
Salivary Glands	Normal	-26	0	No significant findings
Uterus (Horns, Cervix, Body)	Normal	-27	0	Immature
Vagina	Normal	-28	0	Immature
Ovaries	Normal	-29	0	No significant findings
Bladder	Normal	-29	0	No significant findings
Esophagus	Normal	-30	0	No significant findings
Aorta	Normal	-30	0	No significant findings
Trachea	Normal	-31	0	No significant findings

Histopathology Findings

Project: 197253 **Animal:** 014 **Sex:** Female **Pathology No.:** 080160 **Duration:** 15 Days
Group: 3 **Treatment:** Liposomes and α -tocopherol and NAC
Regimen: 60 mg/kg

Tissue	Result	Slide No.	Grade	Description (i.e. No significant findings)
Brain (Hindbrain + Brain Stem)	Normal	-1	0	No significant findings
Brain (Forebrain + Mid Brain)	Normal	-2	0	No significant findings
Adrenals	Normal	-3	0	No significant findings
Pituitary	Normal	-3	0	No significant findings
Sciatic Nerve	Normal	-4	0	No significant findings
Cervical Spinal Cord	Normal	-5	0	No significant findings
Thoracic Spinal Cord	Normal	-6	0	No significant findings
Eye (Left)	Normal	-7	0	No significant findings
Optic Nerve - Left (if present)	Normal	-7	0	No significant findings
Eye (Right)	Normal	-8	0	No significant findings
Optic Nerve - Right (if present)	Normal	-8	0	No significant findings
Heart	Normal	-9	0	No significant findings
Lungs (left & right diaphragmatic lobes)	Normal	-10	0	No significant findings
Liver (sample of central & left lobes)	Normal	-11	0	No significant findings
Kidney (Left)	Normal	-12	0	No significant findings
Kidney (Right)	Normal	-13	0	No significant findings
Pancreas	Normal	-14	0	No significant findings
duodenum	Normal	-14	0	No significant findings
Spleen	Normal	-15	0	No significant findings
Jejunum	Normal	-15	0	No significant findings
Stomach	Normal	-16	0	No significant findings
Ileum	Normal	-17	0	No significant findings
Colon	Normal	-17	0	No significant findings
Mesenteric Lymph Nodes	Normal	-18	0	No significant findings
Cecum	Normal	-18	0	No significant findings
Mandibular Lymph Nodes	Normal	-19	0	No significant findings
Muscle (Quadriceps)	Normal	-20	0	No significant findings
Tongue	Normal	-20	0	No significant findings
Skin	Normal	-21	0	No significant findings
Mammary Gland	Normal	-21	0	No significant findings
Thymus	Normal	-22	0	No significant findings
Lumbar Cord	Normal	-22	0	No significant findings
Thyroid (Left)	Abnormal	-23	2	C-cell hyperplasia
Parathyroid - Left	Normal	-23	0	No significant findings
Thyroid (Right)	Normal	-24	0	No significant findings
Parathyroid - Right	Normal	-24	0	No significant findings
Sterum & Marrow	Normal	-25	0	No significant findings
Salivary Glands	Normal	-26	0	No significant findings
Uterus (Horns, Cervix, Body)	Normal	-27	0	No significant findings
Vagina	Normal	-28	0	No significant findings
Ovaries	Normal	-29	0	No significant findings
Bladder	Normal	-29	0	No significant findings
Esophagus	Normal	-30	0	No significant findings
Aorta	Normal	-30	0	No significant findings
Trachea	Normal	-31	0	No significant findings

Histopathology Findings

Project: 197253 **Animal:** 015 **Sex:** Female **Pathology No.:** 080163 **Duration:** 15 Days
Group: 4 **Treatment:** Liposomes and γ -tocopherol and NAC
Regimen: 60 mg/kg

Tissue	Result	Slide No.	Grade	Description (i.e. No significant findings)
Brain (Hindbrain + Brain Stem)	Normal	-1	0	No significant findings
Brain (Forebrain + Mid Brain)	Normal	-2	0	No significant findings
Adrenals	Normal	-3	0	No significant findings
Pituitary	Normal	-3	0	No significant findings
Sciatic Nerve	Normal	-4	0	No significant findings
Cervical Spinal Cord	Normal	-5	0	No significant findings
Thoracic Spinal Cord	Normal	-6	0	No significant findings
Eye (Left)	Normal	-7	0	No significant findings
Optic Nerve - Left (if present)	Absent	-7	-	
Eye (Right)	Normal	-8	0	No significant findings
Optic Nerve - Right (if present)	Normal	-8	0	No significant findings
Heart	Normal	-9	0	No significant findings
Lungs (left & right diaphragmatic lobes)	Normal	-10	0	No significant findings
Liver (sample of central & left lobes)	Normal	-11	0	No significant findings
Kidney (Left)	Normal	-12	0	No significant findings
Kidney (Right)	Normal	-13	0	No significant findings
Pancreas	Normal	-14	0	No significant findings
duodenum	Normal	-14	0	No significant findings
Spleen	Normal	-15	0	No significant findings
Jejunum	Normal	-15	0	No significant findings
Stomach	Normal	-16	0	No significant findings
Ileum	Normal	-17	0	No significant findings
Colon	Normal	-17	0	No significant findings
Mesenteric Lymph Nodes	Normal	-18	0	No significant findings
Cecum	Normal	-18	0	No significant findings
Mandibular Lymph Nodes	Normal	-19	0	No significant findings
Muscle (Quadriceps)	Normal	-20	0	No significant findings
Tongue	Normal	-20	0	No significant findings
Skin	Normal	-21	0	No significant findings
Mammary Gland	Normal	-21	0	No significant findings
Thymus	Normal	-22	0	No significant findings
Lumbar Cord	Normal	-22	0	No significant findings
Thyroid (Left)	Normal	-23	0	No significant findings
Parathyroid - Left	Normal	-23	0	No significant findings
Thyroid (Right)	Normal	-24	0	No significant findings
Parathyroid - Right	Normal	-24	0	No significant findings
Sterum & Marrow	Normal	-25	0	No significant findings
Salivary Glands	Normal	-26	0	No significant findings
Uterus (Horns, Cervix, Body)	Normal	-27	0	No significant findings
Vagina	Normal	-28	0	No significant findings
Ovaries	Normal	-29	0	No significant findings
Bladder	Normal	-29	0	No significant findings
Esophagus	Normal	-30	0	No significant findings
Aorta	Normal	-30	0	No significant findings
Trachea	Normal	-31	0	No significant findings

Histopathology Findings

Project: 197253 **Animal:** 016 **Sex:** Female **Pathology No.:** 080164 **Duration:** 15 Days
Group: 4 **Treatment:** Liposomes and γ -tocopherol and NAC
Regimen: 60 mg/kg

Tissue	Result	Slide No.	Grade	Description (i.e. No significant findings)
Brain (Hindbrain + Brain Stem)	Normal	-1	0	No significant findings
Brain (Forebrain + Mid Brain)	Normal	-2	0	No significant findings
Adrenals	Normal	-3	0	No significant findings
Pituitary	Abnormal	-3	3	Cyst
Sciatic Nerve	Normal	-4	0	No significant findings
Cervical Spinal Cord	Normal	-5	0	No significant findings
Thoracic Spinal Cord	Normal	-6	0	No significant findings
Eye (Left)	Normal	-7	0	No significant findings
Optic Nerve - Left (if present)	Normal	-7	0	No significant findings
Eye (Right)	Normal	-8	0	No significant findings
Optic Nerve - Right (if present)	Absent	-8	-	
Heart	Normal	-9	0	No significant findings
Lungs (left & right diaphragmatic lobes)	Normal	-10	0	No significant findings
Liver (sample of central & left lobes)	Normal	-11	0	No significant findings
Kidney (Left)	Normal	-12	0	No significant findings
Kidney (Right)	Normal	-13	0	No significant findings
Pancreas	Normal	-14	0	No significant findings
duodenum	Normal	-14	0	No significant findings
Spleen	Normal	-15	0	No significant findings
Jejunum	Normal	-15	0	No significant findings
Stomach	Normal	-16	0	No significant findings
Ileum	Normal	-17	0	No significant findings
Colon	Normal	-17	0	No significant findings
Mesenteric Lymph Nodes	Normal	-18	0	No significant findings
Cecum	Normal	-18	0	No significant findings
Mandibular Lymph Nodes	Normal	-19	0	No significant findings
Muscle (Quadriceps)	Normal	-20	0	No significant findings
Tongue	Normal	-20	0	No significant findings
Skin	Normal	-21	0	No significant findings
Mammary Gland	Absent	-21	-	
Thymus	Normal	-22	0	No significant findings
Lumbar Cord	Normal	-22	0	No significant findings
Thyroid (Left)	Normal	-23	0	No significant findings
Parathyroid - Left	Normal	-23	0	No significant findings
Thyroid (Right)	Normal	-24	0	No significant findings
Parathyroid - Right	Normal	-24	0	No significant findings
Sterum & Marrow	Normal	-25	0	No significant findings
Salivary Glands	Normal	-26	0	No significant findings
Uterus (Horns, Cervix, Body)	Normal	-27	0	Immature
Vagina	Normal	-28	0	Immature
Ovaries	Normal	-29	0	Immature
Bladder	Normal	-29	0	No significant findings
Esophagus	Normal	-30	0	No significant findings
Aorta	Normal	-30	0	No significant findings
Trachea	Normal	-31	0	No significant findings

William L. Stone, Ph.D.

East Tennessee State University,

Johnson City, TN

REPORT DOCUMENTATION PAGE

Form Approved
OMB No. 0704-0188

Public reporting burden for this collection of information is estimated to average 1 hour per response, including the time for reviewing instructions, searching existing data sources, gathering and maintaining the data needed, and completing and reviewing this collection of information. Send comments regarding this burden estimate or any other aspect of this collection of information, including suggestions for reducing this burden to Department of Defense, Washington Headquarters Services, Directorate for Information Operations and Reports (0704-0188), 1215 Jefferson Davis Highway, Suite 1204, Arlington, VA 22202-4302. Respondents should be aware that notwithstanding any other provision of law, no person shall be subject to any penalty for failing to comply with a collection of information if it does not display a currently valid OMB control number. **PLEASE DO NOT RETURN YOUR FORM TO THE ABOVE ADDRESS.**

1. REPORT DATE (DD-MM-YYYY) 29/09/2010		2. REPORT TYPE Final		3. DATES COVERED (From - To) 09/21/2006 – 09/24/2010	
4. TITLE AND SUBTITLE An Overview of the Continuation of the Work of the Mustard Gas Consortium for the Use of the Free and Liposome-Encapsulated Antioxidants as a Counter Measure to Mustards.				5a. CONTRACT NUMBER	
				5b. GRANT NUMBER W81XWH-06-2-0044	
				5c. PROGRAM ELEMENT NUMBER PE 62384BP	
6. AUTHOR(S) William L. Stone, PhD (ETSU subcontract)				5d. PROJECT NUMBER	
				5e. TASK NUMBER	
				5f. WORK UNIT NUMBER	
7. PERFORMING ORGANIZATION NAME(S) AND ADDRESS(ES) East Tennessee State University James H. Quillen College of Medicine Dept of Pediatrics Johnson City, Tennessee 37614-0578				8. PERFORMING ORGANIZATION REPORT NUMBER	
9. SPONSORING / MONITORING AGENCY NAME(S) AND ADDRESS(ES) U.S. Army Medical Research and Materiel Command Fort Detrick, MD 21702-5012				10. SPONSOR/MONITOR'S ACRONYM(S)	
				11. SPONSOR/MONITOR'S REPORT NUMBER(S)	
12. DISTRIBUTION / AVAILABILITY STATEMENT Approved for public release, distribution unlimited.					
13. SUPPLEMENTARY NOTES					
14. ABSTRACT Our overall goal in this research project was to develop therapeutics for human exposure to the dangerous vesicant and chemical warfare agent sulfur mustard [bis-2-(chloroethyl) sulfide, military code HD]. We explored the molecular mechanisms involved in mustard gas toxicity for the basis of the therapeutic(s) design and found that exposure to a high dose of HD or its monofunctional analog 2-chloroethyl-ethyl sulfide (CEES) increases oxidative stress and inflammatory biomarkers. We also provided antioxidant liposomes to other members of the consortium. These liposomes could deliver both nontoxic lipid and water-soluble antioxidants. Our results indicate that antioxidant liposomes are effective in preventing CEES damage to both skin (our work) and lungs (in collaboration with Drs. Ward and Das) even in a post-exposure situation. In addition, our <i>in vitro</i> studies with Dr. Richard Rest suggest that liposomes encapsulated with N-acetyl cysteine (NAC-liposomes) completely inhibited the germination of <i>Bacillus anthracis</i> spores (in the absence of macrophages) and stimulated the ability of macrophages to kill intracellular <i>B. anthracis</i> . These liposome formulations provide a unique therapeutic strategy for injury from both chemical and biological warfare agents.					
15. SUBJECT TERMS HD, CEES, mast cells, lung, oxidative stress, glutathione, liposomes, antioxidant, HD therapeutic, Bacillus anthracis, Vitamin E, N-acetyl-cysteine, Pyruvate					
16. SECURITY CLASSIFICATION OF:			17. LIMITATION OF ABSTRACT	18. NUMBER OF PAGES	19a. NAME OF RESPONSIBLE PERSON
a. REPORT	b. ABSTRACT	c. THIS PAGE			USAMRMC
U	U	U	U	186	19b. TELEPHONE NUMBER (include area code)

Standard Form 298 (Rev. 8-98)
Prescribed by ANSI Std. Z39.18

Table of Contents

	<u>Page</u>
Cover Page	1
Report Documentation Page (SF-298)	2
Table of Contents	3
Introduction	4
Statement of Work.....	5
Body	7
Key Research Accomplishments	33
Reportable Outcomes	35
Conclusion	38
References	40
Appendices	42

Introduction

Our overall goal in this research project was to develop therapeutics for human exposure to the dangerous vesicant and chemical warfare agent sulfur mustard [bis-2-(chloroethyl) sulfide, military code HD]. We explored the molecular mechanisms involved in mustard gas toxicity since this is essential for designing the optimal therapeutics. Accordingly, this report describes molecular mechanisms of inflammation and oxidative stress that we found to play key roles in the toxicity of HD and its monofunctional analog 2-chloroethyl-ethyl sulfide (CEES). A key finding of our research is that antioxidant liposomes provide an effective therapeutic strategy for mustard gas induced injury (dermal and pulmonary).

Antioxidant liposomes provide the ability to deliver both nontoxic lipid and water-soluble antioxidants and can thereby be an effective countermeasure to oxidative stress induced damage caused by HD/CEES. We worked with other members of the consortium by providing well-characterized antioxidant liposomes. Our second generation of liposomes contained isomers of the lipid soluble antioxidant, vitamin E, as well as encapsulated N-acetyl-cysteine (NAC) and pyruvate, both of which are water-soluble antioxidants. Antioxidant-liposomes were found to protect rat and guinea pig lungs from damage and inflammation caused by CEES exposure. We also determined that the addition of pyruvate to liposomes (second generation antioxidant liposomes) may offer additional therapeutic value. Our results to date indicate that antioxidant liposomes are effective in preventing CEES damage to both skin (our work) and lungs (in collaboration with Drs. Ward and Das) even in a post-exposure situation. In addition, our *in vitro* studies with Dr. Richard Rest suggest that liposomes encapsulated with NAC-completely inhibit the germination of *Bacillus anthracis* spores (in the absence of macrophages) and stimulated the ability of macrophages to kill intracellular *B. anthracis*. **These liposome formulations provided a unique therapeutic strategy for injury from both chemical and biological warfare agents.** Our data suggest that antioxidant liposomes can alter the redox status of cells in a manner that protects tissue from sulfur mustard induced injury and provides resistance to the growth and invasiveness of *B. anthracis*.

Our research has documented many of the components of inflammation and oxidative stress that play key roles in the toxicity of HD and its monofunctional analog 2-chloroethyl-ethyl sulfide (CEES). Using proteomics and molecular biology tools, we studied CEES/HD induced oxidative stress in biological samples at the detailed molecular level. We found that immunostimulators like lipopolysaccharide (LPS) induced intracellular generation of NO and reactive oxygen species (ROS) and greatly enhanced CEES toxicity in RAW 264.7 macrophages (Stone et al., 2003). We also found that CEES inhibited NO generation in these cells via down-regulation of inducible NO synthase (iNOS) protein expression (Qui et al., 2006). The generation of NO by iNOS is known to promote wound healing and the inhibition of iNOS expression could account for the slow wound healing following mustard gas exposure.

We utilized redox - proteomics to determine how CEES (or HD/pathogen) treatment influences changes in the levels and distribution of oxidized proteins using either mast cell lines or animal tissue samples obtained from other members of the Consortium. We tested the effect of our liposomes on protein expression and oxidation in mast cells and animal models exposed to CEES or HD. We also initiated work to determine the identities and functional significance of the oxidized proteins.

Skin mast cells have long been suspected of influencing HD-induced cutaneous damage (Graham et al., 1994). Mast cells are known to play a key role in inflammation, but there have been only a few published observations describing the outcome of CEES exposure on mast cells, and these articles provide little detail on the molecular changes that occur when cells are exposed to HD/CEES (Graham et al., 1994; Tewari-Singh et al., 2009; Rikimaru et al., 1991; Dannenburg et al., 1985).

We investigated the effects of CEES on oxidative stress in the rat basophilic leukemia RBL-2H3 mast cell line. Nitric oxide is known to inhibit mast cell degranulation in various species (Eastmond et al., 1997; Iikura et al., 1998). Therefore, we hypothesized that CEES, by inducing oxidative stress and potentially decreasing NO production, would promote mast cell degranulation. Mast cell degranulation could release large amounts of TNF- α , IL-1 β , and other inflammatory cytokines, which could enhance the toxicity of CEES/HD. Our results indicated that *in vitro* exposure of mast cells to CEES does little to increase mast cell degranulation or to decrease NO production (in marked contrast to our previous results with RAW 264.7 murine macrophages). Nevertheless, we found that stimulating mast cell degranulation with a Ca²⁺ ionophore (A-23187) does enhance CEES toxicity.

Oxidative stress occurs when the production of reactive oxygen species (ROS) exceeds the cell's antioxidant defenses thereby causing damage to the cell's proteins, lipids and DNA. Glutathione (GSH), a major cellular antioxidant, helps to protect cells by neutralizing ROS in redox coupled oxidation-reduction reactions. In non-stressed cells, GSH is found almost exclusively in a reduced state at a concentration of approximately ~5 mM, but under conditions of oxidative stress, the balance of reduced glutathione to oxidized glutathione (GSH/GSSG) shifts to a more oxidized state. When the GSH/GSSG ratio is reduced, GSH becomes conjugated to specific proteins; this post-translational modification is defined as glutathionylation. The purpose of protein glutathionylation is now believed to be protective to allow cell repair. For example, glutathionylation has been found to alter protein function by activating cellular repair mechanisms (Townsend et al., 2009). HD and CEES metabolites form GSH-conjugates causing glutathione depletion. Since GSH is a key intracellular antioxidant, its depletion by HD would increase cellular oxidative stress. Exposure to HD also causes macromolecular damage including DNA damage and covalent modifications of proteins. Ultimately, this damage leads to inactivation of enzymes, fragmentation of the extracellular matrix and cell detachment. The damage and oxidative stress finally leads to apoptosis and/or necrosis (Paromov et al., 2007). We described additional effects of CEES cytotoxicity on the rat basophilic leukemia cell line RBL-2H3 by measuring apoptosis, oxidative stress, and glutathionylation in these cells after CEES exposure.

Statement of Work

We found that Immunostimulators like lipopolysaccharide (LPS) induce intracellular generation of NO and reactive oxygen species (ROS) and greatly enhance the toxicity of 2-chloroethyl-ethyl sulfide (CEES, HD analogue) in RAW 264.7 macrophages (Stone et al., 2003). We also found that CEES inhibits NO generation in these cells via downregulation of inducible NO synthase (iNOS) protein expression (Qui et al., 2006). Nitric oxide is known to inhibit mast cell degranulation in

various species (Eastmond et al., 1997; Iikura et al., 1998). Therefore, we hypothesized that CEES might have an effect on mast cell degranulation.

- I. Based on our previous findings, our **first set of goals** was to:
 - a) Investigate the effect of CEES on degranulation/cytokine release of rat basophilic leukemia RBL-2H3.
 - b) Determine if CEES inhibits the production of nitric oxide (NO) in mast cells by use of the cell permeable fluorescent dyes and by measurement of nitrite formed from NO released into the cell medium.
 - c) Determine if antioxidant liposomes inhibit mast cell degranulation induced by CEES.

- II. A **second series of goals** focused on utilizing redox proteomics to determine how CEES (or HD/pathogen) treatment influences changes in the levels and distribution of oxidized proteins using either *in vitro* cellular studies (mast cell lines and human Epiderm skin samples) or the *in vivo* animal models (animal tissue samples snap frozen in liquid nitrogen) obtained from other members of the Mustard Consortium:
 - a) Identify and determine the functional significance of the oxidized proteins. Proteomics of various biological samples exposed to CEES or pathogens were analyzed by 2-dimensional gel electrophoresis (2D-GE). Oxidized proteins from the 2D-GE gels were identified using tandem mass spectrometry.
 - b) Utilize redox proteomics to determine how CEES treatment influenced changes in the levels and distribution of oxidized/glutathionylated proteins expressed in mast cell lines. Focus on determining the identities and functional significance of the oxidized proteins.
 - c) Study the effect of antioxidant liposomes on protein expression and oxidation in both *in vivo* and *in vitro* model systems exposed to CEES or HD.

- III. A **third set of goals** was to continue to supply well characterized antioxidant-liposomes to all other members of the Research Consortium and provide the analytical methodology and services to measure antioxidant (vitamin E and glutathione) levels in tissues collected from the various animal models used by other members of the mustard consortium.
 - a) Continue to supply well characterized antioxidant-liposomes
 - b) Continue to improve the stability and effectiveness of the antioxidant liposomes. Our most recent formulations showed very long term stability during storage.
 - c) Characterize lyophilized antioxidant liposomes (in collaboration with Dr. Zach Suntres) which have a very long shelf life.

Body

I. Investigate the effect of CEES on oxidative stress and degranulation/cytokine release in the rat basophilic leukemia RBL-2H3.

Mast cells are known to play a key role in inflammation. We investigated the effects of CEES on ROS generation and thiol depletion, indicators of oxidative stress, in the rat basophilic leukemia RBL-2H3 mast cell line by performing fluorescent microscopy studies. First, we monitored NO and ROS generation in RBL-2H3 rat mast cells using the specific fluorescent marker carboxy-dichlorofluorescein diacetate (carDCFH-DA). The carDCFH-DA indicates the presence of both NO and ROS. We incubated mast cells for 1.5 hour either with vehicle (1% EtOH), or with 0.5 mM CEES, or with 0.625 μM Ca^{2+} ionophore (A23187, induces degranulation), or with CEES and Ca^{2+} ionophore (A23187 + CEES), or with 0.1 mM tert-butyl hydroperoxide (TBHP, induces oxidative stress) as a positive control. The cells were then stained with the fluorescent dye for 20 min, examined under an inverted fluorescent microscope equipped with a standard FITC filter and digitally photographed. We observed ROS production with carDCFH-DA (**Figure 1**). Mast cells treated with vehicle (not shown) or A23187 did not show any fluorescence (no ROS production), whereas CEES-treated cells showed some signs of oxidative stress, and cells treated with CEES and Ca^{2+} ionophore showed massive oxidative stress (high ROS production, similar to TBHP).

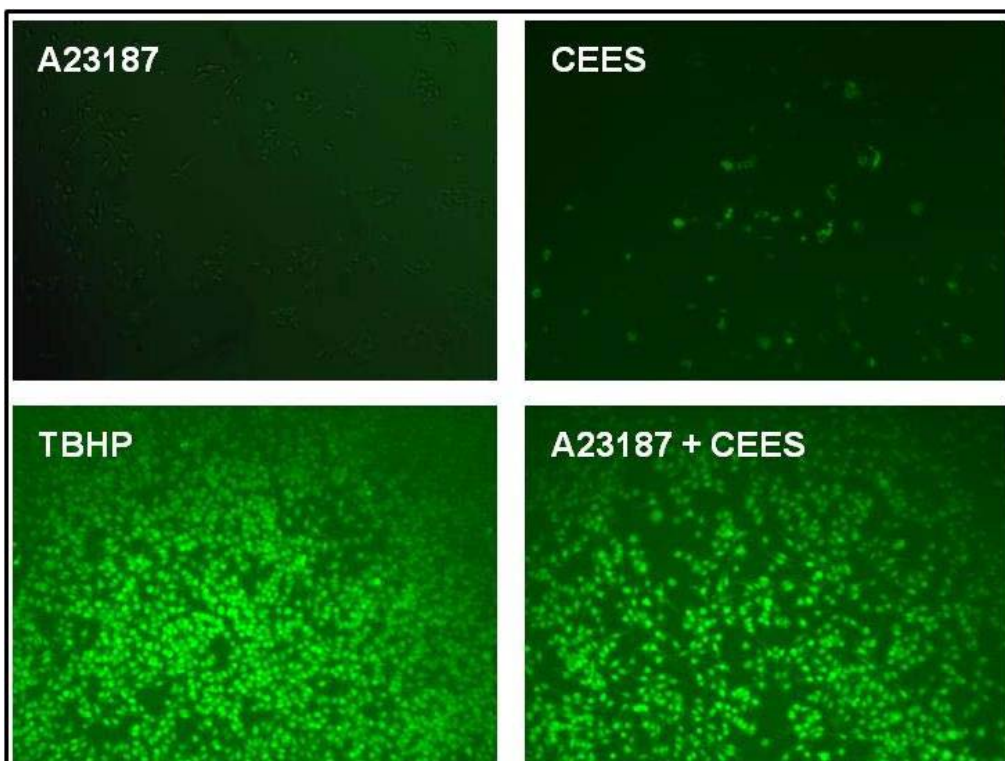


Figure 1. ROS production in rat mast cells: RBL-2H3 cells were incubated with 0.625 μM Ca^{2+} ionophore (**A23187**), or with 0.5 mM CEES (**CEES**), or with CEES and Ca^{2+} ionophore (**A23187 + CEES**), or with 0.1 mM tert-butyl hydroperoxide (**TBHP**) as positive control. ROS production was monitored by car-DCFH DA staining (green fluorescence) under inverted fluorescent microscope.

Second, we monitored another oxidative stress parameter, the depletion of intracellular total thiol and GSH using fluorescent dyes CMF-DA (5-chloromethylfluorescein diacetate) and CMAC (7-amino-4-chloromethylcoumarin), respectively. RBL-2H3 rat mast cells were treated as described for **Figure 1** (see above) and stained either with CMF-DA for 15 min, or with CMAC for 30 min; the cells were then examined with an inverted fluorescent microscope and digitally photographed. **Figure 2** shows total thiol-sensitive green fluorescent staining (CMF-DA); **Figure 3** shows GSH-sensitive blue fluorescent staining (CMAC). RBL-2H3 cells treated with vehicle (not shown) or A23187 did not show any sign of thiol or GSH depletion (high green and blue fluorescence), whereas CEES-treated cells showed moderate depletion of intracellular total thiol and GSH, and cells treated with CEES and Ca²⁺ ionophore were fully depleted from both total thiol and GSH, similar to TBHP treatment (oxidative stress positive control).

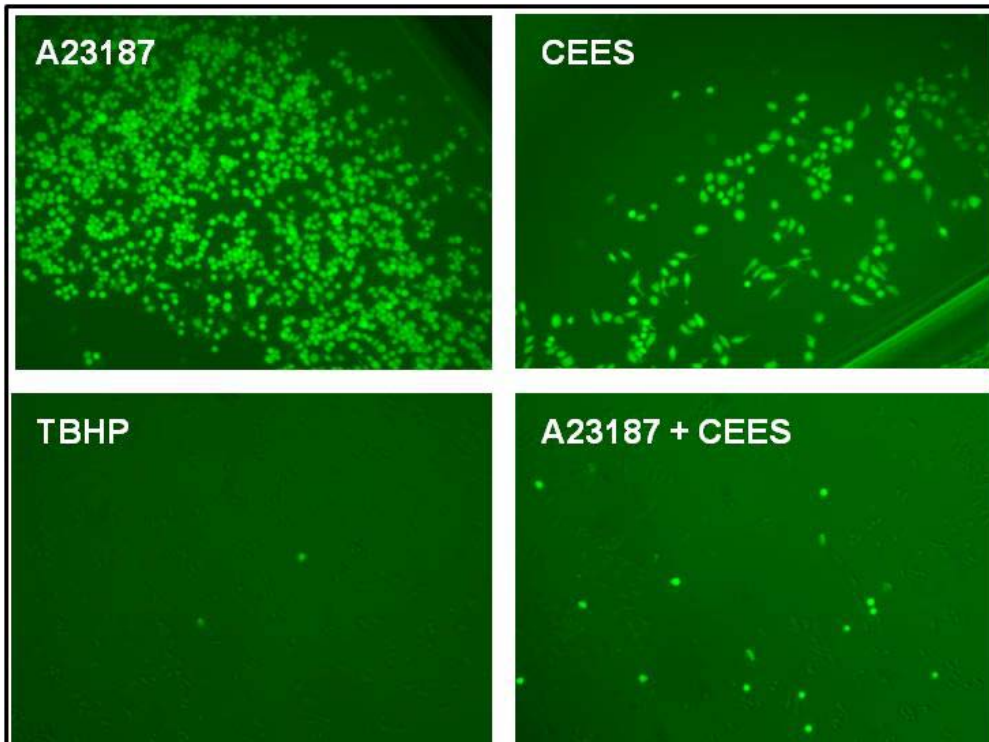
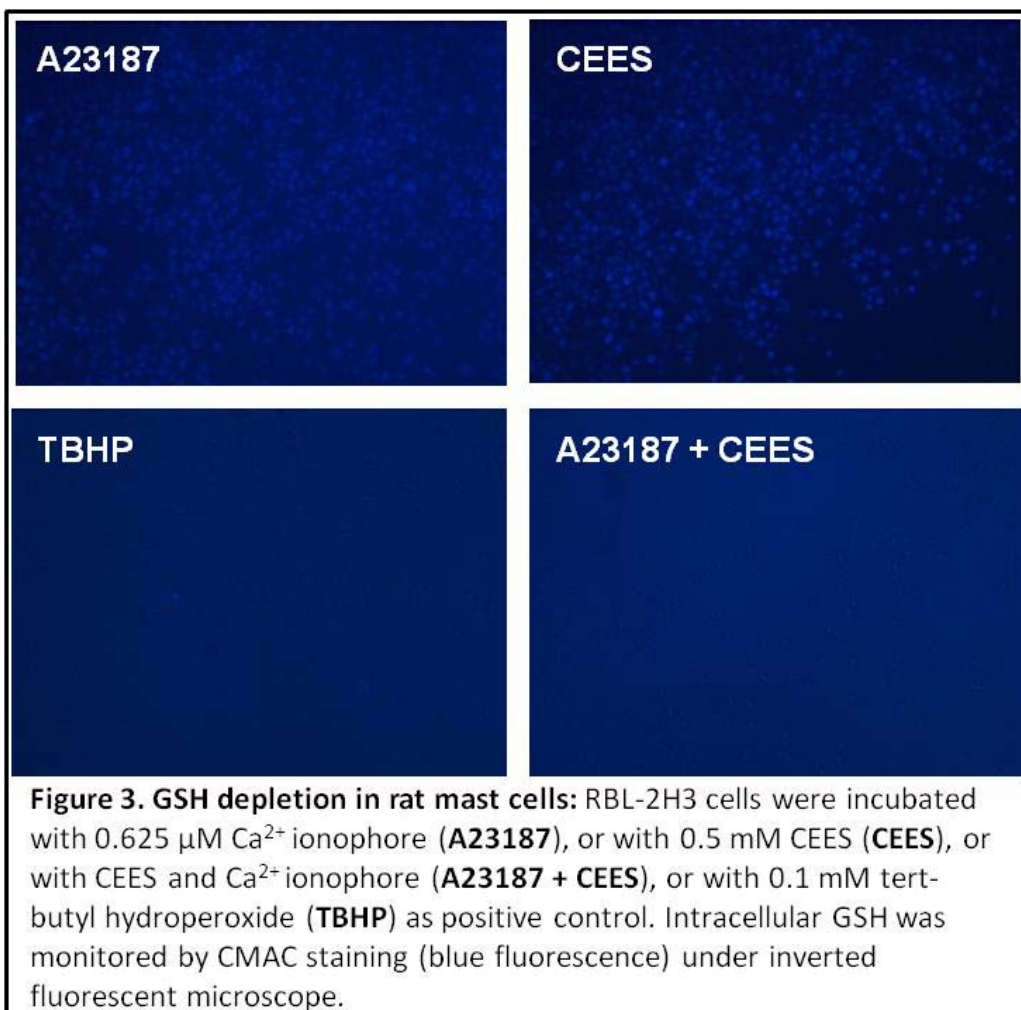


Figure 2. Thiol depletion in rat mast cells: RBL-2H3 cells were incubated with 0.625 μ M Ca²⁺ ionophore (**A23187**), or with 0.5 mM CEES (**CEES**), or with CEES and Ca²⁺ ionophore (**A23187 + CEES**), or with 0.1 mM tert-butyl hydroperoxide (**TBHP**) as positive control. Total cellular thiols were monitored by CMF-DA staining (green fluorescence) under inverted fluorescent microscope.



The results (**Figures 1- 3**) clearly show that combined treatment with CEES and Ca^{2+} ionophore induce massive oxidative stress in rat mast cells as evidenced by free radical production (**Figure 1**), GSH and total thiol depletion (**Figure 3** and **Figure 2**, respectively).

Nitric oxide is known to inhibit mast cell degranulation in various species (Eastmond et al., 1997; Iikura et al., 1998). Therefore, we hypothesized that CEES, by inducing oxidative stress and potentially decreasing NO production, would promote mast cell degranulation. Mast cell degranulation could release large amounts of $\text{TNF-}\alpha$, $\text{IL-1}\beta$, and other inflammatory cytokines, which could enhance the toxicity of CEES/HD.

A colorimetric assay measuring the release of β - hexosaminidase, a component of mast cell granules was used to measure the effect of CEES on degranulation. Degranulation of rat mast cells could not be induced with three different doses of CEES (0.5 mM, 1 mM and 5 mM) whereas the Ca -ionophore A23187 induced 64% degranulation (data not shown). We also determined that pretreatment of the cells with 1 mM CEES for 2 hours before the A23187 stimulation drastically reduced the percentage of degranulated cells when compared with A23187 stimulated cells pretreated with the vehicle only (**Figure 4**). The result was very similar

to another experiment (not shown) in which CEES and A23187 were added to the cells simultaneously.

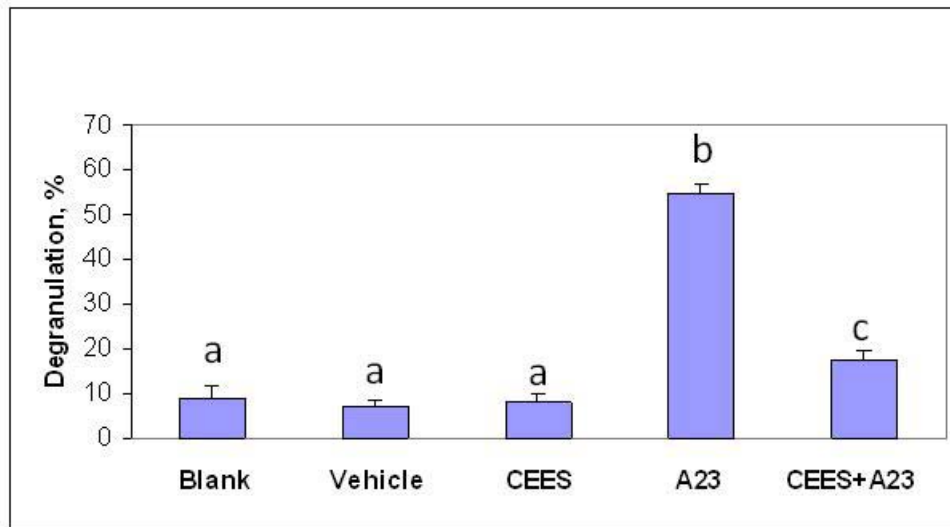


Figure 4. CEES inhibits A-23187-induced mast cell degranulation. RBL-2H3 cells were incubated with 1 mM CEES or 1%EtOH (Vehicle) for 3.5 hours. Blank, no additives. A23, cells were incubated with the vehicle for 2 hours, and then stimulated by additional treatment with 200 nM Ca-ionophore A23187 for 1.5 hour; CEES+A23, cells were pretreated with 1 mM CEES for 2 hours, and then stimulated by additional incubation with 200 nM Ca-ionophore A23187 for 1.5 hour. Mast cell degranulation was measured as β -hexosaminidase release and normalized to the percentage of viable cells (measured in a separate MTT assay). Means not sharing a common letter are significantly different ($P < 0.05$).

Based on the above described experiments **we concluded that toxic doses of CEES impair degranulation in RBL-2H3 rat mast cells.** Initially, we proposed that CEES might stimulate mast cell degranulation since it inhibits the generation of nitric oxide (NO) in RAW 264.7 macrophages (Qui et al., 2006). However, a recent study has shown that endogenous nitric oxide does not modulate degranulation of mesenteric or skin mast cells in rats (Kwasniewski et al., 2003). Alternatively, the rat basophilic leukemia cell line RBL-2H3 represents an immature basophil phenotype and there is some evidence that in this cell line degranulation is not coupled to NO signaling (Koranteng et al., 2000). However, a number of compounds capable of nitric oxide inhibition in RAW 264.7 macrophages also exhibit inhibition of degranulation in RBL-2H3 cells (Seol et al., 2004).

As a next step we further examined the effect of CEES on A23187-induced degranulation and found that experiments in which RBL-2H3 cells were treated with 1 mM CEES and 200 nM A23187 simultaneously produced a marked decrease in cell viability (data not shown), and lower concentrations of CEES and A-23187 also decreased viability suggesting enhanced cytotoxicity (Figure 5). We also found that low levels of CEES did not affect A23187-induced mast cell degranulation (data not shown).

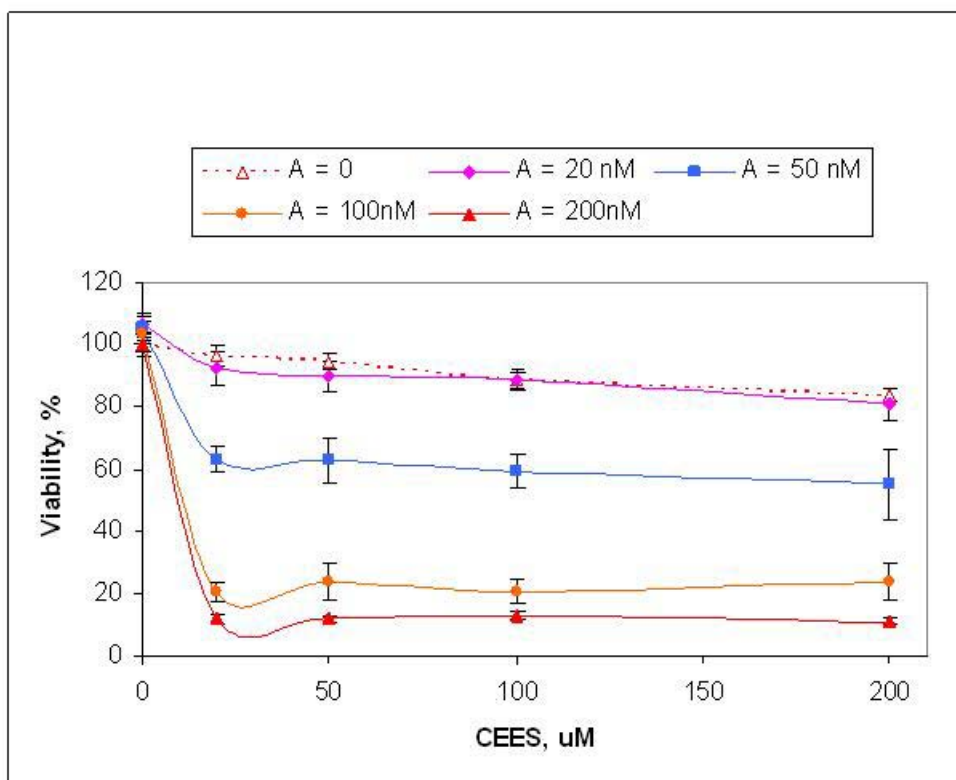


Figure 5. Low levels of CEES ($\geq 25 \mu\text{M}$) combined with A-23187 ($>50 \text{ nM}$) enhance toxicity in RBL-2H3 cells. RBL-2H3 cells were treated with various low levels of CEES and Ca-ionophore A23187 (as indicated) for 24 hours. Both agents were applied simultaneously. Stock solutions of CEES were prepared in ethanol; final concentrations of the vehicles were 1% (vol/vol). Cell viability was measured by the standard MTT assay.

The data support our initial hypothesis that mast cell degranulation (promoted by the Ca-A23187 ionophore) would enhance CEES toxicity.

In the absence of A23187 ionophore, we next found (see Figure 6) that 0.125 mM CEES induced a significant two-fold increase in degranulation in RBL-2H3 cells although the percentage of degranulation was still very low (10% vs. $>25\%$ with A23187 ionophore). The experimental data reveal that CEES at levels greater than 0.125 mM does not promote increased degranulation. Moreover, in the presence of A23187 ionophore, degranulation induced by 0.312 to 0.625 μM A23187 is inhibited at least two-fold when cells are simultaneously treated with 0.5 mM CEES (Figure 6).

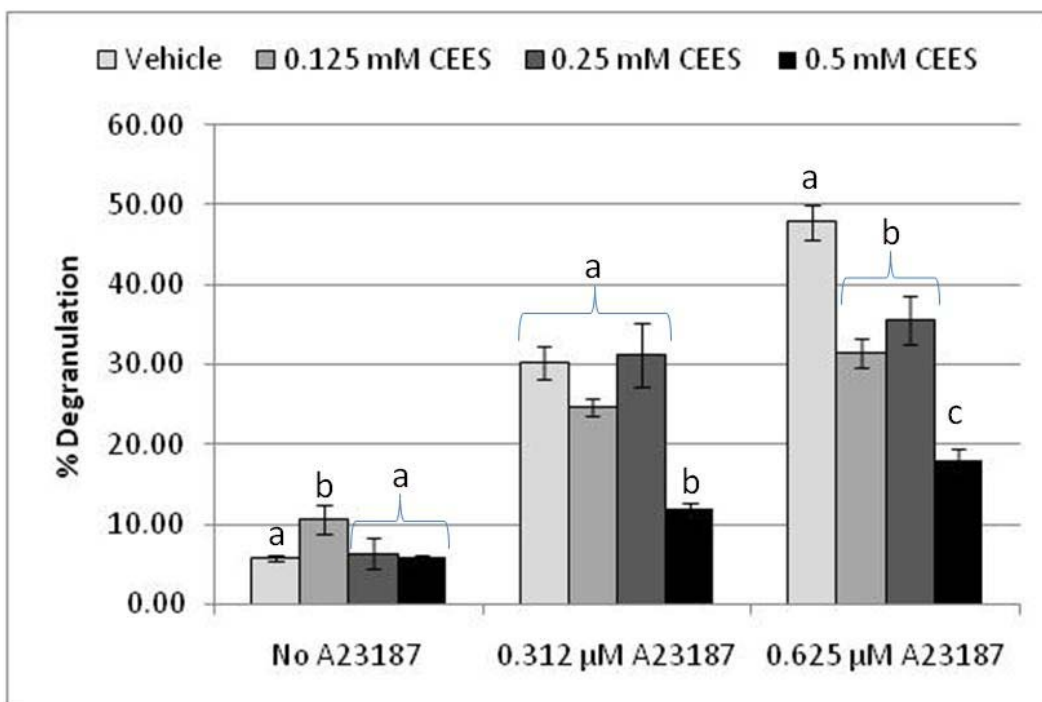


Figure 6. Degranulation of RBL-2H3 cells when simultaneously treated for 1.5 hour with calcium ionophore A23187 (0 to 0.625 μM) and CEES (as indicated). Final concentration of the vehicle (ethanol) was 1.0% (vol/vol). A colorimetric assay was used to measure the release (via degranulation) of β-hexosaminidase, one of the major components of mast cell granules. Degranulation percentage was normalized to cell viability. Cell viability was measured by the MTT assay. Means not sharing a common letter within each group of bars (No, 0.312, or 0.625 μM A23187) are significantly different (P<0.05).

We also compared in RBL-2H3 rat mast cells, the effect of Ca²⁺ ionophore A23187 to the effects of IgE cross-linking antibodies. It is well known that mast cells can be activated for degranulation via cross-linking of anti-dinitrophenol (anti-DNP) Fcε-bound IgE molecules by an IgE-specific antigen (DNP). We found that antibody cross-linking was indeed more effective at inducing degranulation and less toxic to mast cells (data not shown) and therefore included antibody cross-linking to study the effect of CEES on the production of nitric oxide (NO) in mast cells.

Since mast cell degranulation is connected to mast cell NO production, we expected that CEES might reduce NO generation in mast cells stimulated with calcium ionophore A23187. First, we monitored NO generation in RBL-2H3 rat mast cells using specific fluorescent markers 4, 5-diaminofluorescein-2-diacetate (DAF-2 DA) which is specific to intracellular NO. We incubated mast cells for 1.5 hour either with vehicle (1% EtOH), or with 0.5 mM CEES, or with 0.625 μM Ca²⁺ ionophore (A23187), or with CEES and Ca²⁺ ionophore (A23187 + CEES), or with 0.1 mM tert-butyl hydroperoxide (TBHP, induces oxidative stress) as positive control. Then the cells were stained with the DAF-2 DA fluorescent dye for 20 min, examined under an inverted fluorescent microscope equipped with standard FITC filter and photographed digitally. We were unable to register NO generation with DAF-2 DA staining, likely due to the short incubation time or low levels of NO produced (data not shown). We then measured the amount of nitrite accumulation

in the cell medium using a sensitive fluorescent substrate, 2,3-diaminonaphthalene (DAN). We found that mast cells released very low NO levels into the cell medium but that NO production in RBL-2H3 cells was stimulated with increasing levels of A23187, i.e., 1.25 μ M A23187 showed an approximately five-fold increase in NO production compare with 0.5 μ M A23187 (**Figure 7**). CEES did not, however, dramatically alter the levels of nitrite accumulation in marked contrast to the results we observed with RAW 264.7 macrophages.

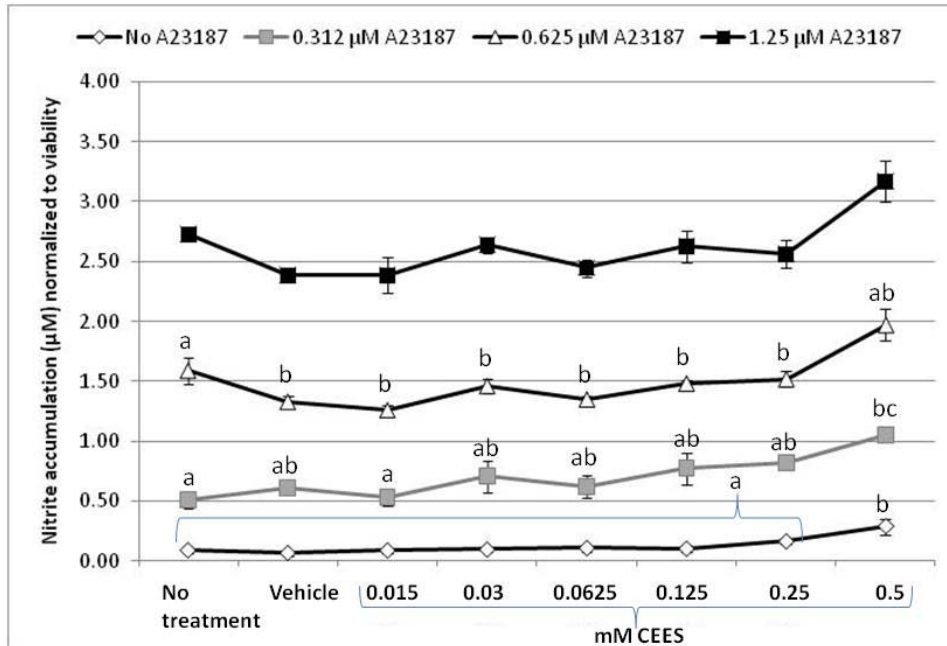


Figure 7. NO generation in RBL-2H3 cells treated with various levels of CEES and stimulated with the calcium ionophore A23187 (as indicated). NO generation was measured as nitrite accumulation in media and normalized to the percentage of viable cells (measured separately by the MTT assay). RBL-2H3 cells were exposed to various levels of CEES (as indicated) in the absence or presence of calcium ionophore A23187 (0 to 1.25 μ M) for 22 hours. Nitrite accumulation was measured using the substrate 2,3-diaminonaphthalene. Final concentration of the vehicle (ethanol) was 1.0% (vol/vol). Means not sharing a common letter within a specific A23187 concentration (0, 0.312, 0.625, or 1.25 μ M A23187) are significantly different ($P < 0.05$).

We also addressed whether the effect of CEES on mast cell degranulation involved endogenous NO generation (in addition to the oxidative stress). Direct measurements of NO accumulation products in cell media did not show useful results because the level of NO in the mast cells remained relatively low (**Figure 7**). We reasoned that if induction of degranulation (using Ca^{2+} ionophore A23187 or IgE cross-linking) is dependent upon endogenous NO levels, a NOS inhibitor would affect the level of degranulation. Experiments inhibiting the production of NO using L-NAME, a specific NO synthase (NOS) inhibitor, provided no useful results (data not shown) most likely because L-NAME decreased mast cell viability (data not shown). We also treated RBL-2H3 cells with tetrahydrobiopterin (BH_4), an essential co-factor in NO formation, or with gamma interferon ($\text{INF-}\gamma$), a cytokine that upregulates the production of NO. Neither BH_4 nor $\text{INF-}\gamma$ increased the production of NO in RBL-2H3 cells (data not shown).

Koranteng et al. (2000) determined that the phenotypic response to INF- γ is dependent on the maturity level of the individual mast cell line. The RBL-2H3 cell line has an immature basophil phenotype and is not likely to be responsive to inducers that upregulate NOS expression. Since we could not increase the level of endogenous NO in RBL-2H3 mast cells, we then asked whether RBL-2H3 cells would respond to an exogenous source of NO. To increase the level of exogenous NO, we used 2,2'-(hydroxynitrosohydrazino)bis-ethanamine (NOC-18), chemical compound that spontaneously releases NO in solution in a rate-controlled manner. Davis et al. (2004) have found that NOC-18 inhibits degranulation in RBL-2H3 cells. We found that 0.25 mM NOC-18 increased NO level in the culture medium up to 40 fold up (data not shown) but also lowered cell viability to 60% (data not shown). However, IgE induced degranulation in RBL-2H3 cells was not significantly affected by NOC-18. Also, NOC-18 did not alter degranulation in the presence of 0.25 mM CEES (**Figure 8**).

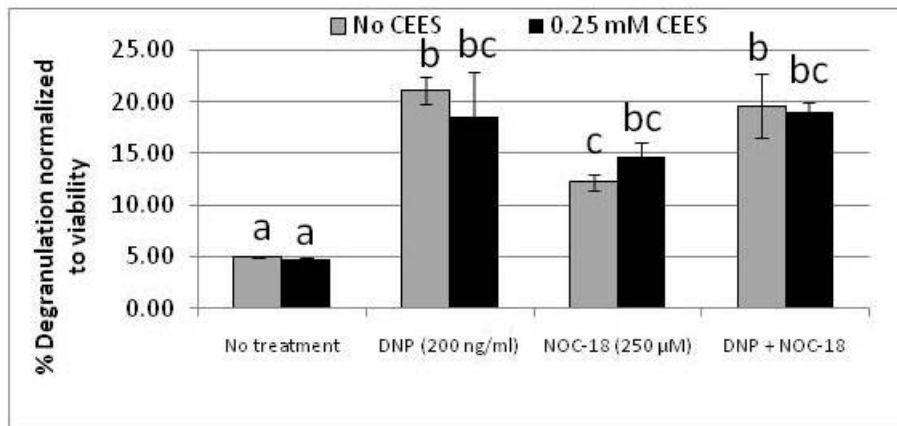


Figure 8. Effect of NOC-18 and CEES on rat mast cell degranulation: RBL-2H3 cells were incubated in the presence or absence of 0.25 mM CEES (as indicated) for one hour and then pretreated with IgE with or without **250 μ M NOC-18** (as indicated) for 18 hours. Cells were then treated with medium with no additives (**no treatment**) or with DNP (**DNP 200 ng/mL**). **DNP+NOC-18**, cells pretreated with NOC-18 and treated with DNP. Percentage of degranulated cells was measured after 40 min by the β -hexosaminidase assay and normalized to cell viability measured separately by the standard MTT assay after 40 min. Means not sharing a common letter are significantly different ($p \leq 0.05$).

It is likely that we did not observe an effect of NOC-18 on RBL-2H3 degranulation due to the toxic dose of the NO producing agent. However, even lower doses of NOC-18 were found to reduce viability (data not shown).

To summarize, we found that CEES drastically enhanced Ca^{2+} ionophore toxicity in mast cells and also inhibited mast cell degranulation. It is very likely that both these effects are due to the oxidative stress. **Thus, antioxidants like NAC, GSH, and vitamin E should be protective in mast cells treated with CEES or CEES and Ca^{2+} ionophore.**

II. Utilize redox proteomics to determine how CEES (or HD/pathogen) treatment influences changes in the levels and distribution of oxidized proteins using either *in vitro* cellular studies (mast cell lines and human Epiderm skin samples) or the *in vivo* animal models (animal tissue samples snap frozen in liquid nitrogen) obtained from other members of the Mustard Consortium.

In our previous published work, we reported that lipopolysaccharide (LPS) was capable of enhancing the cytotoxic effects of CEES. We found that murine RAW264.7 macrophages treated with LPS and CEES show a cytotoxicity that is partially blocked by polymyxin B, an antibiotic capable of binding and blocking the action of LPS (Stone et al., 2003). **These data suggest that non-toxic polymyxin B derivatives (such as polymyxin B nonapeptide) could be useful in minimizing the toxicity of mustard gas.**

The Effect Of Liposomes On Rat Lung Tissues

We also used 2D gel electrophoresis (2D-GE) to analyze rat lung tissue samples (snap frozen in liquid nitrogen) provided by USAMRICD. Prior to lung harvest, these animals had been exposed to CEES or HD and/or treated with antioxidant-liposomes prepared in our laboratory (“Stone” liposomes) or prepared in Dr. Ward’s laboratory (“Ward” liposomes) as well as “blank” liposomes containing no antioxidants. We completed the first phase of this study in which we evaluated the potential influence of blank liposomes (not containing any antioxidants) or antioxidant liposome treatment on the levels and distribution of proteins in rat lung tissue.

Figure 9 shows the results from these analyses. Four gels per sample were simultaneously run under identical conditions in order to minimize differences resulting from experimental variations. The replicate gels were aligned by the Dymension-2 software so that consensus spots could be “warped” together. The spots were then detected and 856, 785 and 914 consensus spots were detected in the Blank, Stone and Ward samples respectively. It should be noted that the differences in the number of consensus spots between the different samples does not always mean differences resulting from the different treatments. It can result from differences in the number of permitted absences (spots that are detected even though they are absent in a set number of gels per sample) or the detection of artifacts. The consensus spots from the three samples were then aligned and matched. A total of 819 matching spots resulted. We found no differences in protein expression between the three different treatments, i.e., **antioxidant-liposomes do not induce any changes in protein expression compared to blank-liposomes.**

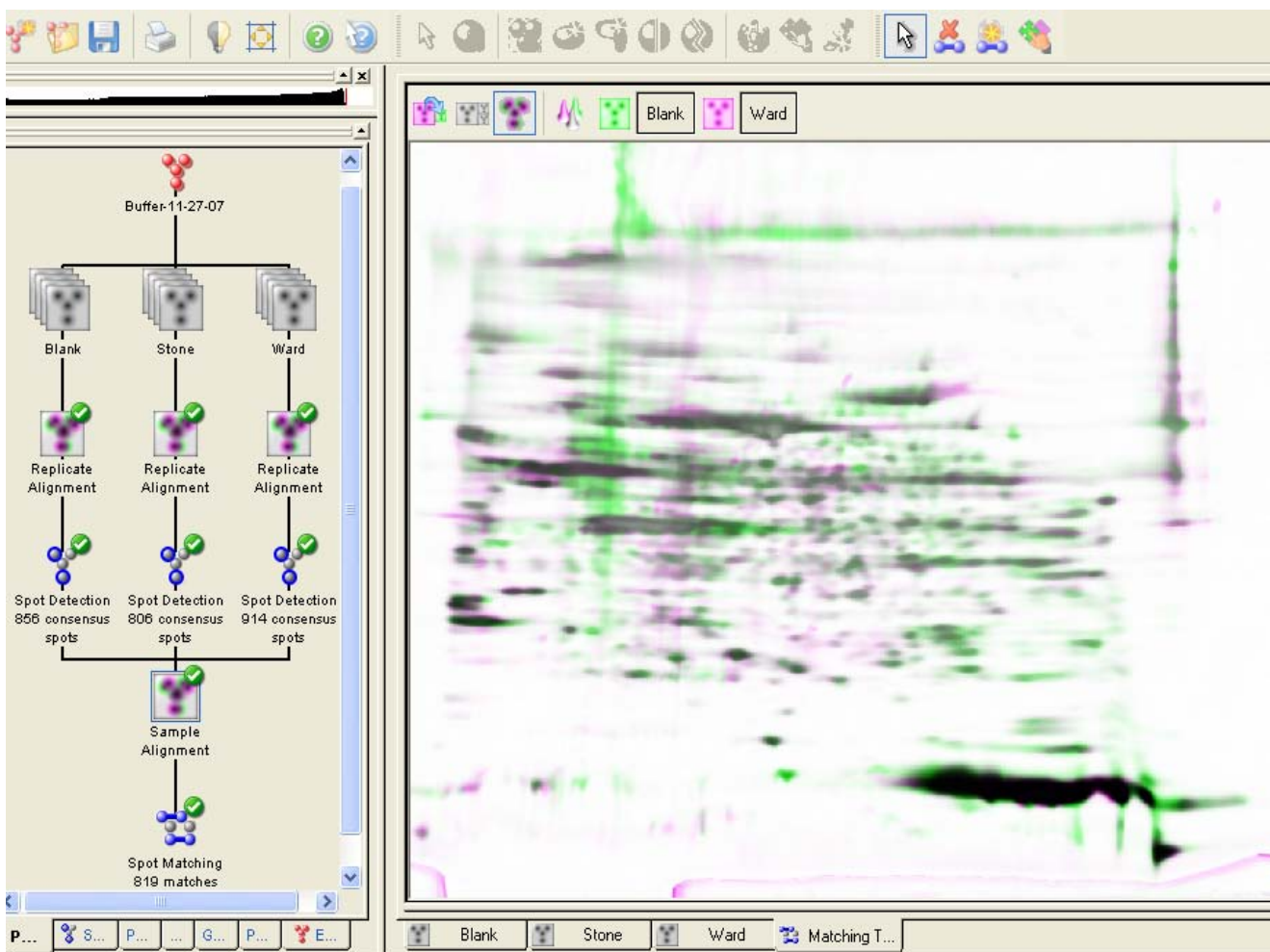


Figure 9. Proteomics Study of the effect of Antioxidant Liposomes in Rat Lung. Frozen tissues samples of rat lungs treated with “Stone” liposomes, “Ward” liposomes or “Blank” liposomes (contain no antioxidants) were obtained from our collaborators. Cell lysates were separated by 2D-GE, silver-stained and photographed (three gels per sample). Average differences in protein expression were quantified with Dymension-2 Software. Left panel shows the software sequence for the image comparison and number of consensus spots for each sample and for the final matching. Right panel shows the aligned image for the “Ward” and “Blank” samples (“Stone” sample showed similar result).

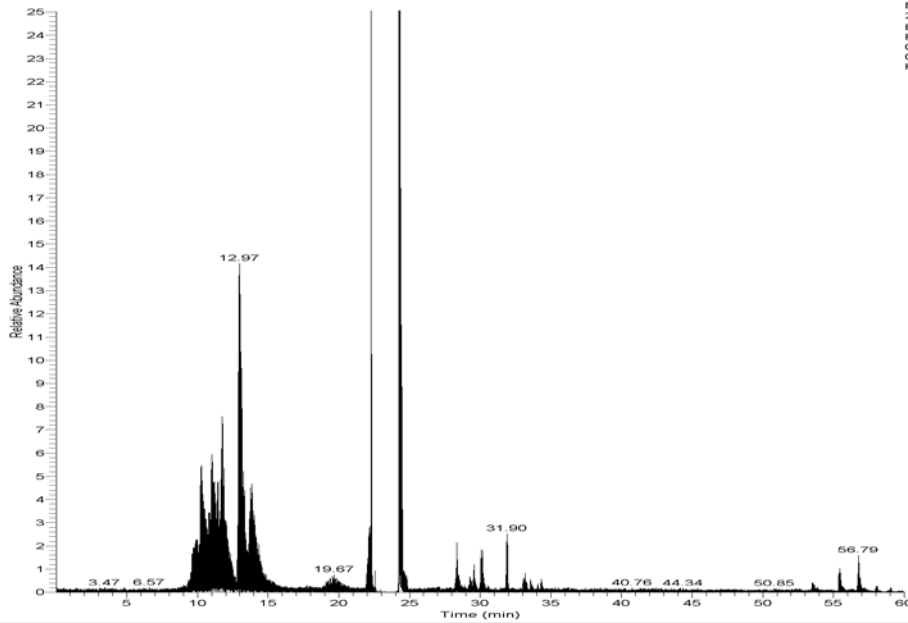
Determination Of HD Induced Post-Translational Modifications In Cellular Proteins From Rat Lung Tissues By Mass Spectrometry

It has been shown that HD exposure causes specific alkylation in various proteins (Noort et al., 2008; Noort et al., 1997; Yeo et al., 2008). We sought to confirm whether it would be possible to find alkylated amino acid residues in the abundant proteins from rat tissues exposed to HD. Rat lung tissues, treated with HD or not treated (100 µg total protein each) were homogenized in the SDS PAGE Sample Buffer and separated on a 4-20% gradient gel. The most abundant protein spot (about 70 kDa) was excised from the gel, destained, trypsinized, and resulting peptide mixtures analyzed using nanospray LS/MS on our LTQ Linear Ion Trap Mass Spectrometer

(Thermo-Fisher). Raw LC/MS data obtained from the mass spectrometer were analyzed with BioWorks 3.3 software (Thermo-Fisher) in order to determine the best matches to all possible tryptic peptides as determined from a recent UniProt 100 protein database.

The most abundant protein in both HD treated and untreated sample was albumin; it was identified with 54% coverage by amino acid residues (**Figure 10**). Albumin was present in the lung tissues since they were not perfused to remove blood proteins before storage. During the SEQUEST analysis with BioWorks software, we searched for the alkylated and oxidized peptides: all H, E, D, C, V, N, Q, K, R and W residues we searched for the addition of a $\text{CH}_2\text{CH}_2\text{SCH}_2\text{CH}_2\text{OH}$ radical to a side chain (104.03 a.e.m. monoisotopic mass addition): all M, C, F, Y, H, K, and W residues we searched for the addition of OH radical to a side chain (15.995 a.e.m. monoisotopic mass addition).

We found one tryptic fragment with both modifications – YNEVLTQCCTESDK. In this peptide, both C residues were oxidized, and the second E residue was alkylated (**Figure 11**): 16 out of 26 Y and B fragment ions were found with high probability level (peptide score $S_f=0.74$). Notably, the modified peptide was found only in the HD treated sample; in the control sample only the unmodified peptide was detected (data not shown). **This example shows that alkylated and/or oxidized proteins can be successfully identified in the tissue samples of HD treated animals.**



NL
2.18E7
Base Peak
F: MS
04-27-
09_rat_tiss+
HD

Reference: gi|19705431|ref|NP_599153.1| albumin [Rattus norvegicus]
Database: C:\local\lib\database\rat_ref.fasta
Number of Amino Acids: 608 Molecular Weight: 66675.0 pI: 6.06



Protein:

MKWTFPLLL FISSGAFSRG VFRREAHKSE IAHFPRDLGE QHFKGLVLA
FSQYLKQCPY EHHIKLVQEV TDFACTVAD ENAENCKEII HTLEFDKLCQ
EPRKIKVYK LAKNCAKQSD EREKCFIQRH DIRMFLPEQ RREARAKTSS
EQRIPTSPFLG HYLHEVAIRH PFFYAPRLLY YARKYNEVIT QCCTESDKAA
CLTPELRVK EKALVAARVQ RREKSRKQF GRATFAVAV RMRGKFFMA
EFAEITKLAT DVTKINKKCC HSDLLECADD RAELAKYKCE NQATISSKIQ
ACCDKVFQK SQCLAEIHD NEDADLPIA ADFVEDKVC RNYARADVF
LGTFLVEYR RHHYFVLLI LRLAKYKAT LRKCCGKDF RACTGVYLA
EQFLVEEKN LVPTNCELYE KGEYGFQNA VLRYTQAP QVSTFLVKA
ARHLGVYTK CCLTPEAQL ECVYEDLRI LRLGVYIEK TVYSEYVTC
CGSLVEEAP CFSALTYDET VYVKEFPAET FTTHSDICTL DDEKCKIKG
TALAEIVQK EIGATEDQLT VGGDFAGVQ KCTHADKDH CFATEGPNLY
ARSEKALA

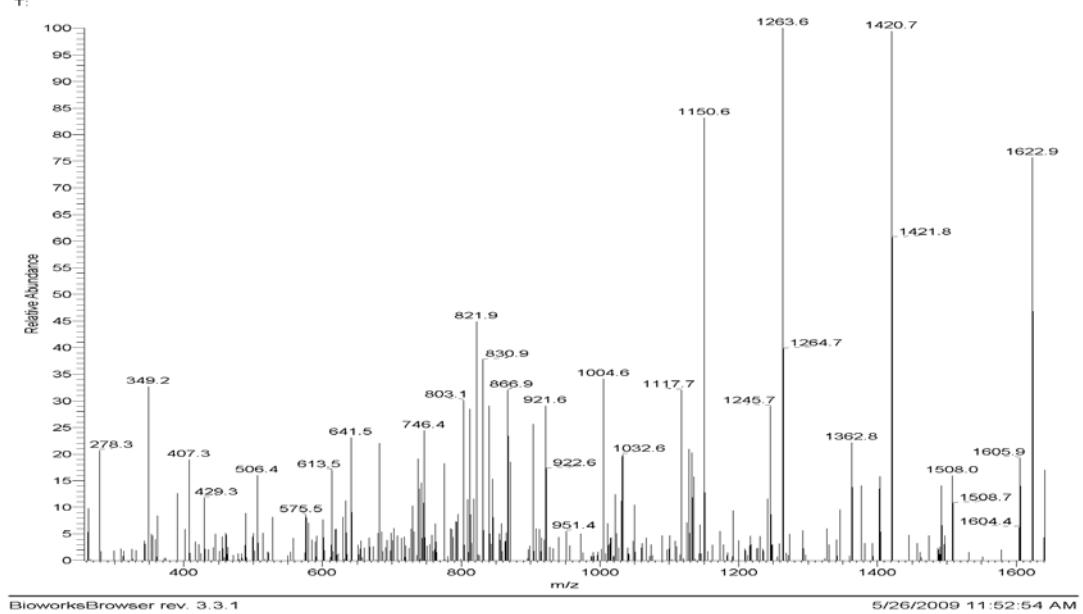
Protein Coverage:

Sequence	MS+	% Mass	AA	% AA
FKDLGEQHFK	1240.64	1.82	35 - 44	1.64
DIGGQHK	973.47	1.42	37 - 44	1.32
GLVLIAPSOYLK	1479.86	2.15	45 - 57	2.14
CYEEIK	1018.47	1.48	58 - 65	1.32
LVQEVDFAK	1149.62	1.67	66 - 75	1.64
TCVADAEKNDK	1411.85	2.04	76 - 88	2.14
QKPEKNCFLQMK	1657.78	2.41	110 - 130	2.14
NKCFLQK	1018.48	1.48	123 - 130	1.32
RHHYFADLRYIAEK	2060.03	3.00	169 - 184	2.63
HPFYAPRLYYIAEK	1903.93	2.77	170 - 184	2.47
YHEVLCCTESDEK	1432.69	2.38	185 - 198	2.30
LDAVK	545.33	0.79	206 - 210	0.82
ALVAAR	699.45	1.02	213 - 219	1.15
EKKK	508.25	0.74	230 - 233	0.66
ANVAAR	673.38	0.98	237 - 242	0.99
EFNAEFAEITK	1246.64	1.84	247 - 257	1.81
LATDVTK	747.42	1.09	258 - 264	1.15
ECKHGLLECAADRAELAK	2090.89	3.04	268 - 286	3.13
YKCNQATISSK	1374.80	2.00	287 - 298	1.97
EQACDKVQK	1345.70	1.96	299 - 310	1.97
SQCLAEIHDNIPADLSIAADFVDEK	2928.36	4.28	311 - 337	4.44
RYIAEK	1495.24	2.12	342 - 347	0.99
DVFLGTFLYEYR	1609.79	2.34	348 - 360	2.14
RHHYFVLELLR	1455.81	2.12	361 - 372	1.97
RHHYFVSLR	1298.71	1.89	362 - 372	1.81
KVEATLEK	981.53	1.43	376 - 383	1.32
CCMGDFACVGVYLAERFPLVEDEK	2766.25	4.03	384 - 409	4.28
NLYK	473.31	0.69	410 - 413	0.66
TNCELYK	999.45	1.46	414 - 421	1.32
LGEYGFQNAVLIR	1465.78	2.13	422 - 434	2.14
APQVSTFLVKAAR	1439.79	2.10	439 - 452	2.30
NLYK	459.27	0.67	453 - 456	0.66
VQTK	404.25	0.59	457 - 460	0.66
CCLTPEAQR	1020.46	1.49	461 - 469	1.48
LPCVVDYLSALLR	1605.83	2.34	470 - 483	2.30
LCVLEK	841.46	1.23	484 - 490	1.15
TFVEEK	660.36	0.96	491 - 496	0.99
CGSELYEYR	953.42	1.39	500 - 508	1.48
RPCFSALTYDETYVPIK	1825.92	2.66	509 - 524	2.63
AEYTFHSDICTLPEK	1824.85	2.66	525 - 543	2.63
AEYTFHSDICTLPEK	2081.98	3.03	526 - 545	2.96
ATFDQLK	804.41	1.17	563 - 569	1.15
TVYKIDFAGVDEK	1267.65	1.88	570 - 581	1.97
AADKDNCFATEGPNVLAAR	1891.90	2.75	585 - 602	2.96
Totals:	36962.72	53.81	328	53.95

Figure 10. Identification of albumin in the rat lung tissue: Nano-chromatogram of the tryptic peptide mixture of albumin containing protein spot from HD-treated rat lung tissue lysate (top panel); protein coverage for the albumin tryptic peptide mixture LC/MS analysis (bottom panel).

File: C:\Xcalibur\data\04-27-09_rat_tiss+HD.RAW
 Enzyme: Trypsin(KR) (2)
 Peptide mass: 1766.91 (± 2.500 peptide, 1.000 fragment)
 Charge: 2
 Activation type: CID
 Mass type: mono
 Search information: 04/29/2009, 03:54 PM., 1.7 secs on ETSU903666
 Database: rat_ref.fasta

04-27-09_rat_tiss+HD #1842 RT: 22.189 NL: 3.17E2



DTA for peak 1842
 Precursor: Ions 894.96
 Mass: 1766.91 mono
 Mod: 01 (C* +57.02146) (HEDCVNQGRW# +104.02960) (HCFYVGRB# +15.99490)

Ion series for charge: +1

AA	A ions	B ions	B* ions	Bo ions	C ions	Y ions	Y* ions	Yo ions	Z ions
Y		364.07							
N		278.31				1605.64			
K		407.16				1491.60			
V		506.22				1362.56			
L		613.32				1263.49			
T		720.36				1150.41			
C		821.42				1049.36			
CP		921.42				921.30			
Q		1032.42				802.30			
T		1150.47				683.29			
E#		1420.54				562.24			
S		1507.57				349.17			
D		1622.60				262.14			
K						147.11			

Figure 11. Determination of the alkylated/oxidized amino-acid residues in the albumin: MS/MS spectra of the YNEVLTCCTESDK albumin fragment (top panel); list of the Y and B ions for the YNEVLTCCTESDK albumin fragment; E#, alkylated glutamic acid residue; C@, oxidized cysteine residue (bottom panel); matched Y and B ions form the MS/MS spectra (top panel) are shown in bold (bottom panel).

The Effects of CEES on the EpiDerm™ Skin Proteomics

In addition to the frozen tissue samples supplied by USAMRICD, we generated a set of fresh cellular lysate samples obtained from EpiDerm skin samples which are an *in vitro* human epidermal model extensively used in toxicology studies. The EpiDerm™ model consists of normal, human-derived epidermal keratinocytes (NHEK) which have been cultured to form a multilayered, highly differentiated model of the human epidermis.

The EpiDerm tissues were treated (or not) with 2.5 mM CEES in the presence or absence of antioxidant liposomes containing reduced glutathione (GSH). Our experiments reported at the Bioscience Review 2008 Meeting (See Bioscience Review 2008 Poster “**The Protective Effect of Antioxidant Liposomes in a Human Epidermal Model Exposed to a Vesicating Agent in Appendix**”), showed that GSH-liposomes increased the viability of keratinocytes (within EpiDerm) exposed to CEES.

We also studied the potential alterations in protein expression due to CEES exposure but restored (fully or partially) by GSH-liposome treatment using 2D-GE. In this experiment, total protein samples from the cellular lysates were separated by the 2D-GE technique and quantitated by using the Dymensions Two software. In order to document only significant differences, each sample was run three times (i.e., three separate 2-D-GE runs) and the resulting images then averaged. **Figure 12** shows differences in the protein expression in EpiDerm due to CEES exposure (red circles) and the differences affected by the GSH-liposomes (green circles). **Table 1** shows the quantitative differences in protein expression for the types of sample (vehicle, CEES, and CEES+GSH-liposomes). In order to perform an LC/MS identification of the proteins, we first tested the experimental procedure by analyzing an abundant protein spot from the sample treated with vehicle and separated on 2D-GE gel. The targeted spot was extracted from the gel, stripped from the silver stain, trypsinized, and resulting peptide mixtures were analyzed using nanospray LS/MS on our LTQ Linear Ion Trap Mass Spectrometer (Thermo-Fisher). The spot appeared to contain three merged protein spots. The three merged spots were, however, unchanged by treatment with CEES or antioxidant liposomes. Raw LC/MS data obtained from the LTQ XL mass spectrometer were analyzed with BioWorks 3.3 software (Thermo-Fisher) in order to determine the best matches to all possible tryptic peptides as determined from a recent UniProt protein database (**Figure 13**).

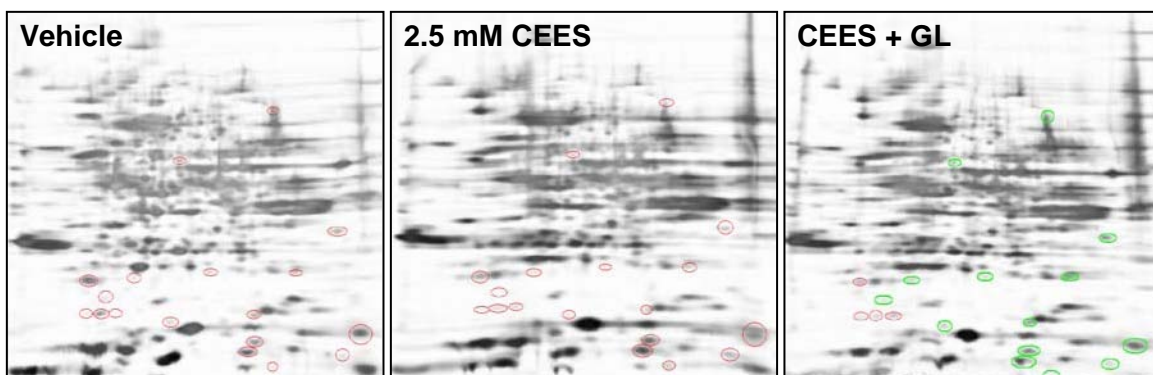


Figure 12. Proteomics Study of CEES toxicity and the effect of GSH-Liposomes in EpiDerm.

Tissues were exposed to vehicle or 2.5 mM CEES in the absence or presence of GSH-liposomes for 18 h. Cell lysates were separated by 2D gel electrophoresis, silver-stained and photographed (three gels per sample). Average differences in protein expression were quantified with Dymension-2 Software. The proteins differentially expressed after CEES exposure are marked with red circles. The proteins, which expression was partially reversed by GSH-liposomes are marked with green circles.

Table 1 Quantitative differences in protein expression in EpiDerm, CEES toxicity and the effect of GSH-Liposomes

The differences are expressed as average 2D-GE protein spot volume ratios normalized to "Vehicle" samples. Vehicle, exposed to 1% EtOH; CEES, exposed to 2.5 mM CEES; CEES+GL, exposed to CEES and GSH-liposomes simultaneously. Positive values mean that the proteins are up-regulated, negative values mean that the proteins are down-regulated.

Spot	MW (kDa)	Volume Ratio		
		Vehicle	CEES	CEES + GL
1	50.6	1	-3.935	-1.322
2	34.1	1	-2.827	-1.049
3	28.3	1	-1.739	1.174
4	19.5	1	-2.92	-1.224
5	13.4	1	-3.186	-1.403
6	12.2	1	-2.02	1.068
7	11.7	1	1.657	-1.028
8	11.3	1	-1.591	-1.198
9	10.8	1	-2.095	-1.465
10	10.2	1	1.731	-1.219
11	9.3	1	1.761	-1.323

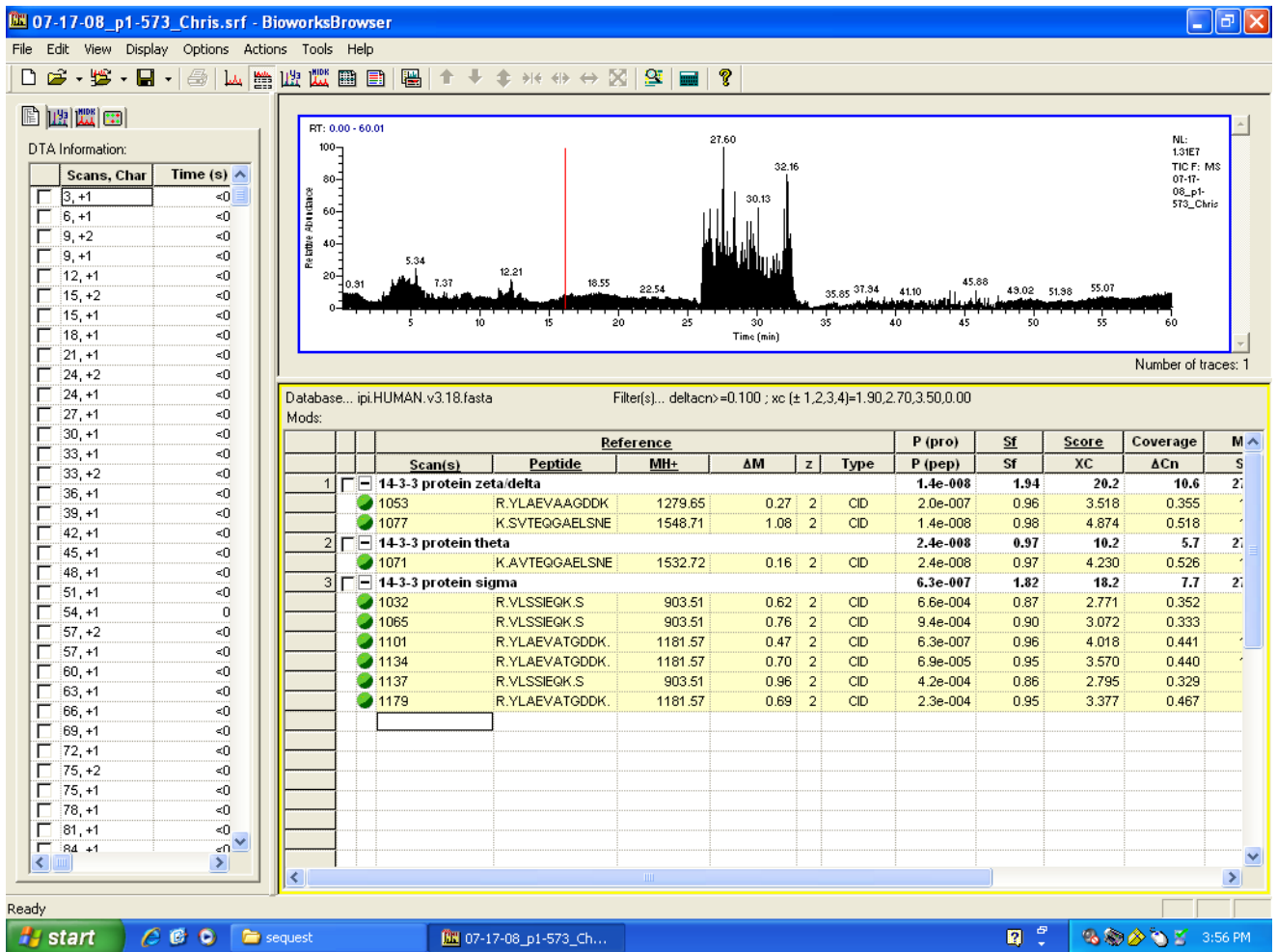


Figure 13. Identification of a set of three proteins from a 2D-GE gel spot (SEQUEST search result). A targeted protein spot from silver stained gel was extracted, destained, and digested by trypsin. Resulting mixture of tryptic peptides was analyzed by LS/MS on the LTQ XL mass spectrometer. Raw data (see the chromatogram at the top right panel) were further analyzed with BioWorks 3.3 software (Thermo-Fisher) in order to determine the best matches to all possible tryptic peptides as determined from a recent UniProt protein database. Computer screen above shows the result of the SEQUEST protein search. Three highly homologous proteins were identified with a high level of significance (see the bottom right panel).

The database search (**Figure 13**) revealed the presence of three highly homologous (97%) human proteins, which belong to the 14-3-3 family of regulatory proteins. The **14-3-3 protein sigma** (Stratifin or Epithelial cell marker protein 1) is an adapter protein implicated in the regulation of a large spectrum of signaling pathways. It binds to a large number of partners, usually by recognition of a phosphoserine or phosphothreonine motif. The binding generally results in the modulation of the activity of the binding partner. The main function is p53-regulated inhibition of G2/M progression.

The **14-3-3 protein theta** (or tau, or Protein HS1) is a negative regulator of transcription. It is involved in the protein kinase C signaling pathway. The **14-3-3 protein zeta** (also known as 14-3-3 delta (a phosphorylated form of 14-3-3 zeta); D14Abb1e; KCIP-1; Tyrosine 3-monooxygenase/tryptophan 5-monooxygenase activation protein, zeta polypeptide; Ywhaz) is another transcription factor involved in the protein kinase C signaling pathway interacting with various serine/threonine protein kinases. It is also an activator of tyrosine 3/tryptophan 5 – monooxygenase.

In skin tissues, it is likely that the **14-3-3 protein zeta** is involved in the synthesis of melanin from tyrosine. **This protein has not, to our knowledge, been identified in human skin and it would be important in preventing skin cancers resulting from prolonged exposure to strong sun light (relevant to military personnel serving in desert environments).**

We attempted LC/MS identification of more of the proteins from the spots that were silver stained in the 2D-GE samples of EpiDerm (**Figure 12**), but due to the low yield of total protein in the Epiderm lysates, the LC/MS/MS analysis of the targeted spots did not allow protein identification. Therefore, we repeated the study using human keratinocytes in order to obtain more concentrated samples. We grew large batches of human keratinocytes (2×10^6 HaCaT cells) and treated them with vehicle (1% DMSO) or with CEES (0.5 mM and 2.5 mM). After an 18 hour incubation cell lysates were separated by 2D-GE and stained with Coomassie Blue (an MS friendly stain). CEES exposure at 0.5 mM did not reveal any significant differences in the protein expression whereas 2.5 mM CEES exposure showed a number of differences. **Figure 14** and **Table 2** show the differences in the protein expression in HaCaT cells due to CEES exposure (circled). In this experiment, total protein samples from the cellular lysates were separated by the 2D-GE technique and quantitated by using the Dymension 2D software.

In order to document only significant differences, each sample was run three times (i.e., three separate gels per sample) and the resulting images then averaged. A few of the targeted proteins were extracted from the gel, stripped from the Coomassie stain, trypsinized, and resulting peptide mixtures analyzed using nanospray LS/MS on our LTQ Linear Ion Trap Mass Spectrometer (Thermo-Fisher), but no data was obtained. We re-examined our method and discovered that the pH of the trypsin digestion buffer was too low (pH of 6.5). We are planning to repeat these experiments using a higher pH (pH 7.5 – 8.0) trypsin digestion buffer.

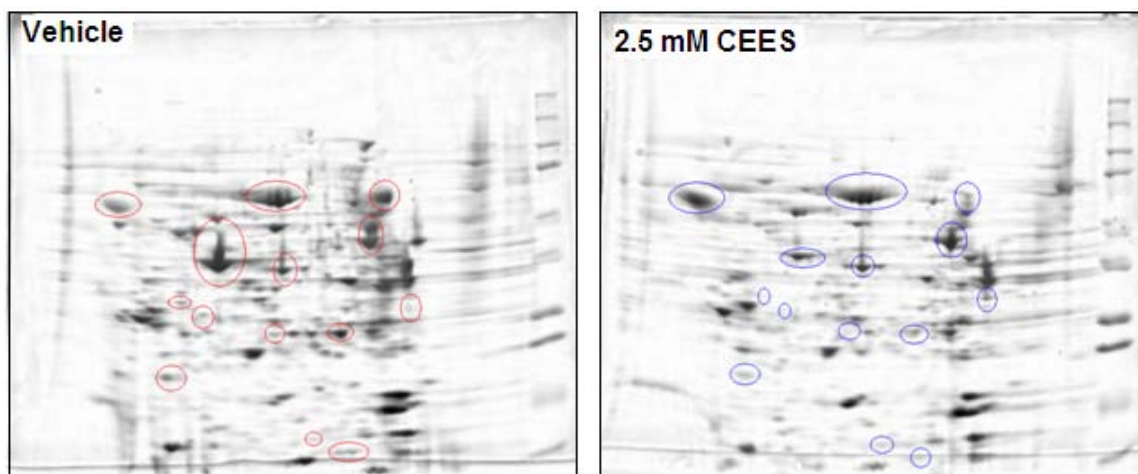


Figure 14. The effect of CEES on Human Skin Proteomics: HaCaT cells were exposed to vehicle (1% DMSO) or 2.5 mM CEES for 18 h. Cell lysate was made and separated by 2D gel Electrophoresis. The resulting gels were stained with Coomassie blue dye and digitally scanned. The images were analyzed using Dymension 2D software (Syngene). The areas circled with red or blue are the representative spots that showed maximum differential expression.

Table 2. Quantitative differences in the EpiDerm protein expression

The differences (see **Figure 12**) for the samples exposed to 2.5 mM CEES are expressed as average 2D gel protein spot volume ratios normalized to Vehicle samples. Positive values show that the proteins are up-regulated, negative values show that the proteins are down-regulated.

Spot No. on Gel	Volume Ratio	MW (Da)	pI
120	-2.667	94118	4.475
141	-2.609	91623	6.325
198	-8.655	77295.5	7.510
201	7.603	75224.5	4.790
211	2.064	74390.0	5.535
212	-3.128	72387.0	5.825
213	7.167	73658.5	4.580
229	-2.743	69236.5	7.545
234	3.386	67468.0	9.295
242	-3.186	65383.0	6.685
243	5.603	65296.0	4.250
280	-5.949	57880.0	8.400
281	4.806	55714.5	3.900
290	-8.482	55692.5	6.860
291	-2.898	55359.0	6.000
294	-3.394	53868.0	7.400
296	-6.397	53730.0	5.330
304	-6.026	51680.0	5.620
326	-7.167	48914.0	8.425

370	-5.725	42101.5	7.060
371	2.888	41829.5	7.920
391	-3.888	39795.0	5.665
392	-3.288	40349.5	6.095
394	-5.929	40547.0	3.510
396	-3.703	40132.0	5.425
435	-3.805	34590.5	3.485
464	-6.594	31618.0	7.940
474	-3.200	31442.5	5.130
482	2.773	30267.5	4.395
612	-2.526	19808.0	7.420
621	-2.414	19098.0	8.260
624	-5.189	18791.0	9.755
625	2.623	18602.0	6.505
640	2.651	18028.5	4.900
696	-5.916	13365.5	7.030

The Effects of CEES on RBL-2H3 Proteomics

We found that RBL-2H3 mast cell viability decreases down to about 20% at CEES concentrations between 1.0 mM – 2.5 mM. In order to study the most prominent differences in protein expression induced by CEES/HD exposure, we compared the proteomics of non-treated mast cells and cells treated with 2.5 mM CEES. RBL-2H3 cells incubated with vehicle (1% DMSO) or treated with 2.5 mM CEES were lysed with 0.1% Triton X-100 solution in PBS by shaking on ice for 30 min. The cell lysates (100 µg total protein each) were separated by 2D-GE. The gel images were analyzed quantitatively by the Dymension 2D software (Syngene). **Figure 15** and **Table 3** show differences in the protein expression in RBL-2H3 mast cells due to CEES exposure. In this experiment, each sample was run in duplicate (i.e., two separate gels per sample) and the resulting images averaged.

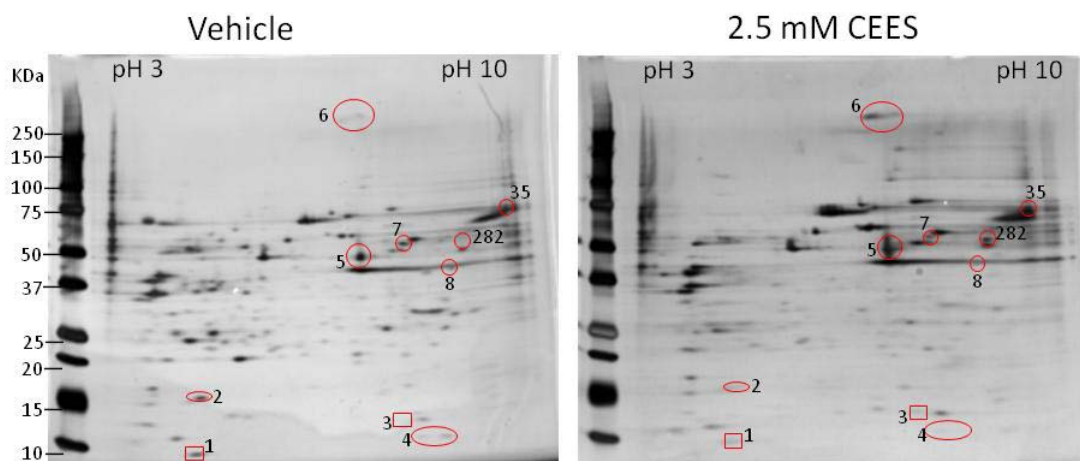


Figure 15. The effect of CEES on rat mast cell proteome: RBL-2H3 cells were exposed to vehicle (1% DMSO) or 2.5 mM CEES for 18 h. Cell lysates were made and separated by 2D-GE. The resulting gels were stained with silver stain and digitally scanned. The images were analyzed using Dymension 2D software (Syngene). The areas circled with red are representative spots that showed differentially expressed proteins.

Table 3. Quantitative differences in protein expression

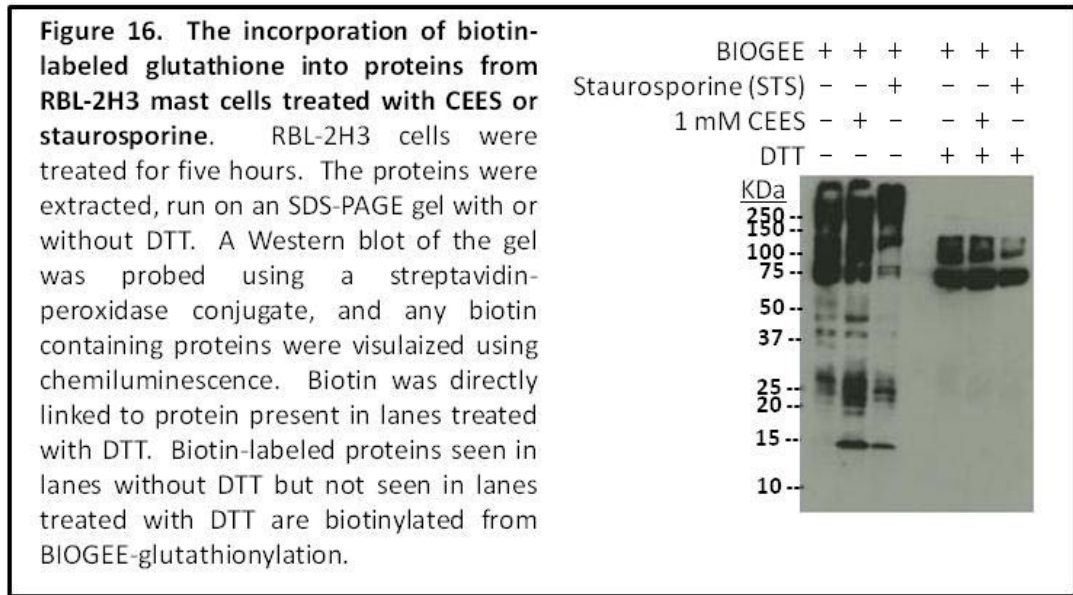
The differences (see Figure 12) for the samples exposed to 2.5 mM CEES are expressed as average 2D gel protein spot volume ratios normalized to Vehicle samples. Positive values show that the proteins are up-regulated, negative values show that the proteins are down-regulated.

Match No. on Gel	Volume Ratio ("CEES"/"Vehicle")	Match No. on Gel	Volume Ratio ("CEES"/"Vehicle")
22	-1.0	195	-1.0
28	-1.0	201	2.0
29	-1.0	222	-1.0
34	-1.0	227	-1.0
57	3.3	228	-1.0
68	3.4	254	No spot for Vehicle-treated
85	1.8	282	"
99	1.7	302	"
102	2.9	314	"
118	-1.0	322	"
159	1.9	323	"
169	2.3	326	"
177	1.7	328	"

The Effects of CEES on RBL-2H3 Protein Glutathionylation

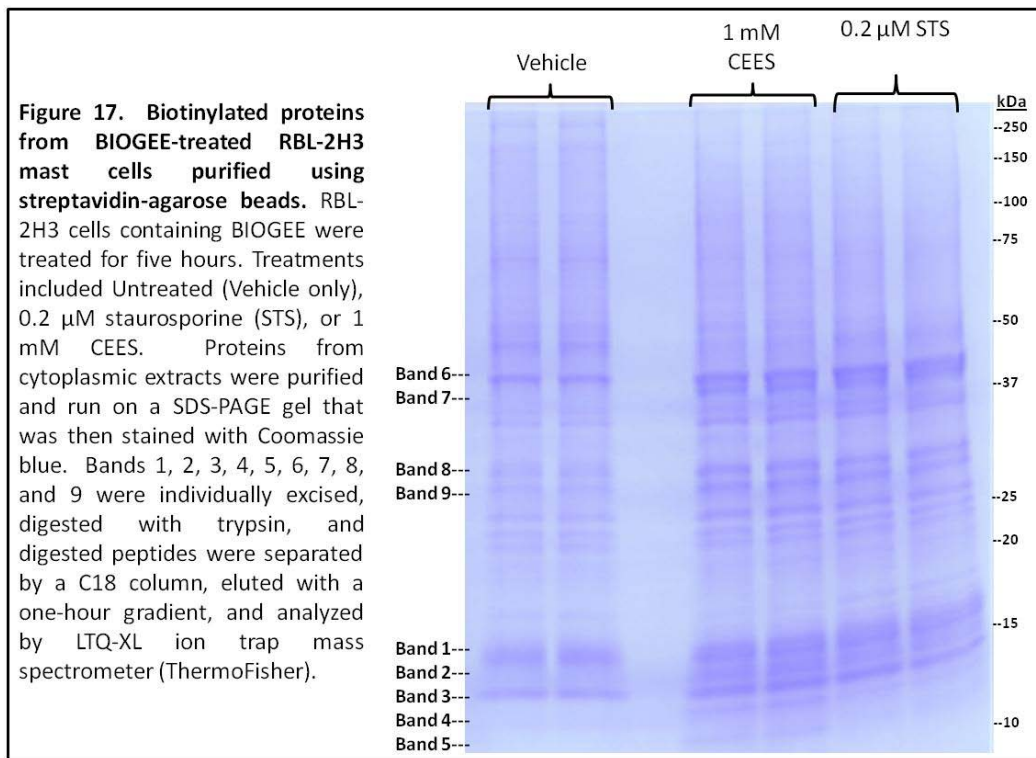
We also utilized redox proteomics to determine how CEES treatment influenced changes in the levels and distribution of oxidized/glutathionylated proteins expressed in the RBL-2H3 mast cell line. **We found that CEES-treated RBL-2H3 cells underwent apoptosis** and that histones were released from nucleosomes into the cytosol during apoptotic cell death. (See 17th Biennial Medical Defense Bioscience Review, “A Sulfur Mustard Analog Induces Oxidative Stress and Apoptotic-specific Glutathionylation of Proteins in Rat Mast Cells”, 2010 in Appendix). We also provided microscopic images of propidium iodide stained mast cells **revealing the presence of some necrotic cells** (data not shown, reported in 2009 Annual Report).

We also investigated the potential effects of CEES on the glutathionylation of RBL-2H3 mast cells. Glutathionylation is the posttranslational modification of a protein by attachment of a GSH molecule by a disulfide bond. It is well established that oxidative stress induces protein glutathionylation. Sullivan et al. (2000) have utilized biotinylated glutathione ethyl ester (BioGEE), a cell-permeant, biotinylated glutathione analog for detecting glutathionylation. Oxidatively stressed cells incubated with BioGEE will incorporate this biotinylated glutathione derivative into proteins thereby facilitating the purification and identification of the modified proteins by mass spectrometry or by Western blotting methods. We added BioGEE to RBL-2H3 mast cells and found that the cells displayed similar glutathionylation protein profiles when they were treated with Staurosporine (STS, an inducer of apoptosis) or with CEES (**Figure 16**). This result provided evidence that mast cells undergoing apoptosis due to either treatment incorporated the biotinylated glutathione derivative from BIOGEE (as a substitute for glutathione) into proteins. The protein bands shown in **Figure 16** that were only observed in CEES- and Staurosporine-treated RBL-2H3 cells could be eliminated when the proteins were run on SDS-PAGE containing dithiothreitol (DTT). DTT removes glutathionylation providing evidence that the CEES- and Staurosporine-specific biotinylation was a result of BIOGEE-glutathionylation. Using an anti-glutathione antibody, we also confirmed by Western blot the increase in protein glutathionylation in CEES-, STS- and H₂O₂-treated RBL-2H3 cells (data not shown).



Biotinylated proteins, directly biotinylated or biotinylated due to BIOGEE (or associated with BioGEE- or biotin-labeled proteins) were affinity-purified using streptavidin-agarose beads (**Figure 17**). Depending on the mast cell treatment, distinctly different proteins were purified especially within the apparent molecular mass range of 20 to 10 kilodaltons (kDa). Shown in **Figure 17**, there were at least five bands (Bands 1 – 5) within this range of purified proteins from mast cells treated with CEES. Only three bands (Bands 1 - 3) were found within the 10-20 kDa range from mast cells treated with vehicle. Four of the five bands (Bands 1, 2, 3, and 4) were found for mast cells treated with STS. In addition, Band 7 was purified only from CEES- and STS-treated mast cells. The higher level of BIOGEE-conjugated proteins found in CEES and STS-treated mast cells indicates that CEES and STS treatments increase the level of protein glutathionylation.

The individual bands shown in **Figure 17** were excised and digested with trypsin. The digested peptides were separated by a C18 column, eluted with a one-hour gradient, and analyzed by LTQ-XL ion trap mass spectrometer (ThermoFisher). A selection of proteins analyzed by the LTQ-XL and identified by SEQUEST search against Uniref 100 UniProt database are shown in **Table 4**.



The affinity purified proteins identified by nanospray LC-MS/MS (**Table 4**) that were unique to CEES treatment were thioredoxin (band 4, **Figure 17**), guanine nucleotide-binding protein beta subunit 2-like 1 (band 9, **Figure 17**), single stranded DNA-binding protein mitochondrial precursor (band 2, **Figure 17**), and mitochondrial ATP synthase e chain (band 5, **Figure 17**). Actin, a protein known to be directly alkylated by HD/CEES during HD/CEES exposure (Sayer et al., 2009), was identified (**Table 4**) in bands 6 and 7 (**Figure 17**) for all treatments. Higher levels of band 7 were observed in CEES- and STS-treated mast cells.

Thioredoxin (Trx) has been shown to be glutathionylated in T cells (Casagrande et al., 2002). Thioredoxin (Trx) plays a major role in redox regulation/oxidative stress through its antioxidant activity by acting as an electron donor to other proteins in the cell. Trx is known to be inhibited upon its glutathionylation in T cells (Casagrande et al., 2002). Thioredoxin reductase (TrxR), a selenocysteine-containing flavoprotein, catalyzes the NADPH-dependent reduction of oxidized Trx. In CEES-exposed lung epithelial cells, TrxR activity is inhibited due to covalent modification of TrxR's reduced selenocysteine-containing active site (Jan et al., 2010). CEES would therefore prevent reduction of Trx by inhibition of TrxR, and would allow oxidized Trx to become glutathionylated as the GSH/GSSG ratio drops during CEES-induced oxidative stress.

In summary, we confirmed that mast cells treated with CEES, staurosporine (STS), an inducer of apoptosis, or H₂O₂, an inducer of oxidative stress, displayed protein profiles with increased protein glutathionylation. Glutathionylation may alter the activity of these proteins defining molecular signaling events involved in HD/CEES cytotoxicity. **Identification of these proteins will aid in the identification of the signal transduction pathway(s) involved in CEES-induced apoptosis/oxidative stress and is an additional step for designing therapeutics that can inhibit/stimulate the pathways playing a role in CEES toxicity.**

Table 4. Selection of proteins identified by SEQUEST search against Uniref 100 UniProt database. Proteins are from mast cells that were incubated with BioGEE and treated with Vehicle, 1 mM CEES, or 0.2 μM Staruosporine (STS). "X" represents positive identification with high confidence; "O" represents protein absent in SEQUEST search.

Band #	Protein		Mast cell treatment		
			Vehicle	1 mM CEES	0.2 μM STS
	Description	MW (kDa)			
1	GTP binding protein Rheb	20.5	O	X	X
	40S and 60S ribosomal proteins	14 – 17	X	X	X
2	SS-DNA-binding protein mit. precursor	17.4	O	X	O
	40S and 60S ribosomal proteins	14 – 17	X	X	X
3	Histone 2a	14.1	X	X	X
	Transcr. Factors or co-activators	10 – 22	O	X	X
	40S and 60S ribosomal proteins	11 – 14	X	X	X
4	Histone H4	11.4	O	X	X
	Thioredoxin	11.5	O	X	O
	40S and 60S ribosomal proteins	11 – 12	X	X	X
5	Mitochondrial ATP synthase e chain	8.1	O	X	O
	40S and 60S ribosomal proteins	10 – 11	X	X	X

6	Actin	41.7	X	X	X
7	Actin	41.7	X	X	X
8	Histone H1.2	21.8	O	X	X
	40S and 60S ribosomal proteins	25 – 30	X	X	X
9	G protein beta subunit 2-like 1	35.4	O	X	O
	40S and 60S ribosomal proteins	27 – 30	X	X	X

III. Continue to supply well characterized antioxidant-liposomes to all other members of the Research Consortium and provide the analytical methodology and services to measure antioxidant (vitamin E and glutathione) levels in tissues collected from the various animal models used by other members of the mustard consortium.

We have prepared liposomes (Yang et al., 2008) using the following instruments: 1) A Model M-110L Microfluidics instrument for 100 ml samples, 2) Lipex Extruder (Northern Lipids, Inc.) for 10 ml samples and 3) Mini-Extruder (Avanti Polar Lipids) for 1 ml samples. The instruments have been used for the preparation of unilamellar antioxidant liposomes containing 6.6 mole percent RRR-alpha-tocopherol (as well as 66.6, 26.5 and 0.66 mole percent of soy lecithin, cholesterol and phosphatidyl serine, respectively). The liposomes have been characterized by measuring: 1) particle size distribution with a dynamic light scattering Model 380 Nicomp particle analyzer; 2) tocopherol content. The vitamin E content does not diminish with up to five passes through the liposome extruder and is stable over four weeks of storage (at 4 deg C). The mean liposome diameter decreases with increasing passes (as expected) of extrusion. The liposome preparation remains unilamellar over a three week period (at 4 deg C). In summary, we prepared batches of up to 100 ml of antioxidant liposomes that had sufficient stability for shipping and further testing. We prepared liposome preparations for Drs. Ward, Das, and Rest groups for *in vivo* and *in vitro* testing.

Liposomes for Dr. Salil Das

Dr. Salil Das at Meharry Medical College found that some of our liposomal formulations were very effective at reducing CEES pulmonary toxicity in a guinea pig model (Das et al., 2003; Mukhopadhyay et al., 2009; Mukherjee et al., 2009; Mukhopadhyay et al., 2010). Five antioxidant liposomes (LIP-1, LIP-2, LIP-3, LIP-4 and LIP-5) were sent to Dr. Das with differing levels of phospholipids, cholesterol, phosphatidic acid, tocopherols, N-acetylcysteine (NAC) and GSH as shown in **Table 5**. Lung damage was measured by albumin leakage from the blood to the lungs (as in our work with Dr. Ward). Maximum lung protection was achieved with two liposomes, LIP-2 (71.5%) and LIP-4 (75.4%), when administered after 5 minutes of CEES exposure. In addition, the vitamin E, NAC-liposomes also provided protection by controlling recruitment of neutrophils, eosinophils, and accumulation of septal and perivascular fibrin and collagen, and parenchymal collapse. Interestingly, liposomes containing delta-tocopherol were found to be particularly effective as counter measures. Delaying the administration of the liposomes after 1 h of CEES exposure decreased the efficacy. **This work clearly suggests that antioxidant liposomes can be used as an effective antidote against CEES-induced lung injury in this animal model.**

Table 5. Antioxidant liposome formulations (LIP-1, LIP-2, LIP-3, LIP-4 and LIP-5) that were sent to Dr. Das. Formulations contain differing levels of phospholipids, cholesterol, phosphatidic acid, tocopherols, N-acetylcysteine (NAC) and GSH.

Liposomes	Concentration in liposomes (mM)							
	Phospholipid (PL90H)	Cholesterol	Phosphatidic acid (PA)	Tocopherol (Vitamin E)			NAC	GSH
				α	γ	δ		
LIP1 (Blank)	71	28	0.67	-	-	-	-	-
LIP 2	55	22	0.6	11	11	5	75	-
LIP 3	62	25	0.6	6	6	-	75	-
LIP 4	55	22	0.6	11	11	-	75	-
LIP 5	55	22	0.6	11	11	-	-	75

Liposomes for Dr. Peter Ward

Dr. Peter Ward's laboratory group demonstrated that acute oxidant-related lung injury (ALI) in rats following instillation of chloroethyl ethyl sulfide (CEES) was attenuated by the airway instillation of anti-oxidant agents (McClintock et al., 2006). This group hypothesized that anti-oxidant containing liposomes would attenuate acute as well as long-term (fibrotic) effects of CEES-induced lung injury. They found that in the acute injury model (at 4 hr), **N-acetylcysteine (NAC)-containing liposomes were protective and reduced to baseline levels both the lung permeability index and the appearance of pro-inflammatory mediators in bronchoalveolar lavage fluids from CEES exposed lungs** (Hoesel et al., 2008). Similar results were obtained when rat alveolar macrophages were incubated *in vitro* with either CEES or lipopolysaccharide (LPS) in the presence of NAC-liposomes. When lung fibrosis three weeks after CEES was quantitated using hydroxyproline content, liposomes containing NAC or NAC + glutathione (GSH) had no effects, but liposomes containing E/ α , γ -tocopherol alone or with NAC significantly suppressed the increase in lung hydroxyproline. Antioxidant-liposomes were effective in treating pulmonary damage (in a rat model) for at least one and half hour post exposure. These findings were confirmed by histopathology evaluation of lung sections. These data demonstrate that **delivery of antioxidants via liposomes to CEES injured lungs are protective against ALI, prevent the appearance of pro-inflammatory mediators, and suppress progressive lung injury (fibrosis)**. A key finding of our work with Dr. Peter Ward (Hoesel et al., 2008) is that liposomes encapsulated with antioxidants are a superior *in vivo* countermeasure to oxidant inducing vesicants compared to the free or unencapsulated antioxidants. In addition, antioxidant-liposomes are effective in treating pulmonary damage (in a rat model) for at least one and half hour post exposure and can also uniquely suppress progressive lung injury. Accordingly, the Ward Group has concluded that **"liposomal strategy may be therapeutically useful in oxidant mediated lung injury in humans."**

Liposomes for Work Dr. Richard Rest

We have supplied NAC-liposomes to Dr. Richard Rest who is studying the influence of redox modulation on the ability of human macrophages to kill *Bacillus anthracis* (BA). **Dr. Rest has found that NAC-liposomes completely delays/inhibits germination of BA spores (in the absence of macrophages) and also stimulates the ability of macrophages to kill intracellular**

BA. These are clearly results with direct military relevance. See in reportable outcomes the manuscript: Bernui, ME, **Stone, WL**, Smith, M, and Rest, RF: N-acetylcysteine (NAC) and STIMAL® (liposome-encapsulated NAC) Increase the Ability of Human Macrophages to Kill Bacillus anthracis) 2010.

Key Research Accomplishments

1. The inhibition of calcium ionophore A23187-induced degranulation by various levels (0.039 – 0.5 mM) of CEES was confirmed in RBL-2H3 rat mast cells.
2. An enhancement of CEES toxicity by non-toxic doses of Ca-ionophore A23187 was documented in RBL-2H3 cells.
3. NO generation was found to be increased in RBL-2H3 cells treated with the calcium ionophore A23187. Various levels of CEES did not inhibit or stimulate NO generation.
4. Various oxidative stress parameters (ROS production, GSH and total thiol depletion, apoptosis and necrosis) were detected in RBL-2H3 rat mast cells treated with CEES or CEES and Ca²⁺ ionophore.
5. A novel effect of CEES in RBL-2H3 mast cells was found. Release of histones from nucleosomes into cytosol was observed along with apoptotic cell death.
6. Different techniques for mast cell activation for degranulation (Ca²⁺ ionophore treatment or IgE cross-linking) were compared (cytotoxicity and percentage of degranulation) in RBL-2H3 rat mast cells.
7. The effect of NOS inhibitor L-NAME on mast cells was studied (cytotoxicity and percentage of degranulation) in RBL-2H3 rat mast cells.
8. The effects of tetrahydrobiopterin (BH₄) and gamma interferon (INF- γ) on the production of NO and degranulation were studied in RBL-2H3 rat mast cells.
9. The effect of 2,2'-(hydroxynitrosohydrazino)bis-ethanamine (NOC-18), source of exogenous NO, on the production of NO and degranulation was studied in RBL-2H3 rat mast cells.
10. The combined effect of NOC-18 and CEES on the production of NO and degranulation was studied in RBL-2H3 rat mast cells.
11. Increased protein glutathionylation of specific proteins from mast cells treated with CEES was measured in two ways: 1) using BIOGEE, a cell-permeant, biotinylated glutathione analog commonly used for detecting protein glutathionylation, and 2) more traditionally by Western blot using an anti-GSH/GSSG antibody.
12. Protein glutathionylation for specific proteins found in CEES-treated mast cells were similar to that found in staurosporine (STS)-treated mast cells. STS is an inducer of apoptosis; therefore we determined that the increased protein glutathionylation pattern for CEES-treated mast cells was similar to that for apoptotic mast cells.
13. H₂O₂, an inducer of oxidative stress, was also used to treat RBL-2H3 mast cells, and we determined that the increased protein glutathionylation protein profile for oxidatively stressed cells was also similar to that for CEES-treated mast cells.

14. We determined that the following proteins are glutathionylated only in CEES-treated and STS-treated mast cells: 1) GTP binding protein Rheb, 2) various transcriptional factors or co-activators, 3) histone H4 and 4) histone H1.2.
15. We determined that glutathionylation of the following proteins is unique to CEES-treatment in RBL-2H3 mast cells: 1) thioredoxin, 2) guanine nucleotide-binding protein beta subunit 2-like 1, 3) single stranded DNA-binding protein mitochondrial precursor, and 4) mitochondrial ATP synthase e chain.
16. We determined that glutathionylation of the following proteins occurs in RBL-2H3 mast cells regardless of treatment (CEES, STS, or vehicle): 1) various 40S and 60S ribosomal proteins, 2) histone 2a, and 3) actin (although glutathionylation of actin appeared to be more abundant in CEES- and STS-treated mast cells).
17. Rat mast cells and various animal tissue samples treated/untreated with CEES or HD were analyzed by 2D-GE separation.
18. Rat lung tissues treated with blank or antioxidant-liposomes were analyzed by 2D-GE gel analysis and no differences in protein expression were found.
19. RBL-2H3 mast cells treated/untreated with 0.5 mM CEES were analyzed by 2D-GE.
20. A number of human Epiderm skin samples exposed to CEES were analyzed by 2D-GE.
21. Proteomic studies of CEES-treated and HD-treated rat tissues were continued. Alkylated and oxidized amino acid residues were found in albumin from HD-treated rat lung tissues.
22. Well-characterized antioxidant liposomes were produced for the members of the Mustard Consortium.
23. Second generation antioxidant liposomes were formulated, prepared and distributed to members of the Consortium. These antioxidant liposomes were found to be particularly effective in preventing both acute and long-term *in vivo* damage to the lungs of rats exposed to CEES.
24. Antioxidant-liposomes prepared by our laboratory are effective in preventing *in vivo* CEES-induced damage to the guinea pig lung.
25. *In vitro* experiments with antioxidant-liposomes (with NAC) have shown an ability to prevent *Bacillus anthracis* spore germination and to enhance the killing of *B. anthracis* by human macrophages.

2007 Reportable Outcomes

Presentations:

1. Advanced Medical Countermeasures Consortium Meeting, June 28, 2007, Crystal City, VA: "Protective effects of anti-oxidant liposomes in acute and progressive lung injury after CEES."
2. BARDA 2007 Industry Day Conference, August 3, 2007, Washington, DC: "Protective effects of anti-oxidant liposomes."
3. Biotech 2007 Poster (Richard Rest, Mariana Bernui, Milton Smith and William Stone). STIMAL (Liposome-Encapsulated N-Acetylcysteine) increases the ability of human macrophages to kill *Bacillus anthracis*.
4. Advanced Medical Countermeasures Consortium Meeting, June 5, 2008, Baltimore, MA: "Effect of low doses of CEES on degranulation of rat mast cells."
5. Bioscience Review 2008 Poster (Victor Paromov, Sudha Kumari, Marianne Brannon, Christian Muenyi, and William Stone). "The Protective Effect of Antioxidant Liposomes in a Human Epidermal Model Exposed to a Vesicating Agent".
6. Bioscience Review 2008 Poster (Peter A. Ward, Laszlo M. Hoesel, Michael A. Flierl, Daniel Rittirsch, Milton Smith, and William Stone). "Liposomal Blockade of Lung Injury after Exposure to 2-Chloroethyl Ethyl Sulfide".
7. SERLC 2008, Cashiers, NC, Victor Paromov, Sudha Kumari, Marianne Brannon, Sasidhar Naga, and William L. Stone: "Antioxidant Liposomes Protect Human Keratinocytes Exposed to a Genotoxic Agent"
8. SERLC 2008, Cashiers, NC, Victor Paromov, Christian Muenyi, Sudha Kumari, Marianne Brannon, and William L. Stone: "Proteomic Alterations in Human Epidermal Model Exposed to a Genotoxic Agent in the Presence of Antioxidant Liposomes"
9. 17th Biennial Medical Defense Bioscience Review, Hunt Valley, Maryland, May 23 – 27, 2010. Marianne Brannon, Victor Paromov, and William L. Stone. A Sulfur Mustard Analog Induces Oxidative Stress and Apoptotic-specific Glutathionylation of Proteins in Rat Mast Cells.

Articles:

Qui M, Paromov VM, Yang H, Smith M, **Stone WL**. Inhibition of inducible Nitric Oxide Synthase by a mustard gas analog in murine macrophages. *BMC Cell Biology* 2006, 7:39.

Viktor Paromov, Zacharias Suntres, Milton Smith, **William L. Stone**. "Sulfur Mustard Toxicity in Human Skin: Role of Oxidative Stress and Antioxidant Therapy" in: *Journal of Burns and Wounds* 2007, 7:e7.

Hoesel LM, Flierl MA, Niederbichler AD, Rittirsch D, McClintock SD, Reuben JS, Pianko MJ, **Stone W**, Yang H, Smith M *et al*: Ability of antioxidant liposomes to prevent acute and progressive pulmonary injury. *Antioxidants & redox signaling* 2008, 10(5):973-981.

Viktor Paromov, Min Qui, Hongsong Yang, Milton Smith, and **William L. Stone** "The influence of N-acetyl-L-cysteine and polymyxin B on oxidative stress and nitric oxide synthesis in stimulated macrophages treated with a mustard gas analog" in: *BMC Cell Biology* 2008, 9:33. (rated "highly accessed" by BMC Central)

Yang H, Paromov V, Smith M, **Stone WL**. Preparation, characterization, and use of antioxidant-liposomes. *Methods Mol Biol*. 2008. 477:277-292.

Mukhopadhyay S, Mukherjee S, **Stone WL**, Smith M, Das SK. Role of MAPK/AP-1 signaling pathway in the protection of CEES-induced lung injury by antioxidant liposome. *Toxicology*. 2009. 261:143-151.

Mukherjee S, **Stone WL**, Yang H, Smith MG, Das SK. Protection of half sulfur mustard gas-induced lung injury in guinea pigs by antioxidant liposomes. *J Biochem Mol Toxicol*. 2009. 23:143-153.

Mukhopadhyay S, Mukherjee S, Ray BK, Ray A, **Stone WL**, Das SK. Antioxidant liposomes protect against CEES-induced lung injury by decreasing SAF-1/MAZ-mediated inflammation in the guinea pig lung. *J. Biochem. Mol. Toxicol*. 2010. 24:187-194.

Book Chapters:

Milton G. Smith, **William L. Stone**, Ren-Feng Guo, Peter A. Ward, Zacharias Suntres, Shyamali Mukherjee and Salil K. Das, Chapter 12 "Vesicants and Oxidative Stress", pp 249-294 in: *Chemical Warfare Agents: Chemistry, Pharmacology, Toxicology and Therapeutics*. Romano editor.

Submitted Manuscripts:

Bernui, ME, **Stone, WL**, Smith, M, and Rest, RF: N-acetylcysteine (NAC) and STIMAL® (liposome-encapsulated NAC) Increase the Ability of Human Macrophages to Kill Bacillus anthracis) 2010 (submitted).

Paromov, V., M. Brannon, S. Kumari, M. Samala, M. Smith, and **W. L. Stone**. Sodium Pyruvate Modulates Cell Death Pathways in Keratinocytes Exposed to a Genotoxic Agent. *Journal of Toxicology*. 2010 (submitted).

Paromov, V., S. Kumari, M. Brannon, S. Naga, H. Yang, M. Smith, and **W. L. Stone**. Protective Effect of Liposome-encapsulated Glutathione in a Human Epidermal Model Exposed to a Mustard Gas Analog. *Journal of Applied Toxicology*. 2010 (submitted)

Brannon, M.F., V. Paromov, M. Smith, and W.L. Stone. A Sulfur Mustard Analog Induces Oxidative Stress and Apoptotic-specific Glutathionylation of Proteins in Rat Mast Cells. (in preparation)

Personnel that was paid during the time frame of August 2006 – September 2010:

William L. Stone

Victor Paromov

Marianne Brannon

Christopher McGoldrick

Mallikarjun Samala

Hongsong Yang

Christian Muenyi

Conclusion

CEES-induced cell injury has a complex molecular mechanism and associated with oxidative stress, gene expression, inflammation, and cell death pathways. The acute phase of injury is an oxidant-mediated process that is associated with intensive inflammatory responses. Liposomes containing antioxidants (GSH, NAC, pyruvates, tocopherols and tocotrienols) were found to be highly protective *in vitro* and *in vivo*. We found that antioxidant-liposomes were effective in preventing CEES induced lung damage in two *in vivo* models, i.e., rats and guinea pigs and also, *in vitro* in human skin EpiDerm model. In addition, antioxidant-liposomes prevented the *in vitro* germination of *Bacillus anthracis* spores and promoted the intracellular killing of this bacterium by human macrophages. **These findings suggest that the antioxidant-liposomes may present promising approach to future effective multi-functional treatment for HD/CEES toxicity.**

We found that toxic doses of CEES impair degranulation in RBL-2H3 rat mast cells. Initially, we proposed that CEES might stimulate mast cell degranulation since we found that CEES inhibits the generation of NO in RAW 264.7 macrophages (Stone et al, 2003). Nitric oxide is known to inhibit mast cell degranulation in various species (Eastmond et al., 1997; Iikura et al., 1998). However, recent study has shown that endogenous nitric oxide does not modulate degranulation of mesenteric or skin mast cells in rats (Kwasniewski et al., 2003). In addition, we found that combined treatment with CEES and Ca²⁺ ionophore (strong degranulating agent) induces massive oxidative stress in rat mast cells as evidenced with free radical production, GSH and total thiol depletion, and apoptotic and necrotic death pathways. It was found that RBL-2H3 mast cells treated with CEES released histones from nucleosomes, a indicator of apoptosis (Wu et al, 2002).. Apoptosis in CEES-treated mast cells was also confirmed by measuring DNA fragmentation and increased caspase-3 activity. **These findings suggest that antioxidants like NAC, GSH, and vitamin E should be protective in mast cells treated with CEES or HD.**

We analyzed overall intracellular changes due to the oxidative stress in CEES/HD treated samples utilizing a systems biology approach. We looked at the differences in protein “finger prints” on the 2D-gels quantitatively using Dymension software (SynGene). In some cases, the most affected proteins were extracted from gels, and identified by nano-spray technique on our LTQ Linear Ion Trap Mass Spectrometer (ThermoFisher). We found that alkylated and/or oxidized proteins can be successfully identified in the tissue samples of HD-treated animals.

It is well established that oxidative stress induces protein glutathionylation. We utilized biotinylated glutathione ethyl ester (BioGEE), a cell-permeant, biotinylated glutathione analog for detecting glutathionylation of proteins in CEES-induced oxidatively stressed RBL-2H3 mast cells. Oxidatively stressed cells incubated with BioGEE incorporated this biotinylated glutathione derivative into proteins thereby facilitating the purification and identification of the modified proteins. The differences in protein glutathionylation were analyzed by Western blotting and by nanospray-LC-MS/MS methods. Depending on the mast cell treatment, distinctly different BIOGEE bound proteins were purified especially within the apparent molecular mass range of 20 to 10 kilodaltons (kDa). There was a higher level of BIOGEE-conjugated proteins found in CEES and STS-treated mast cells indicating that CEES and STS treatments increased the level of protein glutathionylation. The individual BIOGEE-conjugated protein bands run on SDS-PAGE were analyzed by nanospray and LTQ-XL ion trap mass spectrometer (ThermoFisher) and identified by SEQUEST search against Uniref 100 UniProt database. The affinity purified proteins that were identified and were unique to CEES treatment

were: 1) thioredoxin, 2) guanine nucleotide-binding protein beta subunit 2-like 1, 3) single stranded DNA-binding protein mitochondrial precursor, and 4) mitochondrial ATP synthase e chain. Thioredoxin (Trx) has been shown to be glutathionylated in T cells (Casagrande et al., 2002). Actin, a protein known to be directly alkylated by HD/CEES during HD/CEES exposure (Sayer et al., 2009), was identified for all treatments with higher levels of BIOGEE-conjugated actin observed in CEES- and STS-treated mast cells. We also confirmed by Western blotting with an anti-GSH/GSSG antibody probe that mast cells not containing BIOGEE and treated with CEES, Staurosporine (STS), an inducer of apoptosis, or H₂O₂, an inducer of oxidative stress, displayed protein profiles with increased protein glutathionylation. Glutathionylation may alter the activity of these proteins defining molecular signaling events involved in HD/CEES cytotoxicity. Identification of these proteins will aid in the identification of the signal transduction pathway(s) involved in CEES-induced apoptosis. **This work provides new molecular details regarding the mechanisms whereby HD/CEES induced damage causes apoptotic cell death and increase protein glutathionylation of specific proteins in mast cells.**

References

- Casagrande, S., V. Bonetto, M. Fratelli, E. Gianazza, I. Eberini, T. Massignan, M. Salmona, G. Chang, A. Holmgren, and P. Ghezzi. 2002. Glutathionylation of human thioredoxin: a possible crosstalk between the glutathione and thioredoxin systems. *Proc. Natl. Acad. Sci. USA.* 99:9745-9749.
- Das SK, Mukherjee S, Smith MG, Chatterjee D: Prophylactic protection by N-acetylcysteine against the pulmonary injury induced by 2-chloroethyl ethyl sulfide, a mustard analogue. *Journal of biochemical and molecular toxicology* 2003, 17(3):177-184.
- Davis BJ, Flanagan BF, Gilfillan AM, Metcalfe DD, Coleman JW: Nitric oxide inhibits IgE-dependent cytokine production and Fos and Jun activation in mast cells. *J Immunol* 2004, 173(11):6914-6920.
- Eastmond NC, Banks EM, Coleman JW: Nitric oxide inhibits IgE-mediated degranulation of mast cells and is the principal intermediate in IFN-gamma-induced suppression of exocytosis. *J Immunol* 1997, 159(3):1444-1450.
- Graham, J.S, M.A. Bryant, E.H. Braue. 1994. Effect of sulfur mustard on mast cells in hairless guinea pig skin. *J. Toxicol. – Cut. & Ocular Toxicol.* 13:47-54.
- Hoesel LM, Flierl MA, Niederbichler AD, Rittirsch D, McClintock SD, Reuben JS, Pianko MJ, Stone W, Yang H, Smith M *et al*: Ability of antioxidant liposomes to prevent acute and progressive pulmonary injury. *Antioxidants & redox signaling* 2008, 10(5):973-981.
- Iikura M, Takaishi T, Hirai K, Yamada H, Iida M, Koshino T, Morita Y: Exogenous nitric oxide regulates the degranulation of human basophils and rat peritoneal mast cells. *International archives of allergy and immunology* 1998, 115(2):129-136.
- Jan, Y-H., D.E. Heck, J.P. Gray, H. Zheng, R.P. Casillas, D.L. Laskin, and J.D. Laskin. 2010. Selective targeting of selenocysteine in thioredoxin reductase by the half mustard 2-chloroethyl ethyl sulfide in lung epithelial cells. *Chem. Res. Toxicol.* 23:1045-1053.
- Koranteng RD, Dearman RJ, Kimber I, Coleman JW: Phenotypic variation in mast cell responsiveness to the inhibitory action of nitric oxide. *Inflamm Res* 2000, 49(5):240-246.
- Kwasniewski FH, Tavares de Lima W, Bakhle YS, Jancar S: Endogenous nitric oxide does not modulate mesenteric mast cell degranulation in rats. *Biochemical pharmacology* 2003, 65(12):2073-2080.
- McClintock SD, Hoesel LM, Das SK, Till GO, Neff T, Kunkel RG, Smith MG, Ward PA: Attenuation of half sulfur mustard gas-induced acute lung injury in rats. *J Appl Toxicol* 2006, 26(2):126-131.
- Mukherjee S, Stone WL, Yang H, Smith MG, Das SK. Protection of half sulfur mustard gas-induced lung injury in guinea pigs by antioxidant liposomes. *J Biochem Mol Toxicol.* 2009. 23:143-153.

Mukhopadhyay S, Mukherjee S, Ray BK, Ray A, Stone WL, Das SK. Antioxidant liposomes protect against CEES-induced lung injury by decreasing SAF-1/MAZ-mediated inflammation in the guinea pig lung. *J. Biochem. Mol. Toxicol.* 2010. 24:187-194.

Mukhopadhyay S, Mukherjee S, Stone WL, Smith M, Das SK. Role of MAPK/AP-1 signaling pathway in the protection of CEES-induced lung injury by antioxidant liposome. *Toxicology.* 2009. 261:143-151.

Noort D, Fidder A, Degenhardt-Langelaan CE, Hulst AG: Retrospective detection of sulfur mustard exposure by mass spectrometric analysis of adducts to albumin and hemoglobin: an in vivo study. *Journal of analytical toxicology* 2008, 32(1):25-30.

Noort D, Hulst AG, Trap HC, de Jong LP, Benschop HP: Synthesis and mass spectrometric identification of the major amino acid adducts formed between sulphur mustard and haemoglobin in human blood. *Archives of toxicology* 1997, 71(3):171-178.

Paromov, V., Z. Suntres, M. Smith, and W.L. Stone, 2007. Sulfur mustard toxicity following dermal exposure. Role of oxidative stress, and antioxidant therapy. *J. Burns Wounds.* 7:60-85.

Paromov, V., M. Qui, H. Yang, M. Smith, and W.L. Stone, 2008. The influence of N-acetyl-N-cysteine on oxidative stress and nitric oxide synthesis in stimulated macrophages treated with a mustard gas analogue. *BMC Cell Biol.* 9:33.

Qui M, Paromov VM, Yang H, Smith M, Stone WL: Inhibition of inducible Nitric Oxide Synthase by a mustard gas analog in murine macrophages. *BMC cell biology* 2006, 7:39.

Rikimaru T, M. Nakamura, T. Yano, G. Beck, G.S. Habicht, L.L. Rennie, M. Widra, C.A. Hirshman, M.G. Boulay, E.W. Spannhake, et al. 1991. Mediators, initiating the inflammatory response, released in organ culture by full-thickness human skin explants exposed to the irritant, sulfur mustard. *J. Invest. Dermatol.* 96:888-897.

Sayer, N.M., R. Whiting, A.C. Green, K. Anderson, J. Jenner, and C.D. Lindsay. 2010. Direct binding of sulfur mustard and chloroethyl ethyl sulphide to human cell membrane-associated proteins; implications for sulfur mustard pathology. *J. Chromatography B.* 878:1426-1432.

Seol IW, Kuo NY, Kim KM: Effects of dopaminergic drugs on the mast cell degranulation and nitric oxide generation in RAW 264.7 cells. *Archives of pharmacal research* 2004, 27(1):94-98.

Stone WL, Qui M, Smith M: Lipopolysaccharide enhances the cytotoxicity of 2-chloroethyl ethyl sulfide. *BMC cell biology* 2003, 4(1):1.

Sullivan, D.M., N.B. Wehr, M.M. Fergusson, R.L. Levine, and T. Finkel. 2000. Identification of oxidant-sensitive proteins: TNF- α induces protein glutathiolation. *Biochem.* 39:11121-11128.

Tewari-Singh, N., S. Rana, M. Gu, A. Pal, D.J. Orlicky, C.W. White, and R. Agarwal. 2009. Inflammatory biomarkers of sulfur mustard analog 2-chloroethyl sulfide-induced skin injury in SKH-1 hairless mice. *Toxicol. Sci.* 108:194-206.

Townsend, D.M, Y. Manevich, L. He, Y. Xiong, R.R. Bowers, Jr., S. Hutchens, and K.D. Tew. 2009. Nitrosative stress-induced S-glutathionylation of protein disulfide isomerase leads to activation of the unfolded protein response. *Cancer Res.* 69:7626-7634. Graham, J.S, M.A. Bryant, E.H. Braue. 1994. Effect of sulfur mustard on mast cells in hairless guinea pig skin. *J. Toxicol. – Cut. & Ocular Toxicol.* 13:47-54.

Wu, D., A. Ingram, J.H. Lahti, B. Mazza, J. Grenet, A. Kapoor, L. Liu, V.J. Kidd, and D. Tang. 2002. Apoptotic release of histones from nucleosomes. *J.Biol.Chem.* 277:12001-12008.

Yang H, Paromov V, Smith M, Stone WL. Preparation, characterization, and use of antioxidant-liposomes. *Methods Mol Biol.* 2008. 477:277-292.

Yeo TH, Ho ML, Loke WK: Development of a liquid chromatography-multiple reaction monitoring procedure for concurrent verification of exposure to different forms of mustard agents. *Journal of analytical toxicology* 2008, 32(1):51-56.

Appendices (Available as pdf files)

2007 Appendices (available as PDF files)

1. Qui et al. 2006. *BMC Cell Biology.* 7:39
2. Paromov et al. 2007. *Journal of Burns and Wounds.* 7:e7.
3. Paromov et al., 2008. *BMC Cell Biology.* 9:33.
4. Yang et al., 2008. *Methods Mol. Biol.* 477:277-292.
5. SERLC 2008 Poster: “Antioxidant Liposomes...”
6. SERLC 2008 Poster: “Proteomic Alterations ...”
7. Advanced Medical Countermeasures Consortium Meeting, 2008, “Effect of low doses of CEES...”
8. Bioscience Review 2008 Poster, “The Protective Effect of Antioxidant..”
9. 17th Biennial Medical Defense Bioscience Review Poster, 2010.
10. Paromov et al., 2010. *J. Toxicol.* (manuscript)
11. Paromov et al., 2010. *J. Appl. Toxicol.* (manuscript)

Research article

Open Access

Inhibition of inducible Nitric Oxide Synthase by a mustard gas analog in murine macrophages

Min Qui^{†1}, Victor M Paromov^{*†1}, Hongsong Yang^{†1}, Milton Smith² and William L Stone^{†1}

Address: ¹Department of Pediatrics, East Tennessee State University, Johnson City, TN, USA and ²Amox Ltd., Lawton, MI 49605, USA

Email: Min Qui - qui@etsu.edu; Victor M Paromov* - paromov@etsu.edu; Hongsong Yang - yangh@etsu.edu; Milton Smith - mgsmithmd@isp01.net; William L Stone - stone@etsu.edu

* Corresponding author †Equal contributors

Published: 30 November 2006

Received: 22 September 2006

BMC Cell Biology 2006, 7:39 doi:10.1186/1471-2121-7-39

Accepted: 30 November 2006

This article is available from: <http://www.biomedcentral.com/1471-2121/7/39>

© 2006 Qui et al; licensee BioMed Central Ltd.

This is an Open Access article distributed under the terms of the Creative Commons Attribution License (<http://creativecommons.org/licenses/by/2.0>), which permits unrestricted use, distribution, and reproduction in any medium, provided the original work is properly cited.

Abstract

Background: 2-Chloroethyl ethyl sulphide (CEES) is a sulphur vesicating agent and an analogue of the chemical warfare agent 2,2'-dichlorodiethyl sulphide, or sulphur mustard gas (HD). Both CEES and HD are alkylating agents that influence cellular thiols and are highly toxic. In a previous publication, we reported that lipopolysaccharide (LPS) enhances the cytotoxicity of CEES in murine RAW264.7 macrophages. In the present investigation, we studied the influence of CEES on nitric oxide (NO) production in LPS stimulated RAW264.7 cells since NO signalling affects inflammation, cell death, and wound healing. Murine macrophages stimulated with LPS produce NO almost exclusively via inducible nitric oxide synthase (iNOS) activity. We suggest that the influence of CEES or HD on the cellular production of NO could play an important role in the pathophysiological responses of tissues to these toxicants. In particular, it is known that macrophage generated NO synthesised by iNOS plays a critical role in wound healing.

Results: We initially confirmed that in LPS stimulated RAW264.7 macrophages NO is exclusively generated by the iNOS form of nitric oxide synthase. CEES treatment inhibited the synthesis of NO (after 24 hours) in viable LPS-stimulated RAW264.7 macrophages as measured by either nitrite secretion into the culture medium or the intracellular conversion of 4,5-diaminofluorescein diacetate (DAF-2DA) or dichlorofluorescein diacetate (DCFH-DA). Western blots showed that CEES transiently decreased the expression of iNOS protein; however, treatment of active iNOS with CEES *in vitro* did not inhibit its enzymatic activity

Conclusion: CEES inhibits NO production in LPS stimulated macrophages by decreasing iNOS protein expression. Decreased iNOS expression is likely the result of CEES induced alteration in the nuclear factor kappa B (NF- κ B) signalling pathway. Since NO can act as an antioxidant, the CEES induced down-regulation of iNOS in LPS-stimulated macrophages could elevate oxidative stress. Since macrophage generated NO is known to play a key role in cutaneous wound healing, it is possible that this work has physiological relevance with respect to the healing of HD induced skin blisters.

Background

HD is a chemical weapon that can produce casualties in military situations and has been used with devastating results against civilian populations [1]. Extensive and slow healing lesions following exposure to HD can place a heavy burden on the medical services of military and public health organizations. The design of effective countermeasures to HD depends upon a detailed understanding of the molecular mechanisms for its toxicity. Important mechanisms of HD induced skin injury are alkylation of DNA and other macromolecules, accompanied by enhanced reactive oxygen species (ROS) generation and depletion of intracellular glutathione (GSH) [2-5]. Depletion of GSH by HD and its metabolites is known to shift the intracellular redox milieu toward a more oxidized state with a subsequent loss of protection against oxidative free radicals and an activation of inflammatory responses [6,7].

It has been shown that HD induces a vast "spectrum" of inflammatory cytokines released from keratinocytes [8,9]. It is likely that CEES cause similar changes in macrophages and leukocytes. We previously found that LPS, as well as inflammatory cytokines, such as tumor necrosis factor- α (TNF- α) and interleukin one-beta (IL-1 β), significantly amplify the toxicity of CEES in RAW264.7 macrophages [10]. In macrophages, stimulation by LPS, as well as by pro-inflammatory cytokines, leads to the activation and nuclear translocation of NF- κ B [11]. One of the major consequences of such activation in macrophages is an induction of iNOS expression with subsequent elevation of intracellular NO [12]. The effect of CEES on NO generation and on the NF- κ B pathway is potentially significant since NO signalling plays an important role in inflammation, the mechanisms of cell death NF- κ B [13,14], and wound healing [15,16]. The present work describes the inhibition of NO production and iNOS expression in LPS stimulated macrophages treated with CEES.

Results

CEES transiently suppresses NO production and iNOS expression in LPS stimulated cells

In Figure 1a, we examined nitrite secretion into the cell culture medium by RAW 264.7 murine macrophages after 24 hours of treatment with CEES and various levels of LPS. Nitrite level in the cell culture medium, as measured by the Griess reagent, is a reliable indicator of nitric oxide secretion. These data show that CEES (100–500 μ M) inhibited the secretion of NO into the cell medium by LPS stimulated macrophages in a dose-dependent manner. Low levels of CEES (\leq 100 μ M) only partially inhibited NO production, whereas levels higher than 300 μ M completely inhibited NO production. Although CEES does decrease the viability of LPS stimulated macrophages [10],

the decreased generation of NO cannot be accounted simply for the loss of viable cells. Figure 1b shows that in case nitrite levels in the culture medium (as measured by OD at 532 nm) are normalized to the amount of viable cells (OD at 580 nm, MTT assay, measured separately) there is still a significant CEES dose dependent inhibition of NO formation.

In order to determine if CEES influenced cellular levels of iNOS, we performed Western blot analyses (Figure 1c) of the cell lysates using highly selective anti-iNOS antibodies with equal amounts of total protein applied to each lane. Control RAW 264.7 macrophages had no detectable iNOS protein, CEES treatment alone did not induce any iNOS protein but LPS (10 ng/ml for 24 hours) produced a marked induction of iNOS protein. When simultaneously treated with LPS (10 ng/ml) and CEES (300 μ M) there was a marked reduction in the LPS induction of iNOS protein.

We then examined the influence of 300 μ M CEES on the time course of NO production in macrophage stimulated with 10 ng/ml LPS. Figure 2a shows that CEES delays, but does not prevent, the production of NO (as measured by nitrite formation) in LPS-stimulated macrophages. In fact, after 12 hours the rate of NO production is about the same in cells treated with LPS alone compared with cells treated with both LPS and CEES. Western blot data (Figure 2b) from the cells used in Figure 2a show a similar pattern: LPS alone induces robust iNOS protein expression which is completely inhibited by CEES for up to 6 hours. After 12 hours, however, the cells incubated with both CEES and LPS show a rebound in the expression of iNOS and after 24 hours the iNOS protein level in cells treated with both CEES and LPS is very similar to that observed in cells treated with LPS alone. These data show that the influence of CEES on both nitric oxide synthesis and iNOS expression is transient.

CEES does not inhibit iNOS enzymatic activity in vitro

In order to evaluate the possible direct inhibitory effect of CEES on iNOS activity *in vitro*, we measured the intracellular rates of 4,5-diaminofluorescein (DAF-2) or dichlorofluorescein (DCFH) oxidation in intact macrophages. Dichlorofluorescein diacetate (DCFH-DA) is permeable to the cell plasma membrane and intracellular esterases convert it into a membrane impermeable (DCFH) form which is can be oxidized to highly fluorescent dichlorofluorescein (DCF) by free radicals. In macrophages, the oxidation of DCFH has been shown to be a sensitive and relatively selective probe for monitoring intracellular NO formation by iNOS [17].

Using DCFH-DA and DAF-2DA, we were able to continuously monitor NO formation in intact macrophages under a variety of conditions. Previously, we [18] and oth-

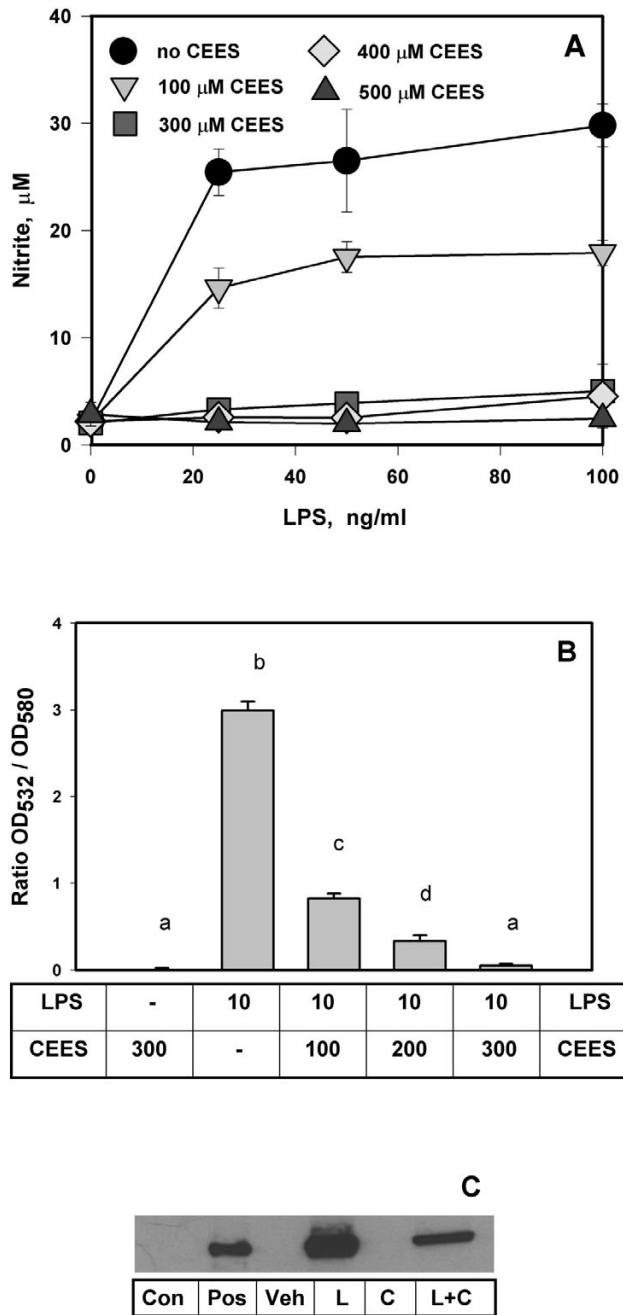


Figure 1
CEES inhibits NO production and iNOS expression in LPS stimulated RAW264.7 macrophages. *Panel A:* Macrophages were simultaneously treated with various levels of CEES (as indicated) and low doses of LPS (as indicated). NO production was monitored as the concentration of nitrite in the culture medium after 24 h. *Panel B:* Cells were treated similarly as for *Panel A*; LPS, 10 ng/ml; CEES, 100, 200, or 300 μM (as indicated). Means not sharing a common letter are significantly different ($p < 0.05$). Nitrite levels in the culture medium (OD at 532 nm) were normalized to the amount of viable cells (OD of the MTT product at 580 nm). *Panel C:* Western blot analysis of iNOS protein from cells simultaneously incubated with 300 μM CEES and/or 10 ng/ml LPS for 24 h; cell lysates were prepared as described in Materials and Methods: Con, control cells; Pos, iNOS protein for positive control; Veh, vehicle; L, 10 ng/ml LPS stimulated cells; C, 300 μM CEES treated cells; L+C, LPS/CEES treated cells.

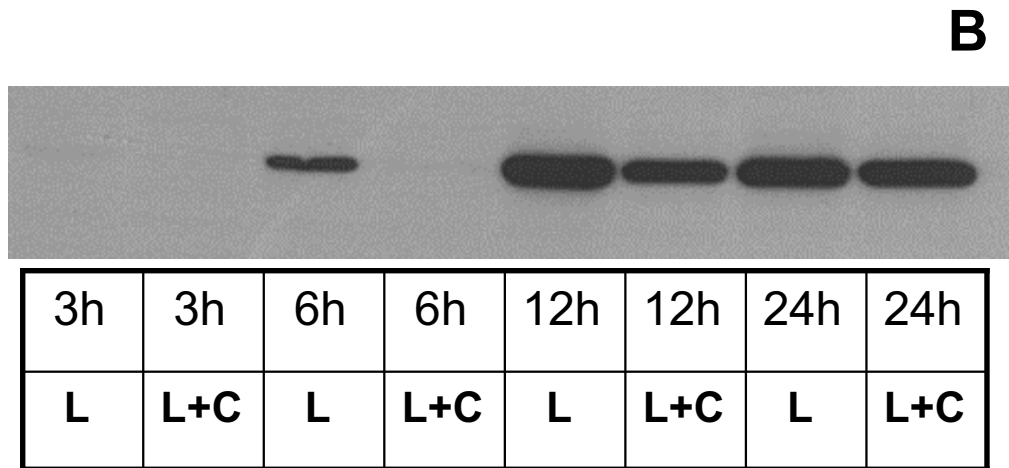
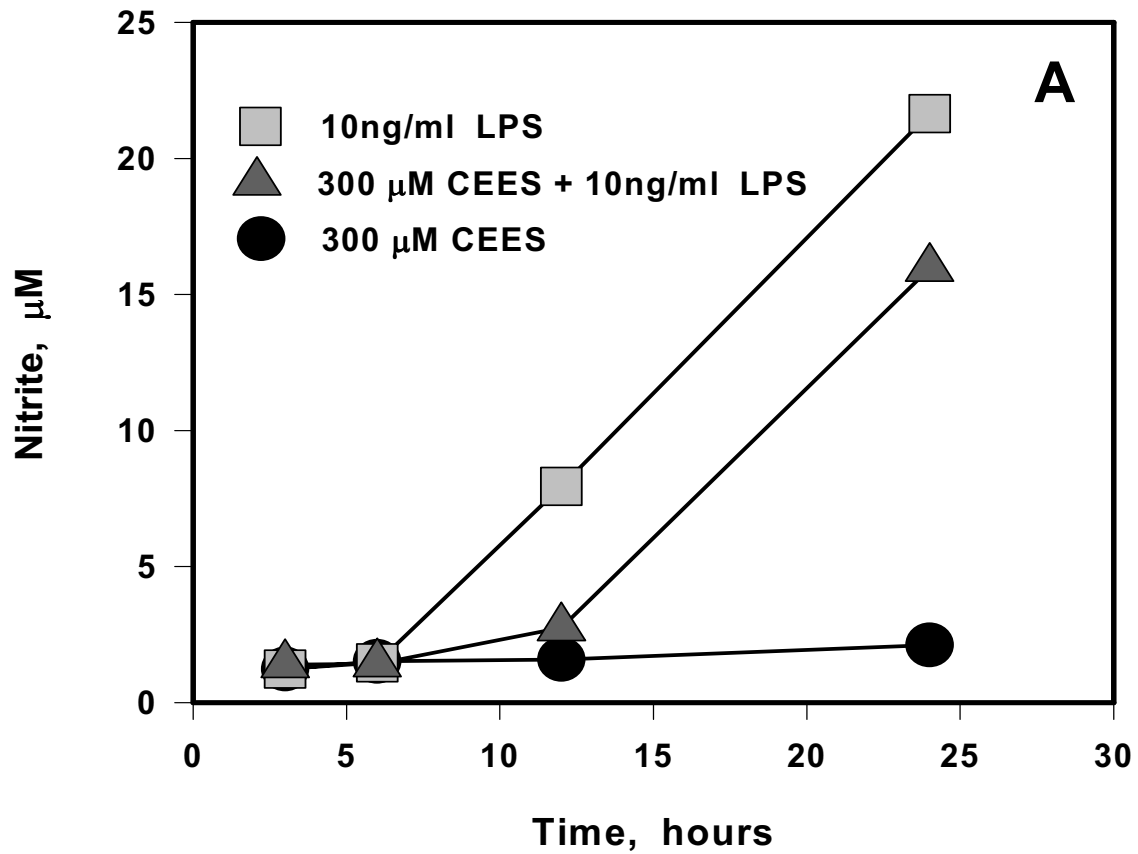


Figure 2

Time course of NO production and iNOS expression in LPS stimulated RAW264.7 macrophages incubated with CEES. Panel A: Macrophages were incubated with 10 ng/ml LPS alone, 300 µM CEES alone or simultaneously with both 300 µM CEES 10 ng/ml LPS for various time intervals (as indicated). NO production measured as concentration of nitrite in culture medium. Panel B: Western blot analysis of iNOS protein from the cells incubated with 300 µM CEES with or without 10 ng/ml LPS; cell lysates were prepared after 3, 6, 12, or 24 hour incubation (as indicated) as described in Materials and Methods; L, LPS; C, CEES.

ers [19] have shown that LPS exclusively induces the iNOS form of nitric oxide synthase in murine macrophages. Figure 3a shows DCFH oxidation in RAW 264.7 cells stimulated with different levels of LPS for 24 hours. In the absence of LPS, the rate of DCFH oxidation was extremely low but increased with increasing exposure to LPS; however, this effect was nearly saturated at LPS levels above 15 ng/ml.

We then measured the rates of DAF-2 oxidation in RAW 264.7 macrophages stimulated with 20 ng/ml LPS in the presence or absence of 500 μ M CEES during 24 hour incubations (Figure 3b). In the absence of LPS or CEES, minimal DAF-2 oxidation was observed. As expected, LPS alone induced a marked increase in DAF-2 oxidation. Next, macrophages incubated with LPS for 24 hours were then exposed (post-treatment) to 500 μ M CEES and the rate of DAF-2 oxidation immediately measured. As shown in Figure 3b, there was no change in rate of DAF-2 oxidation compared to cells treated with LPS alone. These data strongly support the notion that CEES does not directly inhibit iNOS enzymatic activity. Similar results were obtained with DCFH-DA staining (data not shown). As expected, macrophages simultaneously treated with both LPS and CEES for 24 hours show a marked decrease in either DAF-2 or DCFH oxidation.

To further confirm that DCFH oxidation is overwhelmingly due to iNOS, we incubated LPS-stimulated macrophages with ebselen (see Figure 3c). Ebselen is a selenoorganic compound that can inhibit both the activity of iNOS [20] and its induction by LPS [21]. Ebselen (25 μ M) almost completely inhibited the DCFH oxidation in RAW 264.7 cells treated with 10 ng/ml or 20 ng/ml LPS. Ebselen was not cytotoxic at the levels used in Figure 3 (data not shown).

Discussion

Overall, the experiments detailed in this work show that CEES treatment in LPS-stimulated RAW264.7 murine macrophages transiently inhibits intracellular NO generation by interfering with iNOS expression rather than by direct inhibition of iNOS enzymatic activity. CEES (as well as HD) undergo rapid hydrolysis in aqueous solutions and this may account, in part, for the transitory nature of its inhibiting effect on iNOS induction [22]. LPS is a major component of the cell wall of gram-negative bacteria and is known to trigger a variety of inflammatory reactions in macrophages and other cells expressing CD14 receptors [23,24]. LPS is ubiquitous and is present in serum, tap water, and dust. Military and civilian personnel would, indeed, always have some degree of exposure to environmental LPS.

LPS stimulation of macrophages is known to involve the activation of protein phosphorylation by kinases as well as the activation of nuclear transcription factors such as NF- κ B [25-28]. An important consequence of NF- κ B activation in macrophages is the induction of iNOS expression followed with highly elevated NO production [12]. Nitric oxide has been demonstrated to have an important role in promoting cell death; however, the precise nature of this role varies with cell type and the dose. Low levels of nitric oxide protect RAW 264.7 macrophages from hydrogen peroxide induced apoptosis [29], however, nitric oxide has also been reported to induce apoptosis in J774 macrophages [14]. Nitric oxide can induce cell death through energy depletion-induced necrosis and oxidant-induced apoptosis.

We are currently exploring the potential molecular mechanism(s) whereby CEES interferes with iNOS expression in LPS stimulated macrophages. It is possible that GSH depletion caused by CEES determines iNOS expression. There are strong evidences suggesting that thiol depletion and iNOS expression are interrelated [30-32]. For example, LPS stimulated macrophages depleted of GSH exhibit a decreased level of iNOS protein and nitrite production [32]. Similarly, both *in vitro* [30] and *in vivo* [31] studies show that hepatocytes depleted of GSH have a diminished production of nitric oxide which is primarily due to a decreased level of iNOS mRNA. Vos et al. [31] have also presented evidence showing that GSH modulation of iNOS expression in hepatocytes is correlated with NF- κ B activation, i.e., GSH depletion is associated with a lack of NF- κ B activation. The influence of GSH depletion is not, however, consistent in all cell types. Glucose induced reduction of GSH in intestinal epithelial cells is associated with NF- κ B activation and upregulation of iNOS gene expression [33].

It is also possible that CEES decreases iNOS expression by interfering with the LPS-induced activation of transcription factor NF- κ B and/or signal transducer and activator of transcription-1 α (STAT-1 α). It is interesting, therefore, that Gray [34] has found that both CEES and HD inhibit the *in vitro* binding of transcription factor activating protein-2 (AP-2) via alkylating the AP-2 DNA consensus binding sequence rather than by direct damage to the AP-2 protein. Furthermore, it is significant that neither CEES nor its hydrolysis products were found to damage the AP-2 transcription factoring in a manner that prevented its DNA binding [35]. Similar experiments have yet to be done with NF- κ B. Chen et al. [36] have also found that nitrogen mustard (bis(2-chloroethyl) methylamine) similarly inhibits the binding of AP-2 to its consensus sequence. Nitrogen mustard also was shown to inhibit the binding of NF- κ B to the GC-rich consensus sequence due to the interactions with DNA [37]. It is possible, therefore,

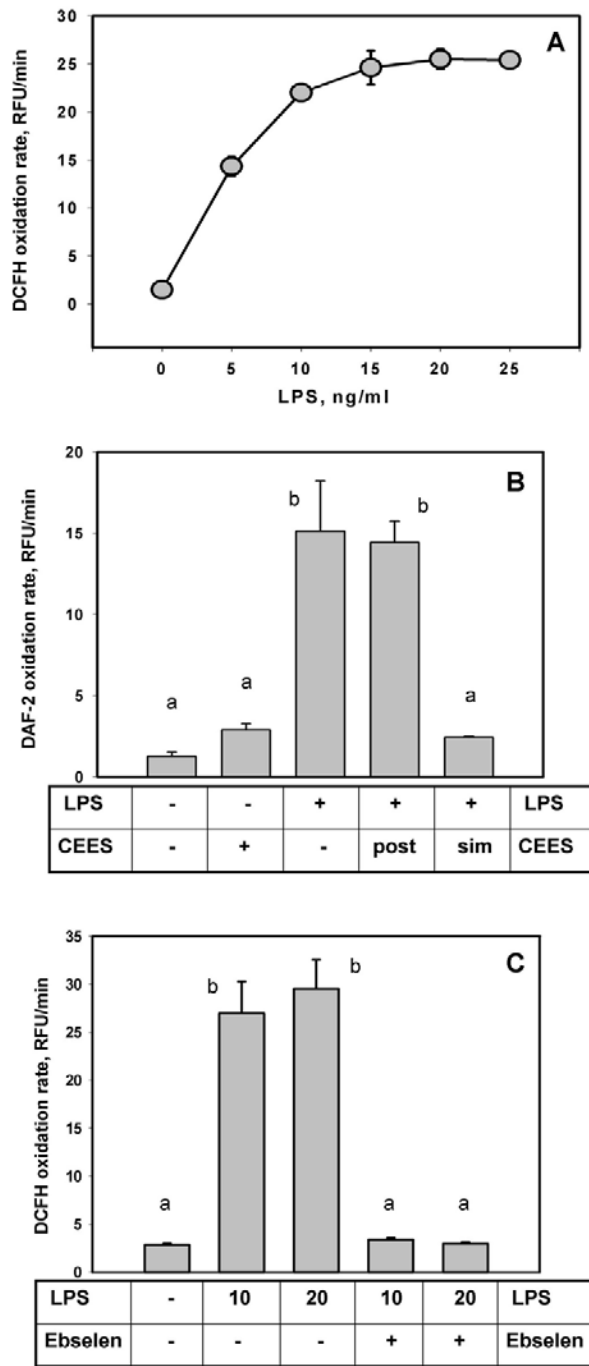


Figure 3
CEES reduces intracellular NO in LPS stimulated RAW264.7 macrophages. *Panel A:* Intracellular DCFH (20 μM) oxidation in LPS stimulated macrophages (as indicated) incubated for 2 h. Fluorescence (excitation 485 nm, emission 520 nm) was measured in Relative Fluorescence Units (RFU); the oxidation rate was expressed as RFU/min. *Panel B:* Macrophages stimulated with 20 ng/ml LPS, were incubated in the presence or absence of 500 μM CEES (as indicated) for 24 h. Post, CEES was applied after the 24 hours of LPS stimulation; Sim, CEES was applied simultaneously with LPS. *Panel C:* LPS stimulated cells were incubated in the presence or absence of 25 μM ebselen, a selective iNOS inhibitor (as indicated). 10, 10 ng/ml LPS; 20, 20 ng/ml LPS. Mean values not sharing a common letter are significantly different (p < 0.05).

that CEES also alkylates the NF- κ B consensus sequence thereby preventing the binding of the NF- κ B to the iNOS promoter. LPS and/or cytokine-inducible NF- κ B binding elements of the murine iNOS promoter have been identified [38], and they are rich of guanine, which is the major alkylation site for HD or CEES. The possible effect of CEES on iNOS promoter regulation is currently being explored.

Although the activation of NF- κ B due to mustard or CEES exposure have been shown in various cell lines [7,37,39], the detailed mechanism of this event is still unclear. Recent report [39] showed that NF- κ B-driven gene expression has maximum at 9 hours in HD treated keratinocytes. In contrast, in a guinea pig model, Chatterjee et al. [40] have shown that NF- κ B activation in lung tissues occurs shortly after CEES expose (1 hour), then disappears within 2 hours completely. However, in our experiments we did not observe any short term stimulating effect of CEES on NO production or iNOS expression (data not shown). Notably, the electrophoretic mobility shift assays used by Chatterjee et al. to measure NF- κ B activation show only the state of NF- κ B protein complex and provide no information regarding its binding to the DNA consensus sequences.

The physiological significance of potentially decreased iNOS expression by exposure to CEES or HD is not known. Considerable evidence, however, supports the view that nitric oxide production via iNOS plays a key role in wound healing [41-43]. Animal studies [16] have shown that the iNOS knockout mice have impaired wound healing that is reversed by iNOS gene transfer. Soneja et al. [44] have suggested that wound healing could be accelerated under circumstances where oxidative stress is minimized and nitric oxide production enhanced. We have initiated work to explore the role of antioxidants in preventing HD induced pathology in skin.

Conclusion

Our results show that CEES transiently inhibits NO production in LPS stimulated macrophages by inhibiting the expression of iNOS protein and not by modulating the enzymatic activity of iNOS. The decreased iNOS expression induced by CEES suggests that this alkylating agent inhibits the LPS stimulated activation of NF- κ B and/or STAT-1 α transcription factors, and this possibility is being investigated. We cannot directly address the physiological significance of our *in vitro* results, however, both decreased expression of iNOS and decreased production of nitric oxide are associated with impaired wound healing [16,41,43,44]. It is likely that the CEES or HD toxicity is modulated by a complex balance between nitric oxide production, thiol depletion and oxidative stress.

Methods

Materials

RPMI-1640 medium without phenol red and fetal bovine serum with a low endotoxin level were purchased from Life Technologies (Gaithersburg, MD). Rabbit anti-mouse iNOS antibody was obtained from Transduction Laboratory (Lexington, KY). Horseradish peroxidase conjugated anti-rabbit polyclonal antibodies, *Escherichia coli* lipopolysaccharide serotype 0111:B4, 3-(4,5-dimethylthiazolyl-2)-2,5-diphenyltetrazolium bromide (MTT), and 2-chloroethyl ethyl sulphide were obtained from Sigma Chemical Company (St. Louis, MO).

Cell culture and treatments

RAW264.7 murine macrophage-like cells (American Type Culture Collection, Rockville, MD) were cultured at 37°C in a humidified incubator with 5% CO₂ in RPMI-1640 medium with 10% fetal bovine serum, 50 U/ml penicillin and 50 mg/ml streptomycin (GiBcoBRL Grand Island, NY). CEES was used as a fresh (2 week old or less) 50 mM stock solution in dried ethanol. LPS was prepared as a 1 mg/ml stock solution in PBS and stored at -20°C for up to 3 months.

MTT assay

The MTT (3-(4,5-dimethylthiazool-2yl)-2,5-diphenyltetrazolium bromide) assay was performed by a slight modification of the method described by Wasserman et al. [45,46]. Briefly, at the end of each experiment, cultured cells in 96 well plates (with 200 μ l of medium per well) were incubated with MTT (20 μ l of 5 μ g/ml per well) at 37°C for 4 hours. The formazan product was solubilized by addition of 100 μ l of dimethyl sulfoxide (DMSO) and 100 μ l of 10% SDS in 0.01 M HCl and the OD measured at 575 nm (Molecular Devices SPECTRAMax Plus microplate reader).

Western blot analysis

Cellular protein lysates were prepared as described in the protocol from Transduction Laboratory (Lexington, KY). Briefly, about 10⁶ adherent cells were rinsed once with cold PBS and solubilized by boiling in 0.1 ml of SDS-PAGE sample buffer for 5 min. Protein concentration was determined by the BCA protein assay (Pierce Chemical Co., Rockford, IL). A 30 μ g aliquot of protein was separated via 8% SDS-PAGE and electrotransferred onto a nitrocellulose membrane. Western blotting was performed with a rabbit polyclonal antiserum against the C-terminal (961 to 1144 amino acids) sequence of mouse iNOS (Transduction Lab, Lexington, KY). The protein was detected using an enhanced chemiluminescence kit from Amersham Life Science (Arlington Heights, IL). Murine iNOS (Calbiochem, CA) was used as a positive control.

Determination of NO production

The production of NO, reflecting cellular NO synthase activity, was estimated from the accumulation of nitrite (NO_2^-), a stable breakdown product of NO, in the medium. Nitrite was measured using the Griess reagent according to the method of Green et al. [47]. Briefly, an aliquot of cell culture medium was mixed with an equal volume of Griess reagent which reacts with nitrite to form an azo-product. Absorbance of the reaction product was determined at 532 nm using a microplate reader (Molecular Devices Microplate Reader). Sodium nitrite was used as a standard to calculate nitrite concentrations.

Intracellular NO measurement

Assays were performed using 96-well tissue culture plates as described by Imrich and Kobzik [17]. The cell density was adjusted to $2 \times 10^5/\text{ml}$, and a 100 μl aliquot of the cell suspension in media was placed put in each well. CEES and LPS solutions to achieve desired concentrations were added and the plate incubated for 24 h at 37°C in 5% CO_2 . Following the removal of media, serum free 1640 RPMI supplemented with 10 mM HEPES containing 20 μM DCFH-DA or 10 μM DAF-2DA (final concentration) was added, and the plates incubated for 2 h at 37°C. Fluorescence intensity (relative fluorescence unit, RFU) was continuously monitored using 485 nm for excitation and 520 nm emission in a fluorescence microplate reader (FluorStar Microplate Reader, BMG).

Statistical analyses

Data were analyzed by followed with the Scheffe test for significance with $p < 0.05$. Results were expressed as the mean \pm SD. In all the Figures, mean values not sharing a common letter are significantly different ($p < 0.05$). Mean values sharing a common letter are not significantly different. The mean values and standard deviations of at least three independent experiments are provided in all the Figures.

Abbreviations

HD, sulphur mustard gas

CEES, 2-chloroethyl ethyl sulphide

LPS, lipopolysaccharide

NO, nitric oxide

iNOS, inducible nitric oxide synthase

NF- κB , nuclear factor kappa B

STAT-1 α , signal transducer and activator of transcription-1 α

DCF, dichlorofluorescein

DCFH, dichlorofluorescein

DCFH-DA, dichlorofluorescein diacetate

TNF- α , tumor necrosis factor-alpha

IL-1 β , interleukin-1 beta

AP2, activating protein 2

MTT, 3-(4,5-dimethylthiazool-2-yl)-2,5-diphenyltetrazolium bromide

DMSO, dimethyl sulfoxide

DEM, diethylmaleate

BSO, buthionine sulfoximine

DAF-2DA, 4,5-diaminofluorescein diacetate

Authors' contributions

WLS supervised the overall conduct of the research, which was performed in his laboratory. MQ and HY carried out all of the experimental work in this study and performed the statistical analyses. WLS and VP analyzed the data and drafted the manuscript. MS (along with WLS) conceived of the study, participated in the study design, and provided continuous evaluation of the experimental data. All authors read and approved the final manuscript.

Acknowledgements

This research was supported by two United States Army Medical Research Command Grants: "The Influence of Antioxidant Liposomes on Macrophages Treated with Mustard Gas Analogues", USAMRMC Grant No. 98164001, and "Topical Application of Liposomal Antioxidants for Protection against CEES Induced Skin Damage", USAMRMC Grant No. W81XWH-05-2-0034.

References

1. Smith KJ, Skelton H: **Chemical warfare agents: their past and continuing threat and evolving therapies. Part I of II.** *Skinmed* 2003, **2(4)**:215-221.
2. Yourick JJ, Dawson JS, Benton CD, Craig ME, Mitcheltree LW: **Pathogenesis of 2,2'-dichlorodiethyl sulfide in hairless guinea pigs.** *Toxicology* 1993, **84(1-3)**:185-197.
3. Elsayed NM, Omaye ST, Klain GJ, Korte DW Jr.: **Free radical-mediated lung response to the monofunctional sulfur mustard butyl 2-chloroethyl sulfide after subcutaneous injection.** *Toxicology* 1992, **72(2)**:153-165.
4. Elsayed NM, Omaye ST: **Biochemical changes in mouse lung after subcutaneous injection of the sulfur mustard 2-chloroethyl 4-chlorobutyl sulfide.** *Toxicology* 2004, **199(2-3)**:195-206.
5. Kadar T, Turetz J, Fishbine E, Sahar R, Chapman S, Amir A: **Characterization of acute and delayed ocular lesions induced by sulfur mustard in rabbits.** *Curr Eye Res* 2001, **22(1)**:42-53.
6. Gross CL, Innace JK, Hovatter RC, Meier HL, Smith WJ: **Biochemical manipulation of intracellular glutathione levels influences**

- cytotoxicity to isolated human lymphocytes by sulfur mustard. *Cell Biol Toxicol* 1993, **9(3)**:259-267.
7. Atkins KB, Lodhi IJ, Hurley LL, Hinshaw DB: **N-acetylcysteine and endothelial cell injury by sulfur mustard.** *J Appl Toxicol* 2000, **20 Suppl 1**:S125-8.
 8. Arroyo CM, Schafer RJ, Kurt EM, Broomfield CA, Carmichael AJ: **Response of normal human keratinocytes to sulfur mustard (HD): cytokine release using a non-enzymatic detachment procedure.** In *Hum Exp Toxicol Volume 18*. Issue 1 ENGLAND ; 1999:1-11.
 9. Sabourin CL, Petrali JP, Casillas RP: **Alterations in inflammatory cytokine gene expression in sulfur mustard-exposed mouse skin.** *J Biochem Mol Toxicol* 2000, **14(6)**:291-302.
 10. Stone WL, Qui M, Smith M: **Lipopolysaccharide enhances the cytotoxicity of 2-chloroethyl ethyl sulfide.** *BMC Cell Biol* 2003, **4(1)**:1.
 11. Li YH, Yan ZQ, Brauner A, Tullus K: **Activation of macrophage nuclear factor-kappa B and induction of inducible nitric oxide synthase by LPS.** *Respiratory research* 2002, **3**:23.
 12. Kleinert H, Pautz A, Linker K, Schwarz PM: **Regulation of the expression of inducible nitric oxide synthase.** *European journal of pharmacology* 2004, **500(1-3)**:255-266.
 13. Borutaite V, Brown G: **What else has to happen for nitric oxide to induce cell death?** *Biochem Soc Trans* 2005, **33(Pt 6)**:1394-1396.
 14. Borutaite V, Brown GC: **Nitric oxide induces apoptosis via hydrogen peroxide, but necrosis via energy and thiol depletion.** *Free Radic Biol Med* 2003, **35(11)**:1457-1468.
 15. Nakai K, Kubota Y, Kosaka H: **Inhibition of nuclear factor kappa B activation and inducible nitric oxide synthase transcription by prolonged exposure to high glucose in the human keratinocyte cell line HaCaT.** *The British journal of dermatology* 2004, **150(4)**:640-646.
 16. Yamasaki K, Edington HD, McClosky C, Tzeng E, Lizonova A, Kovesdi I, Steed DL, Billiar TR: **Reversal of impaired wound repair in iNOS-deficient mice by topical adenoviral-mediated iNOS gene transfer.** *J Clin Invest* 1998, **101(5)**:967-971.
 17. Imrich A, Kobzik L: **Fluorescence-based measurement of nitric oxide synthase activity in activated rat macrophages using dichlorofluorescein.** *Nitric Oxide* 1997, **1(4)**:359-369.
 18. Huang A, Li C, Kao RL, Stone WL: **Lipid hydroperoxides inhibit nitric oxide production in RAW264.7 macrophages.** *Free Radic Biol Med* 1999, **26**:526-537.
 19. Schmidt HH, Warner TD, Nakae M, Forstermann U, Murad F: **Regulation and subcellular location of nitrogen oxide synthases in RAW264.7 macrophages.** *Molecular pharmacology* 1992, **41(4)**:615-624.
 20. Hattori R, Inoue R, Sase K, Eizawa H, Kosuga K, Aoyama T, Masayasu H, Kawai C, Sasayama S, Yui Y: **Preferential inhibition of inducible nitric oxide synthase by ebselen.** *Eur J Pharmacol* 1994, **267(2)**:R1-2.
 21. Zhang N, Weber A, Li B, Lyons R, Contag PR, Purchio AF, West DB: **An inducible nitric oxide synthase-luciferase reporter system for in vivo testing of anti-inflammatory compounds in transgenic mice.** In *J Immunol Volume 170*. Issue 12 UNITED STATES ; 2003:6307-6319.
 22. Gray PJ: **Sulphur mustards inhibit binding of transcription factor AP2 in vitro.** In *Nucleic Acids Res Volume 23*. Issue 21 ENGLAND ; 1995:4378-4382.
 23. Wright SD, Ramos RA, Tobias PS, Ulevitch RJ, Mathison JC: **CD14, a receptor for complexes of lipopolysaccharide (LPS) and LPS binding protein.** *Science* 1990, **249(4975)**:1431-1433.
 24. Downey JS, Han J: **Cellular activation mechanisms in septic shock.** *Front Biosci* 1998, **3**:d468-76.
 25. Chen CC, Wang JK, Lin SB: **Antisense oligonucleotides targeting protein kinase C-alpha, -beta I, or -delta but not -eta inhibit lipopolysaccharide-induced nitric oxide synthase expression in RAW 264.7 macrophages: involvement of a nuclear factor kappa B-dependent mechanism.** In *J Immunol Volume 161*. Issue 11 UNITED STATES ; 1998:6206-6214.
 26. Fujihara M, Connolly N, Ito N, Suzuki T: **Properties of protein kinase C isoforms (beta II, epsilon, and zeta) in a macrophage cell line (J774) and their roles in LPS-induced nitric oxide production.** In *J Immunol Volume 152*. Issue 4 UNITED STATES ; 1994:1898-1906.
 27. Shapira L, Takashiba S, Champagne C, Amar S, Van Dyke TE: **Involvement of protein kinase C and protein tyrosine kinase in lipopolysaccharide-induced TNF-alpha and IL-1 beta production by human monocytes.** *J Immunol* 1994, **153(4)**:1818-1824.
 28. Shapira L, Sylvia VL, Halabi A, Soskolne WA, Van Dyke TE, Dean DD, Boyan BD, Schwartz Z: **Bacterial lipopolysaccharide induces early and late activation of protein kinase C in inflammatory macrophages by selective activation of PKC-epsilon.** *Biochem Biophys Res Commun* 1997, **240(3)**:629-634.
 29. Yoshioka Y, Kitao T, Kishino T, Yamamuro A, Maeda S: **Nitric oxide protects macrophages from hydrogen peroxide-induced apoptosis by inducing the formation of catalase.** *J Immunol* 2006, **176(8)**:4675-4681.
 30. Harbrecht BG, Di Silvio M, Chough V, Kim YM, Simmons RL, Billiar TR: **Glutathione regulates nitric oxide synthase in cultured hepatocytes.** *Ann Surg* 1997, **225(1)**:76-87.
 31. Vos TA, Van Goor H, Tuyt L, De Jager-Krikken A, Leuvenink R, Kuipers F, Jansen PL, Moshage H: **Expression of inducible nitric oxide synthase in endotoxemic rat hepatocytes is dependent on the cellular glutathione status.** *Hepatology* 1999, **29(2)**:421-426.
 32. Buchmuller-Rouiller Y, Corrandin SB, Smith J, Schneider P, Ransijn A, Jongeneel CV, Muel J: **Role of glutathione in macrophage activation: effect of cellular glutathione depletion on nitrite production and leishmanicidal activity.** *Cell Immunol* 1995, **164(1)**:73-80.
 33. Powell LA, Warpeha KM, Xu W, Walker B, Trimble ER: **High glucose decreases intracellular glutathione concentrations and upregulates inducible nitric oxide synthase gene expression in intestinal epithelial cells.** *J Mol Endocrinol* 2004, **33(3)**:797-803.
 34. Gray PJ: **Sulphur mustards inhibit binding of transcription factor AP2.** *Nucleic Acids Research* 1995, **23(Vol. 23)**:4378-4382.
 35. Gray PJ: **Sulphur mustards inhibit binding of transcription factor AP2 in vitro.** *Nucleic Acids Res* 1995, **23(21)**:4378-4382.
 36. Chen XM, Gray PJ, Cullinane C, Phillips DR: **Differential sensitivity of transcription factors to mustard-damaged DNA.** *Chemico-biological interactions* 1999, **118(1)**:51-67.
 37. Fabbri S, Prontera C, Brogini M, D'Incalci M: **Differential inhibition of the DNA binding of transcription factors NF kappa B and OTF-I by nitrogen mustard and quinacrine mustard: transcriptional implications.** *Carcinogenesis* 1993, **14(9)**:1963-1967.
 38. Spink J, Cohen J, Evans TJ: **The cytokine responsive vascular smooth muscle cell enhancer of inducible nitric oxide synthase. Activation by nuclear factor-kappa B.** *The Journal of biological chemistry* 1995, **270(49)**:29541-29547.
 39. Minsavage GD, Dillman 3d JF: **Protective role of CAPE on bifunctional alkylating agent-induced toxicity in keratinocytes via modulation of NF-kappaB, p53 and ARE/EpRE signaling.** In *Bioscience 2006 Medical Defense Review* ; 2006:94-94.
 40. Chatterjee D, Mukherjee S, Smith MG, Das SK: **Signal transduction events in lung injury induced by 2-chloroethyl ethyl sulfide, a mustard analog.** *J Biochem Mol Toxicol* 2003, **17(2)**:114-121.
 41. Schwentker A, Billiar TR: **Nitric oxide and wound repair.** *Surg Clin North Am* 2003, **83(3)**:521-530.
 42. Weller R: **Nitric oxide: a key mediator in cutaneous physiology.** *Clin Exp Dermatol* 2003, **28(5)**:511-514.
 43. Witte MB, Barbul A: **Role of nitric oxide in wound repair.** *Am J Surg* 2002, **183(4)**:406-412.
 44. Soneja A, Drews M, Malinski T: **Role of nitric oxide, nitroxidative and oxidative stress in wound healing.** *Pharmacol Rep* 2005, **57 Suppl**:108-119.
 45. Wasserman TH, Twentyman P: **Use of a colorimetric microtiter (MTT) assay in determining the radiosensitivity of cells from murine solid tumors.** *Int J Radiat Oncol Biol Phys* 1988, **15(3)**:699-702.
 46. Twentyman PR, Luscombe M: **A study of some variables in a tetrazolium dye (MTT) based assay for cell growth and chemosensitivity.** *Br J Cancer* 1987, **56(3)**:279-285.
 47. Green LC, Wagner DA, Glogowski J, Skipper PL, Wishnok JS, Tannenbaum SR: **Analysis of nitrate, nitrite, and [15N]nitrate in biological fluids.** In *Anal Biochem Volume 126*. Issue 1 UNITED STATES ; 1982:131-138.



Sulfur Mustard Toxicity Following Dermal Exposure

Role of Oxidative Stress, and Antioxidant Therapy

Victor Paromov,^a Zacharias Suntres,^b Milton Smith,^c and William L. Stone^a

^aDepartment of Pediatrics, East Tennessee State University, Johnson City; ^bNorthern Ontario School of Medicine, Advanced Technology and Academic Centre, 955 Oliver Road Thunder Bay, ON P7B 5E1; and ^cAMAOX, Ltd., #208, 6300 N. Wickham Rd, Melbourne, Fla.

Correspondence: stone@etsu.edu

Published October 30, 2007

Objective: Sulfur mustard (bis-2-(chloroethyl) sulfide) is a chemical warfare agent (military code: HD) causing extensive skin injury. The mechanisms underlying HD-induced skin damage are not fully elucidated. This review will critically evaluate the evidence showing that oxidative stress is an important factor in HD skin toxicity. Oxidative stress results when the production of reactive oxygen (ROS) and/or reactive nitrogen oxide species (RNOS) exceeds the capacity of antioxidant defense mechanisms. **Methods:** This review will discuss the role of oxidative stress in the pathophysiology of HD skin toxicity in both in vivo and in vitro model systems with emphasis on the limitations of the various model systems. Evidence supporting the therapeutic potential of antioxidants and antioxidant liposomes will be evaluated. Antioxidant liposomes are effective vehicles for delivering both lipophilic (incorporated into the lipid bilayers) and water-soluble (encapsulated in the aqueous inner-spaces) antioxidants to skin. The molecular mechanisms interconnecting oxidative stress to HD skin toxicity are also detailed. **Results:** DNA repair and inflammation, in association with oxidative stress, induce intracellular events leading to apoptosis or to a programmable form of necrosis. The free radical, nitric oxide (NO), is of considerable interest with respect to the mechanisms of HD toxicity. NO signaling pathways are important in modulating inflammation, cell death, and wound healing in skin cells. **Conclusions:** Potential future directions are summarized with emphasis on a systems biology approach to studying sulfur mustard toxicity to skin as well as the newly emerging area of redox proteomics.

SULFUR MUSTARD: A CENTURY OF THREAT

Sulfur mustard (SM) or mustard gas (bis-2-(chloroethyl) sulfide, military code: HD) is a chemical warfare agent classified as a weapon of mass destruction. Mustard gas was one of the first chemical weapons deployed against troops on a battlefield during World War I, almost hundred years ago. Since then, the military use of mustard gas has been documented in a number of situations. In 1988, HD was used with devastating results

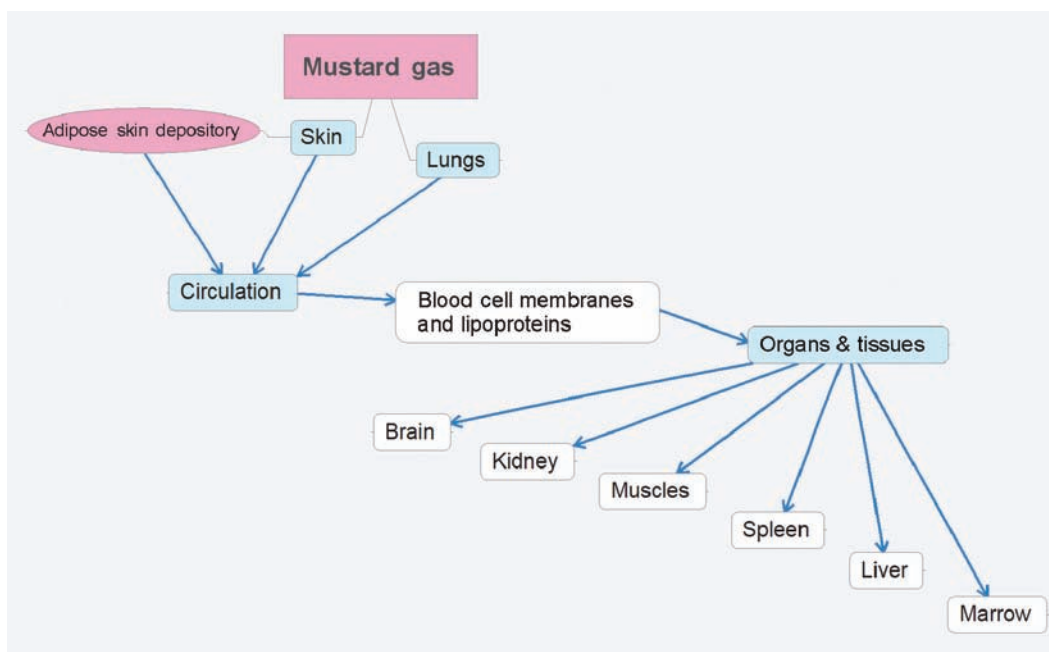


Figure 1. Distribution and accumulation of HD via circulation after dermal/inhalation exposure.

by Saddam Hussein's military forces against civilian targets in Halabja and later during the Iran-Iraq war. Mustard gas produces casualties in the battlefield and forces opposing troops to wear full protective equipment thus slowing the tempo of military operations. It is highly probable that mustard gas could be used by terrorists since it is a simple chemical compound readily synthesized without elaborate technology. Moreover, as a "persistent agent" (US Army classification) aerosolized mustard gas presents a threat for up to 1 week under dry and warm weather conditions because it remains in the environment until fully hydrolyzed. Along with nerve agents, mustard gas presents a major threat as a potential and effective chemical weapon. The possibility of low technology production, easy stockpiling, and difficulty in verifying its storage makes mustard gas a continuing worldwide threat. Presently, there is no antidote or effective treatment for mustard gas intoxication.

PATHOPHYSIOLOGY OF SULFUR MUSTARD ON SKIN

Clinical and physiological characteristics

Mustard gas is lethal in high doses and causes severe damage to the interface organs, that is, skin, lungs, respiratory tract, and eyes. The most prominent toxic effects of HD are on skin where it produces severe damage including extremely slow healing lesions and blisters which can ulcerate, vesicate, and promote secondary infections. Because of its hydrophobic nature, mustard gas easily penetrates and accumulates in the lipid component of exposed tissues. Upon contact with the skin, about 80% of HD evaporates and only about 20% is absorbed by the skin. Skin not only accumulates but also distributes HD to other tissues. Only about 10%–12% of the initially absorbed HD is retained in the skin, whereas up to 90% of HD enters circulation as indicated in Figure 1¹ Extractable skin reservoirs of HD can be

found in the dermis and epidermis even 24 to 48 hours postexposure.² In the case of a lethal poisoning, HD concentration in skin blisters remains very high even 7 days after exposure.³ Consequently, even after the initial exposure, skin reservoirs continue to distribute HD via circulation to the body tissues thereby increasing damage to several organs. Figure 1 schematically shows the distribution pathway of HD toxicity throughout the human body. We would like to point that, although skin is the initial accumulator of HD, its toxic effect is also prominent in distal organs. Therefore, the effect of HD after dermal exposure is not limited only to skin tissues

While the epidermis contains no blood vessels, both the dermis and the subcutaneous regions are rich in blood vessels. Adipose cells in the subcutaneous skin layer are likely to be a depository for HD due to their high lipid content (as indicated in Figure 1). Moreover, HD solubilized in adipose cells would be out of contact with water and thereby resistant to hydrolysis. After acute skin exposure, HD would be systemically delivered to various tissues in the body via lipid rich blood cell membranes and plasma lipoproteins and accumulate in lipid rich tissues (adipose tissues, brain, and skin). Chemical analyses following acute HD exposure show a high accumulation in thigh fat, brain, abdominal skin, kidney, and muscle tissues, in decreasing order.³ In addition, HD can be found in the spleen, liver, and bone marrow.⁴ The organs acquiring the most damage after dermal and/or respiratory exposure are indicated in Figure 1.

Skin damage caused by aerosolized HD appears after a latent period of up to 24 hours. First symptoms, such as itching, burning, and erythema, are followed by hyperpigmentation, tissue necrosis, and blister formation in warm moist areas of the body. When a large skin area is exposed to HD, medical conditions can be complicated by fluid imbalance, general inflammation, systemic intoxication, and secondary infection. At high doses, HD can also produce systemic effects with gastrointestinal symptoms (nausea and vomiting), respiratory distress due to the bronchospasm, temporary blindness as well as corneal damage. In most lethal cases, massive skin burns and wounds, as well as lung damage, are the primary causes of death. Since it damages DNA, mustard gas promotes mutagenesis and carcinogenesis.^{1,5-7} Acute and severe exposures to HD have been shown to produce skin cancers.^{8,9}

A few limited cases of HD exposure in humans provide some evidence for oxidative stress. HD metabolites derived from hydrolysis (thiodiglycol, thiodiglycol sulphoxide), as well as HD metabolites from glutathione (GSH) conjugates by the beta-lyase pathway, can be found in human urine after HD exposure.^{10,11} Both thiodiglycol sulphoxide and beta-lyase metabolites can be detected indicating GSH conjugation. Thiodiglycol has also been detected in urine samples from individuals not exposed to HD and is therefore not useful as a definitive marker for HD exposure.¹¹ In contrast, HD metabolites from the glutathione (GSH)/beta-lyase pathway are specific for HD exposure.^{10,11} These observations suggest that GSH depletion occurs in humans, and that GSH-HD/beta-lyase pathway metabolites provide a specific and useful biomarker for diagnosing HD exposure. GSH is a key intracellular antioxidant and its depletion by HD would be expected to increase oxidative stress.

The effects of HD in humans are very complicated and not fully elucidated. Figure 2 summarizes some of the key potential molecular mechanisms for HD toxicity in skin cells (as discussed in more detail below). Macromolecular damage and thiol depletion are primary and presumably the most dangerous intracellular events following HD exposure to

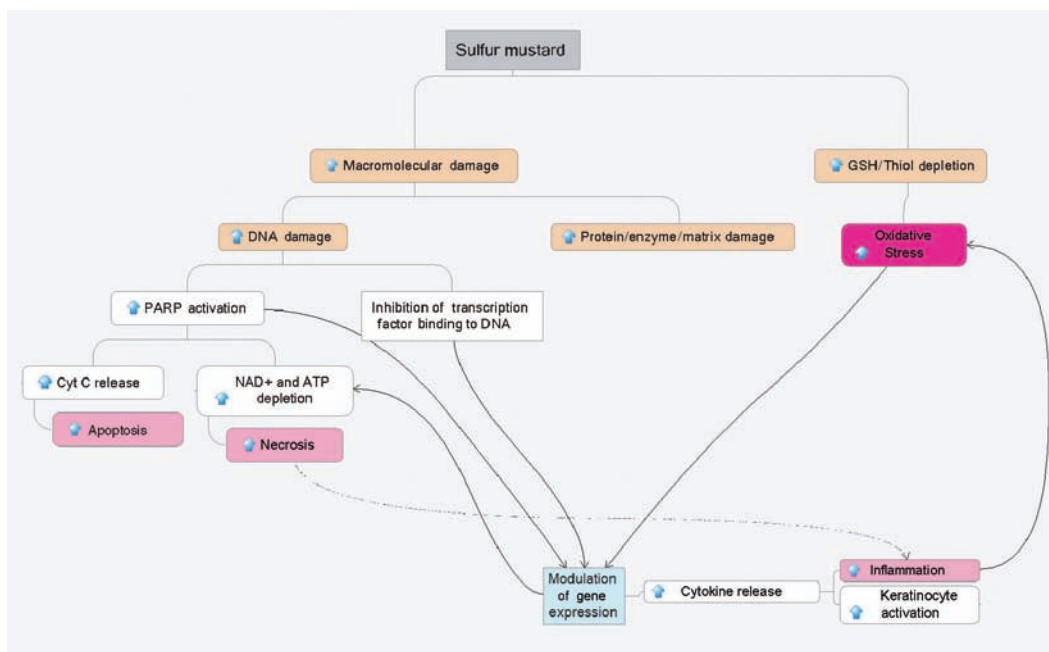


Figure 2. Schematic representation of the hypothesized molecular mechanisms of HD toxicity in skin cells.

skin cells. Macromolecular damage includes DNA damage as well as covalent modification of proteins and inactivation of enzymes. HD can affect cellular proteins indirectly by influencing expression and directly by altering the function of various enzymes and causing fragmentation of the extracellular matrix and cell detachment. GSH and total cellular thiol depletion is considered to be the major source of the oxidative stress. These primary damaging events modulate gene expression and induce inflammation and oxidative stress, which finally leads to apoptosis and/or necrosis (see Fig 2).

GENERAL COUNTERMEASURES

Presently, elimination of contact, decontamination, and supportive therapies are the only primary treatments for vesicant exposure. Respirators and protective masks are effective in preventing inhalation, and special protective clothing can be used to eliminate skin exposure. Various decontaminating agents can eliminate or effectively reduce the toxic effect of HD if used immediately after the exposure. Ambergard XE-555 Resin reactive powder, hypochlorite neutralizing solutions, reactive skin lotions, and absorbent powders can be used to remove HD from human skin. Substantial HD reservoirs can be found in human skin even 24 hours after exposure.¹² These reservoirs can account for up to 35% of the total dose, and it is important, therefore, to develop decontaminating techniques capable of the removing such reservoirs thereby reducing further skin and systemic damage. Graham et al¹³ have provided an excellent review of the strategies and current therapies for treating

cutaneous HD toxicity and promoting wound healing. An optimal therapeutic approach is, however, still lacking.

In this review, we will focus on the potential role of antioxidant therapy; we will review the data from *in vivo* and *in vitro* models suggesting that oxidative stress is an important molecular mechanism underlying HD toxicity and that antioxidants can be therapeutically useful. The strengths and limitations of the *in vivo* and *in vitro* models will be detailed.

MUSTARD GAS/ANALOG-INDUCED OXIDATIVE STRESS IN ANIMAL MODELS AND THE EFFECTS OF ANTIOXIDANTS

Detailed information about HD toxicity to human skin, especially at the molecular level, is very limited. Animal models are, therefore, the major source of information about the pharmacokinetics and the molecular mechanisms of HD skin toxicity. Unfortunately, there is no animal model that exactly mimics the development of HD injury in human skin. Young swine and miniature swine skin are, however, considered to be the best models since they have a similar skin structure (epidermis, dermis, and subcutaneous tissue) and barrier function. Furred animals are poor models probably because their skin is not as well keratinized as human skin, thereby permitting more rapid penetration of drugs or toxins.

Despite limitations, the mouse ear model, the rabbit, the hairless guinea pig, the nude mouse, and the weanling swine have all been useful for studying the (1) pathophysiology, (2) molecular mechanism of action, and (3) efficacy of countermeasures for HD injury. Studies on the Yucatan mini-pig have demonstrated that laminin in the dermo-epithelial junction is a target for partial protease degradation following HD exposure. The protease cleavage of laminin networks may account for the blistering effect of HD.¹⁴ The logistics of dealing with even miniature swine has, however, limited their use in HD studies.

In 2002, Naghii¹⁵ reviewed much of the existing literature connecting HD toxicity and oxidative stress and suggested that further studies in animal models were well justified. Direct evidence for free radical formation in rat lung lavage following inhalation of HD vapor has been obtained by using electron paramagnetic resonance (EPR) and spin trapping techniques.¹⁶ These studies show a rapid formation of ascorbyl radicals followed by the formation of carbon-centered radicals.¹⁶

Elsayed et al^{17,18} have demonstrated that subcutaneous injections of either a butyl 2-chloroethyl sulfide (a monofunctional mustard analog) or 2-chloroethyl 4-chlorobutyl sulfide (a bifunctional mustard gas analog) in animal models caused an elevation in lung tissue lipid peroxidation as assayed by the thiobarbituric acid (TBA) assay. The TBA assay is, however, not very specific: rather than directly measuring levels of lipid hydroperoxide, this assay is generally considered a measure of total “thiobarbituric acid reactive substances” (TBARS). Total (GSH+GSSG) and oxidized (GSSG) glutathione contents in lung tissue were found to increase 1 hour and 24 hours after subcutaneous injection of butyl 2-chloroethyl sulfide.¹⁸ Subcutaneous injection of 2-chloroethyl 4-chlorobutyl sulfide was associated with increased GSSG and decreased GSH at 1 hour postexposure. The increased formation of GSSG and TBARS in lung tissues following subcutaneous injection of mustard analogs is consistent with oxidative stress and suggests that dermal exposure can impact distal organs. This notion is supported by the work of Vijayaraghavan et al,¹⁹ who found that dermally applied HD induces hepatic lipid peroxidation and GSH depletion in mice. In

this study, the generation of malondialdehyde (MDA) was used as an indirect measure of lipid peroxidation. Vitamin E or flavonoids, while not influencing hepatic GSH depletion, did reduce MDA levels, suggesting a therapeutic potential.¹⁹

The effects of topically applied HD on key antioxidant enzymes have been measured but with conflicting results. For example, Husain et al²⁰ found that HD decreased the levels of glutathione peroxidase in white blood cells, spleen, and liver compared to control. Elsayed et al,¹⁸ however, found an increased level of glutathione peroxidase compared to controls. Elsayed¹⁷ interpreted the increased level of glutathione peroxidase (and other antioxidant enzymes) as an upregulation in response to oxidative stress, whereas Husain et al²⁰ interpreted the decreased levels of glutathione peroxidase as a potential cause of oxidative stress. Careful *in vitro* work with purified enzymes may help clarify these issues.

Despite the importance of skin itself as a primary target for HD toxicity, this organ has not been extensively studied with respect to oxidative stress. Yourick et al,²¹ using the hairless guinea pig model, analyzed the skin NAD⁺ and NADP⁺ content as a function of time after HD exposure. Skin NAD⁺ content was found to decrease to a minimum after 16 hours (20% of control) whereas NADP⁺ levels increased (260%) between 1 and 2 hours and returned to control levels at 4 hours. This marked increase in NADP⁺ levels was thought to be an early marker of oxidative stress and a contributory factor for HD toxicity.²¹ Increased NADP⁺ levels are a result of increased NADPH consumption: NADPH is a major source of reducing equivalents for key antioxidant enzymes such as glutathione reductase/peroxidase and thioredoxine reductase/peroxidase and lack of NADPH would be a source of oxidative stress.

The data presented above support the view that diminished antioxidant protective mechanisms are a consequence of HD exposure. It is less clear, however, whether or not the resulting oxidative stress is a direct contributing factor to mustard toxicity or a secondary effect due to inflammation. In any event, the ability of exogenous antioxidants (as discussed below) to decrease HD toxicity supports the hypothesis that decreasing oxidative stress and/or inflammation is a viable therapeutic strategy.

Antioxidant protection in animal models

As early as 1985, work by Vojvodic et al²² demonstrated that vitamin E was very effective in extending the survival time of rats acutely poisoned by HD. Vitamin E is, however, a generic term referring to at least 4 different tocopherols (alpha-, beta-, gamma-, and delta-) and 4 tocotrienols (alpha-, beta-, gamma-, and delta-). The particular form of vitamin E used in the Vojvodic et al experiments was not specified.²² Vitamin E is generally considered to be the primary lipid soluble antioxidant but it is now recognized that vitamin E has important “nonantioxidant” roles in modulating various signal transduction and gene regulation pathways.²³⁻²⁵ Moreover, the different chemical forms of vitamin E are now known to have distinct chemical and biological properties.^{26,27} It is important, therefore, to specify the particular chemical and stereochemical form of vitamin E used in a given experiment.

Superoxide dismutase (SOD, EC 1.15.1.1) is a key antioxidant enzyme that catalyzes the dismutation of superoxide radicals into oxygen and hydrogen peroxide. Eldad et al²⁸ studied the therapeutic role of both Cu-Zn-SOD (cytosolic form) and Mn-SOD (mitochondrial form) in HD skin damage, using the Hartley guinea pig model. Pretreatment of the animals

by intraperitoneal injection with either form of SOD resulted in a dramatically reduced skin lesion area induced by HD.²⁸ Treatment with SOD was, however, not effective when given 1 hour after HD poisoning.²⁸ These data strongly suggest that superoxide radicals play a key role in HD-induced skin toxicity. Superoxide radicals alone are not a particularly damaging form of free radicals but they rapidly react with nitric oxide radicals to form peroxynitrite, which is a potent oxidant capable of causing tissue damage.²⁹⁻³¹

HD and its analogs are alkylating agents that chemically react with and deplete biological thiols such as GSH, which is a key intracellular antioxidant. By promoting ROS generation and lipid peroxidation (as discussed above), HD will also promote the consumption of GSH and a reduced level of NADPH (see above) will inhibit the regeneration of GSH from GSSG. It is reasonable, therefore, that exogenous GSH or *N*-acetyl-L-cysteine (NAC) would help minimize oxidative stress induced by HD or its analogs. Kumar et al³² tested the potential protective effect of GSH given to Swiss albino female mice following acute exposure to HD by either inhalation or percutaneous routes. GSH was administered by intraperitoneal injection and the dose was 400 mg/kg of body weight, which translates into about a 20 mM concentration in blood. Survival time following inhalation exposure to HD was increased by GSH administration as well as 2 other antioxidants: trolox (6-hydroxy-2,5,7,8-tetramethylchroman-2-carboxylic acid), which is a water-soluble derivative of alpha-tocopherol, and quercetin, which a flavonoid.³² Inhalation exposure to HD depleted hepatic GSH levels, and increased hepatic and lung lipid peroxidation (as indirectly measured by MDA levels), and exogenous GSH was able to reduce lung and hepatic lipid peroxidation as well as prevent GSH depletion in these tissues.³² None of the 3 antioxidants tested were able to significantly increase survival time following percutaneous exposure to HD but exogenous GSH was effective in preventing GSH depletion in blood and liver. Surprisingly, lung levels of GSH were not altered by percutaneous HD exposure.³² The data present in work by Kumar et al³² show that the potential effectiveness of antioxidant therapy is dependent on the route of HD exposure.

The role of GSH and NAC (and other antioxidants) in attenuating acute lung injury by 2-chloroethyl ethyl sulfide (CEES) has recently been studied in a rat model in which lung damage was quantitatively measured by the extravasation of¹²⁵I-bovine serum albumin into the extravascular compartment.^{33,34} CEES is a monofunctional analog of HD that has proven very useful in mimicking HD exposure. When the experimental animals were depleted of either complement or neutrophils prior to CEES exposure (by intrapulmonary injection) lung damage was significantly decreased.³⁴ Neutrophil depletion was accomplished by IP injection of rabbit anti-serum to rat polymorphonuclear neutrophils and complement depletion by IP injections cobra venom factor.³⁴ Antioxidants such as catalase, dimethyl sulfoxide, dimethyl urea, resveratrol, and NAC all provided significant protection in this animal model.³⁴ NAC (an acetylated form of L-cysteine) can directly function as free radical scavenger and its metabolites are capable of stimulating GSH synthesis.³⁵ NAC was found to be the most effective antioxidant among those tested^{33,34} and was effective even when given up to 90 minutes after lung exposure to CEES.

In the work of McClintock et al,³³ NAC was superior to GSH. In vitro work by Gross et al³⁶ found that pretreatment of human peripheral blood lymphocytes (PBL) with 10 mM NAC elevated GSH level to 122% of untreated control but caused only a partial protective effect on HD-induced cytotoxicity. These researches also noted work by Meister and Anderson, suggesting³⁷ that exogenously added GSH does not appear to enter the cell very

effectively. This may help explain why NAC is superior to GSH in the work by McClintock et al.³³

Bhat et al³⁸ have studied the potential therapeutic use of lipoic acid to decrease oxidative stress and mustard gas toxicity in a rat model. Lipoic acid is a disulphide derivative of octanoic acid, and it is known to be a crucial prosthetic group for various cellular enzymatic complexes. Lipoic acid has been identified as a potent antioxidant and a potential therapeutic agent for the prevention or treatment of pathological conditions mediated via oxidative stress, as in the case of ischemia-reperfusion injury, diabetes, radiation injury, and oxidative damage of the central nervous system.³⁹⁻⁴³ Lipoic acid is taken up and reduced by cells to dihydrolipoate, a more powerful antioxidant than the parent compound, which is also exported to the extracellular medium; hence, protection is affected in both extracellular and intracellular environments. Both lipoic acid and dihydrolipoate, in addition to their direct antioxidant properties, have been shown to regenerate, through redox cycling, other antioxidants such as vitamin C and vitamin E, and to raise intracellular glutathione levels.^{44,45} Bhat et al³⁸ found that lipoic acid pretreatment decreased the levels of lipid peroxidation (measured as MDA) in lung, skin, and eyes in HD treated rats but was not effective posttreatment.

Antioxidant liposomes as a potential countermeasure

Antioxidant liposomes may represent an optimal means of treating HD-induced skin lesions. The authors' laboratory is currently testing this hypothesis. The term "antioxidant liposome" is relatively new and refers to liposomes containing lipid soluble chemical antioxidants, water-soluble chemical antioxidants, enzymatic antioxidants, or combinations of these various antioxidants. Antioxidant liposomes hold great promise in the treatment of many diseases and conditions in which oxidative stress plays a prominent role.^{46,47} The relative ease of incorporating hydrophilic and lipophilic therapeutic agents into liposomes; the possibility of directly delivering liposomes to an accessible body site; and the relative nonimmunogenicity and low toxicity of liposomes have rendered this system highly attractive for drug delivery. Moreover, several studies have clearly indicated that the liposomal antioxidant formulations, compared to that of the free nonencapsulated antioxidants, exert a far superior protective effect against oxidative stress-induced tissue injuries.⁴⁸

Experimental studies have shown that liposomes and their constituents effectively penetrate skin.^{49,50} Topical application of antioxidant-liposomes is likely, therefore, to be particularly effective in enhancing the antioxidant status of skin. Work by Kirjavainen et al⁴⁹ suggests that liposomes containing dioleoylphosphatidyl ethanolamine (DOPE) are better able to penetrate into the stratum corneum than liposomes without DOPE. Similarly, ultradeformable liposomes, lipid vesicles with special membrane flexibility due to incorporation of an edge activator such as sodium cholate, have been shown to be superior in comparison to ordinary phosphatidylcholine liposomes (see <http://www.skinforum.org.uk/abstracts/ebtassam-essa.php>).

At present there are no data on the potential use of antioxidant liposomes in treating HD-induced skin lesions but McClintock et al³³ have found that liposomes containing pegylated (PEG) catalase, PEG-SOD, or the combination were very effective in reducing

CEES-induced lung injury in a rat model. Similarly, liposomes containing NAC, GSH, or resveratrol also were effective according to this study.

In vitro studies using human skin models

Keratinocyte cell lines

In vivo models are essential for testing countermeasures to HD or its analogs, however, in vitro models are also critical for rapid screening of potential therapeutic agents and for detailed studies at the molecular level. Skin is the largest organ of the human body with a complicated multilayer multicell type structure. As mentioned above, there is no model system perfectly mimicking human skin. Normal or immortalized human keratinocytes cultured on plastic as a monolayer represent the simplest and least inexpensive model and are suitable for an initial approach for HD toxicity studies. Normal human epidermal keratinocytes (NHEK) isolated from adult or infant fetal skin tissue are available commercially. These cells are easy to handle, can be frozen for long-term storage but require special medium containing a mixture of growth factors.⁵¹ Even then, NHEK cells spontaneously transform after 3–5 passages as they continuously undergo terminal differentiation.

Nevertheless, NHEK remains the only commercially available normal cell line possessing all of the structural and functional features of normal skin keratinocytes and is being used by many investigators to study mustard gas toxicity.⁵² However, the requirement of special growth medium and a short lifespan make this model more expensive than immortalized human keratinocytes such as human papilloma virus (HPV)–immortalized cell lines or spontaneously immortalized HaCaT cells. There are also a number of commercially available human keratinocyte cell lines immortalized via transfection with DNA coding E6 and/or E7 viral oncoproteins. All of these cell lines still require special medium with growth factors and, like NHEK, have a limited lifespan since they spontaneously transform after 10 to 15 passages.⁵³

The HaCaT cell line, originating in Germany, has recently become commercially available; it represents spontaneously immortalized adult human keratinocytes.⁵⁴ HaCaT cells are extremely easy to handle and do not require special medium. Theoretically, HaCaT cells have an unlimited lifespan but they do show morphological changes after 10 to 20 passages. Despite the altered growth potential, HaCaT cells still express differentiation-specific markers⁵⁴ and unlike HPV-immortalized cell lines, HaCaT cells are not tumorigenic when transplanted into nude mice.⁵⁴

It is well known that HD, like UV radiation, affects mostly proliferating keratinocytes within the lower dermis and basement membrane. Differentiating keratinocytes of the epidermis are much less susceptible to toxicity since they do not undergo apoptosis and respond weakly to inflammatory stimuli. Normal keratinocytes undergo terminal differentiation (so-called “cornification”) in response to a high (1 mM) exogenous Ca⁺⁺ concentration.⁵¹ Normal keratinocytes in vivo start to differentiate when they detach from the basement membrane and migrate to the suprabasal layers.⁵⁵ Thus, NHEK and HPV-immortalized keratinocytes, unlike HaCaT cells, spontaneously differentiate when subcultured in response to the cell detachment. Therefore, only the first passages of NHEK cells are truly proliferating, whereas every passage of HaCaT culture consists of proliferating cells. On the other hand, HaCaT cells show impaired production and release of IL-1⁵⁶ which is crucial for normal

keratinocyte proliferation and also plays an important role in keratinocyte activation and keratinocyte/fibroblast crosstalk in normal skin.⁵⁷

As previously acknowledged, HD-induced depletion of intracellular glutathione (GSH) is a triggering event for oxidative stress in skin. Smith et al⁵⁸ have shown that pretreatment of the human keratinocyte cell line, SVK-14, with GSH markedly increases the resistance to HD-induced cytotoxicity. Conversely, pretreatment with buthionine sulfoximine (BSO) increases the sensitivity of G361, SVK14, HaCaT, and NCTC 2544 human keratinocytes to HD toxicity.⁵⁹ BSO lowers intracellular GSH by irreversibly inhibiting the rate-limiting GSH synthesis enzyme γ -glutamylcysteine synthetase. Surprisingly, there is no reported direct evidence to date for the enhanced generation of ROS and/or RNOS in HD-treated keratinocytes.

As pointed out earlier, HD and its chemical analogs cause massive leukocyte infiltration in animal skin and lungs^{60,61} It is likely that lymphocytes and macrophages, attracted to the burned area by cytokines released from keratinocytes/fibroblasts, could be a major source of oxidative stress to skin cells. It has been demonstrated that HD-exposed NHEK cells express chemoattractants and cytokine.⁶²⁻⁶⁴ Moreover, an enhanced ability of NHEK cells to attract lymphocytes in vitro was demonstrated in an experiment in which the media from HD-treated keratinocytes was tested for chemoattractant activity to polymorphonuclear leukocytes purified from human blood.⁶⁵

Multilayer keratinocyte tissues

Multilayer skin tissues (so-called “3D skin models”) are a more realistic model for toxicological studies. The simplest models of this class consist only of keratinocytes such as the commercially available Epiderm, which is a few millimeters thick structure of human NHEK cells grown on top of a wet membrane. Epiderm provides the possibility of applying HD (or other gaseous agents) in vapor or aerosol form which closely simulates a real HD attack. However, this model represents differentiating keratinocytes on a collagen matrix and practically all of the cells within the tissue start to cornify at the moment they are fully grown. Blaha et al⁶⁶⁻⁶⁸ have characterized the ultrastructural, histological, and molecular response of the Epiderm model to CEES. The Epiderm system not only has great potential for identifying and developing sulfur mustard therapeutic agents but also has limitations. In vivo, skin damage would be accompanied by the rapid leakage of serum, leukocyte infiltration, and perhaps mast cell degranulation (see below) but these events will not occur in any of the available in vitro skin models.

More advanced tissue models, like EpidermFT full thickness skin tissue model, consist of 2 cell types: a bottom layer of human fibroblasts imbedded in gelatin and an upper multilayer of human keratinocytes. This particular model is particularly valuable for studies involving paracrine signaling (keratinocyte/fibroblast interactions). HaCaT cells, with normal human or mouse fibroblasts, have also been used to construct 3D models of human skin. However, the impaired IL-1 production in these cells presents some technical difficulties that can be overcome with the addition of human growth factors.⁵⁶ These multilayer skin models morphologically mimic the dermis and epidermis of human skin including the cuboidal appearance of the basal cell layer, the presence of the stratum spinosum and stratum granulosum with typical stellate-shaped keratohyalin granules, and the presence of numerous lamellar bodies that are extruded at the stratum granulosum–stratum corneum interface.

In a key experiment, Blaha et al⁶⁷ compared the effects of CEES on the secretion of key inflammatory mediators using 2 model human skin systems, the EpiDerm system (from MatTek Corporation) and the Skin2 system (a 3D skin model) from Advanced Tissue Sciences, which consists of differentiating keratinocytes on a fibroblast-collagen matrix. In the Skin2 system, the proinflammatory cytokine IL-1alpha increased in response to CEES but the proinflammatory cytokine IL-6 decreased: the EpiDerm showed undetectable levels of IL-6 and the levels of IL-1alpha did not change in response to CEES.⁶⁷ These data show that the presence of fibroblasts in the Skin2 model dramatically changes the cytokine secretion response to CEES.

More recently, Hayden et al⁶⁹ evaluated the effects of HD on the EpiDermFT skin model which has a 3D, highly differentiated human skin-like structure with an epidermis and a dermis. This in vitro model permits the study of dermal phenomena in which fibroblast-keratinocyte cell interactions are important as appears to be the case for CEES-induced skin injury (see above). Hayden et al⁶⁹ treated the EpiDerm-FT model with HD for 8 minutes and evaluated the structural effects at 6 and 12 hours postexposure. Histological analyses showed typical HD targeting of basal keratinocytes (cytopathology, condensed chromatin, pyknotic nuclei, and increased eosinophilia) and epidermal cleavage at the dermal/epidermal junction. Transmission electron microscopy showed that lamina densa of the basement membrane to be largely intact. The EpiDerm-FT model represents a major advance in the development of human skin models and its use in studying the molecular mechanisms/proteomics for HD/CEES toxicity is just beginning to be exploited.

Human skin allografts in immunodeficient mice

A third class of human skin model is provided by the use of human skin allografts in immunodeficient mice. Human skin cells, either genetically modified⁷⁰ or normal,⁷¹ were grafted onto nude mice and successfully used to examine HD-induced biochemical alterations in skin. In 1995, Rosenthal et al⁷⁰ described an engineered human skin model, in which human keratinocyte clones, with some genetic modifications, were grafted onto nude mice, where they formed histologically normal human skin. Later, the same group reported an advanced model developed in immunodeficient nude mice, where a pellet of cells containing human keratinocytes and fibroblasts were placed on top of the muscular layer at the graft site and grown for 1 week.⁷¹ Glass bulbs filled with HD can be directly applied to the sections of mouse skin containing the human skin allograft. Although these in vivo models are expensive and complicated, they possess a number of advantages over any of the in vitro cultured skin models. Grafted human skin models make it possible to obtain a detailed picture of HD-induced morphological, ultrastructural, and inflammatory alterations in various layers of skin cells possessing the realistic complexity of multiple cell-cell interactions. Recently, 3D human skin allografts in mice have allowed investigators to identify distinctive pre-vesication and postvesication phases and to monitor both dermal-epidermal separation and basal membrane alterations in response to HD exposure.^{72,73} However, a limitation of this model is the lack of a functional immune response in the recipient mice.

In spite of the ever higher degrees of physiological complexity, there is not a single model that reflects all the features of human skin. The choice of a particular model may, therefore, be dictated by the particular experimental design and goals. Wound healing studies, for example, would require an in vivo system with an intact immune system since

immune cells are known to contribute to skin regeneration. Moreover, immune cells are thought to play important roles both in HD-induced skin inflammation and in postexposure wound healing through the expression of proinflammatory cytokines (such as $\text{IL-1}\beta$, $\text{TNF-}\alpha$, IL-6 , and GM-CSF) within the first hour after exposure and proceeding through vesication and blister formation.⁶⁴ Leukocyte infiltration always starts shortly after HD treatment in mice, rabbits, or guinea pigs. In wound healing, leukocytes and macrophages provide many of the molecular signals regulating fibroblast and keratinocyte proliferation.

The effects of HD on all of the various cell types that come in contact with skin, including macrophages and mast cells, are also important in understanding the overall effects of HD on skin in vivo. Rikimaru et al⁷⁴ have used full-thickness human skin explants to study inflammatory mediators in response to topically applied HD. These investigators found that culture fluids from the HD-treated skin contained increased levels of histamine, plasminogen-activating activity, and prostaglandin E2 compared to control explants. It was concluded that both mast cells and epidermal cells were apparently involved in early mediation of the inflammatory response to HD.⁷⁴ In contrast, Inoue et al⁷⁵ found that the inflammatory response of the mouse ear to HD did not differ in mast cell deficient mice compared to normal mice. At present, there is no obvious explanation for the differences observed between the work of Rikimaru et al⁷⁴ and that of Inoue et al⁷⁵. It may well be that the mouse ear is not an optimal model for human skin. It is critically important to determine whether HD, or other toxic vesicants, degranulate mast cells since this process could be a major source of inflammatory mediators and, therefore, a major factor in modulating the immune response to HD. In particular, mast cell degranulation would release large amounts of $\text{TNF-}\alpha$, which is an inflammatory cytokine.

We have previously reported that lipopolysaccharide (LPS) as well as other inflammatory factors such as $\text{TNF-}\alpha$ and $\text{IL-1-}\beta$ amplify the toxicity of CEES⁷⁶ and that CEES is a potent inhibitor of nitric oxide production from inducible nitric oxide synthase (iNOS).⁷⁷ LPS is a major component of the cell wall of gram-negative bacteria and is known to trigger a variety of inflammatory reactions in macrophages and other cells having CD14 receptors.^{78,79} In particular, LPS is known to stimulate the macrophage secretion of nitric oxide⁸⁰ and inflammatory cytokines such as tumor $\text{TNF-}\alpha$ and $\text{IL-1-}\beta$.⁸¹ Figure 3 shows that RAW 264.7 macrophages stimulated with LPS at 100 ng/mL are markedly more susceptible ($P < .05$) to CEES cytotoxicity (24 hours with 500 μM) than resting macrophages as indicated by a dramatic drop in dehydrogenase activity as measured by the MTT ((3-(4,5-dimethylthiazol-2-yl)-2,5-diphenyltetrazolium bromide) assay. In the absence of LPS, CEES at a level of 500 μM did not significantly affect cell viability.⁷⁶ Figure 4 shows that CEES (100–500 μM for 24 hours) inhibits the secretion of nitric oxide into the cell medium by LPS stimulated macrophages in a dose-dependent manner.⁷⁷ In these experiments, nitrite secretion into the cell culture medium was used as a measure of nitric oxide synthesis. Macrophages (and mast cells) are both present in dermal tissues.

IgE-mediated mast cell degranulation is known to be inhibited by nitric oxide production.⁸² NO is a powerful antioxidant⁸³ and increased intracellular levels of NO are known to inhibit mast cell degranulation.⁸⁴ Significantly, mast cell degranulation and histamine release are stimulated by membrane lipid peroxidation and inhibited by antioxidants such as α -tocopherol.⁸⁵ Collectively, the information presented above suggests that HD/CEES could induce mast cell degranulation by increasing oxidative stress and/or

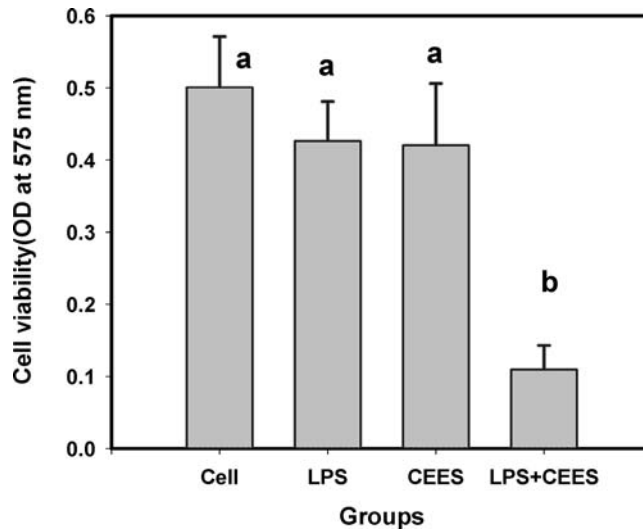


Figure 3. LPS (100 ng/mL) enhances the cytotoxicity of CEES (500 μ M). Means not sharing a common letter are significantly different ($P < .05$). Cytotoxicity was measured after 24 hours by the MTT assay.

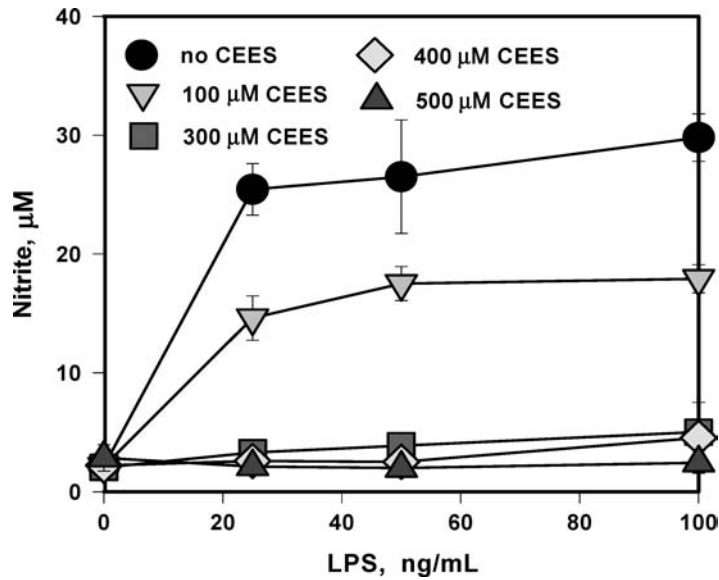


Figure 4. CEES inhibits NO production in LPS stimulated RAW 264.7 macrophages. Cells were simultaneously treated with various levels of CEES (as indicated) and low doses of LPS (as indicated). NO production was monitored as the concentration of nitrite in the culture media after 24 hours.

decreasing nitric oxide production. The subsequent release of TNF-alpha could enhance the cellular toxicity of HD/CEES.

NO generation, mediated by iNOS, is also crucial for the rapid healing of human skin wounds. Although, keratinocytes are known to express iNOS and generate NO in wound healing, it is likely that macrophages, known for their ability to express iNOS and generate high levels of NO, also contribute to the healing stimuli. Thus, it is tempting to suggest that the development of a 3-cell-type (macrophages/fibroblasts/keratinocytes) model would provide a unique and optimal model for studying skin vesication, blistering, and wound healing under very reproducible experimental conditions.

MOLECULAR MECHANISMS FOR MUSTARD TOXICITY

The molecular mechanisms of HD skin toxicity are complex and not yet fully understood. We will focus on 3 major types of interrelated events: primary macromolecule damage, oxidative stress, and inflammation. All of these processes are tightly interconnected and play central roles in HD toxicity. The hypothesized mechanisms of HD toxic effect in skin cells are summarized in Figure 2. In addition, we will discuss the importance of NO signaling modulation in HD toxicity since it is likely to be important for the postexposure wound healing process in skin.

Primary macromolecule damage

HD easily penetrates both cellular and nuclear membranes due to its hydrophobic nature. In the cytosol, it reacts with water forming a highly electrophilic ethylene episulfonium derivative that is the ultimate alkylating agent. DNA alkylation and crosslinking are well-documented primary intracellular damaging reactions of HD. Extensive DNA damage, due to alkylating agents, activates and overloads the DNA repair machinery. In particular, DNA damage induces expression of poly (ADP-ribose) polymerase (PARP), the key regulatory enzyme involved in DNA repair and hypothesized to regulate cell fate by modulating death and survival transcriptional programs.⁸⁶ HD induces PARP expression in normal human keratinocytes and the possible involvement of this nuclear enzyme in the regulation of HD cell death mechanisms has been extensively studied.⁸⁷⁻⁹¹

PARP-1 is the most abundant member of the of PARP protein family. PARP-1 binds to DNA structures that have single- and double-strand breaks, crossovers, cruciforms, or supercoils⁹²; it signals DNA rupture and facilitates base-excision repair.^{93,94} Normally, the intracellular level of PARP-1 is very low, and this enzyme can be detected in the cytosol only under stressful conditions. Upon binding to the damaged DNA sites, PARP-1 metabolizes β -nicotinamide adenine dinucleotide (NAD⁺) into branched polymers of ADP-ribose that are transferred to a set of nuclear proteins. This process also results in a very large decrease in the pyridine nucleotide pool. Poly(ADP-ribosyl)ation is thought to be beneficial for genome repair since modifications of proteins proximal to the DNA breaks facilitate multiple local openings of the condensed chromatin structure allowing the binding of the repair protein complex.^{93,95}

Despite the beneficial effect, PARP can induce apoptosis or necrosis in skin cells treated with HD⁹¹ or other alkylating agents.^{86,96} Thus, limited expression of PARP proteins helps in DNA repair and promotes cell survival but its overexpression (as in case of massive DNA damage) can induce cell death.⁹⁷ PARP overproduction, especially in cells utilizing aerobic glycolysis, can lead to the depletion of cellular NAD⁺ and ATP (see Fig 2) which rapidly promotes general intracellular bioenergetic collapse and oxidative stress resulting in a regulated form of necrosis.^{86,96,98-100} HD is cytotoxic to both dermal fibroblasts and epidermal keratinocytes. It has been suggested that PARP determines the mode of HD-induced cell death in skin fibroblast but not in keratinocytes.⁹¹ In mouse skin fibroblast the absence of PARP shifts the mode of HD-induced cell death shifts from necrosis to apoptosis,⁹¹ whereas keratinocytes, with or without PARP, primarily express an apoptotic form of cell death.⁹¹ HD-treated human keratinocytes show a PARP activation, an upregulation of proapoptotic p53 accompanied by a downregulation of antiapoptotic Bcl-2, and, finally, to caspase activation and apoptosis.^{87,90} This pathway was found to be Ca⁺⁺ and calmodulin dependent.⁹⁰

Necrosis due to PARP-induced depletion of NAD⁺ and ATP exhaustion during aerobic glycolysis is thought to be the main mechanism of cell death induced by DNA damaging agents, especially in proliferating cells.⁹⁶ However, these observations may vary with the dose of alkylating agent, with cell type and perhaps the particular composition of the culture medium (see below) in the case of in vitro studies. HD promotes apoptosis in HeLa cells (10–100 μ M),¹⁰¹ peripheral blood lymphocytes (6–300 μ M),¹⁰² keratinocytes (50–300 μ M),^{53,87} and endothelial cells (<250 μ M).¹⁰³ A time-dependent shift to necrosis was observed in HD-treated lymphocytes.¹⁰² but a shift toward necrosis is observed at higher levels of HD in endothelial cells (>500 μ M)¹⁰³ and HeLa (1 mM)¹⁰¹ Interestingly, human fibroblasts undergo necrosis even at lower concentrations of HD (100–500 μ M).⁹¹ In most human cell types, apoptosis predominates within 6–12 hours of postexposure time, whereas necrotic events markedly increase after 12–24 hours.

Countermeasures capable of preventing rapid ATP depletion and mitochondrial dysfunction could be protective against HD-induced necrosis. Unfortunately, this approach would not eliminate cell death completely since apoptosis would likely proceed. However, a shift from necrosis to the less inflammatory apoptotic pathway could possibly be beneficial by helping eliminate secondary infections and improving wound healing. PARP activation causes NAD⁺ depletion and NAD⁺ is required for glycolysis and pyruvate synthesis.¹⁰⁴ In the absence of pyruvate, mitochondrial respiration fails causing bioenergetic collapse and cell death via necrosis.⁸⁶ Therefore, the addition of a mitochondria substrate, such as pyruvate, glutamate, or glutamine, to the cell medium could be protective against necrosis.¹⁰⁴ A protective effect of pyruvate treatment has, indeed, been documented in genotoxic stress caused by nitrogen mustard or *N*-methyl-*N'*-nitro-*N*-nitrosoguanidine (MNNG), a chemical analog of HD used as anticancer drugs.^{96,100,104}

Alkyl pyruvates, such as methyl pyruvate and ethyl pyruvate, are excellent alternative mitochondrial substrates since they (unlike pyruvate) are stable in solution. In aqueous solutions, pyruvate spontaneously undergoes a series of chemical reactions yielding 2, 4-dihydroxy-2-methylglutarate, which is a mitochondrial poison.¹⁰⁵ In addition, alkyl pyruvates also function as effective and potent scavengers of free radicals. Pyruvates are capable of scavenging hydrogen peroxide (H₂O₂) and the hydroxyl radical (OH[•]).^{106,107} Administration of pyruvates was shown to protect against various types of oxidant-mediated

cellular and organ injuries in numerous in vitro and in vivo studies.^{108,109} These data further suggest that HD activation of PARP and the subsequent depletion of pyruvate is also a contributing factor for HD-induced oxidative stress.

In preliminary results, the authors' laboratory has observed that methyl pyruvate provides protection to human keratinocytes (HaCaT cell line) treated with CEES and a similar effect was observed with ethyl pyruvate (unpublished data). It is worth noting that commercially available serum-free media, formulated to culture NHEK cells, contains 0.5 mM sodium pyruvate. Keratinocyte media from Gibco, Sigma, and Cambrex all contain 0.5 mM pyruvate. It is possible, therefore, that necrosis has not been observed in HD-treated NHEK cells due to the protective effect of sodium pyruvate in the culture media.

In our experiments (unpublished data), however, we used immortalized HaCaT keratinocytes, which proliferate continuously but do not differentiate. Actively proliferating cells utilize aerobic glycolysis and are more susceptible to mitochondrial dysfunction and necrosis.^{86,96,100} After limited number of passages NHEK cells, unlike HaCaT cells, undergo terminal differentiation which is a form of cell death different from either apoptosis or necrosis.⁵⁵ This difference between HaCaT and NHEK cells theoretically could cause discrepancies in the cell death pathway caused by HD. Parallel experiments are now being done with NHEK and HaCaT cells to further characterize the protective effect of pyruvate to HD/CEES.

Inflammation

HD-treated normal human keratinocytes release proinflammatory TNF- α , IL-6, IL-1 β in a dose-dependent manner⁶² but the particular cytokine profiles observed differ depending on the skin model used and the dose of HD.^{63,64,110} Cytokine production and responses are known to be regulated by the activation of nuclear transcription factor-kappaB (NF-kappaB) and this activation also plays a key role in determining the fate of a damaged cell. There are numerous activators of NF-kappaB such as bacterial and viral infections, chemical damage, radiation, and oxidative stress. In response to these stimuli, an active NF-kappaB protein complex is liberated in the cytoplasm and it subsequently translocates to the nucleus and triggers selective gene expression. Among the genes regulated by NF-kappaB are adhesion molecules, pro-inflammatory mediators (IL-1 beta, TNF-alpha, interleukin 6), chemokines, IL-8, iNOS, E-selectin, vascular cell adhesion molecule 1 (ICAM-1), and granulocyte-macrophage colony stimulating factor (GM-CSF).^{34,111-114} In general, NF-kappaB activation also triggers antiapoptotic genes and promotes cell survival.

Although the precise mechanism(s) of HD-induced gene expression has not yet been fully described in skin cells, it is very likely connected to the DNA damaging effect of HD (see Fig 2) and could, therefore, be PARP-dependent. PARP-1 is known to be a coactivator of NF-kappaB.¹¹⁵; however, this pathway has not been fully explored in HD-treated keratinocytes or fibroblasts. It is also possible that HD modulates NF-kappaB and other nuclear factors by covalently modifying DNA binding sequences for transcription factors. Grey et al¹¹⁶ have shown that HD inhibits the in vitro binding of transcription factor activating protein-2 (AP-2) via alkylating the AP-2 DNA consensus binding sequence rather than by direct damage to the AP-2 protein.

In addition, it is highly possible that HD-induced oxidative stress also can stimulate inflammatory responses via transcription factors. Many of the activators of NF-kappaB can

be blocked with the use of antioxidants.^{117,118} Transcription factors AP-1,^{119,120} MAF and NRL,^{121,122} and NF-IL6^{123,124} are regulated by oxygen-dependent mechanisms, and sensitive to ROS. Interestingly, chemical compounds indirectly disrupting NF-kappaB activation induce apoptosis in cancer cells,¹²⁵⁻¹³⁰ whereas inhibitors of NF-kappaB activation protect HD-treated human keratinocytes.^{131,132}

It is also unclear how exactly the proinflammatory cytokines, such as IL-6, contribute to the HD-induced skin damage. It is known, however, that inflammatory processes contribute to the skin damage. In animal models, both skin and lung exposure to HD or CEES causes massive leukocyte infiltration, which starts shortly after the exposure and builds up continuously.^{60,61} The fact that skin burns and blistering have a latent period also suggests that secondary responses in skin cells/immune cells also contribute to the mechanisms of HD toxicity. HD treatment is known to induce NF-kappaB activation and release of inflammatory cytokines in both keratinocytes and macrophages.^{63,110,133-135} TNF-alpha, in general, induces apoptosis in keratinocytes and treatment with anti-TNF-alpha antibodies is protective against UV-induced skin lesions.¹³⁶ However, the effect of TNF-alpha in HD-treated skin is complex and an attempt to reduce cell death in normal human keratinocytes by blocking TNFR1, the major cell receptor for TNH-alphas was not successful.⁷¹

It is likely that keratinocyte activation (see Fig 2) plays an important role in HD toxicity. Activation of keratinocytes is a multistep pathway induced in response to skin injury. Activated keratinocytes are hyperproliferative and able to migrate to the site of injury in order to form layers of fresh cells in the dermis and epidermis. Activation is regulated by various cell signaling pathways including TNF-alpha.^{57,137} Since HD-treated keratinocytes release high levels of TNF-alpha in the medium,¹³³ we suggest that HD promotes keratinocyte activation, subsequent hyperproliferation, and an enhanced susceptibility to the PARP-mediated bioenergetic collapse. This series of molecular events would cause a shift from apoptosis to necrosis. Although a time- or concentration-dependent shift from apoptosis to necrosis has been well documented for HD-treated lymphocytes,¹⁰² endothelial cells,¹⁰³ and HeLa cells,¹⁰¹ such changes have not been noted for human keratinocytes. As discussed above, this may be due to the fact that NHEK cells are always protected from necrosis by pyruvate-containing media. The recently documented protective effect of NF-kappaB inhibitors in NHEK and HaCaT cells treated with HD^{131,132} also supports our speculation since these inhibitors downregulate TNF-alpha which would impair keratinocyte activation.

WOUND HEALING

NO signaling plays a key role in the inflammation and wound healing.¹³⁸⁻¹⁴⁰ Animal studies¹⁴¹ have shown that in iNOS knockout mice, wound healing is impaired but restored by iNOS gene transfer. Lack of NO and impaired expression of iNOS after the HD exposure are thought to be important events promoting skin burns and blistering. We have shown that HD treatment inhibits iNOS expression and NO synthesis (see Fig 4) in LPS-stimulated murine macrophages.⁷⁷ Suppression of iNOS expression and several protein activators of wound healing have also been found in human keratinocytes treated with HD.¹⁴²

In keratinocytes, the beginning stage of the wound healing process is determined by the activation process. Under conditions of physical injury, the keratinocyte cell cycle is activated and the cells become hyperproliferative and migrate to the site of injury in response to chemokines.^{57,137} Activation of keratinocytes, as well as their return to the healthy basal phenotype, is controlled by cytokines and growth factors produced by various cutaneous cell types, including keratinocytes and lymphocytes infiltrated at the wound site. Various intracellular signaling pathways are involved at the different stages of activation. Interestingly, NF-kappaB activation and consequent autocrine TNF-alpha production occur at the initial stages of the activation and allow keratinocytes to become hyperproliferative and migratory.^{57,137} Activation is terminated when lymphocytes, present at the wound site, release interferon-gamma (IFN-gamma), which induces the activation of STAT-1 and makes keratinocytes contract newly deposit fibronectin-rich basement membrane. Finally, transforming growth factor-beta (TGF-beta) secreted by fibroblasts induces the expression of K5 and K14, fully reverting the keratinocytes to a healthy basal phenotype and making them responsive to differentiation stimuli.⁵⁷

In human cells, expression of iNOS, which is the main NO-generating protein in keratinocytes,¹⁴³ is regulated synergistically by 2 major pathways: NF-kappaB and STAT-1.¹⁴⁴ As pointed above, both HD and its chemical analog CEES downregulate iNOS expression in murine macrophages⁷⁷ and human keratinocytes.¹⁴² Since NF-kappaB activation is well documented in NHEK cells,¹³¹⁻¹³³ it is possible that the impaired expression of iNOS in HD-treated cells could be attributed to a STAT-1-dependent mechanisms. In addition, the possible STAT-1 inhibition by HD could disrupt the IFN-gamma signaling pathway resulting in keratinocytes unable to terminate their wound healing state.⁵⁷ Thus, simultaneous HD-induced NF-kappaB activation and STAT-1 inhibition could alter necrosis, inhibit NO generation, prevent wound healing, and possibly affect vesication and blistering.

The molecular mechanisms whereby HD alters transcription factors activation are not fully elucidated. However, it is highly possible that the ability of mustards to alkylate DNA is involved. As pointed above, HD is capable of chemically modifying both proteins (via crosslinking of Cys residues) and DNA (via alkylation of guanine rich sequences, and crosslinking). It seems likely that HD would more effectively damage "more exposed" regions of DNA with accessibility to transcription factors. Interestingly, Gray¹¹⁶ had shown that HD inhibits the *in vitro* binding of transcription factor AP-2 via alkylation of the guanine-rich consensus DNA sequences but not by directly damaging the AP-2 protein. It is tempting to assume that other transcription factor functions could be affected by HD in a similar manner. However, the effects of HD on NF-kappaB and STAT-1 α have not been elucidated and AP-2 remains the only transcription factor studied in relation to HD toxicity.

Since some transcription factors are sensitive to ROS and to the redox state of the cell in general, it is likely that oxidative stress, inflammation, and NO signaling are tightly interconnected in skin and its dynamic responses to toxic agents. Soneja et al¹⁴⁵ have suggested that wound healing could be accelerated under circumstances in which oxidative stress is minimized but NO production remains elevated. On the other hand, under conditions elevating oxidative stress, the toxicity of mustards can be greatly enhanced. For instance, the HD analog CEES shows much higher toxicity in cells stimulated by LPS, TNF-alpha, or IL-1beta, which enhance inflammation and oxidative stress.⁷⁶

FUTURE DIRECTIONS

A systems biology approach to mustard toxicity

As discussed above, HD toxicity in skin results from a multistep complex mechanism involving a number of signaling cascades and various cell types. It is extremely difficult to follow each step in this mechanism even in a simple *in vitro* model. A systems biology approach would view HD toxicity as time-dependent disruption of an integrated and interacting network of genes, proteins, and biochemical reactions. This approach would emphasize integrating data obtained from transcriptomics, metabolomics, and proteomics with the purpose of constructing and validating a comprehensive model of HD toxicity. The computational tools for this task would include network mapping as well as correlation, logical, and kinetic modeling.¹⁴⁶ This comprehensive model would be the best way to address the question: “how relevant to the HD-induced cell death pathways are the direct chemical alterations caused by HD to various cellular proteins (oxidation, cross-linking, and fragmentation) and the indirect chemical protein alterations caused by ROS and RNOS?”

A transcriptomic approach to studying HD toxicity is already yielding useful results. In NHEK cells, DNA array techniques have been applied to studying HD-altered gene expression,^{147,148} and mRNA differential display has been used to examine HD-induced transcriptional modulations in human epidermal keratinocytes.¹⁴⁹ Microarray analyses of gene expression in CEES- or HD-exposed mouse skin *in vivo* have also been accomplished.^{147,150} These studies are providing a deeper insight into the mechanism of HD toxicity since they have identified a number of genes upregulated at the early (0.5–4 hours) and intermediate (24 hours) stages of postexposure. DNA array analyses are capable of providing crucial information regarding the changes in transcriptional activity in the cell and are useful in the search for “the key” signaling pathways involved in HD toxicity. These studies will help in the design of evermore effective countermeasures and help identify key biomarkers for therapeutic efficacy. Proteomic data on HD toxicity are currently very limited but this approach would complement the previously accumulated microarray data by helping identify all the key proteins involved in HD toxicity at different stages.

Collectively, the literature reviewed here supports the notion that oxidative stress, free radical damage to biomolecules, and alterations in redox sensitive signaling pathways are key factors in understanding vesicant toxicology. It is likely, therefore, that the newly emerging area of redox proteomics would be particularly useful in understanding HD damage to skin. Redox proteomics is focused on characterizing (1) the chemical modifications of specific proteins induced by ROS and RNOS; (2) alterations in specific proteins induced by changes in redox sensitive transcription factors; and (3) alterations in the function/structure of specific proteins caused by redox sensitive posttranslational modifications.^{151–153} In this regard, small thiols, like GSH, are no longer viewed just as protective antioxidants but as redox regulators of proteins via glutathionylation or by oxidation of protein cysteine residue.¹⁵² Redox proteomics is rapidly emerging as a very powerful tool for characterizing and identifying proteins based on their redox state.¹⁵³ This approach has recently been used to specifically identify oxidized proteins in Alzheimer’s disease and this information has proven useful in identifying new therapeutic targets and in providing new molecular insights into disease etiology.¹⁵⁴

Multicomponent antioxidant liposomes

HD, due to its hydrophobic nature, effectively penetrates deep into the skin and affects mostly proliferating cells within basement membrane, that is, the lowest layer of proliferating keratinocytes. These growing cells would be highly susceptible to the PARP-mediated bioenergetic collapse since they actively utilize aerobic glycolysis. HD is likely, therefore, to induce necrosis rather than apoptosis in these cells, which would subsequently promote severe inflammation, skin blistering, and vesication. Thus, it is critically important to provide fast and efficient delivery of the desired drugs to the deeper skin layers and liposomes hold promise in this regard. By encapsulating a lipid soluble thiol, antioxidant liposomes could also effectively diminish (by direct covalent reaction) the stores of HD in skin lipid depots. Although this review has emphasized antioxidants, there is practically no limit to the possible encapsulated agents that can be incorporated into liposomes and delivered to the skin cells. These agents could include PARP inhibitors, protease inhibitors, anti-inflammatory agents, and chemical or enzymatic antioxidants. Currently, we are testing novel formulations of multiagent antioxidant liposomes containing both antiapoptotic (NAC) and antinecrotic (ethyl pyruvate) agents. Liposomes can also be formulated with agents designed to accelerate wound healing such as epidermal growth factor, transforming growth factor- β , platelet-derived growth factor, insulin-like growth factor, keratinocyte growth factor, and fibroblast growth factor.

ACKNOWLEDGMENTS

This research was supported by three United States Army Medical Research Command (USAMRMC) Grants: “The Influence of Antioxidant Liposomes on Macrophages Treated with Mustard Gas Analogues”, Grant No. 98164001; “Topical Application of Liposomal Antioxidants for Protection against CEES Induced Skin Damage”, Contract No. W81XWH-05-2-0034, and; “A Proteomic Approach for Studying the Therapeutic Use of Antioxidant Liposomes”, Contract No. W81XWH-06-2-044.

REFERENCES

1. Somani SM, Babu SR. Toxicodynamics of sulfur mustard. *Int J Clin Pharmacol Ther Toxicol*. 1989;27:419–435.
2. Sinclair DC. Disability produced by exposure of skin to mustard-gas vapour. *Br Med J*. 1950;1:346–349.
3. Drasch G, Kretschmer E, Kauert G, von Meyer L. Concentrations of mustard gas [bis(2-chloroethyl)sulfide] in the tissues of a victim of a vesicant exposure. *J Forensic Sci*. 1987;32:1788–1793.
4. Vijayaraghavan R, Kulkarni A, Pant SC, et al. Differential toxicity of sulfur mustard administered through percutaneous, subcutaneous, and oral routes. *Toxicol Appl Pharmacol*. 2005;202:180–188.
5. Papirmeister B, Gross CL, Meier HL, Petrali JP, Johnson JB. Molecular basis for mustard-induced vesication. *Fundam Appl Toxicol*. 1985;5:S134–S149.
6. Langenberg JP, van der Schans GP, Spruit HE, et al. Toxicokinetics of sulfur mustard and its DNA-adducts in the hairless guinea pig. *Drug Chem Toxicol*. 1998;21(suppl 1):131–147.
7. Wormser U. Toxicology of mustard gas. *Trends Pharmacol Sci*. 1991;12:164–167.
8. Hay A. Effects on health of mustard gas. *Nature*. 1993;366:398.
9. Pearson GS. Veterans at risk: the health effects of mustard gas and lewisite. *Nature*. 1993;365:218.
10. Black RM, Read RW. Biological fate of sulphur mustard, 1,1'-thiobis(2-chloroethane): identification of beta-lyase metabolites and hydrolysis products in human urine. *Xenobiotica*. 1995;25:167–73.

11. Boyer AE, Ash D, Barr DB, et al. Quantitation of the sulfur mustard metabolites 1,1'-sulfonylbis[2-(methylthio)ethane] and thiodiglycol in urine using isotope-dilution Gas chromatography-tandem mass spectrometry. *J Anal Toxicol.* 2004;28:327–332.
12. Chilcott RP, Jenner J, Carrick W, Hotchkiss SA, Rice P. Human skin absorption of bis-2-(chloroethyl)sulphide (sulphur mustard) in vitro. *J Appl Toxicol.* 2000;20:349–355.
13. Graham JS, Chilcott RP, Rice P, Milner SM, Hurst CG, Maliner BI. Wound healing of cutaneous sulfur mustard injuries: strategies for the development of improved therapies. *J Burns Wounds.* 2005;4:e1.
14. Lindsay CD, Rice P. Changes in connective tissue macromolecular components of Yucatan mini-pig skin following application of sulphur mustard vapour. *Hum Exp Toxicol.* 1995;14:341–348.
15. Naghii MR. Sulfur mustard intoxication, oxidative stress, and antioxidants. *Mil Med.* 2002;167:573–575.
16. Anderson DR, Yourick JJ, Arroyo CM, Young GD, Harris LW. Use of EPR spin-trapping techniques to detect radicals from rat lung lavage fluid following sulfur mustard vapor exposure. *Med Defense Biosci Rev Proc.* 1993;1:113–121.
17. Elsayed NM, Omaye ST. Biochemical changes in mouse lung after subcutaneous injection of the sulfur mustard 2-chloroethyl 4-chlorobutyl sulfide. *Toxicol.* 2004;199:195–206.
18. Elsayed NM, Omaye ST, Klain GJ, Korte DW Jr. Free radical-mediated lung response to the monofunctional sulfur mustard butyl 2-chloroethyl sulfide after subcutaneous injection. *Toxicol.* 1992;72:153–165.
19. Vijayaraghavan R, Sugendran K, Pant SC, Husain K, Malhotra RC. Dermal intoxication of mice with bis(2-chloroethyl)sulphide and the protective effect of flavonoids. *Toxicol.* 1991;69:35–42.
20. Husain K, Dube SN, Sugendran K, Singh R, Das Gupta S, Somani SM. Effect of topically applied sulphur mustard on antioxidant enzymes in blood cells and body tissues of rats. *J Appl Toxicol.* 1996;16:245–248.
21. Yourick JJ, Dawson JS, Benton CD, Craig ME, Mitcheltree LW. Pathogenesis of 2,2'-dichlorodiethyl sulfide in hairless guinea pigs. *Toxicol.* 1993;84:185–197.
22. Vojvodic V, Milosavljevic Z, Boskovic B, Bojanic N. The protective effect of different drugs in rats poisoned by sulfur and nitrogen mustards. *Fundam Appl Toxicol.* 1985;5:160–168.
23. Azzi A, Gysin R, Kempna P, et al. Vitamin E mediates cell signaling and regulation of gene expression. *Ann N Y Acad Sci.* 2004;1031:86–95.
24. Ricciarelli R, Zingg JM, Azzi A. Vitamin E: protective role of a Janus molecule. *Faseb J.* 2001;15:2314–2325.
25. Zingg JM, Azzi A. Non-antioxidant activities of vitamin E. *Curr Med Chem.* 2004;11:1113–1133.
26. Cooney RV, Franke AA, Harwood PJ, Hatch-Pigott V, Custer LJ, Mordan LJ. Gamma-tocopherol detoxification of nitrogen dioxide: superiority to alpha-tocopherol. *Proc Natl Acad Sci U S A.* 1993;90:1771–1775.
27. Samandari E, Visarius T, Zingg JM, Azzi A. The effect of gamma-tocopherol on proliferation, integrin expression, adhesion, and migration of human glioma cells. *Biochem Biophys Res Commun.* 2006;342:1329–1333.
28. Eldad A, Ben Meir P, Breiterman S, Chaouat M, Shafran A, Ben-Bassat H. Superoxide dismutase (SOD) for mustard gas burns. *Burns.* 1998;24:114–119.
29. Alvarez MN, Trujillo M, Radi R. Peroxynitrite formation from biochemical and cellular fluxes of nitric oxide and superoxide. *Methods Enzymol.* 2002;359:353–366.
30. Beckman JS, Koppenol WH. Nitric oxide, superoxide, and peroxynitrite: the good, the bad, and ugly. *Am J Physiol.* 1996;271:1424–1437.
31. Fukuyama N, Nakazawa H. [Superoxide, nitric oxide and peroxynitrite]. *Nippon Yakurigaku Zasshi.* 1998;112:169–176.
32. Kumar O, Sugendran K, Vijayaraghavan R. Protective effect of various antioxidants on the toxicity of sulphur mustard administered to mice by inhalation or percutaneous routes. *Chem Biol Interact.* 2001;134:1–12.
33. McClintock SD, Hoesel LM, Das SK, et al. Attenuation of half sulfur mustard gas-induced acute lung injury in rats. *J Appl Toxicol.* 2006;26:126–131.
34. McClintock SD, Till GO, Smith MG, Ward PA. Protection from half-mustard-gas-induced acute lung injury in the rat. *J Appl Toxicol.* 2002;22:257–262.
35. Kelly GS. Clinical applications of N-acetylcysteine. *Altern Med Rev.* 1998;3:114–127.
36. Gross CL, Innace JK, Hovatter RC, Meier HL, Smith WJ. Biochemical manipulation of intracellular glutathione levels influences cytotoxicity to isolated human lymphocytes by sulfur mustard. *Cell Biol Toxicol.* 1993;9:259–267.

37. Meister A, Anderson ME. Glutathione. *Annu Rev Biochem.* 1983;52:711–760.
38. Bhat S, Gulati S, Husain K, Milner SM. Lipoic acid decreases oxidative stress in sulphur mustard toxicity. Proceedings of American Burn Association, 38th Annual Meeting, S139. Las Vegas, Nevada: *J Burn Care Res*, 27(2, suppl):S139, 2006.
39. Bast A, Haenen GR. Lipoic acid: a multifunctional antioxidant. *Biofactors.* 2003;17:207–213.
40. Dincer Y, Telci A, Kayali R, Yilmaz IA, Cakatay U, Akcay T. Effect of alpha-lipoic acid on lipid peroxidation and anti-oxidant enzyme activities in diabetic rats. *Clin Exp Pharmacol Physiol.* 2002;29:281–284.
41. Ernst A, Stolzing A, Sandig G, Grune T. Antioxidants effectively prevent oxidation-induced protein damage in OLN 93 cells. *Arch Biochem Biophys.* 2004;421:54–60.
42. Maritim AC, Sanders RA, Watkins JB, III. Effects of alpha-lipoic acid on biomarkers of oxidative stress in streptozotocin-induced diabetic rats. *J Nutr Biochem.* 2003;14:288–294.
43. Wollin SD, Jones PJ. Alpha-lipoic acid and cardiovascular disease. *J Nutr.* 2003;133:3327–3330.
44. Busse E, Zimmer G, Schopohl B, Kornhuber B. Influence of alpha-lipoic acid on intracellular glutathione in vitro and in vivo. *Arzneimittelforschung.* 1992;42:829–831.
45. Han D, Handelman G, Marcocci L, et al. Lipoic acid increases de novo synthesis of cellular glutathione by improving cystine utilization. *Biofactors.* 1997;6:321–338.
46. Stone WL, Mukherjee S, Smith M, Das SK. Therapeutic uses of antioxidant liposomes. *Methods Mol Biol.* 2002;199:145–161.
47. Stone WL, Smith M. Therapeutic uses of antioxidant liposomes. *Mol Biotechnol.* 2004;27:217–230.
48. Fan J, Shek PN, Suntres ZE, Li YH, Oreopoulos GD, Rotstein OD. Liposomal antioxidants provide prolonged protection against acute respiratory distress syndrome. *Surg.* 2000;128:332–338.
49. Kirjavainen M, Urtti A, Jaaskelainen I, et al. Interaction of liposomes with human skin in vitro—the influence of lipid composition and structure. *Biochim Biophys Acta.* 1996;1304:179–189.
50. Kirjavainen M, Urtti A, Valjakka-Koskela R, Kiesvaara J, Monkkonen J. Liposome-skin interactions and their effects on the skin permeation of drugs. *Eur J Pharm Sci.* 1999;7:279–286.
51. Boyce ST, Ham RG. Calcium-regulated differentiation of normal human epidermal keratinocytes in chemically defined clonal culture and serum-free serial culture. *J Invest Dermatol.* 1983;81:33s–40s.
52. Smith WJ, Gross CL, Chan P, Meier HL. The use of human epidermal keratinocytes in culture as a model for studying the biochemical mechanisms of sulfur mustard toxicity. *Cell Biol Toxicol.* 1990;6:285–291.
53. Stoppler H, Stoppler MC, Johnson E, et al. The E7 protein of human papillomavirus type 16 sensitizes primary human keratinocytes to apoptosis. *Oncogene.* 1998;17:1207–1214.
54. Boukamp P, Petrussevska RT, Breitkreutz D, Hornung J, Markham A, Fusenig NE. Normal keratinization in a spontaneously immortalized aneuploid human keratinocyte cell line. *J Cell Biol.* 1988;106:761–771.
55. Lippens S, Denecker G, Ovaere P, Vandenabeele P, Declercq W. Death penalty for keratinocytes: apoptosis versus cornification. *Cell Death Differ.* 2005;12(suppl 2):1497–1508.
56. Maas-Szabowski N, Starker A, Fusenig NE. Epidermal tissue regeneration and stromal interaction in HaCaT cells is initiated by TGF-alpha. *J Cell Sci.* 2003;116:2937–2948.
57. Freedberg IM, Tomic-Canic M, Komine M, Blumenberg M. Keratins and the keratinocyte activation cycle. *J Invest Dermatol.* 2001;116:633–640.
58. Smith CN, Lindsay CD, Upshall DG. Presence of methenamine/glutathione mixtures reduces the cytotoxic effect of sulphur mustard on cultured SVK-14 human keratinocytes in vitro. *Hum Exp Toxicol.* 1997;16:247–253.
59. Simpson R, Lindsay CD. Effect of sulphur mustard on human skin cell lines with differential agent sensitivity. *J Appl Toxicol.* 2005;25:115–128.
60. Wormser U, Sintov A, Brodsky B, Nyska A. Topical iodine preparation as therapy against sulfur mustard-induced skin lesions. *Toxicol Appl Pharmacol.* 2000;169:33–39.
61. Das SK, Mukherjee S, Smith MG, Chatterjee D. Prophylactic protection by N-acetylcysteine against the pulmonary injury induced by 2-chloroethyl ethyl sulfide, a mustard analogue. *J Biochem Mol Toxicol.* 2003;17:177–184.
62. Arroyo CM, Schafer RJ, Kurt EM, Broomfield CA, Carmichael AJ. Response of normal human keratinocytes to sulfur mustard: cytokine release. *J Appl Toxicol. J.* 2000;20(suppl 1):S63–S72.
63. Ricketts KM, Santai CT, France JA, et al. Inflammatory cytokine response in sulfur mustard-exposed mouse skin. *J Appl Toxicol. J.* 2000;20(suppl 1):73–76.

64. Sabourin CL, Petrali JP, Casillas RP. Alterations in inflammatory cytokine gene expression in sulfur mustard-exposed mouse skin. *J Biochem Mol Toxicol*. 2000;14:291–302.
65. Vavra AK, Laurent CJ, Ngo V, Sweeney JF, Levitt JM. Sulfur mustard primes phagocytosis and degranulation in human polymorphonuclear leukocytes. *Int Immunopharmacol*. 2004;4:437–445.
66. Blaha M, Bowers W, Kohl J, DuBose D, Walker J. Il-1-related cytokine responses of nonimmune skin cells subjected to CEES exposure with and without potential vesicant antagonists. 2000;13:99–111.
67. Blaha M, Bowers W, Kohl J, et al. Effects of CEES on inflammatory mediators, heat shock protein 70A, histology and ultrastructure in two skin models. *J Appl Toxicol. Jat*. 2000;20(suppl 1):S101–S108.
68. Blaha M, Kohl J, DuBose D, Bowers W Jr, Walker J. Ultrastructural and histological effects of exposure to CEES or heat in a human epidermal model. *In Vitro Mol Toxicol*. 2001;14:15–23.
69. Hayden PJ, Petrali JP, Hamilton TA, Kubilus J, Smith WJ, Klausner M. Development of a full thickness in vitro human skin equivalent (EpiDerm-FT) for sulfur mustard research, SID Abstract #174. 2005 Society for Investigative Dermatology Annual Meeting, 2005.
70. Rosenthal DS, Shima TB, Celli G, De Luca LM, Smulson ME. Engineered human skin model using poly(ADP-ribose) polymerase antisense expression shows a reduced response to DNA damage. *J Invest Dermatol*. 1995;105:38–43.
71. Rosenthal DS, Veleno A, Chou FP, et al. Expression of dominant-negative Fas-associated death domain blocks human keratinocyte apoptosis and vesication induced by sulfur mustard. *J Biol Chem*. 2003;278:8531–8540.
72. Greenberg S, Margulis A, Garlick JA. In vivo transplantation of engineered human skin. *Methods Mol Biol*. 2005;289:425–430.
73. Greenberg S, Kamath P, Petrali J, Hamilton T, Garfield J, Garlick JA. Characterization of the initial response of engineered human skin to sulfur mustard. *Toxicol Sci*. 2006;90:549–557.
74. Rikimaru T, Nakamura M, Yano T, et al. Mediators, initiating the inflammatory response, released in organ culture by full-thickness human skin explants exposed to the irritant, sulfur mustard. *J Invest Dermatol*. 1991;96:888–897.
75. Inoue H, Asaka T, Nagata N, Koshihara Y. Mechanism of mustard oil-induced skin inflammation in mice. *Eur J Pharmacol*. 1997;333:231–240.
76. Stone WL, Qui M, Smith M. Lipopolysaccharide enhances the cytotoxicity of 2-chloroethyl ethyl sulfide. *BMC Cell Biol*. 2003;4:1.
77. Qui M, Paromov VM, Yang H, Smith M, Stone WL. Inhibition of inducible nitric oxide synthase by a mustard gas analog in murine macrophages. *BMC Cell Biol*. 2006;7:39.
78. Wright SD, Ramos RA, Tobias PS, Ulevitch RJ, Mathison JC. CD14, a receptor for complexes of lipopolysaccharide (LPS) and LPS binding protein. *Sci*. 1990;249:1431–1433.
79. Downey JS, Han J. Cellular activation mechanisms in septic shock. *Front Biosci*. 1998;3:d468–d476.
80. Tepperman BL, Chang Q, Soper BD. Protein kinase C mediates lipopolysaccharide- and phorbol-induced nitric-oxide synthase activity and cellular injury in the rat colon. *J Pharmacol Exp Ther*. 2000;295:1249–1257.
81. Shapira L, Takashiba S, Champagne C, Amar S, Van Dyke TE. Involvement of protein kinase C and protein tyrosine kinase in lipopolysaccharide-induced TNF-alpha and IL-1 beta production by human monocytes. *J Immunol*. 1994;153:1818–1824.
82. Eastmond NC, Banks EM, Coleman JW. Nitric oxide inhibits IgE-mediated degranulation of mast cells and is the principal intermediate in IFN-gamma-induced suppression of exocytosis. *J Immunol*. 1997;159:1444–1450.
83. Wink DA, Miranda KM, Espey MG, et al. Mechanisms of the antioxidant effects of nitric oxide. *Antioxid Redox Signal*. 2001;3:203–213.
84. McCauley SD, Gilchrist M, Befus AD. Nitric oxide: a major determinant of mast cell phenotype and function. *Mem Inst Oswaldo Cruz*. 2005;100(suppl 1):11–14.
85. Masini E, Palmerani B, Gambassi F, et al. Histamine release from rat mast cells induced by metabolic activation of polyunsaturated fatty acids into free radicals. *Biochem Pharmacol*. 1990;39:879–889.
86. Chiarugi A. Poly(ADP-ribose) polymerase: killer or conspirator? The “suicide hypothesis” revisited. *Trends Pharmacol Sci*. 2002;23:122–129.

87. Rosenthal DS, Simbulan-Rosenthal CM, Iyer S, et al. Sulfur mustard induces markers of terminal differentiation and apoptosis in keratinocytes via a Ca^{2+} -calmodulin and caspase-dependent pathway. *J Invest Dermatol*. 1998;111:64–71.
88. Hinshaw DB, Lodhi JJ, Hurley LL, Atkins KB, Dabrowska MI. Activation of poly [ADP-Ribose] polymerase in endothelial cells and keratinocytes: role in an in vitro model of sulfur mustard-mediated vesicitation. *Toxicol Appl Pharmacol*. 1999;156:17–29.
89. Bhat KR, Benton BJ, Rosenthal DS, Smulson ME, Ray R. Role of poly(ADP-ribose) polymerase (PARP) in DNA repair in sulfur mustard-exposed normal human epidermal keratinocytes (NHEK). *J Appl Toxicol*. 2000;20(suppl 1):S13–S17.
90. Rosenthal DS, Simbulan-Rosenthal CM, Iyer S, Smith WJ, Ray R, Smulson ME. Calmodulin, poly(ADP-ribose)polymerase and p53 are targets for modulating the effects of sulfur mustard. *J Appl Toxicol*. 2000;20(suppl 1):S43–S49.
91. Rosenthal DS, Simbulan-Rosenthal CM, Liu WF, et al. PARP determines the mode of cell death in skin fibroblasts, but not keratinocytes, exposed to sulfur mustard. *J Invest Dermatol*. 2001;117:1566–1573.
92. Kim MY, Zhang T, Kraus WL. Poly(ADP-ribosylation) by PARP-1: “PAR-laying” NAD^+ into a nuclear signal. *Genes Dev*. 2005;19:1951–1967.
93. D’Amours D, Desnoyers S, D’Silva I, Poirier GG. Poly(ADP-ribosylation) reactions in the regulation of nuclear functions. *Biochem J*. 1999;342(Pt 2):249–268.
94. Herceg Z, Wang ZQ. Functions of poly(ADP-ribose) polymerase (PARP) in DNA repair, genomic integrity and cell death. *Mutat Res*. 2001;477:97–110.
95. Shall S, de Murcia G. Poly(ADP-ribose) polymerase–1: what have we learned from the deficient mouse model? *Mutat Res*. 2000;460:1–15.
96. Zong WX, Ditsworth D, Bauer DE, Wang ZQ, Thompson CB. Alkylating DNA damage stimulates a regulated form of necrotic cell death. *Genes Dev*. 2004;18:1272–1282.
97. Burkle A. PARP-1: a regulator of genomic stability linked with mammalian longevity. *ChemBiochem*. 2001;2:725–728.
98. Bouchard VJ, Rouleau M, Poirier GG. PARP-1, a determinant of cell survival in response to DNA damage. *Exp Hematol*. 2003;31:446–454.
99. Decker P, Muller S. Modulating poly (ADP-ribose) polymerase activity: potential for the prevention and therapy of pathogenic situations involving DNA damage and oxidative stress. *Curr Pharm Biotechnol*. 2002;3:275–283.
100. Ying W, Alano CC, Garnier P, Swanson RA. NAD^+ as a metabolic link between DNA damage and cell death. *J Neurosci Res*. 2005;79:216–223.
101. Sun J, Wang YX, Sun MJ. Apoptosis and necrosis induced by sulfur mustard in HeLa cells. *Zhongguo Yao Li Xue Bao*. 1999;20:445–448.
102. Meier HL, Millard CB. Alterations in human lymphocyte DNA caused by sulfur mustard can be mitigated by selective inhibitors of poly(ADP-ribose) polymerase. *Biochim Biophys Acta*. 1998;1404:367–376.
103. Dabrowska MI, Becks LL, Lelli JL Jr, Levee MG, Hinshaw DB. Sulfur mustard induces apoptosis and necrosis in endothelial cells. *Toxicol Appl Pharmacol*. 1996;141:568–583.
104. Ying W, Chen Y, Alano CC, Swanson RA. Tricarboxylic acid cycle substrates prevent PARP-mediated death of neurons and astrocytes. *J Cereb Blood Flow Metab*. 2002;22:774–779.
105. Willems JL, de Kort AF, Vree TB, Trijbels JM, Veerkamp JH, Monnens LA. Non-enzymic conversion of pyruvate in aqueous solution to 2,4-dihydroxy-2-methylglutaric acid. *FEBS Lett*. 1978;86:42–44.
106. O’Donnell-Tormey J, Nathan CF, Lanks K, DeBoer CJ, de la Harpe J. Secretion of pyruvate. An antioxidant defense of mammalian cells. *J Exp Med*. 1987;165:500–514.
107. Dobsak P, Courderot-Masuyer C, Zeller M, et al. Antioxidative properties of pyruvate and protection of the ischemic rat heart during cardioplegia. *J Cardiovasc Pharmacol*. 1999;34:651–659.
108. Das UN. Pyruvate is an endogenous anti-inflammatory and anti-oxidant molecule. *Med Sci Monit*. 2006;12:RA79–RA84.
109. Mallet RT, Sun J, Knott EM, Sharma AB, Olivencia-Yurvati AH. Metabolic cardioprotection by pyruvate: recent progress. *Exp Biol Med (Maywood)*. 2005;230:435–443.
110. Sabourin CL, Danne MM, Buxton KL, Casillas RP, Schlager JJ. Cytokine, chemokine, and matrix metalloproteinase response after sulfur mustard injury to weanling pig skin. *J Biochem Mol Toxicol*. 2002;16:263–272.

111. Akira S, Kishimoto T. NF-IL6 and NF-kappa B in cytokine gene regulation. *Adv Immunol.* 1997;65:1–46.
112. Brennan P, O’Neill LA. Effects of oxidants and antioxidants on nuclear factor kappa B activation in three different cell lines: evidence against a universal hypothesis involving oxygen radicals. *Biochim Biophys Acta.* 1995;1260:167–175.
113. Barnes PJ, Adcock IM. Transcription factors and asthma. *Eur Respir J.* 1998;12:221–234.
114. Rahman I, MacNee W. Role of transcription factors in inflammatory lung diseases. *Thorax.* 1998;53:601–612.
115. Martin-Oliva D, O’Valle F, Munoz-Gamez JA, et al. Crosstalk between PARP-1 and NF-kappaB modulates the promotion of skin neoplasia. *Oncog.* 2004;23:5275–5283.
116. Gray PJ. Sulphur mustards inhibit binding of transcription factor AP2 in vitro. *Nucleic Acids Res.* 1995;23:4378–4382.
117. Schulze-Osthoff K, Bauer MK, Vogt M, Wesselborg S. Oxidative stress and signal transduction. *Int J Vitam Nutr Res.* 1997;67:336–342.
118. Schwager J, Schulze J. Influence of ascorbic acid on the response to mitogens and interleukin production of porcine lymphocytes. *Int J Vitam Nutr Res.* 1997;67:10–16.
119. Xanthoudakis S, Miao GG, Curran T. The redox and DNA-repair activities of Ref-1 are encoded by nonoverlapping domains. *Proc Natl Acad Sci U S A.* 1994;91:23–27.
120. Yao KS, Xanthoudakis S, Curran T, O’Dwyer PJ. Activation of AP-1 and of a nuclear redox factor, Ref-1, in the response of HT29 colon cancer cells to hypoxia. *Mol Cell Biol.* 1994;14:5997–6003.
121. Kerppola TK, Curran T. A conserved region adjacent to the basic domain is required for recognition of an extended DNA binding site by Maf/Nrl family proteins. *Oncogene.* 1994;9:3149–3158.
122. Kerppola TK, Curran T. Maf and Nrl can bind to AP-1 sites and form heterodimers with Fos and Jun. *Oncogene.* 1994;9:675–684.
123. Klampfer L, Lee TH, Hsu W, Vilcek J, Chen-Kiang S. NF-IL6 and AP-1 cooperatively modulate the activation of the TSG-6 gene by tumor necrosis factor alpha and interleukin-1. *Mol Cell Biol.* 1994;14:6561–6569.
124. Hsu W, Kerppola TK, Chen PL, Curran T, Chen-Kiang S. Fos and Jun repress transcription activation by NF-IL6 through association at the basic zipper region. *Mol Cell Biol.* 1994;14:268–276.
125. Crispen PL, Uzzo RG, Golovine K, et al. Vitamin E succinate inhibits NF-kappaB and prevents the development of a metastatic phenotype in prostate cancer cells: implications for chemoprevention. *Prostate.* 2007;67:582–590.
126. Campbell SE, Stone WL, Lee S, et al. Comparative effects of RRR-alpha- and RRR-gamma-tocopherol on proliferation and apoptosis in human colon cancer cell lines. *BMC Cancer.* 2006;6:13.
127. Smirnov AS, Ruzov AS, Budanov AV, Prokhortchouk AV, Ivanov AV, Prokhortchouk EB. High constitutive level of NF-kappaB is crucial for viability of adenocarcinoma cells. *Cell Death Differ.* 2001;8:621–630.
128. Dhanalakshmi S, Singh RP, Agarwal C, Agarwal R. Silibinin inhibits constitutive and TNFalpha-induced activation of NF-kappaB and sensitizes human prostate carcinoma DU145 cells to TNFalpha-induced apoptosis. *Oncogene.* 2002;21:1759–1767.
129. Ma Z, Otsuyama K, Liu S, et al. Baicalein, a component of *Scutellaria radix* from Huang-Lian-Jie-Du-Tang (HLJDT), leads to suppression of proliferation and induction of apoptosis in human myeloma cells. *Blood.* 2005;105:3312–3318.
130. Taguchi T, Takao T, Iwasaki Y, Nishiyama M, Asaba K, Hashimoto K. Suppressive effects of dehydroepiandrosterone and the nuclear factor-kappaB inhibitor parthenolide on corticotroph tumor cell growth and function in vitro and in vivo. *J Endocrinol.* 2006;188:321–331.
131. Minsavage GD, Dillman JF 3rd. Protective role of CAPE on bi-functional alkylating agent-induced toxicity in keratinocytes via modulation of NF-kappaB, p53 and ARE/EpRE signaling. *Biosci 2006 Med Defense Rev.* 2006;94–94.
132. Minsavage GD, Dillman JF 3rd. Bifunctional alkylating agent-induced p53 and nonclassical nuclear factor-kappa b (nf- $\{\kappa\}$ b) responses and cell death are altered by caffeic acid phenethyl ester (cape): A potential role for antioxidant/electrophilic response element (ARE/EpRE) signaling. *J Pharmacol Exp Ther.* 2007;321:202–212.
133. Arroyo CM, Burman DL, Kahler DW, et al. TNF-alpha expression patterns as potential molecular biomarker for human skin cells exposed to vesicant chemical warfare agents: sulfur mustard (HD) and Lewisite (L). *Cell Biol Toxicol.* 2004;20:345–359.

134. Atkins KB, Lodhi IJ, Hurley LL, Hinshaw DB. *N*-acetylcysteine and endothelial cell injury by sulfur mustard. *J Appl Toxicol.* 2000;20(suppl 1):S125–S128.
135. Chatterjee D, Mukherjee S, Smith MG, Das SK. Signal transduction events in lung injury induced by 2-chloroethyl ethyl sulfide, a mustard analog. *J Biochem Mol Toxicol.* 2003;17:114–121.
136. Duthie MS, Kimber I, Dearman RJ, Norval M. Differential effects of UVA1 and UVB radiation on Langerhans cell migration in mice. *J Photochem Photobiol B.* 2000;57:123–131.
137. Steffensen B, Hakkinen L, Larjava H. Proteolytic events of wound-healing-coordinated interactions among matrix metalloproteinases (MMPs), integrins, and extracellular matrix molecules. *Crit Rev Oral Biol Med.* 2001;12:373–398.
138. Schwentker A, Billiar TR. Nitric oxide and wound repair. *Surg Clin North Am.* 2003;83:521–530.
139. Weller R. Nitric oxide: a key mediator in cutaneous physiology. *Clin Exp Dermatol.* 2003;28:511–514.
140. Witte MB, Barbul A. Role of nitric oxide in wound repair. *Am J Surg.* 2002;183:406–412.
141. Yamasaki K, Edington HD, McClosky C, et al. Reversal of impaired wound repair in iNOS-deficient mice by topical adenoviral-mediated iNOS gene transfer. *J Clin Invest.* 1998;101:967–971.
142. Ishida H, Ray R, Cao Y, Ray P. Role of nitric oxide (NO) in wound healing. *Biosci 2006 Med Defense Rev.* 2006;1:112.
143. Arany I, Brysk MM, Brysk H, Tyring SK. Regulation of inducible nitric oxide synthase mRNA levels by differentiation and cytokines in human keratinocytes. *Biochem Biophys Res Commun.* 1996;220:618–622.
144. Kleinert H, Schwarz PM, Forstermann U. Regulation of the expression of inducible nitric oxide synthase. *Biol Chem.* 2003;384:1343–1364.
145. Soneja A, Drews M, Malinski T. Role of nitric oxide, nitroxidative and oxidative stress in wound healing. *Pharmacol Rep.* 2005;57(suppl):108–119.
146. Perkel JM. What can systems biology do for you? Four computational modeling strategies and the data that build them. *Scientist.* 2007;21:68.
147. Rogers JV, Choi YW, Kiser RC, et al. Microarray analysis of gene expression in murine skin exposed to sulfur mustard. *J Biochem Mol Toxicol.* 2004;18:289–299.
148. Sabourin CL, Rogers JV, Choi YW, et al. Time- and dose-dependent analysis of gene expression using microarrays in sulfur mustard-exposed mice. *J Biochem Mol Toxicol.* 2004;18:300–312.
149. Platteborze PL. Effects of sulfur mustard on transcription in human epidermal keratinocytes: analysis by mRNA differential display. *J Appl Toxicol.* 2003;23:249–254.
150. Dillman JF, III, Hege AI, Phillips CS, et al. Microarray analysis of mouse ear tissue exposed to bis-(2-chloroethyl) sulfide: gene expression profiles correlate with treatment efficacy and an established clinical endpoint. *J Pharmacol Exp Ther.* 2006;317:76–87.
151. Sultana R, Boyd-Kimball D, Poon HF, et al. Redox proteomics identification of oxidized proteins in Alzheimer's disease hippocampus and cerebellum: an approach to understand pathological and biochemical alterations in AD. *Neurobiol Aging.* 2006;27:1564–1576.
152. Ghezzi P, Bonetto V, Fratelli M. Thiol-disulfide balance: from the concept of oxidative stress to that of redox regulation. *Antioxid Redox Signal.* 2005;7:964–972.
153. Ghezzi P, Bonetto V. Redox proteomics: identification of oxidatively modified proteins. *Proteomics.* 2003;3:1145–1153.
154. Butterfield DA. Proteomics: a new approach to investigate oxidative stress in Alzheimer's disease brain. *Brain Res.* 2004;1000:1–7.

Research article

Open Access

The influence of N-acetyl-L-cysteine on oxidative stress and nitric oxide synthesis in stimulated macrophages treated with a mustard gas analogue

Victor Paromov¹, Min Qui¹, Hongsong Yang¹, Milton Smith² and William L Stone*¹

Address: ¹Department of Pediatrics, College of Medicine, East Tennessee State University, Johnson City, TN 37614, USA and ²AMAOX, Ltd., #208, 6300 N. Wickham Road, Melbourne, FL 32944, USA

Email: Victor Paromov - paromov@etsu.edu; Min Qui - qui@etsu.edu; Hongsong Yang - yangh@etsu.edu; Milton Smith - mgsmithmd@gmail.com; William L Stone* - stone@etsu.edu

* Corresponding author

Published: 20 June 2008

Received: 14 January 2008

BMC Cell Biology 2008, 9:33 doi:10.1186/1471-2121-9-33

Accepted: 20 June 2008

This article is available from: <http://www.biomedcentral.com/1471-2121/9/33>

© 2008 Paromov et al; licensee BioMed Central Ltd.

This is an Open Access article distributed under the terms of the Creative Commons Attribution License (<http://creativecommons.org/licenses/by/2.0>), which permits unrestricted use, distribution, and reproduction in any medium, provided the original work is properly cited.

Abstract

Background: Sulphur mustard gas, 2, 2'-dichlorodiethyl sulphide (HD), is a chemical warfare agent. Both mustard gas and its monofunctional analogue, 2-chloroethyl ethyl sulphide (CEES), are alkylating agents that react with and diminish cellular thiols and are highly toxic. Previously, we reported that lipopolysaccharide (LPS) significantly enhances the cytotoxicity of CEES in murine RAW 264.7 macrophages and that CEES transiently inhibits nitric oxide (NO) production via suppression of inducible NO synthase (iNOS) protein expression. NO generation is an important factor in wound healing. In this paper, we explored the hypotheses that LPS increases CEES toxicity by increasing oxidative stress and that treatment with N-acetyl-L-cysteine (NAC) would block LPS induced oxidative stress and protect against loss of NO production. NAC stimulates glutathione (GSH) synthesis and also acts directly as a free radical scavenger. The potential therapeutic use of the antibiotic, polymyxin B, was also evaluated since it binds to LPS and could thereby block the enhancement of CEES toxicity by LPS and also inhibit the secondary infections characteristic of HD/CEES wounds.

Results: We found that 10 mM NAC, when administered simultaneously or prior to treatment with 500 μ M CEES, increased the viability of LPS stimulated macrophages. Surprisingly, NAC failed to protect LPS stimulated macrophages from CEES induced loss of NO production. Macrophages treated with both LPS and CEES show increased oxidative stress parameters (cellular thiol depletion and increased protein carbonyl levels). NAC effectively protected RAW 264.7 cells simultaneously treated with CEES and LPS from GSH loss and oxidative stress. Polymyxin B was found to partially block nitric oxide production and diminish CEES toxicity in LPS-treated macrophages.

Conclusion: The present study shows that oxidative stress is an important mechanism contributing to CEES toxicity in LPS stimulated macrophages and supports the notion that antioxidants could play a therapeutic role in preventing mustard gas toxicity. Although NAC reduced oxidative stress in LPS stimulated macrophages treated with CEES, it did not reverse CEES-induced loss of NO production. NAC and polymyxin B were found to help prevent CEES toxicity in LPS-treated macrophages.

Background

Mustard gas (HD) is a chemical weapon that can easily and inexpensively be produced and used against military or civilian populations with both acute and devastating long-term effects [1-3]. It produces rapid damage to eyes, skin and pulmonary tissues as well as subsequent damage to many internal organ systems [1,4]. Despite its long history of use, starting in World War I, the molecular mechanisms for HD toxicity are not fully understood and there is continuing research on the design of optimal countermeasures. Mustard gas acts as an alkylating agent covalently modifying DNA, proteins and other macromolecules. There is increasing evidence that HD or CEES toxicity is due, in part, to an enhanced production of inflammatory cytokines [5-9], increased oxidative stress [10] and the generation of damaging reactive oxygen species (ROS) [8,9,11]. HD and CEES have been shown to shift the intracellular redox milieu toward a more oxidized state by reacting with and depleting the intracellular antioxidant GSH with a subsequent loss of protection against ROS and an activation of inflammatory responses [12-14].

In a previous publication, we showed that the cytotoxicity of CEES towards murine RAW 264.7 macrophages was markedly enhanced by the presence of low levels of LPS (25 ng/ml), or pro-inflammatory cytokines, i.e., 50 ng/ml IL-1 β or 50 ng/ml TNF- α [15]. LPS is part of the cell wall of gram negative bacteria: it is ubiquitous and is found in serum, tap water and dust. Both civilian and military personnel would always have some degree of exposure to environmental LPS. HD induced skin lesions often have secondary infections which could markedly increase LPS levels. In macrophages, stimulation by LPS, as well as by pro-inflammatory cytokines, leads to the activation and nuclear translocation of transcription factor NF- κ B (nuclear factor-kappa B). One of the major consequences of such activation in macrophages is an induction of iNOS expression with subsequent elevation of intracellular NO [16,17]. In addition to NF- κ B activation, the binding of transcription factor STAT-1 (signal transducer and activator of transcription-1) to the inducible nitric oxide synthase (iNOS) promoter is required for optimal induction of the iNOS gene by LPS [17].

In a recent publication, we found that CEES transiently inhibits nitric oxide (NO) production by suppressing iNOS protein expression in LPS stimulated macrophages [18]. NO production is an important factor in promoting wound healing [19,20] and iNOS deficiency impairs wound healing in animal models [21]. RAW 264.7 macrophages have undetectable levels of iNOS or NO production in the absence of LPS and in the presence of LPS they show a marked induction of iNOS and NO production [18].

In the present study, we tested the hypothesis that the synergistic cytotoxic effect of CEES with LPS is due to increased oxidative stress with a subsequent depletion of intracellular GSH levels and an increase in protein carbonyls. In some cell types, GSH has also been found to regulate NO generation with decreased GSH levels associated with decreased NO production [22-24]. Vos et al. [25] found that GSH depletion in hepatocytes prevented iNOS induction by cytokines but this effect could be reversed by the addition of NAC. We, therefore, hypothesized that the addition of NAC to stimulated macrophages would reverse the loss of NO production caused by CEES. We also reasoned that polymyxin B, by binding to LPS, would diminish CEES toxicity in LPS treated macrophages.

Results

The influence of NAC on cell viability and NO production in CEES/LPS treated macrophages

Figure 1a shows the effect of NAC treatment on RAW 264.7 macrophages treated with LPS and/or 500 μ M CEES for 24 h. In this experiment, NAC was added simultaneously with LPS and CEES. In the absence of NAC, LPS, at either 50 ng/ml or 100 ng/ml level, markedly decreased cell viability in CEES treated cells compared to cells treated with LPS or CEES alone. This is similar to our previous observations in which cell viability was measured by both the MTT assay and the propidium iodide exclusion assay; the assays were well correlated with each other [15]. The addition of 10 mM NAC increased the viability of macrophages treated with both CEES and LPS (50 ng/ml or 100 ng/ml) to the same level observed for control cells (treated with vehicle alone). It is likely that the differences in the viability of cells treated with NAC and different levels of LPS represent experimental variability since these differences are marginal.

Figure 1b shows NO release, measured as the nitrite levels in the cell culture medium, for the identical cells/treatments used in Figure 1a. As expected, LPS treatment alone resulted in a marked increase of NO generation, and LPS-stimulated macrophages treated with CEES showed a marked reduction in NO production. Surprisingly, NAC treatment did not prevent the decrease in NO production caused by CEES. In cells treated with LPS alone, NAC treatment actually resulted in a decreased production of NO (up to 40% reduction).

In order to further evaluate NAC as a potential protective agent for CEES toxicity in stimulated macrophages, we did two additional experiments in which NAC was added to macrophages 5 h prior to CEES application or 5 h after CEES application. These additional experiments provide a measure of the potential time frame during which NAC could be therapeutically useful. Similar to the previous experiment, LPS and CEES were added simultaneously (as

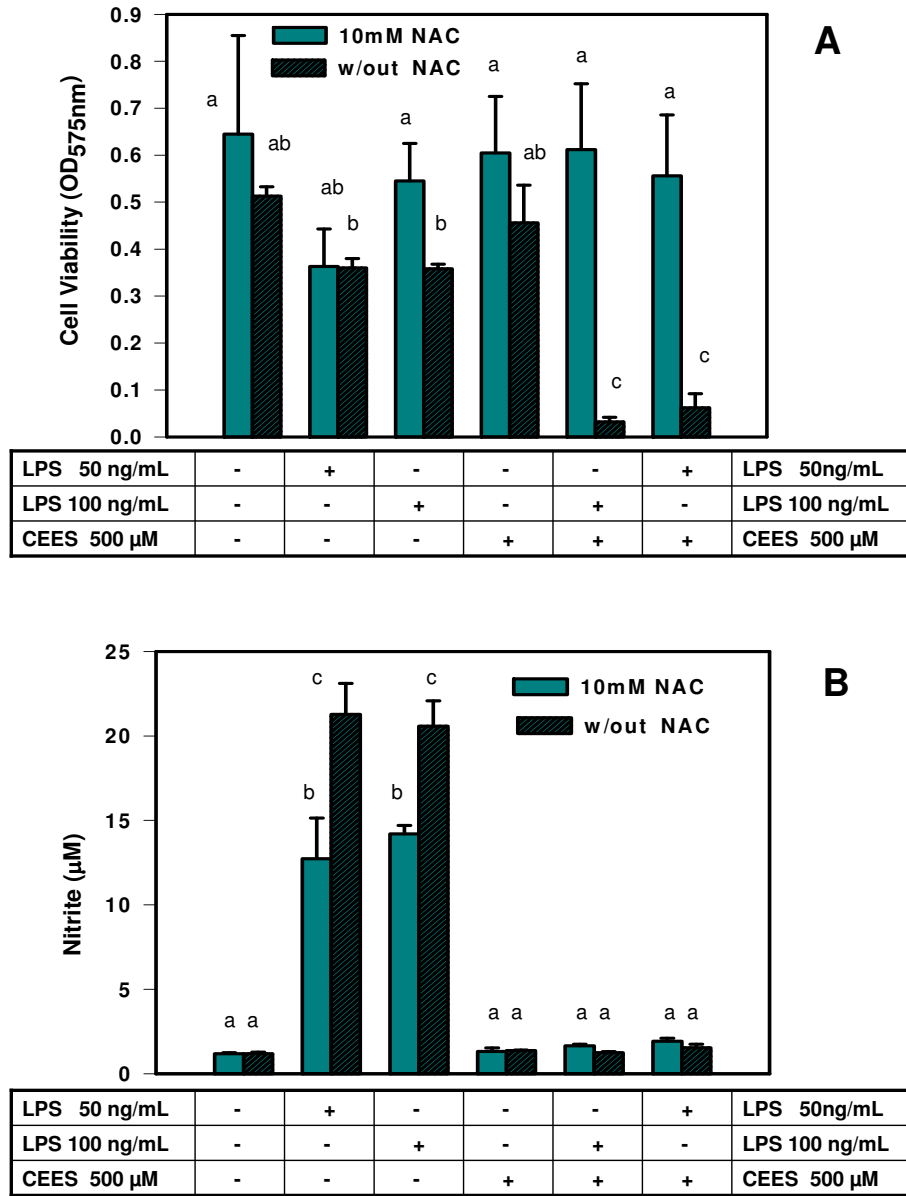


Figure 1
NAC effect on viability and NO production in CEES/LPS treated RAW 264.7 cells (simultaneous NAC/CEES/LPS application). Panel A: Macrophages incubated with 50 or 100 ng/ml of LPS or/and 500 µM CEES were simultaneously treated with or without 10 mM NAC (as indicated) for 24 hours. Cell viability was measured using the MTT assay (see Materials and Methods) and expressed as OD at 575 nm. Panel B: Macrophages were incubated as described above and NO production measured as the concentration of nitrite in the culture media as described in Materials and Methods. Mean values not sharing a common letter are significantly different ($p < 0.05$).

indicated). As shown in Figure 2a, NAC had a substantial protective effect on cell viability when added 5 h before CEES/LPS; however NAC did not protect against loss of NO production in CEES/LPS-treated cells (Figure 2b). When added 5 h after CEES treatment (Figure 3a), NAC was much less effective in protecting the macrophages but still resulted in at least a doubling of the cell viability com-

pared to the cells not treated with NAC. As shown in Figure 3b, NAC added 5 h after CEES/LPS, also failed to restore NO production.

We believe that the difference in viability of cells stimulated with LPS in the absence or in the presence of NAC (Figure 2A) could represent experimental variation since

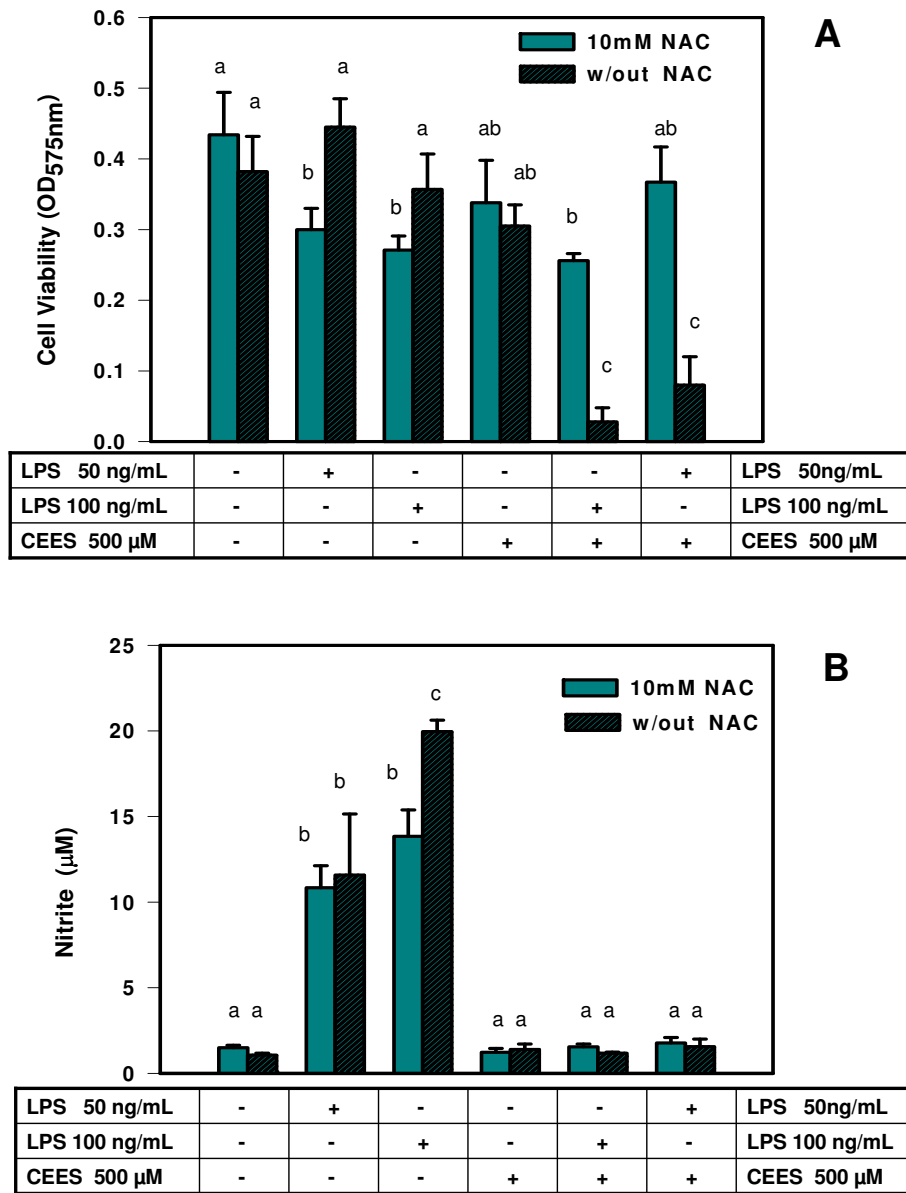


Figure 2

NAC effect on viability and NO production in CEES/LPS incubated RAW 264.7 cells (NAC pre-treatment).

Panel A: Macrophages were pre-treated with or without 10 mM NAC for 5 hours and then incubated with 50 or 100 ng/ml of LPS or/and 500 µM CEES (as indicated) for 24 hours. Cell viability was measured using the MTT assay (see Materials and Methods) and expressed as OD at 575 nm. Panel B: Macrophages were incubated as described above and NO production measured as concentration of nitrite in the culture media as described in Materials and Methods. Mean values not sharing a common letter are significantly different ($p < 0.05$).

relatively small differences are being compared. In the contrast, the protective effect of NAC on CEES+LPS treated macrophages is robust and over seven fold. This point is further reinforced by the data shown in Figure 3A, where viability of cells stimulated with LPS in the absence or in the presence of NAC was not significantly different.

The influence of NAC on oxidative stress and NO production, intracellular GSH and thiols in CEES/LPS treated macrophages by fluorescence microscopy

The influence of NAC on macrophages treated with CEES/LPS was also examined by fluorescent microscopy using three fluorescent probes: a) carboxy-dichlorofluorescein

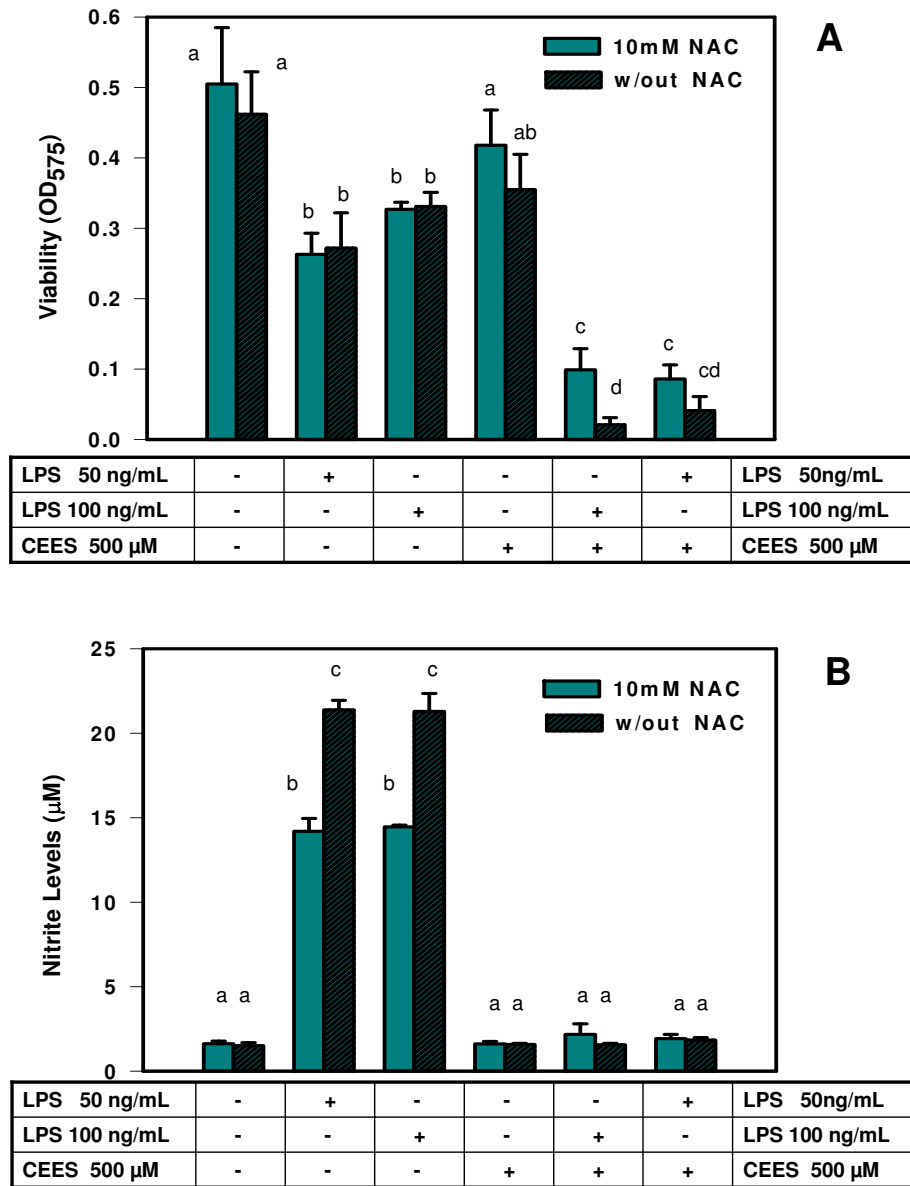


Figure 3
NAC effect on viability and NO production in CEES/LPS treated RAW 264.7 cells (NAC post-treatment). Panel A: Macrophages were incubated with 50 or 100 ng/ml of LPS or/and 500 µM CEES (as indicated) for 24 hours and 10 mM NAC was added to the cell culture medium 5 hours after the CEES/LPS application. Cell viability was measured using the MTT assay (see Materials and Methods) and expressed as OD at 575 nm. Panel B: Macrophages were incubated as described above and NO production measured as concentration of nitrite in the culture media as described in Materials and Methods. Mean values not sharing a common letter are significantly different ($p < 0.05$).

diacetate (carDCFH-DA), a sensor for combined ROS and reactive nitrogen oxide species (RNOS) generation [26-28]; b) 7-amino-4-chloromethylcoumarin (CMAC), an indicator of intracellular GSH [29], and; c) 5-chloromethylfluorescein diacetate (CMF-DA), a probe for total non-protein cellular thiol levels that lacks specificity for GSH [29,30].

Figure 4a shows the results using the lipid soluble carDCFH-DA probe. This probe enters cells and is trapped after being converted to a nonfluorescent polar derivative by cellular esterases. CarDCFH can then be oxidized by either ROS [26,28] or reactive nitrogen oxide species (RNOS) [26,27] to the fluorescent product carboxydichlorofluorescein (car-DCF) and thereby provide a qualitative index

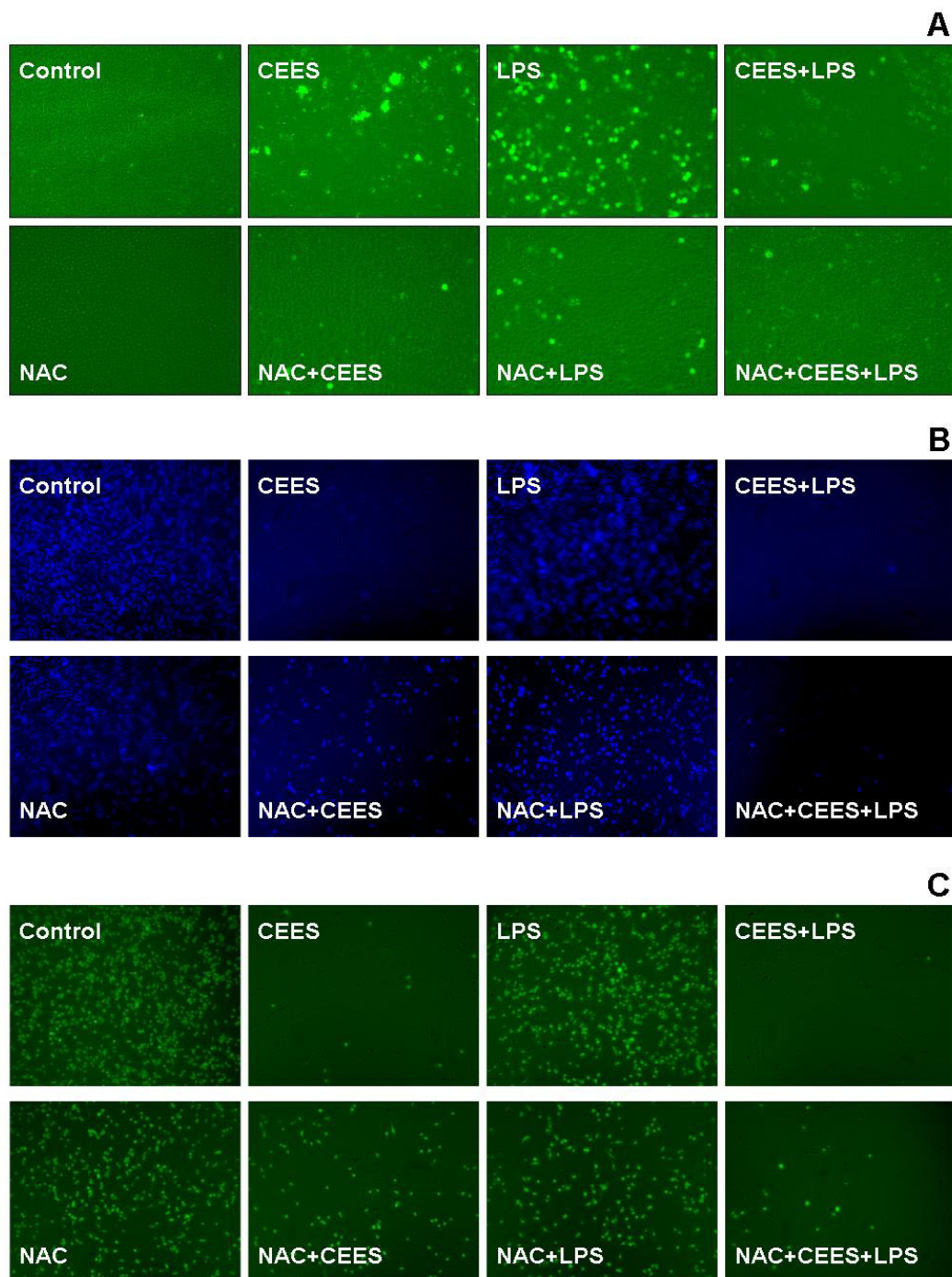


Figure 4

Fluorescent microscopy probes for oxidative stress, GSH and total thiols in RAW 264.7 cells. *Panel A:* Combined generation of ROS and RNOS were monitored using 20 μ M carDCFH-DA; *Panel B:* Intracellular GSH levels were examined using 20 μ M CMAC; *Panel C:* Levels of non-protein cellular thiols were monitored using 20 μ M CMF-DA under a fluorescent microscope. Macrophages were treated with CEES (500 μ M) and/or LPS (50 ng/mL) and incubated in the absence of NAC (top row in each panel) or in the presence of 10 mM NAC for 12 h.

of oxidation stress. As expected, treatment with LPS alone (50 ng/ml for 12 h) induced a marked generation of ROS plus RNOS in macrophages. We and others have shown that car-DCF fluorescence in activated macrophages is almost entirely from NO generation rather than ROS generation [18,27]. Figure 4a also shows that a 12 h treatment with CEES alone (500 μ M) or simultaneous treatment with 500 μ M CEES and 50 ng/ml LPS (CEES+LPS) induces a higher level of car-DCF fluorescence than observed in control cells treated with vehicle alone. We previously reported that CEES markedly reduces NO generation in LPS stimulated cells by reducing the expression of inducible iNOS [18]. The car-DCF fluorescence observed in CEES treated cells or CEES+LPS cells is likely, therefore, to be due to an enhanced generation of ROS alone with a minimal contribution from RNOS.

Simultaneous treatment with 10 mM NAC reduced the car-DCF fluorescence observed in LPS stimulated cells, as well as in CEES or CEES+LPS treated RAW 264.7 macrophages (Figure 4a, compare top row to bottom row). These data qualitatively suggest that CEES and CEES+LPS treatments induce oxidative stress in RAW 264.7 macrophages that can be diminished by NAC treatment.

As a next step we examined intracellular levels of GSH using the CMAC probe (Figure 4b, top row) and levels of total intracellular thiols using the CMF-DA probe (Figure 4c, top row). Both the CMAC and CMF probes revealed similar qualitative patterns: CEES or CEES+LPS treatment for 12 h caused cellular GSH and thiol depletion but treatment with LPS alone did not. These data reinforce the notion that treatment with either CEES alone or treatment with CEES+LPS induces sufficient oxidative stress to

reduce intracellular GSH and thiol levels. LPS alone, however, did not induce GSH or thiol depletion. NAC application was found to inhibit the loss of GSH and thiol levels caused by CEES or CEES+LPS treatment (see Figures 4b and 4c, bottom rows).

The microscopic data (Figure 4) show merged visible/fluorescent images, thus allowing cell counting and the monitoring of cell morphology changes. The counts of live (morphologically unchanged) cells under conditions described above (Figure 4) confirmed the major observations from the MTT-derived data (Figure 1a): (1) NAC treatment enhance (3-fold) the viability of CEES+LPS treated macrophages; (2) CEES+LPS is more toxic than CEES alone. The cells count (as percentage of untreated control cells \pm SEM) were 57% \pm 7, 76% \pm 10, 18% \pm 4, 84% \pm 8, 75% \pm 9, 67% \pm 6, 54% \pm 10, respectively for macrophages treated with CEES (500 μ M), LPS (50 ng/ml), CEES+LPS, NAC (10 mM), NAC+CEES, NAC+LPS and NAC+CEES+LPS.

Quantitative effects of CEES on GSH status and protein carbonyl levels in LPS-stimulated RAW 264.7 macrophages

Since the fluorescence microscopy data presented above are primarily qualitative, we wanted to confirm our results by a more quantitative approach. We, therefore, determined the effect of 500 μ M CEES on the GSH/GSSG status of RAW 264.7 macrophage treated or untreated with 50 ng/ml LPS for 12 h. Total GSH (GSH+GSSG) and GSSG concentrations were measured in cell lysates using a quantitative GSH assay kit and the values normalized to total protein content of the lysate (see Materials and Methods). Figure 5 shows that both total GSH and GSSG levels in macrophages treated with either vehicle alone or LPS were

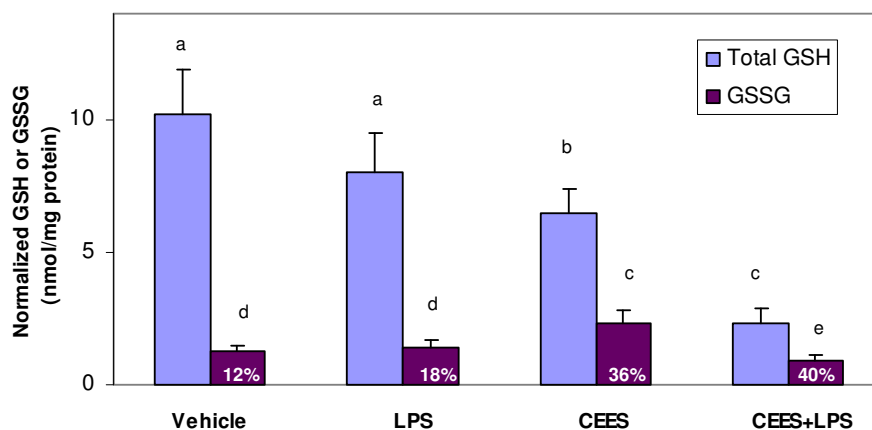


Figure 5
Glutathione status in RAW 264.7 cells incubated with CEES/LPS. Macrophages were incubated with 50 ng/ml LPS or/ and 500 μ M CEES for 12 h. Total GSH (GSH+GSSG) and GSSG levels were measured using a GSH assay kit (see Materials and Methods section) in cell lysates and normalized to total protein. Numbers show the percentage of GSSG in total GSH. Mean values not sharing a common letter are significantly different ($p < 0.05$).

not significantly different, i.e., similar to our fluorescent microscopy data. However, cells treated with CEES alone showed a depletion in total GSH as well as an increase in GSSG levels; cells treated with both CEES and LPS were further depleted in total GSH and the percentage of GSSG in these cells was the highest (40%). These results show that LPS alone does not induce a significant oxidative stress, CEES alone induces a moderate oxidative stress but the combination of both CEES and LPS induces the highest observed level of oxidative stress.

In addition, we measured the protein carbonyl levels in control cells, cells treated with CEES (500 μ M) alone or cells simultaneously treated with both LPS (50 ng/ml) and CEES (500 μ M) for 12 h. Protein carbonyls are stable protein oxidation products. The combination of CEES and LPS produced about 1.5 fold increase in protein carbonyl levels, however cells treated with CEES alone were not significantly different from control cells treated with vehicle alone (data not shown). Cells treated with LPS alone were not assayed in this experiment since both our qualitative (Figure 4b and 4c) and quantitative data (Figure 5) showed no evidence of oxidative stress with this treatment.

The inability of NAC to reverse NO loss in CEES/LPS treated cells is not GSH dependent

The data in Figure 1b show that NAC has almost no ability to restore NO production in LPS-stimulated macrophages treated with CEES. An inability of NAC to prevent the depletion of GSH in LPS-stimulated cells treated with CEES could possibly explain these results. In order to explore this possibility, we examined the ability of 5 mM NAC to prevent GSH depletion in LPS (50 ng/ml) stimulated and CEES treated (500 μ M for 4 h) RAW 264.7 cells. Figure 6 shows that CEES treatment alone decreased intracellular GSH by only about 10% compared to LPS stimulated cells in the absence NAC. As expected, the decrease in GSH levels was quite large in cells treated with both CEES+LPS (in the absence of NAC) but treatment with 5 mM NAC was effective in preventing this loss. The data shown in Figure 6 were obtained by HPLC analyses of the cell lysates but similar results were obtained by using a fluorometric assay for GSH [31] (data not shown). Despite the fact that NAC can increase the GSH level by three fold in CEES+LPS treated cells it does almost nothing to increase NO production (Figure 1a). These data suggest that the loss of NO production in CEES treated stimulated macrophages is not GSH dependent as has been observed in some other cell lines [22-25].

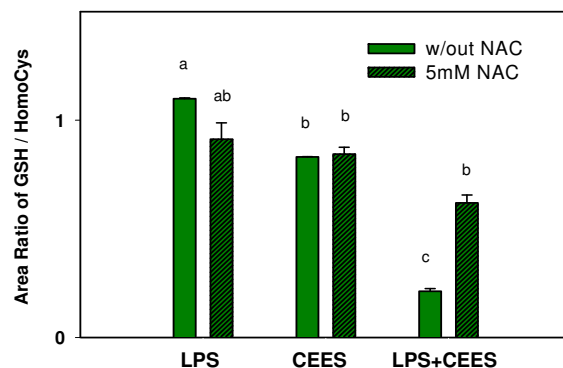


Figure 6
NAC restores intracellular GSH in RAW 264.7 cells incubated with CEES/LPS. Macrophages incubated with 50 ng/ml LPS or/and 500 μ M CEES were simultaneously treated with or without 5 mM NAC (as indicated). Cell lysates were measured for reduced GSH after 4 hour incubation using the HPLC technique described in Materials and Methods. The GSH levels were normalized to an internal homocysteine standard. Mean values not sharing a common letter are significantly different ($p < 0.05$).

Polymyxin B diminishes CEES toxicity in LPS-treated macrophages and partially blocks LPS induced NO production

Polymyxin B is an antibiotic drug, which selectively binds and neutralizes LPS. Since LPS enhances CEES toxicity, we tested the ability of polymyxin B to reduce CEES toxicity (500 μ M) and decrease NO generation in LPS (50 ng/ml) stimulated macrophages. Figure 7a shows that polymyxin B (10 μ g/ml) had no cytotoxic effect on RAW 264.7 macrophages but partially reduced the cytotoxicity of CEES+LPS treated cells (18 h). Nevertheless, polymyxin B produced at least a six fold increase in cell viability compared to cell treated with both LPS and CEES for 18 h. As shown in Figure 7b, polymyxin B effectively blocked the production of NO (measured as nitrite levels) in LPS (50 ng/ml for 18 h) treated macrophages as would be expected if it bound and blocked the action of LPS.

Discussion

The cytotoxic effect of HD, and its analogue CEES, is believed to involve an increased generation of damaging free radicals and ROS [8,11-13,32]. The data presented here show that LPS in combination with CEES induces intracellular GSH and thiol depletion as well as increased levels of protein carbonyls. In experiments with various human cell lines we have found that GSH depletion is relatively rapid as it occurs within first hour of incubation (data not shown). Thus, it is likely that this depletion is due, in large part, by a direct reaction of CEES with GSH. The measurement of protein carbonyls is one of the best

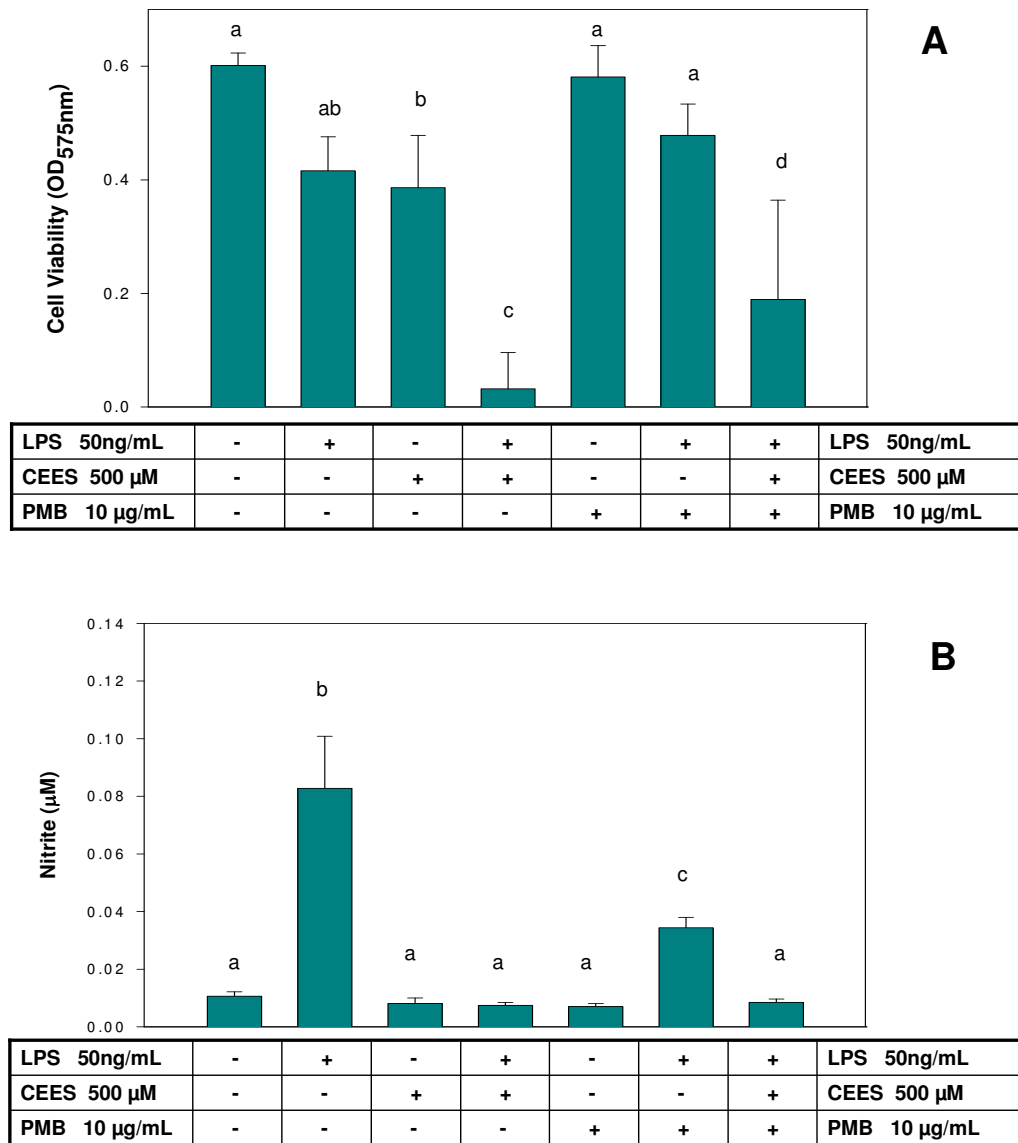


Figure 7
Polmyxin B partially protects LPS stimulated RAW 264.7 cells from CEES toxicity and blocks NO production.
Panel A: Macrophages incubated with 50 ng/ml LPS or/and 500 µM CEES were simultaneously treated with or without 10 µg/mL polymyxin B (as indicated) for 18 hours. Cell viability was measured using the MTT assay (see Materials and Methods) and expressed as OD at 575 nm. *Panel B:* Macrophages were incubated as described above. NO production was measured as nitrite concentration in the culture media as described in Materials and Methods. Mean values not sharing a common letter are significantly different (p < 0.05).

indices for oxidative stress due to the stability of protein carbonyls and sensitivity of the measurement [33]. Cellular thiols are important markers of the redox state of the cell. In particular, GSH is one of the major components of the intracellular redox system and a key intracellular antioxidant that functions as a substrate for glutathione peroxidase which detoxifies both hydrogen peroxide and lipid hydroperoxides [34,35]. Depletion of intracellular

stores of GSH plays an important role in the development of oxidative stress [12,13,36]. Recent work also suggests that the anti-apoptotic protein Bcl-2 directly interacts with GSH to regulate an important mitochondrial GSH pool that influences mitochondrial oxidative stress and subsequent apoptosis [37]. It is highly possible that both sulphur and nitrogen mustards possess a similar ability to deplete cellular thiols and induce protein oxidation.

Taken together, our data strongly suggest that CEES induces oxidative stress in stimulated macrophages. Moreover, the pattern of oxidative stress parallels the pattern observed for CEES cytotoxicity, i.e., cytotoxicity and oxidative stress are amplified in cells treated with both CEES and LPS. The addition of 5–10 mM NAC, a well characterized water-soluble antioxidant, was found to be very effective in minimizing CEES toxicity in stimulated macrophages and in preventing GSH depletion. Our data suggests that NAC can be added five hours before or even five hours after CEES and still exert a cytoprotective effect. Das et al. [9] recently found that NAC in drinking water was effective in reducing CEES-induced lung toxicity to Guinea pigs. Fan et al. [38] have shown that liposomal encapsulated NAC delivered intratracheally was more effective than free NAC against acute respiratory distress syndrome in a rat model. It is interesting, therefore, that McClintock et al. [39] have shown that reducing agents (NAC or GSH), as well as some anti-oxidant enzymes, delivered via liposomes, can substantially diminish CEES-induced injury in rat lungs. We are currently formulating an optimal antioxidant liposome preparation for treating either lung or skin induced CEES/HD injury.

We previously reported that CEES induces a transient loss of iNOS protein expression in LPS stimulated RAW 264.7 macrophages but does not inhibit the enzymatic activity of iNOS. Based on the work of others [22–25], we hypothesized that NAC treatment would not only be protective against CEES toxicity but would also restore NO production in LPS stimulated macrophages treated with CEES. Our results indicate, however, that this was not the case. Our data did, however, show that NAC effectively increases cell viability, increases GSH levels and reduces oxidative stress in LPS stimulated macrophages treated with CEES.

CEES could inhibit iNOS protein synthesis by a number of possible molecular mechanisms which we are currently exploring [18]. It is generally accepted that both the transcription factor NF- κ B and STAT-1 play central roles in the LPS induction of iNOS [17,40]. It is possible that CEES/HD could inhibit the NF- κ B and/or the STAT-1 pathways in RAW 264.7 macrophages and consequently block iNOS gene expression. For instance, CEES could alkylate the NF- κ B consensus nucleotide binding sequences thereby preventing the binding of activated NF- κ B to the iNOS promoter and block the subsequent production of iNOS mRNA and protein expression. Previous studies *in vitro* have shown that DNA alkylation by CEES [41,42] or by nitrogen mustard [43] can inhibit the DNA binding of transcription factor AP2 or NF- κ B.

Alternatively, the DNA binding ability of the NF- κ B and/or STAT-1 transcription factors could be reduced by direct

covalent modification by CEES or as an indirect result of GSH depletion, i.e., redox regulation. Nishi et al. [44] have found, for example, that the cysteine-62 (Cys-62) residue of the p50 NF- κ B protein subunit is oxidized in the cytoplasm but reduced in the nucleus, and that the reduced form is essential for NF- κ B DNA binding. It is possible that CEES could rapidly react with Cys-62 of the p50 NF- κ B subunit and prevent its DNA binding. However, since NAC was found to restore GSH levels without restoring iNOS activity (see Figures 1 and 7), it is unlikely that a GSH redox modulation of the p50 Cys-62 is the molecular mechanism for CEES induced loss of iNOS protein in LPS-stimulated macrophages. This cannot, however, be completely ruled out based on our current data.

Moreover, there is evidence suggesting that alkylating agents do not inhibit but rather promote NF- κ B activation. It is known that CEES or HD treated cells release elevated levels of TNF- α and also show NF- κ B activation both *in vitro* and *in vivo* as measured by electrophoretic mobility shift assays (EMSA)[7,45,46]. Minsavage and Dillman recently demonstrated that NF- κ B is activated by HD treatment in human cell lines via nonclassical p53-dependent pathway [47]. Collectively, these data suggest that the inhibition of iNOS expression by CEES or HD could be due to downregulation of the STAT-1 and/or classical NF- κ B pathway. We are currently exploring these various molecular mechanisms.

In the work presented here, we also tested the ability of polymyxin B to block the effect of LPS. Polymyxin B binds to the lipid A domain of LPS and neutralizes its activity. Our data show that polymyxin B effectively inhibits CEES toxicity in LPS stimulated cells. *In vivo*, LPS could directly enhance CEES/HD toxicity in cells with functional CD14 receptors or by triggering the release of pro-inflammatory cytokines, such as TNF- α and IL-1 β , by immune cells. We have previously demonstrated that inflammatory cytokines also enhance CEES cytotoxicity [15].

Conclusion

Our *in vitro* work presents novel evidence supporting the view that oxidative stress is an important component of CEES/HD toxicity and that antioxidants have therapeutic potential. We anticipated that NAC would prevent GSH depletion and restore the loss of iNOS activity in CEES treated macrophages stimulated with LPS. Although NAC was effective in preventing both CEES toxicity and GSH depletion, it failed to restore iNOS expression. Our results to date indicate that CEES causes a transient decrease in iNOS protein syntheses rather than a direct inhibition of iNOS activity due to covalent modification(s) by CEES. We are currently investigating the molecular mechanism(s) for the down regulation of iNOS expression by CEES.

Inhibition of iNOS and NO production could be an important element in the slow wound healing observed subsequent to CEES/HD injury. Considerable evidence suggests that iNOS is an important component of wound healing [19,20,48]. Although NAC maybe effective at reducing CEES/HD toxicity it is not effective at elevating NO production due to iNOS inhibition by CEES/HD. A more detailed understanding of the molecular mechanism(s) responsible for iNOS inhibition by CEES/HD could, therefore, be useful in the design of more effective countermeasures.

The fact that LPS was found to enhance CEES toxicity highlights the potential importance of preventing secondary infection in the treatment of HD toxicity.

LPS is a component of gram negative bacteria and a ubiquitous environmental contaminant. Its presence at very low levels (ng/ml) amplifies the toxicity of CEES. Polymyxin B, a topically applied antibiotic that binds LPS, was shown to block the iNOS inducing ability of LPS and to reduce CEES toxicity in LPS stimulated cells. Polymyxin B could, therefore, be useful as a supportive treatment in order to prevent secondary infections and to reduce HD toxicity, since it both neutralizes LPS and prevents the growth of gram-negative bacteria in healing wounds.

The path to an optimal countermeasure to CEES/HD exposure may lie in a poly-drug formulation that minimizes oxidative stress, prevents inflammation and secondary infections, and, also, protects iNOS activity. Antioxidant liposomes are currently being investigated as they have unique ability for targeted delivery of both water-soluble and lipid soluble antioxidants [49] or other drugs, for instance, polymyxin B (personal communications, Dr. Zach Suntres) as well as anti-inflammatory agents.

Methods

Materials

RPMI-1640 medium without phenol red and fetal bovine serum with a low endotoxin level were purchased from Life Technologies (Gaithersburg, MD). *Escherichia coli* lipopolysaccharide serotype 0111:B4, 3-(4,5-dimethylthiazolyl-2)-2,5-diphenyltetrazolium bromide (MTT), CEES, NAC, Greiss reagent, GSH, BHT, EDTA, and all organic solvents used were obtained from Sigma Chemical Company (St. Louis, MO). Fluorescent dyes carDCFH-DA, CMAC, and CMF-DA were purchased from Molecular Probes (Invitrogen Corp., Carlsbad, CA).

Cell culture and treatments

RAW264.7 murine macrophage-like cells (American Type Culture Collection, Rockville, MD) were cultured at 37°C in a humidified incubator with 5% CO₂ in RPMI-1640

medium with 10% fetal bovine serum, 100 U/ml penicillin and 100 mg/ml streptomycin (GiBcoBRL Grand Island, NY). Adherent cells were subcultured in 96 well Costar tissue culture plates and treated with CEES and/or LPS in the presence or absence of various concentrations of NAC as indicated in the Figure legends. CEES was used only as a fresh 50 mM stock solution in anhydrous ethanol. LPS was prepared as a 0.5 µg/ml stock solution in PBS, filter-sterilized and stored at -20°C for up to 6 months. NAC was prepared as a 0.5 M stock solution in PBS (pH adjusted to 7.4), filter-sterilized and stored at 4°C for up to two weeks.

MTT assay

MTT assay was performed by a slight modification of the method described by Wasserman et al. [50,51]. Briefly, at the end of each experiment, cultured cells in 96 well plates (with 200 µl of medium per well) were incubated with MTT (20 µl of 5 µg/ml per well) at 37°C for 4 h. The formazan product was solubilized by addition of 100 µl of dimethyl sulfoxide (DMSO) and the OD measured at 575 nm with a Spectramax Plus 384 microplate reader (Molecular Devices Corp, Sunnyvale, CA)

NO generation in RAW264.7 macrophages

The production of NO, reflecting cellular NO synthase activity, was estimated from the accumulation of nitrite (NO₂⁻), a stable breakdown product of NO, in the medium. NO₂⁻ was assayed by the method of Green et al. [52]. Briefly, an aliquot of cell culture medium was mixed with an equal volume of Greiss reagent which reacts with NO₂⁻ to form an azo-product. Absorbance of the reaction product was determined at 532 nm using a Spectramax Plus 384 microplate reader (Molecular Devices Corp, Sunnyvale, CA). Sodium nitrite was used as a standard to calculate NO₂⁻ concentrations.

Quantitative GSH analyses

RAW264.7 macrophages incubated in 96-well plate (~10⁶ adherent cells/well) and treated with LPS/CEES/NAC as indicated in the Figure legends was assayed for total GSH (GSH plus GSSG) using the GSH assay kit (World Precision Instruments, Sarasota, FL) according to the company's protocol. This assay uses the Tietze's enzymatic recycling method [53]. In order to measure just GSSG, 2-vinylpyridine was first used to derivatize GSH alone [54]. Total GSH and GSSG levels were normalized to the total protein (as determined by the standard BCA assay). Alternatively, GSH analyses of the cell lysates were analyzed by isocratic HPLC with electrochemical detector composed of Coulochem II model 5200A and a Coulochem 5011 analytical cell (ESA Inc, Chelmsford, MA) as described by [55]. Since the cell lysates contained no measurable levels of homocysteine, this aminothiols was used as an internal standard.

Protein carbonyl measurement

Protein carbonyl levels were measured by an enzyme immunoassay kit from Cell Biolabs (San Diego, CA) according to the manufacturer's instructions. In this assay, the protein samples are derivatized by making use of the reaction between 2,4-dinitrophenylhydrazine (DNPH) and protein carbonyls to form a DNP hydrazone which is assayed using an anti-DNP antibody and a HRP conjugated secondary antibody. A standard curve from the oxidized BSA standards was run with each microplate. This kit assay is essentially a modification [56] of the method described by Buss et al. [57].

Fluorescent microscopic analyses

The cell density was adjusted to 2×10^5 /ml, and a 100 μ l aliquot of the cell suspension in media was placed in each well of an 8-well Lab-Tek chamber glass slide (Nunc, Rochester, NY). Vehicle alone, CEES alone (500 μ M), CEES+LPS (50 ng/ml) in the presence or absence of NAC (10 mM) were simultaneously added to chamber slides and incubated for 12 h at 37°C in 5% CO₂. At the end of the treatment a stock solution of desired fluorescent probe in DMSO was added and the slides incubated for an additional 30 min at 37°C. The cells were washed with fresh PBS twice, observed and digitally photographed using a MOTIC inverted phase contrast fluorescence microscope equipped with a Nikon Coolpix E4300 4-megapixel camera (Martin Microscope, Easley, SC). A 20 μ M carDCFH-DA and a standard FITC filter were used to monitor combined ROS and RNOS generation; a 20 μ M CMAC and a standard DAPI filter were used to monitor intracellular GSH; a 20 μ M CMF-DA and a standard FITC filter were used to monitor cellular thiol levels. All the optical filters were obtained from Chroma Technology Corp (Rockingham, VT).

Statistical analyses

Data were analyzed ANOVA followed with the Scheffe test for significance with $p < 0.05$ using SPSS 14.0 for Windows (Chicago, IL). Results were expressed as the mean \pm SD. In all the Figures, mean values not sharing a common letter are significantly different ($p < 0.05$). Mean values sharing a common letter are not significantly different. The mean values and standard deviations of at least three independent experiments are provided in all the Figures.

Abbreviations

AP2, activating protein 2; CEES, 2-chloroethyl ethyl sulphide; carDCFH-DA, carboxy-dichlorofluorescein diacetate; CMAC, 7-amino-4-chloromethylcoumarin; CMF-DA, 5-chloromethylfluorescein diacetate; DNPH, 2,4-dinitrophenylhydrazine; GSH, reduced glutathione; GSSG, oxidized glutathione; HD, sulphur mustard gas; IL-1 β , interleukin-1 beta; LPS, lipopolysaccharide; MTT, 3-(4,5-dimethylthiazol-2-yl)-2,5-diphenyltetrazolium bro-

mid; NAC, N-acetyl-L-cysteine; NO, nitric oxide; iNOS, inducible nitric oxide synthase; NF- κ B, nuclear factor kappa B; RNOS, reactive nitrogen oxide species; ROS, reactive oxygen species; STAT-1, signal transducer and activator of transcription-1; TNF- α , tumor necrosis factor- α

Authors' contributions

VP and WLS analyzed the data and drafted the manuscript. WLS supervised the overall conduct of the research, which was performed in his laboratory. VP, MQ and HY carried out the experimental work in this study and performed the statistical analyses. MS (along with WLS) conceived of the study, participated in the study design, and provided continuous evaluation of the experimental data. All authors read and approved the final manuscript.

Acknowledgements

This research was supported by three United States Army Medical Research Command (USAMRMC) Grants: "The Influence of Antioxidant Liposomes on Macrophages Treated with Mustard Gas Analogues", Grant No. 98164001; "Topical Application of Liposomal Antioxidants for Protection against CEES Induced Skin Damage", Contract No. W81XWH-05-2-0034 and; "A Proteomic Approach for Studying the Therapeutic Use of Antioxidant Liposomes", Contract No. W81XWH-06-2-044.

References

1. Paromov V, Suntutres Z, Smith M, Stone WL: **Sulfur mustard toxicity following dermal exposure: role of oxidative stress, and antioxidant therapy.** *J Burns Wounds* 2007, **7**:e7.
2. Balali-Mood M, Hefazi M: **The pharmacology, toxicology, and medical treatment of sulphur mustard poisoning.** *Fundam Clin Pharmacol* 2005, **19**(3):297-315.
3. Smith KJ, Casillas R, Graham J, Skelton HG, Stemler F, Hackley BE Jr.: **Histopathologic features seen with different animal models following cutaneous sulfur mustard exposure.** *Journal of dermatological science* 1997, **14**(2):126-135.
4. Dacre JC, Goldman M: **Toxicology and pharmacology of the chemical warfare agent sulfur mustard.** *Pharmacological reviews* 1996, **48**(2):289-326.
5. Arroyo CM, Burman DL, Kahler DW, Nelson MR, Corun CM, Guzman JJ, Smith MA, Purcell ED, Hackley BE Jr., Soni SD, Broomfield CA: **TNF-alpha expression patterns as potential molecular biomarker for human skin cells exposed to vesicant chemical warfare agents: sulfur mustard (HD) and Lewisite (L).** *Cell biology and toxicology* 2004, **20**(6):345-359.
6. Arroyo CM, Schafer RJ, Kurt EM, Broomfield CA, Carmichael AJ: **Response of normal human keratinocytes to sulfur mustard (HD): cytokine release using a non-enzymatic detachment procedure.** In *Human & experimental toxicology Volume 18. Issue 1 ENGLAND*; 1999:1-11.
7. Arroyo CM, Schafer RJ, Kurt EM, Broomfield CA, Carmichael AJ: **Response of normal human keratinocytes to sulfur mustard: cytokine release.** In *J Appl Toxicol Volume 20 Suppl 1. England*; 2000:S63-72.
8. Arroyo CM, Von Tersch RL, Broomfield CA: **Activation of alpha-human tumour necrosis factor (TNF-alpha) by human monocytes (THP-1) exposed to 2-chloroethyl ethyl sulphide (H-MG).** In *Hum Exp Toxicol Volume 14. Issue 7 ENGLAND*; 1995:547-553.
9. Das SK, Mukherjee S, Smith MG, Chatterjee D: **Prophylactic protection by N-acetylcysteine against the pulmonary injury induced by 2-chloroethyl ethyl sulfide, a mustard analogue.** *Journal of biochemical and molecular toxicology* 2003, **17**(3):177-184.
10. Mukhopadhyay S, Rajaratnam V, Mukherjee S, Smith M, Das SK: **Modulation of the expression of superoxide dismutase gene in**

- lung injury by 2-chloroethyl ethyl sulfide, a mustard analog.** *Journal of biochemical and molecular toxicology* 2006, **20(3)**:142-149.
11. Elsayed NM, Omaye ST, Klain GJ, Korte DW Jr.: **Free radical-mediated lung response to the monofunctional sulfur mustard butyl 2-chloroethyl sulfide after subcutaneous injection.** *Toxicology* 1992, **72(2)**:153-165.
 12. Elsayed NM, Omaye ST: **Biochemical changes in mouse lung after subcutaneous injection of the sulfur mustard 2-chloroethyl 4-chlorobutyl sulfide.** *Toxicology* 2004, **199(2-3)**:195-206.
 13. Han S, Espinoza LA, Liao H, Boulares AH, Smulson ME: **Protection by antioxidants against toxicity and apoptosis induced by the sulphur mustard analog 2-chloroethylethyl sulphide (CEES) in Jurkat T cells and normal human lymphocytes.** *British journal of pharmacology* 2004, **141(5)**:795-802.
 14. Naghii MR: **Sulfur mustard intoxication, oxidative stress, and antioxidants.** *Mil Med* 2002, **167(7)**:573-575.
 15. Stone WL, Qui M, Smith M: **Lipopolysaccharide enhances the cytotoxicity of 2-chloroethyl ethyl sulfide.** *BMC cell biology* 2003, **4(1)**:1.
 16. Ganster RW, Taylor BS, Shao L, Geller DA: **Complex regulation of human inducible nitric oxide synthase gene transcription by Stat 1 and NF-kappa B.** *Proceedings of the National Academy of Sciences of the United States of America* 2001, **98(15)**:8638-8643.
 17. Gao J, Morrison DC, Parmely TJ, Russell SW, Murphy WJ: **An interferon-gamma-activated site (GAS) is necessary for full expression of the mouse iNOS gene in response to interferon-gamma and lipopolysaccharide.** *The Journal of biological chemistry* 1997, **272(2)**:1226-1230.
 18. Qui M, Paromov VM, Yang H, Smith M, Stone WL: **Inhibition of inducible Nitric Oxide Synthase by a mustard gas analog in murine macrophages.** *BMC cell biology* 2006, **7**:39.
 19. Schwentker A, Billiar TR: **Nitric oxide and wound repair.** *The Surgical clinics of North America* 2003, **83(3)**:521-530.
 20. Witte MB, Kiyama T, Barbul A: **Nitric oxide enhances experimental wound healing in diabetes.** *The British journal of surgery* 2002, **89(12)**:1594-1601.
 21. Yamasaki K, Edington HD, McClosky C, Tzeng E, Lizonova A, Kovesdi I, Steed DL, Billiar TR: **Reversal of impaired wound repair in iNOS-deficient mice by topical adenoviral-mediated iNOS gene transfer.** *The Journal of clinical investigation* 1998, **101(5)**:967-971.
 22. Duval DL, Sieg DJ, Billings RE: **Regulation of hepatic nitric oxide synthase by reactive oxygen intermediates and glutathione.** *Archives of biochemistry and biophysics* 1995, **316(2)**:699-706.
 23. Harbrecht BG, Di Silvio M, Chough V, Kim YM, Simmons RL, Billiar TR: **Glutathione regulates nitric oxide synthase in cultured hepatocytes.** *Ann Surg* 1997, **225(1)**:76-87.
 24. Tirmenstein MA, Nicholls-Grzemski FA, Schmittgen TD, Zakrajsek BA, Fariss MW: **Glutathione-dependent regulation of nitric oxide production in isolated rat hepatocyte suspensions.** *Antioxidants & redox signaling* 2000, **2(4)**:767-777.
 25. Vos TA, Van Goor H, Tuyt L, De Jager-Krikken A, Leuvenink R, Kuipers F, Jansen PL, Moshage H: **Expression of inducible nitric oxide synthase in endotoxemic rat hepatocytes is dependent on the cellular glutathione status.** *Hepatology* 1999, **29(2)**:421-426.
 26. Myhre O, Andersen JM, Aarnes H, Fonnum F: **Evaluation of the probes 2',7'-dichlorofluorescein diacetate, luminol, and lucigenin as indicators of reactive species formation.** *Biochemical pharmacology* 2003, **65(10)**:1575-1582.
 27. Imrich A, Kobzik L: **Fluorescence-based measurement of nitric oxide synthase activity in activated rat macrophages using dichlorofluorescein.** *Nitric Oxide* 1997, **1(4)**:359-369.
 28. LeBel CP, Ischiropoulos H, Bondy SC: **Evaluation of the probe 2',7'-dichlorofluorescein as an indicator of reactive oxygen species formation and oxidative stress.** *Chemical research in toxicology* 1992, **5(2)**:227-231.
 29. Sebastia J, Cristofol R, Martin M, Rodriguez-Farre E, Sanfeliu C: **Evaluation of fluorescent dyes for measuring intracellular glutathione content in primary cultures of human neurons and neuroblastoma SH-SY5Y.** *Cytometry A* 2003, **51(1)**:16-25.
 30. Poot M, Kavanagh TJ, Kang HC, Haugland RP, Rabinovitch PS: **Flow cytometric analysis of cell cycle-dependent changes in cell thiol level by combining a new laser dye with Hoechst 33342.** *Cytometry* 1991, **12(2)**:184-187.
 31. Kamencic H, Lyon A, Paterson PG, Juurlink BH: **Monochlorobimane fluorometric method to measure tissue glutathione.** *Analytical biochemistry* 2000, **286(1)**:35-37.
 32. Elsayed NM, Omaye ST, Klain GJ, Inase JL, Dahlberg ET, Wheeler CR, Korte DW Jr.: **Response of mouse brain to a single subcutaneous injection of the monofunctional sulfur mustard, butyl 2-chloroethyl sulfide (BCS)*.** *Toxicology* 1989, **58(1)**:11-20.
 33. Berlett BS, Stadtman ER: **Protein oxidation in aging, disease, and oxidative stress.** *The Journal of biological chemistry* 1997, **272(33)**:20313-20316.
 34. Stone WL, Smith M: **Therapeutic uses of antioxidant liposomes.** *Mol Biotechnol* 2004, **27(3)**:217-230.
 35. Droge W: **Free radicals in the physiological control of cell function.** *Physiological reviews* 2002, **82(1)**:47-95.
 36. Kadar T, Turetz J, Fishbine E, Sahar R, Chapman S, Amir A: **Characterization of acute and delayed ocular lesions induced by sulfur mustard in rabbits.** *Current eye research* 2001, **22(1)**:42-53.
 37. Zimmermann AK, Loucks FA, Schroeder EK, Bouchard RJ, Tyler KL, Linseman DA: **Glutathione binding to the Bcl-2 homology-3 domain groove: a molecular basis for Bcl-2 antioxidant function at mitochondria.** *The Journal of biological chemistry* 2007, **282(40)**:29296-29304.
 38. Fan J, Shek PN, Suntres ZE, Li YH, Oreopoulos GD, Rotstein OD: **Liposomal antioxidants provide prolonged protection against acute respiratory distress syndrome.** *Surgery* 2000, **128(2)**:332-338.
 39. McClintock SD, Hoeseel LM, Das SK, Till GO, Neff T, Kunkel RG, Smith MG, Ward PA: **Attenuation of half sulfur mustard gas-induced acute lung injury in rats.** *J Appl Toxicol* 2006, **26(2)**:126-131.
 40. Kleinert H, Pautz A, Linker K, Schwarz PM: **Regulation of the expression of inducible nitric oxide synthase.** *Eur J Pharmacol* 2004, **500(1-3)**:255-266.
 41. Chen XM, Gray PJ, Cullinane C, Phillips DR: **Differential sensitivity of transcription factors to mustard-damaged DNA.** *Chemico-biological interactions* 1999, **118(1)**:51-67.
 42. Gray PJ: **Sulphur mustards inhibit binding of transcription factor AP2 in vitro.** *Nucleic Acids Res* 1995, **23(21)**:4378-4382.
 43. Fabbri S, Prontera C, Broggin M, D'Incalci M: **Differential inhibition of the DNA binding of transcription factors NF kappa B and OTF-1 by nitrogen mustard and quinacrine mustard: transcriptional implications.** *Carcinogenesis* 1993, **14(9)**:1963-1967.
 44. Nishi T, Shimizu N, Hiramoto M, Sato I, Yamaguchi Y, Hasegawa M, Aizawa S, Tanaka H, Kataoka K, Watanabe H, Handa H: **Spatial redox regulation of a critical cysteine residue of NF-kappa B in vivo.** *The Journal of biological chemistry* 2002, **277(46)**:44548-44556.
 45. Atkins KB, Lodhi JJ, Hurley LL, Hinshaw DB: **N-acetylcysteine and endothelial cell injury by sulfur mustard.** *J Appl Toxicol* 2000, **20 Suppl 1**:S125-8.
 46. Chatterjee D, Mukherjee S, Smith MG, Das SK: **Signal transduction events in lung injury induced by 2-chloroethyl ethyl sulfide, a mustard analog.** *Journal of biochemical and molecular toxicology* 2003, **17(2)**:114-121.
 47. Minsavage GD, Dillman JF: **BIFUNCTIONAL ALKYLATING AGENT-INDUCED p53 AND NONCLASSICAL NUCLEAR FACTOR-KAPPA B (NF- κ B) RESPONSES AND CELL DEATH ARE ALTERED BY CAFFEIC ACID PHENETHYL ESTER (CAPE): A potential role for antioxidant/electrophilic response element (ARE/EpRE) signaling.** *J Pharmacol Exp Ther* 2007, **321(1)**:202-212.
 48. Soneja A, Drews M, Malinski T: **Role of nitric oxide, nitroxidative and oxidative stress in wound healing.** *Pharmacol Rep* 2005, **57 Suppl**:108-119.
 49. Stone WL, Mukherjee S, Smith M, Das SK: **Therapeutic uses of antioxidant liposomes.** *Methods Mol Biol* 2002, **199**:145-161.
 50. Wasserman TH, Twentyman P: **Use of a colorimetric microtiter (MTT) assay in determining the radiosensitivity of cells from murine solid tumors.** *Int J Radiat Oncol Biol Phys* 1988, **15(3)**:699-702.
 51. Twentyman PR, Luscombe M: **A study of some variables in a tetrazolium dye (MTT) based assay for cell growth and chemosensitivity.** *Br J Cancer* 1987, **56(3)**:279-285.
 52. Green LC, Wagner DA, Glogowski J, Skipper PL, Wishnok JS, Tannenbaum SR: **Analysis of nitrate, nitrite, and [15N]nitrate in**

- biological fluids.** In *Analytical biochemistry Volume 126. Issue 1 UNITED STATES*; 1982:131-138.
53. Tietze F: **Enzymic method for quantitative determination of nanogram amounts of total and oxidized glutathione: applications to mammalian blood and other tissues.** *Analytical biochemistry* 1969, **27(3)**:502-522.
 54. Griffith OW: **Determination of glutathione and glutathione disulfide using glutathione reductase and 2-vinylpyridine.** *Analytical biochemistry* 1980, **106(1)**:207-212.
 55. Houze P, Gamra S, Madelaine I, Bousquet B, Gourmel B: **Simultaneous determination of total plasma glutathione, homocysteine, cysteinylglycine, and methionine by high-performance liquid chromatography with electrochemical detection.** *Journal of clinical laboratory analysis* 2001, **15(3)**:144-153.
 56. Alamdari DH, Kostidou E, Paletas K, Sarigianni M, Konstas AG, Karapiperidou A, Koliakos G: **High sensitivity enzyme-linked immunosorbent assay (ELISA) method for measuring protein carbonyl in samples with low amounts of protein.** *Free radical biology & medicine* 2005, **39(10)**:1362-1367.
 57. Buss H, Chan TP, Sluis KB, Domigan NM, Winterbourn CC: **Protein carbonyl measurement by a sensitive ELISA method.** *Free radical biology & medicine* 1997, **23(3)**:361-366.

Publish with **BioMed Central** and every scientist can read your work free of charge

"BioMed Central will be the most significant development for disseminating the results of biomedical research in our lifetime."

Sir Paul Nurse, Cancer Research UK

Your research papers will be:

- available free of charge to the entire biomedical community
- peer reviewed and published immediately upon acceptance
- cited in PubMed and archived on PubMed Central
- yours — you keep the copyright

Submit your manuscript here:
http://www.biomedcentral.com/info/publishing_adv.asp



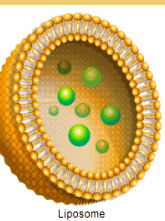
Abstract

Sulfur mustard, 2, 2'-dichlorodiethyl sulfide (HD), is a chemical warfare agent causing extensive skin injury characterized by vesication, slow healing lesions, blistering, and inflammation. Both HD and its monofunctional analogue, 2-chloroethyl ethyl sulfide (CEES), are alkylating agents that induce massive DNA damage followed with oxidative stress. Antioxidant liposomes based on soybean phospholipids (Phospholipon 90G) have the unique ability to deliver water-soluble and lipid-soluble antioxidants through skin tissues. We developed several liposomal formulations containing water-soluble antioxidants (N-acetyl cysteine or reduced glutathione) and/or lipid-soluble antioxidants (tocopherols or alpha-lipoic acid). The protective effects of liposomes were initially studied in HaCaT keratinocytes exposed to 1 mM CEES. N-acetyl cysteine (NAC) and glutathione (GSH) were most protective in reducing CEES-induced toxicity.

The most protective liposomal formulations were then tested in EpiDerm tissues, which model the human epidermis. CEES (0.2 – 5 mM) was quickly mixed with medium and applied topically; tissues were incubated for 18 hours, and cell viability was assayed. NAC or GSH containing liposomes, if applied simultaneously with CEES, markedly increased viability of the tissues exposed to 2.5 mM CEES and restored CEES induced loss of ATP. GSH containing liposomes effectively protected human keratinocytes even if applied 1 hour after the CEES exposure. Microscopic studies revealed that CEES exposure (1 – 5 mM) reduced the number of viable cells, induced fragmentation of extracellular matrix, and altered cellular morphology. Antioxidant-liposome treatment not only effectively restored cell viability but also attenuated changes in cellular morphology. Our results suggest that the encapsulation of antioxidants in soybean phospholipid-based liposomes should be a useful therapeutic strategy for the treatment of mustard toxicity in human skin.

This work was supported by the U.S. Army Medical Research and Materiel Command under Grant W81XWH-05-2-0034.

Antioxidant Liposomes



Liposomes are nano-particles (size 100 – 500 nm)

They consist of a phospholipid bilayer and aqueous inner-space.

Both lipid soluble chemical antioxidants (can be inserted into lipid bilayer) and water-soluble chemical antioxidants (can be encapsulated into aqueous phase) can be delivered by the liposomes

We used liposomes containing encapsulated glutathione (GSH) or N-acetyl-cysteine (NAC)

Results

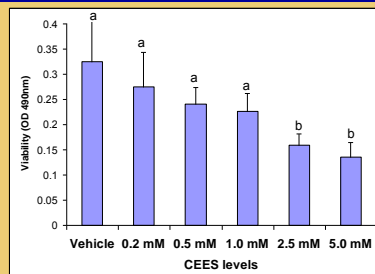


Figure 1. CEES toxicity in the EpiDerm: tissues were topically exposed to vehicle (1% DMSO) or CEES (as indicated) for 18 hours. Cell viability was monitored by the MTS assay. For all graphs: Means not sharing a common letter are significantly different ($p < 0.05$)

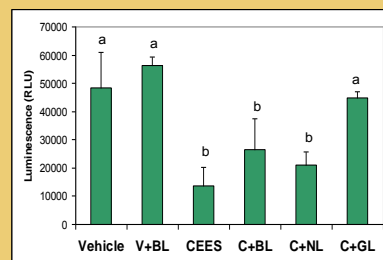


Figure 3. Antioxidant Liposomes prevent cellular ATP depletion in EpiDerm: tissues were exposed to 2.5 mM CEES or vehicle (1% DMSO) in the absence or presence of Blank Liposomes (BL), NAC-Liposomes (NL), GSH-Liposomes (GL) [simultaneously] for 18 hours (as indicated). Cellular ATP was assayed in cell lysates by the ATP assay.

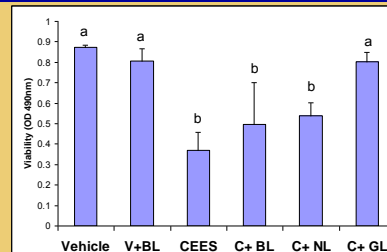


Figure 2. Protective effect of Antioxidant Liposomes in EpiDerm: tissues were exposed to 2.5 mM CEES or vehicle (1% DMSO) in the absence or presence of Blank Liposomes (BL), NAC-Liposomes (NL), GSH-Liposomes (GL) [simultaneously] for 18 hours. Cell viability was monitored by the MTS assay.

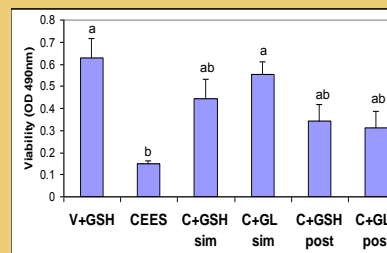


Figure 4. Protective effect of free GSH and GSH-Liposomes in EpiDerm: tissues were exposed topically to vehicle (1% DMSO) and 10 mM free GSH (V+GSH) or 2.5 mM CEES in the absence or presence of free GSH or GSH-Liposomes (GL) [sim, simultaneous application; post, 1 hour post-treatment]. Cell viability was monitored after 18 hours by the MTS assay.

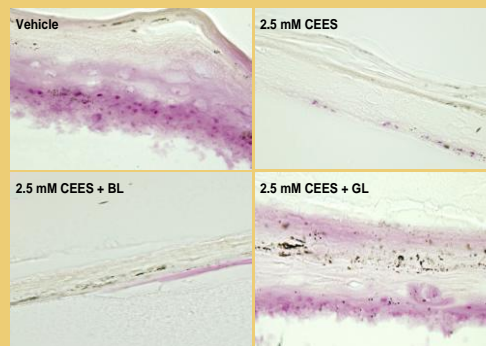


Figure 5. Protective effect of GSH-Liposomes in EpiDerm tissues: EpiDerm tissues were topically exposed to vehicle (1% DMSO) or 2.5 mM CEES in the absence or presence of GSH-Liposomes (GL). After the MTS assay EpiDerm tissues were frozen, dissected, and photographed under a light microscope with 400x magnification.

Conclusions

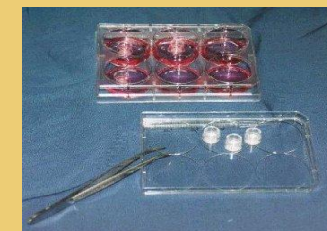
High levels of genotoxic agent CEES (> 2 mM) significantly reduced the viability of human keratinocytes in EpiDerm tissues (Figure 1)

GSH-containing liposomes are effective in blocking CEES toxicity (Figures 2 and 4) and prevented cellular ATP depletion in EpiDerm tissues (Figure 3).

GSH-Liposomes partially reversed morphological changes in keratinocytes exposed to CEES (Figure 5)

Collectively, our data present evidence that Antioxidant Liposomes downregulate necrotic cell death pathway in genotoxic stress

GSH-Liposomes present a promising therapeutic strategy for the treatment of mustard toxicity in human skin



Future Directions

Explore the *in vivo* effect of antioxidant liposomes in an animal model

Study the mechanisms of HD/CEES toxicity and antioxidant protection in human cell lines at the cellular/molecular level

Develop "multi-drug" Phospholipon-based antioxidant liposomes for delivery both antioxidants and anti-inflammatory agents

Abstract

EpiDerm tissues consist of artificially grown epidermal keratinocyte multi-layers and represent a useful model of the human epidermis. We applied a proteomics approach to study how a sulfur mustard analog, 2-chloroethyl ethyl sulfide (CEES), influences protein expression. CEES is an alkylating agent that induces massive DNA damage followed by oxidative stress. Also, we explored whether antioxidant liposomes containing reduced glutathione (GSH) are able to reverse CEES-induced changes in keratinocyte proteomics. GSH containing liposomes were shown to restore cell viability of the tissues exposed to 2.5 mM CEES. Antioxidant liposomes were based on soybean phospholipids (Phospholipon 90G); they are highly effective for delivery water-soluble antioxidants through the skin barrier. Protein expression in human keratinocytes was studied with a standard two-dimensional gel electrophoresis (2D-GE). Protein spots were stained with a mass spectrometry (MS) friendly silver stain and the gel images analyzed with Dymention 2 software in order to target over- or under-expressed proteins. We found 18 protein spots, whose expression was drastically changed when keratinocytes were exposed to 2.5 mM CEES. Notably, the expression of 14 proteins out of those 18 spots was partially reversed when CEES was applied simultaneously with GSH-containing liposomes.

To ensure our ability to identify targeted proteins from silver-stained 2D gels we analyzed a random abundant protein spot from a sample treated with vehicle alone. The spot was extracted from the 2D gel, stripped of the silver stain, trypsinized; and resulting peptide mixture was analyzed using nanospray LS/MS on LTQ Linear Ion Trap Mass Spectrometer (Thermo-Fisher). The spot appeared to contain three highly homologous proteins: 14-3-3 protein sigma, 14-3-3 protein theta, and 14-3-3 protein zeta, as determined via UniProt database search. In the future, we will continue to identify proteins whose expression is altered by CEES exposure but restored due to the antioxidant liposome treatment.

EpiDerm Skin Model

EpiDerm™ consists of normal, human-derived epidermal keratinocytes (NHEK) which have been cultured to form a multilayered, highly differentiated model of the human epidermis. These "ready-to-use" tissues, which are cultured on specially prepared cell culture inserts using serum free medium, attain levels of differentiation on the cutting edge of *in vitro* skin technology. Structurally, the EpiDerm Skin Model closely models human skin, thus providing a useful *in vitro* means to assess toxicology.

Results

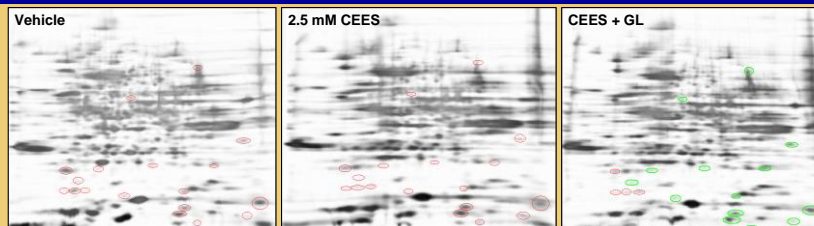


Figure 1: Proteomics Study of CEES toxicity and the effect of GSH-Liposomes in EpiDerm. Tissues were exposed to vehicle or 2.5 mM CEES in the absence or presence of GSH-liposomes for 18 h. Cell lysates were separated by 2D gel electrophoresis, silver-stained and photographed (three gels per sample). Average differences in protein expression were quantified with Dymension-2 Software. The proteins differentially expressed after CEES exposure are marked with red circles. The proteins, which expression was partially reversed by GSH-liposomes are marked with green circles.

Table 1. Quantitative differences in protein expression

Treatment: Vehicle, 1% EtOH; CEES, 2.5 mM CEES; CEES+GL, CEES and GSH-liposomes simultaneously. Positive values show protein up-regulation. Negative values show protein down-regulation

Spot	MW (kDa)	Volume Ratio		
		Vehicle	CEES	CEES + GL
1	50.6	1	-3.935	-1.322
2	34.1	1	-2.827	-1.049
3	28.3	1	-1.739	1.174
4	19.5	1	-2.92	-1.224
5	13.4	1	-3.186	-1.403
6	12.2	1	-2.02	1.068
7	11.7	1	1.657	-1.028
8	11.3	1	-1.591	-1.198
9	10.8	1	-2.095	-1.465
10	10.2	1	1.731	-1.219
11	9.3	1	1.761	-1.323

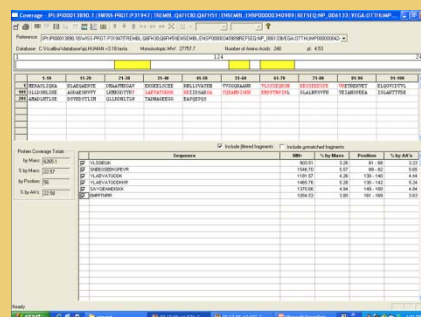


Figure 3: Identification of a set of three proteins from a 2D gel spot (LC/MS/MS data). Coverage for 14-3-3 Protein Sigma: specific peptides identified are listed at the bottom panel and shown in red within the protein sequence at the middle panel.

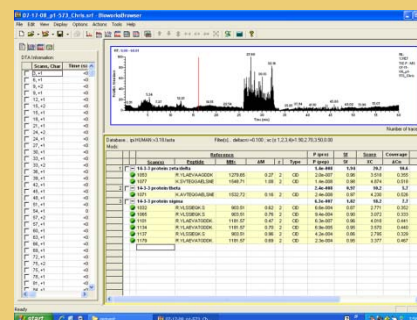


Figure 2: Identification of a set of three proteins from a 2D gel spot (LC/MS/MS data). SEQUEST protein search yielded three highly homologous proteins with a high level of significance (bottom right panel).

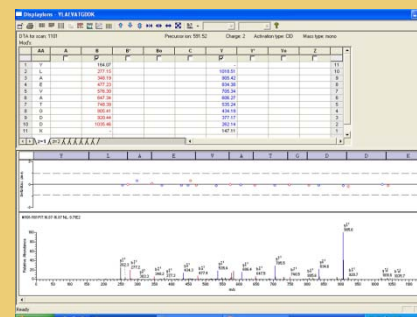
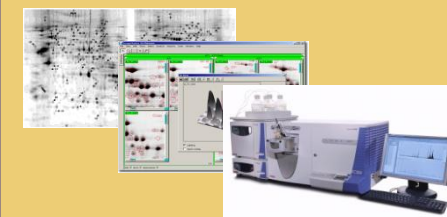


Figure 4: Identification of a set of three proteins from a 2D gel spot (LC/MS/MS data). Ion matches for peptide YLAEVATGDDK (fragment of 14-3-3 Protein Sigma) are shown (matched B ions - red, matched Y ions - blue). The center plot shows mass errors of the measurement.

2D-GE Proteomics Approach

- Obtain cell lysates
- Run 2D-GE for each sample (in triplicates)
- Compare the gels and find changes in protein expression
- Identify target proteins (for each spot):
Cut the spot and trypsinize the protein
Run LS/MS/MS analysis
Identify at least two unique peptides
Find matching proteins from UniProt database



Conclusions

Studies of human keratinocyte proteomics were initiated.

Differentially expressed proteins in EpiDerm tissues exposed to CEES were characterized using 2D gel electrophoresis (2D-GE)

The effect of GSH-Liposomes on proteomic changes in CEES-exposed keratinocytes was explored using 2D-GE technique

Three highly homologous (97%) human proteins, which belong to the 14-3-3 family of regulatory proteins were identified via LC/MS/MS. Notably, the 14-3-3 protein zeta (involved in the synthesis of melanin from tyrosine) has not, to our knowledge, been identified in human skin; it would be important in preventing skin cancers resulting from prolonged exposure to strong sun light (relevant to military personnel serving desert environments).

Proteomic approach presents a promising strategy to study molecular mechanisms of the protective effects of antioxidant liposomes in human cell lines

Future Directions

Study the mechanisms of HD/CEES toxicity and antioxidant protection at the cellular/molecular level applying wide proteomic approach

Identify differentially expressed proteins in human keratinocytes exposed to CEES/HD with and without antioxidant liposome protection using LC-MS analysis

Abstract

Sulfur mustard (bis-2-(chloroethyl) sulfide, military code HD) is an alkylating vesicant and a chemical warfare agent. Exposure to a high dose of HD or its monofunctional analog 2-chloroethyl-ethyl sulfide (CEES) increases oxidative stress and inflammatory biomarkers (Paromov et al., 2007) in dermal tissues. Skin mast cells have long been suspected of playing a key role in HD-induced cutaneous damage (Graham et al., 1994). We investigated the effects of CEES on oxidative stress in the rat basophilic leukemia RBL-2H3 mast cell line. Oxidative stress is known to induce protein S-glutathionylation, a post-translational modification of a protein by disulfide bond attachment with a glutathione (GSH) molecule. Oxidatively stressed cells incubated with biotinylated glutathione ethyl ester (BioGEE) incorporate BioGEE into proteins substituting for GSH. These BioGEE-labeled proteins were detected in RBL-2H3 cells by Western blot using a streptavidin:peroxidase probe. A number of BioGEE-labeled proteins within an apparent molecular weight range of 10 - 25 kDa were found when cells were stressed with either CEES or staurosporine, a general kinase inhibitor used to induce apoptosis. CEES-treated RBL-2H3 cells were also observed to undergo apoptosis. A much lower level of BioGEE-labeled proteins were found in cells treated with vehicle (0.1% ethanol). The BioGEE-labeled proteins have been affinity-purified from streptavidin bead matrices and identified by nanospray liquid chromatography followed by tandem mass spectroscopy (nanospray LC-MS/MS). The identified BioGEE labeled proteins from CEES-treated RBL-2H3 mast cells are compared with those from vehicle-treated mast cells. These data will help define the detailed molecular events in HD/CEES cytotoxicity and help with the design of optimal countermeasure.

This work was supported by the U.S. Army Medical Research and Materiel Command under Grant W81XWH-06-2-0044_2.

HD Induces Glutathione Depletion Resulting in Oxidative Stress

Oxidative stress occurs when the production of reactive oxygen species (ROS) exceeds the cell's antioxidant defenses thereby causing damage to the cell's proteins, lipids and DNA. Glutathione (GSH), a major cellular antioxidant, helps to protect cells by neutralizing ROS in redox coupled oxidation-reduction reactions. In non-stressed cells, GSH is found almost exclusively in a reduced state at a concentration of approximately ~5 mM, but under conditions of oxidative stress, the balance of reduced glutathione to oxidized glutathione (GSH/GSSG) shifts to a more oxidized state. When the GSH/GSSG ratio is reduced, GSH becomes conjugated to specific proteins; this post-translational modification is defined as glutathionylation. The purpose of protein glutathionylation is not well understood. In some cases, glutathionylation alters protein functions changing the cell's response to activating repair mechanisms (Townsend et al., 2009).

HD and CEES metabolites form GSH-conjugates causing glutathione depletion. Since GSH is a key intracellular antioxidant, its depletion by HD would increase cellular oxidative stress. Exposure to HD also causes macromolecular damage including DNA damage and covalent modifications of proteins. Ultimately, this damage leads to inactivation of enzymes, fragmentation of the extracellular matrix and cell detachment. The damage and oxidative stress finally leads to apoptosis and/or necrosis (Paromov et al., 2007).

Results

Figure 1. CEES-treated RBL-2H3 mast cells show increased oxidative stress. RBL-2H3 cells were incubated with 1 mM CEES for 6 hours and stained with 20 µM DCFH-DA for 30 min to detect ROS generation.

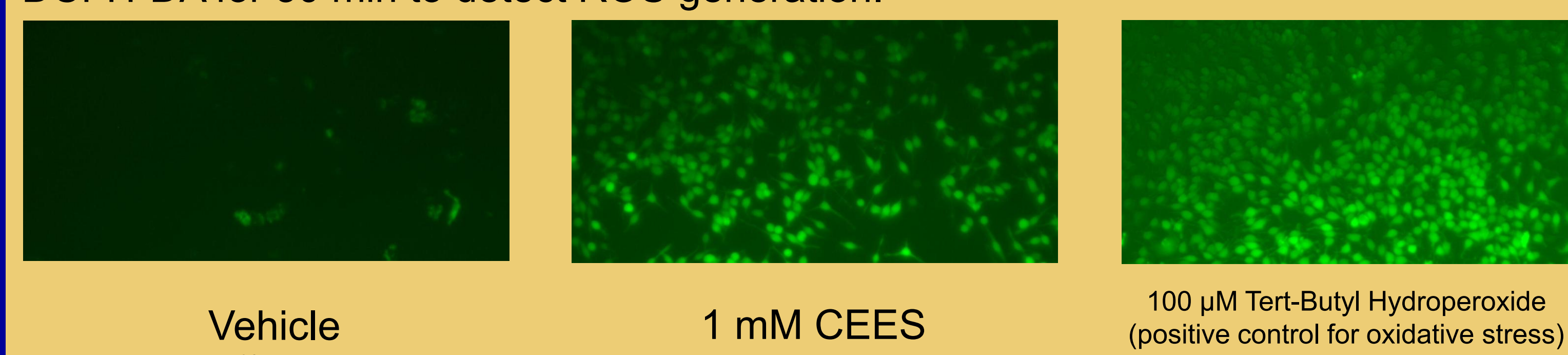


Figure 3. Purification of biotin labeled proteins using streptavidin beads. Biotin label was from biotin in BioGEE (-GSH-Biotin) or direct biotinylation (-Biotin).

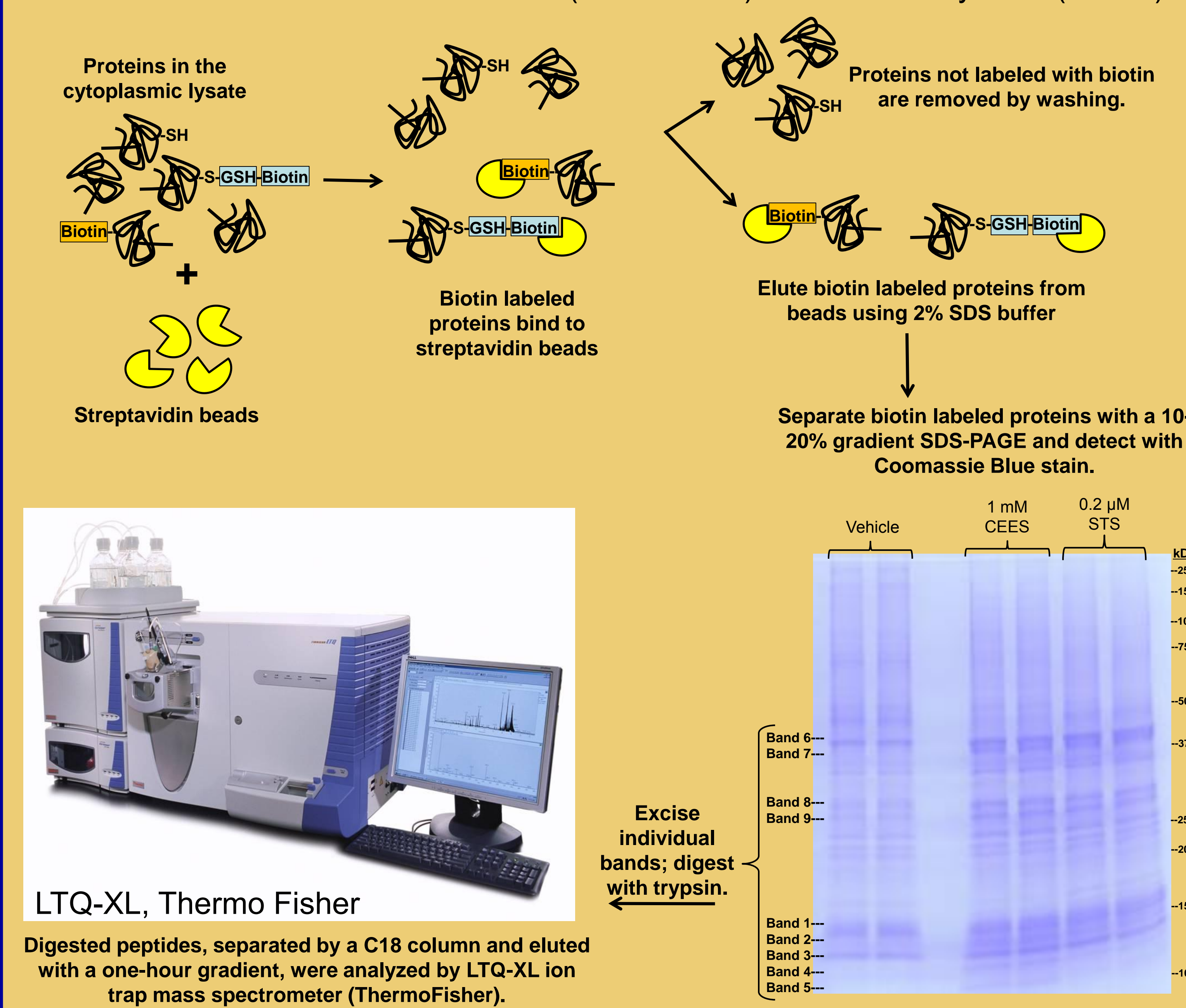


Figure 4. CEES-treated RBL-2H3 mast cells undergo apoptosis.

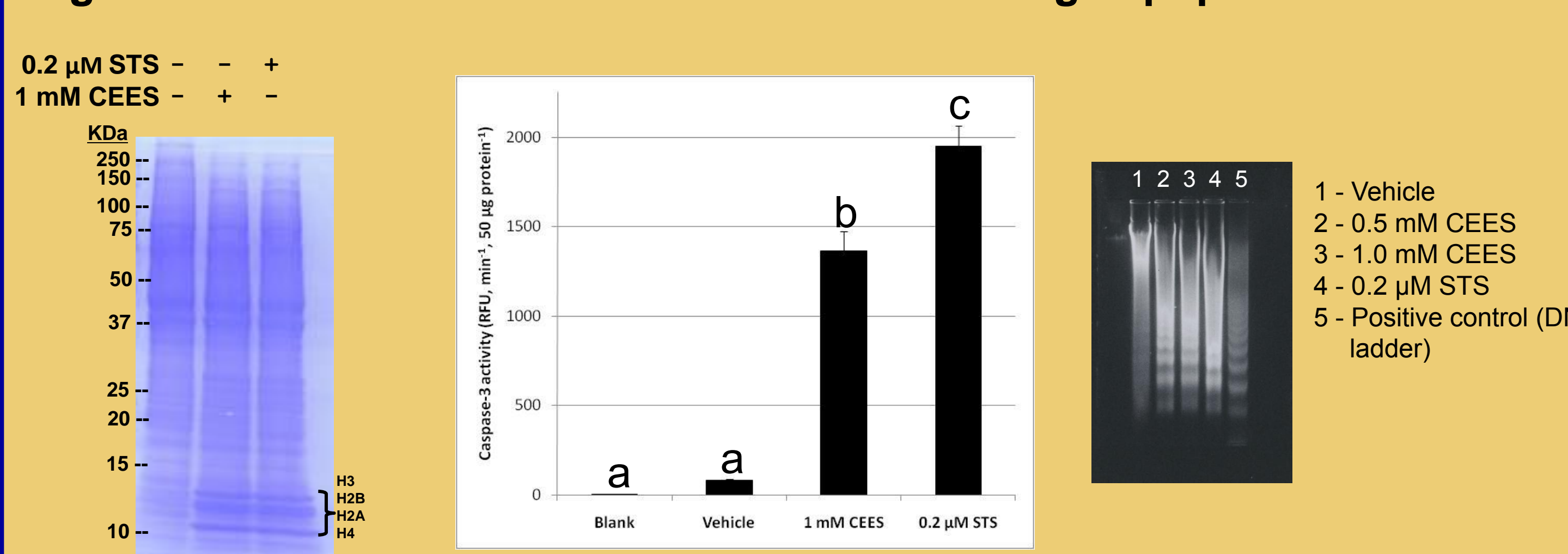


Figure 5A. Apoptotic release of histones from nucleus (as described by Wu et al., 2002). CEES-treated mast cells and apoptotic mast cells release histones (H3, H2B, H2A, H4) from nucleus. RBL-2H3 mast cells were exposed to 1 mM CEES, 0.2 µM Staurosporine (STS, apoptosis inducer) or vehicle (0.1% ethanol) for six hours. Cells were harvested, and cytoplasmic protein (50 µg) from each sample was separated with a 10-20% gradient SDS-PAGE. Total proteins were detected using Coomassie Blue stain.

Figure 5B. Increased caspase-3 activity reveals CEES-treated RBL-2H3 mast cells in the execution phase of apoptosis. Cells were exposed to 1 mM CEES, 0.2 µM Staurosporine (STS, apoptosis inducer) or vehicle (0.1% ethanol) for six hours. Cells were harvested, and cytoplasmic protein (50 µg) from each sample was used to measure caspase-3 activity by the hydrolysis of acetyl-Asp-Glu-Val-Asp 7-amido-4-methylcoumarin (Ac-DEVD-AMC) resulting in the release of the fluorescent 7-amino-4-methylcoumarin (AMC). A negative control containing no cells (blank) was also tested. Means not sharing a common letter are significantly different (p < 0.05).

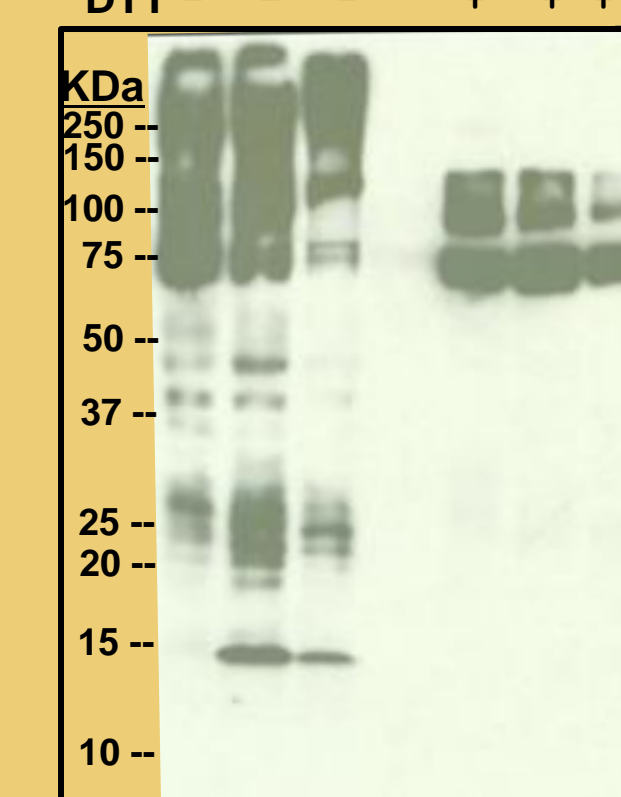
Figure 5C. DNA fragmentation, an apoptotic event, is apparent in CEES-oxidatively stressed mast cells and apoptotic mast cells. RBL-2H3 mast cells were exposed to 0.5 - 1.0 mM CEES, 0.2 µM Staurosporine (STS, apoptosis inducer) or vehicle (0.1% ethanol) for six hours. Cells were harvested, and DNA from from each sample was electrophoretically separated in a 1.5% agarose gel. DNA was detected with ethidium bromide.

Figure 2. CEES-treated cells incubated with biotinylated glutathione ethyl ester (BioGEE) incorporate BioGEE into proteins substituting for GSH.

RBL-2H3 cells were treated with 1 mM CEES or vehicle (0.1% ethanol) for one hour. Cells were washed and serum-free medium containing 10 µM BioGEE with or without 0.2 µM STS was added. Cells were incubated for six hours, and proteins from cytoplasmic lysates were separated with a 10-20% gradient SDS-PAGE and electrotransferred onto a nitrocellulose membrane. The membrane was probed with streptavidin conjugated HRP (Thermo Scientific, Rockford, IL). Biotinylated protein was detected using SuperSignal West Pico Chemiluminescent Substrate (Thermo Scientific).

BIOGEE + + + + +
0.2 µM STS - - - - -
1 mM CEES - - - - -
DTT - - - - -

(BioGEE label was removed in the presence of DTT.)



Chemical structure of BioGEE

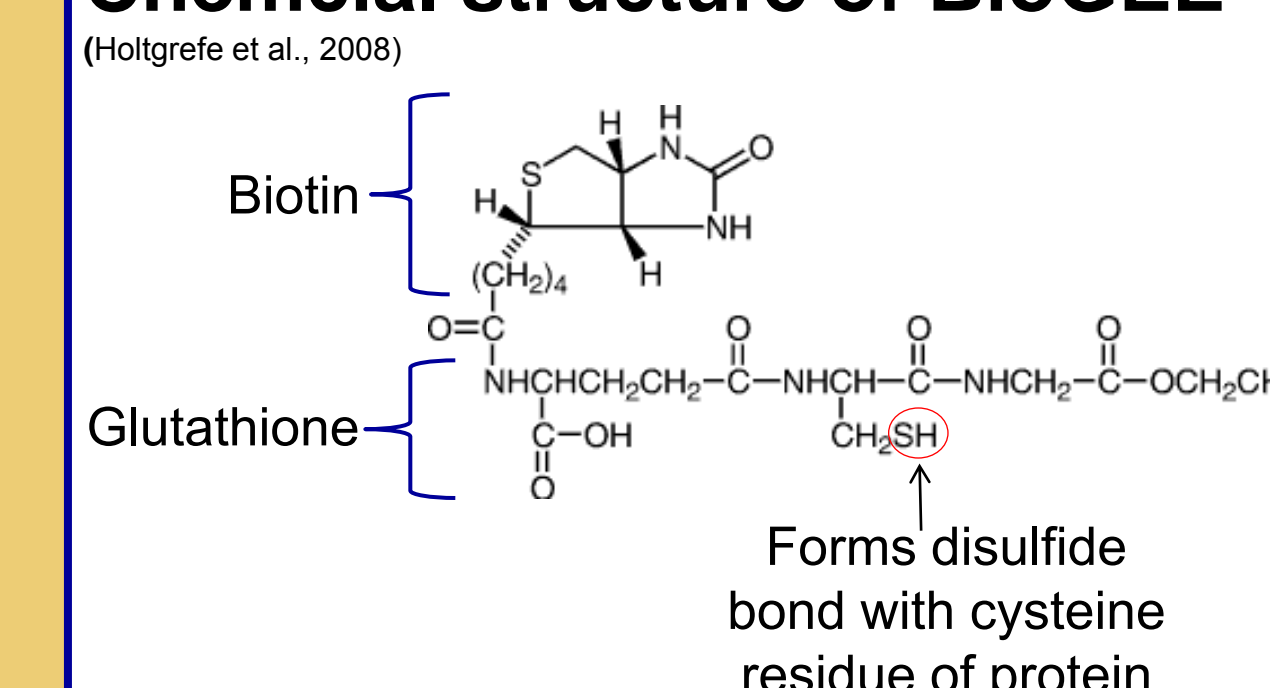


Table 1. Selection of proteins identified by SEQUEST search against Uniref 100 UniProt database. "X" represents positive identification with high confidence; "O" represents protein absent in SEQUEST search.

Band #	Protein	MW (kDa)	Mast cell treatment		
			Vehicle	1 mM CEES	0.2 µM STS
1	GTP binding protein Rheb	20.467	O	X	X
2	40S and 60S ribosomal proteins	14 - 17	X	X	X
	SS DNA-binding protein mit. precursor	17.445	O	X	O
3	40S and 60S ribosomal proteins	14 - 17	X	X	X
	Histone 2a	14.181	X	X	X
	Transcr. factors or co-activators	10 - 22	O	X	X
4	40S and 60S ribosomal proteins	11-14	X	X	X
	Histone H4	11.361	O	X	X
5	Thioredoxin*	11.535	O	X	O
	40S and 60S ribosomal proteins	11-12	X	X	X
6	Mitochondrial ATP synthase e chain	8.119	O	X	O
	40S and 60S ribosomal proteins	10-11	X	X	X
7	Actin	41.710	X	X	X
	Actin	41.710	X	X	X
8	Histone H1.2	21.844	O	X	X
	40S and 60S ribosomal proteins	25-30	X	X	X
9	G protein beta subunit 2-like 1	35.398	O	X	O
	40S and 60S ribosomal proteins	27-30	X	X	X

*glutathionylation confirmed in T cells (Casagrande et al, 2002)

Conclusions

The affinity purified proteins (Figure 3) identified by nanospray LC-MS/MS that were unique to CEES treatment were thioredoxin (band 4), guanine nucleotide-binding protein beta subunit 2-like 1 (band 9), single stranded DNA-binding protein mitochondrial precursor (band 2), and mitochondrial ATP synthase e chain (band 5) (Table 1). These and other proteins were conjugated to BioGEE or directly labeled with biotin or were associated with BioGEE- or biotin-labeled proteins.

Actin, a protein known to be directly alkylated by HD/CEES during HD/CEES exposure (Sayer et al., 2009), was identified in bands 6 and 7 (Table 1) for all treatments. Higher levels of band 7 were observed (Figure 3) in CEES- and STS-treated mast cells.

This is the first report demonstrating glutathionylation of cytoplasmic proteins when cells are CEES-exposed. Glutathionylation may alter the activity of these proteins defining molecular signaling events involved in HD/CEES cytotoxicity.

A number of BioGEE-labeled proteins within an apparent molecular weight range of 10 - 25 kDa were found when cells were stressed with either CEES or staurosporine (STS), an apoptosis inducer. Much lower levels of BioGEE-labeled proteins were found in cells treated with vehicle (Figure 2).

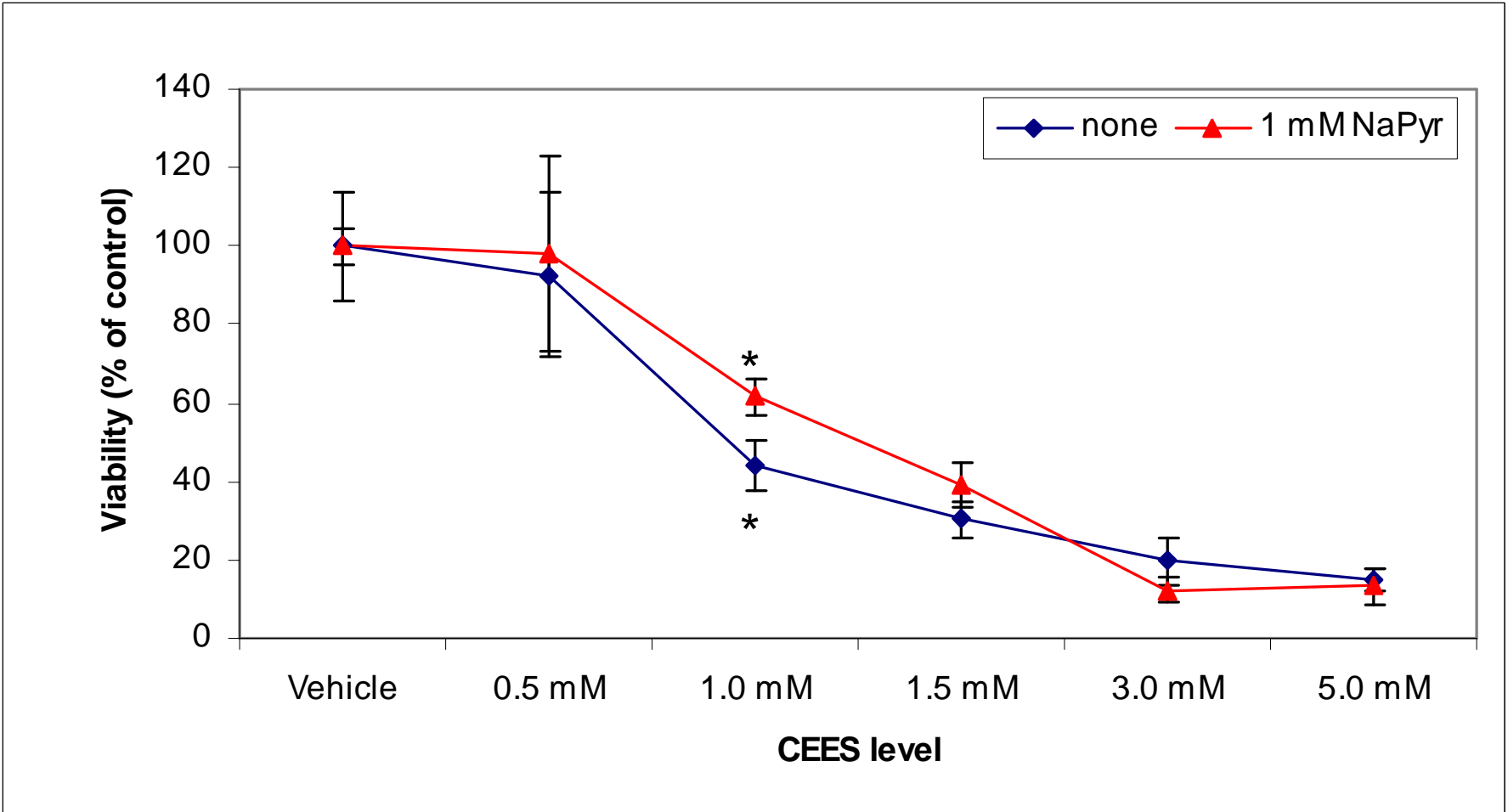
RBL-2H3 cells treated with 1 mM CEES for six hours undergo apoptosis (Figure 4).

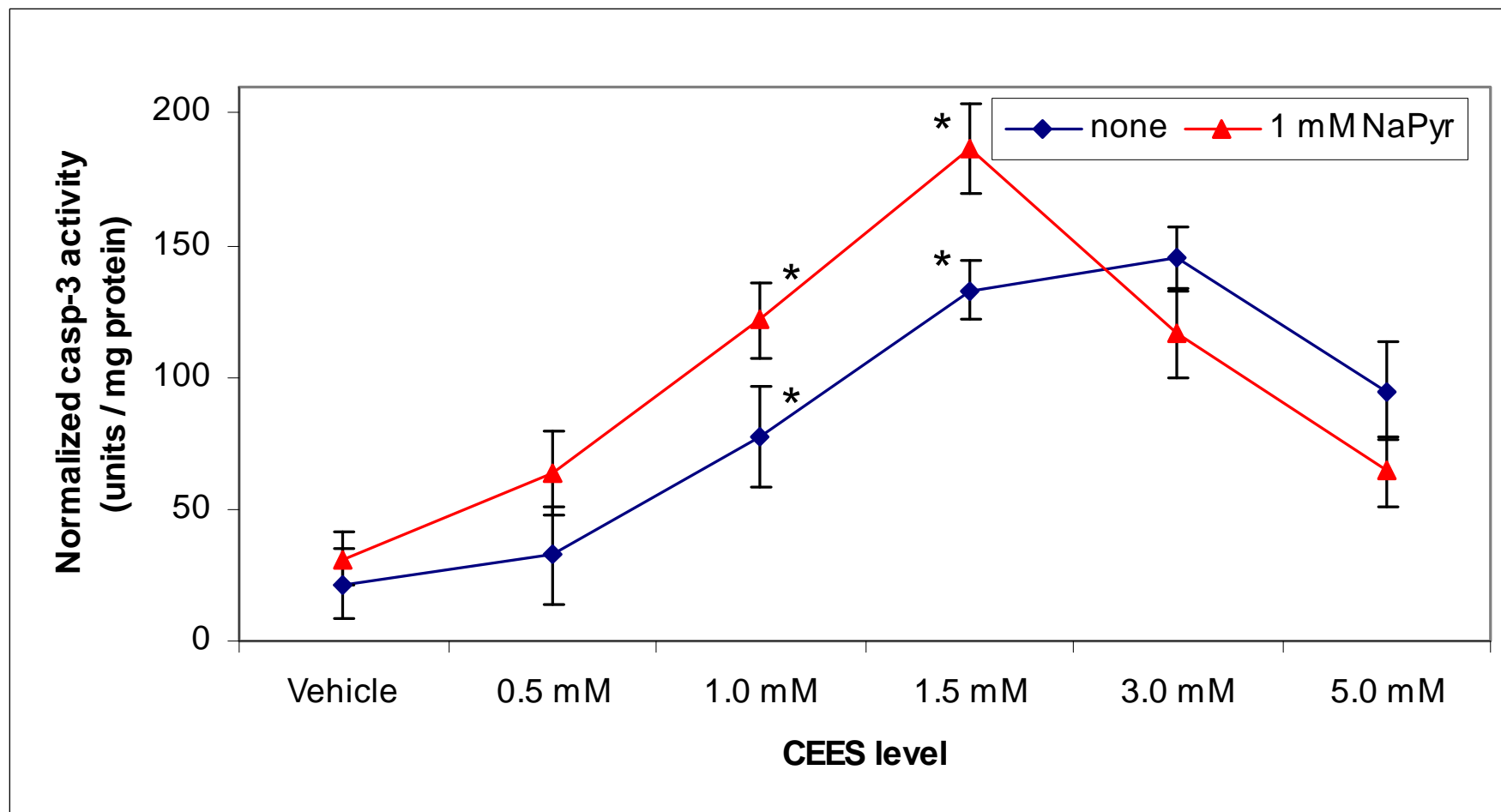
The mechanisms involved with HD/CEES-toxicity in RBL-2H3 mast cells include glutathionylation of a wide variety of proteins and induction of the apoptotic cell death pathway.

References

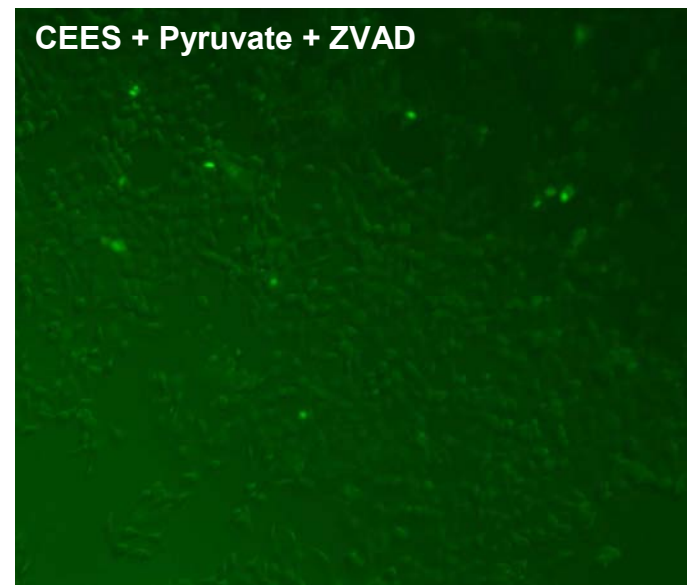
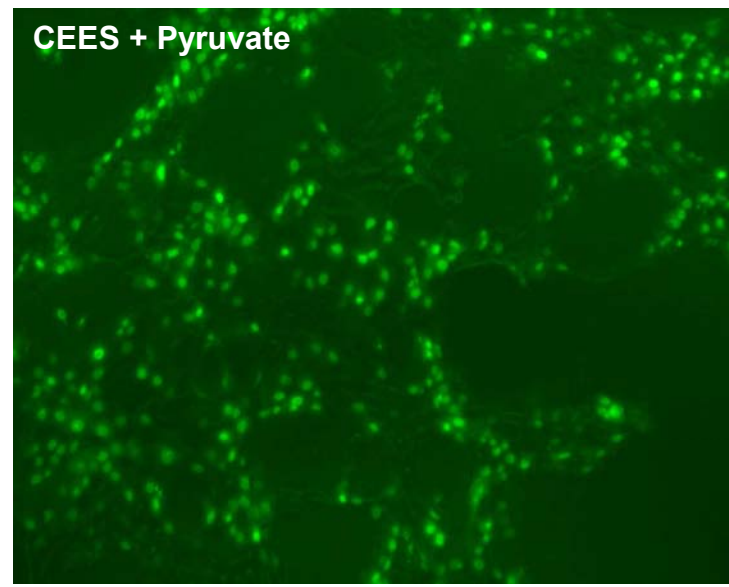
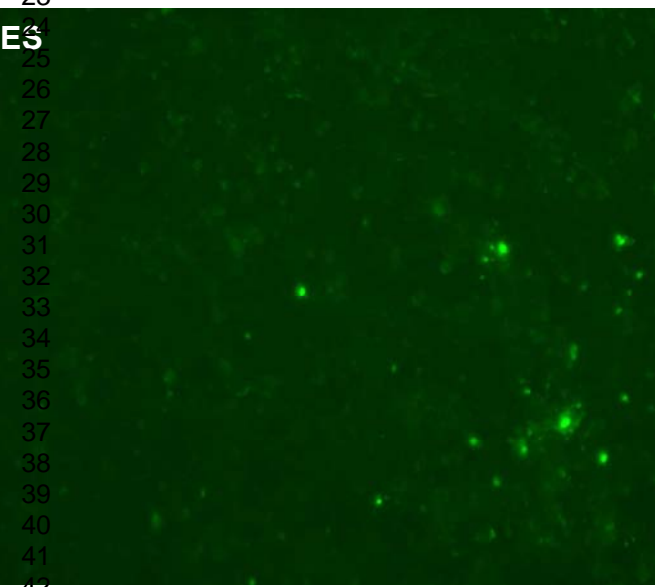
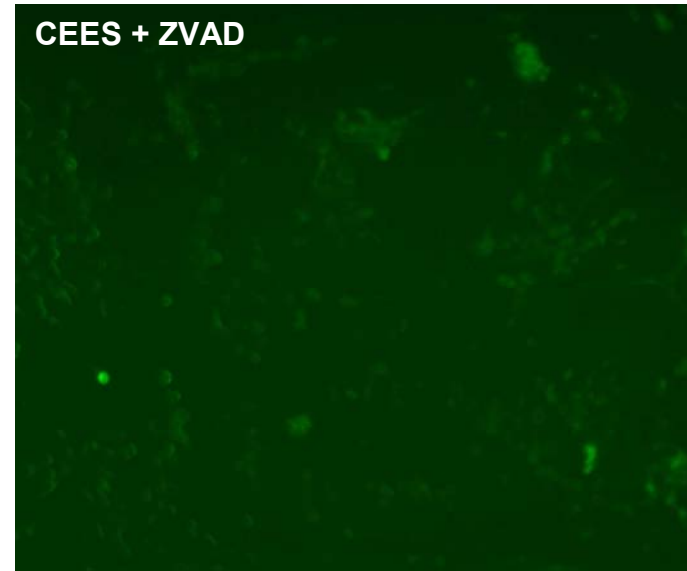
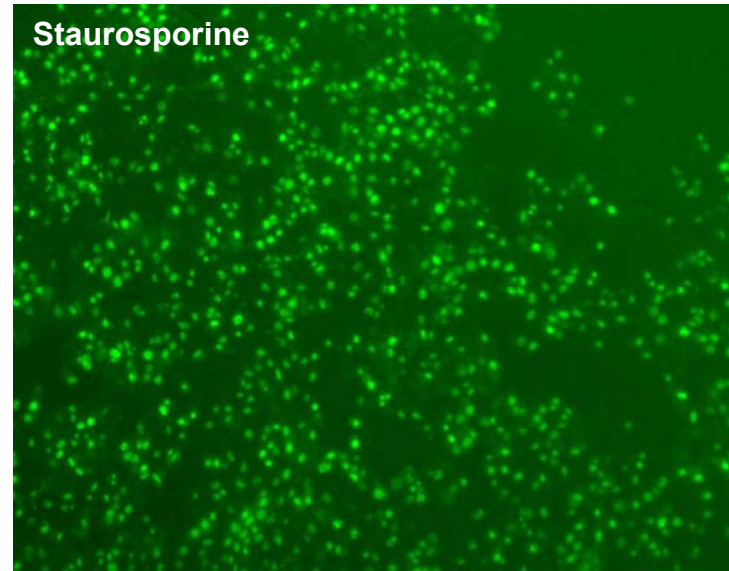
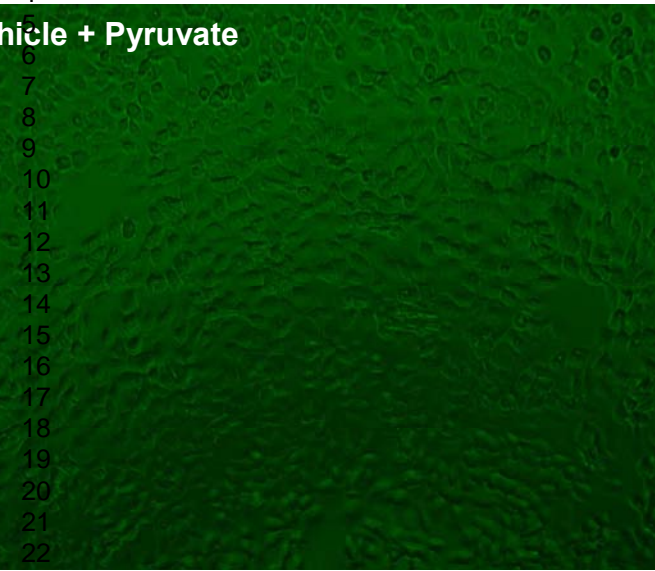
- Casagrande, S., V. Bonetto, M. Fratelli, E. Gianazza, I. Eberini, T. Massignan, M. Salmona, G. Chang, A. Holmgren, and P. Ghezzi. 2002. Glutathionylation of human thioredoxin: a possible crosstalk between the glutathione and thioredoxin systems. Proc. Natl. Acad. Sci. USA. 99:9745-9749.
- Holtgreffe, S., J. Gohike, J. Starmann, S. Druce, S. Klocke, B. Altmann, J. Wojtera, C. Lindermayr, and R. Scheibe. 2008. Regulation of plant cytosolic glyceraldehyde 3-phosphate dehydrogenase isoforms by thiol modifications. Physiol. Plant. 133:211-228.
- Graham, J.S, M.A. Bryant, E.H. Braue. 1994. Effect of sulfur mustard on mast cells in hairless guinea pig skin. J. Toxicol. - Cut. & Ocular Toxicol. 13:47-54.
- Paromov, V., Z. Suntrés, M. Smith, and W.L. Stone. 2007. Sulfur mustard toxicity following dermal exposure. Role of oxidative stress, and antioxidant therapy. J. Burns Wounds. 7:60-85.
- Sayer, N.M., R. Whiting, A.C. Green, K. Anderson, J. Jenner, and C.D. Lindsay. 2010. Direct binding of sulfur mustard and chloroethyl ethyl sulphide to human cell membrane-associated proteins; implications for sulfur mustard pathology. J. Chromatography B. 878:1426-1432.
- Townsend, D.M, Y. Manevich, L. He, Y. Xiong, R.R. Bowers, Jr., S. Hutchens, and K.D. Tew. 2009. Nitrosative stress-induced S-glutathionylation of protein disulfide isomerase leads to activation of the unfolded protein response. Cancer Res. 69:7626-7634.
- Wu, D., A. Ingram, J.H. Lahti, B. Mazza, J. Grenet, A. Kapoor, L. Liu, V.J. Kidd, and D. Tang. 2002. Apoptotic release of histones from nucleosomes. J.B.C. 277:12001-12008.

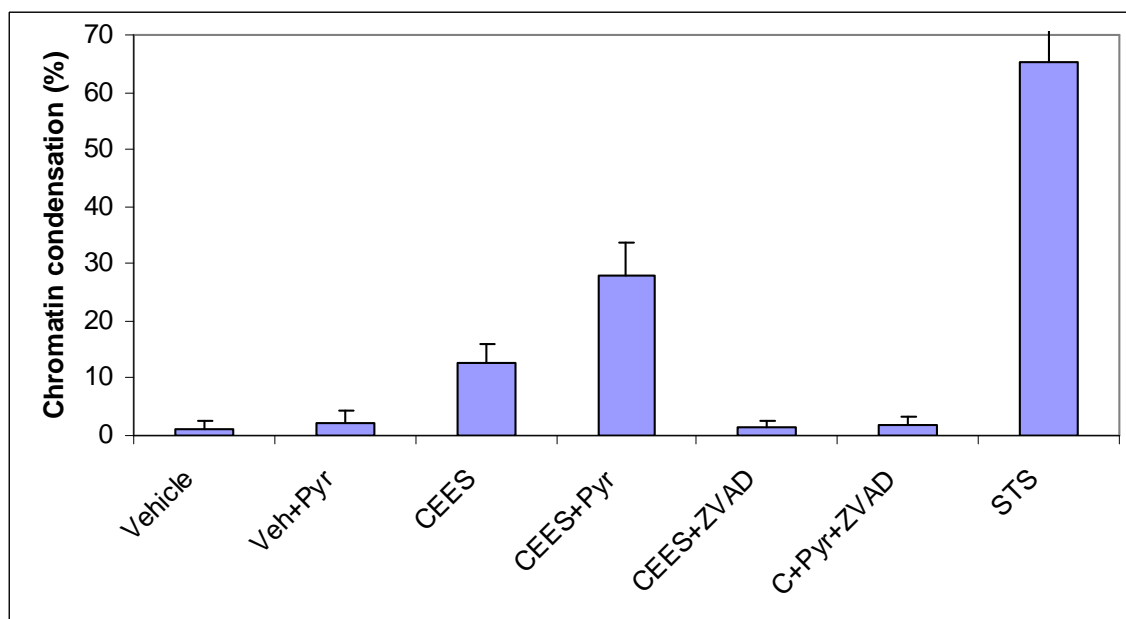
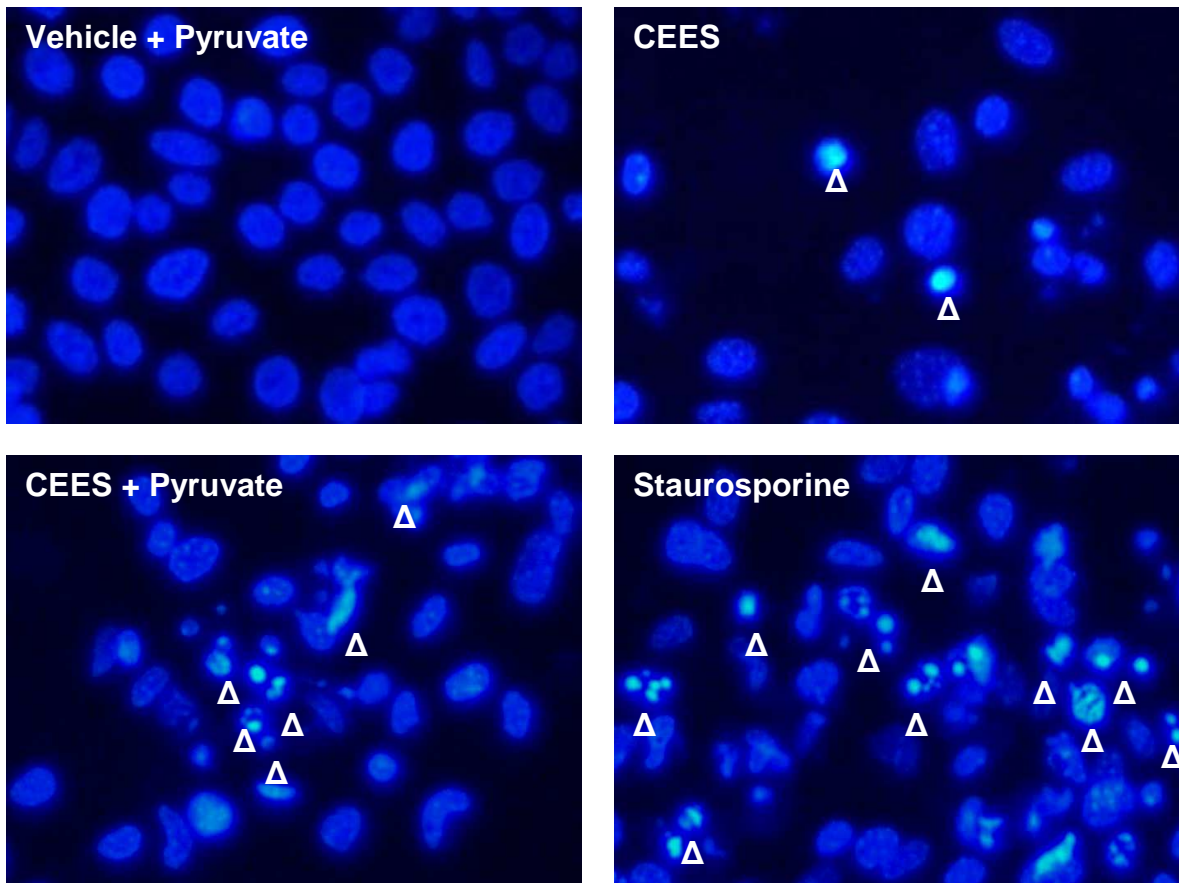
1
2
3
4
5
6
7
8
9
10
11
12
13
14
15
16
17
18
19
20
21
22
23
24
25
26
27
28
29
30
31
32
33
34
35
36
37
38
39
40
41
42
43
44
45
46
47
48
49



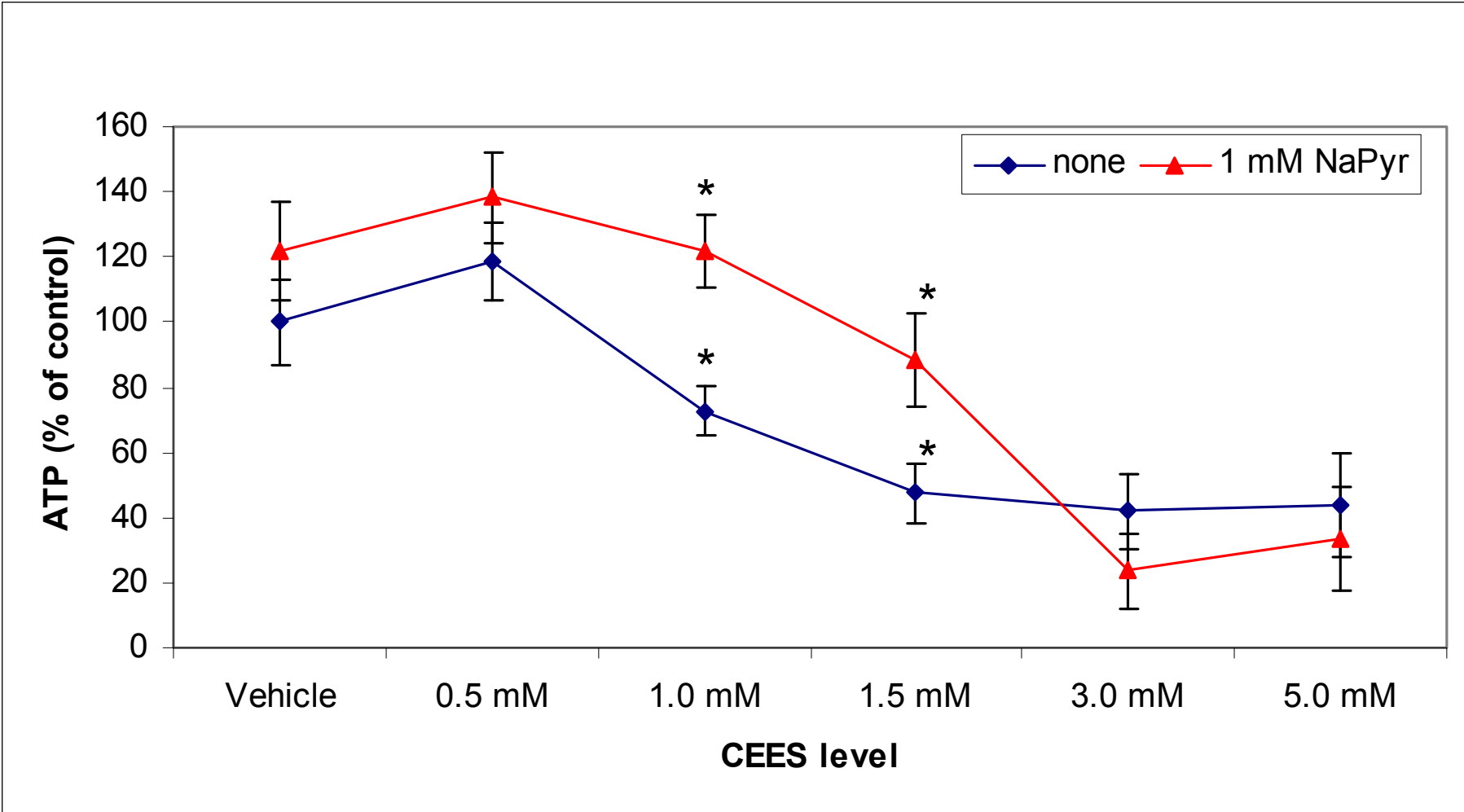
1
2
3
4
5
6
7
8
9
10
11
12
13
14
15
16
17
18
19
20
21
22
23
24
25
26
27
28
29
30
31
32
33
34
35
36
37
38
39
40
41
42
43
44
45
46
47
48
49

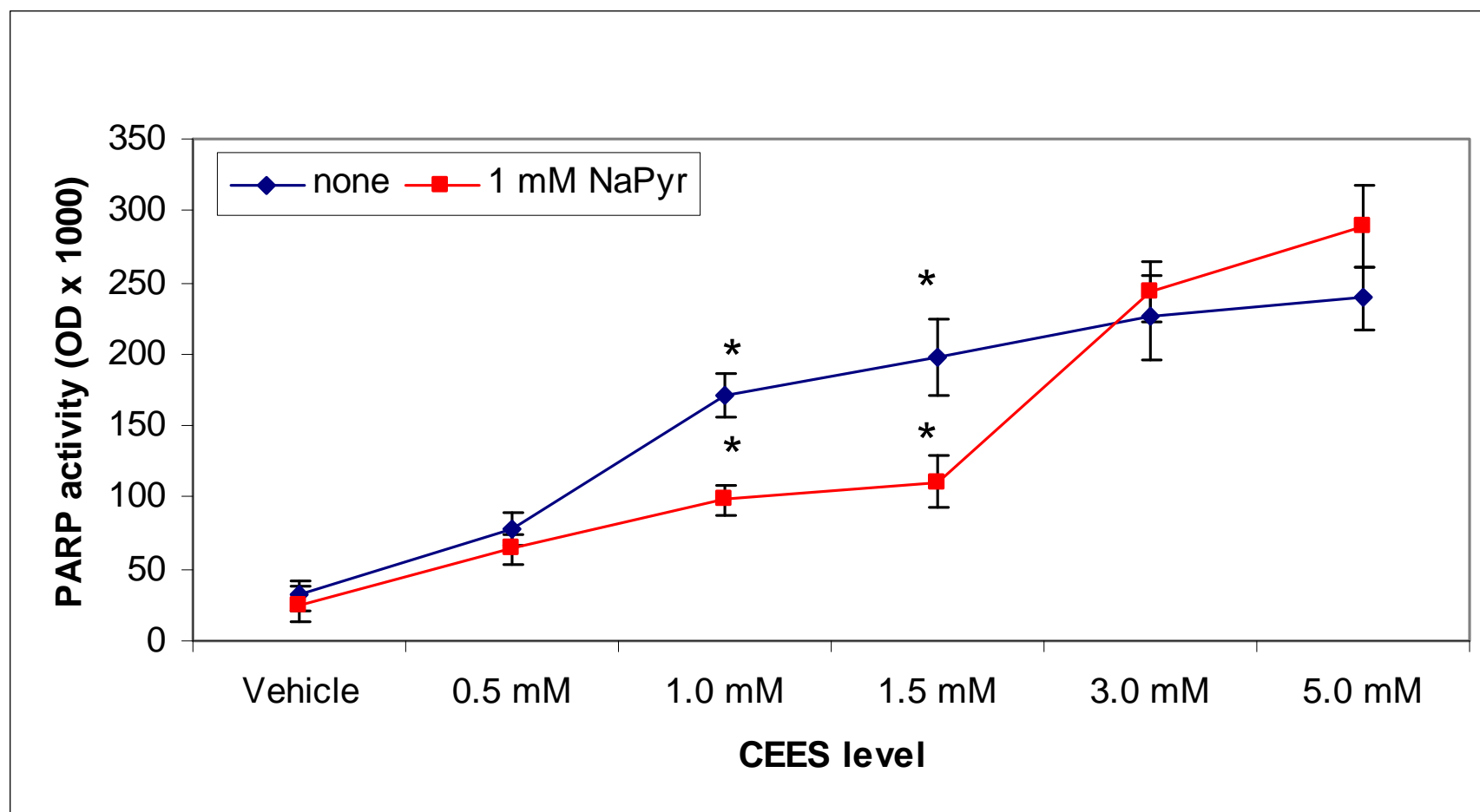
1
2
3
4
5
6
7
8
9
10
11
12
13
14
15
16
17
18
19
20
21
22
23
24
25
26
27
28
29
30
31
32
33
34
35
36
37
38
39
40
41
42
43
44
45
46
47
48
49





1
2
3
4
5
6
7
8
9
10
11
12
13
14
15
16
17
18
19
20
21
22
23
24
25
26
27
28
29
30
31
32
33
34
35
36
37
38
39
40
41
42
43
44
45
46
47
48
49

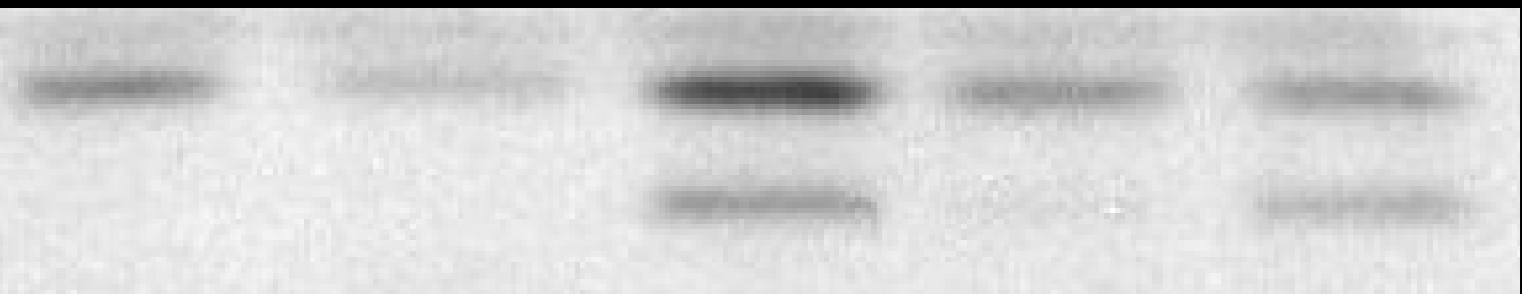




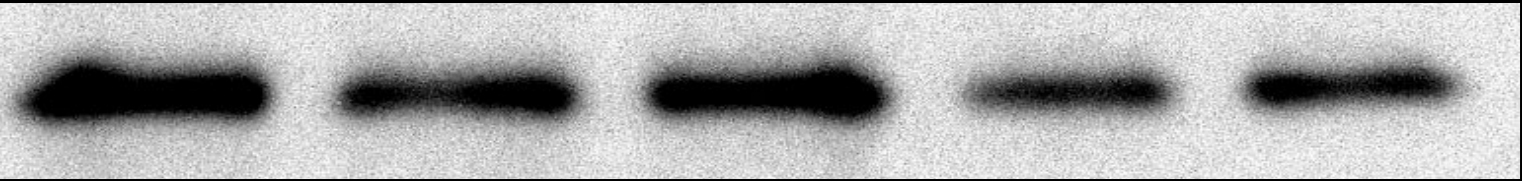
1
2
3
4
5
6
7
8
9
10
11
12
13
14
15
16
17
18
19
20
21
22
23
24
25
26
27
28
29
30
31
32
33
34
35
36
37
38
39
40
41
42
43
44
45
46
47
48
49

Cell lysates, 12 hours

Veh.	Veh.+Pyr.	1mM CEES + Pyr.	1mM CEES	STS
-------------	------------------	----------------------------	-----------------	------------



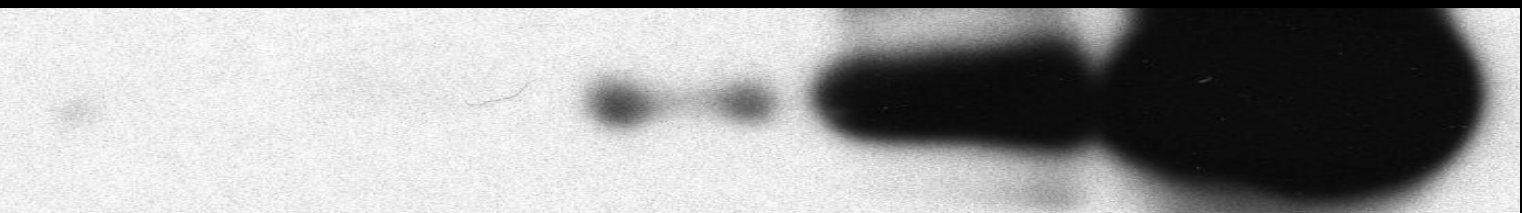
PARP-1



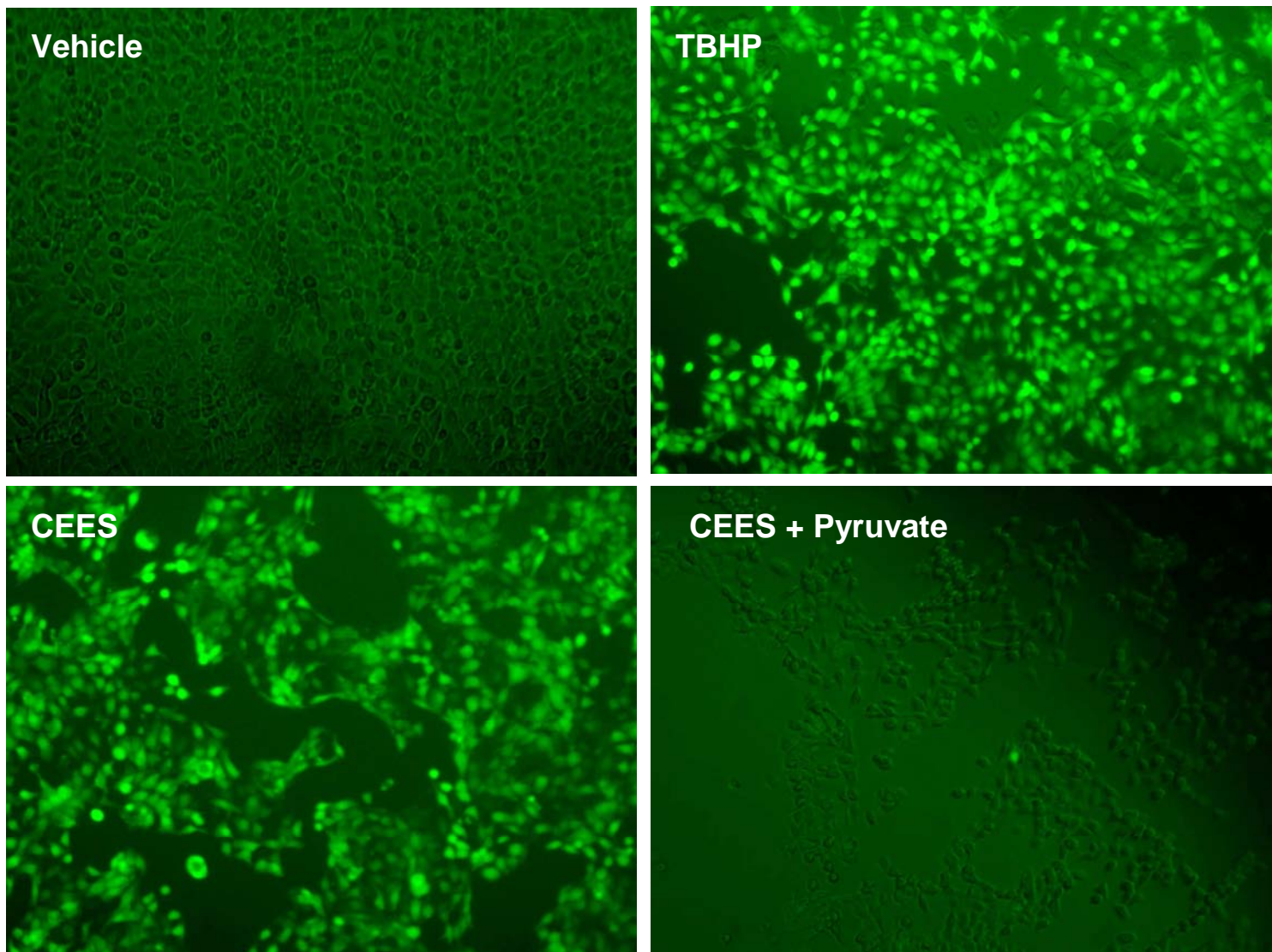
β-actin

Media, 24 hours

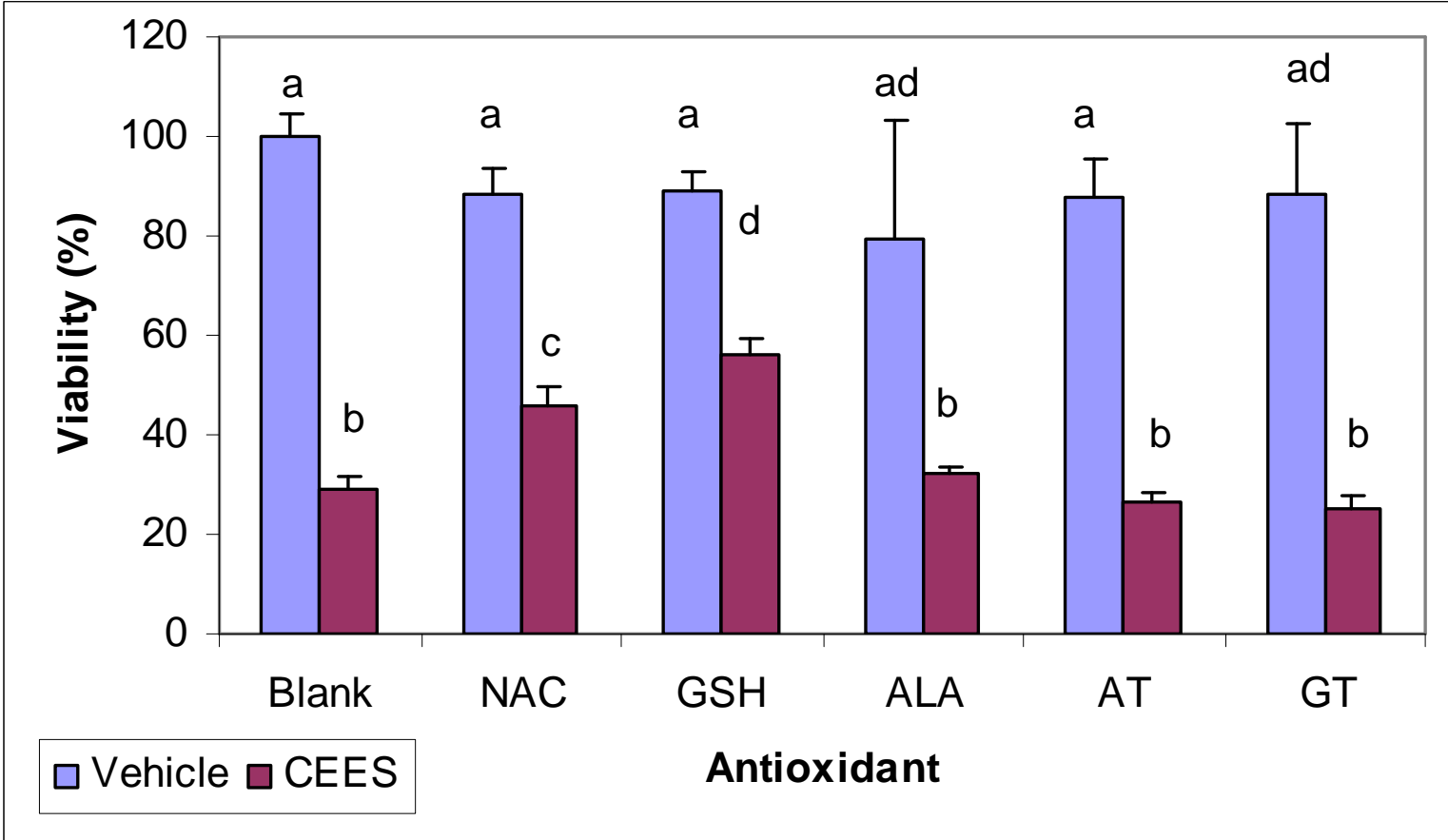
Veh. + Pyr	0.5 mM CEES + Pyr.	0.5 mM CEES	1.5 mM CEES + Pyr.	1.5 mM CEES
-----------------------	-----------------------------------	------------------------	-----------------------------------	------------------------

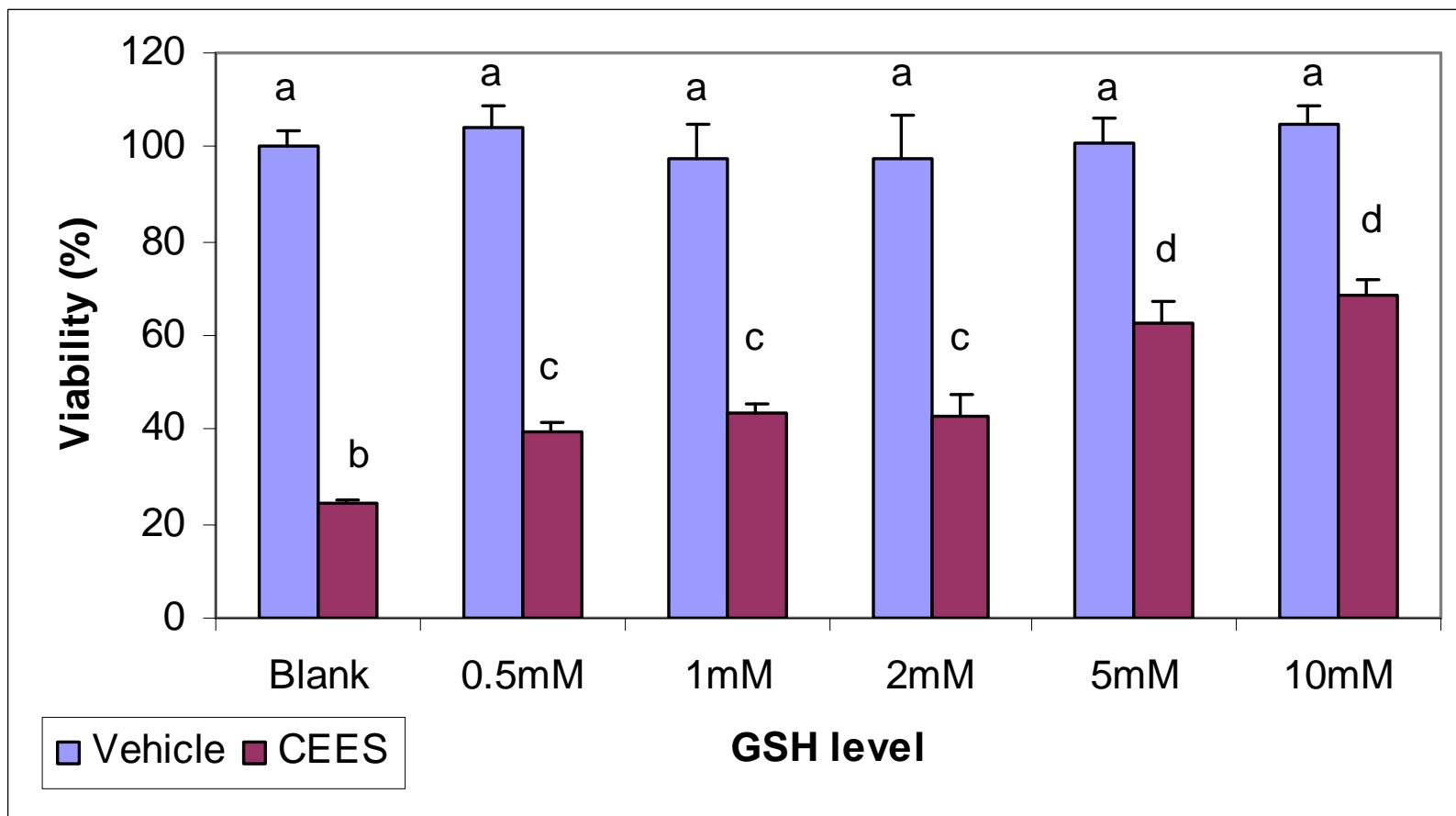


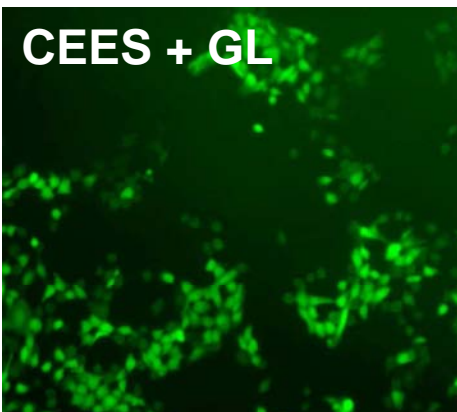
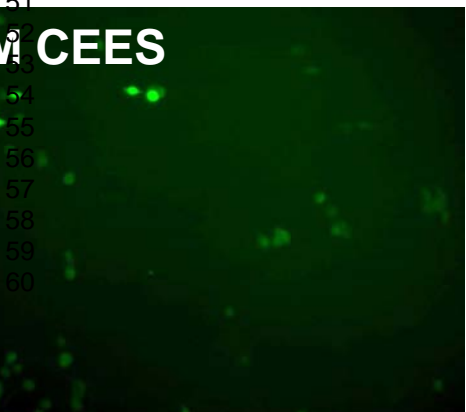
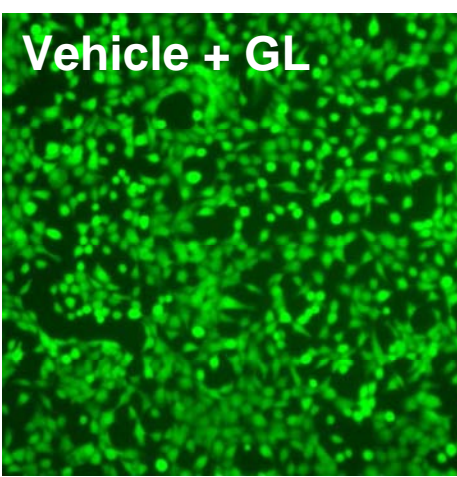
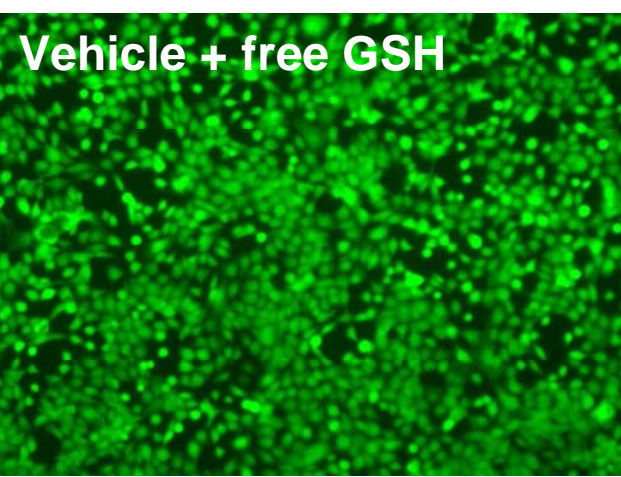
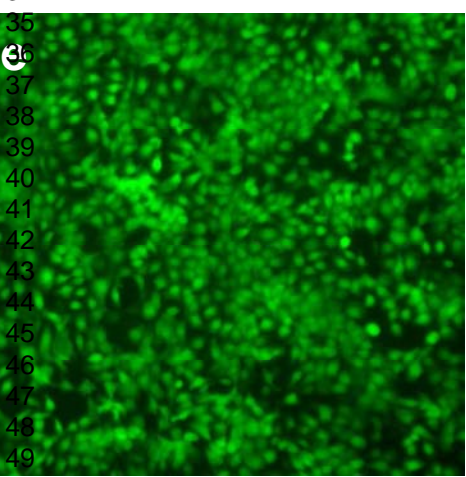
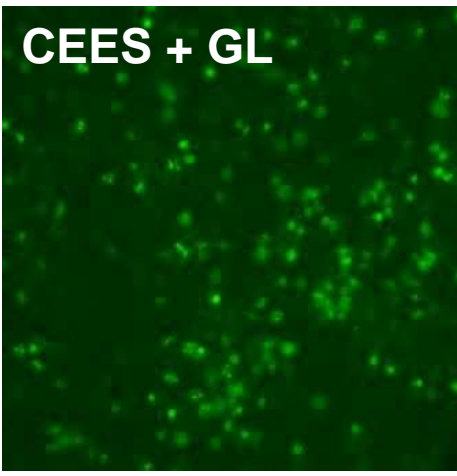
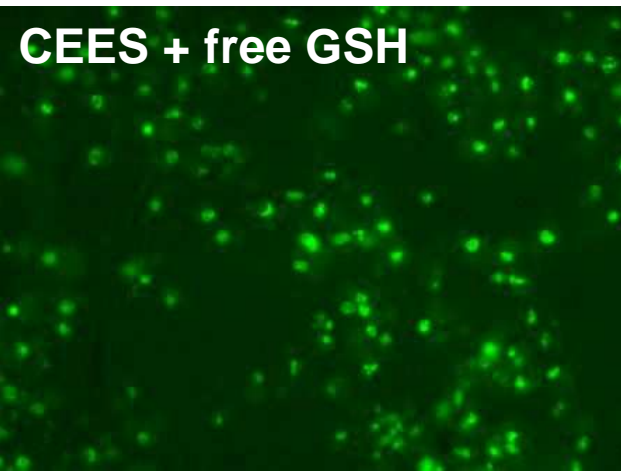
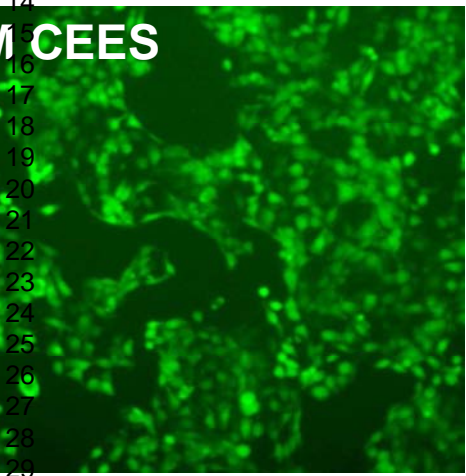
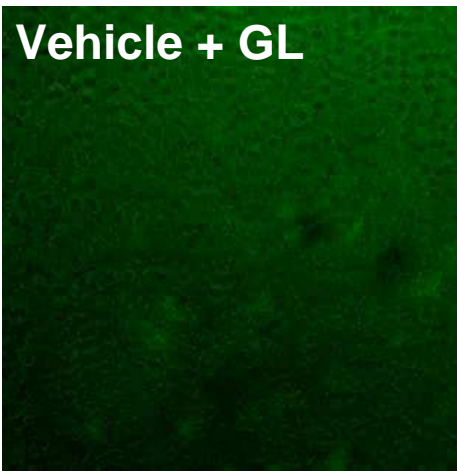
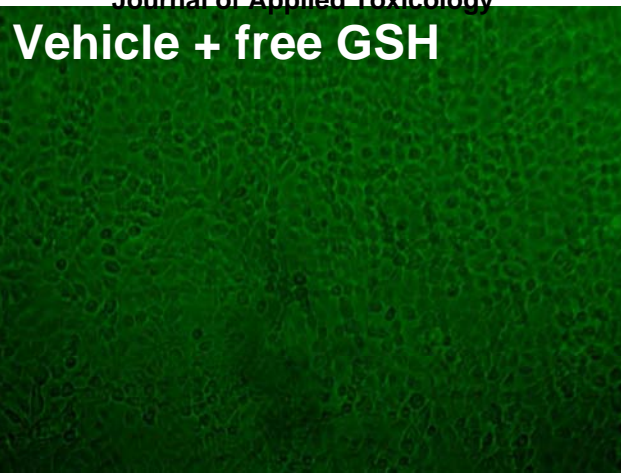
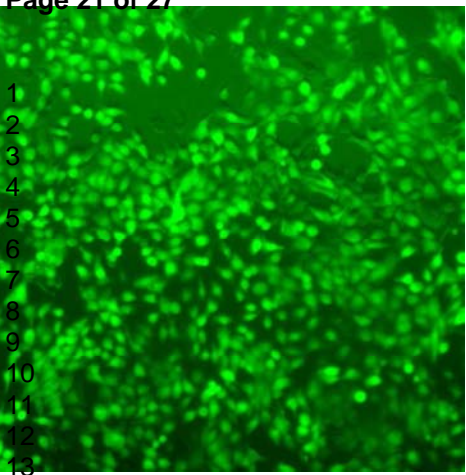
TNF- α

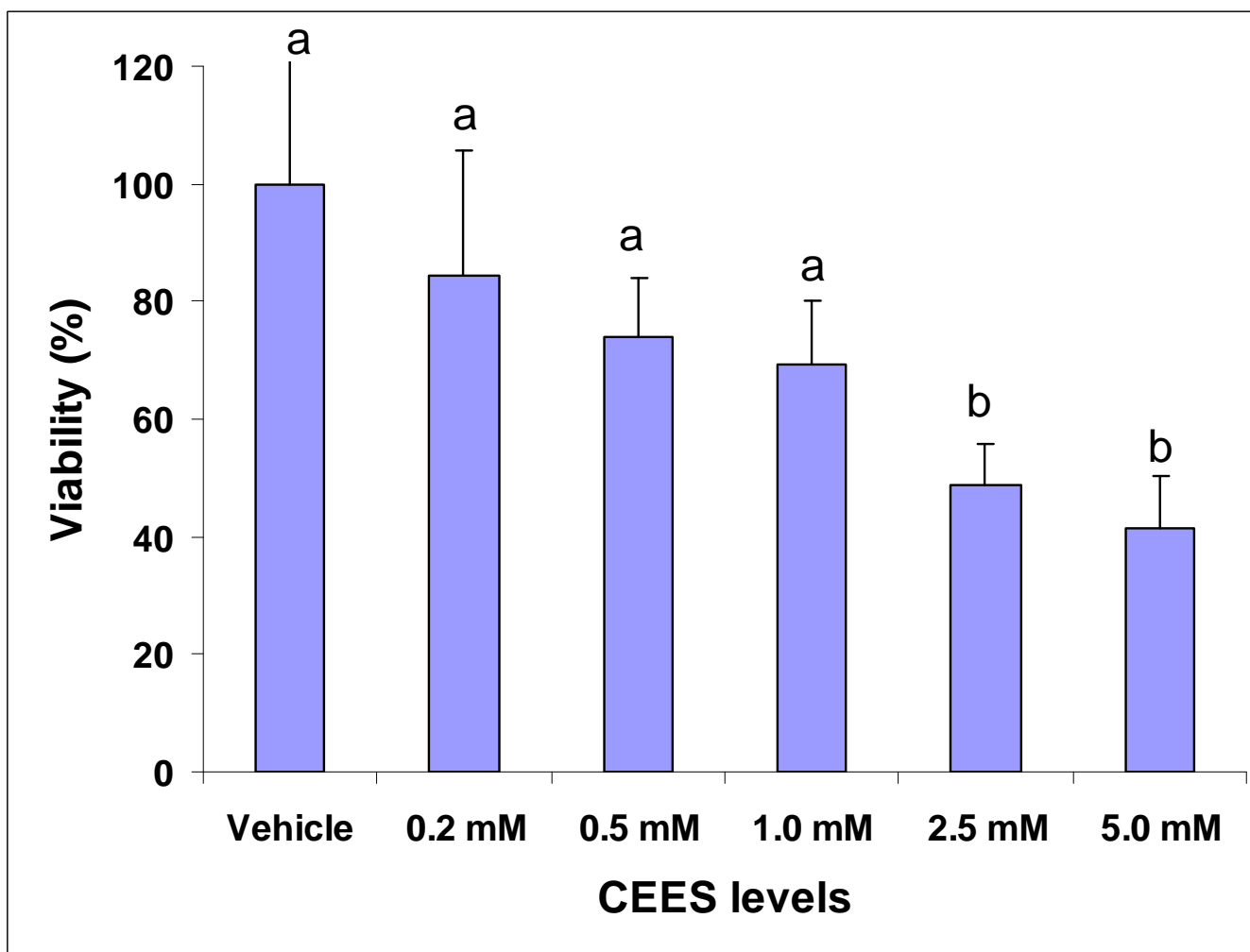


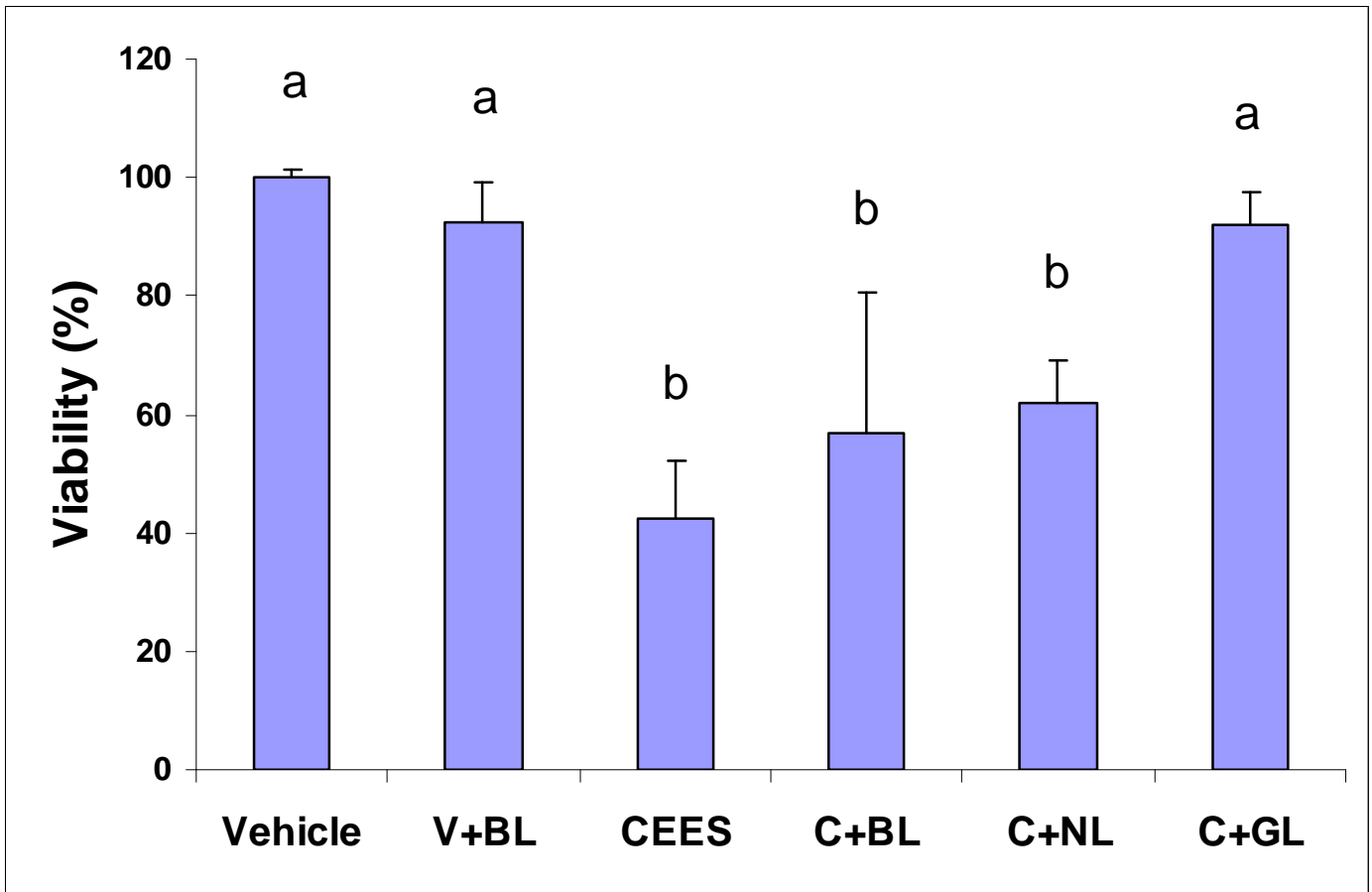
1
2
3
4
5
6
7
8
9
10
11
12
13
14
15
16
17
18
19
20
21
22
23
24
25
26
27
28
29
30
31
32
33
34
35
36
37
38
39
40
41
42
43
44
45
46
47
48
49

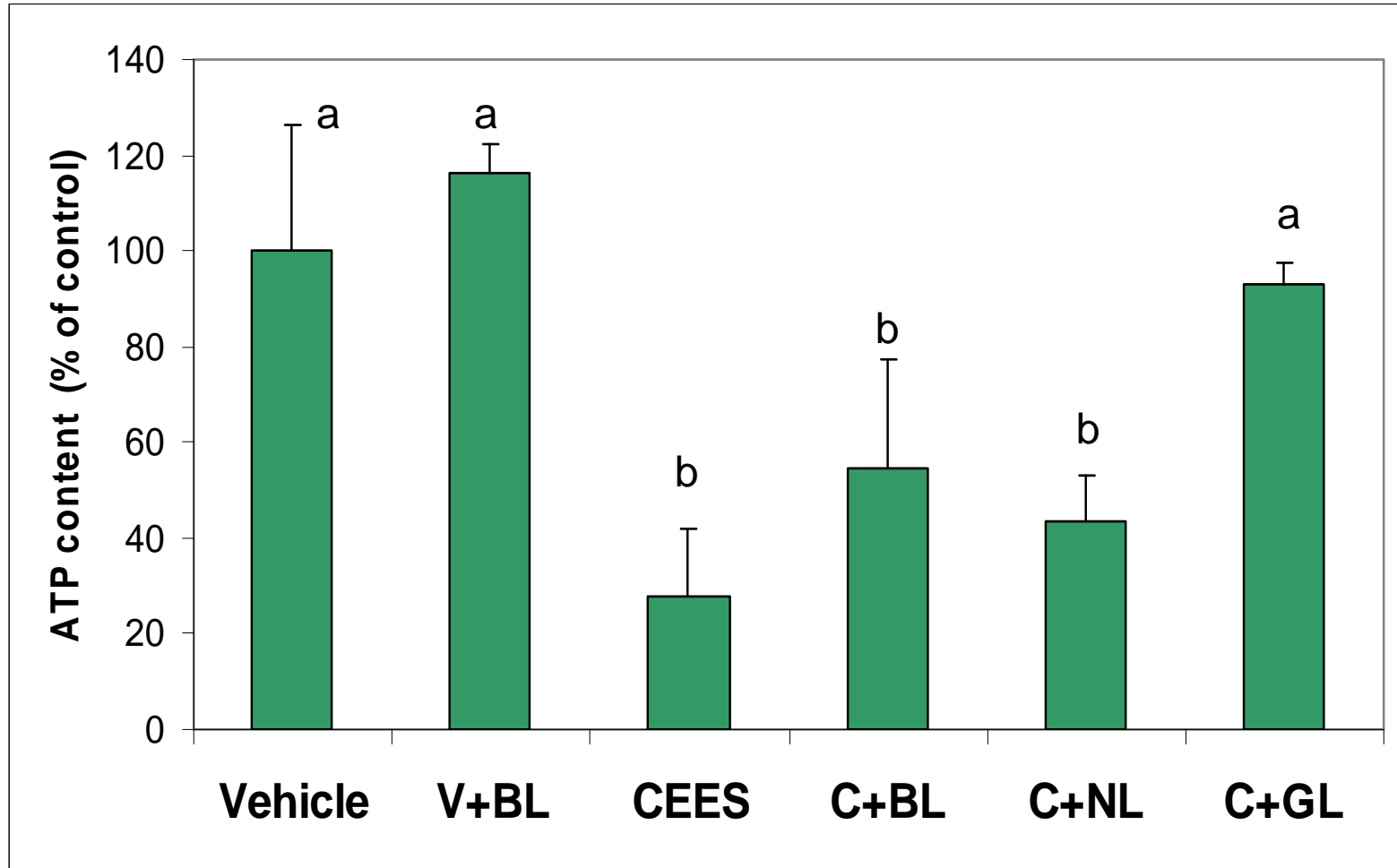


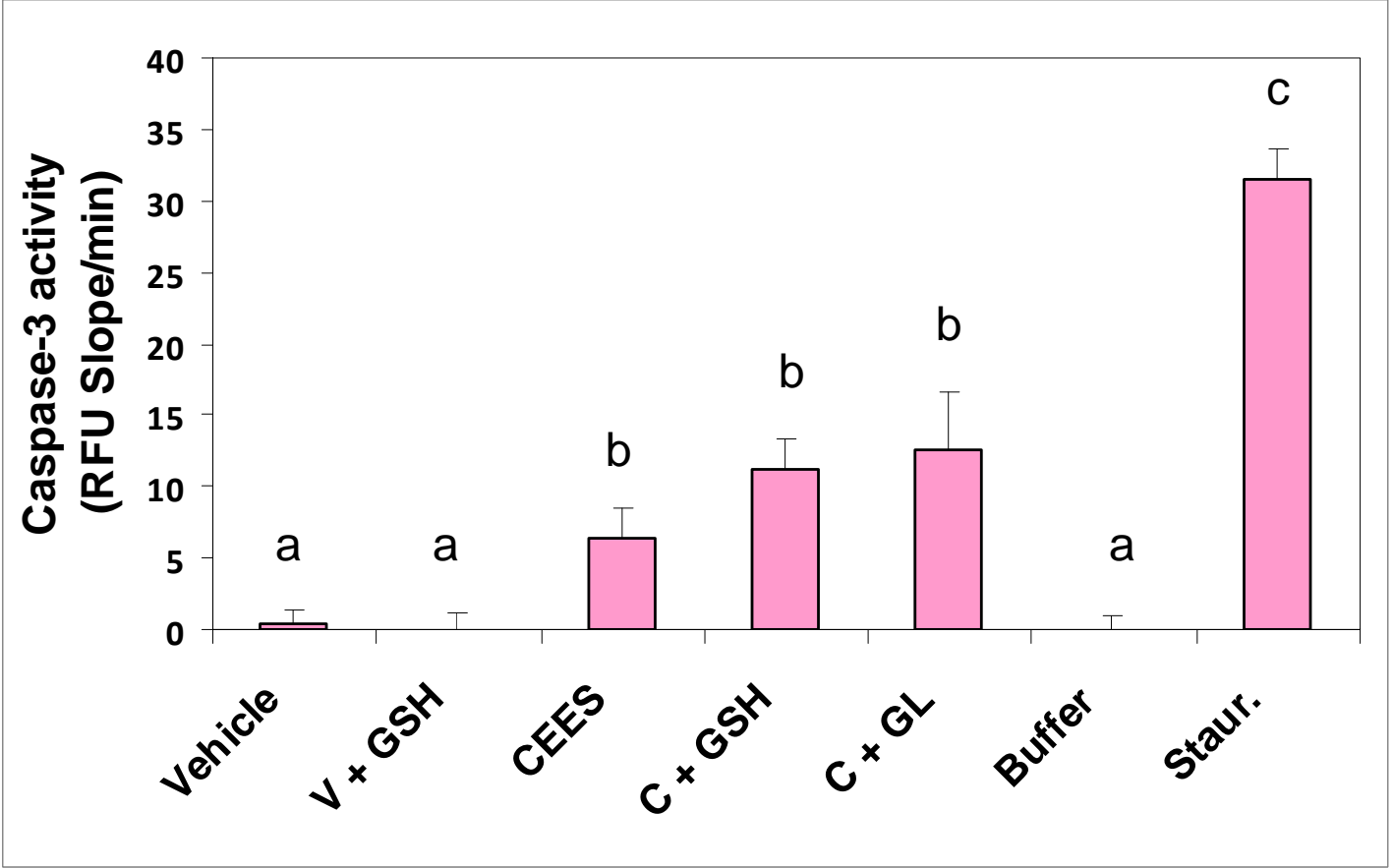




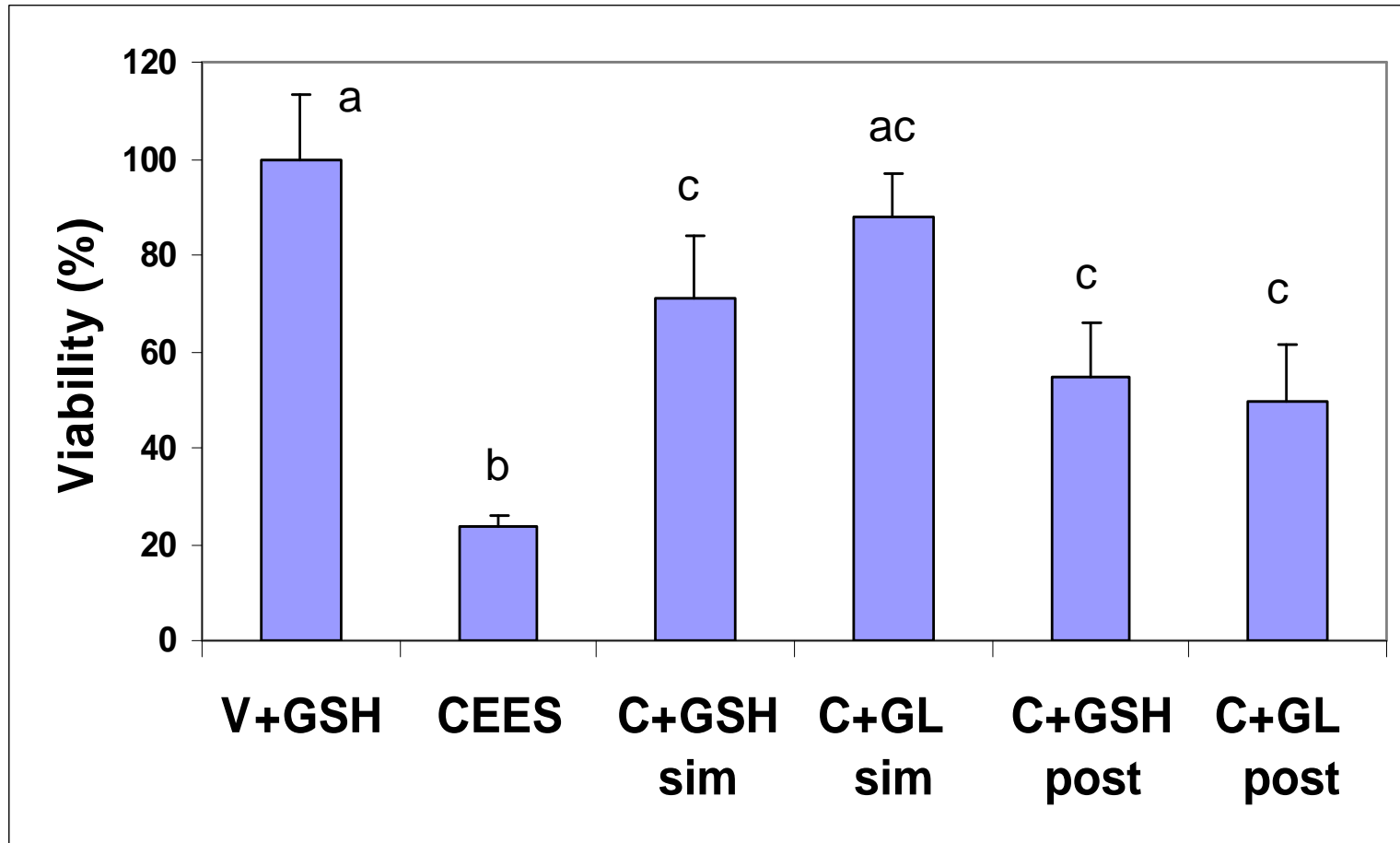




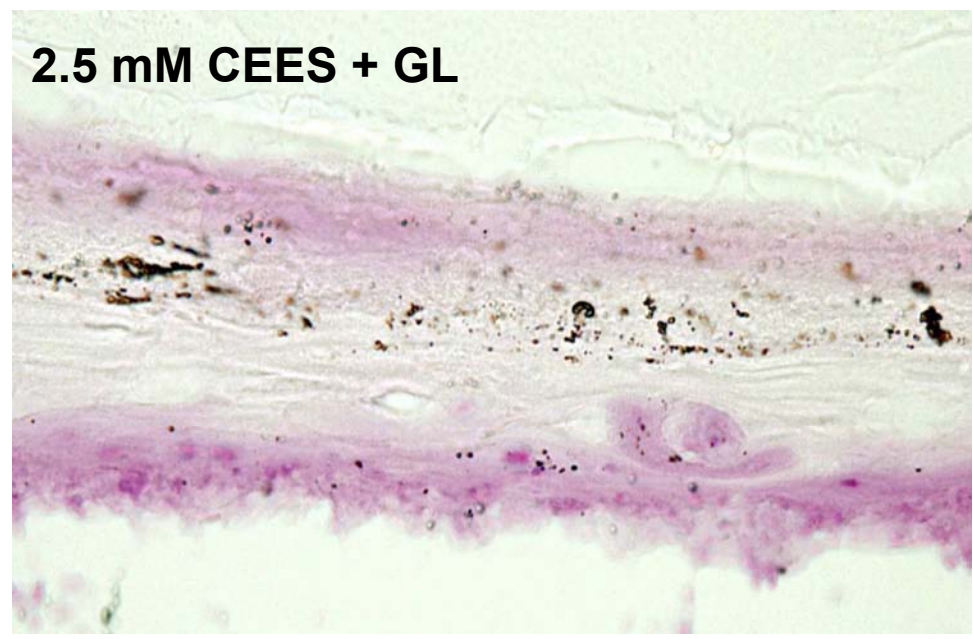
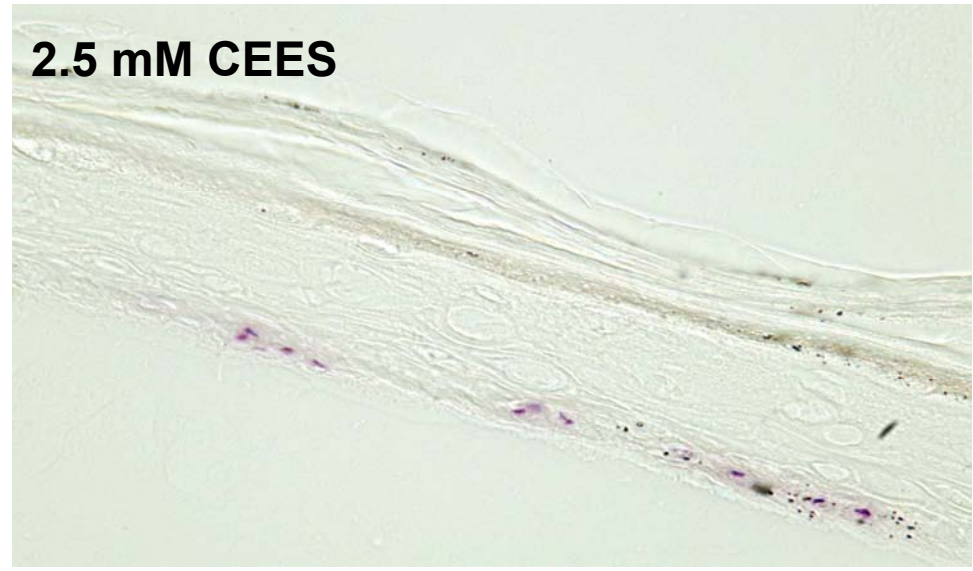
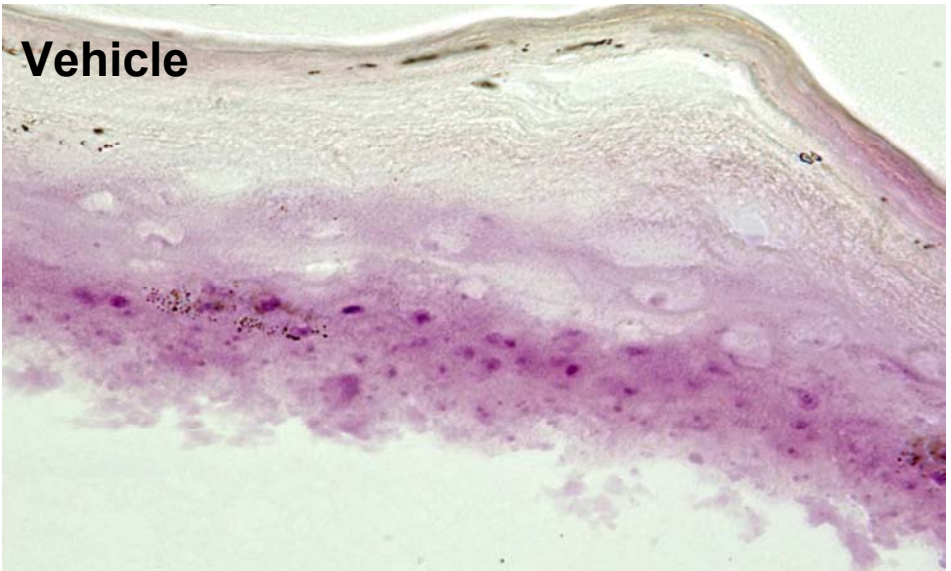




1
2
3
4
5
6
7
8
9
10
11
12
13
14
15
16
17
18
19
20
21
22
23
24
25
26
27
28
29
30
31
32
33
34
35
36
37
38
39
40
41
42
43
44
45
46
47
48
49



1
2
3
4
5
6
7
8
9
10
11
12
13
14
15
16
17
18
19
20
21
22
23
24
25
26
27
28
29
30
31
32
33
34
35
36
37
38
39
40
41
42
43
44
45
46
47
48
49





James H. Quillen
College of Medicine
East Tennessee State University

A Proteomic Approach to Studying Chemical and Biological Weapons

Bill Stone, PhD
Victor Paromov, PhD
Marianne Brannon, PhD
Christian Muenyi, MS
Hongsong Yang, MD
Sudha Kumari

Statement of Work

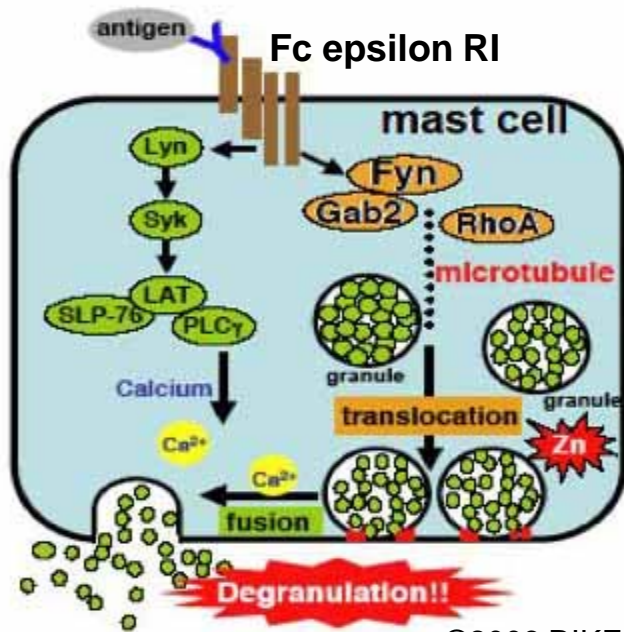
- Is mast cell degranulation induced by 2-chloroethyl ethyl sulfide (CEES) and do antioxidant liposomes influence this degranulation (Dr. Brannon)
- Supply well antioxidant-liposomes to other members of the AMCC (Dr. Hongsong Yang and Sudha Kumari)
- Initiate a proteomic approach to studying the effects of mustard gas/biological weapons in both cellular and animal models
 - Lung samples sent to ETSU by Dr. Dana R Anderson (Mr. Christian Muenyi)
 - Mast cell model
 - Epiderm Skin model



Mast Cell and Sulfur Mustard (HD) Toxicity

- *In vivo* work by John Graham (US Army Medical Research) has shown mast cell degranulation in response to HD (1994)
- Degranulation may play a key role in the inflammatory response caused by HD

Mast Cell Degranulation



©2006 RIKEN RCAI

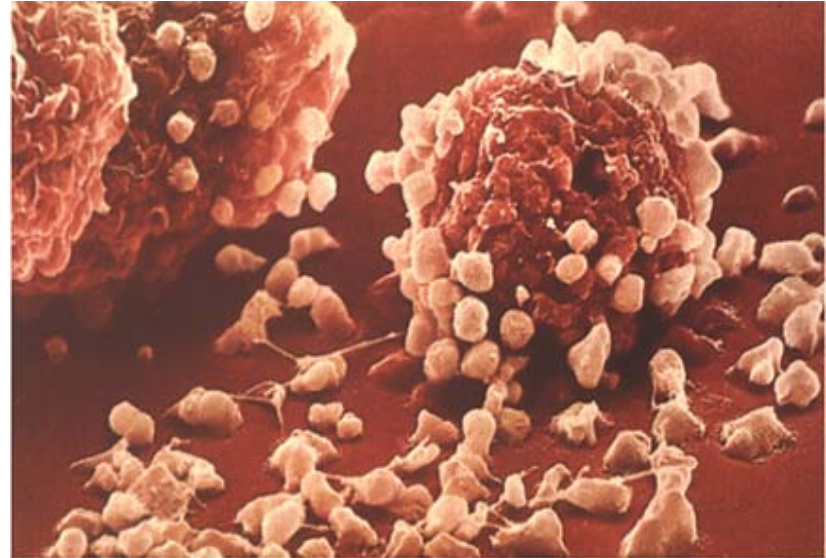


Photo By Diane P. Yolton, PhD, OD

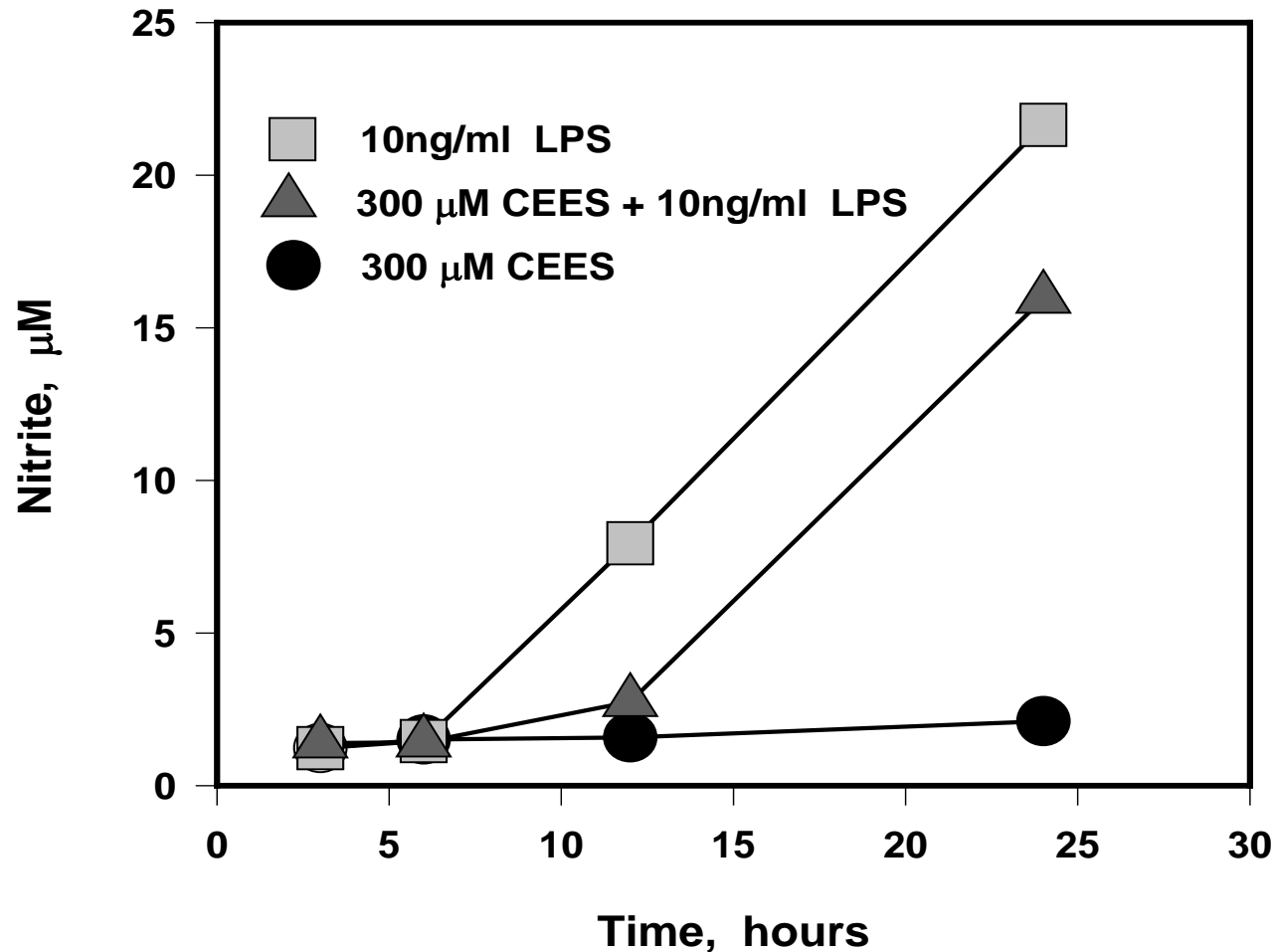
Granule Content:

- Histamine
- Heparin
- Proteases
- Cytokines
- Chemokines
- Leukotrienes
- β -Hexosaminidase

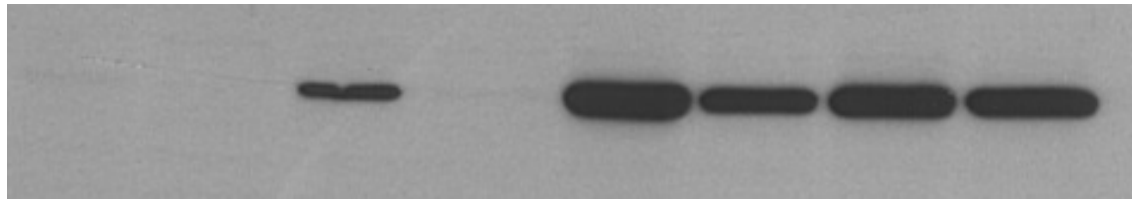
Background Data with RAW264.7 Macrophages

- LPS, IL-1-beta and TNF-alpha enhance the cytotoxicity of CEES (Stone et al., BMC Cell Biology, 2003)
- CEES induces a transient decrease in NO production in activated macrophages that is due to loss of iNOS protein and NOT due to inhibition of iNOS activity (Qui, Paromov, Yang, Smith, Stone, BMC Cell Biology, 2006)

CEES Induces a Transient Decrease in NO Production (RAW 264.7 Macrophages)



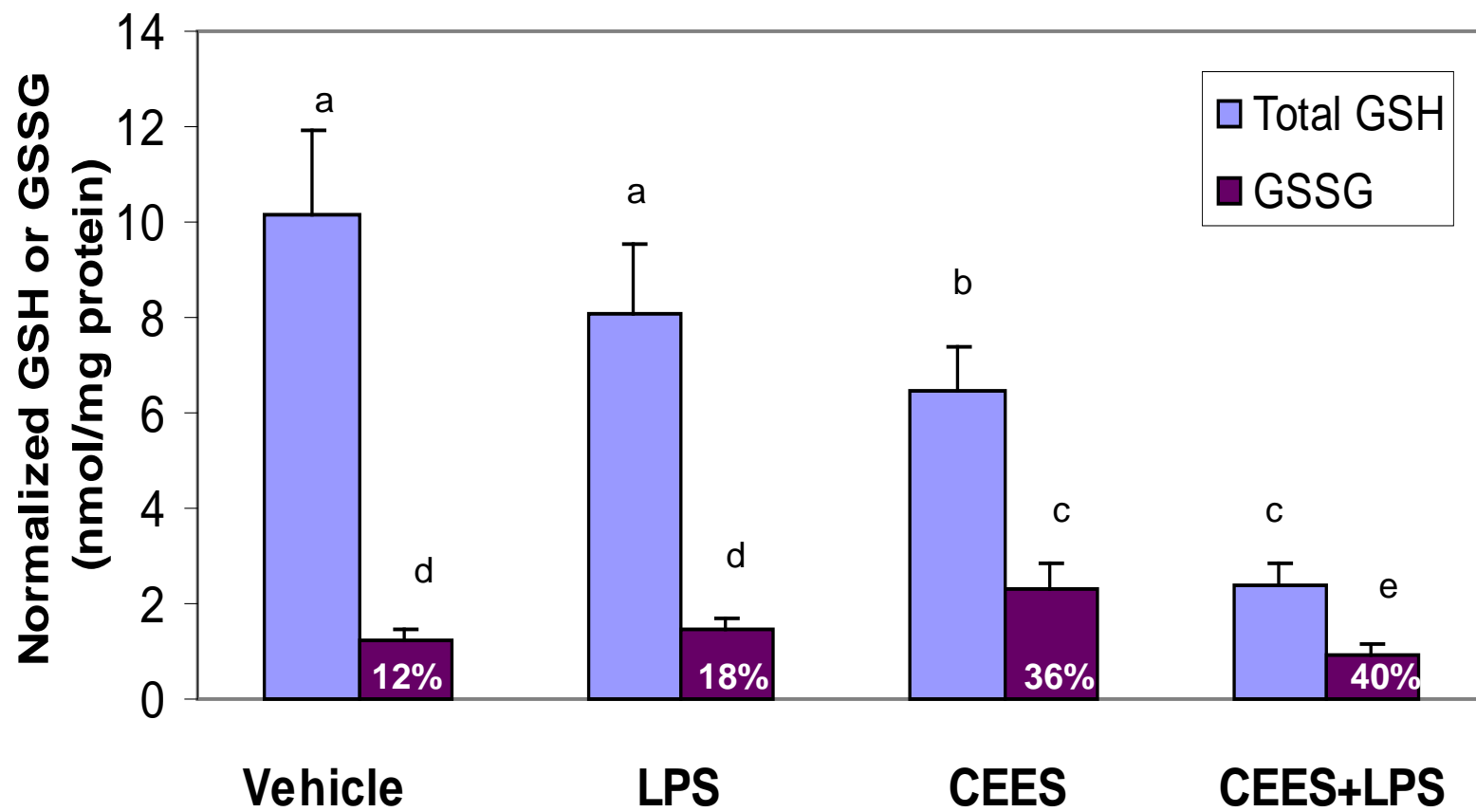
iNOS Expression is Transiently Inhibited by CEES (C) in LPS (L) Stimulated RAW 264.7 Macrophages



3h	3h	6h	6h	12h	12h	24h	24h
L	L+C	L	L+C	L	L+C	L	L+C

What is the Molecular Mechanism for CEES Induced Loss of iNOS activity in RAW 264.7 Cells?

- In some cell types, GSH regulates NO generation with decreased GSH levels associated with decreased NO production
 - This effect could be reversed by the addition of NAC
- We, therefore, hypothesized that the addition of NAC to stimulated macrophages would reverse the loss of NO production caused by CEES



Hypotheses

- CEES, by inducing oxidative stress and decreasing NO production, would promote mast cell degranulation *in vitro*
- Mast cell degranulation would release large amounts of TNF- α , IL-1 β , and other inflammatory cytokines, which could enhance the toxicity of CEES/HD

Colorimetric Degranulation Assay (β -Hexosaminidase Release)



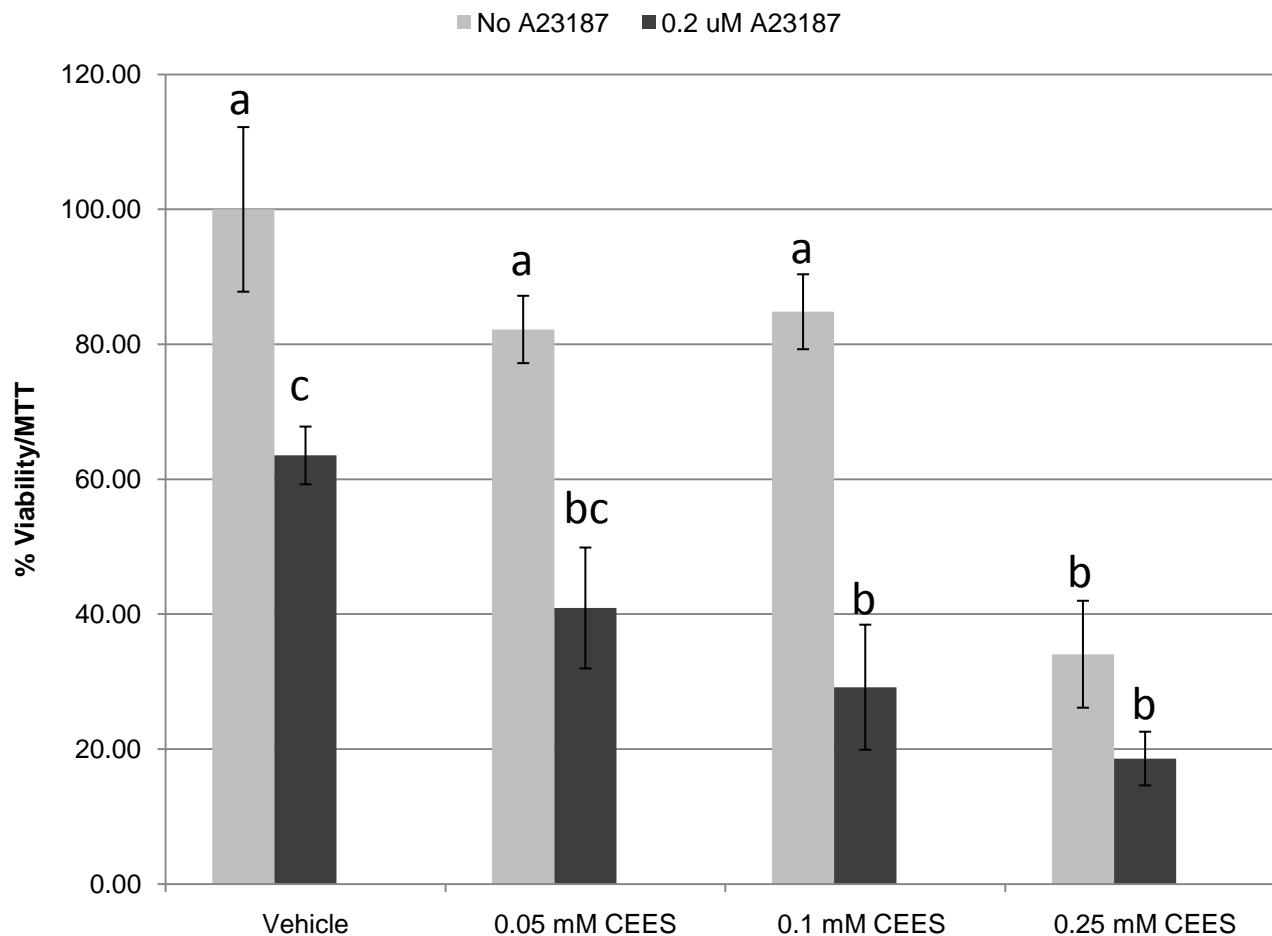
- Stimulate cells
- Incubate for 1.5 h
- Save media
- Prepare cell lysates
- Measure β -Hexosaminidase activity in both media and lysates
- **%Degr = $100 \times \text{Act}_M / (\text{Act}_M + \text{Act}_L)$**

Enzyme: β -Hexosaminidase

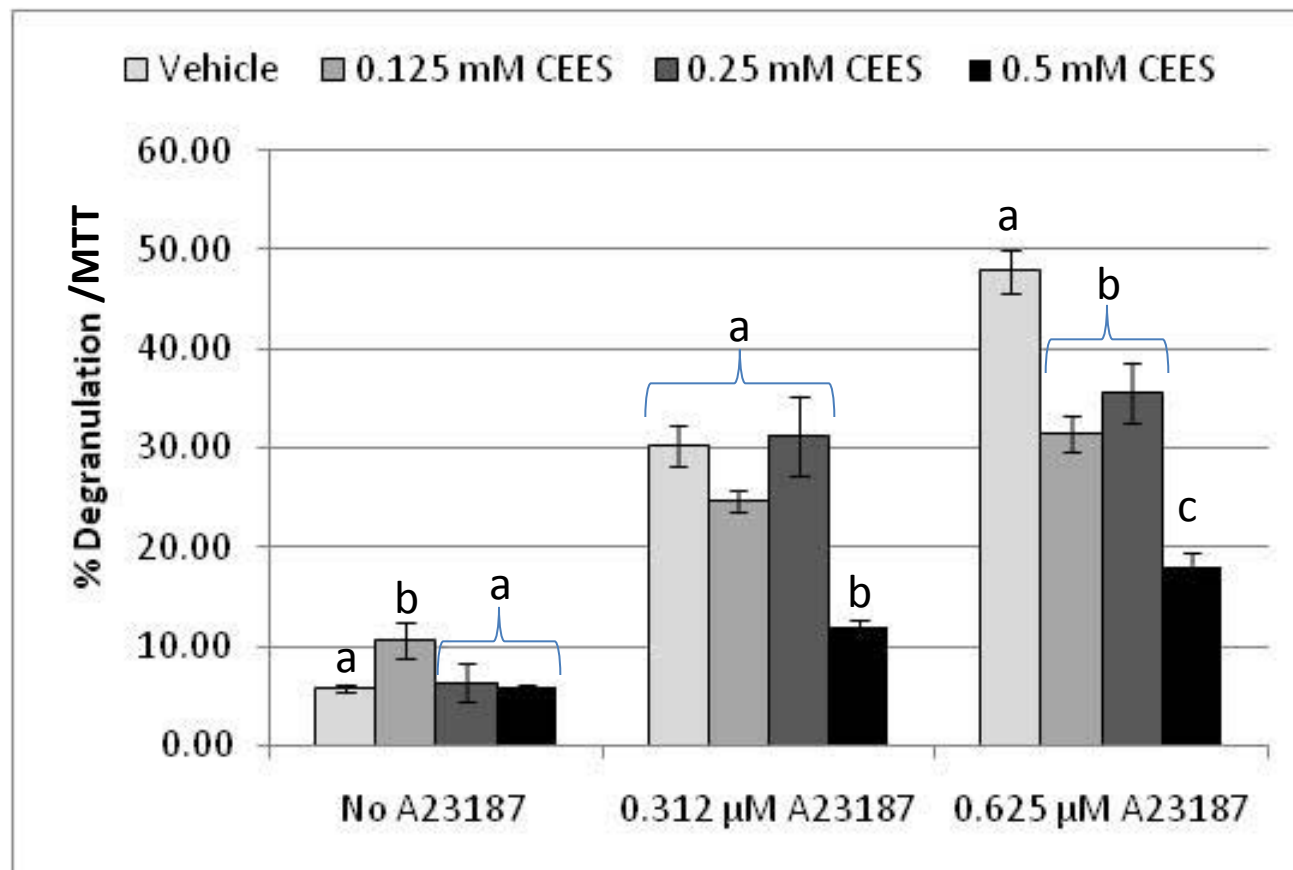
Substrate: 4-Nitrophenyl *N*-acetyl-D-glucosaminide

Product: 4-Nitrophenol (yellow, $\lambda=405$ nm)

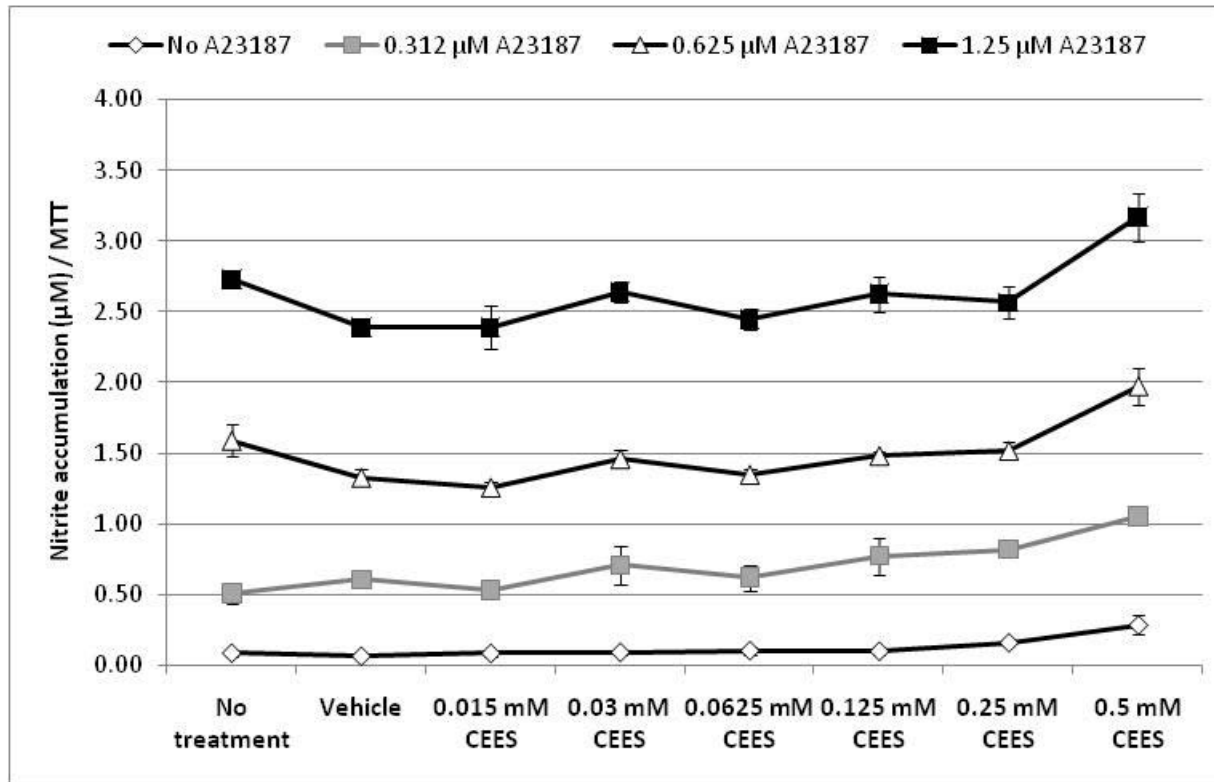
Toxicity (MTT assay) of Ca-ionophore A23187 (0.2 μ M) in the absence or presence of CEES in RBL-2H3 cells after 24 h incubation



Degranulation of RBL-2H3 cells when simultaneously treated for 1.5 hour with Ca ionophore A23187 (0 to 0.625 μ M) and CEES (as indicated). Degranulation percentage was normalized to cell viability



NO generation (normalized to % viable cells) in RBL-2H3 cells treated with CEES and unstimulated or stimulated with the calcium ionophore A23187 (as indicated) for 22 hours



Mast Cells- Conclusions

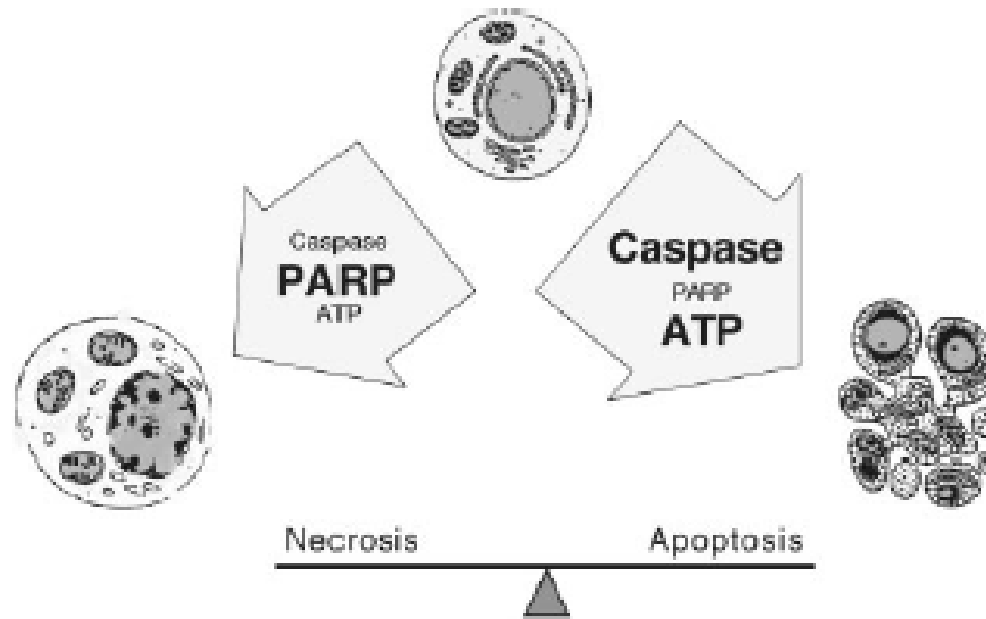
- Mast cell degranulation combined with CEES induces an enhanced cytotoxicity
- A low dose of CEES (0.125 mM) induces a low *in vitro* level of mast cell degranulation
- Ca²⁺ ionophore enhances mast cell degranulation but CEES at 0.5 mM actually inhibits this degranulation

Mast Cells- Continued

- Nitric oxide generation is promoted by the Ca^{2+} ionophore but not influenced by $\text{CEES} \leq 0.5 \text{ mM}$

Second Generation Antioxidant Liposomes

- Oxidative stress and subsequent alterations in redox sensitive signal transduction pathways play a key role in HD toxicity
- Antioxidant liposomes have proven useful in treating HD/CEES induced toxicity
- Second generation antioxidant liposomes maybe even more useful due to insights into the mechanism's) of cell death induced by HD and CEES



PARP as a 'Molecular Switch' between Apoptosis and Necrosis:

Second Generation Antioxidant Liposomes

- GSH and NAC liposomes inhibit HD or CEES induced cell death by blocking apoptosis
- The addition of ethyl pyruvate (also an antioxidant) would prevent necrosis by shifting cell death towards apoptosis (minimizing inflammation) and provide an opportunity for antioxidants-liposomes to rescue apoptotic cells

Proteomic Progress

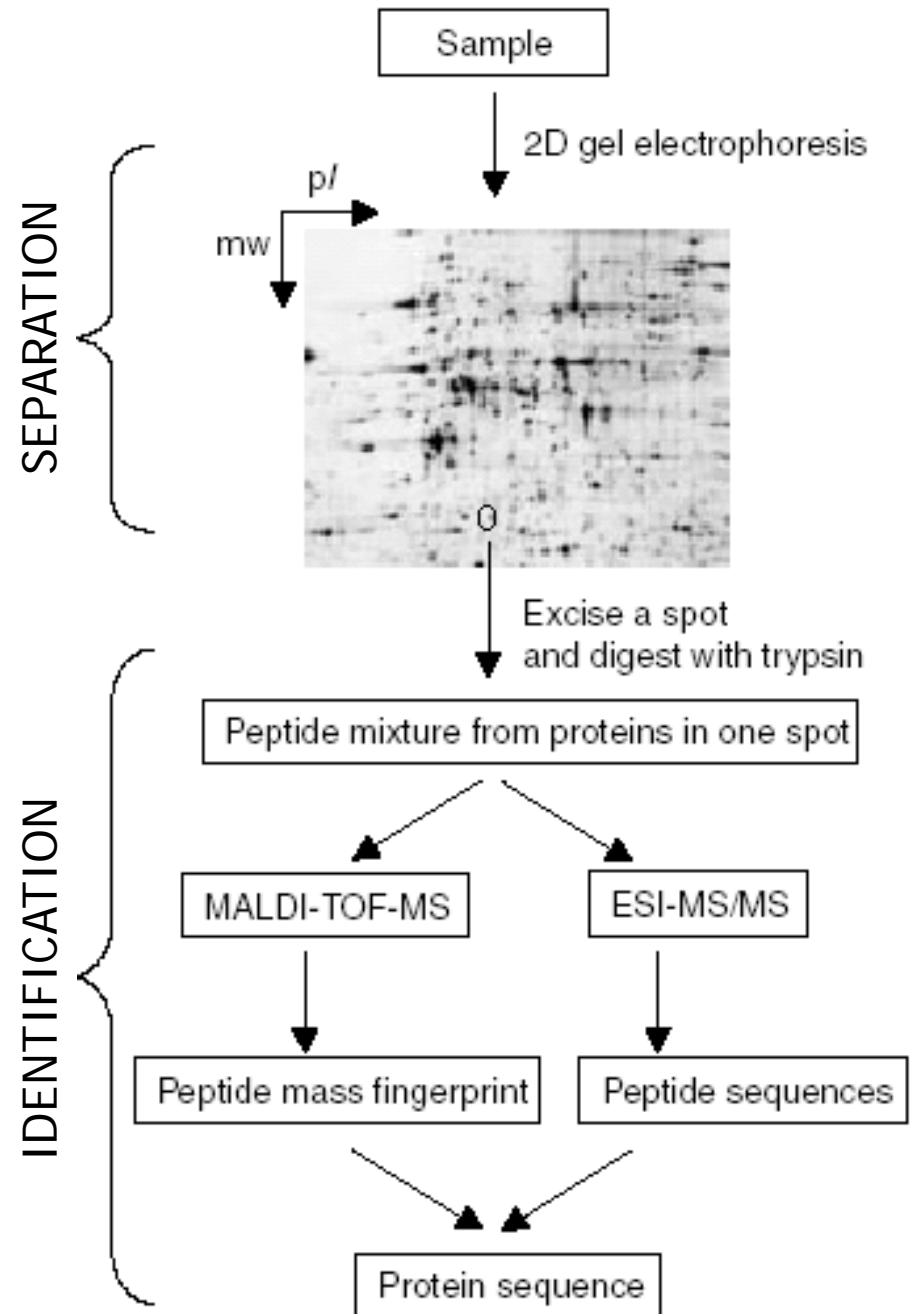
- Proteomics
- State-of-the-art Proteomic System with Finnigan LTQ LX LC/MS system
 - Installed and all laboratory personal have completed the initial training
 - Advanced on site training completed in July 07



Proteomics

- Focuses on the proteins present in a cell/organism, together with their function(s), sub-cellular location, interactions, structure and chemical modifications as function of changing conditions:
 - Disease states (biowarfare agents)
 - Environmental conditions (chemical weapons)

General Flow For Proteomics Analysis



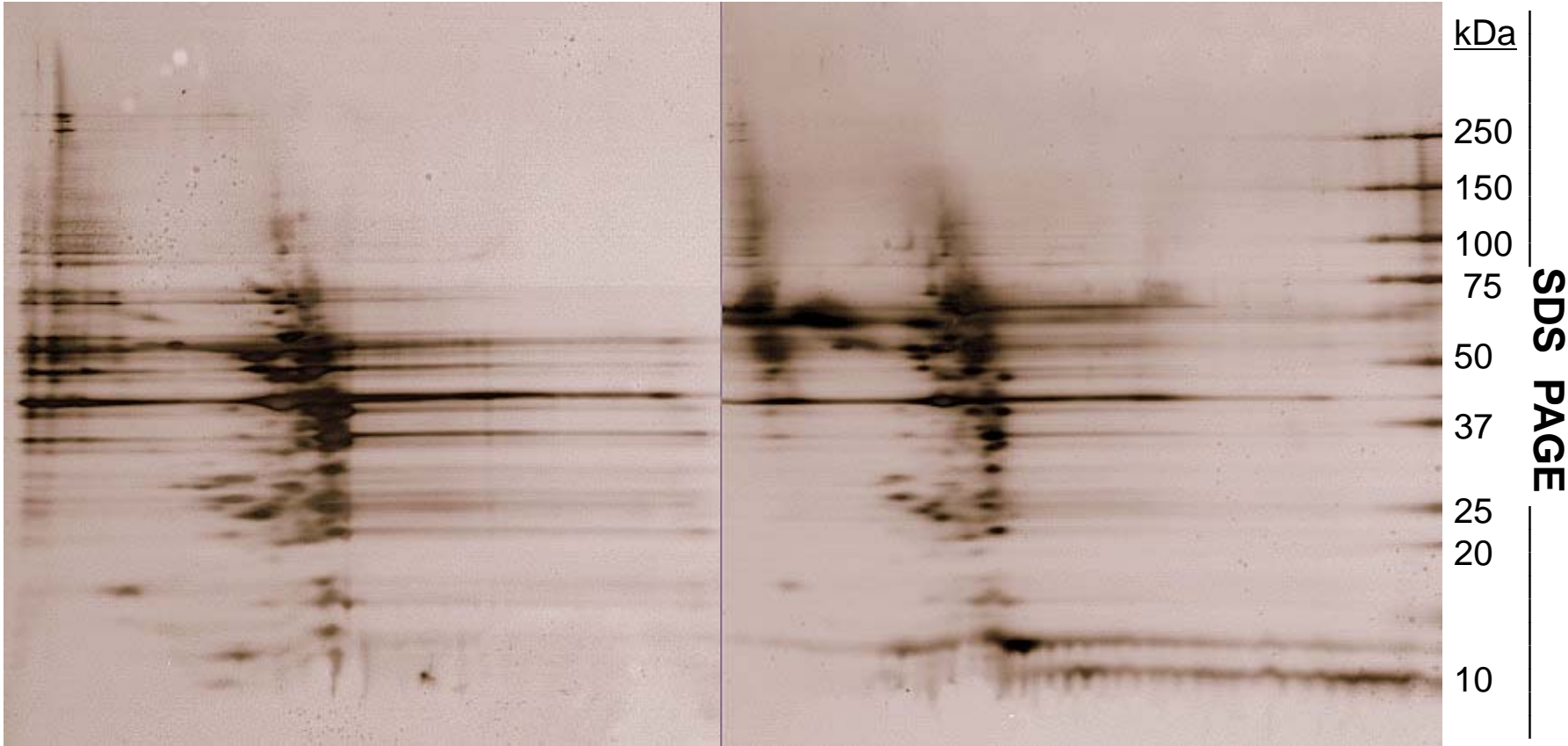
A Proteomic Approach to Studying the Effects Of CEES/HD/Biological Weapons

- Animal Models
 - Rats were exposed to HD and the therapeutic potential of antioxidant-liposomes measured after 6 or 24 hours. Lung samples from these experiment were stored at -80 deg C.
- Cell Models (Mast Cells)
- Epiderm human skin model

Mast Cell Proteomics with/out CEES Exposure

pH 3 to pH 10

pH 3 to pH 10



Vehicle

0.5 mM CEES

Military Significance

- Understanding the molecular mechanisms for HD toxicity will lead to better therapy
 - Antioxidant-liposomes have proven useful in preventing chronic lung fibrosis
 - Acute toxicity could be minimized by antioxidant-liposomes also containing mast cell stabilizers and ethyl pyruvate (second generation therapies)
- Alterations in cellular redox status is an important factor pathogen-host interactions

Salil Das, M.Sc., Sc.D.,D.Sc.

Meharry Medical College

Nashville, TN

REPORT DOCUMENTATION PAGE

Form Approved
OMB No. 0704-0188

Public reporting burden for this collection of information is estimated to average 1 hour per response, including the time for reviewing instructions, searching existing data sources, gathering and maintaining the data needed, and completing and reviewing this collection of information. Send comments regarding this burden estimate or any other aspect of this collection of information, including suggestions for reducing this burden to Department of Defense, Washington Headquarters Services, Directorate for Information Operations and Reports (0704-0188), 1215 Jefferson Davis Highway, Suite 1204, Arlington, VA 22202-4302. Respondents should be aware that notwithstanding any other provision of law, no person shall be subject to any penalty for failing to comply with a collection of information if it does not display a currently valid OMB control number. **PLEASE DO NOT RETURN YOUR FORM TO THE ABOVE ADDRESS.**

1. REPORT DATE (DD-MM-YYYY) 9/24/10		2. REPORT TYPE Final		3. DATES COVERED (From - To) August 21, 2006– Sept 24, 2010	
4. TITLE AND SUBTITLE A. Mechanisms of the Activation of Key Transcription Factors in Mustard Gas - Induced Lung Injury: Protection by Antioxidant Liposomes B. A Feasibility Study on the Development of Lung Injury Model in Guinea Pig by Intratracheal Infusion of Lethal Toxin				5a. CONTRACT NUMBER W81XWH-06-2-0044	
				5b. GRANT NUMBER	
				5c. PROGRAM ELEMENT NUMBER	
6. AUTHOR(S) Salil K. Das				5d. PROJECT NUMBER	
				5e. TASK NUMBER	
				5f. WORK UNIT NUMBER	
7. PERFORMING ORGANIZATION NAME(S) AND ADDRESS(ES) Meharry Medical College, 1005 David Todd Blvd., Nashville, TN 37208				8. PERFORMING ORGANIZATION REPORT NUMBER	
9. SPONSORING / MONITORING AGENCY NAME(S) AND ADDRESS(ES) US Army Medical Research and Materiel Command, Fort Detrick MD 21702-5012				10. SPONSOR/MONITOR'S ACRONYM(S)	
				11. SPONSOR/MONITOR'S REPORT NUMBER(S)	
12. DISTRIBUTION / AVAILABILITY STATEMENT Approved for Public Release, Distributions Unlimited					
13. SUPPLEMENTARY NOTES					
14. ABSTRACT: We reported earlier that intratracheal exposure of 2-chloroethyl ethyl sulfide (CEES) to guinea pigs causes reactive oxygen species (ROS) mediated lung injury by stimulation of inflammatory cytokines, such as TNF- α and activation of the transcription factor NF- κ B. The purpose of the present study was to determine whether CEES-induced activation of TNF- α is followed by activation of several other transcription factors, such as AP-1, SAF-1/MAZ and C/EBP. Increased expression of these genes may lead to altered expression of proteins that may exacerbate the injury in lung or lung cells. Data from the present study reveal that CEES exposure not only activated AP-1/MAPK signaling pathway, but also activated other transcription factors mentioned above. Furthermore, antioxidant liposome treatment had a protective effect against CEES-induced activation of these transcription factors and lung injury. In addition we developed a lung injury model in guinea pig by intratracheal infusion of lethal toxin and established the prophylactic action of antioxidant liposome against lethal toxin-induced lung injury					
15. SUBJECT TERMS CEES, lethal toxin, transcription factors, lung injury, antioxidant liposome, guinea pig					
16. SECURITY CLASSIFICATION OF:			17. LIMITATION OF ABSTRACT	18. NUMBER OF PAGES	19a. NAME OF RESPONSIBLE PERSON
a. REPORT Unclassified	b. ABSTRACT Unclassified	c. THIS PAGE Unclassified			USAMRMC
				106	19b. TELEPHONE NUMBER (include area code)

Table of Contents

	<u>Page</u>
Cover Page.....	1
Report Documentation Page (SF-298).....	2
Table of Contents.....	3
Statement of Work.....	4
Introduction	4
Body.....	4-10
Key Accomplishments.....	10
Reportable Outcomes (Presentations and Manuscripts)	10-11
Conclusion.....	12
References.....	12
Appendices (List of Reprints)	13

Statement of Work

We have established in our laboratory that intratracheal exposure of 2-chloroethyl ethyl sulfide (CEES), a mustard gas analog to guinea pigs causes reactive oxygen species (ROS) mediated lung injury by stimulation of inflammatory cytokines, such as TNF- α . The purpose of this proposal was to determine whether CEES-induced activation of inflammatory cytokines is followed by the activation of several key transcription factors [nuclear factor- κ B (NF- κ B), activation protein-1 (AP-1), serum accelerator factor (SAF), and CCAAT/enhancer binding protein (C/EBP)], and whether antioxidant liposome therapy offers a protection against CEES-induced activation of these transcription factors. These transcription factors induce expression of many target genes including, alpha 1-antitrypsin [α 1-AT], matrix metalloproteinases [MMP], and tissue inhibitors of metalloproteinases [TIMPs]. Increased expression of these genes will lead to altered expression of proteins that may exacerbate the injury in lung or lung cells. Another objective of this investigation was to develop a lung injury model in guinea pig by intratracheal infusion of lethal toxin and explore whether the lethal toxin-induced lung injury can be protected by antioxidant liposome therapy.

We achieved this goal by conducting the following specific aims:

1. Analysis of CEES-induced changes in the transcripts of target genes (alpha 1-antitrypsin [α 1-AT], matrix metalloproteinase [MMP], and tissue inhibitors of metalloproteinases [TIMPs] in lung by Northern blot or RT-PCR.
2. Analysis of CEES-induced changes in the target proteins in the lung by immunohistochemistry.
3. Analysis of CEES-induced changes of SAF-1, AP-1, NF- κ B and C/EBP transcription factor in the lung by immunohistochemistry. Co-localization analysis of transcription factor and target genes.
4. Functional analysis of transcription factor activity in the tracheal epithelial cells by assessing promoter-binding activity followed by CEES exposure.
5. Analysis of the signaling mechanisms [protein kinase A (PKA), protein kinase C (PKC), and mitogen activated protein kinase (MAPK)] involved in the activation of SAF-1 in the lung cells following CEES exposure.
6. Analysis of the effectiveness of the treatment by (a) delivery of a liposome containing an antioxidant, such as N-acetyl cysteine (NAC) either intravenously or subcutaneously, and (b) in combination therapy with a specific inhibitor or inhibitors of transcription factors in abolishing the induction of the transcription factors involved in CEES-induced lung injury.
7. Test whether intratracheal exposure of lethal toxin LeTx in guinea pigs causes lung injury and fibrosis and if so, whether an antioxidant liposome offers any protective action.

Introduction

For several years we have been studying in a guinea pig model the molecular mechanisms by which CEES exposure causes lung injury associated with ARDS. Our earlier publication indicated that CEES causes lung injury and significantly decreases expression and activity of cholinephosphotransferase (CPT), the terminal enzyme in CDP-choline pathway for phosphatidylcholine synthesis [1]. This decrease in CPT activity was not associated with any mutation of the CPT gene and is probably mediated by accumulation of ceramides. CEES induced ceramide accumulation may thus play an important role in the development of ARDS by modulating the expression of CPT. We have previously shown that exposure of CEES to guinea pigs causes an increase in the levels of TNF- α , NF- κ B and ceramides in the lung [2]. However, NF- κ B disappeared after 2 hours indicating an intricate interplay of pro- and anti- apoptotic inflammatory cytokines. In subsequent studies, we utilized a state of the art cytokine array technology to identify other cytokines affected by CEES exposure [3]. The array of cytokine induction within an hour of CEES exposure and dynamic changes in cytokine profile by one day post CEES exposure reveals that following an initial damage, the lung tissue tries to recover and prevent further damage through self defense mechanisms mediated through various classes of cytokines. We also showed that antioxidant liposomes were protective against acute lung injury induced by exposure to CEES [4-6]. We have also observed that CEES exposure causes progressive lung fibrosis [5-7].

Body

1. Induction of cytokines by CEES exposure

Our initial analysis of 60 cytokines showed 16 cytokines up-regulated within 1 hr. in the CEES exposed lungs, 1.5-fold above the control vehicle treated lungs. Among these, 9 cytokines with known or predicted

functions in cellular injury and defense signal (IL-1 α , EOTAXIN, MIP-1 γ), macrophage activation (IFN- γ), inflammatory response (TNF- α), apoptosis (TNF- α), activation of NF- κ B (LIGHT), cell proliferation and wound healing (PDGF-BB, FGF-7 and IGFBP-I) were all induced at higher levels with a minimum cut-off point of 2x above the levels of the control lungs. Eotaxin regulated by both TNF- α and IL-1 α is also known to be induced in response to radiation. We extended our evaluation to additional 60 cytokines (for a total of 120) at one hour and post mustard gas exposure which identified upregulation (>1.5x) of several growth factors (FGF2) chemoattractant proteins (MCP-3) and cytokines involved in extra-cellular (TSP) remodeling (uPAR and TIMPs). To further understand the dynamics of cytokine induction profile we also evaluated the changes in the levels of these 120 cytokines by one-day post mustard gas exposure.

The array of cytokine induction within an hour of CEES exposure and dynamic changes in cytokine profile by one day post mustard gas exposure reveals that following an initial damage, the lung tissue tries to recover and prevent further damage through self defense mechanisms mediated through various classes of cytokines.

2. Activation of angiogenic cytokines by CEES exposure

We reported earlier that guinea pigs exposed to 2-chloroethyl ethyl sulfide (CEES) as a mustard gas analog, accumulate inflammatory cytokines, including TNF- α . Since angiogenesis may play a role, in inflammation and pathophysiology of tissue remodeling, we evaluated the early induction profile of angiogenic cytokines and selected target genes using cytokine antibody arrays. VEGF and bFGF levels showed 1.5-fold increase within 1 hr. of CEES exposure. However, while VEGF remained high after one day, bFGF level was decreased. Increase in VEGF receptors Flk-1 and Flt-1 and MMP-2 were also detected by Western blot analysis in 1 day. Our results strongly suggest that angiogenic cytokines may play an essential role in inducing chronic inflammation following lung injury.

3. Effects of CEES exposure on the protein levels of matrix metalloproteinases and tissue inhibitors of metalloproteinases [TIMPs]

In order to accomplish this goal, we induced lung injury in the guinea pig model in a dose and time dependent manner. Lungs were initially analyzed for changes in the protein levels of the above biochemical parameters by protein antibody array and Western blot analysis. Initial results on Western blot analysis indicated an increase in the protein levels of two metalloproteinases: 1) MMP-2 [72 kd target protein (gelatinase A) for IFN- γ involved in angiogenesis] and 2) MMP-9 [92 kd protein (gelatinase B)], in a dose (0.5 mg – 4 mg/kg of CEES) and time dependent manner (1 h – 14 d). Protein antibody array analysis indicated that while a short-term exposure (1 h) of CEES (0.5 mg/kg) causes an up-regulation of TIMP-2 (an anti-angiogenic cytokine), a longer exposure (24 h) causes its down-regulation. These studies are being continued for statistical validity.

4. Induction of superoxide dismutase gene in CEES-induced lung injury

Mustard gas exposure causes inflammatory lung diseases. Many inflammatory lung diseases are associated with oxidative stress. Reactive oxygen species (ROS) are involved in the maintenance of physiological functions. In tissues, it is therefore essential to maintain a steady-state level of antioxidant activity to allow both for the physiological functions of ROS to proceed and at the same time preventing tissue damage. We have recently reported that mustard gas exposure decreases the overall activity of superoxide dismutase (SOD). In the present study, we investigated the effects of mustard gas on each of the three isozymes [SOD-1 (Cu/Zn), SOD-2 (Mn) and SOD-3 (extracellular)]. Adult guinea pigs were intratracheally injected single doses of CEES (2mg/kg body weight) in ethanol. Control animals were injected with vehicle in the same way. The animals were sacrificed after 7 days and lungs were removed after perfusion with physiological saline. Lung injury was established by measuring the leakage of iodinated-BSA into lung tissue.

Mustard gas exposure caused a significant increase in the activity of SOD-1 (35%). However, the SOD-3 activity which is the predominant type in lung was significantly decreased (62%), whereas, no change was observed in SOD-2 activity. Thus the decrease in the total activity of SOD was primarily due to the SOD-3 isozyme. Northern blot analysis indicated 3.5-fold increased expression of SOD-1 in mustard gas-exposed lung, but no significant change in the expression of SOD-2 and SOD-3 was observed. Mustard gas exposure did not

cause mutation in the coding region of SOD-1 gene while causing modulation in expression levels. The protein levels of SOD-1, SOD-2 and SOD-3 were not altered significantly in the mustard gas exposed lung.

Our results indicate that the overall decrease in the activity of SOD by mustard gas exposure is probably mediated by direct inactivation of the SOD-3 gene or the enzyme itself. This decrease in the activity of SOD-3 may be due to the cleavage of active form of the protein to an inactive form. Existence of active and inactive forms of SOD-3 as a result of shifts in Cys-Cys disulfide bonding has been described in human, recently. Studies are underway in our lab to investigate whether mustard gas-induced inactivation of SOD-3 in lung is similarly mediated by a change in Cys-Cys disulfide bonding.

These results have been recently published [8]. A reprint is included for detailed description.

5. Induction of pulmonary fibrosis by CEES exposure

Cross sectional clinical study on veterans with single heavy exposure to sulfur mustard gas (SMG) revealed that inhalation of SMG can lead to the development of series of chronic destructive pulmonary sequelae such as chronic bronchitis, pulmonary fibrosis (PF), and bronchiectasis. To understand the mechanism by which SMG exposure causes PF, we have used 2-chloroethyl ethyl sulfide (CEES) as a SMG analog to induce lung injury in guinea pigs. Our initial electronmicroscopic studies on lung of guinea pigs exposed to CEES indicate evidence of interstitial pulmonitis with varying degrees of interstitial fibrosis, neutrophilic alveolitis and increased amount of visualized collagen within 7 days [5]. Pulmonary fibrosis has also been demonstrated in rats by our collaborative studies with Dr. Peter Ward [6].

6. Protection of CEES-induced lung injury in guinea pigs by antioxidant liposomes

This study was to develop antioxidant liposomes as antidotes for mustard gas induced lung injury in guinea pigs. Five antioxidant liposomes (LIP-1, LIP-2, LIP-3, LIP-4 and LIP-5) were prepared differing in the levels of phospholipid, cholesterol, phosphatidic acid, tocopherol (α , γ , δ), N-acetylcysteine (NAC) and GSH. A single dose (200 μ l per animal) of each liposome was administered intratracheally after 5 min and 1 h of exposure of 2-chloroethyl ethyl sulfide (CEES). The animals were sacrificed either after 2 h (for lung injury study) or after 30 days (for histology study) of CEES exposure. These antioxidant liposomes offered 9 to 76% protection against lung injury as evidenced by leakage of BSA from blood into the lung. The maximum protection was achieved with two liposomes, LIP-2 (71.5%) and LIP-4 (75.4%), when administered after 5 minutes of CEES exposure. Delaying the administration of the liposomes after 1 h of CEES exposure decreased the efficacy. Both liposomes contained 11 mM α -tocopherol, 11 mM γ -tocopherol and 75 mM NAC. However, LIP-2 contained additionally 5 mM δ -tocopherol. Overall, LIP-2 and LIP-4 offered significant prophylactic protection by controlling recruitment of neutrophils, eosinophils, and accumulation of septal and perivascular fibrin and collagen, and parenchymal collapse. However, LIP-2 showed better protection than LIP-4 in terms of the accumulation of aggregated RBCs in the bronchi, alveolar space, arterioles and veins, and fibrin and collagen deposition in the alveolar space. The protection against CEES-induced lung fibrosis by antioxidant liposomes, particularly LIP-2 was further evident by a decrease in lipid peroxidation and hydroxyproline content in lung. Our study clearly suggests that NAC can be used in combination with vitamin E as a liposome for effective antidote against lung injury.

These results have been recently published [9]. A reprint is included for detailed description

7. Activation of MAPK/AP-1 signaling pathway in lung injury induced by CEES exposure

We reported earlier that the activation of free-radical-mediated TNF- \bullet cascade is the major pathway in the inflammatory lung disease induced by CEES, a mustard gas analog. TNF- \bullet induces AP-1 activation via phosphorylation of MAPKs. The present study examines the relationship between CEES induced lung injury and MAPKs signaling pathway. Adult guinea pigs received single intratracheal injection of different doses of CEES and were sacrificed at different time points. CEES exposure caused lung injury with evidence of fibrosis. The optimum activation of all members of the MAPKs family (ERK1/2, p38 and JNK1/2) was achieved at 0.5 mg/kg dose and at 1 h. No significant change was observed beyond that time point. This led to an activation of AP-1 transcription factors associated with an increase in the protein levels of Fos, ATF and Jun family members. To explore the involvement of AP-1 in cell proliferation, we determined the protein levels of cell cycle protein cyclin D1 and cell differentiation marker PCNA. An up regulation of these proteins was observed. Hence

it is suggested that CEES exposure causes accumulation of TNF- α , which is associated with an activation of MAPK/AP-1 signaling pathway and cell proliferation. Further studies are needed to clarify whether the observed effects are the adaptive responses of the lung or they contribute to the lung injury.

These results have been recently published [10]. A reprint is included for detailed description

8. Protection of CEES-induced activation of MAPK/AP-1 signaling pathway in guinea pig lung by antioxidant liposomes

We recently reported (Mukherjee *et al.*, 2009) that antioxidant liposomes can be used as antidotes for mustard gas induced lung injury in guinea pigs. The maximum protection was achieved with a liposome composed of tocopherols (α , γ , δ) and N-acetylcysteine (NAC) when administered after 5 minutes of exposure of 2-chloroethyl ethyl sulfide (CEES), a half sulfur mustard gas. We also reported an association of mustard gas-induced lung injury with an activation of MAPK/AP-1 signaling pathway and cell proliferation. The objective of the present study was to investigate whether CEES-induced MAPKs/AP-1 signaling pathway is influenced by antioxidant liposome therapy. A single dose (200 μ l) of the antioxidant liposome was administered intratracheally after 5 min of exposure of CEES (0.5 mg/kg). The animals were sacrificed after 1h and 30 days of CEES exposure. Although the liposome treatment did not have any significant effect on the activation of the MAPKs family (ERK1/2, p38 and JNK1/2), it significantly counteracted the CEES-induced activation of AP-1 transcription factors and increase in the protein levels of Fos, ATF and Jun family members. Furthermore, the liposome treatment significantly blocked the CEES-induced increase in the protein levels of cyclin D1, a cell cycle protein and PCNA, a cell differentiation marker. This suggests that the prophylactic protection of antioxidant liposome against CEES-induced lung injury is mediated via control of AP-1 signaling.

These results have been recently published [11]. A reprint is included for detailed description

9. Desensitization of β -adrenergic receptors in lung injury induced by CEES exposure

CEES exposure causes inflammatory lung diseases, including acute respiratory distress syndrome and pulmonary fibrosis. This may be associated with oxidative stress, which has been implicated in the desensitization of beta-adrenergic receptors (β -ARs). The objective of this study was to investigate whether lung injury induced by intratracheal CEES exposure (2 mg/kg b.wt) causes desensitization of β -ARs. The animals were sacrificed after 7 days and lungs were removed. Lung injury was established by measuring the leakage of iodinated-BSA into lung tissue. Receptor binding characteristics were determined by measuring the binding of [3 H]-dihydroalprenolol (0.5-24 nM) to membrane fraction in the presence and absence of DL-propranolol (10 μ M). Both high and low affinity β -ARs were identified in lung. Binding capacity was significantly higher in low affinity site in both control and experimental groups. Although CEES exposure did not change K_D and B_{max} at the high affinity site, it significantly decreased both K_D and B_{max} at low affinity sites. A 20% decrease in β_2 -AR mRNA level and a 60% decrease in membrane protein levels were observed in the experimental group. Furthermore, there was significantly less stimulation of adenylate cyclase activity by both cholera toxin and isoproterenol in the experimental group in comparison to the control group. Treatment of lungs with IBMX, an inhibitor of phosphodiesterase could not abolish the difference between the control group and experimental group on the stimulation of the adenylate cyclase activity. Thus, our study indicates that CEES-induced lung injury is associated with desensitization of β_2 -AR.

These results have been recently published [12]. A reprint is included for detailed description

10. Protection of CEES-induced lung injury by antioxidant liposomes is mediated by decrease in the expression of SAF-1/MAZ

We reported earlier in a guinea pig model that exposure of 2-chloroethyl ethyl sulfide (CEES), a mustard gas analog, causes lung injury associated with the activation of TNF- α , MAPK signaling, and AP-1 transcription factor. Our earlier studies also revealed that antioxidant liposomes can be used as antidotes. Proinflammatory cytokines IL-1, IL-6 and TNF- α , either alone or in combination can induce the activation of another group of transcription factors, namely SAF-1/MAZ. Phosphorylation of SAF-1 via MAPK markedly increases its DNA binding and transactivational potential. The objective of the present study was to investigate whether CEES

exposure causes activation of IL-1 β , IL-6 and SAF-1/MAZ and whether these effects can be prevented by antioxidant liposomes. A single dose (200 μ l) of the antioxidant liposome mixture was administered intratracheally after 5 min of exposure of CEES (0.5 mg/kg). The animals were sacrificed either 1h or 30 days after CEES exposure. CEES exposure caused an up-regulation of proinflammatory cytokines IL-6 and IL-1 β in the lung along with an increased activation of transcription factor SAF -1/MAZ. The antioxidant liposomes treatment significantly blocked the CEES-induced activation of IL-6, IL-1 β , and SAF-1/MAZ. This might suggest that antioxidant liposomes might offer a potential therapeutic strategy against inflammatory diseases associated with activation of these bioactive molecules.

These results have been recently published [13]. A reprint is included for detailed description

11. Effects of intratracheal exposure of CEES on activation of CCAAT-enhancer binding protein (C/EBP) and protection by antioxidant liposome

In our study of “Mechanisms of the activation of key transcription factors in mustard gas-induced lung injury” one of the key transcription factors studied was C/EBP transcription factors. The C/EBP (CCAAT-enhancer binding protein) family of proteins represents a basic leucine zipper transcription factors. There are six known isoforms of C/EBP namely α , β , γ , δ , ϵ and ζ . All the isoforms exhibit similar DNA binding specificities and contain a leucine zipper dimerization region.

It is known from our previous studies that 2-chloroethyl ethyl sulfide (CEES), a sulfur mustard analog induces TNF α in the lung [2]. Our recent studies have shown that this induction of TNF α results in the induction of MAP kinases [10]. Also we reported earlier that the mustard gas exposure in lungs results in lung injury evident from neutrophil accumulation in the interstitial lung spaces [4]. It is known that neutrophil accumulation is mediated by ICAM 1 and C/EBP is implicated in ICAM 1 expression [14]. Also it is known that MAPK activates C/EBP. Therefore, in light of our previous observations, it is important that we look at C/EBP expression and activation with CEES exposure. According to our present knowledge C/EBP β is the most prevalent form of C/EBP transcription factor in the lung [15]. Therefore, we focused our study on C/EBP β . We reported earlier that CEES-induced lung injury is counteracted by intratracheal administration of an antioxidant liposome immediately after CEES exposure [9], we investigated in this study whether this protective effect of the antioxidant liposome is associated with a control in the activation of C/EBP expression.

We adopted two different approaches for looking into C/EBP β expression: TransAM C/EBP α / β ELISA kit (Active Motif) to look for C/EBP β activation and Western blot analysis for C/EBP β protein expression. TransAM C/EBP β ELISA involved plating the tissue extract in triplicate in a 96 well ELISA plate which has an immobilized oligonucleotide that contains C/EBP consensus binding site (5'-GCAAT-3'). C/EBP β contained in the tissue extract specifically binds to this consensus sequence and then the primary antibody used in the kit recognizes an accessible epitope on C/EBP β protein upon DNA binding. Western blot analysis involved running 40 μ g of tissue homogenate on SDS-PAGE and then transferring it to a nitrocellulose membrane and probing it with C/EBP β antibody (sc-150, Santa Cruz Biotechnology). The blots were subsequently stripped and reprobed with actin as the loading control.

Results

Results for C/EBP β activation by TransAM C/EBP α / β ELISA kit (Active Motif) showed activation of CEBP β with mustard gas [Figure 1; increase 226% from control (0.252)]. This activation is negated by application of antioxidant liposome along with mustard gas and the levels came down to that of control (0.463). The western blot analysis also showed increase in the C/EBP β protein as a result of mustard gas (Figure 2; 45% increase from control levels). ICAM-1 protein expression also showed similar pattern (Figure 3; increase of 121% from control). Both protein expressions came back near to the control when antioxidant liposome was administered.

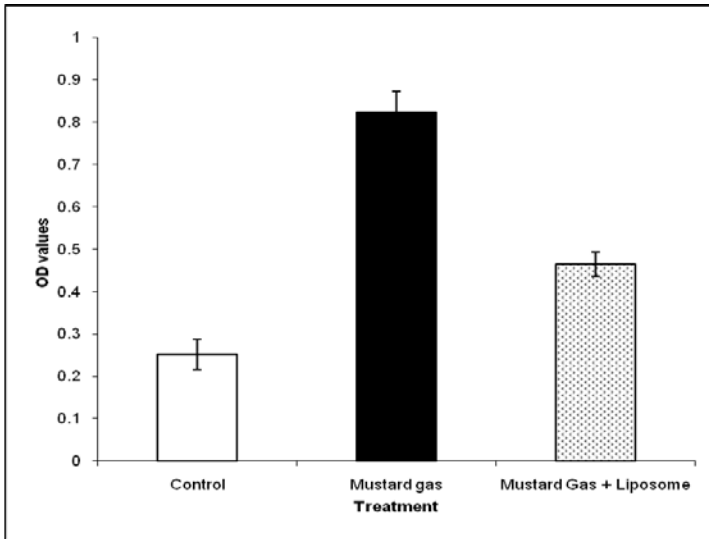


Figure 1: TransAM C/EBP β activation ELISA.

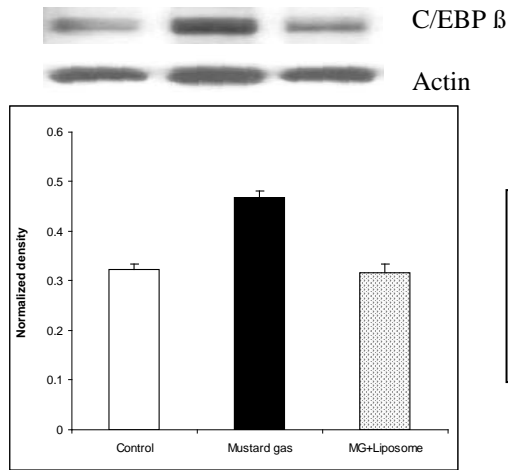


Figure 2: Western blot analysis of the C/EBP β protein. The graph represents normalized value of C/EBP β protein against actin.

We also looked into the downstream target of C/EBP β like ICAM-1 which is involved in the neutrophil accumulation in the lung as the result of mustard gas injury. Western blot analysis for ICAM-1 (ab2213, Abcam) also showed a similar pattern.

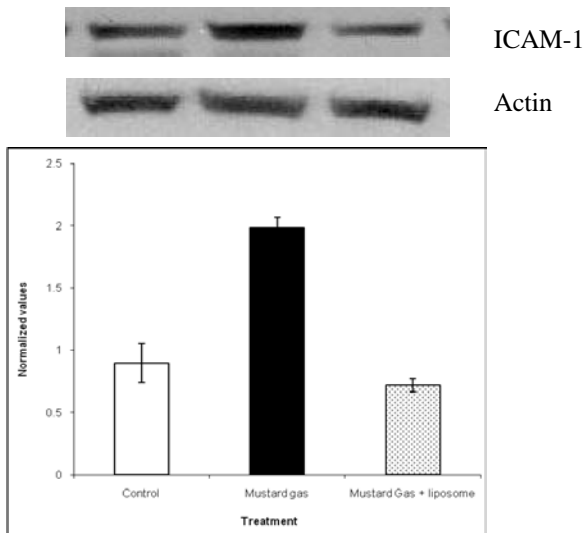


Figure 3: Western blot analysis of ICAM-1. The graph represents normalized value of ICAM-1 against actin.

12. Induction of lung injury by intratracheal exposure of lethal toxin to guinea pigs and protection by antioxidant liposome

In this project period, we studied the effects of intratracheal injection of lethal toxin on lung injury in a guinea pig model and the protective role of antioxidant liposome against lethal toxin-induced lung damage. For this we used three doses of lethal toxin as follows: Low dose: protective antigen (PA) – 50 µg + lethal factor (LF) – 25 µg; Mid dose: PA – 100 µg + LF – 50 µg; High dose: PA – 150 µg + LF – 75 µg. The antioxidant liposome contained NAC (75mM), α -tocopherol (11 mM), δ -tocopherol (5 mM) and γ -tocopherol (11 mM), as described by us earlier [9]. Lung injury was monitored by measuring the leakage of radiolabeled BSA into lung after one hour exposure of the toxin as described earlier [4]. Furthermore, we monitored lung damage by histological studies.

Data indicate that low, mid and high dose of lethal toxin caused 1.36-, 6.9-, and 10.4-fold, respectively increase in lung injury. Furthermore, antioxidant liposome treatment to the animals receiving high dose of the toxin caused 74% decrease in lung injury.

Lethal toxin exposure caused vascular hemorrhage and degeneration, pulmonary edema associated with deposition of alveolar fibrillar acidophilic material, and sloughing bronchiolar epithelium. The blood vessels were congested with loss of endothelial cells. The alveoli contained small collections of extravagated erythrocytes as well as copious amount of edema liquid. There was acute inflammation with infiltration of neutrophils, RBC and eosinophils in alveoli. The lumen of the small bronchus contained bluish firm looking exudates in which there were many leukocytes and macrophages and several apoptotic nuclei. In the wall of the bronchus, there was also a much thicker band of hypertrophic eosinophilic smooth muscle cells and moderate infiltration of leukocytes, PMNs and eosinophil on each side of the smooth muscle. The adjacent alveoli appeared collapsed. Alveoli number was significantly decreased in some area of the lethal toxin exposed lung. These morphological changes seen in lungs of lethal toxin treatment were protected by antioxidant liposome treatment.

Key Research Accomplishments

1. Demonstration of CEES-induced activation of angiogenic cytokines in lung.
2. Demonstration of CEES-induced activation of matrix metalloproteinases and tissue inhibitors of metalloproteinases [TIMPs] in lung.
3. Demonstration of CEES-induced up-regulation of superoxide dismutase gene in lung
4. Development of guinea pig lung fibrosis model by CEES exposure
5. Development of antioxidant liposome as antidote against CEES-induced lung injury
6. Demonstration of the Activation of MAPK/AP-1 signaling pathway in lung injury induced by CEES exposure and protection by antioxidant liposome
7. Demonstration of the desensitization of β -adrenergic receptors in lung injury induced by CEES exposure
8. Demonstration of the activation of SAF-1/MAZ and C/EBP transcription factors in lung by CEES exposure and protection by antioxidant liposomes.
9. Development of guinea pig model of lung injury by intratracheal infusion of CEES and protection by antioxidant liposomes.

Reportable Outcomes

Abstracts

- 1 Das, S.K., Stone, W.L., Smith, M.G. and Mukherjee, S. Protection of Mustard Gas-Induced Lung Injury by Antioxidant Liposomes. 5th International Symposium on Protection Against Toxic Substances, Nov 27-Dec 1, 2006, Singapore.
- 2 Mukherjee S, Stone WL, Yang H, Smith M, and Das SK. Attenuation of Half Sulfur Mustard Gas-Induced Acute Lung Injury in Guinea Pigs by Antioxidant Liposomes., FASEB Meeting, April 28 – May 2, 2007, Washington, DC (FASEB J. 21: A261, 2007)
- 3 Das, S. K. Advanced Medical Countermeasures Consortium Meeting, June 28, 2007, Crystal City, VA: Protection of Mustard Gas-Induced Lung Injury by Antioxidant Liposomes.

- 4 Das SK, Activation of AP-1 Transcription Factors in mustard Gas-Induced Lung Injury. Annual Conference of Association of Clinical Biochemists of India, Dec 18-20, 2007, New Delhi, India, Indian J. Clin. Biochem. Vol 22 (Suppl) 19S6.4, 2007
- 5 Gadsden JL, Mukhopadhyay S, Schaeffer MW, Sinha Roy S, Mukherjee S and Das SK. Effects of 2-Chloroethyl Ethyl Sulfide (CEES), a Mustard Gas Analog, on Serotonin/Dopamine Signaling in Guinea Pig Brain, FASEB Meeting, April 4-9, 2008, San Diego, CA.
- 6 Sinha Roy S, Schaeffer MW, Mukherjee S and Das SK. Mustard Gas-Induced Alteration of Retinoid Metabolism/Signaling in Guinea Pig Lung, FASEB Meeting, April 4-9, 2008, San Diego, CA.
- 7 Mukhopadhyay S, Mukherjee S, Smith M.G. and Das S.K. Activation of MAPK/AP-1 Signaling and Associated Metalloproteinases and Cell Cycle Protein in Guinea Pig Lung by 2-Chloroethyl Ethyl Sulfide (CEES), a Mustard Gas Analog. 2008 Bioscience Review, page 151, Hunt Valley, MD, June 1-6, 2008
- 8 Mukhopadhyay S., Mukherjee S., Smith M., Das S.K. Role of MAPK/AP-1 Signaling in the Protection of 2-Chloroethyl Ethyl Sulfide (CEES)-Induced Lung Injury by Antioxidant Liposomes, ASBMB Meeting, New Orleans, LA, April 18-22, 2009.
- 9 Mukhopadhyay S, Mukherjee S., Das S. K. Protection by Antioxidant Liposomes Against the Mustard Gas-Induced Activation of SAF-1/MAZ Transcription Factor in Guinea Pig Lung, 6th SISPAT Meeting, Singapore, December 8 – 11, 2009.
- 10 Gadsden-Gray J., Mukherjee S., Ogunkua O., Das S.K. Effects of 2-Chloroethyl Ethyl Sulfide (CEES) on Guinea Pig Brain Morphology, Experimental Biology Meeting, Anaheim, CA, April 24 – 28, 2010.

Manuscripts

1. Das SK, Stone WL, Smith M and Mukherjee S. Protection of Mustard Gas-Induced Lung Injury by Antioxidant Liposomes. Proc 5th International SISPAT Symposium on Toxic Substances, Singapore, Nov 27-Dec 2, p 10-15, 2006.
2. Smith M.G., Stone W., Ren-Feng G., Ward, P. A., Suntress Z., Mukherjee, S. and Das, S. K. Vesicants and Oxidative Stress, In: "Chemical Warfare Agents: Chemistry Pharmacology Toxicology, and Therapeutics, eds: J.A. Romano, B. J. Lukey and H. Salem, Taylor & Francis Publisher, pp 247-292, 2008. (Book Chapter)
3. Mukhopadhyay S., Mukherjee S., Smith M.G. and **Das S.K.** Activation of MAPK/AP-1 Signaling Pathway in Lung Injury Induced by 2-Chloroethyl Ethyl Sulfide, a Mustard Gas Analog, Toxicology Letters 181: 112-117, 2008, Epub 2008 Jul 15, PMID 18675330.
4. Kabir S.M., Mukherjee S., Rajaratnam V., Smith M.G. and **Das S.K.** Desensitization in β -Adrenergic Receptors in Lung Injury Induced by 2-Chloroethyl Ethyl Sulfide (CEES), a Mustard Analog. J. Biochem. Mol. Toxicol. 23: 59-70, 2009, Published online in Wiley Interscience (www.interscience.wiley.com). DOI 10:1002/jbt.20265, NIHMSID # 190717, PMCID-PMC2863039, PMID 19202564
5. Mukherjee S., Stone W.L, Yang H., Smith M.G. and **Das S.K.** Protection of Half Sulfur Mustard Gas-Induced Lung Injury in Guinea Pigs by Antioxidant Liposomes. J. Biochem. Mol. Toxicol. 23:143-153, 2009, Published online in Wiley Interscience www.interscience.wiley.com). DOI 10:1002/jbt.20279
6. Mukhopadhyay S., Mukherjee S., Stone W. L., Smith M., and **Das S.K.** Role of MAPK/AP-1 Signaling Pathway in the Protection of CEES-Induced Lung Injury by Antioxidant Liposomes, Toxicology 261: 143-151, 2009, Epub 2009 May 21, PMID 19464336
7. Mukhopadhyay S., Mukherjee S. Ray B.K., Ray A., Stone W. L. and **Das S. K.** Antioxidant Liposomes Protect Against CEES-Induced Lung Injury by Decreasing SAF-1/MAZ- Mediated Inflammation in the Guinea Pig Lung., J. Biochem. Mol. Toxicol., Vol 24, Issue 3, pp 187-194, 2010. DOI 10:1002/jbt.20329, PMID: 20583300
8. Schaeffer M.W., Sinha Roy, S., Mukherjee, S., Ong D., **Das, S.K.** Uptake of all-trans retinoic acid-containing aerosol by inhalation to lungs in a guinea pig model system – a pilot study, In Press, Expt. Lung Res. (Vol 36, Issue9)
9. Schaeffer MW, Sinha Roy S, Mukherjee S, Nohr D, Wolter M, Biesalski HK, Ong DE, **Das SK** . Qualitative and quantitative analysis of retinol, retinyl esters, tocopherols and selected carotenoids out of various internal organs from different species by HPLC. Anal. Methods, DOI: 10.1039/c0ay00288g, 2010

Personnel Funded During the Reporting Period

Salil K. Das
Shyamali Mukherjee
Michael Schaeffer
Somdutta Sinha Roy
Sutapa Mukhopadhyay

Conclusions

CEES exposure causes activation of AP-1/MAPK signaling pathway as well as several other transcription factors, such as SAF-1/MAZ and C/EBP. Furthermore, antioxidant liposome treatment had a protective effect against CEES-induced activation of these transcription factors and lung injury. In addition we developed a lung injury model in guinea pig by intratracheal infusion of lethal toxin and established the prophylactic action of antioxidant liposome against lethal toxin-induced lung injury

References

1. Sinha Roy, S; Mukherjee, S; Kabir, M; Rajaratnam, V; Smith, M and Das, S.K. Inhibition of Cholinephosphotransferase Activity in Lung Injury Induced by 2-Chloroethyl Ethyl Sulfide, a Mustard Analog. *J. Biochem. Molecular Toxicol.* 19: 289-297, 2005.
2. Chatterjee, D; Mukherjee, S; Smith M, and Das, S.K. Signal Transduction Events in Lung Injury Induced by 2-Chloroethyl Ethyl Sulfide, a Mustard Analog. *J. Biochem. Molecular Toxicol.* 17: 114-121, 2003.
3. Rajaratnam VS and Das SK. Array of Cytokine Induction in Early Lung Injury Response to 2-Chloroethyl Ethyl Sulfide, A Mustard Gas Analog. *FASEB J.*, Vol. 19, A852, 2005, FASEB Meeting, April 2-6, 2005, San Diego, CA.
4. Das, S. K., Mukherjee, S., Smith, M and Chatterjee, D. Prophylactic Protection by N-Acetylcysteine Against the Pulmonary Injury Induced by 2-Chloroethyl Ethyl Sulfide, A Mustard Analogue, *J. Biochem. Molecular Toxicol.* 17: 177-184, 2003
5. Mukherjee S and Das SK. Pulmonary Fibrosis in Guinea Pig Induced by 2-Chloroethyl Ethyl Sulfide. *FASEB J.*, Vol. 19, A280, 2005, FASEB Meeting, April 2-6, 2005, San Diego, CA.
6. McClintock, S.D., Hoesel L.M., Das, S. K., Till, G.O., Neff, T., Kunkel R.G., Smith M.G. and Ward, P.A. Attenuation of Half Sulfur Mustard Gas-Induced Acute Lung Injury in Rats. *J. Applied Toxicology.* 26: Issue 2, 126-131, 2006.
7. Das SK, Stone WL, Smith M and Mukherjee S. Protection of Mustard Gas-Induced Lung Injury by Antioxidant Liposomes. *Proc 5th International SISPAT Symposium on Toxic Substances, Singapore, Nov 27-Dec 2, p 10-15, 2006.*
8. Mukhopadhyay S, Rajaratnam V., Mukherjee S., Smith M and Das, S.K. Modulation of the Expression of Superoxide Dismutase Gene in Lung Injury by 2-Chloroethyl Ethyl Sulfide, a Mustard Analog. *J. Biochem Mol. Toxicol.* 20: 142-149, 2006.
9. Mukherjee, S., Stone W.L., Yang H., Smith M.G., Das S.K. Protection of half sulfur mustard gas-induced lung injury by antioxidant liposomes. *J. Biochem. Mol. Toxicol.* 23: 143-153, 2009.
10. Mukhopadhyay S., Mukherjee S., Smith M.G. and **Das S.K.** Activation of MAPK/AP-1 Signaling Pathway in Lung Injury Induced by 2-Chloroethyl Ethyl Sulfide, a Mustard Gas Analog, *Toxicology Letters* 181: 112-117, 2008, Epub 2008 Jul 15, PMID 18675330.
11. Mukhopadhyay S., Mukherjee S., Stone W. L., Smith M., and **Das S.K.** Role of MAPK/AP-1 Signaling Pathway in the Protection of CEES-Induced Lung Injury by Antioxidant Liposomes, *Toxicology* 261: 143-151, 2009, Epub 2009 May 21, PMID 19464336
12. Kabir S.M., Mukherjee S., Rajaratnam V., Smith M.G. and **Das S.K.** Desensitization in β -Adrenergic Receptors in Lung Injury Induced by 2-Chloroethyl Ethyl Sulfide (CEES), a Mustard Analog. *J. Biochem. Mol. Toxicol.* 23: 59-70, 2009, Published online in Wiley Interscience (www.interscience.wiley.com). DOI 10:1002/jbt.20265, NIHMSID # 190717, PMCID-PMC2863039, PMID 19202564
13. Mukhopadhyay S., Mukherjee S. Ray B.K., Ray A., Stone W. L. and Das S. K. Antioxidant Liposomes Protect Against CEES-Induced Lung Injury by Decreasing SAF-1/MAZ- Mediated Inflammation in the Guinea Pig Lung., *J. Biochem. Mol. Toxicol.*, Vol 24, Issue 3, pp 187-194, 2010. DOI 10:1002/jbt.20329, PMID: 20583300

14. Krunkowski T.M., Martin L.D., Fischer B.M., Voynow J.A., Adler K.B. Effects of TNF-alpha on expression of ICAM-1 in human airway epithelial cells in vitro: oxidant-mediated pathways and transcription factors. *Free Radic Biol Med* 35: 1158-1167, 2003
15. Ramji D.P. and Foka P. CCAAT/enhancer-binding proteins: Structure, function and regulation. *Biochem J.* 385: 561-575, 2002.

Appendices (reprints in pdf format) (Aug 21, 06 – Sept 24, 10).

Mukhopadhyay S., Mukherjee S., Smith M.G. and **Das S.K.** Activation of MAPK/AP-1 Signaling Pathway in Lung Injury Induced by 2-Chloroethyl Ethyl Sulfide, a Mustard Gas Analog, *Toxicology Letters* 181: 112-117, 2008, Epub 2008 Jul 15, PMID 18675330.

Kabir S.M., Mukherjee S., Rajaratnam V., Smith M.G. and **Das S.K.** Desensitization in β -Adrenergic Receptors in Lung Injury Induced by 2-Chloroethyl Ethyl Sulfide (CEES), a Mustard Analog. *J. Biochem. Mol. Toxicol.* 23: 59-70, 2009, Published online in Wiley Interscience (www.interscience.wiley.com). DOI 10:1002/jbt.20265, NIHMSID # 190717, PMCID-PMC2863039, PMID 19202564

Mukherjee S., Stone W.L, Yang H., Smith M.G. and **Das S.K.** Protection of Half Sulfur Mustard Gas-Induced Lung Injury in Guinea Pigs by Antioxidant Liposomes. *J. Biochem. Mol. Toxicol.* 23:143-153, 2009, Published online in Wiley Interscience www.interscience.wiley.com). DOI 10:1002/jbt.20279

Mukhopadhyay S., Mukherjee S., Stone W. L., Smith M., and **Das S.K.** Role of MAPK/AP-1 Signaling Pathway in the Protection of CEES-Induced Lung Injury by Antioxidant Liposomes, *Toxicology* 261: 143-151, 2009, Epub 2009 May 21, PMID 19464336

Mukhopadhyay S., Mukherjee S. Ray B.K., Ray A., Stone W. L. and **Das S. K.** Antioxidant Liposomes Protect Against CEES-Induced Lung Injury by Decreasing SAF-1/MAZ- Mediated Inflammation in the Guinea Pig Lung., *J. Biochem. Mol. Toxicol.*, Vol 24, Issue 3, pp 187-194, 2010. DOI 10:1002/jbt.20329, PMID: 20583300

12 Vesicants and Oxidative Stress

*Milton G. Smith, William Stone, Ren-Feng Guo,
Peter A. Ward, Zacharias Suntres, Shyamali Mukherjee,
and Salil K. Das*

CONTENTS

I.	Background	248
II.	Introduction	249
III.	Mustard.....	249
	A. Poly ADP-Ribose Polymerase	250
	B. Metabolites of Sulfur Mustard	251
	C. Signaling	251
	D. Tumor Necrosis Factor-Alpha Increases with CEES Exposure	252
	E. Activation of Sphingomyelinase Activities after CEES Exposure	253
	F. Accumulation of Ceramide in Lungs after CEES Exposure	253
	G. Activation of Nuclear Factor Kappa in Lungs after CEES Exposure	254
	H. Activation of Caspases after CEES Exposure	254
	I. Effects of Ceramide Treatment on Lung Microsomal CPT Activity	258
	J. CEES Induces Oxidative Stress	260
IV.	Chlorine	261
V.	Phosgene.....	261
VI.	Lewisite	262
VII.	Antidotes or Ameliorative Agents.....	262
	A. Lewisite	262
	B. Mustard.....	263
	1. Effect of NAC on Signal Transduction	265
	C. Antioxidant Liposomes	267
	D. Chlorine	269
	E. Phosgene	269
VIII.	Oxidative Stress in Different Organ Systems	271
	A. Lung	271
	1. Monitoring Oxidative Stress in Live Cells	273
	2. Hydrogen Peroxide and Superoxide Radical Generation in Bronchoalveolar Fluids.....	273
	3. Antioxidant Status in Lung	273
	4. Hydroxydeoxyguanosine, an Indicator of DNA Damage	273
	5. Direct Measurements of Oxygen Free Radicals	273
	6. Exhaled Breath Condensate	274
	7. Analysis of Expired Air for Oxidation Products	274

B.	Skin	274
1.	Role of Skin Mast Cells in Vesicant Toxicity.....	274
C.	Eyes	275
1.	Vesicant-Induced Ocular Injury and Oxidative Stress	276
2.	Redox Proteomics	277
IX.	Oxidative Stress: the Concept and the Effect on Gene Expression	277
A.	Definition of Oxidative Stress	277
B.	Molecules that Influence the Redox Potential	278
1.	Nicotinamide Adenosine Dinucleotide Phosphate	278
2.	Thioredoxin.....	279
C.	Apoptosis.....	279
D.	Gene Expression Controlled by Redox-State Transcription Factors.....	279
1.	NF- κ B	280
2.	Ref-1	280
3.	Activator Protein-1.....	280
4.	Heat Shock Transcription Factor	280
X.	Summary	280
A.	Antidotes	281
	References	281

I. BACKGROUND

The primary treatment of vesicant exposure is decontamination and supportive therapies; there is only one vesicant that has an antidote. The paucity of the treatment options continues to confer their tactical advantage. The development of an ameliorative or antidote would accomplish, at a minimum, two goals: (1) effective treatment, if needed, and (2) decreased tactical advantage.

Vesicants are considered to be of low technology and are relatively simple to manufacture. Barrier protection gear, otherwise known as Mission Oriented Protective Posture (MOPP), provides significant protection if donned before exposure. During battlefield conditions, errors would be expected in the use of the MOPP gear because of stressful situations, tears in the suit, false positive or negative alarms, etc.

Vesicants share some common properties that are noteworthy in attempts to achieve a better understanding of their pathogenesis. One characteristic is that they all induce an acute inflammatory reaction (Sidell et al., 1997; Sciuto, 1998; Ricketts et al., 2000; Naghii, 2002; Segal and Lang, 2005), of which a subcomponent is oxidative stress (OS) (Bartsch and Nair, 2006). A consequence of OS is the oxidation of thiol groups, which is seen in all of the vesicant exposures (Vissers and Winterbourn, 1995; Pant et al., 2000; Carr et al., 2001).

The oxidation of thiol groups disrupts redox balance (defined later in this chapter), which can set into motion a cascade of events, such as apoptosis, oxidant production, and increased activity of redox-regulated transcription factors (e.g., nuclear factor kappa beta [NF- κ B]). The occurrence of OS is not isolated to the vesicant class of weapons of mass destruction (WMD). Radiation (Kang et al., 2006), bacterial infections (e.g., anthrax) (Hanna et al., 1994; Kuhn et al., 2006), viral infections (e.g., influenza) (Ghezzi and Ungheri, 2004), and ricin (Kumar et al., 2003; Suntres et al., 2005) exposures also induce OS as part of the host pathogen response, which is acute inflammation.

Sublethal OS induces varying degrees of damage in cellular organelles. Lethal OS occurs when antioxidant defenses completely fail, resulting in necrosis (Virag, 2005) or apoptosis (Haddad, 2004). In this chapter, OS will be discussed as a concept, along with its occurrence in the organ systems that are most notably affected by the vesicants. Antioxidant defenses that are critical to the maintenance of redox balance are also discussed.

Achieving a deeper understanding of OS is important for the elucidation of all acute inflammatory disorders. The OS component of vesicant exposure has not been a focal point of research, by

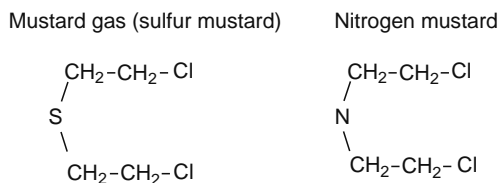


FIGURE 12.1 Chemical structure of sulfur and nitrogen mustards.

and large for vesicants or other WMD. It is hoped that this chapter will help to spur future research in the area.

II. INTRODUCTION

There are four primary vesicating agents—mustard, phosgene, chlorine, and Lewisite. Strategically, they are poor weapons because they are subject to being redirected by the wind. Sulfur mustards (SM) are considered to be one of the vesicants that cause the most concern. There are two types of mustards, sulfur- and nitrogen-based compounds (see Figure 12.1). The nitrogen mustards have been found to be unsuitable for warfare; therefore, there will be no further mention of them. Any further references to mustards will be to SM. Strategically, Lewisite is the least important since there is a proven antidote. British anti-Lewisite, the antidote for Lewisite, has been known for decades (Goldman and Dacre, 1989).

A significant component of acute inflammation is OS (Nonas et al., 2006). One aspect of OS is the production of oxidants and proinflammatory cytokines. It is defined as an imbalance of antioxidant/oxidant ratio, which has a consequent effect on gene expression. The maintenance of the antioxidant/oxidant ratio in the nonstressed cell would be termed redox homeostasis. Thiol groups that are part of intracellular proteins and glutathione (GSH) are critical for the maintenance of redox homeostasis. The vesicants as a class are either oxidants themselves, or they indirectly produce oxidants. Oxidants can be water soluble and fat soluble; therefore, they can arise in any compartment of the cell. They are able to attack any cellular structure, rendering them partially or completely dysfunctional.

The chemical WMD classified as vesicants cause blistering of the skin, which is why they are referred to as blistering agents. They incapacitate more so than kill the exposed person because burns occur on any tissue that it contacts. They all have prolonged systemic effects. The reader is referred to the individual sections of this book and other excellent reviews on the agents for a more detailed classic description of their effects, usage, and history (Goldman and Dacre, 1989; Naghii, 2002; Sciuto and Hurt, 2004; Segal and Lang, 2005). The agents themselves will be reviewed with the features of OS highlighted where information was available.

III. MUSTARD

Vesicants were first deployed against troops during World War I (WWI). They were used as recently as 1988 by Saddam Hussein against the Kurds in Halabja. SM (2-bis-chloroethyl ethyl chloride) is a straw-colored liquid that disseminates with a garlic-like odor on evaporation (Duke-Elder and MacFaul, 1972; Dahl et al., 1985). SM is composed of small, oily droplets with volatility significantly higher in warmer climates (e.g., the Middle East). At a temperature of 38°C, it can be present in the environment for 7 h, whereas at 10°C, it persists for 100 h. The density of mustards is 5.4-fold greater than air and tends to be found 6–12 inches above the ground. This ground-hugging characteristic causes it to sink into trenches and gullies. In WWI, soldiers frequently removed their masks in the morning, assuming that the mustard threat had subsided, and were unaware that the

mustard persisted in the environment. As the ambient temperature increased at sunrise, there was an increase in evaporation of the mustard at the ground-level atmosphere, and the soldiers would unknowingly inhale the newly evaporated gas. Mustard has a high freezing temperature (57°F). This freezing temperature can be reduced by mixing it with other agents, such as chlorobenzene or carbon tetrachloride (Borak and Sidell, 1992; Sidell et al., 1997). Similar reductions in freezing point can be accomplished by mixing it with Lewisite.

SM is commonly referred to as an alkylating agent, but recent evidence has shown it to be a potent inducer of oxidants (Levitt et al., 2003; McClintock et al., 2006). Mustard gas has a strong, irritating effect on living tissue and induces long-lasting, toxic effects (Safarinejad et al., 2001). Additionally, its destructive effects are not localized to the site of application; remote cells and tissues are also affected. SM damages DNA mainly by alkylating and cross-linking the purine bases (Fox and Scott, 1980). Cysteine groups in proteins make them sensitive to SM, resulting in covalently cross-linked dimers on exposure (Byrne et al., 1996). This cross-linking causes conformational change or dysfunction of enzymes. The potent alkylating activity of SM is due to the formation of highly electrophilic ethylene episulphonium derivative (Lundlum et al., 1984; Papirmeister et al., 1991). A portion of the inhalation pathogenesis of SM is due its cholinergic properties (mediating the action of acetylcholine) that stimulates both muscarinic and nicotinic receptors (Anslow, 1946).

On contact with human skin, 80% of the liquid evaporates and 20% penetrates (half remains on the skin and the other half is absorbed systemically). Systemic absorption results in partitioning to organs, such as the spleen, liver, and bone marrow (Langenberg et al., 1998). It is mutagenic and carcinogenic (Papirmeister et al., 1985; Somani and Babu, 1989; Wormser, 1991; Langenberg et al., 1998). The lethal dose for humans is 200 mg if ingested and 3 g with cutaneous exposure (Javadi et al., 2005). A property that has received little attention, but should be kept in mind, is that SM is also a radiomimetic, a property that is shared with other radiation-emitting agents. Additional properties that both radiation and mustards share are the inducement of apoptosis, burns, and OS.

A. POLY ADP-RIBOSE POLYMERASE

Alkylation of DNA by SM leads to the activation of poly ADP-ribose polymerase (PARP), which reduces the availability of oxidized nicotinamide adenine dinucleotide (NAD⁺) and ATP in the cell (Fox and Scott, 1980). The consequent change in cellular bioenergetics leads to the inhibition of glycolysis, activation of hexosemonophosphate shunt, induction of plasminogen activator, and ultimately, production of skin lesions (Mol et al., 1989). Other alterations in cellular metabolism due to the loss of NAD⁺ are microfilament architecture and function in keratinocytes (Papirmeister et al., 1985). PARP uses NAD⁺ for a two-electron donor in an oxidation step to catalyze the polymerization of ADP-ribose units on target proteins to attach PARP. PARP has a multiplicity of functions, such as DNA damage sensor and repair chromatin modification, transcription, cell death pathways, insulator function, and mitotic apparatus function. These processes are important to several physiological and pathophysiological processes that involve genome maintenance, carcinogenesis, aging, inflammation, and neuronal function. Poly ADP-ribose polymerase-1 (PARP-1) is the most abundantly expressed member of the family of PARP proteins; it binds to DNA structures that have single and double strand breaks, crossovers, cruciforms, and supercoils (Kim et al., 2005). During normal cellular metabolism, the level of PARP-1 is very low. The enzymatic activity is greatly increased, as much as 500-fold, with allosteric activators, such as damaged and undamaged DNA occurrence (D'Amours et al., 1998, 1999; Kun and Bauer, 2001; Oei and Shi, 2001).

The attachment of PARP or PARylation, in response to oxidation, alkylation, or ionizing radiation, is dramatic and immediate. At minimal levels of DNA damage, PARP-1 acts as a survival factor involved in DNA damage detections and repair. At high levels of DNA damage, PARP-1 promotes cell death (Burkle, 2001). Elevated levels of PARP in response to DNA damage can promote necrosis secondary to exhaustion of cellular NAD⁺ and ATP (cellular energy failure) (Decker and Muller, 2002; Bouchard et al., 2003). PARP-1 even facilitates apoptosis by a caspase-independent

apoptotic cell death via apoptosis inducing factor (AIF). AIF, a potent trigger of apoptosis, is a flavoprotein, which resides in the mitochondrial intermembrane (similar to cytochrome *c*). However, it is unclear what the exact trigger of AIF release is, but it could be the result of the depletion of NAD⁺ due to excessive PARP synthesis and activity. PARP preferentially depletes cytosolic NAD⁺ (Zong et al., 2004), which would be expected to affect the overall cellular bioenergetics.

B. METABOLITES OF SULFUR MUSTARD

The metabolites of SM are noteworthy because of their utilization of thiol compounds. These metabolites, in addition to OS, diminish the thiol cellular pool. Some metabolites occur by direct hydrolysis, but the majority are conjugates of GSH (Black et al., 1992; Black and Read, 1995); other metabolites are *N*-acetyl-L-cysteine (NAC) conjugates or methylthio/methylsulfanyl derivatives. Enzymatic conjugation of alkylating agents utilizing GSH can occur through glutathione-S-transferase (GST); but alkylating agents can also combine directly with thiols (Moore and Ray 1983; Colvin et al., 1993). Spontaneous or enzymatic conjugation of alkylating agents occurs through an aziridium intermediate (Colvin et al., 1993).

C. SIGNALING

There are a multitude of activators of NF- κ B, such as viral infections, bacterial infections, radiation, interleukin (IL)-1, and tumor necrosis factor (TNF). Most of the activators of NF- κ B can be blocked with the use of antioxidants (Schulze et al., 1997). Other transcription factors, such as AP-1 (Xanthoudakis et al., 1994), MAF, and NRL (Kerppola and Curran, 1994), and NF-IL6 (Hsu et al., 1994) are regulated by oxygen-dependent mechanisms that cause redox cycling of cysteinyl residues.

NF- κ B regulates many genes involved in inflammation, such as inducible nitric oxide synthase (iNOS), proinflammatory cytokines, IL-1, tumor necrosis factor- α (TNF- α), IL-6, chemokine, IL-8, E-selectin, vascular cell adhesion molecule 1 (ICAM-1), and granulocyte-macrophage colony stimulating factor (GM-CSF) (Brennan et al., 1995; Akira and Kishimoto, 1997; Barnes and Adcock, 1998; Rahman and MacNee, 1998; McClintock et al., 2002). Arroyo et al. (2000) found a dose-dependent increase in TNF- α , IL-6, and interleukin-1-beta (IL-1-beta) in SM-treated human keratinocyte cells.

Although inflammatory cytokine profiles differ depending on the skin models used (Ricketts et al., 2000; Sabourin et al., 2002), they were shown to be elevated in response to SM. In contrast, in guinea pig lungs exposed to 2-chloroethyl ethyl sulfide (CEES) (a mustards analog), the inflammatory cytokine TNF- α was found to be markedly elevated (Das et al., 2003). The inflammatory cytokines exacerbate the effects of CEES (Stone et al., 2003), which would imply that there is an amplification of the initial injury by the mustards. Lipopolysaccharide (LPS), a ubiquitous entity in our environment, also upwardly modulates the damage that CEES inherently causes to cells (Stone et al., 2003).

SM activates phospholipase A2 and liberates arachidonic acid by acting on linolenic acid found in cellular membranes. Activated neutrophils show an amplification of their respiratory burst in the presence of arachidonic acid (Bostan et al., 2003). Metabolites of arachidonic acid produce oxidants, which would be additional contributors to OS. Arachidonic acid itself and several of its metabolites, such as 12 HETE and 15 HETE, induce FOS and JUN expression (Haliday et al., 1991; Sellmayer et al., 1991; Rao et al., 1996).

One class of signaling pathways that has received considerable attention involves the action of cytokine-stimulated sphingomyelinase (SHM-ase) (Hannun and Obeid, 1997). Ceramide generated from SHM-ase activation plays a critical role in cytokine-mediated apoptosis, cellular differentiation, and senescence, each of which may be important in the inflammatory response.

Ceramide can be generated through several different pathways, such as synthesis within the cell, hydrolysis of SHM by SHM-ase, and breakdown of glycosphingolipids. The degradation of ceramide by acid ceramidase liberates sphingosine, a free fatty acid in the lysosomal compartment

(Alphonse et al., 2002). Ceramide can also be increased by the inhibition of ceramide breakdown by ceramidase and the inhibition of sphingomyelin synthase.

SHM-ase has been proposed as a key enzyme involved in stress-induced ceramide formation (Hannun and Obeid, 1997). Multiple pathways may be regulated, which in turn ultimately determine the levels of ceramide.

D. TUMOR NECROSIS FACTOR-ALPHA INCREASES WITH CEES EXPOSURE

A single, intratracheal injection (0.5 mg/kg body weight) of CEES in guinea pigs was done at different time points. The guinea pigs were dissected and the lung was removed after perfusion. The lung was lavaged and TNF- α concentrations were measured in lung lavage fluid, lung lavage macrophages, and in lung tissue. The level of TNF- α in lavage fluid was very low, whereas high levels accumulated in lung as well as in lung macrophages within 1 h of CEES exposure. The level of TNF- α decreased rapidly after 1 h and returned to normal levels within 24 h of CEES exposure (Figure 12.2a). Further studies revealed that the induction of TNF- α by CEES is dose dependent, and optimal TNF- α accumulation was observed at 2 mg/kg dose of CEES exposure (Figure 12.2b).

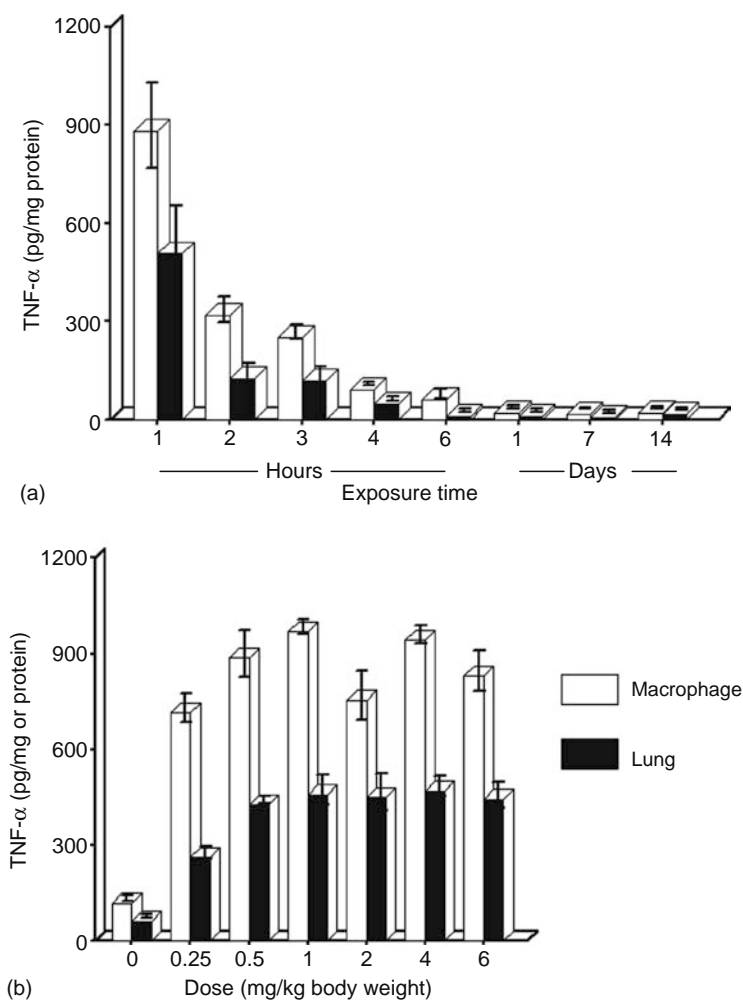


FIGURE 12.2 Accumulation of TNF- α in guinea pig lung and macrophages after exposure to CEES. (a) Time-dependent induction of TNF- α after intratracheal injection of CEES (0.5 mg/kg body weight). (b) Accumulation of TNF- α 1 h after exposure to CEES at different doses (ranging from 0.5 to 6.0 mg/kg body weight).

E. ACTIVATION OF SPHINGOMYELINASE ACTIVITIES AFTER CEES EXPOSURE

Both the neutral and acid SHM-ase activities showed fourfold to fivefold increases after CEES treatment. The basal level of acidic SHM-ase activity (Figure 12.3b and d) was much higher than the basal level of neutral SHM-ase (Figure 12.3a and c).

Both neutral and acid SHM-ase activities started to increase, along with the increase of TNF- α ; these activities reached a maximum peak between 4 and 6 h in the lung and between 3 and 4 h in macrophages. It is not known at this time whether this difference between lung and macrophages is functionally significant or not. The SHM-ase activities (both neutral and acidic) were found to be higher in lavage macrophages than those in the lung tissue. It is possible that macrophages are more sensitive to CEES than other cell types in the lung. The level of SHM-ase decreased rapidly and returned to near normal level within 24 h. It was also found that a 2 mg/kg dose of CEES is sufficient to reach the maximum level of both neutral and acid SHM-ase activity (Figure 12.3c and d).

F. ACCUMULATION OF CERAMIDE IN LUNGS AFTER CEES EXPOSURE

The ceramide accumulation after CEES exposure demonstrated a biphasic pattern. Within 1 h of CEES exposure, ceramide levels became very high and reached a peak accumulation within 2 h (Figure 12.4a). After 2 h, there was some decrease in the ceramide level, but then the level increased very high and remained almost to a steady state, even up to 14 days later (Figure 12.4a). CEES-induced ceramide accumulation was found to be saturated at 4 mg/kg dose of CEES. At 2 mg/kg dose of CEES, about 90% induction of ceramide was achieved (Figure 12.4b).

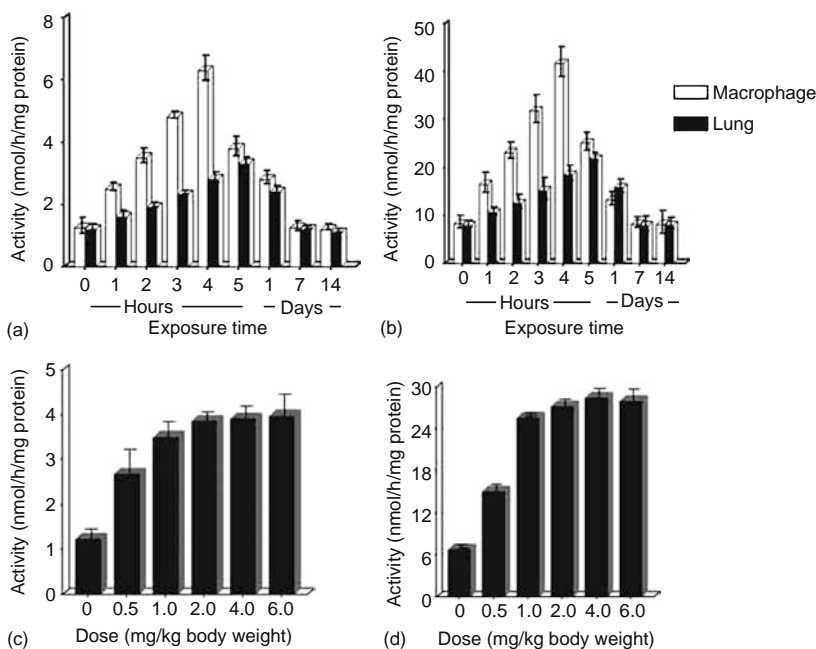


FIGURE 12.3 Activation of acid and neutral sphingomyelinase in guinea pig lung and macrophages following CEES exposure. Time course of induction of neutral (a) and acid (b) sphingomyelinase after intratracheal injection of CEES (0.5 mg/kg body weight). Accumulation of neutral (c) and acid (d) sphingomyelinase at 4 h after exposure to CEES at different doses (ranging from 0.5 to 6.0 mg/kg body weight).

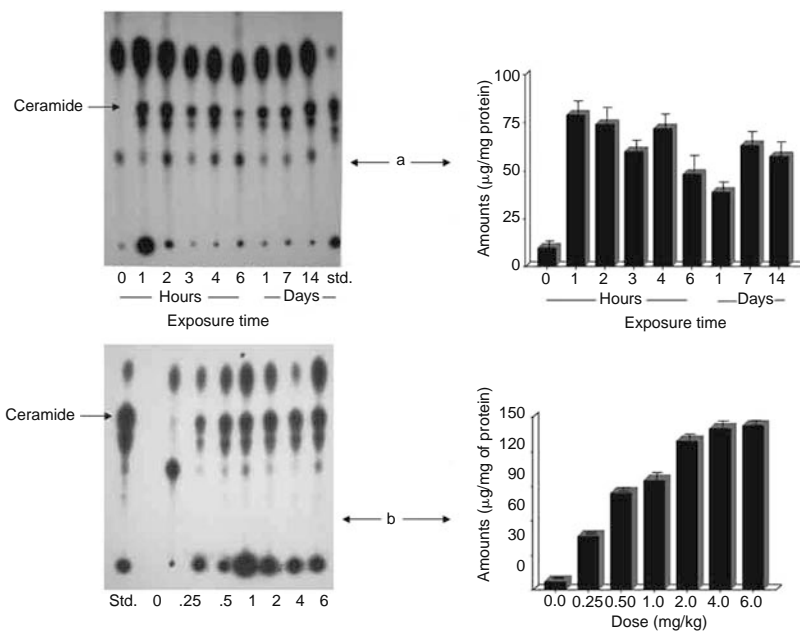


FIGURE 12.4 Accumulation of ceramide in guinea pig lung after CEES exposure. (a) Time course of induction of ceramide after intratracheal injection of CEES (0.5 mg/kg body weight). (b) Accumulation of ceramide at 1 h after exposure to CEES at different doses (ranging from 0.5 to 6.0 mg/kg body weight). In both cases (a and b), the left panel is the autoradiograph showing the accumulated ceramides, and the right panel represents the quantitative analysis of accumulated ceramide as determined by ^{32}P incorporation.

G. ACTIVATION OF NUCLEAR FACTOR KAPPA IN LUNGS AFTER CEES EXPOSURE

The activation of NF- κB was measured in the nuclear extracts of lungs after exposure to CEES. NF- κB , which is well known to inhibit TNF- α -mediated apoptosis, showed activation only up to 1–2 h after CEES exposure (Figure 12.5a). This may explain the biphasic effect of CEES on the lung.

After initial lung damage by TNF- α , within 2 h there was some recovery due to activation of NF- κB . After 2 h, the NF- κB level went down, ceramide level increased, and secondary lung damages were observed. Dose-dependent studies revealed that 4 mg/kg CEES was needed for the optimum activation of NF- κB (Figure 12.5b). Super shift assay using specific antibodies to p50 and p65 revealed that both the p50 and p65 subunits were activated in lung because of CEES exposure (Figure 12.5c).

H. ACTIVATION OF CASPASES AFTER CEES EXPOSURE

Activation of different caspases in guinea pig lung after the CEES exposure is shown in Figure 12.6. Within 1 h of exposure, some activation was observed for all four caspases, but the activity came back to the basal level within 2 h of exposure. The activity of caspase 2, caspase 3, caspase 8, as well as caspase 9 increased significantly between 4 and 6 h of exposure and then declined again. No activity for any of the caspases was observed at 24 h and thereafter. Here also, the activation of caspases was found to be optimum at 2 mg/kg body weight of CEES.

Our study clearly demonstrated the involvement of an SHM-ase/ceramide signal transduction pathway in the mustard gas-mediated lung injury. After intratracheal injection of CEES to guinea pigs, the TNF- α level increased sharply within 1 h of exposure. The TNF- α level started, declined after 1 h, and returned to basal level within 24 h.

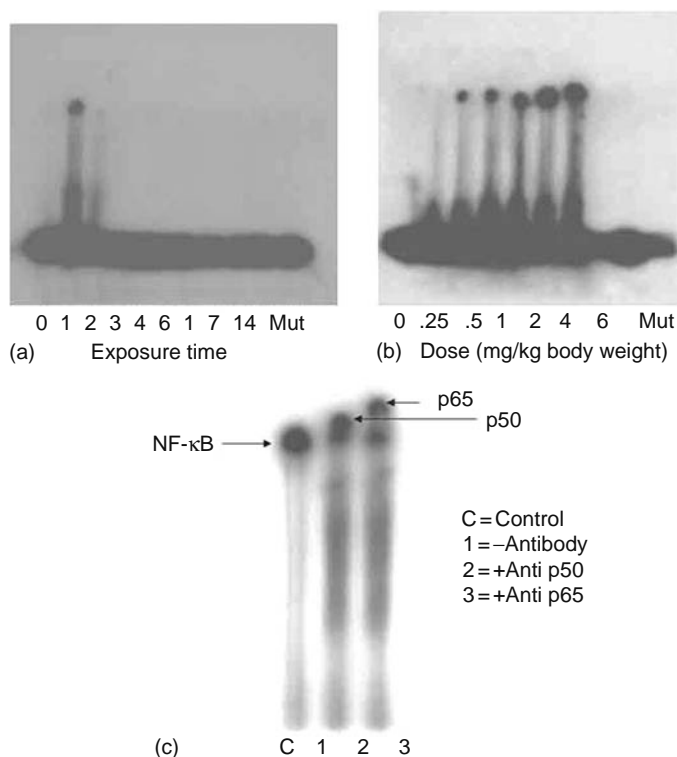


FIGURE 12.5 Activation of NF- κ B in guinea pig lung following CEES exposure. (a) Time-dependent activation of NF- κ B after intratracheal injection of CEES (0.5 mg/kg body weight), as observed by mobility shift assay. (b) Mobility shift assay showing the accumulation of NF- κ B after 1 h of CEES exposure at different doses (ranging from 0.5 to 6.0 mg/kg body weight). (c) Supershift assay, using subunit specific antibodies, to identify the subunits (p50 and p65) of NF- κ B activated due to CEES exposure in guinea pig lung.

Followed by the accumulation of TNF- α , both the acid and neutral SHM-ase activities were stimulated, peaking within 4–6 h after CEES exposure. Though both the acid and neutral SHM-ase activities were stimulated, the level of acid SHM-ase was found to be much higher after CEES exposure.

The higher levels of TNF- α , as well as both the acid and neutral SHM-ase activities in lung macrophages compared with those in lung tissue were expected because lung tissue consists of several types of cells, all of which were not responsive to CEES. We observed a biphasic effect of CEES on lung. After initial damage by TNF- α , there was some recovery due to activation of NF- κ B within 2 h. This biphasic pattern was also observed in caspases activation.

Significant but small activation of caspase 2, caspase 3, caspase 8, and caspase 9 was observed within 1 h of CEES exposure. This activation of caspases declined thereafter and reappeared within 4–6 h, initiating the cell apoptosis in lung as observed by light as well as electron microscopy (unpublished observation). One explanation for this biphasic action of mustard gas is that NF- κ B is activated by TNF- α through a phosphatidylcholine-specific phospholipase C/diacylglycerol (DAG)/protein kinase C (PKC) or phosphatidylcholine-specific phospholipase C/DAG/acid SHM-ase/ceramide model (Chatterjee et al., 2004).

These studies indicate that CEES exposure causes accumulation of TNF- α -activated SHM-ases, resulting in the production of ceramides and simultaneous activation of caspases and finally apoptosis. Ceramides are known to cause apoptosis via the activation of caspases (Alphonse et al., 2002; Hearps et al., 2002; Hetz et al., 2002).

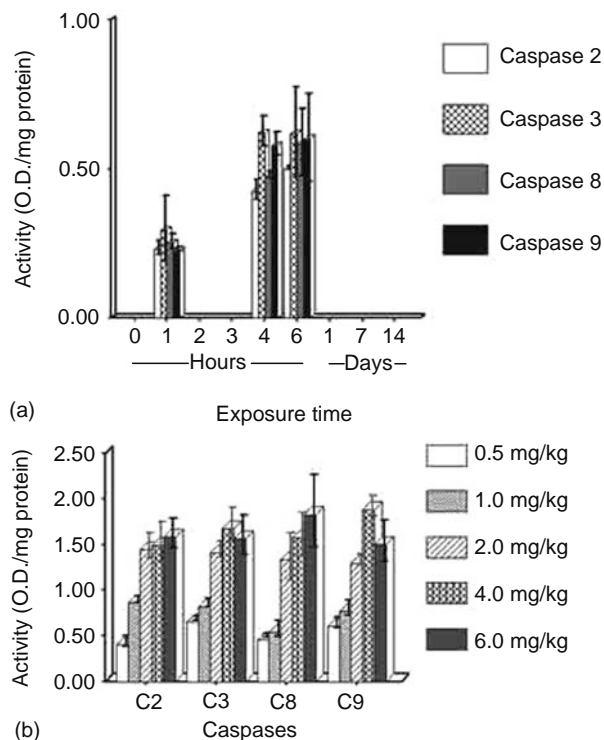


FIGURE 12.6 Activation of different caspases in guinea pig lung after CEES exposure. (a) Time course of activation of different caspases after intratracheal injection of CEES (0.5 mg/kg body weight). (b) Accumulation of different caspases at 4 h after exposure to CEES at different doses (ranging from 0.5 to 6.0 mg/kg body weight).

Our study also revealed that there was some initial damage of the lung tissue when exposed to CEES, but self-defense mechanisms of the lung played a significant role in the recovery from the damage and the prevention of any further damage. Furthermore, the present investigation enhances our understanding of mustard gas-mediated proapoptotic signaling pathways and characterizes the events of mustard gas-induced lung dysfunction.

Mustard gas exposure also causes inflammatory lung diseases, including acute respiratory distress syndrome (ARDS) (Calvet et al., 1994; Sohrabpour, 1984). A defective secretion of surfactant by alveolar type II cells has been implicated as one of the causative factors for the development of ARDS (Ansceschi, 1989). A major component of lung surfactant is DPPC (Stith and Das, 1982). The precursor of DPPC is normally 1-palmitoyl-2-oleoyl PC. DPPC is produced by deacylation and subsequent reacylation with palmitic acid at 2-position of glycerol moiety of the unsaturated phospholipid.

The CDP-choline pathway is the major pathway for the synthesis of PC in the lung, and cholinephosphotransferase (CPT) is a terminal enzyme in this pathway. Regulation of PC metabolism is one of the vital aspects of the cell cycle with implications in the control of cell proliferation as well as in apoptosis (Cui et al., 1996; Baburina and Jackowski, 1998).

PC is the most abundant phospholipid in mammalian cells, and it is synthesized via the CDP-choline pathway (Kent, 1995). CPT is the terminal enzyme of this pathway and plays a direct role in the final production of PC in the lung. This pathway is important for both cell proliferation and cell death (Ghosh et al., 2002; Ryan et al., 2003), and selective inhibition of this pathway has been shown to induce cellular apoptosis (Miquel et al., 1998). Any modulation in the expression and activity of this enzyme is expected to result in abnormal functioning of the cells.

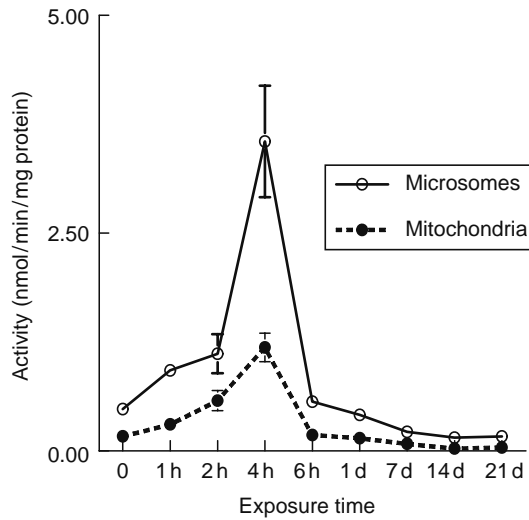


FIGURE 12.7 Time-dependent effects of 0.5 mg/kg body weight CEES treatment on the mitochondrial and microsomal CPT activity. $N = 3$.

The time-dependent effects of CEES treatment showed a biphasic effect on CPT activity in both mitochondria and microsomes. The time-dependent studies indicated that a single infusion of CEES (0.5 mg/kg body weight) caused an increase in the activity for a short time after CEES exposure (up to 4 h), followed by a decrease (6 h onward) (Figure 12.7). The dose-dependent studies indicated that CEES treatment caused an initial increase in the CPT activity at low doses (0–2 mg/kg body weight), followed by a decrease at higher doses (4 and 6 mg/kg body weight) at incubation times of 1 and 4 h. This decrease was more acute in microsomes than in the mitochondria (Figure 12.8).

We have previously demonstrated that in addition to its predominant localization in the microsomes, CPT also exists in the mitochondria (Stith and Das, 1982; Sikpi and Das, 1987). Thus, it is possible that during the early stage of lung injury as observed in this study, cells try to repair the membrane damage by stimulating PC synthesis. Therefore, with increased CPT activity

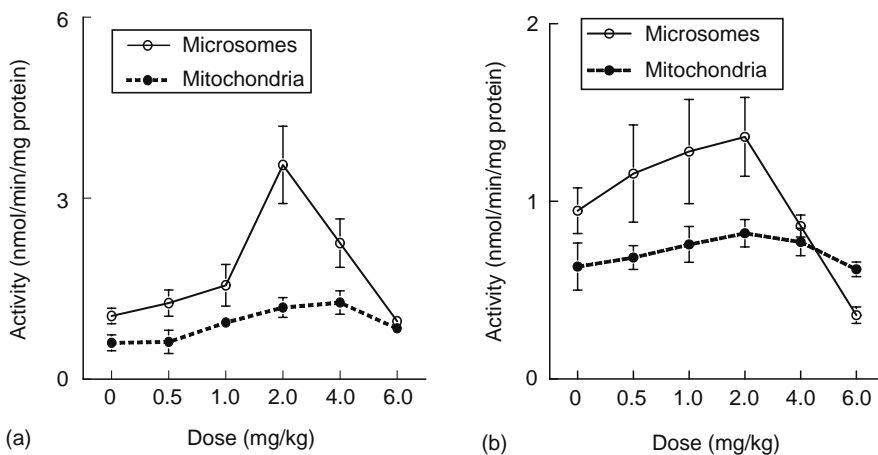


FIGURE 12.8 Dose-dependent effects of CEES on cholinephosphotransferase activity in mitochondria and microsomes. (a) After 1 h CEES treatment. (b) After 4 h CEES treatment. $N = 3$.

over time, lung cells lose their ability to repair membrane damage, as evident from decreased CPT activity in both mitochondria and microsomes isolated from lungs of CEES-treated animals (Figures 12.7 and 12.8). Hence, CEES has both short-term (stimulation) and long-term (inhibition) effects on lung CPT activity. Since CPT activity is crucial to the synthesis of surfactant, these effects may cause ARDS with long-term CEES exposure because of lack of surfactant synthesis.

I. EFFECTS OF CERAMIDE TREATMENT ON LUNG MICROSOMAL CPT ACTIVITY

Ceramides are intracellular signaling molecules implicated in the induction of cellular apoptosis (Kolesnick and Krönke, 1998; Hannun and Luberto, 2000), and are known to induce several protein kinases and phosphatases (Mathias et al., 1991; Dobrowsky et al., 1993; Vietor et al., 1993). Ceramide analogs have been shown to inhibit PC synthesis (Bladergroen et al., 1999; Allan, 2000; Ramos et al., 2000; Vivekananda et al., 2001). Ceramides may directly affect the biosynthesis of PC and phosphatidylethanolamine (PE) by inhibiting the enzymes of the CDP-choline and CDP-ethanolamine pathways (Bladergroen et al., 1999; Awasthi et al., 2001; Ramos et al., 2002).

It has been reported that cells treated with ceramides may undergo programmed cell death, become growth arrested, or in rare cases, become stimulated to proliferate. The diversity of biological responses of cells to ceramides reflects the complexity of the role of these sphingolipids as second signal molecules (van Blitterswijk et al., 2003). Furthermore, ceramide treatment of lung cancer-derived A-549 cells promotes apoptosis in a caspase-dependent process (Kurinna et al., 2004).

Other laboratories have also shown that enzymes of the CDP-choline pathway for the production of PC in the cells, including CPT, show reduced activity when cells are incubated with cell-permeable C₂/C₆ ceramides (Bladergroen et al., 1999; Ramos et al., 2002), and it has been predicted that this inhibition may be due to the competitive inhibition by ceramides owing to the similarity in the structure to one of the substrates for CPT, DAG.

The downstream signal transduction events in lung following CEES exposure involve the induction of TNF- α , which in turn activates both acid and neutral SHM-ases, resulting in the subsequent accumulation of ceramides in the lung (Chatterjee et al., 2003, 2004). The level of ceramide was found to be ~60 μ g/mg protein after 7 days (with 0.5 mg/kg body weight of CEES) and ~130 μ g/mg protein for 2 mg/kg body weight of CEES (after 1 h; Figure 12.4).

When the lung microsomal fraction from control animals was incubated with C₂ ceramide at different concentrations (50, 100, and 200 μ M) and time periods (0, 0.5, 1, and 6 h) before the assay for CPT activity, CPT activity decreased significantly in a time- and dose-dependent manner (Figure 12.9).

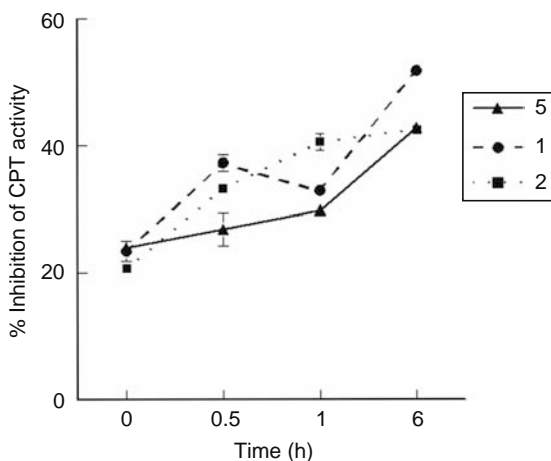


FIGURE 12.9 Effect of C₂ ceramide treatment on lung microsomal CPT activity. $N = 3$.

However, the effect was more pronounced when the microsomal fraction was preincubated with the ceramide before assay of the CPT activity. The degree of inhibition was increased with the increase in incubation time (0.5, 1, and 6 h). The highest inhibition (50%) was achieved after 6 h of incubation. However, only 20% inhibition was observed when ceramide was directly added into the assay mixture.

It has been shown that a 30% inhibition could be obtained in CPT activity when ceramides were directly added to the assay mixture at 50 μ M concentrations (Bladergroen et al., 1999). Since this inhibition of 30% was less than the 64% obtained when cells were incubated directly, it would indicate competitive inhibition was not the only mechanism. In the present work, we found similar results with lung microsomal fraction, that is, with an increase in the incubation time with ceramides, the inhibition of the enzyme activity increases. Therefore, we support the observations by Bladergroen et al. (1999) that ceramide inhibition of CPT activity may be only partially through direct competitive inhibition with DAG; ceramide may act through interaction with other CPT enzyme inhibitors present in the microsomal fraction.

It is known that the short-chain ceramides often do not mimic the endogenous long-chain ceramides produced as a result of SHM-ase activity. However, the lipophilic nature of the both short- and long-chained ceramides makes these molecules likely candidates for altering biological processes as components of the lipid bilayer (Gidwani et al., 2003). We can therefore predict that ceramides accumulated in the lung because of exposure of CEES can alter the activity of the membrane-bound enzymes like CPT and can also act as a membrane perturbant.

This ceramide-induced membrane perturbation can result in mitochondrial release of cytochrome *c* and subsequent release of different caspases (Figure 12.6) (Gidwani et al., 2003; Chatterjee et al., 2004) as a part of the apoptotic pathway. Furthermore, CEES exposure (2.0 mg/kg body weight for 7 days) caused a significant decrease of both CPT activity (\sim 1.5-fold; Figure 12.10) and gene expression (\sim 1.7-fold; Figure 12.11) in the lung (Gidwani et al., 2003; Sinha Roy et al., 2005). This decrease in CPT activity was not associated with any mutation of the CPT gene. Thus, the inhibition of CPT activity as a chronic effect of CEES exposure may be directly responsible for the

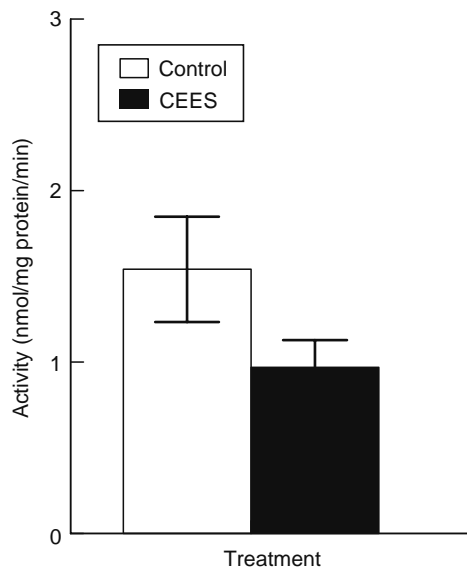


FIGURE 12.10 CPT enzyme activity in the lung microsomal fraction of 2 mg/kg body weight CEES (for 7 days) treated lung as compared with the control (only vehicle) showing significant decrease in activity. $p \leq 0.05$, $N = 3$.

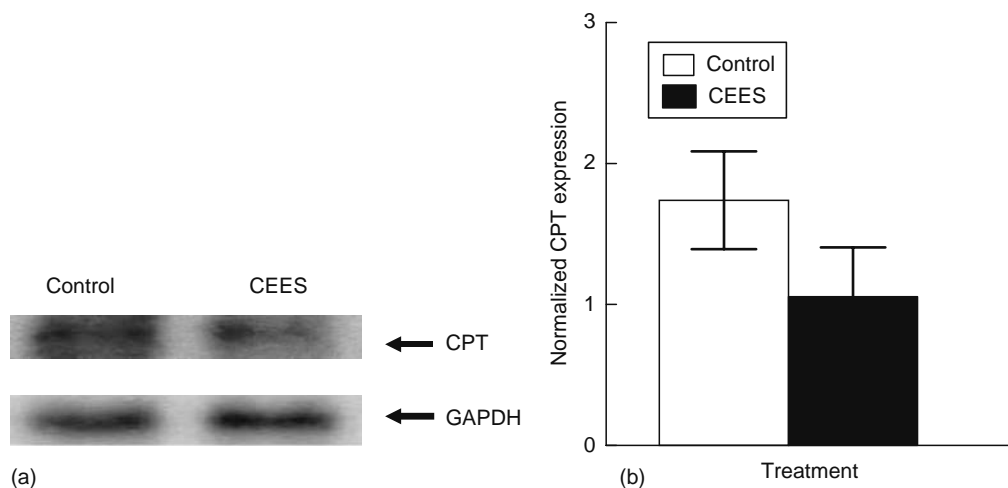


FIGURE 12.11 Northern blot analysis for the expression of the CPT gene. (a) One representative blot for CPT mRNA from control and CEES-treated guinea pig lung and same blot reprobbed for GAPDH expression. (b) Graph showing downregulation of CPT expression as the result of mustards gas treatment normalized with GAPDH. $N=3$.

reduction in the lung surfactant production, resulting in subsequent development of ARDS and pulmonary fibrosis, and is probably mediated by accumulation of ceramides.

J. CEES INDUCES OXIDATIVE STRESS

Stone et al. (2003) have found that OS and inflammatory agents play a key role in the toxicity of CEES. Both HD and CEES are known to provoke acute inflammatory responses in the skin (Blahe et al., 2000a, 2000b; Sabourin et al., 2002). It is interesting that RAW 264.7 macrophages stimulated with LPS or inflammatory cytokines are more susceptible to the cytotoxic effect of CEES than unstimulated macrophages. LPS (bacterial endotoxin) is a well-characterized inflammatory factor found in the cell wall of Gram-negative bacteria and is a ubiquitous natural agent found in the environment. LPS is present in serum, tap water, and dust. Military and civilian personnel would always have some degree of exposure to environmental LPS. Very low levels of LPS (20 ng/mL) were found to dramatically enhance the toxicity of CEES at concentrations greater than 400 μM (Stone et al., 2003). CEES alone is not toxic to RAW 264.7 macrophages at levels lower than about 500 μM (Stone et al., 2003).

LPS is known to trigger a variety of inflammatory reactions in macrophages and other cells having CD14 receptors (Wright et al., 1990; Downey and Han, 1998). In particular, LPS is known to stimulate the macrophage secretion of inflammatory cytokines such as TNF- α and IL-1-beta (Shapira et al., 1994). It is interesting, therefore, that both TNF- α and IL-1-beta were also found to enhance the cytotoxic effects of CEES but to a lesser extent than LPS (Stone et al., 2003). LPS stimulation of macrophages is known to involve the activation of protein phosphorylation by kinases as well as the activation of nuclear transcription factors such as NF- κB (Fujihara et al., 1994; Shapira et al., 1994, 1997; Chen et al., 1998). The activation of PKC by DAG is also a key event in LPS macrophage activation (Downey and Han, 1998). In vitro experiments have shown that the secretion of TNF- α and IL-1-beta by LPS-stimulated monocytes is dependent on PKC activation (Shapira et al., 1997; Coffey et al., 2000). Stone et al. (2003) also determined that phorbol myristate acetate (PMA) activation of PKC also enhanced CEES toxicity. These data suggest that the activation of PKC may play a key role in the molecular mechanism whereby LPS and inflammatory cytokines enhance the cytotoxicity of CEES (and potentially other vesicant weapons

as well). Evidence suggests that LPS (deRojas et al., 1995; Fu et al., 2001) as well as TNF- α (Ye et al., 1999) also stimulate the production of free radicals by macrophages. Collectively, this information supports the view that inflammatory factors and OS are key factors in understanding vesicant toxicity, and are important factors in designing effective countermeasures (Veness-Meehan et al., 1991; Yourick et al., 1991; Elsayed et al., 1992; Pant et al., 2000; Schlager and Hart, 2000; Kadar et al., 2001; Naghii, 2002; Levitt et al., 2003).

IV. CHLORINE

Chlorine is a pulmonary irritant that affects both the upper and the lower respiratory tracts. It is similar to SM in that its density is greater than that of air. Therefore, it characteristically hugs the ground, as does SM when deployed. It is only slightly water soluble; on contact with water or moisture, it forms hypochlorous acid (HClO) and hydrochloric acid (HCl). HClO is unstable and readily decomposes to oxygen-centered radicals. In animal models, 2000 ppm exposure will induce respiratory arrest. Subacute exposures of 9 ppm and acute exposures of 50 ppm can cause chemical pneumonitis (an inflammatory process) and bronchiolitis obliterans (Segal and Lang, 2005).

The LD₅₀ is in the range of 800–1000 ppm. HOCl, whether exogenously obtained from Cl₂ gas, or from an oxidative burst from neutrophils, the product reacts with a number of functional thiol groups present in enzymes (Winterbourn, 1985; Pullar et al., 2002). HOCl reactivity with thiol groups could inactivate such enzymes as GSH peroxidase and catalase (Aruoma and Halliwell, 1987). Inactivation of enzymes involved in antioxidant defense system renders the cell vulnerable to OS (a disruption of redox homeostasis).

Glutamylcysteine synthetase, cysteine, or methionine was 100 times more reactive to hypochlorous acid in comparison with amino acids that did not contain thiol groups (Folkes et al., 1995). Sublethal exposures to HOCl decreased GSH levels in several cell types (Vissers and Winterbourn, 1995; Pullar et al., 1999). In a study by Pullar et al. (1999) using human umbilical vein endothelial cells, doses of 25 nmol of HOCl and less were sublethal; when the exposure was done over 10 min, there was a concentration-dependent loss of intracellular GSH. Tissue exposure to HOCl resulted in a reduction of GSH. The metabolite of the HOCl interaction with GSH was an unexpected cyclic sulfonamide that was exported from the cell. The expected metabolites of glutathione disulfide (GSSH) and GSH sulfonic acid were actually minimal (Pullar et al., 2001). Inactivation of acetylcholinesterase by HOCl could be a contributory cause of airway hyperreactivity (den Hartog et al., 2002).

V. PHOSGENE

Phosgene (COCl₂), also referred to as carbonic dichloride, is extensively used as an industrial chemical. The gas dissolves slowly in water and is hydrolyzed to CO₂ and HCl. It produces little damage to the upper airway, although the lower airways sustain the bulk of the necrosis and inflammation. There is typically a delayed onset of symptoms in the pulmonary system occurring 1–24 h after the initial exposure. The respiratory symptoms of hypoxia (shortness of breath), and in extreme cases, respiratory arrest (discontinuation of spontaneous breathing), are apparently due to leaky alveolar capillaries and the resulting pulmonary edema (Noltkamper and Burgher, 2004); also contributory to the clinical symptoms are arachidonic acid mediators and lipid peroxides (Sciuto and Hurt, 2004).

In rodent models, phosgene elicits decreases in total GSH in lung tissue 48% within 45–60 min after exposure (Sciuto, 1998). Jaskot et al. (1991) confirmed similar results 2 years after the Sciuto publication. The concentration of phosgene exposure inversely affected the GSH levels (Jaskot et al., 1991). In gene expression studies in the inhalation mouse model, GSH regulation and redox regulation, in particular, were affected (Sciuto et al., 2005). A gene expression response can be seen as early as 30 min, wherein glutamate cysteine ligase increases and continues to increase at 8 h. Glutamate cysteine ligase continued to be elevated, approaching control levels in the 24–72 h time period. There was an upregulation of GST α -2, GSH peroxidase-2, glutamate, and γ -glutamyl

cysteine synthetase. At 4–12 h, GSH peroxidase-2, GSH reductase was elevated. GSH synthetase increased in the 4–24 h time frame. Further evidence of the crippling of the antioxidant defense system was the decreased SOD3 gene expression and enzyme activity. Similar results were found in independent experiments by Qin et al. (2004), as were reported by Sciuto in his examination of the antioxidant enzyme defense system. In the exposed rats, the antioxidant defense enzymes GST, superoxide dismutase (SOD), catalase, GSH peroxidase, and nitric oxide synthase in serum, blood, or liver were all increased. In contrast, the nitric oxide content was decreased. Similar changes in enzymes were also noted for other gaseous toxins, such as O₃ and NO₂ (Jaskot et al., 1991).

VI. LEWISITE

The Germans developed several arsenical-based warfare chemical agents circa 1917 (Goldman and Dacre, 1989). The allies, on the other hand, developed Lewisite (2-chlorovinylchloroarsine), adamsite (diphenylaminechloroarsine), methylchloroarsine, and arsine. Lewisite is soluble in organic solvents; it is readily absorbed by rubber, paint, varnish, and porous materials. There are labile chlorine atoms, trivalent arsenic, carbons, and multiple bonds that make it quite reactive. Some of its reactions are due to nucleophilic substitution by water, hydrogen sulfide, thiols, and acid salts.

The reactions with thiol groups (e.g., those that are found in proteins) form an alkylarsine sulfide. Mustard gas, at the same LC₅₀, induces vesication, whereas Lewisite does not. Apparently, Lewisite is more irritating initially to the pulmonary systems than mustard. The hydrolysis products are more persistent in soil in comparison with mustard. In ambient air, Lewisite is about 10 times more volatile than mustard.

The clinical sequelae after Lewisite absorption referred to as “Lewisite Shock” (L shock) are similar to that of severe burns. In dog models at high dosages, exposure resulted in retching, vomiting, extreme salivation, labored breathing, inflammation of the entire respiratory system, and pulmonary edema; respiratory distress was also common, and 80% died. Inhalation of 0.05 mg/L for 15 min results in intoxication and incapacitation for several weeks, whereas 0.5 mg/L for 5 min is lethal. The exact pathophysiology of the pulmonary symptoms seen is unknown, but is likely due to the dilatation of the capillaries. Apparently, the innate immune system is also compromised because of the occurrence of bronchopneumonia. In L shock, a hemolytic anemia can occur; however, it is unclear if this is due to an autoimmune reaction or OS (McMillan et al., 2004; Sato et al., 2006). Other complications of exposure are edema and bleeding that occur in the liver and kidneys (Wardell, 1941).

It is the arsenic in Lewisite that reacts with thiol groups to form alkylarsine sulfides, which is the basic reaction with thiol groups in tissues (Goldman and Dacre, 1989). The degree of enzyme dysfunction is dependent on the affinity of the enzyme to arsine. For example, it binds to the alpha and gamma thiol groups of lipoic acid, a component of pyruvate oxidase, which forms a stable six-membered ring (Stocken, 1949; Johnstone, 1963). Several other known enzymes are also inhibited—alcohol dehydrogenase, succinic oxidase, hexokinase, and succinate dehydrogenase (van Heyningen, 1941; Barron, 1947; Peters, 1946). Lewisite contact with skin results in the immediate elicitation of pain, in contrast to mustard, which would take 4–5 h (Wardell, 1941); it penetrates skin more rapidly than does mustard.

VII. ANTIDOTES OR AMELIORATIVE AGENTS

A. LEWISITE

Partial protection was afforded by monothiols, such as cysteine or GSH, when tested against pyruvate oxidase (Goldman and Dacre, 1989), which was thought to be one of the prime targets of Lewisite. British anti-lewisite or 2,3-dimercaptopropanol preferentially binds with arsenicals over the thiol rings in proteins to form a nontoxic five-membered stable ring, which reverses the lesion induced by

Lewisite. British anti-lewisite is also effective against other heavy metals, such as gold, excessive copper deposition seen in Wilson's disease (El-Youssef, 2003), and mercury (Goldman and Dacre, 1989). Newer analogs of BAL have been synthesized to improve efficacy, such as DMSA, 2,3-dimercapto-1-propane sulfonic acid, and *N*-(2,3 dimercaptopropyl-phthalamidic acid) (DMPA).

B. MUSTARD

Elsayed et al. (1992) performed subcutaneous injections of CEES that resulted in increased GST activity, increased lipid peroxides, and depleted, reduced GSH in lung tissue (Elsayed et al., 1992). Similar findings occurred in the *in vitro* mouse model, a neuroblastoma–rat glioma hybrid cell line, in that there was a reduction in GSH as a function of time after exposure (Moore and Ray, 1983). Within the last 5 years, there has been a greater emphasis on the inhalation effects of SM.

Peter Ward and his group developed a rat instillation CEES model (McClintock et al., 2002). Leakage of radiolabeled albumin ($[^{125}\text{I}]$ BSA) was used as a measure of lung damage, and the rats were sacrificed after 4 h after the installation of CEES into the rat lung with CEES. Neutrophil and complement depletion was found to significantly reduce the injury. Both enzymatic and nonenzymatic protocols were used to examine their ameliorative effect on the model. Dimethyl sulfoxide (DMSO) and dimethyl thiourea (DMTU) resulted in a 51% and 35% reduction in injury, respectively. The enzymatic antioxidants catalase and SOD exhibited 47% and 23% protection, respectively. In contrast, the antioxidant found in red wine, resveratrol (a phytoalexin), showed protection at 61%. Interestingly, the iron chelators 2,3-dihydroxybenzoic acid (DHBA) and deferoxamine mesylate (desferal) did not have any protective effect. NAC was administered 10 min before instillation of CEES. A dose–response curve was generated for 5, 10, 20, 30, and 40 mg/kg⁻¹ body weight. All of the dosages of NAC were found to be protective. The dosage of NAC at 20 mg/kg⁻¹ conferred the best protection out of all antioxidants at 70% protection. *In vitro*, the lethal effects of SM on L-cells were reduced by thiol reagents, namely, dithiothreitol and NAC (Walker, 1967; Walker and Smith, 1969). Several observations support the concept of a pathogenic role for toxic oxygen species in CEES-induced acute lung injury.

Other groups investigated the beneficial effects of agents that scavenge free radicals and other oxidant species (Wormser et al., 2000). They monitored the beneficial effects of those agents mainly by showing the recovery from damaged skin or by showing inhibition of the induction of proteolytic enzymes (Cowan et al., 1992; Cowan and Broomfield, 1993). Systemic and topical steroids administered revealed ameliorative properties in the rabbit SM skin model (Vogt et al., 1984).

The Das Group investigated the effects of orally administered antioxidants on signal transduction in the guinea pig model. A single dose of NAC could not block the CEES-induced lung injury at all. On the other hand, about 76% of lung injury could be blocked by long-term pretreatment (30 days) with NAC. No significant protection of lung injury was observed by pretreatment with either Ondrox (an over-the-counter antioxidant supplement as single-dose or 3 days pretreatment) or GSH (single; Table 12.1). Similarly, a single-dose treatment of NAC just before CEES exposure was found to be ineffective, whereas 76% of lung injury could be blocked by long-term pretreatment (30 days) with NAC. There was no significant protection of lung injury by pretreatment with either Ondrox (single-dose or 3 days pretreatment) or GSH (single dose).

A single-dose treatment of NAC just before CEES exposure was found to be ineffective, whereas 62% of TNF- α induction was inhibited by 3 days pretreatment with NAC. Long-term treatment with NAC gave more protection (inhibition of 73% of TNF- α induction). There was no protection for TNF- α accumulation by single dose of either Ondrox or GSH. Three days pretreatment with Ondrox and DMT could only block 13% and 8% of the TNF- α induction (Table 12.2). Additional support for an involvement of oxidants in the pathogenesis of CEES-induced acute lung injury was provided by the protective effects seen after treatment of CEES-exposed rat with NAC (McClintock et al., 2002). The protective effect of NAC was confirmed in the guinea pig lung model, as well as by others (Wormser et al., 1997).

TABLE 12.1
Effects of *N*-acetyl-L-Cysteine Pretreatment on CEES-Induced Lung Injury in Guinea Pigs

Treatment	Permeability Index
Control	0.20 ± 0.04
Control + NAC (3 days)	0.08 ± 0.01
CEES	2.01 ± 0.16
CEES + NAC (single dose)	2.07 ± 0.11
CEES + NAC (3 days)	0.62 ± 0.09 ^a
CEES + NAC (30 days)	0.48 ± 0.06 ^a
CEES + Ondrox (single dose)	2.04 ± 0.03
CEES + Ondrox (30 days)	2.00 ± 0.08
CEES + GSH (single dose)	1.98 ± 0.10

Note: CEES was infused (6 mg/kg body weight) intratracheally into guinea pigs with or without pretreatment with NAC. NAC was given either in single dose (5 mg) by gavage directly into stomach 10 min before infusion of CEES or with drinking water (0.5 g/day/animal, for either 3 days or 30 days before CEES infusion). Information on treatment with ondrex and GSH is given in text. The lung injury was measured after 1 h of CEES exposure and expressed by permeability index, which is a measure of ¹²⁵I-BSA leakage from damaged blood vessels into lung tissue. Each group had six animals. Values are mean ± SE (*n* = 6).

^a NAC supplementation in drinking water blocked the CEES-induced lung injury significantly (*p* < 0.05).

TABLE 12.2
Inhibition of CEES-Induced TNF- α Accumulation in Guinea Pig Lung by NAC Treatment

Treatment	Level of TNF- α (pg/mg Protein)
Control	20 ± 7
CEES	708 ± 38
CEES + NAC (single dose)	705 ± 24
CEES + NAC (3 days)	270 ± 40 ^a
CEES + NAC (30 days)	190 ± 64 ^a
CEES + Ondrox (single dose)	716 ± 22
CEES + Ondrox (3 days)	610 ± 54
CEES + DMT (3 days)	648 ± 62
CEES + GSH (single dose)	720 ± 41

Note: CEES was injected (4 mg/kg body weight) intratracheally into guinea pigs with or without pretreatment with NAC. NAC was given either in single dose (5 mg) by gavage directly into stomach 10 min before injection of CEES or with drinking water (0.5 g/day/animal, for either 3 days or 30 days before CEES injection). Information on treatment with ondrex, DMT and GSH is given in the text. TNF- α was measured after 1 h exposure of CEES. Values are mean TNF- α ± SE (*n* = 6).

^a NAC supplementation in drinking water blocked the CEES-induced accumulation significantly (*p* of TNF- α < 0.05).

1. Effect of NAC on Signal Transduction

Short-term (3 days) and long-term (30 days) pretreatment with NAC blocked significantly the activation of acid (4% and 49%, respectively, Figure 12.12) and neutral (46% and 61%, respectively, Figure 12.12) SHM-ases and decreased the levels of ceramide by 71% and 77% (Table 12.3). However, pretreatment with a single dose of NAC did not inhibit the activity of either neutral or acid SHM-ase and accumulation of ceramide.

Exposure to CEES significantly inhibited ($p < 0.05$) the activity of SOD (31%), GSH peroxidase (67%), and catalase (25%) (Figure 12.13). Pretreatment of guinea pigs for 3 days with NAC before CEES infusion significantly ($p < 0.05$) decreased CEES-induced inhibition of SOD (from

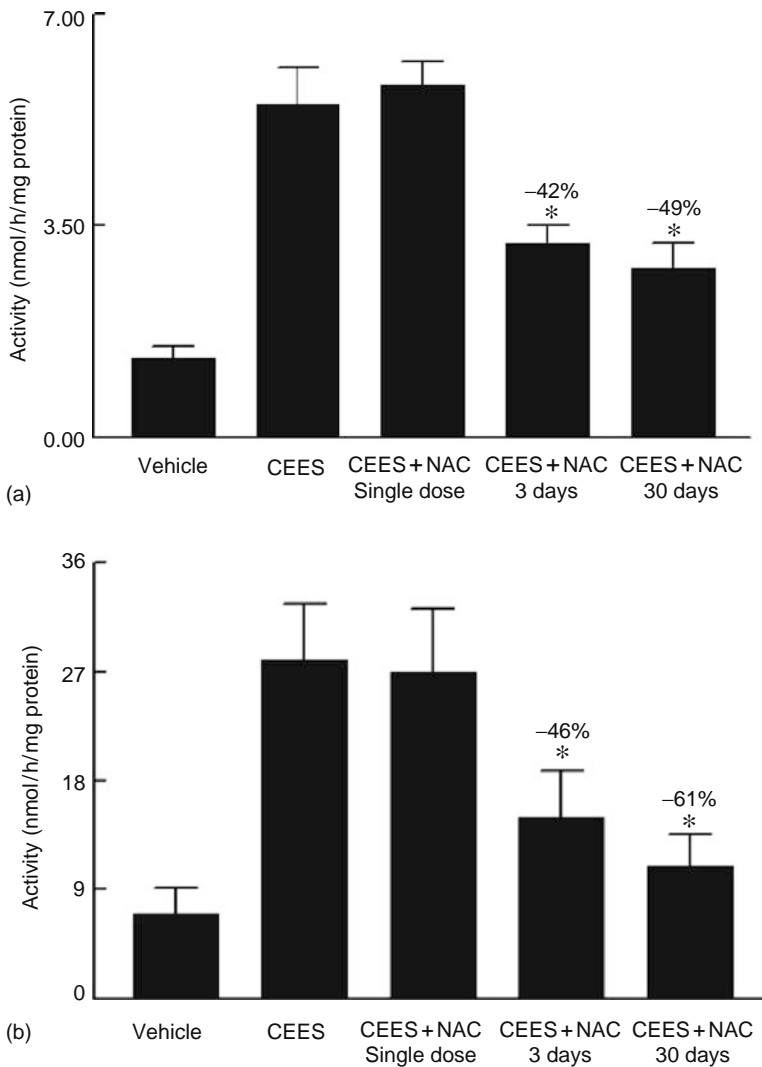


FIGURE 12.12 Inhibition of CEES-induced activation of neutral and acid sphingomyelinases in guinea pig lung by NAC treatment: Accumulation of neutral (a) and acid (b) sphingomyelinases at 4 h after exposure to CEES (4 mg/kg body weight) and their inhibition by 3 and 30 days pretreatment with NAC. Values are mean \pm SE ($n = 6$). Pretreatment with single dose of NAC did not inhibit the activity of either neutral or acid sphingomyelinase. *Pretreatment with NAC for 3 and 30 days before CEES exposure caused a significant inhibition of both neutral and acid sphingomyelinases ($p < 0.05\%$).

TABLE 12.3
Inhibition of CEES-Induced Ceramide Accumulation
in Guinea Pig Lung after NAC Treatment

Treatment	Levels of Ceramide ($\mu\text{g}/\text{mg}$ Protein)
Control	9 ± 2
CEES	148 ± 14
CEES + NAC (single dose)	146 ± 10
CEES + NAC (3 days)	39 ± 8^a
CEES + NAC (30 days)	28 ± 12^a

Note: CEES was infused (4 mg/kg body weight) intratracheally into guinea pigs with or without pretreatment with NAC. NAC was given either in single dose (5 mg) by gavage directly into stomach 10 min before infusion of CEES or with drinking water (0.5 g/day/animal, for either 3 days or 30 days before CEES infusion. Ceramide accumulations were assayed after 1 h of infusion of CEES. Values are mean \pm SE ($n = 6$).

^a NAC supplementation in drinking water blocked the CEES-induced accumulation of ceramide significantly ($p < 0.05$).

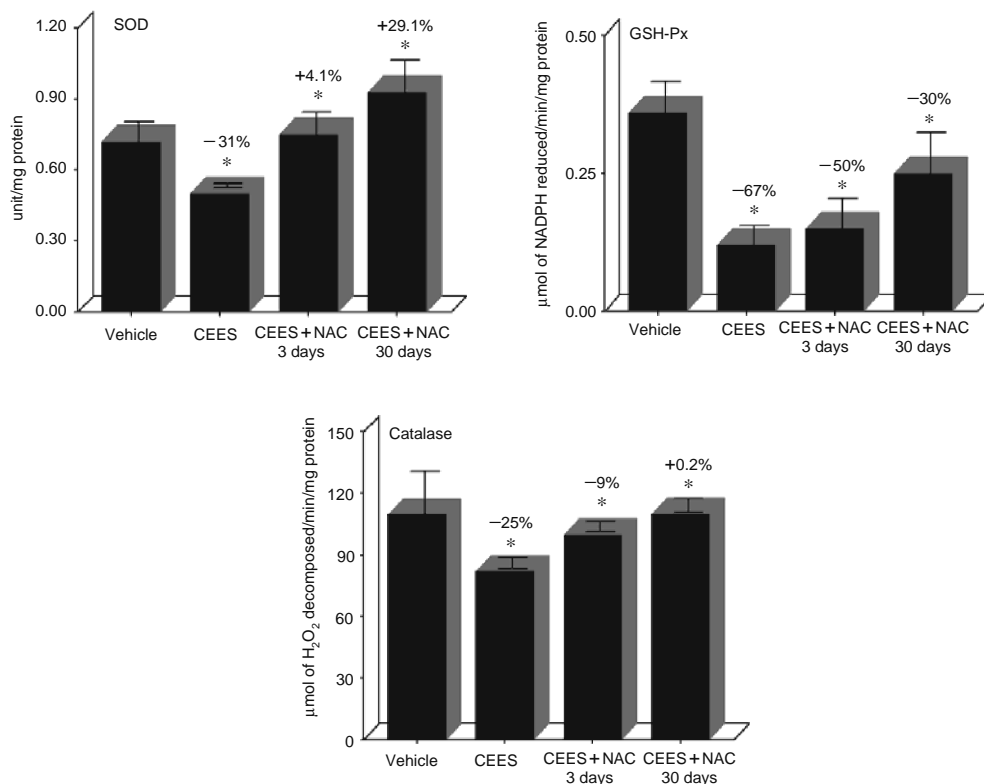


FIGURE 12.13 Effects of NAC pretreatment on the CEES-induced alterations in the free radical-metabolizing enzymes: Guinea pigs were infused with CEES (4 mg/kg body weight) intratracheally and the free radical-metabolizing enzymes (SOD, GSH pretreatment, catalase) were assayed in perfused lung after 4 h of CEES exposure. The samples were taken from guinea pigs with or without pretreatment with NAC for 3 days. *CEES exposure caused a significant decrease in the activity of SOD, GSH pretreatment, and catalase ($p < 0.05$). NAC treatment blocked the CEES-induced changes significantly ($p < 0.05$) for all enzymes.

31% decrease to 4.1% increase), GSH pretreatment (from 67% decrease to 50% decrease), and catalase (from 25% decrease to 9% decrease). Pretreatment of guinea pigs for 30 days with NAC provided additional resistance. For example, the activity of SOD was increased by 29% over the basal value, the activity of GSH pretreatment was decreased by only 30%, and the activity of catalase was brought back to the basal level.

Both short-term (3 days) and long-term (30 days) treatments significantly ($p < 0.05$) blocked the CEES-induced activation of NF- κ B that was observed 1 h after CEES infusion (Figure 12.14a). Furthermore, pretreatment with NAC for 3 days also blocked the activation of caspase 2, caspase 3, caspase 8, and caspase 9 by 41%, 44%, 55%, and 51% (Figure 12.14b).

Protection by NAC from half-mustard, gas-induced, acute lung injury has also been demonstrated recently in rats by McClintock et al. (2006). However, in these studies, NAC was administered by liposome encapsulation directly into the lung as a method of treatment for acute exposure to mustard gas. The co-instillation with CEES of liposomes containing the pegylated (PEG)-catalase, PEG-superoxide, NAC, GSH, resveratrol, or combination greatly attenuated development of rat lung injury (McClintock et al., 2006). Thus, we suggest the following model for the action of NAC on CEES-induced guinea pig lung injury (Figure 12.15).

Morphological analysis indicates that animals exposed to CEES showed symptoms of a chemical burn within 1 h; however, the severity of damage progressively increased with time. At 21 days postexposure, severe bronchial constriction with occasional apoptotic nucleus and accumulation of viscous secretion of mucins were observed in CEES-treated animals. Furthermore, both polymorphonucleus (PMNs) and eosinophilic leukocytes migration were observed in both alveoli and bronchi. However, pretreatment with NAC protected the lung from all these changes remarkably, except mucin secretion (Figure 12.16). How CEES functions as a powerful oxidant and what lung cells are targets of CEES is unclear.

C. ANTIOXIDANT LIPOSOMES

Another method of increasing antioxidant tissue levels is facilitated by using liposomes. Liposomal drug delivery is advantageous to using the oral route in that there is a multiplicity of possible administration routes. They can be used topically, orally (using the gastrointestinal tract), or delivered by aerosol to the lung.

Intact skin allows the passage of small lipophilic substances, but in most cases, efficiently retards the diffusion of water-soluble molecules. Lipid-insoluble drugs generally penetrate the skin slowly in comparison with their rates of absorption through other body membranes. Absorption of drugs through the skin may be enhanced by iontophoresis if the compound is ionized. Certain solvents (e.g., DMSO) may facilitate the penetration of drugs through the skin, but their use for therapeutic applications is controversial. In the formulation of topical dosage forms, attempts are being made to utilize drug carriers to ensure adequate localization or penetration of the drug within or through the skin in order to enhance the local and minimize the systemic effect. For dermatopharmacotherapy, there is a need for a drug delivery system that enhances the penetration of the active ingredient into the skin, localizes the drug at the site of action, and reduces percutaneous absorption. Antioxidant liposomes may prove very useful in this regard.

Liposomes are phospholipid vesicles composed of lipid bilayers enclosing an aqueous compartment. Hydrophilic molecules can be encapsulated in the aqueous spaces, and lipophilic molecules can be incorporated into the lipid bilayers. Liposomes, in addition to their use as artificial membrane systems, are used for the selective delivery of antioxidants and other therapeutic drugs to different tissues in sufficient concentrations to be effective in ameliorating tissue injuries (Stone et al., 2002). Antioxidant liposomes containing combinations of water- and lipid-soluble antioxidants may provide a unique therapeutic strategy for mustard gas exposure because (1) the antioxidants are nontoxic and could, therefore, be used at the earliest stages of exposure; (2) the liposomes themselves are composed of nontoxic, biodegradable, and reusable phospholipids;

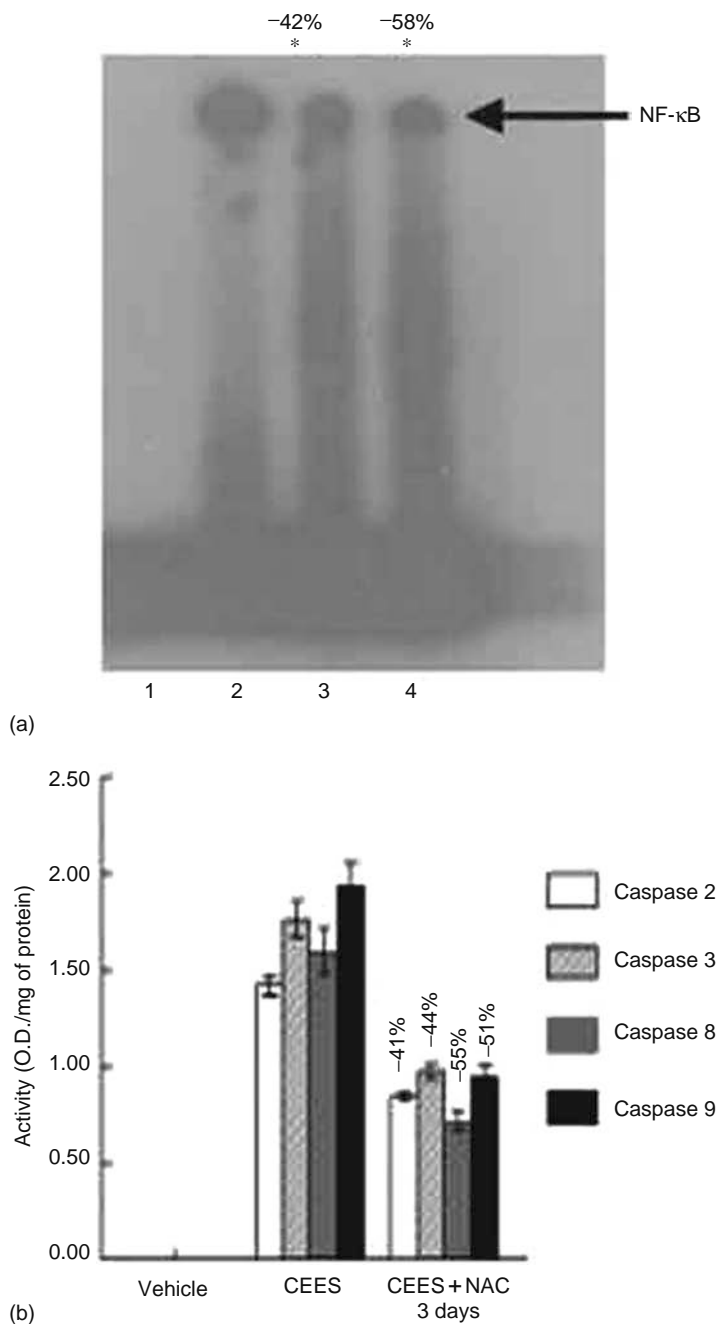


FIGURE 12.14 Inhibition of the activation of NF- κ B (a) and different caspases (b) in guinea pig lung after CEES exposure by pretreatment with NAC. (a) Activation of NF- κ B after 1 h of intratracheal infusion of CEES (4 mg/kg body weight) was monitored by mobility shift assay. The guinea pigs were treated with NAC either for 3 or for 30 days before CEES exposure. Panels 1, 2, 3, and 4 represent vehicle, CEES, CEES + NAC (3 days), and CEES + NAC (30 days), respectively. *NAC treatment caused a significant inhibition (46% and 58% for 3 and 30 days, respectively, $p < 0.05$) in the accumulation of NF- κ B. (b) Accumulation of caspases 2, 3, 8, and 9 at 4 h after exposure to CEES (4 mg/kg body weight) and the prevention of these caspases activation by short-term pretreatment (3 days) with NAC. Values are mean \pm SE ($n = 6$). *NAC treatment inhibited the activation of all caspases significantly ($p < 0.05$).

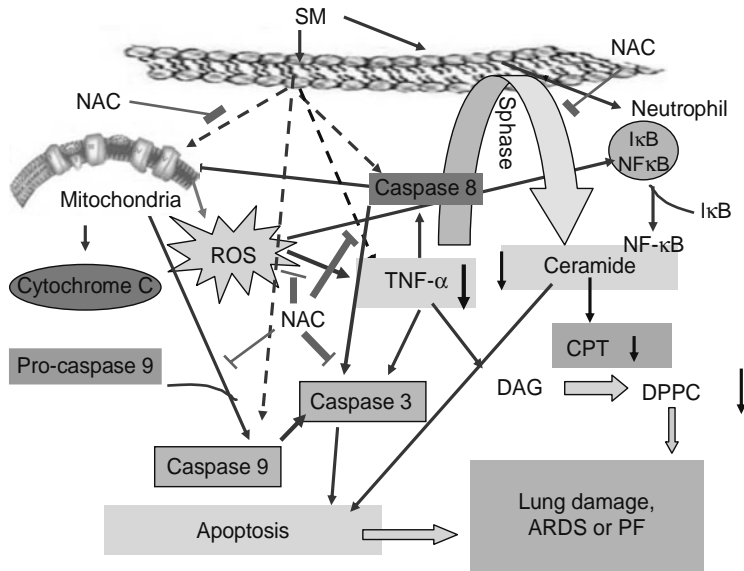


FIGURE 12.15 Proposed mechanism of action of NAC on CEES-induced lung injury.

(3) liposomes are preferentially taken up by the reticuloendothelial system which is an early target of mustards gas toxicity; (4) chemical antioxidants are relatively inexpensive and a wide range of commercial antioxidants are available; and (5) liposomes have low immunogenicity. Furthermore, results from several studies have clearly indicated that the liposomal antioxidant formulations exert a far superior protective effect compared with that of the free (unencapsulated) antioxidants, against OS-induced tissue injuries (Fan et al., 2000).

As shown in Figure 12.17, our preliminary data show that liposomes encapsulated with 5 mM GSH, a major intracellular chemical antioxidant, is effective at preventing CEES cytotoxicity to LPS-stimulated macrophages. We have also found that liposomes encapsulated with either 1 mM NAC (water-soluble antioxidant) or with 13.5 μ M α -tocopherol are also effective in preventing CEES toxicity to stimulated macrophages (data not shown). Preliminary results from our ongoing collaborative research efforts have demonstrated that delivery of antioxidants as liposomal formulations were effective in protecting against CEES-induced cellular injury in an animal model.

D. CHLORINE

Similar to phosgene, chlorine causes a delayed pulmonary edema. There is no specific antidote for chlorine gas inhalational exposure. Treatment for skin or eye contact is irrigation of the site. Inhalation of the gas can be treated supportively by the use of nebulized sodium bicarbonate and bronchodilators (Aslan et al., 2006). Modest improvement in animal models was obtained with the inhalation therapy using corticosteroids (Gunnarsson et al., 2000). Thiol-containing compounds are able to scavenge HOCl, which is suspected to be a significant metabolite of chlorine gas exposure (McKenzie et al., 1999). Enhancement of systemic levels of thiols by the use of orally administered NAC may be a consideration in life-threatening exposures to chlorine gas.

E. PHOSGENE

In experiments using agents as a prophylaxis, there is promise. Rats were exposed to phosgene in a whole-body chamber after 23 days of supplementation of vitamin E (α -tocopherol) or *N*-propyl gallate (nPG) (Sciuto and Moran, 2001). The vitamin E-fed rats did not show any survival

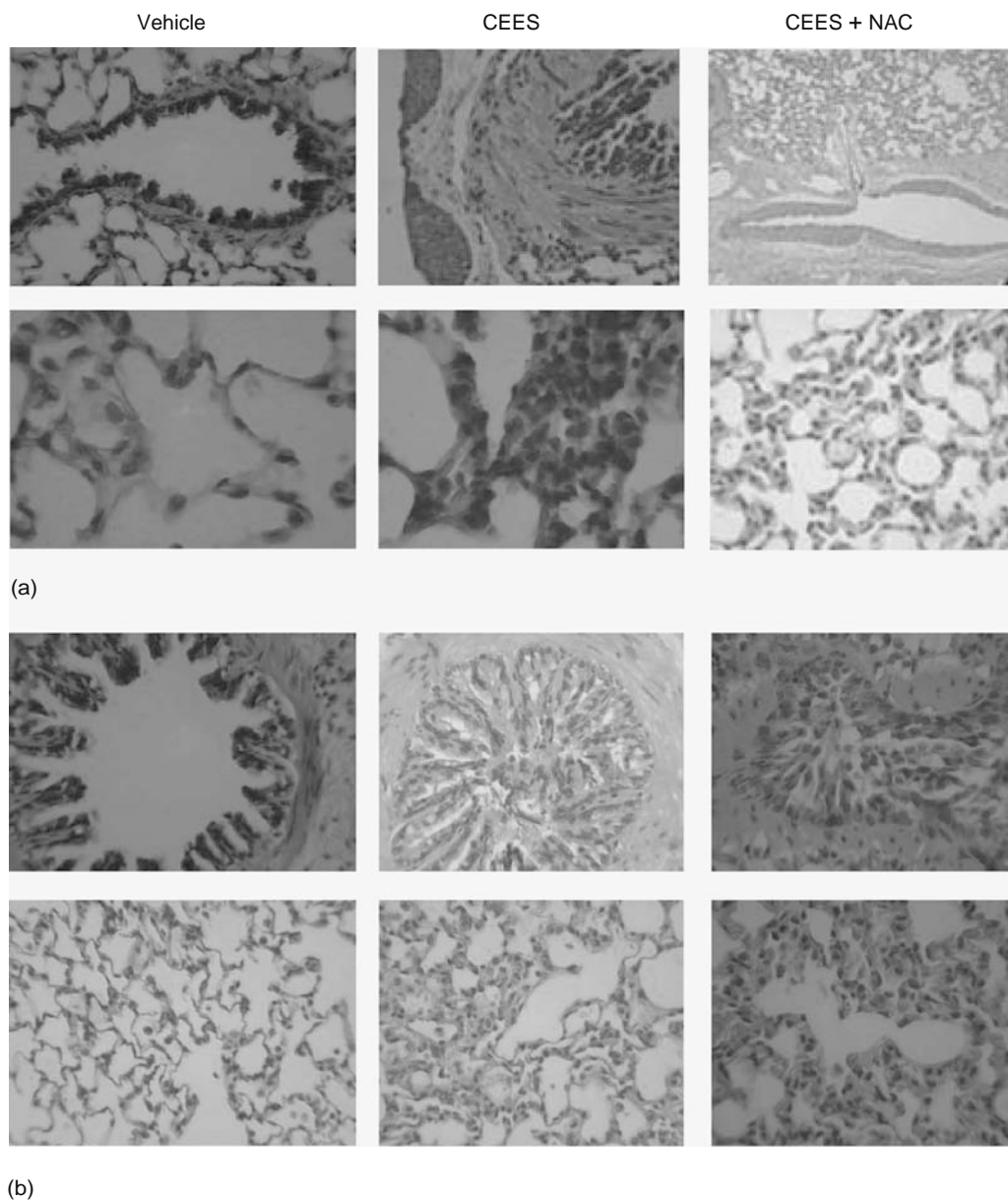


FIGURE 12.16 Histological analysis showing recovery from CEES-induced lung damage by pretreatment of NAC. Guinea pig lungs were examined under light microscope after 1 h (a) and after 21 days (b) of exposure to CEES (0.5 mg/kg body weight). Upper panel represents morphology of bronchi and lower panel represents morphology of the alveoli. Magnifications: 400 \times .

enhancement. The nPG-fed rats fed the lower doses of nPG (0.75%) showed the greatest increase in survival, and the higher dose of nPG (1.5%) was ineffective. In the lower dose of nPG, there was an obvious decrease in lipid peroxidation and increased lung tissue-reduced GSH. Gamma-tocopherol, in comparison with α -tocopherol, is a more potent anti-inflammatory agent and may have produced a much different result under the same experimental conditions that Sciuto and Moran (2001) performed (Jiang and Ames, 2003).

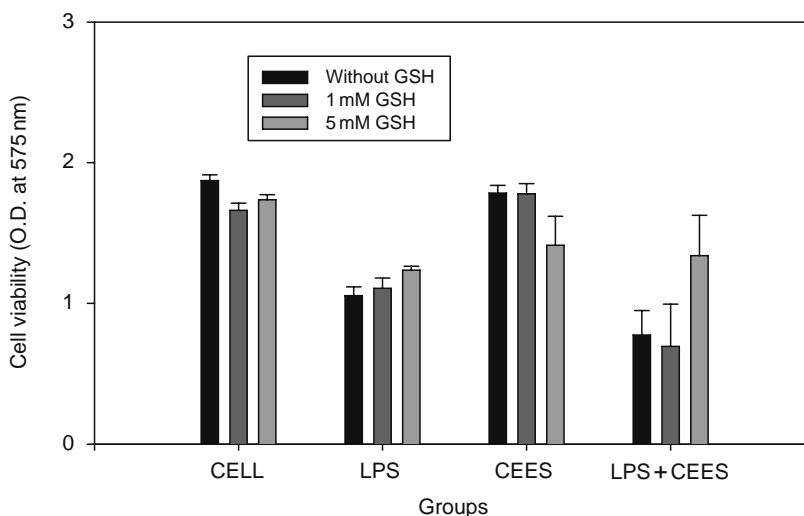


FIGURE 12.17 GSH-liposomes (5 mM) protect simulated macrophages from CEES toxicity.

Postexposure drugs used as a countermeasure to phosgene are more reflective of a clinical application or military theater exposures. The arachidonic acid analog 5-, 8-, 11-, and 14-eicosatraynoic acid (ETYA) inhibits the release of arachidonic acid metabolites, which produce both leukotrienes and prostaglandins (Farrukh et al., 1988). ETYA used as a postexposure treatment in an in situ lung model resulted in less lung edema, as well as increased glutathione levels and lower lipid peroxidation levels. It is questionable as to whether ETYA possesses any antioxidant properties (Sciuto, 2000).

VIII. OXIDATIVE STRESS IN DIFFERENT ORGAN SYSTEMS

A. LUNG

SM inhalation can produce hoarseness, laryngitis, acute airway obstruction, bronchopneumonia, pulmonary edema, and hemorrhage (Calvet et al., 1994). Bronchiolitis and dyspnea are common clinical findings. Examination of the pulmonary tree reveals a mild fibrosis in the parenchyma. Exaggerated fibroblast proliferation and increased collagen synthesis represent two critical events in the pathogenesis of this type of pulmonary fibrosis. The main initial changes are extreme hyperemia, exudation of inflammatory cells, cellular infiltration of the submucosa and detachment, necrosis, and cellular death of the respiratory epithelial lining (Chevallard et al., 1992).

Acute, heavy exposure to SM causes loss of the columnar cells of the upper respiratory tract, peribronchial edema, hyperemia of the blood vessels, cellular infiltrations in the submucosa, and intense vacuolization and disorganization of the cytoplasmic and nuclear structures (Emad and Rezaian, 1997, 1999). Pulmonary hemorrhage, pulmonary edema, and respiratory failure similar to ARDS may also occur. These cytotoxic effects are associated with acute thermal injury sustained by the airway mucosa and lead to scarring and development of stenosis of the tracheobronchial tree as was observed in 9.64% of the SM-exposed patients.

Cross-sectional study on the late pulmonary sequelae of SM-exposed veterans showed airway narrowing or stricture, asthma (10.65%), chronic bronchitis (58.88%), bronchiectasis (8.62%), and pulmonary fibrosis (PF; 12.18%) after 10 years. Crystal et al. (1984) recommended that SM be added to the various causes of interstitial lung diseases and PF (Crystal et al., 1984; DePaso and Winterbauer, 1991; Emad and Rezaian, 1997). The cellular constituents of bronchoalveolar (BAL)

fluid in patients with SM-induced PF are very similar to the cellular constituents seen in patients with idiopathic PF, and this finding indicates the presence of an ongoing active alveolitis in PF (Emad and Rezaian, 1997).

Under normal physiological conditions, airway lining fluids and extracellular spaces are maintained in a highly reduced state. Typically, the levels of antioxidants and oxidants in lung are balanced in favor of a reducing state (redox homeostasis). Decreases in antioxidants or increases in oxidants can disrupt this equilibrium and can cause OS. An imbalance in oxidant–antioxidant system has been recognized as one of the first changes that ultimately lead to inflammatory reactions (Crapo, 2003a).

An increased oxidizing environment can facilitate antigen-presenting cell (APC) maturation and T-cell activation, leading to the activation of the adaptive immune responses and, potentially, a hyperresponsive innate immune system. Thus, OS appears to play an important role in the pathogenesis of the asthmatic reaction. It is not surprising that OS occurs in many forms of lung disorders, such as pneumonia, adult respiratory distress syndrome, idiopathic pulmonary fibrosis, lung transplantation, chronic obstructive pulmonary disease, cystic fibrosis, bronchiectasis ischemia-reperfusion, and lung cancer (Bowler and Crapo, 2002; Crapo, 2003b; Rahman and Kelly, 2003; Rahman et al., 2004).

An oxidizing state in cells can initiate intracellular signaling cascades that lead to the production of inflammatory mediators. Stress kinases (JNK, ERK, p38) and transcription factors, such as NF- κ B and AP-1, are known to be redox sensitive. On their activation, these signaling pathways lead to production of TNF- α , IL-1-beta, IL-6, IL-8, IL-12, adhesion molecules (VCAM-1, ICAM-1), and GM-CSF (Mastruzzo et al., 2002). In addition to protein expression, OS favors uncoiling of DNA, thereby increasing accessibility to transcription factor binding (Rahman et al., 2004). The presence of OS can also damage alveolar epithelial cells by the induction of apoptosis. The angiotensin-converting enzyme system is also known to be redox sensitive. OS facilitates the conversion of angiotensinogen into angiotensin II, which is a bioactive peptide with a broad range of activities, including the induction of apoptosis in epithelial cells and the activation of fibroblasts. Angiotensin II can also increase the lung levels of transforming growth factor (TGF)- α , which is a crucial factor in the development of fibrosis (Mastruzzo et al., 2002).

The maintenance of a reducing environment in lung is considered to be crucial in the lung function. A balance between intracellular and extracellular oxidants and antioxidants is a prerequisite for normal lung homeostasis. The lung has highly specialized and compartmentalized antioxidant defenses to protect against reactive oxygen species (ROS) and RNS. These include the following: (1) small molecular weight antioxidants (e.g., GSH, vitamins, uric acid); (2) mucins; (3) metal-binding proteins (transferrin, lactoferrin, metallothionein, etc.); (4) SODs (e.g., mitochondrial manganese SOD [MnSOD], intracellular copper zinc SOD [CuZnSOD], and extracellular SOD [ECSOD]); (5) a group of enzymes that decomposes hydrogen peroxide (H₂O₂) (numerous GSH-associated enzymes and catalase); (6) detoxification enzyme systems (e.g., GST); and (7) other redox-regulatory thiol proteins (e.g., thioredoxin–peroxiredoxin system and glutaredoxins) (Powis et al., 2000; Fattman et al., 2003; Kinnula and Crapo, 2003).

Reduced GSH appears to be one of the most important antioxidant defense systems. In the extravascular lung fluid that coats the alveolar epithelial surfaces, GSH is present in millimolar quantities. A decrease in the ratio between GSH and oxidized glutathione (GSSG) occurring during OS leads to the activation of a variety of cellular redox-sensitive signaling pathways. Antioxidant enzymes such as SOD and catalase also play an important role in the clearance of oxidative radicals in the lung. The primary oxidant-generating enzyme is nicotinamide adenosine dinucleotide phosphate (NADPH) oxidase in phagocytes such as alveolar macrophages and neutrophils. On activation, phagocytes generate superoxide anions, which lead to the production of H₂O₂ for host defense.

It is clear that a better understanding of the oxidative state in the lung is important for the diagnosis and treatment of lung diseases. There are many methods developed for the detection of free radicals from oxygen, ROS, and their by-products to assess the presence of OS. The techniques

include established standard protocols and advanced methodologies using HPLC, mass spectrometry, and electron paramagnetic resonance (EPR). The following sections describe the most frequently used methods to measure lung oxidative status.

1. Monitoring Oxidative Stress in Live Cells

ROS in live cells can be detected by using fluorogenic marker for ROS and observed under fluorescence microscopy. One of the frequently used markers is carboxy- H_2DCFDA , a permeable fluorogenic marker, which is oxidized during OS in live cells and emits bright green fluorescence (Wan et al., 2005).

2. Hydrogen Peroxide and Superoxide Radical Generation in Bronchoalveolar Fluids

H_2O_2 fluids in BAL can be measured by the simple assay for the detection of the presence of peroxides in both aqueous and lipid environments. The basis of these assays is the complexing of ferrous ion (Fe^{+2}) by H_2O_2 in the presence of xylenol orange. Peroxides oxidize Fe^{+2} to Fe^{+3} , and Fe^{+3} forms a colored complex with xylenol orange that can be read at 560 nm (Jones et al., 1995). Superoxide radical generation can be estimated by nitroblue-tetrazolium reduction assay (Libon et al., 1993).

3. Antioxidant Status in Lung

The antioxidant status in the lungs can be evaluated by lung levels of SOD and catalase and their activities. SOD activity can be assessed by the OxyScan SOD-525 assay, which measures the activity of all forms of SOD. The method is based on the SOD-mediated increase in the rate of autoxidation of 5,6,6a,11b-tetrahydro-3,9,10-trihydroxybenzo[c]fluorene in aqueous alkaline solution to yield a chromophore with maximum absorbance at 525 nm. Catalase activity can be determined by a two-step reaction scheme (Catalase-520 assay). First, catalase reacts with a known quantity of H_2O_2 to generate H_2O and O_2 . In the presence of horseradish peroxidase (HRP), the remaining H_2O_2 reacts with 3,5-dichloro-2-hydroxybenzenesulfonic acid and 4-aminophenazone to form a chromophore with a color intensity. Lipid peroxidation levels in the lung can be measured by thiobarbituric acid reactive substances assay (Erdincler et al., 1997). The GSH/GSSG ratio, a useful measure of OS, can also be determined by a colorimetric method by using Bioxytech GSH/GSSG-412.

4. Hydroxydeoxyguanosine, an Indicator of DNA Damage

The most common type of damage caused by ROS in the body is oxidative damage to DNA. Hydroxydeoxyguanosine (8-OHdG), a product of this type of DNA damage, is used as a biomarker for OS. It can be measured by the immunohistochemical procedure and a high-performance liquid chromatography system equipped with an electrochemical detector (HPLC-ECD) (Mei et al., 2003). More recently, it has been reported that capillary electrophoresis-mass spectrometry (CE/MS) can also be used for the analysis of 8-OHdG to study OS (Weiss and Lunte, 2000).

5. Direct Measurements of Oxygen Free Radicals

It is very difficult to directly measure oxygen-free radicals (OFRs) due to their short half-lives. To study these OFRs, radical spin-trapping agents have to be employed to facilitate the formation of stable radical adducts with the OFRs, for detection by EPR spectroscopy. Trapping agents are generally nitrene or nitroso-containing molecules, such as 5,5-dimethyl-1-pyrroline-*n*-oxide (DMPO), which react with OFRs to form stable nitroxide free radicals. These radical adducts can be analyzed by using EPR (Olea-Azar et al., 2003).

6. Exhaled Breath Condensate

Exhaled breath condensate collected by cooling or freezing the exhaled air is a totally noninvasive procedure. H_2O_2 , leukotrienes, isoprostanes, and 3-nitrotyrosine are good candidates for OS assessments (Paredi et al., 2002). These products have been shown to elevate lung inflammation.

7. Analysis of Expired Air for Oxidation Products

Studies have shown that expired NO and CO can serve as biomarkers for OS, and ethane can serve as a marker of lipid peroxidation (Paredi et al., 2002). CO can be detected electrochemically, and it can also be measured by laser spectrophotometer and near-infrared CO analyzers. The levels of exhaled NO can be assessed by chemiluminescence. Ethane content can be detected using gas chromatography.

B. SKIN

Skin is one of the major sites of damage after exposure to vesicant chemical weapons. In the case of SM, there is a latent period after exposure, followed by an erythematous rash within 4–8 h, and then blistering some 2–18 h later. Elsayed et al. (1992) found that a nonlethal, s.c. dose of the mustard analog chloroethyl 4-chlorobutyl sulfide (CECBS) in mice caused damage to distal tissues, such as the lung, that was consistent with free radical, mediated OS. These authors suggest that “antioxidants could potentially modulate the response and reduce the damage” (Elsayed et al., 1992). Although useful, animal models do not exactly mimic the development of SM injury to human skin. Nevertheless, the mouse ear model, the rabbit, the hairless guinea pig, the nude mouse, and the weanling swine have all been useful for studying the (1) pathophysiology; (2) molecular mechanism of action; and (3) efficacy of countermeasures for SM injury. Similarly, *in vitro* models have major limitations but have the advantage of being cost-effective and potentially very reproducible.

A synthetic human skin model, EpiDerm, showed considerable promise as an *in vitro* model. EpiDerm possessed all the main characteristic features of the native skin tissue, including the cuboidal appearance of the basal cell layer, the presence of the stratum spinosum and stratum granulosum with typical stellate-shaped keratohyalin granules, and the presence of numerous lamellar bodies that are extruded at the stratum granulosum–stratum corneum interface. The EpiDerm system has the potential for identifying and developing SM therapeutic agents but does have its limitations as well. *In vivo*, skin damage can be accompanied by the rapid leakage of serum and leukocyte infiltration but this cannot occur in the *in vitro* skin models.

The U.S. Army Research Institute of Environmental Medicine has used the EpiDerm model to study CEES-induced skin toxicity (Blaha et al., 2000a, 2000b, 2001). Blaha et al. (2000a), for example, studied the potential role of inflammatory cytokines on CEES-induced toxicity. Since CEES or SM is known to provoke an acute inflammatory response in skin, it is reasonable to assume that inflammatory cytokines are involved in this process and that EpiDerm would mimic the *in vivo* responses. Blaha et al. (2000a) found, however, that CEES depressed the levels of IL-1 α and related cytokines. These authors concluded that the inflammatory responses seen *in vivo* are promoted by factors from sources other than keratinocytes (Blaha et al., 2000a). Stone et al. (2003, 2004) found that inflammatory cytokines dramatically enhance the toxicity of CEES in a macrophage model. It would be important, therefore, to determine if inflammatory cytokines increase CEES toxicity in the EpiDerm model. EpiDerm tissues in the presence of inflammatory cytokines may prove to be an excellent model to test the efficacy of countermeasures. Blaha et al. (2001) also demonstrated that CEES induces apoptosis in the EpiDerm model. This is a valuable observation since potential countermeasures could easily be tested for their antiapoptotic effects in this model.

1. Role of Skin Mast Cells in Vesicant Toxicity

Rikimaru et al. (1991) have used full-thickness human skin explants to study inflammatory mediators in response to topically applied SM. These investigators found that culture fluids from

the SM-treated skin contained increased levels of histamine, plasminogen-activating activity, and prostaglandin E2 compared with control explants. It was concluded that both mast cells and epidermal cells were apparently involved in early mediation of the inflammatory response to SM (Rikimaru et al., 1991). In contrast, Inoue et al. (1997) found that the inflammatory response of the mouse ear to SM did not differ in mast cell-deficient mice compared with normal mice. At present, there is no obvious explanation for the differences observed between the work of Rikimaru et al. (1991) and that of Inoue et al. (1997). It may well be that the mouse ear is not an optimal model for human skin. It is, however, critically important to determine if SM, or other toxic vesicants, degranulate mast cells, since this process could be a major source of inflammatory mediators.

C. EYES

The eye is a complex sensory organ, which receives visual information from the environment. It encodes optical information into complex electrical signals, which are transmitted to the cortex for visual imagery through the optical nerve. The visual efficiency primarily depends on the optical clarity of the eye (e.g., cornea, crystalline lens, and intraocular media) and the neural integrity of the visual pathway (e.g., retina, optic nerve, and visual cortex).

The pathogenesis of most age-related eye disorders remain poorly understood. Significant evidence points to oxidative damage as a major factor in the initiation and progression of numerous age-related diseases (Kowluru and Kennedy, 2001; Algvere and Seregard, 2002; Hogg and Chakravarthy, 2004; Shichi, 2004; Ohia et al., 2005; Truscott, 2005). Generally, OS occurs when the level of ROS exceeds the ability of the cell to respond through antioxidant defenses leading to the modification and degradation of carbohydrates, membrane lipids, proteins, and nucleic acids (Gamaley and Klyubin, 1999; Kimura et al., 2005). H₂O₂, a relatively stable oxidant, is present at low concentrations in the normal eye and is found at elevated concentrations in some patients with maturity-onset cataract (Beatty et al., 2001; Ohia et al., 2005; Truscott, 2005). Oxidative damage has also been hypothesized to play a role in the pathogenesis of glaucoma, as the trabecular meshwork is exposed to high levels of OS arising from aerobic metabolism, high aqueous concentrations of H₂O₂, and photochemical reactions in the anterior segment (Shichi, 2004; Ohia et al., 2005). The retina is particularly susceptible to OS because of its high consumption of oxygen, its high proportion of polyunsaturated fatty acids (PUFAs), its abundance of photosensitizers and its exposure to visible light (Sickel, 1972; Beatty et al., 2001). In general, it is well known that the greater the oxygen content of tissues, the more susceptible they are to oxidative and photooxidative damage. The retina is supplied with oxygen by the blood with generally high oxygen content in different portions of the retinal tissues. The lipids present in the membranes of rods contain a high percentage of PUFAs, particularly docosahexanoic acid (DHA) (22:6 ω -3), known to be the most highly PUFA in nature, making the retina inherently susceptible to lipid peroxidation (Sickel, 1972; Bazan, 1989; Beatty et al., 2001).

Although the eye is continuously exposed to OS, cells have numerous protective mechanisms to reduce the incidence of severe oxidative damage. Damage to the eye by increases in ROS is typically avoided because of a very efficient antioxidant system. It is further protected by pigments such as the kynurenines and melanin (Roberts, 2001). The major water-soluble antioxidants are GSH and ascorbic acid (Reddy and Giblin, 1984; Reddy, 1990; Delamere, 1996; Rose et al., 1998; Lou, 2003; Rahman and Kelly, 2003). Ascorbic acid, the most effective aqueous-phase antioxidant in human blood, is present in high concentrations in the lens, cornea, retinal pigment epithelium, and aqueous humor of humans (Delamere, 1996; Rose et al., 1998). GSH is a naturally occurring tripeptide and is found mostly concentrated in the lens epithelium; its concentration in the lens is as high as that seen in the liver. GSH acts as a reductant of peroxides either by a nonenzymatic reaction or by a reaction catalyzed by GSH peroxidase. GSH may be especially important in protecting the thiol groups of crystallins, preventing them from aggregating to form opaque clusters. Aging lenses or lenses under OS show an extensively diminished size of GSH pool, with some protein thiols

being S-thiolated by oxidized nonprotein thiols to form protein thiol-mixed disulfides, as protein-S-S-glutathione (PSSG), protein-S-S-cysteine (PSSC), or protein-S-S-gamma-glutamylcysteine (Megaw, 1984; Reddy and Giblin, 1984; Reddy, 1990; Rose et al., 1998; Beatty et al., 2000; Ganea and Harding, 2006).

The principal lipid-soluble antioxidants are vitamin E and the carotenoids (Hunt et al., 1984; Snodderly, 1995; Khachik et al., 1997; Beatty et al., 2001). Vitamin E is the major chain-breaking, lipid-soluble antioxidant in membranes, and is thus expected to play the most important role in minimizing effects of oxidation of PUFAs. Both vitamin E and the carotenoids scavenge free radicals, particularly hydroxyl radical and singlet oxygen. Vitamin E is recycled by redox coupling with vitamin C. The retina contains high quantities of α -tocopherol (outer segments of rod) and rod and retinal pigmented epithelium (RPE), and the concentrations within these tissues are very sensitive to dietary intake of the vitamin E (Hunt et al., 1984; Beatty et al., 2001). Vitamin E deficiency has been shown to result in retinal degeneration, excessive RPE lipofuscin levels, and a decrease in the PUFA content of rod outer segments and the RPE, suggesting that vitamin E protects against retinal oxidative damage (Hayes, 1974; Beatty et al., 2001). The antioxidant properties of the carotenoids are now well established, and they possess the ability to quench singlet oxygen and triplet sensitizers, interact with free radicals, and prevent lipid peroxidation. Of the many carotenoids circulating in human sera, only lutein and zeaxanthin are accumulated throughout the tissues of the eye, where they reach their highest concentration in the central retina (macula lutea). Lutein and zeaxanthin are more commonly referred to as macular pigments (Snodderly et al., 1984; Khachik et al., 1997).

SOD, catalase, and GSH peroxidase are antioxidant enzymes that play a significant role in protecting the retina from oxidative damage. GSH peroxidase is found in the retina and uses GSH as an electron donor to reduce fatty acid hydroperoxides, phospholipid hydroperoxides, cholesterol hydroperoxides, and H_2O_2 (Beatty et al., 2002; Ganea and Harding, 2006). SOD catalyzes the quenching of the superoxide anion to produce H_2O_2 and oxygen (Beatty et al., 2002; Lin et al., 2005). Catalase is an iron (Fe)-dependent enzyme that scavenges H_2O_2 either catalytically or peroxidatively. Catalase has been demonstrated in human neurosensory retina and RPE (Roberts, 2001; Beatty et al., 2002; Ohia et al., 2005).

1. Vesicant-Induced Ocular Injury and Oxidative Stress

The eyes are the organs most sensitive to vesicants, which cause cellular changes within minutes of contact; however, the onset of signs and symptoms to vesicant exposure may become evident several hours later. The time course of symptom development after exposure between SM and the nitrogen analogs is nearly the same. The initial contact of mustard gas with the eye for the most part does not cause pain and discomfort. Mild ($12\text{--}70\text{ mg/m}^3/\text{min}$) to moderate ($100\text{--}200\text{ mg/m}^3/\text{min}$) exposures might result in irritation, pain, swelling, and tearing that may occur within 3–12 h postexposure. Similar symptoms might appear 1–2 h after severe exposure ($>200\text{ mg/m}^3/\text{min}$) but the symptomatology might also include light sensitivity, severe pain, or temporary blindness. Physical findings include blepharospasm, periorbital edema, conjunctival injection, and inflammation of the anterior chamber (Solberg et al., 1997; Safarinejad et al., 2001; Banin et al., 2003; Javadi et al., 2005).

In the Iran–Iraq conflict, SM was heavily used and even now, about 30,000 victims still suffer from late effects of the agent, for example, chronic obstructive lung disease, lung fibrosis, recurrent corneal ulcer disease, chronic conjunctivitis, abnormal pigmentation of the skin, and several forms of cancer (Kehe and Szinicz, 2005). Evaluation of Iranian survivors with chronic or delayed-onset mustard gas keratitis revealed that mustard gas caused chronic and delayed destructive lesions in the ocular surface and cornea, leading to progressive visual deterioration and ocular irritation. Excised conjunctival and corneal specimens revealed a mixed inflammatory response without any specific features. Light microscopy of conjunctival specimens showed decreased goblet cell density, thickened epithelium, scarring in the substantia propria associated with plasmacytic and lymphocytic

infiltration, and dilated lymphatic vessels. Excised corneal buttons disclosed the absence of epithelium and Bowman's layer, stromal scarring, and vascularization. The pathophysiologic features of these changes are not clearly identified. Based on the clinical appearance of the lesions and the histopathologic findings, an immune-mediated component seems possible (Javadi et al., 2005).

In addition to their alkylating properties, mustards are now being recognized to mediate their toxic actions, at least in part, via the formation and action of ROS (Banin et al., 2003). A dramatic increase in copper levels and a decrease in ascorbic acid within the anterior chamber after ocular exposure to mustard compounds implicates the role of OS in mustard-induced eye injuries (McGahan and Bito, 1982; Kadar et al., 2001; Banin et al., 2003). Mustards are also known to rapidly inactivate sulfhydryl-containing proteins and peptides, such as GSH. These sulfhydryl compounds are critical in maintaining the appropriate oxidation–reduction state of cellular components, and GSH is also thought to be critical in reducing ROS in the cell and preventing peroxidation and loss of membrane integrity (Stadtman, 2001). Furthermore, the amelioration of mustard-induced ocular injuries by antioxidants is also evidence to implicate OS as a potential mechanism of injury (Banin et al., 2003; Morad et al., 2005).

Recognizing the fact that ROS play a role in the pathogenesis of mustard-induced ocular injuries, compounds that inhibit the formation of ROS or prevent their toxic effects would be beneficial in the treatment of mustard-induced ocular injuries. The topical application of low concentrations of Zn/DFO or Ga/DFO after corneal exposure to nitrogen mustards markedly reduced conjunctival, corneal, iris, and anterior chamber injury. In the cornea, the healing of epithelial erosions was faster, the long-term opacification was reduced, and the levels of neovascularization were lowered. In the anterior chamber, decreased inflammation and better maintenance of intraocular pressure were achieved. Cataractous changes were also notably milder (Banin et al., 2003).

A combination of topically applied Zn/DFO and dexamethasone, by virtue of their additive inhibitory effects on free radical formation and inflammation, reduced nitrogen mustard-induced injury to ocular anterior segment structures. Furthermore, the combination treatment of Zn/DFO and dexamethasone resulted in a speedier corneal reepithelization, less-severe corneal neovascularization, and the intraocular pressure was not as severely elevated as in the saline or the Zn/DFO- or dexamethasone-alone groups (Morad et al., 2005).

2. Redox Proteomics

OS induces free radical damage to biomolecules and alterations in redox-sensitive signaling pathways, both of which are key factors in understanding vesicant toxicology. In particular, small thiols, like GSH, are no longer viewed just as protective antioxidants but as redox regulators of proteins via glutathionylation or by oxidation of protein cysteine residue (Ghezzi and Ungheri, 2004). Redox proteomics is rapidly emerging as a very powerful tool for characterizing and identifying proteins based on their redox state (Ghezzi and Ungheri, 2004). This approach has not yet been applied to the study of vesicant toxicity, but studies should soon begin on exploring this area.

IX. OXIDATIVE STRESS: THE CONCEPT AND THE EFFECT ON GENE EXPRESSION

A. DEFINITION OF OXIDATIVE STRESS

Redox potential is defined by the half cell reduction potential that is created by redox couples that are primarily due to GSH, NAD^+ and nicotinamide dinucleotide phosphate. These couples are in ratios of the oxidized to reduced form of the molecules (NAD^+/NAD , $\text{NADP}^+/\text{NADPH}$, and $\text{GSSG}/2\text{GSH}$). The redox couples can be independent, as well linked to each other to form related couples. The redox environment is a reflection of these couples. These ratios can be measured by the Nernst equation, similar to a voltaic cell.

The Nernst equation is

$$E_h = E_0 + (RT/nF) \ln\{[\text{acceptor}]/[\text{donor}]\}$$

E_h is the electromotive force at a particular pH, its units are in volts or millivolts relative to a standard hydrogen electrode (1 atom H_2 , 1M H^+). The electromotive force is a quantitative measurement of a redox-active molecule that donates or accepts electrons.

R is the gas constant, T is the absolute temperature, F is the Faraday's constant, and n is the number of electrons transferred. The steady state of E_h for a redox-active component depends on the kinetic of the transfer of the reduction and oxidation reactions. Under normal homeostatic conditions (absence of OS), the E_h for 2GSH/GSSG relatively reduces because of the NADPH-coupled GSSG reductase. During periods of OS, the E_h becomes more oxidized.

Under normal cellular conditions, the redox potential is reductive. In diseased conditions, wherein OS occurs, the redox potential becomes more oxidative. The redox potential is similar in different cell types, but varies according to the cellular processes: proliferation $E = -240$ mV, differentiation $E = -200$ mV, and apoptosis $E = -170$ mV (Kirlin et al., 1999).

An illustrative experimental example of a cell exposed to an oxidant was carried out by Kirlin et al. (1999). When they used HT29 cells (colon adenocarcinoma) and exposed them to sodium butyrate, it was found that there was an oxidant reaction that caused a drop from -260 to -200 mV in E_h . The 60 mV decrease resulted in a 100-fold change in protein dithiols:disulfide ratio. A correlation was noted between E_h , GST, and NADPH:quinone reductase Kirlin further indicated that the E_h provides two additional pieces of information (1) in reactions that use GSH as a reductant to maintain protein thiol/disulfides in their reduced form, it is an indicator of the reducing power quantitatively and (2) if the redox state is controlled by a GSH redox couple, it is an indication of the functional state of the protein (Kirlin et al., 1999).

B. MOLECULES THAT INFLUENCE THE REDOX POTENTIAL

GSH synthase, a tripeptide (glutamylcysteinylglycine), is not only a water-soluble antioxidant, but is also part of a redox buffer (Smith et al., 1996). It is found in all cells and is used for a multiplicity of cellular functions, such as protein and prostaglandin synthesis, detoxification, etc. Cytosolic concentrations of GSH range from 1 to 11 mM (Smith et al., 1996) and are 100–1000 times greater than the extracellular levels. Many proteins contain sulfhydryl groups because of their cysteine content. The content of thiols in proteins is greater than that of the pool of GSH (Torchinsky, 1981).

The intracellular compartment exchanges GSH with the cytosol (Griffith and Meister, 1985; Schnellmann et al., 1988; Fernandez-Checa et al., 1998). GSH concentrations within the nucleus are critical for maintaining the redox state of protein sulfhydryls that are necessary for DNA repair and expression (Arrigo, 1999). The endoplasmic reticulum has a more oxidizing environment than the cytosol or nucleus. GSH/GSSH in the endoplasmic reticulum is in the range of 1:1 to 3:1, in comparison with the cytosol (Hwang et al., 1992). The ratio of reduced GSH to GSSG influences a variety of cellular signaling processes, such as activation and phosphorylation of stress kinases (JNK, p38, PI-3K) via sensitive cysteine-rich domains, activation of SHM-ase ceramide pathway, and activation of AP-1 and NF- κ B, with subsequent gene transcription (Singh et al., 1998; Arrigo, 1999; Mercurio and Manning, 1999a, 1999b).

1. Nicotinamide Adenosine Dinucleotide Phosphate

NADPH is usually involved in reductive (biosynthetic) reactions and serves as a source of electrons. In contrast, NAD is involved in oxidative reactions and serves as a sink for electrons. In cells and tissues, the ratio of NADPH/NADP⁺ tends to be 1:10 and 1:1000. NADPH is considered the primary source of reducing equivalents for GSH.

2. Thioredoxin

Thioredoxin (TRX) is a pleiotropic polypeptide also known as T-cell leukemia-derived factor (Tagaya et al., 1989; Yodoi and Uchiyama, 1992). It has two redox-reactive cysteine residues in the reactive center (Cys-32 and Cys-35) (Holmgren, 1972, 1985, 1989; Buchanan et al., 1994). Reductases are used to donate electrons from NADPH to facilitate the reduction oxidation reaction between the dithiol or disulfide forms of TRX (Luthman and Holmgren, 1982; Watson et al., 2004).

TRX is responsible for the reduction of cysteine moieties in the DNA-binding sites of several transcription factors (Mathews, 1992; Okamoto, 1992), facilitates the refolding of disulfide-containing proteins, and regulates the DNA-binding activity of some transcription factors (e.g., NF- κ B and Ref-1-dependent AP-1) (Sen, 1998; Arner and Holmgren, 2000). TRX facilitates gene expression in that it enables protein–nucleic acid interactions (Holmgren, 1985); it does so by reducing cysteine in the DNA-binding loop of several transcription factors (Matthews et al., 1992; Okamoto et al., 1992; Xanthoudakis et al., 1992, 1994). The redox state of TRX varies independently to that of GSH/GSSG. GSH forms intermolecular disulfides, whereas TRX is a protein that usually forms intramolecular disulfides. TRX assists in the control of apoptosis signal, regulating kinase-1 (ASK-1) (Saitoh et al., 1998).

C. APOPTOSIS

Apoptosis is induced, when tissue is exposed to SM by a calmodulin- and caspase-dependent pathway (Rosenthal et al., 1998; Sciuto and Hurt, 2004). Zhang et al. (2001) using Jurkat cells exposed to CEES, analyzed gene expression for death and survival pathways. The Akt (PKB) is an important kinase, which can block apoptosis and promote cell survival. It was downregulated in a dose-dependent manner. The antiapoptotic genes, Bcl family, were decreased: Bcl-2, 90%; bax, 80%; bcl-X_L, 67%; Bak and Mcl-1, 70%; and Bik, 57%. Caspases 3, 4, 6, 8, and 9 were upregulated. Crawford et al. (unpublished data) found that CEES-exposed human dendritic cells released cytochrome *c* before detectable levels of ROS generation. NAC was found to inhibit the release of cytochrome *c* and decrease apoptosis. The release of cytochrome *c* was likely due to the opening of the mitochondrial transport permeability transition pores, which is regulated by two redox couples, NADP and GSH (Dalton et al., 1999). It is well known that a portion of the toxicity of mustard is the depletion of NAD (Mol et al., 1989; Byers et al., 2000).

A depletion of GSH alone can act as an early activation of apoptotic signaling (Coffey et al., 2000; Coppola and Ghibelli, 2000; Armstrong and Jones, 2002). Conversion from the procaspase to an active enzyme requires a reduction of the cysteine residue (Hampton et al., 1998). OS can trigger caspase activity, but can also suppress it (Hampton et al., 1998).

Studies conducted by Celli et al. (1998) used BSO (buthionine sulfoximine) to deplete cells of GSH. There was a significant decrease in the Bcl levels and associated time-dependent increase in the number of cells undergoing apoptosis. Maintenance of GSH levels with GSH ethyl ester in the presence of BSO decreased apoptosis and prevented a decrease in Bcl-2 protein. The Celli study, if contrasted to Zhang et al. (2001), one begins to suspect that there may be a strong correlation between the loss of GSH and gene expression in CEES-exposed tissues.

The suppression of Bcl-2 expression induces the relocalization of GSH to the cytosol, whereas the overexpression of Bcl-2 induces a relocalization of GSH to the nucleus. There was a direct correlation between GSH levels and the Bcl-2 nuclear protein levels. It was concluded by Voehringer et al. (1998) that one of the functions of Bcl-2 is to promote the sequestration of GSH into the nucleus.

D. GENE EXPRESSION CONTROLLED BY REDOX-STATE TRANSCRIPTION FACTORS

Redox homeostasis regulates activation and binding by transcription factors at the 5' end of the target gene. In the transcription factors, cysteine residues are frequently located in their protein

sequence localized in their DNA-binding domain. The cysteine molecules are often essential for recognition of the binding site due to electrostatic interactions with specific DNA bases. Inhibition of the binding factor occurs if the cysteine is oxidized, which may be a consequence of an alteration of the tridimensional structure of the transcription factors. The function of several transcription factors could be impaired or inhibited because of oxidation of cysteine groups that result in inter- or intramolecular disulfide bonds (Arrigo, 1999). Several of the transcription factors undergo redox modification posttranslationally. NF- κ B binding with DNA is augmented by TRX *in vitro*. Ref-1 is also modulated by redox compounds (e.g., TRX) (Hirota et al., 1997).

1. NF- κ B

NF- κ B regulates many genes, particularly those involved in immune and inflammatory responses (Baeuerle and Baltimore, 1996). Antioxidants, such as NAC, GSH, and cysteine, inhibit the activation of NF- κ B (Mihm et al., 1995). TRX regulates the binding of NF- κ B to DNA (Matthews et al., 1992).

2. Ref-1

In an oxidizing environment, Ref-1 facilitates the binding transcription factors to DNA by reduction of cysteine residues within the binding domains of these proteins (Xanthoudakis and Curran, 1992; Xanthoudakis et al., 1992; Walker et al., 1993). Under OS, cysteine 65 forms a disulfide bond with cysteine 93, which ceases the stimulatory activity of Rdf-1. Active Ref-1 is recycled by the contribution of hydrogen from TRX (Hirota et al., 1997).

3. Activator Protein-1

Activator protein-1 (ATP-1) binds to an enhancer element (Angel et al., 1987; Lee et al., 1987), and is modified by redox factor 1 (Ref-1), a DNA repair enzyme (Angel et al., 1987; Lee et al., 1987; Arrigo, 1999). It is present in the promoter region of several genes, which are implicated in cell proliferation and tumor promotion. Several growth factors, PKC activators, and intracellular redox activate it (Angel and Karin, 1991). It consists of c-Jun and c-Fos proteins, which are products of the c-jun and c-fos proto-oncogene. Agents that promote intracellular oxidants such as UV irradiation, H₂O₂, and mitogens induce c-fos and c-jun genes (Datta et al., 1992; Lo and Cruz, 1995). Antioxidants that have a phenolic group (e.g., d- α -tocopherol or butylated hydroxytoluene) induce expression of c-fos and c-jun (Choi and Moore, 1993; Stauble et al., 1994). ATP-1 acts as a secondary antioxidant-responsive transcription factor (Meyer et al., 1993).

4. Heat Shock Transcription Factor

Heat shock transcription factor (HSF) is part of the family of heat shock factors that are activated and bind to DNA induced by OS. Several chemicals, heat shock, or conditions that generate abnormally folded proteins activate HSF1 conversion from a monomer to a trimer state (Liu et al., 1996). Iodoacetamide (IDAM), an alkylating agent, activates the transcription of Hsp 70 gene (Liu et al., 1996). The depletion of GSH induces oxidation of protein thiols, denaturation, and aggregation of proteins (Freeman et al., 1997). Alkylating agents that deplete GSH increase HSF1 (Liu et al., 1996) and induce trimerization of HSF1.

X. SUMMARY

Chlorine, phosgene, Lewisite, and SM all react with thiol groups as well as produce oxidants. The arsenic group in Lewisite has a high affinity to the alpha and gamma thiol groups of lipoic acid found in enzymes (e.g., pyruvate oxidase). Oxidants occur as part of the normal metabolism of cells (redox homeostasis). In the diseased state (e.g., exposure to a chemical agent), there is an acute

inflammatory response that is also inclusive of OS (redox imbalance). During significant OS, the oxidant burden exhausts the redox buffer of the cell (e.g., GSH/GSSH, NADP/NADPH, etc.) that consequently alters redox couples. The mitochondrial permeability transition pores (MPTPs) are directly regulated by the redox state. They are a cyclosporine A-sensitive, Ca^{2+} -dependent, and voltage-gated channel. There are two types. One is dependent on the GSH:GSSH ratio (Petronilli et al., 1994; Costantini et al., 1995); the other is a voltage-sensitive gate, regulated by the ratio of pyridine nucleotides (NAD^+/NADP):($\text{NADH}^+/\text{NADPH}$) and is independent of the reduced GSH (Reed and Savage, 1995; Costantini et al., 1996). MPTPs appear to be involved in the toxicity of several chemicals (Dalton et al., 1999). Opening of the pores results in energy uncoupling by a Ca^{2+} -dependent decrease of mitochondrial inner-membrane potential (Petronilli et al., 1994). The collapse of the membrane potential and the inhibition of oxidative phosphorylation result in diminished intracellular ATP. Consequently, there may be the release of inner-membrane cytochrome *c* to the cytosol, which may signal the initiation of apoptosis (Krippner et al., 1996).

In a comparison of SM to CEES done using a histological grading system, SM was shown to be about six times more potent than CEES (Dana Anderson, unpublished results). The doses that were used by our group in the *in vivo* models were found to be equivalent to those used at the U.S. Army Medical Research Institute of Chemical Defense. CEES increases the activity of the transcription factor NF- κ B, and consequently, there is an increase in proinflammatory cytokine production (e.g., TNF- α). PARP activity increases dramatically in both CEES- (Crawford, unpublished results) and SM-exposed tissues (Bhat et al., 2006). Increased PARP activity affects the energy levels of the cell by oxidizing NADPH, which causes a redox imbalance ($\text{NADP}^+/\text{NADPH}$). The transcription factor NF- κ B and caspases are increased in CEES- and SM-exposed tissues. In both CEES and SM exposures, there is a loss of GSH, likely due to direct interaction with thiols and OS. The combined loss of GSH, NADH, and NADPH has far-reaching ramifications on multiple cellular systems, particularly redox-regulated pathways.

A. ANTIDOTES

Lewisite is the only vesicant with a proven antidote—British anti-lewisite (2,3-dimercaptopropanol). Increasing antioxidant levels have been found to be protective against the mustards analog, NAC. NAC, which we have used in our studies with CEES, is immediately clinically available. It is most commonly used for acetaminophen overdose. NAC has a long history of several gram quantities administered in several doses and has minimal adverse reactions. In the case of acetaminophen overdose, it is administered via the oral-gastric route, which increases hepatic GSH levels, and in turn, suppresses inflammatory cytokines (Dambach et al., 2006). Liposome encapsulation of both water- and fat-soluble antioxidants was proven to be more effective in the suppression of OS than the free molecule of NAC.

Antioxidants that are liposome encapsulated are advantageous in that they enhance delivery to sites at which inflammation occurs. In light of the common effect that the vesicants have on redox-regulated pathways and OS, it becomes a compelling reason for additional research. The down-regulation of OS may be a very significant step forward in developing treatment countermeasures against several vesicants and other WMD.

REFERENCES

- Akira, S. and Kishimoto, T. (1997). NF-IL6 and NF- κ B in cytokine gene regulation. *Adv Immunol* 65, 1–46.
- Algvere, P.V. and Seregard, S. (2002). Age-related maculopathy: pathogenetic features and new treatment modalities. *Acta Ophthalmol Scand* 80, 136–43.
- Allan, D. (2000). Lipid metabolic changes caused by short-chain ceramides and the connection with apoptosis. *Biochem J* 345 (Pt 3), 603–10.
- Alphonse, G., Aloy, M.T., Broquet, P., Gerard, J.P., Louisot, P., Rousson, R., and Rodriguez-Lafrasse, C. (2002). Ceramide induces activation of the mitochondrial/caspases pathway in Jurkat and SCC61 cells

- sensitive to gamma-radiation but activation of this sequence is defective in radioresistant SQ20B cells. *Int J Radiat Biol* 78, 821–35.
- Angel, P. and Karin, M. (1991). The role of Jun, Fos and the AP-1 complex in cell-proliferation and transformation. *Biochim Biophys Acta* 1072, 129–57.
- Angel, P., Baumann, I., Stein, B., Delius, H., Rahmsdorf, H.J., and Herrlich, P. (1987). 12-*O*-tetradecanoyl-phorbol-13-acetate induction of the human collagenase gene is mediated by an inducible enhancer element located in the 5'-flanking region. *Mol Cell Biol* 7, 2256–66.
- Anslow, W.P. (1946). *Systemic Pharmacology and Pathology of Sulfur and Nitrogen Mustards*. Washington, DC: Office of Scientific Research and Development, National Defense Research Committee, Div. 9.
- Ansceschi, M. (1989). The alveolar type II cells as a model for investigating the metabolism of surfactant phospholipids. *Eur Respir J Suppl* 3, 10s–12.
- Armstrong, J.S. and Jones, D.P. (2002). Glutathione depletion enforces the mitochondrial permeability transition and causes cell death in Bcl-2 overexpressing HL60 cells. *FASEB J* 16, 1263–5.
- Arner, E.S. and Holmgren, A. (2000). Physiological functions of thioredoxin and thioredoxin reductase. *Eur J Biochem* 267, 6102–9.
- Arrigo, A.P. (1999). Gene expression and the thiol redox state. *Free Radic Biol Med* 27, 936–44.
- Arroyo, C.M., Schafer, R.J., Kurt, E.M., Broomfield, C.A., and Carmichael, A.J. (2000). Response of normal human keratinocytes to sulfur mustards: cytokine release. *J Appl Toxicol* 20 Suppl 1, S63–72.
- Aruoma, O.I. and Halliwell, B. (1987). Action of hypochlorous acid on the antioxidant protective enzymes superoxide dismutase, catalase and glutathione peroxidase. *Biochem J* 248, 973–6.
- Aslan, S., Kandis, H., Akgun, M., Cakir, Z., Inandi, T., and Gorguner, M. (2006). The effect of nebulized NaHCO₃ treatment on “RADS” due to chlorine gas inhalation. *Inhal Toxicol* 18, 895–900.
- Awasthi, S., Vivekananda, J., Awasthi, V., Smith, D., and King, R.J. (2001). CTP: phosphocholine cytidyltransferase inhibition by ceramide via PKC- α , p38 MAPK, cPLA2, and 5-lipoxygenase. *Am J Physiol Lung Cell Mol Physiol* 281, L108–18.
- Baburina, I. and Jackowski, S. (1998). Apoptosis triggered by 1-*O*-octadecyl-2-*O*-methyl-rac-glycero-3-phosphocholine is prevented by increased expression of CTP: phosphocholine cytidyltransferase. *J Biol Chem* 273, 2169–73.
- Bauerle, P.A. and Baltimore, D. (1996). NF- κ B: ten years after. *Cell* 87, 13–20.
- Banin, E., Morad, Y. et al. (2003). Injury induced by chemical warfare agents: characterization and treatment of ocular tissues exposed to nitrogen mustard. *Invest Ophthalmol Vis Sci* 44(7): 2966–2972.
- Barnes, P.J. and Adcock, I.M. (1998). Transcription factors and asthma. *Eur Respir J* 12, 221–34.
- Barron, E.S., Miller, Z.B. et al. (1947). Reactivation by dithiols of enzymes inhibited by lewisite. *Biochem J* 41(1): 69–74.
- Bartsch, H. and Nair, J. (2006). Chronic inflammation and OS in the genesis and perpetuation of cancer: role of lipid peroxidation, DNA damage, and repair. *Langenbecks Arch Surg* 391(5): 499–510.
- Bazan, N.G. (1989). The metabolism of omega-3 polyunsaturated fatty acids in the eye: the possible role of docosahexaenoic acid and docosanoids in retinal physiology and ocular pathology. *Prog Clin Biol Res* 312, 95–112.
- Beatty, S., Koh, H.-H., Phil, M., Henson, D., and Boulton, M.E. (2000). The role of oxidative stress in the pathogenesis of age-related macular degeneration. *Surv Ophthalmol* 45, 115–134.
- Beatty, S., Murray, I.J., Henson, D.B., Carden, D., Koh, H., and Boulton, M.E. (2001). Macular pigment and risk for age-related macular degeneration in subjects from a Northern European population. *Invest Ophthalmol Vis Sci* 42, 439–46.
- Bhat, K.R., Benton, B.J., and Ray, R. (2006). Poly (ADP-ribose) polymerase (PARP) is essential for sulfur mustards-induced DNA damage repair, but has no role in DNA ligase activation. *J Appl Toxicol* 26, 452–7.
- Black, R.M. and Read, R.W. (1995). Biological fate of sulfur mustards, 1,1'-thiobis(2-chloroethane): identification of beta-lyase metabolites and hydrolysis products in human urine. *Xenobiotica* 25, 167–73.
- Black, R.M., Brewster, K., Clarke, R.J., Hambrook, J.L., Harrison, J.M., and Howells, D.J. (1992). Biological fate of sulfur mustards, 1,1'-thiobis(2-chloroethane): isolation and identification of urinary metabolites following intraperitoneal administration to rat. *Xenobiotica* 22, 405–18.
- Bladergroen, B.A., Bussiere, M., Klein, W., Geelen, M.J., Van Golde, L.M., and Houweling, M. (1999). Inhibition of phosphatidylcholine and phosphatidylethanolamine biosynthesis in rat-2 fibroblasts by cell-permeable ceramides. *Eur J Biochem* 264, 152–60.

- Blaha, M., Bowers, W., Kohl, J., DuBose, D., and Walker, J. (2000a). II-1-related cytokine responses of nonimmune skin cells subjected to CEES exposure with and without potential vesicant antagonists. *In Vitro Mol Toxicol* 13, 99–111.
- Blaha, M., Bowers, W., Kohl, J., DuBose, D., Walker, J., Alkhyat, A., and Wong, G. (2000b). Effects of CEES on inflammatory mediators, heat shock protein 70A, histology and ultrastructure in two skin models. *J Appl Toxicol* 20 Suppl 1, S101–8.
- Blaha, M., Kohl, J., DuBose, D., Bowers, W., Jr., and Walker, J. (2001). Ultrastructural and histological effects of exposure to CEES or heat in a human epidermal model. *In Vitro Mol Toxicol* 14, 15–23.
- Borak, J. and Sidell, F.R. (1992). Agents of chemical warfare: sulfur mustards. *Ann Emerg Med* 21, 303–8.
- Bostan, M., Galatiuc, C., Hirt, M., Constantin, M.C., Brasoveanu, L.I., and Iordachescu, D. (2003). Phospholipase A2 modulates respiratory burst developed by neutrophils in patients with rheumatoid arthritis. *J Cell Mol Med* 7, 57–66.
- Bouchard, V.J., Rouleau, M., and Poirier, G.G. (2003). PARP-1, a determinant of cell survival in response to DNA damage. *Exp Hematol* 31, 446–54.
- Bowler, R.P. and Crapo, J.D. (2002). Oxidative stress in allergic respiratory diseases. *J Allergy Clin Immunol* 110, 349–56.
- Brennan, F.M., Maini, R.N., and Feldmann, M. (1995). Cytokine expression in chronic inflammatory disease. *Br Med Bull* 51, 368–84.
- Buchanan, B.B., Schurmann, P., Decottignies, P., and Lozano, R.M. (1994). Thioredoxin: a multifunctional regulatory protein with a bright future in technology and medicine. *Arch Biochem Biophys* 314, 257–60.
- Burkle, A. (2001). PARP-1: a regulator of genomic stability linked with mammalian longevity. *ChemBiochem* 2, 725–8.
- Byers, S., Anderson, D., Brobst, D., and Cowan, F. (2000). Automated assay for nicotinamide adenine dinucleotide (NAD⁺). *J Appl Toxicol* 20 Suppl 1, S19–22.
- Byrne, M.P., Broomfield, C.A., and Stites, W.E. (1996). Mustards gas crosslinking of proteins through preferential alkylation of cysteines. *J Protein Chem* 15, 131–6.
- Calvet, J.H., Jarreau, P.H., Levame M., D'Ortho, M.P., Lorino, H., Harf, A., and Macquin-Mavier, M.I. (1994). Acute and chronic effects of sulfur mustards intoxication in the guinea pig. *J Appl Physiol* 76, 681–8.
- Carr, A.C., Hawkins, C.L., Thomas, S.R., Stocker, R., and Frei, B. (2001). Relative reactivities of *N*-chloramines and hypochlorous acid with human plasma constituents. *Free Radic Biol Med* 30, 526–36.
- Celli, A., Que, F.G., Gores, G.J., and LaRusso, N.F. (1998). Glutathione depletion is associated with decreased Bcl-2 expression and increased apoptosis in cholangiocytes. *Am J Physiol* 275, G749–57.
- Chatterjee, D., Mukherjee, S., Smith, M.G., and Das, S.K. (2003). Signal transduction events in lung injury induced by 2-chloroethyl ethyl sulfide, a mustards analog. *J Biochem Mol Toxicol* 17, 114–21.
- Chatterjee, D., Mukherjee, S., Smith, M.G., and Das, S.K. (2004). Role of sphingomyelinase in the environmental toxin induced apoptosis of pulmonary cells. In: *In Lipids: Sphingolipid Metabolizing Enzymes*, eds. Dipak, Haldar, and Salil K Das, Research Signpost, pp. 117–139, Trivandrum, Kerala, India.
- Chen, C.C., Wang, J.K., and Lin, S.B. (1998). Antisense oligonucleotides targeting protein kinase C- α , - β I, or - δ but not - ϵ inhibit lipopolysaccharide-induced nitric oxide synthase expression in RAW 264.7 macrophages: involvement of a nuclear factor kappa B-dependent mechanism. *J Immunol* 161, 6206–14.
- Chevillard, M., Laine, P., Robineau, P., and Puchelle, E. (1992). Toxic effects of sulfur mustards on respiratory epithelial cells in culture. *Cell Biol Toxicol* 8, 171–81.
- Choi, H.S. and Moore, D.D. (1993). Induction of c-fos and c-jun gene expression by phenolic antioxidants. *Mol Endocrinol* 7, 1596–602.
- Coffey, R.N., Watson, R.W., Hegarty, N.J., O'Neill, A., Gibbons, N., Brady, H.R., and Fitzpatrick, J.M. (2000). Thiol-mediated apoptosis in prostate carcinoma cells. *Cancer* 88, 2092–104.
- Colvin, O.M., Friedman, H.S., Gamcsik, M.P., Fenselau, C., and Hilton, J. (1993). Role of glutathione in cellular resistance to alkylating agents. *Adv Enzyme Regul* 33, 19–26.
- Coppola, S. and Ghibelli, L. (2000). GSH extrusion and the mitochondrial pathway of apoptotic signalling. *Biochem Soc Trans* 28, 56–61.
- Costantini, P., Petronilli, V., Colonna, R., and Bernardi, P. (1995). On the effects of paraquat on isolated mitochondria. Evidence that paraquat causes opening of the cyclosporin A-sensitive permeability transition pore synergistically with nitric oxide. *Toxicology* 99, 77–88.

- Costantini, P., Chernyak, B.V., Petronilli, V., and Bernardi, P. (1996). Modulation of the mitochondrial permeability transition pore by pyridine nucleotides and dithiol oxidation at two separate sites. *J Biol Chem* 271, 6746–51.
- Cowan, F.M. and Broomfield, C.A. (1993). Putative roles of inflammation in the dermato-pathology of sulfur mustards. *Cell Biol and Toxicol* 9, 201–213.
- Cowan, F.M., Broomfield, C.A., and Smith, W.J. (1992). Inhibition of sulfur mustards-increased protease activity by niacinamide, *N*-acetyl cysteine or dexamethasone. *Cell Biol Toxicol* 8, 129–138.
- Crapo, J.D. (2003a). Oxidative stress as an initiator of cytokine release and cell damage. *Eur Respir J Suppl* 44, 4s–6s.
- Crapo, J.D. (2003b). Redox active agents in inflammatory lung injury. *Am J Respir Crit Care Med* 168, 1027–8.
- Crystal, R.G., Bitterman, P.B., Rennard, S.I., Hance, A.J., and Keogh, B.A. (1984). Interstitial lung diseases of unknown cause. Disorders characterized by chronic inflammation of the lower respiratory tract. *N Engl J Med* 310, 235–44.
- Cui, Z., Houweling, M., Chen, M.H., Record, M., Chap, H., Vance, D.E., and Terce, F. (1996). A genetic defect in phosphatidylcholine biosynthesis triggers apoptosis in Chinese hamster ovary cells. *J Biol Chem* 271, 14668–71.
- D'Amours, D., Germain, M., Orth, K., Dixit, V.M., and Poirier, G.G. (1998). Proteolysis of poly(ADP-ribose) polymerase by caspase 3: kinetics of cleavage of mono(ADP-ribosyl)ated and DNA-bound substrates. *Radiat Res* 150, 3–10.
- D'Amours, D., Desnoyers, S., D'Silva, I., and Poirier, G.G. (1999). Poly(ADP-ribosylation) reactions in the regulation of nuclear functions. *Biochem J* 342 (Pt 2), 249–68.
- Dahl, H., Gluud, B., Vangsted, P., and Norm, M. (1985). Eye lesions induced by mustards gas. *Acta Ophthalmol Suppl* 173, 330–35.
- Dalton, T.P., Shertzer, H.G., and Puga, A. (1999). Regulation of gene expression by reactive oxygen. *Annu Rev Pharmacol Toxicol* 39, 67–101.
- Dambach, D.M., Durham, S.K., Laskin, J.D., and Laskin, D.L. (2006). Distinct roles of NF- κ B p50 in the regulation of acetaminophen-induced inflammatory mediator production and hepatotoxicity. *Toxicol Appl Pharmacol* 211, 157–65.
- Das, S.K., Mukherjee, S., Smith, M.G., and Chatterjee, D. (2003). Prophylactic protection by *N*-acetylcysteine against the pulmonary injury induced by 2-chloroethyl ethyl sulfide, a mustards analogue. *J Biochem Mol Toxicol* 17, 177–84.
- Datta, R., Hallahan, D.E., Kharbanda, S.M., Rubin, E., Sherman, M.L., Huberman, E., Weichselbaum, R.R., and Kufe, D.W. (1992). Involvement of reactive oxygen intermediates in the induction of c-jun gene transcription by ionizing radiation. *Biochemistry* 31, 8300–6.
- Decker, P. and Muller, S. (2002). Modulating poly (ADP-ribose) polymerase activity: potential for the prevention and therapy of pathogenic situations involving DNA damage and oxidative stress. *Curr Pharm Biotechnol* 3, 275–83.
- Delamere, N.A. (1996). Ascorbic acid and the eye. *Subcell Biochem* 25, 313–29.
- den Hartog, G.J., Vegt, E., van der Vijgh, W.J., Haenen, G.R., and Bast, A. (2002). Hypochlorous acid is a potent inhibitor of acetylcholinesterase. *Toxicol Appl Pharmacol* 181, 228–32.
- DePaso, W.J. and Winterbauer, R.H. (1991). Interstitial lung disease. *Dis Mon* 37, 61–133.
- deRojas Walker, T., Tamir, S., Ji, H., Wishnok, J.S., and Tannenbaum, S.R. (1995). Nitric oxide induces oxidative damage in addition to deamination in macrophage DNA. *Chem Res Toxicol* 8, 473–7.
- Dobrowsky, R.T., Kamibayashi, C., Mumby, M.C., and Hannun, Y.A. (1993). Ceramide activates heterotrimeric protein phosphatase 2A. *J Biol Chem* 268, 15523–30.
- Downey, J.S. and Han, J. (1998). Cellular activation mechanisms in septic shock. *Front Biosci* 3, d468–76.
- Duke-Elder, S. and MacFaul, P.A. (1972). *Injuries, Part 2 Non-mechanical Injuries*, Henry Kimpton, London.
- El-Youssef, M. (2003). Wilson disease. *Mayo Clin Proc* 78, 1126–36.
- Elsayed, N.M., Omaye, S.T., Klain, G.J., and Korte, D.W., Jr. (1992). Free radical-mediated lung response to the monofunctional sulfur mustards butyl 2-chloroethyl sulfide after subcutaneous injection. *Toxicology* 72, 153–65.
- Emad, A. and Rezaian, G.R. (1997). The diversity of the effects of sulfur mustards gas inhalation on respiratory system 10 years after a single, heavy exposure: analysis of 197 cases. *Chest* 112, 734–8.

- Emad, A. and Rezaian, G.R. (1999). Immunoglobulins and cellular constituents of the BAL fluid of patients with sulfur mustards gas-induced pulmonary fibrosis. *Chest* 115, 1346–51.
- Erdinçler, D.S., Seven, A., İnci, F., Beger, T., and Candan, G. (1997). Lipid peroxidation and antioxidant status in experimental animals: effects of aging and hypercholesterolemic diet. *Clin Chim Acta* 265, 77–84.
- Fan, J., Shek, P.N., Suntres, Z.E., Li, Y.H., Oreopoulos, G.D., and Rotstein, O.D. (2000). Liposomal antioxidants provide prolonged protection against acute respiratory distress syndrome. *Surgery* 128, 332–8.
- Farrukh, I.S., Michael, J.R., Peters, S.P., Sciuto, A.M., Adkinson, N.F., Jr., Freeland, H.S., Paky, A., Spannhake, E.W., Summer, W.R., and Gurtner, G.H. (1988). The role of cyclooxygenase and lipoxygenase mediators in oxidant-induced lung injury. *Am Rev Respir Dis* 137, 1343–9.
- Fattman, C.L., Schaefer, L.M., and Oury, T.D. (2003). Extracellular superoxide dismutase in biology and medicine. *Free Radic Biol Med* 35, 236–56.
- Fernandez-Checa, J.C., Kaplowitz, N., Garcia-Ruiz, C., and Colell, A. (1998). Mitochondrial glutathione: importance and transport. *Semin Liver Dis* 18, 389–401.
- Folkes, L.K., Candeias, L.P., and Wardman, P. (1995). Kinetics and mechanisms of hypochlorous acid reactions. *Arch Biochem Biophys* 323, 120–6.
- Fox, M. and Scott, D. (1980). The genetic toxicology of nitrogen and sulfur mustards. *Mut Res* 75, 131–68.
- Freeman, M.L., Huntley, S.A., Meredith, M.J., Senisterra, G.A., and Lepock, J. (1997). Destabilization and denaturation of cellular protein by glutathione depletion. *Cell Stress Chaperones* 2, 191–8.
- Fu, Y., McCormick, C.C., Roneker, C., and Lei, X.G. (2001). Lipopolysaccharide and interferon-gamma-induced nitric oxide production and protein oxidation in mouse peritoneal macrophages are affected by glutathione peroxidase-1 gene knockout. *Free Radic Biol Med* 31, 450–9.
- Fujihara, M., Connolly, N., Ito, N., and Suzuki, T. (1994). Properties of protein kinase C isoforms (beta II, epsilon, and zeta) in a macrophage cell line (J774) and their roles in LPS-induced nitric oxide production. *J Immunol* 152, 1898–906.
- Gamaley, I.A. and Klyubin, I.V. (1999). Roles of reactive oxygen species: signaling and regulation of cellular functions. *Int Rev Cytol* 188, 203–55.
- Ganea, E. and Harding, J.J. (2006). Glutathione-related enzymes and the eye. *Curr Eye Res* 31, 1–11.
- Ghezzi, P. and Ungheri, D. (2004). Synergistic combination of *N*-acetylcysteine and ribavirin to protect from lethal influenza viral infection in a mouse model. *Int J Immunopathol Pharmacol* 17, 99–102.
- Ghosh, A., Akech, J., Mukherjee, S., and Das, S.K. (2002). Differential expression of cholinephosphotransferase in normal and cancerous human mammary epithelial cells. *Biochem Biophys Res Commun* 297, 1043–8.
- Gidwani, A., Brown, H.A., Holowka, D., and Baird, B. (2003). Disruption of lipid order by short-chain ceramides correlates with inhibition of phospholipase D and downstream signaling by FcepsilonRI. *J Cell Sci* 116, 3177–87.
- Goldman, M. and Dacre, J.C. (1989). Lewisite: its chemistry, toxicology, and biological effects. *Rev Environ Contam Toxicol* 110, 75–115.
- Griffith, O.W. and Meister, A. (1985). Origin and turnover of mitochondrial glutathione. *Proc Natl Acad Sci U S A* 82, 4668–72.
- Gunnarsson, M., Walther, S.M., Seidal, T., and Lennquist, S. (2000). Effects of inhalation of corticosteroids immediately after experimental chlorine gas lung injury. *J Trauma* 48, 101–7.
- Haddad, J.J. (2004). Redox and oxidant-mediated regulation of apoptosis signaling pathways: immunopharmacoredox conception of oxidative siege versus cell death commitment. *Int Immunopharmacol* 4, 475–93.
- Haliday, E.M., Ramesha, C.S., and Ringold, G. (1991). TNF induces c-fos via a novel pathway requiring conversion of arachidonic acid to a lipoxygenase metabolite. *EMBO J* 10, 109–15.
- Hampton, M.B., Fadeel, B., and Orrenius, S. (1998). Redox regulation of the caspases during apoptosis. *Ann N Y Acad Sci* 854, 328–35.
- Hanna, P.C., Kruskal, B.A., Ezekowitz, R.A., Bloom, B.R., and Collier, R.J. (1994). Role of macrophage oxidative burst in the action of anthrax lethal toxin. *Mol Med* 1, 7–18.
- Hannun, Y.A. and Obeid, L.M. (1997). Mechanisms of ceramide-mediated apoptosis. *Adv Exp Med Biol* 407, 145–9.
- Hannun, Y.A. and Luberto, C. (2000). Ceramide in the eukaryotic stress response. *Trends Cell Biol* 10, 73–80.

- Hayes, K.C. (1974). Retinal degeneration in monkeys induced by deficiencies of vitamin E or A. *Invest Ophthalmol* 13, 499–510.
- Hearps, A.C., Burrows, J., Connor, C.E., Woods, G.M., Lowenthal, R.M., and Ragg, S.J. (2002). Mitochondrial cytochrome *c* release precedes transmembrane depolarisation and caspase-3 activation during ceramide-induced apoptosis of Jurkat T cells. *Apoptosis* 7, 387–94.
- Hetz, C.A., Hunn, M., Rojas, P., Torres, V., Leyton, L., and Quest, A.F. (2002). Caspase-dependent initiation of apoptosis and necrosis by the Fas receptor in lymphoid cells: onset of necrosis is associated with delayed ceramide increase. *J Cell Sci* 115, 4671–83.
- Hirota, K., Matsui, M., Iwata, S., Nishiyama, A., Mori, K., and Yodoi, J. (1997). AP-1 transcriptional activity is regulated by a direct association between thioredoxin and Ref-1. *Proc Natl Acad Sci U S A* 94, 3633–8.
- Hogg, R. and Chakravarthy, U. (2004). AMD and micronutrient antioxidants. *Curr Eye Res* 29, 387–401.
- Holmgren, A. (1972). Tryptophan fluorescence study of conformational transitions of the oxidized and reduced form of thioredoxin. *J Biol Chem* 247, 1992–8.
- Holmgren, A. (1985). Thioredoxin. *Annu Rev Biochem* 54, 237–71.
- Holmgren, A. (1989). Thioredoxin and glutaredoxin systems. *J Biol Chem* 264, 13963–6.
- Hsu, W., Kerppola, T.K., Chen, P.L., Curran, T., and Chen Kiang, S. (1994). Fos and Jun repress transcription activation by NF-IL6 through association at the basic zipper region. *Mol Cell Biol* 14, 268–76.
- Hunt, D.F., Organisciak, D.T., Wang, H.M., and Wu, R.L. (1984). Alpha-tocopherol in the developing rat retina: a high pressure liquid chromatographic analysis. *Curr Eye Res* 3, 1281–8.
- Hwang, C., Sinskey, A.J., and Lodish, H.F. (1992). Oxidized redox state of glutathione in the endoplasmic reticulum. *Science* 257, 1496–502.
- Inoue, H., Asaka, T., Nagata, N., and Koshihara, Y. (1997). Mechanism of mustards oil-induced skin inflammation in mice. *Eur J Pharmacol* 333, 231–40.
- Jaskot, R.H., Grose, E.C., Richards, J.H., and Doerfler, D.L. (1991). Effects of inhaled phosgene on rat lung antioxidant systems. *Fundam Appl Toxicol* 17, 666–74.
- Javadi, M.A., Yazdani, S., Sajjadi, H., Jadidi, K., Karimian, F., Einollahi, B., Ja'farinasab, M.R., and Zare, M. (2005). Chronic and delayed-onset mustards gas keratitis: report of 48 patients and review of literature. *Ophthalmology* 112, 617–25.
- Jiang, Q. and Ames, B.N. (2003). Gamma-tocopherol, but not alpha-tocopherol, decreases proinflammatory eicosanoids and inflammation damage in rats. *FASEB J* 17, 816–22.
- Johnstone, R.M. (1963). Sulfhydryl Agents: Arsenicals. In *Metabolic Inhibitors* R.M. Hochester and J.H. Quastel (Eds.), New York: Academic Press, 99–118.
- Jones, D.P., Maellaro, E., Jiang, S., Slater, A.F., and Orrenius, S. (1995). Effects of *N*-acetyl-L-cysteine on T-cell apoptosis are not mediated by increased cellular glutathione. *Immunol Lett* 45, 205–9.
- Kadar, T., Turetz, J., Fishbine, E., Sahar, R., Chapman, S., and Amir, A. (2001). Characterization of acute and delayed ocular lesions induced by sulfur mustards in rabbits. *Curr Eye Res* 22, 42–53.
- Kang, K.A., Zhang, R., Lee, K.H., Chae, S., Kim, B.J., Kwak, Y.S., Park, J.W., Lee, N.H., and Hyun, J.W. (2006). Protective effect of triphlorethol-A from *Ecklonia cava* against ionizing radiation in vitro. *J Radiat Res (Tokyo)* 47, 61–8.
- Kehe, K. and Szinicz, L. (2005). Medical aspects of sulphur mustard poisoning. *Toxicology* 214(3): 198–209.
- Kent, C. (1995). Eukaryotic phospholipid biosynthesis. *Annu Rev Biochem* 64, 315–43.
- Kerppola, T.K. and Curran, T. (1994). Maf and Nrl can bind to AP-1 sites and form heterodimers with Fos and Jun. *Oncogene* 9, 675–84.
- Khachik, F., Bernstein, P.S., and Garland, D.L. (1997). Identification of lutein and zeaxanthin oxidation products in human and monkey retinas. *Invest Ophthalmol Vis Sci* 38, 1802–11.
- Kim, M.Y., Zhang, T., and Kraus, W.L. (2005). Poly(ADP-ribosylation) by PARP-1: 'PAR-laying' NAD⁺ into a nuclear signal. *Genes Dev* 19, 1951–67.
- Kimura, H., Sawada, T., Oshima, S., Kozawa, K., Ishioka, T., and Kato, M. (2005). Toxicity and roles of reactive oxygen species. *Curr Drug Targets Inflamm Allergy* 4, 489–95.
- Kinnula, V.L. and Crapo, J.D. (2003). Superoxide dismutases in the lung and human lung diseases. *Am J Respir Crit Care Med* 167, 1600–19.
- Kirlin, W.G., Cai, J., Thompson, S.A., Diaz, D., Kavanagh, T.J., and Jones, D.P. (1999). Glutathione redox potential in response to differentiation and enzyme inducers. *Free Radic Biol Med* 27(11–12): 1208–18.
- Kolesnick, R.N. and Krönke, M. (1998). Regulation of ceramide production and apoptosis. *Annu Rev Physiol* 60, 643–65.

- Kowluru, R.A. and Kennedy, A. (2001). Therapeutic potential of anti-oxidants and diabetic retinopathy. *Expert Opin Investig Drugs* 10, 1665–76.
- Krippner, A., Matsuno-Yagi, A., Gottlieb, R.A., and Babior, B.M. (1996). Loss of function of cytochrome *c* in Jurkat cells undergoing fas-mediated apoptosis. *J Biol Chem* 271, 21629–36.
- Kuhn, J.F., Hoerth, P., Hoehn, S.T., Preckel, T., and Tomer, K.B. (2006). Proteomics study of anthrax lethal toxin-treated murine macrophages. *Electrophoresis* 27, 1584–97.
- Kumar, O., Sugendran, K., and Vijayaraghavan, R. (2003). Oxidative stress associated hepatic and renal toxicity induced by ricin in mice. *Toxicol* 41, 333–8.
- Kun, E. and Bauer, P.I. (2001). Cell biological functions of PARP I: an overview. *Ital J Biochem* 50, 15–8.
- Kurinna, S.M., Tsao, C.C., Nica, A.F., Jiffar, T., and Ruvolo, P.P. (2004). Ceramide promotes apoptosis in lung cancer-derived A549 cells by a mechanism involving c-Jun NH₂-terminal kinase. *Cancer Res* 64, 7852–6.
- Langenberg, J.P., van der Schans, G.P., Spruit, H.E., Kuijpers, W.C., Mars-Groenendijk, R.H., van Dijk Knijnenburg, H.C., Trap, H.C., van Helden, H.P., and Benschop, H.P. (1998). Toxicokinetics of sulfur mustards and its DNA-adducts in the hairless guinea pig. *Drug Chem Toxicol* 21 Suppl 1, 131–47.
- Lee, W., Mitchell, P., and Tjian, R. (1987). Purified transcription factor AP-1 interacts with TPA-inducible enhancer elements. *Cell* 49, 741–52.
- Levitt, J.M., Lodhi, I.J., Nguyen, P.K., Ngo, V., Clift, R., Hinshaw, D.B., and Sweeney, J.F. (2003). Low-dose sulfur mustards primes oxidative function and induces apoptosis in human polymorphonuclear leukocytes. *Int Immunopharmacol* 3, 747–56.
- Libon, C., Forestier, F., Cotte-Laffitte, J., Labarre, C., and Quero, A.M. (1993). Effect of acute oral administration of alcohol on superoxide anion production from mouse alveolar macrophages. *J Leukoc Biol* 53, 93–8.
- Lin, D., Barnett, M. et al. (2005). Expression of superoxide dismutase in whole lens prevents cataract formation. *Mol Vis* 11, 853–858.
- Liu, H., Lightfoot, R., and Stevens, J.L. (1996). Activation of heat shock factor by alkylating agents is triggered by glutathione depletion and oxidation of protein thiols. *J Biol Chem* 271, 4805–12.
- Lo, Y.Y. and Cruz, T.F. (1995). Involvement of reactive oxygen species in cytokine and growth factor induction of c-fos expression in chondrocytes. *J Biol Chem* 270, 11727–30.
- Lou, M.F. (2003). Redox regulation in the lens. *Prog Retin Eye Res* 22, 657–82.
- Ludlum, D.B., Tong, P.A., Mehata, J.R., Kirk, M.C., and Papirmeister, B. (1984). Formation of ethylthioethyl deoxy guanosine from the reaction of chloroethyl ethyl sulphide with deoxyguanosine. *Cancer Res*, 44, 12(1): 5698–5701.
- Luthman, M. and Holmgren, A. (1982). Rat liver thioredoxin and thioredoxin reductase: purification and characterization. *Biochemistry* 21, 6628–33.
- Mastruzzo, C., Crimi, N., and Vancheri, C. (2002). Role of oxidative stress in pulmonary fibrosis. *Monaldi Arch Chest Dis* 57, 173–6.
- Mathias, S., Dressler, K.A., and Kolesnick, R.N. (1991). Characterization of a ceramide-activated protein kinase: stimulation by tumor necrosis factor alpha. *Proc Natl Acad Sci U S A* 88, 10009–13.
- Matthews, J.R., Wakasugi, N., Virelizier, J.L., Yodoi, J., and Hay, R.T. (1992). Thioredoxin regulates the DNA binding activity of NF- κ B by reduction of a disulphide bond involving cysteine 62. *Nucleic Acids Res* 20, 3821–30.
- McClintock, S.D., Till, G.O., Smith, M.G., and Ward, P.A. (2002). Protection from half-mustards-gas-induced acute lung injury in the rat. *J Appl Toxicol* 22, 257–62.
- McClintock, S.D., Hoesel, L.M., Das, S.K., Till, G.O., Neff, T., Kunkel, R.G., Smith, M.G., and Ward, P.A. (2006). Attenuation of half sulfur mustards gas-induced acute lung injury in rats. *J Appl Toxicol* 26, 126–31.
- McKenzie, S.M., Doe, W.F., and Buffinton, G.D. (1999). 5-aminosalicylic acid prevents oxidant mediated damage of glyceraldehyde-3-phosphate dehydrogenase in colon epithelial cells. *Gut* 44, 180–5.
- McMillan, D.C., Sarvate, S.D., Oatis, J.E., Jr., and Jollow, D.J. (2004). Role of oxidant stress in lawsone-induced hemolytic anemia. *Toxicol Sci* 82, 647–55.
- Megaw, J.M. (1984). Glutathione and ocular photobiology. *Curr Eye Res* 3, 83–7.
- Mei, N., Tamae, K., Kunugita, N., Hirano, T., and Kasai, H. (2003). Analysis of 8-hydroxydeoxyguanosine 5'-monophosphate (8-OH-dGMP) as a reliable marker of cellular oxidative DNA damage after gamma-irradiation. *Environ Mol Mutagen* 41, 332–8.

- Mercurio, F. and Manning, A.M. (1999a). Multiple signals converging on NF- κ B. *Curr Opin Cell Biol* 11, 226–32.
- Mercurio, F. and Manning, A.M. (1999b). NF- κ B as a primary regulator of the stress response. *Oncogene* 18, 6163–71.
- Meyer, M., Schreck, R., and Baeuerle, P.A. (1993). H₂O₂ and antioxidants have opposite effects on activation of NF- κ B and AP-1 in intact cells: AP-1 as secondary antioxidant-responsive factor. *EMBO J* 12, 2005–15.
- Mihm, S., Galter, D., and Droge, W. (1995). Modulation of transcription factor NF kappa B activity by intracellular glutathione levels and by variations of the extracellular cysteine supply. *FASEB J* 9, 246–52.
- Miquel, K., Pradines, A., Terce, F., Selmi, S., and Favre, G. (1998). Competitive inhibition of choline phosphotransferase by geranylgeraniol and farnesol inhibits phosphatidylcholine synthesis and induces apoptosis in human lung adenocarcinoma A549 cells. *J Biol Chem* 273, 26179–86.
- Mol, M.A., van de Ruit, A.M., and Kluivers, A.W. (1989). NAD⁺ levels and glucose uptake of cultured human epidermal cells exposed to sulfur mustards. *Toxicol Appl Pharmacol* 98, 159–65.
- Moore, L., and Ray, P. (1983). Enhanced inhibition of hepatic microsomal calcium pump activity by CCl₄ treatment of isopropanol-pretreated rats. *Toxicol Appl Pharmacol* 71, 54–8.
- Morad, Y., Banin, E. et al. (2005) Treatment of ocular tissues exposed to nitrogen mustard: beneficial effects of zinc desferrioxamine combined with steroids. *Invest Ophthalmol Vis Sci* 46(5): 1640–1646.
- Naghii, M.R. (2002). Sulfur mustards intoxication, oxidative stress, and antioxidants. *Mil Med* 167, 573–5.
- Noltkamper, D. and Burgher, S.W. (2004). Toxicity, phosgene. *eMedicine*.
- Nonas, S., Miller, I., Kawkitinarong, K., Chatchavalvanich, S., Gorshkova, I., Bochkov, V.N., Leitinger, N., Natarajan, V., Garcia, J.G., and Birukov, K.G. (2006). Oxidized phospholipids reduce vascular leak and inflammation in rat model of acute lung injury. *Am J Respir Crit Care Med* 173, 1130–8.
- Oei, S.L. and Shi, Y. (2001). Poly(ADP-ribosylation) of transcription factor Yin Yang 1 under conditions of DNA damage. *Biochem Biophys Res Commun* 285, 27–31.
- Ohia, S.E., Opere, C.A., and Leday, A.M. (2005). Pharmacological consequences of oxidative stress in ocular tissues. *Mutat Res* 579, 22–36.
- Okamoto, T., Ogiwara, H., Hayashi, T., Mitsui, A., Kawabe, T., and Yodoi, J. (1992). Human thioredoxin/adult T cell leukemia-derived factor activates the enhancer binding protein of human immunodeficiency virus type 1 by thiol redox control mechanism. *Int Immunol* 4, 811–9.
- Olea-Azar, C., Rigol, C., Mendizabal, F., Morello, A., Maya, J.D., Moncada, C., Cabrera, E., Di Maio, R., Gonzalez, M., and Cerecetto, H. (2003). ESR spin trapping studies of free radicals generated from nitrofurantoin derivative analogues of nifurtimox by electrochemical and Trypanosoma cruzi reduction. *Free Radic Res* 37, 993–1001.
- Pant, S.C., Vijayaraghavan, R., Kannan, G.M., and Ganesan, K. (2000). Sulfur mustards induced oxidative stress and its prevention by sodium 2,3-dimercapto propane sulphonic acid (DMPS) in mice. *Biomed Environ Sci* 13, 225–32.
- Papirmeister, B., Gross, C.L., Meier, H.L., Petrali, J.P., and Johnson, J.B. (1985). Molecular basis for mustard-induced vesication. *Fundam Appl Toxicol* 5, S134–49.
- Papirmeister, B., Feister, A.J., Robinson, S.I., and Ford, R.D. (1991). *Mustards Gas. Toxic Mechanisms and Pharmacological Implications*, CRC Press, Boca Raton, FL.
- Paredi, P., Kharitonov, S.A., and Barnes, P.J. (2002). Analysis of expired air for oxidation products. *Am J Respir Crit Care Med* 166, S31–7.
- Peters, R.A., Sinclair, H.M. et al. (1946). An analysis of the inhibition of pyruvate oxidation by arsenicals in relation to the enzyme theory of vesication. *Biochem J* 40(4): 516–524.
- Petronilli, V., Costantini, P., Scorrano, L., Colonna, R., Passamonti, S., and Bernardi, P. (1994). The voltage sensor of the mitochondrial permeability transition pore is tuned by the oxidation–reduction state of vicinal thiols. Increase of the gating potential by oxidants and its reversal by reducing agents. *J Biol Chem* 269, 16638–42.
- Powis, G., Mustacich, D., and Coon, A. (2000). The role of the redox protein thioredoxin in cell growth and cancer. *Free Radic Biol Med* 29, 312–22.
- Pullar, J.M., Winterbourn, C.C., and Vissers, M.C.M. (1999). Loss of GSH and thiol enzymes in endothelial cells exposed to sublethal concentrations of hypochlorous acid. *Am J Physiol Heart Circ Physiol* 277(4): H1505–12.

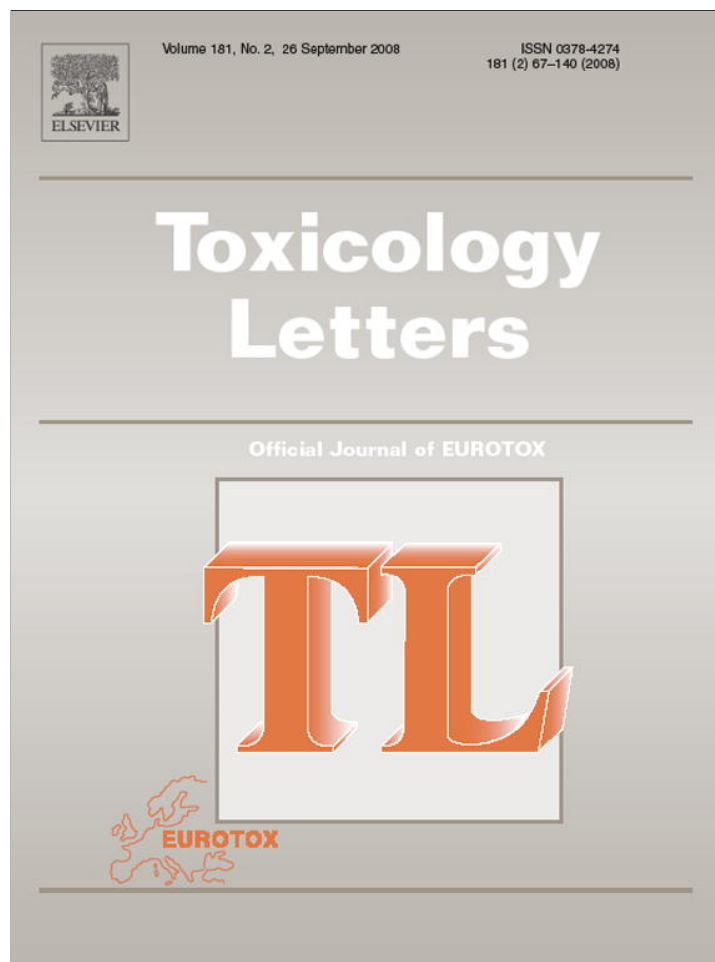
- Pullar, J.M., Vissers, M.C., and Winterbourn, C.C. (2001). Glutathione oxidation by hypochlorous acid in endothelial cells produces glutathione sulfonamide as a major product but not glutathione disulfide. *J Biol Chem* 276, 22120–5.
- Pullar, J.M., Winterbourn, C.C., and Vissers, M.C. (2002). The effect of hypochlorous acid on the expression of adhesion molecules and activation of NF- κ B in cultured human endothelial cells. *Antioxid Redox Signal* 4, 5–15.
- Qin, X.J., Hai, C.X., Liang, X., Wang, P., Chen, H.L., and Liu, R. (2004). [Effect of acute phosgene inhalation on antioxidant enzymes, nitric oxide and nitric-oxide synthase in rats]. *Zhonghua Lao Dong Wei Sheng Zhi Ye Bing Za Zhi* 22, 200–2.
- Rahman, I. and Kelly, F. (2003). Biomarkers in breath condensate: a promising new non-invasive technique in free radical research. *Free Radic Res* 37, 1253–66.
- Rahman, I. and MacNee, W. (1998). Role of transcription factors in inflammatory lung diseases. *Thorax* 53, 601–12.
- Rahman, I., Marwick, J., and Kirkham, P. (2004). Redox modulation of chromatin remodeling: impact on histone acetylation and deacetylation, NF- κ B and pro-inflammatory gene expression. *Biochem Pharmacol* 68, 1255–67.
- Ramos, B., Salido, G.M., Campo, M.L., and Claro, E. (2000). Inhibition of phosphatidylcholine synthesis precedes apoptosis induced by C2-ceramide: protection by exogenous phosphatidylcholine. *Neuroreport* 11, 3103–8.
- Ramos, B., El Mouedden, M., Claro, E., and Jackowski, S. (2002). Inhibition of CTP: phosphocholine cytidylyltransferase by C(2)-ceramide and its relationship to apoptosis. *Mol Pharmacol* 62, 1068–75.
- Rao, G.N., Glasgow, W.C., Eling, T.E., and Runge, M.S. (1996). Role of hydroperoxyeicosatetraenoic acids in oxidative stress-induced activating protein 1 (AP-1) activity. *J Biol Chem* 271, 27760–4.
- Reddy, V.N. (1990). Glutathione and its function in the lens—an overview. *Exp Eye Res* 50, 771–8.
- Reddy, V.N. and Giblin, F.J. (1984). Metabolism and function of glutathione in the lens. *Ciba Found Symp* 106, 65–87.
- Reed, D.J. and Savage, M.K. (1995). Influence of metabolic inhibitors on mitochondrial permeability transition and glutathione status. *Biochim Biophys Acta* 1271, 43–50.
- Ricketts, K.M., Santai, C.T., France, J.A., Graziosi, A.M., Doyel, T.D., Gazaway, M.Y., and Casillas, R.P. (2000). Inflammatory cytokine response in sulfur mustards-exposed mouse skin. *J Appl Toxicol* 20 Suppl 1, S73–6.
- Rikimaru, T., Nakamura, M., Yano, T., Beck, G., Habicht, G.S., Rennie, L.L., Widra, M., Hirshman, C.A., Boulay, M.G., Spannhake, E.W. et al. (1991). Mediators, initiating the inflammatory response, released in organ culture by full-thickness human skin explants exposed to the irritant, sulfur mustards. *J Invest Dermatol* 96, 888–97.
- Roberts, J.E. (2001). Ocular phototoxicity. *J Photochem Photobiol B* 64(2–3): 136–143.
- Rose, R.C., Richer, S.P., and Bode, A.M. (1998). Ocular oxidants and antioxidant protection. *Proc Soc Exp Biol Med* 217, 397–407.
- Rosenthal, D.S., Simbulan Rosenthal, C.M., Iyer, S., Spoonde, A., Smith, W., Ray, R., and Smulson, M.E. (1998). Sulfur mustards induces markers of terminal differentiation and apoptosis in keratinocytes via a Ca²⁺-calmodulin and caspase-dependent pathway. *J Invest Dermatol* 111, 64–71.
- Ryan, A.J., McCoy, D.M., McGowan, S.E., Salome, R.G., and Mallampalli, R.K. (2003). Alveolar sphingolipids generated in response to TNF-alpha modifies surfactant biophysical activity. *J Appl Physiol* 94, 253–8.
- Sabourin, C.L., Danne, M.M., Buxton, K.L., Casillas, R.P., and Schlager, J.J. (2002). Cytokine, chemokine, and matrix metalloproteinase response after sulfur mustards injury to weanling pig skin. *J Biochem Mol Toxicol* 16, 263–72.
- Safarinejad, M.R., Moosavi, S.A., and Montazeri, B. (2001). Ocular injuries caused by mustards gas: diagnosis, treatment and medical defense. *Mil Med* 166, 67–70.
- Saitoh, M., Nishitoh, H., Fujii, M., Takeda, K., Tobiume, K., Sawada, Y., Kawabata, M., Miyazono, K., and Ichijo, H. (1998). Mammalian thioredoxin is a direct inhibitor of apoptosis signal-regulating kinase (ASK) 1. *EMBO J* 17, 2596–606.
- Sato, S., Furuta, K., Miyake, T., Mishiro, T., Kohge, N., Akagi, S., Uchida, Y., Rumi, M.A., Ishihara, S., Adachi, K., and Kinoshita, Y. (2006). Hemolytic anemia during 24 weeks of ribavirin and interferon-alpha2b combination therapy does not influence the cardiac function of patients with viral hepatitis C. *J Clin Gastroenterol* 40, 88–9.

- Schlager, J.J. and Hart, B.W. (2000). Stress gene activity in HepG2 cells after sulfur mustards exposure. *J Appl Toxicol* 20, 395–405.
- Schnellmann, R.G., Gilchrist, S.M., and Mandel, L.J. (1988). Intracellular distribution and depletion of glutathione in rabbit renal proximal tubules. *Kidney Int* 34, 229–33.
- Schulze-Osthoff, K., Bauer, M.K., Vogt, M., and Wesselborg, S. (1997). Oxidative stress and signal transduction. *Int J Vitam Nutr Res* 67, 336–42.
- Sciuto, A.M. (1998). Assessment of early acute lung injury in rodents exposed to phosgene. *Arch Toxicol* 72, 283–8.
- Sciuto, A.M. (2000). Posttreatment with ETYA protects against phosgene-induced lung injury by amplifying the glutathione to lipid peroxidation ratio. *Inhal Toxicol* 12, 347–56.
- Sciuto, A.M., and Hurt, H.H. (2004). Therapeutic treatments of phosgene-induced lung injury. *Inhal Toxicol* 16, 565–80.
- Sciuto, A.M. and Moran, T.S. (2001). Effect of dietary treatment with n-propyl gallate or vitamin E on the survival of mice exposed to phosgene. *J Appl Toxicol* 21, 33–9.
- Sciuto, A.M., Phillips, C.S., Orzolek, L.D., Hege, A.I., Moran, T.S., and Dillman, J.F., III. (2005). Genomic analysis of murine pulmonary tissue following carbonyl chloride inhalation. *Chem Res Toxicol* 18, 1654–60.
- Segal, E. and Lang, E. (2005). Toxicity, chlorine gas. *eMedicine*.
- Sellmayer, A., Uedelhoven, W.M., Weber, P.C., and Bonventre, J.V. (1991). Endogenous non-cyclooxygenase metabolites of arachidonic acid modulate growth and mRNA levels of immediate-early response genes in rat mesangial cells. *J Biol Chem* 266, 3800–7.
- Sen, C.K. (1998). Redox signaling and the emerging therapeutic potential of thiol antioxidants. *Biochem Pharmacol* 55, 1747–58.
- Shapira, L., Takashiba, S., Champagne, C., Amar, S., and Van Dyke, T.E. (1994). Involvement of protein kinase C and protein tyrosine kinase in lipopolysaccharide-induced TNF-alpha and IL-1 beta production by human monocytes. *J Immunol* 153, 1818–24.
- Shapira, L., Sylvia, V.L., Halabi, A., Soskolne, W.A., Van Dyke, T.E., Dean, D.D., Boyan, B.D., and Schwartz, Z. (1997). Bacterial lipopolysaccharide induces early and late activation of protein kinase C in inflammatory macrophages by selective activation of PKC-epsilon. *Biochem Biophys Res Commun* 240, 629–34.
- Shichi, H. (2004). Cataract formation and prevention. *Expert Opin Investig Drugs* 13, 691–701.
- Sickel, W. (1972). *Retinal Metabolism in Dark and Light*, Springer-Verlag, Berlin.
- Sidell, F., Urbanetti, J.S., Smith, W.J., and Hurst, C.G. (1997). Vesicants. In textbook of military medicine. Washington, DC: Borden Institute, Walter Reed Army Medical Center.
- Sidell, F., Urbanetti, J.S., Smith, W.J., and Hurst, C.G. (1997). *Chapter 7 – Vesicants*.
- Sikpi, M. and Das, S. (1987). Development of cholinephosphotransferase in guinea pig lung mitochondria and microsomes. *Biochim Biophys Acta* 899, 35–43.
- Singh, I., Pahan, K., Khan, M., and Singh, A.K. (1998). Cytokine-mediated induction of ceramide production is redox-sensitive. Implications to proinflammatory cytokine-mediated apoptosis in demyelinating diseases. *J Biol Chem* 273, 20354–62.
- Sinha Roy, S., Mukherjee, S., Kabir, S., Rajaratnam, V., Smith, M., and Das, S.K. (2005). Inhibition of cholinephosphotransferase activity in lung injury induced by 2-chloroethyl ethyl sulfide, a mustards analog. *J Biochem Mol Toxicol* 19, 289–97.
- Smith, C.V., Jones, D.P., Guenther, T.M., Lash, L.H., and Lauterburg, B.H. (1996). Compartmentation of glutathione: implications for the study of toxicity and disease. *Toxicol Appl Pharmacol* 140, 1–12.
- Snodderly, D.M., Brown, P.K., Delori, F.C., and Auran, J.D. (1984). The macular pigment. I. Absorbance spectra, localization, and discrimination from other yellow pigments in primate retinas. *Invest Ophthalmol Vis Sci* 25, 660–673.
- Snodderly, D.M. (1995). Evidence for protection against age-related macular degeneration by carotenoids and antioxidant vitamins. *Am J Clin Nutr* 62, 1448S–61.
- Sohrappour, H. (1984). Clinical manifestations of chemical agents on Iranian combatants during Iran–Iraq conflict. *Arch Belg Suppl*, 291–7.
- Solberg, Y., Alcalay, M. et al. (1997). Ocular injury by mustard gas. *Surv Ophthalmol* 41(6): 461–466.
- Somani, S.M. and Babu, S.R. (1989). Toxicodynamics of sulfur mustards. *Int J Clin Pharmacol Ther Toxicol* 27, 419–35.
- Stadtman, E.R. (2001). Protein oxidation in aging and age-related diseases. *Ann NY Acad Sci* 928: 22–38.

- Stauble, B., Boscoboinik, D., Tassinato, A., and Azzi, A. (1994). Modulation of activator protein-1 (AP-1) transcription factor and protein kinase C by hydrogen peroxide and D-alpha-tocopherol in vascular smooth muscle cells. *Eur J Biochem* 226, 393–402.
- Stith, I.E. and Das, S.K. (1981). Pulmonary surfactant lipids: studies on cholinephosphotransferase in developing guinea pig lung. *Indian Biologist* 13, 120–8.
- Stith, I.E. and Das, S.K. (1982). Development of cholinephosphotransferase in guinea pig lung and mitochondria and microsomes. *Biochem Biophys Acta* 714, 250–6.
- Stocken, L.A. and Thompson, R.H.S. (1946c). British anti-lewisite. 3. Arsenic and thiol excretion in animals after treatment of lewisite burns. *Biochem J* 40: 548–554.
- Stone, W.L., Mukherjee, S., Smith, M., and Das, S.K. (2002). Therapeutic uses of antioxidant liposomes. *Methods Mol Biol* 199, 145–61.
- Stone, W.L., Qui, M., and Smith, M. (2003). Lipopolysaccharide enhances the cytotoxicity of 2-chloroethyl ethyl sulfide. *BMC Cell Biol* 4, 1.
- Stone, W.L., Qui, M., Yang, H., and Smith, M. (2004). Lipopolysaccharide enhances the cytotoxicity of 2-chloroethyl ethyl sulfide. *Bioscience Proceedings* Chapter 236, 1–9.
- Suntres, Z., Stone, W., and Smith, M.G. (2005). Ricin-induced tissue toxicity: the role of oxidative stress. *J Med CBR Def* 3, http://www.jmedcbr.org/Issue-0301/Suntres/Suntres_1205.html.
- Tagaya, Y., Maeda, Y., Mitsui, A., Kondo, N., Matsui, H., Hamuro, J., Brown, N., Arai, K., Yokota, T., Wakasugi, H., and et al. (1989). ATL-derived factor (ADF), an IL-2 receptor/Tac inducer homologous to thioredoxin; possible involvement of dithiol-reduction in the IL-2 receptor induction. *EMBO J* 8, 757–64.
- Torchinsky, Y.M. (1981). *Sulfur in Proteins*, Pergamon, Oxford, UK.
- Truscott, R.J. (2005). Age-related nuclear cataract-oxidation is the key. *Exp Eye Res* 80, 709–25.
- van Blitterswijk, W.J., van der Luit, A.H., Veldman, R.J., Verheij, M., and Borst, J. (2003). Ceramide: second messenger or modulator of membrane structure and dynamics? *Biochem J* 369, 199–211.
- van Heyningen, R. (1941). The properties and -SH nature of hexokinase. *Report ETF*, Military Intelligence Division. Great Britain.
- Veness-Meehan, K.A., Cheng, E.R., Mercier, C.E., Blixt, S.L., Johnston, C.J., Watkins, R.H., and Horowitz, S. (1991). Cell-specific alterations in expression of hyperoxia-induced mRNAs of lung. *Am J Respir Cell Mol Biol* 5, 516–21.
- Victor, I., Schwenger, P., Li, W., Schlessinger, J., and Vilcek, J. (1993). Tumor necrosis factor-induced activation and increased tyrosine phosphorylation of mitogen-activated protein (MAP) kinase in human fibroblasts. *J Biol Chem* 268, 18994–9.
- Virag, L. (2005). Structure and function of poly(ADP-ribose) polymerase-1: role in oxidative stress-related pathologies. *Curr Vasc Pharmacol* 3, 209–14.
- Vissers, M.C. and Winterbourn, C.C. (1995). Oxidation of intracellular glutathione after exposure of human red blood cells to hypochlorous acid. *Biochem J* 307 (Pt 1), 57–62.
- Vivekananda, J., Smith, D., and King, R.J. (2001). Sphingomyelin metabolites inhibit sphingomyelin synthase and CTP: phosphocholine cytidyltransferase. *Am J Physiol Lung Cell Mol Physiol* 281, L98–107.
- Voehringer, D.W., McConkey, D.J., McDonnell, T.J., Brisbay, S., and Meyn, R.E. (1998). Bcl-2 expression causes redistribution of glutathione to the nucleus. *Proc Natl Acad Sci U S A* 95, 2956–60.
- Vogt, R.F., Dannenberg, A.L., Schofiels, B., Hynes, N., and Papirmeister, B. (1984). Pathogenesis of skin caused by sulfur mustards. *Fundam Appl Toxicol* 4: 571–583.
- Walker, I. (1967). *Protection of Animal Cells Against Mustards Gas by Pretreatment with Dithiothreitol*. Proceeding of the 5th International Congress Chemotherapy, Vienna.
- Walker, I.G. and Smith, W. (1969). Protection of L-cells by thiols against the toxicity of sulfur mustards. *Can J Physiol Pharmacol* 47, 143–51.
- Walker, L.J., Robson, C.N., Black, E., Gillespie, D., and Hickson, I.D. (1993). Identification of residues in the human DNA repair enzyme HAP1 (Ref-1) that are essential for redox regulation of Jun DNA binding. *Mol Cell Biol* 13, 5370–6.
- Wan, X.S., Zhou, Z., Ware, J.H., and Kennedy, A.R. (2005). Standardization of a fluorometric assay for measuring oxidative stress in irradiated cells. *Radiat Res* 163, 232–40.
- Wardell, B.L. (1941). Lewisite (M-1): Summary of physiologic and toxicologic data. *Report No. EATR 285*. Edgewood Arsenal, MD: Chemical Warfare Service.
- Watson, W.H., Yang, X., Choi, Y.E., Jones, D.P., and Kehrer, J.P. (2004). Thioredoxin and its role in toxicology. *Toxicol Sci* 78, 3–14.

- Weiss, D.J. and Lunte, C.E. (2000). Detection of a urinary biomaker for oxidative DNA damage 8-hydroxydeoxyguanosine by capillary electrophoresis with electrochemical detection. *Electrophoresis* 21, 2080–5.
- Winterbourn, C.C. (1985). Comparative reactivities of various biological compounds with myeloperoxidase-hydrogen peroxide-chloride, and similarity of the oxidant to hypochlorite. *Biochim Biophys Acta* 840, 204–10.
- Wormser, U. (1991). Toxicology of mustards gas. *Trends in Pharmacological Sciences* 12, 164–7.
- Wormser, U., Brodsky, B., Green, B.S., Arad-Yellin, R., and Nyska, A. (1997). Protective effect of povidone-iodine ointment against skin lesions induced by sulfur mustards and by non-mustards vesicants. *Arch Toxicol* 71, 165–70.
- Wormser, U., Brodsky, B., Green, B.S., Arad-Yellin, R., and Nyska, A. (2000). Protective effect of povidone iodine ointment against skin lesions induced by chemical and thermal stimuli. *J Appl Toxicol* 20 Suppl 1, S183–5.
- Wright, S.D., Ramos, R.A., Tobias, P.S., Ulevitch, R.J., and Mathison, J.C. (1990). CD14, a receptor for complexes of lipopolysaccharide (LPS) and LPS binding protein. *Science* 249, 1431–3.
- Xanthoudakis, S. and Curran, T. (1992). Identification and characterization of Ref-1, a nuclear protein that facilitates AP-1 DNA-binding activity. *EMBO J* 11, 653–65.
- Xanthoudakis, S., Miao, G., Wang, F., Pan, Y.C., and Curran, T. (1992). Redox activation of Fos-Jun DNA binding activity is mediated by a DNA repair enzyme. *EMBO J* 11, 3323–35.
- Xanthoudakis, S., Miao, G.G., and Curran, T. (1994). The redox and DNA-repair activities of Ref-1 are encoded by nonoverlapping domains. *Proc Natl Acad Sci U S A* 91, 23–7.
- Ye, J., Wang, S., Leonard, S.S., Sun, Y., Butterworth, L., Antonini, J., Ding, M., Rojanasakul, Y., Vallyathan, V., Castranova, V., and Shi, X. (1999). Role of reactive oxygen species and p53 in chromium(VI)-induced apoptosis. *J Biol Chem* 274, 34974–80.
- Yodoi, J. and Uchiyama, T. (1992). Diseases associated with HTLV-I: virus, IL-2 receptor dysregulation and redox regulation. *Immunol Today* 13, 405–11.
- Yourick, J.J., Clark, C.R., and Mitcheltree, L.W. (1991). Niacinamide pretreatment reduces microvesicle formation in hairless guinea pigs cutaneously exposed to sulfur mustards. *Fundam Appl Toxicol* 17, 533–42.
- Zhang, J., Johnston, G., Stebler, B., and Keller, E.T. (2001). Hydrogen peroxide activates NFkappaB and the interleukin-6 promoter through NFkappaB-inducing kinase. *Antioxid Redox Signal*, 3(3): 493–504.
- Zong, W.X., Ditsworth, D., Bauer, D.E., Wang, Z.Q., and Thompson, C.B. (2004). Alkylating DNA damage stimulates a regulated form of necrotic cell death. *Genes Dev* 18, 1272–82.

Provided for non-commercial research and education use.
Not for reproduction, distribution or commercial use.



This article appeared in a journal published by Elsevier. The attached copy is furnished to the author for internal non-commercial research and education use, including for instruction at the authors institution and sharing with colleagues.

Other uses, including reproduction and distribution, or selling or licensing copies, or posting to personal, institutional or third party websites are prohibited.

In most cases authors are permitted to post their version of the article (e.g. in Word or Tex form) to their personal website or institutional repository. Authors requiring further information regarding Elsevier's archiving and manuscript policies are encouraged to visit:

<http://www.elsevier.com/copyright>



Contents lists available at ScienceDirect

Toxicology Letters

journal homepage: www.elsevier.com/locate/toxlet

Activation of MAPK/AP-1 signaling pathway in lung injury induced by 2-chloroethyl ethyl sulfide, a mustard gas analog

Sutapa Mukhopadhyay^a, Shyamali Mukherjee^a, Milton Smith^b, Salil K. Das^{a,*}^a Department of Cancer Biology, Meharry Medical College, 1005 David Todd Blvd., Nashville, TN 37208, United States^b AMAOX Ltd, Melbourne, FL 32944, USA

ARTICLE INFO

Article history:

Received 7 May 2008

Received in revised form 2 July 2008

Accepted 2 July 2008

Available online 15 July 2008

Keywords:

MAPK

AP-1

Lung injury

CEES

ABSTRACT

We reported earlier that the activation of free-radical-mediated tumor necrosis factor- α (TNF- α) cascade is the major pathway in the inflammatory lung disease induced by 2-chloroethyl ethyl sulfide (CEES), a mustard gas analog. TNF- α induces activating protein 1 (AP-1) activation via phosphorylation of mitogen activated protein kinases (MAPKs). The present study examines the relationship between CEES induced lung injury and MAPKs signaling pathway. Adult guinea pigs received single intratracheal injection of different doses of CEES and were sacrificed at different time points. CEES exposure caused lung injury with evidence of fibrosis. The optimum activation of all members of the MAPKs family (ERK1/2, p38 and JNK1/2) was achieved at 0.5 mg/kg dose and at 1 h. No significant change was observed beyond that time point. This led to an activation of AP-1 transcription factors associated with an increase in the protein levels of Fos, activating transcription factor (ATF) and Jun family members. To explore the involvement of AP-1 in cell proliferation, we determined the protein levels of cell cycle protein cyclin D1 and cell differentiation marker proliferating cell nuclear antigen (PCNA). An up regulation of these proteins was observed. Hence it is suggested that CEES exposure causes accumulation of TNF- α , which is associated with an activation of MAPK/AP-1 signaling pathway and cell proliferation. Further studies are needed to clarify whether the observed effects are the adaptive responses of the lung or they contribute to the lung injury.

© 2008 Elsevier Ireland Ltd. All rights reserved.

1. Introduction

Mustard gas is a well-known chemical warfare agent which was extensively used in World War I (Willems, 1989; Mellor et al., 1991). This poisonous chemical agent exerts its effects on eyes, skin, and respiratory tissue, and thereby impairment of nervous, cardiac, and digestive systems in humans and laboratory animals (Elsayed et al., 1989a,b; Momeni et al., 1992; Debrowska et al., 1996; Dacre and Goldman, 1996). Inhalation of mustard gas causes hemorrhagic inflammation to the tracheobronchial tree, with severe pulmonary complications, including adult respiratory distress syndrome (ARDS) (Elsayed et al., 1989a,b). Long-term exposure of mustard gas at low doses may lead to lung cancer (Calvet et al., 1994).

The basis for the tissue injuries caused by mustard gas is not fully understood. Mustard gas belongs to a group of bifunctional alkylating agents that has electrophilic properties. Several studies in rats and mice have shown that the mechanism of mustard gas

action on lung, skin, or other organ includes DNA alkylation; cross-linking of DNA (Gross et al., 1985; Elsayed et al., 1992; Yamakido et al., 1996); activation of proteases, resulting in proteolysis of several vital intracellular enzymes and structural proteins (Cowman and Broomfield, 1993); production of free radicals and free radical-mediated oxidative stress (Kopff et al., 1994; Husain et al., 1996).

Mustard gas induced lung injury is associated with pulmonary fibrosis (McClintock et al., 2006). Tumor necrosis factor- α (TNF- α) is an important cytokine involved in the pathogenesis of inflammatory diseases of the lung. We have established earlier that the initiation of free-radical-mediated TNF- α cascade is the major pathway in the mustard gas mediated lung injury in guinea pigs (Chatterjee et al., 2003; Das et al., 2003). TNF- α induces transcriptional factor activating protein 1 (AP-1) activation via phosphorylation and activation of mitogen activated protein kinases (MAPKs) (Cohen et al., 2006). Interestingly, the promoter regions of many inflammatory cytokines and chemokines contain AP-1 binding sites (Koj, 1996; Zagariya et al., 1998; Roebuck et al., 1999) suggesting that AP-1 activation may be necessary for the induction of acute, cytokine-mediated inflammation. However, it is not known whether a similar mechanism is responsible for mustard gas induced lung injury in guinea pigs.

* Corresponding author. Tel.: +1 615 327 6988; fax: +1 615 327 6442.
E-mail address: sdas@mmc.edu (S.K. Das).

MAPKs cascades are multi-functional signaling pathways that are evolutionally well conserved in all eukaryotic cells. MAPKs are serine/threonine kinases that are sequentially phosphorylated by upstream kinases. Three major pathways, such as extracellular signal-regulating kinases (ERKs), c-Jun N-terminal kinases (JNKs, also referred to as stress-activated protein kinases), and p38 MAP kinases have been characterized (Kyriakis and Avruch, 2001; Takeda et al., 2003). They mediate signal transduction from the cell surface to the nucleus. Activation of ERK is primarily involved in growth factor- and phorbol ester-stimulated responses. Responses to pro-inflammatory cytokines, UV radiation, and other stresses are mostly dependent on JNK and p38 activation (Karin, 1995; Shaulian and Karin, 2001).

MAPK signaling pathways have been shown to affect AP-1 activity by direct phosphorylation of AP-1 proteins and by influence on the abundance of individual AP-1 components in a cell (Karin, 1995; Whitmarsh and Davis, 1996). AP-1 is an important regulatory protein involved in cell growth, differentiation, transformation, and apoptosis (Angel and Karin, 1991; Shaulian and Karin, 2001). The AP-1 complex consists of homo- or heterodimers of Fos families (c-Fos, Fos-B, Fra-1 and Fra-2), activating transcription factor families (ATF-1 and ATF-2) and Jun subfamilies (c-Jun, Jun-B and Jun-D) of basic-region leucine-zipper (B-ZIP) proteins (Herdegen and Leah, 1998; Steinmuller et al., 2001; Shaulian and Karin, 2002). These transcription factors act as converging points to MAPK signal transduction pathways activated by toxic or mitogenic stimuli. Upon activation, AP-1 binds to DNA sequences, such as 5'-TGAG/CTCA-3' [TPA response element (TRE) or AP-1 site], and regulates the transcription of multiple genes, including themselves, in a context (promoter and cell type) - dependent manner (Angel and Karin, 1991; Zhang et al., 2004). Activation of JNK leads to the phosphorylation and activation of c-Jun, and ATF-2, that form heterodimers and preferentially bind to TRE to activate c-Jun transcription, and activation of p38 can also phosphorylate and activate ATF-2 (Karin, 1995). AP-1 proteins have been suggested to play both pro- and anti-regulatory roles

in pulmonary defense, injury, and repair (Reddy and Mossman, 2002).

Based on this knowledge, it is important to evaluate the role of MAPK phosphorylation and subsequent AP-1 activation on the mustard gas induced lung injury. We hypothesized that exposure of 2-chloroethyl ethyl sulfide (CEES), a mustard gas analog modulates AP-1 family member expression in lung tissue, thereby altering protein-protein interactions between themselves and other members of the leucine-zipper super family of transcription factors. In this study, we investigated the roles of MAPK signaling pathways in the regulation of AP-1 transcriptional activity as well as AP-1 dependent cell cycle proteins.

2. Materials and methods

2.1. Animals and CEES treatment

Male guinea pigs (Hartley strain, 5–6 weeks old, 400 g body weight) were obtained from Harlan Sprague-Dawley Inc. (Indianapolis, IN). To determine the optimum treatment time, animals were infused intratracheally with a single dose (0.5 mg/kg body wt.) of CEES (Sigma Chemicals, St. Louis, MO) in ethanol (infusion volume was 100 μ l/animal). Control animals were infused with 100 μ l of ethanol in the same way. The animals were then sacrificed after different time points of 1 h and 1, 7, 14 and 30 days post-CEES infusion. For dose-dependent studies, animals were intratracheally infused with single injection of different doses (0.5, 2 and 4 mg/kg body wt.) of CEES in ethanol for 1 h. Lungs were perfused with 2.6 mM phosphate buffered saline containing 5.6 mM glucose, removed from the chest cavity and immediately flash frozen in liquid nitrogen and stored at -80°C for further experiment.

2.2. AP-1 activation assay

The activation of individual family member of AP-1 in the lung tissues was measured by TransAM AP-1 ELISA kits (Active Motif, Carlsbad, CA) according to the manufacturer's protocol.

2.3. Western blot analysis

Lung tissues were homogenized in a 5 volume of ice cold lysis buffer (Biosource, Camarillo, CA) containing protease inhibitor cocktail (0.01%, Sigma Chemicals, St. Louis, MO) by using a Brinkman Polytron (setting 6–7, 30 s). Proteins were measured by Bio-Rad protein assay (Bio-Rad, Hercules, CA) and 50 μ g protein was separated by

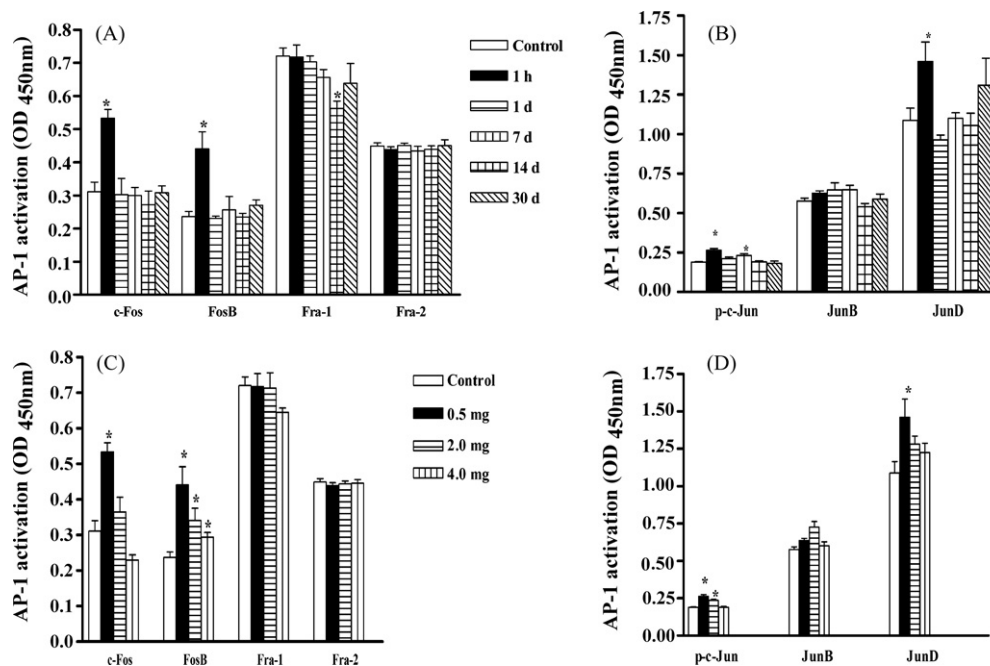


Fig. 1. CEES-induced activation of DNA binding of AP-1 family members in guinea pig lung. (A) Time dependent induction of AP-1 DNA binding activity after intratracheal injection of CEES (0.5 mg/kg body wt.). (B) DNA binding activity of AP-1 1 h after exposure to CEES at different doses (ranging from 0.5 to 4.0 mg/kg body wt.). Statistical significance was determined by Dunnett's test after one-way ANOVA. Results are expressed as mean \pm S.E. ($N = 3$), * $p < 0.05$ compared to control.

12% SDS polyacrylamide gel electrophoresis (SDS-PAGE). Proteins were transferred electrophoretically onto PVDF membranes Immobilon-P (Millipore, Bedford, MA). The membrane was immunoblotted with primary antibodies: MAPK (Cell Signaling Tech., Danvers, MA), c-Fos, FosB, Fra-1, Fra-2, c-Jun, JunB, JunD, ATF-2, L-ZIP, cyclin D1 and proliferating cell nuclear antigen (PCNA) (Santa Cruz Biotechnology Inc., Santa Cruz, CA) and horseradish peroxidase (HRP)-conjugated anti mouse, anti-goat and anti-rabbit secondary antibodies. Binding of antibodies to the blots was detected with an ECL-detection system (PerkinElmer, Boston, MA) following manufacturer's instructions. Stripped blots were re-probed with β -actin specific polyclonal antibodies (Santa Cruz Biotechnology Inc., Santa Cruz, CA) to enable normalization of signals between samples. Band intensities were analyzed using Bio-Rad Gel Doc (Bio-Rad, Hercules, CA).

2.4. Statistical analysis

Data were expressed as means \pm standard error (S.E.). Statistical significance was determined by the Student's *t*-test or by Dunnett's test after one-way analysis of variance (ANOVA), when multiple comparisons were made, using GraphPad prism Version 4.0 (GraphPad software, San Diego, CA). Results were considered statistically significant at $p < 0.05$.

3. Results

3.1. AP-1 family profiling for DNA binding activation after CEES exposure

To determine the time at which maximal activation of AP-1 is expressed, we have given single intratracheal injection (0.5 mg/kg body weight) of CEES to guinea pigs. At different time points, the guinea pigs were sacrificed and lungs were removed after perfusion and AP-1 activation were measured. Fig. 1A shows the effects of CEES on activation of AP-1 over time. The DNA binding activity of c-Fos, FosB, p-c-Jun and JunD was increased within 1 h of CEES exposure, but the activity decreased rapidly after 1 h and came to the normal level up to 30 days. No effect was noticed on Fra-1, Fra-2 and JunB. Fig. 1B shows the dose-dependent effects of CEES on AP-1 activation after 1 h. These studies revealed that optimal DNA activation of c-Fos, Fos B, p-c-Jun and JunD was observed at 0.5 mg/kg dose of CEES exposure.

3.2. Effects of CEES on MAPK activity

The optimum activation of individual family member of AP-1 was achieved at 0.5 mg dose and at 1 h; hence we focused our research on that particular dose and time point. CEES exposure caused a 100%, 33% and 42% increase in the phosphorylation of ERK1/2 (p44/42), p38 and JNK 1/2 (p54/46), respectively (Fig. 2).

3.3. Western blot analysis of AP-1 transcription factors

Since we observed a higher DNA binding activity of AP-1 transcription factor in CEES-exposed lung (Fig. 1), we determined the protein levels of individual members of AP-1 family. First we studied the protein levels of ATF-2 and L-ZIP. CEES exposure caused a significant increase in the protein level of only ATF-2 (68%) and not L-ZIP (Fig. 3A).

Among Fos members of the AP-1 transcription factors family, the optimum activation was achieved at 0.5 mg dose and at 1 h. The protein level was significantly increased in all four members of Fos family (Fig. 3B). CEES exposure caused a 134%, 75%, 250%, and 51% increase in the protein levels of c-Fos, FosB, Fra-1 and Fra-2, respectively. It should be noted however that even though protein levels of Fra-1 and Fra-2 were increased due to CEES exposure, we did not find any increase on their DNA binding activity (Fig. 1).

All members of the Jun family were activated optimally at 0.5 mg dose and at 1 h of CEES exposure. The protein level was significantly increased in all three members of Jun family (Fig. 3C). CEES exposure caused a 140%, 90%, and 300% increase in the protein levels of c-Jun, JunB, and JunD, respectively. DNA binding activity of JunB however was not changed (Fig. 1).

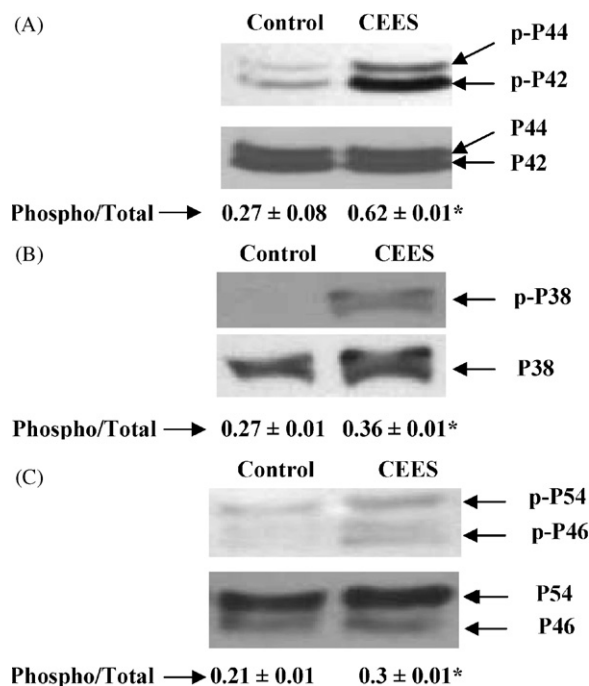


Fig. 2. CEES-induced activation of MAPKs in guinea pig lung. Western blot analysis of ERK 1/2 (A), p38 (B), JNK 1/2 (C) ($N = 3$ in each group). Statistical significance was determined by the Student's *t*-test. Results are expressed as mean \pm S.E., * $p < 0.05$ compared to control.

3.4. Up regulation of AP-1 dependent cell cycle proteins by CEES exposure

To further explore the involvement of AP-1 in cell proliferation, we determined the protein levels of cell cycle proteins, PCNA and cyclin D1 (Fig. 4). Both dose- and time-response effects were studied. The optimum effect was observed at 0.5 mg dose for both proteins. The optimum activation was achieved at 1 h (data not shown). Fig. 4 demonstrates that CEES exposure caused a 49% and 93% increase in the protein levels of cyclin D1 and PCNA, respectively.

4. Discussion

We observed that exposure of CEES to guinea pigs resulted an immediate and severe injury to lung epithelium. It is evident from our earlier findings (Sinha Roy et al., 2005) that CEES exposure causes a clear morphological change in the type II alveolar cells and disruption in their secretory function due to accumulation of lamellar bodies. These cells are responsible for the secretion of lung surfactant, and any injury to these cells is expected to cause a modulation in surfactant secretion.

We already reported that the initiation of free-radical-mediated TNF- α cascade is the major pathway in the mustard gas mediated adult respiratory distress syndrome (Chatterjee et al., 2003). TNF- α induces the activation of AP-1 in alveolar epithelial cells (Rahman, 2000). TNF- α promoter itself contains AP-1 binding sites and is subject to positive auto regulation (Baud and Karin, 2001). We found earlier that TNF- α increased within 1 h of CEES exposure (Chatterjee et al., 2003). Similarly, we found that exposure with 0.5 mg/kg dose of CEES after 1 h significantly induced the basal level of AP-1 activation in guinea pig lung (Fig. 1). Thus, we chose this concentration to investigate the possible signaling pathways involved in the regulation of AP-1 activation.

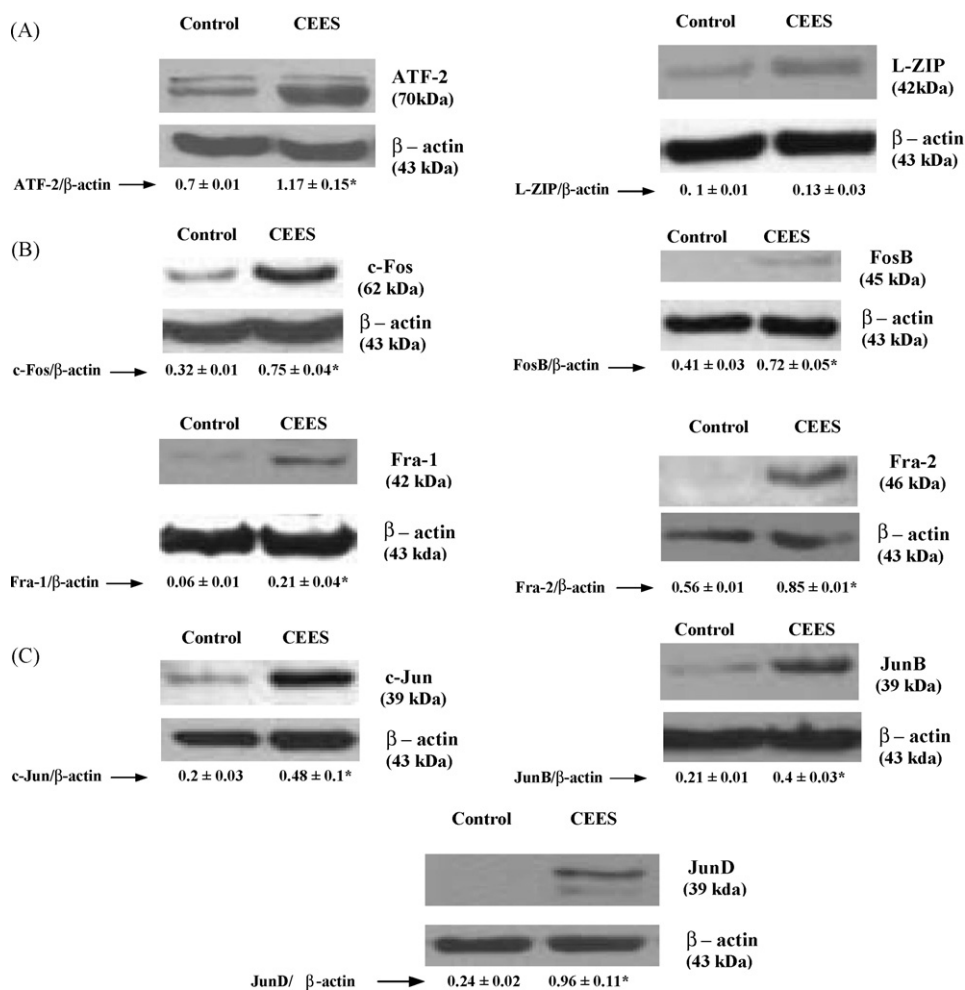


Fig. 3. CEES-induced increase in protein levels of AP-1 transcription factors in guinea pig lung. Western blot analysis of ATF-2 and L-ZIP (A); c-Fos, Fos-B, Fra-1, Fra-2 (B); c-Jun, JunB, JunD (C) (N=3 in each group). Statistical significance was determined by the Student's *t*-test. Results are expressed as mean ± S.E., **p* < 0.05 compared to control.

The present study examines the relationship between mustard gas induced lung injury and MAPKs signaling pathway in guinea pig. To elucidate the mechanisms, we measured the activity (total and phospho) of individual members of the MAPK family (p38, JNK1/2, and ERK1/2) in the lung tissues. According to our results, a significant increase was observed in the phosphorylation of all three

MAPKs (ERK, JNK and p38) in CEES-exposed animals (Fig. 2). These results are in agreement with previous finding that JNK cascade is activated following exposure to inflammatory cytokines (Karin, 1995). In addition to that, Carter et al. (1999) also demonstrated that activation of both the ERK and p38 kinase pathways is necessary for optimal accumulation of IL-6 and TNF mRNAs and cytokine release from endotoxin (LPS)-stimulated alveolar macrophages (AM). Inhibition of either of these pathways only partially reduced cytokine gene expression, but simultaneous inhibition of both pathways resulted in a marked reduction in expression of these genes. Our result also suggests that mustard gas induced induction of inflammatory cytokines trigger the ERK, JNK and p38 MAPK signal transduction pathways that may cause the ultimate lung damage.

Distinct MAPK pathways are responsible for the phosphorylation and activation of AP-1 proteins (Zhong et al., 2005). The stress-responsive p38 and JNK MAPK pathways regulate cell cycle and apoptosis (Zhang et al., 2005). MAPKs have significant roles in mediating signals triggered by cytokines, growth factors, and environmental stress; and are involved in controlling cell proliferation, cell differentiation, and death (Franklin et al., 1994; Rincon, 2001).

AP-1 is the down stream signal of MAPKs signaling pathways (Karin, 1995), and the blocking of MAPKs leads to the inhibition of AP-1 transactivation and subsequent cell transformation (Dong et al., 1997). AP-1 activity plays a critical role in the process of tumorigenesis (Angel and Karin, 1991; Sun and Oberley, 1996). AP-1 regulates cellular proliferation, differentiation, apoptosis, cancer

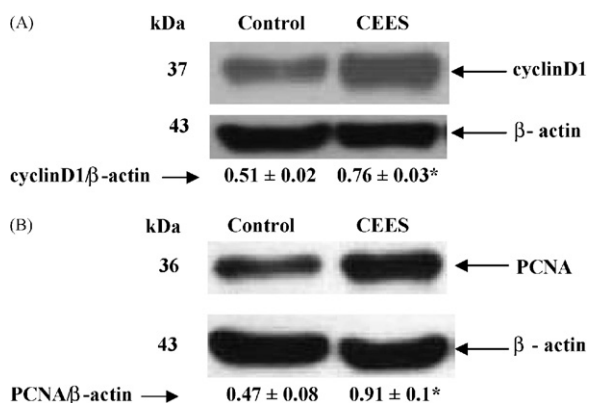


Fig. 4. CEES-induced activation of AP-1 dependent cell cycle protein in guinea pig lung. Western blot analysis of cyclin D1 (A) and PCNA (B) (N=3 in each group). Statistical significance was determined by the Student's *t*-test. Results are expressed as mean ± S.E., **p* < 0.05 compared to control.

cell invasion and oncogene-induced transformation (McDonnell et al., 1990; Szabo et al., 1991; Brown et al., 1993).

To elucidate whether any down stream signal of MAPK pathway is affected by CEES exposure, we monitored the protein levels of AP-1 family. Since AP-1 is a homo or hetero dimers of Fos family, activating transcription factor (ATF) and Jun subfamilies of basic-region leucine-zipper (L-ZIP) proteins, we measured the protein levels of individual components. We observed a significant increase in ATF-2 protein level (Fig. 3A). At the transcription level, ATF-2 is phosphorylated and activated by all three MAPKs, supporting our observation that increased MAPK activity may result in an increase in ATF-2. We measured the protein level of individual family members of both Fos (c-Fos, Fra-1, Fra-2 and Fos-B) and Jun (c-Jun, Jun-B and Jun-D) families. We found a significant increase of c-Fos, FosB, Fra-1 and Fra-2 in the CEES-exposed animals (Fig. 3B). A significant increase in the protein levels of c-Jun, JunB and Jun-D was also observed in animals exposed to CEES in contrast to the control animals (Fig. 3C). Since c-Jun is phosphorylated by JNK, observed increased level of phosphorylated JNK is responsible for the increase in phosphorylated c-Jun level (Figs. 1 and 2). Phosphorylation of c-Jun stimulates their ability to activate transcription, thereby leading to c-Jun induction (Karin, 1995).

Jun and Fos proteins differ significantly in both their DNA binding and transactivation potential as well as their target gene regulation (Zhong et al., 2005). In vitro studies have shown that Jun/Fos heterodimers are more stable and have a stronger DNA binding activity than Jun homodimers (Ryseck and Bravo, 1991). Thus, increased activation of AP-1 in CEES-exposed lung was due to c-Fos and c-Jun dimerization.

PCNA is a cofactor of DNA polymerase delta and is required for DNA synthesis. The PCNA gene contains AP-1 sites in the promoter region and its expression is regulated by AP-1 activity (Yamaguchi et al., 1991; Gillardon et al., 1995). Our result shows an up-regulation of PCNA in CEES-exposed animal compared with control (Fig. 4). Cyclin D1, the regulatory subunit of several cyclin-dependent kinases, is required for, and capable of shortening, the G1 phase of the cell cycle. AP-1 proteins bind the cyclin D1-954 region. Cyclin D1 promoter activity is stimulated by over expression of mitogen-activated protein kinase through the proximal 22 base pairs (Albanese et al., 1995). Several AP-1 proteins are shown to bind these sites and activate cyclin D1 expression (Albanese et al., 1995; Brown et al., 1998; Beier et al., 1999). Our results show that up regulation of AP-1 dependent cell cycle proteins as well as cell differentiation marker occur in the lung of animals exposed to CEES (Fig. 4).

In conclusion, it is evident that CEES-induced activation of TNF- α is associated with an increase in MAPKs/AP-1 signaling, a stimulation of cell proliferation and lung injury. Further studies are needed to clarify whether the observed effects are the adaptive responses of the lung or they contribute to the lung injury.

Conflict of interest

None.

Acknowledgement

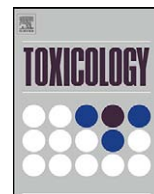
This study was supported by the US Army Grant W81XWH-06-2-0044.

References

Albanese, C., Johnson, J., Watanabe, G., Eklund, N., Vu, D., Arnold, A., Pestell, R.G., 1995. Transforming p21ras mutants and c-Ets-2 activate the cyclin D1 promoter through distinguishable regions. *J. Biol. Chem.* 270, 23589–23597.

- Angel, P., Karin, M., 1991. The role of Jun, Fos and the AP-1 complex in cell-proliferation and transformation. *Biochim. Biophys. Acta* 1072, 129–157.
- Baud, V., Karin, M., 2001. Signal transduction by tumor necrosis factor and its relatives. *Trends Cell Biol.* 11, 372–377.
- Beier, F., Lee, R.J., Taylor, A.C., Pestell, R.G., LuValle, P., 1999. Identification of the cyclin D1 gene as a target of activating transcription factor 2 in chondrocytes. *Proc. Natl. Acad. Sci. U.S.A.* 96, 1433–1438.
- Brown, J.R., Nigh, E., Lee, R.J., Te, H., Thompson, M.A., Saudou, F., Pestell, R.G., Greenberg, M.E., 1998. Fos family members induce cell cycle entry by activating cyclin D1. *Mol. Cell Biol.* 18, 5609–5619.
- Brown, P.H., Alani, R., Preis, L.H., Szabo, E., Birrer, M.J., 1993. Suppression of oncogene-induced transformation by a deletion mutant of c-jun. *Oncogene* 8, 877–886.
- Calvet, J.H., Jarreau, P.H., Levame, M., D'ortho, M.P., Lorino, H., Harf, A., Mavrier, I.M., 1994. Acute and chronic respiratory effects of sulfur mustard intoxication in guinea pigs. *J. Appl. Physiol.* 76, 681–688.
- Carter, A.B., Monick, M.M., Hunninghake, G.W., 1999. Both Erk and p38 kinases are necessary for cytokine gene transcription. *Am. J. Respir. Cell Mol. Biol.* 20, 751–758.
- Chatterjee, D., Mukherjee, S., Smith, M.G., Das, S.K., 2003. Signal transduction events in lung injury induced by 2-chloroethyl ethyl sulfide, a mustard analog. *J. Biochem. Mol. Toxicol.* 17, 114–121.
- Cohen, M., Meisser, A., Haeggeli, L., Bischof, P., 2006. Involvement of MAPK pathway in TNF-alpha-induced MMP-9 expression in human trophoblastic cells. *Mol. Human Reprod.* 12, 225–232.
- Cowman, F.M., Broomfield, C.A., 1993. Putative roles of inflammation in the dermatopathology of sulfur mustard. *Cell Biol. Toxicol.* 9, 201–213.
- Dacre, J.C., Goldman, M., 1996. Toxicology and pharmacology of the chemical warfare agent sulfur mustard. *Pharmacol. Rev.* 48, 289–326.
- Das, S.K., Mukherjee, S., Smith, M., Chatterjee, D., 2003. Prophylactic protection by N-acetylcysteine against the pulmonary injury induced by 2-chloroethyl ethyl sulfide, a mustard analogue. *J. Biochem. Mol. Toxicol.* 17, 177–184.
- Debrowska, M.I., Becks, L.L., Lelli, J.L., Levee, M.G., Hinshaw, D.B., 1996. Sulfur mustard induces apoptosis and necrosis in endothelial cells. *Toxicol. Appl. Pharmacol.* 141, 568–583.
- Dong, Z., Ma, W., Huang, C., Yang, C.S., 1997. Inhibition of tumor promoter-induced activator protein 1 activation and cell transformation by tea polyphenols, (-)-epigallocatechin gallate, and theaflavins. *Cancer Res.* 57, 4414–4419.
- Elsayed, N.M., Omaye, S.T., Klain, G.J., Inase, J.L., Dahlberg, E.T., Wheeler, C.R., Korte, D.W., 1989a. Response of mouse brain to a single subcutaneous injection of the monofunctional sulfur mustard, butyl-2-chloroethyl sulfide (BCS). *Toxicology* 58, 11–20.
- Elsayed, N.M., Omaye, S.T., Klain, G.J., Korte, D.W., 1992. Free radical mediated lung response to the monofunctional sulfur mustard, butyl-2-chloroethyl sulfide after subcutaneous injection. *Toxicology* 72, 153–165.
- Elsayed, N.M., Ta, P.N., Korte, D.W., 1989b. Biochemical alterations in mouse liver induced by nitrogen mustard. *Toxicologist* 9, 26–34.
- Franklin, R.A., Tordai, A., Patel, H., Gardner, A.M., Johnson, G.L., Gelfand, E.W., 1994. Ligation of the T-cell receptor complex results in activation of the Ras/Raf-1/MEK/MAPK cascade in human T lymphocytes. *J. Clin. Invest.* 93, 2134–2140.
- Gillardard, F., Moll, I., Uhlmann, E., 1995. Inhibition of c-Fos expression in the UV-irradiated epidermis by topical application of antisense oligodeoxynucleotides suppresses activation of proliferating cell nuclear antigen. *Carcinogenesis* 16, 1853–1856.
- Gross, C.L., Meier, H.L., Papirmeister, B., Brinkley, F.B., Johnson, J.B., 1985. Sulfur mustard lowers nicotinamide adenine dinucleotide concentrations in human skin grafted to nude mice. *Toxicol. Appl. Pharmacol.* 81, 85–90.
- Herdegen, T., Leah, J.D., 1998. Inducible and constitutive transcription factors in the mammalian nervous system: control of gene expression by Jun, Fos and Krox, and CREB/ATF proteins. *Brain Res. Brain Res. Rev.* 28, 370–490.
- Husain, K., Dube, S.N., Sugendran, K., Singh, R., DasGupta, S., Somani, S.M., 1996. Effect of topically applied sulphur mustard on antioxidant enzymes in blood cells and body tissues of rats. *J. Appl. Toxicol.* 16, 245–248.
- Karin, M., 1995. The regulation of AP-1 activity by mitogen-activated protein kinases. *J. Biol. Chem.* 270, 16483–16486.
- Koj, A., 1996. Initiation of acute phase response and synthesis of cytokines. *Biochim. Biophys. Acta* 1317, 84–94.
- Kopff, M., Zakrzewska, I., Strzelczyk, M., Klem, J., Dubiecki, W., 1994. Superoxide dismutase and catalase activity in psoriatic patients treated topically with ointment containing 2-chloroethyl-3-chloropropyl sulfide. *Pol. J. Pharmacol.* 46, 439–444.
- Kyriakis, J.M., Avruch, J., 2001. Mammalian mitogen-activated protein kinase signal transduction pathways activated by stress and inflammation. *Physiol. Rev.* 81, 807–869.
- McClintock, S.D., Hoesel, L.M., Das, S.K., Till, G.O., Neff, T., Kunkel, R.G., Smith, M.G., Ward, P.A., 2006. Attenuation of half sulfur mustard gas-induced acute lung injury in rats. *J. Appl. Toxicol.* 26, 126–131.
- McDonnell, S.E., Kerr, L.D., Matrisian, L.M., 1990. Epidermal growth factor stimulation of stromelysin mRNA in rat fibroblasts requires induction of proto-oncogenes c-fos and c-jun and activation of protein kinase C. *Mol. Cell Biol.* 10, 4284–4293.
- Mellor, S.G., Rice, P., Cooper, G.C., 1991. Vesicant burns. *Br. J. Plast. Surg.* 44, 434–437.
- Momeni, A.Z., Enshaeih, S., Meghadadi, M., Amindjavaheri, M., 1992. Skin manifestations of mustard gas: a clinical study of 535 patients exposed to mustard gas. *Arch. Dermatol.* 128, 775–780.
- Rahman, I., 2000. Regulation of nuclear factor-kappa B, activator protein-1, and glutathione levels by tumor necrosis factor-alpha and dexamethasone in alveolar epithelial cells. *Biochem. Pharmacol.* 60, 1041–1049.

- Reddy, S.P., Mossman, B.T., 2002. Role and regulation of activator protein-1 in toxicant-induced responses of the lung. *Am. J. Physiol. Lung Cell Mol. Physiol.* 283, L1161–L1178.
- Rincon, M., 2001. MAP-kinase signaling pathways in T-cell. *Curr. Opin. Immunol.* 13, 339–345.
- Roebuck, K.A., Carpenter, L.R., Lakshminarayanan, V., Page, S.M., Moy, J.N., Thomas, L.L., 1999. Stimulus-specific regulation of chemokine expression involves differential activation of the redox-responsive transcription factors AP-1 and NF-kappaB. *J. Leukoc. Biol.* 65, 291–298.
- Ryseck, R.P., Bravo, R., 1991. c-Jun, JunB, JunD differ in their binding affinities to AP-1 and CRE consensus sequences: effects of fos proteins. *Oncogene* 6, 533–542.
- Shaulian, E., Karin, M., 2001. AP-1 in cell proliferation and survival. *Oncogene* 20, 2390–2400.
- Shaulian, E., Karin, M., 2002. AP-1 as a regulator of cell life and death. *Nat. Cell Biol.* 4, E131–E136.
- Sinha Roy, S., Mukherjee, S., Kabir, S., Rajaratnam, V., Smith, M., Das, S.K., 2005. Inhibition of cholinephosphotransferase activity in lung injury induced by 2-chloroethyl ethyl sulfide, a mustard analog. *J. Biochem. Molec. Toxicol.* 19, 289–297.
- Steinmuller, L., Cibelli, G., Moll, J.R., Vinson, C., Thiel, G., 2001. Regulation and composition of activator protein 1 (AP-1) transcription factors controlling collagenase and c-Jun promoter activities. *Biochem. J.* 360, 599–607.
- Sun, Y., Oberley, L.W., 1996. Redox regulation of transcriptional activators. *Free Radic. Biol. Med.* 21, 335–348.
- Szabo, E., Presis, L.H., Brown, P.H., Birrer, M.J., 1991. The role of jun and fos gene family members in 12-O-tetradecanoylphorbol-13-acetate induced hemopoietic differentiation. *Cell Growth Differ.* 2, 475–482.
- Takeda, K., Matsuzawa, A., Nishitoh, H., Ichijo, H., 2003. Roles of MAPKKK ASK1 in stress-induced cell death. *Cell Struct. Funct.* 28, 23–29.
- Whitmarsh, A.J., Davis, R.J., 1996. Transcription factor AP-1 regulation by mitogen-activated protein kinase signal transduction pathways. *J. Mol. Med.* 74, 589–607.
- Willems, J.L., 1989. Clinical management of mustard gas casualties. *Annal. Med. Milit. Belg.* 3, 1–61.
- Yamaguchi, M., Hayashi, Y., Hirose, F., Matsuoka, S., Moriuchi, T., Shiroishi, T., Moriwaki, K., Matsukage, A., 1991. Molecular cloning and structural analysis of mouse gene and pseudogenes for proliferating cell nuclear antigen. *Nucleic Acids Res.* 19, 2403–2410.
- Yamakido, M., Ishinka, S., Hiyama, K., Maeda, A., 1996. Former poison gas workers and cancer: Incidence and inhibition of tumor formation by treatment with biological response modifier N-CWS. *Environ. Health Perspect.* 104, 485–488.
- Zagariya, A., Mungre, S., Lovis, R., Birrer, M., Ness, S., Thimmapaya, B., Pope, R., 1998. Tumor necrosis factor alpha gene regulation: enhancement of C/EBPbeta-induced activation by c-Jun. *Mol. Cell Biol.* 18, 2815–2824.
- Zhang, N., Ahsan, M.H., Zhu, L., Sambucetti, L.C., Purchio, A.F., West, D.B., 2005. NF-kB and not the MAPK signaling pathway regulates GADD45 β expression during acute inflammation. *J. Biol. Chem.* 280, 21400–21408.
- Zhang, Q., Kleeberger, S.R., Reddy, S.P., 2004. DEP-induced fra-1 expression correlates with a distinct activation of AP-1-dependent gene transcription in the lung. *Am. J. Physiol. Lung Cell Mol. Physiol.* 286, L427–L436.
- Zhong, C.Y., Zhou, Y.M., Douglas, G.C., Witschi, H., Pinkerton, K.E., 2005. MAPK/AP-1 signal pathway in tobacco smoke-induced cell proliferation and squamous metaplasia in the lungs of rats. *Carcinogenesis* 26, 2187–2195.



Role of MAPK/AP-1 signaling pathway in the protection of CEES-induced lung injury by antioxidant liposome

Sutapa Mukhopadhyay^a, Shyamali Mukherjee^a, William L. Stone^b, Milton Smith^c, Salil K. Das^{a,*}

^a Department of Cancer Biology, Meharry Medical College, 1005 David Todd Blvd., Nashville, TN 37208, USA

^b Department of Pediatrics, East Tennessee State University, Johnson City, TN 37614, USA

^c AMAOX Ltd, Melbourne, FL 32944, USA

ARTICLE INFO

Article history:

Received 12 January 2009

Received in revised form 28 April 2009

Accepted 12 May 2009

Available online 21 May 2009

Keywords:

MAPK

AP-1

Lung injury

CEES

Antioxidant liposome

ABSTRACT

We have recently reported that antioxidant liposomes can be used as antidotes for mustard gas induced lung injury in guinea pigs. The maximum protection was achieved with a liposome composed of tocopherols (α , γ , δ) and N-acetylcysteine (NAC) when administered after 5 min of exposure of 2-chloroethyl ethyl sulfide (CEES), a half sulfur mustard gas. We also reported an association of mustard gas-induced lung injury with an activation of MAPK/AP-1 signaling pathway and cell proliferation. The objective of the present study was to investigate whether CEES-induced MAPKs/AP-1 signaling pathway is influenced by antioxidant liposome therapy. A single dose (200 μ l) of the antioxidant liposome was administered intratracheally after 5 min of exposure of CEES (0.5 mg/kg). The animals were sacrificed after 1 h and 30 days of CEES exposure. Although the liposome treatment did not have any significant effect on the activation of the MAPKs family (ERK1/2, p38 and JNK1/2), it significantly counteracted the CEES-induced activation of AP-1 transcription factors and corresponding increase in the protein levels of Fos, ATF and Jun family members. The liposome treatment significantly blocked the CEES-induced increase in the protein levels of cyclin D1, a cell cycle protein and PCNA, a cell differentiation marker. Furthermore, it protected lung against CEES-induced inflammation and infiltration of neutrophils, eosinophils and erythrocytes in the alveolar space. This suggests that the protective effect of antioxidant liposome against CEES-induced lung damage is mediated via control of AP-1 signaling.

© 2009 Elsevier Ireland Ltd. All rights reserved.

1. Introduction

Mustard gas is a well-known chemical warfare agent which was extensively used in World War I (Willems, 1989; Mellor et al., 1991). It exerts a local action on eyes, skin, and respiratory tissue followed by impairment of nervous, cardiac, and digestive systems in humans and laboratory animals (Papirmeister et al., 1991; Dacre and Goldman, 1996; Smith et al., 2003).

Although the exact mechanism is not well understood, it is reasonable to postulate a causal role of oxidative stress in the pathology that follows exposure to mustard gas. Many inflammatory lung diseases, including adult respiratory distress syndrome (ARDS), are associated with oxidative stress (Leff et al., 1993). For example, inflammatory cytokines, such as tumor necrosis factor- α (TNF- α), provoke the generation of reactive oxygen species (ROS), mediators of oxidative stress (Lloyd et al., 1993). The contribution of these ROS to tissue injury is best demonstrated by the ability of antioxidants to prevent injury in various experimental models (Kehrer,

1993). Oxidants, such as hydrogen peroxide, have been shown to induce the expression of several of the early response genes and to activate the transcription factors activating protein 1 (AP-1) and NF- κ B (Devary et al., 1991; Schreck et al., 1991). Antioxidant therapy therefore might act by reducing inflammatory response through the impairment of cell signaling processes (Fan et al., 2000).

AP-1 is an important regulatory protein involved in cell growth, differentiation, transformation, and apoptosis (Angel and Karin, 1991; Shaulian and Karin, 2001). The AP-1 complex consists of homo- or heterodimers of Fos families (c-Fos, Fos-B, Fra-1 and Fra-2), activating transcription factor families (ATF-1 and ATF-2) and Jun subfamilies (c-Jun, Jun-B and Jun-D) of basic-region leucine zipper (B-ZIP) proteins (Herdegen and Leah, 1998; Steinmuller et al., 2001; Shaulian and Karin, 2002). AP-1 proteins have been suggested to play both pro- and anti-regulatory roles in pulmonary defense, injury, and repair (Reddy and Mossman, 2002).

We have recently demonstrated that CEES-induced activation of TNF- α is associated with an increase in mitogen activated protein kinases (MAPKs)/AP-1 signaling, a stimulation of cell proliferation and lung injury (Mukhopadhyay et al., 2008). In addition, the delivery of an antioxidant N-acetylcysteine (NAC) via drinking water was shown to have prophylactic protection against 2-chloroethyl ethyl

* Corresponding author. Tel.: +1 615 327 6988; fax: +1 615 327 6442.

E-mail address: sdas@mmc.edu (S.K. Das).

sulfide (CEES)-induced lung injury (Das et al., 2003). This protection was associated with inhibition of CEES-induced activation of TNF- α , NF- κ B, and reactive oxygen species (Das et al., 2003). A similar protection against CEES-induced lung injury with antioxidant liposomes containing NAC and tocopherols (α , γ , δ) was demonstrated in our laboratory recently (McClintock et al., 2006; Mukherjee et al., 2009).

The present study investigates whether antioxidant liposome therapy counteracts the CEES-induced activation of MAPK/AP-1 signaling pathway and cell proliferation in guinea pig lung.

2. Materials and methods

2.1. Animal model of lung injury

Male guinea pigs (Hartley strain, 5–6 weeks old, 400 g body weight) were obtained from Charles River (Wilmington, MA). Animals were infused intratracheally with a single dose (0.5 mg/kg b.wt.) of CEES (Sigma Chemicals, St. Louis, MO) in ethanol (infusion volume was 100 μ l/animal). Control animals were infused with 100 μ l of ethanol in the same way. All animal experiments were in accordance with the standards in the Guide for the Care and Use of Laboratory Animals, and were supervised by veterinarians from the Unit for Laboratory and Animal Care of the Meharry Medical College.

2.2. Treatment of animals with antioxidant liposome

The antioxidant liposome was prepared as described elsewhere (Mukherjee et al., 2009). The blank liposome (LIP1) contained only soybean phospholipids, cholesterol and phosphatidic acid in mole fraction ratio of 71:28:0.67, respectively, and no antioxidant. The antioxidant liposome (LIP2) contained soybean phospholipids, cholesterol and phosphatidic acid (mole fraction ratio of 55:22:0.6) and in addition 11 mM α -tocopherol, 11 mM γ -tocopherol, 5 mM δ -tocopherol and 75 mM NAC. Animals were divided into five groups. Animals of group 1 served as control and received LIP1 (200 μ l) after 5 min of vehicle exposure and sacrificed after 1 h. After 5 min of CEES exposure, animals of groups 2 and 4 received LIP1 (200 μ l) and sacrificed after 1 h and 30 days post CEES exposure, respectively. Similarly 5 min after CEES exposure, the animals of groups 3 and 5 received LIP2 (200 μ l) and sacrificed after 1 h and 30 days post CEES exposure, respectively. Since there

was no difference in lung morphology between 1 h and 30-day control groups (Mukherjee et al., 2009), we did not include any control group for 30 days post vehicle exposure in this study. Lungs were perfused with 2.6 mM phosphate buffered saline containing 5.6 mM glucose, removed from the chest cavity and immediately flash frozen in liquid nitrogen and stored at -80°C for further experiment. A section of the lung was fixed in buffered formalin for morphological assessment.

2.3. Morphological assessment of lung injury

Morphological assessment of lung tissues was carried out as described before (Mukherjee et al., 2009). Briefly, a portion of lung tissue was fixed over night in neutral buffered formalin (10%), pH 7.2, and embedded in paraffin for light microscopy. Lung sections were obtained for histological examination by staining with hematoxylin and eosin.

2.4. Assay of TNF- α

Lung tissues were sonicated in Tris buffered saline (0.05 M Tris-HCl, 0.15 M sodium chloride, pH 7.4), centrifuged at 10,000 rpm for 10 min. TNF- α was measured in the supernatant using TNF- α enzyme-linked immunosorbent assay (ELISA) kit (Biosource, Camarillo, CA). Supernatants were added to TNF- α antibody-coated micro wells (supplied with the kit) along with biotin-conjugated secondary antibody and incubated for 1 h 30 min at room temperature. After washing, the wells were incubated with streptavidin-horseradish peroxidase complex. The wells were washed and color reactions were carried out using horseradish peroxidase substrate. The color developments were measured using Bio-Rad ELISA platereader (Bio-Rad, Hercules, CA) after addition of stop solution.

2.5. Evaluation of DNA binding activity of AP-1 by ELISA

The DNA binding activity of AP-1 was quantified by ELISA using the TransAMTM AP-1 transcription factor family assay kit (Active Motif, Carlsbad, CA), according to the manufacturer's protocol. Briefly, lung tissues were homogenized in a 5 volume of ice-cold lysis buffer (Biosource, Camarillo, CA) containing protease inhibitor cocktail (0.01%, Sigma Chemicals, St. Louis, MO) and incubated in 96-well plates to which oligonucleotide containing a TPA responsive element (TRE) was immobilized. AP-1 binding to the target oligonucleotide was detected by incubation with primary antibodies specific for c-Fos, Fos-B, Fra-1, Fra-2, p-c-Jun, JunB, JunD and visualized with anti-IgG horseradish peroxidase conjugate and developing solution, and quantified at 450 nm with a reference wavelength of 655 nm.

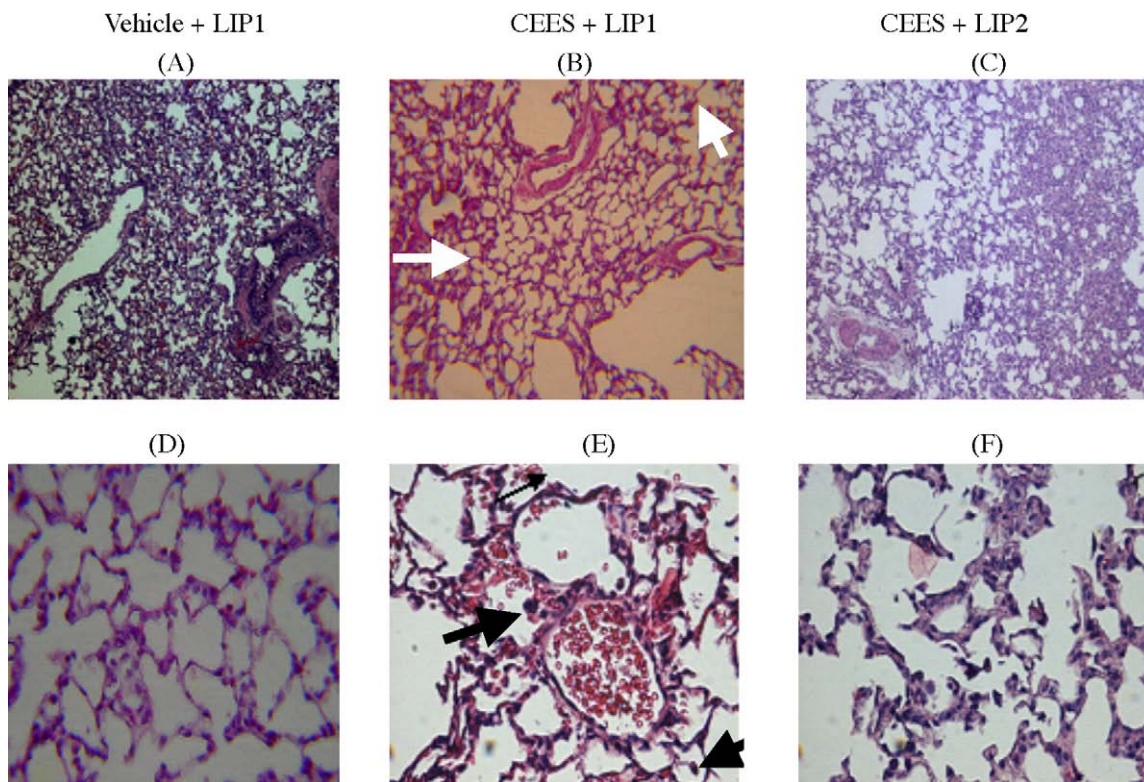


Fig. 1. Effect of antioxidant liposome treatment on CEES-induced lung injury in guinea pigs. Section of lungs were stained with H&E stain. Lungs were obtained at 1 h after tracheal instillation of either vehicle or CEES. In each case liposomes (LIP1 and LIP2) were administered intratracheally 5 min after vehicle or CEES exposure. A and D = Vehicle + LIP1; B and E = CEES + LIP1; C and F = CEES + LIP2. A, B and C = 10 \times ; D, E and F = 40 \times .

2.6. Western blot analysis

Lung tissues were homogenized in a 5 volume of ice-cold lysis buffer (Biosource, Camarillo, CA) containing protease inhibitor cocktail (0.01%, Sigma Chemicals, St. Louis, MO) by using a Brinkman Polytron (setting 6–7, 30 s). Proteins were measured by Bio-Rad protein assay (Bio-Rad, Hercules, CA) and 50 µg protein was separated by 12% SDS polyacrylamide gel electrophoresis (SDS-PAGE). Proteins were transferred electrophoretically onto PVDF membranes Immobilon-P (Millipore, Bedford, MA). The membrane was immunoblotted with primary antibodies: MAPK (Cell Signaling Tech., Danvers, MA), c-Fos, FosB, Fra-1, Fra-2, c-Jun, JunB, JunD, ATF-2, cyclin D1 and proliferating cell nuclear antigen (PCNA) (Santa Cruz Biotechnology Inc., Santa Cruz, CA) and horseradish peroxidase (HRP)-conjugated anti-mouse, anti-goat and anti-rabbit secondary antibodies. Binding of antibodies to the blots was detected with an ECL-detection system (PerkinElmer, Boston, MA) following manufacturer's instructions. Stripped blots were re-probed with β -actin specific polyclonal antibodies (Santa Cruz Biotechnology Inc., Santa Cruz, CA) to enable normalization of signals between samples. Same blots were stripped and re-probed for Fra-1 and Fra-2. Band intensities were analyzed using Bio-Rad Gel Doc (Bio-Rad, Hercules, CA).

2.7. Statistics

Data were presented as means \pm standard error (SE). Statistical comparisons between groups were determined by the Tukey test after one-way analysis of variance (ANOVA), using GraphPad prism Version 5.0 (GraphPad software, San Diego, CA). A p -value of less than 0.05 was considered statistically significant.

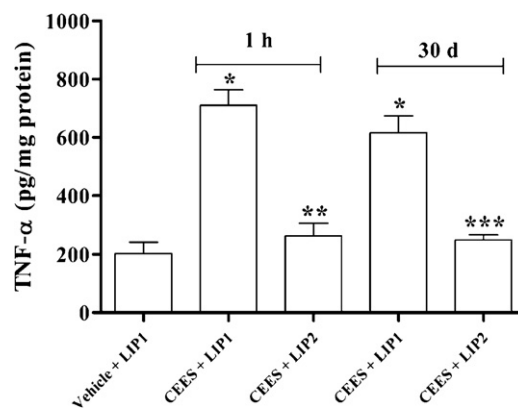


Fig. 2. Attenuation of CEES-induced activation of TNF- α by antioxidant liposome. Accumulation of TNF- α was measured by ELISA at 1 h and 30 days after exposure to CEES (0.5 mg/kg body weight) and their inhibition by 1 h and 30 days treatment with antioxidant liposome. Statistical significance was determined by Tukey test after one-way ANOVA. Values are mean \pm SE ($N=3$), * $p < 0.05$ compared to control; ** $p < 0.05$ compared to CEES exposure for 1 h; *** $p < 0.05$ compared to CEES exposure for 30 days.

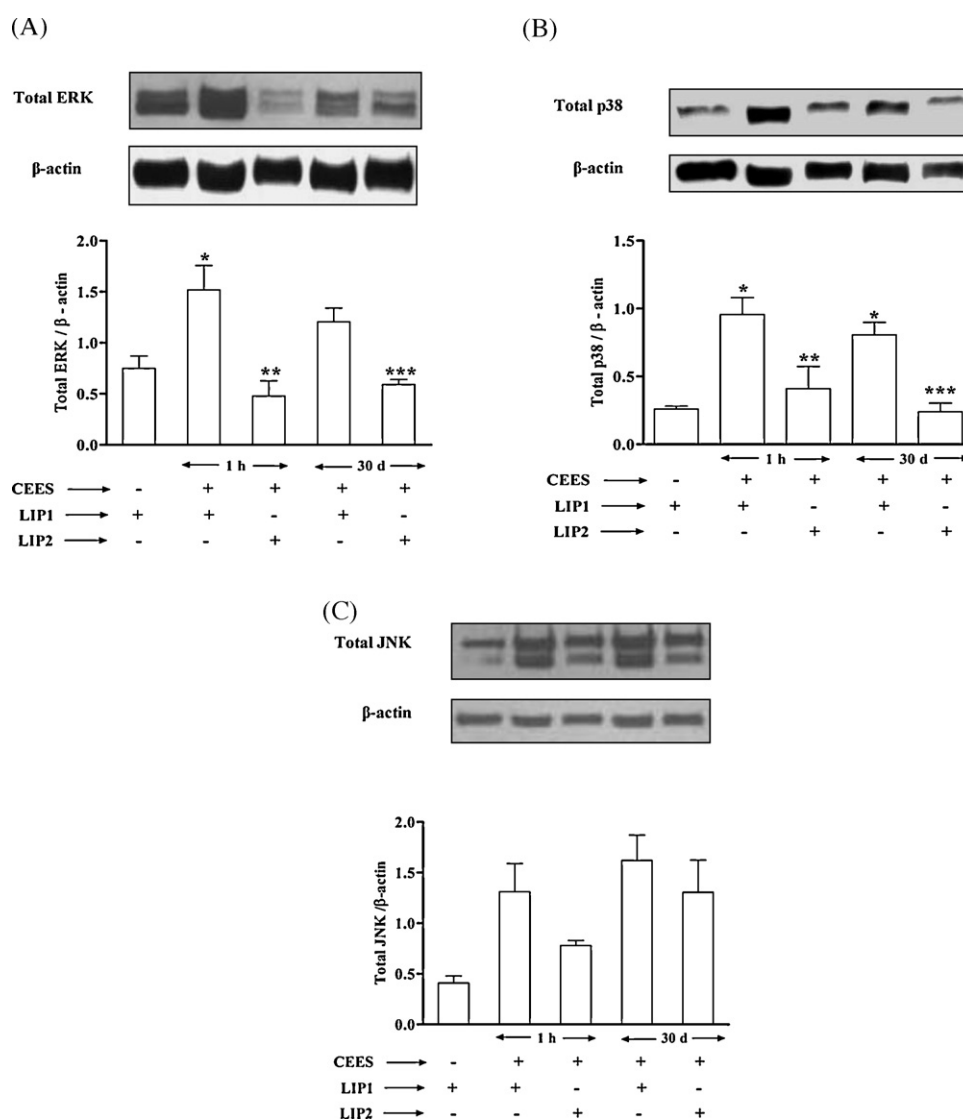


Fig. 3. Effects of antioxidant liposome on CEES-induced changes in MAPKs in guinea pig lung. Western blot analysis of total ERK 1/2 (A), p38 (B), JNK 1/2 (C) ($N=3$ in each group). Statistical significance was determined by Tukey test after one-way ANOVA. Results are expressed as mean \pm SE ($N=3$), * $p < 0.05$ compared to control; ** $p < 0.05$ compared to CEES exposure for 1 h; *** $p < 0.05$ compared to CEES exposure for 30 days.

3. Results

3.1. Attenuation of CEES-induced morphological changes by antioxidant liposome

Fig. 1A and D shows the histological characteristic of lung after 1 h of exposure of vehicle and LIP1. The overall pulmonary architecture, including bronchus, bronchioles, alveolar ducts, alveoli, vascular endothelium, and smooth muscle layers are well maintained. Fig. 1B and E shows the histological characteristic of lung after 1 h of exposure of CEES and LIP1. These specimens

showed acute inflammation with infiltration of 1–2 neutrophils and eosinophils per alveoli in a patchy distribution through out the sections (arrow, Fig. 1B and E). Furthermore, there are several air spaces with erythrocytes. Bronchial epithelium shows no difference from untreated lung whereas detachment of endothelium indicates contraction of the smooth muscle cells, many of which had slight edema. Alveoli number is decreased in some area (Fig. 1E). This could be due to CEES burn. Fig. 1C and F shows the histological characteristic of lung after 1 h of exposure of CEES and LIP2. Although treatment with LIP2 did not control the burn, it decreased acute inflammation and corresponding infiltration of

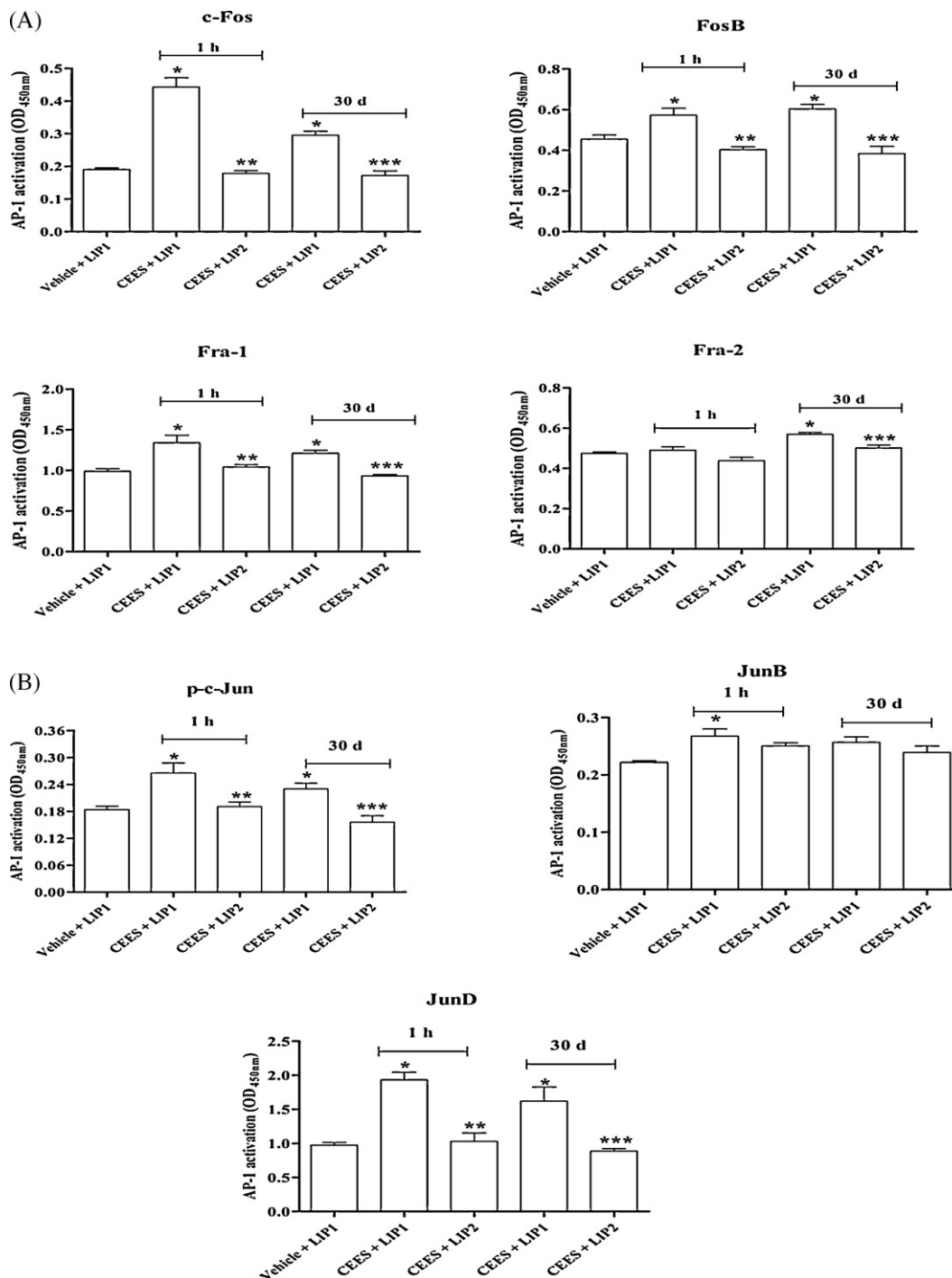


Fig. 4. Protection of CEES-induced activation of DNA binding of AP-1 family members by antioxidant liposome in guinea pig lung. Evaluation of DNA Binding Activity of AP-1 by ELISA: Fos family (A) and Jun family (B). Statistical significance was determined by Tukey test after one-way ANOVA. Results are expressed as mean \pm SE ($N=3$), * $p < 0.05$ compared to control; ** $p < 0.05$ compared to CEES exposure for 1 h; *** $p < 0.05$ compared to CEES exposure for 30 days.

neutrophils, eosinophils and erythrocytes in the alveolar space (Fig. 1F).

3.2. Attenuation of CEES-induced activation of TNF- α by antioxidant liposome

The data on the effects of the liposome on CEES-induced induction of TNF- α in lung are presented in Fig. 2. CEES caused a 3.5- and 3-fold increase in the TNF- α level after 1 h and 30 days of exposure, respectively. Liposome treatment completely blocked the CEES-induced activation of TNF- α at both time points.

3.3. Attenuation of CEES-induced MAPK activation by antioxidant liposome

CEES exposure caused an increase in the protein levels of all members of MAPK family [ERK 1/2 (p44/42), p38 and JNK (p54/46)] at both time points [1 h and 30 days] (Fig. 3). CEES-induced increase in the protein level of each member of the MAPK family was blocked by liposome treatment at 1 h. This attenuation by antioxidant liposome was evident for all members of MAPK family except JNK in 30 days. However, while CEES exposure caused a significant increase in the levels of phosphoMAPKs, liposome treatment did not block the phosphorylation of MAPKs (data not shown).

3.4. Attenuation of CEES-induced activation of DNA binding of AP-1 family members by antioxidant liposome

3.4.1. Fos family members

Data are presented in Fig. 4A. CEES caused a 2.3-, 1.3- and 1.4-fold increase in the DNA binding activity of c-Fos, FosB, and Fra-1, respectively, after 1 h of exposure. Similarly, CEES caused a 1.6-, 1.3- and 1.2-fold increase in the DNA binding activity of c-Fos, FosB, and Fra-1, respectively, after 30 days of exposure. Fra-2 was activated by CEES only after 30 days (1.2-fold) and not after 1 h. Liposome treatment completely blocked the CEES-induced activation of DNA binding of all members of the Fos family except Fra-2 at both time points. Liposome reduced the activation of Fra-2 only at 30 days.

3.4.2. Jun family members

Data are presented in Fig. 4B. CEES caused a 1.4- and 2-fold increase in the DNA binding activity of p-c-Jun, and JunD, respectively, after 1 h of exposure. Similarly, CEES caused a 1.2- and 1.7-fold increase in the DNA binding activity of p-c-Jun and JunD, respectively, after 30 days of exposure. JunB was activated by CEES only after 1 h (1.2-fold) and the activity came back to the basal level in 30 days. Liposome treatment completely blocked the CEES-induced activation of DNA binding of all members of the Jun family except JunB at both time points.

3.5. Attenuative effect of antioxidant liposome on protein levels of AP-1 transcription factors

Since antioxidant liposome attenuated the CEES-induced activation of DNA binding of AP-1 transcription factors (Fig. 4), we determined the effect of antioxidant liposome treatment on the protein levels of individual members of AP-1 family. First we studied the protein levels of ATF-2. CEES exposure caused a significant increase in the protein level of ATF-2 (65.8%) (Fig. 5). However, this increased activation was down-regulated by 31.8% in 1 h when antioxidant liposome was administered after 5 min of CEES exposure. Similarly, liposome treatment attenuated CEES-induced activation (51.8%) of ATF-2 protein levels by 40.6% after 30 days of CEES exposure.

Among Fos members of the AP-1 transcription factors family, the protein level was significantly increased in all four members

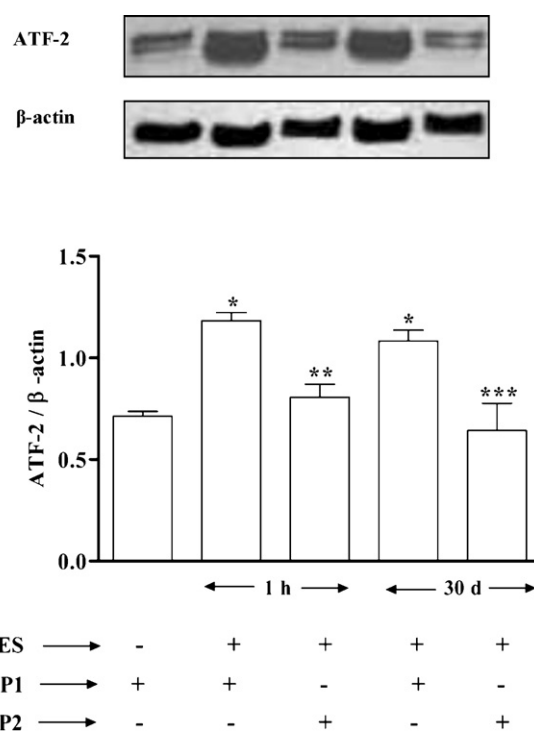


Fig. 5. Effects of antioxidant liposome on CEES-mediated activation of ATF-2 transcription factors in guinea pig lung by Western blot analysis. Statistical significance was determined by Tukey test after one-way ANOVA. Results are expressed as mean \pm SE ($N=3$), * $p < 0.05$ compared to control; ** $p < 0.05$ compared to CEES exposure for 1 h; *** $p < 0.05$ compared to CEES exposure for 30 days.

of Fos family after CEES exposure (Fig. 6). CEES exposure caused a 95.3%, 82.6%, 216.9%, and 58.7% increase in the protein levels of c-Fos, FosB, Fra-1 and Fra-2, respectively, after 1 h. It should be noted, however, that even though protein levels of Fra-2 were increased due to CEES exposure, we did not find any increase on their DNA binding activity (Fig. 4A). However, the antioxidant liposome treatment down-regulated the CEES-induced increase in the protein level by 38.8%, 76.3%, 86.1%, and 77.2%, respectively, in 1 h after liposome administration. Similarly, liposome treatment attenuated CEES-induced activation of cFos (77.5%), FosB (49%), Fra-1 (222.6%) and Fra-2 (26.1%) protein levels by 41.6%, 84.9%, 80.3% and 58.6%, respectively, after 30 days of CEES exposure.

All members of the Jun family were activated upon CEES exposure. The protein level was significantly increased in all three members of Jun family (Fig. 7). CEES exposure caused a 132.9%, 71.9%, and 279.5% increase in the protein levels of c-Jun, JunB, and JunD, respectively, after 1 h. This increased activation was down-regulated by 90.2%, 55.7%, and 76.7%, respectively, when antioxidant liposome was treated for 1 h along with CEES. Similarly, liposome treatment attenuated CEES-induced activation of c-Jun (44.6%), JunB (72.4%) and JunD (180.8%) protein levels by 72%, 60%, and 57.1%, respectively, after 30 days of CEES exposure.

It should be noted, however, that even though protein levels of JunB were increased due to CEES exposure in 30 days, we did not find any increase on their DNA binding activity (Fig. 4B).

3.6. Protection against CEES-induced increase in the AP-1-dependent cell cycle protein levels by antioxidant liposome

To further explore the involvement of AP-1 in cell proliferation, we determined the protein levels of cell cycle proteins, PCNA and cyclin D1 (Fig. 8). Fig. 8 demonstrates that CEES exposure caused a 155% and 97.4% increase in the protein levels of cyclin D1 and PCNA, respectively, after 1 h of CEES exposure. However, this increased

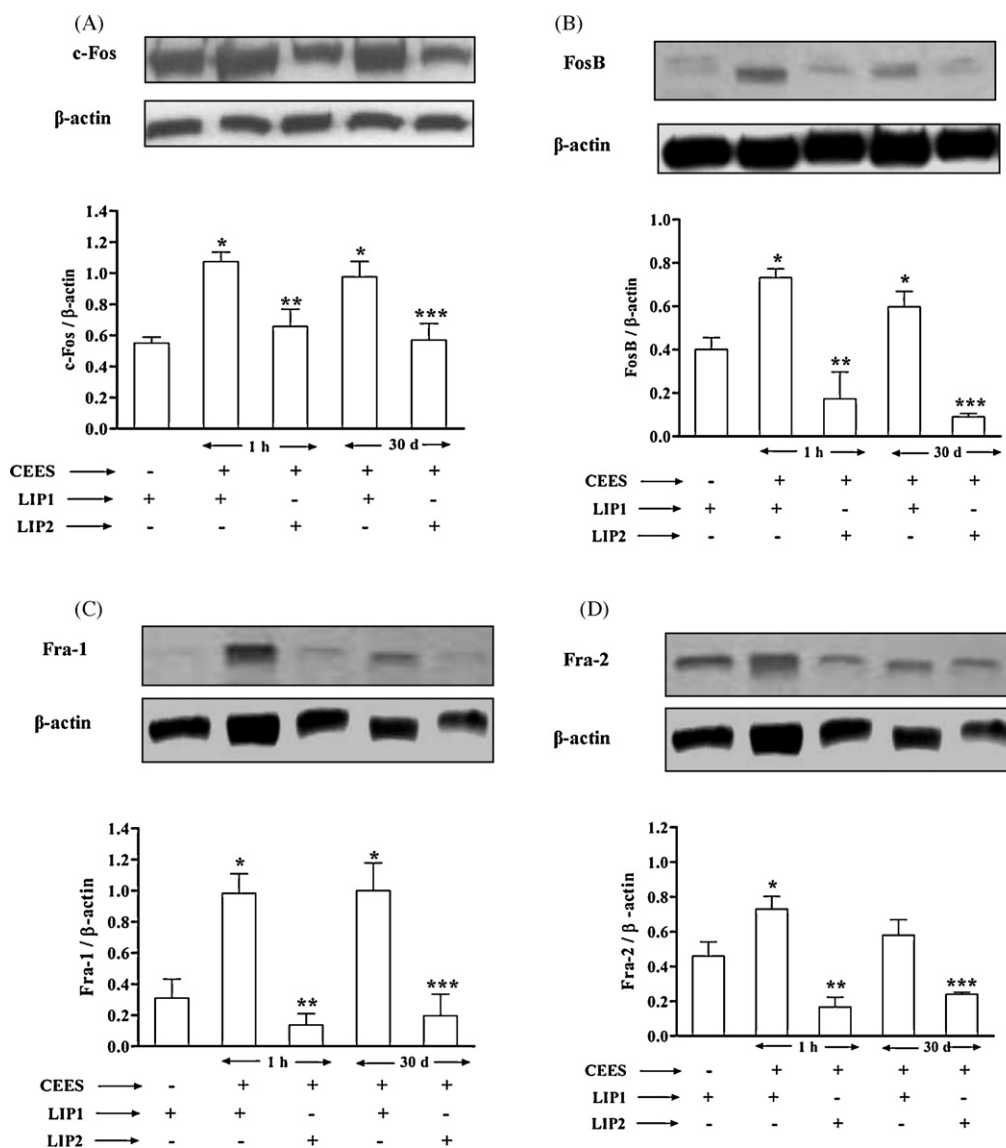


Fig. 6. Inhibition of CEES-induced increase in protein levels of AP-1 transcription factors by antioxidant liposome in guinea pig lung. Western blot analysis of (A) c-Fos, (B) Fos-B, (C) Fra-1, and (D) Fra-2 ($N=3$ in each group). Statistical significance was determined by the Tukey test after one-way ANOVA. Results are expressed as mean \pm SE, * $p < 0.05$ compared to control; ** $p < 0.05$ compared to CEES exposure for 1 h; *** $p < 0.05$ compared to CEES exposure for 30 days.

activation was down-regulated by 80.4% and 51.1%, respectively, when antioxidant liposome was administered 5 min after CEES exposure. Similarly, liposome treatment attenuated CEES-induced activation of cyclinD1 (145.5%) and PCNA (74%) protein levels by 33.3% and 67%, respectively, after 30 days of CEES exposure.

4. Discussion

We previously reported that intratracheal infusion of CEES produces acute lung injury associated with production of reactive oxygen species (Chatterjee et al., 2003). This notion was further evident by the attenuative effects of antioxidant liposome containing NAC and tocopherols on CEES-induced lung injury (Das et al., 2003; Mukherjee et al., 2009). Our previous study also reported that CEES exposure not only initiate a series of signaling events but also causes oxidative stress (Chatterjee et al., 2003; Das et al., 2003). Liposomes are considered to be an acceptable drug delivery system because they are biocompatible, biodegradable, and relatively non-toxic (Taylor and Farr, 1993). The present study clearly indicates that antioxidant liposome (LIP2) therapy protects lung against

CEES-induced acute inflammation, infiltration of neutrophils and eosinophils as well as accumulation of erythrocytes in the alveoli.

We reported earlier that tocopherols cause more protection than NAC alone (McClintock et al., 2006; Mukherjee et al., 2009). Furthermore, it has been reported that alpha tocopherol reduces transendothelial migration of neutrophils and prevents lung injury from toxicants (Rocksén et al., 2003; Suntres and Shek, 1997). Our morphological study (Fig. 1) indicates that antioxidant liposome treatment may inhibit the transendothelial migration of neutrophils and eosinophils from the blood vessels by stabilizing the capillary membrane. Tocopherols are considered the most important naturally antioxidative defense agents against lipid peroxidation and a membrane stabilizer. It can be implied from our previous study that liposomal delivery selectively enhances reducing environment in lung macrophages and epithelial cells and thereby protects against CEES toxicity in these cells (Mukherjee et al., 2009).

It has been well known that lung epithelium presents the first physical barrier to inhaled toxicants. In addition to direct toxicant–epithelial interactions, proinflammatory mediators

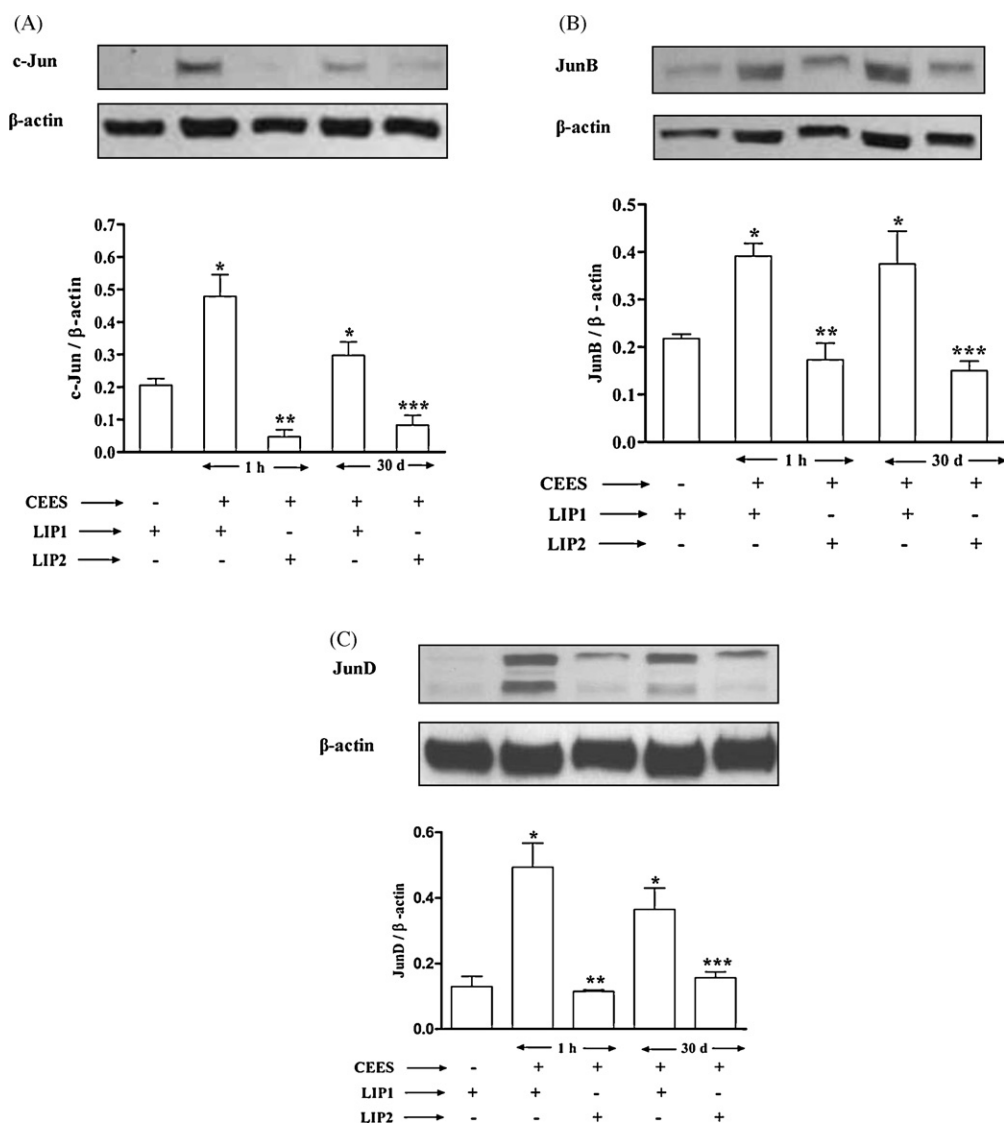


Fig. 7. Protection of CEES-induced increase in protein levels of AP-1 transcription factors by antioxidant liposome in guinea pig lung. Western blot analysis of (A) c-Jun, (B) JunB, and (C) JunD ($N=3$ in each group). Statistical significance was determined by the Tukey test after one-way ANOVA. Results are expressed as mean \pm SE, * $p < 0.05$ compared to control; ** $p < 0.05$ compared to CEES exposure for 1 h; *** $p < 0.05$ compared to CEES exposure for 30 days.

secreted from other pulmonary cells in response to toxicant challenge can also act upon epithelial cells indirectly. It has been reported previously that TNF- α activates intracellular signal transduction pathways in bronchial epithelial cells resulting in increased cell surface expression of adhesion molecules implicated in the recruitment of leukocytes to inflammatory loci (Krunkosky et al., 2000). In addition, TNF- α can induce epithelial cells to secrete other cytokines, such as interleukin (IL-8), an important neutrophil chemoattractant (Cromwell et al., 1992).

We already reported that the initiation of free-radical-mediated TNF- α cascade is the major pathway in the mustard gas-mediated ARDS (Chatterjee et al., 2003). We also showed that consumption of the antioxidant in drinking water prior to CEES exposure significantly inhibited the induction of TNF- α (Das et al., 2003). In the present study we report that only a single dose of antioxidant liposome significantly protected lung against the CEES-induced production of TNF- α (Fig. 2). Furthermore, the effect of antioxidant liposome was almost same as acute treatment up to 30 days.

In this study, however, the TNF- α level remained high in 30 days post CEES exposure contrary to our earlier studies (Chatterjee et al., 2003). We do not know at this time whether the blank liposome

(LIP1) is responsible for this high cytokine level. However, we have reported earlier that lung morphology remained abnormal after 30 days of CEES exposure (Mukherjee et al., 2009). It is interesting to note that in bleomycin-induced lung injury TNF- α level remains high even after 14 days of bleomycin instillation (Mata et al., 2003).

TNF- α induces the activation of AP-1 in alveolar epithelial cells (Rahman, 2000). TNF- α promoter itself contains AP-1 binding sites and is subject to positive auto regulation (Baud and Karin, 2001). We also found that exposure with 0.5 mg/kg dose of CEES after 1 h significantly increased AP-1 activation in guinea pig lung (Fig. 4). This is further evident by our observation that antioxidant liposomes offer a protection against AP-1 activation induced by CEES exposure (Fig. 4).

CEES exposure caused a significant increase in the phosphorylation/activation of MAPKs. However, antioxidant liposome treatment did not reduce the CEES-induced phosphorylation/activation of MAPK (data not shown). Antioxidant liposome treatment led to reduction of the AP-1 activity, without the reduction of MAPK activity. Masuya et al. (1999) also reported that calmodulin-dependent protein kinase II rather than the MAPK family regulates the induction of the human c-fos gene expression by hemin. We can conclude

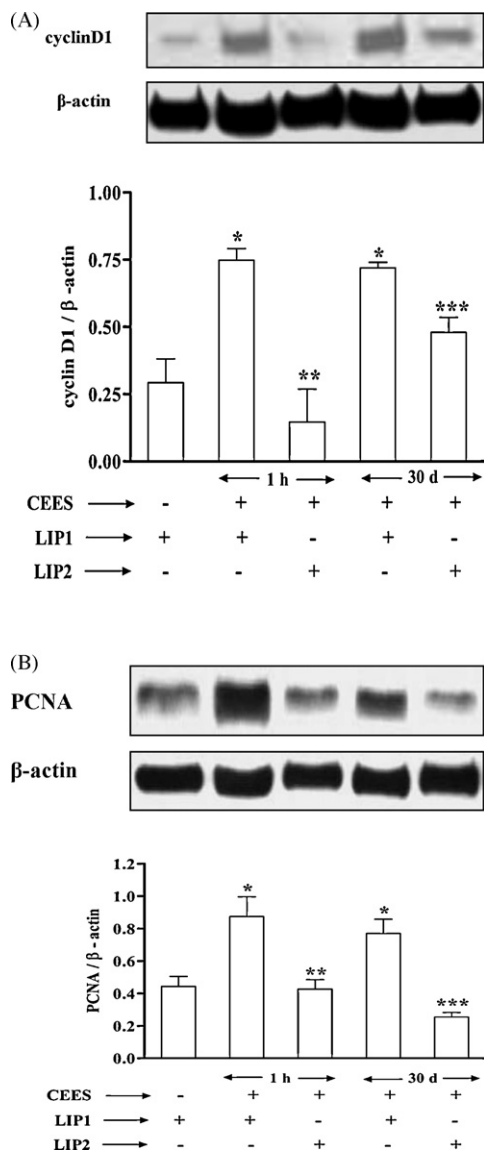


Fig. 8. Protection against CEES-induced increase in AP-1-dependent cell cycle proteins by antioxidant liposome. Western blot analysis of cyclinD1 (A) and PCNA (B) ($N=3$ in each group). Statistical significance was determined by the Tukey test after one-way ANOVA. Results are expressed as mean \pm SE, * $p < 0.05$ compared to control; ** $p < 0.05$ compared to CEES exposure for 1 h; *** $p < 0.05$ compared to CEES exposure for 30 days.

that antioxidant liposome may work in a different pathway other than the MAPK pathway to down-regulate AP-1 signaling.

AP-1 activity plays a critical role in the process of tumorigenesis (Angel and Karin, 1991; Sun and Oberley, 1996). AP-1 regulates cellular proliferation, differentiation, apoptosis, cancer cell invasion and oncogene-induced transformation (McDonnell et al., 1990; Szabo et al., 1991; Brown et al., 1993). The increased activation of AP-1 in CEES-exposed lung was reduced by antioxidant liposome treatment (Figs. 4–7). It should be noted that while in our previous study (Mukhopadhyay et al., 2008), no significant change was observed on AP-1 activation beyond 1 h after CEES exposure; we observed a continued activation up to 30 days in the present study. We do not know at this time whether the blank liposome (LIP1) is responsible for this continued activation of AP-1 due to CEES exposure.

PCNA is a cofactor of DNA polymerase delta and is required for DNA synthesis. The PCNA gene contains AP-1 sites in the promoter region and its expression is regulated by AP-1 activity (Yamaguchi

et al., 1991; Gillardon et al., 1995). Our result show that antioxidant liposome treatment down-regulates the CEES-induced increase in PCNA protein levels (Fig. 8). Cyclin D1, the regulatory subunit of several cyclin-dependent kinases, is required for, and capable of shortening, the G1 phase of the cell cycle. AP-1 proteins bind the cyclin D1-954 region. Cyclin D1 promoter activity is stimulated by over expression of mitogen-activated protein kinase through the proximal 22 base pairs (Albanese et al., 1995). Several AP-1 proteins are shown to bind these sites and activate cyclin D1 expression (Albanese et al., 1995; Brown et al., 1998; Beier et al., 1999). Our results also show that CEES-induced increase in the AP-1-dependent cell cycle proteins as well as cell differentiation marker is blocked by antioxidant liposome treatment (Fig. 8).

Thus, antioxidant liposomes offer a protection against CEES-induced activation of AP-1 signaling. We have previously reported that antioxidant liposomes protect against CEES-induced lung fibrosis (Mukherjee et al., 2009). The effect is probably modulated via AP-1 signaling pathway. Our studies also indicate that early inhibition of proinflammatory mediators and transendothelial migration of neutrophils and eosinophils could be key regulators for CEES-induced lung fibrosis and/or ARDS.

Conflict of interest

None.

Acknowledgement

This study was supported by the US Army Grant W81XWH-06-2-0044.

References

- Albanese, C., Johnson, J., Watanabe, G., Eklund, N., Vu, D., Arnold, A., Pestell, R.G., 1995. Transforming p21ras mutants and c-Ets-2 activate the cyclin D1 promoter through distinguishable regions. *J. Biol. Chem.* 270, 23589–23597.
- Angel, P., Karin, M., 1991. The role of Jun, Fos and the AP-1 complex in cell-proliferation and transformation. *Biochim. Biophys. Acta* 1072, 129–157.
- Baud, V., Karin, M., 2001. Signal transduction by tumor necrosis factor and its relatives. *Trends Cell Biol.* 11, 372–377.
- Beier, F., Lee, R.J., Taylor, A.C., Pestell, R.G., LuValle, P., 1999. Identification of the cyclin D1 gene as a target of activating transcription factor 2 in chondrocytes. *Proc. Natl. Acad. Sci. U.S.A.* 96, 1433–1438.
- Brown, P.H., Alani, R., Preis, L.H., Szabo, E., Birrer, M.J., 1993. Suppression of oncogene-induced transformation by a deletion mutant of c-jun. *Oncogene* 8, 877–886.
- Brown, J.R., Nigh, E., Lee, R.J., Te, H., Thompson, M.A., Saudou, F., Pestell, R.G., Greenberg, M.E., 1998. Fos family members induce cell cycle entry by activating cyclin D1. *Mol. Cell Biol.* 18, 5609–5619.
- Chatterjee, D., Mukherjee, S., Smith, M.G., Das, S.K., 2003. Signal transduction events in lung injury induced by 2-chloroethyl ethyl sulfide, a mustard analog. *J. Biochem. Mol. Toxicol.* 17, 114–121.
- Cromwell, O., Hamid, Q., Corrigan, C.J., Barkans, J., Meng, Q., Collins, P.D., Kay, A.B., 1992. Expression and generation of interleukin-8, IL-6 and granulocyte-macrophage colony-stimulating factor by bronchial epithelial cells and enhancement by LI-1 beta and tumor necrosis factor-alpha. *Immunology* 77, 330–337.
- Dacre, J.C., Goldman, M., 1996. Toxicology and pharmacology of the chemical warfare agent sulfur mustard. *Pharmacol. Rev.* 48, 289–326.
- Das, S.K., Mukherjee, S., Smith, M.G., Chatterjee, D., 2003. Prophylactic protection by N-acetylcysteine against the pulmonary injury induced by 2-chloroethyl ethyl sulfide, a mustard analogue. *J. Biochem. Mol. Toxicol.* 17, 177–184.
- Devary, Y., Gottlieb, R.A., Lau, L.F., Karin, M., 1991. Rapid and preferential activation of the c-Jun gene during the mammalian UV response. *Mol. Cell Biol.* 11, 2804–2811.
- Fan, J., Shel, P.N., Sontres, Z.E., Li, Y.H., Oreopoulos, G.D., Rotstein, O.D., 2000. Liposomal antioxidants provide prolonged protection against acute respiratory distress syndrome. *Surgery* 128, 332–338.
- Gillardon, F., Moll, I., Uhlmann, E., 1995. Inhibition of c-Fos expression in the UV-irradiated epidermis by topical application of antisense oligodeoxynucleotides suppresses activation of proliferating cell nuclear antigen. *Carcinogenesis* 16, 1853–1856.
- Herdegen, T., Leah, J.D., 1998. Inducible and constitutive transcription factors in the mammalian nervous system: control of gene expression by Jun, Fos and Krox, and CREB/ATF proteins. *Brain Res. Brain Res. Rev.* 28, 370–490.
- Kehrer, J.P., 1993. Free radicals as mediators of tissue injury and disease. *Crit. Rev. Toxicol.* 23, 21–48.

- Krunkosky, T.M., Fischer, B.M., Martin, L.D., Jones, N., Akley, N.J., Adler, K.B., 2000. Effects of TNF- α expression of ICAM-1 in human airway epithelial cells *in vitro*. *Am. J. Respir. Cell Mol. Biol.* 22, 685–692.
- Leff, J.A., Parsons, P.E., Day, C.E., Taniguchi, N., Jochum, M., Fritz, H., Moore, F.A., Moore, E.E., McCord, J.M., Repine, J.E., 1993. Serum antioxidants as predictors of adult respiratory distress syndrome in patients with sepsis. *Lancet* 341, 777–780.
- Lloyd, S.S., Cheng, A.K., Taylor, F.B., McCay, J.E.G., 1993. Free radicals and septic shock in primates: the role of tumor necrosis factor. *Free Radic. Biol. Med.* 14, 233–242.
- Masuya, Y., Kameshita, I., Fujisawa, H., Kohno, H., Hioki, K., Tokunaga, R., Taketani, S., 1999. MAP kinase-independent induction of proto-oncogene *c-fos* mRNA by hemin in human cells. *Biochem. Biophys. Res. Commun.* 260, 289–295.
- Mata, M., Ruiz, A., Cerdá, M., Martínez-Losa, M., Cortijo, J., Santangelo, F., Serrano-Mollar, A., Llombart-Bosch, A., Morcillo, E.J., 2003. Oral N-acetylcysteine reduces bleomycin-induced lung damage and mucin Muc5ac expression in rats. *Eur. Respir. J.* 22, 900–905.
- McClintock, S.D., Hoesel, L.M., Das, S.K., Till, G.O., Neff, T., Kunkel, R.G., Smith, M.G., Ward, P.A., 2006. Attenuation of half sulfur mustard gas-induced acute lung injury in rats. *J. Appl. Toxicol.* 26, 126–131.
- McDonnell, S.E., Kerr, L.D., Matrisian, L.M., 1990. Epidermal growth factor stimulation of stromelysin mRNA in rat fibroblasts requires induction of proto-oncogenes *c-fos* and *c-jun* and activation of protein kinase C. *Mol. Cell Biol.* 10, 4284–4293.
- Mellor, S.G., Rice, P., Cooper, G.C., 1991. Vesicant burns. *Br. J. Plast. Surg.* 44, 434–437.
- Mukherjee, S., Stone, W.L., Yang, H., Smith, M.G., Das, S.K., 2009. Protection of half sulfur mustard gas-induced lung injury in guinea pig by antioxidant liposome. *J. Biochem. Mol. Toxicol.* 23, 143–153.
- Mukhopadhyay, S., Mukherjee, S., Smith, M., Das, S.K., 2008. Activation of MAPK/AP-1 signaling pathway in lung injury induced by 2-chloroethyl ethyl sulfide, a mustard gas analog. *Toxicol. Lett.* 181, 112–117.
- Papirmeister, B., Fenster, A.J., Robinson, S.I., Ford, R.D., 1991. Sulfur mustard injury: description of lesions and resulting incapacitations. In: Fenster, A.J., Boca Raton, F.L. (Eds.), *Medical Defense Against Mustard Gas. Toxic Mechanisms and Pharmacological Implications*. CRC, pp. 13–42.
- Rahman, I., 2000. Regulation of nuclear factor-kappa B, activator protein-1, and glutathione levels by tumor necrosis factor-alpha and dexamethasone in alveolar epithelial cells. *Biochem. Pharmacol.* 60, 1041–1049.
- Reddy, S.P., Mossman, B.T., 2002. Role and regulation of activator protein-1 in toxicant-induced responses of the lung. *Am. J. Physiol. Lung Cell Mol. Physiol.* 283, L1161–1178.
- Rocksén, D., Ekstrand-Hammarström, B., Johansson, L., Bucht, A., 2003. Vitamin E reduces transendothelial migration of neutrophils and prevents lung injury in endotoxin-induced airway inflammation. *Am. J. Respir. Cell Mol. Biol.* 28, 199–207.
- Schreck, R., Rieber, P., Bauerle, P.A., 1991. Reactive oxygen intermediates as apparently widely used messengers in the activation of the NF-kappa B transcription factor and HIV-1. *EMBO J.* 10, 2247–2258.
- Shaulian, E., Karin, M., 2001. AP-1 in cell proliferation and survival. *Oncogene* 20, 2390–2400.
- Shaulian, E., Karin, M., 2002. AP-1 as a regulator of cell life and death. *Nat. Cell Biol.* 4, E131–136.
- Smith, M.G., Stone, W., Crawford, K., Ward, P., Till, G.O., Das, S.K., 2003. A promising new treatment for mustard gas with the potential to substantially reduce the threat posed by chemical, biological and radiological agents. *Jane's Chem-Bio Web*, 1–5.
- Steinmuller, L., Cibelli, G., Moll, J.R., Vinson, C., Thiel, G., 2001. Regulation and composition of activator protein 1 (AP-1) transcription factors controlling collagenase and c-Jun promoter activities. *Biochem. J.* 360, 599–607.
- Sun, Y., Oberley, L.W., 1996. Redox regulation of transcriptional activators. *Free Radic. Biol. Med.* 21, 335–348.
- Suntres, Z.E., Shek, P.N., 1997. Protective effect of liposomal alphotocopherol against bleomycin-induced lung injury. *Biomed. Environ. Sci.* 10, 47–59.
- Szabo, E., Presis, L.H., Brown, P.H., Birrer, M.J., 1991. The role of jun and fos gene family members in 12-O-tetradecanoylphorbol-13-acetate induced hemopoietic differentiation. *Cell Growth Differ.* 2, 475–482.
- Taylor, K.M.G., Farr, S.J., 1993. Liposomes for drug delivery to the respiratory track. *Drug Dev. Ind. Pharm.* 19, 123–142.
- Willems, J.L., 1989. Clinical management of mustard gas casualties. *Ann. Med. Milit. Belg.* 3, 1–61.
- Yamaguchi, M., Hayashi, Y., Hirose, F., Matsuo, S., Moriuchi, T., Shiroishi, T., Moriwaki, K., Matsukage, A., 1991. Molecular cloning and structural analysis of mouse gene and pseudogenes for proliferating cell nuclear antigen. *Nucleic Acids Res.* 19, 2403–2410.

Protection of Half Sulfur Mustard Gas-Induced Lung Injury in Guinea Pigs by Antioxidant Liposomes

Shyamali Mukherjee,¹ William L. Stone,² Hongsong Yang,² Milton G. Smith,³ and Salil K. Das¹

¹Department of Cancer Biology, Meharry Medical College, Nashville, TN 37208, USA; E-mail: sdas@mmc.edu

²Department of Pediatrics, East Tennessee State University, Johnson City, TN 37614, USA

³Amaox Ltd., Melbourne, FL 32944, USA

Received 15 September 2008; revised 13 November 2008; accepted 15 November 2008

ABSTRACT: The purpose of this study was to develop antioxidant liposomes as an antidote for mustard gas-induced lung injury in a guinea pig model. Five liposomes (LIP-1, LIP-2, LIP-3, LIP-4, and LIP-5) were tested with differing levels of phospholipid, cholesterol, phosphatidic acid, tocopherol (α , γ , δ), *N*-acetylcysteine (NAC), and glutathione (GSH). A single dose (200 μ L) of liposome was administered intratracheally 5 min or 1 h after exposure to 2-chloroethyl ethyl sulfide (CEES). The animals were sacrificed either 2 h after exposure (for lung injury study) or 30 days after exposure (for histology study). The liposomes offered 9%–76% protection against lung injury. The maximum protection was with LIP-2 (71.5% protection) and LIP-4 (75.4%) when administered 5 min after CEES exposure. Delaying the liposome administration 1 h after CEES exposure decreased the efficacy. Both liposomes contained 11 mM α -tocopherol, 11 mM γ -tocopherol, and 75 mM NAC. However, LIP-2 contained additionally 5 mM δ -tocopherol. Overall, LIP-2 and LIP-4 offered significant protection by controlling the recruitment of neutrophils, eosinophils, and the accumulation of septal and perivascular fibrin and collagen. However, LIP-2 showed better protection than LIP-4 against the accumulation of red blood cells in the bronchi, alveolar space, arterioles and veins, and fibrin and collagen deposition in the alveolar space. The antifibrotic effect of the liposomes, particularly LIP-2, was further evident by a decreased level of lipid peroxidation and hydroxyproline in the lung. Thus, antioxidant liposomes containing both NAC and vitamin E are an effective antidote against CEES-induced lung injury. © 2009 Wiley Periodicals, Inc. *J Biochem Mol Toxicol* 23:143–153, 2009; Published online in Wiley InterScience (www.interscience.wiley.com). DOI 10.1002/jbt.20279

KEYWORDS: 2-Chloroethyl Ethyl Sulfide (CEES); Lung Injury; Liposomes; Collagen; Pulmonary Fibrosis

INTRODUCTION

Mustard gas is a chemical warfare agent known to exert toxic effects on eyes, skin, and respiratory tissue followed by impairment of the nervous, cardiac, and digestive systems in humans and laboratory animals [1–3]. Upper and lower respiratory tracts may be acutely damaged because of hemorrhagic inflammation after inhalation of mustard gas. Subsequently, a variety of chronic pulmonary complications may develop, including acute respiratory distress syndrome, chronic bronchitis, and pulmonary fibrosis [4–8].

Although the exact mechanism is not well understood, it is not unreasonable to postulate a causal role of oxidative stress in the pathology that follows exposure to mustard gas. Many inflammatory lung diseases, including acute respiratory distress syndrome, are associated with oxidative stress [9]. For example, inflammatory cytokines, such as tumor necrosis factor- α (TNF- α), provoke the generation of reactive oxygen species, mediators of oxidative stress [10].

Recently, we reported that intratracheal exposure of sulfur mustard analog, 2-chloroethyl ethyl sulfide (CEES), to guinea pigs caused a high accumulation of TNF- α in the lung [11]. TNF- α elevations resulted in activation of acid and neutral sphingomyelinases and the production of excessive ceramides, a second messenger involved in programmed cell death (apoptosis) [11]. In addition, intratracheal exposure to CEES leads to an immediate but transient activation of NF- κ B, which is regarded as an antiapoptotic signaling molecule. The abrupt disappearance of NF- κ B, however, resulted in activation of several caspases, leading to apoptosis [11].

Correspondence to: Salil K. Das.

Contract Grant Sponsors: US Department of Army W81XWH-06-2-0044.

© 2009 Wiley Periodicals, Inc.

Ultrastructural assessment of the lungs from guinea pigs exposed to a single low dose of CEES (0.5 mg/kg body weight) showed an increase in neutrophilic alveolitis and varying degrees of interstitial fibrosis [8,12]. The lung injury was characteristic of that caused by oxidative stress secondary to the inhibition of defense enzymes against oxygen injury, such as superoxide dismutase (SOD), glutathione peroxidase, and catalase [12].

Recently, we reported that drinking water with an antioxidant *N*-acetylcysteine (NAC) provided protection against CEES-induced lung injury [12]. This protection was associated with (a) inhibition of CEES-induced activation of TNF- α , NF- κ B, sphingomyelinases, and caspases; (b) inhibition of CEES-induced accumulation of ceramides; and (c) protection of the oxygen defense system by counteracting CEES-induced inhibition of SOD, glutathione peroxidase, and catalase activities [12]. We also observed protection against CEES-induced lung injury in rats by intratracheal administration of liposomes containing catalase, SOD, or the reducing agents NAC, GSH, or resveratrol [13].

It is known that skin injured by mustard gas exposure can be treated by rapidly decontaminating or detoxifying the contaminated sites and applying ointment to the surface [14,15]. Those kinds of treatments, however, are not possible for lung injury and no prophylactic treatment has been available for pulmonary injury by mustards. Because of this lack of a prophylactic treatment, the unprotected civilian is at risk for pulmonary injury from mustards. Therefore, it is important to develop a suitable antioxidant liposome therapy for the protection of injury induced by mustard gas exposure. The present study reports data on the attenuation of CEES-induced acute lung injury in guinea pigs by five antioxidant liposomes differing in the levels of phospholipid, cholesterol, phosphatidic acid, tocopherol (α , γ , δ), NAC, and GSH.

MATERIALS AND METHODS

Chemicals

Except where noted, all chemicals and reagents were purchased from Sigma-Aldrich (St. Louis, MO).

Animal Model

Male guinea pigs (Hartley strain, 5–6 weeks old, 400-g body weight) were obtained from Harlan Sprague Dawley Inc (Indianapolis, IN). Animals were infused intratracheally with single doses of CEES (2 mg/kg body weight) in ethanol (infusion volume was 100 μ L/animal). Control animals were infused with 100 μ L of ethanol in the same way. All animal

experiments were in accordance with the standards in the Guide for the Care and Use of Laboratory Animals and were supervised by veterinarians from the Unit for Laboratory and Animal Care of the Meharry Medical College.

Liposome Preparation

Antioxidant liposomes were prepared using a model M-110L Microfluidizer (Microfluidics Headquarters, Newton, MA) as described earlier [16]. Soybean phospholipids (as PL90H from Lipoid LLC, Newark, NJ), phosphatidic acid (Avanti Polar Lipids Inc., Alabaster, AL), cholesterol (Sigma-Aldrich, St. Louis, MO), RRR- α -tocopherol and RRR- γ -tocopherol (Cognis Corporation, LaGrange, IL), and RRR- δ -tocopherol (Cayman Chemicals, Ann Arbor, MI) were dissolved in dichloromethane and added (in various combinations) to a round bottom flask. The solvent was removed with a rotary film evaporator and the lipid film hydrated by rapid mixing with sterile phosphate buffer saline (PBS) buffer containing various water-soluble antioxidants, that is, reduced glutathione or *N*-acetyl-*L*-cysteine. The hydrated lipids were then passed three times through the M-110L microfluidizer. The liposomes were characterized by measuring their particle size distribution using a dynamic light scattering Model 380 Nicomp particle analyzer (Particle Sizing Systems, Santa Barbara, CA). The particle size of the liposomes was large with an average diameter of 1000 nm. It has been established earlier that a large particle size facilitates cellular uptake of liposomes [16,17].

Liposome Treatment

Altogether, five different antioxidant liposome preparations were tested, as outlined in Table 1 which shows the composition and concentrations of the stock liposomal formulations. Liposomes were injected intratracheally in a volume of 200 μ L per animal through the same catheter setup used for CEES instillation. Liposomes were given 5 and 60 min after CEES exposure and sacrificed after 2 h.

Measurement of Lung Injury by Leakage of Plasma Albumin Into the Lung

Lung injury was monitored by studying the leakage of 125 I-BSA into lung after CEES exposure [12]. 125 I-BSA solution (8 μ Ci/animal) was slowly injected into the guinea pigs' ear vein and CEES (2 mg/kg body weight) was infused into the animals intratracheally 3 h after 125 I-BSA injection. Control animals were infused intratracheally with 100 μ L of solvent alone. The animals were sacrificed 5 h after 125 I-BSA injection

TABLE 1. Composition of Antioxidant Liposomes

Liposomes	Liposome Content							
	Phospholiposome (PL90H) Mole Fraction	Cholesterol Mole Fraction	Phosphatidic Acid (PA) Mole Fraction	Tocopherol (mM) (Vitamin E)			NAC mM	GSH (mM)
				α	γ	δ		
LIP-1 (Blank)	71	28	0.67	–	–	–	–	–
LIP-2	55	22	0.6	11	11	5	75	–
LIP-3	62	25	0.6	6	6	–	75	–
LIP-4	55	22	0.6	11	11	–	75	–
LIP-5	55	22	0.6	11	11	–	–	75

(i.e., 2 h after CEES infusion) and 1 mL of blood was collected. The chest cavity was opened and lung perfused with buffer to remove any residual blood. The perfused lung was taken out and after removal of the heart and trachea, the radioactivity content of the lung was monitored using a gamma counter. Lung injury was expressed as permeability index that was obtained by dividing total radioactive counts in the lung by counts in 1 mL of blood from the same animal.

Morphological Assessment of Lung Injury

For morphological assessment of lung injury, animals were sacrificed 30 days after CEES exposure. Lungs were isolated and fixed by intratracheal instillation of 10 mL buffered (pH 7.2) formalin (10%). Lung sections were obtained for histological examination by staining with hematoxylin and eosin. In addition, lung sections were stained with trichrome for assessment of fibrin and collagen deposition [13]. For morphometric analysis of specific inflammatory cells [polymorphonucleus (PMN) and eosinophilic leukocytes], seven fields of the lung sections were used under the microscope.

Assessment of Oxidative Stress in Lung by Measurement of Lipid Peroxidation

All animals were sacrificed 30 days after CEES exposure. For experiments with the liposomal protection, a single dose (200g μ L per animal) of each liposome was administered intratracheally 5 min after CEES exposure. For assessment of oxidative stress in lung, the lipid peroxidation profile was determined by measuring the formation of malonaldehyde–thiobarbituric acid derivative as described by us earlier [18].

Assessment of Lung Fibrosis by Measurement of Hydroxyproline Content

All animals were sacrificed 30 days after CEES exposure. For experiments with the liposomal protection,

a single dose (200g μ L per animal) of each liposome was administered intratracheally 5 min after CEES exposure. For assessment of fibrosis in lung, the hydroxyproline content was determined as described by Fujita et al. [19]. In brief, lung specimens were lyophilized, pulverized, and incubated overnight with 6 N HCl at 120°C. The acid hydrolysates (5 μ L) and hydroxyproline standards (Sigma-Aldrich, St. Louis, MO) were applied to an enzyme-linked immunosorbent assay plate along with 5 μ L of citric acid/acetate buffer and 100 μ L of chloramine T solution. The plates were incubated for 20 min at room temperature and then 100 μ L of Ehrlich's solution was added and incubated further at 65°C for 15 min. The reaction product was read at 550 nm.

Statistical Analysis

We subjected all parameters to two-group repeated measures analysis of variance. Data are expressed as means \pm SE. $p < 0.05$ was used as the significance level for all tests.

RESULTS

Leakage of Plasma Albumin Into the Lung

CEES-induced lung injury is expressed as permeability index, which is a measure of 125 I-BSA leakage from blood into the lung. The data presented in Table 2 indicate that all liposomes offered protection; however, the efficacy varied (9.2%–75.4%) depending on the liposomal composition. Two liposome preparations offered maximum protection (LIP 2 at 71.5%, LIP-4 at 75.4%) when given within 5 min of CEES exposure. Liposome 2 contained 11 mM α -Vit E, 11 mM γ -Vit E, 5 mM δ -Vit E, and 75 mM NAC. The only difference between LIP-2 and LIP-4 is that LIP-4 did not have any δ -Vit E. The protection was diminished if the liposome delivery was delayed for 1 h. Maximum protection was 43% if the liposome was given 1 h after CEES exposure.

TABLE 2. Effects of Liposome Treatment on CEES-Induced Lung Injury in Guinea Pigs (Leakage of ¹²⁵I-BSA From Blood Into the Lung)

Treatment	Permeability Index	
	Liposomes Injected 5 (min) After CEES Exposure	Liposomes Injected 60 (min) After CEES Exposure
Control (No CEES)	0.20 ± 0.04	
CEES only	1.30 ± 0.22	
CEES + LIP-1	1.18 ± 0.03	1.11 ± 0.21
CEES + LIP-2	0.37 ± 0.03*	0.74 ± 0.04*
CEES + LIP-3	0.60 ± 0.02	0.80 ± 0.06
CEES + LIP-4	0.32 ± 0.01*	0.76 ± 0.03*
CEES + LIP-5	0.64 ± 0.05	0.83 ± 0.04

Guinea pigs were infused intratracheally with CEES (2 mg/kg body weight) with or without antioxidant liposomes. Liposomes (LIP-1, LIP-2, LIP-3, LIP-4, and LIP-5) were infused intratracheally either 5 or 60 min after CEES exposure. The lung injury was measured after 2 h of CEES exposure and expressed as permeability index, which is a measure of ¹²⁵I-BSA leakage from damaged blood vessels into lung tissue. ¹²⁵I-BSA was injected into the ear veins 3 h prior CEES exposure. Each group had three animals. Values are mean ± SE. Asterisks indicate statistically different from CEES-exposed groups without any liposomes LIP-1 ($p < 0.05$).

Furthermore, LIP-4 offered better protection than LIP-5. Although both contained α -Vit E and γ -Vit E, they differed in the concentration of NAC and GSH. LIP-4 contained 75 mM NAC and no GSH, whereas LIP-5 contained 75 mM GSH and no NAC. It suggests that NAC has a better protective effect than GSH.

Morphological Assessment of Lung Injury

Figure 1 shows the histological characteristics of the control lung. The overall pulmonary architecture, including bronchus, bronchioles, alveolar ducts, alveoli, vascular endothelium, and smooth muscular layers are well maintained (Figures 1a–1f). The alveoli contain alveolar macrophages (thick arrow, Figure 1f) and occasionally PMNs (Figure 1e). The type II alveolar epithelial cells are cuboidal of normal size with unremarkable nucleus and cytoplasm (thin arrow, Figure 1f). The type I alveolar epithelial cells are intact and present a flat profile (Figures 1e and 1f). The alveolar capillaries show normal luminal size and overall architecture (Figure 1c). Trichrome stain revealed the usual perivascular and septal evidence of fibrin and collagen (arrow, Figures 1g–1l).

Figure 2 shows the histological characteristic of CEES-exposed lung. CEES exposure causes acute inflammation with infiltration of several PMNs (2.10 ± 0.25 /mm of visual field) and eosinophils (1.48 ± 0.29 /mm of visual field) in alveoli. Bronchial constriction is pronounced (thick arrow, Figures 2a and 2g). Almost all of small or large diameter bronchus show evidence of smooth muscle contraction. The lumen of the

small bronchus contains pale bluish firm-looking exudates in which there are many cells, mostly eosinophilic leukocytes (thick arrow Figures 2d and 2e). In the wall of the bronchus, there is also a much thicker band of hypertrophic eosinophilic smooth muscle cells (thin arrow, Figure 2d) beneath the basement membrane and a moderate infiltrate of eosinophilic leukocytes and PMNs on each side of the smooth muscle. The bronchus is lined by a single layer of large palisade epithelial cells, distended with mucus on a relatively thick basement (Figure 2d). The adjacent alveoli appear collapsed or big hollow due to CEES burn (Figures 2c, 2e, and 2f). There are also several apoptotic nuclei in the bronchial epithelial layers. But it is not clear whether these cells are inflammatory or bronchiolar epithelial in origin. Furthermore, there are several foci of intraepithelial, intramuscular, and interstitial aggregation of red blood cells (RBCs) in the bronchi, alveolar space, arterioles, and veins (thin arrow, Figures 2c, 2e, 2f, and 2i). Alveoli number is significantly decreased in some area of the lung (Figures 2b, 2i, and 2l). Trichrome stains revealed the deposition of severe trichrome-positive (blue dye) materials in bronchial smooth muscle, alveolar walls, and interstitial and intra-alveolar region of lung than normal, suggesting deposition of fibrin and collagen fibers (thin arrow, Figures 2j–2l). Intra-alveolar hemorrhage, edema, and intra-alveolar accumulation of macrophages and mononuclear cells were evident. Furthermore, extensive confluent collagen deposition was observed throughout the lung sections (Figure 2) together with a collapse of alveolar structure (Figures 2b, 2e, 2f, 2i, and 2l).

Figure 3 and Figure 4 show histological characteristic of lungs from CEES-exposed animals that received treatment of LIP-2 and LIP-4 antioxidant liposomes, respectively, 5 min after CEES exposure. Both antioxidant liposomes-treated lungs show less inflammation with very few PMNs (0.20 ± 0.05 /mm for LIP-2 and 0.32 ± 0.06 /mm for LIP-4) and eosinophils (0.48 ± 0.09 /mm for LIP-2 and 0.52 ± 0.07 /mm for LIP-4) in alveoli throughout the sections. Both bronchioles and terminal bronchioles (thick arrow, Figures 3b and 3d; Figures 4b and 4j) have more or less similar histological feature as seen in the control lungs. However, while LIP-4 did not have any significant effect against accumulation of CEES-induced aggregated RBCs (thick arrow, Figures 4e and 4h) in the lung, LIP-2 treatment reduced the number of aggregated RBCs. The alveoli contained less type II or type I cells in both LIP-2- and LIP-4-treated groups than control (Figures 3c, 3e, and 3f and Figures 4c, 4e, and 4f). Furthermore, big hollow areas due to CEES burn are still present in both liposome-treated groups (Figure 3a and Figure 4a). Trichrome stains revealed that there are normal levels of perivascular and septal collagen in both liposome-treated groups as seen

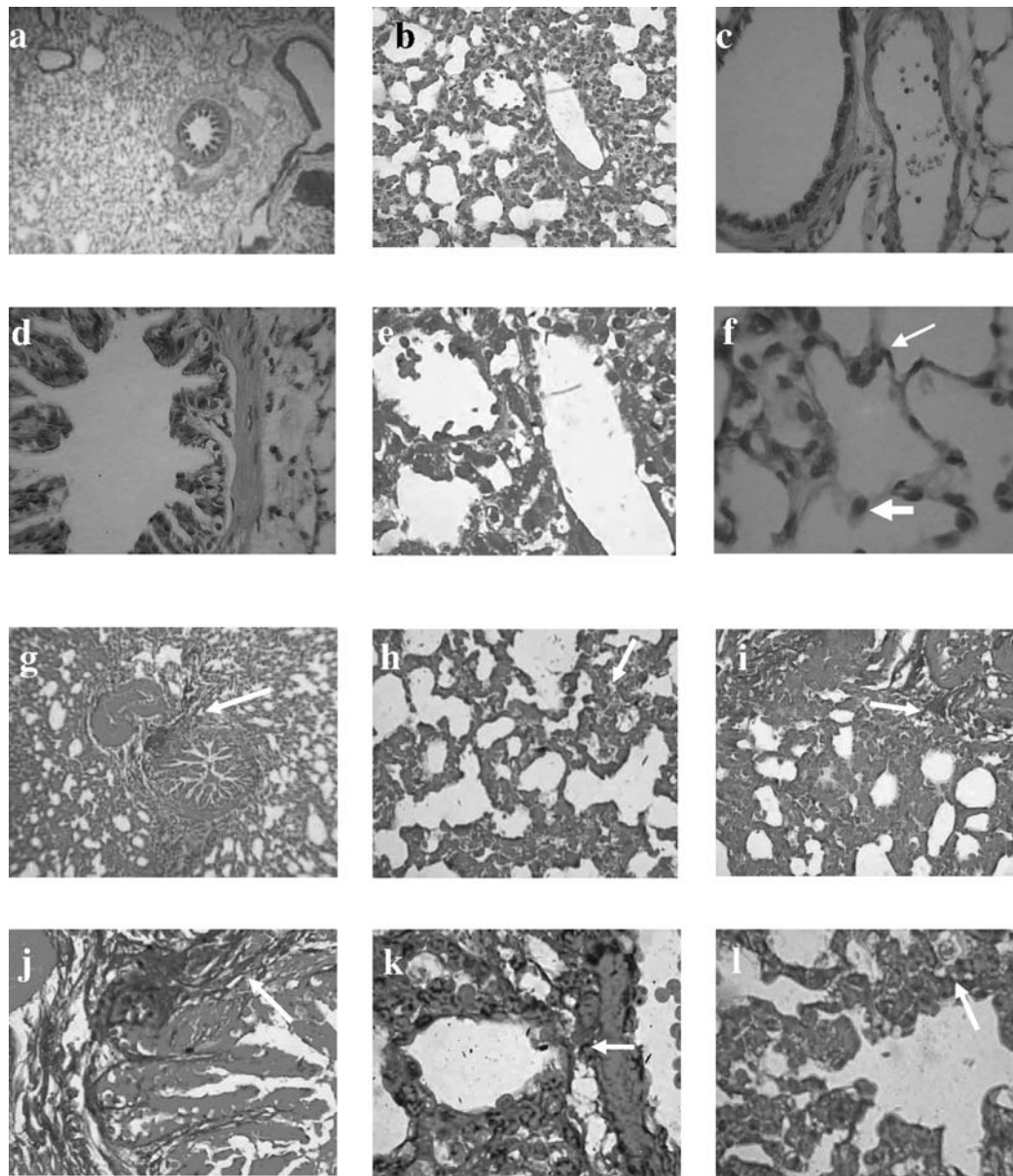


FIGURE 1. Sections of control lungs with h and e (a–f) and trichrome stain (g–l). Lungs were obtained after tracheal instillation of vehicle at 30 days (a, g 10 \times ; b, c, h, i 40 \times ; d, e, f, j, k, and l 100 \times).

in control lung (Figures 3g–3l and Figures 4g–4k). However, the alveolar space of LIP-4-treated lung (Figure 4l) contained more trichrome-positive materials in comparison with the control and LIP-2-treated lungs.

Assessment of Lipid Peroxidation in Lung

Data on the lipid peroxidation are shown in Figure 5. There was a significant increase in the *in vitro* lipid peroxidation potential of the lungs exposed to CEES. The lipid peroxidation was significantly decreased by both antioxidant liposomes (LIP-2 and LIP-4). However, the protection was higher in LIP-2

group than LIP-4 group. The blank liposome (LIP-1) did not have any significant effect on the CEES-exposed group, although it reduced the peroxidation potential in the control group.

Assessment of Lung Fibrosis

Data on the levels of hydroxyproline in lung are shown in Figure 6. There was a significant increase in the levels of hydroxyproline in lungs exposed to CEES. Both antioxidant liposomes (LIP-2 and LIP-4) reduced the hydroxyproline levels significantly; however, the protection was much higher in the LIP-2 group than

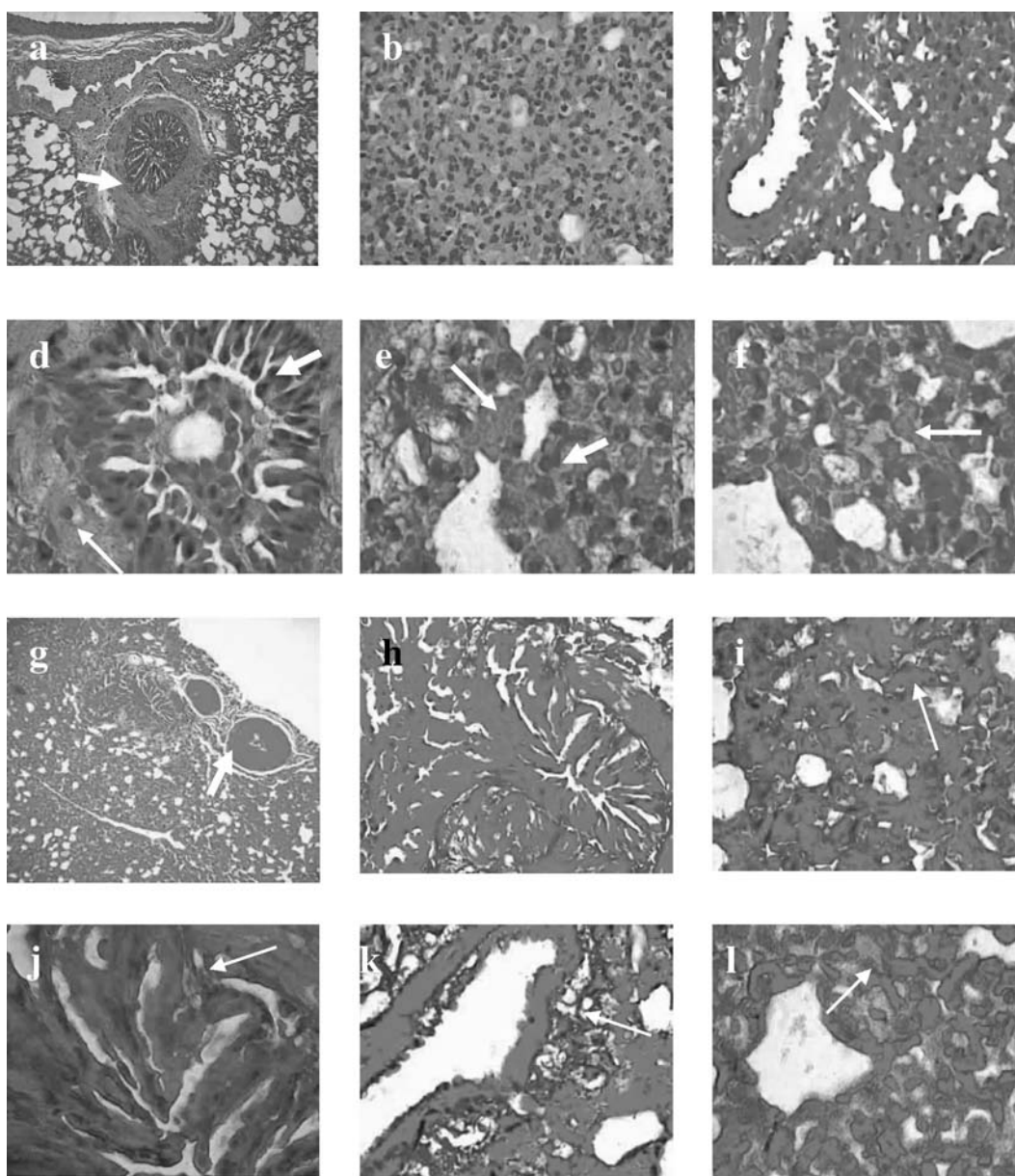


FIGURE 2. Sections of CEES-exposed lungs with h and e (a–f) and trichrome stain (g–l). Lungs were obtained after 30 days of single exposure of CEES (2 mg/kg) (a, g 10 \times ; b, c, h, i 40 \times ; d, e, f, j, k, l 100 \times).

LIP-4 group. It is interesting that the blank liposome (LIP-1) caused a significant decrease in both control and CEES-exposed groups. However, the decrease was significantly less than that in LIP-2 group and equal in comparison with the LIP-4 group.

DISCUSSION

Sulfur mustard and CEES are known to cause oxidative stress and lipid peroxidation [12]. A number of other mechanisms have also been proposed for their

cytotoxic effects including DNA damage. Furthermore, we previously reported that intratracheal infusion of CEES produces acute lung injury in a manner that seems related to the loss of the redox balance in the lung, although our study did not demonstrate this directly. This conclusion was based on the attenuative effects of reducing agents (NAC, GSH) or changes of peroxide scavenger status in the CEES-exposed guinea pig lung [12]. The data described here indicate that intratracheal infusion of CEES causes not only an increase in the permeability index of lung but also an increase in lung damage as evidenced by lung histopathology.

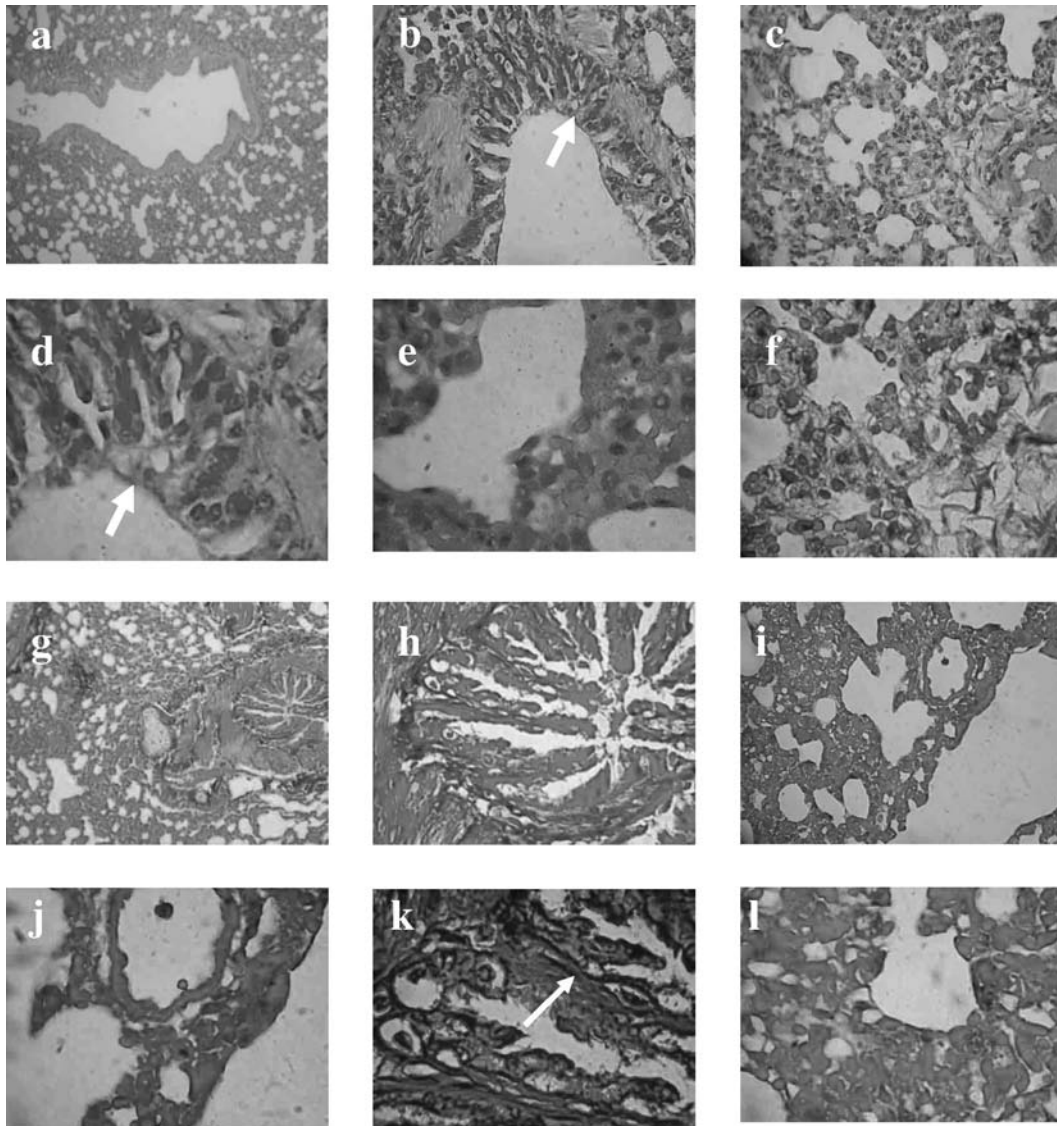


FIGURE 3. Sections of lungs exposed to CEES and LIP-2. Guinea pigs were exposed to CEES (2 mg/kg) intratracheally and 5 min later received a single tracheal instillation of 200 μ L LIP-2. After 30 days of CEES exposure, lung sections were stained with h and e (a–f) and trichrome stain (g–l) (a, g 10 \times ; b, c, h, i 40 \times ; d, e, f, j, k, l 100 \times).

The morphological features described in this report are consistent with our previous findings in rat lung after CEES infusion [13].

Lung parenchymal damage, occlusion of bronchial lumen, and pseudomembrane formation observed in this study have also been observed by others [20,21]. The presence of alveolar hemorrhage and edema indicates a severe disruption of vascular and distal airway barrier (Figure 2). Masson's trichrome staining revealed an accumulation of fibrin and or collagen within interstitial and alveolar spaces (Figures 2g–2l). Deposition of fibrin and collagen indicates that CEES exposure causes development of interstitial fibrosis. Furthermore, the

recruitment of neutrophils in the air spaces and interstitium indicates that CEES causes acute pulmonary inflammation. It has been well documented that cells activated at the inflamed site can release a variety of cytotoxic agents, such as proteases and free radicals, thereby injuring parenchymal cells [22–24]. It has also been reported that sulfur mustard gas causes pulmonary parenchymal cell death and this is associated with lipid peroxidation and depletion of glutathione [25,26].

The death following sulfur mustard gas exposure is attributed mainly to hypoxia resulting from the occlusion of bronchioles and airways [2,27]. In this study,

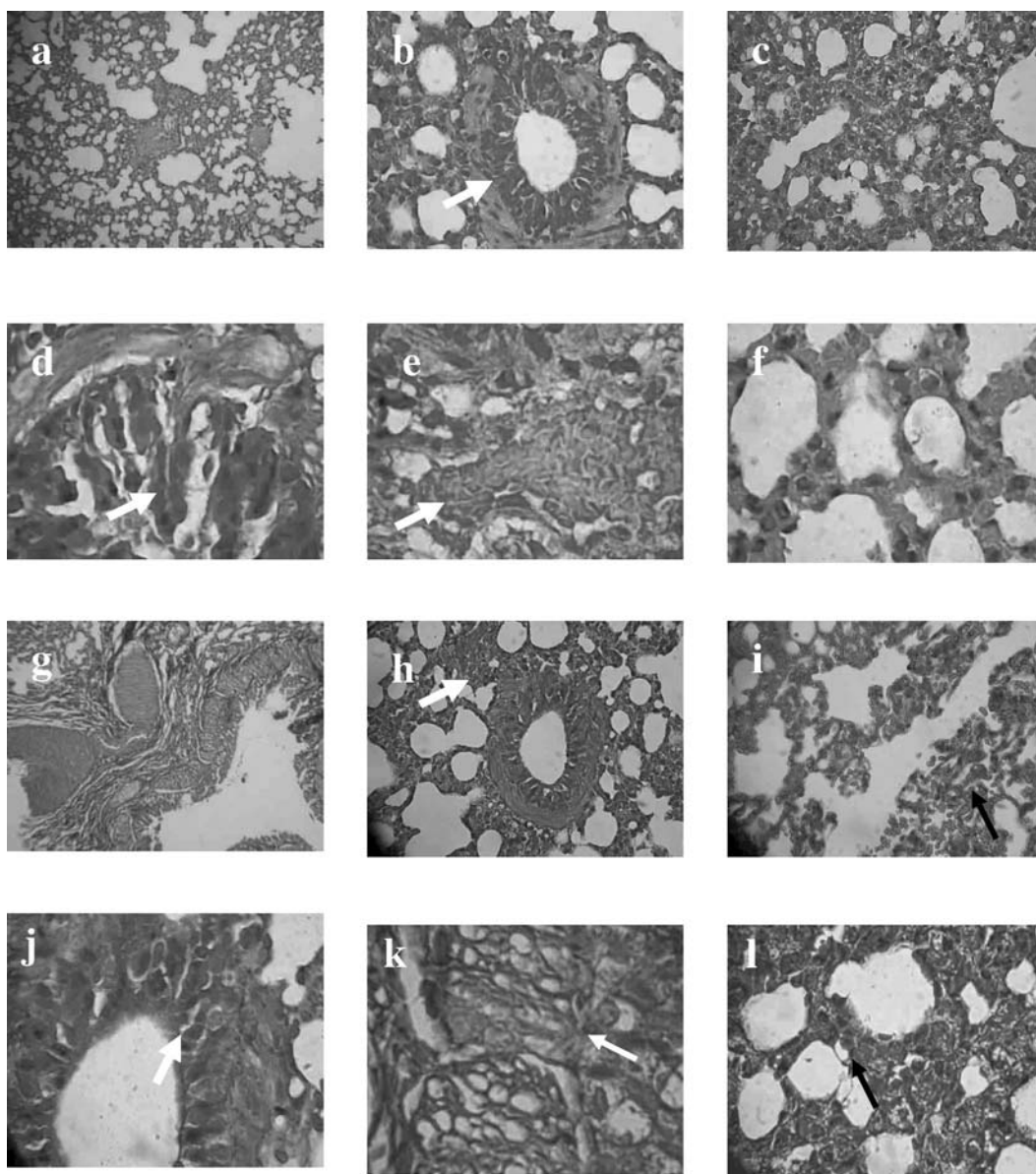


FIGURE 4. Sections of lungs exposed to CEES and LIP-4. Guinea pigs were exposed to CEES (2 mg/kg) intratracheally and 5 min later received a single tracheal instillation of 200 μ L LIP-4. After 30 days of CEES exposure, lung sections were stained with h and e (a–f) and trichrome stain (g–l) (a, g 10 \times ; b, c, h, i 40 \times ; d, e, f, j, k, l 100 \times).

we also observed occlusion of bronchioles and airways, pyknosis/necrosis of bronchiole-associated lymphoid tissue due to CEES exposure (Figure 2). The alveolar walls of CEES-infused animals became lined with waxy hyaline membranes (Figure 2) that are similar to those seen in hyaline membrane disease of neonates [23]. Furthermore, the presence of alveolar hemorrhage and edema indicates a severe disruption of vascular and distal airway barrier (Figures 2c and 2e). It also appears that CEES exposure causes epithelial and endothelial damage as well as migration of PMN and eosinophils. These changes lead to interstitial and alveolar accu-

mulation of collagen thereby resulting in parenchymal collapse and honeycombing changes similar to those observed in human with pulmonary fibrosis. Numerous macrophages, PMNs, and eosinophils in areas of collagen deposition in the lung may be associated with the release of mediators such as TNF- α and TGF- β that promote lung production of collagen [28–30]. We previously reported that CEES exposure not only initiates a series of signaling events but also causes oxidative stress [11,12]. However, we still do not know how CEES acts as a powerful oxidant and which cells are affected first by CEES.

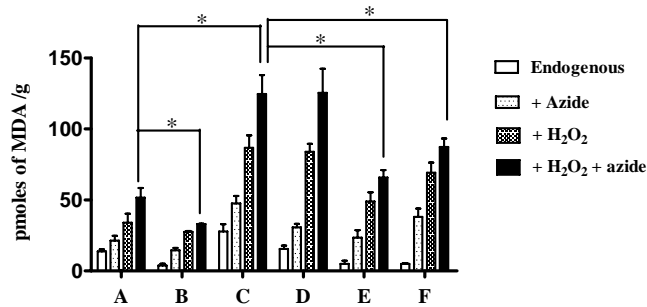


FIGURE 5. Effect of CEES exposure on *in vitro* lipid peroxidation of lung: protection by liposome treatment. Guinea pigs were exposed to CEES (2 mg/kg) intratracheally and 5 min later received a single tracheal instillation of 200 μ L of liposomes (LIP-1, LIP-2, and LIP-4) and lungs were removed after 30 days of CEES exposure for measurement of lipid peroxidation. Lipid peroxidation was measured in the presence and absence of Na-azide, an irreversible inhibitor of catalase. A = vehicle, B = vehicle + blank liposome (LIP-1), C = CEES, D = CEES + LIP-1, E = CEES + LIP-2, and F = CEES + LIP-4. * $p < 0.05$.

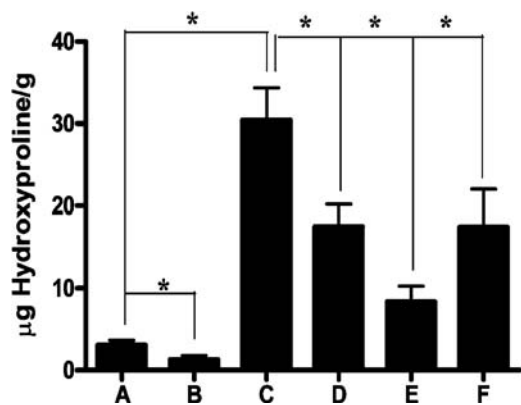


FIGURE 6. Effect of CEES exposure on the hydroxyproline content of lung: Protection by liposome treatment. Guinea pigs were exposed to CEES (2 mg/kg) intratracheally and 5 min later received a single tracheal instillation of 200 μ L of liposomes (LIP-1, LIP-2, and LIP-4) and lungs were removed after 30 days of CEES exposure for measurement of hydroxyproline. A = vehicle, B = vehicle + blank liposome (LIP-1), C = CEES, D = CEES + LIP-1, E = CEES + LIP-2, and F = CEES + LIP-4. * $p < 0.05$.

The extensive leakage of albumin into the lung after intratracheal infusion of CEES indicates that the blood-gas barrier has been seriously compromised and that causes a functional impairment or destruction of both vascular endothelial and alveolar epithelial cells resulting in hypoxia. In the present study, we report data on the attenuation of CEES-induced acute lung injury in guinea pigs by five antioxidant liposomes differing in the levels of phospholipid, cholesterol, phosphatidic acid, tocopherol (α , γ , δ), NAC, and GSH. Empty liposome (LIP-1) infusion did not change the permeability index. LIP-2 and LIP-4 offered substantial attenuation of the massive leak of blood albumin into the lung

(Table 2). Furthermore, a matter of considerable interest is that delayed delivery (for as long as 60 min) of liposomes into the lung after CEES infusion still provides substantial attenuation of lung injury. It is well-known that liposomes delivered into the airways are phagocytized by macrophages and internalized [31]. Thus, it can be implied from the current studies that liposomal delivery selectively enhances reducing environment in lung macrophages and thereby protects against CEES toxicity in these cells. Another interesting observation here is that LIP-2 is better than LIP-4 in terms of protecting the lung from aggregation of RBCs and collagen deposit. It is known that RBC interacts with extracellular matrix and this interaction causes recruitment of inflammatory cells by stimulating fibroblasts to secrete variety of mediators including IL-8 [32]. Thus, LIP-2 may offer a protective mechanism regulating repair after lung injury.

Our results indicate that addition of tocopherols causes more protection than NAC or GSH only. Vitamin E is believed to be involved in a variety of physiological and biochemical functions. The molecular mechanism of these functions is believed to be mediated by either the antioxidant action of the vitamin or by its action as a membrane stabilizer and most potent lipid-soluble antioxidants in blood, breaking free radical chain reactions of lipid peroxidation [33]. Furthermore, the antioxidative roles of the different tocopherol isoforms are highly interdependent and may be complimentary in function.

There is some evidence suggesting that tocopherol isoforms concentrations relative to each other may be important in preventing specific types of oxidative damage, with γ -tocopherol possibly being more important than α -tocopherol in removing nitrogen oxides and other electrophilic mutagens [34]. Recent evidence has suggested that γ -tocopherol and its metabolites are more potent inhibitors of cyclooxygenase-2 than α -tocopherol [35]. Furthermore, *in vitro* studies suggest that other tocopherols and tocotrienols have chemopreventive effects. γ -tocopherol is more effective than α -tocopherol in inhibiting prostate cancer cell growth, reducing oxidative DNA, increasing SOD activity, and scavenging mutagenic electrophiles such as peroxynitrite, a potent nitrating and oxidizing compound and exhibits greater anti-inflammatory effects than α -tocopherol, whereas δ -tocopherol has stronger antiproliferative effect than α - and γ -tocopherol [35,36].

It can be implied from this study that liposomal delivery selectively enhances reducing environment in lung macrophages and thereby protects against CEES toxicity in these cells. This is further evident by our observation that antioxidant liposomes, such as LIP-2 and LIP-4, offer protection against lipid peroxidation induced by CEES exposure (Figure 5). Our data

(Figure 6) clearly indicate that delivery of antioxidant liposomes, particularly LIP-2, significantly protects against CEES-induced lung fibrosis by controlling the accumulation of fibrin and collagen in lung.

ACKNOWLEDGMENT

This work was supported by grant from the US Department of Army (W81XWH-06-2-0044).

REFERENCES

- Papirmeister B, Fenster AJ, Robinson SI, Ford RD. Sulfur mustard injury: Description of lesions and resulting incapacitations. In: Boca AJ, Raton FL, editors. *Medical Defense Against Mustard Gas. Toxic Mechanisms and Pharmacological Implications*. Fenster: CRC; 1991. pp 13–42.
- Dacre JC, Goldman M. Toxicology and pharmacology of the chemical warfare agent sulfur mustard. *Pharmacol Rev* 1996;48:289–326.
- Smith MG, Stone W, Crawford K, Ward P, Till GO, Das SK. A promising new treatment for mustard gas with the potential to substantially reduce the threat posed by chemical, biological and radiological agents. *Jane's Chem-Bio Web* 2003;1–5.
- Wormser U. Toxicology of mustard gas. *Trends Pharmacol Sci* 1991;12:164–167.
- Momeni AZ, Enshaeh S, Meghdadi SM, Amindjavaheri M. Skin manifestation of mustard gas. Clinical study of 535 patients exposed to mustard gas. *Arch Dermatol* 1992;128:775–780.
- Calvet JH, Jarrean PH, Levame M, D'ortho MP, Lorino H, Harf A, Mavier IM. Acute and chronic respiratory effects of sulfur mustard intoxication in guinea pigs. *J Appl Physiol* 1994;76:681–688.
- Emad A, Rezaian GR. The diversity of the effects of sulfur mustard gas inhalation on respiratory system 10 years after a single, heavy exposure: Analysis of 197 cases. *Chest* 1997;112:734–738.
- Mukherjee S, Das SK. Pulmonary fibrosis in guinea pig by 2-chloroethyl ethyl sulfide. *FASEB J* 2005;19:A280.
- Leff JA, Parsons PE, Day CE, Taniguchi N, Jochum M, Fritz H, Moore FA, Moore EE, McCord JM, Repine JE. Serum antioxidants as predictors of adult respiratory distress syndrome in patients with sepsis. *Lancet* 1993;341:777–780.
- Lloyd SS, Cheng AK, Taylor FB, McCay JEG. Free radicals and septic shock in primates: The role of tumor necrosis factor. *Free Radic Biol Med* 1993;14:233–242.
- Chatterjee D, Mukherjee S, Smith MG, Das SK. Signal transduction events in lung injury induced by 2-chloroethyl ethyl sulfide (CEES), a mustard analog. *J Biochem Mol Toxicol* 2003;17:1–8.
- Das SK, Mukherjee S, Smith MG, Chatterjee D. Prophylactic protection by *N*-acetylcysteine against the pulmonary injury induced by 2-chloroethyl ethyl sulfide, a mustard analogue. *J Biochem Mol Toxicol* 2003;17:177–184.
- McClintock SD, Hoesel LM, Das SK, Till GO, Neff T, Kunkel RG, Smith MG, Ward PA. Attenuation of half sulfur mustard gas-induced acute lung injury in rats. *J Appl Toxicol* 2006;26(2):126–131.
- Wormser U, Brodsky B, Green BS, Arad-Yellin R, Nyska A. Protective effect of povidone-iodine ointment against skin lesions induced by sulphur and nitrogen mustards and by non-mustard vesicants. *Arch Toxicol* 1997;71:165–170.
- Wormser U, Brodsky B, Green BS, Arad-Yellin R, Nyska A. Protective effect of povidone-iodine ointment against skin lesions induced by chemical and thermal stimuli. *J Appl Toxicol* 2001;20:S183–S185.
- Yang H, Paromov V, Smith M, Stone WL. Preparation, characterization and use of antioxidant liposomes. In: Armstrong D, editor. *Advanced Protocols in Oxidative Stress 1 Series: Methods in Molecular Biology*. New York: Humana Press; 2008. Vol 477, XIV, pp 277–292. ISBN: 978-1-60327-218-6.
- Chono S, Tanino T, Seki T, Morimoto K. Uptake characteristics of liposomes by rat alveolar macrophages: Influence of particle size and surface mannose modification. *J Pharm Pharmacol* 2007;59:75–80.
- Mukherjee S, Woods L, Weston Z, Williams AB, Das SK. The effect of mainstream and sidestream cigarette smoke exposure on oxygen defense mechanisms of guinea pig erythrocytes. *J Biochem Toxicol* 1993;8:119–125.
- Fujita M, Shannon JM, Morikawa O, Gaudie J, Hara N, Mason RJ. Overexpression of tumor necrosis factor- μ diminishes pulmonary fibrosis induced by bleomycin or transforming growth factor- μ . *Am J Respir Cell Mol Biol* 2003;29:669–676.
- Beheshti J, Mark EJ, Akbaei HMH, Aslani J, Ghanei M. Mustard lung secrets: Long term clinicopathological study following mustard gas exposure. *Pathol Res Pract* 2006;202:739–744.
- Ghanei M, Tazelaar HD, Chilosi M, Harandi AA, Peyman M, Akbari HM, Shamsaei H, Bahadori M, Aslani J, Mohammadi A. An international collaborative pathologic study of surgical lung biopsies from mustard gas-exposed patients. *Respir Med* 2008;102:825–830.
- Fantone JC, Ward PA. Role of oxygen-derived free radicals and metabolites in leukocyte-dependent inflammatory reactions. *Am J Pathol* 1982;107:395–418.
- Willoughby WF, Willoughby JB. Immunologic mechanism of parenchymal lung injury. *Environ Health Perspect* 1984;55:239–257.
- Strausz J, Muller-Quernheim J, Stepling H, Ferlinz R. Oxygen radical production by alveolar inflammatory cells in idiopathic pulmonary fibrosis. *Am Rev Respir Dis* 1990;41:124–128.
- Papirmeister B, Fenster AJ, Robinson SI, Ford RD. *Medical defense against mustard gas: Molecular mechanisms of cytotoxicity*. Boca Raton, FL: CRC Press; 1991. pp 155–209.
- Elsayed NM, Omaye ST, Klain GJ, Korte DW Jr. Free radical-mediated lung response to the monofunctional sulfur mustard butyl 2-chloroethyl sulfide after subcutaneous injection. *Toxicology* 1992;72:153–165.
- Sidell FR, Urbanetti JS, Smith WJ, Hurst CG. Vesicant. In: Zajchuk R, editor. *Textbook of Military Medicine. Medical Aspects of Chemicals and Biological Warfare*. Office of Surgeon General; 1997.
- Piguet PF, Tacchini-Cottier F, Vesin C. Administration of anti-TNF- α or anti-CD11a antibodies to normal adult mice decreases lung and bone collagen content: Evidence for an effect of platelet consumption. *Am J Respir Cell Mol Biol* 1995;12:227–231.

29. Redlich CA, Delisser HM, Elias JA. Retinoic acid inhibition of transforming growth factor-beta-induced collagen production by human lung fibroblasts. *Am J Respir Cell Mol Biol* 1995;12:287-295.
30. Venkatesan N, Roughley PJ, Ludwig MS. Proteoglycan expression in bleomycin lung fibroblasts: Role of transforming growth factor-beta (1) and interferon-gamma. *Am J Physiol Lung Cell Mol Physiol* 2002;283:L806-L814.
31. Gonzalez-Rothi RJ, Straub I, Cacace JL, Schreier H. Liposomes and pulmonary alveolar macrophages: Functional and morphologic interactions. *Exp Lung Res* 1991;17:687-705.
32. Fredriksson K, Lundahl J, Palmberg L, Romberger DJ, Liu XD, Rennard SI, Skold CM. Red blood cells stimulate lung fibroblasts to secrete interleukin-8. *Inflammation* 2003;27:71-78.
33. Wang X, Quinn PJ. Vitamin E and its function in membranes. *Prog Lipid Res* 1999;38:309-336.
34. Christen S, Woodall AA, Shigenaga MK, Southwell-Keely PT, Duncan MW, Ames BN. Gamma-tocopherol traps mutagenic electrophiles such as NO₂ and complements alpha-tocopherol: Physiological implications. *Proc Natl Acad Sci USA* 1997;94:3217-3222.
35. Jiang Q, Elson-Schwab I, Courtemanche C, Ames BN. Gamma-tocopherol and its major metabolite, in contrast to alpha-tocopherol, inhibit cyclooxygenase activity in macrophages and epithelial cells. *Proc Natl Acad Sci USA* 2000;97:11494-11499.
36. McIntyre BS, Briski KP, Tirmenstin MA, Fariss MW, Gapor A, Sylvester PW. Antiproliferative and apoptotic effects of tocopherols and tocotrienols on normal mouse mammary epithelial cells. *Lipids* 2000;35:171-180.

Desensitization of β -Adrenergic Receptors in Lung Injury Induced by 2-Chloroethyl Ethyl Sulfide, a Mustard Analog

Syeda M. Kabir,¹ Shyamali Mukherjee,² Veera Rajaratnam,¹ Milton G. Smith,³ and Salil K. Das^{1*}

¹Department of Cancer Biology, Meharry Medical College, 1005 David Todd Blvd., Nashville, TN 37208, USA; E-mail: sdas@mmc.edu

²Department of Professional and Medical Education, Meharry Medical College, 1005 David Todd Blvd., Nashville, TN 37208, USA

³Amaox Ltd., Melbourne, FL 32944, USA

Received 23 April 2008; revised 25 August 2008; accepted 14 September 2008

ABSTRACT: 2-Chloroethyl Ethyl Sulfide (CEES) exposure causes inflammatory lung diseases, including acute respiratory distress syndrome (ARDS) and pulmonary fibrosis. This may be associated with oxidative stress, which has been implicated in the desensitization of beta-adrenergic receptors (β -ARs). The objective of this study was to investigate whether lung injury induced by intratracheal CEES exposure (2 mg/kg body weight) causes desensitization of β -ARs. The animals were sacrificed after 7 days and lungs were removed. Lung injury was established by measuring the leakage of iodinated-bovine serum albumin ($[^{125}\text{I}]$ -BSA) into lung tissue. Receptor-binding characteristics were determined by measuring the binding of $[^3\text{H}]$ dihydroalprenolol ($[^3\text{H}]$ DHA) (0.5–24 nM) to membrane fraction in the presence and absence of DL-propranolol (10 μM). Both high- and low-affinity β -ARs were identified in the lung. Binding capacity was significantly higher in low-affinity site in both control and experimental groups. Although CEES exposure did not change K_D and B_{max} at the high-affinity site, it significantly decreased both K_D and B_{max} at low affinity sites. A 20% decrease in β_2 -AR mRNA level and a 60% decrease in membrane protein levels were observed in the experimental group. Furthermore, there was significantly less stimulation of adenylate cyclase activity by both cholera toxin and isoproterenol in the experimental group in comparison to the control group. Treatment of lungs with 3-isobutyl-1-methylxanthine (IBMX), an inhibitor of phosphodiesterase (PDE) could not abolish the difference between the control group and the experimental group on the stimulation of the

adenylate cyclase activity. Thus, our study indicates that CEES-induced lung injury is associated with desensitization of β_2 -AR. © 2009 Wiley Periodicals, Inc. *J Biochem Mol Toxicol* 23:59–70, 2009; Published online in Wiley InterScience (www.interscience.wiley.com). DOI 10:1002/jbt.20265

KEYWORDS: 2-Chloroethyl Ethyl Sulfide (CEES); Lung Injury; β -Adrenergic Receptors; cAMP; Guinea Pig

INTRODUCTION

Mustard gas, an alkylating agent, is an extensively used chemical warfare agent and upon exposure is known to exert local action on eyes, skin, and respiratory tissue followed by impairment of nervous, cardiac, and digestive systems in humans and laboratory animals [1,2]. The upper and lower respiratory tracts may be damaged acutely due to hemorrhagic inflammation after its inhalation and subsequently, a variety of chronic pulmonary sequelae may develop, including acute respiratory distress syndrome (ARDS), chronic bronchitis, and pulmonary fibrosis [3–6]. Yet the exact mechanism is not well understood.

Many inflammatory lung diseases including ARDS are associated with oxidative stress and accumulation of free radicals [7]. Inflammatory cytokines, such as tumor necrosis factor- α (TNF- α), play an important role in the generation of reactive oxygen species (ROS) [8]. Recently, we have reported that guinea pigs exposed intratracheally to a mustard analog, 2-chloroethyl ethyl sulfide (CEES) accumulate high levels of TNF- α , which leads to activation of both acid and neutral sphingomyelinase resulting in high accumulation of

*Correspondence to: Salil K. Das.

Contract Grant Sponsor: US Army.

Contract Grant Number: W81XWH-06-2-0044.

Contract Grant Sponsor: NIH.

Contract Grant Number: 5T32HL-07751-09.

© 2009 Wiley Periodicals, Inc.

ceramides, a second messenger involved in cell apoptosis [9,10]. In addition, CEES activated NF- κ B, which rapidly disappeared after 2 h, and because of the disappearance of NF- κ B, the cells were damaged continually owing to accumulation of ceramides and activation of several caspases, leading to apoptosis. A subsequent study further revealed that an antioxidant *N*-acetylcysteine, offers prophylactic protection against the CEES-induced lung injury [11].

Beta-adrenergic receptors (β -ARs) are prototypic members of the G-protein-coupled receptors that regulate the intracellular concentration of important second messenger molecules such as cyclic AMP (cAMP) and play important roles in a variety of cells and organ systems [12,13]. To date, three subtypes of β -ARs (β_1 , β_2 , and β_3) that differ in their affinities for endogenous catecholamine as well as synthetic ligands have been identified. All three receptors couple to the stimulatory guanine nucleotide binding protein G_s and the agonist binding to the receptor causes activation of G_s -coupled adenylate cyclase, which leads to elevation of intracellular cAMP [14–16].

In the lung, β -ARs especially the β_2 -ARs play a major role in the secretion of surfactant by the alveolar-type cells [17,18] and clearance of alveolar fluid [19]. Recently, we have reported that isoproterenol, a β_2 -AR ligand, causes an increase in the secretion of surfactant by stimulating release of Ca^{2+} from intracellular stores in guinea pig alveolar type II cells [20]. A defect in the β -ARs system in alveolar type II cells has been thought to be a contributing factor in the development of respiratory diseases [21,22]. In addition, oxidative stress has been implicated in the desensitization of β -ARs [23]. Receptor desensitization is a phenomenon in which cellular responsiveness is ultimately diminished when cells are subjected to a continuous stimulus. The important mechanism is the loss of cellular receptors due to desensitization of the β -ARs [24,25]. Desensitization of the β_2 -AR-adenylate cyclase system characterized by reduction of cAMP production has been observed in expression systems and different cell lines [14–16].

Surfactant defects have been demonstrated in a number of alveolar and airway diseases. In ARDS, deficiencies in surfactant components such as phospholipids, surfactant protein SP-A, and SP-B are evident, and may be caused by proinflammatory cytokines, e.g. TNF- α that decreases surfactant components [26]. Hence, the surfactant defects may additionally play an undefined role in chronic obstructive pulmonary disease (COPD) [27]. Therefore, we can hypothesize that the CEES treatment causes desensitization of β -ARs by up-regulating proinflammatory cytokines; as a result, it causes a defect in surfactant production and secretion, which is very relevant to ARDS.

In order to test this hypothesis, the objective of this study was to investigate whether lung injury induced by CEES exposure causes modification in the structure of alveolar type II cells and desensitization of β -ARs in the lung. Although, both β_1 and β_2 ARs are present in the lung, there are more β_2 than β_1 ARs [17,18]. Furthermore, it has been demonstrated by our laboratory [20] and others [28,29] that the release of surfactant is mediated by β_2 rather than β_1 ARs. Thus, ARDS induced due to exposure to mustard gas could be the result of reduction in responsiveness of the β_2 -ARs. The prominent mechanism during long-term desensitization of the β -ARs is the loss of cellular receptors [30].

β -ARs gene expression has been shown to be regulated at the transcriptional level by various factors, including steroid hormones such as glucocorticoids [31] and by chronic treatment with β -agonists [32]. It has been reported that down-regulation of β_2 -AR following long-term agonist exposure is accompanied by a decrease in β_2 -AR mRNA levels [33]. Thus, in the present study, we also investigated whether CEES exposure causes any change in β_2 -AR gene expression and its signaling capabilities in the lung.

MATERIALS AND METHODS

Chemicals

2-Chloroethyl ethyl sulfide (CL- $CH_2CH_2-S-CH_2CH_2$, CEES), DL-propranolol, atenolol, and ICI-118, 551 hydrochloride were purchased from Sigma Chemicals (St. Louis, MO). [3H] dihydroalprenolol ([3H] DHA) (40 Ci/mmol) was purchased from NENTM Life Science products Inc. (Boston, MA), [^{32}P]- α -ATP was obtained from Amersham Pharmacia Biotech (Piscataway, NJ), and [^{125}I]-bovine serum albumin ([^{125}I]-BSA) was purchased from ICN (Aurora, OH).

Animals and the CEES Treatment

Male guinea pigs (Harley strain, 5–6 weeks old, 400 g body weight) were obtained from Harlan Sprague Dawley, Inc. (Indianapolis, IN). Animals were infused intratracheally with single doses of CEES (2.0 mg/kg body weight). Control animals were infused with ethanol as vehicle. The animals were sacrificed after 7 days of CEES exposure.

Lung Injury Study

Lung injury was monitored by studying the leakage of [^{125}I]-BSA from the lung after CEES exposure

according to the method of Ward et al. [34] as described by us [10].

Ultrastructural Analysis

Lung samples were fixed with 2.5% glutaraldehyde in 0.1 M Sorensen's phosphate buffer (pH 7.2) followed by osmium tetroxide in the same buffer as described by us [35]. The specimens were dehydrated through an upgraded ethanol series at room temperature. Preparations were embedded in epon 812. Poststaining was done in a saturated solution of uranyl acetate in 50% ethanol followed by Reynolds' lead citrate. Sections were examined with a Philips 301 transmission electron microscope.

β -Adrenergic Receptors Binding Assay

The binding of [3 H] DHA to lung membrane fraction was determined as described earlier [18,36]. This was done in a volume of 0.5 mL containing: 0.1 mL membrane protein (50–100 mg), 0.1 mL radioligand (0.125–40 nM), 0.1 mL DL-propranolol (10 mM) (or buffer), and 0.2 mL assay buffer (10 mM Tris-HCl, 1 mM dithiothreitol (DTT), pH 7.6). The reaction was initiated by the addition of membrane protein and terminated after 40 min at room temperature by rapid filtration over a Brandel GF/B filtering manifold, with two 5 mL washes of ice-cold 0.85% NaCl. The specific binding of [3 H] DHA was defined as the difference in binding obtained in the presence and absence of propranolol (10 mM). Based on our earlier finding with guinea pig lung [18], two binding sites of β -ARs were identified for β -ARs in this study, one as high-binding sites ($K_D < 1$ nM) and the other as low-binding sites ($K_D > 4$ nM).

In order to characterize these two subtypes, other experiments were carried out in which the incubation medium contained varied concentrations (10^{-12} – 10^{-3} M) of either atenolol (β_1 -antagonist) or ICI 118,551 (β_2 -antagonist) at two fixed concentrations of DHA (2 and 8 nM), and IC_{50} values were determined. IC_{50} was defined as the concentration of the antagonist producing 50% inhibition of DHA binding. Protein concentration was determined according to modified Lowry's method [37] using BSA as a standard.

Isolation of RNA and Reverse Transcriptase-Polymerase Chain Reaction

Immediately after sacrifice, lungs were perfused with physiological saline, removed, and flash-frozen in liquid nitrogen and stored at -80°C . Total RNA was extracted using a Qiagen RNeasy kit. The concen-

tration and purity of the RNA was analyzed in a UV spectrophotometer.

Reverse transcriptase-polymerase chain reaction (RT-PCR) of β -ARs and glyceraldehydes-3-phosphate dehydrogenase (GAPDH) genes were performed using DNase-treated RNA from each sample, using the One-Step RT-PCR kit (Invitrogen, MD). Both forward and reverse primers were designed based on the sequences from the GenBank Accession No. AJ459814 (*cavia porcellus* β_2 -ARs) and U51572 (*c. porcellus* GAPDH). The RT-PCR products were separated by electrophoresis on a 1% agarose gel, purified using QIAquick PCR purification kit (Qiagen, CA), and sequenced using BidDye-terminators kit (Applied Biosystems, CA). The sequences were analyzed using Applied Biosystems Automated Sequencer (ABI 3700 model).

Northern Blot Hybridization

Total RNA (30 μg) was loaded on a 1.6% agarose gel containing 2.2 M formaldehyde and 0.2 M 3-[N-morpholino]propane sulfonic acid (MOPS) buffer. After 6 h of electrophoresis at 70 V, RNA was transferred overnight onto a Bright Star (Ambion) nylon membrane in $20\times$ sodium chloride-sodium citrate (SSC buffer) and UV cross-linked. Total RNA was DNase-treated to remove genomic DNA before being reverse-transcribed into cDNA for PCR amplification of the β -AR and GAPDH probes. The primers for the probe are the same used for RT-PCR. After RT-PCR, guinea pig β_2 -AR cDNA (600 bp) and the GAPDH cDNA (400 bp) were gel-purified using a Qiagen Kit (Cat no. 28104). The fragments were labeled with [$\alpha^{32}\text{P}$] ATP (3,000 Ci/mmol) using DNA polymerase Nick Translation kit (Invitrogen). Following a three-hour prehybridization at 42°C , the filters were hybridized overnight at 42°C with the ^{32}P -labeled β_2 -AR probe added in ultrahybridization buffer (Ambion). Blots were washed twice in $2\times$ SSC/0.1% sodium dodecyl sulfate (SDS) for 30 min, once with $1\times$ SSC/0.1% SDS at 42°C for 30 min, $0.5\times$ SSC/0.1% SDS at 50°C for 30 min, and finally with $0.1\times$ SSC/0.1% SDS at 55°C for 30 min, and exposed at -80°C to Kodak OMAT Xs film for development. Following autoradiography, blots were stripped and reprobed with a ^{32}P -labeled guinea pig GAPDH cDNA probe, to enable standardization between samples. Band intensities on films were analyzed using Alpha Imager (Inontech) densitometric scan.

Measurement of β_2 -ARs Level by Western Blot Analysis

Both control and CEES-treated lungs were homogenized in 5 volumes of ice-cold buffer [Manitol (210 mM)/Sucrose(70 mM)/EDTA(1 mM)/CaCl₂

(2 mM), pH 7.2] containing 0.1 mM phenylmethylsulfonyl fluoride (PMSF), 1 mM DTT, and aprotinin (2 $\mu\text{g}/\text{mL}$) by using a Brinkman Polytron (setting 6–7, 30 s). The homogenates were filtered through a 100 μm Nylon mesh and divided into two parts. One part was used as total homogenate and the other part was then centrifuged at $20,000\times g$ for 20 min at 4°C and washed three times and resuspended in 50 mM Tris-HCl, containing 0.1 mM PMSF, 1 mM DTT, and aprotinin (2 $\mu\text{g}/\text{mL}$), pH 7.4. Protein concentrations of both total homogenate and membrane fraction were measured according to the modified Lowry's method [37], using BSA as a standard. Protein (50 μg) of total homogenate and membrane protein from each group were resolved by 10% SDS-PAGE. Proteins were transferred onto polyvinylidene difluoride (PVDF) membranes Immobilon-P (Millipore, Bedford, MA), as described by us [38]. Following incubation with β_2 -specific polyclonal antibodies raised in rabbit (1:500; sc 9042, Santa Cruz Biotechnology Inc., CA), blots were washed and incubated with HRP-conjugated anti-rabbit goat antibody (1:1000; sc 2350, Santa Cruz Biotechnology). Binding of antibodies to the blots was detected with an ECL detection system (Amersham Life Sciences, Arlington Heights, IL) following manufacturer's instructions. Stripped blots were re probed with β -actin-specific polyclonal antibodies (1:500; H-196, sc 7120, Santa Cruz Biotechnology) to enable standardization of signals between samples. Band intensities were acquired by Alpha Imager (Inontech).

cAMP Production in the Presence of Isoproterenol, Cholera Toxin, and IBMX

Lung homogenate (100 μg of protein) from both control and CEES-treated groups were incubated in the presence or absence of different concentrations of isoproterenol (6.25 nM–100 μM) at 37°C for 30 min as described by us [39]. The reaction was terminated with 6% trichloroacetic acid and centrifuged at $14,000\times g$ for 15 min. The deproteinized supernatants were washed 10 times with water-saturated diethyl ether and dried by lyophilization and dissolved in water. The levels of cAMP in the extracts were measured by a radio-binding assay described in the instruction material supplied with the Biotrak cAMP assay system (Amersham Life Science).

To determine if there is any difference in the stability of cAMP between control and CEES-treated groups, we measured cAMP production in the presence and absence of 12.5 nM isoproterenol at different times (15–60 min). We also measured cAMP production in the

presence or absence of cholera toxin (50 ng/mL) at 60 min.

Furthermore, we studied the effects of 3-isobutyl-1-methylxanthine (IBMX), an inhibitor of phosphodiesterase (PDE) on cAMP production in both control and experimental groups. For this, we incubated homogenates (1 mg protein/mL) with 50 μg IBMX at 37°C for 10 min, and afterwards centrifuged at $105,000 g$ for 30 min. The pellet was treated with 12.5 nM isoproterenol for 1 h, and analyzed for cAMP levels.

Statistical Analysis

Differences between the control samples and the samples treated with mustard gas were assessed by using ANOVA, and the significance level was set for $p \leq 0.05$ using Graph Pad Prism 4 software program.

RESULTS

Effects of CEES Exposure on Lung Injury

Guinea pigs exposed to CEES had a 5-fold increase in lung permeability as measured by leakage of [^{125}I]-BSA (Figure 1). This lung injury was further evident by ultrastructural analysis (photographs not shown because similar observations were reported earlier; see reference 40). Mustard gas exposure caused irregular expansion of alveolar spaces that contained surfactant lamellae and extruded type II cells, indicating disruption of surfactant secretion. Type II cells had irregular outlines and contained large number of lamellar bodies. No protrusion of type II cells was observed in the alveolar spaces in the vehicle-treated control animals.

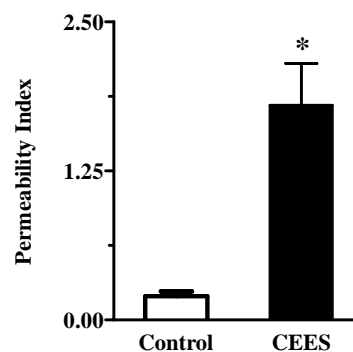


FIGURE 1. CEES-induced lung injury. Lung injury was expressed as permeability index, which was obtained by dividing total radioactive counts of [^{125}I]-BSA in lung by counts in 1 mL of blood from the same animal ($n = 3$). Asterisks indicate statistically different compared to control ($p < 0.05$).

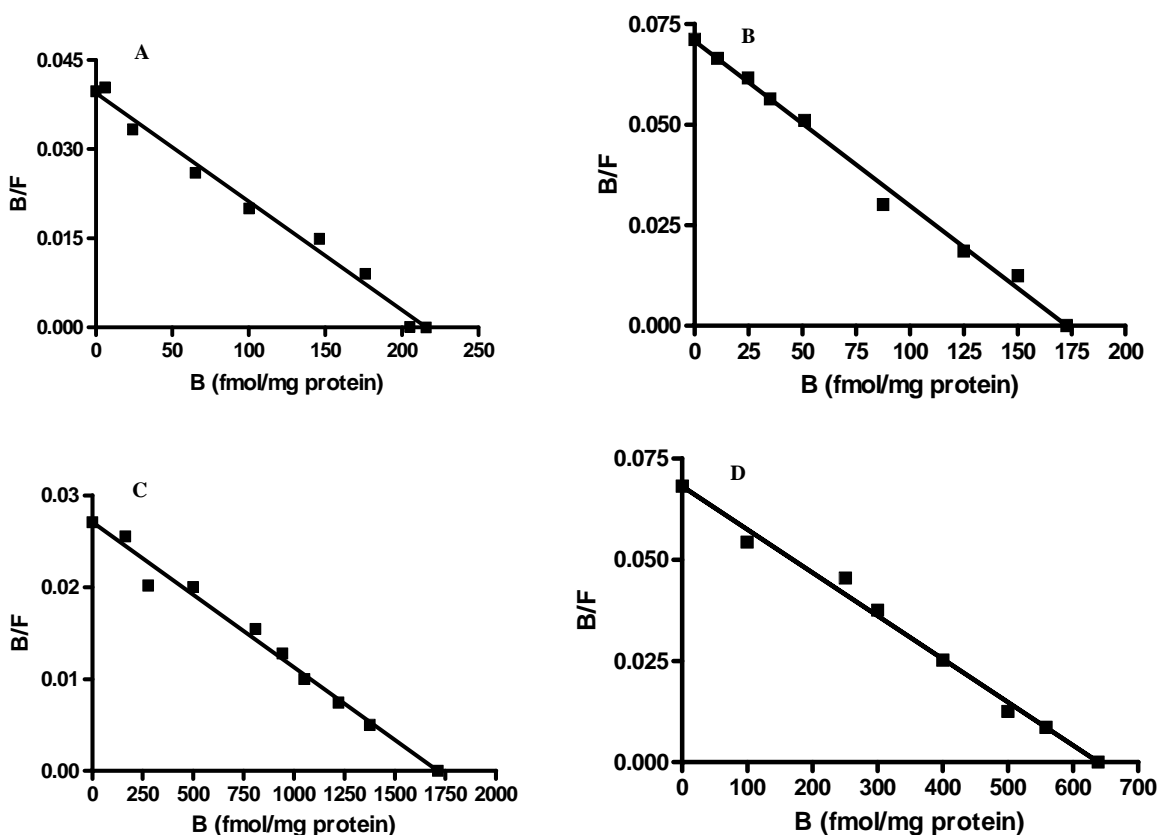


FIGURE 2. Representative Scatchard analysis of [^3H] DHA binding to β -ARs in guinea pig lung membranes: (A) high-affinity (control), (B) high-affinity (CEES-exposed), (C) low-affinity (control), (D) low-affinity (CEES-exposed). The binding of [^3H] DHA to the membrane was measured as described in the "Materials and Methods" section ($n = 3$). B = Specific binding of ligand and F = Free ligand concentration.

Effects of CEES Exposure on the Binding Characteristics of β -Adrenergic Receptors

The Scatchard plot (Figure 2) by Graph Pad PRISM 4 software program revealed that [^3H] DHA binds to whole lung membrane extract at two binding sites with different affinities; high [$K_D = (0.68 \pm 0.17)$ nM] and low [$K_D = (6.40 \pm 2.1)$ nM] affinities in control animals. Binding capacity (B_{\max}) of the low-affinity site [$B_{\max} = (2087 \pm 370)$ fmol/mg protein] was significantly higher than that at the high-affinity site [$B_{\max} = (221.2 \pm 56.0)$ fmol/mg protein], as previously reported by us in guinea pig alveolar type II cells [18]. Lung membranes from CEES-exposed animals also revealed two binding sites with different affinities; $K_D = (0.62 \pm 0.15)$ nM and $K_D = (2.85 \pm 0.9)$ nM, respectively. Although CEES exposure did not change K_D and B_{\max} at the high-affinity site, it significantly decreased both K_D by 2.2 folds and B_{\max} by 2.7 folds at the low-affinity site (Table 1).

In order to characterize the high- and low-affinity DHA binding sites in our whole lung membrane preparation, we used subtype-specific antagonists [18,36]. Binding experiments were done in the presence of either atenolol, a β_1 -specific antagonist or ICI 118,551, a

β_2 -specific antagonist. Both atenolol and ICI 118,551 inhibited the putative binding sites in a dose-dependent manner (Figure 3). The inhibition of DHA binding showed a biphasic distribution by both atenolol and ICI 118,551. Atenolol was more potent in displacing [^3H] DHA at a low concentration (2 nM; Figure 3) than at a higher concentration (8 nM) of DHA (Figure 3). With 2 nM and 8 nM concentrations of [^3H] DHA, IC_{50} for atenolol at high-affinity sites were 6×10^{-10} M and 2×10^{-7} M, respectively. On the other hand, at both low and high [^3H] DHA concentrations, IC_{50} for ICI 118,551 for low-affinity sites were 2×10^{-6} M and 18×10^{-6} M, respectively. Hence, β -ARs in guinea pig lung are heterogeneous and contain both β_1 (high affinity) and β_2 (low affinity) as previously reported by us in alveolar type II cells [18]. Furthermore, the CEES treatment affects both K_D and B_{\max} of β_2 subtype, but not β_1 subtype of the β -ARs (Table 1).

Effects of CEES Exposure on β_2 -Adrenergic Receptor Gene Expression

To verify whether a mutation in the coding region of the gene and thus a defect in protein could explain

TABLE 1. Effects of Mustard Gas Exposure on Binding Characteristics of β -Adrenoreceptors

Samples	High Affinity		Low Affinity	
	K_D (nM)	B_{max} (fmol/mg protein)	K_D (nM)	B_{max} (fmol/mg protein)
Control	0.68 \pm 0.17	221.2 \pm 56.9	6.40 \pm 2.1	2087 \pm 370
CEES-exposed	0.62 \pm 0.15	203.8 \pm 69.0	2.85 \pm 0.9	765.4 \pm 164.1*

* B_{max} at low-affinity sites is significantly reduced by mustard gas exposure ($p = 0.03$) ($n = 3$ for each group).

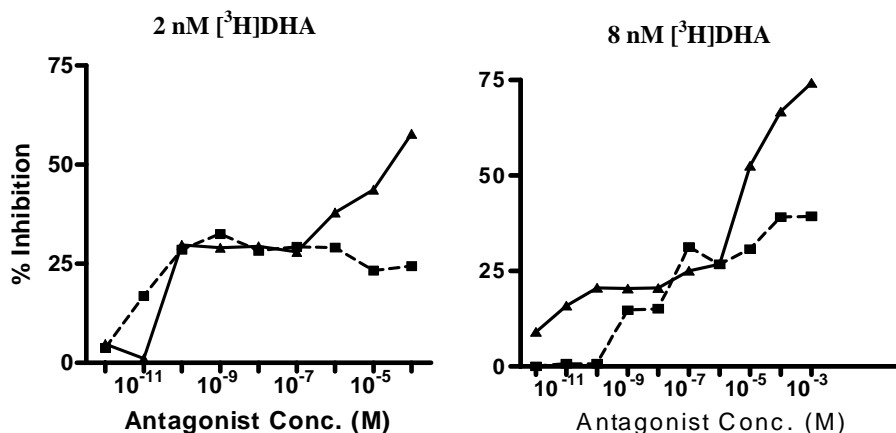


FIGURE 3. Inhibition of [³H] DHA binding to the lung membrane by β -antagonists. (■—■, Atenolol; ▲—▲, ICI-118, 551). The binding of [³H] DHA to the membrane and IC_{50} for the two antagonists were measured as described in the "Materials and Methods" section ($n = 3$).

this reduction in B_{max} , the β_2 -AR cDNA from control and CEES-exposed animals were sequenced. The β_2 -AR cDNA products were obtained by reverse transcription of RNA isolated from the control and CEES-exposed lung tissues, using β_2 -AR-specific primers. However, when compared by BLAST, no differences in nucleotide sequences between the RT-PCR products (Figure 4) from the control and experimental lungs were observed. The observed sequence had 100% identity with the sequence reported for *c. porcellus* β_2 -AR gene in NCBI GenBank (Accession No. AJ459814).

In order to evaluate whether the CEES treatment exerts an inhibitory effect on β_2 -AR gene expression,

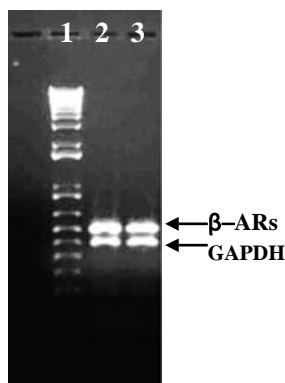


FIGURE 4. RT-PCR products of β -ARs gene of lung; 1 = kb⁺ DNA ladder; 2 = Control; 3 = CEES-exposed.

Northern blot analysis was performed. In both control and CEES-exposed lungs, we consistently detected a distinct band at 2.2 kb as expected for the expressed β_2 -AR message (Figure 5A). However, densitometry evaluation and comparison after normalization with the housekeeping gene GAPDH, indicates only a 20% reduction in β_2 gene expression in CEES-exposed lungs (Figure 5B). However, this minimal reduction was not statistically significant.

To further characterize whether the CEES treatment has any effect on translation of β_2 -AR mRNA, both whole lung homogenate and membrane isolated from both control and CEES-exposed lungs were

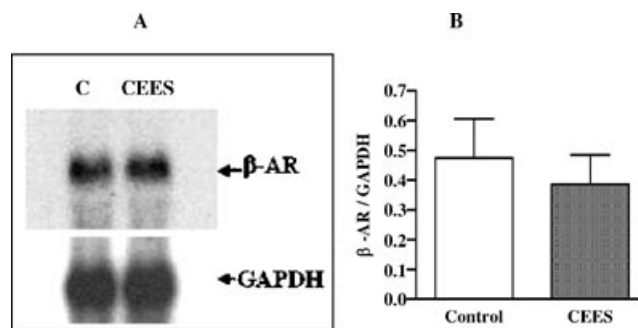


FIGURE 5. Effect of mustard gas on guinea pig lung β_2 -AR receptor gene expression. (A) A representative autoradiogram of Northern blot analysis, (B) bar graph of normalized densitometric values ($n = 3$).

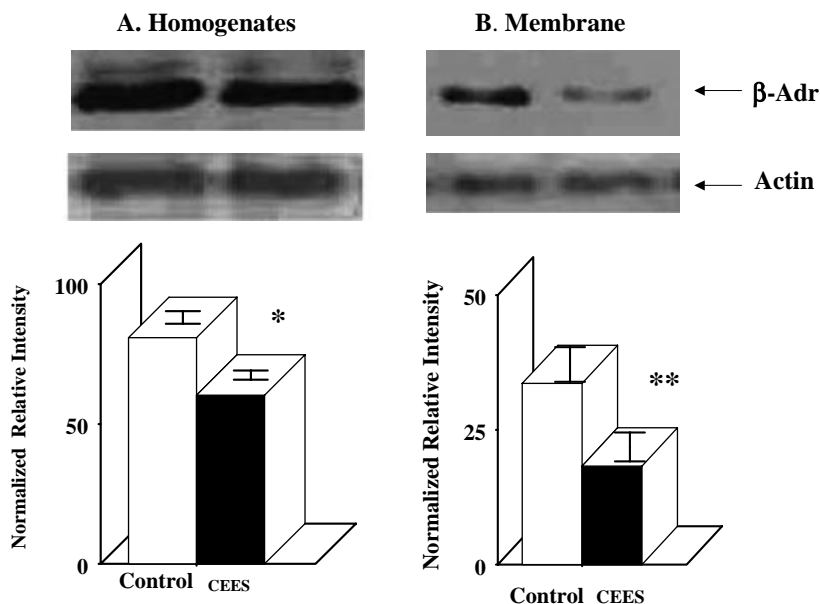


FIGURE 6. Effect of mustard gas on guinea pig lung β_2 -AR receptor levels. (A) Homogenate ($n = 3$), (B) membrane ($n = 3$).

immunodetected by using β_2 -AR-specific polyclonal antibody by Western blot (Figure 6). The protein level of β_2 -AR after normalization with β -actin levels indicates a 25% reduction in total lung homogenate (Figure 6A) and 60% reduction in the membrane (Figure 6B) from CEES-treated animals compared to the corresponding control. Furthermore, the CEES-induced decrease in β_2 -AR level was more in the membrane fraction than that in whole homogenate fraction. This indicates that the CEES treatment causes rapid internalization and degradation of β_2 -AR in the lung.

Effects of CEES Exposure on cAMP Production

Binding of agonists to the β_2 -AR stimulates adenylate cyclase activity and converts ATP to cAMP [12,13]. In order to assess whether the decrease in the expression of β_2 -ARs by CEES exposure causes a decreased response to β -agonists due to desensitization of β_2 -ARs, we measured the effects of CEES exposure on isoproterenol-induced cAMP production. Figure 7A shows a dose-dependent production of cAMP in response to isoproterenol treatment for 30 min of lung homogenate in both control and CEES-treated groups. The maximal induction was at 12.5 nM in both control (150 fmol/mg) and experimental lungs (212.5 fmol/mg). Thus, the stimulation was 29.4% less in the CEES-exposed group in comparison to the control group. The same degree of less stimulation by isoproterenol was observed at all dose levels in the

experimental group than in the control group. There was a significant decrease ($p < 0.001$) in endogenous cAMP level in a time-dependent manner when incubated with optimum dose of isoproterenol (12.5 nM) in the CEES-exposed lungs compared to the control lungs (Figure 7B).

The cAMP production in response to cholera toxin, a direct activator of adenylate cyclase, was significantly less in the CEES-exposed group compared to the control group. For example, the stimulation was 21.1-fold for control group whereas it was 16-fold for the experimental group (Table 2). Hence, it indicates that the CEES treatment not only affects the agonist-mediated cellular response, but also stimulated degradation of cAMP. This is also evident from the results obtained from the study with IBMX (Figure 7C). The cAMP level was significantly lower in the CEES-exposed group than in the control group in the presence of both isoproterenol and IBMX.

In addition to the morphological changes in alveolar Type II cells that correlate with functional compromise, our binding studies and gene expression analysis strongly indicate that CEES exposure indeed down-regulates β -AR, especially the β_2 subtype in the lung at both expression and functional levels.

DISCUSSION

Our recent studies with the guinea pig as an experimental model indicated that within 1 h of CEES

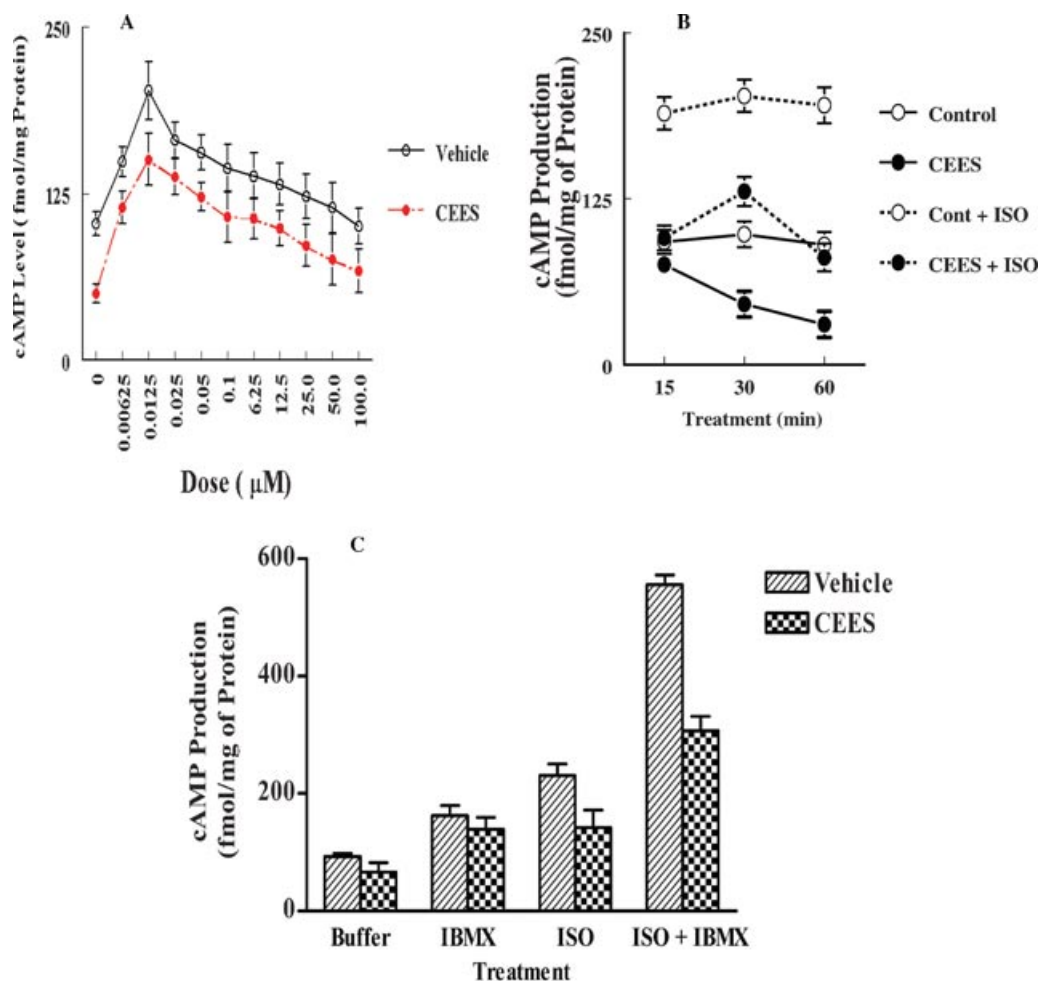


FIGURE 7. Effects of mustard gas exposure on cAMP production in guinea pig lung. (A) Dose-response curve in the presence and absence of isoproterenol ($n = 3$), (B) time-response curve in the presence and absence of isoproterenol ($n = 3$), (C) response in the presence of isoproterenol and IBMX singly or in combination ($n = 3$).

exposure, there is induction of TNF- α [9] that initiates a series of signaling events leading to cellular apoptosis [10]. In this study, we investigated whether CEES exposure induced lung injury by modulating the binding characteristics and/or the expression of the β -ARs in lung. In fact, our results clearly show that the CEES treatment not only causes lung injury, ultrastructural modification of alveolar type II cells, and decrease in

binding capacity of β -ARs, but also inhibits β_2 -AR gene expression as well as induces desensitization, internalization, and degradation of the β_2 -ARs.

We have previously reported the presence of high- and low-binding sites of β -ARs in the guinea pig lung alveolar Type II cells [18]. It was also established in that study that the high-affinity site is the β_1 subtype and the low-affinity site is the β_2 receptor subtype. The widely used β -AR ligand [3 H] DHA binding to both control and experimental lung membrane preparations showed saturable characteristics. Binding characteristics of both the β_1 and β_2 subtypes in the whole lung membrane preparations in the current study is in good agreement with the previous observations [18] with alveolar type II cells from guinea pig. The β -AR ligand [3 H] DHA exhibited two binding sites with different affinities, in both control and experimental lungs. The binding studies with control and experimental lungs we report here clearly indicate the presence of two

TABLE 2. Intracellular Level of cAMP in Cholera toxin-Treated Guinea Pig Lung: Role of the CEES Treatment

Addition	cAMP (fmol/mg of Protein)	
	Vehicle	CEES
Endogenous	98.20 \pm 2.65	35.62 \pm 0.67
Cholera toxin (50 ng/mL)	2074.51 \pm 6.77	1050.34 \pm 6.87

The values are mean \pm SEM of four samples.

β -AR subtypes and prominent reduction in binding capacity of the β_2 subtype due to CEES exposure.

It has been reported that CEES acts as a mutagen. In humans, several single nucleotide polymorphisms that affect the function of β_2 -AR have been identified [40]. Since we did not observe any change in nucleotide sequences between the RT-PCR products from the control and experimental lungs, the reduction in binding due to CEES exposure is not due to any mutation. However, the data related to the gene expression (Figure 5) and protein level (Figure 6) indicate that CEES exposure causes reduction of the β_2 -ARs expression, and also induces internalization of β_2 -AR. We observed an overall 20% reduction in β_2 receptor message levels in the lung tissues exposed to CEES.

In recent years, substantial evidence has been accumulated in support of the concept that cytokines are key regulators of the cascade of cellular events associated with airway inflammation in asthma and COPD [42–45]. Moreover, there is increasing evidence that cytokines may contribute to the β -AR responsiveness that is observed in asthma [45]. Cells in the airway wall also show that there is a close relationship between increased expression of IL- β , TNF- α , and IL-5 with reduced capacity of airway smooth muscle to generate cAMP or to relax in response to β -agonists. A decrease in β -AR-mediated relaxation of airway smooth muscle caused by IL-1 β and/or TNF- α has also been described in guinea pigs, rats, rabbits, and dogs [46,47]. Finally, administration of specific cytokines has been shown to induce impairment of β -AR-mediated airway relaxation in the isolated guinea pig trachea [48]. Furthermore, we previously reported that the CEES treatment causes increased TNF- α in both lung tissue and macrophage [9,10]. Hence, we can postulate that CEES may affect both transcription and translation of β -ARs by stimulating inflammatory cytokines, such as TNF- α .

The protein level of β_2 -ARs significantly decreased in membrane fraction (Figure 6B; 60%) more than that in total homogenate (Figure 6A; 25%) isolated from CEES-treated lungs (but not from control lung) control. A significant difference of protein level between homogenate and membrane fraction indicates that the CEES treatment increases uncoupling of β_2 -ARs from G_s , and as a result internalization of β_2 -ARs. Then internalized β_2 -ARs may be either reactivated and recycled to the plasma membrane following dephosphorylation in intracellular vesicles or degraded in lysosomes. Both the above-mentioned processes can contribute to a reduction in the β_2 -ARs level in the plasma membrane of the guinea pig lung. Mounting evidence suggests that the physiological function of the various subtypes of adrenergic receptors is controlled by phosphorylation/dephosphorylation reactions. Dif-

ferent types of kinases appear to be involved. On the other hand, phosphorylation reactions may operate in a classical feedback regulatory sense. Thus cAMP-dependent kinase, once activated by a β -agonist, can feedback-regulate the function of the receptors by phosphorylating and desensitizing them. There may also be “cross-talk” between systems. Lefkowitz and Caron [49] reported that the cAMP-dependent protein kinases could phosphorylate the alpha 1 adrenergic receptor *in vitro*. Moreover, protein kinases C, when stimulated by phorbols, are able to phosphorylate and desensitize the β -ARs. Thus, one transmembrane-signaling system can regulate the function of another, which indicates that receptor-mediated signals are tightly regulated by feedback inhibition and act to prevent signal overload and reset the receptor to a changing environment. It has also been shown that short-term regulation i.e. uncoupling of β -ARs involves receptor phosphorylation and uncoupling of the receptor from the G protein G_s [50].

Chronic exposure to ligand leads to reduced receptor number, i.e. down-regulation, which results from a combination of receptor internalization, and degradation and decreased mRNA abundance. It has also been reported that regulation of β -ARs is species- and subtype-specific, with a rank order of β_2 -ARs > β_1 -ARs > β_3 -ARs, and most tissues express more than one subtype [50]. Several reports have shown that oxidative stress modulates differentially various receptor responses in guinea pig and β -AR response is more susceptible than muscarinic receptor response [51–53]. Our observation is in parallel with previous reports of a reduction in β -AR mRNA after chronic *in vivo* β -agonist treatment [30,32,54]. Nishikawa et al. [54] reported that β_2 -AR mRNA was significantly reduced as early as one day and persisted at day 7 after isoproterenol infusion. The mechanism by which CEES exerts its effect on the β_2 -AR mRNA levels is not known.

We previously reported that the CEES treatment causes not only increase of TNF- α , but also oxidative stress in guinea pig lung [9–11]. CEES may affect transcription, translation, and degradation of β_2 -ARs as a result of desensitization of β -AR by increasing production of TNF- α , generation of ROS, and endogenous catecholamine. Zang et al. [55] have shown that oxygen radicals play an important role in the nonvagal component of the noncholinergic bronchoconstriction in guinea pigs *in vivo*. Morken et al. [56] have shown that there is an immediate and sustained systemic elevation of catecholamines including epinephrine, which may set the stage for development of neutrophil-mediated acute lung injury. Furthermore, it has been reported that stress and hypoxia of anaphylaxis cause catecholamine release, loss of choline-containing phospholipids, and thereby ARDS [57]. A decrease in both β_2 -AR receptor and mRNA levels in response to chronic

stimulation by β -AR agonists has been reported [33]. In addition, the β_2 -AR gene contains cAMP and glucocorticoid receptor response elements (CRE and GRE), and studies indicate regulation of β_2 -receptor by cAMP (and/or corticosteroids) at the gene expression level [33,58]. CRE-binding protein is also believed to maintain the basal transcription of β_2 -receptor gene [8,32]. Reduced cAMP regulatory element binding (CREB) activity has been suggested to result in reduced β_2 mRNA in rat and guinea pig lungs following prolonged exposure to β -agonist [32]. Endogenous catecholamines may increase due to CEES-induced stress and trauma, and thereby modulate basal transcription of β_2 -AR gene.

The early signaling event in classical G-protein-coupled receptor signal transduction pathway induced upon β_2 -ARs binding to endogenous catecholamines is the activation of adenylate cyclase activity [30,59]. Our results with *in vitro* treatment of isoproterenol show a dose-dependent decrease of β -agonist-induced activation of adenylate cyclase activity as expressed in terms of cAMP production, in CEES-treated lungs in comparison to control lungs (Figure 7A). The potent activator of adenylate cyclase, cholera toxin causes 50% reduced stimulation of adenylate cyclase in CEES-treated lungs than control lungs (Table 2). This seems to suggest that the CEES treatment may cause β -ARs ligand-mediated desensitization in guinea pig lung. The β -AR ligand-mediated desensitization has been demonstrated in several *in vitro* systems, including ventricular strips, adipocytes, and a variety of cell lines [60]. The CEES treatment causes a 2.8-fold decrease in endogenous cAMP compared to the levels in control lungs. Moreover, the fold stimulation from basal level is higher than control, but stability of cAMP is significantly decreased ($p < 0.001$) in CEES-treated lungs than in control lungs (Figure 7B). This indicates that the CEES treatment not only affects the β_2 -AR responsiveness to agonists, but also increases the rapid degradation of cAMP. It has been reported that the cyclic nucleotides are synthesized by adenylate cyclase or guanylate cyclase and degraded by PDEs [61]. Desensitization may also involve activation of G_i and inhibition of adenylate cyclase [62]. It has been shown that protein kinase A (PKA) phosphorylation of β -AR increases the affinity for G_i , thus effectively switching signaling pathways G_s to G_i [61]. Hence, the CEES treatment may modulate directly or indirectly multiple events of β_2 -ARs signaling.

Fivefold increases in leakage of [125 I]-BSA (Figure 1) and altered alveolar Type II cell morphology [41] indicate that lung injury is induced and surfactant secretion may be compromised following CEES exposure. In healthy and diseased animals/or humans, oxidative stress has been shown to compromise host defense (e.g. excess mortality from bacterial infections in

rodents) and cause lung injury and inflammation (e.g., alveolar protein leak, neutrophils influx, etc). The impaired host defense may arise from increased alveolar macrophage (AM) apoptosis and polymorphonucleus phagocytosis and respiratory burst, whereas inflammation appears to arise from increased NF- κ B activity, leading to the up-regulation of cytokines and adhesion molecules in endothelial and epithelial cells [63,64]. cAMP and PKA have been implicated in cell migration and wound repair. It has been shown that isoproterenol increased the migration of cells to speed up closing of mechanically and enzymatically induced wounds of submerged monolayers of bovine bronchial and human airway epithelial cells [65,66]. Dumasius et al. [67] have demonstrated that alveolar β_2 -AR overexpression improves β_2 -AR function and maximally up-regulates β -agonist responsive active Na^+ transport by improving responsiveness to endogenous catecholamines, and as a result accelerates clearance of the alveolar fluid. Previously, we have reported that the NF- κ B level increases within 1 h of the CEES treatment, leading to the up-regulation of cytokines and causing oxidative stress.

Here we report that the CEES treatment results in down-regulation of β_2 -AR and causes lung injury and inflammation as evident by alveolar leakages. In summary, the CEES treatment causes desensitization of β_2 -AR by (a) up-regulating TNF α ; (b) increasing generation of ROS; (c) enhancing infiltration of inflammatory cells, and probably (d) increasing stress-related endogenous catecholamine. Therefore, the CEES treatment may not only cause agonist-stimulated cAMP-dependent receptor phosphorylation, but also cAMP-independent receptor phosphorylation, and as a consequence, it will reduce responsiveness of the β_2 -ARs. Furthermore, the CEES treatment directly or indirectly stimulates PDEs activity (Figure 7B), which not only could cause the loss in responsiveness of the β_2 -ARs, but also could stimulate degradation of cAMP and affect the repairing of CEES-induced lung injury and inflammation as evident by leakage of [125 I]-BSA (Figure 1). Furthermore, the CEES treatment causes down-regulation of mRNA (Figure 5) following an increase in TNF α and ROS and causes desensitization of β_2 -ARs, which is relevant to ARDS, since β_2 -ARs are responsible for surfactant secretion by alveolar type II cells.

REFERENCES

1. Smith MG, Stone W, Crawford K, Ward P, Till GO, Das SK. A promising new treatment for mustard gas with the potential to substantially reduce the threat posed by chemical, biological and radiological agents. *Jane's Chem-Bio Web* 2003;1-5.

2. Papirmeister B, Fenster AJ, Robinson SI, Ford RD. Sulfur mustard injury: Description of lesions and resulting incapacitations. In: Fenster AJ, editor. Medical defense against mustard gas. Toxic mechanisms and pharmacological implications. Boca Raton, FL: CRC; 1991. pp 13–42.
3. Worwser U. Toxicology of mustard gas. *Trends Pharmacol Sci* 1991;12:164–167.
4. Momeni AZ, Enshaelh S, Meghdadi SM, Amindjavaheri M. Skin manifestation of mustard gas. Clinical study of 535 patients exposed to mustard gas. *Arch Dermatol* 1992;128:775–780.
5. Calvet JH, Jarrean PH, Levame M, D'ortho MP, Lorino H, Harf A, Mavier IM. Acute and chronic respiratory effects of sulfur mustard intoxication in guinea pigs. *J Appl Physiol* 1994;76:681–688.
6. Emad A, Rezaian GR. The diversity of the effects of sulfur mustard gas inhalation on respiratory system 10 years after a single, heavy exposure: Analysis of 197 cases. *Chest* 1997;112:734–738.
7. Leff JA, Parsons PE, Day CE, Taniguchi N, Jochum M, Fritz H, Moore FA, Moore EE, McCord JM, Repine JE. Serum antioxidants as predictors of adult respiratory distress syndrome in patients with sepsis. *Lancet* 2003;341:777–780.
8. Lloyd SS, Cheng AK, Taylor FB, McCay JEG. Free radicals and septic shock in primates: The role of tumor necrosis factor. *Free Radic Biol Med* 1993;14:233–242.
9. Rajaratnam VS, Das SK. Array of cytokine induction in early lung injury response to 2-chloroethyl ethyl sulfide, a mustard gas analog. *FASEB J* 2005;19:A852.
10. Chatterjee D, Mukherjee S, Smith MG, Das SK. Signal transduction events in lung injury induced by 2-chloroethyl ethyl sulfide (CEES), a mustard analog. *J Biochem Mol Toxicol* 2003;17:1–8.
11. Das SK, Mukherjee S, Smith MG, Chatterjee D. Prophylactic protection by *N*-acetylcysteine against the pulmonary injury induced by 2-chloroethyl ethyl sulfide, a mustard analogue. *J Biochem Mol Toxicol* 2003;17:177–184.
12. Liggett SB. Update on current concepts of the molecular basis of beta-2 adrenergic receptor signaling. *J Allergy Clin Immunol* 2002;110:S223–S227.
13. Hein L, Kobilka BK. Adrenergic receptor signal transduction and regulation. *Neuropharmacology* 1995;34:357–366.
14. Collins S, Caron MG, Lefkowitz RJ. From ligand binding to gene expression: New insight into the regulation of G-protein-coupled receptors. *Trends Biochem Sci* 1992;17:37–40.
15. Brady AE, Limbird LE. G protein-coupled receptor interacting proteins: Emerging roles in localization and signal transduction. *Cell signal* 2002;14:297–309.
16. Penn RB, Benovic JL. Desensitization of G protein-coupled receptors. In: Conn PM, editor. *Handbook of physiology*. New York: Oxford University Press; 1998. Vol 1 pp 125–164.
17. Brown LA, Longmore WJ. Adrenergic and cholinergic regulation of lung surfactant secretion in the isolated perfused rat lung and in the alveolar type II cell in culture. *J Biol Chem* 1981;256:66–72.
18. Das SK, Sikpi MO, Skolnick P. Heterogeneity of beta adrenoceptors in guinea pig alveolar type II cells. *Biochem Biophys Res Commun* 1987;142:898–903.
19. McGraw DW, Fukuda N, James PF, Fobes SL, Woo AL, Lingrel JB, Witte DP, Matthay MA, Liggett SB. Targeted transgenic expression of beta (2)-adrenergic receptors to type II cells increases alveolar fluid clearance. *Am J Physiol Lung Cell Mol Physiol* 2001;281:L895–903.
20. Das SK, Mukherjee S. Role of peripheral benzodiazepines receptors on secretion of surfactant in guinea pig alveolar type II cells. *Biosci Rep* 1999;19:461–471.
21. Peterson JW, Luich KM, Goldie RG. The role of beta-adrenoreceptors in hyperreactivity. In: Morley J, editor. *Perspectives in asthma*. London: Academic Press; 1982. pp 245–268.
22. Pauwels R. Bronchial adrenergic receptors and asthma, tachyphylaxis and its prevention. *Allerg Immunol (Paris)* 1988;20:261–265.
23. Persad S, Elimban V, Kaila J, Dhalla NS. Biphasic alterations in cardiac Beta-adrenoceptor signal transduction mechanism due to oxyradicals. *J Pharmacol Exp Ther* 1997;282:1623–1631.
24. Ferguson SSG. Evolving concepts in G protein-coupled receptor endocytosis: The role in receptor desensitization and signaling. *Pharmacol Rev* 2001;53:1–24.
25. Stadel JM, Nambi P, Shorr RGL, Sawyer DF, Caron MG, Lefkowitz RJ. Catecholamine-induced desensitization of Turkey erythrocyte adenylate cyclase is associated with phosphorylation of the β -adrenergic receptor. *Proc Natl Acad Sci USA* 1983;80:3173–3177.
26. Profita M, Chiappara G, Mirabella F, Di Giorgi R, Chimenti L, Costanzo G, Riccobono L, Bellia V, Bousquet J, Vignola AM. Effect of cilomilast (Ariflo) on TNF α , IL-8 and GM-CSF release by airway cells of patients with COPD. *Thorax* 2003;58:573–579.
27. Hall M, Glumoff V, Ramet M. Surfactant in respiratory distress syndrome and lung injury. *Comp Biochem Physiol* 2001;129:287–294.
28. Dobbs LG, Mason RJ. Pulmonary alveolar type II cells isolated from rats: Release of phosphatidylcholine in response to β -adrenergic stimulation. *J Clin Invest* 1979;63:378–387.
29. Whitsett JA, Manton MA, Darovec-Beckerman C, Adams KG, Moore JJ. Beta-adrenergic receptors in the developing rabbit lung. *Am J Physiol* 1981;240:E351–357.
30. Mills HE. Implications of feedback regulation of beta-adrenergic signaling. *J Anim Sci* 2001;80 (E Suppl. 1):E30–E35.
31. Davies AO, Lefkowitz RJ. Regulation of β -adrenergic receptors by steroid hormones. *Annu Rev Physiol* 1984;46:119–130.
32. Mak JCW, Nishikawa M, Shirasaki H, Miyayasu K, Barnes PJ. Protective effects of glucocorticoids on down regulation of pulmonary β_2 -Adrenergic receptors in vivo. *J Clin Invest* 1995;96:99–106.
33. Hadcock JR, Malbon CC. Regulation of β -adrenergic receptors by permissive hormones; glucocorticoids increase steady state levels of receptor mRNA. *Proc Natl Acad Sci USA* 1988;85:8415–8419.
34. Ward PA, Till GO, Kunel R, Beaucham C. Evidence for role of hydroxyl radical in complement and neutrophil-dependent tissue injury. *J Clin Invest* 1983;72:789–801.
35. Mukherjee S, Nayyar T, Chytil F, Das SK. Mainstream and sidestream cigarette smoke exposure increases retinol in guinea pig lungs. *Free Radic Biol Med* 1995;18:507–514.
36. Das SK, Mukherjee S, Banerjee D. β -adrenoreceptors of multiple affinities in a clonal capillary endothelial cell line and its functional implication. *Mol Cell Biochem* 1994;140:49–54.

37. Peterson GL. A simplification of the protein assay method of Lowry et al. Which is more generally applicable. *Anal Biochem* 1977;83:346–356.
38. Das SK, Tsao FHC, Mukherjee S. Mainstream and sidestream cigarette smoke exposure increases Ca²⁺-dependent phospholipid binding proteins in guinea pig alveolar type II cell. *Mol Cell Biochem* 2002;231:37–42.
39. Mukherjee S, Coaxum SD, Maleque M, Das SK. Effects of oxidized low-density lipoprotein on nitric oxide synthetase and protein kinase C activities in bovine endothelial cells. *Cell Mol Biol* 2001;47:1051–1058.
40. Belfer I, Buzas B, Evans C, Hipp H, Phillips G, Taubman J, Lorincz I, Lipsky RH, Enoch MA, Max MB, Goldman D. Haplotype structure of the beta adrenergic receptor genes in US Caucasians and African Americans. *Eur J Hum Genet* 2004;13:341–351.
41. Sinha Roy S, Mukherjee S, Kabir S, Rajaratnam V, Smith M, Das SK. Inhibition of cholinephosphotransferase activity in lung injury induced by 2-chloroethyl ethyl sulfide, a mustard analog. *J Biochem Mol Toxicol* 2005;19:289–297.
42. Watson ML, Smith D, Bourne AD, Thompson RC, Westwick J. Cytokines contribute to airway dysfunction in antigen-challenged guinea pigs: Inhibition of airway hyperreactivity, pulmonary eosinophil accumulation and tumor necrosis factor by pretreatment with an interleukin-1 receptor antagonist. *Am J Respir Cell Mol Biol* 1993;8:365–369.
43. Hakonarson H, Herrick DJ, Gonzalez P, Grunstein MM. Mechanism of cytokine-induced modulation of β -adrenoceptor responsiveness in airway smooth muscle. *J Clin Invest* 1996;97:2593–2600.
44. Moore PE, Lahiri T, Laporte JD, Church T, Panettieri Jr. RA, Shore SA. Signal transduction in smooth muscle selected contribution: Synergism between TNF α and IL-1 β in airway smooth muscle cells: Implications for β -adrenergic responsiveness. *J Appl Physiol* 2001;91:1467–1474.
45. Hegab AE, Sakamoto T, Saitoh W, Massoud HH, Massoud HM, Hassanein KM, Sekizawa K. Polymorphisms of IL4, IL13 and ADR2 gene in COPD. *Chest* 2004;126:1832–1839.
46. Wills-Krap M, Uchida Y, Lee JY, Jinot J, Hirata A, Hirata F. Organ culture with proinflammatory cytokines reproduces impairment of the beta-adrenoreceptor-mediated relaxation in tracheas of a guinea pig antigen model. *Am J Respir Cell Mol Biol* 1993;8:153–159.
47. Koto H, Mak JC, Haddad EB, Xu WB, Salmon M, Barnes PJ, Chung KR. Mechanisms of impaired beta-adrenoceptor-induced airway relaxation by interleukin-1 beta in vivo in the rat. *J Clin Invest* 1996;98:1780–1787.
48. Boskabady MH, Teymoory S. The influence of epithelium on the responsiveness of guinea-pig trachea to -adrenergic agonist and antagonist. *Med Sci Monit* 2003;9(9):BR336–342.
49. Lefkowitz RJ, Caron MG. Regulation of adrenergic receptor function by phosphorylation. *Curr Top Cell Regul* 1986;28:209–231.
50. Mills SE. Implications of feedback regulation of beta-adrenergic signaling. *J Anim Sci* 2003;80(E Suupl. 1):E30–E35.
51. Van Hoof IH, Van Bree L, Bast A. Changes in receptor function by oxidative stress in guinea pig tracheal smooth muscle. *Cent Eur J Public Health* 1996;4(Suppl): 3–5.
52. Doelman CJ, Leurs R, Oosterom WC, Bast A. Mineral dust exposure and free radical-mediated lung damage. *Exp Lung Res* 1990;16:41–55.
53. Doelman CJ, De Vlieger JF, Sprong RC, Bast A. Oxidative stress and receptor responses in guinea-pig tracheal tissue. *Agents Actions Suppl* 1990;31:143–145.
54. Nishikawa M, Mak JCW, Shirasaki H, Harding SE, Barnes PJ. Differential down-regulation of pulmonary β_1 - and β_2 -adrenergic receptor messenger RNA with prolonged in vivo infusion of isoprenaline. *Eur J Pharmacol Mol Pharmacol* 1993;247:131–138.
55. Zhang HQ, Tai HH, Lai YL. Oxygen radicals in the nonvagal component of cholinergic airway constriction. *Respir Physiol* 1996;104:213–220.
56. Morken JJ, Warren KU, Xie Y, Rodriguez JL, Lyte M. Epinephrine as a mediator of pulmonary neutrophils sequestration. *Shock* 2002;18:46–50.
57. Goadby P. Release of adrenaline by anaphylaxis in the guinea pig: Its effect on lung surfactant. *J Pharm Pharmacol* 1975;27:254–261.
58. Collins S, Altschmied J, Herbsman O, Caron MG, Mellon PL, Lefkowitz RJ. A cAMP response element in the β_2 -adrenergic receptor gene confers transcriptional autoregulation by cAMP. *J Biol Chem* 1990;265:19330–19335.
59. Tran TM, Friedman J, Qunaibi F, Baameur F, Moore RH, Clark RB. Characterization of agonist stimulation of cAMP-dependent protein kinase and G-protein-coupled receptor kinase phosphorylation of the β_2 -adrenergic receptor using phosphoserine-specific antibodies. *Mol Pharmacol* 2004;65:106–206.
60. Penn RB, Benovic JL. Regulation of G protein coupled receptors. In: Conn PM, editor. *Handbook of physiology*. Oxford: Oxford University Press; 1998. pp 125–164.
61. Raeburn D, Adrenier C. Isoenzyme-selective cyclic nucleotide phospho-diesterase inhibitors: Effects on airways smooth muscle. *Int J Biochem Cell Biol* 1995;27:29–37.
62. Tepe NM, Liggett SB. Functional receptor coupling to Gi a mechanism of an agonist-promoted desensitization of the beta2-adrenergic receptor. *J Recept Signal Transduct Res* 2000;20:75–85.
63. Lakshminarayanan V, Drab-Weiss EA, Roeback KA. Hydrogen peroxide and tumor necrosis factor- α induce differential binding of the redox-responsive transcription factors AP-1 and NF- κ B to the interleukin-8 promoters in endothelial and epithelial cells. *J Biol Chem* 1996;273:32670–32678.
64. Rahman I, MacNee W. Role of transcription factors in inflammatory lung diseases. *Thorax* 1998;53:601–612.
65. Spurzem JR, Gupta J, Veys T, Kneifl KR, Rennard SI, Wyatt TA. Activation of protein kinase A accelerates bovine bronchial epithelial cell migration. *Am J Physiol Lung Cell Mol Physiol* 2002;282:L1108–L1116.
66. Nishimura K, Tamaoki J, Isono K, Aoshiba K, Nagai A. Beta-adrenergic receptor-mediated growth of human airway epithelial cell lines. *Eur Respir J* 2002;20:353–358.
67. Dumasius V, Sznajder JL, Azzam ZS, Boja J, Mutlu GM, Maron MB, Factor P. Beta (2)-adrenergic receptor overexpression increases alveolar fluid clearance and responsiveness to endogenous catecholamines in rats. *Circ Res* 2001;89:907–914.

Antioxidant Liposomes Protect against CEES-Induced Lung Injury by Decreasing SAF-1/MAZ-Mediated Inflammation in the Guinea Pig Lung

Sutapa Mukhopadhyay,¹ Shyamali Mukherjee,¹ Bimal K. Ray,² Alpana Ray,² William L. Stone,³ and Salil K. Das¹

¹Department of Cancer Biology, Meharry Medical College, Nashville, TN 37208, USA; E-mail: sdas@mmc.edu

²Department of Veterinary Pathobiology, University of Missouri, Columbia, MO 65211, USA

³Department of Pediatrics, East Tennessee State University, Johnson City, TN 37614, USA

Received 24 September 2009; accepted 26 September 2009

ABSTRACT: We reported earlier in a guinea pig model that exposure of 2-chloroethyl ethyl sulfide (CEES), a mustard gas analog, causes lung injury associated with the activation of tumor necrosis factor alpha (TNF- α), mitogen activated protein kinases (MAPK) signaling, and activator protein-1 (AP-1) transcription factor. Our earlier studies also revealed that antioxidant liposomes can be used as antidotes. Proinflammatory cytokines IL-1, IL-6, and TNF- α , either alone or in combination, can induce the activation of another group of transcription factors, namely SAF-1 (serum accelerator factor-1)/MAZ (Myc-associated zinc finger protein). Phosphorylation of SAF-1 via MAPK markedly increases its DNA-binding and transactivational potential. The objective of the present study was to investigate whether CEES exposure causes activation of IL-1 β , IL-6, and SAF-1/MAZ and whether these effects can be prevented by antioxidant liposomes. A single dose (200 μ L) of the antioxidant liposome mixture was administered intratracheally after 5 min of exposure of CEES (0.5 mg/kg). The animals were sacrificed either 1 h or 30 days after CEES exposure. CEES exposure caused an upregulation of proinflammatory cytokines IL-6 and IL-1 β in the lung along with an increase in the activation of transcription factor SAF-1/MAZ. The antioxidant liposomes treatment significantly blocked the CEES-induced activation of IL-6, IL-1 β , and SAF-1/MAZ. This might suggest that antioxidant liposomes might offer a potential therapeutic strategy against inflammatory diseases associated with activation of these bioactive molecules. © 2010 Wiley Periodicals, Inc. J

Biochem Mol Toxicol 24:187–194, 2010; Published online in Wiley InterScience (www.interscience.wiley.com). DOI 10.1002/jbt.20329

KEYWORDS: IL-6; IL-1 β ; SAF-1/MAZ; Lung Injury; CEES; Antioxidant Liposome

INTRODUCTION

Inflammation is a host response to external insults, and it is manifested both locally and systemically. Normally, this cellular process is designed to defend the host from the deleterious effect of external factors. However, the host response may become uncontrolled causing more harm to the host by eliciting abnormal gene expression [1–3]. 2-Chloroethyl ethyl sulfide (CEES) exposure of lung cells may trigger this type of host response leading to massive damage to the organ [4,5] and perhaps an adverse systemic effect. The process presumably begins with chemical exposure of the epithelial cells of the lung, infiltration of circulating macrophage cells and other immune cells, and production of inflammatory cytokines. This latter event subsequently triggers a cascade of intracellular events in those cells having appropriate receptors to these bioactive ligands. The most critical intracellular event is the activation of transcription factors, which subsequently induce many genes whose abnormal expression have an adverse physiological effect [6]. Such genes include, among others, α 1-antitrypsin, matrix metalloproteinases, and tissue inhibitors of metalloproteinases.

The question that remains unanswered is how these genes are activated. Obviously, transcription

Correspondence to: Salil K. Das.

Contract Grant Sponsor: U.S. Army.

Contract Grant Number: W81XWH-06-2-0044.

© 2010 Wiley Periodicals, Inc.

factors are considered major regulatory molecules and their control may provide a basis for therapeutic intervention of inflammatory diseases. There are a number of transcription factors, which are activated by inflammatory cytokines, and these include nuclear factor kappa B (NF- κ B), CCAAT/enhancer-binding protein, and activator protein-1 (AP-1) among others. Another transcription factor has recently been reported to be highly induced by inflammation is serum accelerator factor-1 (SAF-1) [7,8].

SAF-1 is a member of those transcriptional factors regulating serum amyloid A (SAA) protein. This protein contains multiple Cys₂-His₂-type zinc finger domains most of which are located at its C-terminal half, which are activated by a number of inflammatory stimuli, including cytokines, phorbol 12-myristate 13-acetate, lipopolysaccharide, and oxidized low-density lipoproteins [8–11]. Proinflammatory cytokines interleukin-1 (IL-1), IL-6, and tumor necrosis factor alpha (TNF- α), either alone or in combination, can increase the transcription of the gene for SAA [10,12–15]. Phosphorylation of SAF-1 via mitogen activated protein kinases (MAPK), protein kinase C, or protein kinase A markedly increases its DNA-binding and DNA transactivational potential [16–18]. SAF-1 shows a high degree of homology with Myc-associated zinc finger protein (MAZ)/Pur-1 proteins, and this suggests that SAF-1 is an ortholog of MAZ/Pur-1 [19,20].

The 60-kDa MAZ (also designated ZF87, and Pur-1 in mouse) is a transcription factor that functions in both the initiation and termination of the transcription of target genes [19]. It binds to two sites (ME1a1 and ME1a2) within the c-myc promoter but has a greater affinity for ME1a1 [21]. MAZ and SV40 promoter-activating factor 1 (Sp1) [22] regulate expression of the serotonin 1A receptor gene promoter, suggesting that MAZ may act on a variety of promoters through G-C rich sequences, which serve as binding sites for the Sp1 family of transcription factors [23,24].

We reported earlier that the initiation of free-radical-mediated TNF- α cascade is the major pathway in mustard gas-induced acute lung injury [25]. We have recently demonstrated that CEES-induced activation of TNF- α is associated with an increase in MAPKs/AP-1 signaling, a stimulation of cell proliferation and lung injury [26]. Our earlier study also revealed that consumption of *N*-acetylcysteine (NAC), an antioxidant in drinking water prior to CEES exposure, significantly inhibits the induction of TNF- α [4].

The role of SAF-1/MAZ in the inflammation of the lung epithelium after CEES exposure is not yet known. Therefore, it is important to elucidate the mechanism by which CEES exposure causes SAF-1/MAZ-mediated inflammation and injury in lung. The present study also investigates whether the CEES-induced activation of

SAF-1 is associated with activation of proinflammatory cytokines, particularly IL-1 β and IL-6. Furthermore, the study also reveals data on the protective effect of antioxidant liposome against CEES-induced lung damage by reducing activation of IL-6, IL-1 β , and SAF-1/MAZ.

MATERIALS AND METHODS

Exposure of Animals to CEES

Male guinea pigs (Hartley strain, 5–6 weeks old, 400 g body weight) were obtained from Charles River (Wilmington, MA). Animals were infused intratracheally with a single dose (0.5 mg/kg body wt.) of CEES (Sigma Chemicals, St. Louis, MO) in ethanol (infusion volume was 100 μ L/animal) [4]. Control animals were infused with 100 μ L of ethanol in the same way. All animal experiments were performed in accordance with the standards in the *Guide for the Care and Use of Laboratory Animals* and were supervised by veterinarians from the Unit for Laboratory and Animal Care of Meharry Medical College.

Treatment of Animals with Antioxidant Liposomes

The antioxidant liposome fraction was prepared as described elsewhere [27]. The blank liposomes (LIP1) contained only soybean phospholipids, cholesterol, and phosphatidic acid in a mole fraction ratio of 71:28:0.67, respectively, with no antioxidants. The antioxidant liposome fraction (LIP2) contained soybean phospholipids, cholesterol, and phosphatidic acid (mole fraction ratio of 55:22:0.6) along with 11 mM α -tocopherol, 11 mM γ -tocopherol, 5 mM δ -tocopherol, and 75 mM NAC. Liposomes were given intratracheally to the animals. Animals were divided into five groups. Animals of group 1 served as controls and received LIP1 (200 μ L) after 5 min of vehicle exposure (100 μ L of ethanol) and were sacrificed after 1 h. After 5 min of CEES exposure, animals of groups 2 and 4 received LIP1 (200 μ L) and were sacrificed either after 1 h or 30 days post-CEES exposure, respectively. Similarly 5 min after CEES exposure, the animals of groups 3 and 5 received LIP2 (200 μ L) and sacrificed either after 1 h or 30 days post-CEES exposure, respectively. Since there was no difference in lung morphology between 1-h and 30-day control groups in our previous study [27], we did not include a control group for 30 days postvehicle exposure in this study. Furthermore, since LIP1 had no effect on CEES-induced lung injury [27], we did not include a group with CEES only. Animals were sacrificed, and lungs were immediately perfused with ice-cold 2.6 mM phosphate buffered saline containing 5.6 mM glucose, removed from the chest

cavity and immediately flash frozen in liquid nitrogen and stored at -80°C for further experiment. A section of the lung was fixed in buffered formalin for morphological assessment.

Morphological Assessment of Lung Injury

Morphological assessment of lung tissues was carried out as described before [28]. Briefly, a portion of lung tissue was fixed overnight in neutral buffered formalin (10%), pH 7.2, and embedded in paraffin for light microscopy. Lung sections were obtained for histological examination by staining with hematoxylin and eosin.

Assay of IL-6 and IL-1 β by ELISA

Lung tissues were sonicated in Tris buffered saline (0.05 M Tris-HCl, 0.15 M sodium chloride, pH 7.4), centrifuged at 10,000 rpm for 10 min. IL-6 and IL-1 β were measured in the supernatant using an IL-6 and IL-1 β enzyme-linked immunosorbent assay (ELISA) kit (Invitrogen Corporation, Camarillo, CA). Supernatants were added to IL-6 and IL-1 β antibody-coated micro wells (supplied with the kit) and incubated for 2 h at 37°C followed by 3 h at room temperature. After washing, the wells were incubated with biotin-conjugated secondary antibody for 1 h. The wells were washed and incubated with streptavidin-horseradish peroxidase complex. The color reactions were carried out using horseradish peroxidase substrate after washing. The color developments were measured using a Bio-Rad microplate spectrophotometer (Bio-Rad, Hercules, CA) after addition of stop solution.

Western Blot Analysis of SAF-1 and MAZ

Lung tissues were homogenized in 5 volumes of ice-cold lysis buffer (Biosource, Camarillo, CA) containing protease inhibitor cocktail (0.01%, Sigma Chemicals, St. Louis, MO) by using a Brinkman Polytron (setting 6–7, 30 s). Proteins were measured by Bio-Rad protein assay (Bio-Rad, Hercules, CA), and 50 μg protein extract was separated by 12% SDS polyacrylamide gel electrophoresis (SDS-PAGE). Proteins were transferred electrophoretically onto PVDF membranes (Immobilon-P Millipore, Bedford, MA). The membrane was immunoblotted with SAF-1 [11] and MAZ (University of New York at Stony Brook) antibodies and horseradish peroxidase (HRP)-conjugated anti-mouse, anti-goat, and anti-rabbit secondary antibodies. Binding of antibodies to the blots was detected with an ECL-detection system (Perkin Elmer, Boston, MA) following the manufacturer's instructions. Stripped blots were re probed with β -actin specific polyclonal antibod-

ies (Santa Cruz Biotechnology Inc., Santa Cruz, CA) to enable normalization of signals between samples. Band intensities were analyzed using Bio-Rad Gel Doc (Bio-Rad, Hercules, CA).

Immunohistochemical Staining of MAZ

Deparaffinized formalin (10%) fixed sections were incubated with normal rabbit serum for 30 min to block nonspecific binding. After rinses in PBS and incubation in 0.3% H_2O_2 to block endogenous peroxidase activity, the sections were incubated overnight at 4°C with MAZ monoclonal antibody. The sections were then incubated with HRP-streptavidin (Jackson ImmunoResearch Laboratories, West Grove, PA) for 60 min at room temperature and reacted with diaminobenzamine until a reddish brown color developed. Sections were then counterstained with Gill's hematoxylin solution and cover slipped. Reactivity was evaluated by the number of positive and negative epithelial cells in several randomly selected fields in each section.

Immunofluorescence Staining of MAZ

The deparaffinized sections were incubated overnight at 4°C with a monoclonal antibody for MAZ. The sections were incubated with a fluorescein isothiocyanate (FITC)-conjugated secondary antibody for 1 h, treated with vectashield mounting medium (Vector Laboratories), cover slipped, and viewed on a TE2000 C1 laser scanning confocal microscope operated with Nikon EZC1 3.2 software (Tokyo, Japan). FITC was excited using a 488-nm laser, and the emitted light was captured with a bandpass filter (505–550 nm). Images were collected using a 60×1.4 numerical aperture (N.A.) oil immersion objective.

Statistical Analysis

Data were presented as mean \pm standard error (SE). Statistical comparisons between groups were determined by the Tukey test after one-way analysis of variance (ANOVA), using GraphPad prism version 5.0 (GraphPad software, San Diego, CA). A *P* value of less than 0.05 was considered statistically significant.

RESULTS

Attenuation of CEES-Induced Morphological Changes by Antioxidant Liposomes

The intratracheal infusion of CEES to guinea pigs caused an immediate and severe injury to lung epithelium, and these morphological changes were protected

by intratracheal infusion of the antioxidant liposome (LIP2) given after 5 min of CEES exposure. Photographs are not shown since these have been described earlier [27].

Attenuation of CEES-Induced Activation of IL-6 and IL-1 β by Antioxidant Liposomes

The data on the effects of liposomes on CEES-induced induction of IL-6 and IL-1 β in lung are presented in Figure 1. CEES caused a 4.7-fold and 3.7-fold increase in the IL-6 level after 1 h and 30 days of exposure, respectively. LIP2 treatment significantly blocked

the CEES-induced activation of IL-6 at both time points (Figure 1A).

CEES caused a 2.3-fold increase in the IL-1 β level after 1 h and 30 days of exposure, respectively. LIP2 treatment significantly blocked the CEES-induced activation of IL-1 β at both time points (Figure 1B).

Western Blot Analysis of SAF-1 and MAZ

For Western blot analysis, we used rabbit polyclonal anti SAF-1 antibody. We got a band close to 50 kDa with this antibody (Figure 2). However, this

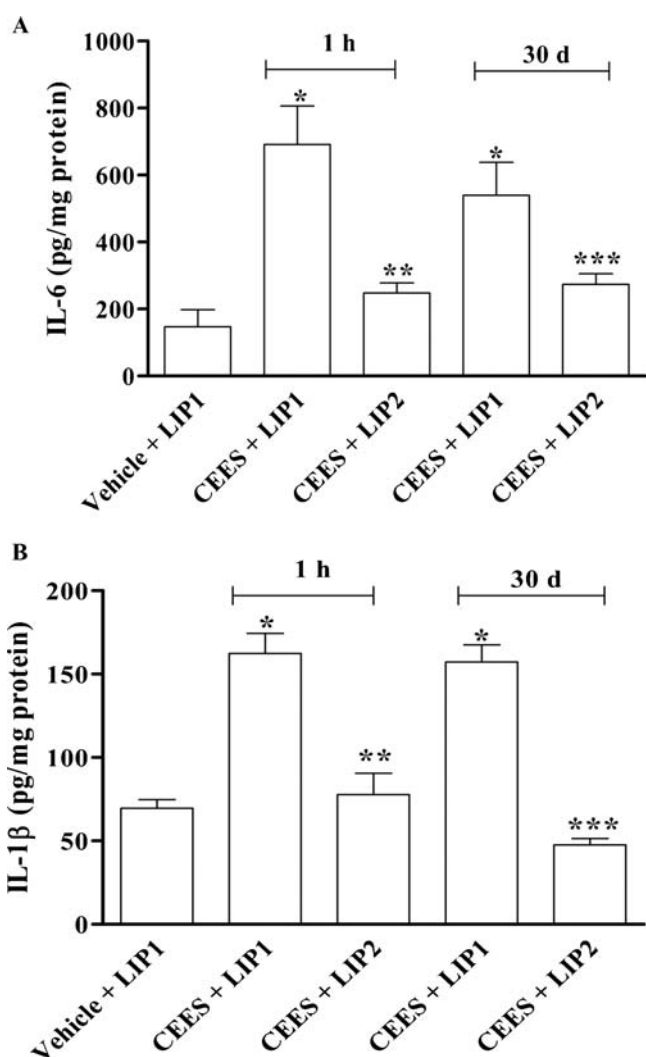


FIGURE 1. Attenuation of CEES-induced activation of (A) IL-6 and (B) IL-1 β by antioxidant liposome. Accumulation of IL-6 and IL-1 β was measured by ELISA at 1 h and 30 days after exposure to CEES (0.5 mg/kg body weight) + control liposomes (LIP1) and 1 h or 30 days following CEES exposure and antioxidant liposome (LIP2) treatment. Statistical significance was determined by the Tukey test after one-way ANOVA. Values are mean \pm SE ($N = 3$). * $P < 0.05$ compared to vehicle control; ** $P < 0.05$ compared to CEES + LIP1 exposure for 1 h; *** $P < 0.05$ compared to CEES + LIP1 exposure for 30 days.

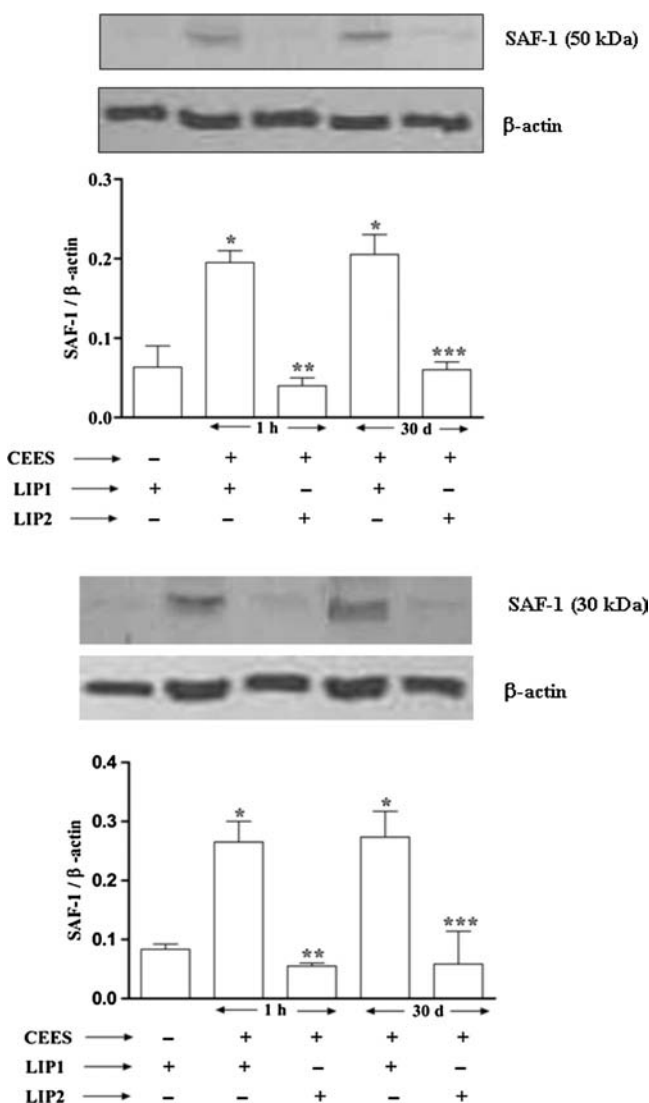


FIGURE 2. Effects of antioxidant liposomes on CEES-mediated activation of SAF-1 transcription factor (shown as 50 and a 30 kDa, presumed cleavage product) in guinea pig lung by Western blot analysis. Statistical significance was determined by the Tukey test after one-way ANOVA. Results are expressed as mean \pm SE ($N = 3$). * $P < 0.05$ compared to vehicle control; ** $P < 0.05$ compared to CEES exposure + LIP1 for 1 h; *** $P < 0.05$ compared to CEES exposure + LIP1 for 30 days.

antibody also elicited a second band at 30 kDa (Figure 2), which may be a cleaved product of the 50-kDa protein. Indeed earlier report [18] indicated that SAF-1 can be proteolytically truncated, generating a highly active form of this protein. Our current data provides evidence for a possible accumulation of such truncated form of SAF-1 in the lung during CEES-induced inflammatory condition.

Figure 2 clearly indicates that CEES exposure caused a transient activation of SAF-1 (50 kDa) within 1 h (207.9%) followed by a slight increase after 30 days (223.7%). LIP2 treatment completely blocked the CEES-induced activation of SAF-1 at both time points. CEES exposure caused an increase in the activation of SAF-1 (30 kDa) protein level within 1 h (218%) followed by a slight increase after 30 days (228%). LIP2 treatment completely blocked the CEES-induced activation of SAF-1 at both time points.

Figure 3 demonstrated that CEES exposure causes a transient activation of MAZ (60 kDa) within 1 h (160.7%) followed by a slight decrease after 30 days (123%). However, even at 30 days there was a significantly higher level of MAZ in comparison to the control levels. The activation of MAZ was significantly decreased when treated with LIP2 (Figure 3).

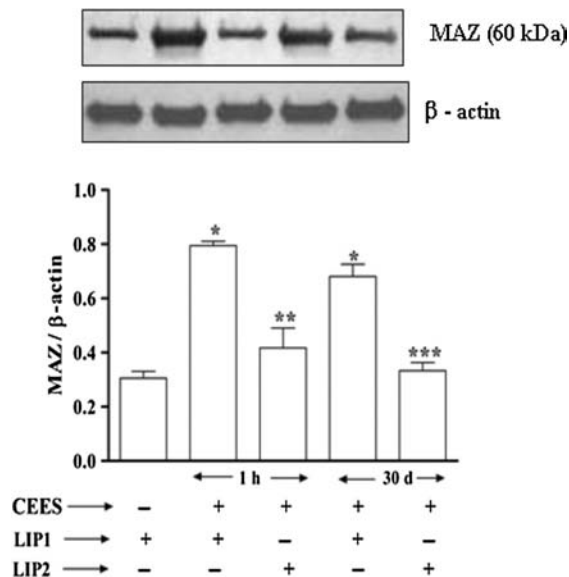


FIGURE 3. Inhibition of CEES-induced increase in protein levels of the MAZ transcription factor by antioxidant liposomes in guinea pig lung by Western blot analysis ($N = 3$ in each group). Statistical significance was determined by the Tukey test after one-way ANOVA. Results are expressed as mean \pm SE, * $P < 0.05$ compared to vehicle control; ** $P < 0.05$ compared to CEES exposure +LIP1 for 1 h; *** $P < 0.05$ compared to CEES exposure +LIP1 for 30 days.

Immunohistochemical and Immunofluorescence Staining of MAZ

We demonstrated by immunohistochemistry (Figure 4) and immunofluorescence (Figure 5) the increase in the protein level of MAZ following CEES exposure and protection against this increase by LIP2. CEES-exposed animals showed more immunopositive staining against MAZ antibody (Figures 4B and 4D) at inflammatory sites of both airway and infiltrating cells present in alveolar space, indicating a much higher level of inflammation at both time points. In contrast, only a few cells of control lungs showed little or no staining with this antibody (Figure 4A). The staining was almost negligible when CEES-exposed animals were treated with LIP2 (Figures 4C and 4E).

Immunofluorescence with anti-MAZ antibody showed higher levels of nuclear MAZ protein in the CEES-exposed lung compared to the control lung (Figure 5). The staining was almost negligible when CEES-exposed animals were treated with LIP2 (Figure 5).

DISCUSSION

We reported earlier that intratracheal exposure of CEES to guinea pigs causes acute lung injury and fibrosis associated with activation of free-radical-mediated TNF- α cascade [4,25,27]. CEES-induced lung damage was characterized by histological demonstration of loss of type II cells and increase in the number of neutrophils and eosinophils in the bronchi and alveolar space as well as accumulation of septal and perivascular fibrin and collagen [27]. The lung fibrosis was confirmed by quantitative assessment of hydroxyproline content [27]. Furthermore, this report revealed that antioxidant liposomes containing NAC and tocopherols infused intratracheally within 5 min of exposure of CEES offer a significant protection against lung damage [27]. The protection of lung damage by antioxidant liposomes was mediated by inhibiting the recruitment of neutrophils, eosinophils, and red blood cells in the bronchi, alveolar space, arterioles and veins, as well as deposition of fibrin and collagen in the alveolar space.

It is evident from our previous study [26] that CEES-induced activation of TNF- α is associated with an increase in MAPKs/AP-1 signaling, a stimulation of cell proliferation, infiltration of neutrophils, eosinophils, and erythrocytes in the alveolar space, and lung injury. It has been reported that the cytokine-mediated induction of DNA-binding activity and the transcriptional activation of SAF-1 is regulated by a MAPK-signaling pathway [16]. We also found that

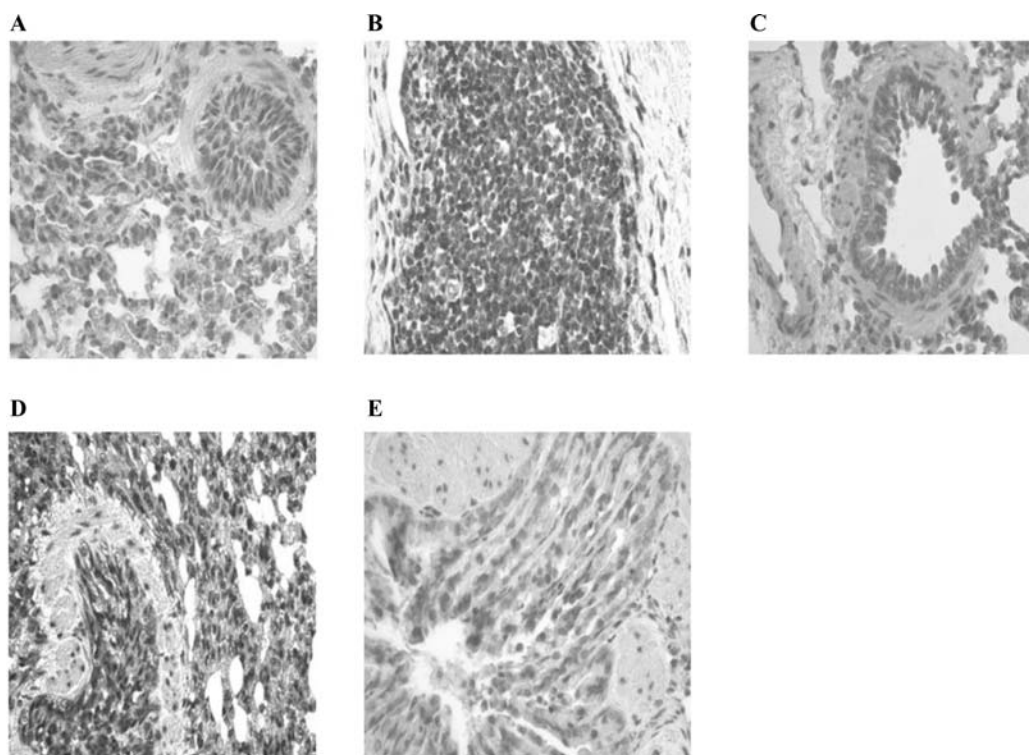


FIGURE 4. Immunohistochemical analysis of MAZ in control and CEES-induced guinea pig lung (40 \times). (A) Control (animals injected with LIP1); (B and D) CEES-exposed animals in 1 h and 30 day, respectively; (C and E) CEES-exposed animals treated with antioxidant liposomes.

exposure with 0.5 mg/kg dose of CEES after 1 h significantly increased SAF-1 and MAZ activation in guinea pig lung (Figures 2–5). It has also been reported that the levels of SAF-1 remains moderately high under chronic inflammatory conditions [29], which is in accordance with our results after 30 days of CEES exposure (Figure 2).

An interesting observation of the Western immunoblot analysis in Figures 2 and 3 is the multiple sizes of the SAF-1 and MAZ proteins. It is tempting to speculate that 50 and 30 kDa fragments as detected by the polyclonal anti-SAF-1 antibody (Figure 2) might be derived from a precursor molecule of about 60 kDa, detected by the monoclonal anti-MAZ antibody (Figure 3). Proteolytic processing of transcription factors is quite evident in nature, which provides diversity in the activity of these bioactive molecules [30,31]. It will be interesting to assess whether functional diversity of MAZ/SAF-1 involves a proteolytic processing event.

In many tissues, low levels of SAF-1 DNA-binding activity have been detected normally. However, many inflammatory agents, including IL-6 [9] are known to increase its DNA-binding activity and its overall transactivating potential. Ray et al. reported that activation of SAF-1 in response to IL-1 and IL-6 is mediated via

MAPK-regulated phosphorylation [16]. Previously, we reported that CEES causes an acute lung injury via induction of MAPK/AP-1 regulation [26]. According to Figure 1, there is also an increase in IL-6 and IL-1 β when animals are exposed to CEES.

Liposomes are considered to be an acceptable drug delivery system because they are biocompatible, biodegradable, and relatively nontoxic [32]. We have previously reported that antioxidant liposomes protect against CEES-induced lung fibrosis [27]. The effect is probably modulated via AP-1 signaling pathway. Antioxidant liposomes offer a protection against CEES-induced activation of AP-1 signaling [28]. This is evident by our observation that antioxidant liposomes offer a protection against SAF-1 and MAZ activation induced by CEES exposure (Figures 2–5).

Thus, antioxidant liposomes offer a protection against CEES-induced activation of SAF-1 and MAZ. We reported earlier that antioxidant liposomes containing NAC and tocopherols α , γ , and δ offer a protection against CEES-induced lung fibrosis by modulating AP-1 signaling pathway. Our present study also indicates that early inhibition of proinflammatory modulators, such as IL-1, IL-6, and SAF-1/MAZ transcription factor, could be key regulators for CEES-induced lung fibrosis and/or ARDS.

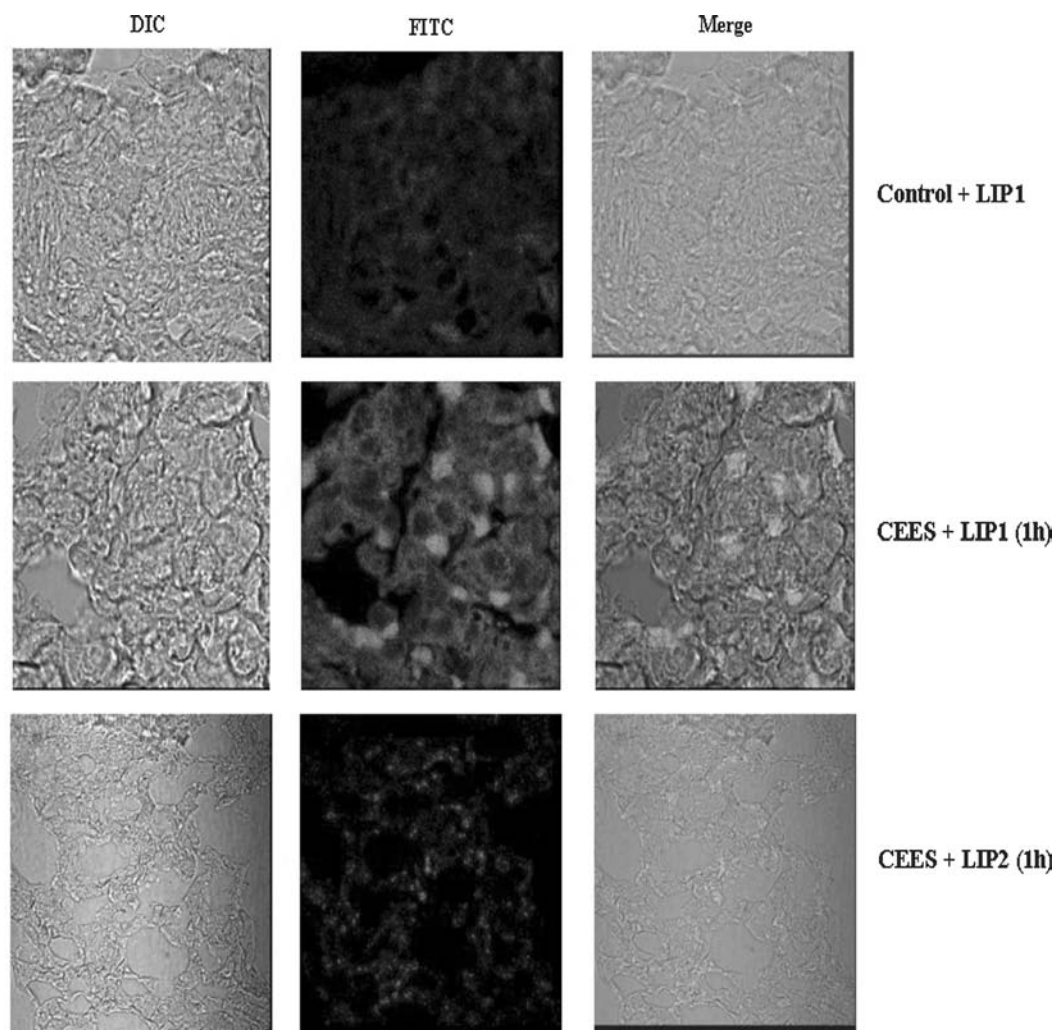


FIGURE 5. Immunofluorescence analysis of MAZ in control and CEES-induced guinea pig lung (60 \times). DIC stands for differential interference contrast.

ACKNOWLEDGMENTS

The authors thank Dr. J. Shawn Goodwin for the use of the Morphology Core Facility, which is supported by an NIH grant to Meharry (U54NS 041071). The authors also thank Dr. Milton Smith (Amax Ltd., Melbourne, FL) for his encouragement.

REFERENCES

- Adcock IM, Caramori G. Cross-talk between pro-inflammatory transcription factors and glucocorticoids. *Immunol Cell Biol* 2001;79:376–384.
- Keyszer GM, Heer AH, Gay S. Cytokines and oncogenes in cellular interactions of rheumatoid arthritis. *Stem Cells* 1994;12:75–86.
- Ray A. A SAF binding site in the promoter region of human gamma-fibrinogen gene functions as an IL-6 response element. *J Immunol* 2000;165:3411–3417.
- Das SK, Mukherjee S, Smith MG, Chatterjee D. Prophylactic protection by *N*-acetylcysteine against the pulmonary injury induced by 2-chloroethyl ethyl sulfide, a mustard analogue. *J Biochem Mol Toxicol* 2003;17:177–184.
- Chatterjee D, Mukherjee S, Smith MG, Das SK. Role of sphingomyelinase in the environmental toxin induced apoptosis of pulmonary cells. In: Haldar D, Das SK, editors. *Lipids: Sphingolipid metabolizing enzymes*. Trivandrum, Kerala, India: Research Signpost Publishers; 2004. pp. 117–139.
- McKay S, Bromhaar MM, de Jongste JC, Hoogsteden HC, Saxena PR, Sharma HS. Pro-inflammatory cytokines induce *c-fos* expression followed by IL-6 release in human airway smooth muscle cells. *Mediators Inflamm* 2001;10:135–142.

7. Ray BK, Ray A. Induction of serum amyloid A (SAA) gene by SAA-activating sequence-binding factor (SAF) in monocyte/macrophage cells. Evidence for a functional synergy between SAF and Sp1. *J Biol Chem* 1997;272:28948–28953.
8. Ray A, Ray BK. Isolation and functional characterization of cDNA of serum amyloid A-activating factor that binds to the serum amyloid A promoter. *Mol Cell Biol* 1998;18:7327–7335.
9. Ray A, Schatten H, Ray BK. Activation of Sp1 and its functional co-operation with serum amyloid A-activating sequence binding factor in synoviocyte cells trigger synergistic action of interleukin-1 and interleukin-6 in serum amyloid A gene expression. *J Biol Chem* 1999;274:4300–4308.
10. Ray BK, Chatterjee S, Ray A. Mechanism of minimally modified LDL-mediated induction of serum amyloid A gene in monocyte/macrophage cells. *DNA Cell Biol* 1999;18:65–73.
11. Ray BK, Ray A. Involvement of an SAF-like transcription factor in the activation of serum amyloid A gene in monocyte/macrophage cells by lipopolysaccharide. *Biochemistry* 1997;36:4662–4668.
12. Betts JC, Cheshire JK, Akira S, Kishimoto T, Woo P. The role of NF- κ B and NF-IL6 transactivating factors in the synergistic activation of human serum amyloid A gene expression by interleukin-1 and interleukin-6. *J Biol Chem* 1993;268:25624–25631.
13. Edbrooke MR, Burt DW, Cheshire JK, Woo P. Identification of cis-acting sequences responsible for phorbol ester induction of human serum amyloid A gene expression via a nuclear factor kappa B-like transcription factor. *Mol Cell Biol* 1989;9:1908–1916.
14. Mackiewicz A, Ganapathi MK, Schultz D, Samols D, Reese J, Kushner I. Regulation of rabbit acute phase protein biosynthesis by monokines. *Biochem J* 1988;253:851–857.
15. Ray A, Hannink M, Ray BK. Concerted participation of NF- κ B and C/EBP heteromer in lipopolysaccharide induction of serum amyloid A gene expression in liver. *J Biol Chem* 1995;270:7365–7374.
16. Ray A, Yu GY, Ray BK. Cytokine-responsive induction of SAF-1 activity is mediated by a mitogen-activated protein kinase signaling pathway. *Mol Cell Biol* 2002;22:1027–1035.
17. Ray A, Fields AP, Ray BK. Activation of transcription factor SAF involves its phosphorylation by protein kinase C. *J Biol Chem* 2000;275:39727–39733.
18. Ray A, Ray P, Guthrie N, Shakya A, Kumar D, Ray BK. Protein kinase A signaling pathway regulates transcriptional activity of SAF-1 by unmasking its DNA-binding domains. *J Biol Chem* 2003;278:22586–22595.
19. Bossone SA, Asselin C, Patel AJ, Marcu KB. MAZ, a zinc finger protein, binds to c-MYC and C2 gene sequences regulating transcriptional initiation and termination. *Proc Natl Acad Sci USA* 1992;89:7452–7456.
20. Kennedy GC, Rutter WJ. Pur-1, a zinc-finger protein that binds to purine-rich sequences, transactivates an insulin promoter in heterologous cells. *Proc Natl Acad Sci USA* 1992;89:11498–11502.
21. Pyrc JJ, Moberg KH, Hall DJ. Isolation of a novel cDNA encoding a zinc-finger protein that binds to two sites within the c-myc promoter. *Biochemistry* 1992;31:4102–4110.
22. Dynan WS, Tjian R. Isolation of transcription factors that discriminate between different promoters recognized by RNA polymerase II. *Cell* 1983;32:669–680.
23. Her S, Bell RA, Bloom AK, Siddall BJ, Wong DL. Phenylethanolamine N-methyltransferase gene expression. Sp1 and MAZ potential for tissue-specific expression. *J Biol Chem* 1999;274:8698–8707.
24. Parks CL, Shenk T. The serotonin 1a receptor gene contains a TATA-less promoter that responds to MAZ and Sp1. *J Biol Chem* 1996;271:4417–4430.
25. Chatterjee D, Mukherjee S, Smith MG, Das SK. Signal transduction events in lung injury induced by 2-chloroethyl ethyl sulfide, a mustard analog. *J Biochem Mol Toxicol* 2003;17:114–121.
26. Mukhopadhyay S, Mukherjee S, Smith M, Das SK. Activation of MAPK/AP-1 signaling pathway in lung injury induced by 2-chloroethyl ethyl sulfide, a mustard gas analog. *Toxicol Lett* 2008;181:112–117.
27. Mukherjee S, Stone WL, Yang H, Smith MG, Das SK. Protection of half sulfur mustard gas-induced lung injury in guinea pig by antioxidant liposome. *J Biochem Mol Toxicol* 2009;23:143–153.
28. Mukhopadhyay S, Mukherjee S, Stone WL, Smith M, Das SK. Role of MAPK/AP-1 signaling pathway in the protection of CEES-induced lung injury by antioxidant liposome. *Toxicology* 2009;261:143–151.
29. Ray A, Ray BK. Persistent expression of serum amyloid A during experimentally induced chronic inflammatory condition in rabbit involves differential activation of SAF, NF- κ B, and C/EBP transcription factors. *J Immunol* 1999;163:2143–2150.
30. Krupnik VE, Sharp JD, Jiang C, Robison K, Chickering TW, Amaravadi L, Brown DE, Guyot D, Mays G, Leiby K, Chang B, Duong T, Goodearl AD, Gearing DP, Sokol SY, McCarthy SA. Functional and structural diversity of the human Dickkopf gene family. *Gene* 1999;238:301–313.
31. Brown MS, Goldstein JL. The SREBP pathway: regulation of cholesterol metabolism by proteolysis of a membrane-bound transcription factor. *Cell* 1997;89:331–340.
32. Taylor KMG, Farr SJ. Liposomes for drug delivery to the respiratory track. *Drug Dev Ind Pharm* 1993;19:123–142.